

# Geotechnical Design Manual

## 2019



Version 2.0

Issued in January 2019

## PREFACE

The South Carolina Department of Transportation (SCDOT) Geotechnical Design Manual (GDM) has been developed to provide uniform practices for SCDOT's designers to complement the Mission of SCDOT by providing for safe, economical, effective and efficient geotechnical designs.<sup>1</sup>

GDM Version 2.0, January 2019, supersedes all previous editions (Version 1.0, August 2008, and Version 1.1, June 2010) of the GDM and all publications relating to the geotechnical aspects of transportation projects.

---

<sup>1</sup>SCDOT's Mission (SC Code Section 57-1-30): *"The department shall have as its functions and purposes the systematic planning, construction, maintenance, and operation of the state highway system and the development of a statewide intermodal and freight system that is consistent with the needs and desires of public.*

*"The department shall coordinate all state and federal programs relating to highways among all departments, agencies and other bodies politic and legally constituted agencies of this State and the performance of such other duties and matters as may be delegated to it pursuant to law. The goal of the department is to provide adequate, safe, and efficient transportation services for the movement of people and goods."*



<b>Table of Contents</b>	
<b>Preface</b>	
<b>Chapter 1 – Introduction</b>	
<b>Chapter 2 – Glossary</b>	
<b>Chapter 3 – Reserved</b>	
<b>Chapter 4 – Subsurface Investigation Guidelines</b>	
<b>Chapter 5 – Field and Laboratory Testing Procedures</b>	
<b>Chapter 6 – Materials Description, Classification, and Logging</b>	
<b>Chapter 7 – Geomechanics</b>	
<b>Chapter 8 – Geotechnical LRFD Design</b>	
<b>Chapter 9 – Geotechnical Resistance Factors</b>	
<b>Chapter 10 – Geotechnical Performance Limits</b>	
<b>Chapter 11 – South Carolina Geology and Seismicity</b>	
<b>Chapter 12 – Geotechnical Earthquake Engineering</b>	
<b>Chapter 13 – Geotechnical Seismic Hazards</b>	
<b>Chapter 14 – Geotechnical Seismic Design</b>	
<b>Chapter 15 – Shallow Foundations</b>	
<b>Chapter 16 – Deep Foundations</b>	
<b>Chapter 17 – Embankments</b>	
<b>Chapter 18 – Earth Retaining Structures</b>	
<b>Chapter 19 – Ground Improvement</b>	
<b>Chapter 20 – Geosynthetic Design</b>	
<b>Chapter 21 – Geotechnical Reports</b>	
<b>Chapter 22 – Plan Preparation</b>	
<b>Chapter 23 – Specifications and Special Provisions</b>	
<b>Chapter 24 – Construction QA/QC</b>	
<b>Chapter 25 – Reserved</b>	
<b>Chapter 26 – Geotechnical Software</b>	

<b>Index</b>
<b>Appendix A – Geotechnical Design Section Forms</b>
<b>Appendix B – Reserved</b>
<b>Appendix C – MSE Walls</b>
<b>Appendix D – Reinforced Soil Slopes</b>
<b>Appendix E – Geotechnical Template Plans</b>
<b>Appendix F – Geotechnical Specifications List</b>
<b>Appendix G – SCDOT Software List</b>
<b>Appendix H – Shear Wave Velocity Profiles</b>
<b>Appendix I – Shear Strength Ratio Triggering Method</b>
<b>Appendix J – Flow Charts</b>
<b>Appendix K – Performance Objective Development</b>



# **CHAPTER 1 INTRODUCTION**

## **GEOTECHNICAL DESIGN MANUAL**

*January 2019*





**Table of Contents**

<b><u>Section</u></b>		<b><u>Page</u></b>
1.1	Introduction.....	1-1
1.2	Revision Process.....	1-1





# CHAPTER 1

## INTRODUCTION

### 1.1 INTRODUCTION

The South Carolina Department of Transportation (SCDOT) Geotechnical Design Manual (GDM) has been established to provide uniform guidance for the development of field explorations, resistance factors ( $\phi$ ), performance limits, design processes and project deliverables. The GDM applies to all projects on the SCDOT system when required by SCDOT. The engineer should meet all criteria and practices presented in the GDM, while fulfilling SCDOT's operational and safety requirements. However, the criteria presented in the GDM shall not be considered as a standard that must be met in all circumstances. Engineers must consider economic impacts, aesthetics, and the social and cultural resources of the project area, and other factors as appropriate and shall request modifications to the criteria in writing to the appropriate Preconstruction – Geotechnical Design Section (PC/GDS) and shall include a technical justification as to why the modification is necessary. The GDM presents most of the information normally required in the geotechnical design of transportation projects; however, because it is impossible to address every issue that geotechnical engineers will encounter, sound engineering judgment must be exercised when conditions arise that are not specifically covered in the GDM. Frequently, geotechnical engineers must be innovative in their approach to geotechnical design. This may require, for example, additional research into geotechnical literature. Any questions concerning the applicability or interpretation of any procedure, analysis, or method contained in the GDM shall be directed to the Preconstruction Support – Geotechnical Design Section (PCS/GDS) for review and comment.

For this Manual, the Geotechnical Engineer-of-Record (GEOR) includes the Regional Production Group – Geotechnical Design Section (RPG/GDS), the Geotechnical Engineering Consultant (GEC) whether for design-bid-build or a design build team.

The current version of the GDM was prepared based on the 8<sup>th</sup> Edition of the American Association of State Highway and Transportation Officials (AASHTO) LRFD Bridge Design Specifications (2017) (AASHTO LRFD Specifications) and shall be used whenever the GDM refers to the AASHTO LRFD Specifications. The applicability of future editions and interims shall be determined by the PC/GDS in conjunction with the PCS/GDS when requested in writing from the GEOR.

### 1.2 REVISION PROCESS

The GDM is intended to provide current geotechnical design policies and procedures for use in developing State highway projects. To ensure that the GDM remains up-to-date and appropriately reflects changes in SCDOT's needs and requirements, its contents will be updated on an ongoing basis. Updates and revisions released between editions of the GDM will be published as *Geotechnical Design Bulletin (GDB)* and made available on the SCDOT website. It is the responsibility of the GDM holder to keep their copy of the GDM updated.

It is important that users of the GDM inform SCDOT of any inconsistencies, errors, need for clarification, or new ideas to support the goal of providing the best and most up-to-date information practical. Comments may be forwarded to the PCS/GDS.

# **CHAPTER 2**

# **GLOSSARY**

## **GEOTECHNICAL DESIGN MANUAL**

*January 2019*





**Table of Contents**

<b><u>Section</u></b>		<b><u>Page</u></b>
2.1	Introduction.....	2-1
2.2	Definitions.....	2-1



# CHAPTER 2

## GLOSSARY

### 2.1 INTRODUCTION

The purpose of this Chapter is to provide consistent definitions of key words and concepts that will be used throughout the GDM. Some of the definitions used herein are exclusive to the GDM, while others are borrowed from the SCDOT Bridge Design Manual (2006) (BDM) or from the SCDOT Seismic Design Specifications for Highway Bridges (2017) (Seismic Specs). Additional definitions are also borrowed from the AASHTO LRFD Specifications referenced in either the BDM or the Seismic Specs. Where there is potential conflict between the GDM and any of these other sources, the GDM shall govern, unless specifically indicated otherwise.

### 2.2 DEFINITIONS

**Active Earth Pressure  
Coefficient,  $K_a$**

The coefficient of lateral pressure that is developed when a structure, either an ERS or an abutment wall moves away from the backfill resulting in a decrease in pressure on the structure relative to the at-rest pressure

**Alternate Profiles**

Alternate profiles are sometimes necessary when evaluating settlements; these profiles are typically parallel to the alignment of the roadway at a location that is subject to larger settlements than those at the Profile Grade location; alternately, this profile may be transverse to the Profile Grade and is used to determine differential settlement

**Apparent Opening Size,  
AOS ( $O_{95}$ )**

A property which indicates the approximate largest particle that would effectively pass through a geotextile

**Approach Slab**

A reinforced concrete structural slab placed on the embankment to transition from the roadway pavement to the bridge surface at the end bent; approach slabs are typically 20 feet in length

**Argillaceous Geomaterials**

Geomaterials that contain a significant clay fraction (CF) (12 to 40 percent) within the soil matrix

**At-Rest Earth Pressure  
Coefficient,  $K_o$**

The coefficient of lateral pressure that exists in level ground for the condition of no lateral deformation

**Blinding**

Condition whereby soil particles block the surface openings of a geotextile, thereby reducing the hydraulic conductivity

**Bridge Embankment**

The longitudinal length of embankment where mitigation is required to meet the Global Performance Objectives of the Bridge System as contained in the Seismic Specs or 3.25 times the height of the backwall (see Chapter 14), whichever is longer; in the event mitigation is not required, this embankment shall encompass the front slope and shall extend 3.25 times the height

of the backwall

**California Bearing Ratio (CBR)**

The ratio of (1) the force per unit area required to penetrate a soil mass with a 3-square-inch circular piston (approximately 2-inch diameter) at the rate of 0.05 inches/minute to (2) the force per unit area required for corresponding penetration of a standard method

**Cantilever ERS**

An ERS that prevents the advance of an in situ soil mass and is typically constructed from the top of the wall to the base concurrent with excavation operations of the in-situ soil to be removed; cantilever retaining ERS can either be constructed with or without anchors; typical cantilever ERSs used are Sheet Pile Wall with and without anchors, Soldier Pile Wall and Lagging with and without anchors, Tangent/Secant Pile Wall with and without anchors, and Soil Nailed Wall

**Check Flood**

Storm surge, tide or mixed population flood shall be the more severe of the 500-year flow event or from an overtopping flood of lesser recurrence interval; the Extreme Event II limit state shall apply

**Clogging**

Condition where soil particles move into and are retained in the openings of a geotextile, thereby reducing hydraulic conductivity

**Cross-machine Direction**

The direction in the plane of the geosynthetic perpendicular to the direction of manufacture

**Cross Section**

A slice or section taken perpendicular to the roadway alignment at a specific location (station) of the road

**DB/GDS**

Design Build – Geotechnical Design Section

**Design Flood**

Storm surge, tide or mixed population flood shall be the more severe of the 100-year flow event or from an overtopping flood of lesser recurrence interval

**Drained Strength**

Shear strength when there is no change in effective stress on the failure plane

**Earth Retaining Structure (ERS)**

An engineered structural system that prevents the lateral advance of a soil mass by resisting the lateral earth pressures exerted by the soil; ERSs shall have a face angle greater than or equal to 70° above the horizontal; ERSs have been classified for Strength limit state design by the type of retaining system as follows:

- Rigid Gravity ERS
- Flexible Gravity ERS
- Cantilever ERS

Further, ERSs are also classified based on the construction method Fill ERS, bottom-up, or Cut ERS, top-down

<b>Effective Stress</b>	The stress that includes only the forces (loads) that are transmitted (carried) by grain-to-grain contact
<b>Embankment</b>	An earthen mass structure constructed from select fill material placed in compacted lifts over competent soil (natural or improved) capable of supporting the structure; there are 2 types of embankments: bridge and roadway; embankments have face angles of less than 70° above the horizontal
<b>Embankment Widening</b>	An embankment is considered to be widened when the centerline of the embankment is shifted more than 1/2 of the width of the travelway (all travel lanes combined) in either transverse direction or if 1 travel lane is added in each direction and the centerline of the embankment does not change
<b>ERS Profile</b>	A profile of the wall that indicates the top of the wall, the location where the wall intersects the natural ground and the bottom of the wall (embedment depth of the wall below natural ground); wall profiles typically have their own alignment and stationing and are tied in to the project alignment
<b>ERS Cross Section</b>	A slice or section taken perpendicular to the wall profile at a specific location (station)
<b>Failure Surface</b>	An approximation of the most likely shear failure surface that will develop as a result of instability of an earthen mass; typically this surface has the highest resistance factor ( $\phi > 1.0$ ); a failure surface is not considered present if the resistance factor is equal to or less than 1.0 ( $\phi \leq 1.0$ ); the surface may be either circular or non-circular.
<b>Filtration</b>	The process of retaining soils while allowing the passage of water (fluid)
<b>Flexible Gravity ERS</b>	Flexible gravity walls are typically constructed bottom-up (fill) that have flexible facings and flexible structural elements such as those used in Gabion Wall, MSE (Full Height Panel Facing), MSE (Modular Block Facing), MSE (Precast Panel Facing), MSE (Gabion Facing), and Geosynthetic Reinforced Soil Slopes (face slopes greater than or equal to 70°)
<b>Front Slope</b>	The embankment that extends beneath the bridge and to the end of the approach slab (see Figure 10-1); the front slope begins at the end bent and extends longitudinally from the existing ground surface in front of the end bent to the end of the approach slab and extends transversely to existing ground surface on the sides; front slope grades are given in ratios of horizontal distance to vertical height (i.e., 2(H):1(V)); for bridges without approach slabs, the front slope shall extend 20 feet from either “begin” or “end” of bridge

**Functional Evaluation**

<b>Earthquake (FEE)</b>	The ground shaking having a 15 percent probability of exceedance in 75 years (15%/75yr) and is equal to the 10 percent probability of exceedance in 50 years (10%/50yr); the FEE PGA and PSA are used for the functional evaluation of transportation infrastructure; annual probability of exceedance ( $P_E$ ) is $2.11 \times 10^{-3}$
<b>GEC</b>	Geotechnical Engineering Consultant, a consultant, specializing in geotechnical engineering, hired by SCDOT to provide geotechnical services including field, laboratory and engineering services, that SCDOT either does not perform or has insufficient personnel to provide the service
<b>Geocell</b>	A 3-dimensional comb-like structure, that may be filled with soil, aggregate or concrete
<b>Geocomposite</b>	A geosynthetic material manufactured of 2 or more geo-materials (i.e., geomembrane and geonet combination)
<b>Geogrid</b>	A geosynthetic formed by a regular network of tensile elements and apertures, typically used for reinforcement applications
<b>Geomembrane</b>	An essentially impermeable geosynthetic, typically used to control fluid migration
<b>Geonet</b>	A geosynthetic consisting of integrally connected parallel sets of ribs overlying similar sets of ribs, for planar drainage of liquids or gases
<b>GEOR</b>	Geotechnical Engineer-of-Record
<b>Geosynthetic</b>	A planar product manufactured from polymeric material used with soil, aggregate, or other geotechnical engineering materials
<b>Geotextile</b>	A permeable geosynthetic comprised solely of textiles
<b>Global Instability</b>	An imbalance of the driving and resisting forces of an earthen mass that causes a shear failure surface to occur and consequently causing the earthen mass to deform
<b>Global Stability Analysis</b>	An estimation of the balance between the driving forces (demand) and resisting forces (capacity) within an earthen mass that is seeking to maintain equilibrium
<b>Gravity ERS</b>	An ERS that prevents the advance of select fill materials placed during construction and is constructed from the base to the top of the wall
<b>HEOR</b>	Hydraulic Engineer-of-Record
<b>Index Test</b>	A test procedure which may contain a known bias but which may be used to establish an order for a set of specimens with respect to the property of interest

<b>Intermediate Geomaterials (IGM)</b>	Earth materials with properties at the boundary between soil and rock that display properties of both materials; the required properties are discussed in Chapter 6.
<b>Machine Direction</b>	The direction in the plane of the geosynthetic parallel to the direction of manufacture
<b>Maximum Average Roll Value (MaxARV)</b>	A quality control tool used by geosynthetic manufacturers to establish and publish <u>maximum</u> property values
<b>Minimum Average Roll Value (MARV)</b>	A quality control tool used by geosynthetic manufacturers to establish and publish <u>minimum</u> property values
<b>Passive Earth Pressure Coefficient, <math>K_p</math></b>	The coefficient of lateral pressure that is developed when, either an ERS or an abutment wall moves toward the backfill resulting in an increase in pressure on the structure relative to the at-rest pressure
<b>PC/GDS</b>	Preconstruction – Geotechnical Design Section includes Geotechnical Design Sections within each Regional Production Group, the Design Build Section and Preconstruction Support
<b>PC/SDS</b>	Preconstruction – Structural Design Section includes Structural Design Sections within each Regional Production Group, the Design Build Section and Preconstruction Support
<b>PCS/GDS</b>	Preconstruction Support – Geotechnical Design Section
<b>PCS/HDS</b>	Preconstruction Support – Hydraulic Design Section
<b>PCS/SDS</b>	Preconstruction Support – Structural Design Section
<b>Peak Shear Strength</b>	The maximum shear stress that a soil can withstand, $\tau_{Peak}$
<b>Permeability</b>	The rate of flow of a fluid under a differential pressure through a material
<b>Permittivity</b>	The volumetric flow rate of water per unit cross sectional area per unit head under laminar flow conditions, in the normal direction through a geotextile
<b>Pore Pressure</b>	The force (load) transmitted (carried) by the interstitial water (i.e., the water contained in the pore spaces)
<b>Profile Grade</b>	Roadway plans typically have plan and profile sheets; the profiles are given along a specific location of the pavement surface that is referred to in the plans as the Profile Grade (P.G.) or Finished



	Grade (F.G.); often this location is the same as the centerline of the road; there may be multiple profile grades along a divided roadway or intersection for each traffic direction; the location of the roadway alignment in plan view typically coincides with the location of the profile grade
<b>Reinforced Embankment</b>	An embankment that typically has a face angle less than 1H:1V but greater than 2H:1V, and requires the use of geosynthetic reinforcement within the embankment to maintain stability; a reinforced embankment can use borrow materials as defined in the Standard Specifications
<b>Reinforced Soil Slope (RSS)</b>	An embankment that typically has a face angle greater than or equal to 1H:1V but less than 70°, has geosynthetic or metallic reinforcement within the embankment and generally has a face element of some kind (see Chapter 17 for face elements)
<b>REOR</b>	Roadway Engineer-of-Record
<b>Residual Shear Strength</b>	The minimum shear stress that a soil can maintain regardless of the amount of displacement, $\tau_r$
<b>Right-of-Way (ROW)</b>	A privilege to pass over the land of another in some particular path; usually an easement over the land of another; a strip of land used in this way for railroad or highway purposes, for pipelines or pole lines, and for private or public passage
<b>Rigid Gravity ERS</b>	Rigid gravity ERSs are typically constructed bottom-up (fill) that have rigid facings and rigid structural elements such as those used in Concrete Barrier Walls, Concrete Retaining Walls, and Concrete Stem (cantilever) walls with and without buttresses; rigid gravity ERSs depend on the mass (weight) of the concrete to resist the driving forces placed on the wall
<b>Roadway Embankment</b>	The portion of the embankment that extends beyond the bridge embankment and extends between the toes of the slopes on either side
<b>Rock</b>	Naturally occurring solid aggregate of minerals that occur in large masses or fragments; consolidated accumulation of solid particles
<b>RPG/GDS</b>	Regional Production Group – Geotechnical Design Section
<b>Safety Evaluation Earthquake (SEE)</b>	The ground shaking having a 3 percent probability of exceedance in 75 years (3%/75yr) and is equal to the 2 percent probability of exceedance in 50 years (2%/50yr); the SEE PGA and PSA are used for the safety evaluation of transportation infrastructure. Annual probability of exceedance ( $P_E$ ) is $4.04 \times 10^{-4}$
<b>SEOR</b>	Structural Engineer-of-Record

<b>Side Slopes</b>	The embankment that extends perpendicular to the travelway and has been graded to meet traffic safety and stability requirements; the side slope begins at the shoulder break and extends to the existing ground surface; side slope grades are given in ratios of horizontal distance to vertical height (i.e., 3(H):1(V)), transverse to the roadway travel direction
<b>Standard Specifications</b>	The <u>Standard Specifications for Highway Construction</u> , latest version as published by SCDOT; the Standard Specifications also includes Supplemental Specifications, Supplemental Technical Specifications and Special Provisions
<b>Soil</b>	Sediment or other unconsolidated accumulation of solid particles produced by the physical and chemical disintegration of rock materials which may or may not contain organic matter
<b>Soil Shear Strength Loss (SSL)</b>	The reduction in soil shear strength caused by seismically induced cyclic loading of soil; in loose cohesionless soils this is termed cyclic liquefaction while in plastic cohesive soils, SSL is termed cyclic softening
<b>Station</b>	Locations along a reference base line on the plan or profile that is based on measurements from a reference point (i.e., Sta. 1+00.00 = 100.00 feet)
<b>Temporary</b>	Structure or embankment having design life of 5 years or less
<b>Transmissivity</b>	The volumetric flow rate of water per unit cross sectional area per unit head under laminar flow conditions, in the in-plane direction through a geotextile
<b>Total Stress</b>	The stress that includes all of the forces (loads) that are transmitted (carried) by not only grain-to-grain contact but also by the interstitial water
<b>Undrained Strength</b>	Shear strength when there is no change in water content (i.e., no volume change)
<b>Unreinforced Embankment</b>	An embankment that typically has a face angle flatter than or equal to 2H:1V; an unreinforced embankment can use borrow materials as defined in the Standard Specifications

**CHAPTER 3**  
**RESERVED**

**GEOTECHNICAL DESIGN MANUAL**

*January 2019*



# **CHAPTER 3**

## **RESERVED**

Chapter 3 – *Consultant Services and Review* of GDM versions 1.0 (2008) and 1.1 (2010) has been deleted. This Chapter is reserved for future use by SCDOT.

**CHAPTER 4**  
**SUBSURFACE INVESTIGATION**  
**GUIDELINES**

**GEOTECHNICAL DESIGN MANUAL**

*January 2019*



**Table of Contents**

<b><u>Section</u></b>		<b><u>Page</u></b>
4.1	Introduction.....	4-1
4.2	Subsurface Investigation.....	4-2
	4.2.1 Preliminary Subsurface Investigation .....	4-2
	4.2.2 Final Subsurface Investigation .....	4-4
4.3	Subsurface Investigation Methods .....	4-5
	4.3.1 Bridge Foundations .....	4-6
	4.3.2 Earth Retaining Structures .....	4-7
	4.3.3 Embankments .....	4-8
	4.3.4 Cut Excavations .....	4-8
	4.3.5 Culverts/Pipes .....	4-9
	4.3.6 Sound Barrier Walls .....	4-9
	4.3.7 Ground Improvement Methods.....	4-9
	4.3.8 Miscellaneous Structures .....	4-10
	4.3.9 Pavement Structures.....	4-10



**List of Tables**

<b><u>Table</u></b>	<b><u>Page</u></b>
Table 4-1, Bridge Foundation Minimum Requirements.....	4-6
Table 4-2, Minimum DOSI.....	4-7

# CHAPTER 4

## SUBSURFACE INVESTIGATION GUIDELINES

### 4.1 INTRODUCTION

A subsurface investigation is typically required for new or replaced structures and roadway alignments, including realignments involving earthwork. Examples of this include bridge replacements, widening of existing bridges, roadway realignments including widenings, pedestrian and wildlife bridges, ERSs, pipes or culverts (greater than or equal to 30 inches in diameter), overhead sign-structures, sound barrier walls, and other miscellaneous structures.

This Chapter presents guidelines to be used in the development of subsurface investigations, both preliminary and final. The actual type of subsurface investigation, depth, location, and frequency of all testing locations shall be based on project specific information. Subsurface investigations shall also indicate the testing intervals to be used if different from the standard intervals contained in this Chapter. The specific process requirements for conducting field and laboratory testing are contained in Chapter 5. The requirements of this Chapter shall be applied to all projects prepared by or provided to SCDOT (regardless of contracting method including encroachment permit requests).

The subsurface investigation shall include all backup documentation available. This backup documentation may include, but is not limited to, previous soil borings in the general vicinity of the project; USDA soils maps, USGS topographic maps, aerial photographs, and wetland inventory maps. In addition, the backup documentation should include information pertaining to the existence or extent of geologic conditions (including but not limited to artesian conditions, karstic formations, etc.) that may be present at the project site or in the immediate vicinity of the site that may affect the project. Further, geologic conditions shall be noted on the boring records and the geotechnical reports shall discuss the impacts of geologic conditions on the construction of the project.

A detailed subsurface investigation plan (including preliminary and final explorations, if possible) shall be prepared prior to the commencement of any field operations. For consultant projects, regardless of contracting method, the GEC shall submit the subsurface investigation plan to the respective PC/GDS, for review and acceptance. The plan shall describe the soil or rock stratification anticipated as the basis of the planned exploration. The plan shall outline the proposed testing types (borings/soundings), depths, and locations of all testing. The subsurface investigation plan shall conform to the requirements of this Manual. In addition, the GEC is responsible for ascertaining that all testing locations are clear of utilities. In addition, the GEC shall prepare and submit an encroachment permit with the respective Resident Maintenance Engineer (RME) for all testing locations located in the SCDOT Right-of-Way (ROW). The encroachment permit application will follow the guidelines established by SCDOT and will be copied to the appropriate PC/GDS. For all testing locations located outside of the SCDOT ROW, prepare a plan (see GDF 004 in Appendix A) indicate all testing locations and forward the plan the SCDOT Right-of-Way Office (ROWO). The ROWO will obtain the necessary access permissions for the affected property owners. The ROWO will inform the PC/GDS once these permissions have been obtained or not. Frequently, explorations must be conducted in sensitive environmental areas or in high hazard traffic areas. The GEC's exploration plan shall describe any special access requirements or traffic control requirements necessary to protect the interests of SCDOT during the field investigation phase and shall be included with the encroachment permit application. The GEC is responsible for all special access requirements and traffic control and shall coordinate these activities with the RME. All traffic control shall conform to the latest Department guidelines.

## 4.2 SUBSURFACE INVESTIGATION

Subsurface investigations are typically conducted in 2 phases; preliminary and final. The location and spacing of all testing locations shall be coordinated between the preliminary and final subsurface investigations. The preliminary subsurface investigation should be conducted early enough in the design process to assist in the selection of foundation types, in determining location and length of the bridge/structure, and to identify areas requiring additional exploration during the final exploration. The testing locations for the preliminary subsurface investigation should be easily accessible and within the current SCDOT ROW. The final subsurface investigation should take into account the testing locations from the preliminary subsurface investigation. Boring locations that require construction of access entry ways shall be provided to the Environmental Services Office (ESO) for inclusion in a Programmatic Categorical Exclusion (CE). Coordinate with the ESO to determine what documentation will be required. The requirements for the preliminary and final subsurface investigations, including frequency and spacing of testing locations, are presented in the following Sub-sections and Sections.

### 4.2.1 Preliminary Subsurface Investigation

The purpose of the preliminary subsurface investigation is to collect enough basic information to assist in development of preliminary plans. The results of the preliminary subsurface exploration shall be presented as indicated in Chapter 21. The testing locations should be located in readily accessible locations within the SCDOT ROW and should, as indicated previously, be coordinated with the final subsurface investigation. Any testing locations that need to be located outside of the SCDOT ROW will require review by the ESO. Coordinate with the ESO to determine what documentation will be required. The preliminary subsurface investigation shall include the collection of shear wave velocity data to depths of at least 100 feet beneath the existing ground surface, but may be extended to the practical limit of the equipment used to measure the shear wave velocities. Perform 1 shear wave velocity test for bridges with a length of less than or equal to 500 feet. For bridges with lengths greater than or equal to 1,000 feet perform 1 shear wave velocity test per 500 feet of bridge. For bridges between 500 and 1,000 feet contact the PC/GDS for guidance. In addition, if surface methods are used to determine the shear wave velocity, then either testing shall be conducted adjacent to a proposed boring or a boring shall be performed in the area of the surface method. The shear wave velocity profile shall be calibrated with the boring. These shear wave velocities shall be used as described in Chapter 12.

The preliminary subsurface investigation shall include a laboratory testing program that will consist primarily of index testing. For bridge and structure borings, index testing shall be performed on all of the samples collected that have an  $N_{60}$  less than or equal to 35 blows per foot (bpf) and having an estimated age of Pleistocene and younger. The exception to this is if the bridge has a Seismic Design Category (SDC) of A, as defined in the Seismic Specs, and the PGA is less than or equal to 0.20g ( $PGA \leq 0.20g$ ), then a SSL analysis will not be required (see Chapter 13); therefore, the GEOR shall determine how many index tests will be performed. Index testing shall consist of the following tests:

- Grain-size Distribution with wash No. 200 Sieve
- Moisture-Plasticity Relationship Determination (Atterberg Limits)
  - Performed only on samples with more than 20 percent passing #200 sieve
- Natural Moisture Content

The geologic age shall be estimated using the information presented in Chapter 11 and other publically available geologic information/literature. All publically used resources shall be documented in accordance with accepted industry reference standards.

The laboratory testing program shall also include grain-size analysis, including hydrometer, on all soil samples within the upper 15 feet of the bottom of the water crossing. However, if the scour depth and/or elevation is known or estimated and is deeper than 15 feet below the bottom of the water crossing, then grain-size analysis including hydrometer will be conducted to this scour depth and/or elevation. This analysis is required in determining the amount of scour predicted for a bridge over a body of water and shall be provided to the HEOR; however, the HEOR shall be consulted to determine if this analysis is required. If the analysis is required, the GEOR and HEOR shall discuss the proposed locations of the soil testing locations and sample depths from where the grain-size analysis with hydrometer shall come from.

Electro-chemical testing (pH, resistivity, chloride, and sulfate testing) shall be performed to determine the potential impacts of the soils, groundwater, and surface water on the structural components. Electro-chemical testing of soil samples should be considered from the existing ground surface to a depth of at least 6 pile diameters below the groundwater interface or 3 feet below the deepest anticipated groundwater depth, whichever is deeper. Surface water shall also be tested in coastal regions where the potential intrusion of brackish (higher salinity) water may occur in tidal streams. In addition, surface water shall also be tested when in the opinion of the GEOR there is potential source of environmental concern along a stream or river. A field resistivity test may also be conducted in addition to laboratory resistivity testing.

In addition, a composite bulk sample shall be obtained of the existing embankment material. The composite sample shall have the following laboratory tests performed:

- Moisture-density Relationship (Standard Proctor)
- Grain-size Distribution with wash No. 200 Sieve
- Moisture-Plasticity Relationship Determination (Atterberg Limits)
  - Performed only on samples with more than 20 percent passing #200 sieve
- Natural Moisture Content
- Direct Simple Shear Test
  - Performed only on samples with less than or equal to 20 percent passing #200 sieve
  - Sample remolded to 95 percent of Standard Proctor value
  - Sample moisture content shall be between -1 percent to +2 percent of optimum moisture content
- Consolidated-Undrained Triaxial Shear Test with pore pressure measurements
  - Performed only on samples with more than 20 percent passing #200 sieve
  - Sample remolded to 95 percent of Standard Proctor value
  - Sample moisture content shall be between -1 percent to +2 percent of optimum moisture content

For projects located in the Piedmont Physiographic Province unconfined compression testing of rock core samples is required. The unconfined compression testing should be performed on more than 50 percent of the rock cores with lowest Rock Quality Designation (RQD). Provided enough sample is available to meet the length to diameter ratio required for testing. The remaining unconfined compression tests shall be performed on rock cores with the highest RQD values and the longest coring rates (see Chapters 5 and 6). While the compression results on the lowest RQD specimens will typically govern design, the compression results on the highest RQD specimens will help determine the size of the construction equipment required.

The information (i.e. field and laboratory data) collected during the preliminary subsurface investigation will be used to refine the final subsurface investigation. All field and laboratory data and any preliminary recommendations shall be reported as required in Chapter 21 and shall include a completed GeoScoping form. The preliminary geotechnical recommendations provided are used to evaluate the Design Field Review (DFR) plans. After the DFR has been conducted, a detailed final subsurface soil exploration is conducted based on the required structures or geotechnical issues identified during the DFR.

#### **4.2.2 Final Subsurface Investigation**

The purpose of the final subsurface investigation is to collect detailed subsurface information for use in developing final reports and construction plans. The results of the final subsurface exploration shall be presented as indicated in Chapter 21. The final testing locations shall be located along the proposed alignment of the roadway and bridge structure whether within or outside of the existing SCDOT ROW. The testing locations should be coordinated with the preliminary exploration to avoid testing in the same location and to assure that the entire construction area is adequately explored. If the preliminary subsurface investigation encounters thick deposits (i.e. strata thickness greater than 3 feet) of fine-grained very soft to firm soils, then a field vane shear test (FVST) should be performed in the layer during the final subsurface investigation. In addition, a pore pressure dissipation test should also be conducted using the electro-piezocone (CPTu). The PC/GDS shall be contacted to provide a review and acceptance of the final subsurface investigation testing locations prior to commencement of the final subsurface investigation. At this time it will be determined if the FVST and pore pressure dissipation test is to be performed. Further, an explanation of how the FVST and pore pressure dissipation test results are anticipated being incorporated into the design shall be provided. The information collected during the final subsurface investigation shall be used to develop the final foundation and earthwork recommendations for the project.

The final subsurface investigation shall include additional laboratory analyses. These additional laboratory analyses should include additional index property testing as well as sophisticated shear and consolidation testing. Index testing (see previously presented list) should be performed on 100 percent of the samples from the borings located at the ends of the bridge and 100 feet from the end of the bridge. Further, index testing should be performed on 75 percent of the samples from the interior bridge bent borings. As in the Preliminary Subsurface Exploration, if the site meets the criteria for no SSL (see Section 4.2.1 and Chapter 13), this index testing requirement is removed and the GEOR shall determine how many index tests will be performed. The shear testing shall meet the requirements presented below. The amount of index testing outside of the limits defined previously shall be at the discretion of the GEOR.

- Grain-size Distribution with wash No. 200 Sieve
- Moisture-Plasticity Relationship Determination (Atterberg Limits)
  - Performed only on samples with more than 20 percent passing #200 sieve
- Natural Moisture Content
- Direct Simple Shear Test
  - Performed only on samples with less than or equal to 20 percent passing #200 sieve
  - Sample remolded to 95 percent of Standard Proctor value
  - Sample moisture content shall be between -1 percent to +2 percent of optimum moisture content
- Consolidated-Undrained Triaxial Shear Test with pore pressure measurements
  - Performed only on samples with more than 20 percent passing #200 sieve
  - Sample remolded to 95 percent of Standard Proctor value

- Sample moisture content shall be between -1 percent to +2 percent of optimum moisture content

For projects located in the Piedmont Physiographic Province unconfined compression testing of rock core samples is required. The unconfined compression testing should be performed on more than 50 percent of the rock cores with lowest Rock Quality Designation (RQD). Provided enough sample is available to meet the length to diameter ratio required for testing. The remaining unconfined compression tests shall be performed on rock cores with the highest RQD values. While the compression results on the lowest RQD specimens will typically govern design, the compression results on the highest RQD specimens will help determine the size of the construction equipment required.

### 4.3 SUBSURFACE INVESTIGATION METHODS

This Section discusses the number, location and anticipated depth of all testing locations. As indicated previously, the preliminary and final subsurface investigations shall be coordinated to assure that the complete structure (whether bridge or roadway embankment) is adequately explored. The frequency and spacing of test locations will depend on the anticipated variation in subsurface conditions and the type of facility to be designed. A surveyor licensed pursuant to the laws of South Carolina shall locate (station, offset, and GPS coordinates (latitude and longitude)) and establish ground elevation at all testing locations. The testing location frequency/spacing and depth criteria indicated below are the minimum requirements. Any requests to deviate from these minimum requirements shall be made in writing and shall be forwarded to the PC/GDS for consideration and acceptance. All testing shall be to a sufficient depth to effectively evaluate the appropriate limit state conditions and shall fully penetrate any formation that will affect performance (e.g., settlement or slope instability of a roadway embankment or roadway structure). Soil test borings, CPTu soundings, FVST and/or dilatometer (DMT) soundings are to be conducted at test locations. No more than half of the testing locations can be CPTu or DMT soundings. The use of "soil test boring" shall include the Standard Penetration Test (SPT) unless specifically indicated otherwise. In addition, 1 soil test boring shall be performed adjacent to a CPTu sounding to allow for correlation of the CPTu sounding to the actual soils encountered on site. Further, this soil test boring shall be continuously sampled for the upper 50 feet and sampled every 5 feet thereafter to the anticipated depth of CPTu sounding or to the actual termination depth of CPTu sounding, whichever is shallower. The soil test boring shall be located no more than 5 feet from the location of the CPTu sounding and shall be at the same approximate elevation as the CPTu sounding.

Soil test borings shall include the SPT and the SPTs shall be conducted as indicated in Chapter 5. Since SPT samples are highly disturbed, these samples can only be used for index and classification testing. If high quality consolidation and shear strength data are required then undisturbed samples will be required. The collection of undisturbed samples (location and depth) shall be determined by the GEOR of the project. Wash rotary drilling methods (see Chapter 5) shall be used for projects in the following counties: Aiken, Allendale, Bamberg, Barnwell, Beaufort, Berkeley, Calhoun, Charleston, Chesterfield, Clarendon, Colleton, Darlington, Dillon, Dorchester, Florence, Georgetown, Hampton, Horry, Jasper, Kershaw, Lee, Lexington, Marion, Marlboro, Orangeburg, Richland, Sumter, and Williamsburg. These counties are typically located within the Coastal Plain Physiographic Province of South Carolina, with the remaining South Carolina Counties located in the Piedmont Physiographic Province of South Carolina (see Chapter 11 for a detailed geologic discussion). However, the Coastal Plain extends into Edgefield, Fairfield, Lancaster and Saluda Counties, even though these counties are normally considered to be Piedmont counties; therefore, for those portions of these counties that are located in the Coastal Plain, wash rotary drilling methods shall be required. Variations

to this requirement shall be made in writing and shall be forwarded to the PC/GDS for review and concurrence.

In areas of difficult access beneath proposed fill embankments or along crossline pipes, manual augers (MA) with dynamic cone penetrometers (DCPs) may be utilized to evaluate undercutting requirements. The DCPs should be performed approximately on 1 foot increments.

#### 4.3.1 Bridge Foundations

All bridges (vehicular, pedestrian, wildlife, etc.) shall have soil testing taken at each end bent and at interior bents to meet the minimum geotechnical site investigation indicated below:

**Table 4-1, Bridge Foundation Minimum Requirements**

Bridge Foundation Type	Minimum Geotechnical Site Investigation
Pile Foundation	Minimum 1 testing location per interior bent <sup>1,2</sup>
	Minimum 2 testing locations per end bent <sup>3,4</sup>
Single Foundation - Drilled Shaft (hammerhead)	Minimum 1 testing location per foundation location
Multiple Foundation – Drilled Shaft	Minimum 2 testing locations per bent location <sup>5,6</sup>
Shallow Foundation – Founded on Soil	Minimum 3 testing locations per bent location
Shallow Foundation – Founded on Rock	Minimum 2 testing locations per bent location

<sup>1</sup>Spacing between testing locations may be increased, but shall be approved prior to field operations and shall include justification; spacing may not exceed 100 feet except on pedestrian bridges where the spacing may not exceed 200 feet, longitudinally.

<sup>2</sup>An additional boring shall be required if the interior bent width is 100 feet or more. The bent length is typically transverse to the centerline of the bridge.

<sup>3</sup>One testing location shall be a soil test boring.

<sup>4</sup>Includes both driven and drilled piles. Drilled piles are only allowed at end bents. Prior approval of the PC/GDS and the PC/SDS shall be required prior to using drilled piles at interior bents.

<sup>5</sup>An additional boring is required if 5 or more drilled shafts will support the bent/footing. To reduce design and construction risk due to subsurface condition variability and the potential for construction claims, at least 1 exploration per shaft should be considered for large diameter shafts (e.g., greater than 5 ft in diameter), especially when shafts are socketed into bedrock.

<sup>6</sup>Minimum 1 testing location per bent is allowed in Aiken, Allendale, Bamberg, Barnwell, Beaufort, Berkeley, Calhoun, Charleston, Chesterfield, Clarendon, Colleton, Darlington, Dillon, Dorchester, Florence, Georgetown, Hampton, Horry, Jasper, Kershaw, Lee, Marion, Marlboro, Orangeburg, Sumter, and Williamsburg Counties.

All boring/soundings taken for deep foundations shall extend below the anticipated pile or drilled shaft tip elevation a minimum of 3 times the diameter/width of the shaft/pile or a minimum of 2 times the minimum pile group dimension, whichever is deeper.

All boring/soundings taken for shallow foundations shall extend beneath the anticipated bearing elevation to the Depth of Significant Influence (DOSI) as indicated in the following table:

**Table 4-2, Minimum DOSI**

Shallow Foundation Case	Minimum Testing Depth <sup>1</sup>
$L < 2B$	2B
$2B \leq L \leq 5B$	3B
$5B < L < 10B$	4B
$10B \leq L$	6B

<sup>1</sup>Beneath the anticipated bearing elevation

L = Length of spread footing; B = Width of spread footing (minimum side dimension of footing)

All bridge foundations (deep and shallow) bearing on rock shall have a minimum of 10 feet of rock coring or the minimum testing depth requirements listed above, whichever is greater. It is highly recommended to have rock coring done as close to the proposed shaft or pile location as possible. South Carolina geology can have a rock formation that changes in a number of feet along the length or the width of the bridge.

#### 4.3.1.1 Bridge Scour Analysis Requirements

As indicated previously, all of the soil samples obtained from beneath a stream channel shall have grain-size including hydrometer analyses performed, if requested/required by the HEOR. This testing shall be performed at both end bents, regardless of whether the bridge is single span or multi-span, from depths that approximate the bottom of the stream channel and extend to a depth of least 15 feet below the approximate bottom of the stream channel. However, if the scour depth and/or elevation is known or estimated and is deeper than 15 feet below the bottom of the water crossing, then additional grain-size analysis including hydrometer will be conducted to this scour depth and/or elevation. For multi-span bridges, laboratory testing samples shall be obtained from the SPT samples obtained from the soil test borings located at the interior bent locations to the depths described previously. In addition, a soil test boring to a depth of least 15 feet beneath the bottom of the stream channel shall be performed for a single span bridge, if requested by the HEOR. If the bottom of the stream channel for single span bridge is comprised of Partially Weather Rock (PWR), then extend the boring to a depth of 10 feet beneath the bottom of the stream channel unless otherwise requested by the HEOR. For stream channels, beneath single span bridges, that are comprised of rock, extend the boring to a depth of 5 feet for rock with a Rock Quality Designation (RQD, see Chapter 6) greater than 0. For rock with a RQD of 0 extend the boring 10 feet. The GEOR shall coordinate with the HEOR concerning the requirement for a soil test boring in the interior of a single span bridge. This boring may be extended to a deeper depth if the scour depth and/or elevation is preliminarily estimated to be deeper than 15 feet. Similarly to the soil samples obtained from the end bents, all of the soil samples obtained from this boring shall have grain-size including hydrometer analyses performed to a depth of 15 feet below the bottom of the stream channel. The results of the laboratory testing shall be reported as indicated in Chapter 7.

#### 4.3.2 Earth Retaining Structures

All ERSs shall have a minimum of 2 testing locations per ERS with additional testing locations performed at least every 50 feet along the ERS line, if the ERS is within 100 feet of bridge abutments. ERSs more than 100 feet from the bridge abutment shall have a minimum of 2 testing locations per ERS with additional testing locations performed at least every 100 feet along the ERS line. ERSs with heights of less than 5 feet do not require a geotechnical exploration unless in the opinion of the GEOR an exploration is warranted, except if the ERS is part of a compound slope (i.e. the ground surface either slopes up from the top of the wall or



slopes down from the bottom of the wall (see Figure 18-18)). Mechanically Stabilized Earth (MSE) walls shall have testing locations at both the wall line and within the reinforced zone at the same intervals specified above. The testing locations within the reinforced zone shall be located approximately a distance equal to the wall height from the wall line. In addition, all anchored walls shall have testing locations at both the wall line and within the anchored zone at the same intervals specified above with the testing locations within the anchored zone located approximately a distance equal to the height of the wall from the wall line. The testing at the locations indicated shall extend to depths sufficient to effectively evaluate all the limit states for the roadway structure. At a minimum, the testing locations shall extend to a depth of at least twice the height of the wall beneath the anticipated bearing elevation or to auger refusal, whichever is shallower.

### **4.3.3 Embankments**

All roadway embankments shall have 1 testing location at least every 500 feet along the roadway embankment; however at the discretion of the GEOR, testing locations along the roadway embankment may be drilled at a shorter interval. In addition, the bridge embankment (embankments within 100 feet of a bridge end) shall have a minimum of 3 testing locations; 2 at the bridge end (which are also used for bridge foundation design) and 1 at a point 100 feet from the bridge end. The testing location 100 feet from the bridge end must be extended to a depth that is sufficient to effectively evaluate the Extreme Event (EE) I limit state for the roadway embankment design (i.e. the side and end slopes). Reinforced Soil Slopes (RSS) located outside of the bridge embankment shall have a minimum of 2 testing locations, with 1 test located at either end of the RSS section. An additional testing location shall be added for every 200 feet of length of RSS. The testing locations shall extend to a sufficient depth to effectively evaluate the Service limit state. RSSs beyond the bridge embankment shall not be analyzed for the EE I limit state. RSSs that are bridge embankments shall have 1 test located every 100 feet of total RSS length, in addition, to the soil test borings located at either end of the RSS. These testing locations shall extend to a sufficient depth to effectively evaluate all limit state conditions.

### **4.3.4 Cut Excavations**

All cut excavations having an exposed height of greater than 5 feet shall have 1 test location performed to the depths indicated below. Cut excavations greater than 300 feet in length shall have 2 test locations per cut excavation with additional testing locations performed at least every 300 feet along the cut area. All testing locations shall be performed to a depth of at least twice the depth of the cut below the anticipated bottom depth of the cut or to auger refusal, whichever is shallower. Begin rock coring operations at auger refusal. Rock coring is to extend to at least 5 feet below the anticipated bottom depth of the cut. In addition, a composite bulk sample shall be collected from the area of the cut excavations, but no less than every 300 feet. The composite sample shall have the following laboratory tests performed:

- Moisture-density Relationship (Standard Proctor)
- Grain-size Distribution with wash No. 200 Sieve
- Moisture-Plasticity Relationship Determination (Atterberg Limits)
  - Performed only on samples with more than 20 percent passing #200 sieve
- Natural Moisture Content
- Direct Simple Shear Test
  - Performed only on samples with less than or equal to 20 percent passing #200 sieve
  - Sample remolded to 95 percent of Standard Proctor value
  - Sample moisture content shall be between -1 percent to +2 percent of optimum moisture content

- Consolidated-Undrained Triaxial Shear Test with pore pressure measurements
  - Performed only on samples with more than 20 percent passing #200 sieve
  - Sample remolded to 95 percent of Standard Proctor value
  - Sample moisture content shall be between -1 percent to +2 percent of optimum moisture content

#### **4.3.5 Culverts/Pipes**

New pipes and culverts that cross the project alignment in a transverse direction (i.e., an open drainage system), with an ADT  $\geq$  5,000 vehicles per day (vpd), having a diameter or an inside cross-sectional dimension greater than or equal to 48 inches, and are being founded at or below the original grade, shall have a minimum of 1 test location at each end of the pipe or culvert and every 100 feet along the pipe or culvert. Pipe and culvert extensions, having a diameter or an inside cross-sectional dimension greater than or equal to 48 inches, shall have a minimum of 1 test location at each extension. For extensions greater than 50 feet, testing locations shall be spaced every 50 feet. All testing locations shall extend to a depth sufficient to effectively evaluate all limit states as directed by the SEOR and/or the HEOR. The testing depths shall be measured from the anticipated bearing elevation. Testing may be terminated above the anticipated depth if auger refusal is encountered. For all other pipe and culverts (smaller diameter, less ADT, pipe and culverts regardless of size or ADT that are founded within the proposed embankment or that run parallel (longitudinal) (i.e., a closed drainage system) to the roadway centerline, the exploration requirements shall conform to the requirements for embankments. Pipe and culverts located in the Piedmont Counties (see Chapter 11 for a more detailed discussion) having a diameter or an inside cross-sectional dimension greater than or equal to 48 inches that are to be founded in the existing subgrade and that run parallel (longitudinal) (i.e., a closed drainage system) to the roadway centerline shall have test locations every 500 feet or where shallow rock is anticipated and shall extend to a depth of 5 feet deeper than the proposed invert elevation or to auger refusal, whichever is shallower. The RME may request additional testing locations for smaller diameter pipes and culverts. The subsurface investigation should attempt to characterize possible unsuitable soil conditions for which pipes and culverts are anticipated to be founded in.

#### **4.3.6 Sound Barrier Walls**

Sound barrier walls may be supported by either shallow foundations or deep foundations. Testing locations for sound barrier walls shall be placed at the beginning and ending of the wall, at the location of major changes in the wall alignment and at a maximum spacing of 200 feet. For sound barrier walls located on top of a berm, the testing locations shall extend a minimum of twice the berm height plus twice the height of the proposed sound barrier wall for shallow foundations and shall extend to a depth sufficient to effectively evaluate the appropriate limit state requirements for this type of foundation. For sound barrier walls not located on top of a berm, the testing locations shall extend a minimum of twice the height of the proposed sound barrier wall for shallow foundations and shall extend to a depth sufficient to effectively evaluate the appropriate limit state requirements for this type of foundation. If deep foundations are used to support the sound barrier walls, the testing shall extend a minimum of 5 feet beneath the anticipated deep foundation tip elevation.

#### **4.3.7 Ground Improvement Methods**

Certain ground improvement methods will require additional geotechnical investigations, both in the field as well as the laboratory. The GEOR is required to understand which ground improvement methods require additional geotechnical investigation and to establish the scope of services required to meet the requirements for the anticipated ground improvement method.

The additional geotechnical investigation may be conducted during the Final Subsurface Investigation, but may also need to be conducted in a Supplemental Subsurface Investigation. Prior approval will be required for all Supplemental Subsurface Investigations.

#### **4.3.8 Miscellaneous Structures**

Miscellaneous structures such as overhead signs and light poles should have a minimum of 1 test location performed per foundation location unless directed otherwise by the PC/GDS. All test locations shall extend to the same depth criteria as specified for the bridge test locations for the same type of foundation.

#### **4.3.9 Pavement Structures**

Subsurface investigation requirements for pavement structure design vary with location, traffic level, and project size. Requirements for pavement structure design subsurface investigations are provided in SCDOT's Pavement Design Guidelines (latest edition), which is published by the Office of Materials and Research (OMR). Contact the OMR Geotechnical Materials Engineer for further information.

**CHAPTER 5**  
**FIELD AND LABORATORY**  
**TESTING PROCEDURES**

**GEOTECHNICAL DESIGN MANUAL**

*January 2019*



## Table of Contents

<u>Section</u>	<u>Page</u>
5.1 Introduction .....	5-1
5.2 Sampling Procedures .....	5-1
5.2.1 Soil Sampling.....	5-1
5.2.2 Rock Core Sampling.....	5-3
5.3 Field Testing Procedures.....	5-3
5.3.1 Test Pits.....	5-4
5.3.2 Soil Borings.....	5-4
5.3.3 Standard Penetration Test .....	5-5
5.3.4 Dynamic Cone Penetrometer Test .....	5-6
5.3.5 Cone Penetrometer Test.....	5-6
5.3.6 Dilatometer Test.....	5-8
5.3.7 Pressuremeter Test .....	5-9
5.3.8 Field Vane Shear Test .....	5-10
5.3.9 Double-Ring Infiltrometer Test .....	5-12
5.3.10 Geophysical Testing Methods.....	5-12
5.4 Soil/Rock Laboratory Testing.....	5-19
5.4.1 Grain-Size Analysis.....	5-19
5.4.2 Moisture Content.....	5-20
5.4.3 Atterberg Limits.....	5-20
5.4.4 Specific Gravity of Soils .....	5-20
5.4.5 Undisturbed Sample Preparation .....	5-21
5.4.6 Strength Tests .....	5-21
5.4.7 Consolidation Test .....	5-27
5.4.8 Organic Content.....	5-33
5.4.9 Shrinkage and Swell .....	5-34
5.4.10 Permeability .....	5-34
5.4.11 Compaction Tests.....	5-35
5.4.12 Relative Density Tests .....	5-35
5.4.13 Electro-Chemical Tests.....	5-36
5.4.14 Rock Cores.....	5-37
5.5 Quality Assurance/Quality Control .....	5-38
5.5.1 Field Testing QA/QC Plan.....	5-38
5.5.2 Laboratory Testing QA/QC Plan.....	5-38
5.6 References.....	5-38

**List of Tables**

<b><u>Table</u></b>	<b><u>Page</u></b>
Table 5-1, Expected Calibration Values .....	5-8
Table 5-2, Consolidation Parameters and Symbols .....	5-28
Table 5-3, Determination of Preconsolidation Stress .....	5-29

**List of Figures**

<b>Figure</b>	<b>Page</b>
Figure 5-1, Pressuremeter Curve.....	5-10
Figure 5-2, Field Vane Devices.....	5-11
Figure 5-3, SASW Shear Wave Velocity Testing.....	5-13
Figure 5-4, Downhole Shear Wave Velocity Testing.....	5-14
Figure 5-5, Crosshole Shear Wave Velocity Testing.....	5-15
Figure 5-6, Suspension Logging Schematic.....	5-16
Figure 5-7, Acoustic Televiewer Image.....	5-17
Figure 5-8, Seismic Refraction Testing.....	5-18
Figure 5-9, Data Reduction Example for Determining Depth to Hard Layer.....	5-18
Figure 5-10, Interpretation of UU Test Data.....	5-22
Figure 5-11, Mohr Circle Depicting Mohr-Coulomb Failure Criterion.....	5-24
Figure 5-12, Stress Path ( $p'$ - $q'$ ) Plot.....	5-24
Figure 5-13, Direct Shear Test Results.....	5-26
Figure 5-14, Void Ratio versus log Time.....	5-28
Figure 5-15, Normally Consolidated.....	5-30
Figure 5-16, Overconsolidated.....	5-30
Figure 5-17, Under Consolidated.....	5-30
Figure 5-18, Determination of Preconsolidation Stress from $e$ -log $p$ .....	5-31
Figure 5-19, Determination of Preconsolidation Stress from $\epsilon$ -log $p$ .....	5-31
Figure 5-20, Change in Work vs. Vertical Effective Stress.....	5-32





# CHAPTER 5

## FIELD AND LABORATORY TESTING PROCEDURES

### 5.1 INTRODUCTION

This Chapter discusses items related to field and laboratory testing procedures. Sections 5.2 and 5.3 discuss sampling procedures and the different methods of retrieving soil and rock samples. These Sections also discuss drilling procedures and what types of equipment are typically available. Section 5.4 discusses soil/rock laboratory testing and the different types of testing procedures. Tests shall be performed in accordance with ASTM and/or AASHTO standards. Where applicable the appropriate SCDOT testing procedures shall be used. Any deviations from the accepted testing procedures (includes both field and laboratory) shall be made in writing to the PC/GDS prior to the testing for review and acceptance. As appropriate the PC/GDS shall consult with either the PCS/GDS or OMR. All tests shall be performed by a certified AASHTO Materials Reference Laboratory (AMRL) for the specific test being performed. As required, the GEC shall provide Excel<sup>®</sup> spreadsheets that contain data from various tests. In addition, the GEC shall contact the PC/GDS to ascertain the current version of Excel<sup>®</sup> being used by SCDOT.

### 5.2 SAMPLING PROCEDURES

#### 5.2.1 Soil Sampling

ASTM and AASHTO have procedures that must be followed for the collection of field samples. All samples must be properly obtained, preserved, and transported to a laboratory facility in accordance with these procedures in order to preserve the samples as best as possible. There are several procedures that can be used for the collection of samples as described below. See ASTM D4220 - *Standard Practices for Preserving and Transporting Soil Samples*.

##### 5.2.1.1 Bulk Samples

Bulk samples are highly disturbed samples obtained from auger cuttings or test pits. The quantity of the sample depends on the type of testing to be performed, but can range up to 50 lb. or more. Typical testing performed on bulk samples include moisture-density relationship, moisture-plasticity relationship, grain-size distribution, natural moisture content, and triaxial compression or direct shear testing on remodeled specimens.

##### 5.2.1.2 Split-Barrel Sampling

The most commonly used method for obtaining samples is the split-barrel sampler, also known as the standard split-spoon. The split-spoon has an interior length that ranges from 18 to 30 inches not including the length of the shoe, typically 1 to 2 inches. This sampler is used in conjunction with the Standard Penetration Test (SPT). The sampler is driven into soil by means of hammer blows. The number of blows required for driving the sampler through multiple 6-inch intervals is recorded. The 2<sup>nd</sup> and 3<sup>rd</sup> 6-inch intervals are added to make up the standard penetration number,  $N_{meas}$ . The split-spoon shall not be driven more than the interior length into the subsurface soils. After driving is completed the sampler is retrieved and the soil sample is removed and placed into air tight containers. The entire retrieved sample shall be placed in the air tight container (i.e., plastic bag). For those split-spoons that encounter a change in soil type, each soil type will be placed in a separate air tight container to prevent combination of the

samples. The SPT and collection of samples is to be done at 5-foot intervals, except in the upper 10 feet where samples will be collected every 2 feet. This type of sampling is adequate for natural moisture content, grain-size distribution, moisture-plasticity relationship (Atterberg Limit tests), and visual identification. See ASTM D1586 - *Standard Test Method for Standard Penetration Test (SPT) and Split-Barrel Sampling of Soils* (AASHTO T206 - *Standard Method of Test for Penetration Test and Split-Barrel Sampling of Soils*).

### 5.2.1.3 Shelby Tube Sampling

The Shelby tube is a thin-walled steel tube pushed into the soil to be sampled by hydraulic pressure and spun to shear off the base. Shelby tube sampling is also known as undisturbed (UD) sampling. After the sampler is pulled out, the sampler is immediately sealed and taken to the laboratory facility. This process allows the sample to be undisturbed as much as possible and is suitable for fine-grained soils that require strength and consolidation tests. See ASTM D1587 – *Standard Practice for Thin-Walled Tube Sampling of Soils for Geotechnical Purposes* (AASHTO T207 – *Standard Method of Test for Thin-Walled Tube Sampling of Soils*). There are a variety of methods that may be used to collect Shelby tube samples. Listed in the following Sections are the types of sampling methods commonly used. It is not the intention of this Manual that this list be comprehensive. Prior approval is required to use other sampling procedures, contact the PC/GDS for review and acceptance. A soil test boring log shall be prepared for all locations where UD samples are not collected within an existing soil test boring. The location (depth) of UD taken in an existing soil test boring shall be indicated on the soil test boring log. See Chapter 6 for the preparation and presentation of the UD soil test boring log.

#### 5.2.1.3.1 Fixed Head or Shelby Sampler

The simplest means of obtaining a Shelby tube sample is through the use of a fixed head attachment that allows a Shelby tube to be connected to the drill string. The head contains a check valve that allows water and drilling mud to exit the head as the sampler is lowered to the bottom of the borehole and pushed into the soil using the drill rig. This sampling method is typically used for firm to stiff fine-grained soils that are not very susceptible to disturbance and are strong enough to stay in the tube during retrieval.

#### 5.2.1.3.2 Fixed Piston Sampler

This sampler has the same standard dimensions as the Shelby sampler above, but with the addition of a piston that fits inside the tube. The sampler is connected to the drilling rods and a small diameter activation rod extends through the drill string from the piston up to the ground surface. The piston is positioned at the bottom of the thin-wall tube while the sampler is lowered to the bottom of the hole, thus preventing disturbed materials from entering the tube. The piston is fixed in place on top of the soil to be sampled by locking the activation rods to a point of fixity on the ground surface (e.g., a sawhorse, the drill rig, etc.). A sample is obtained by pressing the tube into the soil with a continuous, steady thrust using the drill rig. The stationary piston is held fixed on top of the soil while the sampling tube is advanced. This reduces the stress on the soil during the sampling process and creates suction while the sampling tube is retrieved thus aiding in retention of the sample. This sampler is suitable for soft to firm clays and silts as well as some clayey or silty sands. As compared to other thin-walled tube sampling methods, fixed piston sampling reduces disturbance and increases sample recovery.

#### 5.2.1.3.3 Floating Piston Sampler

This sampler is similar to the fixed method above, except that activation rods are not used and the piston is not fully fixed. A wedge mechanism limits piston movement to 1 direction, which is towards the top of the sampling tube. As with the fixed piston sampler, the piston is initially

positioned at the bottom of the tube. As the tube is pushed into the soil, the piston rides on the top of the sample. Since the piston is not fixed in place and is free to move down as the tube is being pushed, it applies a load to the soil. If the soil is soft, the loading from the piston may create significant sample disturbance and may even exceed the soil shear strength. Therefore, this method should be limited to firm to stiff soils. When the tube is retrieved, the wedge mechanism fixes the piston in place and thereby aids in sample retention, which is the principal benefit of the floating piston sampler.

#### 5.2.1.3.4 Hydraulic (Osterberg) Piston Sampler

The principle of the hydraulic piston sampler is the same as a fixed piston sampler but the 2 devices differ in their operation. Rather than using activation rods to maintain the piston elevation during sampling, the hydraulic piston sampler uses the drill string for this purpose. Additionally, rather than using the drill string to push the sampling tube into the soil, the hydraulic sampler uses the drill rig water pump. The sampling tube is advanced hydraulically using the drilling water delivered to the sampler through the drill rods. The elimination of the activation rods makes this method faster than the fixed piston process. However, the push capacity using the available pressure from the drill rig water pump is less than the push capacity using the drill rig crowd. Therefore, use of the hydraulic piston sampler is limited to very soft to firm soils. See ASTM D6519 – *Standard Practice for Sampling of Soil Using the Hydraulically Operated Stationary Piston Sampler*.

#### 5.2.1.3.5 Retractable Piston Sampler

This sampler is similar to the fixed piston sampler; however, after lowering the sampler into position the piston is retracted and locked in place at the top of the sampling tube. A sample is then obtained by pushing the entire assembly downward. This sampler is used for loose or soft soils.

### 5.2.2 Rock Core Sampling

The most common method for obtaining rock samples is diamond core drilling. There are 3 basic types of core barrels: single tube, double tube, and triple tube. All rock cores shall be N-size and shall have an approximate 2-inch diameter; however, larger rock core diameters may be obtained with prior approval of the PC/GDS. See ASTM D2113 - *Standard Practice for Rock Core Drilling and Sampling of Rock for Site Investigation* (AASHTO T225 - *Standard Method of Test for Diamond Core Drilling for Site Investigation*).

## 5.3 FIELD TESTING PROCEDURES

After access and utility clearances have been obtained and a survey base line has been established in the field, begin field explorations based on the subsurface exploration plan prepared by the GEOR. Many methods of field exploration exist; some of the more common are described below. These methods are often augmented by in-situ testing. The testing described in this Chapter provides the GEOR with soil and rock parameters determined in-situ. This is important on all projects, especially those involving soft clays, loose sands, or sands below the water table, due to the difficulty of obtaining representative samples suitable for laboratory testing. For each test included, a brief description of the equipment, the test method, and the use of the data is presented.

### **5.3.1 Test Pits**

These are the simplest methods of inspecting subsurface soils. Test pits consist of excavations performed by hand, backhoe, or dozer. Hand excavations are often performed with posthole diggers. Test pits offer the advantages of speed and ready access for sampling; however, test pits are severely hampered by limitations of depth and by the fact that advancement through soft or loose soils or below the water table can be extremely difficult. Test pits are used to examine large volumes of near surface soils and can be used to obtain bulk samples for additional testing. Test pits are particularly useful in characterizing existing fill material when buried debris, trash, organics, etc., may be present or are suspected.

### **5.3.2 Soil Borings**

Soil borings are the most common method of exploration. The results of the soil borings are presented on a Soil Test Log (see Chapter 6 for detailed description of the information presented on the log). In addition, to the description of the soils encountered, the Soil Test Log shall include the depth to groundwater both at the completion of the soil test boring and at least 24 hours later. Soil borings can be advanced using a number of methods. In addition, several different in-situ tests can be performed in the open borehole. The methods for advancing the boreholes will be discussed first followed by the methods of in-situ testing.

#### **5.3.2.1 Manual Auger Borings**

Manual auger borings are advanced using hand held equipment. Typically, these borings are conducted in areas where access for standard drilling equipment is severely restricted. Manual auger borings are limited in depth by the presence of ground water or collapsible soils that cause caving of the borehole. The Dynamic Cone Penetrometer test is usually conducted in conjunction with this boring method. A Manual Auger Boring Log and the results of the Dynamic Cone Penetrometer shall be prepared as indicated in Chapter 6.

#### **5.3.2.2 Hollow Stem Auger Borings**

A hollow-stem auger (HSA) consists of a continuous flight auger surrounding a hollow drill stem. The hollow-stem auger is advanced similar to other augers; however, removal of the hollow-stem auger is not necessary for sampling. SPT and undisturbed samples are obtained through the hollow drill stem, which acts like a casing to hold the borehole open. This increases usage of hollow-stem augers in soft and loose soils. See ASTM D6151 - *Standard Practice for Using Hollow-Stem Augers for Geotechnical Exploration and Soil Sampling* (AASHTO T306 - *Standard Method of Test for Progressing Auger Borings for Geotechnical Explorations*). This drilling method is not appropriate in sand below the water table and therefore shall not be used in soils where sand below the water table is anticipated. This includes any Coastal county; the coastal portion of a Piedmont county; or river flood plain regardless of where the river is located. The use of HSA to start a wash rotary boring is not allowed without the express written permission of the PC/GDS.

#### **5.3.2.3 Wash Rotary Borings**

In this method, the boring is advanced by a combination of the cutting action of a light bit and the flushing action of water flowing upward from the bit. A downward pressure applied during rapid rotation advances the hollow drill rods with a cutting bit attached to the bottom. The drill bit cuts the material and drilling fluid, discharged from ports on the side of the drill bit, washes the cuttings from the borehole. This is, in most cases, the fastest method of advancing the borehole and can be used in any type of soil except those containing considerable amounts of large gravel or boulders. Drilling mud or casing can be used to keep the borehole open in soft

or loose soils, although the former makes identifying strata change by examining the cuttings difficult. SPT and undisturbed samples are obtained through the drilling fluid, which holds the borehole open. This method of drilling shall be required in the following counties: Aiken, Allendale, Bamberg, Barnwell, Beaufort, Berkeley, Calhoun, Charleston, Chesterfield, Clarendon, Colleton, Darlington, Dillon, Dorchester, Florence, Georgetown, Hampton, Horry, Jasper, Kershaw, Lee, Lexington, Marion, Marlboro, Orangeburg, Richland, Sumter, and Williamsburg. These counties are typically located within the Coastal Plain Physiographic Province of South Carolina, with the remaining counties are located in the Piedmont Physiographic Province of South Carolina (see Chapter 11 for a detailed geologic discussion). However, the Coastal Plain extends into Edgefield, Fairfield, Lancaster and Saluda Counties, even though these counties are considered to be Piedmont counties. For those portions of these counties that are located in the Coastal Plain, wash rotary drilling methods shall be required. Additionally, wash rotary drilling methods shall be used at any locations where alluvium below the water table is anticipated, regardless of the county or proximity to the Coastal Plain. As previously indicated the use of HSAs to start wash rotary borings is not permitted without the express written permission of the PC/GDS. However, if the use of HSAs is permitted, the HSA drilling should not extend more than 3 feet below the existing ground surface.

#### 5.3.2.4 Coring

A core barrel is advanced through rock by the application of downward pressure during rotation. Circulating water removes ground-up material from the hole while also cooling the bit. The rate of advance is controlled so as to obtain the maximum possible core recovery. See ASTM D2113 – *Standard Practice for Rock Core Drilling and Sampling of Rock for Site Investigation* (AASHTO T225 - *Standard Method of Test for Diamond Core Drilling for Site Investigation*). A professional geologist or engineer, with experience in geotechnical engineering, shall be on-site during coring operations to perform measurements in the core hole to allow for determination of the Geological Strength Index (GSI) and the Rock Mass Rating (RMR) (see Chapter 6) and other rock properties. Rock coring, as indicated in Chapter 6, should begin when drilling refusal is encountered and an SPT N-value of 50 blows per 2 inches or less of penetration is encountered.

#### 5.3.3 Standard Penetration Test

The SPT is 1 of the most widely used in-situ test in the United States. It has the advantages of simplicity, the availability of a wide variety of correlations for its data, and the fact that a sample is obtainable with each test. A standard split-barrel sampler (discussed previously) is advanced into the soil by dropping a 140-pound manual safety or automatic hammer attached to the drill rod from a height of 30 inches. **[Note: Use of a donut hammer is not permitted].** The sampler is advanced a total of 18 inches. The number of blows required to advance the sampler for each of 3 6-inch increments is recorded. The sum of the number of blows for the 2<sup>nd</sup> and 3<sup>rd</sup> increments is called the Standard Penetration Value, or more commonly, N-value ( $N_{meas}$ ) (blows per foot). Tests shall be performed in accordance with ASTM D1586 - *Standard Test Method for Standard Penetration Test (SPT) and Split-Barrel Sampling of Soils* (AASHTO T206 - *Standard Method of Test for Penetration Test and Split-Barrel Sampling of Soils*). The Standard Penetration Test shall be performed every 2 feet in the upper 10 feet ( $5 N_{meas}$ ) and every 5 feet thereafter. The exception is beneath embankments, where the Standard Penetration Test shall also be performed every 2 feet in the first 10 feet below the original ground surface. The depth to the original ground surface may be estimated based on the height of the existing embankment.

When the SPT is performed in soil layers containing large shells, gravels or similar materials, the sampler may become plugged. A plugged sampler will cause the SPT N-value to be much larger than for an unplugged sampler and, therefore, not a representative index of the soil layer properties. In this circumstance, a realistic design requires reducing the N-value used for design to the trend of the N-values which do not appear distorted. However, the actual N-values should be presented on the Soil Test Logs (see Chapter 6). A note shall be placed on the Soil Test Logs indicating that the sampler was likely plugged.

The SPT values should not be used indiscriminately. They are sensitive to the fluctuations in individual drilling practices and equipment. Studies have also indicated that the results are more reliable in sands than clays. Although extensive use of this test in subsurface exploration is recommended, it should always be augmented by other field and laboratory tests, particularly when dealing with clays. The type of hammer (safety or automatic) shall be noted on the boring logs, since this will affect the actual input driving energy.  $N_{meas}$  requires correction prior to being used in engineering analysis (see Chapter 7).

The amount of driving energy shall be measured using ASTM D4633 - *Standard Test Method for Energy Measurement for Dynamic Penetrometers*. Since there is a wide variability of performance in SPT hammers, this method is used to evaluate an individual hammer's performance. The energy of a hammer can be effected by the mechanical state of the hammer system (i.e., maintained or not), the condition of the rope, the experience of the driller, the time of day, and the weather. A Quality Assurance/Quality Control (QA/QC) plan for measuring hammer energy shall be submitted for review and acceptance by the PC/GDS, prior to being used in the field.

The SPT installation procedure is similar to pile driving because it is governed by stress wave propagation. As a result, if force and velocity measurements are obtained during a test, the energy transmitted can be determined.

### **5.3.4 Dynamic Cone Penetrometer Test**

The Dynamic Cone Penetrometer (DCP) Test is a dynamic penetration test usually performed in conjunction with manual auger borings. DCP testing shall be conducted using the procedure presented by Sowers and Hedges (1966). The DCP resistance values shall be correlated to  $N_{meas}$ , by performing an SPT adjacent to a DCP test location. As an alternate to the Sowers and Hedges (1966) procedure, the DCP may also be conducted using ASTM D6951 – *Standard Test Method for Use of the Dynamic Cone Penetrometer in Shallow Pavement Applications*.

### **5.3.5 Cone Penetrometer Test**

The Cone Penetrometer Test is a quasi-static penetration test in which a cylindrical rod with a conical point is advanced through the soil at a constant rate and the resistance to penetration is measured. A series of tests performed at varying depths at 1 location is commonly called a sounding.

Several types of cone penetrometers have been historically used, including the mechanical (Dutch) cone, mechanical friction-cone, electric cone, and electric friction-cone but these are now obsolete. All Cone Penetrometer Testing on SCDOT projects shall use electro-piezocone (CPTu) penetrometers. Standard cone penetrometers measure 3 main parameters: 1) resistance to penetration at the conical tip of the penetrometer, 2) resistance acting on a cylindrical friction sleeve which is mounted behind the conical tip, and 3) water pressure acting at the joint between the conical tip and the friction sleeve also known as the  $u_2$  position. All 3 measurements are made nearly continuously (e.g., every 2 cm (~3/4-inch)) with depth. Many cone penetrometers also have the ability to measure inclination during penetration and

specialized cones may include additional capabilities (e.g., instrumentation for shear wave velocity measurements, resistivity, fuel fluorescence, etc.).

For all types of penetrometers, cone dimensions of a 60-degree tip angle and a 10 cm<sup>2</sup> (1.55 in<sup>2</sup>) or 15 cm<sup>2</sup> (2.33 in<sup>2</sup>) projected end area are standard. Friction sleeve outside diameter is the same as the base of the cone. Penetration rates should be between 10 to 20 mm/sec. Tests shall be performed in accordance with ASTM D5778 - *Standard Test Method for Electronic Friction Cone and Piezocone Penetration Testing of Soils*. Prior to being used on a SCDOT project, all electro-piezocones shall be calibrated to ascertain that the internal components of the cone are working correctly. Calibration of the cone shall comply with the requirements of Section 5.5. In addition, prior to performing each sounding and immediately after completion of the sounding, the zero readings of the cone shall be obtained. If the before “zero reading” is different from the after “zero reading”, the GEC shall determine if the cone is working properly. Further, the GEC shall determine if the different “zero readings” affect the results of the sounding. If the sounding is affected, then the GEC shall contact the PC/GDS with this information along with recommendations as to what corrective action is required. If there is no change between the before “zero reading” and the after “zero reading”, then the “zero reading” shall be used to correct the results of the sounding.

The measured parameters (i.e, tip resistance, sleeve resistance, and pore pressure) can be used with various classification methods to determine the soil behavior type. Many correlations of the cone test results to other soil parameters have been made, and design methods are available for spread footings and piles. The cone penetrometer can be used in sands or clays, but not in rock or other extremely dense soils. Since samples are not obtained during a CPTu sounding, the exploration should be augmented by push-tube sampling, SPT borings or other borings with soil samples taken. On SCDOT projects, the CPTu soil behavior type ( $I_c$ ) shall be correlated to the in-situ soils by performing a boring adjacent to the sounding. Only a single correlation boring shall be required, if in the opinion of the GEOR the site is uniform. If the site is not uniform, then the GEOR shall determine if additional correlation borings are required. The soil test boring shall be continuously sampled for the upper 50 feet and sampled every 5 feet thereafter to the anticipated depth of CPTu sounding termination or the actual depth of CPTu sounding termination whichever is shallower. The soil test boring shall be located no more than 5 feet from the location of the CPTu sounding and shall be located at the same approximate elevation. A professional engineer or professional geologist shall classify the soil samples obtained from the boring using both visual classification methods as well as index testing. Then the professional engineer or professional geologist shall compare the classifications from the soil test boring to the soil behavior type classifications indicated by the CPTu sounding. Differences between the soil classification of the samples from the boring and the soil behavior type from the CPTu data shall be reflected in subsequent use and presentation of the CPTu data (e.g., on subsurface cross sections).

As indicated in Chapter 4, the CPTu may be used to measure the dissipation rate of the excessive pore water pressure for all soils identified as fine-grained with a thickness of more than 3 feet. At the option of the GEOR, thinner layers may have pore pressure dissipation tests. The cone should be equipped with a pressure transducer that is capable of measuring the induced water pressure. To perform this test, the cone will be advanced into the subsoil at a standard rate of 20 mm/sec. Excess pore water pressures will be measured immediately and at several time intervals thereafter. Use the recorded data to plot pore pressure dissipation versus log-time graph. Using this graph, an estimate of the permeability and/or coefficient of consolidation can be made. In addition an Excel<sup>®</sup> spreadsheet shall be provided that contains the data from the test (indicated in Chapter 6).



### 5.3.6 Dilatometer Test

The dilatometer is a 3.75-inch wide and 0.55-inch thick stainless steel blade with a thin 2.4-inch diameter expandable metal membrane on 1 side. While the membrane is flush with the blade surface, the blade is pushed into the subsurface. The thrust required to insert the dilatometer ranges from 2 to 15 tons, but should be limited to less than 5 tons to prevent damage to the dilatometer. Alternatively, the dilatometer can be driven to the required testing interval using a SPT hammer. However, extreme caution is required when driving the dilatometer to prevent damage to the instrument. Rods carry pneumatic and electrical lines from the membrane to the surface. Individual dilatometer tests are typically conducted at depth intervals of 12 inches. Tests shall be performed in accordance with ASTM D6635 - *Standard Test Method for Performing the Flat Plate Dilatometer*. A pressurized gas (a bottle of nitrogen) is used to expand the membrane into the soil. Three readings or pressures are measured during the test. According to The Flat Dilatometer Test, Publication No. FHWA-SA-91-044 (Briaud and Miran (1992)), these readings are:

1. A-pressure – gas pressure against the inside of the membrane when the center of the membrane has lifted above its support and moved horizontally into the surrounding soil 0.05 mm
2. B-pressure – gas pressure against the inside of the membrane when the center of the membrane has lifted above its support and moved horizontally into the surrounding soil 1.1 mm
3. C-pressure – gas pressure against the inside of the membrane obtained by slowly deflating the membrane until contact is reestablished

According to Briaud and Miran (1992), the dilatometer is calibrated in the air under atmospheric pressure, both before and after the test: “The gas pressure necessary to overcome the membrane stiffness and move it in the air to both the A position and B position are referred to as  $\Delta A$  and  $\Delta B$ , respectively; they are not negligible.” If the membrane calibration is conducted using the same gauge as used in the field testing, then  $Z_M$  (see Chapter 6) shall be set to 0. The reason is that the  $Z_M$  correction is already accounted for in the membrane calibration. New membranes will have calibration values outside of the anticipated values (see Table 5-1). In order to get the membrane calibration values into the range of anticipated values the new membrane should be exercised prior to being used for testing. Exercising should continue until the calibration values are within the anticipated values. “S” (standard) type membranes are relatively soft and should only be used when the anticipated thrust to advance the dilatometer is less than 2 tons. “H” (high strength) type membranes are strong and can be used in any soil. Therefore, the “H” type membrane should be the membrane typically used. The Excel<sup>®</sup> spreadsheet shall indicate the type of membrane used.

**Table 5-1, Expected Calibration Values  
(Briaud and Miran (1992))**

Membrane Type	$\Delta A$ Calibration (bars)			$\Delta B$ Calibration (bars)		
	Minimum	Maximum	Average	Minimum	Maximum	Average
Standard “S”	0.10	0.20	0.13	0.10	0.70	0.35
High Strength “H”	0.10	0.25	0.19	0.10 <sup>1</sup>	1.50	0.90 <sup>2</sup>

<sup>1</sup> $\Delta B < 0.30$  is unusual for “H” membranes and may indicate damage

<sup>2</sup>Considerable variation

The thrust ( $q_d$ ) is typically measured at the ground surface; therefore, the resistance of the rods will need to be subtracted from the total thrust to obtain the thrust just to insert the blade. The resistance of the rods may be determined in several ways, first, estimate the required resistance on the push rods and reduce the total thrust to get the blade thrust. Second, measure the thrust encountered during dilatometer insertion, measure the thrust required to extract the dilatometer,

with the difference between the 2 measurements being the thrust required to insert just the dilatometer blade. The final way to estimate thrust is to assume the tip stress ( $q_c$ ) required to insert a nearby cone is the same as the thrust required to insert the dilatometer. In addition, an Excel<sup>®</sup> spreadsheet shall be provided that contains the data (indicated in Chapter 6) from the test.

### **5.3.7 Pressuremeter Test**

This test is performed with a cylindrical probe placed at the desired depth in a borehole. The Menard type pressuremeter requires pre-drilling of the borehole; the self-boring type pressuremeter advances the hole itself, thus reducing soil disturbance. The PENCEL pressuremeter can be set in place by pressing it to the test depth or by direct driving from ground surface or from within a predrilled borehole. The hollow center PENCEL probe can be used in series with the static cone penetrometer. The borehole should have a diameter ranging from 1.03D to 1.2D, where D is the diameter of the pressuremeter. The Menard type pressuremeter shall have a length to diameter (L/D) ratio of at least 6.5:1 to minimize end effects. The pressuremeter membrane typically has a slotted tube or a Chinese screen covering to protect the membrane from punctures during inflation. In soils the membrane is inflated using either water (typical) or gas, while in weathered and fractured rocks hydraulic oil is used. Tests shall be performed in accordance with ASTM D4719 - *Standard Test Methods for Prebored Pressuremeter Testing in Soils*.

Prior to proposing or conducting the Pressuremeter Test (PMT), the GEOR shall contact the PC/GDS to discuss the anticipated testing results and the use of these testing results in design. In addition to the plotted pressuremeter data, the GEC shall provide to the PC/GDS an electronic file in Excel<sup>®</sup> format providing at least the following data:

1. Depth (feet)
2.  $p_o$  (psf)
3.  $p_f$  (psf)
4.  $p_u$  (psf)
5.  $p_r$  (psf)
6.  $p_L$  (psf)
7. Creep Test

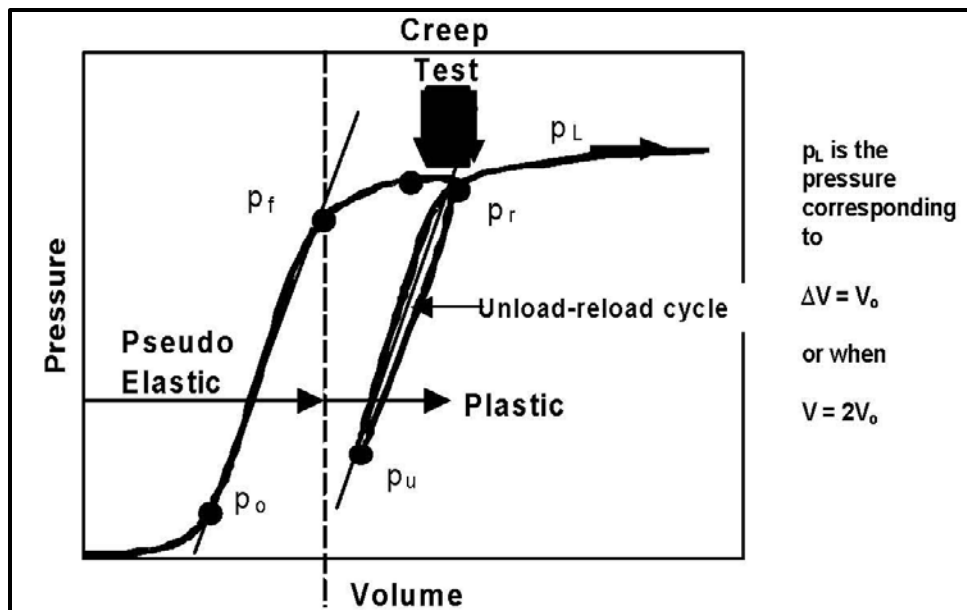


**Figure 5-1, Pressuremeter Curve  
(Sabatini, Bachus, Mayne, Schneider and Zettler (2002))**

Where,

- $p_o$  – Pressure at which recompression of the disturbed soil is complete and expansion into undisturbed soil begins
  - $p_f$  – Pressure where the soil changes from pseudo-elastic to plastic shear
  - $p_u$  – Minimum pressure during unloading, in the unload-reload cycle
  - $p_r$  – Pressure at the point during the reload portion in the unload-reload cycle where recompression ends and plastic shearing reinitiates
  - $p_L$  – Pressure at which curve becomes asymptotic to pressure regardless of the increase of volume; extrapolated as the pressure when the volume is equal to twice the initial volume of the pressuremeter
- Creep Test – Prior to performing an unload-reload test, a creep test should be performed, continued deformation at a constant pressure until strain rates of 0.1 percent per minute are recorded

In addition, the PC/GDS will determine what correlated design parameters from the PMT shall be provided. Contact the PC/GDS for instructions on log preparation and presentation of PMT data.

Results are interpreted based on semi-empirical correlations from past tests and observation. In-situ horizontal stresses, shear strength, bearing capacities, and settlement can be estimated using these correlations. The pressuremeter test results can be used to obtain load displacement curves ( $p$ - $y$  curves) for lateral load analyses. The pressuremeter test is very sensitive to borehole disturbance and the data may be difficult to interpret for some soils.

### **5.3.8 Field Vane Shear Test**

The Field Vane Shear Test (FVST) consists of advancing a 4-bladed vane into cohesive soil to the desired depth. The field vane should be advanced a minimum of 4 times the diameter of the borehole to allow for testing undisturbed soils. The field vane shall have a minimum height ( $H$ ) to diameter ( $D$ ) ratio of at least 2 (see Figure 5-2). In addition, the field vane has 2 basic configurations rectangular or tapered (see Figure 5-2). In the tapered configuration some vanes only have a tapered edge along the bottom of the vane which affects the way the undrained shear strength is determined (see Chapter 7). Torque is applied at a constant rate (6°/min

(0.1°/sec)) until the soil fails in shear along a cylindrical surface. The torque measured ( $T_{net}$ ) at failure provides the undrained shear strength ( $(S_u)_{fvst}$ ) of the soil. After determining the torque required for initial failure ( $(S_u)_{fvst}$ ), the vane is quickly rotated through 10 complete revolutions and the remolded undrained shear strength ( $(S_{urem})_{fvst}$ ) is determined using  $T_{net}$  for these revolutions. Using the undrained shear strengths (peak and remolded) the sensitivity of the soil may be determined. Tests shall be performed in accordance with ASTM D2573 - *Standard Test Method for Field Vane Shear Test in Cohesive Soil* (AASHTO T223 - *Standard Method of Test for Field Vane Shear Test in Cohesive Soil*).

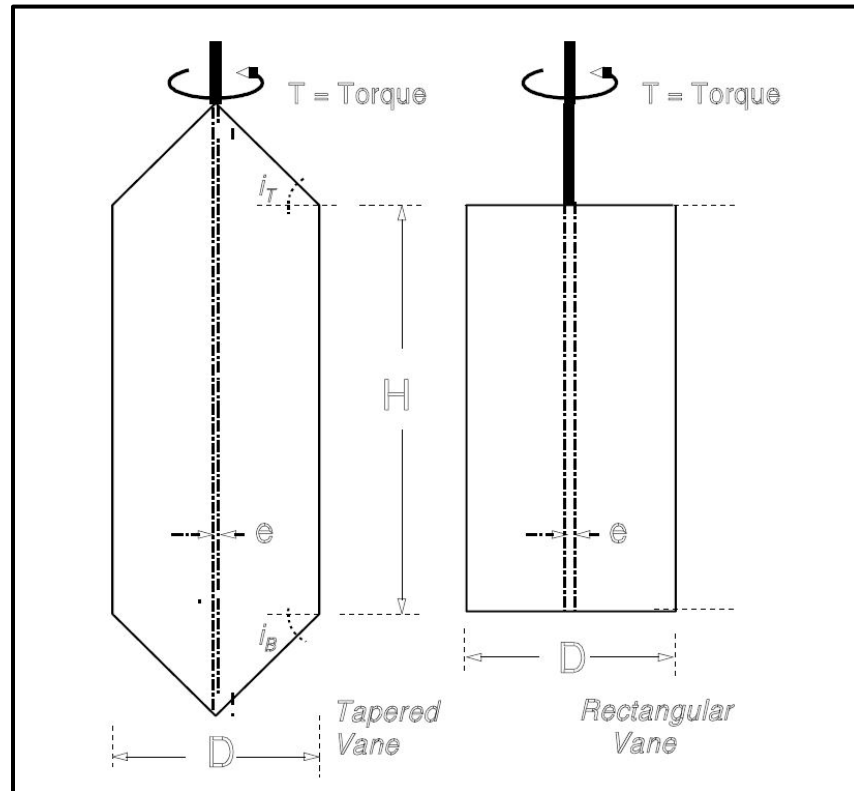


**Figure 5-2, Field Vane Devices  
(Mayne, Christopher and DeJong (2002))**

$$T_{net} = T_{max} - T_{rod}$$

**Equation 5-1**

Where,

D – Diameter of the field vane

H – Height of the field vane (see Figure 5-2)

e – thickness of the vanes

$i_T$  and  $i_B$  – Angle measured from the horizontal of the taper (up (T) or down (B))

$T_{net}$  – Net torque

$T_{max}$  – Maximum torque at peak undrained shear strength

$T_{rod}$  – Torque on rod caused by skin friction

The correlations for  $(S_u)_{fvst}$ ,  $(S_{urem})_{fvst}$  and  $S_{t(fvst)}$  (sensitivity) shall conform to the requirements of Chapter 7. The GEC shall provide the results of the FVST in an Excel® spreadsheet. The data from the FVST shall be presented as indicated in Chapter 6. This method is commonly used for measuring shear strength in soft clays (anticipated shear strength less than 2 tsf) and organic deposits. It should not be used in stiff and hard clays. Results can be affected by the presence of gravel, shells, roots, or sand layers. Shear strength may be overestimated in plastic clays ( $PI > 5$ ) and a correction factor ( $\mu_v$ ) should be applied.

$$\tau_{mobilized} = \mu_v * (S_u)_{fvst} \quad \text{Equation 5-2}$$

$$\mu_v = 1.05 - 0.45 * (PI)^{0.5} \quad \text{Equation 5-3}$$

Where,

PI – Plasticity index

$\mu_v$  – Empirical correction factor

$\tau_{mobilized}$  – Mobilized shear strength

### 5.3.9 Double-Ring Infiltrometer Test

The double-ring infiltrometer test is used to determine the rate of water infiltration into the subgrade soils. Infiltration rates are typically required in the design of storm water retention structures. The test consists of using 2 concentric metal rings that are inserted into the ground. Water is added to the outer ring and allowed to soak into the soil, with more water added to keep the water in the outer ring at the same depth. Once the water level in the outer ring stays constant, water is added to the inner ring until the water level in the inner ring is the same as the level in the outer ring. As soon as the water level in the 2 rings is the same, the change in the water level of the inner ring is recorded with time. The test is repeated with successively longer time intervals until the infiltration rate is constant with time and the infiltration rate can be determined. Tests shall be performed in accordance with ASTM D3385 - *Standard Test Method for Infiltration Rate of Soils in Field Using Double-Ring Infiltrometer*. Contact the PC/GDS for instructions on presentation of data.

### 5.3.10 Geophysical Testing Methods

Geophysical testing methods are non-destructive testing procedures which can provide general information on the general subsurface profile, depth to bedrock or water, location of granular borrow areas, peat deposits or subsurface anomalies and provide an indication of certain material properties (i.e., compression wave ( $V_p$ ) and shear wave velocity ( $V_s$ )). Geophysical testing methods are not limited to subsurface conditions, but can also be used to evaluate existing bridge decks, foundations and pavements. The reader should see Application of Geophysical Methods to Highway Related Problems, FHWA-IF-04-021 (Wightman, et al. (2003)), for additional information on the application of geophysical test methods to other areas other than subsurface conditions.

#### 5.3.10.1 Surface Shear Wave Velocity Methods

Surface wave methods consist of Spectral Analysis of Surface Waves (SASW) or Multi-channel Analysis of Surface Waves (MASW). The SASW and MASW are used to measure layer thickness, depth and the shear wave velocity ( $V_s$ ) of the layer. The shear wave velocity is more of bulk (general) velocity than a discrete velocity of a layer. Discrete shear wave velocity may be determined by crosshole or downhole methods. While the SASW will typically have 2 geophones (see Figure 5-3), the MASW will have additional geophones spread over a larger area. Typically SASW and the MASW profiles are limited to a depth of approximately 130 feet using man portable equipment. Additional depth can be obtained but heavier motorized equipment is required. The GEC shall provide the results of the testing in an Excel<sup>®</sup> spreadsheet. See Chapter 6 for presentation of SASW/MASW data.

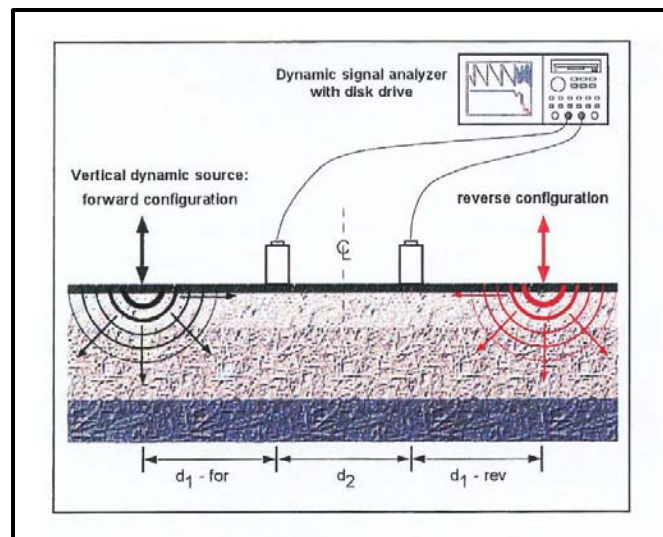


**Figure 5-3, SASW Shear Wave Velocity Testing (Mayne et al. (2002))**

### 5.3.10.2 Downhole Shear Wave Velocity Methods

Downhole methods for determining shear wave velocity differ from surface methods in that equipment is placed in the ground (see Figure 5-4). In downhole methods, either, a casing is placed in the ground and a pair geophones are lowered into the casing or a seismic cone penetrometer (SCPTu) is pushed into the ground. The SCPTu should have 2 geophones or accelerometers mounted above the friction sleeve on the cone. The transducers in either method shall be capable of measuring in orthogonal directions (i.e., 1 vertical and 2 horizontal at 90° to each other). With either method, a shear wave is induced at the ground surface and the time for arrival is determined. For conventional downhole testing in a borehole, the casing must be grouted in place with a non-shrink grout. As compared to the casing method, SCPTu is much faster but has the major limitation of refusal to advance in dense soils. Tests shall be performed in accordance with ASTM D7400 – *Standard Test Methods for Downhole Seismic Testing*. The GEC shall provide the results of the testing in an Excel® spreadsheet. The spreadsheet shall include both  $V_p$  and  $V_s$  determinations as well as the depth of each reading. See Chapter 6 for presentation of Downhole Shear Velocity data.

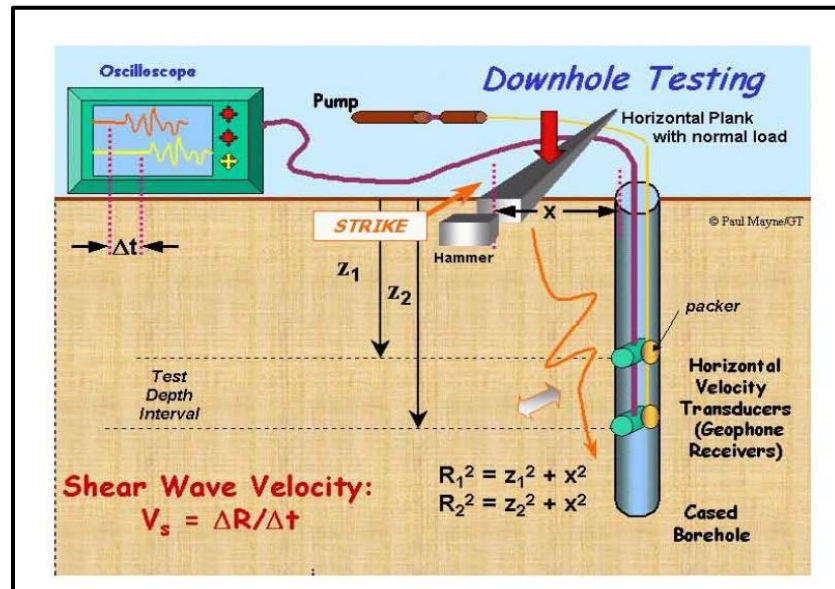


**Figure 5-4, Downhole Shear Wave Velocity Testing  
(Mayne et al. (2002))**

### 5.3.10.3 Crosshole Shear Wave Velocity Methods

In crosshole shear wave velocity testing, shear wave velocities are determined between a series of cased boreholes (see Figure 5-5). A downhole hammer and geophone are lowered to the same depth, but in different holes. The hammer is tripped and time for the shear wave to travel to the geophone is recorded. The major limitation to the crosshole method is the expense of the installation of the required cased borehole. In addition, care must be taken during the construction of the casings to assure that the casings are plumb and in the same horizontal plane and are in good contact with the surrounding soil. Depending on the depth and spacing between the cased boreholes, a verticality survey with an inclinometer may be necessary to determine the actual spacing between the boreholes at the test depths. Tests shall be performed in accordance with ASTM D4428 – *Standard Test Methods for Crosshole Seismic Testing*. The GEC shall provide the results of the testing in an Excel® spreadsheet. The spreadsheet shall include both  $V_p$  and  $V_s$  determinations as well as the depth of each reading. See Chapter 6 for presentation of Crosshole Shear Wave Velocity data.

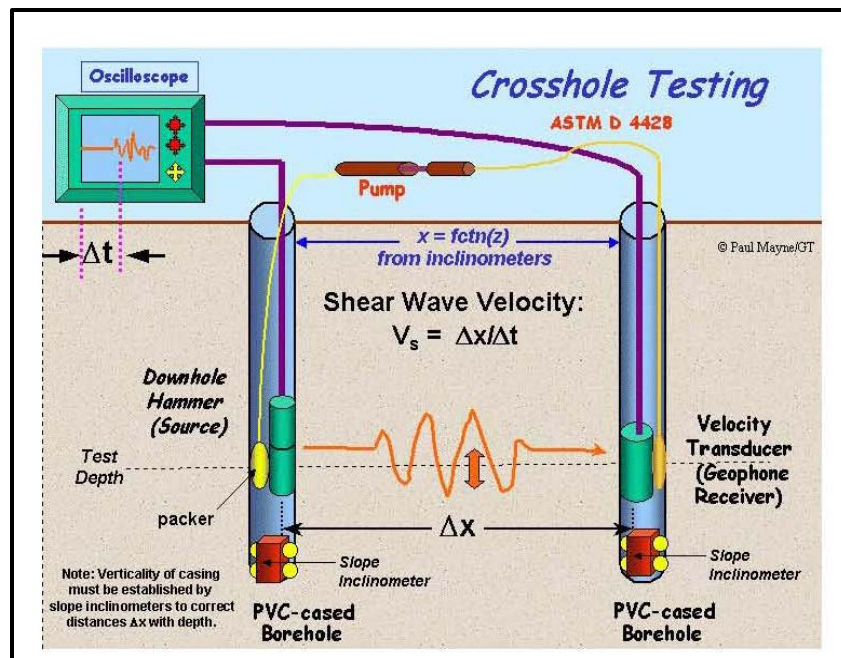


**Figure 5-5, Crosshole Shear Wave Velocity Testing  
(Mayne et al. (2002))**

#### 5.3.10.4 Suspension Logging

Suspension logging is a borehole geophysical technique used to measure compression and shear wave ( $V_p$  and  $V_s$ , respectively) velocities. Unlike the downhole or crosshole methods, the use of casing is not required; in fact the use of no casing is preferred. The receivers and source have the same polarity (axis). A schematic diagram of suspension logging is depicted in Figure 5-6. Energy from the source is transmitted through the borehole fluid to the borehole walls, where the energy is converted into P- and S-waves radiating out from the borehole wall. These waves travel up the soil column and pass the 2 receivers, which are located 1 meter apart. The time between energy wave generation and the time for first arrival at each receiver is recorded. The  $V_p$  and  $V_s$  can be developed from the arrival times and the distance between the receivers. Advantages and limitations are presented in Diehl, Martin and Steller (2006). Suspension logging shall conform to the requirements of ASTM D5753 – *Standard Guide for Planning and Conducting Borehole Geophysical Logging*. In addition, the testing methodology for the suspension logging shall be provided by the GEC to the PC/GDS prior to commencing field work. The GEC shall provide the results of the testing in an Excel<sup>®</sup> spreadsheet. The spreadsheet shall include both  $V_p$  and  $V_s$  determinations as well as the depth of each reading.



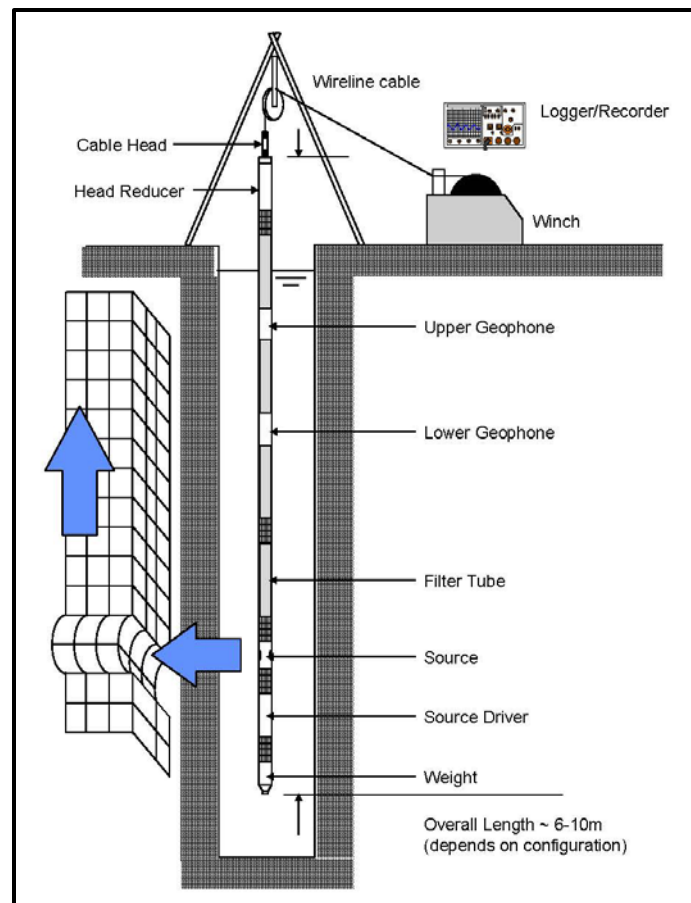


**Figure 5-6, Suspension Logging Schematic  
(Diehl, Martin and Steller (2006))**

### 5.3.10.5 Acoustic Televiwer

The acoustic televiwer uses an acoustic signal to obtain an oriented image of a borehole. It is anticipated that this testing method will only be used in boreholes that extend into rock where obtaining cores is difficult, expensive or are simply not available. The acoustic signal is generated by a rotating sonar transducer, which produces an “image” of the borehole. The image can be presented 2 different ways either as a wrapped core (Figure 5-7 – left hand image) or as an unwrapped image, viewed from the center of the borehole (Figure 5-7 – right hand image). From the data obtained void and joint data may be presented in terms of depth, direction of dip (with respect to North), dip angle and strike.

The preferred piece of equipment is a high-resolution acoustic televiwer. The use of a high-resolution acoustic televiwer allows the “image” to be presented in “pseudo-color”. Breaks and voids in the rock will appear as dark lines on the image. The acoustic televiwer shall conform to the requirements of ASTM D5753 - *Standard Guide for Planning and Conducting Borehole Geophysical Logging*. In addition, the testing methodology for the acoustic televiwer shall be provided by the GEC to the PC/GDS prior to commencing field work. The GEC shall provide the results of the testing in an Excel<sup>®</sup> spreadsheet. Contact the PC/GDS for instructions on data presentation.

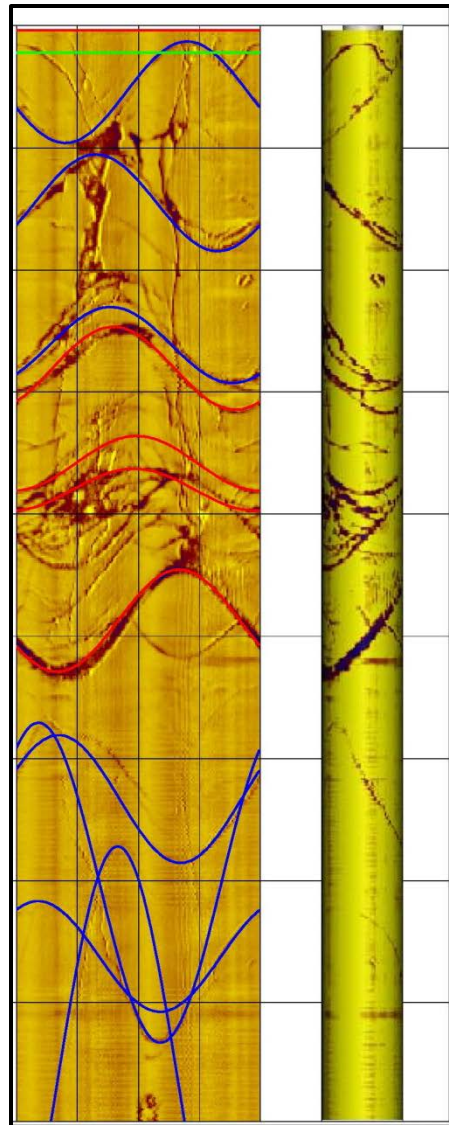


Figure 5-7, Acoustic Televiewer Image  
(GEOVision (2014))

### 5.3.10.6 Seismic Refraction

Seismic refraction is primarily used to determine the depth to bedrock. This method works well for depths less than 100 feet. A seismic energy source is required for producing seismic waves (see Figure 5-8). A sledge hammer is typically used for depths less than 50 feet and either a drop weight or a black powder charge is used for depths between 50 and 100 feet. The seismic compression waves penetrate the overburden material and refract along the bedrock surface. This method can be used for up to 4 soil layers on rock layers; however, each layer must have a higher shear wave velocity than the overlying layer. Figure 5-9 provides an example of determining the depth to rock in a 2-layer system. Tests shall be performed in accordance with ASTM D5777 – *Standard Guide for Using the Seismic Refraction Method for Subsurface Investigation*. The GEC shall provide the results of the testing in an Excel<sup>®</sup> spreadsheet. Contact the PC/GDS for instructions on data presentation.

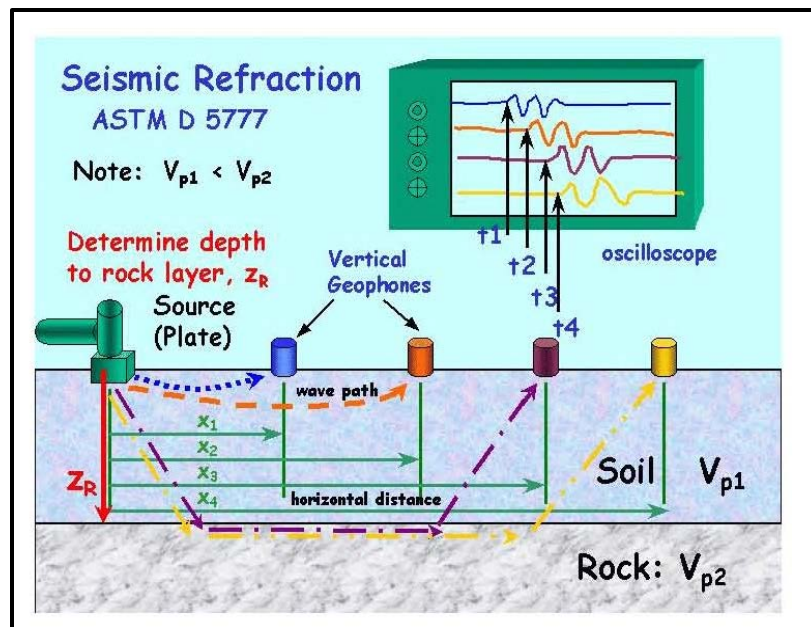


Figure 5-8, Seismic Refraction Testing (Mayne et al. (2002))

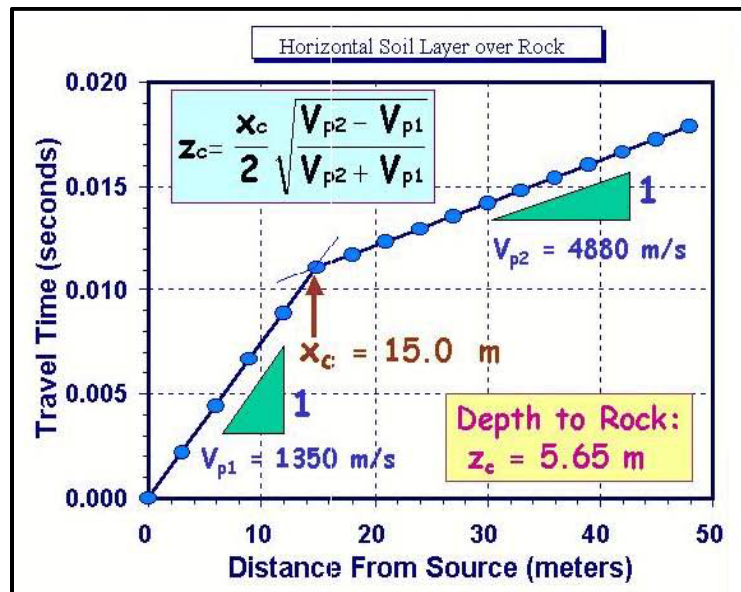


Figure 5-9, Data Reduction Example for Determining Depth to Hard Layer (Mayne et al. (2002))

### 5.3.10.7 Seismic Reflection

Seismic reflection uses a surface seismic wave source to create seismic waves that can penetrate the subsurface. The waves are reflected at interfaces that have either a change in shear wave velocity and/or a change in density. Changes in velocity or density are termed impedance contrasts. At impedance contrasts, a portion of the seismic wave is reflected back to the ground surface and a portion continues into the subsurface where it is reflected at the next impedance contrast. Seismic reflection techniques can obtain information in excess of 100 feet. Tests shall be performed in accordance with ASTM D7128 – *Standard Guide for Using the Seismic-Reflection Method for Shallow Subsurface Investigation*. Contact the PC/GDS for instructions on the presentation of the data.

### 5.3.10.8 Resistivity

Resistivity is used to find the depth to bedrock since soil and rock typically have different electrical resistances. The depth of the resistivity survey is typically 1/3 of the electrode spacing. For example, to reach a depth of 50 feet an electrode spacing of 150 feet is required. Resistivity surveys can reach depths of 160 feet. Resistivity testing is affected by the moisture content of the soil and the presence or lack of metals, salts and clay particles. In addition, resistivity surveys may be used to model ground water flow through the subsurface. Further, resistivity surveys may also be used to determine the potential for corrosion of foundation materials for the in-situ subsurface materials. Tests shall be performed in accordance with either ASTM D6431 – *Standard Guide for Using the Direct Current Resistivity Method for Subsurface Investigation* or ASTM G57 – *Standard Test Method for Field Measurement of Soil Resistivity Using the Wenner Four-Electrode Method*. Contact the PC/GDS for instructions on the presentation of data.

## 5.4 SOIL/ROCK LABORATORY TESTING

### 5.4.1 Grain-Size Analysis

There are 2 types of grain-size analysis tests: grain-size with wash No. 200 and the hydrometer test. Grain-size with wash No. 200, also known as Sieve Analysis, is for coarse-grained soils (sand, gravels) while the hydrometer test mainly is used for fine-grained soils (clays, silts). The results of the analyses are presented as depicted in Chapter 6.

The grain-size analysis can also be used for obtaining 3 basic soil parameters from the curves. These parameters are: effective size ( $D_{10}$ ), Coefficient of Uniformity ( $C_u$ ), and Coefficient of Curvature ( $C_c$ ). As required in Chapter 4, a hydrometer test and grain-size analysis shall be performed on selected samples to determine the  $D_{50}$ , which is used in scour analysis by the HEOR. The results of the testing are presented as indicated in Chapter 7.

#### 5.4.1.1 Sieve Analysis

The sieve analysis is a method used to determine the grain-size distribution of soils between the 3-inch sieve and the No. 200 sieve. The soil is passed through a series of woven wires with square openings of decreasing sizes. The test gives a soil classification based on the percentage retained on each sieve. See ASTM D6913 - *Standard Test Method for Particle-Size Distribution (Gradation) of Soils Using Sieve Analysis*. The amount passing the No. 200 sieve shall be determined in accordance with ASTM D1140 – *Standard Test Method for Amount of Material in Soils Finer than No. 200 (75- $\mu$ m) Sieve*. For gradations of particles greater than the 3-inch sieve in accordance with ASTM D5519 – *Standard Test Method for Particle Size Analysis of Natural and Man-Made Riprap Materials*.

#### 5.4.1.2 Hydrometer

The hydrometer analysis is used to determine the particle size distribution in a soil that is finer than a No. 200 sieve size (0.075 mm), which is the smallest standard size opening in the sieve analysis. The procedure is based on the sedimentation of soil grains in water. It is expressed by Stokes Law, which states that the velocity of the soil sediment is based on the soil particles shape, size and weight, as well as the viscosity of the water. Thus, the hydrometer analysis measures the change in specific gravity of a soil-water suspension as soil particles settle out over time. See ASTM D7928 - *Standard Test Method for Particle-Size Distribution (Gradation) of Fine-Grained Soils Using the Sedimentation (Hydrometer) Analysis* (AASHTO T88 - *Standard Method of Test for Particle Size Analysis of Soils*).

## 5.4.2 Moisture Content

The moisture content ( $w$ ) is defined as the ratio of the weight of water in a sample to the weight of solids. The weight of the solids must be oven dried and is considered as weight of dry soil. Organic soils can have the moisture content determined, but must be dried at a lower temperature for the weight of dry soil to prevent degradation of the organic matter. See ASTM D2216 - *Standard Test Methods for Laboratory Determination of Water (Moisture) Content of Soil and Rock by Mass* (AASHTO T265 - *Standard Method of Test for Laboratory Determination of Moisture Content of Soils*). It is noted that the terms “moisture content” and “water content” are used interchangeably.

## 5.4.3 Atterberg Limits

The Atterberg Limits are different descriptions of the moisture content of fine-grained soils as it transitions from a solid to a liquid-state (also termed the moisture-plasticity relationship). For classification purposes the 2 primary Atterberg Limits used are the plastic limit (PL) and the liquid limit (LL). The plasticity index (PI) is also calculated for soil classification.

### 5.4.3.1 Plastic Limit

The PL is the moisture content at which a soil transitions from being in a semisolid state to a plastic state. Tests shall be performed in accordance with ASTM D4318 - *Standard Test Methods for Liquid Limit, Plastic Limit, and Plasticity Index of Soils* (AASHTO T90 - *Standard Method of Test for Determining the Plastic Limit and Plasticity Index of Soils*).

### 5.4.3.2 Liquid Limit

The LL is defined as the moisture content at which a soil transitions from a plastic state to a liquid state. Tests shall be performed in accordance with ASTM D4318 - *Standard Test Methods for Liquid Limit, Plastic Limit, and Plasticity Index of Soils* (AASHTO T89 - *Standard Method of Test for Determining the Liquid Limit of Soils*).

### 5.4.3.3 Plasticity Index

The PI is defined as the difference between the LL and the PL of a soil. The PI represents the range of moisture contents within which the soil behaves as a plastic solid.

$$PI = LL - PL \qquad \text{Equation 5-4}$$

## 5.4.4 Specific Gravity of Soils

The specific gravity of soil,  $G_s$ , is defined as the ratio of the unit weight of a given material to the unit weight of water. The procedure is applicable only for soils composed of particles smaller than the No. 4 sieve (4.75 mm). This test shall be performed in conjunction with all consolidation tests. See ASTM D854 - *Standard Test Methods for Specific Gravity of Soil Solids by Water Pycnometer* (AASHTO T100 - *Standard Method of Test for Specific Gravity of Soils*). If the soil contains particles larger than the No. 4 sieve (4.75 mm), use ASTM C127- *Standard Test Method for Density, Relative Density (Specific Gravity), and Absorption of Coarse Aggregate*.

### 5.4.5 Undisturbed Sample Preparation

Strength and consolidation testing require the use of undisturbed (Shelby tube) samples, to avoid unnecessarily compromising the samples, extreme care is required in the transportation and handling of this samples. These samples shall be transported in a manner to minimize shaking and shall be oriented vertically with the top of the sample at the top of the carrier used to hold the tubes during transportation to the laboratory. Upon arrival at the testing laboratory all samples will maintain the same vertical orientation. The Shelby tube shall be cut in approximate 6-inch lengths with stiff (i.e.,  $N_{60}$ -value greater than or equal to 9 blows per foot) shall be extruded in the same direction as the sample was pushed i.e., extrude the sample toward the top of the tube. For soft soils (i.e.,  $N_{60}$ -value less than 9 blows per foot) cut the Shelby tube in approximate 6-inch lengths and very carefully cut the Shelby tube off the sample using something similar to a Dremel<sup>®</sup> tool. Prise the cut carefully off the sample to minimize disturbance. At no time shall the sample be extruded from the Shelby tube, since this may potentially disturb the sample. Prepare an Undisturbed Shelby Tube log as indicated in Chapter 6. Provide the Undisturbed Shelby Tube log to the GEOR prior to commencing any strength or consolidation testing. Based on the results of the log, the GEOR will determine which individual specimens will be used in testing.

### 5.4.6 Strength Tests

The shear strength is the internal resistance per unit area that the soil can handle before failure and is expressed as a stress. There are 2 components of shear strength, a cohesive element (expressed as the cohesion,  $c$ , in units of force/unit area) and a frictional element (expressed as the angle of internal friction,  $\phi$ , in units of degrees, °). These parameters are expressed in the form of total stress ( $c, \phi$ ) or effective stress ( $c', \phi'$ ). The total stress on any subsurface element is produced by the overburden pressure plus any applied loads. The effective stress equals the total stress minus the pore water pressure. The common methods of ascertaining these parameters in the laboratory are discussed below. All of these tests are normally performed on undisturbed samples, but may also be performed on remolded samples. Further, the moisture-plasticity (Atterberg Limits), moisture content, and grain-size analysis with wash #200 sieve shall be performed on all samples that are tested for shear strength.

#### 5.4.6.1 Unconfined Compression Tests

The unconfined compression test is a quick method of determining the value of undrained strength ( $(S_u)_{UC}$  or  $(\tau_{max})_{UC}$ ) for clay soils. The test involves a clay specimen with no confining pressure and an axial load being applied to observe the axial strains corresponding to various stress levels. The stress at failure is referred to as the unconfined compression strength,  $q_u$ . If failure has not occurred prior to 15 percent strain, then the sample at 15 percent strain is considered to have failed and the stress at this strain shall be reported as  $q_u$ . See ASTM D2166 - *Standard Test Method for Unconfined Compressive Strength of Cohesive Soil* (AASHTO T208 - *Standard Method of Test for Unconfined Compressive Strength of Cohesive Soil*).

$$(\tau_{max})_{UC} = (S_u)_{UC} = \left(\frac{q_u}{2}\right) \quad \text{Equation 5-5}$$

#### 5.4.6.2 Triaxial Compression Tests

The triaxial compression test is a more sophisticated testing procedure, as compared to the unconfined compression test, for determining the shear strength of a soil. The test involves a soil specimen subjected to an axial load until failure while also being subjected to confining



pressure that approximates the in-situ stress conditions. The GEOR shall be responsible for determining the required confining pressures ( $\sigma_3$ ). The confining pressures shall model the existing loading conditions on the soil as well as future loading conditions. There are 3 types of triaxial tests which are described below.

#### 5.4.6.2.1 Unconsolidated-Undrained (UU), or Q Test

In unconsolidated-undrained (UU) tests, the specimen is not permitted to change its initial water content before or during shear (i.e., the volume of the sample doesn't change). It should be noted that the results of this test are predicated on the assumption that the soil sample is 100 percent saturated. Typically, a UU test is performed on samples that will mechanically behave as a Clay-Like soil (see Chapter 7 for an explanation of Clay-Like). The results are expressed in total stress parameters,  $(S_u)_{UU}$  (see Figure 5-10; where each test is considered independent of the other tests). In addition to  $(S_u)_{UU}$ , the  $\sigma_3$  for each undrained shear strength shall be indicated. The  $\sigma_3$  should range from the existing overburden pressure to the anticipated full embankment height. The interpretation of  $c$  and  $\phi$  from an UU test is incorrect and shall not be accepted. The failure mode of the soil specimen shall also be indicated (i.e., bulging, shear plain, etc.). This test is used primarily in the calculation of immediate embankment stability during quick-loading conditions. Refer to ASTM D2850 - *Standard Test Method for Unconsolidated-Undrained Triaxial Compression Test on Cohesive Soils* (AASHTO T296 - *Standard Method of Test for Unconsolidated, Undrained Compressive Strength of Cohesive Soils in Triaxial Compression*).

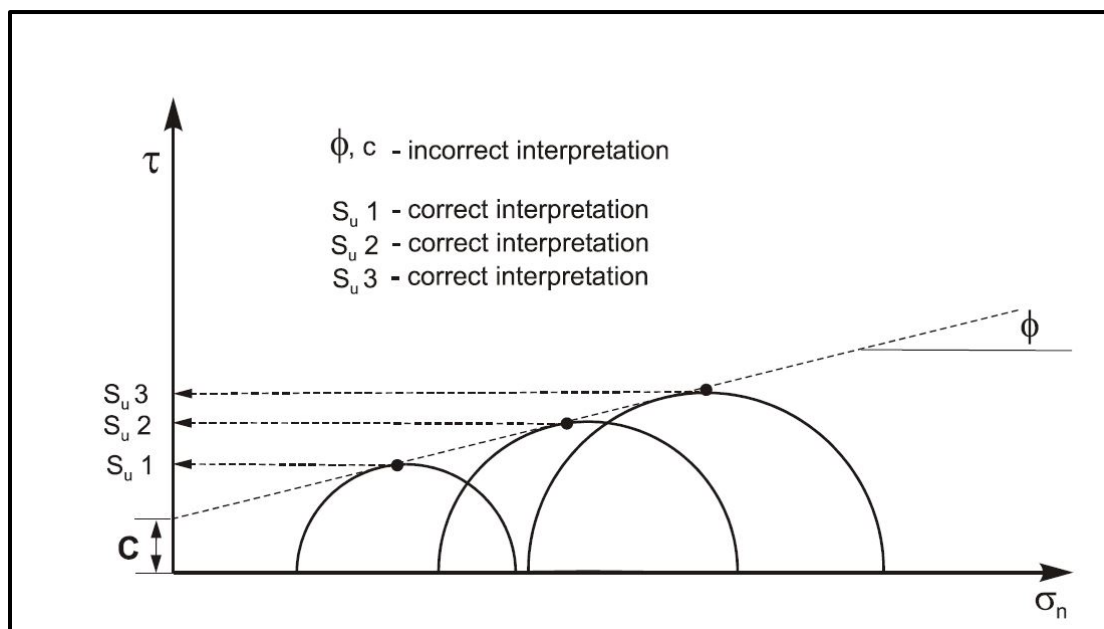


**Figure 5-10, Interpretation of UU Test Data  
(Sabatini et al. (2002))**

#### 5.4.6.2.2 Consolidated-Undrained (CU), or R Test

The consolidated-undrained (CU) test is the most common type of triaxial test. This test allows the soil specimen to be isotropically consolidated under a confining (also called consolidation) pressure ( $\sigma_3$  or  $\sigma_c$ ) prior to shear. In some of the literature this test is also designated CIU (consolidated isotropic undrained) shear strength test. When pore pressures are also measured during testing, the test is designated CUw/pp (CIUw/pp), both effective and total stress soil shear strength parameters may be developed. Therefore, CU tests with pore pressure

measurements (CUw/pp) are required. As presented below, when selecting  $\sigma_3$  for use in testing account for the effects of sample disturbance. Effective stress parameters,  $\phi'$  and  $c'$ , for soils that behave mechanically as a Clay-Like soil (see Chapter 7 for an explanation of Clay-Like) can be directly developed from the results of the testing and used in long-term stability analyses. For the same soil type, short-term stability analyses should be performed using total stress parameters. In the total stress analyses the ratio of the undrained shear strength  $((S_u)_{CU})$  to effective overburden pressure ( $\sigma'_{vo}$ ) or in the case of laboratory testing ( $\sigma'_3$ ),  $((S_u)_{CU})/\sigma'_{vo}$  or  $((S_u)_{CU})/\sigma'_3$  should be used. It is noted that in this approach to total stress analyses, it is assumed that  $\phi = 0$ .

Where,

$\phi$  = Total stress friction angle  
 $\sigma'_3$  = Effective confining pressure

$$\sigma'_3 = \sigma_3 - \Delta u \quad \text{Equation 5-6}$$

Where:

$\sigma_3$  = Total confining pressure  
 $\Delta u$  = Change in pore pressure

According to Sabatini et al. (2002), a confining pressure ( $\sigma_3$ ) approximately equal to the in-situ effective overburden stress ( $\sigma'_{vo}$ ) will overestimate the undrained shear strength of the soil. This overestimation of undrained shear strength is caused by sample disturbance. During drilling, sampling, transportation, extrusion and sample trimming the sample will become denser (i.e., the void ratio,  $e$ , will decrease). When confined at the same approximate overburden pressure, the denser sample will tend to have higher shear strength than the actual soil would have. To compensate for this apparent overestimation of undrained shear strength, the use of a confining stress in excess of the effective overburden stress should be used. Sabatini et al. (2002) states:

Because consolidation to higher pressures will result in higher undrained strengths, the undrained strength measured using a CU test at consolidation pressures (*confining stress*) greater than those corresponding to the depth at which the sample was taken is not a correct measure of the undrained strength for the depth in the ground where the sample for the CU test was taken.

To compensate for this overestimation of undrained shear strength, the undrained shear strength should be normalized by the effective overburden pressure ( $\sigma'_{vo}$ ) or the confining pressure ( $\sigma'_3$ ) as discussed previously.

The results of the CUw/pp testing shall include the following information and graphs:

1. Mohr's Circle (total stress) including undrained shear strength at failure
  - a.  $((S_u)_{UC})/\sigma'_{vo}$  or  $((S_u)_{UC})/\sigma'_3$
2. Mohr's Circle (effective stress) including best fit line – see Figure 5-11
  - a.  $\phi'$
  - b.  $c'$
3. p'-q' plots (effective stress) – see Figure 5-12
  - a.  $\alpha'$
  - b.  $a'$
4. p-q plots (total stress) including undrained shear strength at failure
  - a.  $((S_u)_{UC})/\sigma'_{vo}$  or  $((S_u)_{UC})/\sigma'_3$



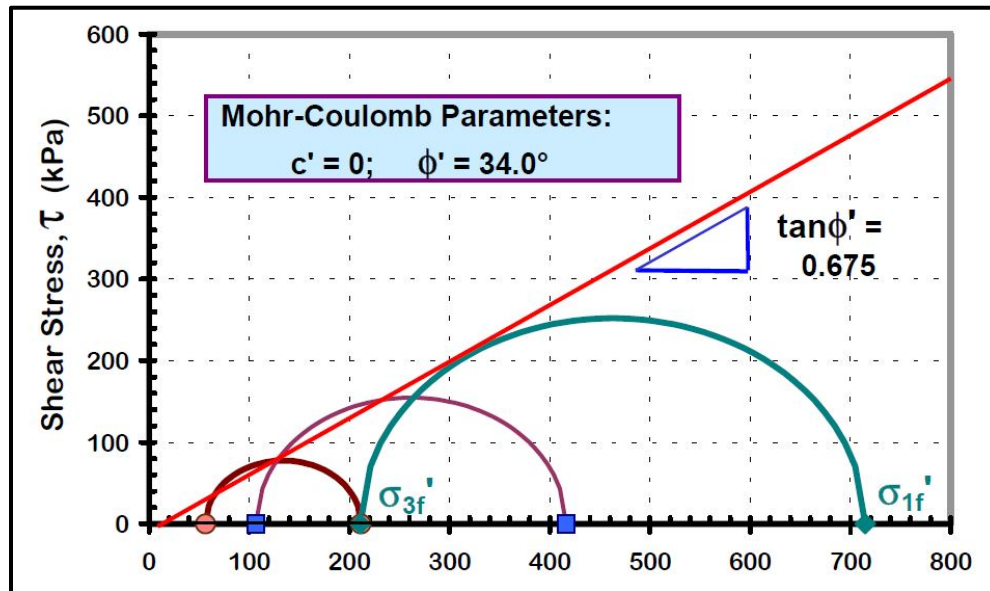


Figure 5-11, Mohr Circle Depicting Mohr-Coulomb Failure Criterion (Mayne et al. (2002))

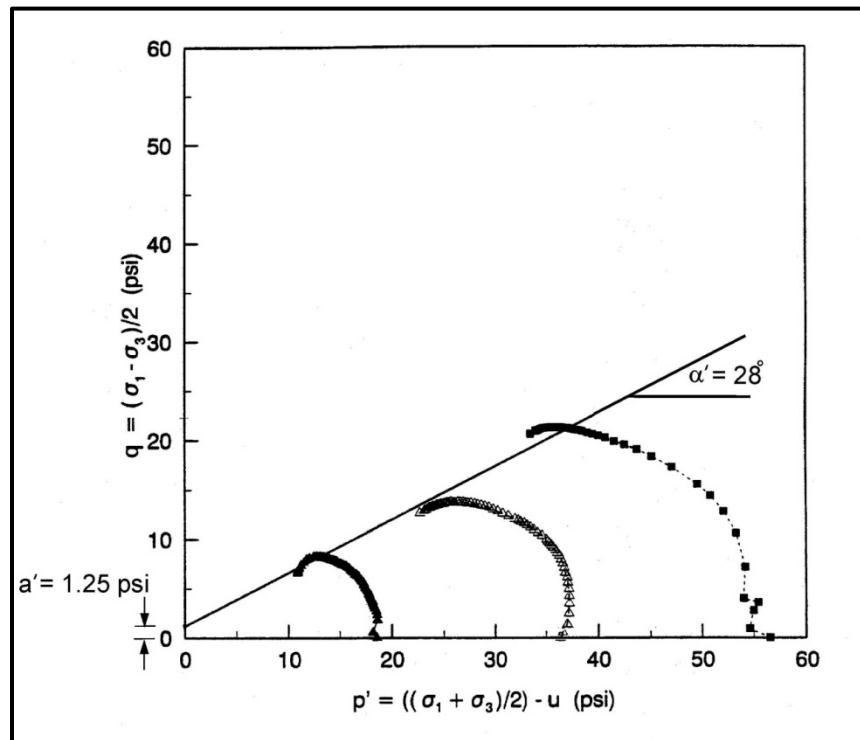


Figure 5-12, Stress Path (p'-q') Plot (Sabatini et al. (2002))

Effective stress soil parameters ( $\phi'$  and  $c'$ ) can be derived from the stress path plot using the following equations:

$$\phi' = \sin^{-1} \tan \alpha' \tag{Equation 5-7}$$

$$c' = \frac{a'}{\cos \phi'} \tag{Equation 5-8}$$

The failure mode of the soil specimen shall also be indicated (i.e., bulging, shear plain, etc.). In addition, the procedure for determining failure shall also be indicated. See ASTM D4767 - *Standard Test Method for Consolidated Undrained Triaxial Compression Test for Cohesive Soils* (AASHTO T297 - *Standard Method of Test for Consolidated, Undrained Triaxial Compression Test on Cohesive Soils*).

#### 5.4.6.2.3 Consolidated-Drained (CD), or S Test

The consolidated-drained (CD) test is similar to the consolidated-undrained test except that drainage is permitted during shear and the rate of shear is very slow. Thus, the buildup of excess pore pressure is prevented. Because of the length of time to conduct this test, it is typically not performed on SCDOT projects. The exception to this is if the sample is Sand-Like (see Chapter 7 for an explanation of Sand-Like) then a consolidated-drained triaxial shear test may be considered. Prior to performing this test, the PC/GDS shall review the purpose of the test and the anticipated outcome. This test is used to determine parameters for calculating long-term stability of embankments. The failure mode of the soil specimen shall also be indicated (i.e., bulging, shear plain, etc.). In addition, the procedure for determining failure shall also be indicated. Refer to ASTM D7181 – *Standard Test Method for Consolidated Drained Triaxial Compression Test for Soils*.

#### 5.4.6.3 Resonant-Column Test

The resonant-column test is used to determine the shear modulus,  $G$ ; shear damping,  $\lambda$ ; and Young's modulus,  $E$ . This test may be performed on either undisturbed or remolded specimens. In addition, the specimen may be unconfined or the specimen may have a confining pressure applied to it. If confining pressure is to be used the procedures discussed in Section 5.4.5.2.1 shall be used in regards the confining pressure. The GEOR shall be responsible for determining the required  $\sigma_3$ . See ASTM D4015 – *Standard Test Methods for Modulus and Damping of Soils by Resonant-Column Method*.

#### 5.4.6.4 Direct Shear

The direct shear test is the oldest and simplest form of shear test. A soil sample is placed in a metal shear box and undergoes a horizontal force, typically designated  $T$  (tangential force). While the horizontal force is being applied, a normal force ( $N$  ( $P$  in Figure 5-13)) is applied to the top of the direct shear box. The application of a higher  $N$  causes  $T$  to increase. The forces are often expressed as stresses ( $\sigma_N$  and  $\tau$ ). Because of the way the shear test is conducted, the soil fails along a horizontal plane. The test is performed using strain-control and is performed slowly enough to allow drainage to prevent the buildup of excess pore pressures. There are 2 types of direct shear test; simple and torsional, each test is described in the following Sub-sections. Similarly, to the triaxial tests, the GEOR shall be responsible for determining  $N$  for both test types.

##### 5.4.6.4.1 Direct Simple Shear Test

The direct simple shear test is applicable to all soil types; however, it is typically performed on Sand-Like (see Chapter 7 for an explanation of Sand-Like). The results of the test shall be presented as indicated in Figure 5-13. In addition, a table of  $\sigma_N$  and  $\tau$  shall also be provided.

The test is typically performed as consolidated-drained test on Sand-Like soils; however, there is a test method available to perform a consolidated-undrained test (ASTM D6528 – *Standard Test Method for Consolidated Undrained Direct Simple Shear Testing of Cohesive Soils*). The

use of ASTM D6528 will require approval by the PC/GDS. See ASTM D3080 - *Standard Test Method for Direct Shear Test of Soils Under Consolidated Drained Conditions* (AASHTO T236 - *Standard Method of Test for Direct Shear Test of Soils Under Consolidated Drained Conditions*).

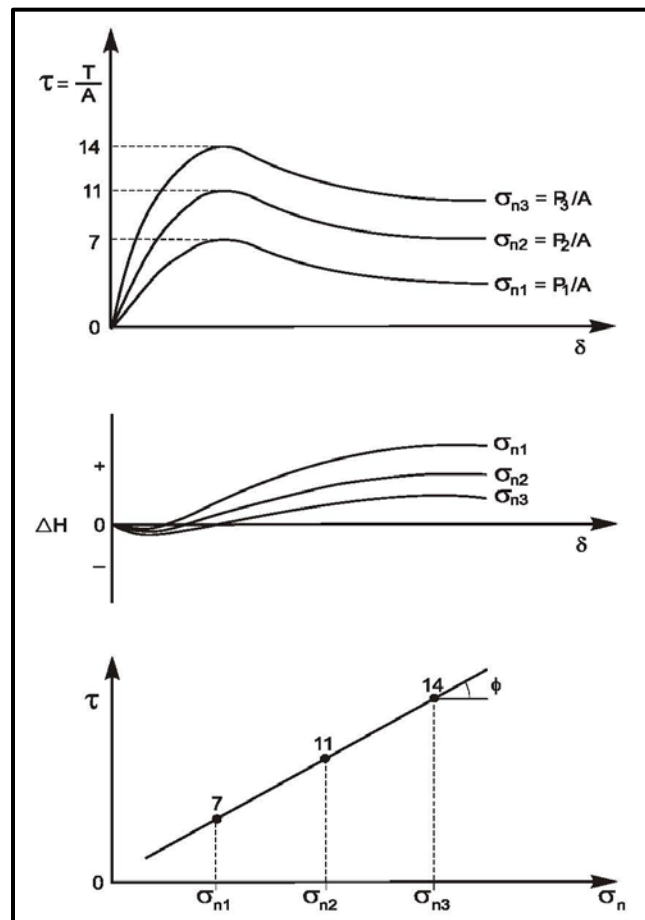


**Figure 5-13, Direct Shear Test Results  
(Sabatini et al. (2002))**

#### 5.4.6.4.2 Torsional Ring Shear Test

According to Terzaghi, Peck and Mesri (1996), triaxial and direct simple shear testing "...lack the ability to investigate the shearing resistance of soils at very large strains or displacements;...". Therefore, to account for the application of very large strains the torsional ring shear test device was developed by a joint effort of the Norwegian Geotechnical Institute and Imperial College (Terzaghi, Peck and Mesri (1996)). This test method should not be used on Sand-Like (see Chapter 7 for an explanation of Sand-Like). Torsional shear testing should be used on Clay-Like (see Chapter 7 for an explanation of Clay-Like). There are 2 testing methods, ASTM D6467 – *Standard Test Method for Torsional Ring Shear Test to Determine Drained Residual Shear Strength of Cohesive Soils* and ASTM D7608 – *Standard Test Method for Torsional Ring Shear Test to Determine Drained Fully Softened Shear Strength and Nonlinear Strength Envelope of Cohesive Soils (Using Normally Consolidated Specimen) for Slopes with No Preexisting Shear Surface*. The GEOR shall determine which test method is to be used based on the project requirements.

#### 5.4.6.5 Miniature Vane Shear (Torvane) and Pocket Penetrometer

The miniature vane shear and the pocket penetrometer tests are performed to obtain undrained shear strength ( $(S_u)_{iv}$  or  $(S_u)_{pp}$ , respectively) for plastic cohesive soils. Both of these tests consist of hand-held devices that are pushed into the sample and either a torque resistance (Torvane) or a tip resistance (pocket penetrometer) is measured. They can be performed in the lab or in the field. See ASTM D4648 - *Standard Test Method for Laboratory Miniature Vane Shear Test for Saturated Fine-Grained Clayey Soil* for the miniature vane shear test only.

#### 5.4.7 Consolidation Test

The amount of settlement ( $S_t$  or  $\Delta_v$ ) induced by the placement of load bearing elements (i.e., ERSs or bridges) on the ground surface or the construction of earthen embankments will affect the performance of the structure. The amount of settlement is a function of the increase in pore water pressure caused by the loading and the reduction of this pressure over time. The reduction in pore pressure and the rate of the reduction are a function of the permeability of the in-situ soil. All soils undergo elastic compression ( $S_i$ ), primary consolidation ( $S_c$ ) and secondary compression ( $S_s$ ). Sand-Like soils tend to be relatively permeable and will therefore, undergo settlement much faster. The amount of elastic compression settlement can vary depending on the soil type; however, the time for this settlement to occur is relatively quick and will normally occur during construction.

Clay-Like soils tend to have a much lower permeability and will, therefore, take longer to settle. Clay-Like soils undergo elastic compression during the initial stages of loading (i.e., the soil particles rearrange due to the loading). After elastic compression of Clay-Like soils is complete, primary consolidation begins. Saturated Clay-Like soils have a lower coefficient of permeability, thus the excess pore water pressure generated by loading will gradually dissipate over a longer period of time. Therefore in saturated clays, the amount and rate of settlement is of great importance in construction. For example, an embankment may settle until a gap exists between an approach and a bridge abutment. The calculation of settlement involves many factors, including the magnitude of the load, the effect of the load at the depth at which compressible soils exist, the water table, and characteristics of the soil itself. Consolidation testing is performed to ascertain the nature of these characteristics. The most commonly used test procedure is the incremental load method of 1-dimensional consolidation testing. See ASTM D2435 - *Standard Test Methods for One-Dimensional Consolidation Properties of Soils Using Incremental Loading* (AASHTO T216 - *Standard Method of Test for One-Dimensional Consolidation Properties of Soils*). In addition, the moisture-plasticity (Atterberg Limits), moisture content, grain-size analysis with wash #200 sieve and specific gravity shall be performed on all samples tested using this test method. ASTM D4186 – *Standard Test Method for One-Dimensional Consolidation Properties of Saturated Cohesive Soils Using Controlled Strain Loading* shall not be allowed.

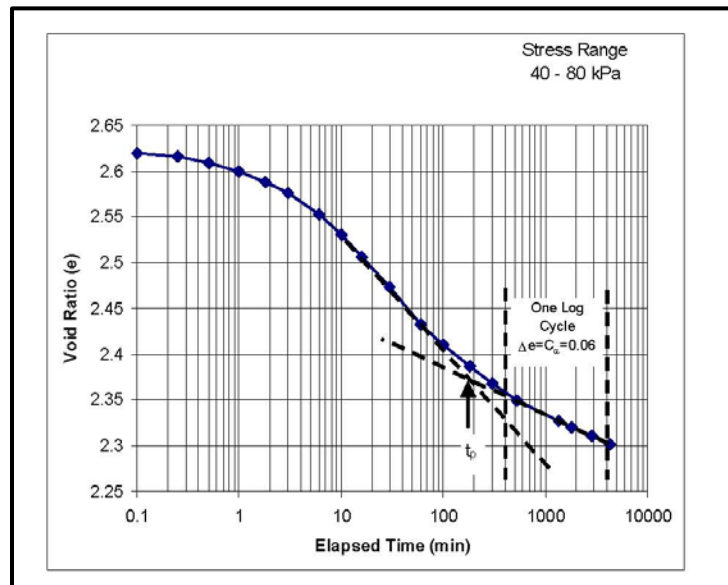
The consolidation test unit consists of a consolidometer (or alternatively, an oedometer) and a loading device. The soil sample is placed between 2 porous stones, which permit drainage (i.e., double drainage). Load is applied incrementally and is typically held up to 24 hours. The loading increments shall be determined by the GEOR. The GEOR shall review the results of each load increment (i.e.,  $e$  versus log time plots (see Figure 5-14), alternatively  $\varepsilon$  versus log time plots may be used) to determine if the load has been held a sufficient length of time to determine the secondary compression ( $c_\alpha$ ) index. The next load increment shall only be applied as approved by the GEOR. The secondary compression index shall be determined as indicated in the following paragraphs. The test measures the change in height (strain) of the specimen after each loading is applied. In addition, the GEOR shall determine if an unload/reload cycle is to be included and at which load increment the cycle shall begin and end. Typically the

unload/reload cycle should begin when the loading exceeds the preconsolidation pressure ( $\sigma'_p$ ) by at least 1 loading increment. A first-order estimate of the  $\sigma'_p$  shall be made using the correlations provided in Chapter 7. Further, the consolidation testing shall extend to loads of 8 times the first-order estimate of  $\sigma'_p$ . After the maximum loading has been reached, the loading is removed in appropriate decrements. Contact the PC/GDS for guidance if the anticipated range of loading exceeds the load limits of the testing apparatus. It is noted that a consolidation test with unload/reload cycle should require between 14 and 16 loading increments to form a complete test. The 1-dimensional consolidation test is used to determine the parameters for use in 1-dimensional consolidation theory. These parameters are indicated in Table 5-2.

**Table 5-2, Consolidation Parameters and Symbols**

Symbol	Parameter
$C_c$ or $C_{cc}$	Compression Index
$C_r$ or $C_{cr}$	Recompression Index
$C_{\alpha}$ or $C_{\epsilon\alpha}$	Secondary Compression Index
$\sigma'_p$ or $p'_c$	Effective Preconsolidation Stress
$c_v$	Coefficient of Consolidation
$m_v$	Coefficient of Vertical Compression

The results of each load increment are plotted on a deformation (void ratio) versus log time plot (see Figure 5-14). Alternatively, the strain versus log time plot may be used. From this curve, 2 parameters can be derived: coefficient of consolidation ( $c_v$ ) and secondary compression ( $C_{\alpha}$ ) index. These parameters are used to predict the rate of primary settlement and the amount of secondary consolidation. Further this curve is used to determine when primary consolidation is complete for each load increment.



$t_p$  = time to 100 percent consolidation (i.e., end of primary consolidation)

**Figure 5-14, Void Ratio versus log Time (Sabatini et al. (2002))**

The coefficient of consolidation ( $c_v$ ) shall be determined using both Casagrande’s logarithm of time and Taylor’s square root of time method. Casagrande’s method uses the time to 50 percent of primary consolidation and Taylor’s method use the time to 90 percent of primary consolidation and determines  $c_v$  using:

$$c_v = \frac{0.197 * H_{DR}^2}{t_{50}} \quad \text{Equation 5-9}$$

$$c_v = \frac{0.848 * H_{DR}^2}{t_{90}} \quad \text{Equation 5-10}$$

Where,

$H_{DR}$  – Height of the drainage path (assumed to be ½ of specimen thickness at each load increment to account for double drainage), inches

$t_{50}$  – Time required to achieve 50 percent primary consolidation, seconds

$t_{90}$  – Time required to achieve 90 percent primary consolidation, seconds

It is noted that both Casagrande's and Taylor's methods are included in the ASTM and shall be used to determine  $c_v$  for each load increment. Both sets of  $c_v$  shall be plotted and provided to the GEOR. The  $c_v$ , typically is higher for load increments under  $\sigma'_p$  and lower when the load increments are over the  $\sigma'_p$ .

After the time-deformation plots are obtained, the void ratio and the strain can be calculated. Two more plots can be presented; an  $e$ -log  $p$  curve, which plots void ratio ( $e$ ) as a function of the log of pressure ( $p$ ), or an  $\varepsilon$ -log  $p$  curve where  $\varepsilon$  equals percent strain. The parameters necessary for settlement calculation can be derived from the corrected  $e$ -log  $p$  curve and are: compression index ( $C_c$ ), recompression index ( $C_r$ ), preconsolidation pressure ( $\sigma'_p$ ), and initial void ratio ( $e_o$ ). Alternatively, the corrected  $\varepsilon$ -log  $p$  curve provides the compression index ( $C_{cc}$ ), the recompression index ( $C_{cr}$ ), and the preconsolidation pressure ( $\sigma'_p$ ). The 1-dimensional consolidation test is sensitive to sample disturbance; therefore, the results of the test must be corrected, by the GEOR, using the procedures provided in Chapter 7.

Casagrande (1936) developed a graphical procedure for determining the preconsolidation stress. The Casagrande procedure for determining preconsolidation stress is outlined in Table 5-3. While the Casagrande procedure was applicable to both  $e$ -log  $p$  and  $\varepsilon$ -log  $p$  curves, SCDOT prefers the use of the  $\varepsilon$ -log  $p$  curve for data presentation. The effective preconsolidation stress ( $\sigma'_p$ ) is extremely important because it is used to determine if a soil is normally consolidated (NC) or overconsolidated (OC). In normally consolidated soils, the effective preconsolidation stress is equal to the existing effective overburden stress (i.e.,  $\sigma'_{vo} = \sigma'_p$ ) (see Figure 5-15). Normally consolidated soils tend to have large settlements. Overconsolidated soils have an effective preconsolidation stress greater than the existing effective overburden stress (i.e.,  $\sigma'_{vo} < \sigma'_p$ ) (see Figure 5-16). Overconsolidated soils do not tend to have large settlements. In some locations within South Carolina, under consolidated soils (i.e.,  $\sigma'_{vo} > \sigma'_p$ ) (see Figure 5-17) are known to exist. These soils are still consolidating under the weight of the soil and should be anticipated to have very large amounts of settlement.

**Table 5-3, Determination of Preconsolidation Stress  
(Duncan and Buchignani (1976))**

Step	Description
1	Locate the point of sharpest curvature on the $e$ -log $p$ or $\varepsilon$ -log $p$ curve
2	From this point (a) (see Figures 5-18 or 5-19), draw a horizontal line (b) and a tangent (b) to the curve
3	Bisect the angle formed by these 2 lines (c)
4	Extend the virgin curve (d) backward to intersect the bisector (c)
5	The point where these lines (d and c) cross determines the preconsolidation pressure ( $\sigma'_p$ or $p'_c$ )

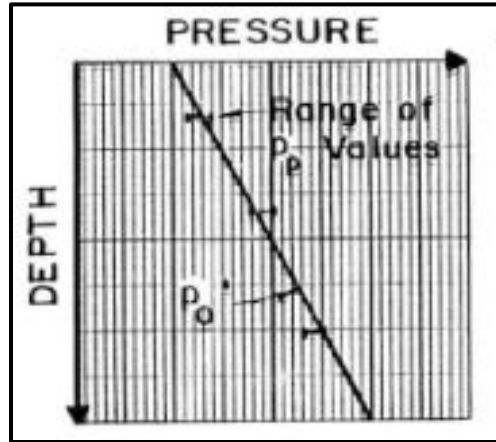


Figure 5-15, Normally Consolidated (Duncan and Buchignani (1976))

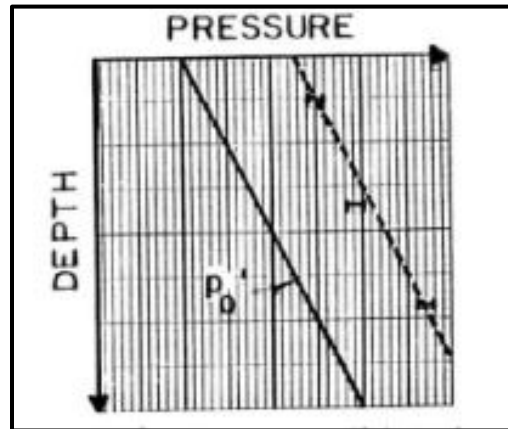


Figure 5-16, Overconsolidated (Duncan and Buchignani (1976))

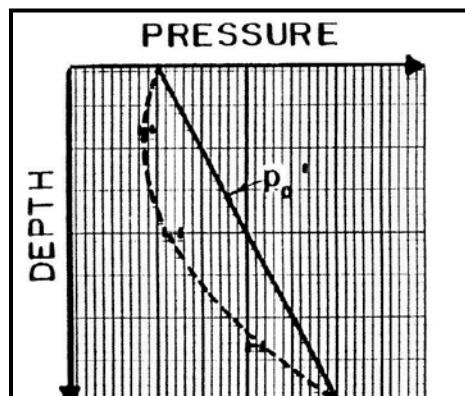


Figure 5-17, Under Consolidated (Duncan and Buchignani (1976))

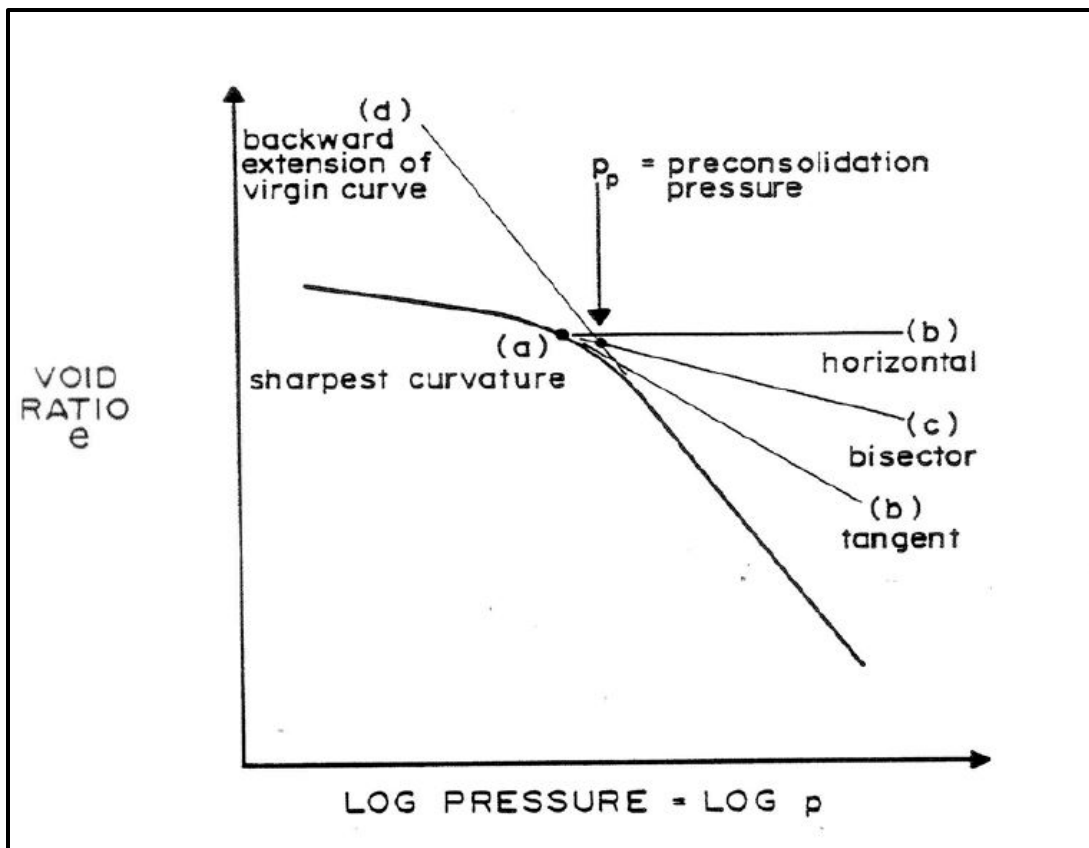


Figure 5-18, Determination of Preconsolidation Stress from  $e$ - $\log p$  (Duncan and Buchignani (1976))

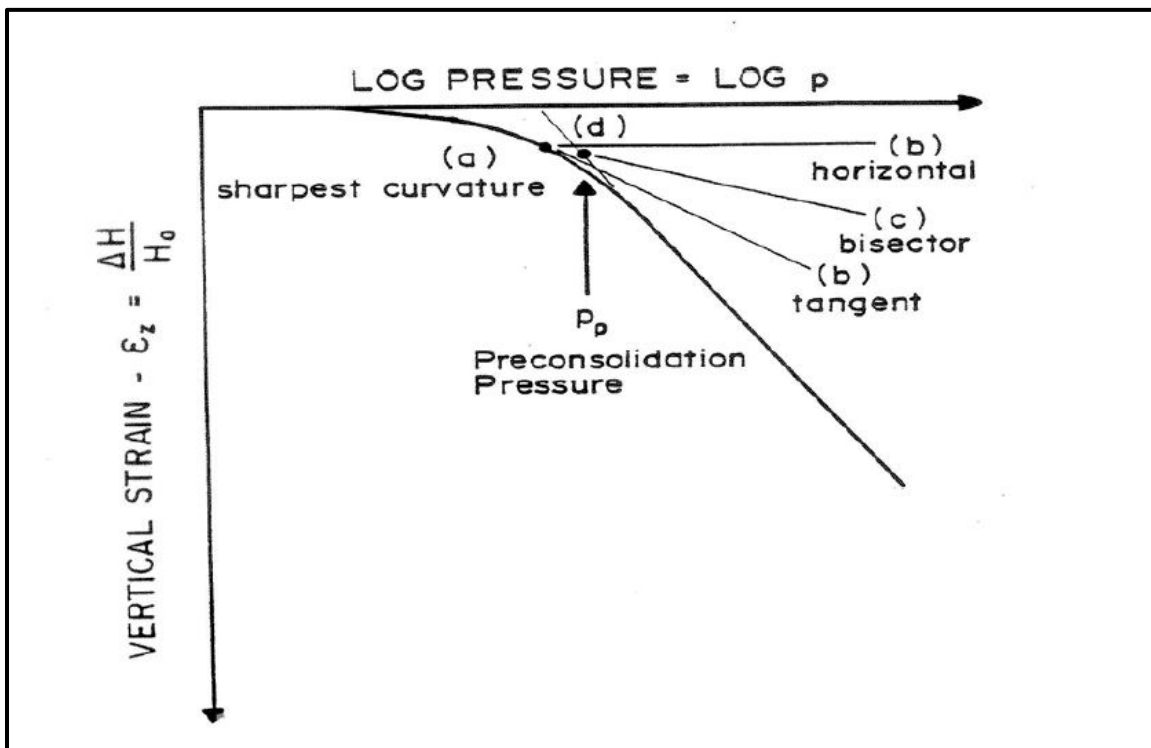


Figure 5-19, Determination of Preconsolidation Stress from  $\epsilon$ - $\log p$  (Duncan and Buchignani (1976))



In addition to using the Casagrande reconstruction method to determine  $\sigma'_p$ , the Strain-Energy method (Becker, Crooks, Been and Jefferies (1987)) shall also be used. The Strain-Energy method involves plotting the cumulative strain energy (i.e., the product of stress times strain) for each load increment in a laboratory consolidation test. The point where the strain energy plot exhibits a large incremental increase represents the preconsolidation stress,  $\sigma'_p$ , for the soil. The first step in determining  $\sigma'_p$  using the Strain-Energy method is determining the change in work (energy) per unit volume using the following equation:

$$\Delta W = \left( \frac{\sigma'_i + \sigma'_f}{2} \right) * \left( \ln \frac{1 - \varepsilon_i}{1 - \varepsilon_f} \right) \quad \text{Equation 5-11}$$

Where,

$\Delta W$  = Change in work (energy) per unit volume (units of stress (tsf (kJ/m<sup>3</sup> or kPa)))

$\sigma'_i$  = Stress at beginning of strain increment (units of stress (tsf))

$\sigma'_f$  = Stress at end of strain increment (units of stress (tsf))

$\varepsilon_i$  = Strain at beginning of increment (dimensionless)

$\varepsilon_f$  = Strain at end of increment (dimensionless)

The second step is to plot the stress versus the summation of work for each stress increment (see Figure 5-20). It is assumed that the stress value corresponding to the summation of work is the stress at the end of the strain increment. A noticeable change in slope should be evident when the data are plotted. A curve connecting the data should have a sharp transition from a flatter slope in the recompression range (slope 1) to a steeper slope (slope 2) in the virgin compression range. Construct a trend line through the data that represent a line with slope 1. Construct a second trend line through the data that represent a line with slope 2. The stress where these 2 trend lines intersect is the preconsolidation stress,  $\sigma'_p$ .

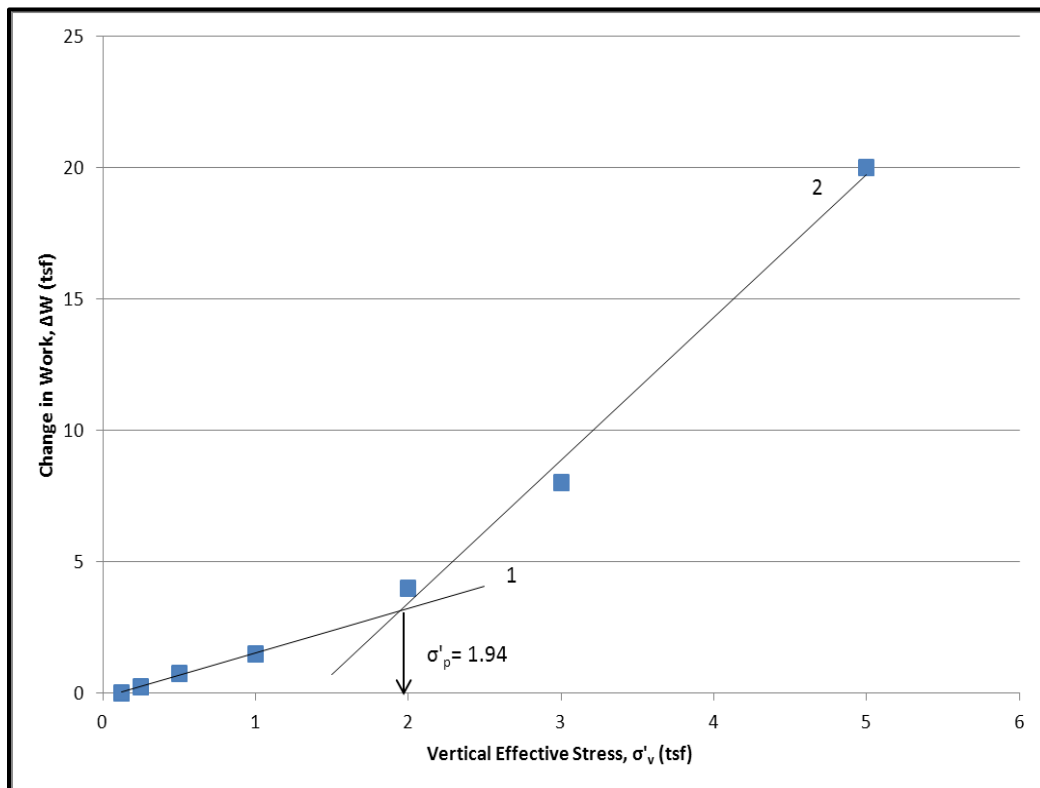


Figure 5-20, Change in Work vs. Vertical Effective Stress  
(Sabatini et al. (2002))

The preconsolidation stress,  $\sigma'_p$ , determined from both the Casagrande reconstruction method and from the Strain-Energy method shall be provided. In addition, all results provided shall be indicated as being uncorrected.

The secondary compression ( $C_\alpha$  or  $C_{\varepsilon\alpha}$ ) index shall be determined for each loading increment and shall be reported graphically similarly to the coefficient of consolidation ( $c_v$ ) versus the log of pressure. Secondary compression settlement begins at the completion of primary consolidation and in certain soils including highly organic soils secondary compression settlement can exceed the amount of settlement caused by consolidation. The secondary compression index is determined from the void ratio ( $C_\alpha$ ) (strain ( $C_{\varepsilon\alpha}$ )) versus log time graph (see Figure 5-14) and is determined using the following equations:

$$C_\alpha = \frac{e_2 - e_1}{\log\left(\frac{t_2}{t_1}\right)} \quad \text{Equation 5-12}$$

$$C_{\varepsilon\alpha} = \frac{\varepsilon_2 - \varepsilon_1}{\log\left(\frac{t_2}{t_1}\right)} \quad \text{Equation 5-13}$$

Where:

$e_2$  = Void ratio at time 2

$e_1$  = Void ratio at time 1

$\varepsilon_2$  = Strain at time 2

$\varepsilon_1$  = Strain at time 1

$t_1$  and  $t_2$  = Time that occurs after the time to end primary consolidation, seconds

For highly organic materials (organic content greater than 50%), research sponsored by the Florida Department of Transportation has shown that the end of primary consolidation occurs quickly in the laboratory and field, and that a major portion of the total settlement is due to secondary compression (creep). As a result, differentiating between primary consolidation and secondary compression settlement can be very difficult and generate misleading results. To analyze results from 1-dimensional consolidation tests for these types of materials, use the Square Root (Taylor) Method to identify the end of primary consolidation for each load sequence. In addition, each load sequence must be maintained for at least 24 hours to identify a slope for the secondary consolidation portion of the settlement versus time plot.

#### **5.4.8 Organic Content**

Organic soils demonstrate very poor engineering characteristics, most notably low strength and high compressibility. In the field these soils can usually be identified by their dark color, musty odor and low unit weight. The most used laboratory test for quantification purposes is the Ignition Loss test, which measures how much of a sample's mass burns off when placed in a muffle furnace. The results are presented as a percentage of the total sample mass. Tests shall be performed in accordance with ASTM D2974 - *Standard Test Methods for Moisture, Ash, and Organic Matter of Peat and Other Organic Soils* (AASHTO T267 - *Standard Method of Test for Determination of Organic Content in Soils by Loss on Ignition*).

## **5.4.9 Shrinkage and Swell**

Certain soil types (highly plastic) have a large potential for volumetric change depending on the moisture content of the soil. These soils can shrink with decreasing moisture or swell with increasing moisture. Shrinkage can cause soil to pull away from structure thus reducing the bearing area or causing settlement of the structure beyond that predicted by settlement analysis. Swelling of the soil can cause an extra load to be applied to the structure that was not accounted for in design. Therefore, the potential for shrinkage and swelling should be determined for soils that have high plasticity.

### **5.4.9.1 Shrinkage**

These tests are performed to determine the limits of a soil's tendency to lose volume during decreases in moisture content. The shrinkage limit (SL) is presented as a percentage in moisture content, at which the volume of the soil mass ceases to change. See ASTM D4943 – *Standard Test Method for Shrinkage Factors of Soils by the Wax Method* (AASHTO T92 - *Standard Method of Test for Determining the Shrinkage Factors of Soils*).

### **5.4.9.2 Swell**

There are certain types of soils that can swell, particularly clay in the montmorillonite family. Swelling occurs when the moisture is allowed to increase causing the clay soil to increase in volume. There are a number of reasons for this to occur: the elastic rebound of the soil grains, the attraction of the clay mineral for water, the electrical repulsion of the clay particles and their adsorbed cations from one another, or the expansion of the air trapped in the soil voids. In the montmorillonite family, adsorption and repulsion predominate and this can cause swelling. Testing for swelling is difficult, but can be done. It is recommended that these soils not be used for roadway construction. The swell potential can be estimated from the test methods shown in AASHTO T258 - *Standard Method of Test for Determining Expansive Soils*.

## **5.4.10 Permeability**

Permeability, also known as hydraulic conductivity, has the same units as velocity and is generally expressed in ft/min or m/sec. The coefficient of permeability is dependent on void ratio, grain-size distribution, pore-size distribution, roughness of mineral particles, fluid viscosity, and degree of saturation. There are 3 standard laboratory test procedures for determining the coefficient of soil permeability, constant and falling head tests, and flexible wall test.

### **5.4.10.1 Constant Head Test**

In the constant head test, water is poured into a sample of soil, and the difference of head between the inlet and outlet remains constant during the testing. After the flow of water becomes constant, water that is collected in a flask is measured in quantity over a time period. This test is more suitable for coarse-grained soils that have a higher coefficient of permeability. See AASHTO T215 - *Standard Method of Test for Permeability of Granular Soils (Constant Head)*.

### **5.4.10.2 Falling Head Test**

The falling head test uses a similar procedure to the constant head test, but the head is not kept constant. The permeability is measured by the decrease in head over a specified time. This test is more appropriate for fine-grained soils. Tests shall be performed in accordance with ASTM D5856 - *Standard Test Method for Measurement of Hydraulic Conductivity of Porous Material Using a Rigid-Wall, Compaction-Mold Permeameter*.

### 5.4.10.3 Flexible Wall Permeability

For fine-grained soils, tests performed using a triaxial cell are generally preferred. In-situ conditions can be modeled by application of an appropriate confining pressure. The sample can be saturated using back pressuring techniques. Water is then allowed to flow through the sample and measurements are taken until steady-state conditions occur. Tests shall be performed in accordance with ASTM D5084 - *Standard Test Methods for Measurement of Hydraulic Conductivity of Saturated Porous Materials Using a Flexible Wall Permeameter*.

### 5.4.11 Compaction Tests

There are 2 types of tests that can be used to determine the optimum moisture content and maximum dry density of a soil (also termed the moisture-density relationship); the standard Proctor and the modified Proctor. The results of the tests are used to determine appropriate methods of field compaction and to provide a standard by which to judge the acceptability of field compaction.

The results of the compaction tests are typically plotted as dry density versus moisture content. Moisture content has a great influence on the degree of compaction achieved by a given type of soil. In addition to moisture content, there are other important factors that affect compaction. The soil type has a great influence because of its various classifications, such as grain-size distribution, shape of the soil grains, specific gravity of soil solids, and amount and type of clay mineral present. The compaction energy also has an effect because it too has various conditions, such as number of blows, number of layers, weight of hammer, and height of the drop.

#### 5.4.11.1 Standard Proctor

This test method uses a 5-1/2-pound rammer dropped from a height of 12 inches. The sample is compacted in 3 layers. See ASTM D698 - *Standard Test Methods for Laboratory Compaction Characteristics of Soil Using Standard Effort (12,400 ft-lbf/ft<sup>3</sup> (600 kN-m/m<sup>3</sup>))* (AASHTO T99 - *Standard Method of Test for Moisture-Density Relations of Soils Using a 2.5-kg (5.5-lb) Rammer and a 305-mm (12-in.) Drop*).

#### 5.4.11.2 Modified Proctor

This test method uses a 10-pound rammer dropped from a height of 18 inches. The sample is compacted in 5 layers. See ASTM D1557 - *Standard Test Methods for Laboratory Compaction Characteristics of Soil Using Modified Effort (56,000 ft-lbf/ft<sup>3</sup> (2,700 kN-m/m<sup>3</sup>))* (AASHTO T180 - *Standard Method of Test for Moisture-Density Relations of Soils Using a 4.54-kg (10-lb) Rammer and a 457-mm (18-in.) Drop*).

### 5.4.12 Relative Density Tests

The relative density tests are most commonly used for granular or unstructured soils. It is used to indicate the in-situ denseness or looseness of the granular soil. In comparison, Proctor tests often do not produce a well-defined moisture-density curve for cohesionless, free-draining soils. Therefore relative density is expressed in terms of maximum and minimum possible dry unit weights and can be used to measure compaction in the field.

#### 5.4.12.1 Maximum Index Density

In this test, soil is placed in a mold of known volume with a 2-psi surcharge load applied to it. The mold is then vertically vibrated at a specified frequency for a specified time. At the end of the vibrating period, the maximum index density can be calculated using the weight of the sand and the volume of the sand. See ASTM D4253 - *Standard Test Methods for Maximum Index Density and Unit Weight of Soils Using a Vibratory Table*.

#### 5.4.12.2 Minimum Index Density

The test procedure requires sand being loosely poured into a mold at a designated height. The minimum index density can be calculated using the weight of the sand required to fill the mold and the volume of the mold. See ASTM D4254 - *Standard Test Methods for Minimum Index Density and Unit Weight of Soils and Calculation of Relative Density*.

#### 5.4.13 Electro-Chemical Tests

Electro-chemical tests provide quantitative information related to the aggressiveness of the subsurface environment, the surface water environment, and the potential for deterioration of foundation materials. Electro-chemical testing includes pH, resistivity, sulfate, and chloride contents. The electro-chemical tests shall be performed on soil samples. In addition, surface water shall also be tested in coastal regions where the potential intrusion of brackish (higher salinity) water may occur in tidal streams. All water (surface or subsurface) samples shall be obtained in accordance with sampling and chain-of-custody procedures prepared by the South Carolina Department of Health and Environmental Control (SCDHEC). In lieu of using ASTM or AASHTO testing procedures, testing procedures established by the US Environmental Protection Agency (EPA) may be used, provided the laboratory conducting the tests is certified to perform the test by either the EPA or SCDHEC. If EPA testing standards are used, the GEC shall be required to indicate which EPA standard was used and to provide proof that the laboratory performing the test is certified by either the EPA or SCDHEC.

##### 5.4.13.1 pH Testing

pH testing is used to determine the acidity or alkalinity of the subsurface or surface water environments. Acidic or alkaline environments have the potential for being aggressive on structures placed within these environments. Soil samples collected during the normal course of a subsurface exploration should be used for pH testing. The pH of soils shall be determined ASTM G51 – *Standard Test Method for Measuring pH of Soil for Use in Corrosion Testing* (AASHTO T289 - *Standard Method of Test for Determining pH of Soil for Use in Corrosion Testing*). The surface water samples shall have the pH determined using ASTM D1293 – *Standard Test Methods for pH of Water*.

##### 5.4.13.2 Resistivity Testing

Resistivity testing is used to determine the electric conduction potential of the subsurface environment. The ability of soil to conduct electricity can have a significant impact on the corrosion of steel components. If a soil has a high potential for conducting electricity, then sacrificial anodes may be required on the structure or the metal will need to be galvanized. This type of testing can be performed in the laboratory or in the field. For the field testing procedure see Section 5.3.10.6. Field resistivity measurements shall be determined using ASTM G57 – *Standard Test Method for Field Measurement of Soil Resistivity Using the Wenner Four-Electrode Method*. Laboratory resistivity shall be determined using either ASTM G57 (laboratory procedure) or AASHTO T288 – *Standard Method of Test for Determining Minimum Laboratory Soil Resistivity*. It is noted that AASHTO T288 will produce 2 resistivities, the first at

100 percent saturation and the second when the soil is in a slurry condition. The resistivity of surface water samples can be determined using ASTM D1125 – *Standard Test Methods for Electrical Conductivity and Resistivity of Water*.

#### **5.4.13.3 Chloride Testing**

Subsurface soils and surface water should be tested for chloride if the presence of sea or brackish water is suspected or if a source of groundwater contamination is known. Chloride testing for soils shall be determined using AASHTO T291 – *Standard Method of Test for Determining Water-Soluble Chloride Ion Content in Soil*. The chloride testing for the surface water shall be performed in accordance with ASTM D512 – *Standard Test Methods for Chloride Ion in Water*.

#### **5.4.13.4 Sulfate Testing**

Subsurface soils and surface water should be tested for sulfate, especially if a source of groundwater contamination is known to exist in the general vicinity of the project. Sulfate testing for soils shall be determined using ASTM C1580 – *Standard Test Method for Water-Soluble Sulfate in Soil* (AASHTO T290 – *Standard Method of Test for Determining Water-Soluble Sulfate Ion Content in Soil*). The sulfate testing for the surface water shall be performed in accordance with ASTM D516 – *Standard Test Method for Sulfate Ion in Water*.

#### **5.4.14 Rock Cores**

Rock coring, as indicated in Chapter 6, should begin when drilling refusal is encountered. At each core run, the length of the rock sample obtained and the distance the core run is drilled will give a recovery ratio. The recovery ratio is expressed in percentage with 100% being intact rock and 50% or below as highly fractured rock. Further, the time required to drill specific rock core shall also be recorded and reported as required in Chapter 6. Another way to evaluate rock is rock quality designation (RQD) which is also expressed in percentage (See ASTM D6032 - *Standard Test Method for Determining Rock Quality Designation (RQD) of Rock Core*). The time rate and RQD allow the engineer to determine which core samples can/should be tested for compressive strength. In addition, all rock cores shall be N-size and shall have an approximate 2-inch diameter.

##### **5.4.14.1 Unconfined Compression Strength Test**

This test is performed on intact rock core specimens, usually with a rock sample length of at least 2 times the diameter. All core samples shall be prepared for testing using ASTM D4543 – *Standard Practices for Preparing Rock Core as Cylindrical Test Specimens and Verifying Conformance to Dimensional Shape and Tolerances*. Provide the information contained in the report section of the ASTM. The specimen is tested using unconfined compression or uniaxial compression. The test provides data used in determining the strength of the rock, namely the uniaxial strength ( $q_u$ ), shear strengths at varying pressures and varying temperatures, angle of internal friction, (angle of shearing resistance), and cohesion intercept. Unconfined compression strength testing shall be performed in accordance with ASTM D7012 - *Standard Test Methods for Compressive Strength and Elastic Moduli of Intact Rock Core Specimens under Varying States of Stress and Temperatures*. ASTM D7012 Methods C or D (unconfined compression) shall be used; however, Methods A or B (triaxial compression) may be used if required on a project.

## 5.5 QUALITY ASSURANCE/QUALITY CONTROL

The Quality Assurance/Quality Control (QA/QC) of the field and laboratory testing procedures/methods can have a significant impact on the results obtained from the testing. Therefore, all field and laboratory testing will require a QA/QC plan to be developed, maintained and implemented. The QA/QC plan shall follow the appropriate national, state or approved industrial standards.

### 5.5.1 Field Testing QA/QC Plan

All field testing shall be performed in accordance with an accepted QA/QC plan. The plan shall at a minimum establish the calibration schedule for the equipment, the method of calibration and provide circumstances when calibration is required differently from the regularly scheduled calibration. The QA/QC plan shall be submitted to and accepted by the PC/GDS, if requested, and shall comply with the general requirements of ASTM D3740 – *Standard Practice for Minimum Requirements for Agencies Engaged in Testing and/or Inspection of Soil and Rock as Used in Engineering Design and Construction*.

### 5.5.2 Laboratory Testing QA/QC Plan

All laboratories conducting geotechnical testing shall be AASHTO re:source (formerly AMRL) certified. The laboratories shall only conduct those tests for which that specific laboratory is certified. If the laboratory is not certified to conduct the test, the laboratory may contract to another laboratory that is certified. If no laboratory is certified, then a QA/QC plan for that particular test shall be developed and submitted to the PC/GDS for review and approval prior to testing. The QA/QC plan shall indicate which test method is being followed, the most recent calibration of the laboratory equipment to be used and the qualifications of the personnel performing the test. For tests where there is not an established ASTM, AASHTO or State testing standard, then the laboratory may use a testing method established by another Federal or State agency. The use of other agency standards shall be approved in writing by the PC/GDS prior to conducting the test. The laboratory requesting the use of another agency standard shall prove proficiency in the standard as well as submitting a QA/QC plan for the test method.

## 5.6 REFERENCES

ASTM International, (2012), Annual Book of ASTM Standards, Section 4 – Construction, Volume 04.08 – Soil and Rock (I): D420 – D5876.

ASTM International, (2012), Annual Book of ASTM Standards, Section 4 – Construction, Volume 04.09 – Soil and Rock (II): D5877 - Latest.

Becker, D. E., Crooks, J. H. A., Been, K., and Jeffries, M. G. (1987), “Work as a Criterion for Determining In Situ and Yield Stresses in Clays,” *Canadian Geotechnical Journal*, Vol. 24, No. 4.

Briaud, J.-L. and Miran, J., (1992), The Cone Penetrometer Test, (Publication No. FHWA-SA-91-043), US Department of Transportation, Office of Technology Applications, Federal Highway Administration, Washington, D.C.

Briaud, J.-L. and Miran, J., (1992), The Flat Dilatometer Test, (Publication No. FHWA-SA-91-044), US Department of Transportation, Office of Technology Applications, Federal Highway Administration, Washington, D.C.

Casagrande, A. (1936), "The Determination of Pre-Consolidation Load and Its Practical Significance," Proceedings of the First International Conference on Soil Mechanics, Harvard University, Cambridge, Massachusetts.

Das, M. Braja, (1994), Principles of Geotechnical Engineering, 3<sup>rd</sup> Edition, PWS Publishing Company, Boston MA.

Diehl, J. G., Martin, A. J., and Steller, R. A., (2006), "Twenty Year Retrospective on the Oyo P-S Suspension Logger" Proceedings of the 8<sup>th</sup> U.S. National Conference on Earthquake Engineering, San Francisco, California, USA.

Duncan, J. M. and Buchignani, A. L., (1976), *An Engineering Manual for Settlement Studies*, University of California at Berkeley, Berkeley, California.

GEOVision, (2014), *Sample Acoustic Televiewer*, provided via E-mail from J. G. Diehl, President, GEOVision, Inc.

Marchetti, S., Monaco, P., Totani, G., and Calabrese, M., (2001), "The Flat Dilatometer Test (DMT) in Soil Investigations" Proceedings In-Situ 2001, International Conference on In-Situ Measurement of Soil Properties, Bali, Indonesia.

Mayne, P. W., Christopher, B. R., and DeJong, J., (2002), Subsurface Investigations - Geotechnical Site Characterization, (Publication No. FHWA-NHI-01-031). US Department of Transportation, National Highway Institute, Federal Highway Administration, Washington, D.C.

Sabatini, P. J., Bachus, R. C., Mayne, P. W., Schneider, J. A., and Zettler, T. E. (2002), Evaluation of Soil and Rock Properties, Geotechnical Engineering Circular No. 5, (Publication No. FHWA-IF-02-034). US Department of Transportation, Office of Bridge Technology, Federal Highway Administration, Washington, D.C.

Sowers, George F., (1970), Introductory Soil Mechanics and Foundations: Geotechnical Engineering, 4<sup>th</sup> Edition, Macmillan Publishing Co., Inc., New York, NY.

Sowers, George F. and Hedges, Charles S, (1966) "Dynamic Cone for Shallow In-Situ Penetration Testing", Vane Shear and Cone Penetration Resistance Testing of In-Situ Soils, ASTM STP399.

Spangler, Merlin G., and Handy, Richard L., (1982), Soil Engineering, 4<sup>th</sup> Edition, Harper & Row, Publishers, New York, NY.

Terzaghi, K., Peck, R. B., and Mesri, G., (1996), Soil Mechanics In Engineering Practice, 3<sup>rd</sup> Edition, John Wiley & Sons, Inc., New York.

Wightman, W. E., Jalinoos, F., Sirles, P., and Hanna, K. (2003), Application of Geophysical Methods to Highway Related Problems, (Publication No. FHWA-IF-04-021). US Department of Transportation, Central Federal Lands Highway Division, Federal Highway Administration, Lakewood, Colorado.



**CHAPTER 6**

**MATERIAL DESCRIPTION,  
CLASSIFICATION, AND  
LOGGING**

**GEOTECHNICAL DESIGN MANUAL**

*January 2019*



**Table of Contents**

<b><u>Section</u></b>		<b><u>Page</u></b>
6.1	Introduction.....	6-1
6.2	Soil Description and Classification .....	6-2
6.2.1	Soil Test Borings.....	6-2
6.2.2	Cone Penetrometer Test.....	6-17
6.2.3	Dilatometer Test.....	6-20
6.3	Rock Description and Classification.....	6-21
6.3.1	Rock Type.....	6-23
6.3.2	Rock Color .....	6-23
6.3.3	Grain-size and Shape .....	6-23
6.3.4	Texture (stratification/foliation) .....	6-24
6.3.5	Mineral Composition .....	6-24
6.3.6	Weathering and Alteration.....	6-25
6.3.7	Strength .....	6-25
6.3.8	Rock Discontinuity.....	6-28
6.3.9	Rock Fracture Description.....	6-29
6.3.10	Other Pertinent Information .....	6-31
6.3.11	Geological Strength Index .....	6-31
6.3.12	Rock Mass Rating .....	6-33
6.4	Field and Laboratory Testing Records .....	6-34
6.4.1	Field Testing Records .....	6-34
6.4.2	Laboratory Testing Records .....	6-34
6.5	References .....	6-35

**List of Tables**

<b><u>Table</u></b>	<b><u>Page</u></b>
Table 6-1, SPT Relative Density / Consistency Terms .....	6-3
Table 6-2, Moisture Condition Terms .....	6-4
Table 6-3, Particle Angularity and Shape .....	6-4
Table 6-4, HCl Reaction .....	6-4
Table 6-5, Cementation .....	6-5
Table 6-6, Coarse-Grained Soil Constituents .....	6-6
Table 6-7, Adjectives For Describing Size Distribution .....	6-6
Table 6-8, Soil Plasticity Descriptions.....	6-8
Table 6-9, Letter Designations .....	6-8
Table 6-10, AASHTO Gradation Requirements.....	6-14
Table 6-11, AASHTO Plasticity Requirements.....	6-14
Table 6-12, CPT Soil Behavior Type .....	6-20
Table 6-13, CPT Relative Density / Consistency Terms .....	6-20
Table 6-14, DMT Material Index .....	6-21
Table 6-15, Rock Classifications .....	6-22
Table 6-16, Grain-size Terms.....	6-24
Table 6-17, Grain Shape Terms for Sedimentary Rocks .....	6-24
Table 6-18, Stratification/Foliation Thickness Terms .....	6-24
Table 6-19, Weathering/Alteration Terms .....	6-25
Table 6-20, Rock Strength Terms.....	6-25
Table 6-21, Rock Quality Description Terms .....	6-26
Table 6-22, Rock Hardness Terms.....	6-26
Table 6-23, Discontinuity Type .....	6-28
Table 6-24, Discontinuity Spacing .....	6-28
Table 6-25, Aperture Size Discontinuity Terms.....	6-28
Table 6-26, Discontinuity Width Terms.....	6-29
Table 6-27, Surface Shape of Joint Terms .....	6-29
Table 6-28, Surface Roughness Terms.....	6-29
Table 6-29, Filling Amount Terms.....	6-29
Table 6-30, Classification of Rock Masses .....	6-33
Table 6-31, Relative Rating Adjustment for Joint Orientations.....	6-34
Table 6-32, Rock Mass Class Determination.....	6-34

### List of Figures

<u>Figure</u>	<u>Page</u>
Figure 6-1, Moisture Content versus Volume Change .....	6-7
Figure 6-2, Plasticity Chart .....	6-7
Figure 6-3, Group Symbol and Group Name Coarse-Grained Soils (Gravel).....	6-9
Figure 6-4, Group Symbol and Group Name for Coarse-Grained Soils (Sand).....	6-10
Figure 6-5, Group Symbol and Group Name for Fine-Grained Soils ( $LL \geq 50$ ).....	6-11
Figure 6-6, Group Symbol and Group Name for Fine-Grained Soils ( $LL < 50$ ).....	6-12
Figure 6-7, Group Symbol and Group Name for Organic Soils .....	6-13
Figure 6-8, Range of LL and PI for Soils in Groups A-2 through A-7 .....	6-15
Figure 6-9, AASHTO Soil Classification System.....	6-16
Figure 6-10, Standard Electro-Piezocone.....	6-18
Figure 6-11, Normalized CPT Soil Behavior Chart Using $Q_T$ versus $F_R$ .....	6-19
Figure 6-12, RQD Determination.....	6-27
Figure 6-13, GSI Determination.....	6-32
Figure 6-14, SCDOT Soil Test Log Template .....	6-36
Figure 6-15, SCDOT Soil Test Log Descriptors – Soil .....	6-37
Figure 6-16, SCDOT Soil Test Log Descriptors – Rock .....	6-38
Figure 6-17, SCDOT Soil Test Log Descriptors – Rock (con't) .....	6-39
Figure 6-18, SCDOT Manual Auger Log Template .....	6-40
Figure 6-19, Soil Test Log Example .....	6-41
Figure 6-20, Soil Test Log Example (con't).....	6-42
Figure 6-21, Manual Auger Log Example .....	6-43
Figure 6-22, Field Vane Shear Testing Log Example .....	6-44
Figure 6-23, Undisturbed Sampling Log Example .....	6-45
Figure 6-24, Electro-Piezocone Sounding Record Example .....	6-46
Figure 6-25, Dilatometer Sounding Record Example.....	6-47
Figure 6-26, Shear and Compression Wave Velocity Profile vs. Depth .....	6-48
Figure 6-27, Shear and Compression Wave Velocity Profile Table.....	6-49
Figure 6-28, Summary of Laboratory Testing Results.....	6-50
Figure 6-29, Index Properties versus Depth .....	6-51
Figure 6-30, Moisture-Plasticity Relationship Testing Results .....	6-52
Figure 6-31, Grain-Size Analysis Results .....	6-53
Figure 6-32, Moisture-Density Relationship Testing Results.....	6-54
Figure 6-33, Shelby Tube Log Example .....	6-55
Figure 6-34, Shelby Tube Log Photograph Example .....	6-56
Figure 6-35, Shelby Tube Log Photograph Example .....	6-57
Figure 6-36, Consolidation Testing Results .....	6-58
Figure 6-37, Unconfined Compression Testing Results.....	6-59
Figure 6-38, Direct Shear Testing Results.....	6-60
Figure 6-39, Triaxial Shear Testing Results.....	6-61
Figure 6-40, p-q Plot - Triaxial Shear Testing .....	6-62
Figure 6-41, Rock Coring Summary .....	6-63
Figure 6-42, Rock Core Testing Results.....	6-64
Figure 6-43, Rock Core Testing Stress versus Strain Graph .....	6-65



# CHAPTER 6

## MATERIAL DESCRIPTION, CLASSIFICATION, AND LOGGING

### 6.1 INTRODUCTION

Geomaterials (soil and rock) are naturally occurring materials used in highway construction by SCDOT. Understanding soil and rock behavior is critical to the design and construction of any project. Soil and rock classification is an essential element of understanding the behavior of geomaterials. Field explorations in South Carolina encounter 3 types of geomaterials (i.e., soil, IGM and rock).

Soil and rock are either unconsolidated or consolidated solid particles, respectively, while IGM is a material with both soil and rock characteristics and properties. Soil is the result of the weathering of rock and may be transported to another location or may be left in-place. Consolidated soils typically have some degree of cementation while unconsolidated soils typically have no cementation. Rock is normally a durable, hard naturally occurring material. IGM is used only in the design of drilled shafts (see Chapter 16 for discussion on how IGM is applied to design). O'Neill, Townsend, Hassan, Buller and Chan (1996) defined IGM more specifically as:

- argillaceous geomaterials – heavily overconsolidated clays, clay shales, and saprolites that are prone to smearing when drilled
- calcareous rocks – limestone and limerock and argillaceous materials that are not prone to smearing when drilled
- very dense granular geomaterials – residual and completely decomposed rock with an SPT N-value between 50 and 100 blows per foot

The first 2 IGM types indicated above are considered Cohesive IGM, while the 3<sup>rd</sup> is considered Cohesionless IGM. The argillaceous IGMs composed of transported materials containing between 12 and 40 percent clay fraction (CF) while the saprolites are the result of in-situ chemical weathering of the parent rock material that contains between 12 and 40 percent CF. If design dictates that the type of IGM needs to be determined, then the percent CF shall be determined using ASTM D7928 (hydrometer analysis). The unconfined compressive strength,  $q_u$ , ranges from 5 tons per square foot (tsf) to 50 tsf; therefore, for a soil to be considered Cohesive IGM, both conditions (i.e., the CF and  $q_u$ ) must be met for the argillaceous geomaterials. For calcareous rocks only  $q_u$  must be met (i.e.,  $q_u$  ranges from 5 to 50 tsf) for the geomaterials to be considered cohesive IGM. The  $q_u$  shall be determined by laboratory shear strength testing on undisturbed samples. The use of field methods to determine shear strength shall be allowed only when approved in writing by the PC/GDS prior to the field testing. The Cohesionless IGM is treated as very dense sand in the design of drilled shafts (see Chapter 16).

As required in Chapter 4 and indicated in Chapter 5 soils are typically drilled using either hollow stem augers (HSA) or rotary wash (RW) methods (see Chapter 5 for drilling method to be used where). The problem in the field is when rock coring is required as opposed to drilling methods. Coring shall begin at drilling refusal. An SPT shall be performed at drilling refusal. Drilling refusal is defined as the inability to advance the auger in areas where HSA are allowed. In borings using RW methods, drilling refusal is defined as the inability to advance a roller cone (tricone) bit.

As indicated in Chapter 5, there are numerous field and laboratory testing procedures used by SCDOT to explore project sites. Included in this Chapter is a discussion of the presentation of only some of these methods, specifically soil test borings (including SPT and rock coring results), CPT and DMT test results. Also indicated in this Chapter is the manner in which to present the results of shear wave velocity testing. For convenience, the classification of soil will be discussed first for the soil borings, CPT and DMT with the classification of rock following. In addition, figures indicating the presentation of the field data are included.

Details of the subsurface conditions encountered, including basic material descriptions and details of the drilling and sampling methods shall be recorded. See ASTM D5434 - *Standard Guide for Field Logging of Subsurface Explorations of Soil and Rock*. During field exploration, specifically soil borings, a field log shall be kept of the materials encountered. In addition, the field log shall also include driller notes concerning the advancement of the test method (i.e., were hard layers encountered between SPT samples, etc.). The field personnel keeping the field logs shall have a minimum of 2 years of soil classification experience using ASTM D2488 – *Standard Practice for Description and Identification of Soils (Visual-Manual Procedure)*. The exception to this is for rock coring. All rock coring shall be observed and all rock cores shall be logged by either a registered engineer or registered geologist with a minimum of 4 years of rock coring observation and logging experience. Daily, copies of driller field logs shall be scanned and forwarded to the GEOR for review. The GEOR, at his/her discretion, may make changes to the field operations based on observations from the field logs.

Upon delivery of the samples to the laboratory, a registered engineer or registered geologist shall verify and modify as necessary the material descriptions and classifications based on the results of a more detailed visual-manual inspection of samples. Draft logs shall only be submitted to the PC/GDS after verification of the classifications in the laboratory. The PC/GDS shall use the draft logs to assign laboratory testing as required for those projects conducted by the PC/GDS. Classifications shall be further modified based on the results of the laboratory testing and final logs shall be prepared based on the revised classifications.

Material descriptions, classifications, and other information obtained during the subsurface explorations are heavily relied upon throughout the remainder of the investigation program and during the design and construction phases of a project. It is therefore necessary that the method of reporting this data be standardized. Records of subsurface explorations should follow as closely as possible the standardized format presented in this Chapter.

This Chapter is divided into 2 primary sections, the first is associated with the description and classification of soil and the second section will discuss the description and classification of rock. The soil description and classification section will discuss the 2 soil classification systems used by SCDOT (i.e., the USCS and AASHTO).

## **6.2 SOIL DESCRIPTION AND CLASSIFICATION**

### **6.2.1 Soil Test Borings**

A detailed description for each material stratum encountered should be included on the Soil Test Log (see Figures 6-14, 6-19 and 6-20) and on the Manual Auger Log (see Figures 6-18 and 6-21). The extent of detail will be somewhat dependent upon the material itself and on the purpose of the project. However, the descriptions should be sufficiently detailed to provide the GEOR with an understanding of the material present at the site. The descriptions should be



sufficiently detailed to permit grouping of similar materials and aid in the selection of representative samples for testing.

Soils should be described with regard to soil type, color, relative density/consistency, etc. The description shall match the requirements of the Unified Soil Classification System (USCS) and the AASHTO soil classification system. A detailed soil description shall include the following items and shall match the descriptive terms discussed in the following sections, in order:

1. Relative Density/Consistency
2. Moisture Condition
3. Soil Color
4. Particle Angularity and Shape (for coarse-grained soils)
5. Hydrochloric (HCl) Reaction
6. Cementation
7. Gradation
  - a. Coarse-Grained Soils
  - b. Fine-Grained Soils
8. Unified Soil Classification System (USCS)
9. AASHTO Soil Classification System (AASHTO)
10. Other pertinent information

### 6.2.1.1 Relative Density/Consistency

Relative density refers to the degree of compactness of a coarse-grained soil. Consistency refers to the stiffness of a fine-grained soil. When evaluating subsurface soil conditions using correlations based on SPT N-values, the N-values shall be corrected (see Chapter 7 for correction). However, only actual field recorded (uncorrected) SPT N-values ( $N_{meas}$ ) shall be included on the Soil Test Boring Log and shall be used to determine the relative density and/or consistency.

Standard Penetration Test N-values (blows per foot) are usually used to define the relative density and consistency as follows:

**Table 6-1, SPT Relative Density / Consistency Terms**

Relative Density <sup>1,2</sup>			Consistency <sup>1,3</sup>		
Descriptive Term	Relative Density	SPT Blow Count (bpf) <sup>4</sup>	Descriptive Term	Unconfined Compression Strength ( $q_u$ ) (tsf)	SPT Blow Count (bpf) <sup>4</sup>
Very Loose	0 to 15%	≤ 4	Very Soft	≤0.25	≤2
Loose	16 to 35%	5 to 10	Soft	0.26 to 0.50	3 to 4
Medium Dense	36 to 65%	11 to 30	Firm	0.51 to 1.00	5 to 8
Dense	66 to 85%	31 to 50	Stiff	1.01 to 2.00	9 to 15
Very Dense	86 to 100%	≥51	Very Stiff	2.01 to 4.00	16 to 30
			Hard	≥4.01	≥ 31
<sup>1</sup> For Classification only, not for design					
<sup>2</sup> Applies to coarse-grained soils (major portion retained on No. 200 sieve)					
<sup>3</sup> Applies to fine-grained soils (major portion passing No. 200 sieve)					
<sup>4</sup> bpf – blows per foot of penetration at 60 percent ER (see Chapter 7 for ER determination)					

### 6.2.1.2 Moisture Condition

The in-situ moisture condition shall be determined using the visual-manual procedure. The term “saturated” shall not be used, unless the degree of saturation is actually determined. The moisture condition is defined using the following terms:

**Table 6-2, Moisture Condition Terms**

<b>Descriptive Term</b>	<b>Criteria</b>
Dry	Absence of moisture, dusty, dry to the touch
Moist	Damp but no visible water
Wet	Visible free water, usually in coarse-grained soils below the water table

### 6.2.1.3 Soil Color

The color of the soil shall be determined using the Munsell color chart and shall be described while the soil is still at or near the in-situ moisture condition. The Munsell color designation shall be provided at the end of the soils description.

### 6.2.1.4 Particle Angularity and Shape

Coarse-grained soils are described as angular, subangular, subrounded, or rounded. Gravel and cobbles can be described as flat, elongated, or flat and elongated. Descriptions of fine-grained soils will not include a particle angularity or shape.

**Table 6-3, Particle Angularity and Shape**

<b>Descriptive Term</b>	<b>Criteria</b>
Angular	Particles have sharp edges and relatively plane sides with unpolished surfaces
Subangular	Particles are similar to angular description but have rounded edges
Subrounded	Particles have nearly plane sides but have well-rounded corners and edges
Rounded	Particles have smoothly curved sides and no edges
Flat	Particles with a width to thickness ratio greater than 3
Elongated	Particles with a length to width ratio greater than 3
Flat and Elongated	Particles meeting the criteria for both Flat and Elongated

### 6.2.1.5 HCl Reaction

The terms presented below describe the reaction of soil with HCl (hydrochloric acid). Since calcium carbonate is a common cementing agent, a report of its presence on the basis of the reaction with dilute hydrochloric acid is important.

**Table 6-4, HCl Reaction**

<b>Descriptive Term</b>	<b>Criteria</b>
None	No visible reaction
Weakly	Some reaction, with bubbles forming slowly
Strongly	Violent reaction, with bubbles forming immediately

### 6.2.1.6 Cementation

The terms presented below describe the cementation of intact coarse-grained soils.

**Table 6-5, Cementation**

Descriptive Term	Criteria
Weakly Cemented	Crumbles or breaks with handling or little finger pressure
Moderately Cemented	Crumbles or breaks with considerable finger pressure
Strongly Cemented	Will not crumble or break with finger pressure

### 6.2.1.7 Gradation

The classification of soil is divided into 2 general categories based on gradation, coarse-grained and fine-grained soils. Coarse-grained soils (gravels and sands) have more than or equal to 50 percent (by weight) of the material retained on the No. 200 sieve, while fine-grained soils (silts and clays) have more than 50 percent of the material passing the No. 200 sieve. Gravels and sands are typically described in relation to the particle size of the grains. Silts and clays are typically described in relation to plasticity. The primary constituents are identified considering grain-size distribution. In addition to the primary constituent, other constituents which may affect the engineering properties of the soil should be identified. Secondary constituents are generally indicated as modifiers to the principal constituent (e.g., sandy clay or silty gravel, etc.). Other constituents can be included in the description using the terminology of ASTM D2488 through the use of terms such as trace (<5%), few (5-10%), little (15-25%), some (30-45%), and mostly (50-100%).

#### 6.2.1.7.1 Coarse-Grained Soils

Coarse-grained soils are those soils with more than or equal to 50 percent by weight retained on or above the No. 200 sieve. Coarse-grained soils divided into 2 categories, well- and poorly-graded with the difference between well- and poorly-graded depending upon the Coefficient of Curvature ( $C_c$ ) and the Coefficient of Uniformity ( $C_u$ ). Coarse-grained soils with a  $C_c$  between 1 and 3 ( $1 \leq C_c \leq 3$ ) and a  $C_u$  greater than or equal to 4 ( $C_u \geq 4$ ) are considered to be well-graded.  $C_c$  and  $C_u$  are determined using the following equations.

$$C_c = \frac{(D_{30})^2}{[(D_{10})(D_{60})]} \quad \text{Equation 6-1}$$

$$C_u = \frac{(D_{60})}{(D_{10})} \quad \text{Equation 6-2}$$

Where,

$D_{10}$  = Diameter of particle at 10% finer material, millimeters (mm)

$D_{30}$  = Diameter of particle at 30% finer material, mm

$D_{50}$  = Diameter of particle at 50% finer material, mm

$D_{60}$  = Diameter of particle at 60% finer material, mm

$D_{85}$  = Diameter of particle at 85% finer material, mm

% Fines = Percent passing the No. 200 Sieve

The  $D_{50}$  is the mean grain size and is used in scour analysis and is provided to the HEOR. The  $D_{10}$  is also termed the effective size of the soil. The  $D_{85}$  is used in the design of geosynthetic

filtration requirements. The percent pass the No. 200 sieve is termed the fines content. The  $D_{10}$ ,  $D_{30}$ ,  $D_{50}$ ,  $D_{60}$ ,  $D_{85}$  and percent fines shall be graphically determined.

The particle size for gravels and sands are provided in Table 6-6 and the adjectives used for describing the possible combinations of particle size are provided in Table 6-7.

**Table 6-6, Coarse-Grained Soil Constituents**

Soil Component	Grain-size
<b>Gravel</b>	
Coarse	3" to $\frac{3}{4}$ "
Fine	$\frac{3}{4}$ " to No. 4 sieve
<b>Sand</b>	
Coarse (c)	No. 4 to No. 10 sieve
Medium (m)	No. 10 to No. 40 sieve
Fine (f)	No. 40 to No. 200 sieve

**Table 6-7, Adjectives For Describing Size Distribution**

Particle-Size Adjective	Abbreviation	Size Requirements
Coarse	c	< 30% m/f Sand or < 12% f Gravel
Coarse to medium	c/m	< 12% f Sand
Medium to fine	m/f	< 12% c Sand and > 30% m Sand
Fine	f	< 30% m Sand or < 12% c Gravel
Coarse to fine	c/f	> 12% of each size

#### 6.2.1.7.2 Fine-Grained Soils

Fine-grained soils are those soils with more than 50 percent passing the No. 200 sieve. Silt size particles range from the No. 200 Sieve (0.074 mm) to 0.002 mm ( $0.002 \leq D \leq 0.074$ ). Clays have particle sizes less than 0.002 mm. These materials are defined using moisture-plasticity relationships that were developed in the early 1900's by the Swedish soil scientist A. Atterberg. Atterberg developed 5 moisture-plasticity relationships, of which 3 are used in engineering practice and are known as the Atterberg Limits. These limits are the shrinkage limit (SL), the plastic limit (PL) and the liquid limit (LL). The SL is defined as the moisture content at which there is no additional volume change in soil sample with further reduction in moisture content and is the moisture content when a soil behaves as a solid. The PL is defined as the moisture content at which a 1/8-inch diameter thread can be rolled out and at which the thread just begins to crumble and is the moisture content when soil begins behaving plastically. The LL is the moisture content at which a soil will flow when dropped a specified distance and a specified number of times and is the moisture content when a soil begins behave as liquid material and begins to flow. In addition, the plasticity index (PI) is the range between the liquid limit and the plastic limit (LL-PL). Figure 6-1 provides a chart indicating the relationship between increasing moisture content (X-axis) and increasing volume (Y-axis). The Plasticity Chart, Figure 6-2, is used to determine low and high plasticity and whether a soil will be Silt or Clay. If the results of the LL and PI plot above or to the left of the "U" Line, the testing procedure and results should be checked. Table 6-8 provides the adjectives used to describe plasticity and the applicable plasticity range.

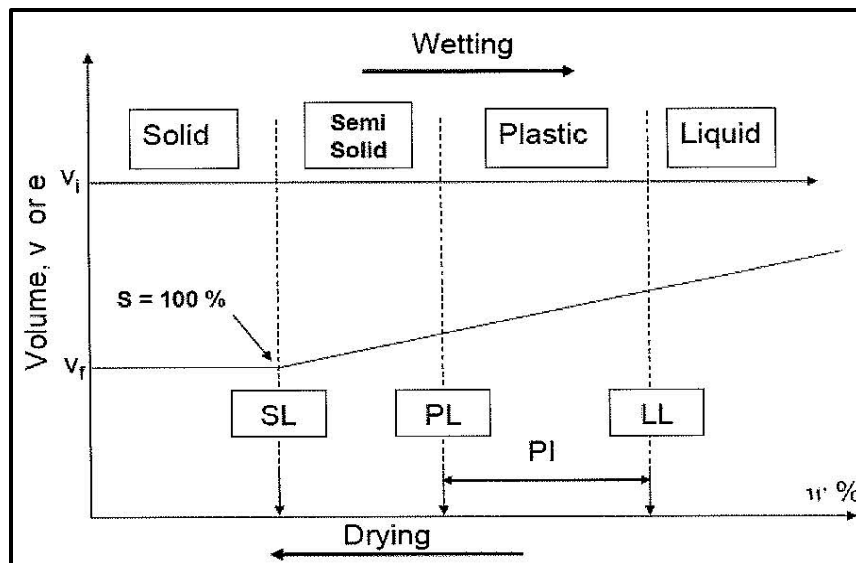


Figure 6-1, Moisture Content versus Volume Change

Because of the extremely hazardous nature of determining the SL (i.e., mercury is used), SL testing will typically not be performed. If SL testing is required, contact the PC/GDS for concurrence on the proposed testing method and provide an explanation as to how the results of the testing will be used or benefit the project.

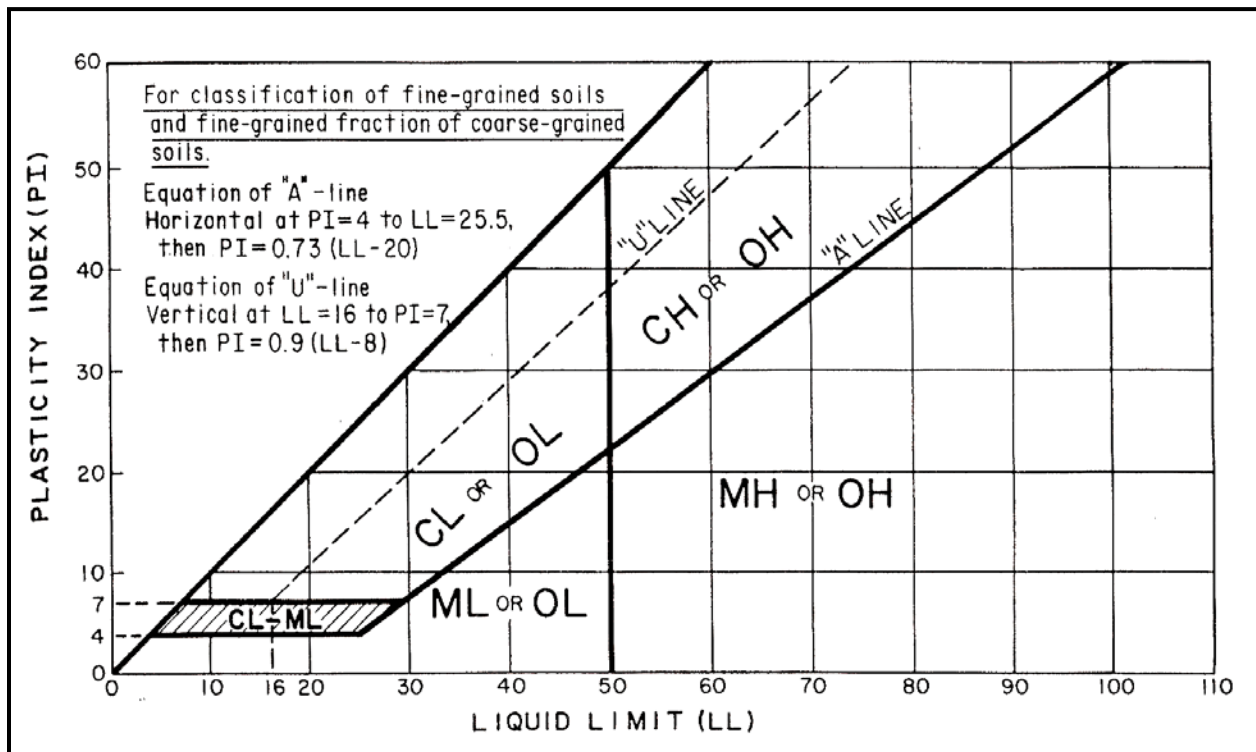


Figure 6-2, Plasticity Chart

**Table 6-8, Soil Plasticity Descriptions**

PI Range	Adjective	Dry Strength
0	non-plastic	none – crumbles into powder with mere pressure
1 – 10	low plasticity	low – crumbles into powder with some finger pressure
11 – 20	medium plasticity	medium – breaks into pieces or crumbles with considerable finger pressure
21 – 40	high plasticity	high – cannot be broken with finger pressure
> 41	very plastic	very high – cannot be broken between thumb and a hard surface

### 6.2.1.8 Unified Soil Classification System (USCS)

Dr. A. Casagrande developed the USCS for the classification of soils used to support Army Air Corps bomber bases. This system incorporates textural (grain-size) characteristics into the engineering classification. The system has 15 different potential soil classifications with each classification having a 2-letter designation. The basic letter designations are listed in Table 6-9.

**Table 6-9, Letter Designations**

Letter Designation	Meaning	Letter Designation	Meaning
G	Gravel	O	Organic
S	Sand	W	Well-graded
M	Non-plastic or low plasticity fines (Silt)	P	Poorly-graded
C	Plastic fines (Clay)	L	Low liquid limit
Pt	Peat	H	High liquid limit

The classification of soil is divided into 2 general categories, coarse-grained and fine-grained soils. Coarse-grained soils (gravels and sands) have more than or equal to 50 percent (by weight) of the material retained on the No. 200 sieve, while fine-grained soils (silts and clays) have more than 50 percent of the material passing the No. 200 sieve. Gravels and sands are typically described in relation to the particle size of the grains (See Section 6.2.1.7.1). Silts and clays are typically described in relation to plasticity (see Section 6.2.1.7.2).

In many soils, 2 or more soil types are present. When the percentage of the minor soil type is equal to or greater than 30 percent and less than 50 percent of the total sample (by weight), the minor soil type is indicated by adding a “y” to its name; i.e., Sandy SILT, Silty SAND, Silty CLAY, etc.

Figures 6-3, 6-4, 6-5, 6-6, and 6-7 provide the flow charts for the classification of coarse- and fine-grained soils using the USCS. See ASTM D2487 – *Standard Practice for Classification of Soils for Engineering Purposes (Unified Soil Classification System)*.

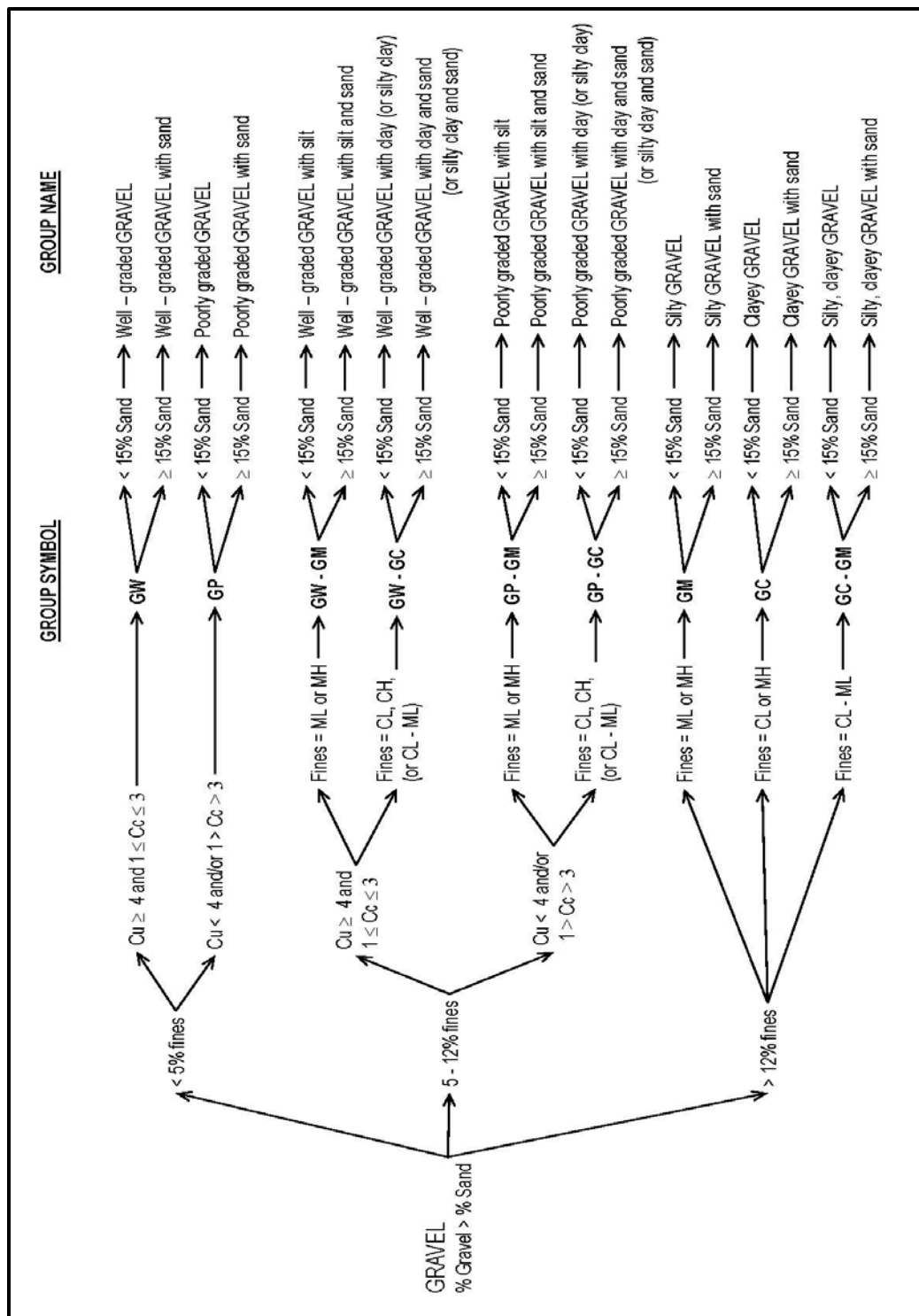
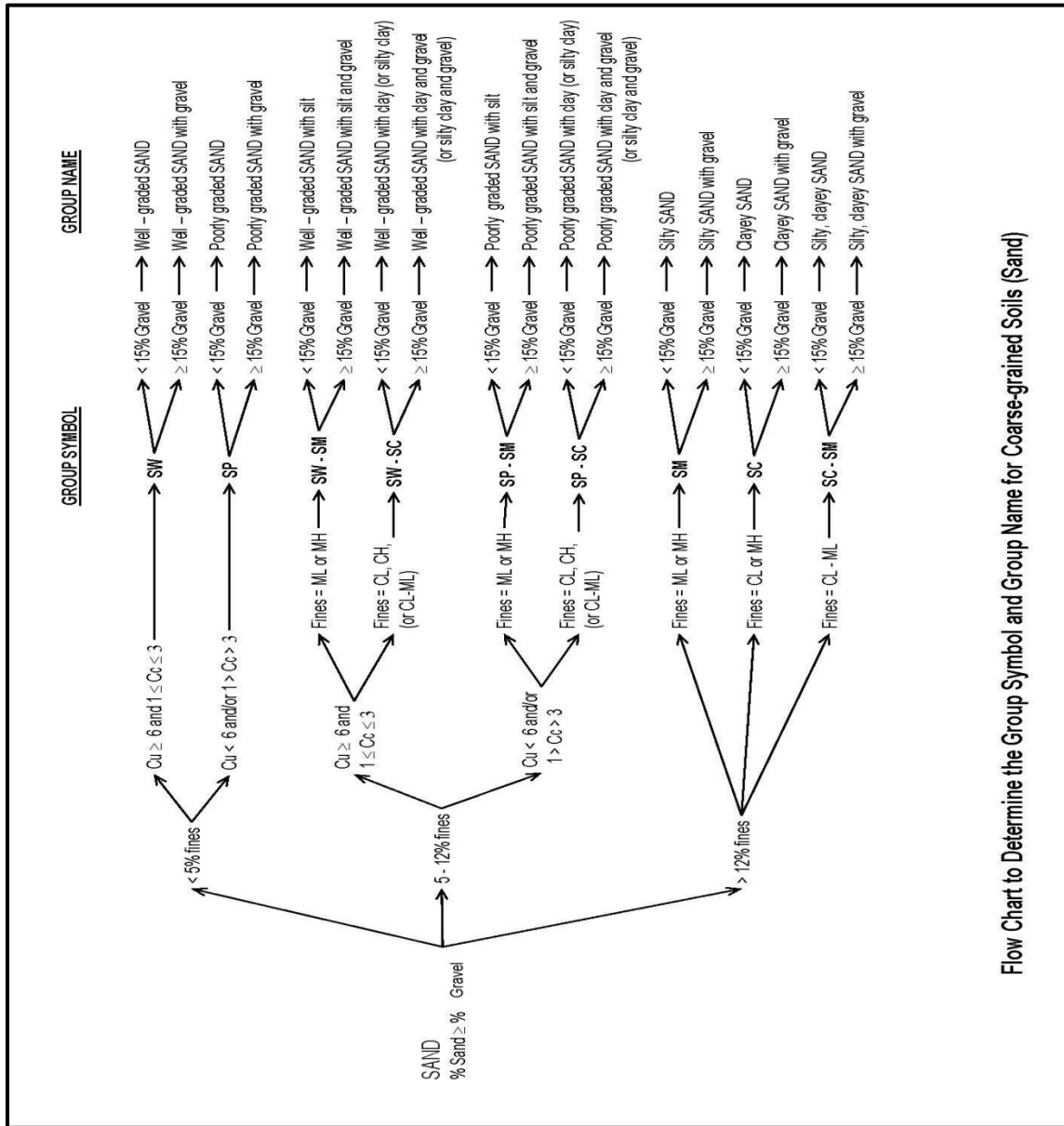


Figure 6-3, Group Symbol and Group Name Coarse-Grained Soils (Gravel) (Mayne, Christopher and DeJong (2002))



Flow Chart to Determine the Group Symbol and Group Name for Coarse-grained Soils (Sand)

Figure 6-4, Group Symbol and Group Name for Coarse-Grained Soils (Sand) (modified Mayne, et al. (2002))



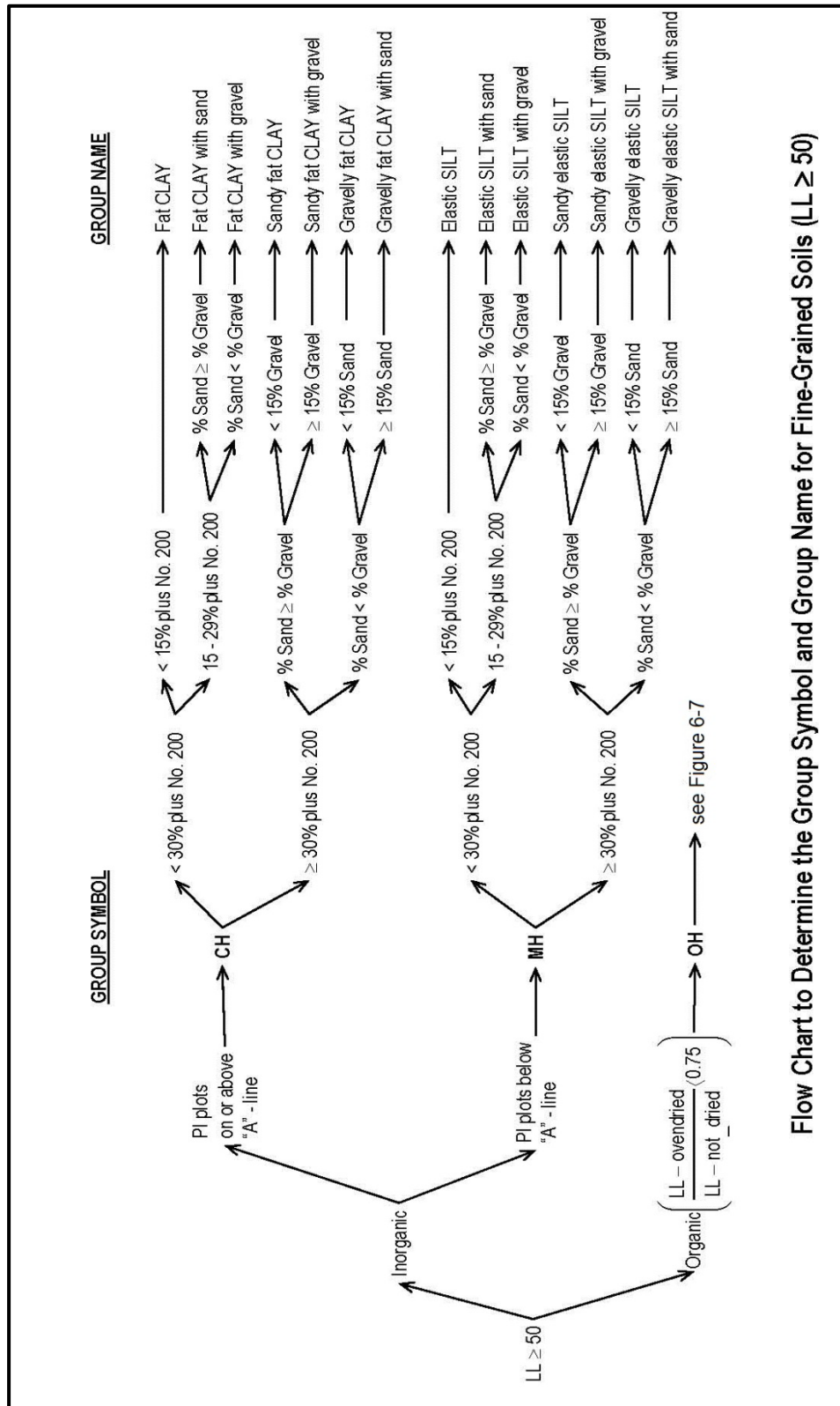


Figure 6-5, Group Symbol and Group Name for Fine-Grained Soils (LL ≥ 50) (Mayne, et al. (2002))

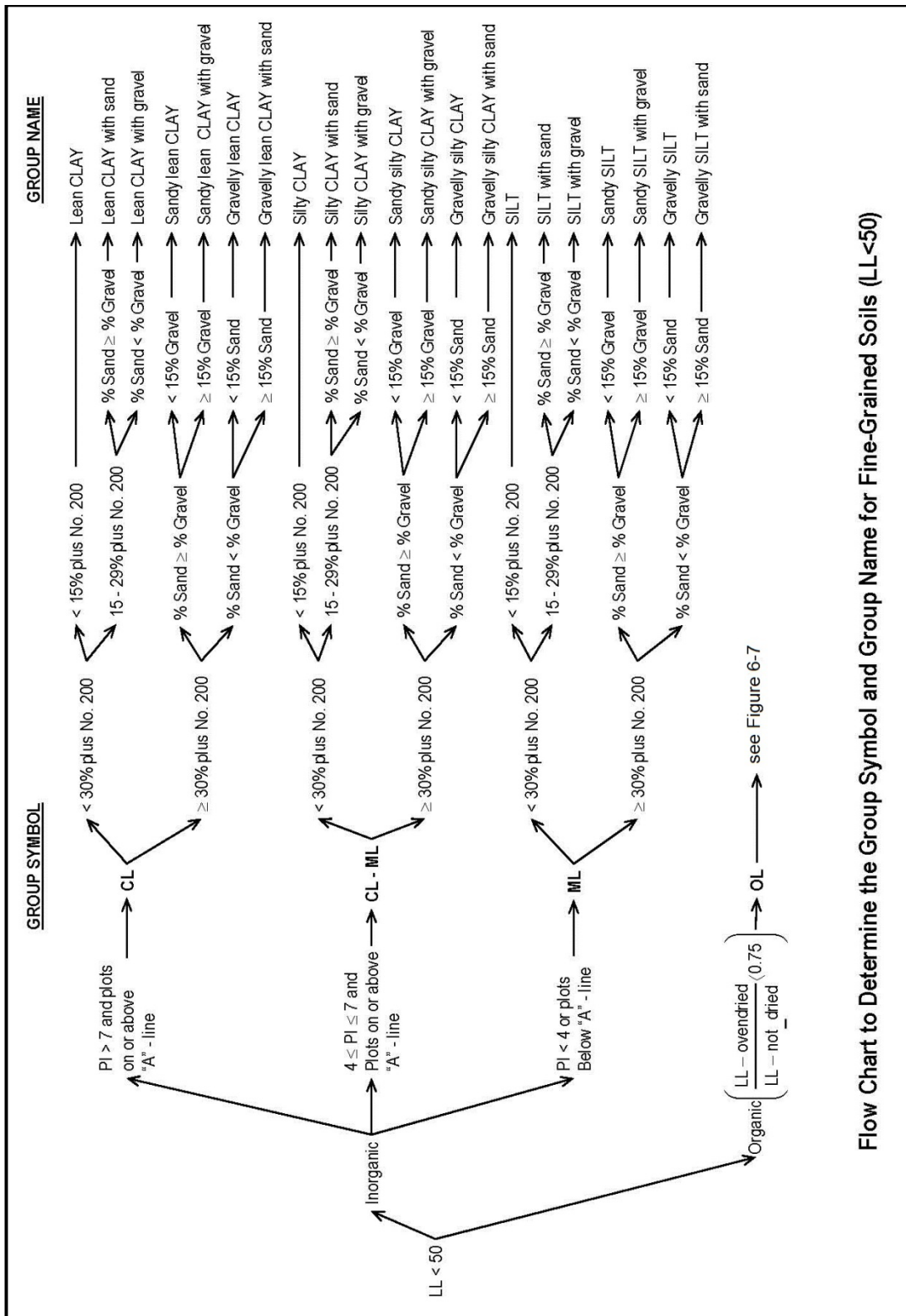


Figure 6-6, Group Symbol and Group Name for Fine-Grained Soils (LL < 50) (Mayne, et al. (2002))

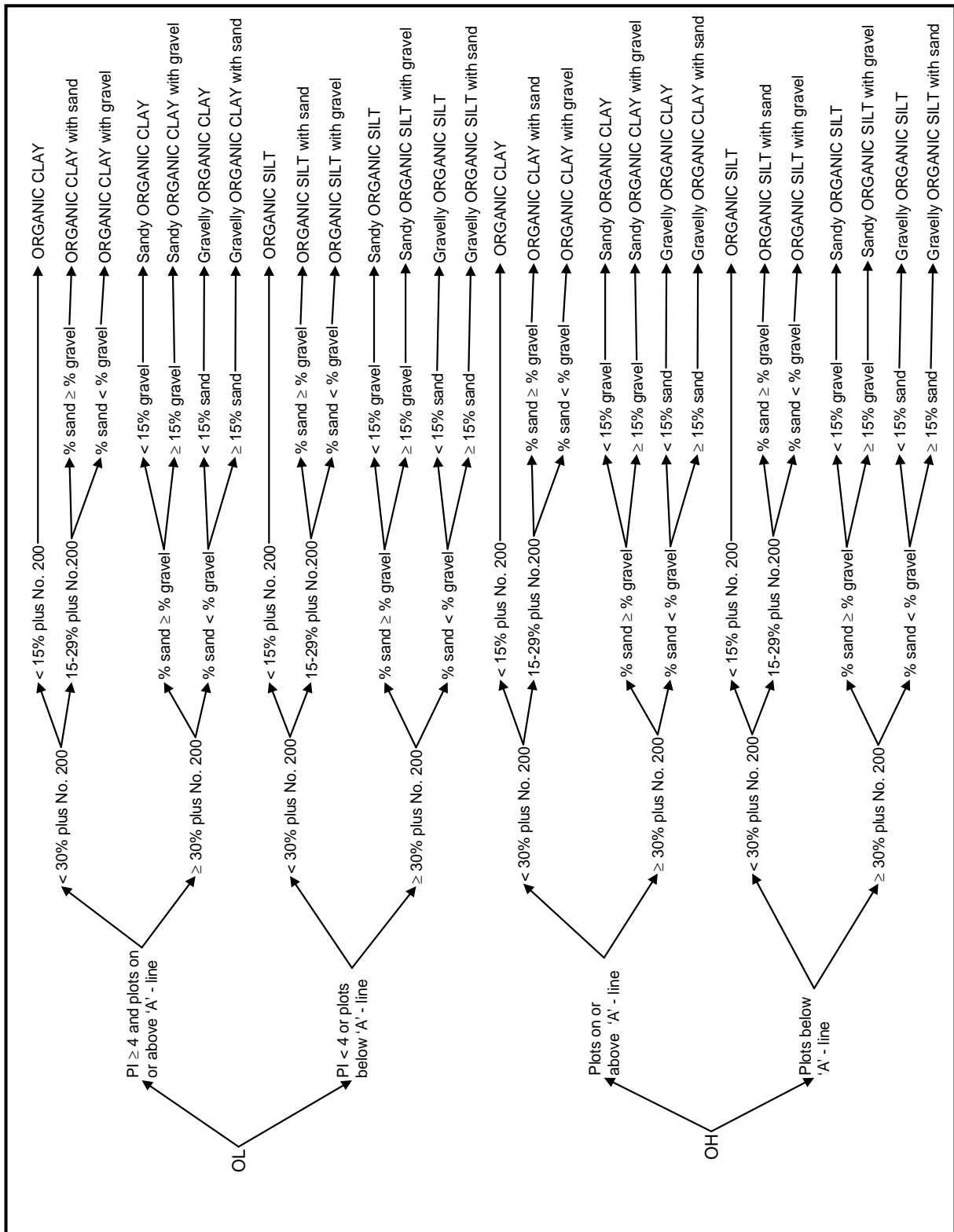


Figure 6-7, Group Symbol and Group Name for Organic Soils (Mayne, et al. (2002))

### 6.2.1.9 AASHTO Soil Classification System (AASHTO)

Terzaghi and Hogentogler originally developed this classification system for the U.S. Bureau of Public Roads in the late 1920s. This classification system divides all soils into 8 major groups designated A-1 through A-8 (see Figures 6-8 and 6-9). In this classification system, the lower the number the better the soil is for subgrade materials. Coarse-grained soils are defined by groups A-1 through A-3, while groups A-4 through A-7 define the fine-grained soils. Group A-4 and A-5 are predominantly silty soils and group A-6 and A-7 are predominantly clayey soils. Group A-8 refers to peat and muck soils.

Groups A-1 through A-3 have 35 percent or less passing the No. 200 sieve, while groups A-4 through A-7 have more than 35 percent passing the No. 200 sieve. The classification system is presented in Figure 6-9. Table 6-10 indicates the gradation requirements used in the AASHTO classification system.

**Table 6-10, AASHTO Gradation Requirements**

Soil Component	Grain-size
Gravel	between 3" to No. 10
Sand	between No. 12 to No. 200
Silt and Clay	less than No. 200

For soils in Groups A-2, A-4, A-5, A-6 and A-7 the plasticity of the fines is defined in Table 6-11.

**Table 6-11, AASHTO Plasticity Requirements**

Soil Component	Plasticity Index
Silty	≤ 10%
Clayey	≥ 11%

To evaluate the quality of a soil as a highway subgrade material, a number called the Group Index (GI) is incorporated with the groups and subgroups of the soil. The GI is written in parenthesis after the group or subgroup designation and is determined by the following equation:

$$GI = (F - 35)[0.2 + 0.005(LL - 40)] + 0.01(F - 15)(PI - 10) \quad \text{Equation 6-3}$$

Where:

F = percent passing No. 200 sieve (in percent)

LL = Liquid Limit

PI = Plasticity Index

Listed below are some rules for determining the GI:

- If the equation yields a negative value for the GI, use zero;
- Round the GI to the nearest whole number, using proper rules of rounding;
- For the upper limit of GI see Figure 6-9;
- Groups A-1-a, A-1-b, A-2-4, A-2-5, and A-3, will always have a GI of zero;
- The GI for groups A-2-6 and A-2-7 is calculated using the following equation:

$$GI = 0.01(F - 15)(PI - 10) \quad \text{Equation 6-4}$$

Figure 6-7 provides the range of liquid limit and plasticity index for group A-2 to A-7 soils.

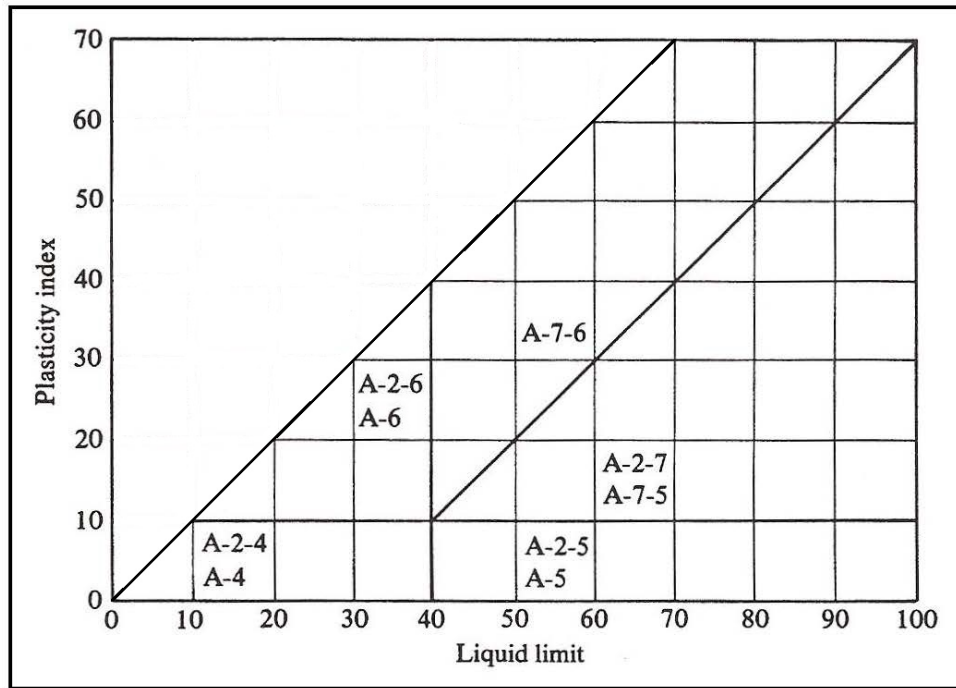


**Figure 6-8, Range of LL and PI for Soils in Groups A-2 through A-7 (modified from Mayne, et al. (2002))**

GENERAL CLASSIFICATION	GRANULAR MATERIALS (35 percent or less of total sample passing No. 200)				SILT-CLAY MATERIALS (More than 35 percent of total sample passing No. 200)						
	A-1		A-3	A-2		A-4	A-5	A-6	A-7		
GROUP CLASSIFICATION	A-1-a	A-1-b	A-3	A-2-4	A-2-5	A-2-6	A-2-7	A-4	A-5	A-6	A-7
Sieve analysis, percent passing:											
2 mm (No. 10)	50 max.										
0.425 mm (No. 40)	30 max.	50 max.									
0.075 mm (No. 200)	15 max.	25 max.	51 min. 10 max.	35 max.	35 max.	35 max.	35 max.	36 min.	36 min.	36 min.	36 min.
Characteristics of fraction passing 0.425 mm (No. 40)											
Liquid limit											
Plasticity index	6 max.		NP					40 max. 10 max.	41 min. 10 max.	40 max. 10 max.	41 min. 11 min. 11 min.*
Usual significant constituent materials	Stone fragments, gravel and sand		Fine sand	Silty or clayey gravel and sand				Silty soils		Clayey soils	
Group Index**	0	0	0	0	0	4 max.		8 max.	12 max.	16 max.	20 max.

Classification procedure: With required test data available, proceed from left to right on chart; correct group will be found by process of elimination. The first group from left into which the test data will fit is the correct classification.

\*Plasticity Index of A-7-5 subgroup is equal to or less than LL minus 30. Plasticity Index of A-7-6 subgroup is greater than LL minus 30 (see Fig 4-9).

\*\*See group index formula (Eq. 4-1) Group index should be shown in parentheses after group symbol as: A-2-6(3), A-4(5), A-6(12), A-7-5(17), etc.

Figure 6-9, AASHTO Soil Classification System (Mayne, et al. (2002))

### 6.2.1.10 Soil Electro-Chemical Classifications

Electro-chemical testing is required for soil and water samples collected from project sites, so that appropriate materials may be used on the project site. Electro-chemical testing is performed in accordance with the requirements contained in Chapter 5 and consists of pH, resistivity, sulfate and chloride contents. Soils are considered aggressive if the pH is less than 4.5; more than 8.0; or the resistivity is less than 1,000 ohms per centimeter (ohms/cm). Non-aggressive soils have a pH greater than or equal to 4.5 or a resistivity greater than or equal to 5,000 ohms/cm. Soils with resistivity between 1,000 and 5,000 ohms/cm shall have sulfate and chloride ion content checked. Soils with chloride ion contents greater than 100 parts per million (ppm) or sulfate ion contents greater than 200 ppm shall be considered aggressive. In addition, to the electro-chemical tests, the location of the ground water table should also be noted. Fluctuations in the ground water table may lead to aggressive soil environments by allowing increased oxygen content around the foundation. The results of all electro-chemical testing shall be reported to the SEOR and project team for their consideration in the design of the structure.

### 6.2.1.11 Other Pertinent Information

Additional information that adds to the description of the soil may be included. This information should enhance the soil description. This may include the geologic formation to which the soil belongs. The determination and designation of geologic formations is the responsibility of the GEOR and not the GEC providing the field and laboratory services. The depth to ground water at both the time of boring and approximately 24 hours after drilling are required to be indicated on the Soil Test Boring Log. In some cases the borehole collapses prior to obtaining the ground water reading. The depth of caving shall be indicated on the Soil Test Boring Log. For Sand-Like soils the caved depth may be interpreted as the depth of ground water. In Clay-Like soils the depth to ground water may be interpreted as possibly within 3 or 4 feet above or below the caved depth.

## 6.2.2 Cone Penetrometer Test

The Cone Penetrometer Test shall be conducted in accordance with Chapter 5. The penetrometer data is plotted showing the tip stress ( $q_t$  – corrected), the friction resistance ( $f_s$  – measured), the friction ratio ( $R_f$ ) and the pore pressures vs. depth (see Figure 6-24). Typically, the cone penetrometers used in South Carolina have a porous element located just behind the cone tip (shoulder) as depicted in Figure 6-10. Prior to using a cone penetrometer with a different porous element location, approval shall be obtained from the PC/GDS. In addition, to the plotted penetrometer data, the GEC shall provide to the PC/GDS an electronic file in Excel<sup>®</sup> format providing the following data in the order shown:

1. Depth, feet
2.  $q_c$  – Uncorrected/measured tip resistance, tons per square foot (tsf)
3.  $f_s$  – Measured friction resistance, tsf
4.  $u_2$  – Pore pressure behind tip, tsf
5.  $u_0$  – Hydrostatic pore pressure, tsf
6.  $q_t$  – Corrected tip resistance (see Equation 6-5), tsf
7.  $R_f$  – Friction ratio (see Equation 6-6), percent
8.  $\sigma_{vo}$  – Total overburden stress, tsf
9.  $\sigma'_{vo}$  – Effective overburden stress, tsf
10.  $B_q$  – Pore pressure parameter, dimensionless (see Equation 7-15)

11.  $Q_T$  – Normalized tip resistance, dimensionless (see Equation 7-13)
12.  $F_R$  – Normalized sleeve resistance, dimensionless (see Equation 7-14)
13.  $I_c$  – Soil behavior type, dimensionless (see Equation 7-17)
14. Zone # corresponding to  $I_c$ , dimensionless (see Figure 6-11 and Table 6-12)
15.  $N_{60}$  – Estimated N-value at 60 percent energy, bpf (see Equation 7-21)
16.  $N_k$  – Cone factor as known as  $N_{kt}$ , dimensionless
17.  $(S_u)_{cpt}$  – Undrained shear strength, pounds per square foot (psf) (see Equation 7-33)
18.  $\phi'$  – Effective friction angle, degree (see Equation 7-46)
19.  $S_t$  – Sensitivity, dimensionless (see Equation 7-40)
20.  $V_s$  – Shear wave velocity, feet per second (fps) (if measured)

Further the GEC shall indicate the equations used for all normalized parameters and correlations and how  $u_0$ ,  $\sigma_{vo}$  and  $\sigma'_{vo}$  were determined. The correlations shall conform to the requirements of Chapter 7.

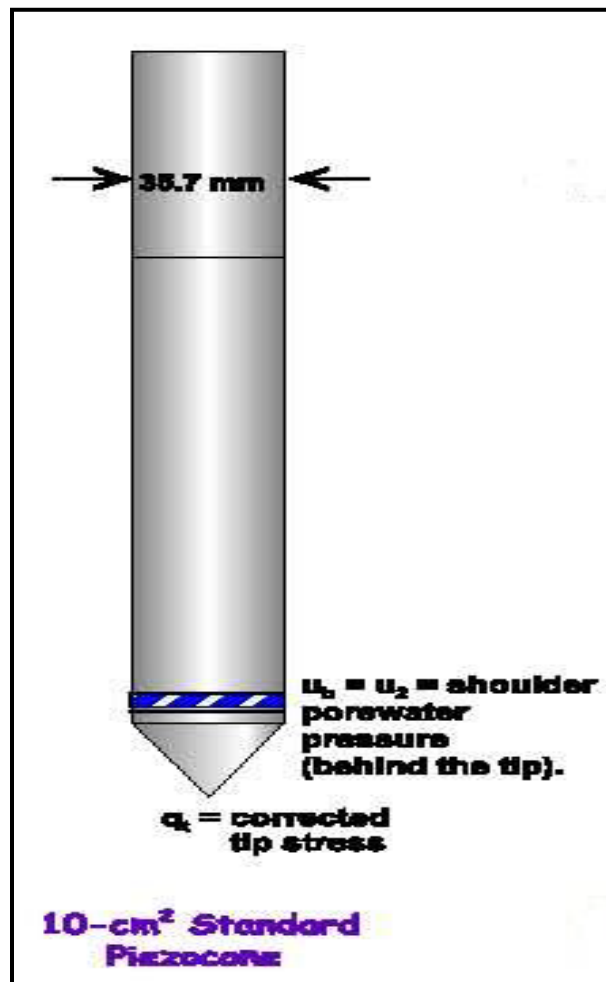


Figure 6-10, Standard Electro-Piezocone  
(Mayne, et al. (2002))

$$q_t = q_c + (1 - a_n) * u_2 \quad \text{Equation 6-5}$$

$$R_f = \frac{f_s}{q_t} * (100\%) \quad \text{Equation 6-6}$$



Where:

$a_n$  = Net area ratio developed from calibration testing

Provide the  $a_n$  value used to compute the corrected tip resistance and the cone factor ( $N_k$ ) used to compute the undrained shear strength in the Excel<sup>®</sup> spreadsheet. Similarly to Soil Test Borings, the CPT can be used to classify the soils at a site. However, the classification is based on soil behavior rather than grain-size and plasticity and the various classification systems yield a Soil Behavior Type (SBT or  $I_c$ ) rather than a USCS soil type. The basic classification is between coarse-grained and fine-grained soils, the differences are indicated below:

1. Coarse-grained
  - a. High end resistance, tip stress, ( $q_c$ )
  - b. Low Friction Ratio, ( $R_f$ )
  - c. Low pore pressure, ( $u_2$ )
2. Fine-grained
  - a. Low end resistance, tip stress, ( $q_c$ )
  - b. High Friction Ratio, ( $R_f$ )
  - c. High pore pressure, ( $u_2$ )

Soil classifications are based on the relationship between normalized Friction Ratio ( $F_R$  ( $F_r$  in Figure 6-11)) and normalized tip resistance ( $Q_t$  ( $Q_{tn}$  in Figure 6-11)) as shown in Figure 6-11. Table 6-12 provides the description of the soils by zone as well as the  $I_c$  for each zone. Similarly to Soil Test Borings, the relative density and/or consistency can be assigned to a soil layer. The relative density and/or consistency is based on the corrected tip resistance ( $q_t$ ). Table 6-13 provides the relative density/consistency versus correct tip resistance.

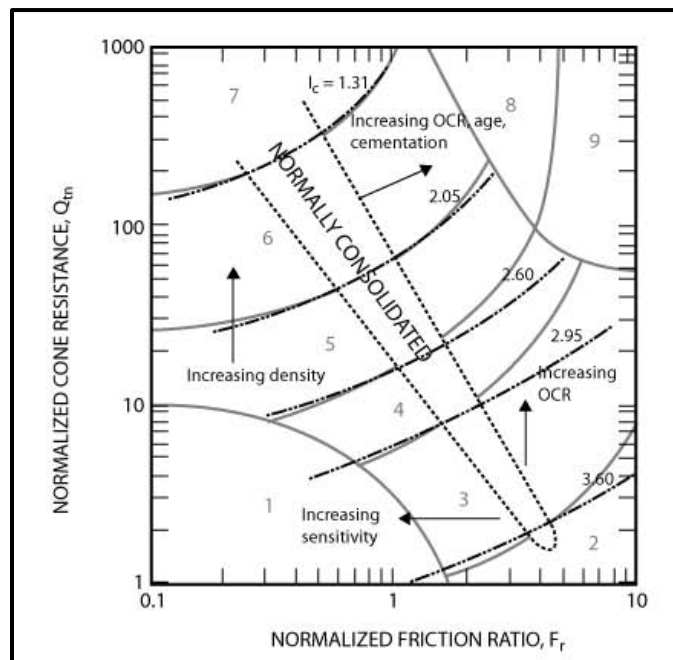


Figure 6-11, Normalized CPT Soil Behavior Chart Using  $Q_T$  versus  $F_R$  (Robertson and Cabal (2015))

**Table 6-12, CPT Soil Behavior Type  
(Robertson and Cabal (2015))**

Soil Behavior Type			
Zone #	Description	$I_c$	
		Min	Max
1	Sensitive, fine-grained	N/A	
2	Organic soils – peats	$\geq 3.6$	
3	Clays – Silty Clay to Clay	2.95	3.59
4	Silt mixtures – Clayey Silt to Silty Clay	2.60	2.94
5	Sand mixtures – Silty Sand to Sandy Silt	2.05	2.59
6	Sands – clean Sand to Silty Sand	1.31	2.04
7	Gravelly Sand to dense Sand	$\leq 1.30$	
8	Very stiff Sand to Clayey Sand (high OCR or cemented)	N/A	
9	Very stiff, fine-grained (high OCR or cemented)	N/A	

**Table 6-13, CPT Relative Density / Consistency Terms**

Relative Density <sup>1,2</sup>			Consistency <sup>1,3</sup>	
Descriptive Term	Relative Density	$q_t^4$ (tsf)	Descriptive Term	$q_t^4$ (tsf)
Very Loose	0 to 15%	$\leq 50$	Very Soft	$\leq 5$
Loose	16 to 35%	51 to 100	Soft to Firm	6 to 15
Medium Dense	36 to 65%	101 to 150	Stiff	16 to 30
Dense	66 to 85%	151 to 200	Very Stiff	31 to 60
Very Dense	86 to 100%	$\geq 201$	Hard	$\geq 61$
<sup>1</sup> For Classification only, not for design				
<sup>2</sup> Applies to coarse-grained soils (major portion retained on No. 200 sieve)				
<sup>3</sup> Applies to fine-grained soils (major portion passing No. 200 sieve)				
<sup>4</sup> Corrected Tip Resistance				

### 6.2.3 Dilatometer Test

The Dilatometer Test (DMT) shall be conducted in accordance with Chapter 5. In addition, to the plotted dilatometer data (see Figure 6-25); the GEC shall provide to the PC/GDS an electronic file in Excel<sup>®</sup> format providing the following data in the order shown (1 bar  $\approx$  1 tsf):

1. Depth, feet
2. A-pressure, bars
3. B-pressure, bars
4. C-pressure, bars
5.  $\Delta A$  – Corrections from membrane calibration, bars
6.  $\Delta B$  – Corrections from membrane calibration, bars
7.  $p_0$  – Corrected A-pressure (see Equation 6-7), bars
8.  $p_1$  – Corrected B-pressure (see Equation 6-8), bars
9.  $p_2$  – Corrected C-pressure (see Equation 6-9), bars
10.  $Z_M$  – Pressure gauge reading when vented to atmospheric pressure, bars
11.  $q_d$  – Corrected thrust required to insert dilatometer, tons
12.  $\sigma_{vo}$  – Total overburden stress, tsf
13.  $\sigma'_{vo}$  – Effective overburden stress, tsf
14.  $u_0$  – Equilibrium pore pressure, tsf
15.  $I_D$  – Material index (soil type), dimensionless

16.  $K_D$  – Horizontal stress index, dimensionless
17.  $E_D$  – Dilatometer Modulus, bars
18.  $U_D$  – Pore Pressure Index, dimensionless
19.  $(S_u)_{DMT}$  – Undrained shear strength, psf

The correlated information requested above shall also be included in the Excel<sup>®</sup> spreadsheet. Further the equations for determining these correlations shall be indicated. The GEC shall also indicate how  $\sigma_{v0}$  and  $\sigma'_{v0}$  were determined. The correlations shall conform to the requirements of Chapter 7. Through developed correlations (see Chapter 7), information can be deduced concerning material type, pore water pressure, in-situ horizontal and vertical stresses, void ratio or relative density, modulus, shear strength parameters, and consolidation parameters.

Where:

$p_0$  – Corrected A-pressure

$$p_0 = 1.05 * (A - Z_M + \Delta A) - 0.05 * (B - Z_M - \Delta B) \quad \text{Equation 6-7}$$

$p_1$  – Corrected B-pressure

$$p_1 = (B - Z_M - \Delta B) \quad \text{Equation 6-8}$$

$p_2$  – Corrected C-pressure ( $u_0$  – Equilibrium pore pressure)

$$u_0 = p_2 = (C - Z_M + \Delta A) \quad \text{Equation 6-9}$$

Similarly to CPT, the DMT can be used to classify the soils at a site based on behavior. Soil classifications are based on the material index ( $I_D$ ) as indicated in Table 6-14.

**Table 6-14, DMT Material Index  
(Marchetti, et al. (2001))**

Soil Type	Material Index, ( $I_D$ )	
	Min	Max
Clay	0.1	0.6
Silt	0.6	1.8
Sand	$\geq 1.8$	

Another general indicator of soil type is the pore pressure index ( $U_D$ ). A  $U_D$  of between 0.0 and approximately 0.2 indicates that the soils are “free-draining”. “Free-draining” (permeable) soils are typically coarse-grained (i.e., clean sands and gravels) soils. Impermeable soils are typically fine-grained (clays (lean and fat) and elastic silts) soils and have a  $U_D$  of 0.7 or greater. Soils with a  $U_D$  between 0.2 and 0.7 have an intermediate permeability. A wide range of soils can have an intermediate permeability.  $U_D$  provides a general indication of soil type and is not considered exact; therefore,  $U_D$  should be used in conjunction with  $I_D$  to determine soil type.

### 6.3 ROCK DESCRIPTION AND CLASSIFICATION

Rock descriptions should use technically correct geologic terms, although accepted local terminology may be used provided the terminology helps to describe distinctive characteristics. Rock cores shall be logged when wet for consistency of color description and greater visibility of rock features. Geologists classify all rocks according to their origin and into 3 distinctive types

as indicated in Table 6-15. All 3 rock types are found here in South Carolina: igneous rocks are found in the Piedmont region, metamorphic rocks are found in the Piedmont and Blue Ridge regions, and sedimentary rocks are found in the Coastal Plain. The Department uses both the geological history as well as the engineering properties to describe rock materials.

**Table 6-15, Rock Classifications**

<b>Rock Type</b>	<b>Definition</b>
Igneous	Derived from molten material
Sedimentary	Derived from settling, depositional, or precipitation processes
Metamorphic	Derived from preexisting rocks due to heat, fluids, and/or pressure.

The geologic conditions of South Carolina have a direct bearing on the activities of SCDOT. This is because the geological history of a rock will determine its mechanical behavior. Therefore, construction costs for a project, especially a new project with substantial foundation construction, are frequently driven by geological, subsurface factors. It is for this reason that much of the initial site investigation for a project requiring foundation work focuses on mechanical behavior of the subsurface materials within the construction limits. A detailed geologic description shall include the following items, in order:

1. Rock Type
2. Rock Color
3. Grain-Size and Shape
4. Texture (stratification/foliation)
5. Mineral Composition
6. Weathering and Alteration
7. Strength
8. Rock Discontinuity
9. Rock Fracture Description
10. Other pertinent information
11. Geologic Strength Index
12. Rock Mass Rating

In addition to the above information being included on the boring record, a photographic log of the cores shall also be provided. The photographic log shall be obtained in the field upon completion of the specific core run. The top and bottom of each individual core run shall be clearly labeled. The label shall include the top and bottom depth of each core run as well as the core run number. A tape measure or ruler shall be placed cross the top or bottom edge of the core box to provide a scale for the photograph. The ruler shall be large enough and provide enough contrast to allow for differentiation between the markings on the ruler. All breaks that occur during coring or are required to fit the core run into the core box shall be indicated to be mechanical breaks.

Rock Quality Designation (RQD) is used to indicate the quality of the rock and is frequently accompanied with descriptive words. It is always expressed as a percent. Percent recovery can be greater than 100 percent if the core from a prior run is recovered during a later run. Figure 6-12 further illustrates the determination of the RQD.

### **6.3.1 Rock Type**

The rock type shall be identified by either a licensed geologist or geotechnical engineer with a minimum of 4 years of experience classifying rock. Rocks are classified according to origin into the 3 major groups: igneous, sedimentary and metamorphic. These groups are subdivided into types based on mineral and chemical composition, texture, and internal structure.

#### **6.3.1.1 Igneous**

Intrusive, or plutonic, igneous rocks have coarse-grained (large, intergrown crystals) texture and are believed to have been formed below the earth's surface. Granite and gabbro are examples of intrusive igneous rocks found in South Carolina. Extrusive, or volcanic, igneous rocks have fine-grained (small crystals) texture and have been observed to form at or above the earth's surface. Basalt and tuff are examples of an extrusive igneous rocks found in South Carolina. Pyroclastic igneous rocks are the result of a volcanic eruption and the rapid cooling of lava, examples of this type of rock are pumice and obsidian. Pyroclastic igneous rocks are not native to South Carolina.

#### **6.3.1.2 Sedimentary**

Sedimentary rocks are the most common form of rock and are the result of weathering of other rocks and the deposition of the rock sediment and soil. Sedimentary rocks are classified into 3 groups called clastic, chemical, and organic. Clastic rocks are composed of sediment (from weathering of rock or erosion of soil). Mudstone and sandstone are examples of clastic sedimentary rock found in South Carolina. Chemical sedimentary rocks are formed from materials carried in solution into lakes and seas. Limestone, dolomite, and halite are examples of this type of sedimentary rock. Organic sedimentary rocks are formed from the decay and deposition of organic materials in relatively shallow water bodies. Examples of organic sedimentary rocks are chalk, shale, coal, and coquina. Coquina is found within South Carolina.

#### **6.3.1.3 Metamorphic**

Metamorphic rocks result from the addition of heat, fluid, and/or pressure applied to preexisting rocks. This rock is normally classified into 3 types, strongly foliated, weakly foliated, and nonfoliated. Foliation refers to the parallel, layered minerals orientation observed in the rock. Schist is an example of a strongly foliated rock. Gneiss (pronounced "nice") is an example of a weakly foliated rock, while marble is an example of a nonfoliated rock. Schist, gneiss, slate and marble are metamorphic rocks found in South Carolina.

### **6.3.2 Rock Color**

The color of the rock shall be determined using the Munsell Color Chart and shall be described while the rock is still at or near the in-situ moisture condition. The Munsell color designation shall be provided at the end of the rock description.

### **6.3.3 Grain-size and Shape**

Grain-size is dependent on the type of rock as described previously; sedimentary rocks will have a different grain-size and shape, when compared to igneous rocks. Metamorphic rocks may or may not display relict grain-size of the original parent rock. The grain-size description should be classified using the terms presented in Table 6-16. Angularity is a geologic property

of particles and is also used in rock classification. Table 6-17 shows the grain shape terms and characteristics used for sedimentary rocks.

**Table 6-16, Grain-size Terms**

Description	Diameter (mm)	Characteristic
Very coarse-grained	> 4.75	Grain-sizes greater than popcorn kernels
Coarse-grained	2.00 – 4.75	Individual grains easy to distinguish by eye
Medium grained	0.425 – 2.00	Individual grains distinguished by eye
Fine-grained	0.075 – 0.425	Individual grains distinguished with difficulty
Very fine-grained	< 0.075	Individual grains cannot be distinguished by unaided eye

**Table 6-17, Grain Shape Terms for Sedimentary Rocks**

Description	Characteristic
Angular	Shows little wear; edges and corners are sharp, secondary corners are numerous and sharp
Subangular	Shows definite effects of wear; edges and corners are slightly rounded off; secondary corners are less numerous and less sharp than angular grains
Subrounded	Shows considerable wear; edges and corners are rounded to smooth curves; secondary corners greatly reduced and highly rounded
Rounded	Shows extreme wear; edges and corners smoother to broad curves; secondary corners are few and rounded
Well-rounded	Completely worn; edges and corners are not present; no secondary edges

#### 6.3.4 Texture (stratification/foliation)

Significant nonfracture structural features should be described. Stratification refers to the layering effects within sedimentary rocks, while foliation refers to the layering within metamorphic rocks. The thickness of the layering should be described using the terms of Table 6-18. The orientation of the stratification/foliation should be measured from the horizontal with a protractor.

**Table 6-18, Stratification/Foliation Thickness Terms**

Descriptive Term	Layer Thickness
Very Thickly Bedded	>1.0 m
Thickly Bedded	0.5 to 1.0 m
Thinly Bedded	50 to 500 mm
Very Thinly Bedded	10 to 50 mm
Laminated	2.5 to 10 mm
Thinly Laminated	<2.5 mm

#### 6.3.5 Mineral Composition

The mineral composition shall be identified by a geologist or geotechnical engineer based on experience and the use of appropriate references. The most abundant mineral should be listed first, followed by minerals in decreasing order of abundance. For some common rock types, mineral composition need not be specified (e.g., dolomite and limestone).

### 6.3.6 Weathering and Alteration

Weathering as defined here (see Table 6-19) is due to physical disintegration of the minerals in the rock by atmospheric processes while alteration is defined here as due to geothermal processes.

**Table 6-19, Weathering/Alteration Terms**

Description	Recognition
Residual Soil	Original minerals of rock have been entirely decomposed to secondary minerals, and original rock fabric is not apparent; material can be easily broken by hand
Completely Weathered / Altered	Original minerals of rock have been almost entirely decomposed to secondary minerals, although the original fabric may be intact; material can be granulated by hand
Highly Weathered / Altered	More than half of the rock is decomposed; rock is weakened so that a minimum 1-7/8 inch diameter sample can be easily broken readily by hand across rock fabric
Moderately Weathered / Altered	Rock is discolored and noticeably weakened, but less than half is decomposed; a minimum 1-7/8 inch diameter sample cannot be broken readily by hand across rock fabric
Slightly Weathered / Altered	Rock is slightly discolored, but not noticeably lower in strength than fresh rock
Fresh	Rock shows no discoloration, loss of strength, or other effect of weathering / alteration

### 6.3.7 Strength

Table 6-20 presents guidelines for common qualitative assessment of strength while mapping or during primary logging of rock cores at the site by using a geologic hammer and pocketknife. The field estimates should be confirmed where appropriate by comparisons with selected laboratory test.

**Table 6-20, Rock Strength Terms**

Description	Recognition	Approximate Uniaxial Compressive Strength (psi)
Extremely Weak Rock	Can be indented by thumbnail	35 – 150
Very Weak Rock	Can be peeled by pocket knife	150 – 700
Weak Rock	Can be peeled with difficulty by pocket knife	700 – 3,500
Medium Strong Rock	Can be indented 3/16 inch with sharp end of pick	3,500 – 7,200
Strong Rock	Requires one hammer blow to fracture	7,200 – 14,500
Very Strong Rock	Requires many hammer blows to fracture	14,500 – 35,000
Extremely Strong Rock	Can only be chipped with hammer blows	> 35,000

A popular classification system based on quantifying discontinuity spacing is known as the RQD (see ASTM D6032 – *Standard Test Method for Determining Rock Quality Designation (RQD) of Rock Core*). RQD is illustrated in Figure 6-12 and is defined as the total combined length of all the pieces of the intact core that are longer than twice the diameter of the core (normally 2

inches) recovered during the core run divided by the total length of the core run (e.g., the summation of rock pieces greater than 4 inches in length is 4 feet for a 5-foot run indicating an RQD of 80 percent). The RQD can be used to describe the quality of the rock as indicated in Table 6-21. An additional qualitative measure of rock strength is the time to advance the core barrel. The time should be recorded as minutes per foot and should only include the time spent actually advancing the core barrel into the rock mass.

**Table 6-21, Rock Quality Description Terms**

<b>Description</b>	<b>RQD</b>
Very poor	0 - 25%
Poor	26% - 50%
Fair	51% - 75%
Good	76% - 90%
Excellent	91% - 100%

The scratch hardness test can also be used to provide an indication of the hardness of a rock sample. The terms to describe rock hardness are provided in Table 6-22.

**Table 6-22, Rock Hardness Terms**

<b>Description</b>	<b>Characteristic</b>
Soft (S)	Plastic materials only
Friable (F)	Easily crumbled by hand, pulverized or reduced to powder
Low Hardness (LH)	Can be gouged deeply or carved with a pocketknife
Moderately Hard (MH)	Can be readily scratched by a knife blade
Hard (H)	Can be scratched with difficulty
Very Hard (VH)	Cannot be scratched by pocketknife



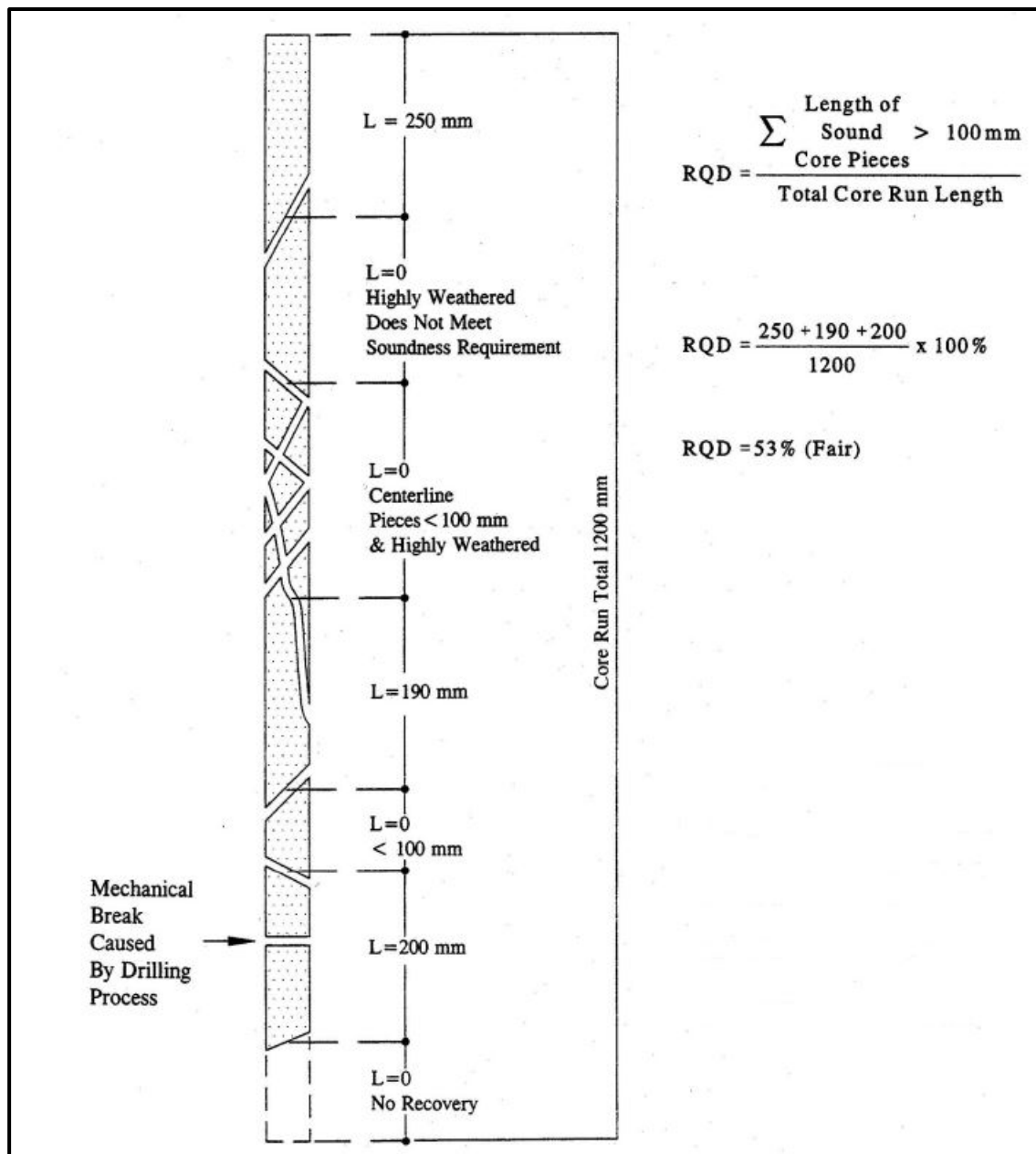


Figure 6-12, RQD Determination (Mayne, et al., 2002)

### 6.3.8 Rock Discontinuity

Discontinuity is the general term for any mechanical crack or fissure in a rock mass having no or low tensile strength. It is the collective term for most types of joints, weak bedding planes, weak schistosity planes, weakness zones, and faults. The symbols recommended for the type of rock mass discontinuities are listed in Table 6-23.

**Table 6-23, Discontinuity Type**

Symbol	Description
F	Fault
J	Joint
Sh	Shear
Fo	Foliation
V	Vein
B	Bedding

The spacing of discontinuities is the perpendicular distance between adjacent discontinuities. The spacing is measured in feet, perpendicular to the planes in the set. Table 6-24 presents guidelines to describe discontinuity.

**Table 6-24, Discontinuity Spacing**

Symbol	Description
EW	Extremely Wide (> 65 feet)
W	Wide (22 – 65 feet)
M	Moderate (7.5 – 22 feet)
C	Close (2 – 7.5 feet)
VC	Very Close (< 2 feet)

The discontinuities should be described as closed, open, or filled. Aperture is used to describe the perpendicular distance separating the adjacent rock walls of an open discontinuity in which the intervening space is air or water filled. Width is used to describe the distance separating the adjacent rock walls of filled discontinuities. The terms presented in Table 6-25 and Table 6-26 should be used to describe apertures and widths, respectively. Terms such as “wide”, “narrow”, and “tight” are used to describe the width of discontinuities such as thickness of veins, fault gouge filling, or joint openings. For the faults or shears that are not thick enough to be represented on the soil test boring log, the measured thickness is recorded numerically in millimeters (mm).

**Table 6-25, Aperture Size Discontinuity Terms**

Aperture Opening	Description	
<0.1 mm	Very tight	Closed Features
0.1 – 0.25 mm	Tight	
0.25 – 0.5 mm	Partly open	
0.5 – 2.5 mm	Open	Gapped Features
2.5 – 10 mm	Moderately open	
>10 mm	Wide	
1 – 10 cm	Very wide	Open Features
10 – 100 cm	Extremely wide	
>1m	Cavernous	

**Table 6-26, Discontinuity Width Terms**

Symbol	Description
W	Wide (12.5 – 50 mm)
MW	Moderately Wide (2.5 – 12.5 mm)
N	Narrow (1.25 – 2.5 mm)
VN	Very Narrow (<1.25 mm)
T	Tight (0 mm)

In addition to the above characterizations, discontinuities are further characterized by the surface shape of the joint and the roughness of its surface (see Tables 6-27 and 6-28).

**Table 6-27, Surface Shape of Joint Terms**

Symbol	Description
Wa	Wavy
Pl	Planar
St	Stepped
Ir	Irregular

**Table 6-28, Surface Roughness Terms**

Symbol	Description
Slk	Slickensided (surface has smooth, glassy finish with visual evidence of striations)
S	Smooth (surface appears smooth and feels so to the touch)
SR	Slightly Rough (asperities on the discontinuity surfaces are distinguishable and can be felt)
R	Rough (some ridges and side-angle steps are evident; asperities are clearly visible, and discontinuity surface feels very abrasive)
VR	Very Rough (near-vertical steps and ridges occur on the discontinuity surface)

Filling is the term for material separating the adjacent rock walls of discontinuities. Filling is characterized by its type, amount, width (i.e., perpendicular distance between adjacent rock walls (see Table 6-26)), and strength. Table 6-29 presents guidelines for characterizing the amount of filling.

**Table 6-29, Filling Amount Terms**

Symbol	Description
Su	Surface Stain
Sp	Spotty
Pa	Partially Filled
Fi	Filled
No	None

### 6.3.9 Rock Fracture Description

The location of each naturally occurring fracture and mechanical break should be shown in the fracture column of the rock core log. The naturally occurring fractures are numbered and described using the terminology presented above for discontinuities.

The naturally occurring fractures and mechanical breaks are sketched in the drawing column of the Soil Test Log (see Figures 6-19 and 6-20). Dip angles of fractures shall be measured using a protractor and marked on each log. If the rock is broken into many pieces less than 1 inch long, the log may be crosshatched in that interval or the fracture may be shown schematically. Strike (dip orientation or direction (i.e., north, south, etc.)) should be estimated based on rock cores, local outcrops, and geologic experience in the immediate area.

The number of naturally occurring fractures observed in each 1 foot of core should be recorded in the fracture frequency column. Mechanical breaks, thought to have occurred due to drilling, are not counted. The following criteria can be used to identify natural breaks:

- A rough brittle surface with fresh cleavage planes in individual rock minerals indicates an artificial fracture.
- A generally smooth or somewhat weathered surface with soft coating or infilling materials, such as talc, gypsum, chlorite, mica, or calcite obviously indicates a natural discontinuity.
- In rocks showing foliation, cleavage, or bedding it may be difficult to distinguish between natural discontinuities and artificial fractures when these are parallel with the incipient weakness planes. If drilling has been carried out carefully, then the questionable breaks should be counted as natural features, to be on the conservative side.
- Depending upon the drilling equipment, part of the length of core being drilled may occasionally rotate with the inner barrels in such a way that grinding of the surfaces of discontinuities and fractures occur. In weak rock types, it may be very difficult to decide if the resulting rounded surfaces represent natural or artificial features. When in doubt, the conservative assumption should be made; i.e., assume that the discontinuities are natural.

The results of core logging (frequency and RQD) can be strongly time dependent and moisture content dependent in cases of certain varieties of shales and mudstones having relatively weakly developed diagenetic bonds. A frequent problem is “discing”, in which an initially intact core separates into discs on incipient planes, the process becoming noticeable perhaps within minutes of core recovery. This phenomenon is experienced in several different forms:

- Stress relief cracking (and swelling) by the initially rapid release of strain energy in cores recovered from areas of high stress, especially in the case of shaley rocks.
- Dehydration cracking experienced in the weaker mudstones and shales which may reduce RQD from 100 percent to 0 percent in a matter of minutes, the initial integrity possibly being due to negative pore pressure.
- Slaking cracking experienced by some of the weaker mudstones and shales when subjected to wetting and drying.

All these phenomena may make core logging of fracture frequency and RQD unreliable. Whenever such conditions are anticipated, cores shall be logged by an experienced geologist or geotechnical engineer as it is recovered and at subsequent intervals when the phenomenon is predicted.

### **6.3.10 Other Pertinent Information**

Additional information that adds to the description of the rock may be included. This may include the geologic formation to which the rock belongs. This information should enhance the description.

### **6.3.11 Geological Strength Index**

In the prior versions of this Manual (Version 1.0 and 1.1) the Rock Mass Rating (RMR) was determined and used in the development of the Hoek-Brown criteria used in rock design. In the most recent version of the Hoek-Brown criteria (Hoek, Carranza-Torres and Corkum (2002)), RMR has been replaced by the Geological Strength Index (GSI) classification system. However, the RMR shall still also be determined. According to Marinos, Marinos and Hoek (2005):

This index (*GSI*) is based upon an assessment of the lithology, structure and condition of discontinuity surfaces in the rock mass and it is estimated from visual examination of the rock mass exposed in outcrops, in surface excavations such as road cuts and in tunnel faces and borehole cores. The GSI, by combining the two fundamental parameters of the geological process, the blockiness of the mass and the conditions of the discontinuities, respects the main geological constraints that govern a formation and is thus a geologically sound index that is simple to apply in the field.

The use of GSI is only applicable to rock masses whose behavior is controlled by the overall mass response and not by failure along pre-existing structural discontinuities. Rock mass is used to describe the system comprised of intact rock, the consolidated and cemented assemblage of mineral particles, and discontinuities, joints, bedding planes, minor faults, or other recurrent planar features. Intact rock characteristics are determined from index and laboratory tests on core samples, while the rock mass properties are estimated from intact rock properties plus the characteristics of discontinuities.

Figure 6-13 provides the chart for determining GSI from rock core samples or exposed outcrops on a site. The GSI is estimated based on, first, the structure of the rock mass and second, on the condition of the rock surfaces. Combining the rock type and the uniaxial compressive (unconfined) strength of intact ( $q_u$ ) with the GSI provides a practical means to assess rock mass strength and modulus for foundation design.

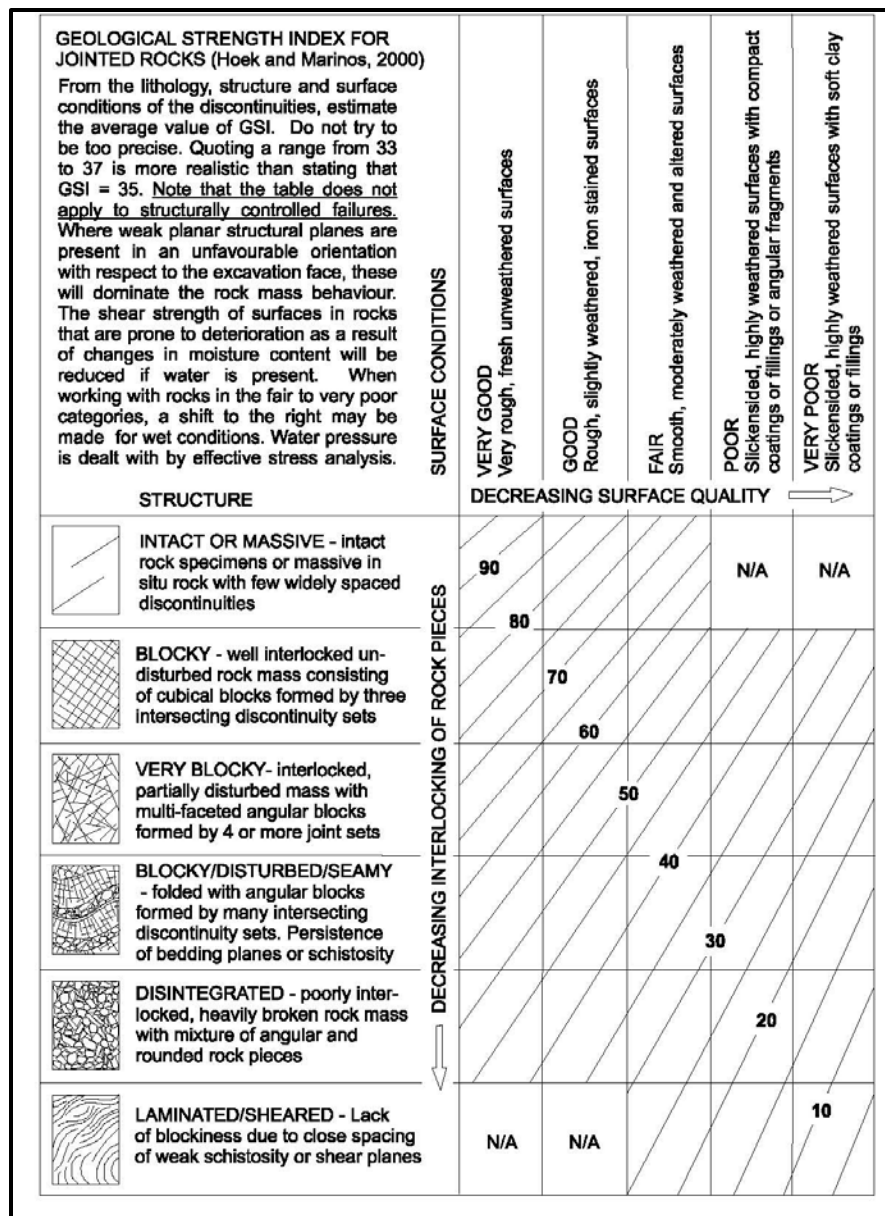


**Figure 6-13, GSI Determination (Brown, Turner and Castelli (2010))**

Marinos, et al. (2005) have identified some limitations to the use of the GSI. The GSI classification system should only be applied to those rock masses that are isotropic (i.e., behavior of the rock mass is independent on loading direction). If a clearly defined dominant structural orientation is present (i.e., slate or bedded shales) then the GSI classification system shall not be used. The exception is in slope stability: if the bedding planes are oriented 90° to the slope (i.e., the bedding planes dip into the slope), then the GSI classification system, may be used with caution. Another limitation that needs to be accounted for is the aperture of the discontinuities within the rock mass, since these openings can significantly affect the rock mass properties. The size of the apertures is termed a “disturbance factor” (D) in the latest version of the Hoek-Brown criterion. The disturbance factor ranges from 0 for intact rock to 1 for extremely disturbed rock masses. This factor allows for the disruption of the interlocking on individual rock pieces as result of the opening of the discontinuities. The GSI classification system is a

qualitative system that is subjective to the engineer or geologist logging the borehole. Therefore a range of GSI values shall be determined from Figure 6-13.

### 6.3.12 Rock Mass Rating

The information obtained in the preceding Sections is also used to develop the Rock Mass Rating (RMR). The RMR is used to determine how the mass of rock will behave as opposed to the samples used in unconfined compression, which typically tend to represent the firmest materials available. Discontinuities affect the ability of rock to carry load and to resist deformations. The RMR is the sum of the relative ratings (RR) for 5 parameters adjusted for joint orientations. Table 6-30 provides the 5 parameters and the range of values. The RMR is adjusted to account for joint orientation depending on the favorability of the joint orientation for the specific project. Table 6-31 contains the relative rating adjustments (RRA) for joint orientation. The adjusted RMR is determined using Equation 6-10. The description of the rock mass is based on the adjusted RMR as defined in Table 6-32. The adjusted RMR can be used to estimate the rock mass shear strength and the deformation modulus (see Chapter 7).

$$RMR = RR1 + RR2 + RR3 + RR4 + RR5 + RRA \quad \text{Equation 6-10}$$

**Table 6-30, Classification of Rock Masses**

Parameter		Range of Values						
1	Strength of intact rock material	Point load strength index	>1,215 psi	1,215 – 1,100 psi	300 – 1,100 psi	150 – 300 psi	For this low range, uniaxial compressive test is preferred	
		Uniaxial compressive strength	>30,000 psi	30,000 – 15,000 psi	7,500 – 15,000 psi	3,600 – 7,500 psi	1,500 – 3,600 psi	500 – 1,500 psi
	Relative Rating (RR1)	15	12	7	4	2	1	0
2	Drill core quality RQD	90 – 100%		75 – 90%	50 – 75%	25 – 50%	<25%	
	Relative Rating (RR2)	20		17	13	8	3	
3	Spacing of Joints	>10 ft		3 – 10 ft	1 – 3 ft	2 in – 1 ft	<2 in	
	Relative Rating (RR3)	30		25	20	10	5	
4	Condition of Joints	- Very rough surfaces - Not continuous - No separation - Hard joint wall rock		- Slightly rough surfaces - Separation <0.05 in - Hard joint wall rock	- Slightly rough surfaces - Separation <0.05 in - Soft joint wall rock	- Slicken-sided surfaces or - Gouge <0.2 in thick or - Joints open 0.05 – 0.2 in - Continuous joints	- Soft gouge >0.2 in thick or - Joints open >0.2 in - Continuous joints	
		Relative Rating (RR4)	25		20	12	6	0
5	Ground water conditions	Ratio – joint water pressure/major principal stress	0	0.0 – 0.2	0.2 – 0.5		>0.5	
		General conditions	Completely dry	Moist only (interstitial water)	Water under moderate pressure		Severe water problems	
	Relative Rating (RR5)	10	7	4		0		

**Table 6-31, Relative Rating Adjustment for Joint Orientations**

Strike and Dip Orientations of Joints		Very Favorable	Favorable	Fair	Unfavorable	Very Unfavorable
Relative Ratings (RRA)	Foundations	0	-2	-7	-15	-25
	Slopes	0	-5	-25	-50	-60

**Table 6-32, Rock Mass Class Determination**

RMR Rating	81 – 100	61 – 80	41 – 60	21 – 40	<20
Class No.	I	II	III	IV	V
Description	Very good rock	Good rock	Fair rock	Poor rock	Very poor rock

## 6.4 FIELD AND LABORATORY TESTING RECORDS

This Section discusses the presentation of field and laboratory data on SCDOT projects.

### 6.4.1 Field Testing Records

The results of Soil Test Borings shall be preliminarily prepared and forwarded to the GEOR for review and editing as well as for the selection of samples for laboratory testing. At the completion of laboratory testing, the preliminary logs shall be corrected to conform to the results of the laboratory testing and final Soil Test Logs shall be prepared and submitted. Figure 6-14 provides the template for the preparation of a soil test log for use on SCDOT projects. Figures 6-15, 6-16 and 6-17 provide the descriptors to be used in preparing the logs. Figure 6-18 provides a template for a manual auger log for use on SCDOT projects. Figures 6-19 and 6-20 provide an example of a completed Soil Test Log. Figure 6-21 presents an example of a completed Manual Auger Log. The results of Field Vane Shear Testing (FVST) shall be presented on soil test boring record as indicated in Figure 6-22, with “FV” inserted after the boring number (i.e., B-1FV). As indicated in Chapter 5, a record is required for Shelby tube (undisturbed, UD) sampling, if the UD is not obtained within a soil test boring. See Figure 6-23 for an example. The record of UD sampling shall consist of the soil test boring designation with a “U” after the number (i.e., B-1U). The results of the CPTu and DMT soundings shall be as presented in Figures 6-24 and 6-58, respectively. The shear wave velocity ( $V_s$ ) profile versus depth shall be presented as indicated in Figure 6-26. In addition, the  $V_s$  profile versus depth shall also be included in the Excel<sup>®</sup> spreadsheet as well as provided as a table (see Figure 6-27). In addition, to the information previously indicated, the Soil Test Boring records shall indicate the termination depth, if auger refusal was encountered and what depth. Further, the Soil Test Boring records shall indicate the depth of caving, if encountered and whether the caving was indicated at the completion of the boring or at some other time.

### 6.4.2 Laboratory Testing Records

In an effort to standardize the appearance of laboratory testing results, all laboratory testing results shall be processed using gINT<sup>®</sup> as produced by Bentley Systems, Incorporated. Those tests that do not have presentation forms in gINT<sup>®</sup> shall use the forms currently being used by the GEC. A summary of all laboratory testing results shall be provided (see Figure 6-28). Following the laboratory results summary, provide a graph of index properties (liquid and plastic limits, natural moisture content and percent fines) versus depth. Figure 6-29 provides an example of this graph. The results of moisture-plasticity relationship testing results and grain-



size analysis shall also be presented graphically as depicted in Figures 6-30 and 6-31, respectively. The moisture-density relationship testing results shall be depicted as shown in Figure 6-32. In addition, each UD sample is required to have an extraction log (i.e., Shelby Tube Log) indicating the soil encountered in each undisturbed specimen. Further photos of each specimen will also be presented see Figures 6-33, 6-34 and 6-35 for examples. The results of consolidation testing may be shown as depicted in Figure 6-36; however, alternate presentations of consolidation testing results may be presented with prior approval of the PC/GDS. The results of unconfined compression testing may be shown as depicted in Figure 6-37. The results of direct shear testing may be shown as depicted in Figure 6-38. The results of triaxial testing should be shown as indicated in Figures 6-39 and 6-40. In addition, photographs of the triaxial sample immediately after it has been extracted from the Shelby tube, after the sample has been trimmed and placed in the loading cell and after failure shall also be provided. Figure 6-41 provides a summary of the results of rock core testing and Figures 6-42 and 6-43 provide an example of an individual unconfined rock core test result.

## 6.5 REFERENCES

ASTM International, (2012), Annual Book of ASTM Standards, Section 4 – Construction, Volume 04.08 – Soil and Rock (I): D420 – D5876.

ASTM International, (2012), Annual Book of ASTM Standards, Section 4 – Construction, Volume 04.09 – Soil and Rock (II): D5877 - Latest.

Brown, D. A., Turner, J. P., and Castelli, R. J., (2010), Drilled Shafts: Construction Procedures and LRFD Design Methods, Geotechnical Engineering Circular No. 10, (Publication No. FHWA-NHI-10-016), US Department of Transportation, National Highway Institute, Federal Highway Administration, Washington, DC.

Hoek, E., Carranza-Torres, C., and Corkum, B., (2002), “Hoek-Brown Failure Criterion – 2002 Edition,” Mining and Tunnelling Innovation and Opportunity: Proceedings of the 5th North American Rock Mechanics Symposium and the 17th Tunnelling Association of Canada Conference : NARMS-TAC 2002, Toronto, Ontario, Canada.

Marchetti, S., Monaco, P., Totani, G., and Calabrese, M., (2001), “The Flat Dilatometer Test (DMT) in Soil Investigations,” Proceedings of In-Situ 2001, International Conference on In-Situ Measurement of Soil Properties, Bali, Indonesia.

Marinos, V., Marinos, P., and Hoek, E., (2005), “The Geological Strength Index: Applications and Limitations,” *The Bulletin of Engineering Geology and the Environment*, Volume 64, Number 1.

Mayne, P. W., Christopher, B. R., and DeJong, J., (2002), Subsurface Investigations - Geotechnical Site Characterization, (Publication No. FHWA-NHI-01-031). US Department of Transportation, National Highway Institute, Federal Highway Administration, Washington, D.C.

O'Neill, M. W., Townsend, F. C., Hassan, K. M., Buller, A., and Chan, P. S., (1996), Load Transfer for Drilled Shafts in Intermediate Geomaterials, (Publication No. FHWA-RD-95-172), US Department of Transportation, Office of Engineering and Highway Operations R&D, Federal Highway Administration, McLean, Virginia.

Robertson, P. K. and Cabal (Robertson), K. L., (2015), “Guide to Cone Penetration Testing for Geotechnical Engineering,” 6<sup>th</sup> Edition, Gregg Drilling & Testing, Inc., Signal Hill, California.

Soil Test Log

<b>Project ID:</b> 0041401-B01		<b>County:</b> Beaufort/Jasper		<b>Boring No.:</b> B-722	
<b>Site Description:</b> RBO New River			<b>Route:</b> SC 170/46		
<b>Eng./Geo.:</b> A. Bore		<b>Boring Location:</b> 722+00		<b>Offset:</b> 5 ft LT	<b>Alignment:</b> Mainline
<b>Elev.:</b> 1,500 ft	<b>Latitude:</b> 34.3750	<b>Longitude:</b> 81.0944	<b>Date Started:</b> 07/15/03		
<b>Total Depth:</b> 45 ft	<b>Soil Depth:</b> 39 ft	<b>Core Depth:</b> 6 ft	<b>Date Completed:</b> 07/16/03		
<b>Bore Hole Diameter (in):</b> 4.5		<b>Sampler Configuration</b>		<b>Liner required:</b> Y N	<b>Liner used:</b> Y N
<b>Drill Machine:</b> CME-750	<b>Drill Method:</b> Wash Rotary	<b>Hammer Type:</b> Automatic		<b>Energy Ratio:</b> 100%	
<b>Core Size:</b> NQ Wireline	<b>Driller:</b> I. Core	<b>Groundwater:</b> TOB		7.5 ft	24 hr 15 ft

Depth (feet)	Elevation (ft msl)	MATERIAL DESCRIPTION	Graphic Log	Sample Depth (feet)	Sample Type / No.	SPT N-Value	● - SPT N-Value (blows / foot) PL MC LL X-----O-----X ▲ - % fines									
					1 st 2 nd 3 rd 4 th		1	2	3	4	5	6	7	8	9	10
		Soil Description [a] , [b] , [c] , [d] , [e] , [f] , [g] [h] , [i] , [j] , [Munsell] , [LL] [PL] , [PI] , [NMC] , [%#200] Munsell = Munsell Color Chart Designation LL = Liquid Limit PL = Plastic Limit PI = Plasticity Index NMC = Natural Moisture Content %#200 = Percent Passing #200 Sieve														
		Rock Description (as required) [k] , [l] , [m] , [n] , [o] , [p] , [q] [r] , [s] , [t] , [u] , [v] , [w] , [x] [Munsell] , [RQD] , [%REC] , [GSI] [RMR] , [q <sub>u</sub> ] , [Time Rate] Munsell = Munsell Color Chart Designation RQD = Rock Quality Designation %REC = Percent Recovery GSI = Geological Strength Index RMR = Rock Mass Rating q <sub>u</sub> = Unconfined Compressive Strength Time Rate = Time required to drill a core														

Figure 6-14, SCDOT Soil Test Log Template

**SCDOT** Soil Test Log Descriptors

**a - Relative Density / Consistency Terms**

<u>Relative Density<sup>1</sup></u>			<u>Consistency<sup>2</sup></u>		
Descriptive Term	Relative Density	SPT Blow Count	Descriptive Term	Unconfined Compression Strength (q <sub>u</sub> ) (tsf)	SPT Blow Count
Very Loose	0 to 15%	< 4	Very Soft	<0.25	<2
Loose	16 to 35%	5 to 10	Soft	0.26 to 0.50	3 to 4
Medium Dense	36 to 65%	11 to 30	Firm	0.51 to 1.00	5 to 8
Dense	66 to 85%	31 to 50	Stiff	1.01 to 2.00	9 to 15
Very Dense	86 to 100%	>51	Very Stiff	2.01 to 4.00	16 to 30
			Hard	>4.01	> 31

**b - Moisture Condition**

<u>Descriptive Term</u>	<u>Criteria</u>
Dry	Absence of moisture, dusty, dry to the touch
Moist	Damp but no visible water
Wet	Visible free water, usually in coarse-grained soils below the water table

**c - Color**

Describe the sample color while sample is still moist, using Munsell color chart.

**d - Angularity<sup>1</sup>**

<u>Descriptive Term</u>	<u>Criteria</u>
Angular	Particles have sharp edges and relatively plane sides with unpolished surfaces
Subangular	Particles are similar to angular description but have rounded edges
Subrounded	Particles have nearly plane sides but have well-rounded corners and edges
Rounded	Particles have smoothly curved sides and no edges

**e - HCl Reaction<sup>3</sup>**

<u>Descriptive Term</u>	<u>Criteria</u>
None Reactive	No visible reaction
Weakly Reactive	Some reaction, with bubbles forming slowly
Strongly Reactive	Violent reaction, with bubbles forming immediately

**f - Cementation<sup>3</sup>**

<u>Descriptive Term</u>	<u>Criteria</u>
Weakly Cemented	Crumbles or breaks with handling or little finger pressure
Moderately Cemented	Crumbles or breaks with considerable finger pressure
Strongly Cemented	Will not crumble or break with finger pressure

**g - Particle-Size Range<sup>1</sup>**

<u>Gravel</u>			<u>Sand</u>		
	mm	Sieve size		mm	Sieve size
Fine	4.76 to 19.1	#4 to ¾ inch	Fine	0.074 to 0.42	#200 to #40
Coarse	19.1 to 76.2	¾ inch to 3 inch	Medium	0.42 to 2.00	#40 to #10
			Coarse	4.00 to 4.76	#10 to #4

**h - Primary Soil Type<sup>1,2</sup>**

The primary soil type will be shown in all capital letters

**i - USCS Soil Designation**

Indicate USCS soil designation as defined in ASTM D-2487 and D-2488

**j - AASHTO Soil Designation**

Indicate AASHTO soil designation as defined in AASHTO M-145 and ASTM D-3282

<sup>1</sup>Applies to coarse-grained soils (major portion retained on No. 200 sieve)  
<sup>2</sup>Applies to fine-grained soils (major portion passing No. 200 sieve)  
<sup>3</sup>Use as required

Figure 6-15, SCDOT Soil Test Log Descriptors – Soil

**SCDOT** Soil Test Log Descriptors

**k** **Rock Type**  
Indicate type of rock encountered (i.e. granite, limestone, shale, slate, etc.)

**l** **Color**  
Describe the sample color while sample is still moist, using Munsell color chart.

**m** **Texture**  
Describe the nonfracture structural features. Stratification is the layering of sedimentary rock and foliation is the layering of metaphoric rock

<u>Descriptive Term</u>	<u>Criteria</u>
Very Thickly Bedded	> 1.0 m
Thickly Bedded	0.5 to 1.0 m
Thinly Bedded	50 to 500 mm
Very Thinly Bedded	10 to 50 mm
Laminated	2.5 to 10 mm
Thinly Laminated	< 2.5 mm

**n** **Grain Size and Shape**  
Describe the size and shape of all visible grains, typically used on sedimentary rock.

<u>Descriptor</u>	<u>mm</u>	<u>Sieve size</u>
Very coarse grained	> 4.75	Grain sizes greater than popcorn kernels
Coarse grained	2.00 – 4.75	Individual grains easy to distinguish by eye
Medium grained	0.425 – 2.00	Individual grains distinguished by eye
Fine grained	0.075 – 0.425	Individual grains distinguished with difficulty
Very Fine grained	< 0.075	Individual grains cannot be distinguished by unaided eye

<u>Descriptive Term</u>	<u>Criteria</u>
Angular	Shows little wear; edges and corners are sharp
Subangular	Shows definite effects of wear; edges and corners are slightly rounded off
Subrounded	Shows considerable wear; edges and corners are rounded to smooth curves
Rounded	Shows extreme wear; edges and corners are smoother to broad curves
Well-rounded	Completely worn; edges and corners are not present

**o** **Weathering / Alteration**  
Weathering is the physical disintegration of the minerals by atmospheric processes. Alteration is disintegration of the minerals by geothermal processes.

<u>Description</u>	<u>Recognition</u>
Residual Soil	Original minerals of rock have been entirely decomposed to secondary minerals, and original rock fabric is not apparent; material can be easily broken by hand
Completely Weathered / Altered	Original minerals of rock have been almost entirely decomposed to secondary minerals, although the original fabric may be intact; material can be granulated by hand
Highly Weathered / Altered	More than half of the rock is decomposed; rock is weakened so that a minimum 1-7/8 inch diameter sample can be easily broken readily by hand across rock fabric
Moderately Weathered / Altered	Rock is discolored and noticeably weakened, but less than half is decomposed; a minimum 1-7/8 inch diameter sample cannot be broken readily by hand across rock fabric
Slightly Weathered / Altered	Rock is slightly discolored, but not noticeably lower in strength than fresh rock
Fresh	Rock shows no discoloration, loss of strength, or other effect of weathering / alteration

Figure 6-16, SCDOT Soil Test Log Descriptors – Rock

**SCDOT** Soil Test Log Descriptors

**p** **Rock Strength**  
 Provide a qualitative assessment of the rock strength using either a geologic hammer or knife.

Description	Recognition	Approximately Uniaxial Compressive Strength (psi)
Extremely Weak Rock	Can be indented by thumbnail	35 – 150
Very Weak Rock	Can be peeled by pocket knife	150 – 700
Weak Rock	Can be peeled with difficulty by pocket knife	700 – 3,500
Medium Strong Rock	Can be indented 3/16 inch with sharp end of pick	3,500 – 7,200
Strong Rock	Requires one hammer blow to fracture	7,200 – 14,500
Very Strong Rock	Requires many hammer blows to fracture	14,500 – 35,000
Extremely Strong Rock	Can only be chipped with hammer blows	> 35,000

**q** **Strike and Dip**  
 Dip of fracture surface measured relative to horizontal with bearing and direction (i.e. N30°down, etc.)

<b>r</b> Discontinuity Type	<b>s</b> Discontinuity Width (millimeters)	<b>t</b> Amount of Infilling
F - Fault	W - Wide (12.5 – 50)	Su - Surface Stain
J - Joint	MW - Moderately Wide (2.5 – 12.5)	Sp - Spotty
Sh - Shear	N - Narrow (1.25 – 2.5)	Pa - Partially Filled
Fo - Foliation	VN - Very Narrow (< 1.25)	Fi - Filled
V - Vein	T - Tight (0)	No - None
B - Bedding		

<b>u</b> Type of Infilling	<b>v</b> Surface Shape of Joint	<b>w</b> Discontinuity Spacing (feet)
Cl - Clay	Wa - Wavy	EW Extremely Wide (> 65)
Ca - Calcite	Pl - Planar	W Wide (22 – 65)
Ch - Chloride	St - Stepped	M Moderate (7.5 – 22)
Fe - Iron Oxide	Ir - Irregular	C Close (2 – 7.5)
Gy - Gypsum/Talc		VC Very Close (< 2)
H - Healed		
No - None		

**x** **Roughness of Surface**

- Slk - Slickensided (surface has smooth, glassy finish with visual evidence of striations)
- S - Smooth (surface appears smooth and feels so to the touch)
- SR - Slightly Rough (asperities on the discontinuity surfaces are distinguishable and can be felt)
- R - Rough (some ridges and side-angle steps are evident; asperities are clearly visible, and discontinuity surface feels very abrasive)
- VR - Very Rough (near-vertical steps and ridges occur on the discontinuity surface)

Figure 6-17, SCDOT Soil Test Log Descriptors – Rock (con't)

Manual Auger Log

<b>Project ID:</b> 0041401-B01		<b>County:</b> Beaufort/Jasper		<b>Boring No.:</b> MA-1	
<b>Site Description:</b> RBO New River				<b>Route:</b> SC 170/46	
<b>Driller:</b> A. Bore	<b>Boring Location:</b> 722+00		<b>Offset:</b> 5 ft LT	<b>Alignment:</b> Mainline	
<b>Elev.:</b> 1,500 ft	<b>Latitude:</b> 34.3750	<b>Longitude:</b> 81.0944	<b>Date Started:</b> 07/15/03		
<b>Total Depth:</b> 5 ft	<b>Groundwater:</b> TOB	5 ft	<b>24 hr</b> 3 ft	<b>Date Completed:</b> 07/16/03	
<b>Dynamic Cone Penetrometer Test Procedure:</b> Sowers and Hedges (1966)			<b>ASTM D6951</b>		

Depth (feet)	Elevation (ft msl)	MATERIAL DESCRIPTION	Graphic Log	Sample Depth (feet)	Sample Type / No.	DCP N-Value	• - DCP N-Value (blows / foot) PL MC LL X-----O-----X ▲ - % fines												
							1 st	2 nd	3 rd	1	2	3	4	5	6	7	8	9	10
		Soil Description <div style="display: flex; justify-content: space-between; margin-top: 5px;"> <span>[ a ] , [ b ] , [ c ] , [ d ] , [ e ] , [ f ] , [ g ]</span> </div> <div style="display: flex; justify-content: space-between; margin-top: 5px;"> <span>[ h ] , [ i ] , [ j ] , [ Munsell ] , [ LL ]</span> </div> <div style="display: flex; justify-content: space-between; margin-top: 5px;"> <span>[ PL ] , [ PI ] , [ NMC ] , [ %#200 ]</span> </div> <p style="font-size: small; margin-top: 5px;">                         Munsell = Munsell Color Chart Designation                          LL = Liquid Limit                          PL = Plastic Limit                          PI = Plasticity Index                          NMC = Natural Moisture Content                          %#200 = Percent Passing #200 Sieve                     </p>																	

Figure 6-18, SCDOT Manual Auger Log Template

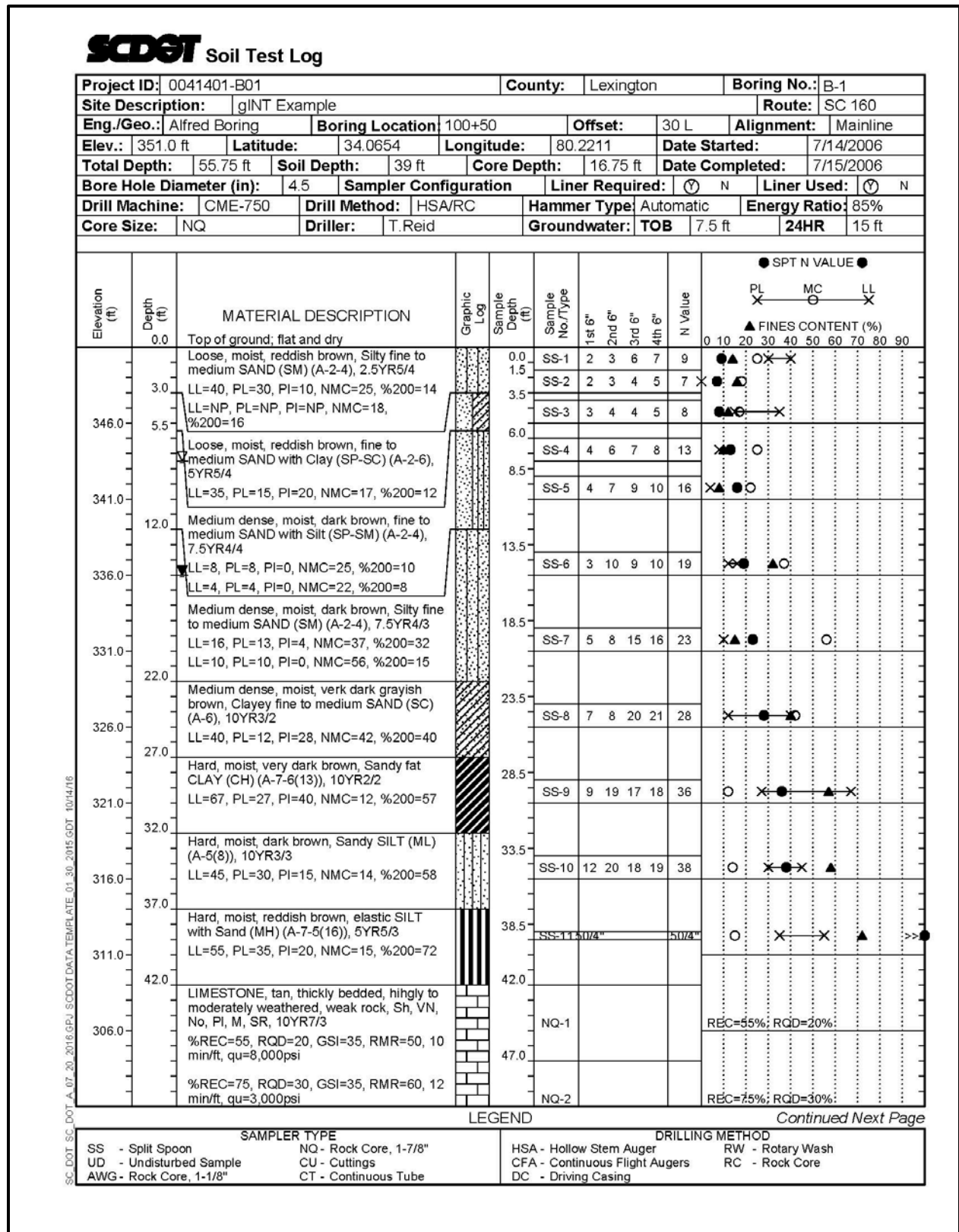


Figure 6-19, Soil Test Log Example

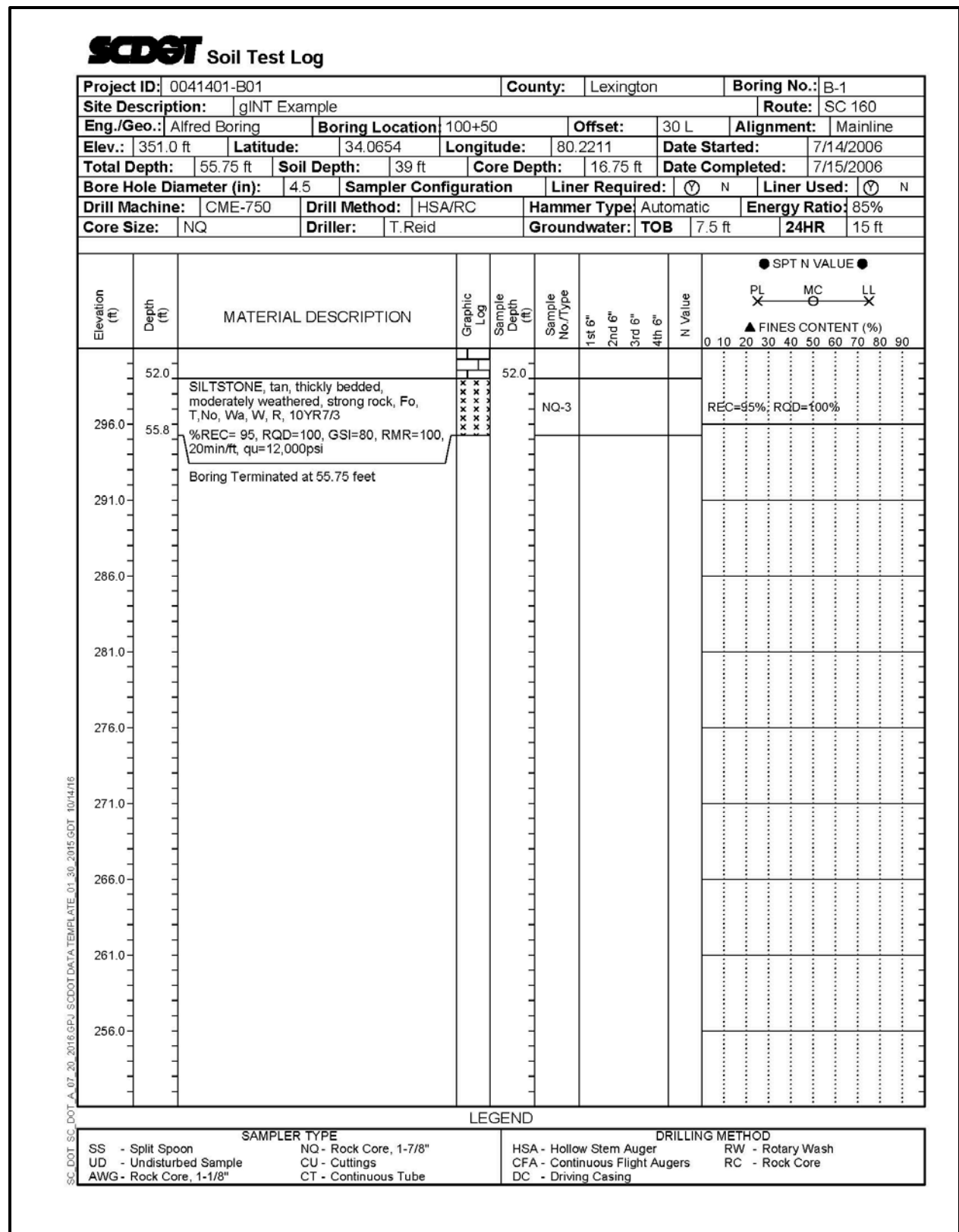


Figure 6-20, Soil Test Log Example (con't)



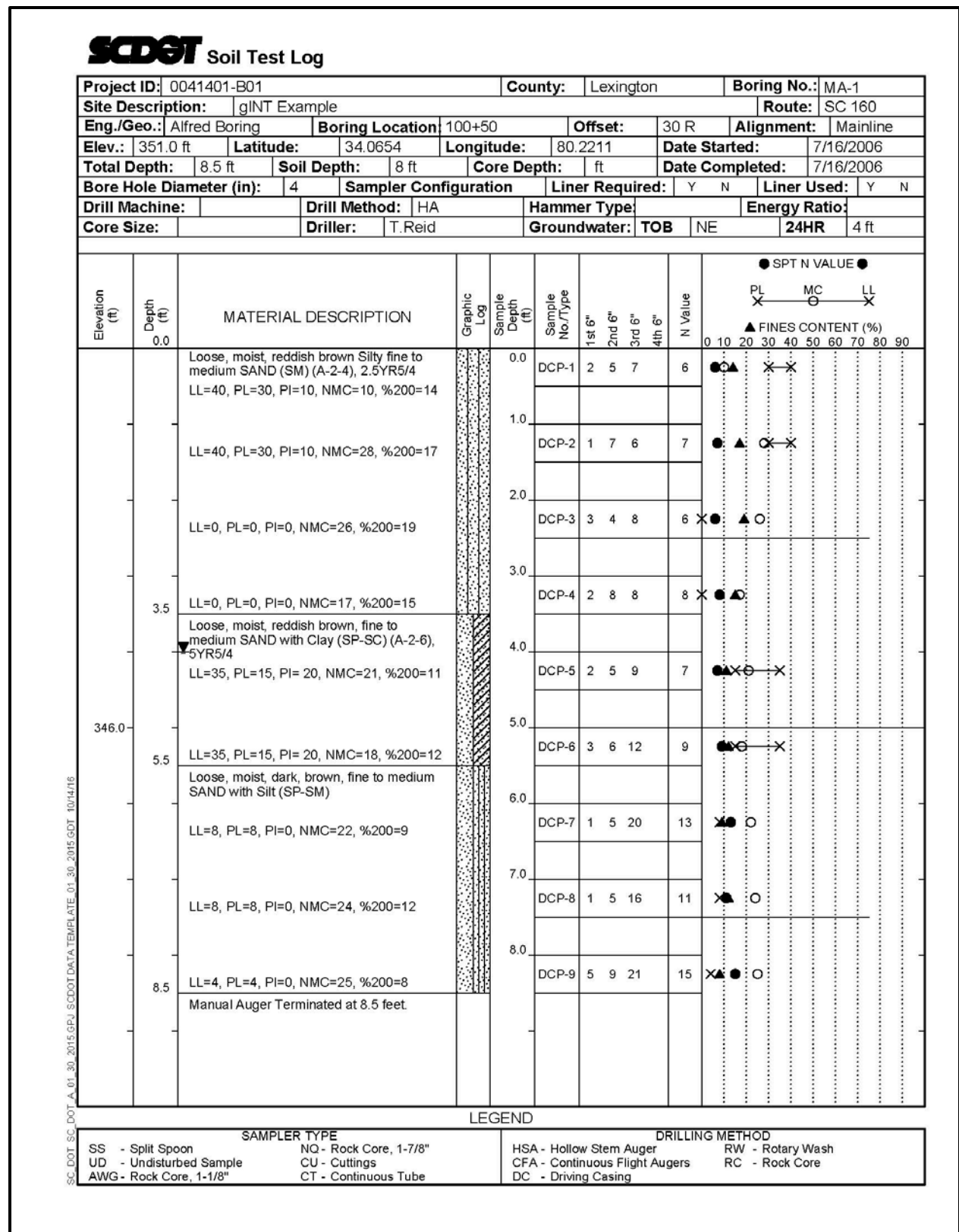


Figure 6-21, Manual Auger Log Example

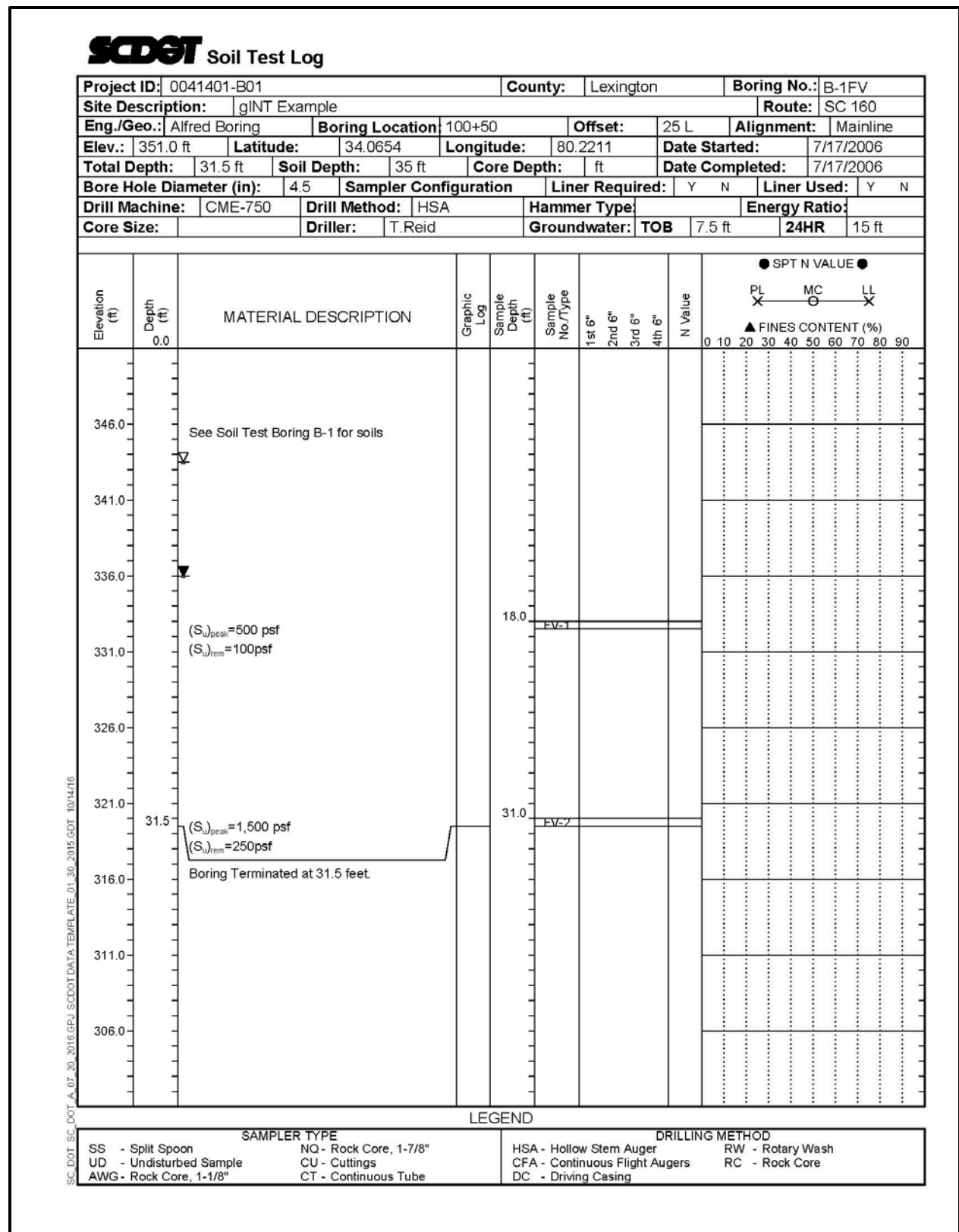


Figure 6-22, Field Vane Shear Testing Log Example



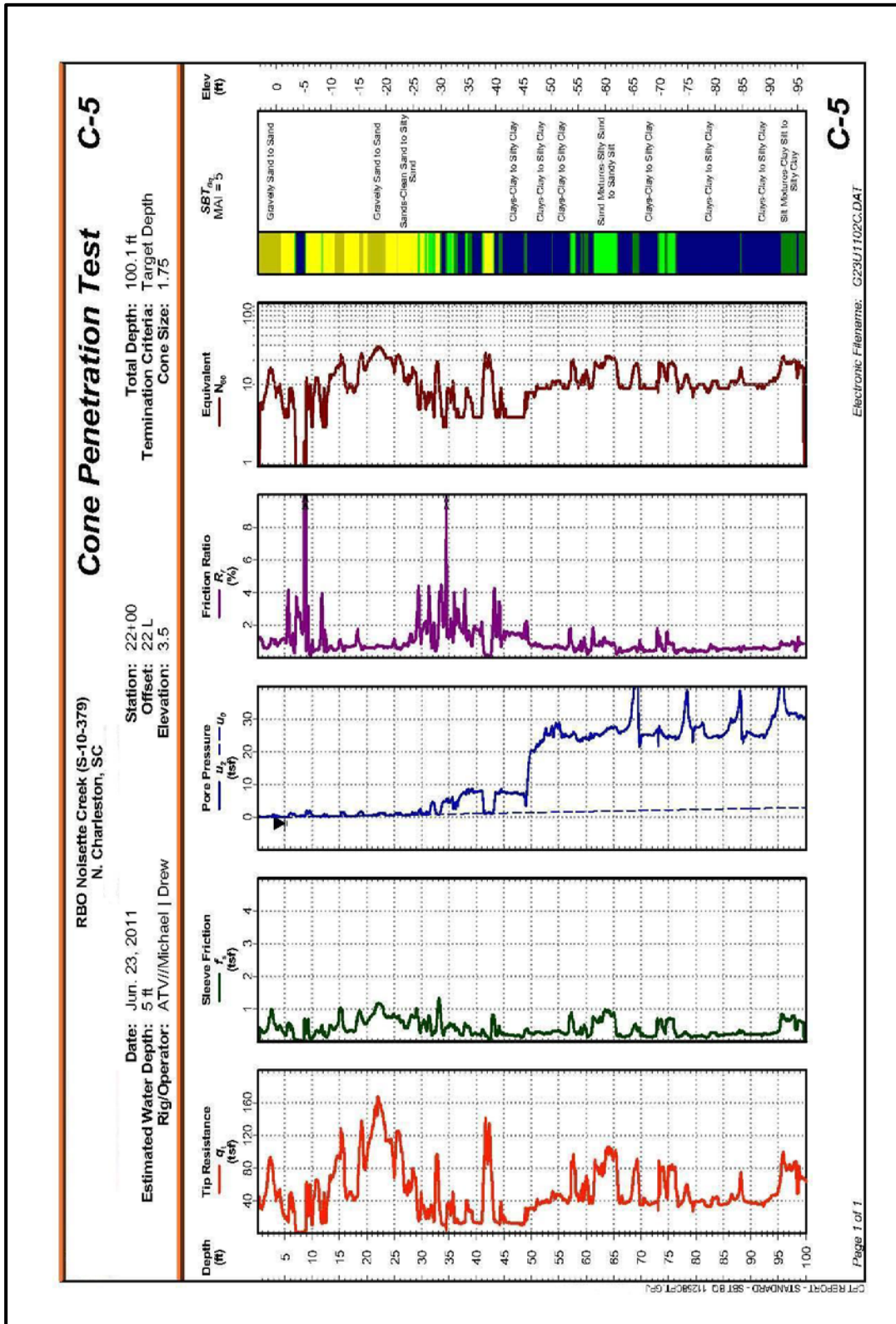


Figure 6-24, Electro-Piezocone Sounding Record Example

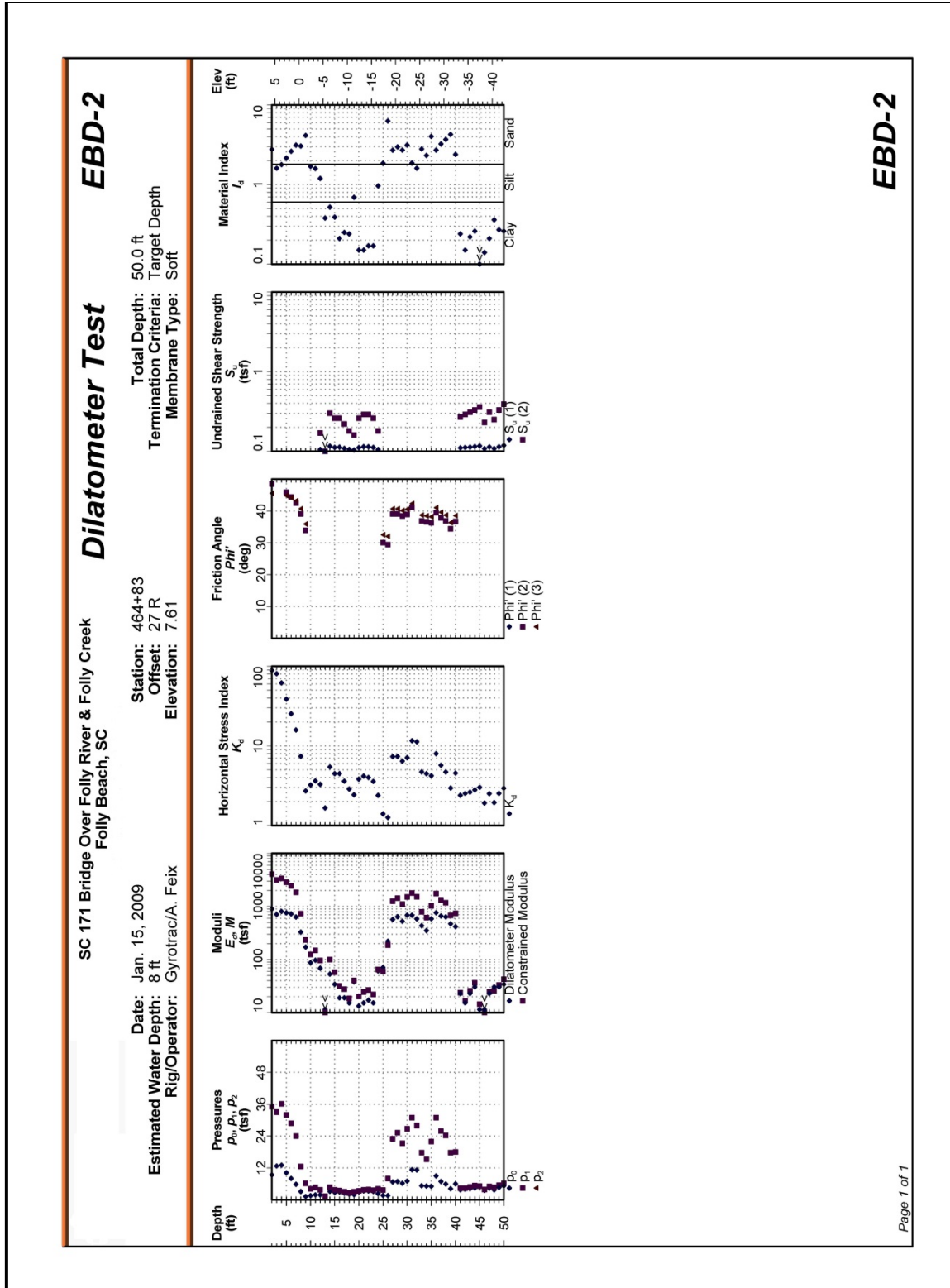
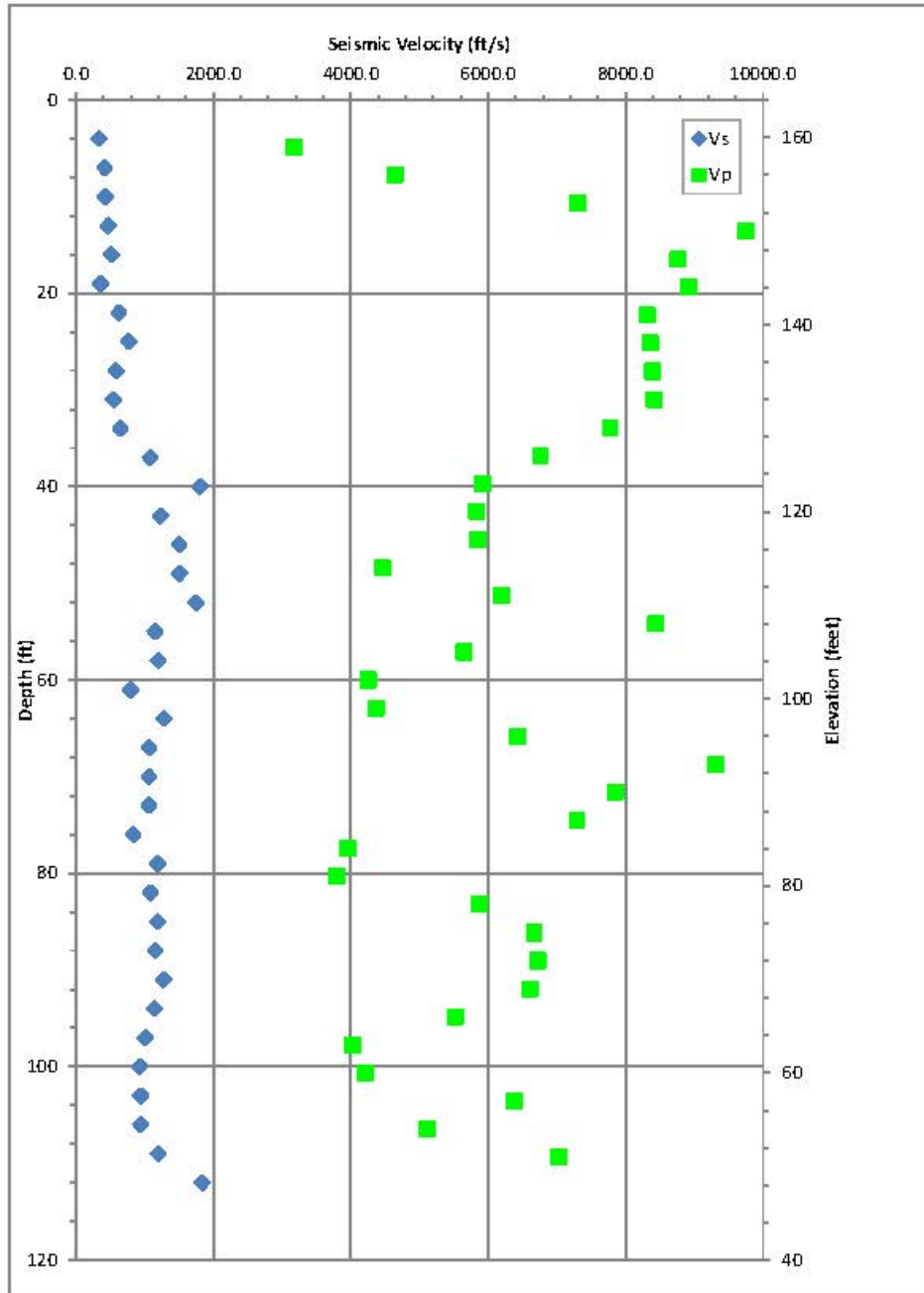


Figure 6-25, Dilatometer Sounding Record Example



1 of 1

Figure 6-26, Shear and Compression Wave Velocity Profile vs. Depth



**Shear Wave Velocity Calculation**

Project ID:	36261	County:	16 - Darlington	Sounding ID:	STB-3
Project Descrip.:	RBO High Hill Creek		Route:	US 401	
Geopone Offset:	0	feet	Elevation:	163	feet NAVD 88
Casing Stickup:	0	feet	Date:	9/24/2015	
Source Offset:	6	feet	Eng. Firm:	Any Firm	

Interval Depth (feet)	Interval Elevation (feet)	$V_s$ (ft/s)	$V_p$ (ft/s)	Poissons Ratio, $\nu$
-----------------------	---------------------------	--------------	--------------	-----------------------

4	159	337.1	3176.4	0.494
7	156	417.7	4640.6	0.496
10	153	426.8	7298.1	0.498
13	150	466.3	9747.6	0.499
16	147	513.8	8765.4	0.498
19	144	361.0	8925.8	0.499
22	141	624.4	8313.0	0.497
25	138	765.7	8359.8	0.496
28	135	584.5	8394.1	0.498
31	132	553.1	8420.0	0.498
34	129	646.0	7774.9	0.497
37	126	1083.4	6758.0	0.487
40	123	1805.4	5923.1	0.449
43	120	1225.6	5835.3	0.477
46	117	1504.8	5841.2	0.464
49	114	1506.0	4452.0	0.435
52	111	1746.5	6188.5	0.457
55	108	1152.2	8440.6	0.491
58	105	1198.6	5645.5	0.476
61	102	797.2	4246.8	0.482
64	99	1279.8	4361.0	0.453
67	96	1064.6	6427.8	0.486
70	93	1064.9	9303.3	0.493
73	90	1065.2	7845.2	0.491
76	87	834.6	7288.7	0.493
79	84	1188.6	3946.2	0.450
82	81	1085.2	3794.0	0.455
85	78	1189.0	5875.4	0.479
88	75	1157.1	6668.2	0.484
91	72	1274.1	6723.2	0.481
94	69	1139.6	6601.5	0.485
97	66	1008.7	5512.8	0.483
100	63	927.8	4028.3	0.472
103	60	943.7	4209.7	0.474
106	57	943.8	6369.5	0.489
109	54	1197.5	5100.7	0.471
112	51	1834.1	7029.2	0.463

1 of 1

**Figure 6-27, Shear and Compression Wave Velocity Profile Table**



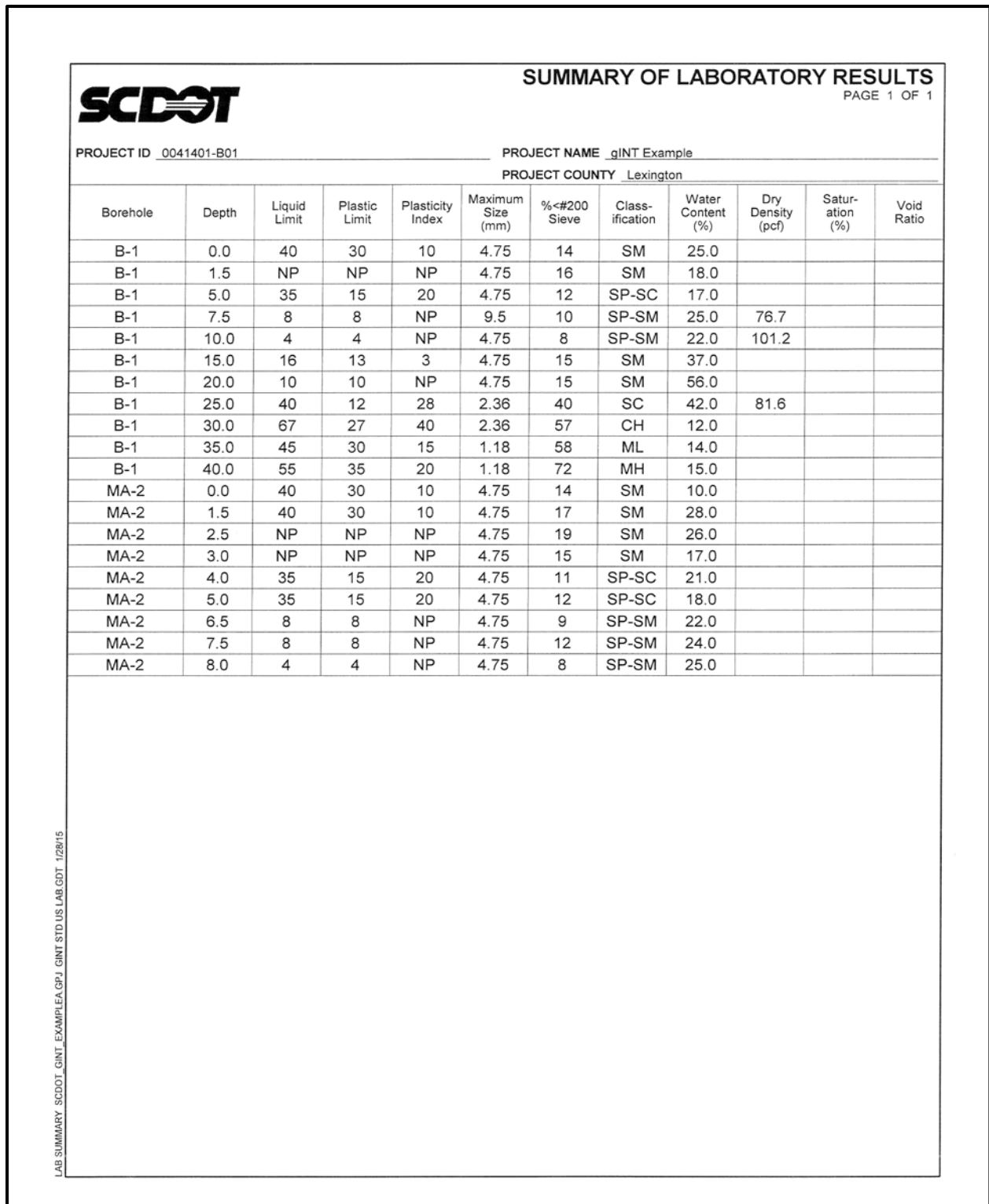


Figure 6-28, Summary of Laboratory Testing Results



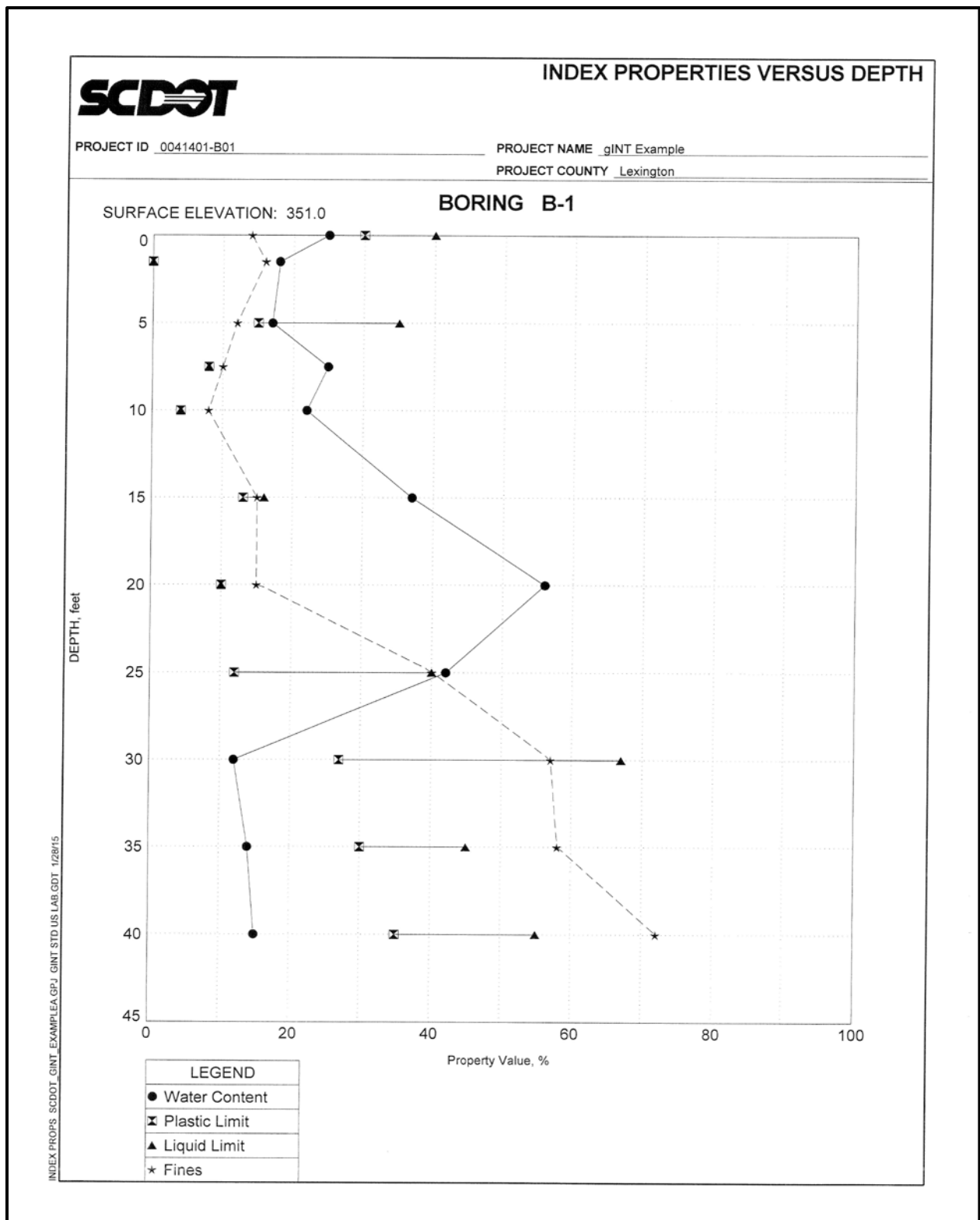


Figure 6-29, Index Properties versus Depth

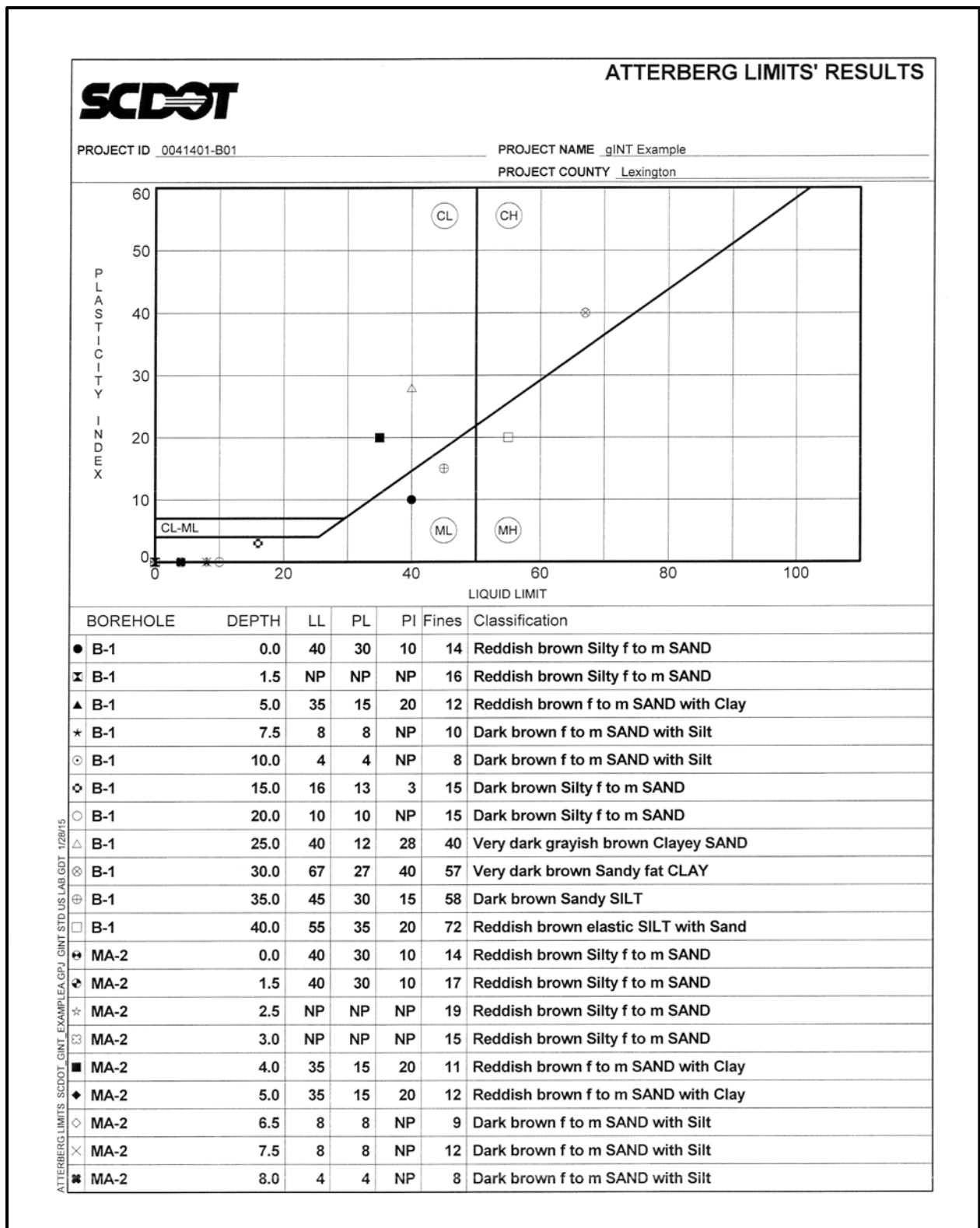


Figure 6-30, Moisture-Plasticity Relationship Testing Results

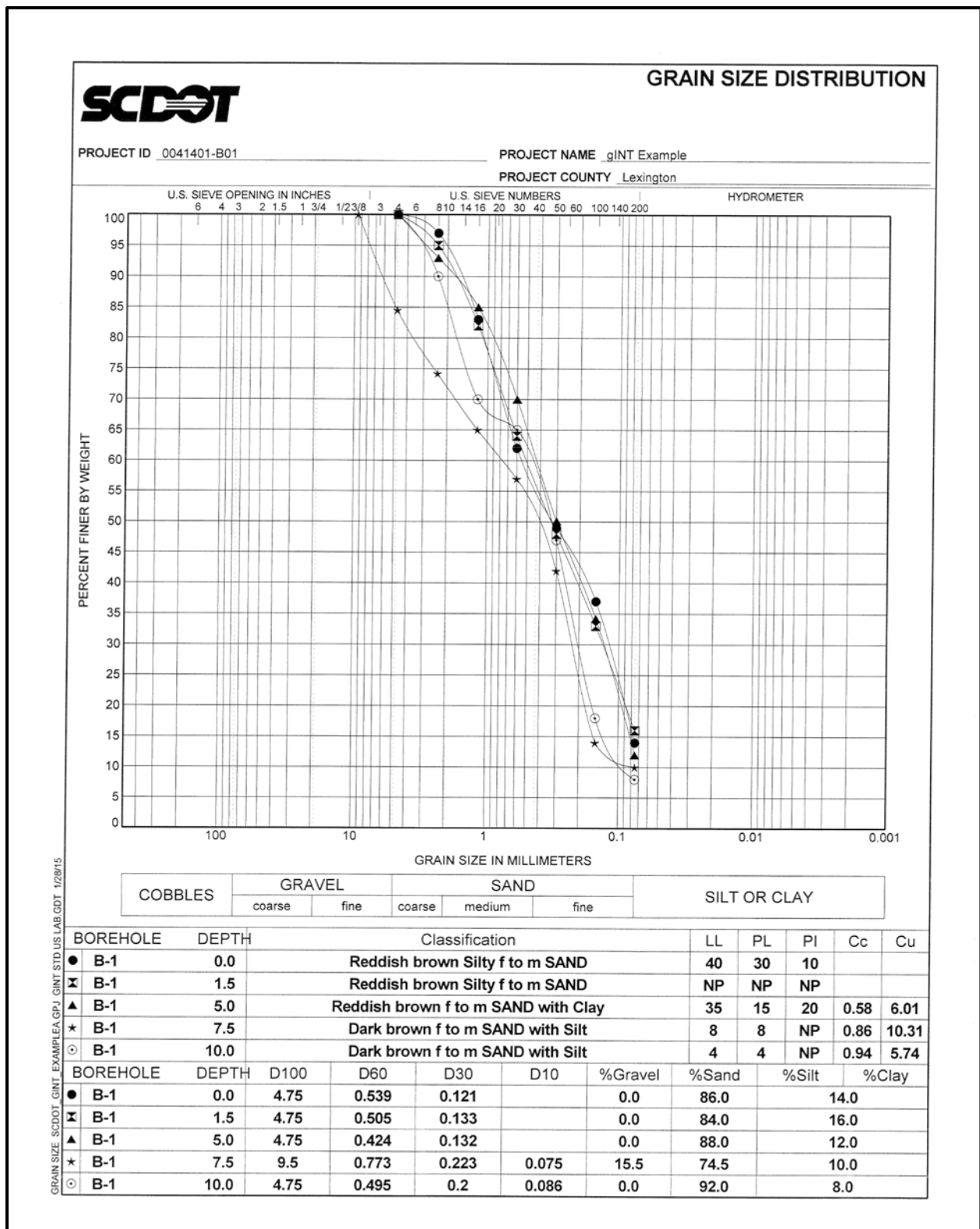


Figure 6-31, Grain-Size Analysis Results

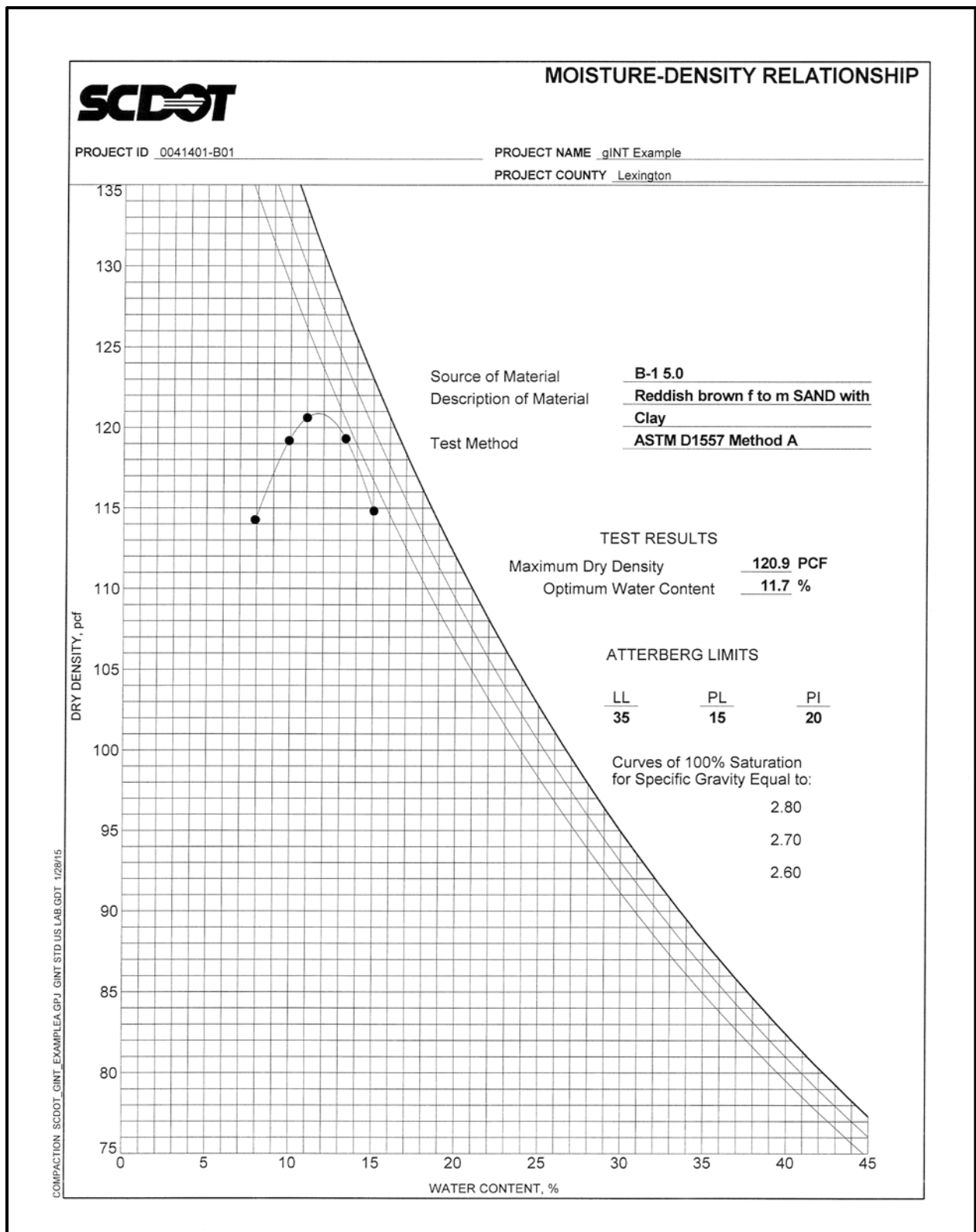


Figure 6-32, Moisture-Density Relationship Testing Results



Project ID:	36261	County:	16 - Darlington	Boring No:	B-9U
Project Descrip.:	RBO Jefferies Creek		Route:	US 401	
UD Sample No.:	ST-1	Depth:	8.0' - 10.0'		
Date Sampled:	5/25/2016	Date Extracted:	7/14/2016		
Extracted By:	Z. Bore	Eng. Firm:	Any Firm		

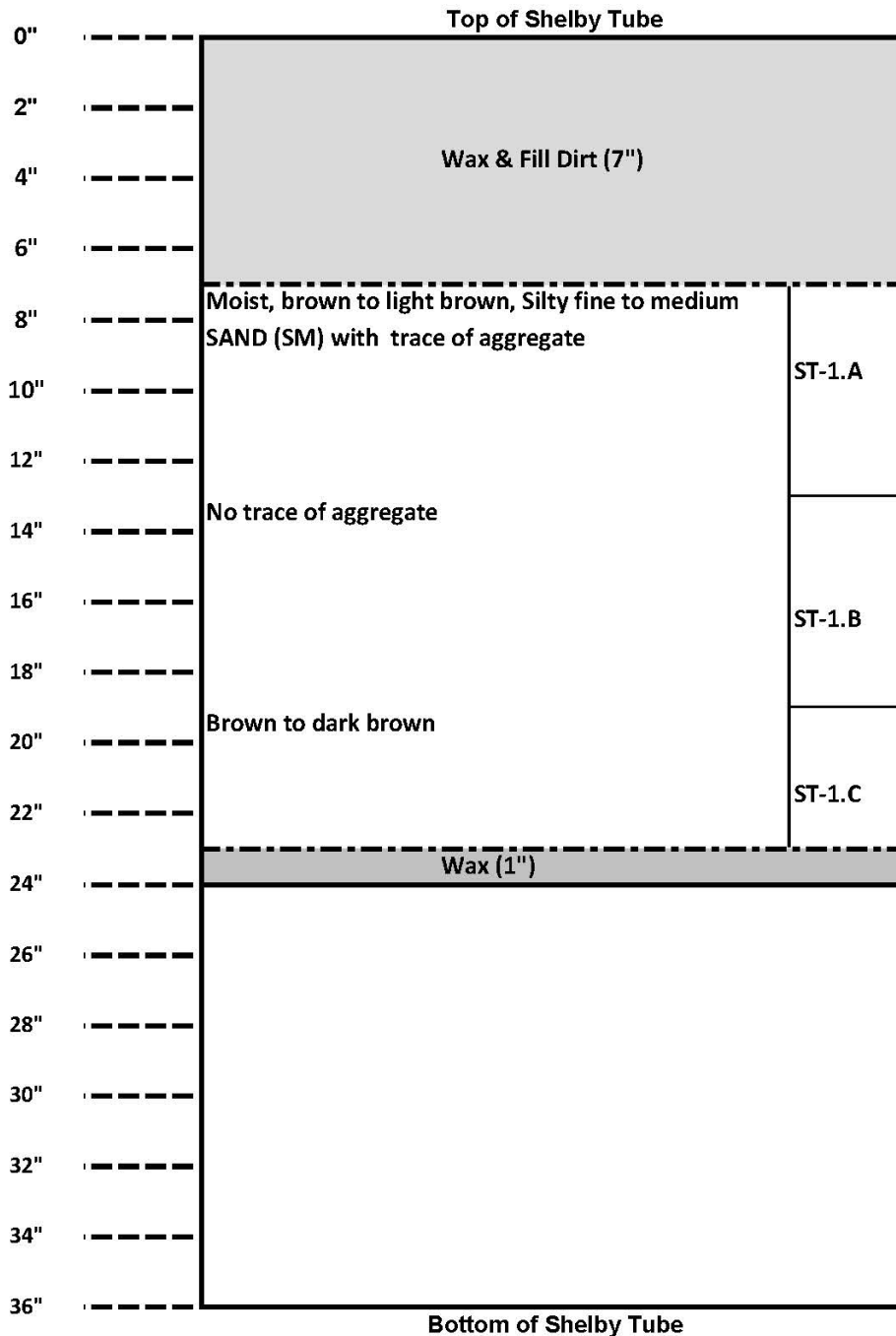


Figure 6-33, Shelby Tube Log Example

**SCDOT**

Project ID:	36261	County:	16 - Darlington	Boring No:	B-9U
Site Description:	RBO Jefferies Creek		Route:	US 401	
UD Sample No.:	ST-1	Depth:	8.0' - 10.0'		
Date Sampled:	42515	Date Extracted:	42565		
Extracted By:	Z. Bore		Eng. Firm:	Any Firm	

Specimen No.

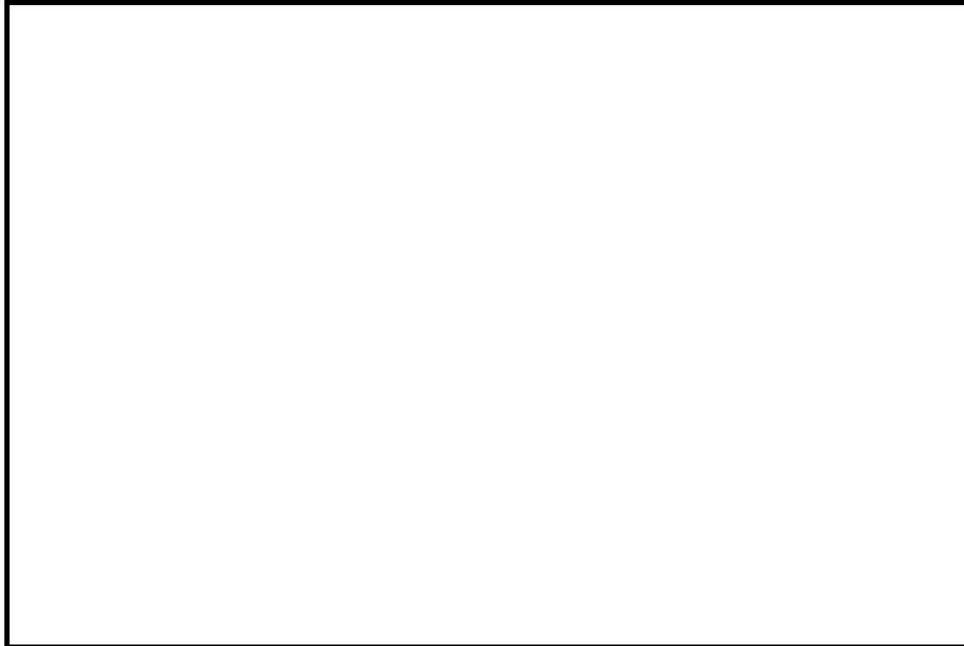
  

Specimen No.

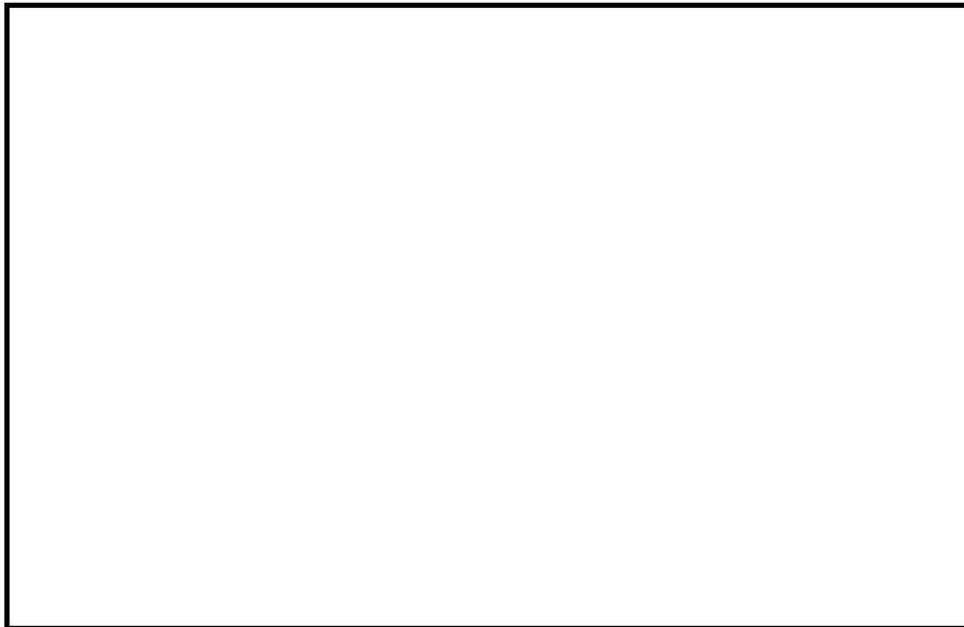
Figure 6-34, Shelby Tube Log Photograph Example



Project ID:	36261	County:	16 - Darlington	Boring No:	B-9U
Site Description:	RBO Jefferies Creek		Route:	US 401	
UD Sample No.:	ST-1	Depth:	8.0' - 10.0'		
Date Sampled:	42515	Date Extracted:	42565		
Extracted By:	Z. Bore	Eng. Firm:	Any Firm		



Specimen No.



Specimen No.

Figure 6-35, Shelby Tube Log Photograph Example

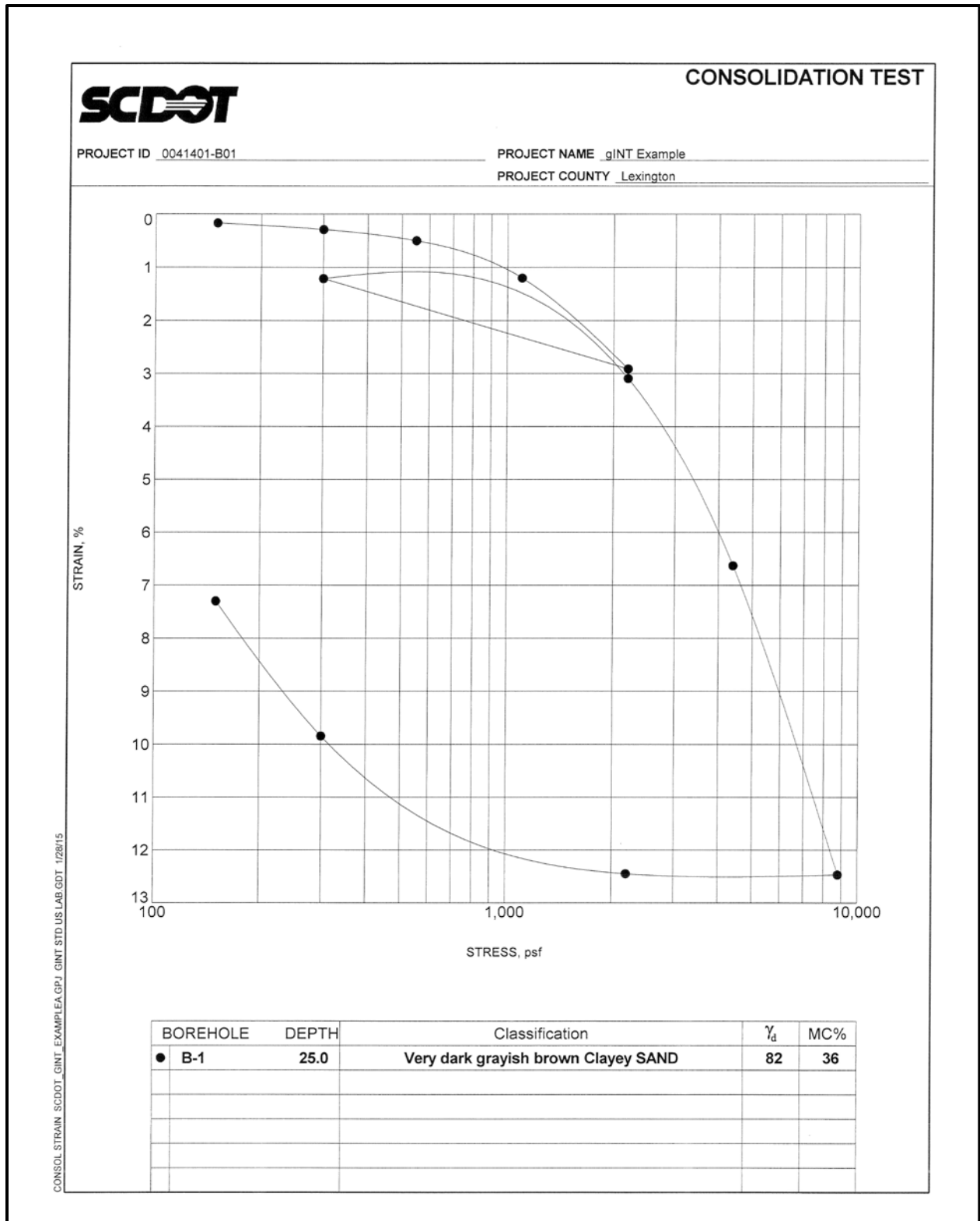


Figure 6-36, Consolidation Testing Results



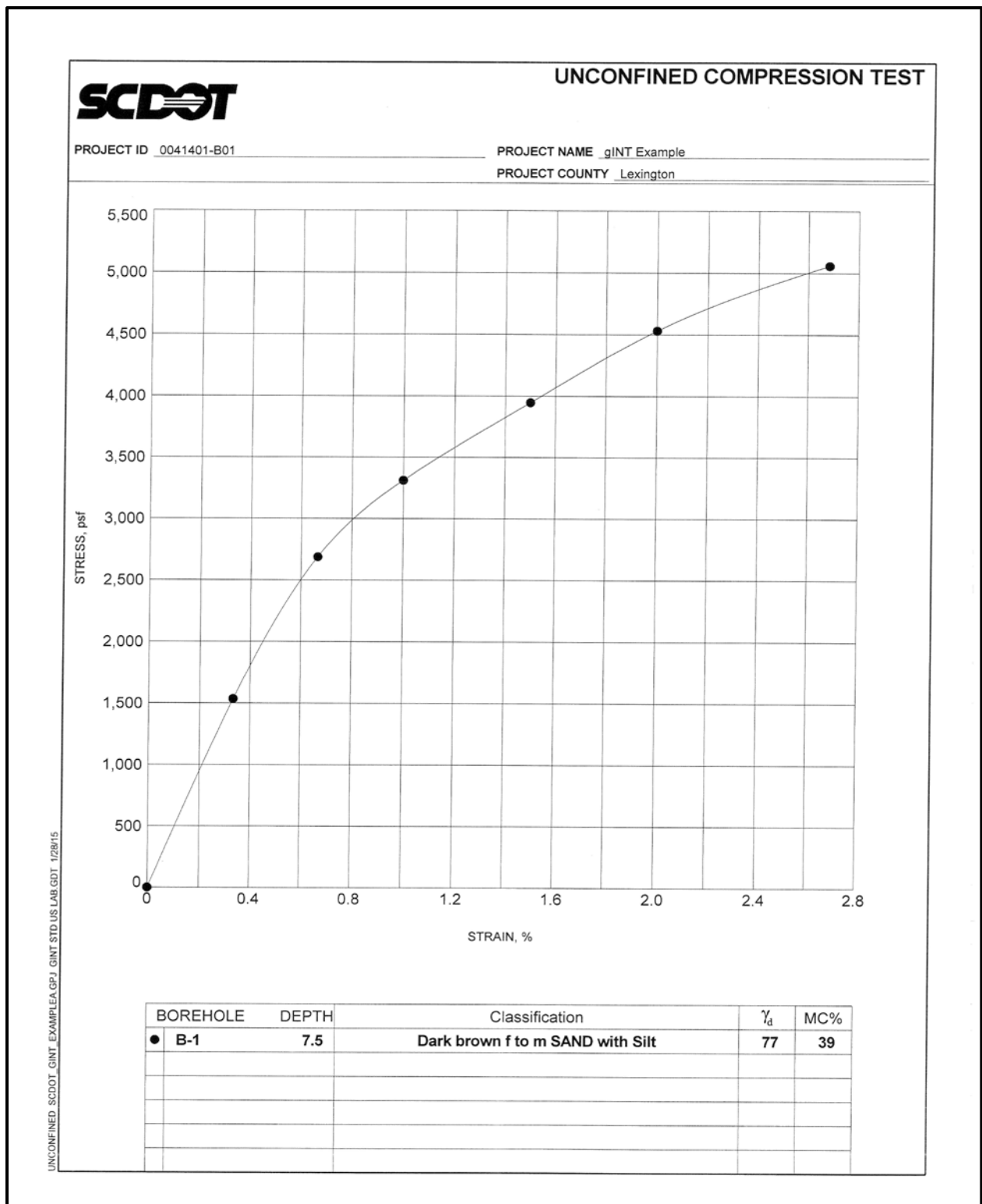


Figure 6-37, Unconfined Compression Testing Results

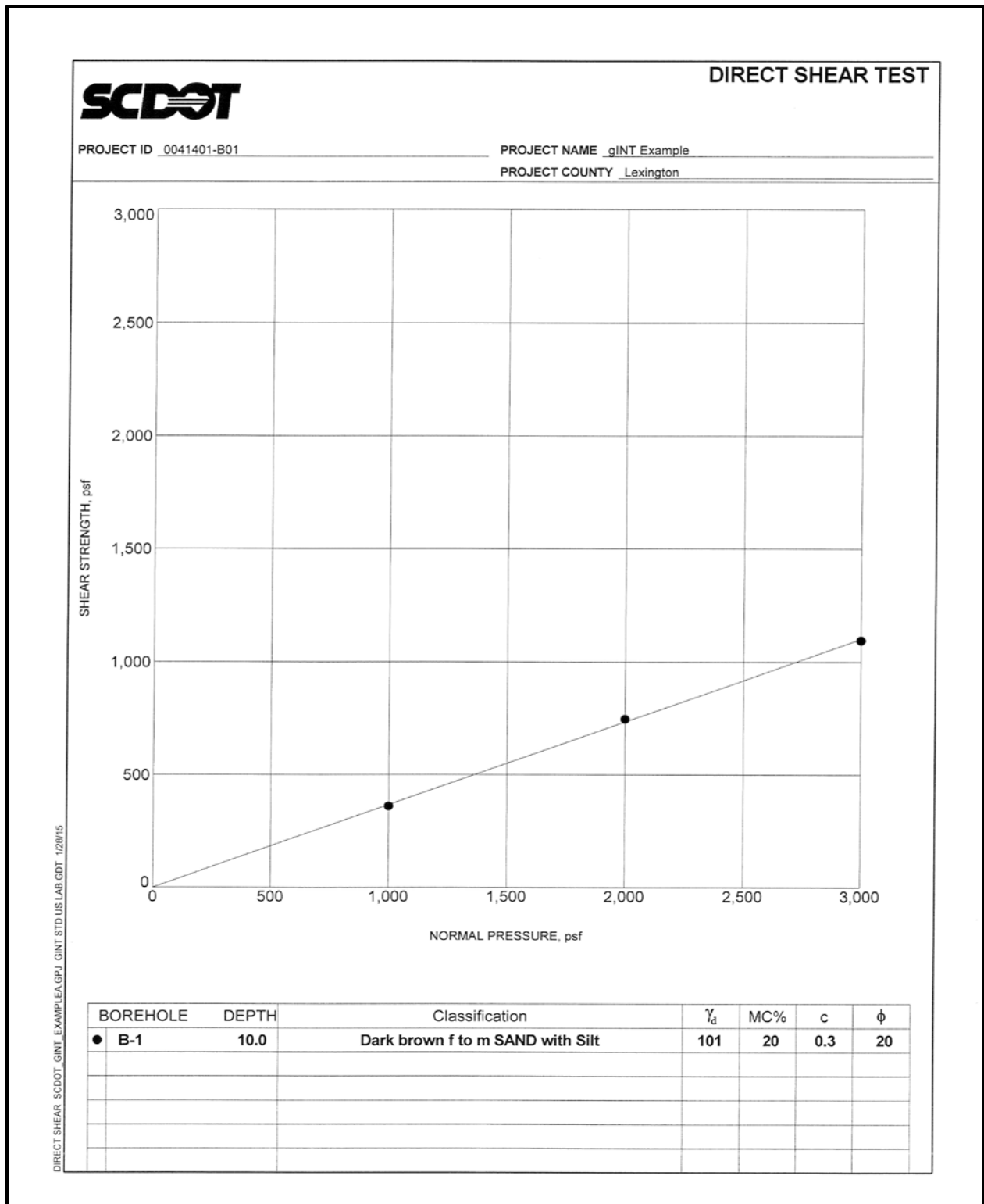
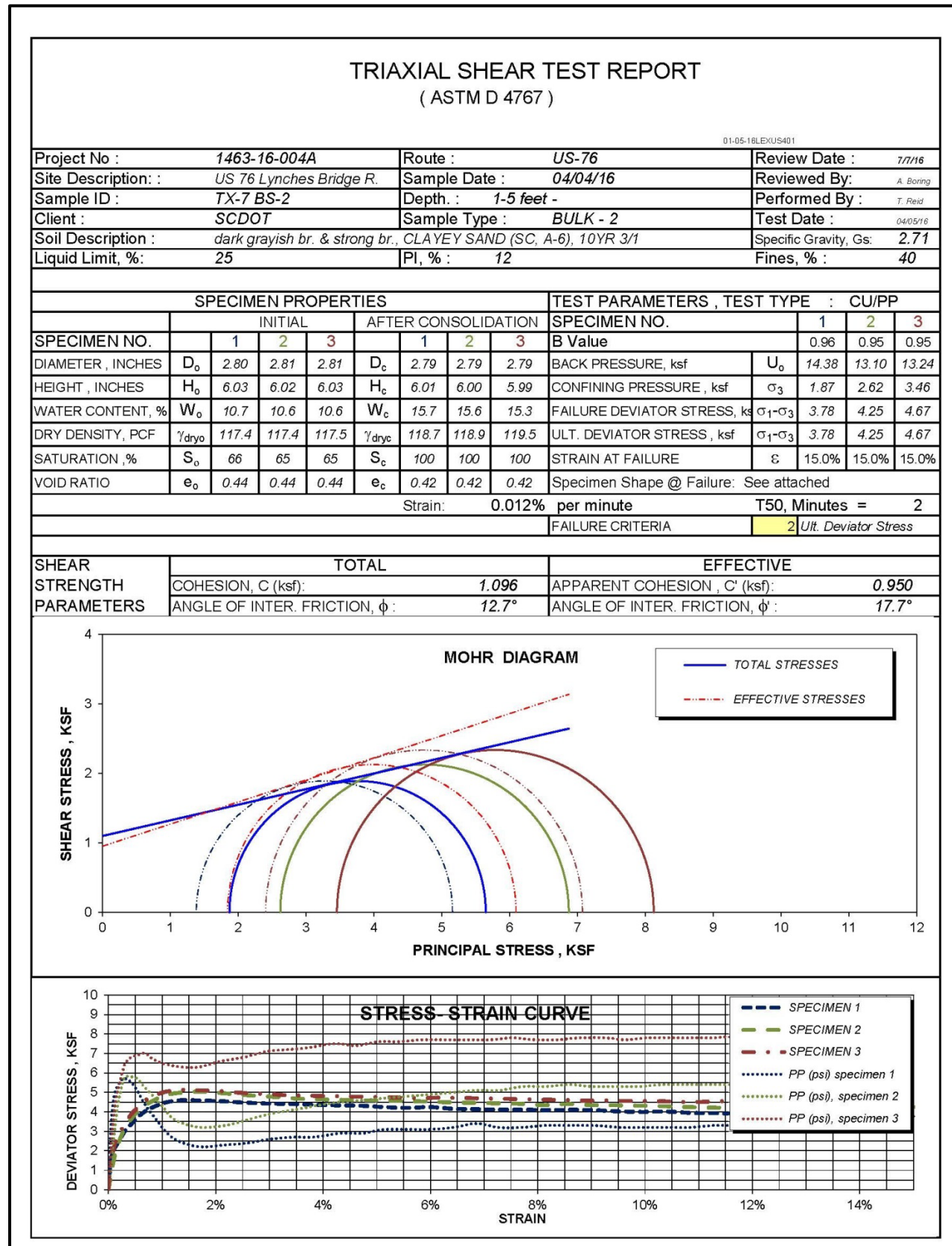


Figure 6-38, Direct Shear Testing Results



**Figure 6-39, Triaxial Shear Testing Results**

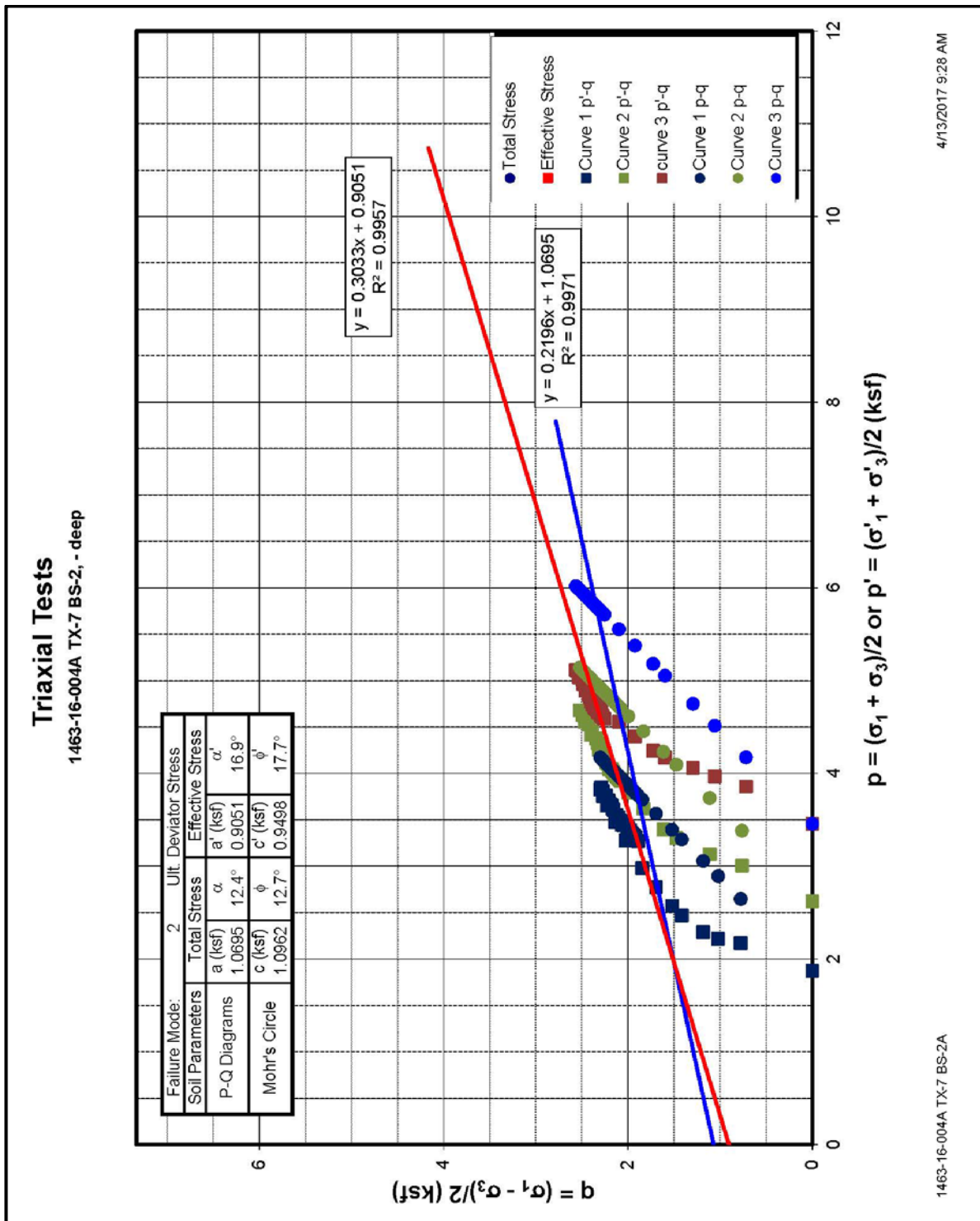


Figure 6-40, p-q Plot - Triaxial Shear Testing





<b>Project</b>	SC-823 BRO Little River		<b>Diameter, in.:</b>	1.99	<b>Date:</b>	5/10/2016	
<b>Project No.:</b>	1461-15-030		<b>Length, in.:</b>	4.49	<b>Tested by:</b>	BKP	
<b>Boring Id:</b>	B-7		<b>Unit Weight, pcf:</b>	189.5	<b>Reviewed by:</b>	JBB	
<b>Sample No.:</b>	Run 1		<b>Moisture Content, %:</b>	0.1			
<b>Depth (ft):</b>	22.9-23.6		<b>Load Rate, psi/sec:</b>	70			
Data Point	Strain(10 <sup>-6</sup> )		Load (lb)	Compressive stress (psi)	Secant Modulus x10 <sup>6</sup> (psi)	Poisson's Ratio	Remarks Failure
	axial	radial					
1	0	0	0	0	0.00	0.00	
2	-50	12	2,000	643	12.86	0.24	
3	-94	27	4,000	1,286	13.68	0.29	
4	-146	39	6,000	1,929	13.21	0.27	
5	-198	54	8,000	2,572	12.99	0.27	
6	-253	68	10,000	3,215	12.71	0.27	
7	-302	82	12,000	3,859	12.78	0.27	
8	-355	97	14,000	4,502	12.68	0.27	
9	-404	113	16,000	5,145	12.73	0.28	
10	-462	130	18,000	5,788	12.53	0.28	
11	-513	145	20,000	6,431	12.54	0.28	
12	-569	161	22,000	7,074	12.43	0.28	
13	-623	179	24000	7,717	12.39	0.29	
14	-679	196	26,000	8,360	12.31	0.29	
15	-732	212	28,000	9,003	12.30	0.29	
16	-790	231	30,000	9,646	12.21	0.29	
17	-849	249	32,000	10,289	12.12	0.29	
18	-961	287	36,000	11,576	12.05	0.30	
19	-1,078	324	40,000	12,862	11.93	0.30	
20	-1,197	366	44,000	14,148	11.82	0.31	
21	-1,321	410	48,000	15,434	11.68	0.31	
22	-1,443	459	52,000	16,720	11.59	0.32	
23	-1,577	513	56,000	18,006	11.42	0.33	
24	-1,710	571	60,000	19,293	11.28	0.33	
25	-1,843	638	64,000	20,579	11.17	0.35	
28	-1,989	714	68,000	21,865	10.99	0.36	
29	-2,131	801	72,000	23,151	10.86	0.38	
30	-2,287	906	76,000	24,437	10.69	0.40	
31	-2,457	1,048	80,000	25,724	10.47	0.43	
32	-2,627	1,221	84,000	27,010	10.28	0.46	
33	-2,829	1,541	88,000	28,296	10.00	0.54	
34			89,530	28,788			Failure



Figure 6-42, Rock Core Testing Results

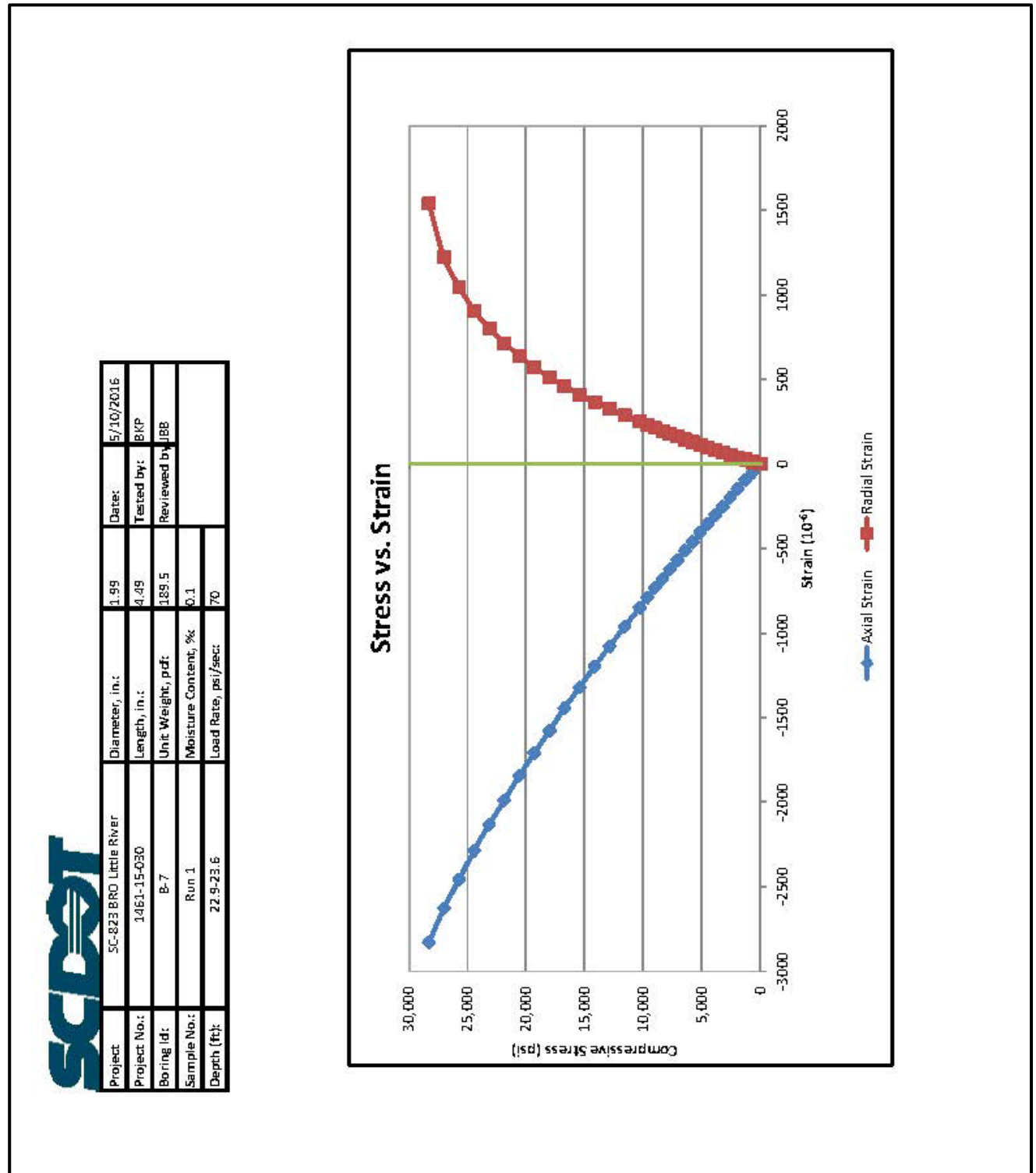


Figure 6-43, Rock Core Testing Stress versus Strain Graph

**Chapter 7**  
**GEOMECHANICS**

**GEOTECHNICAL DESIGN MANUAL**

*January 2019*





## Table of Contents

<u>Section</u>	<u>Page</u>
7.1	Introduction.....7-1
7.2	Geotechnical Design Approach.....7-1
7.3	Geotechnical Engineering Quality Control .....7-2
7.4	Development Of Subsurface Profiles .....7-2
7.5	Site Variability.....7-2
7.6	Preliminary Geotechnical Subsurface Exploration.....7-3
7.7	Final Geotechnical Subsurface Exploration .....7-4
7.8	Field Data Corrections and Normalization.....7-4
	7.8.1 SPT Corrections.....7-4
	7.8.2 CPTu Corrections.....7-7
	7.8.3 Correlations for Relative Density From SPT and CPTu .....7-10
	7.8.4 Dilatometer Correlation Parameters .....7-11
7.9	Soil Loading Conditions And Soil Shear Strength Selection.....7-12
	7.9.1 Soil Loading .....7-12
	7.9.2 Soil Response.....7-13
	7.9.3 Soil Strength Testing.....7-21
7.10	Total Stress .....7-28
	7.10.1 Sand-Like Soils .....7-28
	7.10.2 Clay-Like Soils .....7-29
	7.10.3 Transitional Soils.....7-35
	7.10.4 Maximum Allowable Total Soil Shear Strengths .....7-35
7.11	Effective Stress.....7-35
	7.11.1 Sand-Like Soils .....7-36
	7.11.2 Clay-Like Soils .....7-39
	7.11.3 Transitional Soils.....7-47
	7.11.4 Maximum Allowable Effective Soil Shear Strength .....7-47
7.12	Borrow Materials Soil Shear Strength Selection.....7-48
	7.12.1 SCDOT Borrow Specifications .....7-49
	7.12.2 USDA Soil Survey Maps .....7-50
	7.12.3 Compacted Soils Shear Strength Selection.....7-52
	7.12.4 Allowable Soil Shear Strengths of Compacted Soils.....7-53
7.13	Soil Settlement Parameters .....7-54
	7.13.1 Elastic Parameters.....7-54
	7.13.2 Consolidation Parameters .....7-56
7.14	Rock Parameter Determination.....7-62
	7.14.1 Shear Strength Parameters.....7-62
	7.14.2 Settlement Parameters.....7-63
7.15	Scour.....7-64
	7.15.1 Soil.....7-65
	7.15.2 Rock.....7-65
7.16	Dynamic Properties – General .....7-69
7.17	Soil Dynamic Properties.....7-70
	7.17.1 Soil Consistency.....7-70
	7.17.2 Shear Wave Velocity/Initial Shear Modulus .....7-71
	7.17.3 Cyclic Stress-strain Behavior.....7-75
	7.17.4 Cyclic Residual Shear Strength.....7-85
7.18	Rock Dynamic Properties .....7-85
7.19	Electro-Chemical Properties .....7-85
7.20	References .....7-86

**List of Tables**

<b><u>Table</u></b>	<b><u>Page</u></b>
Table 7-1, Site Variability Defined By $\overline{COV}$ .....	7-3
Table 7-2, Assumed Energy Ratio by Hammer Type ( $C_E$ ) .....	7-5
Table 7-3, Rod Length Correction ( $C_R$ ).....	7-6
Table 7-4, Sampler Configuration Correction ( $C_S$ ).....	7-6
Table 7-5, Borehole Diameter Correction ( $C_B$ ).....	7-6
Table 7-6, Soil Response Classification .....	7-14
Table 7-7, OCR Values .....	7-19
Table 7-8, Soil Shear Strength Selection Based on Strain Level .....	7-21
Table 7-9, Bridge Foundation Soil Parameters.....	7-22
Table 7-10, Earth Retaining Structures & Embankment Soil Parameters .....	7-23
Table 7-11, Laboratory Testing Soil Shear Strength Determination.....	7-25
Table 7-12, In-Situ Testing - Soil Shear Strength Determination .....	7-26
Table 7-13, Soil Suitability of In-Situ Testing Methods.....	7-27
Table 7-14, Sensitivity of Cohesive Soils.....	7-33
Table 7-15, Residual Shear Strength Loss Factor ( $\lambda_r$ ) .....	7-34
Table 7-16, Maximum Allowable Total Soil Shear Strengths .....	7-35
Table 7-17, Maximum Allowable Effective Soil Shear Strengths .....	7-48
Table 7-18, Elastic Modulus Correlations For Soil Using SPT N-values .....	7-54
Table 7-19, Typical Elastic Modulus and Poisson Ratio Values for Soil .....	7-56
Table 7-20, Correction of the e-log p Curve for Disturbance.....	7-57
Table 7-21, Correction of the $\epsilon$ -log p Curve for Disturbance .....	7-58
Table 7-22, Constants m and s based on RMR.....	7-63
Table 7-23, Values of Rock Mass Strength Parameter, $M_s$ .....	7-66
Table 7-24, Rock Joint Set Number $J_n$ .....	7-67
Table 7-25, Joint Roughness Number, $J_r$ .....	7-67
Table 7-26, Joint Alteration Number, $J_a$ .....	7-67
Table 7-27, Relative Orientation Parameter, $J_s$ .....	7-69
Table 7-28, Typical Small-Strain Shear Wave Velocity and Initial Shear Modulus.....	7-72
Table 7-29, Recommended Values $\gamma_{cr1}$ , $\alpha$ , and k for SC Soils.....	7-79
Table 7-30, Procedure for Computing $G/G_{max}$ .....	7-80
Table 7-31, Recommended Value $\lambda_{min1}$ (%) for SC Soils .....	7-81
Table 7-32, Procedure for Computing Damping Ratio .....	7-83
Table 7-33, Alternate Correlations for Determining Soil Stiffness Based on $G_{max}$ .....	7-84
Table 7-34, Criteria for Substructure Environmental Classifications .....	7-86

**List of Figures**

<b>Figure</b>	<b>Page</b>
Figure 7-1, Schematic of Thin Layer Effects.....	7-8
Figure 7-2, CPTu Thin Layer Correction ( $C_{Thin}$ ) .....	7-9
Figure 7-3, Normalized CPT Soil Behavior Chart Using $Q_T$ versus $B_q$ .....	7-10
Figure 7-4, Drainage Time Required.....	7-15
Figure 7-5, Drained Stress-Strain Behavior .....	7-16
Figure 7-6, Shear Strength Sands (Direct Shear-Test).....	7-17
Figure 7-7, Shear Strength of Clay Consolidated Drained Triaxial.....	7-20
Figure 7-8, Shear Strength of Clay Consolidated Undrained Triaxial.....	7-20
Figure 7-9, Shear Modes for Embankment Stability Shear Failure Surface .....	7-24
Figure 7-10, $\tau$ of Clays and Shales as Function of Failure Orientation .....	7-24
Figure 7-11, Shear Strength Measured by In-Situ Testing.....	7-26
Figure 7-12, Total Principal Stresses .....	7-28
Figure 7-13, Undrained Shear Strength – SPT Relationship .....	7-30
Figure 7-14, Undrained Shear Strength Ratio and OCR Relationship .....	7-32
Figure 7-15, Sensitivity based on Liquidity Index and $\sigma'_{vo}$ .....	7-33
Figure 7-16, Remolded Shear Strength vs Liquidity Index.....	7-34
Figure 7-17, Effective Principal Stresses.....	7-36
Figure 7-18, Effective Peak Friction Angle and SPT ( $N_{1,60}^*$ ) Relationship .....	7-37
Figure 7-19, Effective Peak Friction Angle and CPT ( $q_t$ ) Relationship .....	7-38
Figure 7-20, Effective Peak Friction Angle and DMT ( $K_D$ ) Relationship .....	7-38
Figure 7-21, Overconsolidated Clay Failure Envelope (CUw/pp Triaxial Test) .....	7-39
Figure 7-22, Plasticity Index versus Drained Friction Angle for NC Clays.....	7-40
Figure 7-23, Plasticity Index versus Drained Shear Resistance for NC Clays .....	7-41
Figure 7-24, Plasticity Index versus Drained Shear Resistance for OC Clays .....	7-42
Figure 7-25, Undrained Shear Strength versus Drained Shear Resistance for OC Clays.....	7-43
Figure 7-26, Drained Residual Friction Angle and Liquid Limit Relationship.....	7-44
Figure 7-27, Updated Drained Residual Friction Angle and Liquid Limit Relationship .....	7-44
Figure 7-28, Borrow Material Specifications By County.....	7-50
Figure 7-29, USDA Soil Map – Newberry County, South Carolina.....	7-51
Figure 7-30, USDA Roadfill Source Map - Newberry County, South Carolina .....	7-52
Figure 7-31, Corrected e-log p Normally Consolidated Curve .....	7-57
Figure 7-32, Corrected e-log p Overconsolidated Curve .....	7-57
Figure 7-33, Corrected $\epsilon$ -log p Normally Consolidated Curve.....	7-58
Figure 7-34, Corrected $\epsilon$ -log p Overconsolidated Curve.....	7-58
Figure 7-35, Secondary Compression Index Chart.....	7-60
Figure 7-36, Consolidation Coefficient and Liquid Limit Relationship .....	7-61
Figure 7-37, Stresses Induced in a Soil Element by Vertical Shear Wave.....	7-75
Figure 7-38, Hysteretic Stress-Strain Loop for Uniform Cyclic Loading .....	7-76
Figure 7-39, Example Shear Modulus Reduction and Damping Ratio Curve.....	7-77
Figure 7-40, $\lambda_{min1}$ , Small-Strain Damping @ $\sigma'_m = 1$ atm.....	7-81
Figure 7-41, $(\lambda - \lambda_{min})$ vs. $(G/G_{max})$ Relationship .....	7-82



# CHAPTER 7

## GEOMECHANICS

### 7.1 INTRODUCTION

This Chapter presents the geotechnical design philosophy of SCDOT. This philosophy includes the approach to the geotechnical investigations of the project and the correlations that link the field and laboratory work that precedes this Chapter to the engineering analysis that is subsequent to this Chapter. The approach to the geotechnical investigation of transportation projects entails the use of preliminary and final explorations and reports. The development of an understanding of the regional and local geological environment and the effect of seismicity on the project is required. The geotechnical approach provided in this Chapter is not meant to be the only approach, but a representative approach of the thought process expected to be used on SCDOT projects. The GEOR shall develop a design approach that reflects both the requirements of this Manual as well as a good standard-of-practice. While there is some flexibility in the approach to the design process, the correlations provided in this Chapter shall be used unless written permission is obtained in advance. All requests for changes shall be submitted to the PCS/GDS for review and approval. These correlations were adopted after a review of the geotechnical state-of-practice within the United States and the experience of SCDOT.

### 7.2 GEOTECHNICAL DESIGN APPROACH

Geotechnical engineering requires the use of science, art, and economics to perform analyses and designs that are suitable for the public use. The science of geotechnical engineering consists of using the appropriate theories to interpret field data; develop geologic profiles; select foundation types; perform analyses; develop designs, plans and specifications; construction monitoring; maintenance; etc.

The art of geotechnical engineering is far more esoteric and relies on the judgment and experience of the engineer. This is accomplished by knowing the applicability and limitations of the geotechnical analytical theories and assessing the uncertainties associated with soil properties, design methodologies, and the resulting impact on structural performance. The engineer is required to evaluate the design or analysis and decide if it is “reasonable” and whether it will meet the performance expectations that have been established. Reasonableness is a subjective term that depends on the engineer’s experience, both in design and construction. If the solution does not appear reasonable, the engineer should make the appropriate changes to develop a reasonable solution. In addition, the engineer should document why the first solution was not reasonable and why the second solution is reasonable. This documentation is an important part of the development of the design approach. If the solution appears reasonable, then the design proceeds to the economics of geotechnical engineering.

The economics of geotechnical engineering assesses the effectiveness of the solution from a cost perspective. Sometimes geotechnical engineers get caught up in the science and art of geotechnical engineering and do not evaluate other non-geotechnical solutions that may be cost effective both in design and construction. For example, alternate alignments could be explored to avoid poor soils, decreasing vertical alignment to reduce surface loads, placing alternate designs on the plans to facilitate competitive bidding, etc. The science, art, and economics are not sequential facets of geotechnical engineering but are very often intermixed throughout the design process.

### 7.3 GEOTECHNICAL ENGINEERING QUALITY CONTROL

A formal internal geotechnical engineering Quality Control plan shall be established for all phases of the geotechnical engineering process and shall be made available to SCDOT upon request. The first-line geotechnical engineer is expected to perform analyses with due diligence and a self-prescribed set of checks and balances. The geotechnical Quality Control plan should include milestones in the project development where analysis, recommendations, etc. are reviewed. The review shall be conducted by at least 1 other geotechnical engineer of equal experience or higher seniority. Formal documentation of the Quality Control process shall be detectable upon review of geotechnical calculations, reports, etc. All engineering work shall be performed under the direct supervision of a Professional Engineer (P.E.) licensed by the South Carolina State Board of Registration for Professional Engineers and Surveyors in accordance with Chapter 22 of Title 40 of the 1976 Code of Laws of South Carolina, latest amendment.

### 7.4 DEVELOPMENT OF SUBSURFACE PROFILES

The SCDOT geotechnical field exploration process indicated in Chapter 4, allows for a preliminary and a final geotechnical exploration program for all projects. The primary purpose of the preliminary exploration is to provide a first glance at the project, while the final exploration is to provide all of the necessary geotechnical information to complete the final design.

It is incumbent upon the GEOR to understand the geology of the project site and determine the potential effects of the geology on the project. The GEOR should also have knowledge of the regional geology that should be used in the development of the exploration program for the project. In addition to the geologic environment, the GEOR shall be aware of the seismic environment (see Chapters 11 and 12). The GEOR is also required to know and understand the impacts of the design earthquake event on the subsurface conditions at the project site (see Chapters 13 and 14 for the impacts and designs, respectively). The geologic formation and local seismicity may have a bearing on the selection of the foundation type and potential capacity. For example, for driven piles bearing in the Cooper Marl formation of the Charleston area, prestressed concrete piles should penetrate the formation approximately 5 feet, with most of the capacity being developed by steel H-pile extensions, penetrating into the Marl.

The GEOR shall develop a subsurface profile for both the preliminary and final geotechnical subsurface explorations. The subsurface profile developed shall take into consideration the site variability as indicated in Section 7.5. The profile should account for all available data and is normally depicted along the longitudinal axis of the structure or roadway. The bridge profile shall extend from 100 feet from either end of the bridge, inclusively. However, in some cases, cross-sectional subsurface profiles transverse to the axis of the structure or roadway may be required to determine if a formation is varying (i.e., sloping bearing strata) along the transverse axis.

### 7.5 SITE VARIABILITY

Keeping in mind the geologic framework of the site, the GEOR shall evaluate the site variability (SV) or site uniformity. The SV is used in determining the resistance factor,  $\phi$ , and the required amount of load testing for deep foundations (see Chapter 9). A site with "Low" SV is more uniform than a site with "High" SV. A "High" SV shall not be allowed except with review and approval by the PC/GDS. All "High" variability, unless previously approved, sites shall be subdivided into smaller "sites" such that the SV is either "Low" or "Medium". All "sites" shall be geologically continuous (i.e., shall contain similar soils). The SV shall be determined using energy corrected SPT N-values ( $N_{60}$ ) (see Section 7.8.1.6 and Equation 7-6), or the corrected tip resistance ( $q_t$ ) from the CPT or the RQD for rock cores. Other site factors such as undrained shear strength, etc., may be used to determine the SV, only with the prior written permission of

the PC/GDS. The Coefficient of Variation (COV) shall be determined on the bearing stratum at each testing location using the following equation.

$$COV = \frac{\sigma}{\bar{x}} \quad \text{Equation 7-1}$$

Where,

$\sigma$  = Standard deviation

$\bar{x}$  = Mean (average) value

The  $\sigma$  and  $\bar{x}$  shall be determined using statistical equations that are generally recognized. An average COV ( $\overline{COV}$ ) shall be developed based on the results of the individual test location COVs. The  $\overline{COV}$  shall be used to determine the SV using Table 7-1.

**Table 7-1, Site Variability Defined By  $\overline{COV}$**

Site Variability (SV)	$\overline{COV}$
Low	< 25%
Medium	25% ≤ $\overline{COV}$ < 40%
High	40% ≤

## 7.6 PRELIMINARY GEOTECHNICAL SUBSURFACE EXPLORATION

Prior to the commencement of the preliminary exploration, the GEOR shall visit the site and conduct a GeoScoping. The GeoScoping consists of the observation of the project site to identify areas that may impact the project from the geotechnical perspective. These areas shall be selected for exploration during the preliminary exploration if the site is located within the existing SCDOT ROW. If the areas of concern are located outside of the existing SCDOT ROW, then these areas shall be investigated as early as possible in the project development process. For projects conducted by SCDOT, the results of the GeoScoping shall be reported on the appropriate forms (see Appendix A). For non-in-house projects, the GEC shall use the form developed and approved by the GEC firm. The form shall be included in the Appendix to the preliminary geotechnical report. An engineering professional with experience in observing and reviewing sites for potential geotechnical concerns shall be responsible for conducting the GeoScoping.

The preliminary exploration requirements are detailed in Chapter 4, while the contents of the preliminary geotechnical report are detailed in Chapter 21. The primary purpose of the preliminary exploration is to provide an initial assessment of the project. Typically, there will be few project details available prior to conducting the preliminary exploration; however, the most important details that will be known are what type of project it is (i.e., bridge replacement, new road, intersection improvement, etc.) and where the project is located. In many cases, the final alignment and structure locations may not be known. The primary purpose of this type of exploration is not to provide final designs, but to determine if there are any issues that could significantly affect the project. These issues should be identified and the potential impacts and consequences of these design issues should be evaluated by the project design team. Design issues should be identified and documented for additional exploration during the final geotechnical exploration. If the project is located completely within the SCDOT ROW, then the entire exploration may be performed during the preliminary exploration phase of the project; however, the report prepared shall be a preliminary report that meets the requirements of Chapter 21.



## 7.7 FINAL GEOTECHNICAL SUBSURFACE EXPLORATION

The final geotechnical exploration shall conform to the requirements detailed in Chapter 4, while the contents of the final geotechnical report shall conform to the requirements detailed in Chapter 21. The final exploration shall be laid out to use the testing locations from the preliminary exploration to the greatest extent possible without compromising the results of the final exploration. The final exploration shall include those areas identified during the preliminary exploration or during the GeoScoping as requiring additional investigation. If these areas impact the performance of the project, these impacts shall be brought to the immediate attention of the Design/Program Manager or the project team leader for consultant designed projects. In addition, the GEOR shall also include recommended mitigation methods.

## 7.8 FIELD DATA CORRECTIONS AND NORMALIZATION

In-situ testing methods such as the SPT, the CPTu, and the DMT may require corrections or adjustments prior to using the results for soil property correlation or in design. These in-situ testing methods are described in Chapter 5. The SPT and CPTu field data are the most commonly corrected or normalized to account for overburden pressure, energy, rod length, non-standard sampler configuration, borehole diameter, fines content, and the presence of thin very stiff layers. The data obtained from the DMT is corrected for the effects of the instrument operation on the results of the testing. All corrections for in-situ testing methods that are used in geotechnical design and analyses shall be documented in the geotechnical report. The following sections discuss corrections and adjustments in greater detail.

### 7.8.1 SPT Corrections

Many correlations exist that relate the corrected N-values to relative density ( $D_r$ ), peak effective angle of internal friction ( $\phi$ ), undrained shear strength ( $S_u$ ), and other parameters; therefore it is incumbent upon the designer to understand the correlations being used and the requirements of the correlations for corrected N-values. Design methods are available for using N-values directly in the design of driven piles, embankments, spread footings, and drilled shafts. These corrections are especially important in soil Shear Strength Loss (SSL) potential assessments (Chapter 13). Design calculations using SPT N-value correlations should be performed using corrected N-values; however, only the actual field SPT  $N_{meas}$ -values should be plotted on the soil test boring logs and profiles depicting the results of SPT borings. Each of the corrections is discussed in greater detail in the following Sub-sections.

#### 7.8.1.1 Energy Correction ( $C_E$ )

The type of hammer used to collect split-spoon samples shall be noted on the boring logs. Typically correlations used between soil parameters and N-values are based on a hammer system having a transferred energy of 60 percent of the theoretical maximum. A split-spoon sampler advanced with a manual safety hammer has historically been assumed to have an approximate transferred energy of 60 percent ( $ER \approx 60\%$ ); although, the relatively recent ability to make actual energy measurements has indicated that this assumption is not necessarily valid. The energy ratio (ER) is the measured energy divided by the theoretical maximum (i.e., 140-pound hammer dropping 30 inches or 4,200 inch-pounds). The measured energy is determined as discussed in Chapter 5.

The split-spoon sampler is also advanced with either an automatic hammer (measured ER is typically greater than 60%); a manual safety hammer (measured ER is typically 60%); or a manual donut hammer (measured ER is typically less than 60%) **[Reminder: The use of the donut hammer is not permitted]**. The corrections for the donut hammer are provided for

information only since some past projects were performed using the donut hammer. N-values obtained using either the automatic or the manual safety hammer will require correction prior to being used in engineering analysis. As indicated in Chapter 5, the measured transferred energy (ER) for each drill-rig and hammer shall be determined. The energy correction factor ( $C_E$ ) shall be determined using the following equation.

$$C_E = \frac{ER}{60} \quad \text{Equation 7-2}$$

$$ER = \frac{E_{meas}}{E_{theor}} = \frac{E_{meas}}{4,200} \quad \text{Equation 7-3}$$

Where,

$E_{meas}$  = Measured energy (see Chapter 5 for determination)

ER is expressed as an integer (i.e., 90 percent energy is ER = 90) in Equation 7-2. The  $C_E$  values provided in Table 7-2 for each hammer type shall only be used on boring logs where the hammer energy transfer ratio is not provided. In addition, if the hammer type is not indicated and the boring was obtained prior to the year 2000, the hammer shall be assumed to be a manual safety hammer.

**Table 7-2, Assumed Energy Ratio by Hammer Type ( $C_E$ )**

Hammer Type	Energy Ratio (ER) %	$C_E$
Automatic	80	1.33
Safety	60	1.00
Donut	45	0.75

### 7.8.1.2 Overburden Correction ( $C_N$ )

$N_{meas}$ -values in coarse-grained soils will increase with depth due to increasing overburden pressure. The overburden correction is used to standardize all N-values to a reference overburden pressure. The reference overburden pressure is 1 ton per square foot (tsf) (1 atmosphere). The overburden correction factor ( $C_N$ ) (Liao and Whitman (1986)) for coarse-grained soils is provided below. A  $C_N$  of 1.0 shall be used for fine-grained soils.

$$C_N = \left(\frac{1}{\sigma'_v}\right)^{0.5} \leq 1.7 \quad \text{Equation 7-4}$$

Where,

$\sigma'_v$  = Effective overburden stress, tsf

### 7.8.1.3 Rod Length Correction ( $C_R$ )

$N_{meas}$ -values measured in the field should be corrected for the length of the rod used to obtain the sample. The original  $N_{60}$ -value measurements were obtained using long rods (i.e., rod length greater than 33 feet); therefore, a correction to obtain "equivalent"  $N_{60}$ -values for short rod length (i.e., rod length less than 33 feet) is required. Typically, the rod length will be the depth of the sample (d) plus an assumed 5 feet of stick up above the ground surface. The rod length correction factor ( $C_R$ ) equation is provided below with typical values presented in Table 7-3 (McGregor and Duncan (1998)).

$$C_R = e^{-e^{(-0.11d-0.55)}} \quad \text{Equation 7-5}$$

Where,

d = Depth of sample, ft

**Table 7-3, Rod Length Correction ( $C_R$ )**

Rod Length (feet)	$C_R$
< 13	0.75
13 – 20	0.85
20.1 – 33	0.95
> 33	1.00

#### 7.8.1.4 Sampler Configuration Correction ( $C_S$ )

The sampler configuration correction factor ( $C_S$ ) (Cetin et al. (2004)) is used to account for samplers designed to be used with liners, but the liners are omitted during sampling. If the sampler is not designed for liners or if the correct size liner is used no correction is required (i.e.,  $C_S = 1.0$ ). When liners are omitted there is an increase to the inside diameter of the sampler; therefore, the friction between the soil and the sampler is reduced. The sampler configuration correction factor is presented in Table 7-4.

**Table 7-4, Sampler Configuration Correction ( $C_S$ )**

Sampler Configuration	$C_S$
Standard Sampler not designed for liners	1.0
Standard Sampler designed for and used with liners	1.0
Standard Sampler designed for liners and used without liners:	
$N_{meas} \leq 10$	1.1
$11 \leq N_{meas} \leq 29$	$1 + N_{meas}/100$
$30 \leq N_{meas}$	1.3

#### 7.8.1.5 Borehole Diameter Correction ( $C_B$ )

The borehole diameter affects the  $N_{meas}$ -value if the borehole diameter is greater than 4.5 inches. Large diameter boreholes allow for stress relaxation of the soil materials. This stress relaxation can be significant in Sand-Like soils, but has a negligible effect in Clay-Like soils. Therefore, for Clay-Like soils use  $C_B$  equal to 1.0. Listed in Table 7-5 are the borehole diameter correction factors ( $C_B$ ) for Sand-Like soils (McGregor and Duncan (1998)).

**Table 7-5, Borehole Diameter Correction ( $C_B$ )**

Borehole Diameter (inches)	$C_B$
2-1/2 – 4-1/2	1.00
6	1.05
8	1.15

#### 7.8.1.6 Corrected N-values

As indicated previously, the N-values measured in the field ( $N_{meas}$ ) require corrections or adjustments prior to being used for the selection of design parameters or in direct design

methods. The N-value requirements of the correlations or the direct design methods should be well understood and known to the GEOR. Please note that the correction for fines content has been intentionally left out of this Section. The correction for fines content is used only in the determination of soil SSL (see Chapter 13). Corrections typically applied to the  $N_{meas}$ -values are listed in the following equations.

$$N_{60} = N_{meas} * C_E \quad \text{Equation 7-6}$$

$$N_{1,60} = N_{60} * C_N \quad \text{Equation 7-7}$$

$$N_{60}^* = N_{60} * C_R * C_S * C_B \quad \text{Equation 7-8}$$

$$N_{1,60}^* = N_{60}^* * C_N \quad \text{Equation 7-9}$$

## 7.8.2 CPTu Corrections

The CPTu corrected tip resistance ( $q_t$ , see Chapter 6) and sleeve resistance ( $f_s$ ) require corrections to account for the effect of overburden on the tip and sleeve resistance. The tip resistance may also be corrected to account for thin stiff layers located between softer soil layers. These corrections are discussed in the following Sub-sections.

### 7.8.2.1 Effective Overburden Normalization

The corrected CPTu tip resistance ( $q_t$ ) and sleeve resistance ( $f_s$ ) in sands are influenced by the effective overburden stress. This effect is accounted for by normalizing the measured resistances to a standard overburden stress of 1 tsf (1 atm). The normalized and corrected CPTu tip resistance ( $q_{t,1}$ ) and sleeve resistance ( $f_{s,1}$ ), for coarse-grained soils are provided below. A  $C_N$  of 1.0 shall be used for fine-grained soils.

$$q_{t,1} = C_N * q_t \quad \text{Equation 7-10}$$

$$f_{s,1} = C_N * f_s \quad \text{Equation 7-11}$$

Where,

$q_t$  = Corrected CPTu tip resistance, tsf (1 MPa  $\cong$  10.442 tsf)

$f_s$  = Measured CPTu sleeve resistance, tsf (1 MPa  $\cong$  10.442 tsf)

$C_N$  = Overburden normalization factor is the same for  $q_{t,1}$  and  $f_{s,1}$  as indicated in Equation 7-4.

### 7.8.2.2 Thin Layer Correction

When the corrected CPTu tip resistance ( $q_t$ ) is obtained in a thin layer of granular soil that is embedded between softer surrounding soils, the corrected tip resistance ( $q_t$ ) will be reduced due to the effects of the underlying softer soils. This commonly occurs in fluvial environments where granular soils are interbedded between layers of fine-grained soils. Granular soils that are affected by this reduction in corrected tip resistance ( $q_t$ ) are typically sand layers that are less than 3-1/2 feet (~1,074 mm) thick and where the ratio of the corrected tip resistance of the sand ( $q_{tA}$ ) is twice the corrected tip resistance of the cohesive soil ( $q_{tB}$ ) (see Figure 7-1). This correction only applies to thin sand layers (i.e., less than 3-1/2 feet thick). The CPTu tip resistance for this special case is normalized and corrected for the thin layer ( $q_{t,1,Thin}$ ) and is computed as indicated in the following equation.

$$q_{t,1,Thin} = C_{Thin} * (q_{t,1}) \tag{Equation 7-12}$$

Where,

$q_{t,1}$  = Normalized and corrected CPTu tip resistance, MPa (1 MPa  $\cong$  10.442 tsf)

$C_{Thin}$  = Thin layer correction factor and is determined from the following equation and is depicted in Figure 7-2.

$$C_{Thin} = 1.0 + 0.25 \left[ \left( \frac{H}{d_c} \right) - 1.77 \right]^2 \tag{Equation 7-13}$$

Where,

H = Thickness of the soil layer less than or equal to 1,074 mm, millimeters (mm)

$d_c$  = diameter of cone, mm (35.7 mm for a standard 10 cm<sup>2</sup> cone)

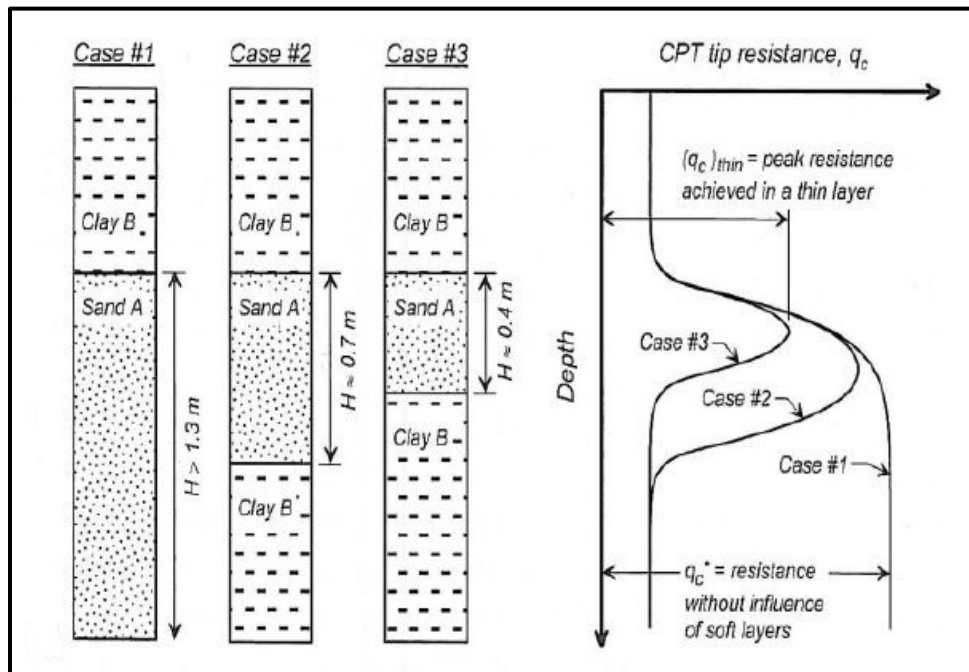
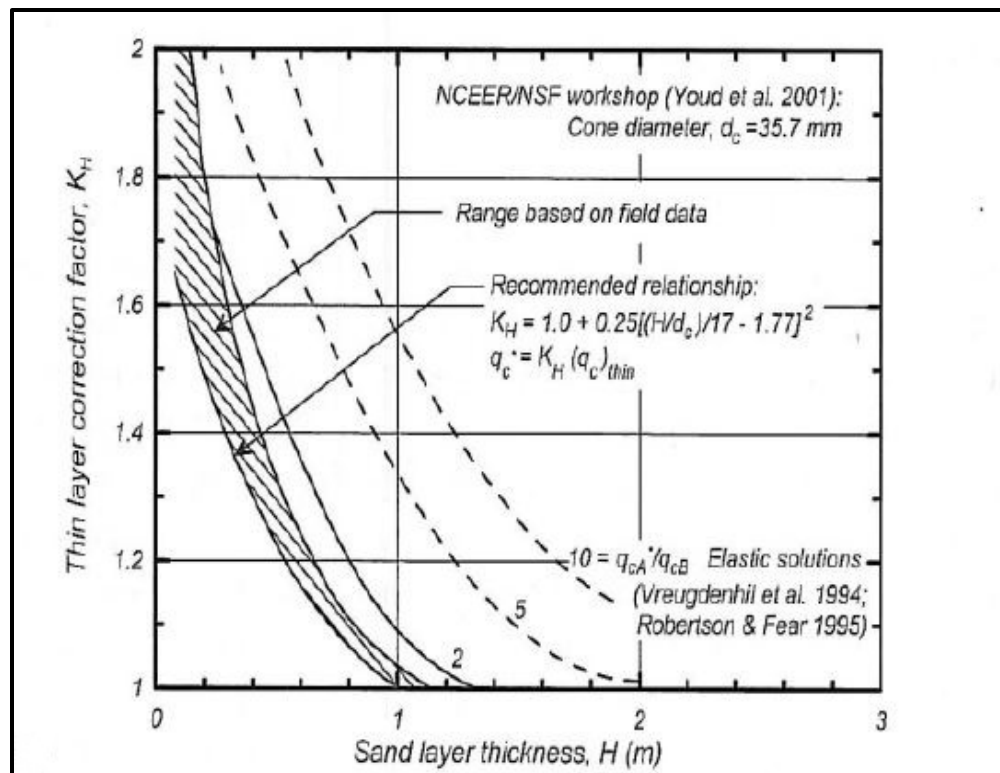


Figure 7-1, Schematic of Thin Layer Effects (Idriss and Boulanger (2008))



Note:  $K_H = C_{Thin}$

**Figure 7-2, CPTu Thin Layer Correction ( $C_{Thin}$ ) (Idriss and Boulanger (2008))**

**7.8.2.3 Soil Behavior Type and Normalization of CPTu Data**

The Soil Behavior Type,  $I_c$ , is computed using normalized tip resistance ( $Q_T$ ) and normalized sleeve friction ( $F_R$ ). The normalized corrected CPTu tip resistance ( $q_{t,1,Thin,N}$ ) is computed by dividing the corrected CPTu resistance ( $q_{t,1,Thin}$ ) by the atmospheric pressure ( $P_a = 1 \text{ atm} = 1 \text{ tsf}$ ) to eliminate units. The following equations should be used.

$$Q_T = \frac{q_{t,1,Thin} - \sigma_v}{\sigma'_v} \tag{Equation 7-14}$$

$$F_R = \left( \frac{f_{s,1}}{q_{t,1,Thin} - \sigma_v} \right) * 100 \tag{Equation 7-15}$$

$$B_q = \frac{(u_2 - u_0)}{(q_{t,1,Thin} - \sigma_v)} \tag{Equation 7-16}$$

$$q_{t,1,Thin,N} = \frac{q_{t,1,Thin}}{P_a} \tag{Equation 7-17}$$

Where,

$q_{t,1,Thin}$  = Normalized, corrected and thin layer corrected tip resistance, tsf

$f_{s,1}$  = Where  $f_s$  is the normalized CPTU cone tip resistance, tsf

$\sigma'_v$  = Effective overburden pressure, tsf

$\sigma_v$  = Total overburden pressure, tsf

$u_2$  = Pore pressure measurement located on the tip shoulder, tsf

$u_0$  = Hydrostatic water pressure, tsf

The Soil Behavior Type,  $I_c$ , is computed using the following equation.

$$I_c = \sqrt{(3.47 - \log Q_T)^2 + (1.22 + \log F_R)^2} \quad \text{Equation 7-18}$$

The  $I_c$  can be generally correlated to a soil classification as indicated in Chapter 6 and using Figure 7-3 to relate  $Q_T$  to  $B_q$ . The numbers indicated in each zone correspond to the CPTu soil behavior type indicated in Chapter 6.

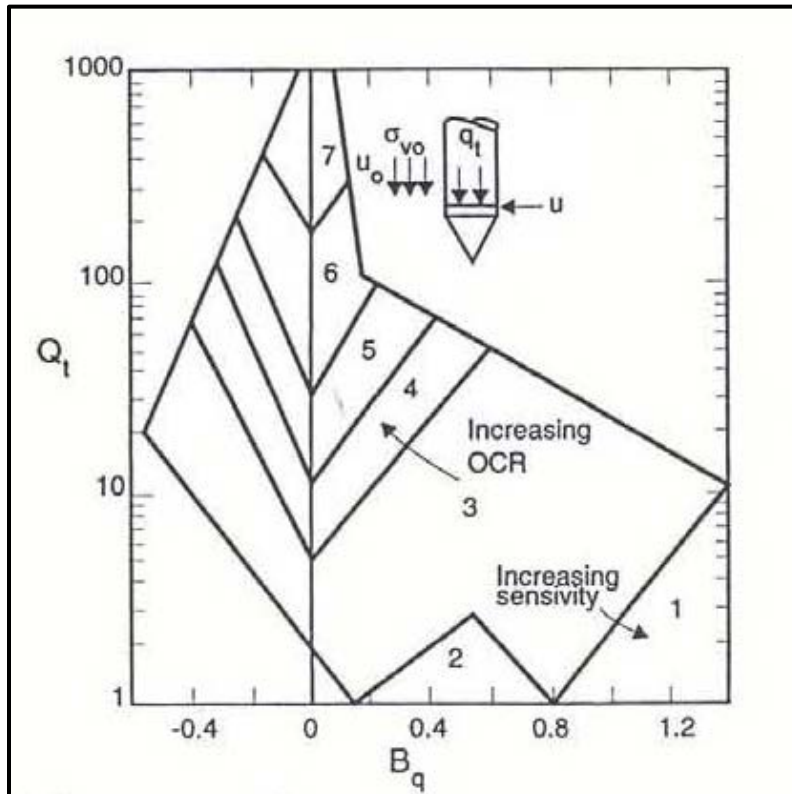


Figure 7-3, Normalized CPT Soil Behavior Chart Using  $Q_T$  versus  $B_q$  (Robertson and Cabal (2015))

### 7.8.3 Correlations for Relative Density From SPT and CPTu

Correlations to compute relative density ( $D_r$ ) from SPT and CPTu testing may be required for soil SSL analyses. The correlations proposed by Boulanger (2003) to relate SPT N-values ( $N_{1,60}^*$ ) and CPTu tip resistance ( $q_{t,1,Thin,N}$ ) to relative density ( $D_r$ ) are provided below.

$$D_r = \left[ \left( \frac{N_{1,60}^*}{46} \right)^{0.5} \right] * 100\% \quad \text{Equation 7-19}$$

Where,

$$N_{1,60}^* \leq 46 \text{ bpf}$$

Equation 7-20

$$D_r = \left[ 0.478 * (q_{t,1,Thin,N})^{0.264} - 1.063 \right] * 100\%$$

Where,

$$q_{t,1,Thin,N} \leq 254$$

Where,

$N_{1,60}^*$  = Corrected SPT N-value, blows per foot

$q_{t,1,Thin,N}$  = Normalized, corrected and thin layer corrected tip resistance, unitless

$D_r$  = Relative Density in percent

The relative density correlations (Equations 7-19 and 7-20) for SPT and CPTu results can be combined to develop an SPT equivalent correlation for normalized CPTu tip resistance as indicated by the following equation.

$$N_{1,60}^* = 46 * \left[ 0.478 * (q_{t,1,Thin,N})^{0.264} - 1.063 \right]^2 \quad \text{Equation 7-21}$$

Alternatively, Jefferies and Davies (1993) recommend a correlation between  $q_t$  and  $N_{60}$ . This correlation has modified to the following equation.

$$N_{60} = \frac{\left( \frac{q_t}{p_a} \right)}{\left[ 8.5 - \left( 1 - \frac{I_c}{4.6} \right) \right]} \quad \text{Equation 7-22}$$

Where,

$q_t$  = Corrected CPTu tip resistance, tsf

$p_a$  = Atmospheric Pressure (1 tsf = 1 atm), tsf

$I_c$  = Soil Behavior Type, dimensionless

#### 7.8.4 Dilatometer Correlation Parameters

Using the corrected pressure readings,  $p_0$ ,  $p_1$  and  $p_2$  (see Chapter 6), the horizontal stress index ( $K_D$ ), the material index ( $I_D$ ), the Dilatometer modulus ( $E_D$ ) and the pore pressure index ( $U_D$ ) shall be reported for all DMT results. The following equations shall be used.

$$K_D = \frac{(p_0 - u_0)}{\sigma'_{v0}} \quad \text{Equation 7-23}$$

$$I_D = \frac{(p_1 - p_0)}{(p_0 - u_0)} \quad \text{Equation 7-24}$$

$$E_D = 34.7 * (p_1 - p_0) \quad \text{Equation 7-25}$$

$$U_D = \frac{(p_2 - u_0)}{(p_0 - u_0)} \quad \text{Equation 7-26}$$

Where,

$p_0$  = Corrected A-pressure, bars (1 bar  $\approx$  1 tsf)

$p_1$  = Corrected B-pressure, bars (1 bar  $\approx$  1 tsf)

$p_2$  = Corrected C-pressure, bars (1 bar  $\approx$  1 tsf)



$\sigma'_{vo}$  = Effective overburden stress, tsf (1 bar  $\approx$  1 tsf)

$u_0$  = Equilibrium pore pressure, bars (1 bar  $\approx$  1 tsf)

## 7.9 SOIL LOADING CONDITIONS AND SOIL SHEAR STRENGTH SELECTION

Geotechnical engineering as presented in this Manual has a statistical (LRFD) and performance-based design component that requires selection of appropriate soil properties in order to design within an appropriate margin of safety consistent with Chapter 9 and also to predict as reasonably as possible the geotechnical performance required in Chapter 10. The selection of soil shear strengths by the GEOR requires that the designer have a good understanding of the loading conditions and soil behavior, high quality soil sampling and testing, and local geotechnical experience with the various geologic formations. This Section provides guidance in the selection of shear strengths for Clay-Like soils (i.e., clays and plastic silts) and Sand-like soils (i.e., sands and nonplastic silts) for use in geotechnical design. The selection of shear strength parameters for rock is covered in Section 7.14.

An in-depth review of the topics addressed in this Section is provided in Sabatini, Bachus, Mayne, Schneider and Zettler (2002) and Duncan and Wright (2005).

Geotechnical load resisting analyses that are typically performed in the design of transportation facilities are bearing resistance of a shallow foundation, axial (tension and compression) load resistance of deep foundations (drilled shafts and piles), lateral load resistance of deep foundations, stability analyses of hillside slopes and constructed embankments, sliding resistance of ERSs, and passive soil resistance. Each of these analyses can have various loading conditions that are associated with the limit state (Strength, Service, and Extreme Event) under evaluation.

Soil shear strength is not a unique property and must be determined based on the anticipated soil response for the loading condition being evaluated. This requires the following 3-step evaluation process:

1. **Evaluate the Soil Loading:** The soil loading should be investigated based on the soil loading rate, the direction of loading, and the boundary conditions for the limit state (Strength, Service, Extreme Event) being evaluated.
2. **Evaluate Soil Response:** The soil response should be evaluated based on pore pressure build-up ( $\Delta u$ ), the soil's state of stress, and volumetric soil changes during shearing, and the anticipated magnitude of soil deformation or strain for the soil loading being applied.
3. **Evaluate Appropriate Soil Strength Determination Method:** This consists of determining the most appropriate soil testing method that best models the loading condition and the soil response for determination of soil shear strength design parameters. Also included in this step is the review of the results for reasonableness based on available correlations and regional experience.

The 3-step evaluation process is discussed in detail in the following Sections.

### 7.9.1 Soil Loading

The soil loading can be evaluated with respect to loading rate, direction of loading, and boundary conditions. The loading rate primarily affects the soil's response with respect to pore water pressure build-up ( $\Delta u$ ). When the loading rate either increases or decreases the pore water pressure ( $\Delta u \neq 0$ ), the loading is referred to as short-term loading. Short-term loading, during or immediately after construction, typically occurs in fine-grained soils, because these

soils drain much slower than coarse-grained soils which allows for an increase or decrease in pore pressures ( $\Delta u$ ) during loading. Conversely, if the loading rate does not affect the pore water pressure ( $\Delta u = 0$ ), the loading is referred to as a long-term loading. Coarse-grained soils, typically, do not build pore pressures, because drainage is relatively rapid. Therefore, long-term loading conditions would be applicable even immediately after the completion of construction. The next Section discusses the response of the soil in greater detail.

Short-term loadings typically occur during construction such as when earth-moving equipment places large soil loads within a relatively short amount of time. The actual construction equipment (cranes, dump trucks, compaction equipment, etc.) should also be considered during the evaluation of construction loadings. Construction loadings are typically evaluated under the Strength limit state. Earthquakes or impacts (vessel or vehicle collisions) that can apply a significant amount of loading on the soil within a short amount of time are also referred to as short-term loadings; however, because of the relative transient and infrequent nature of earthquake and impact loadings, geotechnical design for these types of loadings are performed under the Extreme Event limit state. It is noted that coarse-grained soils during an Extreme Event loading may experience an increase in pore pressure ( $\Delta u > 0$ ) that may significantly affect the soil response (see Chapter 13).

Long-term loadings are typically the result of static driving loads placed on the soils when performing limit state equilibrium analyses such as those that occur with embankments, retaining walls, or foundations that have been in place for a sufficient length of time that the pore water pressures have dissipated. These types of loadings are typically evaluated under the Strength and Service limit states.

The direction of loading is directly related to the critical failure surface and its angle of incidence with respect to the soil element under evaluation. This becomes important when analyzing the soil shear strength with respect to a base of a retaining wall sliding over the foundation or during the analysis of soil stability where the failure surface intersects the soil at various angles within the soil mass. The shear strength is also affected by plane strain loading condition as is typically observed under structures such as continuous wall footings. Plane strain loading occurs when the strain in the direction of intermediate principal stress is zero.

Soil loading boundary conditions result from the soil-structure interaction between the loads imposed by the structure and the soil. The loadings and soil response are interdependent based on the stress-strain characteristics of the structure and the soil. Boundary conditions also include the frictional interface response between the structure and the soil. These boundary conditions can be very complex and affect the magnitude of the soil loadings, magnitude of the soil resistance, the distribution of the soil loading (rigid or flexible foundation), and the direction of the loading.

### **7.9.2 Soil Response**

The application of load to a soil results in a change in either pore pressures ( $\Delta u$ ) and/or a change in soil volume ( $\delta_v$ ). How the soil responds to these changes in part determines whether drained or undrained shear strengths are required. Further how fast the load is applied also affects these changes. The following discussion is based on the assumptions that the soil is completely saturated ( $S = 100$  percent) and that the load is instantaneously placed. If the load is placed incrementally, it is assumed that each increment is placed instantaneously. Guidance will be provided at the end of the Section on how to handle unsaturated soil. The following paragraphs discuss in greater detail the effects of loading on the soil.

The ability of a soil to behave in an undrained ( $\Delta u \neq 0$ ) or a drained ( $\Delta u = 0$ ) condition is controlled by the percentage of fines and the plasticity of the fines. For the purpose of determining soil response, the soil behaviors provided in Table 7-6 shall be used. The use of Sand-Like soils strictly as a frictional material and Clay-Like soils as a strictly cohesive material is only anticipated when using correlations. The results of actual shear strength testing will determine shear strength parameters (i.e.,  $\phi$  and  $c$ ) that are to be used in design. In addition, the Soil Behavior Type,  $I_c$ , from CPTu and the material index,  $I_D$ , from DMT testing is also included.

**Table 7-6, Soil Response Classification**

Percent Fines	Soil Behavior	LL	PI	$I_c^{1,2}$	$I_D^1$	Loading Condition	Shear Strength	Stress Condition	Settlement	AASHTO (USCS) Classification
≤ 20	Sand-Like	N/A <sup>3</sup>	N/A <sup>3</sup>	≤ 2.05	≥ 1.8	Short-term	Drained	Effective	Elastic	A-1-a, A-1-b, A-3 (SP, SP-SM, SP-SC, SM, SC, SC-SM) <sup>4</sup>
						Long-term	Drained	Effective		
> 20	Sand-Like	≤ 40	≤ 10	≤ 2.05	≥ 1.8	Short-term	Drained	Effective	Elastic	A-1-b, A-2-4, A-4 (SM, SC, SC-SM, ML, CL-ML, CL)
						Long-term	Drained	Effective		
	Clay-Like	> 40	> 10	≥ 2.6	≤ 0.6	Short-term	Undrained	Total	Consolidation	A-2-7, A-7-5, A-7-6 (SM, SC, ML, CL, MH, CH)
						Long-term	Drained	Effective		
	Clay-Like <sup>5,6</sup>	≤ 40	> 10	> 2.05 to < 2.6	> 0.6 to < 1.8	Short-term	Undrained	Total	Consolidation	A-2-6, A-6 (SC, SM, CL, ML)
						Long-term	Drained	Effective		
	Sand-Like <sup>5,6</sup>	> 40	≤ 10	> 2.05 to < 2.6	> 0.6 to < 1.8	Short-term	Drained	Effective	Elastic	A-2-5, A-5 (SM, ML, MH)
						Long-term	Drained	Effective		

<sup>1</sup>These are typical values and may change based on the correlation between CPTu or DMT and soil test boring.

<sup>2</sup> $I_c$  to be correlated with Soil Test Boring to verify soil classification.

<sup>3</sup>Not Applicable – plasticity not expected to affect these soils

<sup>4</sup>Does not include gravels (GW, GP, etc.) and well graded sands (SW, etc.)

<sup>5</sup>Possible Transitional Soil may be either Sand-Like or Clay-Like. Additional laboratory testing may be required and shall be approved by PC/GDS

<sup>6</sup>Pore pressure dissipation test during CPTu testing may be required to determine difference between Sand-Like and Clay-Like

The pore water pressure response ( $\Delta u$ ) that allows water to move in or out of the soil over time is dependent on the soil drainage characteristics (i.e., percent fines) and the drainage path length. The time for drainage to occur can be estimated by using Terzaghi’s theory of 1-dimensional consolidation where the time required to reach 99% of the equilibrium volume change,  $t_{99}$ , is determined by the following equation.

$$t_{99} = 4 * \left( \frac{D^2}{c_v} \right) \quad \text{Equation 7-27}$$

Where,

D = Longest distance that water must travel to flow out of the soil mass, ft

$c_v$  = Coefficient of vertical consolidation,  $ft^2/sec$

Typical drainage times for various types of soil deposits based on Equation 7-27 are provided in Figure 7-4. It can readily be seen that Sand-Like soils (see Table 7-6) drain within minutes to months while Clay-Like soils drain within months to years. Please note that it is assumed that Sand-Like soils will behave cohesionlessly (i.e., in frictional manner) and that Clay-Like soils will behave cohesively. The transitional soils may behave as either Sand-Like or Clay-Like depending on percent fines and plasticity. The behavior of the transitional soils is anticipated to be a combination of cohesionless and cohesive. The determination of the behavior of these soils will be the responsibility of the GEOR. Depending on the percent fines and the plasticity these soils may drain in days to years. Even though a soil formation may behave in an undrained condition at the beginning of the load application with excess pore water pressures ( $\Delta u \neq 0$ ), with sufficient time to allow for pore pressure dissipation, the soils will reach a drained condition where static loads are in equilibrium and there is no excess pore water pressure ( $\Delta u = 0$ ). Because soil layers may have different drainage characteristics and drainage paths within a soil profile, soil layers may be at various stages of drainage with some soil layers responding in an undrained condition while other layers respond in a drained condition.

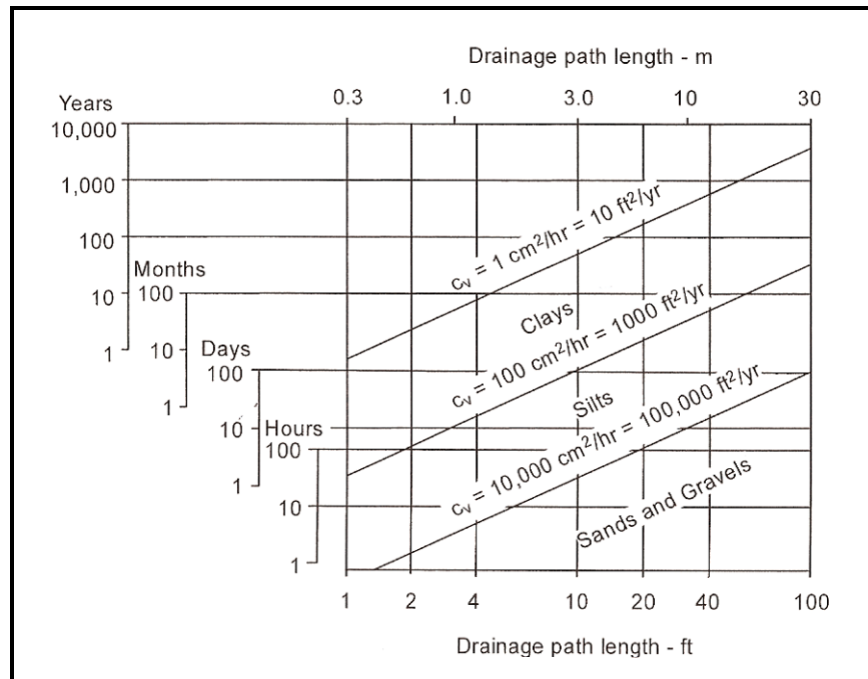


**Figure 7-4, Drainage Time Required  
(Duncan and Wright (2005))**

Volumetric change ( $\delta_v$ ) during shearing can significantly affect the shear strength behavior of the soils. When the soil response is a decrease ( $-\delta_v$ ) in volume during soil shearing the soils are termed to have **contractive** behavior. Loose sands and soft clays typically have contractive behavior. When the soil response is an increase ( $+\delta_v$ ) in volume during soil shearing these soils are termed to have **dilative** behavior. Overconsolidated clays and medium-dense sands typically have dilative behavior. Soils that do not exhibit volumetric change during shearing ( $\delta_v = 0$ ) are termed to have **steady state** behavior.

For typical Sand-Like or Clay-Like soils, it has been observed that the soil shear stress ( $\tau$ ) varies as the soil strains or deforms during soil shearing. Selection of the appropriate soil shear strength to be used in design must be compatible with the deformation or strain that the soil will exhibit under the loading. This is best illustrated in Figure 7-5, where the drained behavior of 2 stress-strain curves is depicted, with each curve representing a different effective consolidation stress ( $\sigma'_{v1}$  and  $\sigma'_{v2}$ ) shown. On the left of Figure 7-5 is a shear stress vs. shear strain plot ( $\tau$ - $\gamma_s$  plot). Because there is a well-defined peak shear stress ( $\tau_{max}$ ) in the plots this would be indicative of dilative soil behavior of either dense sand or overconsolidated clay. The maximum shear stress ( $\tau_{max}$ ) is termed the **peak shear strength** ( $\tau_{Peak} = \tau_{max}$ ). In overconsolidated clay soils, as the maximum shear stress ( $\tau_{max}$ ) is exceeded, post-peak strain softening occurs until a **fully-softened strength** ( $\tau_{NC}$ ) is reached. The fully-softened strength is a post-peak strain softening strength that is considered to be the shear strength that is equivalent to peak shear strength of the same soil in the normally consolidated (NC) stress state ( $\tau_{Peak} \approx \tau_{NC}$ ). For very large shearing strains in soils (cohesive or cohesionless), the shear stress value is reduced further to a residual shear strength ( $\tau_r$ ). The Mohr-Coulomb effective shear strength envelopes for peak shear strength ( $\tau_{Peak} = \tau_{max}$ ), fully-softened shear strength ( $\tau_{Peak} \approx \tau_{NC}$ ), and residual shear strength ( $\tau_r$ ) are illustrated on the right side of Figure 7-5.

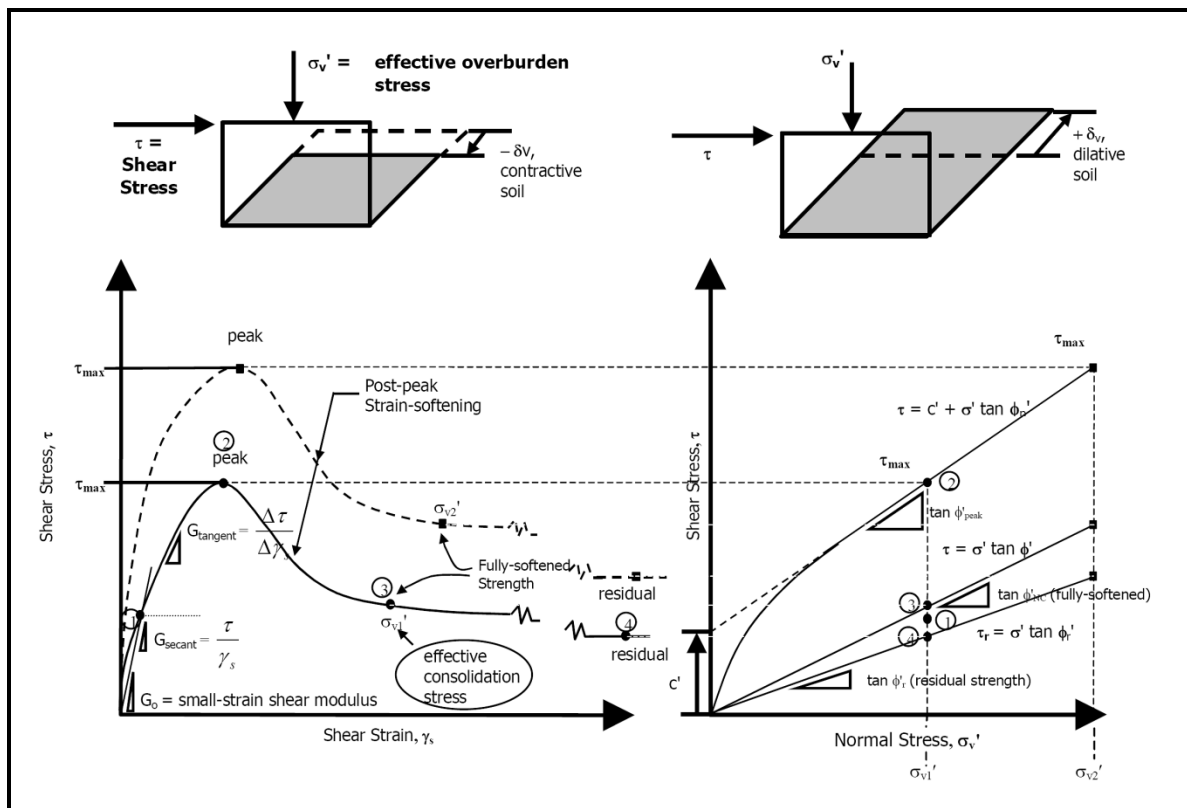


**Figure 7-5, Drained Stress-Strain Behavior (Sabatini, et al. (2002))**

There are various soil models that are used to characterize soil shear strength. The simplest and most commonly used soil shear strength model is the Mohr-Coulomb soil failure criteria. More sophisticated soil shear strength models such as critical state soil mechanics and numerical models (finite element constitutive soil models) exist and are to be used when simpler models such as the Mohr-Coulomb soil failure criteria cannot accurately predict the soil response.

**7.9.2.1 Soil Response – Sand-Like**

The soils included in this category are typically clean to dirty sands and inelastic silts (AASHTO classifications A-1-a, A-1-b, A-2-4, A-3 and A-4). Refer to Table 7-6 for the fine contents and plasticity requirements for Sand-Like soils. The fines content and plasticity of these soils is such that the effect on the rate of loading will be minimal. An  $I_c$  less than or equal to 2.05 ( $I_c \leq 2.05$ ) from CPTu testing is also indicative of sandy type soil behavior. This is a nominal value from Robertson and Cabal (2015); however, the actual soil behavior shall be determined from the correlation boring obtained adjacent to the CPTu as required in Chapter 4. If the  $I_c$  value for sandy type soil behavior is shown to be different, then that  $I_c$  shall be used for the entire project site. It is noted that  $I_c$  is not a soil classification, but an indication of Soil Behavior Type. In addition, a material index,  $I_D$ , of greater than or equal to 1.8 ( $I_D \geq 1.8$ ) is also indicative of sandy behavior from the DMT. These soils will have cohesionless behavior. Because of the relatively rapid drainage anticipated for these soils, less than 100 hours (see Figure 7-4), no excess pore pressures are anticipated ( $\Delta u = 0$ ) (i.e., drained conditions and effective stresses are applicable) and all changes in volume will occur either during loading or immediately after the completion of loading (i.e., all settlement will be elastic).

When drained conditions exist ( $\Delta u = 0$ ), effective stress parameters are used to evaluate soil shear strength. Effective stress is characterized by using effective shear strength parameters

( $c'$ ,  $\phi'$ ) and effective stress,  $\sigma'_{vo}$ , (use total unit weights above the water table and buoyant (total unit weight minus the unit weight of water) unit weight below the water table). The basic Mohr-Coulomb soil failure criteria for effective stress shear strength ( $\tau'$ ) is shown in the following equation.

$$\tau' = c' + \sigma'_{vo} \tan \phi' \quad \text{Equation 7-28}$$

Where,

$c'$  = Effective soil cohesion. The effective cohesion for cohesionless soils is typically assumed to equal zero ( $c' = 0$ ), psf.

$\sigma'_{vo}$  = Effective vertical overburden pressure. Buoyant unit weights ( $\gamma_B = \gamma_T - \gamma_w$ ) are used below the water table and total unit weights ( $\gamma_T$ ) are used above the water table, psf.

$\phi'$  = Effective internal soil friction angle. The effective internal soil friction angle ( $\phi'$ ) for a cohesionless soil is typically greater than the total internal soil friction angle ( $\phi$ ), degrees.

The soil behavior of typical Sand-Like soils can be further illustrated by comparing the stress-strain behavior of granular soils having various densities as shown in Figure 7-6. Medium and dense sands typically reach a peak shear strength ( $\tau_{Peak} = \tau_{max}$ ) value and then decrease to a residual shear strength value at large displacements. The volume of medium and dense sands initially decreases (contractive behavior) and then increases as the soil grains dilate (dilative behavior) with shear displacement until it reaches a point of almost constant volume (steady state behavior). The shear stress in loose sands increases with shear displacement to a maximum value and then remains constant. The volume of loose sands gradually decrease (contractive behavior) until it reaches a point of almost constant volume (steady state behavior).

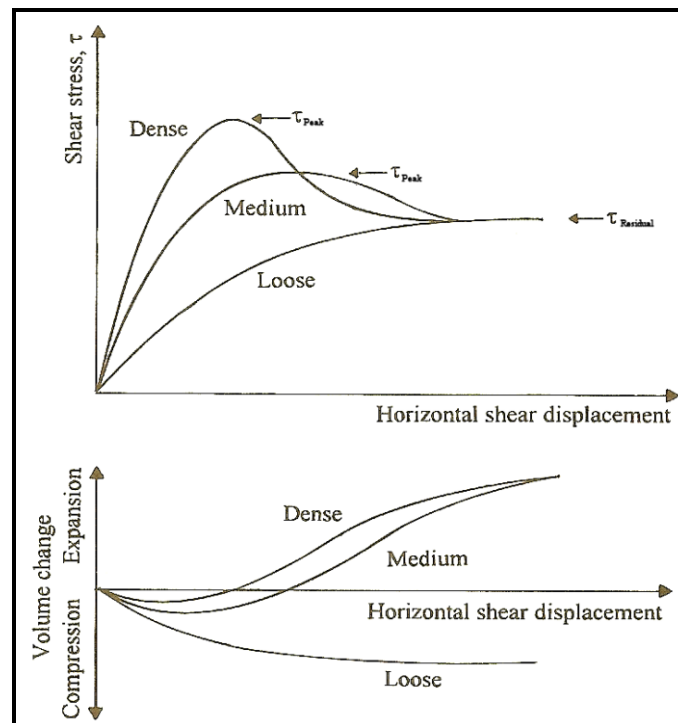


Figure 7-6, Shear Strength Sands (Direct Shear-Test)  
(Das (1997))

The soil response is influenced significantly by the soils pore water pressure response ( $\Delta u$ ) resulting from the rate of loading as the soils attempt to reach a state of equilibrium. The undrained condition is a soil response that occurs when there is either an increase (+) in pore water pressure ( $\Delta u > 0$ ) or a decrease (-) in pore water pressure ( $\Delta u < 0$ ) within the soil during soil loading. The drained condition is a soil response that occurs when there is no change in pore water pressure ( $\Delta u = 0$ ) as a result of the soil loading.

### 7.9.2.2 Soil Response – Clay-Like

The soils in this category are typically elastic silts and fat (plastic) clays (AASHTO classifications A-2-7, A-7-5, and A-7-6). Clay-Like soils will have more than 20 percent fines. Refer to Table 7-6 for the plasticity requirements for Clay-Like soils. Where the rate of loading and plasticity can have a significant impact on how these soils perform. An  $I_c$  greater than or equal to 2.6 ( $2.6 \leq I_c$ ) from CPTu testing is also indicative of clayey type soil behavior. This is a nominal value from Robertson and Cabal (2015); however, the actual soil behavior shall be determined from the correlation boring obtained adjacent to the CPTu as required in Chapter 4. If the  $I_c$  value for clayey type soil behavior is shown to be different, then that  $I_c$  shall be used for the entire project site. It is noted that  $I_c$  is not a soil classification, but an indication of Soil Behavior Type. In addition, an  $I_D$  of less than or equal to 0.6 ( $I_D \leq 0.6$ ) is also indicative of clayey behavior from the DMT. These soils will have cohesive behavior. Typically, these soils will have drainage times measured in months to years, pore pressures are anticipated to change ( $\Delta u \neq 0$ ) and any changes in volume ( $\pm \delta_v$ ) will occur over time. Undrained shear strengths and total stress conditions are applicable to these types of soils for short-term loading conditions. Under long-term loading conditions, drained shear strengths and effective stress conditions are applicable. See the previous Section for the discussion on the development of drained shear strengths and effective stress conditions.

When undrained conditions exist ( $\Delta u \neq 0$ ), total stress parameters are used to evaluate soil shear strength. The total stress condition is characterized by using total shear strength parameters ( $c$ ,  $\phi$ ) and total stress,  $\sigma_{v0}$ , (total unit weights). The basic Mohr-Coulomb soil failure criteria for total stress shear strength ( $\tau$ ), also referred to as the undrained shear strength ( $S_u$ ), is shown in the following equation.

$$\tau = c + \sigma_{v0} \tan \phi \quad \text{Equation 7-29}$$

Where,

$c$  = Total soil cohesion, psf.

$\sigma_{v0}$  = Total vertical overburden pressure. Total unit weights ( $\gamma_T$ ) are used, psf.

$\phi$  = Total internal soil friction angle. The total internal soil friction angle for cohesive soils is typically assumed to equal zero ( $\phi = 0$ ). Total internal soil friction angle ( $\phi$ ) for a cohesionless soil is typically less than the effective internal soil friction angle ( $\phi'$ ), degrees.

Another factor that affects soil response of these soils is the in-situ stress state. The stress state is defined by either total ( $\sigma_{v0}$ ) or effective ( $\sigma'_{v0}$ ) vertical stress, total ( $\sigma_{h0}$ ) or effective ( $\sigma'_{h0}$ ) horizontal stress, and the effective preconsolidation stress ( $\sigma'_p$  or  $p'_c$ ). The effective preconsolidation stress is the largest state of stress that the soil has experienced. The state of stress is often quantified by the overconsolidation ratio (OCR) as indicated by the following equation.

$$OCR = \frac{\sigma'_p}{\sigma'_{vo}} \quad \text{Equation 7-30}$$

Clay-Like soils are often defined by the in-situ state of stress as indicated in Table 7-7:

**Table 7-7, OCR Values**

Description	State of Stress	OCR
Underconsolidated, UC	$\sigma'_p < \sigma'_{vo}$	< 1.0
Normally Consolidated, NC	$\sigma'_{vo} = \sigma'_p$	1.0
Overconsolidated, OC	$\sigma'_{vo} < \sigma'_p$	1.1 - 4.0
Heavily Overconsolidated, OC	$\sigma'_{vo} \ll \sigma'_p$	> 4.0

The soil behavior of typical Clay-Like soils can be further illustrated by comparing the stress-strain behavior of normally consolidated clays ( $OCR = 1$ ) with the stress-strain behavior of overconsolidated clays ( $OCR > 1$ ) for consolidated drained and undrained Triaxial tests in Figures, 7-7 and 7-8, respectively. The stress-strain behavior for overconsolidated clays ( $OCR > 1$ ) indicates that they are subject to strain softening, similar to medium-dense sands shown in Figure 7-6, and that normally consolidated clays ( $OCR = 1$ ) increase in strength, similar to loose sands also shown in Figure 7-6. Overconsolidated (drained or undrained) clays typically reach peak shear strength ( $\tau_{Peak} = \tau_{max}$ ) and then decrease to a fully-softened strength that is approximately equal to the peak shear strength of a normally consolidated clay ( $\tau_{Peak} \approx \tau_{NC}$ ). The volume change of overconsolidated clays in a drained test is very similar to the volume change in medium-dense sand; the volume initially decreases (contractive behavior) and then increases (dilative behavior). The pore pressures in an undrained test of overconsolidated clays initially increase slightly and then become negative as the soil begins to expand or dilate. The shear stress (drained or undrained test) of a normally consolidated ( $OCR = 1$ ) clay increases with shear displacement to a maximum value ( $\tau_{Peak} = \tau_{NC}$ ). The volume of normally consolidated clays in a drained test gradually decreases (contractive behavior) as it reaches a point of almost constant volume (steady state behavior). The pore pressure in an undrained test of normally consolidated clay increases until failure and remains positive for the entire test.



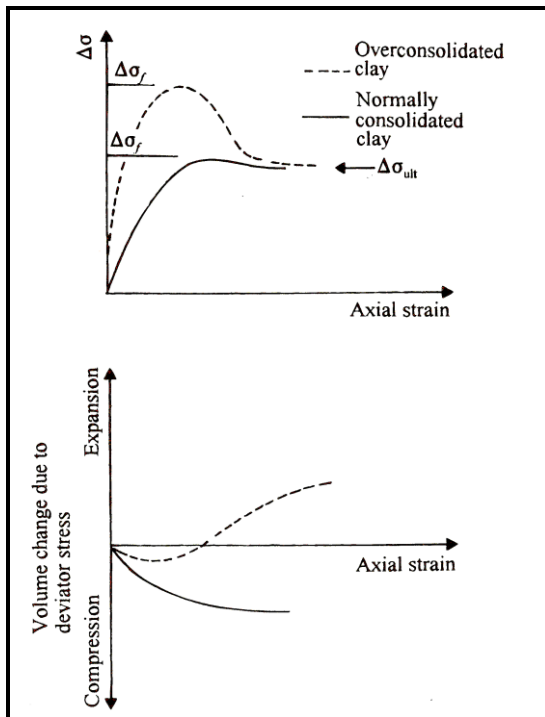


**Figure 7-7, Shear Strength of Clay Consolidated Drained Triaxial (Das (1997))**

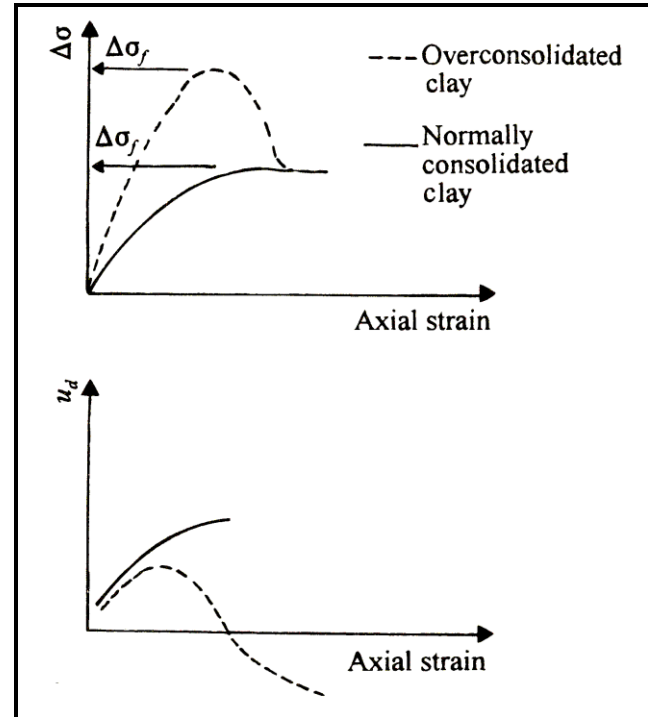


**Figure 7-8, Shear Strength of Clay Consolidated Undrained Triaxial (Das (1997))**

### 7.9.2.3 Soil Response – Transitional Soils

As indicated in Table 7-6, these soils can behave either as Sand-Like or Clay-Like depending on the plasticity of the soil. The GEOR will be responsible for determining whether these soils will behave as Sand-Like or Clay-Like and determining whether undrained or drained shear strengths are to be used. These soils will typically have more than 20 percent fines and will classify as sands with fines to elastic silts and clays (AASHTO classification A-2-5, A-2-6, A-5, and A-6). An  $I_c$  greater than 2.05 and less than 2.6 ( $2.05 < I_c < 2.6$ ) from CPTu testing is also indicative of soil behavior between cohesionless and cohesive. This is nominal value from Robertson and Cabal (2015); however, the actual soil behavior shall be determined from the correlation boring obtained adjacent to the CPTu as required in Chapter 4. If the  $I_c$  value for silty type soil behavior is shown to be different, then that  $I_c$  shall be used for the entire project site. It is noted that  $I_c$  is not a soil classification, but an indication of Soil Behavior Type. In addition, the  $I_D$  will range from greater than 0.6 to less than 1.8 ( $0.6 < I_D < 1.8$ ). See the previous Sections for a discussion of drained and undrained shear strengths.

### 7.9.2.4 Soil Response – Unsaturated Soils

The preceding Sections assume that the soils are 100 percent saturated. For unsaturated soils ( $S < 100$  percent), the GEOR should be aware of the impacts that unsaturated soils can cause. First, there could be volumetric change ( $-\delta_v$ ) without an associated increase in pore pressure ( $+\Delta u$ ). For Clay-Like soils, the air in the soil voids will eventually be squeezed out and the sample will become fully saturated and should be treated accordingly. The time required for this to occur is not easily determined. Further the determination of when to use undrained or drained shear strengths will not be clear. Therefore, SCDOT recommends that all soils are assumed to 100 percent saturated and that all design analysis be based on this assumption.

### 7.9.3 Soil Strength Testing

Selection of soil shear strengths should be made based on laboratory testing and soil strain level anticipated from analyses. Table 7-8 provides a summary of published stress-strain behavior from Holtz and Kovacs (1981), Terzaghi, Peck, and Mesri (1996), and Duncan and Wright (2005) for various soils types. This table is provided for “general” guidance in the selection of shear strengths and soil strain level anticipated from equilibrium analyses.

**Table 7-8, Soil Shear Strength Selection Based on Strain Level**

Sand-Like	Strain Level <sup>1</sup>		
	<b>±5% Strains</b>	<b>15–20% Strains</b>	<b>Large Strains &gt;20%</b>
Med. To Dense Sand	$\tau_{Peak}$	$\tau_r$	$\tau_r$
Non-Liquefying Loose Sands	$\tau_{Peak}$	$\tau_{Peak}$	$\tau_r$
Clay-Like	Strain Level <sup>1</sup>		
	<b>±2% Strains</b>	<b>10–15% Strains</b>	<b>Large Strains &gt;15%</b>
Clay (OCR = 1)	$\tau_{Peak} = \tau_{NC}$	$\tau_{Peak} = \tau_{NC}$	$\tau_{Peak} = \tau_{NC}$
Clay (OCR >1)	$\tau_{Peak}$	$\approx \tau_{NC}$	$\tau_r$
<b>Shear Strength Nomenclature:</b> $\tau_{Peak}$ = Peak Soil Shear Strength $\tau_{NC}$ = Normally Consolidated Soil Shear Strength $\tau_r$ = Residual Soil Shear Strength			
<sup>1</sup> Strain levels indicated are generalizations and are dependent on the stress-strain characteristics of the soil and should be verified by laboratory testing.			

Once the soil loading and soil response has been evaluated, the next step is to select the method of evaluating the soil shear strength. The shear strength can be evaluated by one of the following methods:

1. Soil shear strength determined by geotechnical laboratory testing.
2. Soil shear strength correlations with in-situ field testing results.
3. Soil shear strength correlations based on index parameters.

The laboratory testing should be selected based on shear strength testing method and the testing parameters best suited to model the loading condition and the soil response. Shear strength laboratory testing methods are described in Chapter 5. A summary of the design parameters that should be used in selection of the appropriate testing method and procedure is provided below:

1. **Total or Effective Stress:** Selection of soil shear strength parameters based on total or effective stress state (drained or undrained). Guidance for typical geotechnical analyses for each limit state (Strength, Service, and Extreme Event) being analyzed is provided for bridge foundations in Table 7-9 and for earth retaining structures and embankments in Table 7-10. Total and effective shear strength determination guidelines for laboratory and in-situ testing are provided in Sections 7.10 and 7.11, respectively.
2. **Soil Shear Strength:** Soil shear strength parameters ( $\tau_{Peak}$  or  $\tau_r$ ) selection should be based on strain level anticipated from equilibrium analyses. See Table 7-8 for guidance. Seismic soil shear strengths used to design for the Extreme Event I limit state are discussed in Chapter 13.

- Loading Direction:** The shearing direction should be compatible with how the soil is being loaded or unloaded and the angle of incidence with respect to soil normal stress. Figure 7-9 illustrates test methods that would be appropriate for shear modes for embankment instability shear surface. Figure 7-10 provides undrained strength (UU Triaxial) of typical clays and shales as a function of stress orientation.

**Table 7-9, Bridge Foundation Soil Parameters**

Limit State		Strength		Service	Extreme Event			
Load Combinations		Strength I, II, III, IV, V		Service I	Extreme Events I & II <sup>2</sup>			
Seismic Event		N/A			FEE & SEE			
Loading Condition		Static			During Earthquake Shaking		Post-Earthquake	
Soil Shear Strength Stress State		Total	Effective	Effective	Total <sup>1</sup>	Effective	Total <sup>(1)</sup>	Effective
Shallow Foundation Design	Soil Bearing Resistance	√	√	---	√	√	√	---
	Sliding Frictional Resistance	√	√	---	√	√	√	---
	Sliding Passive Resistance	√	√	---	√	√	√	---
	Structural Capacity	√	√	---	√	√	√	---
	Lateral Displacement	√	√	√	√	√	√	---
	Vertical Settlement	√	√	∇	∇	∇	∇	∇
	Overall Stability	---	---	√	√	√	√	---
Deep Foundation Design	Axial Capacity	√	•	---	---	√	√	---
	Structural Capacity	√	√	---	---	√	√	---
	Lateral Displacements	√	√	√	√	√	√	---
	Vertical Settlement	√	√	∇	∇	∇	∇	∇

<sup>1</sup> Residual soil shear strengths of liquefied soils must include effects of strain softening due to liquefaction.  
<sup>2</sup> For Extreme Event II use During Earthquake Shaking – Total.

**Soil Stress State Legend:**  
 √ Indicates that soil stress state indicated requires analysis  
 --- Indicates that soil stress state does not require analysis  
 • Indicates that soil stress state may need to be evaluated depending on method of analysis  
 ∇ Indicates that soil stress state transitions from undrained to drained (i.e., consolidation)

**Table 7-10, Earth Retaining Structures & Embankment Soil Parameters**

Limit State		Strength		Service		Extreme Event			
Load Combinations		Strength I, II, III, IV, V		Service I		Extreme Events I & II <sup>2</sup>			
Seismic Event		N/A				FEE & SEE			
Loading Condition		Static				During Earthquake Shaking		Post-Earthquake	
Soil Shear Strength Stress State		Total	Effective	Total	Effective	Total <sup>1</sup>	Effective	Total <sup>(1)</sup>	Effective
Earth Retaining Structure Design	Soil Bearing Resistance	√	√	---	---	√	√	---	√
	Sliding Frictional Resistance	√	√	---	---	√	√	---	√
	Sliding Passive Resistance	√	√	---	---	√	√	---	√
	Structural Capacity	√	√	---	---	√	√	---	√
	Lateral Load Analysis (Lateral Displacements)	√	√	√	√	√	√	---	√
	Settlement	√	√	▽	▽	▽	▽	▽	▽
	Global Stability	---	---	√	√	√	√	---	√
Embankment Design	Soil Bearing Resistance	√	√	---	---	√	√	---	√
	Lateral Spread	√	√	---	---	√	√	---	√
	Lateral Squeeze	√	√	---	---	√	√	---	√
	Lateral Displacements	---	---	√	√	√	√	---	√
	Vertical Settlement	√	√	▽	▽	▽	▽	▽	▽
	Global Stability	---	---	√	√	√	√	---	√

<sup>1</sup> Residual soil shear strengths of liquefied soils must include effects of strain softening due to liquefaction  
<sup>2</sup> For Extreme Event II use During Earthquake Shaking – Total.

Soil Stress State Legend:  
 √ Indicates that soil stress state indicated requires analysis  
 --- Indicates that soil stress state does not require analysis  
 • Indicates that soil stress state may need to be evaluated depending on method of analysis  
 ▽ Indicates that soil stress state transitions from undrained to drained (i.e., consolidation)

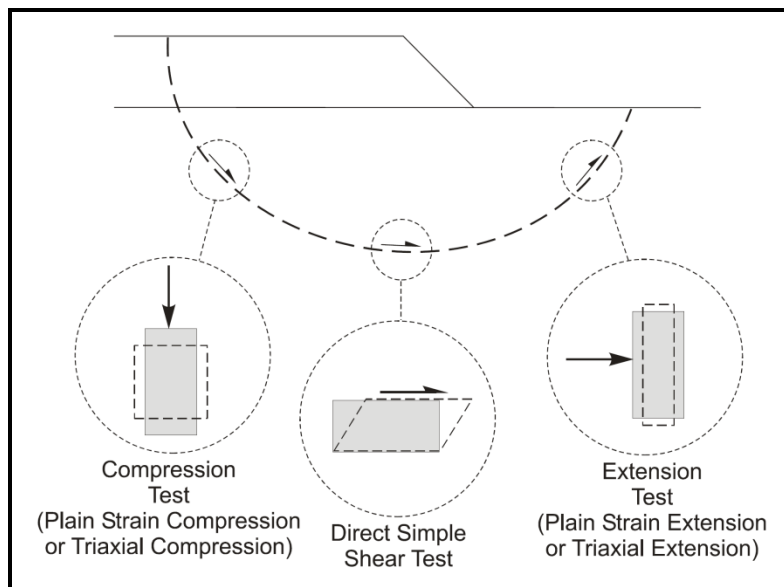


**Figure 7-9, Shear Modes for Embankment Stability Shear Failure Surface (Sabatini, et al. (2002))**

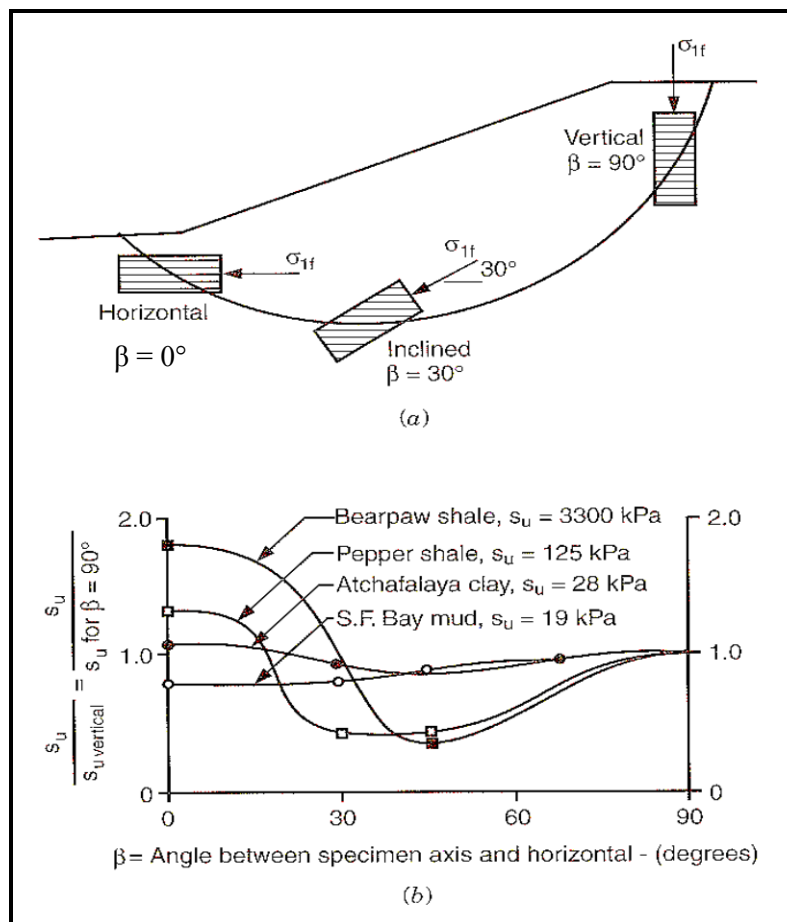


**Figure 7-10,  $\tau$  of Clays and Shales as Function of Failure Orientation (modified from Duncan and Wright (2005))**

The undrained and drained shear strengths of soils can be obtained from laboratory testing. The laboratory testing procedures are described in Chapter 5. A summary of laboratory testing methods suitable for determining the undrained and drained shear strengths of cohesive and cohesionless soils is provided in Table 7-11.

Table 7-11, Laboratory Testing Soil Shear Strength Determination

Laboratory Testing Method	Undrained Shear Strength				Drained Shear Strength			
	Cohesive		Cohesionless		Cohesive		Cohesionless	
	$\tau_{Peak}$	$\tau_r$	$\tau_{Peak}$	$\tau_r$	$\tau'_{Peak}$	$\tau'_r$	$\tau'_{Peak}$	$\tau'_r$
Unconfined Compression (UC) Test	√	√	---	---	---	---	---	---
Unconsolidated Undrained (UU) Test <sup>2</sup>	√	√	---	---	---	---	---	---
Direct Simple Shear (DS) Test <sup>2</sup>	---	---	---	---	---	---	√	√
Consolidated Drained (CD) Test <sup>2</sup>	---	---	---	---	√ <sup>1</sup>	√ <sup>1</sup>	√	√
Consolidated Undrained (CU) Test with Pore Pressure Measurements <sup>2</sup>	√	√	√	√	√	√	√	√

√ - Indicates laboratory method provides indicated shear strength  
 √<sup>1</sup> - Test not considered practical due to time required to perform test  
<sup>2</sup> - Confining stress for triaxial tests and the normal stress for direct shear test shall be determined by GEOR  
 --- - N/A  
**Definitions:**  
 $\tau_{Peak}$  = Peak Undrained Shear Strength       $\tau'_{Peak}$  = Peak Drained Shear Strength  
 $\tau_r$  = Residual Undrained Shear Strength       $\tau'_r$  = Residual Drained Shear Strength

In-situ testing methods (Chapter 5), such as the SPT, the CPTu, the DMT, and the FVST, can be used to evaluate soil shear strength parameters by the use of empirical/semi-empirical correlations. Even though the torvane (TV) or the pocket penetrometer (PP) are soil field testing methods, their use is restricted to only qualitative evaluation of relative shear strength during field visual classification of soil stratification. The major drawback to the use of in-situ field testing methods to obtain soil shear strength parameters is that the empirical/semi-empirical correlations are based on a limited soil database that is typically material or soil formation specific and therefore, the reliability of these correlations must be verified for each project site until sufficient substantiated regional experience is available. Poor correlation between in-situ testing results and soil shear strength parameters may also be due to the poor repeatability of the in-situ testing methods. The CPTu, in all versions, has been shown to be more repeatable while the SPT has been shown to be highly variable. Another source of variability is the sensitivity of the test method to different soil types with different soil consistency (very soft to hard cohesive soils) or density (very loose to very dense cohesionless soils). In-situ penetration testing values correspond to the peak of the stress-strain shear strength curve as indicated in Figure 7-11. Since deformations induced from penetration tests are close to the initial stress state, correlations have been developed for the soil modulus.

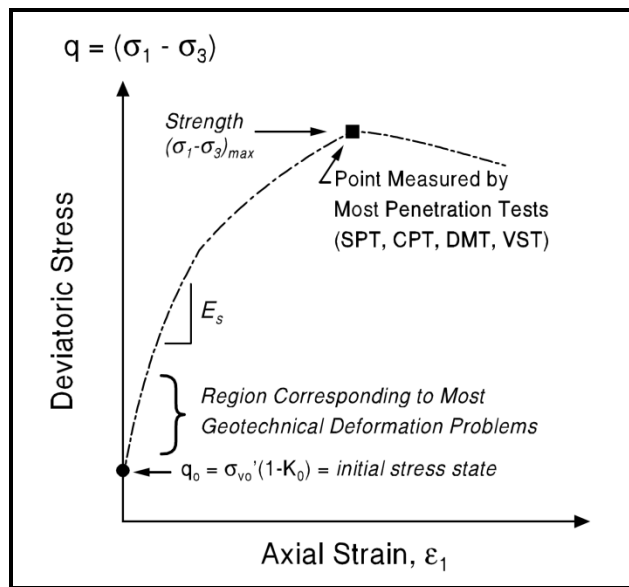


Figure 7-11, Shear Strength Measured by In-Situ Testing (Sabatini, et al. (2002))

A summary of in-situ testing methods suitable for determining the undrained and drained shear strengths of cohesive and cohesionless soils is provided in Table 7-12. The suitability of in-situ testing methods to provide soil shear strength parameters is provided in Table 7-13.

Table 7-12, In-Situ Testing - Soil Shear Strength Determination

In-Situ Testing Method	Undrained Shear Strength				Drained Shear Strength			
	Cohesive		Cohesionless		Cohesive		Cohesionless	
	$\tau_{Peak}$	$\tau_r$	$\tau_{Peak}$	$\tau_r$	$\tau'_{Peak}$	$\tau'_r$	$\tau'_{Peak}$	$\tau'_r$
Standard Penetrometer Test (SPT)	√	---	---	---	---	---	√	---
Piezococone with pore pressure measurements (CPTu)	√	√	---	---	---	---	√	---
Flat Plate Dilatometer Test (DMT)	√	---	---	---	---	---	√	---
Field Vane Shear Test (FVST)	√	√	---	---	---	---	---	---

√ - Indicates in-situ method provides indicated shear strength  
 --- - N/A

**Definitions:**  
 $\tau_{Peak}$  = Peak Undrained Shear Strength       $\tau'_{Peak}$  = Peak Drained Shear Strength  
 $\tau_r$  = Residual Undrained Shear Strength       $\tau'_r$  = Residual Drained Shear Strength

**Table 7-13, Soil Suitability of In-Situ Testing Methods  
(Modified from Canadian Geotechnical Society (2006) and Holtz and Kovacs (1981))**

<b>In-Situ Test Method</b>	<b>Suitable Soils<sup>1</sup></b>	<b>Unsuitable Soils</b>	<b>Correlated Properties</b>	<b>Remarks</b>
Standard Penetrometer Test (SPT)	Sand, Clay, Residual Soils	Gravel	Sand and residual soil effective peak internal friction angle, clay undrained peak shear strength, soil modulus.	SPT repeatability is highly variable. Disturbed samples. Very variable $S_u$ correlations are available for clays.
Piezocone with pore pressure measurements (CPTu)	Sand, Silt, Clay, Residual Soil	Gravel	Sand, silt, and residual soil effective peak internal friction angle, clay and residual soil undrained peak shear strength, soil modulus.	Continuous evaluation of soil properties. CPT is very repeatable. No samples recovered.
Flat Plate Dilatometer Test (DMT)	Sand, Clay, and Residual Soil	Gravel	Sand, silt, and residual soil effective peak internal friction angle, clay and undrained peak shear strength, overconsolidation ratio, at-rest pressure coefficient, soil modulus.	Unreliable results may occur with very dense sand, cemented sand, and gravel. No samples recovered.
Field Vane Shear Test (FVST)	Clay	Sand, Residual Soil, and Gravel	Clay undrained peak shear strength.	May overestimate shear strength. Very soft clays need to be corrected. Unreliable results may occur with fissured clays, varved clays, and highly plastic clays, sand, residual soil, and gravel. FVST repeatability may be variable with rate of rotation. No samples recovered.

<sup>1</sup> The suitability of testing Piedmont residual soils should be based on Mayne et al. (2002). Residual soils frequently have a dual USCS description of SM-ML and behave as both cohesive soils and cohesionless soils because the Piedmont residuum soil is close to the opening size of the U.S. No. 200 Sieve (0.075 mm).

Shear strength of cohesive and cohesionless soils can also be estimated based on effective overburden stress ( $\sigma'_{vo}$ ), effective preconsolidation stress ( $\sigma'_p$  or  $p'_c$ ), the overconsolidation ratio (OCR), and index properties such as grain-size distribution (Fines Content – FC), moisture content ( $w$ ), and Atterberg Limits (LL, PI). Index properties are described in Chapter 6. Unless indicated otherwise, these correlations are used only for preliminary analyses or for evaluating reasonableness of laboratory or in-situ shear strength results.



## 7.10 TOTAL STRESS

Total stress is the force per unit area carried by both the soil grains and the water located in the pores between the soil grains. The total stress state uses undrained soil shear strengths ( $\Delta u \neq 0$ ) and is typically used to resist short-term loadings (i.e., construction loading, earthquake loadings, etc.). The Mohr-Coulomb undrained shear strength equation ( $\tau = S_u$ ) is defined as follows:

$$\tau = c + \sigma_v \tan \phi \quad \text{Equation 7-31}$$

The deviator compression stress at failure ( $\Delta\sigma_f$ ) for unconfined compression tests ( $\sigma_3 = 0$ ) on clays is equal to the unconfined compression strength ( $\sigma_1 = q_u = c$ ). The deviator compression stress at failure ( $\Delta\sigma_f$ ) for undrained triaxial testing (unconsolidated or consolidated) is equal to the total major principal stress ( $\sigma_1$ ) minus the total minor principal stress ( $\sigma_3$ ) (see Figure 7-12).

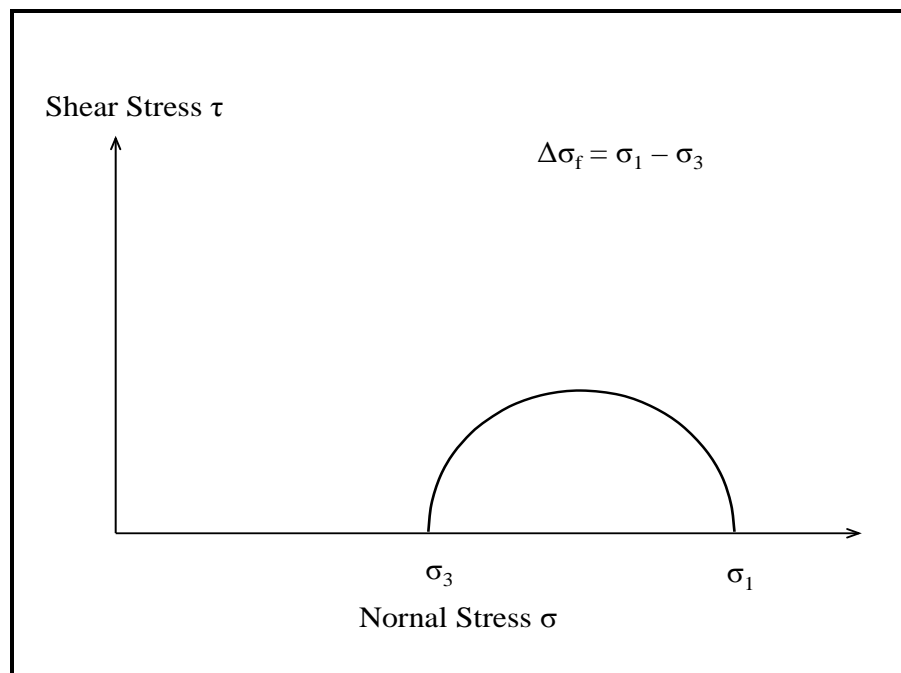


Figure 7-12, Total Principal Stresses

### 7.10.1 Sand-Like Soils

Undrained shear strengths for Sand-Like soils (cohesionless soils) should be used when the rate of loading is so fast that the soil does not have sufficient time to drain such as in the case of rapid draw-down (specifically not addressed in this Manual), cyclic loadings (typically caused by machine loading and are not anticipated on SCDOT projects), and earthquake loadings. Based on Table 7-6 Sand-Like soils are not anticipated to require undrained shear strengths; therefore, no undrained shear strengths will be used or provided. The only exception is during earthquake loadings; see Chapter 13 for the development of undrained shear strengths for use during seismic events. Undrained residual shear strength ratio of liquefied soils ( $\tau_{rl}/\sigma'_{vo}$ ) as proposed by Idriss and Boulanger (2008) are presented in Chapter 13.

### 7.10.2 Clay-Like Soils

The  $\tau$  for Clay-Like soils should be determined using UC tests, UU triaxial tests, or CU triaxial tests of undisturbed samples. The undrained shear strength for these soils should be compatible with the level of strain anticipated under Service conditions (see Table 7-8). Undrained shear strengths are used for short-term loading conditions, the length of time to reduce pore pressures induced by loading may require months to years, in a total stress analysis. Typically the total internal friction angle is negligible and assumed equal to zero ( $\phi = 0$ ) and the Mohr-Coulomb shear strength equation for the  $\tau$  of cohesive soils can be expressed as indicated by the following equation.

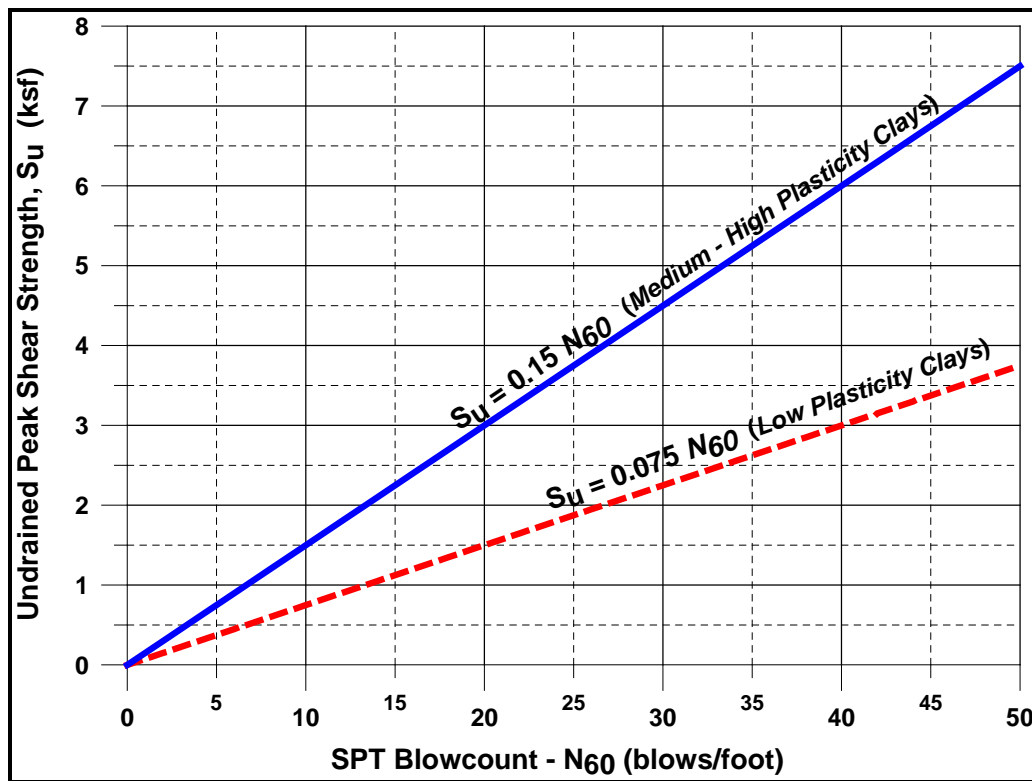
$$\tau = c = \frac{\Delta\sigma_f}{2} \quad \text{Equation 7-32}$$

The undrained shear strength of Clay-Like soils may also be determined by in-situ testing such as the SPT, the CPTu, the DMT, or the FVST as described in Chapter 5. As stated previously, in Section 7.9.3, the biggest drawback to the use of in-situ field testing methods to obtain undrained shear strengths of Clay-Like soils is that the empirical correlations are based on a soil database that is material or soil formation specific and therefore the reliability of these correlations must be verified for each project site by substantiated regional experience or by conducting laboratory testing and calibrating the in-situ testing results.

The SPT can provide highly variable results in Clay-Like soils as indicated in Table 7-13. However, the following correlations may be used if laboratory undrained shear strengths are correlated to the corrected  $N_{60}$  value obtained from the SPT. Peak undrained shear strength ( $\tau = (S_u)_{SPT}$ ), in units of ksf, for Clay-Like soils (McGregor and Duncan (1998)) can be computed for low plasticity clays using Equation 7-33 and medium to high plasticity clays using Equation 7-34. Plasticity is defined in Chapter 6.

$$\tau = (S_u)_{SPT} = 0.075 * N_{60} \quad \text{Equation 7-33}$$

$$\tau = (S_u)_{SPT} = 0.15 * N_{60} \quad \text{Equation 7-34}$$



Note:  $N_{60} = N_{60}^*$

**Figure 7-13, Undrained Shear Strength – SPT Relationship  
(modified from McGregor and Duncan (1998))**

The peak undrained shear strength ( $\tau = (S_u)_{cpt}$ ) of cohesive soils can also be obtained from the CPTu (Mayne (2007)) as indicated by the following equation.

$$\tau = (S_u)_{cpt} = \frac{(q_t - \sigma_{vo})}{N_k} \quad \text{Equation 7-35}$$

Where,

$q_t$  = Corrected CPT tip resistance, tsf (see Chapter 5)

$\sigma_{vo}$  = total overburden pressure at test depth, tsf

$N_k$  = cone factor (see Chapter 6)

According to Robertson and Cabal (2015),  $N_k$  can vary between 10 and 18 and is typically set at 14.  $N_k$  tends to increase with increasing plasticity and decrease with increasing soil sensitivity.  $N_k$  will be determined on a site-specific basis and reported as required in Chapter 6. As the parameter  $B_q$  increases  $N_k$  decreases such that is very sensitive fine-grained soils as  $B_q$  approaches 1.0,  $N_k$  can be as low as 6. As can be seen from Equation 7-35 an accurate determination of  $N_k$  is required, especially in soft fine-grained (Clay-Like) soils. The use of the typical value could under estimate the shear strength.

The peak undrained shear strength ( $\tau = (S_u)_{DMT}$ ) of Clay-Like soils can also be obtained from the DMT (Marchetti, Monaco, Totani, and Calabrese (2001)) as indicated by the following equation.

$$\tau = (S_u)_{DMT} = 0.22 * \sigma'_{vo} * (0.5 * K_D)^{1.25} \quad \text{Equation 7-36}$$

Where,

$\sigma'_{vo}$  = effective overburden pressure at test depth, psf

$K_D$  = horizontal stress index

The peak undrained shear strength ( $\tau = (S_u)_{FVST}$ ) and the remolded shear strength  $(S_{urem})_{FVST}$  of Clay-Like soils can also be obtained from the FVST (Mayne, Christopher and DeJong (2002)) using Equation 7-37.  $(S_{urem})_{FVST}$  is substituted for  $(S_u)_{FVST}$  after the 10 revolutions have been completed.

$$\tau = (S_u)_{FVST} = \frac{12T_{net}}{\pi D^2 \left( \frac{D}{\cos i_T} + \frac{D}{\cos i_B} + 6*H \right)} \quad \text{Equation 7-37}$$

Where,

- $T_{net}$  = Net torque, inch-pounds (see Chapter 5)
- D = Diameter of the field vane, inches (see Chapter 5)
- H = Height of the field vane, inches (see Chapter 5)
- $i_T$  and  $i_B$  = Taper angle, degrees (see Chapter 5)

Correction of  $(S_u)_{FVST}$  is required prior to use in engineering design to account for rate effects in the test. Mayne, et al. (2002) recommends using the following equations to correct the undrained shear strength for testing rate effects based on plasticity ( $PI > 5$ ):

$$\tau_{mobilized} = \mu_R * (S_u)_{FVST} \quad \text{Equation 7-38}$$

$$\mu_R = 1.05 - 0.045 * (PI)^{0.5} \quad \text{Equation 7-39}$$

Where,

- PI = Plasticity Index

Empirical correlations based on SHANSHEP (Stress History and Normalized Soil Engineering Parameters) laboratory testing results can be used for preliminary designs and to evaluate the peak undrained shear strength ( $S_u$ ) obtained from laboratory testing or in-situ testing. This method is only applicable to clays without sensitive structure where undrained shear strength increases proportionally with the effective overburden pressure ( $\sigma'_{vo}$ ). The SHANSHEP laboratory test results of Ladd, Foot, Ishihara, Schlosser, and Poulos (1977) revealed trends in undrained shear strength ratio ( $S_u / \sigma'_v$ ) as a function of overconsolidation ratio as indicated in Figure 7-14.

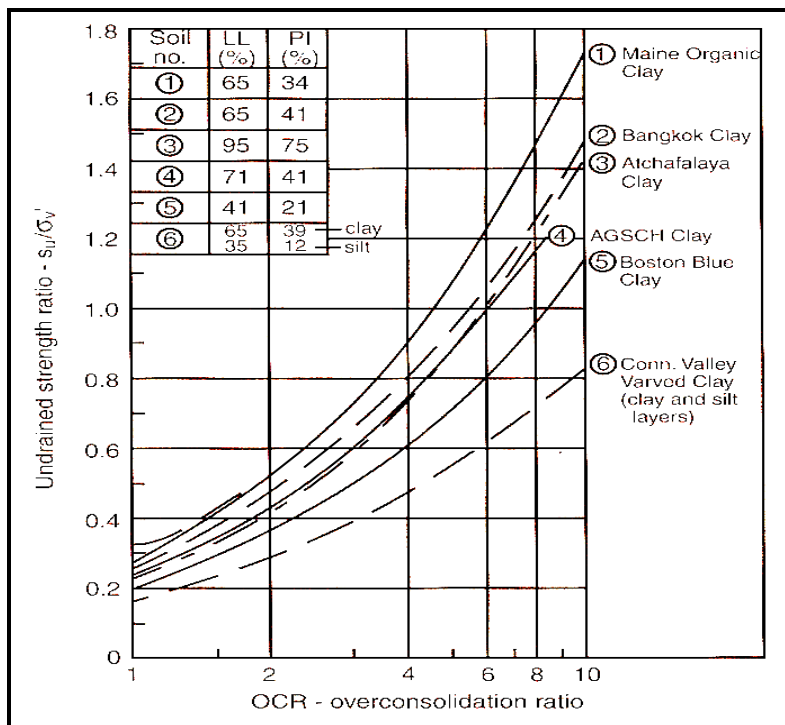


**Figure 7-14, Undrained Shear Strength Ratio and OCR Relationship (Ladd, et al. (1977))**

The average peak undrained shear strengths ( $\tau$ ) shown in Figure 7-14 can be approximated by an empirical formula developed by Jamiolkowski, Ladd, Germaine, and Lancellotta (1985) as indicated by the following equation.

$$\tau = (0.23 * (OCR)^{0.8}) * \sigma'_{vo} \tag{Equation 7-40}$$

Where,

- $\tau$  = Undrained shear strength, tsf
- OCR = Overconsolidation ratio
- $\sigma'_{vo}$  = Effective overburden pressure at test depth, tsf

The  $\tau$  can be compared to the remolded shear strength ( $\tau_{rem}$ ) or  $\tau_r$  to determine the sensitivity ( $S_t$ ) of cohesive soils. Sensitivity is the measure of the breakdown and loss of interparticle attractive forces and bonds within Clay-Like soils. Typically in dispersed Clay-Like soils the loss is relatively small, but in highly flocculated structures the loss in strength can be large. Sensitivity is determined using the following equation.

$$S_t = \frac{\tau}{\tau_{rem}} = \frac{\tau}{\tau_r} \tag{Equation 7-41}$$

Sensitivity may also be estimated directly from CPT results using the following equation,

$$S_t \cong \frac{(q_t - \sigma_{vo})}{f_s * N_k} \tag{Equation 7-42}$$

The description of sensitivity is defined in the following table.

**Table 7-14, Sensitivity of Cohesive Soils  
(Modified from Spangler and Handy (1982))**

Sensitivity	Descriptive Term
< 1	Insensitive
1 - 2	Slightly Sensitive
3 - 4	Medium Sensitive
5 - 8	Sensitive
9 - 16	Very Sensitive
17 - 32	Slightly Quick
33 - 64	Medium Quick
>64	Quick

The  $\tau_{rem}$  of Clay-Like soils can be determined from remolded triaxial specimens or from in-situ testing methods (CPTu or FVST). Triaxial specimens should have the same moisture content as the undisturbed sample as well as the same degree of saturation and confining pressure. Sensitivity can also be related to the liquidity index using the following figure.

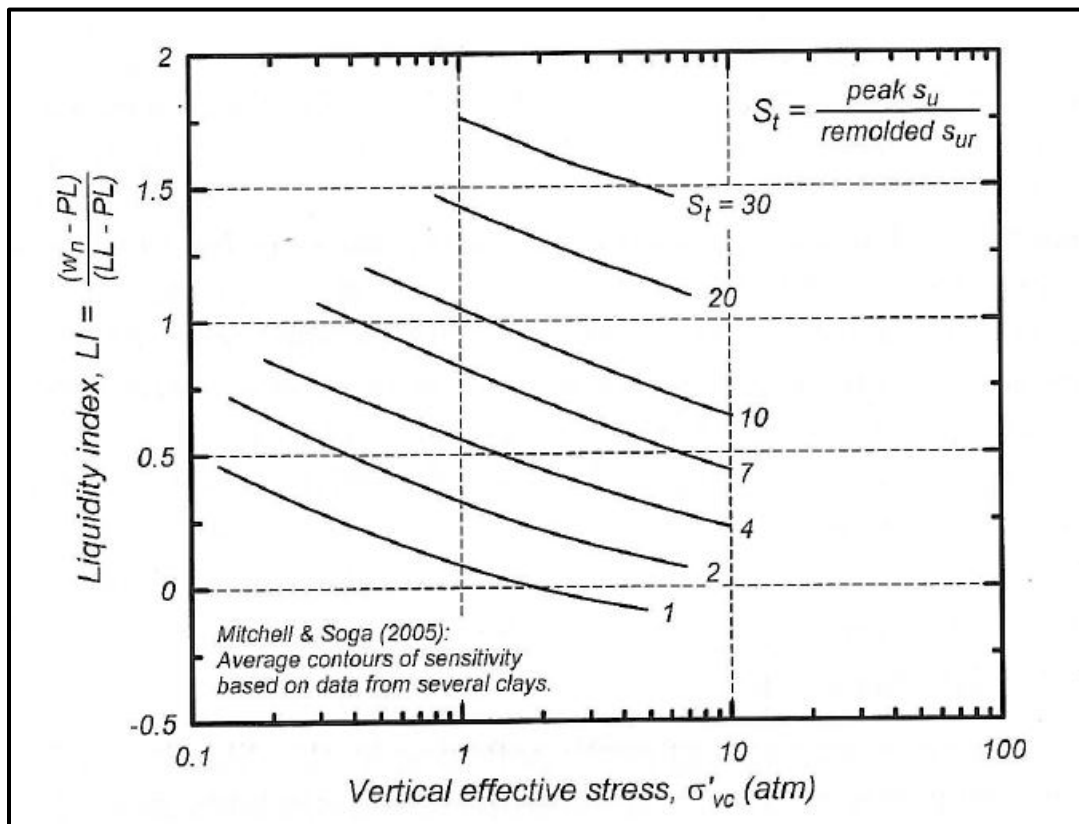
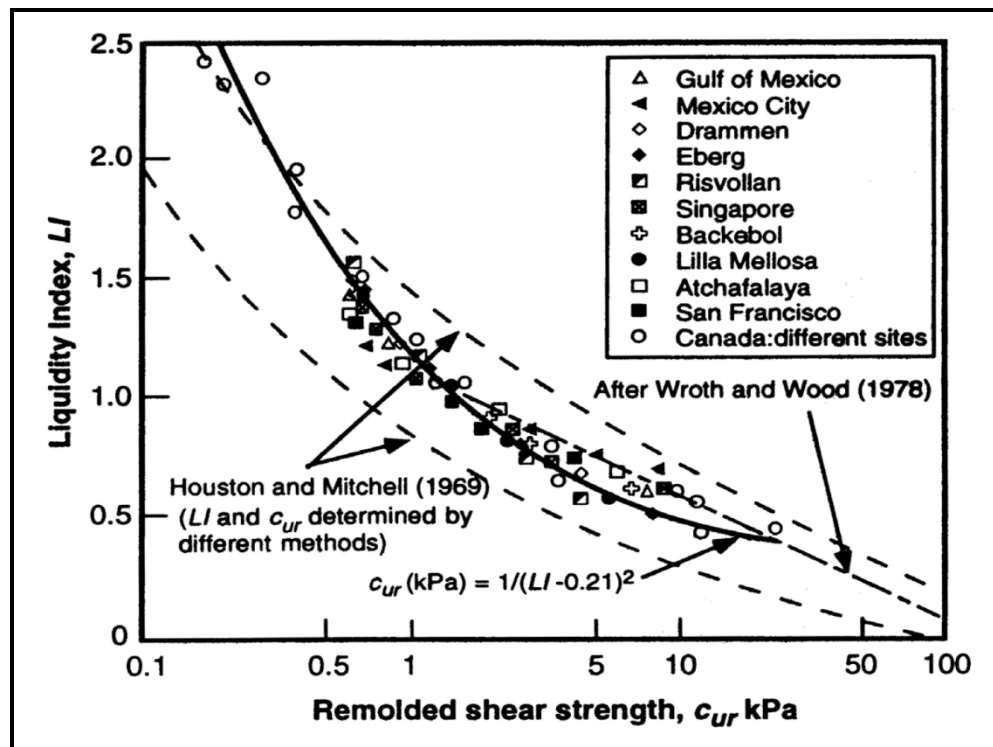


**Figure 7-15, Sensitivity based on Liquidity Index and  $\sigma'_{vc}$   
(Idriss and Boulanger (2008))**

The Liquidity Index (LI) can also be related to remolded shear strength ( $\tau_{rem} = c_{urem} = S_{urem}$ ) as indicated in the following.



1 kPa = 0.0209 ksf = 20.89 psf

**Figure 7-16, Remolded Shear Strength vs Liquidity Index (Mitchell (1993))**

The Liquidity Index (LI) is the relationship between  $w$ ,  $PL$ , and the  $LL$ . The LI is a measure of the relative softness of a Clay-Like soil as indicated by the closeness of the  $w$  to the  $LL$ . The LI can be determined by the following equation.

$$LI = \frac{(w-PL)}{(LL-PL)} \tag{Equation 7-43}$$

An LI equal to 1 is general indication that a Clay-Like soil is normally consolidated and an LI equal to 0 is a general indication that a Clay-Like soil is overconsolidated.

The undrained residual shear strength of Clay-Like soils ( $S_t < 2$ ) can be estimated for preliminary design and to evaluate the  $\tau_r$  ( $S_{ur}$ ) obtained from laboratory testing or in-situ testing. In addition, the  $\tau_r$  ( $S_{ur}$ ) can be estimated by reducing  $\tau_{Peak}$  by a residual shear strength loss factor ( $\lambda_\tau$ ) as indicated in the following equation.

$$\tau_r = \lambda_\tau * \tau \tag{Equation 7-44}$$

The  $\lambda_\tau$  factor typically ranges from 0.50 to 0.67 depending on the type of clay soil. The  $\lambda_\tau$  factors recommended in Table 7-15 are based on the results of a pile soil set-up factor study prepared by Rausche, Thendean, Abou-matar, Linkins and Goble (1997)

**Table 7-15, Residual Shear Strength Loss Factor ( $\lambda_\tau$ )**

Soil Type		Residual Shear Strength Loss Factor ( $\lambda_\tau$ )
USCS	Description	
Low Plasticity Clay	CL-ML	0.57
Medium to High Plasticity Clay	CL & CH	0.50

### 7.10.3 Transitional Soils

The undrained shear strength of transitional materials may have both  $\phi$  and  $c$  components which should be determined in the laboratory using the appropriate testing methods. However, if samples for this type of testing have not been obtained (e.g., during the preliminary exploration), then the GEOR should review the percent fines and the plasticity of the soil to determine whether the soil will behave Sand-Like or Clay-Like. If transitional soils are identified in the preliminary exploration, obtaining undisturbed samples of these materials should be attempted during the final exploration. For soils that are difficult to determine the approximate classification, the undrained shear strength parameters for both Sand-Like and Clay-Like soils should be determined and the more conservative design should be used.

### 7.10.4 Maximum Allowable Total Soil Shear Strengths

SCDOT has established maximum allowable peak ( $c$ ,  $\phi$ ) and residual ( $c_r$ ,  $\phi_r$ ) undrained soil shear strength design parameters for in-situ soils shown in Table 7-16, for use in design. These soil shear strength design parameters may be exceeded with appropriate laboratory testing results (see Table 7-11). Alternately, these shear strengths may be exceeded using correlations with field testing results (see Table 7-12) and the express written permission of the PC/GDS.

**Table 7-16, Maximum Allowable Total Soil Shear Strengths**

Soil Type		Peak		Residual	
		$c$ (psf)	$\phi$ (degrees)	$c_r$ (psf)	$\phi_r$ (degrees)
USCS	Description				
ML, MH, SC	Silt, Clayey Sand, Clayey Silt	1,500	15	1,200	6
SM, ML	Residual Soils	900	14	700	6
CL-ML	NC Clay (Low Plasticity)	1,500	0	900	0
CL, CH	NC Clay (Med-High Plasticity)	2,500	0	1250	0
CL-ML	OC Clay (Low Plasticity)	2,500	0	1400	0
CL, CH	OC Clay (Med-High Plasticity)	4,000	0	2000	0

## 7.11 EFFECTIVE STRESS

Effective stress is the force per unit area carried by the soil grains. The effective stress state uses drained soil shear strengths ( $\Delta u = 0$ ). The Mohr-Coulomb drained shear strength equation is defined as follows.

$$\tau' = c' + \sigma'_v * \tan \phi' \quad \text{Equation 7-45}$$

The deviator compression stress at failure ( $\Delta\sigma_i$ ) for undrained triaxial testing (consolidated) is equal to the total or effective major principal stress ( $\sigma_1$ ) minus the total or effective minor principal stress ( $\sigma_3$ ). The effective major and minor principal stresses are the total major and minor principal stresses minus the pore pressure at failure ( $u_f$ ) (see Figure 7-17).



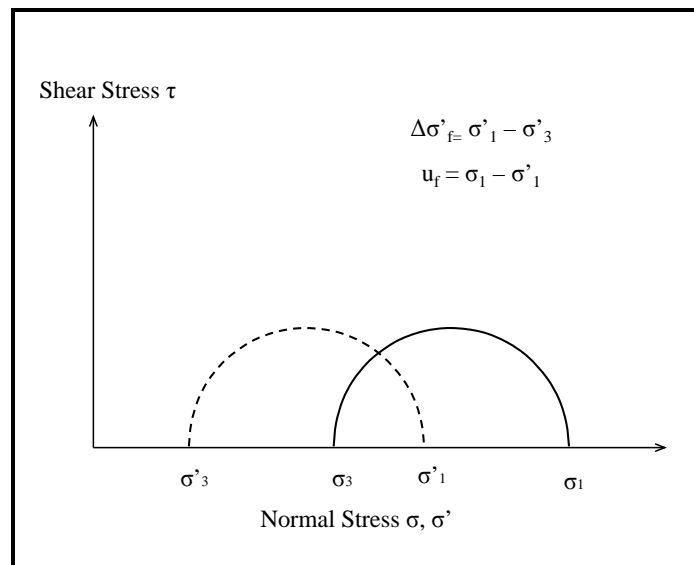


Figure 7-17, Effective Principal Stresses

### 7.11.1 Sand-Like Soils

Drained shear strengths for Sand-Like soils should be used when there is relatively no change in pore water pressure ( $\Delta u \approx 0$ ) as a result of soil loading. The drained shear strength for these soils should be compatible with the level of strain anticipated under service conditions (see Table 7-8). Sand-Like soils that are subjected to construction loads and static driving loads typically use peak or residual drained shear strengths due to the relatively rapid (minutes to hours) drainage characteristics of granular soils as indicated in Section 7.9.2. The peak or residual drained soil shear strength parameters can be obtained from CD triaxial tests, CU triaxial tests with pore pressure measurements, or DS tests. Typically the effective cohesion ( $c'$ ) is negligible and assumed to be equal to zero ( $c' = 0$ ) and the Mohr-Coulomb shear strength criteria for drained shear strength of Sand-Like soils can then be expressed as indicated in the following equation.

$$\tau' = \sigma'_v * \tan \phi' \quad \text{Equation 7-46}$$

The peak drained shear strength of Sand-Like soils may also be determined by in-situ testing methods such as the SPT, the CPTu, or the DMT. As stated previously, in Section 7.9.3, the biggest drawback to the use of in-situ field testing methods to obtain drained shear strengths of Sand-Like soils is that the empirical correlations are based on a soil database that is material or soil formation specific and therefore the reliability of these correlations must be verified for each project site by either using substantiated regional experience or conducting laboratory testing and calibrating the in-situ testing results.

The effective peak friction angle,  $\phi'$ , of Sand-Like soils can be obtained from the SPT. Most SPT correlations were developed for clean sands and their use for micaceous sands/silts, silty soils, and gravelly soils may be may be unreliable as indicated below:

- SPT blow counts in micaceous sands or silts may be significantly reduced producing very conservative correlations.
- SPT blow counts in silty soils may produce highly variable results and may require verification by laboratory triaxial testing depending on a sensitivity analysis of the impact of the variability of results on the analyses and consequently the impact on the project.

- SPT blow counts in gravelly soils may overestimate the penetration resistance. Conservative selection of shear strength parameter or substantiated local experience should be used in lieu of laboratory testing.

The effective peak friction angle,  $\phi'$ , of Sand-Like soils can be estimated using the relationship of Hatanaka and Uchida (1996) for corrected N-values ( $N_{1,60}^*$ ) as indicated below or using Figure 7-18:

$$\phi' = (15.4 * N_{1,60}^*)^{0.5} + 20^\circ \quad \text{Equation 7-47}$$

Where,

$$4 \text{ blows per foot} \leq N_{1,60}^* \leq 50 \text{ blows per foot}$$



**Figure 7-18, Effective Peak Friction Angle and SPT ( $N_{1,60}^*$ ) Relationship  
(Based on Hatanaka and Uchida (1996))**

The effective friction angle,  $\phi'$ , of Sand-Like soils can also be estimated by the CPTu based on Robertson and Campanella (1983). This method requires the estimation of the effective overburden pressure ( $\sigma'_{vo}$ ) and the corrected tip resistance ( $q_t$ ) using the relationship in Figure 7-19. This relationship may be approximated by the following equation.

$$\phi' = \tan^{-1} \left[ 0.1 + 0.38 * \log \left( \frac{q_t}{\sigma'_{vo}} \right) \right] \quad \text{Equation 7-48}$$

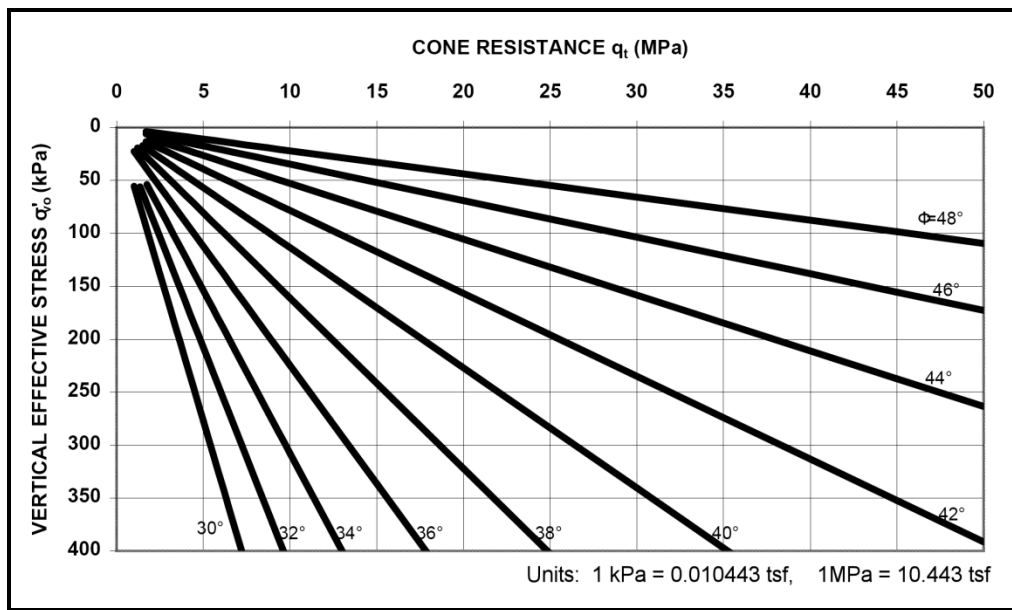


Figure 7-19, Effective Peak Friction Angle and CPT ( $q_t$ ) Relationship (Robertson and Campanella (1983))

The effective friction angle,  $\phi'$ , of Sand-Like soils can also be estimated by the DMT using the Marchetti (1997) relationship shown in Figure 7-20. The Marchetti (1997) relationship may be approximated by the following equation.

$$\phi' = 28^\circ + 14.6^\circ * \log K_D - 2.1^\circ \log^2 K_D \quad \text{Equation 7-49}$$

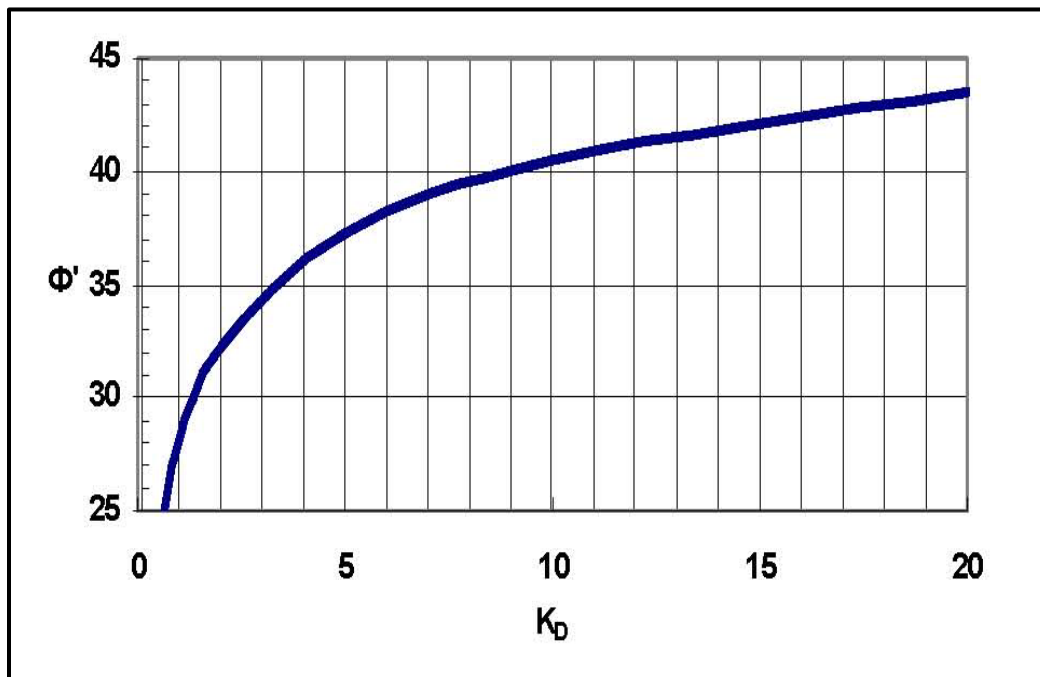


Figure 7-20, Effective Peak Friction Angle and DMT ( $K_D$ ) Relationship (Sabatini, et al. (2002))

### 7.11.2 Clay-Like Soils

Drained shear strengths for Clay-Like soils should be used when there is relatively no change in pore water pressure ( $\Delta u \approx 0$ ) as a result of soil loading such as static driving loads. The drained shear strength for these soils should be compatible with the level of strain anticipated under service conditions (see Table 7-8). Drained shear strengths are used for long-term loading conditions, geotechnical analyses for these types of loadings are based on effective stress analyses. The peak or residual drained soil shear strength parameters can be obtained from CD triaxial testing (this test is normally not performed because of the time requirements for testing), or CU triaxial testing with pore pressure measurements. It is noted that use of the following methods should only be used if the appropriate laboratory testing for shear strength has not been performed and that preference is that the testing should be performed. Typically for normally consolidated ( $OCR = 1$ ; see Table 7-7) Clay-Like soils the effective cohesion ( $c'$ ) is negligible and is assumed to be equal to zero ( $c' = 0$ ) and the Mohr-Coulomb shear strength equation for drained shear strength for Clay-Like soils can be expressed as indicated in the following equation.

$$\tau' = \sigma'_v * \tan \phi'_{NC} \quad \text{Equation 7-50}$$

Typically for overconsolidated Clay-Like soils the effective cohesion is greater than zero with the effective friction angle less than that determined for normally consolidated Clay-Like soils. When the preconsolidation pressure ( $\sigma'_p$  or  $p'_c$ ) is exceeded the overconsolidated Clay-Like soil becomes normally consolidated (see Figure 7-21).

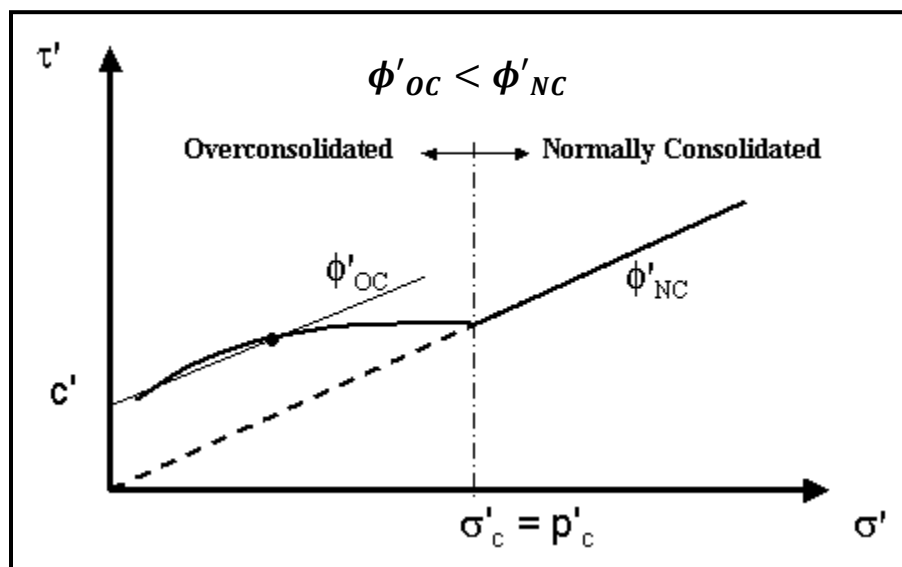


Figure 7-21, Overconsolidated Clay Failure Envelope (CUw/pp Triaxial Test)

The effective peak and residual drained shear strength of Clay-Like soils should not be evaluated using in-situ testing methods. Drained shear strengths should be developed using appropriate laboratory testing. However, SCDOT recognizes the fact that this type of testing may not be practicable; therefore, the correlations provided in the following paragraphs may be used.

Correlations have been developed between drained shear strengths of Clay-Like soils and index parameters such as plasticity index (PI or  $I_p$ ), LL, clay fraction (CF) and effective overburden pressure ( $\sigma'_{vo}$  = effective normal stress). Similarly to relationships developed for in-situ testing methods, these relationships for drained shear strengths of Clay-Like soils were developed

based on a soil database that is typically material or soil formation specific and may require verification by laboratory triaxial testing depending on a sensitivity analysis of the impact of the variability of results on the analyses and consequently the impact on the project. These relationships should be used to evaluate the validity of laboratory testing results and to improve the relationship database for regional soil deposits by SCDOT.

In normally consolidated Clay-Like soils ( $OCR = 1.0$ ) the shear strength test will result in a peak effective friction angle ( $\phi'$ ). Terzaghi, et al. (1996) proposed the relationship in Figure 7-22 between peak effective friction angle ( $\phi'$ ) for normally consolidated clays and the plasticity index ( $I_p$  or  $PI$ ). For plasticity indices above 60 percent, the peak effective friction angle ( $\phi'$ ) should be determined from laboratory testing. The Terzaghi, et al. (1996) relationship between peak effective friction angle ( $\phi'$ ) for normally consolidated clays and the plasticity index ( $I_p$  or  $PI$ ) may be estimated by the following equation.

$$\phi'_{NC} = 35.7^\circ - [0.28^\circ * (PI)] + [0.00145^\circ * (PI)^2] \pm 4^\circ \quad \text{Equation 7-51}$$

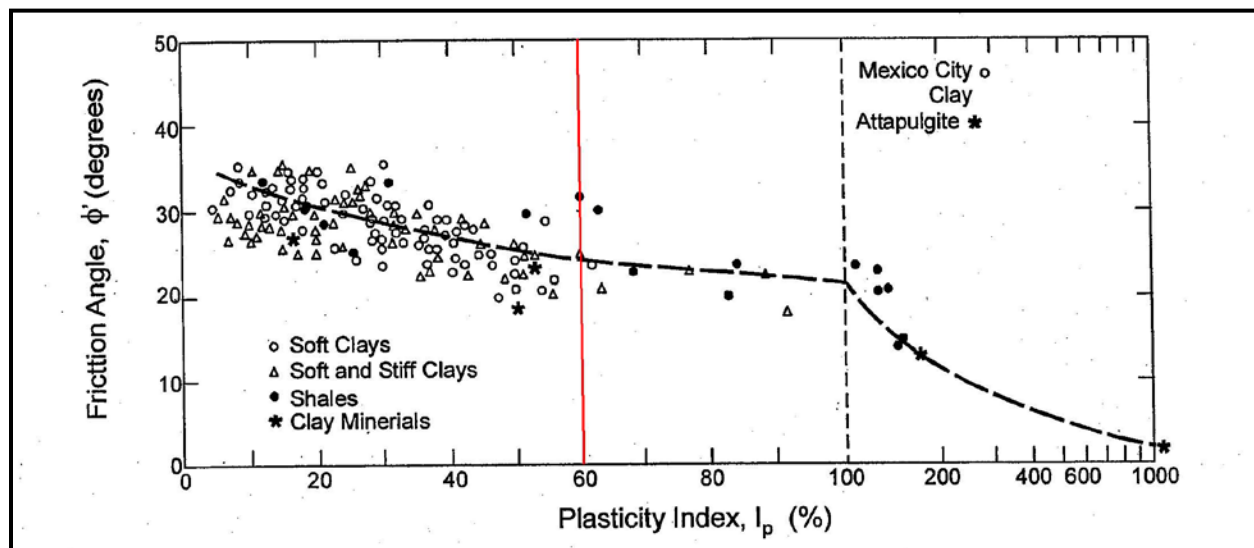


Figure 7-22, Plasticity Index versus Drained Friction Angle for NC Clays (Terzaghi, et al. (1996))

As an alternate to Terzaghi, et al. (1996), Sorensen and Okkels (2013) may be used. Sorensen and Okkels (2013) have developed 2 equations for obtaining the drained friction angle for normally consolidated Clay-Like soils ( $\phi'_{NC}$ ) using  $PI$  and  $CF$ . These equations apply for  $CF$  less than 90 percent ( $CF < 90\%$ ) because the available data from which this equation is based did not have any samples with  $CF$ s greater than about 90 percent. However, it is noted that  $PI$  has a greater influence on  $\phi'_{NC}$  than does  $CF$ . Figure 7-23 depicts the data set used by Sorensen and Okkels (2013) to develop these equations. As can be seen in Figure 7-23, a mean equation and a lower bound equation have been developed. The lower bound equation should have no more than 5 percent of the data points below the lower bound line. SCDOT recommends that the lower bound curve be used first to develop the normally consolidated drained shear strength for use in design. The mean equation should be used if the lower bound equation does not achieve the required resistances.

Lower Bound Equation

$$\phi'_{NC} = 39^\circ - 11^\circ * \log PI \quad \text{Equation 7-52}$$

Mean Equation

$$\phi'_{NC} = 43^\circ - 10^\circ * \log PI \quad \text{Equation 7-53}$$

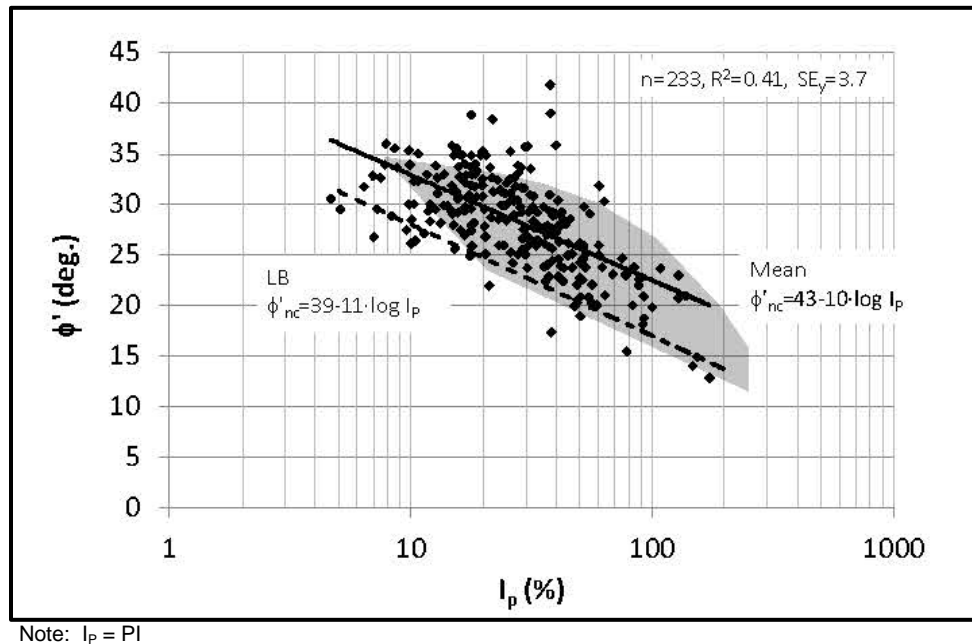
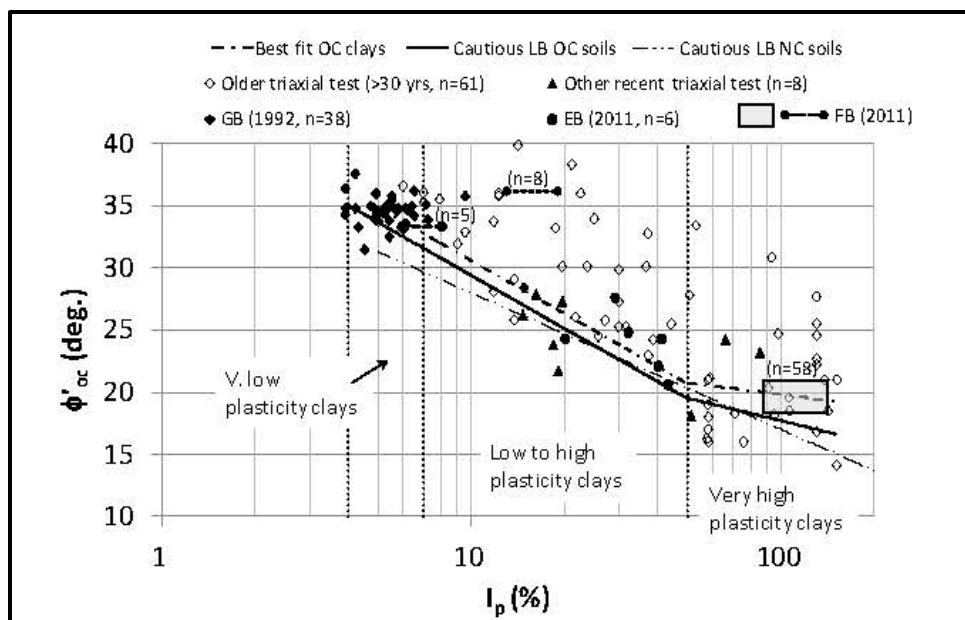


**Figure 7-23, Plasticity Index versus Drained Shear Resistance for NC Clays (Sorensen and Okkels (2013))**

Sorensen and Okkels (2013) have also developed procedures for determining the drained shear strength ( $c'_{OC}$  and  $\phi'_{OC}$ ) for overconsolidated Clay-Like soils ( $OCR \geq 1.1$ ). For overconsolidated Clay-Like soils the Mohr-Coulomb shear strength equation for drained shear strength can be expressed as indicated in the following equation.

$$\tau' = c'_{OC} + \sigma'_v * \tan \phi'_{OC} \quad \text{Equation 7-54}$$

Sorensen and Okkels (2013) have demonstrated that drained shear strength of overconsolidated Clay-Like soils are related not only to PI but also the CF of the material. Similarly to the development of drained shear strength for normally consolidated Clay-Like soils, Sorensen and Okkels have developed 2 equations based on both best fit of the drained shear strength data for overconsolidated Clay-Like soils as well as a lower bound equation for which approximately 95 percent of the available data points are above the lower bound line (see Figure 7-24). SCDOT recommends that the lower bound curve be used first to develop the overconsolidated drained shear strength for use in design. The best fit equation should be used if the lower bound equation does not achieve the required resistances.



Note:  $I_p = PI$

**Figure 7-24, Plasticity Index versus Drained Shear Resistance for OC Clays (Sorensen and Okkels (2013))**

As can be seen from the lower bound curve in Figure 7-24, both the lower bound and best fit curves kink at a PI of approximately 50 percent ( $50\% < PI$ ); therefore 2 equations will be required to describe each curve based on PI.

Lower Bound Equations

$$4 < PI < 50 \quad \phi'_{oc} = 44^\circ - 14^\circ * \log PI \quad \text{Equation 7-55}$$

$$50 \leq PI < 150 \quad \phi'_{oc} = 30^\circ - 6^\circ * \log PI \quad \text{Equation 7-56}$$

Best Fit Equations

$$4 < PI < 50 \quad \phi'_{oc} = 45^\circ - 14^\circ * \log PI \quad \text{Equation 7-57}$$

$$50 \leq PI < 150 \quad \phi'_{oc} = 26^\circ - 3^\circ * \log PI \quad \text{Equation 7-58}$$

These equations are for soils that CFs less than 80 percent ( $CF < 80\%$ ). These equations may be used for soils with CFs greater 80 percent ( $CF \geq 80\%$ ); however, extreme caution should be exercised in the use of these equations at greater CFs. Soils with greater CFs were not part of the data set used to develop these equations.

As indicated previously, overconsolidated Clay-Like soils can have a drained cohesion ( $c'_{oc}$ ). Sorensen and Okkels (2013) have developed equations relating  $c'_{oc}$  to PI; however, since  $c'_{oc}$  is more related to soil structure than  $\phi'_{oc}$  the use of their equations may not be appropriate. Considering the fact that  $\phi'_{oc}$  is based on soil mineralogy, which is partially based on PI, while  $c'_{oc}$  is more based soil structure which is lost during the sample preparation for PI determination. Therefore, Sorensen and Okkels (2013) recommends using a relationship between  $c'_{oc}$  and  $S_u$  (see Figure 7-25). This relationship is applicable for clays having PIs greater than or equal to 7 ( $PI \geq 7$ ). For clays with PI less than 7 ( $PI < 7$ ), Sorensen and Okkels (2013) recommend  $c'_{oc}$  be assumed to be 0 psf.

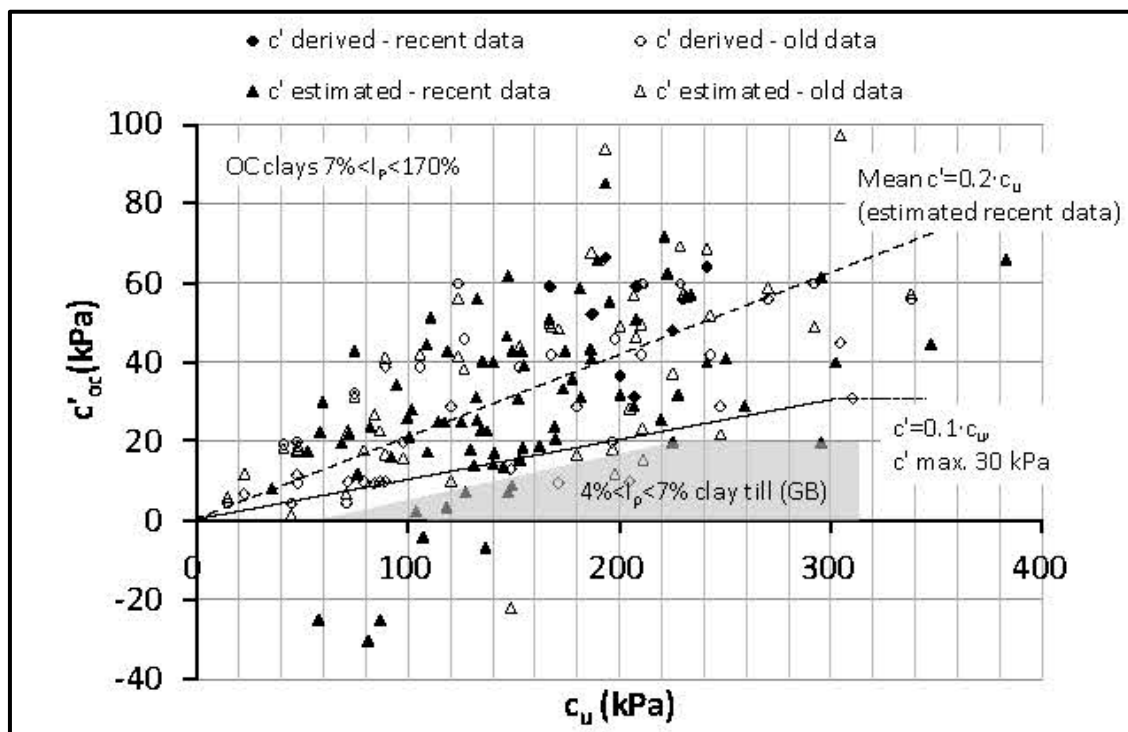


Figure 7-25, Undrained Shear Strength versus Drained Shear Resistance for OC Clays (Sorensen and Okkels (2013))

$$PI < 7 \quad c'_{oc} = 0 \text{ psf} \quad \text{Equation 7-59}$$

$$7 \leq PI < 150 \quad c'_{oc} = 0.1 * S_u \leq 630 \text{ psf} \quad \text{Equation 7-60}$$

It is noted that the  $c'_{oc}$  has a maximum value of 630 psf.

The preceding paragraphs discussed the development of the peak drained shear strength for normally ( $\phi'_{NC}$ ) and overconsolidated ( $\phi'_{OC}$  and  $c'_{OC}$ ) Clay-Like soils. The following paragraphs discuss the development of drained residual shear strength. Stark and Eid (1994 and 1997) developed a graphical relationship between PI, CF and  $\sigma'_{vo}$  (effective normal stress) to obtain the drained shear strength of Clay-Like soils (see Figure 7-26). This graph was used for heavily overconsolidated ( $OCR > 4$ ) Clay-Like soils. This method for determining drained residual shear strength has been updated by Stark and Hussain (2013) (see Figure 7-27). The Stark and Hussain (2013) procedure shall be used to determine the drained residual shear strength ( $\phi'_r$ ). Stark and Hussain (2013) have developed 3 sets of equations based on CF with individual equations based on LL (surrogate for PI) and  $\sigma'_{vo}$ .

- $CF \leq 20\%$
- $25\% \leq CF \leq 45\%$
- $CF \geq 50\%$

Each set of equations also has a range of LL over which the equations apply. The limitations imposed by the LL are a result of the testing results used to develop the equations.



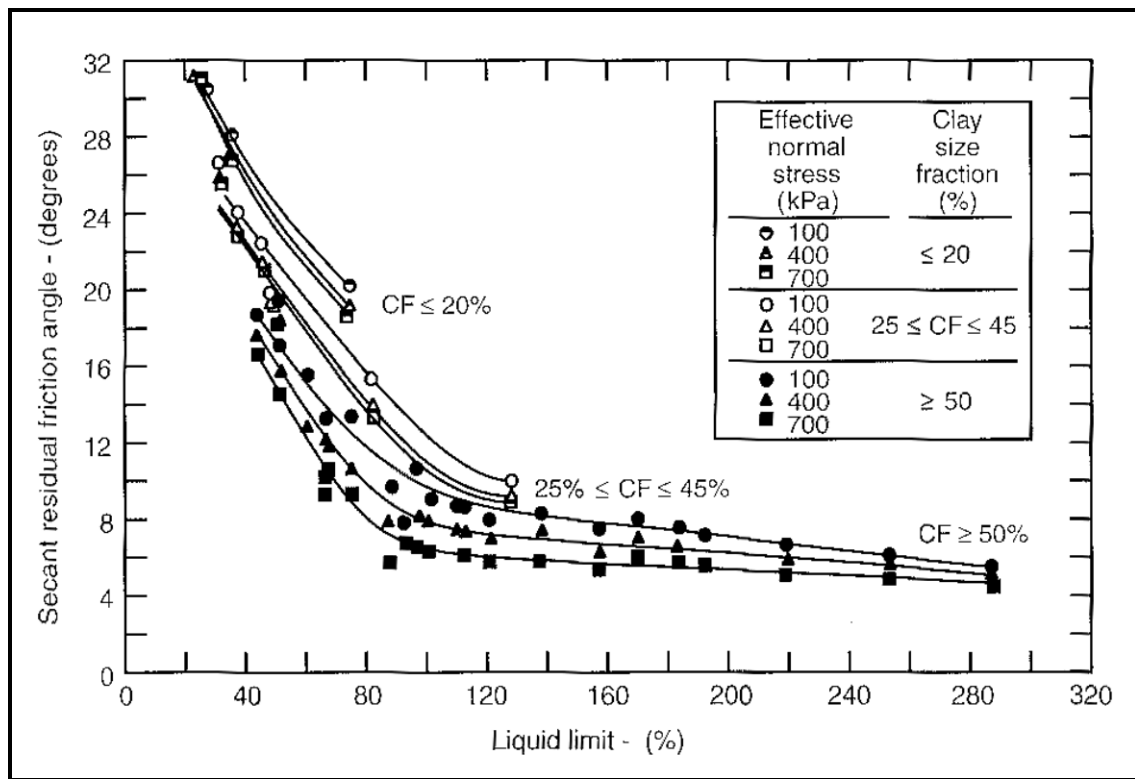


Figure 7-26, Drained Residual Friction Angle and Liquid Limit Relationship (Stark and Eid (1994) with permission from ASCE)

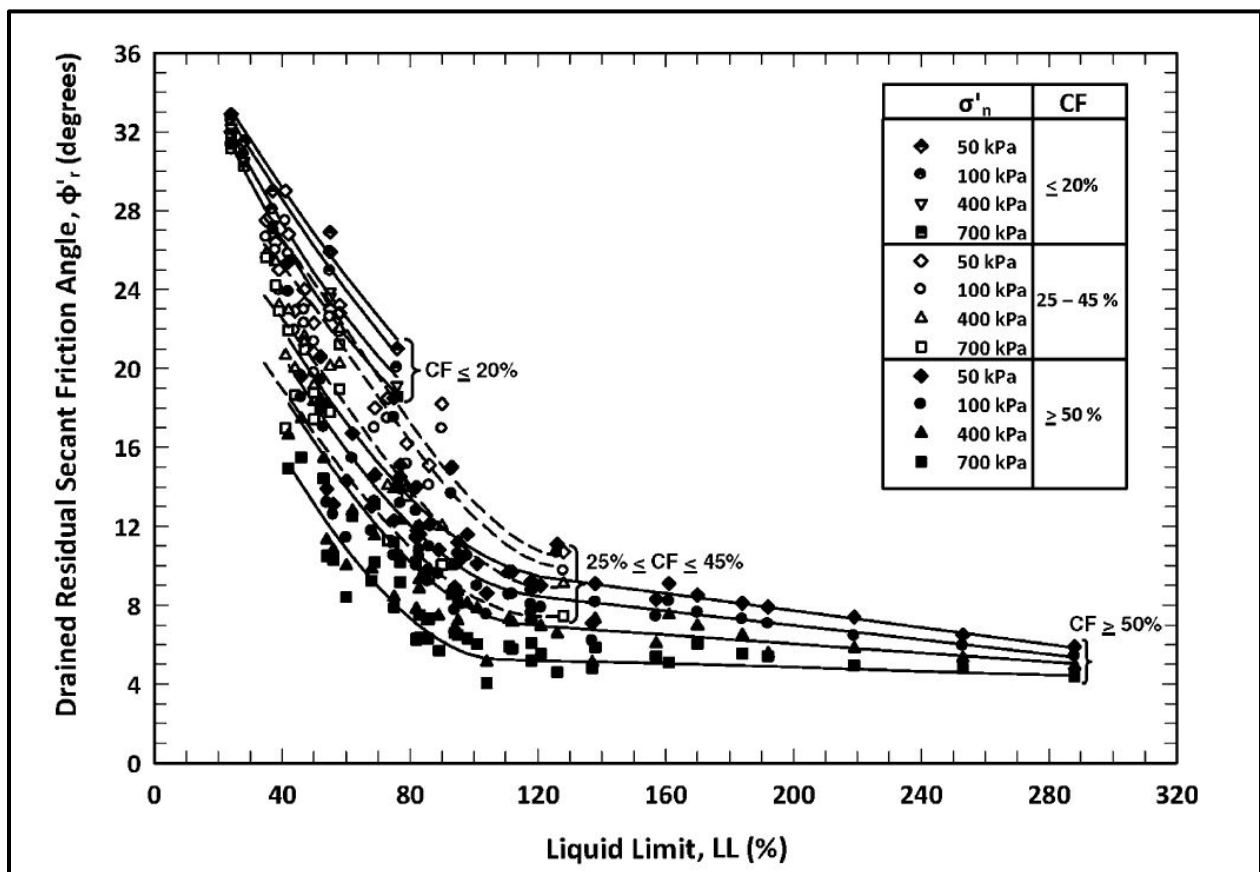


Figure 7-27, Updated Drained Residual Friction Angle and Liquid Limit Relationship (Stark and Hussain (2013) with permission from ASCE)

The first set of equations ( $CF \leq 20\%$ ) for determining the drained residual shear strength are presented below. These equations should be used for soils that have  $30\% \leq LL < 80\%$ ; however, these equations may be used with extreme caution on soils having LLs outside of this range.

$$(\phi'_r)_{\sigma'_{vo}=50kPa} = 39.71 - 0.29 * (LL) + [6.63 * 10^{-4} * (LL)^2] \quad \text{Equation 7-61}$$

Equation 7-62

$$(\phi'_r)_{\sigma'_{vo}=100kPa} = 39.41 - 0.298 * (LL) + [6.81 * 10^{-4} * (LL)^2]$$

$$(\phi'_r)_{\sigma'_{vo}=400kPa} = 40.24 - 0.375 * (LL) + [1.36 * 10^{-3} * (LL)^2] \quad \text{Equation 7-63}$$

Equation 7-64

$$(\phi'_r)_{\sigma'_{vo}=700kPa} = 40.34 - 0.412 * (LL) + [1.683 * 10^{-3} * (LL)^2]$$

Note 1 kPa is equal to approximately 20.89 psf.

The second set of equations ( $25\% \leq CF \leq 45\%$ ) for determining the drained residual shear strength are presented below. These equations should be used for soils that have  $30\% \leq LL < 130\%$ ; however, these equations may be used with extreme caution on soils having LLs outside of this range.

Equation 7-65

$$(\phi'_r)_{\sigma'_{vo}=50kPa} = 31.4 - 6.79 * 10^{-3} * (LL) - 3.616 * 10^{-3} (LL)^2 + 1.864 * 10^{-5} * (LL)^3$$

Equation 7-66

$$(\phi'_r)_{\sigma'_{vo}=100kPa} = 29.8 - 3.627 * 10^{-4} * (LL) - 3.584 * 10^{-3} (LL)^2 + 1.854 * 10^{-5} * (LL)^3$$

Equation 7-67

$$(\phi'_r)_{\sigma'_{vo}=400kPa} = 28.4 - 5.622 * 10^{-2} * (LL) - 2.952 * 10^{-3} (LL)^2 + 1.721 * 10^{-5} * (LL)^3$$

Equation 7-68

$$(\phi'_r)_{\sigma'_{vo}=700kPa} = 28.05 - 0.2083 * (LL) - 8.183 * 10^{-4} (LL)^2 + 9.372 * 10^{-6} * (LL)^3$$

The third set of equations ( $CF \geq 50\%$ ) for determining the drained residual shear strength are presented below; however, a review of Figure 7-27 indicates that the 2 equations for each curve

will be required. For soils that have  $30\% \leq LL < 120\%$  a third-degree polynomial will be required to describe this portion of the curve, while for soils having  $120\% \leq LL < 300\%$  a linear equation may be used. For each effective overburden pressure, the third-degree polynomial is provided first followed by the linear equation. Extreme caution should be used when applying these to soils having LLs outside of this range.

$30\% \leq LL < 120\%$

$$(\phi'_r)_{\sigma'_{vo}=50kPa} = 33.5 - 0.31 * (LL) + 3.9 * 10^{-4}(LL)^2 + 4.4 * 10^{-6} * (LL)^3 \quad \text{Equation 7-69}$$

$120\% \leq LL < 300\%$

$$(\phi'_r)_{\sigma'_{vo}=50kPa} = 12.03 - 0.0215 * (LL) \quad \text{Equation 7-70}$$

$30\% \leq LL < 120\%$

$$\quad \text{Equation 7-71}$$

$$\begin{aligned} (\phi'_r)_{\sigma'_{vo}=100kPa} \\ = 30.7 - 0.2504 * (LL) - 34.2053 * 10^{-4}(LL)^2 + 8.0479 \\ * 10^{-6} * (LL)^3 \end{aligned}$$

$120\% \leq LL < 300\%$

$$(\phi'_r)_{\sigma'_{vo}=100kPa} = 10.64 - 0.0183 * (LL) \quad \text{Equation 7-72}$$

$30\% \leq LL < 120\%$

$$\quad \text{Equation 7-73}$$

$$\begin{aligned} (\phi'_r)_{\sigma'_{vo}=400kPa} \\ = 29.42 - 0.2621 * (LL) - 4.011 * 10^{-4}(LL)^2 + 8.718 * 10^{-6} \\ * (LL)^3 \end{aligned}$$

$120\% \leq LL < 300\%$

$$(\phi'_r)_{\sigma'_{vo}=400kPa} = 8.32 - 0.0114 * (LL) \quad \text{Equation 7-74}$$

$30\% \leq LL < 120\%$

$$\quad \text{Equation 7-75}$$

$$\begin{aligned} (\phi'_r)_{\sigma'_{vo}=700kPa} \\ = 27.7 - 0.3233 * (LL) + 2.896 * 10^{-4}(LL)^2 + 7.1131 * 10^{-6} \\ * (LL)^3 \end{aligned}$$

$120\% \leq LL < 300\%$

$$(\phi'_r)_{\sigma'_{vo}=700kPa} = 5.84 - 0.0049 * (LL) \quad \text{Equation 7-76}$$

As indicated previously the above approach for developing drained residual shear strength is for heavily overconsolidated Clay-Like soils. Typically most heavily overconsolidated Clay-Like soils are indurated (hard) and aggregated (i.e., the clay particles stick together) additional processing of the samples is required to get accurate CFs and LLs. Using the appropriate ASTM procedures, the samples will be processed using a mortar and pestle with the sample being passed through a No. 40 sieve. The CF and LL for the material passing the No. 40 sieve

is then determined ( $CF_{No. 40}$  and  $LL_{No. 40}$ ). The equations presented above are typically based on some of the samples being processed using ball milling to completely disaggregate the sample and then pass the sample through the No. 200 sieve. The material passing the No. 200 sieve is then tested for CF and LL ( $CF_{No. 200}$  and  $LL_{No. 200}$ ) using the appropriate ASTM testing method. Typically, the  $CF_{No. 200}$  and  $LL_{No. 200}$  are greater than the  $CF_{No. 40}$  and  $LL_{No. 40}$ . The use of ball milling is not a typical testing preparation method. Stark and Hussain (2013) have developed based on the available data correlations between  $CF_{No. 40}$  and  $CF_{No. 200}$ ; and  $LL_{No. 40}$  and  $LL_{No. 200}$ . These correlations shall only be used with this procedure.

$$LL_{No.200} = 0.003 * (LL_{No.40})^2 + 1.23 * LL_{No.40} \quad \text{Equation 7-77}$$

Equation 7-78

$$CF_{No.200} = 0.0002 * (CF_{No.40})^3 - 0.0278 * (CF_{No.40})^2 + 2.15 * (CF_{No.40})$$

Please note that these equations have been slightly rearranged from the way Stark and Hussain (2013) presented.

### 7.11.3 Transitional Soils

The drained shear strength of transitional soils may have both  $\phi'$  and  $c'$  components; these components should be determined in the laboratory using the appropriate testing methods. However, if samples for this type of testing have not been obtained (e.g., during the preliminary exploration), then the GEOR should review the percent fines and the plasticity of the soil to determine whether the soil will behave Sand-Like or Clay-Like. If transitional soils are identified in the preliminary exploration, obtaining undisturbed samples of these materials should be attempted during the final exploration. For soils that are difficult to determine the approximate classification, the undrained shear strength parameters for both Sand-Like and Clay-Like soils should be determined and the more conservative design should be used.

### 7.11.4 Maximum Allowable Effective Soil Shear Strength

SCDOT has established maximum allowable peak ( $c, \phi$ ) and residual ( $c_r, \phi_r$ ) undrained soil shear strength design parameters for in-situ soils shown in Table 7-17, for use in design. These soil shear strength design parameters may be exceeded with appropriate laboratory testing results (see Table 7-11). Alternately, these shear strengths may be exceeded using correlations with field testing results (see Table 7-12) and the express written permission of the PC/GDS.

**Table 7-17, Maximum Allowable Effective Soil Shear Strengths**

Soil Description		Peak <sup>1</sup>		Residual	
		c' (psf)	φ' (degrees)	c' (psf)	φ' (degrees)
USCS	Description				
GW, GP, GM, GC	Stone and Gravel	0	40	0	34
SW	Coarse-grained Sand	0	38	0	32
SM, SP	Fine-grained Sand	0	36	0	30
SP	Uniform Rounded Sand	0	32	0	32
ML, MH, SC	Silt, Clayey Sand, Clayey Silt	0	30	0	27
SM, ML	Residual Soils	0	27	0	22
CL-ML	NC Clay (Low Plasticity)	0	35	0	31
CL, CH	NC Clay (Med-High Plasticity)	0	26	0	16
CL-ML	OC Clay (Low Plasticity)	0	34	0	31
CL, CH	OC Clay (Med-High Plasticity)	0	28	0	16

<sup>1</sup> The same maximum peak effective shear strength parameters shall be used for peak effective internal friction angle of normally consolidated cohesive soils and to the fully-softened internal friction angle of overconsolidated cohesive soils.

## 7.12 BORROW MATERIALS SOIL SHEAR STRENGTH SELECTION

This Section pertains to the selection of soil shear strength design parameters for borrow materials used in embankments or behind retaining walls (other than MSE walls or Reinforced Soil Slopes (RSSs)). Soil shear strength selection shall be based on the soil loading and soil response considerations presented in Section 7.9. The soil shear strength design parameters selected must be locally available, cost effective, and be achievable during construction. The selection of soil shear strength design parameters that require the importation of materials from outside of the general project area should be avoided. To this end, bulk samples will be obtained from existing fill embankments or from proposed cut areas and tested as indicated in Chapter 4. The purpose of sampling and testing the existing fill is the assumption that similar fill materials will be available locally. The purpose of sampling and testing proposed cut areas is to determine the suitability of the material for use as fill. The selection of design soil shear strengths required for borrow sources should take into consideration the construction borrow specifications as indicated in Section 7.12.1.

The procedure for selecting soil shear strength design parameters varies depending on the type of project as indicated below:

1. **Traditional Design-Bid-Build W/Existing Embankments:** This type of project can occur when existing roads are being improved by widening the existing embankment. An investigation of locally available materials should be made to confirm that the existing embankment soils are still locally available. If the existing embankment soils are available, the selection of soil shear strength design parameters for these types of projects will be based on using laboratory testing from composite bulk sample obtained from the existing embankment as required in Chapter 4 and appropriately selecting the drained and undrained soil shear strength design parameters for the borrow material. The plans and contract documents may specify the minimum required soil shear strength parameters for the borrow sources based on the existing embankment soils, if necessary. If the existing embankment soils are not locally available, the borrow

material shear strength parameters will be determined as if the project were on a new alignment.

2. **Traditional Design-Bid-Build On New Alignment:** This type of project requires the pre-selection of soil shear strength design parameters without performing any laboratory testing. The preliminary subsurface investigation may need to identify locally available soils (or borrow sources) and appropriately select soil shear strength design parameters for the borrow materials. Locally available soils can be investigated by using USDA Soil Survey maps as indicated in Section 7.12.2. The plans and contract documents may specify the minimum required soil shear strength parameters for the borrow sources, if necessary.

### 7.12.1 **SCDOT Borrow Specifications**

The SCDOT Standard Specifications for Highway Construction (latest edition), Section 203, provides the requirements for borrow material. Embankment material must not have optimum moisture content greater than 25.0% as defined in accordance with SC-T-29. Acceptable soils for use in embankments and as subgrade vary by county indicated by the following 2 Groups.

**Group A:** Includes the following counties: Abbeville, Anderson, Cherokee, Chester, Edgefield, Fairfield, Greenville, Greenwood, Lancaster, Laurens, McCormick, Newberry, Oconee, Pickens, Saluda, Spartanburg, Union, and York. Below the upper 5 feet of embankment, any soil that does not meet the description of muck may be used provided it is stable when compacted to the required density.

**Group B:** Aiken, Allendale, Bamberg, Barnwell, Beaufort, Berkeley, Calhoun, Charleston, Chesterfield, Clarendon, Colleton, Darlington, Dillon, Dorchester, Florence, Georgetown, Hampton, Horry, Jasper, Kershaw, Lee, Lexington, Marion, Marlboro, Orangeburg, Richland, Sumter, and Williamsburg. The soil material below the upper 5 feet of embankment is soil that classifies as A-1, A-2, A-3, A-4, A-5, and A-6.

Groups A and B are shown graphically on a South Carolina map in Figure 7-28.

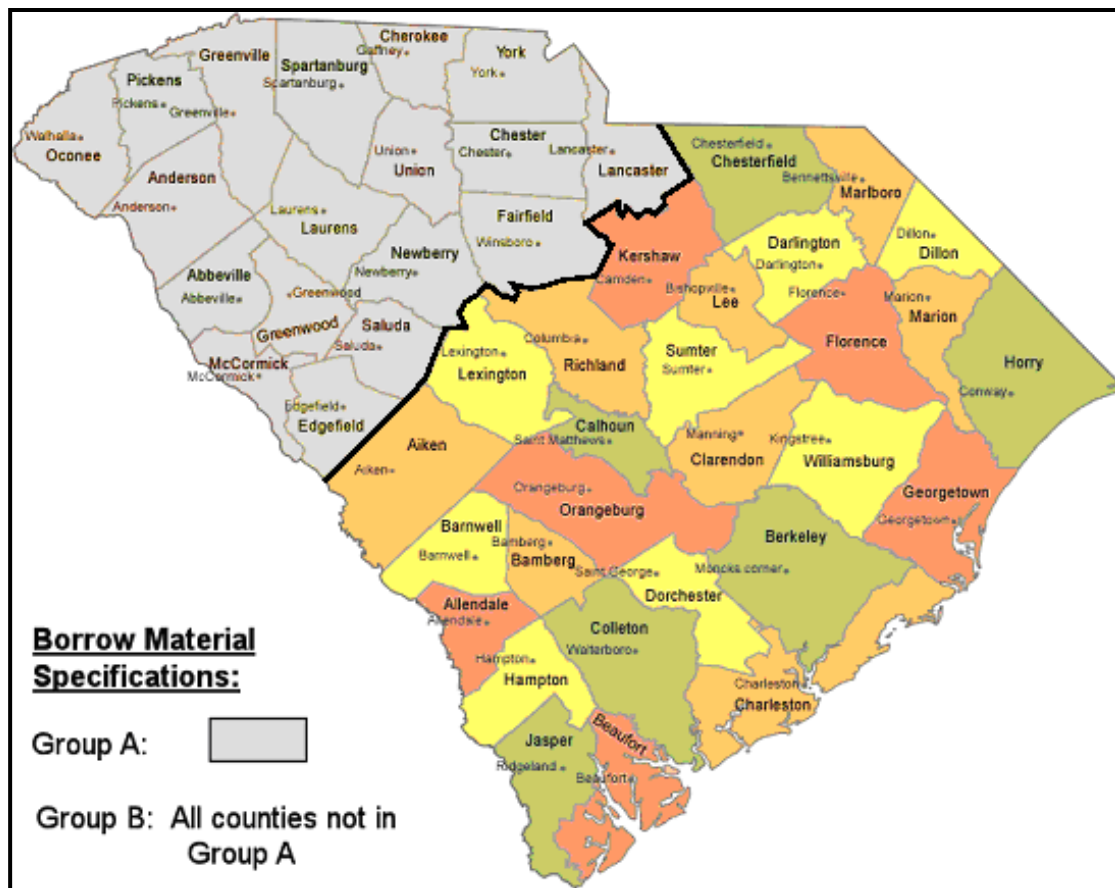


Figure 7-28, Borrow Material Specifications By County

A brief geologic description of the surface soils in Groups A and B are provided below and for more detail see Chapter 11.

**Group A:** This group is located northwest of the “Fall Line” in the Blue Ridge and Piedmont physiographic geologic units. The Blue Ridge unit surface soils typically consist of residual soil profile consisting of clayey soils near the surface where weathering is more advanced, underlain by sandy silts and silty sands. There may be colluvial (old land-slide) material on the slopes. The Piedmont unit has a residual soil profile that typically consists of clayey soils near the surface, where soil weathering is more advanced, underlain by sandy silts and silty sands. The residual soil profile exists in areas not disturbed by erosion or the activities of man.

**Group B:** This group is located south and east of the “Fall Line” in the Coastal Plain physiographic geologic unit. Sedimentary soils are found at the surface consisting of unconsolidated sand, clay, gravel, marl, cemented sands, and limestone.

### 7.12.2 USDA Soil Survey Maps

Locally available borrow sources can be researched by using the United States Department of Agriculture (USDA) Soil Survey Maps. A listing of USDA Soil Surveys that are available can be obtained by selecting “South Carolina” at [http://soils.usda.gov/survey/printed\\_surveys/](http://soils.usda.gov/survey/printed_surveys/) and reviewing results by county. Soil surveys can be obtained as either printed documents, CD-ROM, downloading online .pdf documents, or generated using USDA Web Soil Survey (WSS) Internet application.





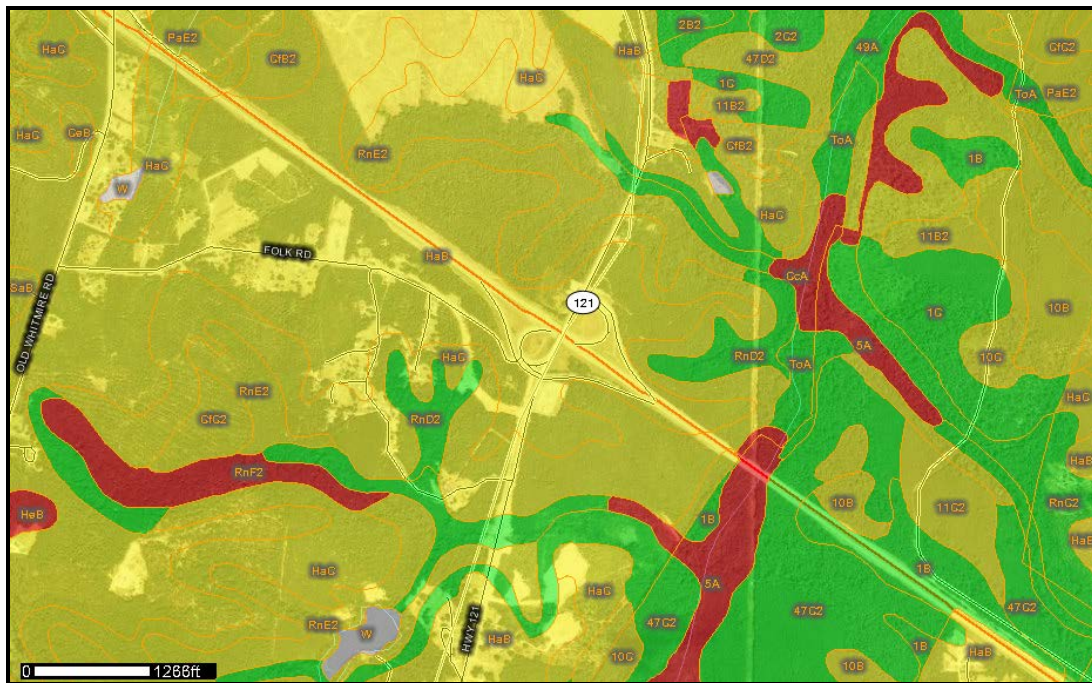


Figure 7-30, USDA Roadfill Source Map - Newberry County, South Carolina (USDA Web Soil Survey)

### 7.12.3 Compacted Soils Shear Strength Selection

Compacted soils are used to construct roadway embankments, bridge approaches, and backfill behind retaining walls. This Section does not govern the selection of backfill soil properties for MSE walls or RSSs. The method of selecting soil shear strength parameters for compacted soils will be either:

- Measured using appropriate laboratory shear strength tests or
- Conservatively selected based on drained soil shear strength parameters typically encountered in South Carolina soils.

The method to be used for selection will be dependent on the type of project as discussed previously.

SCDOT experience with borrow materials typically found in Group A are Piedmont residual soils. These borrow materials are typically classified as micaceous clayey silts and micaceous sandy silts, clays, and silty soils in partially drained conditions. These soils may have USCS classifications of either ML or MH and typically have LL greater than 30. Published laboratory shear strength testing results for Piedmont residual soils (Sabatini, et al. (2002), Appendix A, page A-40) indicate an average effective friction angle of  $35.2^\circ$  with a  $\pm 1$  standard deviation range of  $29.9^\circ < \phi' < 40.5^\circ$ . A conservative lower bound of  $27.3^\circ$  is also indicated.

SCDOT experience with borrow materials typically found in Group B are Coastal Plain soils that are typically uniform fine sands that are sometimes difficult to compact and behave similar to silts. When these soils are encountered, caution should be used in selecting effective soil shear strength friction angles since values typically range from  $28^\circ < \phi' < 32^\circ$ .

### 7.12.4 Allowable Soil Shear Strengths of Compacted Soils

SCDOT has determined, through a research project, the effective and total soil strength parameters (i.e.,  $c'$  and  $\phi'$  or  $c$  and  $\phi$ ) that are typically available for each South Carolina County. The results of this research and the allowable parameters are available on the SCDOT website ([http://www.scdot.org/doing/geoTech\\_Design.aspx](http://www.scdot.org/doing/geoTech_Design.aspx)). If the results of the on-site soil testing or the selected shear strength parameters are less than the shear strength parameters provided on the SCDOT website then shear strength verification testing during construction should not be required during compaction. However, the GEOR may select a project-specific soil classification (i.e., AASHTO and USCS Classifications (see Chapter 6)) in order to assure that the borrow materials meet the shear strength requirements. This project-specific soil classification shall be provided on the project plans. The required testing for this verification, is not anticipated to be different than the classification testing already currently being performed during construction. If the on-site soil has a shear strength greater than the allowed for the county, the GEOR may elect to use this higher shear strength without the requirement for shear strength verification testing during construction. However, a project-specific classification (i.e., AASHTO and USCS Classifications) shall be required to be indicated on the project plans. If the GEOR's design needs to exceed the on-site shear strength parameters and the county shear strength values, the GEOR shall use the proposed plan notes (see Chapter 22) to convey the required soil strength properties to the Contractor. The following testing shall be required to confirm the anticipated revised shear strength parameters:

- Moisture-density Relationship (Standard Proctor)
- Grain-size Distribution with wash No. 200 Sieve
- Moisture-Plasticity Relationship Determination (Atterberg Limits)
  - Performed only on samples with more than 20 percent passing #200 sieve
- Natural Moisture Content
- Direct Simple Shear Test
  - Performed only on samples with less than or equal to 20 percent passing #200 sieve
  - Sample remolded to 95 percent of Standard Proctor value
  - Sample moisture content shall be between -1 percent to +2 percent of optimum moisture content
- Consolidated-Undrained Triaxial Shear Test with pore pressure measurements
  - Performed only on samples with more than 20 percent passing #200 sieve
  - Sample remolded to 95 percent of Standard Proctor value
  - Sample moisture content shall be between -1 percent to +2 percent of optimum moisture content

Once a borrow source achieving the required shear strength parameters has been located, additional shear strength testing during construction will be required every approximate 50,000 CY. Classification testing performed at the intervals required by the SCDOT Standard Specifications for Highway Construction, latest edition, will be required to assure that the borrow materials continue to be similar to the materials used in the shear strength testing. The GEOR shall determine when and if additional shear strength testing is required if the classification testing indicates a change in classification.

If stone (e.g., Nos. 57, 67, 789 or No. 4 ballast) is selected as the borrow material, large scale direct shear (minimum size of direct shear box of 12 inches square by 8 inches deep) should be required. However, to avoid the cost and time for testing these materials a maximum  $\phi'$  of 46° shall be assumed for all of the stones. If a  $\phi'$  greater than this value is required, then testing will be required. However, prior to testing the GEOR shall obtain approval from the appropriate

PC/GDS for the increased  $\phi'$  and will provide the name of the laboratory performing the tests. It is noted that this  $\phi'$  does not apply to MSE wall design. See Supplemental Technical Specification (STS) *Mechanically Stabilized Earth (MSE) Walls*, SC-M-713, for the  $\phi'$  that applies to MSE wall design.

### 7.13 SOIL SETTLEMENT PARAMETERS

Settlements are caused by the introduction of loads (stresses,  $+\Delta\sigma$ ) on to the subsurface soils located beneath a site. These settlements can be divided into 2 primary categories, elastic and time-dependent settlements (consolidation). Settlements (strains) are a function of the load (stress) placed on the subsurface soils. Elastic settlements typically predominate in Sand-Like soils or soils with 0 to 20 percent fines regardless of the plasticity of the fines. Time-dependent settlements predominate in Clay-Like soils or soils with more than 20 percent fines and with LL greater than 40 ( $LL > 40$ ) and PI greater than 10 ( $PI > 10$ ). The GEOR should evaluate soils with either LL greater than 40 ( $LL > 40$ ) or PI greater than 10 ( $PI > 10$ ) as to whether the soils will behave elastically or have time-dependent settlement characteristics. The GEOR is responsible for making this determination for these soils (see Table 7-6 for guidance).

Settlement parameters can be developed from high quality laboratory testing (triaxial shear for elastic parameters and consolidation testing for time-dependent parameters). However, for cohesionless soils, obtaining high quality samples for testing can be extremely difficult. Therefore, in-direct methods (correlations) for measuring the elastic parameters are used. Time-dependent settlement parameter correlations for cohesive soils also exist. These correlations should be used for either preliminary analyses or for evaluating the reasonableness of laboratory consolidation testing.

#### 7.13.1 Elastic Parameters

Elastic settlements are instantaneous and are considered recoverable. These settlements are calculated using elastic theory. The determination of elastic settlements is provided in Chapter 17. In the determination of the elastic settlements the elastic modulus,  $E$ , (tangent or secant) and the Poisson's ratio,  $\nu$ , are used. Since  $E$  and  $\nu$  are both dependent on the laboratory testing method (unconfined, confined, undrained, drained), the overconsolidation ratio, water content, strain rate and sample disturbance, considerable engineering judgment is required to obtain reasonable values for use in design. Provided in Table 7-18 are elastic modulus correlations with  $N_{1.60}^*$  values. Table 7-19 provides typical values of soil elastic modulus and Poisson's ratio for various soil types.

**Table 7-18, Elastic Modulus Correlations For Soil Using SPT N-values  
(AASHTO LRFD Specifications (2017))**

Soil Type	Elastic Modulus, $E_s$ (psi)
Silts, sandy silts, slightly cohesive mixtures	$56^*(N_{1.60}^*)$
Clean fine to medium sands and slightly silty sands	$97^*(N_{1.60}^*)$
Coarse sands	$139^*(N_{1.60}^*)$
Sandy gravels and gravels	$167^*(N_{1.60}^*)$

The elastic modulus of soil may also be correlated to corrected tip resistance ( $q_t$ ) and the soil behavior type ( $I_c$ ) according to Robertson and Cabal (2015), using the following equations:

$$E_s = \alpha_E * (q_t - \sigma_{vo}) \quad \text{Equation 7-79}$$

$$\alpha_E = 0.015 * [10^{(0.55 * I_c + 1.68)}] \quad \text{Equation 7-80}$$

Where,

$q_t$  = Corrected tip resistance (see Chapter 5)

$\sigma_{vo}$  = Total overburden stress at depth of  $q_t$  (see Chapter 5)

$I_c$  = Soil behavior type (see Chapter 5)

$E_s$  = Elastic modulus, same units as  $q_t$  and  $\sigma_{vo}$

According to Marchetti, et al. (2001), the elastic modulus of soil,  $E_s$ , may be correlated from the DMT using the constrained modulus,  $M_{DMT}$ .

$$E_s = \left[ \frac{(1+\nu) * (1-2\nu)}{(1-\nu)} \right] * M_{DMT} \quad \text{Equation 7-81}$$

Where,

$\nu$  = Poisson's ratio

$M_{DMT}$  = constrained modulus (bars) (1 bar  $\approx$  1 tsf)

$$M_{DMT} = R_M * E_D \quad \text{Equation 7-82}$$

Where,

$E_D$  = Dilatometer modulus (bars) (1 bar  $\approx$  1 tsf)

The term  $R_M$  is a function of the Material Index and the Horizontal Stress Index ( $f(I_D, K_D)$ ).  $R_M$  is determined using the following equations when  $K_D$  is less than or equal to 10 ( $K_D \leq 10$ ).

$$I_D \leq 0.6 \quad R_M = 0.14 + 2.36 * \log K_D \quad \text{Equation 7-83}$$

$$0.6 < I_D < 3 \quad R_M = R_{M,0} + (2.5 - R_{M,0}) * \log K_D \quad \text{Equation 7-84}$$

$$R_{M,0} = 0.14 + 0.15 * [I_D - 0.6] \quad \text{Equation 7-85}$$

$$I_D \geq 3 \quad R_M = 0.5 + 2 * \log K_D \quad \text{Equation 7-86}$$

If  $K_D$  is greater than 10 ( $K_D > 10$ ), then use the following equation:

$$R_M = 0.32 + 2.18 * \log K_D \quad \text{Equation 7-87}$$

If  $R_M$  determined using the above equations is less than 0.85, set  $R_M$  equal to 0.85.

For soils with a Poisson's ratio,  $\nu$ , ranging from 0.25 to 0.30, the following equation may be used. A Poisson's ratio in this range is typical of coarse-grained soils (see Table 7-19).

$$E_s \approx 0.8 M_{DMT} \quad \text{Equation 7-88}$$

**Table 7-19, Typical Elastic Modulus and Poisson Ratio Values for Soil  
(AASHTO LRFD Specifications (2017))**

Soil Type	Typical Elastic Modulus Values, E (ksi)	Poisson's Ratio, $\nu$
Clay:		0.4 – 0.5 (Undrained)
Soft sensitive	0.347 – 2.08	
Medium stiff to stiff	2.08 – 6.94	
Very stiff	6.94 – 13.89	
Silt	0.278 – 2.78	0.3 – 0.35
Fine Sand:		0.25
Loose	1.11 – 1.67	
Medium dense	1.67 – 2.78	
Dense	2.78 – 4.17	
Sand:		
Loose	1.39 – 4.17	0.20 – 0.36
Medium dense	4.17 – 6.94	0.25 – 0.40
Dense	6.94 – 11.11	0.30 – 0.40
Gravel:		
Loose	4.17 – 11.11	0.20 – 0.35
Medium dense	11.11 – 13.89	0.25 – 0.40
Dense	13.89 – 27.78	0.30 – 0.40

### 7.13.2 Consolidation Parameters

Consolidation settlement involves the removal of water from the interstitial spaces (pores) between soil grains and the rearrangement of the soil grains. Typically, Clay-Like soils are considered to undergo consolidation settlements. However, soils with either LL greater than 40 ( $LL > 40$ ) or PI greater than 10 ( $PI > 10$ ) also undergo consolidation settlements depending on the moisture-plasticity relationship. Clay-Like soils are typically more impervious and therefore will require more time to settle. Further these soil types may also undergo more settlement than Sand-Like soils because of the volume of water within these soils. To determine the amount of consolidation settlement that a soil will undergo, the following soil parameters are required: compression ( $C_c$  or  $C_{ec}$ ), recompression ( $C_r$  or  $C_{er}$ ), and secondary ( $C_{\alpha}$  or  $C_{e\alpha}$ ) compression indices, coefficient of consolidation ( $c_v$ ) and the effective preconsolidation pressure ( $\sigma'_p$  or  $p'_c$ ). These parameters are normally determined from consolidation testing (see Chapter 5).

Prior to obtaining the parameters indicated previously, the curves obtained from the consolidation test require correction by the GEOR. Curve correction is applied to the test results presented as  $e$ -log  $p$  and  $\varepsilon$ -log  $p$  curves. Duncan and Buchignani (1976) provide methods for correcting both  $e$ -log  $p$  and  $\varepsilon$ -log  $p$  for both normally consolidated and overconsolidated soils. The procedures for correcting the  $e$ -log  $p$  curves (normally consolidated and overconsolidated) are presented in Table 7-20 and for the  $\varepsilon$ -log  $p$  curves (normally consolidated and overconsolidated) are presented in Table 7-21.

**Table 7-20, Correction of the e-log p Curve for Disturbance  
(modified from Duncan and Buchignani (1976))**

Step	Description
<b>Normally Consolidated Soil (<math>\sigma'_{vo} = \sigma'_p</math>) (Figure 7-31)</b>	
1	Locate point A at the intersection of $e_o$ and $\sigma'_p$ ( $P_p$ )
2	Locate point B on the virgin curve or extension where $e = 0.4e_o$
3	Connect points A and B with a straight line – this is the corrected virgin curve
<b>Overconsolidated Soil (<math>\sigma'_{vo} &lt; \sigma'_p</math>) (Figure 7-32)</b>	
1	Locate point A at the intersection of $e_o$ and $\sigma'_{vo}$ ( $P_o'$ )
2	Draw a line from point A parallel to the rebound curve and locate point B where this line intersects $\sigma'_p$ ( $P_p$ )
3	Locate point C on the virgin curve or extension where $e = 0.4e_o$
4	Connect points B and C with a straight line – this is the corrected virgin curve

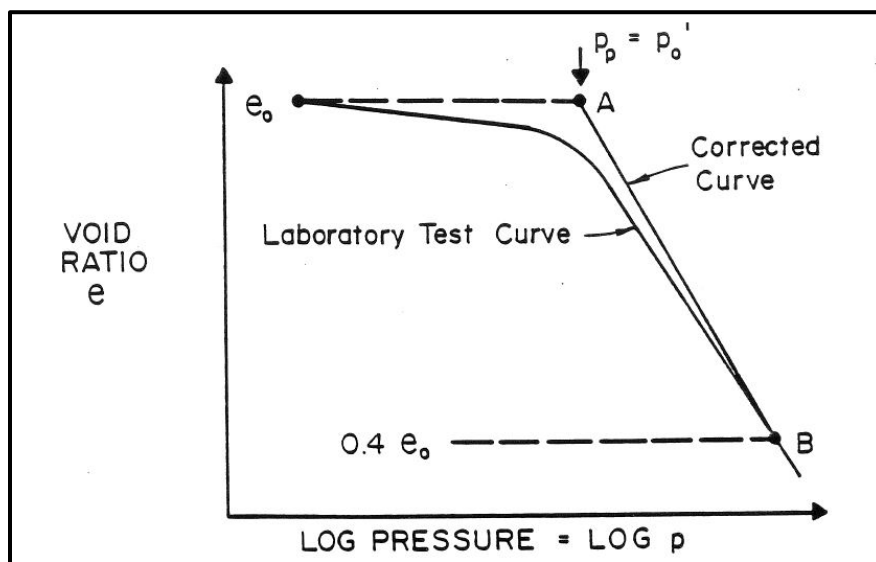


**Figure 7-31, Corrected e-log p Normally Consolidated Curve  
(Duncan and Buchignani (1976))**

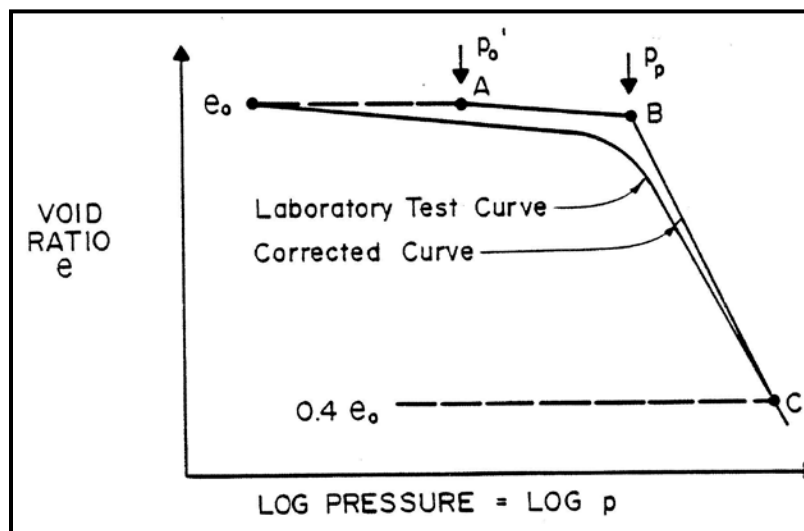


**Figure 7-32, Corrected e-log p Overconsolidated Curve  
(Duncan and Buchignani (1976))**

**Table 7-21, Correction of the  $\epsilon$ -log p Curve for Disturbance  
(modified from Duncan and Buchignani (1976))**

Step	Description
<b>Normally Consolidated Soil (<math>\sigma'_{vo} = \sigma'_p</math>) (Figure 7-33)</b>	
1	Locate point A at the intersection of $\epsilon = 0$ and $\sigma'_p$ ( $P_p$ )
2	Locate point B on the virgin curve or extension where $\epsilon = 0.4$
3	Contact points A and B with a straight line – this is the corrected virgin curve
<b>Overconsolidated Soil (<math>\sigma'_{vo} &lt; \sigma'_p</math>) (Figure 7-34)</b>	
1	Locate point A at the intersection of $\epsilon = 0$ and $\sigma'_{vo}$ ( $P_o'$ )
2	Draw a line from point A parallel to the rebound curve and locate point B where this line intersects $\sigma'_p$ ( $P_p$ )
3	Locate point C on the virgin curve or extension where $\epsilon = 0.4$
4	Contact points B and C with a straight line – this is the corrected virgin curve

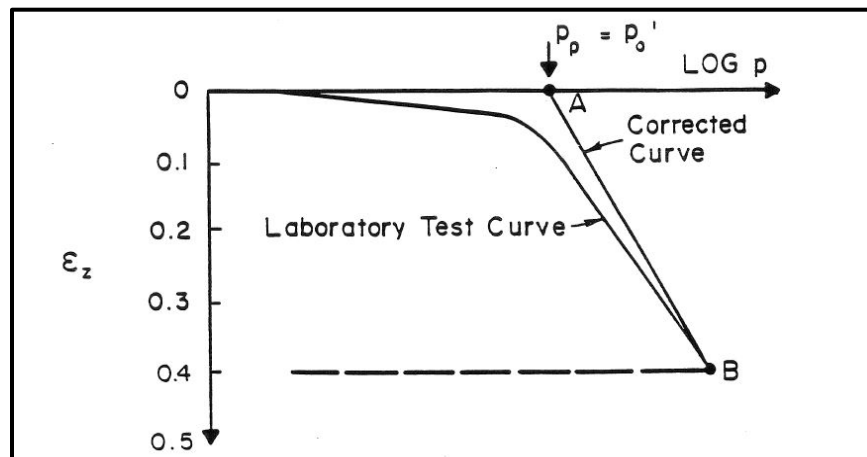


**Figure 7-33, Corrected  $\epsilon$ -log p Normally Consolidated Curve  
(Duncan and Buchignani (1976))**

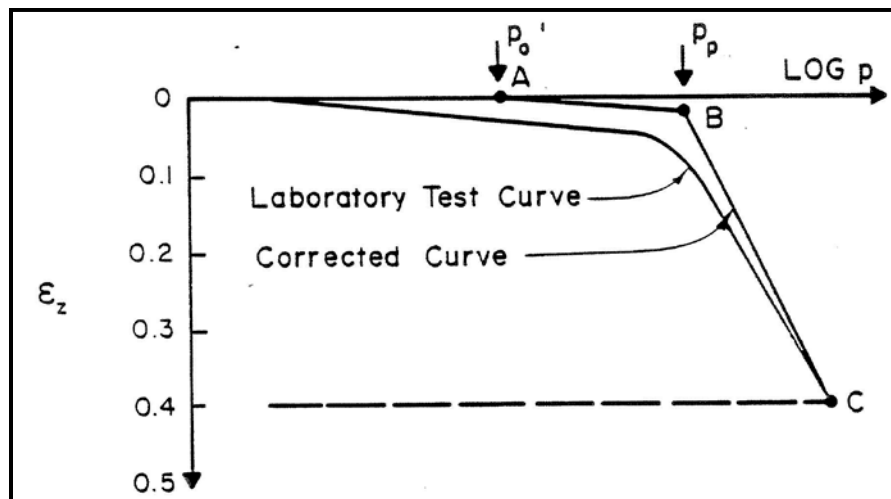


**Figure 7-34, Corrected  $\epsilon$ -log p Overconsolidated Curve  
(Duncan and Buchignani (1976))**

The compression ( $C_c$  or  $C_{ec}$ ) and recompression ( $C_r$  or  $C_{er}$ ) indices are determined from the corrected curves. The compression ( $C_c$  or  $C_{ec}$ ) index is the slope of the virgin portion of the corrected curve, either  $e$ -log  $p$  ( $C_c$ ) or  $\epsilon$ -log  $p$  ( $C_{ec}$ ), over a full logarithmic cycle. The

recompression index is the slope of the recompression portion of the corrected curve, either  $e$ -log  $p$  ( $C_r$ ) or  $\varepsilon$ -log  $p$  ( $C_{\varepsilon r}$ ) over a full logarithmic cycle. If the slope of either portion of the curve does not extend over a full logarithmic cycle extend the line in both directions to cover a full logarithmic cycle.

For preliminary estimates and to verify the results of the consolidation testing the correlations listed in the following Sections may be used. These correlations should not be used for final design, except where the GEOR considers the results of the consolidation testing to be questionable. The GEOR shall document the reason for the use of the correlations. In addition, all of the consolidation parameters shall be clearly provided in the geotechnical report.

### 7.13.2.1 Compression Index

Similarly to the other consolidation parameters, the  $C_c$  is best determined from consolidation testing. The Compression Index ( $C_c$ ) has been related to the Atterberg Limits by Tiwari and Ajmera (2012); however, this correlation should only be used for either preliminary analyses (first order estimates) or for evaluating the reasonableness of laboratory consolidation testing.

$$C_c = 0.014 * (PI) \quad \text{Equation 7-89}$$

Where,

PI = Plasticity Index (%)

The Compression Index may also be related to strain as indicated below.

$$C_{\varepsilon c} = \frac{C_c}{(1+e_o)} \quad \text{Equation 7-90}$$

Where,

$e_o$  = Initial void ratio

$C_c$  = Compression Index

### 7.13.2.2 Recompression Index

The Recompression Index ( $C_r$ ) can be correlated to the  $C_c$  values. Ladd (1973) indicates the  $C_r$  value is approximately 10 to 20 percent of the  $C_c$  value. The Recompression Index may also be related to strain as indicated by the following equation.

$$C_{\varepsilon r} = \frac{C_r}{(1+e_o)} \quad \text{Equation 7-91}$$

Where,

$e_o$  = Initial void ratio

$C_r$  = Recompression Index

### 7.13.2.3 Secondary Compression Index

Secondary compression occurs after the completion of elastic and primary consolidation settlements. The amount of secondary compression settlement should be determined and included in the estimate of total settlement for a given project. The Secondary Compression Index ( $C_{\alpha}$ ) like the other consolidation settlement parameters is best determined from consolidation testing; however, correlations exist that may be used to provide a preliminary



estimate of secondary compression settlement. In addition, these correlations may be used to verify the results of the consolidation testing. Provided in Figure 7-35 is a chart of  $C_{\alpha}$  versus the natural moisture content of soil.

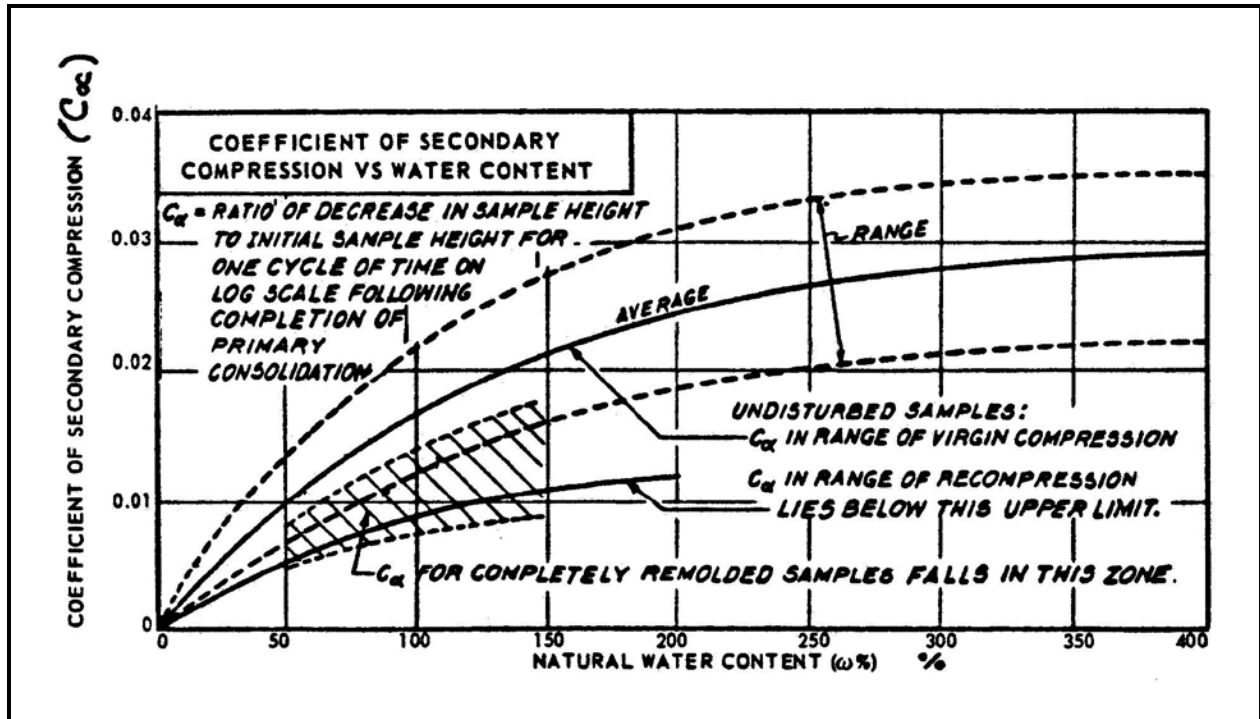


Figure 7-35, Secondary Compression Index Chart (NAVFAC DM-7.1 (1982))

The Secondary Compression Index may also be related to strain as indicated below.

$$C_{\epsilon\alpha} = \frac{C_{\alpha}}{(1+e_o)} \quad \text{Equation 7-92}$$

Where,

$e_o$  = Initial void ratio

$C_{\alpha}$  = Secondary Compression Index

For normally consolidated soils, the ratio of the coefficient of secondary compression to the compression index ( $C_{\alpha}/C_c = C_{\epsilon\alpha}/C_{\epsilon c}$ ) is relatively constant for a given soil. On average, the value of  $C_{\alpha}/C_c$  is  $0.04 \pm 0.01$  for inorganic clays and silts. For organic clays and silts the value averages  $0.05 \pm 0.01$ . For peats, the value averages  $0.06 \pm 0.01$ . These values may be used to assess actual values from laboratory tests or for preliminary analyses. If the final effective stress in the ground is less than the preconsolidation stress, the  $C_r$  should be used instead of  $C_c$  to estimate the coefficient of secondary compression.

### 7.13.2.4 Consolidation Coefficient

The preceding Sections dealt with the parameters required to determine the amount of settlement that could be anticipated at a project location; while this Section provides a means to estimate the time for consolidation settlement. As indicated previously, elastic settlements are anticipated to occur relatively instantaneously (i.e., during construction) while consolidation settlements are anticipated to occur at some time after the structure has been completed. The rate of consolidation is directly related to the permeability of the soil. As with the consolidation

parameters, the coefficient of consolidation ( $c_v$ ) should be determined from the results of consolidation testing. Correlations exist that may be used to provide a preliminary estimate of  $c_v$ . In addition, these correlations may be used to verify the results of the consolidation testing. Provided in Figure 7-36 is a chart of  $c_v$  versus the LL of soil.

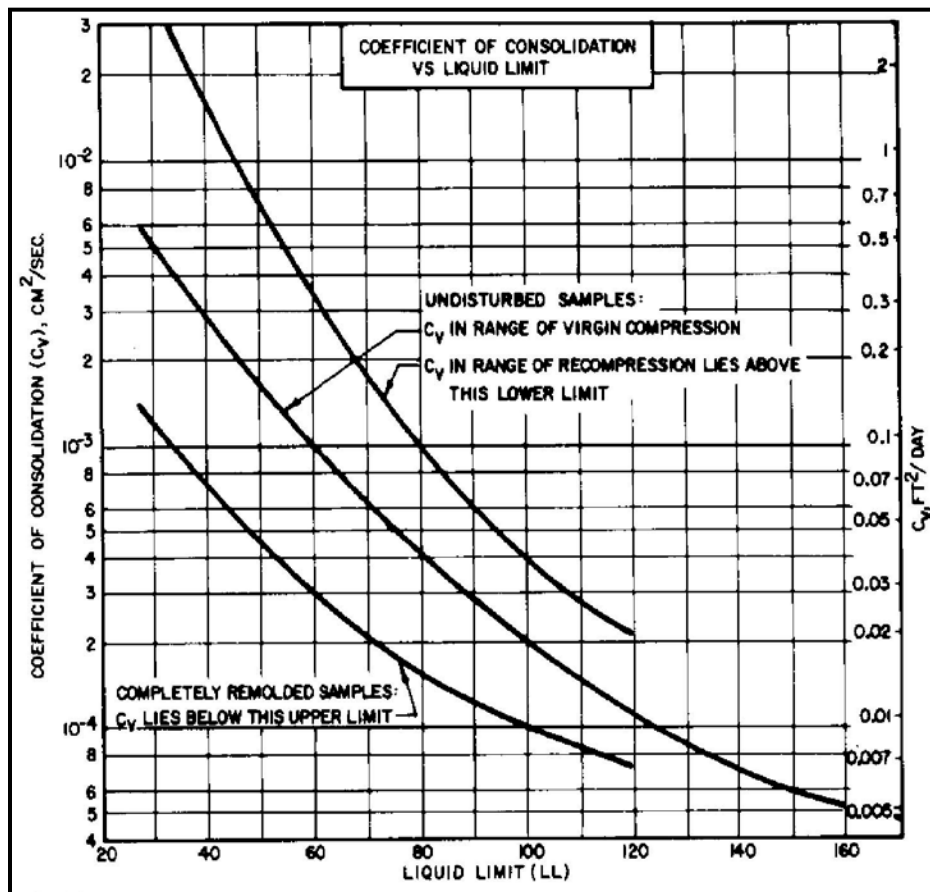


Figure 7-36, Consolidation Coefficient and Liquid Limit Relationship (NAVFAC DM-7.1 (1982))

### 7.13.2.5 Effective Preconsolidation Stress

The effective preconsolidation stress ( $\sigma'_p$  or  $p'_c$ ) in soils is used to determine whether to use the Compression or Recompression Index. The effective preconsolidation stress ( $\sigma'_p$ ) is the maximum past pressure that a soil has been exposed to since deposition. Similarly to the other consolidation parameters the  $\sigma'_p$  is best determined from consolidation testing. Correlations also exist; however, these correlations should only be used for either preliminary analyses (first order estimates) or for evaluating the reasonableness of laboratory consolidation testing. The effective preconsolidation stress ( $\sigma'_p$  or  $p'_c$ ) can be correlated to total cohesion,  $c$  (NAVFAC DM-7.1 (1982)). As with the other consolidation parameters the correlated  $\sigma'_p$  should be used for preliminary estimates only.

$$\sigma'_p = \frac{c}{(0.11 + 0.0037 * PI)} \quad \text{Equation 7-93}$$

The  $\sigma'_p$  can also be estimated from the CPTu using the following equations (Sabatini, et al. (2002)).

$$\sigma'_p = 0.33 * (q_t - \sigma_{vo}) \quad \text{Equation 7-94}$$

CPT Piezocone (shoulder element):

$$\sigma'_p = 0.53 * (u_2 - u_0) \quad \text{Equation 7-95}$$

$$\sigma'_p = 0.60 * (q_t - u_2) \quad \text{Equation 7-96}$$

## 7.14 ROCK PARAMETER DETERMINATION

While the shear strength of individual rock cores is obtained from unconfined axial compression testing, the shear strength of the entire rock mass should be used for design. Therefore, the shear strength and consolidation parameters for the rock mass shall be developed using both the GSI and the RMR methods as defined in Chapter 6. In addition, the GEOR should consider the time rate of rock coring, since typically harder rock masses will take longer to core through than weaker rock masses. There are many factors besides the strength of the rock that will affect the time rate of rock coring including condition of the core barrel, the condition of the drill rig, experience of the driller rig operator in rock operations, etc. The GEOR should be aware of all of these conditions when developing a profile of the rock encountered at a site.

### 7.14.1 Shear Strength Parameters

#### 7.14.1.1 GSI

The rock mass shear strength from the GSI should be evaluated using the Hoek-Brown failure criterion (Hoek, Carranza-Torres, and Corkum (2002)). The shear strength of the rock mass is represented by a curved envelope that is a function of the unconfined (uniaxial) compressive strength of the intact rock,  $q_u$ , and 2 dimensionless factors. The rock mass compressive shear strength,  $\tau$  is defined as indicated below. This rock mass compressive shear strength is used in design, provided there is no structural defect in the rock mass that would predominate over the rock mass compressive shear strength.

$$\tau = q_u * s^a \quad \text{Equation 7-97}$$

$$s = e^{\left(\frac{GSI-100}{9-3D}\right)} \quad \text{Equation 7-98}$$

$$a = \frac{1}{2} + \frac{1}{6} * \left( e^{\left(\frac{-GSI}{15}\right)} - e^{\left(\frac{-20}{3}\right)} \right) \quad \text{Equation 7-99}$$

Where,

$q_u$  = Unconfined compressive strength of intact rock specimen

GSI = Geological Strength Index (see Chapter 6)

D = Disturbance factor (see Chapter 6)

e = Mathematical constant (i.e., Euler's number)

#### 7.14.1.2 RMR

The rock mass shear strength should be evaluated using the Hoek and Brown criterion as presented in AASHTO LRFD Specifications. The shear strength of the rock mass is represented by a curved envelope that is a function of the unconfined (uniaxial) compressive

strength of the intact rock,  $q_u$ , and 2 dimensionless factors. The rock mass shear strength,  $\tau$ , (in ksf) is defined as indicated below.

$$\tau = (\cot \phi'_i - \cos \phi'_i) * m * \frac{q_u}{8} \tag{Equation 7-100}$$

$$\phi'_i = \tan^{-1} \left\{ 4h * \cos^2 \left[ 30 + 0.33 * \sin^{-1} \left( h^{\left(\frac{-3}{2}\right)} \right) \right] - 1 \right\}^{\left(\frac{-1}{2}\right)} \tag{Equation 7-101}$$

$$h = 1 + \frac{[16 * (m * \sigma'_n + s * q_u)]}{3 * m^2 * q_u} \tag{Equation 7-102}$$

Where,

- $\phi'_i$  = instantaneous friction angle of the rock mass (degrees)
- $q_u$  = average unconfined rock core compressive strength (ksf)
- $\sigma'_n$  = effective normal stress (ksf)
- m and s = Constants, from Table 7-22

**Table 7-22, Constants m and s based on RMR  
(AASHTO LRFD Specifications (2017))**

Rock Quality	Constants	<u>Rock Type:</u>				
		A	B	C	D	E
Intact rock samples RMR = 100	m	7.00	10.00	15.00	17.00	25.00
	s	1.00	1.00	1.00	1.00	1.00
Very good quality rock mass RMR = 85	m	2.40	3.43	5.14	5.82	8.567
	s	0.082	0.082	0.082	0.082	0.082
Good quality rock mass RMR = 65	m	0.575	0.821	1.231	1.395	2.052
	s	0.00293	0.00293	0.00293	0.00293	0.00293
Fair quality rock mass RMR = 44	m	0.128	0.183	0.275	0.311	0.458
	s	0.00009	0.00009	0.00009	0.00009	0.00009
Poor quality rock mass RMR = 23	m	0.029	0.041	0.061	0.069	0.102
	s	$3 * 10^{-6}$	$3 * 10^{-6}$	$3 * 10^{-6}$	$3 * 10^{-6}$	$3 * 10^{-6}$
Very poor quality rock mass RMR = 3	m	0.007	0.010	0.015	0.017	0.025
	s	$1 * 10^{-7}$	$1 * 10^{-7}$	$1 * 10^{-7}$	$1 * 10^{-7}$	$1 * 10^{-7}$

### 7.14.2 Settlement Parameters

Rocks will primarily undergo elastic settlements. The elastic settlements will be instantaneous and considered recoverable. These settlements are calculated using elastic theory. The determination of elastic settlements is provided in Chapter 17. In the determination of the elastic settlements, the elastic modulus of the rock mass,  $E_m$ , is required.

### 7.14.2.1 GSI

The elastic modulus of a rock mass,  $E_m$ , is the lesser of modulus determined from intact rock core testing,  $E_R$ , or from the equations below (Turner (2006)).

$$q_u \leq 100 \text{ MPa} \quad E_m = \left[ \left( \sqrt{\frac{q_u}{100}} \right) * 10^{\left( \frac{GSI-10}{40} \right)} \right] \quad \text{Equation 7-103}$$

$$q_u > 100 \text{ MPa} \quad E_m = 10^{\left( \frac{GSI-10}{40} \right)} \quad \text{Equation 7-104}$$

$$E_m = \frac{E_R}{100} * \left( e^{\left( \frac{GSI}{21.7} \right)} \right) \quad \text{Equation 7-105}$$

Where,

$q_u$  = unconfined (uniaxial) compressive strength of the intact rock, MPa

$E_m$  = elastic modulus of rock mass, GPa

$E_R$  = elastic modulus of intact rock, GPa

1MPa = 10.44 tsf = 20.88 ksf

1GPa = 145 ksi

### 7.14.2.2 RMR

The elastic modulus of a rock mass is the lesser of modulus determined from intact rock core testing or from the equations below (AASHTO LRFD Specifications).

$RMR \leq 85$

$$E_m = 145 * \left( 10^{\left( \frac{RMR-10}{40} \right)} \right) \quad \text{Equation 7-106}$$

$60 < RMR < 85$

$$E_m = (290 * RMR) - 14,500 \quad \text{Equation 7-107}$$

Where,

$E_m$  = Elastic modulus of rock mass, ksi

RMR = Adjusted Rock Mass Rating from Chapter 6

For RMR greater than or equal to 85 ( $RMR \geq 85$ ), use either the modulus determined from intact rock core testing or 10,150 ksi whichever is less.

## 7.15 SCOUR

This Section of the GDM is concerned with the soil and rock properties that are provided to the HEOR for use in scour analysis and design. According to the AASHTO Transportation Glossary (2009) scour is defined as:

The washing away of streambed material by water channel flow. General (*contraction*) scour occurs as a result of a constriction in the water channel openings; local scour occurs as a result of local flow changes in a channel due to constrictions caused by the presence of bridge piers or abutments.

Scour is typically determined during 2 different hydraulic events; typically the 100-year flow (design flood) event and the 500-year flow (check flood) event. The scour caused by the design flood is used in the Strength and Service limit state checks; while the check flood is part of the Extreme Event II limit state check (see Chapter 8 for more discussion on limit states). Regardless of the flow event used to determine scour, certain soil and rock properties are required to be provided to the HEOR for use in analysis and design. According to the SCDOT Requirements for Hydraulic Design Studies (HDS) (2009), “Scour analysis will be performed for all bridge type (*bridge, wall and culverts*) structures *that are exposed to storm event waters*, utilizing USGS envelope curves and methods found in HEC-18.”

### 7.15.1 Soil

As required in Chapter 4, grain-size analyses including hydrometers are to be conducted on samples within the potential scour zone both at the interior bents of the bridge as well as at the end bents of the bridge. For each grain-size test performed, the  $D_{50}$  shall be reported in millimeters to the HEOR.

### 7.15.2 Rock

In addition to classifying rock using the RMR and GSI systems, rock should also be classified in regards to the erosion potential of the rock to flowing water. Fortunately, most of the information previously used to describe the rock using the RMR and GSI systems is used to describe the erodibility of the rock. Arneson, Zevenbergen, Lagasse, and Clooper (2012) use the Erodibility Index to describe this erodibility of rock. The Erodibility Index,  $K$ , is determined using the following equation. The GEOR shall coordinate with the HEOR to determine when  $K$  is required and how  $K$  will be communicated between the GEOR and HEOR.

$$K = (M_s) * (K_b) * (K_d) * (J_s) \quad \text{Equation 7-108}$$

Where,

$M_s$  = Intact rock mass strength parameter

$K_b$  = Block size parameter

$K_d$  = Shear strength parameter

$J_s$  = Relative orientation parameter

The intact rock mass strength parameter,  $M_s$ , is related to the unconfined compressive strength as indicated in Table 7-23.

According to Arneson, et al. (2012):

Joint spacing and the number of joint sets within a rock mass determines the value of  $K_b$  for rock. Joint spacing is estimated from borehole data by means of the rock quality designation (RQD) and the number of joint sets is represented by the joint set number ( $J_n$ ). The values of the joint set numbers ( $J_n$ ) are found in Table 7-24. As seen in the table,  $J_n$  is a function of the number of joint sets, ranging from rock with no or few joints (essentially intact rock), to rock formations consisting of one to more than 4 joint sets. The classification accounts for rock that displays random discontinuities in addition to regular joint sets. Random joint discontinuities are discontinuities that do not form regular patterns. For example, rock with two joint sets and random discontinuities is classified as having 2 joint

sets plus random. Having determined the values of RQD and  $J_n$ ,  $K_b$  is calculated as:

$$K_b = \frac{RQD}{J_n} \quad \text{Equation 7-109}$$

The discontinuity or shear strength number ( $K_d$ ) is the parameter that represents the relative strength of discontinuities in rock. In rock, it is determined as the ratio between joint wall roughness ( $J_r$ ) and joint wall alteration ( $J_a$ ), where  $J_r$  represents the degree of roughness of opposing faces of a rock discontinuity, and  $J_a$  represents the degree of alteration of the materials that form the faces of the discontinuity. Alteration relates to amendments of the rock surfaces, for example weathering or the presence of cohesive material between the opposing faces of a joint. Values of  $J_r$  and  $J_a$  can be found in Tables 7-25 and 7-26. The values of  $K_d$  calculated with the information in these tables change with the relative degree of resistance offered by the joints. Increases in resistance are characterized by increases in the value of  $K_d$ . The shear strength of a discontinuity is directly proportional to the degree of roughness of opposing joint faces and inversely proportional to the degree of alteration.

$$K_d = \frac{J_r}{J_a} \quad \text{Equation 7-110}$$

**Table 7-23, Values of Rock Mass Strength Parameter,  $M_s$   
(Arneson, et al. (2012))**

Strength/Hardness		Recognition	Unconfined Compressive Strength (psi)	Mass Strength Number, $M_s$
Extremely Weak Rock	Very Soft Rock	Material crumbles under firm (moderate) blows from sharp end of geological pick	< 250	0.87
Very Weak Rock	Very Soft Rock	Can be peeled with knife	250 – 480	1.86
Weak Rock	Soft Rock	Can just be scraped and peeled with a knife	480 – 950	3.95
Medium Strong Rock	Soft Rock	Indentations up to 3/16-inch in specimen with firm (moderate) blows of pick point	950 – 1,915	8.39
Strong Rock	Hard Rock	Cannot be scraped or peeled with knife; specimen can be broken with hammer end of geological pick with a single firm (moderate) blow	1,915 – 3,825	17.70
Very Strong Rock	Very Hard Rock	Specimen breaks with hammer end of pick under more than 1 blow	3,825 – 7,685 7,685 – 15,300	35.0 70.0
Extremely Strong Rock	Extremely Hard Rock	Many blows with geological pick to break through intact material	> 30,750	280.0

**Table 7-24, Rock Joint Set Number  $J_n$   
(Arneson, et al. (2012))**

Number of Joint Sets	Joint Set Number, $J_n$
Intact, no or few joint/fissures	1.00
One joint/fissure set	1.22
One joint/fissure set plus random	1.50
Two joint/fissure sets	1.83
Two joint/fissure sets plus random	2.24
Three joint/fissure sets	2.73
Three joint/fissure sets plus random	3.34
Four joint/fissure sets	4.09
Multiple joint/fissure sets	5.00

**Table 7-25, Joint Roughness Number,  $J_r$   
(Arneson, et al. (2012))**

Condition of Joint	Joint Roughness Number, $J_r$
Stepped Joints/fissures	4.0
Rough or irregular, undulating	3.0
Smooth undulating	2.0
Slickensided undulating	1.5
Rough or irregular, planar	1.5
Smooth planar	1.0
Slickensided planar	0.5
Joints/fissures either open or containing relatively soft gouge of sufficient thickness to prevent joint/fissure wall contact upon excavation	1.0
Shattered or micro-shattered clays	1.0

**Table 7-26, Joint Alteration Number,  $J_a$   
(Arneson, et al. (2012))**

Description of Gouge	Joint Alteration Number, $J_a$ for Joint Separation (mm)		
	1.00 <sup>1</sup>	1.01 – 5.00 <sup>2</sup>	> 5.01 <sup>3</sup>
Tightly healed, hard, non-softening impermeable filling	0.75	-	-
Unaltered joint walls, surface staining only	1.0	-	-
Slightly altered, non-softening, non-cohesive rock mineral or crushed rock filling	2.0	2.0	4.0
Non-softening, slightly clayey non-cohesive filling	3.0	6.0	10.0
Non-softening, strongly over-consolidated clay mineral filling, with or without crushed rock	3.0	6.0**	10.0
Softening or low friction clay mineral coatings and small quantities of swelling clays	4.0	8.0	13.0
Softening moderately over-consolidated clay mineral filling, with or without crushed rock	4.0	8.0**	13.0
Shattered or micro-shattered (swelling) clay gouge, with or without crushed rock	5.0	10.00**	18.0

<sup>1</sup> Joint walls effectively in contact.  
<sup>2</sup> Joint walls come into contact after approximately 100 mm shear.  
<sup>3</sup> Joint walls do not come into contact at all upon shear.  
\*\*Also applies when crushed rock occurs in clay gouge without rock wall contact.

Relative orientation, in the case of rock, is a function of the relative shape of the rock and its dip and dip direction relative to the direction of flow. The relative



orientation parameter  $J_s$  represents the relative ability of earth material to resist erosion due to the structure of the ground. This parameter is a function of the dip and dip direction of the least favorable discontinuity (most easily eroded) in the rock with respect to the direction of flow, and the shape of the material units. These 2 variables (orientation and shape) affect the ease by which the stream can penetrate the ground and dislodge individual material units.

Conceptually, the function of the relative orientation parameter  $J_s$  incorporating shape and orientation is as follows. If rock is dipped against the direction flow, it will be more difficult to scour the rock than when it is dipped in the direction of flow. When it is dipped in the direction of flow, it is easier for the flow to lift the rock, penetrate underneath and remove it. Rock that is dipped against the direction of flow will be more difficult to dislodge. The shape of the rock, represented by the length to width ratio  $r$ , impacts the erodibility of rock in the following manner. Elongated rock will be more difficult to remove than equi-sided blocks of rock. Therefore, large ratios of  $r$  represent rock that is more difficult to remove because it represents elongated rock shapes. Values of the relative orientation parameter  $J_s$  are provided in Table 7-27.

**Table 7-27, Relative Orientation Parameter,  $J_s$   
(Arneson, et al. (2012))**

Dip Direction of Closer Spaced Joint Set	Dip Angle of Closer Spaced Joint Set (degrees)	Ratio of Joint Spacing, r			
		Ratio 1:1	Ratio 1:2	Ratio 1:4	Ratio 1:8
Dip Direction	Dip Angle	Ratio 1:1	Ratio 1:2	Ratio 1:4	Ratio 1:8
180/0	90	1.14	1.20	1.24	1.26
In direction of stream flow	89	0.78	0.71	0.65	0.61
In direction of stream flow	85	0.73	0.66	0.61	0.57
In direction of stream flow	80	0.67	0.60	0.55	0.52
In direction of stream flow	70	0.56	0.50	0.46	0.43
In direction of stream flow	60	.050	0.46	0.42	0.40
In direction of stream flow	50	0.49	0.46	0.43	0.41
In direction of stream flow	40	0.53	0.49	0.46	0.45
In direction of stream flow	3	0.63	0.59	0.55	0.53
In direction of stream flow	20	0.84	0.77	0.71	0.67
In direction of stream flow	10	1.25	1.10	0.98	0.90
In direction of stream flow	5	1.39	1.23	1.09	1.01
In direction of stream flow	1	1.50	1.33	1.19	1.10
0/180	0	1.14	1.09	1.05	1.02
Against direction of stream flow	-1	0.78	0.85	0.90	0.94
Against direction of stream flow	-5	0.73	0.79	0.84	0.88
Against direction of stream flow	-10	0.67	0.72	0.78	0.81
Against direction of stream flow	-20	0.56	0.62	0.66	0.69
Against direction of stream flow	-30	0.50	0.55	0.58	0.60
Against direction of stream flow	-40	0.49	0.52	0.55	0.57
Against direction of stream flow	-50	0.53	0.56	0.59	0.61
Against direction of stream flow	-60	0.63	0.68	0.71	0.73
Against direction of stream flow	-70	0.84	0.91	0.97	1.01
Against direction of stream flow	-80	1.26	1.41	1.53	1.61
Against direction of stream flow	-85	1.39	1.55	1.69	1.77
Against direction of stream flow	-89	1.50	1.68	1.82	1.91
180/0	-90	1.14	1.20	1.24	1.26

Notes:

1. For intact material take  $J_s = 1.00$
2. For values of r greater than 8 take  $J_s$  as for  $r = 8$
3. If the flow direction, FD, is not in the direction of the true dip, TD, the effective dip, ED, is determined by adding the ground slope, GS, to the apparent dip AD:  $ED = AD + GS$

## 7.16 DYNAMIC PROPERTIES – GENERAL

Soil and rock dynamic properties are required in developing the site characterization model. The site characterization model is used in the development of the site response analysis under the EE I limit state. Chapter 12 provides details on conducting a site response analysis. The static site characterization model (i.e., subsurface profile) has been developed in Section 7.4. This static model forms the basis for the dynamic site characterization model. The dynamic site characterization model consists of the following soil parameters:

- Initial (small strain) dynamic shear modulus.
- The small strain viscous damping ratio.
- Shear modulus reduction and strain-dependent hysteretic damping characteristics.

- Dynamic shear strength.
- Liquefaction (SSL) resistance parameters.
- Post-liquefaction (post-SSL) residual shear strength.

These parameters may be developed using the standard geotechnical exploration as indicated in Chapter 4. Further these parameters may be developed using more advanced in-situ testing techniques or from geophysical surveys. The CPTu is beneficial in the development of the dynamic site characterization because the CPTu can identify thin (~3-inch thick) layers that might be missed in the standard soil test boring. However, it is possible to discover these thin layers in standard soil test borings using continuous sampling techniques and careful logging of each sample obtained. These thin layers, if continuous, could consist of weak or potentially liquefiable soils that could lead to slope instability issues.

The ideal dynamic site characterization profile should extend to competent bedrock. Competent bedrock is defined as having a shear wave velocity of at least 2,500 feet per sec (ft/s), which is indicative, of the B-C Boundary (see Chapter 12). The physical properties (static and dynamic) of the soil should be known over the entire interval from the ground surface to the top of the competent rock. However, in most of the South Carolina, this will not be possible because of the depth of the B-C Boundary. Therefore, the physical properties (static and dynamic) shall be developed for the deepest testing location within the project limits. Because the B-C Boundary is typically found at deeper depths in the Coastal Plain (see Chapter 11), the profile from beneath the deepest boring to the top of the B-C Boundary may be established using previously obtained data. Contact the PC/GDS for this additional data.

## 7.17 SOIL DYNAMIC PROPERTIES

The same parameters used to describe soil properties used in static analyses are the same for seismic analyses. During a geotechnical subsurface investigation conducted in accordance with this Manual, the following information should be obtained for each soil layer of interest:

- Soil classification.
- Index parameters (LL, PL, PI,  $w$ , etc.).
- Unit weight of the soil ( $\gamma_d$ ,  $\gamma_{max}$ , etc.).
- Compressibility parameters ( $C_c$ ,  $C_r$ ,  $\sigma'_p$ , etc.).
- Shear strength parameters ( $\phi$ ,  $c$ ,  $\phi'$ ,  $c'$ , etc.).

For a site response analysis the following seismic parameters will be required:

1. Consistency of the soil (e.g., relative density,  $D_r$ , or overconsolidation ratio, OCR).
2. Shear wave velocity,  $V_s$ , or initial (small strain) shear modulus,  $G_{max}$ .
3. Cyclic stress-strain behavior.
4. Residual shear strength,  $\tau_r$ .

### 7.17.1 Soil Consistency

The consistency of the soil is composed of 2 indicators, relative density,  $D_r$ , for Sand-Like soils and the overconsolidation ratio, OCR, for Clay-Like soils. The  $D_r$  can be determined from the following equation,

$$D_r = \frac{e_{max} - e_o}{e_{max} - e_{min}} = \left( \frac{1 - \frac{\gamma_{dmin}}{\gamma_{do}}}{1 - \frac{\gamma_{dmin}}{\gamma_{dmax}}} \right) * 100\% \quad \text{Equation 7-111}$$

Where,

- $e_{max}$  = Maximum void ratio
- $e_{min}$  = Minimum void ratio
- $e_o$  = In-situ void ratio
- $\gamma_{dmax}$  = Maximum dry unit weight
- $\gamma_{dmin}$  = Minimum dry unit weight
- $\gamma_{do}$  = In-situ dry unit weight

The information required to develop the  $D_r$  using Equation 7-111 must be obtained through relative density testing and consolidation testing (see Chapter 5); therefore, the  $D_r$  is normally correlated to the SPT N-value or the CPTu tip resistance (see 7.8.3). The  $D_r$  is normally used on cohesionless (coarse-grained) soils.

As discussed previously, the OCR is the ratio of the past effective overburden to the existing overburden and is typically used for Clay-Like (fine-grained) soils. Table 7-7 indicates that soils with OCRs greater than 1 are overconsolidated; however, in addition to the OCR, the sensitivity,  $S_t$ , is also required.  $S_t$  and OCR are used in Chapter 13 in the selection of the residual shear strength to be used in design. Soils with a  $S_t$  less than 5 use a cyclic residual shear strength, while soils with a  $S_t$  greater than or equal to 5 use the remolded shear strength.

### 7.17.2 Shear Wave Velocity/Initial Shear Modulus

One of the required soil properties needed to perform a soil response analysis is the soil stiffness. Soil stiffness is characterized by either small-strain shear-wave velocity,  $V_s$ , or small-strain shear modulus,  $G_{max}$ . The measurement of  $V_s$  is required in Chapter 4 and is measured in the field as indicated in Chapter 5 and reported as indicated in Chapter 6. The small-strain shear wave velocity,  $V_s$ , is related to small-strain shear modulus,  $G_{max}$ , by the following equation.

$$G_{max} = \rho * V_s^2 \quad \text{Equation 7-112}$$

$$\rho = \frac{\gamma_t}{g} \quad \text{Equation 7-113}$$

Where,

- $V_s$  = Shear wave velocity of the soil, feet per sec (ft/s)
- $\rho$  = Mass density of the soil, (pound\*second squared) per square foot ((lb\*s<sup>2</sup>)/ft<sup>2</sup>)
- $\gamma_t$  = Total unit weight, pounds per cubic foot (lb/ft<sup>3</sup>)
- $g$  = Acceleration due to gravity, 32.174 feet per second squared (ft/s<sup>2</sup>)

The Theory of Elasticity relates  $G_{max}$  to the small strain Young's modulus,  $E_{max}$ , as a function of the Poisson's ratio,  $\nu$ , using the following equation:

$$E_{max} = 2 * (1 + \nu) * G_{max} \quad \text{Equation 7-114}$$

Poisson's ratio for uncemented Sand-Like materials may be assumed to be approximately 0.35 and for Clay-Like materials Poisson's ratio may be assumed to be approximately 0.48. For transitional materials, review the PI as indicated in Table 7-6 and determine whether the soil will behave as either a Sand-Like material or a Clay-Like material. Alternately, the Poisson's ratio may be determined from the results of geophysical testing using the following equation:

$$v = 1 - \left\{ \frac{1}{2 * \left[ 1 - \left( \frac{V_s}{V_p} \right)^2 \right]} \right\} \quad \text{Equation 7-115}$$

Where,

- $V_s$  = Shear wave velocity, ft/sec
- $V_p$  = Compression wave velocity, ft/sec

Typical values of small-strain shear wave velocity,  $V_s$ , and small-strain shear modulus,  $G_{max}$ , for various soil types are shown in Table 7-28.

**Table 7-28, Typical Small-Strain Shear Wave Velocity and Initial Shear Modulus (Based on Hunt (2005) and Kavazanjian, Matasovic, Hadj-Hamou, and Wang (1998))**

Soil Type	Mass Density, $\rho$	Total Unit Weight, $\gamma_t$	Small-strain Shear Wave Velocity, $V_s$		Initial Shear Modulus, $G_{max}$	
	kg/m <sup>3</sup>	pcf	m/s	ft/s	kPa	psi
Soft Clay	1,600	100	40 – 90	130 – 300	2,600 – 13,000	400 – 2,000
Stiff Clay	1,680	105	65 – 140	210 – 500	7,000 – 33,000	1000 – 5,700
Loose Sand	1,680	105	130 – 280	420 – 920	28,400 – 131,700	4,000 – 19,200
Dense Sand and Gravel	1,760	110	200 - 410	650 – 1,350	70,400 – 300,000	10,000 – 43,300
Residual Soil (PWR, IGM)	2,000	125	300 - 600	1,000 – 2,000	180,000 – 720,000	27,000 – 108,000
Piedmont Metamorphic and Igneous Rock (Highly – Moderately Weathered)	2,500	155	760 – 3,000	2,500 – 10,000	1,400,00 – 22,500,000	209,000 – 3,400,000
0 <RQD < 50			600	2,000		
RQD = 65 <sup>(1)</sup>			760	2,500		
RQD = 80 <sup>(1)</sup>			1,500	5,000		
RQD = 90 <sup>(1)</sup>			2,500	8,000		
RQD = 100 <sup>(1)</sup>	3,400	11,000				
Basement Rock (Moderately Weathered to Intact)	2,600	165	> 3,400	> 11,000	> 30,000	> 4,300,000

<sup>(1)</sup> Typical Values, Linear interpolate between RQD values

When site-specific shear wave velocities,  $V_s$ , are not available or need to be supplemented, an estimation of the shear wave velocity,  $V_s$ , can be made by the use of correlations with in-situ testing such as the SPT or the CPTu. Procedures for estimating dynamic properties of soils have been developed by Andrus, Hayati, and Mohanan (2009). The procedures for correlating SPT and CPTu results with shear wave velocity,  $V_s$ , have been summarized in Sections 7.17.2.1 and 7.17.2.2, respectively. These correlated  $V_s$  are for Holocene age clean sands. In addition,  $V_s$  is also normalized to 1.0 tsf overburden ( $V_{s1}$ ). Therefore,  $(V_s)_{meas}$  requires correction for fines content and normalization for overburden using the following equations.

$$(V_{s,1,CS})_{meas} = C_{Nvs} * K_{cvs} * (V_s)_{meas} \quad \text{Equation 7-116}$$

$$C_{Nvs} = \left(\frac{1}{\sigma'_v}\right)^{0.25} \leq 1.4 \quad \text{Equation 7-117}$$

$$(V_{s,1})_{meas} = C_{Nvs} * (V_s)_{meas} \quad \text{Equation 7-118}$$

$K_{cvs}$  should only be applied to  $V_s$  less than or equal to 1,300 ft/sec. For  $V_s$  greater than 1,300 ft/sec, set  $K_{cvs}$  equal to 1.0.

Where,

$\sigma'_{vo}$  = Effective normal stress, tsf

$$FC \leq 5\%$$

$$K_{cvs} = 1.0 \quad \text{Equation 7-119}$$

$$5\% < FC < 35\%$$

$$K_{cvs} = 1 + (FC - 5) * T \quad \text{Equation 7-120}$$

$$35\% \leq FC$$

$$K_{cvs} = 1 + 30 * T \quad \text{Equation 7-121}$$

Where,

$$T = 0.009 - 0.0109 * \left[\frac{(V_{s,1})_{meas}}{328}\right] + 0.0038 \left[\frac{(V_{s,1})_{meas}}{328}\right]^2 \quad \text{Equation 7-122}$$

### 7.17.2.1 SPT - Shear Wave Velocity, $V_s$ , Estimation

Andrus, et al. (2009) have developed a correlation for determining  $V_{s,1,CS}$  from  $N_{1,60,CS}$ , where  $N_{1,60,CS}$  is the standard penetration resistance normalized for overburden pressure and corrected for energy and fines content.  $N_{1,60}$  is obtained from Equation 7-6.  $N_{1,60,CS}$  is obtained from the following equation.

$$N_{1,60,CS} = \alpha + \beta * (N_{1,60}) \quad \text{Equation 7-123}$$

Where,

$$FC \leq 5\%$$

$$\alpha = 0.0$$

$$\beta = 1.0$$

$$\text{Equation 7-124}$$

$$5\% \leq FC \leq 35\%$$

$$\alpha = e^{\left(1.76 - \frac{190}{FC^2}\right)}$$

$$\beta = 0.99 + \frac{FC^{1.5}}{1000}$$

$$\text{Equation 7-125}$$

$$35\% \leq FC$$

$$\alpha = 5.0 \qquad \beta = 1.2 \qquad \text{Equation 7-126}$$

Where,

$$(V_{s,1,CS})_{SPT} = 288 * (N_{1,60,CS})^{0.253} \qquad \text{Equation 7-127}$$

Where,

$(V_{s,1,CS})_{SPT}$  = Corrected and normalized shear wave velocity based on SPT N-values for uncemented, Holocene age sands, ft/sec

### 7.17.2.2 CPTu - Shear Wave Velocity, $V_s$ , Estimation

Similarly to the N-value correlation presented previously for  $V_s$ , Andrus, et al. (2009) have developed a correlation between  $V_s$  and  $q_{t,1,N,CS}$ . Use Equation 7-9 to develop  $q_{t,1}$ . Normalization of  $q_{t,1}$  is required and determined using the following equation.

$$q_{t,1,N} = \frac{q_{t,1}}{P_a} \qquad \text{Equation 7-128}$$

Where,

$q_{t,1}$  = Corrected tip resistance, tsf  
 $P_a$  = Atmospheric pressure, assumed to be 1.0 tsf

Therefore,  $q_{t,1,N,CS}$  is determined using the following equation.

$$q_{t,1,N,CS} = K_c * q_{t,1,N} \qquad \text{Equation 7-129}$$

Where,

$$I_c \leq 1.64 \qquad K_c = 1.0 \qquad \text{Equation 7-130}$$

$$I_c > 1.64 \qquad \text{Equation 7-131}$$

$$K_c = -0.403 * (I_c)^4 + 5.581 * (I_c)^3 - 21.631 * (I_c)^2 + 33.75 * (I_c) - 17.88$$

Where,

$I_c$  = Soil Behavior Type (see Equation 7-17)

Once  $q_{t,1,N,CS}$  is determined the  $(V_{s,1,CS})_{CPT}$  may be determined using the following equation.

$$(V_{s,1,CS})_{CPT} = 205 * (q_{t,1,N,CS})^{0.231} \qquad \text{Equation 7-132}$$

Where,

$(V_{s,1,CS})_{CPT}$  = Corrected and normalized shear wave velocity based on CPT tip resistances for uncemented, Holocene age sands, ft/sec

### 7.17.3 Cyclic Stress-strain Behavior

An additional requirement of the site response analysis is an understanding of how the cyclic loading of the design seismic event (EE I limit state) affects the stress-strain behavior of the soil. This stress-strain behavior of soil is complex due to the cyclic ground motions induced by the design seismic event (i.e., strong motion). Figure 7-37 provides a schematic of this complexity. In Step 1, the soil element is sheared toward the right, while in Step 2, the soil element is sheared toward the left. While the soil element is sheared right and left, the shear wave that causes this shearing is considered to be vertically propagating and is considered to be normal to the ground surface.

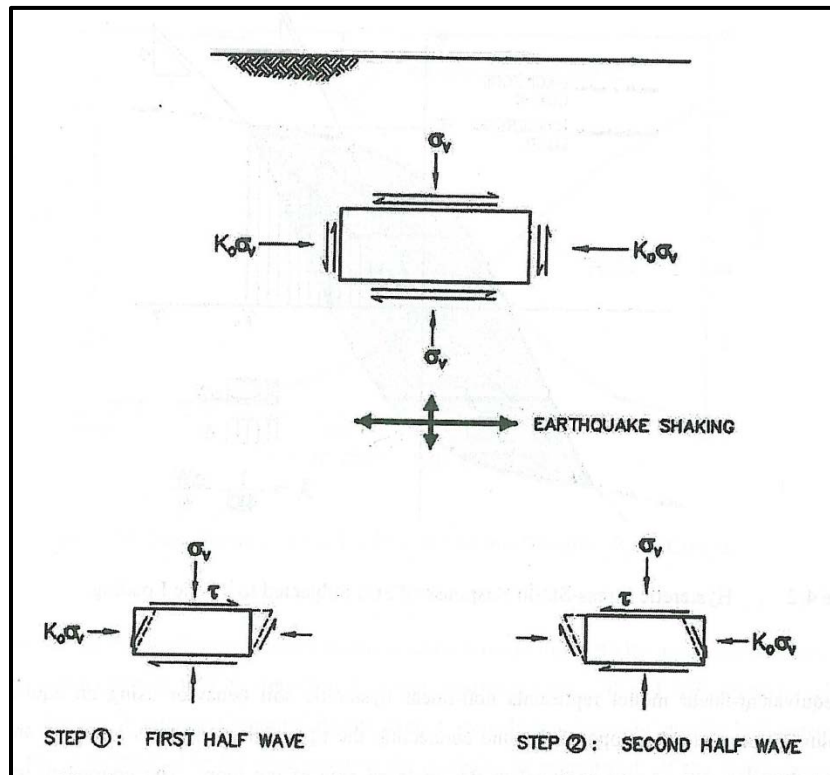


**Figure 7-37, Stresses Induced in a Soil Element by Vertical Shear Wave (Kavazanjian, et al. (2011))**

The cyclic shearing stress and strain,  $\tau_c$  and  $\gamma_c$ , is generally considered to be the source of most of the damage caused by a seismic event. The response of the soil to cyclic shear stress and strain is commonly characterized by hysteresis. Figure 7-38 shows a hysteretic loop for uniform cyclic loading. This hysteretic loop would apply to soil that is perfectly elastic, but soils are not perfectly elastic and will deform (strain) under the induced shear loading. Therefore, the hysteretic loop “leans” toward increasing shear strain, both positive and negative. A line drawn through the tips of each hysteretic loop is called a “backbone curve” (see Figure 7-38). This “backbone curve” further indicates that under cyclic loading soils will behave non-linearly (i.e., inelastically), but for easier understanding and modeling of the soil in these loading conditions an equivalent linear model is used. The following equation shows that the shear modulus,  $G$ , of the soil is related directly to the cyclic shear stress and strain:

$$G = \frac{\tau_c}{\gamma_c} \quad \text{Equation 7-133}$$



Where,

$\tau_c$  = Cyclic shear stress

$\gamma_c$  = Cyclic shear strain

As can be seen in Figure 7-38,  $G_{\max}$  occurs at zero shear strain ( $\gamma_c = 0$ ) at least theoretically. However, in reviewing Equation 7-133 at  $\gamma_c = 0$ ,  $G_{\max}$  has no solution; therefore,  $G_{\max}$  is normally determined at very small shear strains,  $\gamma_c = 10^{-4}$  or smaller.

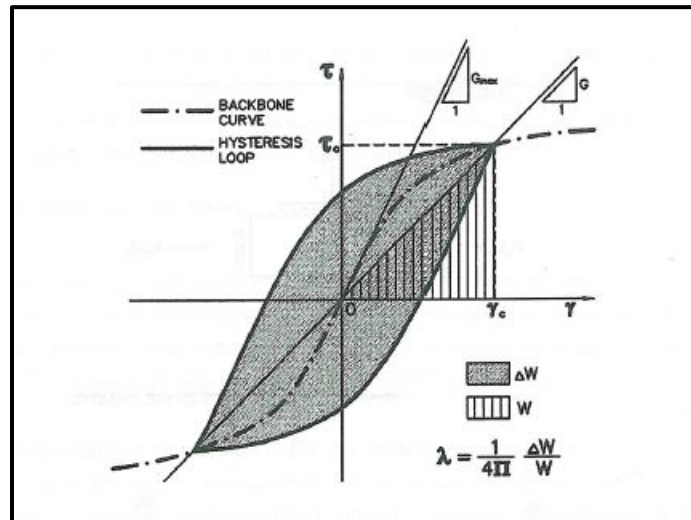


Figure 7-38, Hysteretic Stress-Strain Loop for Uniform Cyclic Loading (Kavazanjian, et al. (2011))

According to Kavazanjian, et al. (2011):

The equivalent-linear model represents non-linear hysteretic soil behavior using an equivalent shear modulus,  $G$ , equal to the slope of the line connecting the tips of the hysteresis loop and an equivalent viscous damping ratio,  $\lambda$ , proportional to the enclosed areas of the loop. ... The shear strain dependence of the equivalent modulus and damping ratio are described by the modulus reduction and damping curves shown in Figure 7-39.

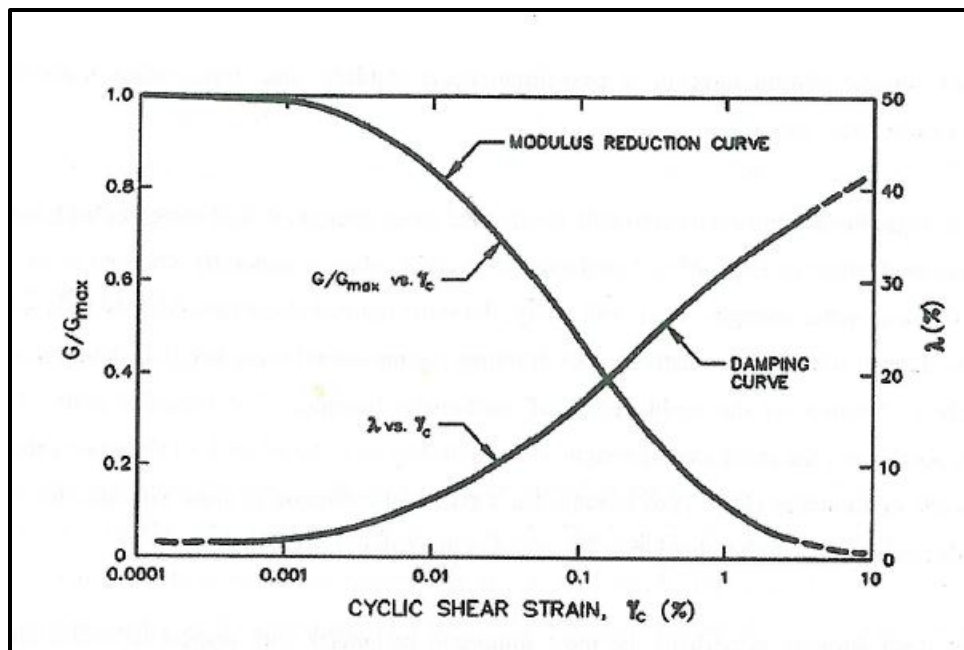


Figure 7-39, Example Shear Modulus Reduction and Damping Ratio Curve (Kavazanjian, et al. (2011))

### 7.17.3.1 Shear Modulus Reduction Curves

Shear modulus reduction curves are typically presented as normalized shear modulus,  $G/G_{max}$  versus cyclic shear strain ( $\gamma_c$ ). These curves are used for performing site-specific response analyses. These shear modulus reduction curves are primarily influenced by the strain amplitude, confining pressure, soil type, and plasticity. The shear modulus reduction curve is typically obtained by using a hyperbolic model. A modified hyperbolic model by Stokoe, Darendeli, Andrus and Brown (1999) has been used by Andrus, et al. (2003) to develop shear modulus reduction curves for South Carolina soils. The hyperbolic model by Stokoe, et al. (1999) is shown in the following equation.

$$\frac{G}{G_{max}} = \frac{1}{1 + \left(\frac{\gamma_c}{\gamma_{cr}}\right)^\alpha} \quad \text{Equation 7-134}$$

Where,

$\alpha$  = Curvature coefficient

$\gamma_c$  = Cyclic shear strain

$\gamma_{cr}$  = Cyclic reference shear strain

The curvature coefficient,  $\alpha$ , and cyclic reference shear strain,  $\gamma_{cr}$ , have been estimated by Andrus, et al. (2003) to provide the most accurate values for South Carolina Soils. Because it was found that the cyclic reference shear strain,  $\gamma_{cr}$ , varied based on effective confining pressure,  $\gamma_{cr}$  values are computed using cyclic reference shear strain at 1 tsf (100 kPa, 1 atm),  $\gamma_{cr1}$ , as shown in the following equation.

$$\gamma_{cr} = \gamma_{cr1} * \left(\frac{\sigma'_m}{P_a}\right)^k \quad \text{Equation 7-135}$$

The mean confining pressure,  $\sigma'_m$ , at depth (Z) is computed as shown in Equation 7-136 in units of kPa, where  $P_a$  is the reference pressure of 100 kPa, and k is an exponent that varies based on the geologic formation and PI. Laboratory studies by Stokoe, Hwang, Darendeli, and Lee (1995) indicate that the mean confining pressure,  $\sigma'_m$ , values of each layer within a geologic unit should be within  $\pm 50$  percent of the range of  $\sigma'_m$  for the major geologic unit.

$$\sigma'_m = \sigma'_v * \left( \frac{1+2*K_o}{3} \right) \quad \text{Equation 7-136}$$

Where,

$\sigma'_v$  = Vertical effective pressure, kPa  
 $K_o$  = At-rest earth pressure coefficient

The  $K_o$  is defined as the ratio of horizontal effective pressure,  $\sigma'_h$ , to vertical effective pressure,  $\sigma'_v$  and is discussed in greater detail in Chapter 18. Values for the reference strain at 1 tsf (100 kPa, 1 atm),  $\gamma_{cr1}$ , curvature coefficient,  $\alpha$ , and k exponent are provided for South Carolina soils based on Andrus, et al. (2003) in Table 7-29.

**Table 7-29, Recommended Values  $\gamma_{cr1}$ ,  $\alpha$ , and k for SC Soils  
(Andrus, et al. (2003))**

Geologic Age and Location of Deposits <sup>(1)</sup>	Variable	Soil Plasticity Index, PI (%)					
		0	15	30	50	100	150
Holocene	$\gamma_{cr1}$ (%)	0.073	0.114	0.156	0.211	0.350	0.488
	$\alpha$	0.95	0.96	0.97	0.98	1.01	1.04 <sup>(2)</sup>
	k	0.385	0.202	0.106	0.045	0.005	0.001 <sup>(2)</sup>
Pleistocene (Wando)	$\gamma_{cr1}$ (%)	0.018	0.032	0.047	0.067	0.117	0.166
	$\alpha$	1.00	1.02	1.04	1.06	1.13	1.19
	k	0.454	0.402	0.355	0.301	0.199	0.132
Tertiary Ashley Formation (Cooper Marl)	$\gamma_{cr1}$ (%)	---	---	0.030 <sup>(2)</sup>	0.049	0.096 <sup>(2)</sup>	---
	$\alpha$	---	---	1.10 <sup>(2)</sup>	1.15	1.28	---
	k	---	---	0.497 <sup>(2)</sup>	0.455	0.362 <sup>(2)</sup>	---
Tertiary (Stiff Upland Soils)	$\gamma_{cr1}$ (%)	---	---	0.023	0.041 <sup>(2)</sup>	---	---
	$\alpha$	---	---	1.00	1.00 <sup>(2)</sup>	---	---
	k	---	---	0.102	0.045 <sup>(2)</sup>	---	---
Tertiary (All soils at SRS except Stiff Upland Soils)	$\gamma_{cr1}$ (%)	0.038	0.058	0.079	0.106	0.174 <sup>(2)</sup>	---
	$\alpha$	1.00	1.00	1.00	1.00	1.00 <sup>(2)</sup>	---
	k	0.277	0.240	0.208	0.172	0.106 <sup>(2)</sup>	---
Tertiary (Tobacco Road, Snapp)	$\gamma_{cr1}$ (%)	0.029	0.056	0.082	0.117	0.205 <sup>(1)</sup>	---
	$\alpha$	1.00	1.00	1.00	1.00	1.00 <sup>(1)</sup>	---
	k	0.220	0.185	0.156	0.124	0.070 <sup>(1)</sup>	---
Tertiary (Soft Upland Soils, Dry Branch, Santee, Warley Hill, Congaree)	$\gamma_{cr1}$ (%)	0.047	0.059	0.071	0.086	0.125 <sup>(1)</sup>	---
	$\alpha$	1.00	1.00	1.00	1.00	1.00 <sup>(1)</sup>	---
	k	0.313	0.299	0.285	0.268	0.229 <sup>(1)</sup>	---
Residual Soil and Saprolite	$\gamma_{cr1}$ (%)	0.040	0.066	0.093 <sup>(1)</sup>	0.129 <sup>(1)</sup>	---	---
	$\alpha$	0.72	0.80	0.89	1.01 <sup>(1)</sup>	---	---
	k	0.202	0.141	0.099	0.061 <sup>(2)</sup>	---	---

<sup>(1)</sup> SRS = Savannah River Site

<sup>(2)</sup> Tentative Values – Andrus et al. (2003)

The procedure for computing the  $G/G_{max}$  correlation using Equation 7-134 is provided in Table 7-30.

**Table 7-30, Procedure for Computing  $G/G_{max}$** 

Step	Procedure Description
1	Perform a geotechnical subsurface exploration and identify subsurface soil geologic units, approximate age, and formation.
2	Develop soil profiles based on geologic units, soil types, average PI, and soil density. Subdivide major geologic units to reflect significant changes in PI and soil density. Identify design ground water table based on seasonal fluctuations and artesian pressures.
3	Calculate the average $\sigma'_m$ and determine the corresponding $\pm 50\%$ range of $\sigma'_m$ for each major geologic unit using Equation 7-136.
4	Calculate $\sigma'_m$ for each <u>layer</u> within each major geologic unit. If the values for $\sigma'_m$ of each layer are within a geologic unit's $\pm 50\%$ range of $\sigma'_m$ (Step 3) then assign the average $\sigma'_m$ for the major geologic unit (Step 3) to all layers within it. If the $\sigma'_m$ of each layer within a geologic unit is not within the $\pm 50\%$ range of $\sigma'_m$ for the major geologic unit, then the geologic unit needs to be "subdivided" and more than one average $\sigma'_m$ needs to be used, provided the $\sigma'_m$ remain within the $\pm 50\%$ range of $\sigma'_m$ for the "subdivided" geologic unit.
5	Select the appropriate values for each <u>layer</u> of cyclic reference strain, $\gamma_{cr1}$ , at 1 tsf (1 atm), curvature coefficient, $\alpha$ , and k exponent from Table 7-29. These values may be selected by rounding to the nearest PI value in the table or by interpolating between listed PI values in the table.
6	Compute the cyclic reference strain, $\gamma_{cr}$ , based on Equation 7-135 for each <u>geologic unit</u> (or "subdivided" geologic unit) that has a corresponding average $\sigma'_m$ .
7	Compute the design shear modulus reduction curves ( $G/G_{max}$ ) for each <u>layer</u> by substituting cyclic reference strain, $\gamma_{cr}$ , and curvature coefficient, $\alpha$ , for each layer using Equation 7-134. Tabulate values of normalized shear modulus, $G/G_{max}$ with corresponding cyclic shear strain, $\gamma_c$ , for use in a site-specific response analysis.

### 7.17.3.2 Equivalent Viscous Damping Ratio Curves

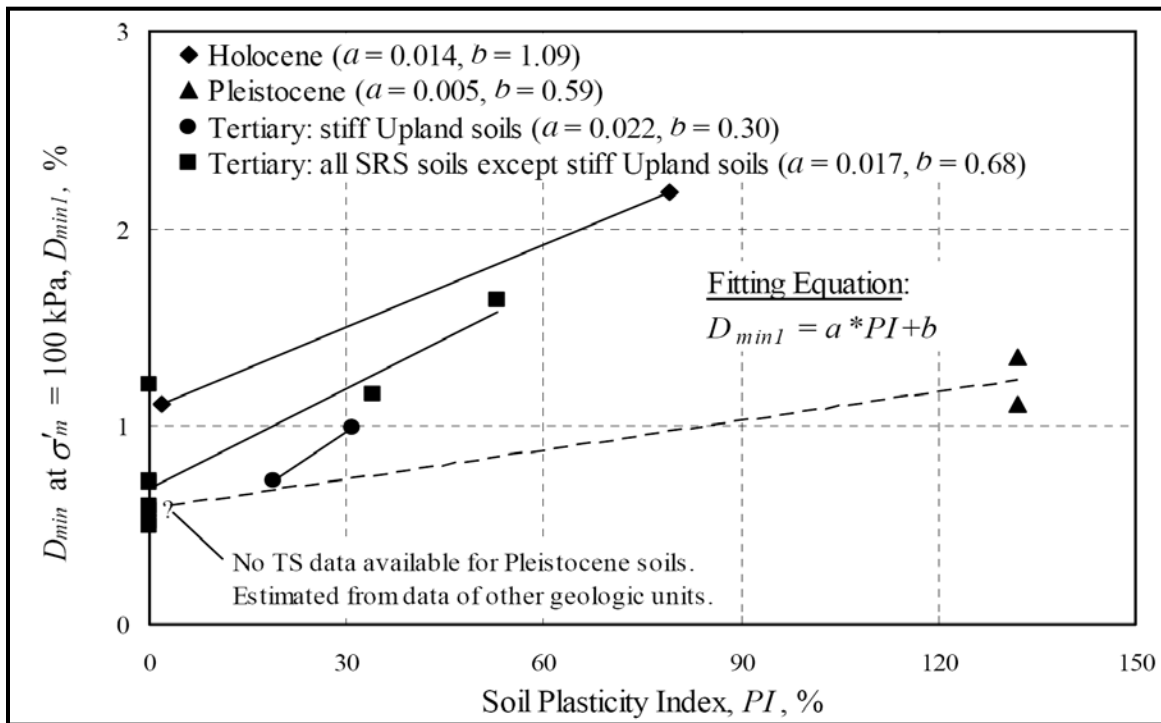
Equivalent Viscous Damping Ratio curves are presented in the form of a Soil Damping Ratio,  $\lambda^1$  vs. Shear Strain,  $\gamma$ . The Soil Damping Ratio represents the energy dissipated by the soil and is related to the stress-strain hysteresis loops generated during cyclic loading. Energy dissipation or damping is due to friction between soil particles, strain rate effects, and nonlinear behavior of soils. The damping ratio is never zero, even when soils are straining within the linear elastic range of the cyclic loading. The damping ratio,  $\lambda$ , is constant during the linear elastic range of the cyclic loading and is referred to as the small-strain material damping,  $\lambda_{min}$ . The small-strain material damping,  $\lambda_{min}$ , can be computed using the equations developed by Stokoe, et al. (1995).

$$\lambda_{min} = \lambda_{min1} * \left( \frac{\sigma'_m}{P_a} \right)^{-0.5*k} \quad \text{Equation 7-137}$$

Where  $\lambda_{min1}$  is the small-strain damping at  $\sigma'_m$  of 1 tsf (1 atm). The mean confining pressure,  $\sigma'_m$ , at depth (Z) is computed as shown in Equation 7-136 in units of kPa. The k exponent is provided for South Carolina soils based on Andrus, et al. (2003) in Table 7-29. A relationship for  $\lambda_{min1}$  based on soil plasticity index, PI, and fitting parameters "a" and "b" for specific geologic units has been developed by Darendeli (2001) as indicated in Figure 7-40. Values for  $\lambda_{min1}$ ,

<sup>1</sup>Editor's Note: In the previous versions of this Manual, the Soil Damping Ratio was identified using "D", as indicated in Andrus, et al. (2003). The Soil Damping Ratio has also been identified using " $\xi$ " in Kramer (1996) and " $\lambda$ " in Kavazanjian, et al. (2011). To be consistent with current NHI standards " $\lambda$ " will be used to identify Soil Damping Ratio in this version of the GDM.

small-strain damping @  $\sigma'_m = 1$  atm are provided for South Carolina soils based on Andrus, et al. (2003) in Table 7-33.



Note:  $D_{min1} = \lambda_{min1}$

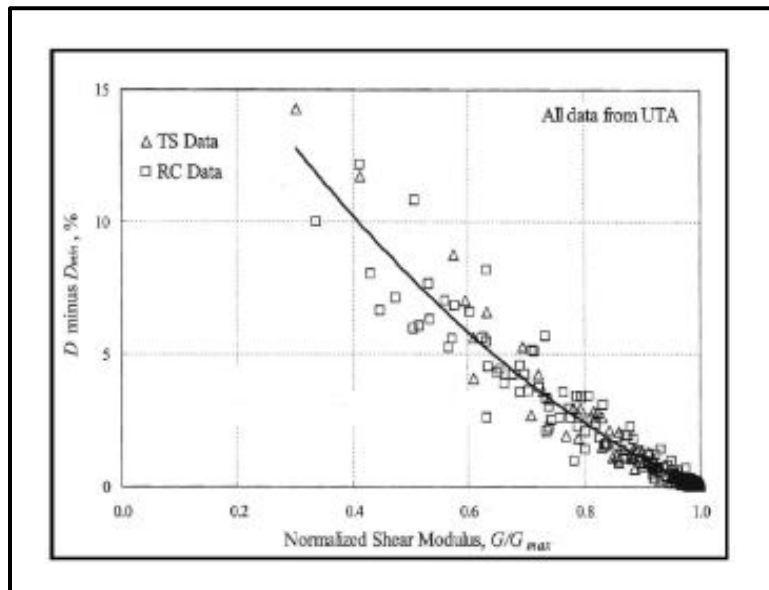
Figure 7-40,  $\lambda_{min1}$ , Small-Strain Damping @  $\sigma'_m = 1$  atm (Andrus, et al. (2003))

Table 7-31, Recommended Value  $\lambda_{min1}$  (%) for SC Soils (Andrus, et al. (2003))

Geologic Age and Location of Deposits	Soil Plasticity Index, PI (%)					
	0	15	30	50	100	150
Holocene	1.09	1.29	1.50	1.78	2.48	3.18 <sup>(1)</sup>
Pleistocene (Wando)	0.59	0.66	0.73	0.83	1.08	1.32
Tertiary Ashley Formation (Cooper Marl)	---	---	1.14 <sup>(1)</sup>	1.52 <sup>(1)</sup>	2.49 <sup>(1)</sup>	---
Tertiary (Stiff Upland Soils)	---	---	0.98	1.42 <sup>(1)</sup>	---	---
Tertiary (All soils at SRS except Stiff Upland Soils)	0.68	0.94	1.19	1.53	2.37 <sup>(1)</sup>	---
Tertiary (Tobacco Road, Snapp)	0.68	0.94	1.19	1.53	2.37 <sup>(1)</sup>	---
Tertiary (Soft Upland Soils, Dry Branch, Santee, Warley Hill, Congaree)	0.68	0.94	1.19	1.53	2.37 <sup>(1)</sup>	---
Residual Soil and Saprolite	0.56 <sup>(1)</sup>	0.85 <sup>(1)</sup>	1.14 <sup>(1)</sup>	1.52 <sup>(1)</sup>	---	---

<sup>(1)</sup> Tentative Values – Andrus, et al. (2003)

Data compiled by the University of Texas at Austin (UTA) for  $(\lambda - \lambda_{min})$  vs.  $(G/G_{max})$  is plotted in Figure 7-41.



Note:  $D = \lambda$

**Figure 7-41,  $(\lambda - \lambda_{min})$  vs.  $(G/G_{max})$  Relationship  
(Andrus, et al. (2003))**

Equation 7-137 represents a best-fit equation (UTA Correlation) of the observed relationship of  $(\lambda - \lambda_{min})$  vs.  $(G/G_{max})$  indicated below:

**Equation 7-138**

$$\lambda - \lambda_{min} = 12.2 * \left( \frac{G}{G_{max}} \right)^2 - 34.2 * \left( \frac{G}{G_{max}} \right) + 22.0$$

If we substitute Equation 7-134 into Equation 7-138 and solve for the damping ratio,  $\lambda$ , the Equivalent Viscous Damping Ratio curves can be generated using the following equation.

**Equation 7-139**

$$\lambda = \lambda_{min} + 12.2 * \left[ \frac{1}{1 + \left( \frac{\gamma_c}{\gamma_{cr}} \right)^\alpha} \right]^2 - 34.2 * \left[ \frac{1}{1 + \left( \frac{\gamma_c}{\gamma_{cr}} \right)^\alpha} \right] + 22.0$$

Where values of reference strain,  $\gamma_{cr}$ , are computed using Equation 7-135.

The procedures for using Equation 7-139 are provided in Table 7-32.

**Table 7-32, Procedure for Computing Damping Ratio**

Step	Procedure Description
1	Perform a geotechnical subsurface exploration and identify subsurface soil geologic units, approximate age, and formation.
2	Develop soil profiles based on geologic units, soil types, average PI, and soil density. Subdivide major geologic units to reflect significant changes in PI and soil density. Identify design ground water table based on seasonal fluctuations and artesian pressures.
3	Calculate the average $\sigma'_m$ and determine the corresponding $\pm 50\%$ range of $\sigma'_m$ for each major <u>geologic unit</u> using Equation 7-136.
4	Calculate $\sigma'_m$ for each <u>layer</u> within each major geologic unit. If the values for $\sigma'_m$ of each layer are within a geologic unit's $\pm 50\%$ range of $\sigma'_m$ (Step 3) then assign the average $\sigma'_m$ for the major geologic unit (Step 3) to all layers within it. If the $\sigma'_m$ of each layer within a geologic unit is not within the $\pm 50\%$ range of $\sigma'_m$ for the major geologic unit, then the geologic unit needs to be "subdivided" and more than one average $\sigma'_m$ needs to be used, provided the $\sigma'_m$ remain within the $\pm 50\%$ range of $\sigma'_m$ for the "subdivided" geologic unit.
5	Select appropriate small-strain material Damping @ $\sigma'_m = 1 \text{ atm}$ , $\lambda_{\min 1}$ , from Table 7-31 for each <u>layer</u> within a geologic unit.
6	Compute the small-strain material Damping, $\lambda_{\min}$ , for each <u>layer</u> within a geologic unit using Equation 7-137.
7	Select the appropriate values for each <u>layer</u> of cyclic reference strain, $\gamma_{cr1}$ , @ $\sigma'_m = 1 \text{ atm}$ , curvature coefficient, $\alpha$ , and k exponent from Table 7-29. These values may be selected by rounding to the nearest PI value in the table or by interpolating between listed PI values in the table.
8	Compute the cyclic reference strain, $\gamma_{cr}$ , based on Equation 7-135 for each <u>geologic unit</u> that has a corresponding average $\sigma'_m$ .
9	Compute the design equivalent viscous damping ratio curves ( $\lambda$ ) for each layer by substituting cyclic reference strain, $\gamma_{cr}$ , and curvature coefficient, $\alpha$ , and small-strain material Damping, $\lambda_{\min}$ , for each layer using Equation 7-139. Tabulate values of Soil Damping Ratio, $\lambda$ , with corresponding cyclic shear strain, $\gamma_c$ , for use in a site-specific site response analysis.

### 7.17.3.3 Alternate Dynamic Property Correlations

#### 7.17.3.3.1 Soil Stiffness

The SPT and CPTu shear wave,  $V_s$ , correlations provided in Sections 7.17.2.1 and 7.17.2.2 are based on studies performed by Andrus, et al. (2009) for South Carolina soils. If the Andrus, et al. (2009) shear wave correlations are not appropriate (i.e., embankment fill) for the soils encountered at a specific project site, the GEOR can use alternate correlations. Documentation is required explaining the use of the alternate correlation and that the correlation is nationally or regionally recognized. Acceptable correlations for  $G_{\max}$  that can be used are listed in Table 7-33 and may be substituted into rearranged Equation 7-112.



**Table 7-33, Alternate Correlations for Determining Soil Stiffness Based on  $G_{max}$** 

Reference	Correlation Equation	Units	Comments																
Seed, Wong, Idriss and Tokimatsu (1986)	$G_{max} = 220 * (K_2)_{max} * (\sigma'_m)^{0.5}$ $(K_2)_{max} \approx 20 * (N_{1,60})^{0.33}$	kPa	$(K_2)_{max} \approx 30$ for loose sands and 75 for very dense sands; $\approx 80$ -180 for dense well graded gravels; Limited to cohesionless soils																
Imai and Tonouchi (1982)	$G_{max} = 15,560 * (N_{60})^{0.68}$	kPa	Limited to cohesionless soils																
Hardin (1978)	$G_{max} = \left(\frac{625}{\chi}\right) * (K)^{0.5} * OCR^k$ $\chi = 0.3 + 0.7 * e_o^2$ $K = (P_a * \sigma'_m)^{0.5}$	kPa <sup>(1)</sup>	Limited to cohesive soils $P_a$ = atmospheric pressure $P_a$ and $\sigma'_m$ in kPa																
Jamiolkowski, Leroueil, and Lo Presti (1991)	$G_{max} = \left(\frac{625}{e_o^{1.3}}\right) * K * OCR^k$ $K = (P_a * \sigma'_m)^{0.5}$	kPa <sup>(1)</sup>	Limited to cohesive soils $P_a$ and $\sigma'_m$ in kPa																
Mayne and Rix (1993)	$G_{max} = 99.5 * (P_a)^{0.305} * \left(\frac{q_c^{0.695}}{e_o^{1.13}}\right)$	kPa	Limited to cohesive soils $P_a$ and $q_c$ in kPa																
<sup>(1)</sup> The parameter k is related to the plasticity index, PI, as follows: <table border="1" style="margin-left: 20px;"> <thead> <tr> <th>PI</th> <th>k</th> <th>PI</th> <th>k</th> </tr> </thead> <tbody> <tr> <td>0</td> <td>0.00</td> <td>60</td> <td>0.41</td> </tr> <tr> <td>20</td> <td>0.18</td> <td>80</td> <td>0.48</td> </tr> <tr> <td>40</td> <td>0.30</td> <td>&gt;100</td> <td>0.50</td> </tr> </tbody> </table>				PI	k	PI	k	0	0.00	60	0.41	20	0.18	80	0.48	40	0.30	>100	0.50
PI	k	PI	k																
0	0.00	60	0.41																
20	0.18	80	0.48																
40	0.30	>100	0.50																

### 7.17.3.3.2 Shear Modulus Reduction Curves

The shear modulus reduction curves provided in Section 7.17.3.1 are based on studies performed by Andrus, et al. (2009). If the Andrus, et al. (2009) shear modulus reduction curves are not appropriate (i.e., embankment fill) for the soils encountered at a specific project site, the GEOR may use alternate shear modulus reduction curve correlations. Documentation is required explaining the use of the alternate curve and that the alternate curve is nationally or regionally recognized. Acceptable correlations that may be used are listed below:

- Andrus, Zhang, Ellis and Juang (2003)
- Seed and Idriss (1970)
- Vucetic and Dobry (1991)
- Ishibashi and Zhang (1993)
- Idriss (1990)
- Seed et al. (1986)

### 7.17.3.3.3 Equivalent Viscous Damping Ratio Curves

The equivalent viscous damping ratio curves provided in Section 7.17.3.2 are based on studies performed by by Andrus, et al. (2009). If the by Andrus, et al. (2009) equivalent viscous damping ratio curves are not appropriate (i.e., embankment fill) for the soils encountered at a project site the GEOR may use alternate equivalent viscous damping ratio curves. Documentation is required explaining the use of the alternate curve and that the alternate curve is nationally or regionally recognized. Acceptable correlations that may be used are listed below:

- Andrus, Zhang, Ellis and Juang (2003)

- Seed et al. (1986)
- Idriss (1990)
- Vucetic and Dobry (1991)

#### **7.17.4 Cyclic Residual Shear Strength**

Cyclic residual shear strengths are an important element in the evaluation of seismic slope stability. Two different residual shear strengths may be developed depending on whether the soils are susceptible to soil shear strength loss or not. The use of residual shear strengths in the Service or Strength limit states is not anticipated for slope stability analysis. However, the residual shear strengths discussed previously in this Chapter should be used for those soils that are not susceptible to soil shear strength loss, but are anticipated to undergo significant movement (typically greater than 10 inches) caused by the induced seismic motion. Typically these soils are anticipated to be above the groundwater level. Chapter 13 provides the methods for determining the residual shear strength of soils that will undergo shear strength losses. Chapter 14 provides the discussion of when to use these residual shear strengths.

### **7.18 ROCK DYNAMIC PROPERTIES**

According to Kavazanjian, et al. (2011):

In a seismic analysis, rock may be treated as either a linear elastic material with a constant shear modulus and no damping or as an equivalent linear material with an initial small strain modulus, a slight potential for modulus degradation, and a small amount of damping. The elastic modulus for the rock mass is generally based upon either shear wave velocity measurements or, in cases where the value of the modulus is not critical (i.e., when the modulus is merely used to characterize the impedance contrast at the bottom of a soil column), using typical properties. Modulus reduction and damping typically based upon generic equivalent linear modulus reduction and damping curves (e.g., the generic curves for soft rock from Silva, et al. (1996)).

### **7.19 ELECTRO-CHEMICAL PROPERTIES**

The GEOR is required to test soil and water, both surface and subsurface as required, to determine the electro-chemical properties of the respective materials. Two general environments are established:

- Aggressive
- Non-aggressive

The SCDOT BDM (2006) defines the substructure “as any component or element located below the bearings.” The superstructure is defined as the “bearings and all of the components and elements resting upon them.” For superstructures the environmental classification will be determined by the SEOR. Substructures are classified as indicated in Table 7-34.

**Table 7-34, Criteria for Substructure Environmental Classifications**

Environmental Classification	Electro-Chemical Component	Units	Soil	Water
Aggressive (if any of these conditions exist)	pH	-	< 5.5	< 5.5
	Cl	ppm <sup>1</sup>	N.A.	> 500
	SO <sub>4</sub>	ppm <sup>1</sup>	> 1,000	> 500
	Resistivity	Ohm-cm	< 2,000	N.A.
Non-aggressive	This classification must be used at all sites not meeting the requirements for Aggressive Environments			
pH = acidity (-log <sub>10</sub> H <sup>+</sup> ; potential of hydrogen); Cl = chloride content; SO <sub>4</sub> = sulfate content				

<sup>1</sup> ppm (part per million) = mg/L (milligram per liter)

These criteria do not apply to MSE walls, RSSs or reinforced embankments; see the appropriate STS.

## 7.20 REFERENCES

American Association of State Highway and Transportation Officials, (2017), LRFD Bridge Design Specifications Customary U.S. Units, 8<sup>th</sup> Edition, American Association of State Highway and Transportation Officials, Washington, D.C.

American Association of State Highway and Transportation Officials, (2009), Transportation Glossary, 4<sup>th</sup> Edition, American Association of State Highway and Transportation Officials, Washington, D.C.

Arneson, L. A., Zevenbergen, L. W., Lagasse, P. F., and Clooper, P. E., (2012), Evaluating Scour at Bridges, Hydraulic Engineering Circular 18, (Publication No. FHWA-HIF-12-003), 5<sup>th</sup> Edition, US Department of Transportation, Office of Bridge Technology, Federal Highway Administration, Washington, D.C.

Andrus, R. D., Hayati, H., and Mohanan, N. P., (2009), "Correcting Liquefaction Resistance for Aged Sands Using Measured to Estimated Velocity Ratio." *Journal of Geotechnical and Geoenvironmental Engineering*, ASCE, Volume 135, Issue 6, pp. 735-744.

Andrus, R. D., Zhang, J., Ellis, B. S., and Juang, C. H., (2003), "Guide for Estimating the Dynamic Properties of South Carolina Soils for Ground Response Analysis", South Carolina Department of Transportation, SC-DOT Research Project No. 623, FHWA-SC-03-07.

Boulanger, R. W. (2003), "Relating Ka to a Relative State Parameter Index." *Journal of Geotechnical and Geoenvironmental Engineering*, ASCE, Volume 129, Issue 8, pp. 770-773.

Canadian Geotechnical Society, (2006), Canadian Foundation Engineering Manual, 4<sup>th</sup> Edition.

Cetin, K. O., Seed, R. B., Der Kiureghian, A., Tokimatsu, K., Harder, L. F., Kayen, R. E. and Moss, R. E. S., (2004), "Standard Penetration Test-Based Probabilistic and Deterministic Assessment of Seismic Soil Liquefaction Potential", *Journal of Geotechnical and Geoenvironmental Engineering*, ASCE, Vol. 130, Issue 12, pp. 1314-1340.

Darendeli, M. B., (2001), Development of a New Family of Normalized Modulus Reduction and Material Damping Curves, Ph.D. Dissertation, The University of Texas at Austin, Austin, TX.

Das, B. M., (1997), Advanced Soil Mechanics, 2<sup>nd</sup> Edition, Taylor & Francis, Washington, DC.

Department of Defense, Department of the Navy, Naval Facilities Engineering Command, (1986), Soil Mechanics – Design Manual 7.1, (Publication No. NAVFAC DM-7.01), Alexandria, Virginia.

Duncan, J. M. and Buchignani, A. L., (1976), An Engineering Manual for Settlement Studies, Virginia Polytechnic Institute and State University.

Duncan, J. M. and Wright, S. G., (2005), Soil Strength and Slope Stability, John Wiley & Sons, Inc., New Jersey.

Hardin, B. O., (1978), "The Nature of Stress-Strain Behavior of Soils", Proc. Earthquake Engineering and Soil Dynamics, ASCE, Pasadena, California, Vol. 1, pp. 3-89.

Hatanaka, M. and Uchida, A., (1996), "Empirical Correlation Between Penetration Resistance and Internal Friction Angle of Sandy Soils", Soils and Foundations, Japanese Geotechnical Society, Volume 36, No. 4, pp. 1-9.

Hoek, E., (2007), Practical Rock Engineering, Rocscience, Available at: [http://www.rocscience.com/education,hoeks\\_corner](http://www.rocscience.com/education,hoeks_corner).

Hoek, E., Carranza-Torres, C., and Corkum, B., (2002), "Hoek-Brown Failure Criterion – 2002 Edition," Mining and Tunnelling Innovation and Opportunity: Proceedings of the 5th North American Rock Mechanics Symposium and the 17th Tunnelling Association of Canada Conference : NARMS-TAC 2002, Toronto, Ontario, Canada.

Holtz, R. D. and Kovacs, W. D., (1981), An Introduction to Geotechnical Engineering, Prentice Hall, New Jersey.

Hunt, R. E., (2005), "Geotechnical Engineering Investigation Handbook", 2<sup>nd</sup> Edition, Taylor & Francis, Boca Raton, Florida.

Idriss, I. M., (1990), "Response of Soft Soil Sites During Earthquakes", H. Bolton Seed Memorial Symposium Proceedings, Volume 2, BiTech, Vancouver, British Columbia, Canada.

Idriss, I.M. and Boulanger, R.W., (2008), "Soil Liquefaction During Earthquakes." Earthquake Engineering Research Institute (EERI), EERI Monograph MNO-12.

Imai, T. and Tonouchi, K., (1982), "Correlation of N-Value with S-Wave Velocity and Shear Modulus", Proc. 2nd European Symposium on Penetration Testing, Amsterdam, The Netherlands, pp. 67-72.

Ishibashi, I. and Zhang, X. J., (1993), "Unified Dynamic Shear Moduli and Damping Ratios of Sand and Clay", Soils and Foundations, Japanese Society of Soil Mechanics and Foundation Engineering, Volume 33, No. 1, pp. 182-191.

Jamiolkowski, M., Ladd, C. C., Germaine, J., and Lancellotta, R., (1985), "New Developments in Field and Lab Testing of Soils", 11<sup>th</sup> International Conference on Soil Mechanics and Foundations Engineering Proceedings, Volume 1.

Jamiolkowski, M., Leroueil, S. and Lo Presti, D. C. F. (1991), "Theme Lecture: Design Parameters from Theory to Practice", Proc. Geo-Coast '91, Yokohama, Japan, pp. 1-41.

Jefferies, M. G. and Davies, M. P., (1993), "Use of CPTu to Estimate SPT  $N_{60}$ ," Geotechnical Testing Journal, ASTM, Volume 16, Number 4, pp. 458-468.

Kavazanjian, E., Wang, J-N. J., Martin, G. R., Shamsabadi, A., Lam, I., Dickenson. S. E., and Hung, C. H., (2011), LRFD Seismic Analysis and Design of Transportation Geotechnical Features and Structural Foundations, Geotechnical Engineering Circular No. 3, (Publication No. FHWA-NHI-11-032), US Department of Transportation, Office of Bridge Technology, Federal Highway Administration, Washington, D.C.

Kramer, S. L., (1996), Geotechnical Earthquake Engineering, Prentice Hall, New Jersey.

Ladd, C. C., (1973), "Settlement Analysis of Cohesive Soils," Research Report 71-2, No. 272, Department of Civil Engineering, MIT, Cambridge, MA.

Ladd, C. C., Foot, R., Ishihara, K., Schlosser, F., and Poulos, H. G. (1977). "Stress Deformation and Strength Characteristics." Proceedings 9th International Conference on Soil Mechanics and Foundation Engineering, Volume 2, Tokyo, Japan.

Liao, S. S. C. and Whitman, R. V., (1986), "Overburden Correction Factors for SPT in Sand", *Journal of Geotechnical Engineering*, ASCE, Volume 112, Issue 3, pp. 373-377.

Marchetti, S. (1997). "The Flat Dilatometer: Design Applications." Proceedings, 3rd International Geotechnical Engineering Conference, Soil Mechanics and Foundations Research Laboratory, Cairo University, Egypt.

Marchetti, S., Monaco, P., Totani, G., and Calabrese, M., (2001) "The Flat Dilatometer Test (DMT) in soil investigations, A Report by the ISSMGE Committee TC16," Proceedings In-Situ 2001, International Conference on In Situ Measurement of Soil Properties, Bali, Indonesia.

Marinos, P. and Hoek, E., (2000), "GSI: A Geologically Friendly Tool for Rock Mass Strength Estimation," Proceedings, Geo-Engineering 2000, International Conference on Geotechnical and Geological Engineering, Melbourne, Australia.

Mayne, P. W. (2007), Cone Penetration Testing, NCHRP Synthesis 368, National Cooperative Highway Research Program, Transportation Research Board, Washington, DC.

Mayne, P. W. and Rix, G. J., (1993), " $G_{max}$ - $q_c$ , Relationships for Clays", *Geotechnical Testing Journal*, ASTM, Volume 16, No. 1, pp. 54-60.

Mayne, P. W., Christopher, B. R., and DeJong, J., (2002), Subsurface Investigations - Geotechnical Site Characterization, (Publication No. FHWA-NHI-01-031), US Department of Transportation, National Highway Institute, Federal Highway Administration, Washington, D.C.

McGregor, J. A. and Duncan, J. M., (1998) Performance and Use of the Standard Penetration Test in Geotechnical Engineering Practice, Virginia Polytechnic Institute and State University.

Mitchell, J. K., (1993), Fundamentals of Soil Behavior, 2<sup>nd</sup> Edition, John Wiley and Sons, Inc.

Munfakh, G., Arman, A., Samtani, N., and Castelli, R., (1997), Subsurface Investigations, (Publication No. FHWA-HI-97-021), US Department of Transportation, National Highway Institute, Federal Highway Administration, Washington D.C.

Munfakh, G., Kavazanjian, E., Matasovic, N., Hadj-Hamou, T., and Wang, J., (1998), Geotechnical Earthquake Engineering, Reference Manual, NHI Course No. 13239, (Publication No. FHWA HI-99-012), U.S. Department of Transportation, National Highway Institute, Federal Highway Administration, Arlington, Virginia.

Rausche, F., Thendean, G., Abou-matar, H., Linkins, G. E., and Goble, G. G., (1997), Determination of Pile Driveability and Capacity from Penetration Tests – Volume I: Final Report, (Report No. FHWA-RD-96-179), U. S. Department of Transportation, Office of Engineering R&D, Federal Highway Administration, McLean, Virginia.

Robertson, P. K., and Campanella, R. G., (1983), *Interpretation of Cone Penetration Tests*, *Canadian Geotechnical Journal*, Volume 20, Issue 4, pp. 718-745.

Roberston, P. K. and Cabal (Roberston) K. L., (2015), Guide to Cone Penetration Testing for Geotechnical Engineering, 6<sup>th</sup> Edition, Gregg Drilling and Testing, Signal Hill, California.

Sabatini, P. J., Bachus, R. C., Mayne, P. W., Schneider, J. A., and Zettler, T. E., (2002), Evaluation of Soil and Rock Properties, Geotechnical Engineering Circular No. 5, (Publication No. FHWA-IF-02-034). US Department of Transportation, Office of Bridge Technology, Federal Highway Administration, Washington, D.C.

Seed, H. B., and Idriss, I. M., (1970), “Soil Moduli and Damping Factors for Dynamic Response Analysis”, Report EERC 70-10, Earthquake Engineering Research Institute, Berkeley, CA.

Seed, H. B., Wong, R. T., Idriss, I. M., and Tokimatsu, K., (1986), “Moduli and Damping Factors for Dynamic Analysis of Cohesionless Soils”, *Journal of the Geotechnical Engineering Division*, ASCE, Volume 112, Issue 11, pp. 1016-1031.

Silva, W., Abrahamson, N. A., Toro, G. R., and Constantino, C., (1996), “Description and Validation of the Stochastic Ground Motion Model”, Report prepared for the Engineering Research and Applications Division, Department of Nuclear Energy, Pacific Engineering and Analysis, El Cerrito, California.

Sorensen, H. K. and Okkels, N., (2013), “Correlation between drained shear strength and plasticity index of undisturbed overconsolidated clays”, Challenges and Innovations in Geotechnics, Proceedings of the 18<sup>th</sup> International Conference on Soil Mechanics and Geotechnical Engineering, Paris, France.

South Carolina Department of Transportation, (2009), Requirements for Hydraulic Design Studies, South Carolina Department of Transportation, <http://www.scdot.org/doing/technicalPDFs/hydraulic/requirements2009.pdf>.

Spangler, M. G. and Handy, R. L., (1982), Soil Engineering, 4<sup>th</sup> Edition, Harper & Row.

Stark, T. D. and Eid, H. T., (1994), “Drained Residual Strength of Cohesive Soil”, *Journal of Geotechnical Engineering*, ASCE, Volume 120, Issue 5, pp. 856-871.

Stark, T. D. and Eid, H. T., (1997), “Slope Stability Analyses in Stiff Fissured Clays”, *Journal of Geotechnical and Geoenvironmental Engineering*, ASCE, Volume 123, Issue 4, pp. 335-343.

Stark, T. D. and Hussain M., (2013), "Empirical Correlations: Drained Shear Strength for Slope Stability Analyses", *Journal of Geotechnical and Geoenvironmental Engineering*, ASCE, Volume 139, Issue 6, pp. 853-862.

Stokoe, K. H., II, Hwang, S. K., Darendeli, M. B., and Lee, N. J., (1995), "Correlation Study of Nonlinear Dynamic Soils Properties", final report to Westinghouse Savannah River Company, The University of Texas at Austin, Austin, TX.

Stokoe, K. H., II, Darendeli, M. B., Andrus, R. D., and Brown, L. T., (1999). "Dynamic Soil Properties: Laboratory, Field and Correlation Studies", *Proceedings, 2<sup>nd</sup> International Conference on Earthquake Geotechnical Engineering*, Vol. 3, Lisbon, Portugal, 811-845.

Terzaghi, K., Peck, R. B., and Mesri, G., (1996), Soil Mechanics In Engineering Practice, 3<sup>rd</sup> Edition, John Wiley & Sons, Inc., New York.

Tiwari, B. and Ajmera, B., (2012), "New Correlation Equations for Compression Index of Remolded Clays", *Journal of Geotechnical and Geoenvironmental Engineering*, ASCE, Volume 138, Issue 6, pp. 757-762.

Turner, J., (2006), Rock-Socketed Shafts for Highway Structure Foundations, NCHRP Synthesis 360, National Cooperative Highway Research Program, Transportation Research Board, Washington, D.C.

Vucetic, M., and Dobry, R., (1991), "Dynamic Effect of Soil Plasticity on Cyclic Response", *Journal of Geotechnical Engineering*, ASCE, Volume 117, No. 1, pp. 89-107.

**Chapter 8**  
**GEOTECHNICAL**  
**LRFD DESIGN**

**GEOTECHNICAL DESIGN MANUAL**

*January 2019*





## Table of Contents

<u>Section</u>	<u>Page</u>
8.1 Introduction .....	8-1
8.2 LRFD Design Philosophy.....	8-2
8.3 Limit States .....	8-2
8.4 Types of Loads.....	8-3
8.4.1 Permanent Loads.....	8-3
8.4.2 Transient Loads .....	8-5
8.5 Load Combination Limit States.....	8-8
8.6 Load Modifiers.....	8-9
8.7 Load Combination and Load Factors.....	8-9
8.8 Load Combinations and Factors For Construction Loads .....	8-13
8.9 Operational Classification .....	8-13
8.10 LRFD Geotechnical Design and Analysis .....	8-14
8.10.1 Bridge Foundations.....	8-14
8.10.2 Embankments .....	8-15
8.10.3 Earth Retaining Structures .....	8-16
8.11 References.....	8-17

**List of Tables**

<b><u>Title</u></b>	<b><u>Page</u></b>
Table 8-1, Limit States .....	8-3
Table 8-2, Permanent Load Descriptions .....	8-4
Table 8-3, Transient Load Descriptions.....	8-5
Table 8-4, Load Combination Limit State Considerations.....	8-8
Table 8-5, Load Combination and Load Factors.....	8-9
Table 8-6, Load Factors for Permanent Loads, $\gamma_p$ .....	8-11
Table 8-7, Uniform Surcharge Pressures .....	8-12
Table 8-8, Unit Weights of Common Materials .....	8-13
Table 8-9, Shallow Foundation Limit States .....	8-15
Table 8-10, Deep Foundation Limit States .....	8-15
Table 8-11, Embankment Limit States .....	8-16
Table 8-12, Earth Retaining Structures Limit States.....	8-17

# CHAPTER 8

## GEOTECHNICAL LRFD DESIGN

### 8.1 INTRODUCTION

Geotechnical engineering analyses and designs for transportation structures have traditionally been based on Allowable Stress Design (ASD), also known as Working Stress Design (WSD). Transportation structures that require geotechnical engineering are bridge foundations, sign and lighting foundations, Earth Retaining Structures (ERSs: MSE walls, reinforced concrete walls, cantilever walls, etc.), and embankments (both bridge and road). The primary guidance for the ASD design methodology has been the AASHTO Standard Specifications for Highway Bridges (17<sup>th</sup> edition – last edition published 2002) and various Federal Highway Administration (FHWA) geotechnical engineering publications. The ASD methodology is based on limiting the stresses induced by the applied loads ( $Q$ , which includes dead loads - DL and live loads - LL) on a component/member from exceeding the allowable (or working) stress of the material ( $R_{all}$ ). The allowable stress of a material is computed by dividing the nominal strength of the material ( $R_n$ ) by an appropriate factor of safety (FS) as indicated in the following equation.

$$Q = \sum DL + \sum LL \leq R_{all} = \frac{R_n}{FS} \quad \text{Equation 8-1}$$

This design approach uses a single factor of safety to account for all of the geotechnical engineering uncertainties. The ASD factors of safety do not appropriately take into account variability associated with the predictive accuracy of dead loads, live loads, wind loads, and seismic loads or the different levels of uncertainty associated with design methodology, material properties, site variability, material sampling, and material testing. The assignment of ASD factors of safety has traditionally been based on experience and judgment. This methodology does not permit a consistent or rational method of accessing risk.

In 1986 an NCHRP study (20-7/31) concluded that the AASHTO Standard Specifications for Highway Bridges contained gaps and inconsistencies, and did not use the latest design philosophy and knowledge. In response, AASHTO adopted the Load and Resistance Factor Design (LRFD) Bridge Design Specification in 1994 and the Load and Resistance Factor Rating (LRFR) Guide Specification in 2002. The current AASHTO LRFD Specifications incorporate state-of-the-art analysis and design methodologies with load and resistance factors based on the known variability of applied loads and material properties. These load and resistance factors are calibrated from actual statistics to ensure a uniform level of safety. Because of LRFD's impact on the safety, reliability, and serviceability of the Nation's bridge inventory, AASHTO, in concurrence with the FHWA, set a transition deadline of 2007 for bridges and 2010 for culverts, retaining walls and other miscellaneous structures. After this date, States must design all new structures in accordance with the LRFD design methodology.

SCDOT is committed to using the LRFD design methodology on structures including all aspects of geotechnical engineering analysis and design. In this Manual the term AASHTO LRFD Specifications refers to the AASHTO LRFD Bridge Design Specifications, 8<sup>th</sup> Edition (2017), unless indicated otherwise. The LRFD geotechnical design approach is presented in Chapters 8, 9, and 10 of this Manual. All tables in this Chapter have been modified and adapted from the AASHTO LRFD Specifications unless indicated otherwise. The geotechnical design methodology presented in this Manual provides guidance on how to apply the LRFD geotechnical design approach into geotechnical engineering analyses for SCDOT projects.

## 8.2 LRFD DESIGN PHILOSOPHY

Basic to all good engineering design methodologies (including ASD and LRFD) is that when a Load (Q or Demand) is placed on a component/member, there is sufficient Resistance (R or Capacity) to insure that an established performance criterion is not exceeded. This concept is illustrated by the following equation:

$$\mathbf{Load (Q) \leq RESISTANCE (R)} \qquad \mathbf{Equation 8-2}$$

The Load and Resistance quantities can be expressed as force, stress, strain, displacement, number of cycles, temperature, or some other parameter that results in structural or performance failure of a component/member. The level of inequality between the Load and Resistance side of Equation 8-2 represents the uncertainty. In order to have an acceptable design the uncertainties must be mitigated by applying an appropriate margin of safety in the design.

The LRFD design methodology mitigates the uncertainties by applying individual load factors ( $\gamma$ ) and a load modifier ( $\eta$ ) to each type of load ( $Q_i$ ). On the resistance side of the equation a resistance factor ( $\phi$ ) is applied to the nominal resistance ( $R_n$ ). The sum of the factored loads, Q, placed on the component/member must not exceed the factored resistance of the component/member in order to have satisfactory performance. The following equation illustrates the basic LRFD design concept.

$$\mathbf{Q = \sum \eta_i \gamma_i Q_i \leq \phi R_n = R_r} \qquad \mathbf{Equation 8-3}$$

Where,

- Q = Factored Load
- $Q_i$  = Force Effect
- $\eta_i$  = Load modifier
- $\gamma_i$  = Load factor
- $R_r$  = Factored Resistance
- $R_n$  = Nominal Resistance (i.e., ultimate capacity)
- $\phi$  = Resistance Factor

Equation 8-3 is applicable to more than 1 load combination as defined by the condition that defines the “Limit State”.

## 8.3 LIMIT STATES

A “Limit State” is a condition beyond which a component/member of a foundation or other structure ceases to satisfy the provisions for which the component/member was designed. The AASHTO LRFD Specifications has defined the following limit states for use in design:

- Strength Limit State
- Service Limit State
- Extreme Event Limit State
- Fatigue Limit State

The Fatigue Limit State is the only limit state that is not used in geotechnical analyses or design. A description of the limit states that are used in geotechnical engineering are provided in the following table.

**Table 8-1, Limit States  
(Modified from Wilson, et al. (2007))**

Limit State	Description
<b>Strength</b>	A design boundary condition considered to ensure that strength and stability are provided to resist specified load combinations, and avoid the total or partial collapse of the structure. Examples of Strength limit states in geotechnical engineering include bearing failure, sliding, and earth loadings for structural analysis.
<b>Service</b>	A design boundary condition for structure performance under intended service loads, and accounts for some acceptable measure of structure movement throughout the structure's performance life. Examples include vertical settlement of a foundation or lateral displacement of a retaining wall. Another example of a Service limit state condition is the rotation of a rocker bearing on an abutment caused by instability of the earth slope that supports the abutment.
<b>Extreme Event (EE)</b>	Evaluation of a structural member/component at this limit state considers a loading combination that represents an excessive or infrequent design boundary condition. Such conditions may include vessel impacts, vehicle impact, check flood (500-year flow event), and seismic events. Because the probability of these events occurring during the life of the structure is relatively small, a smaller margin of safety is appropriate when evaluating this limit state.

## 8.4 TYPES OF LOADS

AASHTO specifications classify loads as either permanent loads or transient loads.

### 8.4.1 Permanent Loads

Permanent loads are present for the life of the structure and do not change over time. Permanent loads are generally very predictable. The following is a list of all loads identified by AASHTO LRFD Specifications as permanent loads:

- Force Effects Due to Creep – CR
- Dead Load of Components – DC
- Downdrag – DD
- Dead Load of Wearing Surface and Utilities – DW
- Horizontal Earth Pressures – EH
- Locked-In Erection Stresses – EL
- Vertical Earth Pressure – EV
- Earth Load Surcharge – ES
- Secondary Forces from Post-tensioning – PS
- Force Effects Due to Shrinkage – SH

A brief description for each of these permanent loads is provided in Table 8-2. For a complete description and method of computing these loads see the AASHTO LRFD Specifications.

**Table 8-2, Permanent Load Descriptions**  
**(Modified from AASHTO LRFD Specifications (2017) and Wilson, et al. (2007))**

AASHTO Designation	Definition	Description
CR	Creep	These loads are internal force effects that develop on structure components as a result of creep and shrinkage of materials. These forces should be considered for substructure design when applicable.
DC	Dead load of structural components and nonstructural attachments	These loads include the weight of both fabricated structure components (e.g., structural steel girders and prestressed concrete beams) and cast-in-place structure components (e.g., deck slabs, abutments, and footings). DC loads also include nonstructural attachments such as lighting and signs.
DD	Downdrag	When a deep foundation is installed through a soil layer that is subject to relative settlement of the surrounding soil to the deep foundation, downdrag forces are induced on the deep foundation. The magnitude of DD load may be computed in a similar manner as the positive shaft resistance calculation. Allowance may need to be made for the possible increase in undrained shear strength as consolidation occurs. For the strength limit state, the factored downdrag loads are added to the factored vertical dead load in the assessment of pile capacity. For the Service limit state, the downdrag loads are added to the vertical dead load in the assessment of settlement. Downdrag forces can also occur in the EE I limit state due to downdrag forces resulting from soil liquefaction of loose sandy soil. Measures to mitigate downdrag are typically used by applying a thin coat of bitumen on the deep foundation surface or some other means of reducing surface friction on the pile may reduce downdrag forces.
DW	Dead load of wearing surfaces and utilities	These loads include asphalt wearing surfaces, future overlays and planned widening, as well as miscellaneous items (e.g., scuppers, railings and supported utility services).
EH	Horizontal earth pressure load	<p>These loads are the force effects of horizontal earth pressures due to partial or full embedment into soil. These horizontal earth pressures are those resulting from static load effects.</p> <p>The magnitude of horizontal earth pressure loads on a substructure are a function of:</p> <ul style="list-style-type: none"> <li>• Structure type (e.g., gravity, cantilever, anchored, or MSE wall)</li> <li>• Type, unit weight, and shear strength of the retained earth</li> <li>• Anticipated or permissible magnitude and direction of horizontal substructure movement</li> <li>• Compaction effort used during placement of soil backfill</li> <li>• Location of the ground water table within the retained soil</li> </ul>

**Table 8-2 (Continued), Permanent Load Descriptions  
(Modified from AASHTO LRFD Specifications (2017) and Wilson, et al. (2007))**

<b>EL</b>	Locked-in erection stresses	These loads are accumulated locked-in force effects resulting from the construction process, typically resulting from segmental superstructure construction. These would include precast prestressed or post-tensioned concrete structures. For substructure designs, these force effects are small enough and can be ignored.
<b>EV</b>	Vertical pressure from dead load of earth fill	The vertical pressure of earth fill dead load acts on the top of footings and on the back face of battered wall and abutment stems. The load is determined by multiplying the volume of fill by the density and the gravitational acceleration (unit weight).
<b>ES</b>	Earth surcharge load	Surcharge loads are the force effects on the backs of ERSs. These effects must be considered in the design of walls and bridge abutments.
<b>PS</b>	Post-tensioning forces	The post-tensioning forces imposed on a continuous structure supports and any internal forces.
<b>SH</b>	Shrinkage	These loads are internal force effects that develop on structure components as a result of shrinkage of materials. These forces should be considered for substructure design when applicable.

#### 8.4.2 Transient Loads

Transient loads may only be present for a short amount of time, may change direction, and are generally less predictable than permanent loads. Transient loads include the following:

- Blast Loading – BL
- Vehicular braking force – BR
- Vehicular centrifugal force – CE
- Vehicular collision force – CT
- Vessel collision force – CV
- Earthquake – EQ
- Friction – FR
- Ice load – IC
- Vehicular dynamic load allowance – IM
- Vehicular live load – LL
- Live load surcharge – LS
- Pedestrian live load – PL
- Settlement – SE
- Temperature gradient – TG
- Uniform temperature – TU
- Water load and stream pressure – WA
- Wind on live load – WL
- Wind load on structure – WS

A brief description for each of these transient loads is provided in Table 8-3. For a complete description and method of computing these loads see the AASHTO LRFD Specifications.

**Table 8-3, Transient Load Descriptions  
(Modified from AASHTO LRFD Specifications (2017) and Wilson, et al. (2007))**

<b>AASHTO Designation</b>	<b>Definition</b>	<b>Description</b>
<b>BL</b>	Blast Loading	The force effects of a blast loading, either intentional or unintentional, on either a bridge or bridge component.
<b>BR</b>	Vehicular braking force	The force effects of vehicle braking that are represented as a horizontal force effect along the length of a bridge that is resisted by the structure foundations.



**Table 8-3 (Continued), Transient Load Descriptions  
(Modified from AASHTO LRFD Specifications (2017) and Wilson, et al. (2007))**

<b>CE</b>	Vehicular centrifugal force	These loads are the force effects of vehicles traveling on a bridge located along a horizontal curve and that generate a centrifugal force effect that must be considered in design. For substructure design, centrifugal forces represent a horizontal force effect.
<b>CT</b>	Vehicular collision force	These loads are the force effects of collisions by roadway and rail vehicles.
<b>CV</b>	Vessel collision force	These loads are the force effects of vessel collision by ships and barges due to their proximity to navigable waterways. The principal factors affecting the risk and consequences of vessel collisions with substructures in a waterway are related to vessel, waterway, and bridge characteristics.
<b>EQ</b>	Earthquake	<p><b><u>(DO NOT USE AASHTO FOR DETERMINATION OF EQ LOADS)</u></b> These loads are the earthquake force effects that are predominately horizontal and act through the center of mass of the structure. Because most of the weight of a bridge is in the superstructure, seismic loads are assumed to act through the bridge deck. These loads are due to inertial effects and therefore are proportional to the weight and acceleration of the superstructure. The effects of vertical components of earthquake ground motions are typically small and are usually neglected except for complex bridges. The SCDOT Seismic Specs specifies 2 design earthquakes to be used:</p> <ul style="list-style-type: none"> <li>• Functional Evaluation Earthquake (FEE). The ground shaking having a 15% probability of exceedance in 75 years</li> <li>• Safety Evaluation Earthquake (SEE). The ground shaking having a 3% probability of exceedance in 75 years</li> </ul> <p>For information on how to compute EQ loads for geotechnical earthquake engineering analyses see Chapters 11, 12, 13 and 14 of this Manual and the SCDOT Seismic Specs.</p>
<b>FR</b>	Friction	Forces due to friction as a result of sliding or rotation of surfaces.
<b>IC</b>	Ice Load	Ice force effects on piers as a result of ice flows, thickness of ice, and geometry of piers. In South Carolina this factor is typically not used on bridges. Ice force effects (i.e., the weight of ice) should be considered in the design of overhead signs, signals and sound walls.
<b>IM</b>	Vehicular dynamic load allowance	These loads are the force effects of dynamic vehicle loading on structures. For foundations and abutments supporting bridges, these force effects are incorporated into the loads used for superstructure design. For retaining walls not subject to vertical superstructure reactions and for foundation components completely below ground level, the dynamic load allowance is not applicable.

**Table 8-3 (Continued), Transient Load Descriptions  
(Modified from AASHTO LRFD Specifications (2017) and Wilson, et al. (2007))**

<b>LL</b>	Vehicular live load	These loads are the force effects of vehicular live load (truck traffic). The force effects of truck traffic are in part modeled using a highway design “umbrella” vehicle designated HL-93 to represent typical variations in axle loads and spacing. The HL-93 vehicular live load consists of a combination of a design truck HS20-44 and a design lane loading that simulates a truck train combined with a concentrated load to generate a maximum moment or shear effect for the component being designed, and an impact load (not used on lane loadings) to account for the sudden application of the truck loading to the structure.
<b>LS</b>	Live load surcharge	These loads are the force effects of traffic loads on backfills that must be considered in the design of walls and abutments. These force effects are considered as an equivalent surcharge. Live load surcharge effects produce a horizontal pressure component on a wall in addition to horizontal earth loads. If traffic is expected within a distance behind a wall equal to about half of the wall height, the live load traffic surcharge is assumed to act on the retained earth surface.
<b>PL</b>	Pedestrian live load	These loads are the force effects of pedestrian and/or bicycle traffic loads that are placed on bridge sidewalks or pedestrian bridges.
<b>SE</b>	Settlement	These loads are internal force effects that develop on structure components as a result of differential settlement between substructures and within substructure units.
<b>TG</b>	Temperature gradient	These loads are internal force effects and deformations that develop on structure components as a result of positive and negative temperature gradients with depth in component’s cross-section. These forces should be considered for substructure design when applicable.
<b>TU</b>	Uniform temperature	These loads are internal force effects that develop on structure components as a result of thermal movement associated with uniform temperature changes in the materials. These forces should be considered for substructure design when applicable.
<b>WA</b>	Water load and stream pressure	These loads are the force effects on structures due to water loading and include static pressure, buoyancy, and stream pressure. Static water and the effects of buoyancy need to be considered whenever substructures are constructed below a temporary or permanent ground water level. Buoyancy effects must be considered during the design of a spread footing or pile cap located below the water elevation. Stream pressure effects include stream currents and waves, and floating debris.
<b>WL</b>	Wind on live load	These loads are the wind force effects on live loads. The WL force should only be applied to portions of the structure that add to the force effect being investigated.

**Table 8-3 (Continued), Transient Load Descriptions  
(Modified from AASHTO LRFD Specifications (2017) and Wilson, et al. (2007))**

<b>WS</b>	Wind load on structure	<p>These loads are the wind force effects of horizontal wind pressure on the structure. The effects of vertical wind pressure on the underside of bridges due to an interruption of the horizontal flow of air and the effects of aero-elastic instability represent special load conditions that are typically taken into account for long-span bridges. For small and/or low structures, wind loading does not usually govern the design. However, for large and/or tall bridges, wind loading can govern the design and should be investigated.</p> <p>Where wind loading is important, the wind pressure should be evaluated from 2 or more different directions for the windward (facing the wind), leeward (facing away from the wind), and side pressures to determine which produce the most critical loads on the structure.</p>
-----------	------------------------	---

## 8.5 LOAD COMBINATION LIMIT STATES

The limit states are subdivided based on consideration of applicable load. The design of foundations supporting bridge piers or abutments should consider all limit state loading conditions applicable to the structure being designed. A description of the load combination limit states that are used in geotechnical engineering is provided in Table 8-4. Most substructure designs will require the evaluation of foundation and structure performance at the Strength I and Service I limit states. These limit states are generally similar to evaluations of ultimate capacity and deformation behavior in ASD, respectively.

**Table 8-4, Load Combination Limit State Considerations  
(Modified from Wilson, et al. (2007))**

Load Combination Limit State	Load Combination Considerations
<b>Strength I</b>	Basic load combination relating to the normal vehicular use of the bridge without wind.
<b>Strength II</b>	Load combination relating to the use of the bridge by Owner-specified special design vehicles and/or evaluation permit vehicles, without wind.
<b>Strength III</b>	Load combination relating to the bridge exposed to wind velocity exceeding 55 mph without live loads.
<b>Strength IV</b>	Load combination relating to very high dead load to live load force effect ratios in the bridge substructures exceeding about 7.0 (e.g., for spans greater than 250 ft.).
<b>Strength V</b>	Load combination relating to normal vehicular use of the bridge with wind velocity of 55 mph.
<b>Extreme Event I</b>	Load combination including the effects of the design earthquakes. South Carolina uses 2 design earthquakes (SEE and FEE).
<b>Extreme Event II</b>	Load combination relating to collision by vessels and vehicles, check flood (500-year flow event), and certain hydraulic events.
<b>Service I</b>	Load combination relating to the normal operational use of the bridge with 55 mph wind.

### 8.6 LOAD MODIFIERS

AASHTO LRFD methodology allows each factored load to be adjusted by a load modifier,  $\eta_i$ . This load modifier,  $\eta_i$ , accounts for the combined effects of ductility,  $\eta_D$ , redundancy,  $\eta_R$ , and operational importance,  $\eta_I$ . In geotechnical design load modifiers are not used to account for the influence of ductility, redundancy, and operational importance on structure performance. The influences of redundancy and operational importance have been incorporated into the selection of the geotechnical resistance factors. Therefore, a load modifier of 1.0 shall be used by the SCDOT for all geotechnical engineering analyses.

### 8.7 LOAD COMBINATION AND LOAD FACTORS

Load factors vary for different load types and limit states to reflect either the certainty with which the load can be estimated or the importance of each load category for a particular limit state. Table 8-5 provides load combinations and appropriate load factors to be used on SCDOT geotechnical designs. This table is based on the AASHTO LRFD Specifications.

These load factors apply only to geotechnical structures. For bridges and structures located along roadways, the SEOR is responsible for evaluating the load combinations and load factors and providing the loads to the geotechnical engineers for analyses. For geotechnical structures, the GEOR will be responsible for determining the load combinations and load factors for their geotechnical structure (embankments, MSE walls-external stability, reinforced slopes, etc.). Some analytical methods have not been calibrated for LRFD design methodology. Geotechnical analyses that have not been calibrated include, global stability analyses (static and seismic), and liquefaction induced geotechnical seismic hazards. For these analyses a load factor ( $\gamma$ ) of unity (1.0) shall be used.

**Table 8-5, Load Combination and Load Factors  
(Modified from AASHTO LRFD Specifications (2017))**

Load Combination Limit State	DC DD DW EH EV ES EL PS CR SH	LL IM CE BR PL LS	WA	WS	WL	FR	TU		TG	SE	<i>Note: Use Only One of These Load Types at a Time</i>				
							Min	Max							
							EQ	BL			IC	CT	CV		
<b>Strength I</b>	$\gamma_P$	1.75	1.00	----	----	1.00	0.50	1.20	$\gamma_{TG}$	$\gamma_{SE}$	----	----	----	----	----
<b>Strength II</b>	$\gamma_P$	1.35	1.00	----	----	1.00	0.50	1.20	$\gamma_{TG}$	$\gamma_{SE}$	----	----	----	----	----
<b>Strength III</b>	$\gamma_P$	----	1.00	1.00	----	1.00	0.50	1.20	$\gamma_{TG}$	$\gamma_{SE}$	----	----	----	----	----
<b>Strength IV</b>	$\gamma_P$	----	1.00	----	----	1.00	0.50	1.20	----	----	----	----	----	----	----
<b>Strength V</b>	$\gamma_P$	1.35	1.00	1.00	1.00	1.00	0.50	1.20	$\gamma_{TG}$	$\gamma_{SE}$	----	----	----	----	----
<b>Extreme Event I</b>	1.00	$\gamma_{EQ}$	1.00	----	----	1.00	----	----	----	----	1.00	----	----	----	----
<b>Extreme Event II</b>	1.00	0.50	1.00	----	----	1.00	----	----	----	----	----	1.00	1.00	1.00	1.00
<b>Service I</b>	1.00	1.00	1.00	1.00	1.00	1.00	1.00	1.20	$\gamma_{TG}$	$\gamma_{SE}$	----	----	----	----	----

Observations about the magnitude and relationship between various the load factors indicated in Table 8-5 are listed below:

- A load factor of 1.00 is used for all permanent and most transient loads for Service I.
- The live load factor for Strength I is greater than that for Strength II (i.e., 1.75 versus 1.35) because variability of live load is greater for normal vehicular traffic than for a permit vehicle.
- The live load factor for Strength I is greater than that for Strength V (i.e., 1.75 versus 1.35) because variability of live load is greater for normal vehicular use without wind than for a bridge subjected to a wind of 55 mph, and because less traffic is anticipated during design wind conditions.
- The live load factor for Strength III is zero because vehicular traffic is considered unstable and therefore unlikely under extreme wind conditions.

The load factor temperature gradient ( $\gamma_{TG}$ ) shall be selected by the SEOR in accordance with AASHTO LRFD Specifications or other governing design specifications. The load settlement factor ( $\gamma_{SE}$ ) should be selected on a project-specific basis, typically it is taken as  $\gamma_{SE} = 1.0$ . The blast load factor ( $\gamma_{BL}$ ) shall only be used as directed by the Department and is not anticipated being required in geotechnical design.

AASHTO requires that certain permanent loads and transient loads be factored using maximum and minimum load factors, as shown in Table 8-6. The concept of using maximum and minimum factored loads in geotechnical engineering can be associated with using these load factors (max. and min.) to achieve a load combination that produces the largest driving force and the smallest resisting force. Criteria for the application of the permanent load factors ( $\gamma_P$ ,  $\gamma_{EQ}$ ) are presented below:

- Load factors should be selected to produce the largest total factored force effect under investigation.
- Both maximum and minimum extremes should be investigated for each load combination.
- For load combinations where a force effect decreases the effect of another force, the minimum value should be applied to the load that reduces the force effect.
- The load factor that produces the more critical combination of permanent force effects should be selected from Table 8-6.
- If a permanent load increases the stability or load-carrying capacity of a structural component (e.g., load from soil backfill on the heel of a wall), the minimum value for that permanent load must also be investigated.

**Table 8-6, Load Factors for Permanent Loads,  $\gamma_p$   
(Modified from AASHTO LRFD Specifications (2017))**

Type of Load		Load Factor	
		Maximum	Minimum
<b>DC:</b> Component and Attachment		1.25	0.90
<b>DC:</b> Strength IV Only		1.50	0.90
<b>DD:</b> Downdrag on Deep Foundations	Driven Piles ( $\alpha$ (Tomlinson) Method)	1.40	0.25
	Driven Piles ( $\lambda$ Method)	1.05	0.30
	Drilled Shafts (O'Neill & Reese 2010 Method)	1.25	0.35
<b>DW:</b> Wearing Surface and Utilities		1.50	0.65
<b>EH:</b> Horizontal Earth Pressure	Active	1.50	0.90
	At-Rest	1.35	0.90
	Apparent Earth Pressure (AEP) for Anchored Walls	1.35	N/A
<b>EL:</b> Locked-in Erection Stresses		1.00	1.00
<b>EV:</b> Vertical Earth Pressures	Overall Stability	1.00	N/A
	Retaining Walls and Abutments	1.35	1.00
	Rigid Buried Structure	1.30	0.90
	Rigid Frames	1.35	0.90
	Flexible Buried Structures		
	Metal Box Culverts, Structural Plate Culverts with Deep Corrugations, and Fiberglass Culverts	1.50	0.90
	Thermoplastic Culverts	1.30	0.90
	All Others	1.95	0.90
<b>ES:</b> Earth Surcharge		1.50	0.75

The load factors for downdrag loads (DD) are specific to the method used to compute the load. Only maximum load factors for permanent loads ( $\gamma_p$ ) are applicable for downdrag loads (DD), these represent the uncertainty in accurately estimating downdrag loads on piles. If the downdrag load acts to resist a permanent uplift force effect, the minimum load factor will be utilized.

Typically in South Carolina the earthquake load factor ( $\gamma_{EQ}$ ) used in Extreme Event I (EE I) live load combinations is 0.0, unless otherwise determined by the Department.

Typical transient loads used to design geotechnical structures for pedestrian live loads (PL), and live load surcharge (LS) shall be computed using the values indicated in Table 8-7. When traffic live loads (LL) are necessary, the AASHTO LRFD Specifications shall be used.

**Table 8-7, Uniform Surcharge Pressures**

Material Description		Uniform Pressure (psf)
<b>PL:</b> Pedestrian Live Load	Sidewalk widths 2.0 ft or wider	75
	Bridge walkways or bicycle pathways	90
<b>LS<sup>(1)</sup></b> : Live load uniform surcharge at bridge abutments perpendicular to traffic Where $H_{abut}$ = Abutment Height	$H_{abut} \leq 5$ ft.	500
	$H_{abut} = 10$ ft. <sup>(3)</sup>	375
	$H_{abut} \geq 20$ ft.	250
<b>LS<sup>(1,2)</sup></b> : Live Load Surcharge on Retaining Walls Parallel To Traffic Where $H_{wall}$ = Wall Height and distance from back of wall = 0.0 ft.	$H_{wall} \leq 5$ ft.	625
	5 ft. < $H_{wall} \leq 20$ ft.	440
	$H_{wall} > 20$ ft.	250
<b>LS<sup>(1,2)</sup></b> : Live Load Surcharge on Retaining Walls Parallel To Traffic Where $H_{wall}$ = Wall Height and distance from back of wall $\geq 1.0$ ft	$H_{wall} \leq 5$ ft.	250
	5 ft. < $H_{wall} \leq 20$ ft.	250
	$H_{wall} > 20$ ft.	250
<b>LS<sup>(1)</sup></b> : Live Load Surcharge on embankments		250

<sup>(1)</sup> Uniform Pressure equal to  $\gamma_s h_{eq}$  as per AASHTO specifications distributed over the traffic lanes. Where the unit weight of the soil,  $\gamma_s$ , is taken as 125 pcf and the surcharge equivalent height is  $h_{eq}$ .

<sup>(2)</sup> Traffic lanes shall be assumed to extend up to the location of a physical barrier such as a guardrail. If no guardrail or other type of barrier exists, traffic shall be assumed to extend to the back of the wall.

<sup>(3)</sup> For abutment heights between 5 and 10 feet and 10 and 20 feet linearly interpolate uniform pressure.

Dead loads computed for components (DC), wearing surfaces and utilities (DW), and vertical earth pressures (EV) shall be computed using the unit weights of the materials. In the absence of specific unit weights of materials, the values indicated in Table 8-8 should be used.

**Table 8-8, Unit Weights of Common Materials  
(Modified from AASHTO LRFD Specifications (2017))**

Material Description		Unit Weight (pcf)
<b>Bituminous (AC) Wearing Surfaces</b>		140
<b>Steel</b>		490
<b>Wood</b>	Hard	60
	Soft	50
<b>Unreinforced Concrete<sup>(1)</sup></b>	Lightweight	110 - 135
	Normal Weight ( $f_c \leq 5.0$ ksi)	145
	Normal Weight ( $5.0 \text{ ksi} < f_c \leq 15.0 \text{ ksi}$ ) ( $f_c - \text{ksi}$ )	$140 + 0.001 * f_c$
<b>Soils (moist)</b>	Compacted Soils	120
	Very Loose to Loose Sand	100
	Medium to Dense Sand	125
	Dense to Very Dense Sand	130
	Very Soft to Soft Clay	110
	Medium Clay	118
	Stiff to Very Stiff Clay	125
<b>Rock</b>	Rolled Gravel or ballast	140
	Crushed Stone	95
	Gravel	100
	Weathered Rock (PWR)	155
	Basement Metamorphic or Igneous Rock	165
<b>Water</b>	Fresh	62.4
	Salt	64.0

<sup>1</sup> For reinforced concrete, add 5 pcf

## 8.8 LOAD COMBINATIONS AND FACTORS FOR CONSTRUCTION LOADS

In the design of geotechnical structures the GEOR must take into consideration potential construction loadings and sequence of construction into the design of geotechnical structures. When a construction method is specified, such as staged construction, and specialty ground improvement (prefabricated vertical drains (PVDs), surcharges, geosynthetic reinforcement, aggregate columns, etc.), or when temporary structures such as temporary MSE walls, sheet piling, etc. are designed, the Strength I limit state shall be used with the following modifications to the load factors. The maximum permanent load factor ( $\gamma_P$ ) for permanent loads DC and DW shall be at least 1.25 and the maximum load factor for transient loads LL, PL, and LS shall be at least 1.30. Construction plans and specifications of construction methods and temporary construction structures must include construction limitations and sequence of construction used in developing the design.

## 8.9 OPERATIONAL CLASSIFICATION

An Operational classification (OC) has been developed for all “typical” bridges on the South Carolina transportation system. “Typical” bridges are those bridges whose design is governed by the Seismic Specs. These classifications have been developed specifically for the South Carolina transportation system and are defined in the Seismic Specs. OC serves to assist in providing guidance as to the operational (i.e., the post-seismic event Service and Damage Level) requirements of the structure being designed as well as the design effort that will be required. The Performance Limits in Chapter 10 have been established for the various structures based on the OC. This is particularly evident when evaluating geotechnical earthquake engineering analyses/designs.



## 8.10 LRFD GEOTECHNICAL DESIGN AND ANALYSIS

The limit state that is selected for geotechnical engineering analyses/designs is dependent on the performance limit state and the probability of the loading condition. Guidance in selecting limit states for geotechnical analyses of Bridge Foundations, Embankments, and ERSs are provided in the following subsections.

### 8.10.1 Bridge Foundations

The design of foundations supporting bridge piers or abutments should consider all limit state loading conditions applicable. Strength limit states are used to evaluate a condition of total or partial collapse. The Strength limit state is typically evaluated in terms of shear or bending stress failure.

The Service limit state is typically evaluated in terms of excessive deformation in the forms of settlement, lateral displacement, or rotation. The Service II, III and IV limit states are used to evaluate specific critical structural components and are not generally applicable to foundation design.

The EE I limit state is used to evaluate seismic loadings and its effect on the bridge. The EE II limit state is used for the evaluation of vessel impact or vehicle impact and for the effect of the check flood on the bridge structure. The EE I limit state may control the design of foundations in seismically active areas. The EE II limit state may control the design of foundations or piers that may be exposed to vehicle or vessel impacts or may be exposed to the check flood (500-year flow event).

With respect to deformation, (i.e., horizontal deflection or settlement), the Service I limit state or the EE I limit state will control the design. Performance measures and the corresponding limit states for design of shallow foundations and deep foundations are provided in Tables 8-9 and 8-10, respectively.

Bridge foundation design for a given limit state shall take into account the change in foundation condition resulting from scour analyses.

- Strength – used to determine nominal resistance for axial stability and critical penetration depth for lateral stability (includes design (100-yr) flood scour);
- Service – used to determine displacements (includes design (100-yr) flood scour);
- Extreme Event I – used to determine axial resistance and lateral stability in seismic;
- Extreme Event II – 1) used to determine axial resistance and lateral stability for impact (vessel/vehicle) load, and 2) used to determine axial resistance and lateral stability for the check (500-yr) flood scour.

**Table 8-9, Shallow Foundation Limit States**

Performance Measure	Limit States		
	Strength	Service	Extreme Event
Soil Bearing Resistance	√		√
Sliding Frictional Resistance	√		√
Sliding Passive Resistance	√		√
Structural Capacity	√		√
Lateral Displacement		√	√
Vertical Settlement		√	√

**Table 8-10, Deep Foundation Limit States**

Performance Measure	Limit States		
	Strength	Service	Extreme Event
Axial Compression Load	√		√
Axial Uplift Load	√		√
Structural Capacity	√		√
Lateral Displacements		√	√
Settlement		√	√

### 8.10.2 Embankments

The predominant loads influencing the stability of an embankment are dead weight, earth pressure, and live load surcharge. According to Abu-Hejleh, et al. (2011):

Overall stability should be theoretically addressed under the Strength limit state because it is the shear strength that is being evaluated and the consequence of failure is global instability. However, it is investigated under the Service limit state (Article 11.6.2.3, *AASHTO LRFD Specifications quoted below*) because soil weight appears on both the load and resistance sides of the equation and the analytical consequence is complex.

AASHTO LRFD Specifications (2017) states:

The overall stability of the retaining wall, retained slope and foundation soil or rock shall be evaluated for all walls using limiting equilibrium methods of analysis. The overall stability of temporary cut slopes to facilitate construction shall also be evaluated....

The evaluation of overall stability of earth slopes (*embankments*) with or without a foundation unit should be investigated at the Service I Load Combination and an appropriate resistance factor.

The Service I limit state and the EE limit states will control the deformation and overall stability of the embankment design. When evaluating the embankment with respect to seismic loads, the EE I limit state is used; however, see Chapter 17 for no analysis condition requirements.

The EE I limit state may control the design in seismically active areas. All bridge embankments shall be designed for Service and EE limit states. Roadway embankments shall be designed for the Service limit state only. It is noted the vessel/vehicle impact loading of EE II shall not be used in the design of embankments.

- Service – used to determine the nominal stability of the slope (includes design (100-yr) flood scour);
- Extreme Event I – used to determine the stability of the slope in seismic events;
- Extreme Event II – used to determine the stability of the slope including the check (500-yr) flood scour

Both the SEE and FEE events shall be used in EE I design; however, if adequate resistance factors and displacements are achieved using the SEE EE I loads, then the GEOR may elect not to use the FEE event. The report shall indicate that the FEE event was not used and shall indicate why this event was not used. Performance measures and corresponding limit state for design of embankments are provided in Table 8-11.

**Table 8-11, Embankment Limit States**

Performance Measure	Limit States		
	Strength	Service	Extreme Event
Lateral Squeeze	√		√
Lateral Displacements		√	√
Vertical Settlement		√	√
Overall Stability		√	√

### 8.10.3 Earth Retaining Structures

The predominant loads influencing the stability of ERSs are dead weight, earth pressure, and live load surcharge. The Strength I and IV limit state load combinations have the largest dead, earth and live load factors and therefore control the design at the Strength limit state. The Strength limit state is evaluated for bearing, sliding, and overturning. The Service I limit state and the EE limit states will control the deformation performance limits for ERSs. When evaluating the ERSs with respect to seismic loads, the EE I limit state is used. The EE I limit state may control the design in more seismically active areas. All ERSs shall be designed for Strength, Service and EE limit states.

- Strength – used to determine nominal resistance for bearing, sliding (including frictional and passive) as well as structural capacity (includes design (100-yr) flood scour);
- Service – used to determine the nominal stability, the vertical and horizontal displacements (includes design (100-yr) flood scour);
- Extreme Event I – used to determine resistance for bearing, sliding (including frictional and passive) as well as structural capacity and the nominal stability, the vertical and horizontal displacements during seismic events
- Extreme Event II – used to determine the stability of the slope including the check (500-yr) flood scour

Both the SEE and FEE events shall be used in EE I design of ERSs located within the bridge embankment. The EE I design of ERSs located within the roadway embankment shall use the SEE only. It is noted that vehicular impact on ERSs is not used in slope stability analysis. Performance measures and corresponding limit states for design of earth retaining structures are provided in Table 8-12.

**Table 8-12, Earth Retaining Structures Limit States**

Performance Measure	Limit States		
	Strength	Service	Extreme Event
Soil Bearing Resistance	√		√
Sliding Frictional Resistance	√		√
Sliding Passive Resistance	√		√
Structural Capacity	√		√
Lateral Load Analysis (Lateral Displacements)		√	√
Settlement		√	√
Overall Stability		√	√

## 8.11 REFERENCES

Abu-Hejleh, N., DiMaggio, J. A., Kramer, W. M., Anderson, S., and Nichols, S., (2011), Implementation of LRFD Geotechnical Design for Bridge Foundations, (Publication No. FHWA NHI-10-039), National Highway Institute, Federal Highway Administration, US Department of Transportation, Washington, D.C.

American Association of State Highway and Transportation Officials, (2017), AASHTO LRFD Bridge Design Specifications, 8<sup>th</sup> Edition, American Association of State Highway and Transportation Officials, Washington, D.C.

NCHRP Project 20-7/31, (1986), "Development of Comprehensive Bridge Specifications and Commentary," National Cooperative Highway Research Program (NCHRP), August 1986.

South Carolina Department of Transportation, (2006), Bridge Design Manual, South Carolina Department of Transportation, [http://www.scdot.org/doing/structural\\_Bridge.aspx](http://www.scdot.org/doing/structural_Bridge.aspx).

South Carolina Department of Transportation, (2017), Seismic Design Specifications for Highway Bridges, South Carolina Department of Transportation, [http://www.scdot.org/doing/structural\\_Seismic.aspx](http://www.scdot.org/doing/structural_Seismic.aspx).

Wilson, K. E., Kimmerling, R. E., Goble, G. C., Sabatini, P. J., Zang, S. D., Zhou, J. Y., Amrhein, W. A., Bouscher, J. W., and Danaovich, L. J., (2007), LRFD for Highway Bridge Substructures and Earth Retaining Structures, (Publication No. FHWA-NHI-05-094) National Highway Institute, Federal Highway Administration, US Department of Transportation, Washington, D.C.

**Chapter 9**

**GEOTECHNICAL  
RESISTANCE FACTORS**

GEOTECHNICAL DESIGN MANUAL

*January 2019*



**Table of Contents**

<b><u>Section</u></b>	<b><u>Page</u></b>
9.1 Introduction .....	9-1
9.2 Soil Properties .....	9-2
9.3 Resistance Factors for LRFD Geotechnical design .....	9-2
9.4 Shallow Foundations .....	9-3
9.5 Deep Foundations .....	9-4
9.5.1 Driven Piles.....	9-5
9.5.2 Drilled Shafts .....	9-8
9.6 Embankments .....	9-9
9.7 Earth Retaining Structures.....	9-10
9.8 Reinforced Soil (Internal Stability).....	9-12
9.9 SSL Induced Geotechnical Seismic Hazards.....	9-13
9.10 References.....	9-13

**List of Tables**

<b><u>Title</u></b>	<b><u>Page</u></b>
Table 9-1, Resistance Factors for Shallow Foundations.....	9-4
Table 9-2, Geotechnical Resistance Factors for Driven Piles .....	9-7
Table 9-3, Number of Static Load Tests per Site .....	9-8
Table 9-4, Resistance Factor for Drilled Shafts .....	9-9
Table 9-5, Resistance Factors for Embankments (Fill / Cut Section).....	9-10
Table 9-6, Resistance Factors for Rigid Gravity Retaining Walls.....	9-11
Table 9-7, Resistance Factors for Flexible Gravity Retaining Walls.....	9-11
Table 9-8, Resistance Factors for Cantilever Retaining Walls .....	9-12
Table 9-9, Resistance Factors for Reinforced Soils (Internal).....	9-13
Table 9-10, Resistance Factors for Soil Shear Strength Loss .....	9-13
Table 9-11, Resistance Factors for Soil SSL Induced Seismic Hazards.....	9-13



# CHAPTER 9

## GEOTECHNICAL RESISTANCE FACTORS

### 9.1 INTRODUCTION

As described in Chapter 8, Resistance Factors ( $\phi$ ) are used in LRFD design to account for the variability associated with the resistance side of the basic LRFD Equation.

$$Q \leq \phi R_n = R_r \quad \text{Equation 9-1}$$

Where,

- Q = Factored Load
- R<sub>r</sub> = Factored Resistance
- R<sub>n</sub> = Nominal Resistance (i.e., ultimate resistance)
- $\phi$  = Resistance Factor

AASHTO and FHWA have conducted studies to develop geotechnical Resistance Factors ( $\phi$ ) based on reliability theory that accounts for the uncertainties presented below:

- Accuracy of Prediction Models (Design Methodology)
- Site Characterization
- Reliability of material property measurements
- Material properties relative to location, direction, and time
- Material Resistance
- Sufficiency and applicability of sampling
- Soil Behavior
- Construction Effects on Designs

When insufficient statistical data was available, the studies performed a back-analysis of the geotechnical designs to obtain a resistance factor that maintains the current level of reliability that is inferred by the ASD design methodology using the appropriate Factors of Safety.

The LRFD geotechnical design philosophy and load factors for geotechnical engineering are provided in Chapter 8. The Performance Limits for the Service and Extreme Event limit states are provided in Chapter 10. The design methodology used in the application of the design criteria (load factors, resistance factors, and performance limits) is based on AASHTO design methodology with modifications/deviations as indicated in the following Chapters of this Manual:

- Chapter 12 – Geotechnical Seismic Analysis
- Chapter 13 – Geotechnical Seismic Hazards
- Chapter 14 – Geotechnical Seismic Design
- Chapter 15 – Shallow Foundations
- Chapter 16 – Deep Foundations
- Chapter 17 – Embankments
- Chapter 18 – Earth Retaining Structures
- Chapter 19 – Ground Improvement
- Chapter 20 – Geosynthetic Design
- Appendix C – MSE Walls
- Appendix D – Reinforced Soil Slopes

## 9.2 SOIL PROPERTIES

The geotechnical Resistance Factors ( $\phi$ ) provided in this Chapter are only appropriate when soil material properties are based on sampling/testing frequency and testing methods as defined in this Manual. Geotechnical designs and/or analyses should be performed after establishing a “site” based on the site variability with respect to the soil properties that most affect the design or geotechnical analysis. A site variability of “Medium” or lower shall be selected based on the requirements of Chapter 7.

Engineering judgment is important in the selection of soil properties but must be used judiciously in a manner that is consistent with the method used to develop the resistance factors and should not be used as a method to account for insufficient geotechnical information due to an inadequate subsurface investigation. As indicated above, the AASHTO resistance factors were developed by either reliability theory or by ASD back-calculation. LRFD resistance factors that were based on reliability theory were developed based on using “average” soil shear properties for each identified geologic unit. LRFD resistance factors that were developed based on a back-analysis of ASD design methodology should use the same method of selecting soil properties (lower bound, average, etc.) as previously used in ASD design. For further information into how the resistance factors were developed the AASHTO LRFD Specifications and supporting reference documents should be consulted.

When sufficient subsurface information is available, soil properties should be rationally selected and substantiated by the use of statistical analyses of the geotechnical data. To arbitrarily select conservative soil properties may invalidate the assumptions made in the development of LRFD resistance factors by accounting for uncertainties multiple times; therefore, producing geotechnical designs which are more conservative and consequently have higher costs than the ASD design methodology previously used. When limited amounts of subsurface information is available or the subsurface information is highly variable, it may not be possible to select an “average” soil property for design and a conservative selection of soil properties may be required so as to reduce the risk of poor performance of the structure being designed.

## 9.3 RESISTANCE FACTORS FOR LRFD GEOTECHNICAL DESIGN

The geotechnical Resistance Factors ( $\phi$ ) that are provided in this Chapter are distinguished by the type of geotechnical structure being designed as listed below:

- Shallow Foundations
- Deep Foundations
- Embankments
- Earth Retaining Structures
- Reinforced Earth Internal Stability

Resistance factors for the determination of SSL induced geotechnical earthquake hazards are also provided.

As indicated in Chapter 8, the Fatigue limit state is the only limit state that is not used in geotechnical analyses or designs. Geotechnical resistance factors are provided for the following limit state load combinations:

- Strength – This includes Strength I, II, III, IV, and V; includes the design flood (100-year flow event)
- Service – This includes Service I; includes the design flood (100-yr flow event)

- Extreme Event – This includes Extreme Event I (Seismic loadings) and Extreme Event II (Impact loadings and check flood (500-yr flow event))

Resistance factors are provided based on the type of analysis being performed and the method of determination. When resistance factors are not applicable to the limit state the term “N/A” has been used in the resistance factor tables included in this Chapter. The method of determination shall either be based on the method of construction control or the analytical method used in the design. For details of the analytical methods used in the design see the appropriate Chapters in this Manual.

Geotechnical analyses that have not been calibrated for LRFD design methodology include, global stability analyses (static and seismic), and SSL induced geotechnical earthquake hazards. The resistance factors ( $\phi$ ) provided for these analyses are the inverse of the Factor of Safety (1/FS) and consequently have the same margin of safety as previously used in ASD designs. For global stability, Equation 9-1 can be written as indicated below.

$$\frac{R_n}{Q} = \frac{\text{Resisting Forces}}{\text{Driving Forces}} = FS \geq \frac{1}{\phi} \quad \text{Equation 9-2}$$

Where,

- $R_n$  = Nominal Resistance (i.e., ultimate resistance)
- $Q$  = Factored Load (With load factor,  $\gamma = 1.0$ )
- FS = Factor of Safety
- $\phi$  = Resistance Factor

The geotechnical Resistance Factors ( $\phi$ ) provided in this Chapter have been selected by the SCDOT based on the standard-of-practice that is presented in this Manual, South Carolina geology, and local experience. Although statistical data combined with calibration have not been used to select regionally specific geotechnical resistance factors, the resistance factors presented in AASHTO and FHWA publications have been adjusted based on substantial successful experience to justify these values. The AASHTO LRFD Specifications should be consulted for any geotechnical resistance factors not provided in this Chapter. The PCS/GDS shall review the AASHTO LRFD geotechnical resistance factors that are not included in this Manual prior to use and shall provide acceptance.

## 9.4 SHALLOW FOUNDATIONS

Geotechnical Resistance Factors ( $\phi$ ) for shallow foundations have been modified slightly from those specified in the AASHTO LRFD Specifications. Resistance factors for shallow foundations are shown in Table 9-1. Resistance factors for bearing resistance are specified for soil and rock. Resistance factors for sliding are based on the materials at the sliding interface.

**Table 9-1, Resistance Factors for Shallow Foundations**

Performance Limit	Limit States		
	Strength	Service	Extreme Event
Soil Bearing Resistance (Soil)	0.45	N/A	1.00
Soil Bearing Resistance (Rock)	0.45	N/A	1.00
Sliding Frictional Resistance (Cast-in-place Concrete on Sand)	0.80	N/A	1.00
Sliding Frictional Resistance (Cast-in-place or Precast Concrete on Clay)	0.85	N/A	1.00
Sliding Frictional Resistance (Precast Concrete on Sand)	0.90	N/A	1.00
Sliding (Soil on Soil)	0.90	N/A	1.00
Sliding Passive Resistance (Soil)	0.50	N/A	1.00
Lateral Displacement	N/A	1.00	1.00
Vertical Settlement	N/A	1.00	1.00

## 9.5 DEEP FOUNDATIONS

The design of deep foundations requires that foundations supporting bridge piers or abutments consider all limit state loading conditions applicable to the structure being designed. In addition, deep foundations may also be used to support ancillary transportation structures such as overhead signs, light fixtures, noise walls or ground improvement methods. Deep foundations consist of driven piles, drilled piles, drilled shafts, continuous flight auger piles and micro-piles. Continuous flight auger piles and micro-piles are not used to support SCDOT bridge structures. The resistance factors provided in this Section shall be used for driven piles, drilled piles and drilled shafts regardless of the structure supported. See Chapter 16 for the design methodology for drilled piles. Drilled piles designed as driven piles shall use the driven pile resistance factors while drilled piles designed as drilled shafts shall use the drilled shaft resistance factors. Contact the PCS/GDS for resistance factors for continuous flight auger piles and micro-piles. SCDOT has deviated in its application of LRFD design of deep foundations as presented in the AASHTO LRFD Specifications. The deviations are a result of current design and construction practice, design policies, and experience obtained evaluating field load tests of driven piles and drilled shafts.

The resistance factors used to determine the nominal resistance for single piles or drilled shafts in axial compression or uplift shall be based on the method of deep foundation load resistance verification during construction. The foundation resistance verification will typically be conducted at Test Pile (non-production pile) locations or at Index Pile (production pile) locations. Foundation resistance verification may be required at any foundation that does not meet foundation installation criteria or whose load carrying resistance is in question. A description of deep foundation load resistance verification methods (wave equation, static load testing, including the Osterberg® cell; rapid load testing (i.e., Statnamic® testing); high strain load testing (i.e., dynamic testing using either PDA or Apple® testing) are presented in Chapters 16 and 24. All other resistance factors are based on the design methodology used for deep foundations presented in Chapter 16. The frequency of deep foundation load resistance verification is dependent on the Site Variability as defined in Chapter 7.

A very widely accepted method to verify the axial load resistance of deep foundations is the use of the static load testing either uni-directional or bi-directional (i.e., Osterberg® Cell). The resistance factor for bi-directional load testing methods shall be the same as for conventional static load tests indicated in Tables 9-2 and 9-4.

The rapid load testing method has been included as a method of verifying pile resistance due to its regional popularity and its economic advantages. The rapid load testing methodology is a relatively new load testing method compared to static load testing or dynamic testing and has yet to be included in the AASHTO LRFD Specifications. The Statnamic® load test is regarded as a rapid load testing method that induces a “fast push” on the deep foundation element. The load applied to the top of the foundation is applied dynamically although at a much slower rate as compared to dynamic testing (PDA). The analysis of the rapid load test data requires that the dynamic resistance from the soil be subtracted from the total load applied to obtain the static resistance. Regional experience using rapid load testing has shown that dynamic resistance is greater for friction piles/drilled shafts in cohesive soils and consequently the reliability of this method is less for this type of foundation. For friction piles/drilled shafts in cohesionless soils or end-bearing piles/drilled shafts on rock, IGM or dense sands the dynamic resistance is less and therefore the reliability of the rapid load testing method is better when compared to rapid load testing of friction piles/drilled shafts in cohesive soils. The method used to separate the dynamic resistance from the static resistance has not been nationally accepted (AASHTO) and the method’s reliability has not been independently verified.

SCDOT has conservatively assigned resistance factors for rapid load testing based on the limited regional practice. Since cohesive soils tend to produce higher dynamic resistances as compared to cohesionless soils, a lower reliability has been assumed for friction piles/drilled shafts installed in cohesive soils. No increases in resistance factors will be allowed when performing multiple rapid load tests within a “Site” as indicated in Table 9-4. In order to increase the resistance factors indicated in this Section, a full-scale static load test per “Site” will be required to calibrate the rapid load test method of analysis, with the approval of the PCS/GDS. The term “Site” is defined as indicated in Chapter 7.

For high strain load testing SCDOT uses (i.e., PDA or Apple®) to verify the capacity of either driven piles or drilled shafts. Typically the PDA is performed on driven piles, while the Apple® load test is performed on drilled shafts.

### **9.5.1 Driven Piles**

AASHTO LRFD Specifications for driven piles differentiate between the predicted nominal axial capacities ( $R_{nstatic}$ ) based on static analyses and the field verified pile capacities ( $R_n$ ) by applying different geotechnical Resistance Factors ( $\phi$ ) for each of these axial capacities. Upon review of the AASHTO LRFD Specifications recommended geotechnical Resistance Factors ( $\phi_{stat}$ ) for the static resistance prediction, it was observed that the AASHTO geotechnical Resistance Factors ( $\phi_{stat}$ ) inherently presume a substantial amount of uncertainty in the predicted nominal axial resistance with respect to the field verified pile resistance using either dynamic formula, dynamic analysis, or static load tests. This presumption of greater uncertainty of predicted values vs. field verified values is logical and has merit for a national specification but it does not take into account the regional experience of predicting pile capacities. SCDOT has observed that when using the nominal axial compression pile resistance design methods presented in this Manual that there is rarely a need to extend the pile lengths in the field because the required pile resistance is achieved during pile driving. Driven piles are typically installed in cohesionless soils where pile resistance is most likely underpredicted. It has been observed that the pile resistance methods predict fairly accurately when pile resistance verification is made using pile re-strikes with the Pile Driving Analyzer (PDA). Typically, pile lengths provided in the plans have sufficient length to achieve the required ultimate pile resistance at the end-of-driving or re-strikes when verified by wave equation, dynamic load testing (PDA), or static load tests.

SCDOT has elected to use resistance factors ( $\phi$ ) based on the construction pile resistance verification method required in the plans to predict the nominal axial capacities (static

determination of ultimate pile resistance) during design, which is used to select the number of piles and pile plan lengths.

Additional considerations that have gone into the selection of SCDOT geotechnical resistance factors are as follows:

- The definition of a “Site” is the same as presented in the AASHTO LRFD specifications with the exception that a “Site” cannot have a variability greater than “Medium”. If a “Site” classifies as a “High” variability, the “Site” shall be reduced in size to maintain a variability of “Low” or “Medium.” The Site Variability shall be determined as indicated in Chapter 7.
- Resistance factors are based on a Site Variability of “Low” or “Medium”
- When field load testing is used, a minimum of 1 test pile is required per “Site” and it is typically placed at the weakest location based on the subsurface soil investigation and design methodology.
- The Contractor’s pile installation plan is reviewed by SCDOT and the pile driving installation equipment is evaluated using the Wave Equation
- Wave Equation Analysis is used to verify the field pile resistance during pile driving. The Wave Equation is calibrated using signal matching (CAPWAP) with the dynamic testing results.
- When load tests are performed, the test pile installation is monitored with the Pile Driving Analyzer (PDA).
- All bridges, regardless of the OC, will be designed using the same geotechnical Resistance Factors to maintain the same level of variability.

Load modifiers presented in Chapter 8 are not used to account for the influence of redundancy in geotechnical foundation design. Redundancy in deep foundation design is taken into account by the selection of the geotechnical resistance factor. Non-redundant pile foundations are those foundations that have pile footings with less than 5 piles supporting a single column, or less than 5 piles in a pile bent. Otherwise the foundations are redundant.

A resistance factor of 1.0 should be used for soils encountered in scour zones or zones neglected in design when performing pile driveability evaluations or when determining the required driving resistance. A resistance factor 10 percent greater than that shown in Table 9-2 can be used for the pile tested, but shall not exceed a resistance factor of 0.80. Except for redundant piles in low and medium site variability conditions when 2 or more piles are statically tested, the resistance factors provided in Table 9-3 shall be used.

**Table 9-2, Geotechnical Resistance Factors for Driven Piles**

Analysis and Method of Determination	Limit States			
	Strength		Service	Extreme Event
	Redundant	Non-Redundant		
Nominal Resistance Single Pile in Axial Compression (soil) with Wave Equation <sup>(1)</sup>	0.50	0.40	N/A	1.00
Nominal Resistance Single Pile in Axial Compression (rock) with Wave Equation <sup>(1)</sup>	0.60	0.50	N/A	1.00
Nominal Resistance Single Pile in Axial Compression with High Strain Load Testing (PDA) and calibrated Wave Equation <sup>(2)</sup>	0.65	0.55	N/A	1.00
Nominal Resistance Single Pile in Axial Compression with Static Load Testing. Dynamic Monitoring (PDA) of test pile installation and calibrated Wave Equation <sup>(2,3)</sup> .	See Table 9-3		N/A	1.00
Nominal Resistance Single Pile in Axial Compression with Rapid Load Testing For Friction Piles. Dynamic Monitoring (PDA) of test pile installation and calibrated Wave Equation <sup>(2)</sup>	0.65	0.55	N/A	1.00
Nominal Resistance Single Pile in Axial Compression with Rapid Load Testing For End Bearing Piles in Rock or Very Dense Sand. Dynamic Monitoring (PDA) of test pile installation and calibrated Wave Equation <sup>(2)</sup> .	0.70	0.55	N/A	1.00
Pile Group Block Failure (Clay)	0.60	N/A	N/A	1.00
Nominal Resistance Single Pile in Axial Uplift Load with High Strain Load Testing (PDA) and calibrated Wave Equation <sup>(2)</sup>	0.50	0.40	N/A	0.80
Nominal Resistance Single Pile in Axial Uplift Load with Static Load Testing	0.60	0.50	N/A	0.80
Group Uplift Resistance	0.50	N/A	N/A	N/A
Single or Group Pile Lateral Load Geotechnical Analysis (Lateral Displacements)	1.00	1.00	1.00	1.00
Single or Group Pile Vertical Settlement	1.00	1.00	1.00	1.00
Pile Driveability – Geotechnical Analysis	1.00	1.00	N/A	N/A

<sup>(1)</sup> Applies only to factored loads less than or equal to 600 kips.

<sup>(2)</sup> Dynamic testing is required on at least 2 piles per pile type and per "site", but no less than 2 percent of the total production piles per pile type for each approved hammer type used.

<sup>(3)</sup> See Table 9-3 for number of static load testing required.

Dynamic testing is used to control the construction of pile foundations by verifying pile resistance (signal matching required - CAPWAP), calibrating wave equation inspector charts based on signal matching, and monitoring the pile driving hammer performance throughout the project.

All test and index piles should require dynamic testing to monitor pile installation. The number

of dynamic tests shall conform to the requirements of Note 2 to Table 9-2. Include an equal number of additional dynamic tests if restrikes are required for test piles or index piles. For bridges with more than 200 piles, a minimum 3.0 percent of the piles for “Sites” with “Low” variability or 6.0 percent of the piles for “Sites” with “Medium” variability should be included in the contract as test piles to allow for evaluation of poor or highly variable hammer performance or pile restrikes to verify pile resistance throughout the project. The additional dynamic testing of production piles shall be used uniformly throughout the “Site” for QC of the Contractor’s pile driving operations.

**Table 9-3, Number of Static Load Tests per Site**

Number of Static Load Tests per Site	Resistance Factor ( $\phi$ )			
	Low Site Variability		Medium Site Variability	
	Redundant	Non-Redundant	Redundant	Non-Redundant
1	0.80	0.65	0.70	0.60
2	0.90	0.70	0.75	0.65
3 or more	0.90	0.70	0.85	0.70

### 9.5.2 Drilled Shafts

Drilled shaft geotechnical resistance factors ( $\phi$ ) have been provided in Table 9-4. Resistance factors are provided for Clay, Sand, Rock, and IGM as well as dynamic, static and rapid load testing.

Additional considerations that have gone into the selection of SCDOT geotechnical resistance factors are as follows:

- The definition of a “Site” is provided in Chapter 7 of this Manual. A “Site” cannot have a variability greater than “Medium”. If a “Site” classifies as a “High” variability, the “Site” shall be reduced in size to maintain a variability of “Low” or “Medium.”
- Resistance factors are based on a site variability of “Low” or “Medium.”
- When field load testing is used, a minimum of 1 test shaft is required per “Site” and it is typically placed at the weakest location based on the subsurface soil investigation and design methodology.

As discussed in Chapter 8, load modifiers will not be used to account for the influence of redundancy in geotechnical foundation design. Redundancy in deep foundations is taken into account by the selection of the geotechnical resistance factor. Non-redundant foundations are those drilled shaft footings with 4 or less drilled shafts supporting a single column or individual drilled shafts supporting individual columns in a bent regardless of the number of columns in the bent. Drilled shaft footings with 5 or more drilled shafts are classified as redundant drilled shaft foundations. If the foundation is a hammerhead (1 shaft and 1 column per bent) reduce the non-redundant resistance factor by 20 percent.

Because drilled shaft capacities cannot be verified individually during construction (only drilled shaft installation monitoring), a single resistance factor will be provided on the plans for both redundant and non-redundant drilled shafts. No increases in resistance factors will be allowed when performing multiple load tests within a “Site” as indicated in Table 9-3. A resistance factor 10 percent greater than that shown in Table 9-4 can be used for the drilled shaft tested, but shall not exceed a resistance factor of 0.80.



**Table 9-4, Resistance Factor for Drilled Shafts**

Performance Limit			Limit States			
			Strength		Service	Extreme Event
			Redundant	Non-Redundant <sup>(1)</sup>		
Nominal Resistance Single Drilled Shaft in Axial Compression	Clay	Side	0.55	0.45	N/A	1.00
		Tip	0.50	0.40	N/A	1.00
	Sand	Side	0.65	0.55	N/A	1.00
		Tip	0.60	0.50	N/A	1.00
	IGM	Side	0.70	0.60	N/A	1.00
		Tip	0.65	0.55	N/A	1.00
	Rock	Side	0.60	0.50	N/A	1.00
		Tip	0.60	0.50	N/A	1.00
Nominal Resistance Single Drilled Shaft in Axial Compression with High Strain Load Testing			0.65	0.65	N/A	1.00
Nominal Resistance Single Drilled Shaft in Axial Compression with Static Load Testing			0.70	0.70	N/A	1.00
Nominal Resistance Single Drilled Shaft in Axial Compression with Rapid Load Testing.			0.65	0.65	N/A	1.00
Nominal Resistance Single Drilled Shaft in Axial Uplift Load (Side Resistance)	Clay	0.45	0.35	N/A	1.00	
	Sand	0.55	0.45	N/A	1.00	
	IGM	0.55	0.45	N/A	1.00	
	Rock	0.50	0.40	N/A	1.00	
Nominal Resistance Single Drilled Shaft in Axial Uplift with Static Load Testing			0.60	0.60	N/A	1.00
Drilled Shaft Group Block Failure (Clay)			0.55	N/A	N/A	1.00
Drilled Shaft Group Uplift Resistance			0.45	N/A	N/A	1.00
Single or Group Drilled Shaft Lateral Load Geotechnical Analysis (Structural Resistance)			1.00	1.00	1.00	1.00
Single or Group Drilled Shaft Lateral Load Geotechnical Analysis (Lateral Displacements)			1.00	1.00	1.00	1.00
Single or Group Drilled Shaft Vertical Settlement			1.00	1.00	1.00	1.00

<sup>(1)</sup> If foundation is a hammerhead (1 shaft and 1 column per bent) reduce the non-redundant resistance factor by 20 percent.

## 9.6 EMBANKMENTS

Geotechnical Resistance Factors ( $\phi$ ) for both bridge and roadway embankments (both unreinforced and reinforced) have been modified slightly from those specified in the AASHTO LRFD Specifications. Resistance factors for embankments (fill) sections and cut-sections are shown in Table 9-5. The  $\phi$  for temporary embankments is indicated in Table 9-5. The global stability resistance factors for the EE I limit state check includes the inertial effects (i.e., PGA) of the seismic event as determined in Chapter 12. Should the presence of soils that will undergo SSL be encountered on a site, see Section 9.9 for the required resistance factors. The GEOR should use engineering judgment to possibly lower the resistance factor for the possible

consequences of failure.

**Table 9-5, Resistance Factors for Embankments (Fill / Cut Section)**

Performance Limit	Limit States		
	Service		Extreme Event
	Temporary <sup>1</sup>	Perm.	
Lateral Squeeze	0.90	0.75	1.00
Lateral Displacement	1.00	1.00	1.00
Vertical Settlement	1.00	1.00	1.00
Global Stability Embankment (Fill)	0.90	0.75	1.00 <sup>2</sup>
Global Stability Cut Section	0.90	0.75	1.00 <sup>2</sup>

<sup>1</sup>Use if vertical staging is required or if temporary condition will exist.

<sup>2</sup>Global stability analyses for Extreme Event I limit state that have resistance factors greater than specified require a displacement analysis to determine if it meets the performance limits presented in Chapter 10.

## 9.7 EARTH RETAINING STRUCTURES

Geotechnical Resistance Factors ( $\phi$ ) for ERSs have been modified slightly from those specified in the AASHTO LRFD Specifications by varying resistance factors based on the retaining wall system type. Resistance factors are provided for external stability of the structure with respect to bearing, sliding, and passive resistance. Resistance factors for bearing resistance are specified for soil and rock. Resistance factors for sliding are based on the materials at the sliding interface. The  $\phi$  provide in Tables 9-6 and 9-7 may require modification downward for both the Service and the EE limit states depending on what the ERS is supporting (i.e., a building or bridge (supported on shallow foundations)). For  $\phi$  due to internal stability of Mechanically Stabilized Earth (MSE) walls see Section 9.8. Resistance factors for Rigid Gravity Retaining Walls are provided in Table 9-6; Flexible Gravity Retaining Walls are provided in Table 9-7 and Cantilever Retaining Walls with or without anchors are provided in Table 9-8. The  $\phi$  provided in these tables apply to both permanent and temporary ERSs. The use of rigid gravity ERSs as temporary ERSs is not anticipated; therefore,  $\phi$  will not be provided. The global stability resistance factors for the EE I limit state check include the inertial effects (i.e., PGA) of the seismic event as determined in Chapter 12. Should the presence of soils that will undergo SSL be encountered on a site, see Section 9.9 for the required resistance factors. The GEOR should use engineering judgment to lower the resistance factor for the possible consequences of failure.

Rigid gravity retaining walls include cast-in-place concrete walls typically used in roadway projects. Flexible gravity retaining wall systems include bin walls; panel and block face MSE walls. Cantilever walls include sheet pile walls and soldier pile walls.

**Table 9-6, Resistance Factors for Rigid Gravity Retaining Walls**

Performance Limit	Limit States		
	Strength	Service	Extreme Event
Soil Bearing Resistance (Soil)	0.55	N/A	1.00
Soil Bearing Resistance (Rock)	0.55	N/A	1.00
Sliding Frictional Resistance (Cast-in-place Concrete on Sand)	1.00	N/A	1.00
Sliding Frictional Resistance (Cast-in-place or Precast Concrete on Clay)	1.00	N/A	1.00
Sliding Frictional Resistance (Precast Concrete on Sand)	1.00	N/A	1.00
Lateral Squeeze	N/A	0.75	1.00
Lateral Displacement	N/A	1.00	1.00
Vertical Settlement	N/A	1.00	1.00
Global Stability Fill Walls	N/A	0.75	1.00 <sup>1</sup>
Global Stability Cut Walls	N/A	0.75	1.00 <sup>1</sup>

<sup>1</sup>Global stability analyses for Extreme Event I limit state that have resistance factors greater than specified require a displacement analysis to determine if it meets the performance limits presented in Chapter 10.

**Table 9-7, Resistance Factors for Flexible Gravity Retaining Walls**

Performance Limit	Limit States			
	Strength	Service		Extreme Event
		Temporary <sup>1</sup>	Perm.	
Soil Bearing Resistance (Soil)	0.65	N/A	N/A	1.00
Soil Bearing Resistance (Rock)	0.65	N/A	N/A	1.00
Sliding Frictional Resistance	0.90	N/A	N/A	1.00
Lateral Squeeze	N/A	0.80	0.75	1.00
Lateral Displacement	N/A	1.00	1.00	1.00
Vertical Settlement	N/A	1.00	1.00	1.00
Global Stability Fill Walls	N/A	0.80	0.75	1.00 <sup>2</sup>
Global Stability Cut Walls	N/A	0.80	0.75	1.00 <sup>2</sup>

<sup>1</sup>Use if vertical staging is required or if temporary condition will exist.

<sup>2</sup>Global stability analyses for Extreme Event I limit state that have resistance factors greater than specified require a displacement analysis to determine if it meets the performance limits presented in Chapter 10.

**Table 9-8, Resistance Factors for Cantilever Retaining Walls**

Performance Limit	Limit States			
	Strength	Service		Extreme Event
Axial Compressive Resistance of Vertical Elements	Sections 9.4 and 9.5 Apply			
Passive Resistance of Vertical Element	0.75	N/A		0.85
Flexural Resistance of Vertical Element	0.90	N/A		0.90
Tensile Resistance of Anchor <sup>(1)</sup>	Mild Steel (ASTM A615)	N/A	0.900 <sup>1</sup>	
	High Strength Steel (ASTM A722)		0.80 <sup>1</sup>	
Pullout Resistance of Anchors <sup>(2)</sup>	Sand and Silts	N/A	0.65 <sup>2</sup>	
	Clay		0.70 <sup>2</sup>	
	Rock		0.50 <sup>2</sup>	
Anchor Pullout Resistance Test <sup>(3)</sup> (With proof test of every production anchor)	N/A	1.00 <sup>3</sup>		1.00 <sup>3</sup>
		<b>Temporary<sup>4</sup></b>	<b>Final</b>	
Lateral Displacement	N/A	1.00	1.00	1.00
Vertical Settlement	N/A	1.00	1.00	1.00
Global Stability Fill Walls	N/A	0.80	0.75	1.00 <sup>5</sup>
Global Stability Cut Walls	N/A	0.80	0.75	1.00 <sup>5</sup>

<sup>1</sup>Apply to maximum proof test load for the anchor. For mild steel apply resistance factor to  $F_y$ . For high-strength steel apply the resistance factor to guaranteed ultimate tensile strength.

<sup>2</sup>Apply to presumptive ultimate unit bond stresses for preliminary design only. See AASHTO LRFD (C11.9.4.2) specifications for additional information.

<sup>3</sup>Apply where proof tests are conducted on every production anchor to load of 1.0 or greater times the factored load on the anchor.

<sup>4</sup>Use if vertical staging is required or if temporary condition will exist.

<sup>5</sup>Global stability analyses for Extreme Event I limit state that have resistance factors greater than specified require a displacement analysis to determine if it meets the performance limits presented in Chapter 10.

## 9.8 REINFORCED SOIL (INTERNAL STABILITY)

Geotechnical Resistance Factors ( $\phi$ ) for analysis of internal stability of reinforced soils are based on AASHTO LRFD Specifications. Resistance factors for internal stability of reinforced soils are shown in Table 9-9. Resistance factors may be used in reinforced soil slopes or MSE walls. The external stability of MSE walls shall be governed by the resistance factors provided for flexible walls in Table 9-7. The external stability of RSSs with slopes less than 70° shall be governed by the resistance factors provided for embankments in Table 9-5.

**Table 9-9, Resistance Factors for Reinforced Soils (Internal)**

Performance Limit		Limit States		
		Strength	Service	Extreme Event
Tensile Resistance of Metallic Reinforcement and Connectors <sup>(1)</sup>	Strip Reinforcement	0.75	N/A	1.00
	Grid Reinforcement <sup>(2)</sup>	0.65		0.85
Tensile Resistance of Geosynthetic Reinforcement And Connectors		0.90	N/A	1.20
Pullout Resistance of Tensile Reinforcement		0.90	N/A	1.20

<sup>1</sup>Apply to gross cross-section less sacrificial area. For sections with holes, reduce the gross area and apply to net section less sacrificial area.

<sup>2</sup>Applies to grid reinforcements connected to a rigid facing element (concrete panel or block). For grid reinforcements connected to a flexible facing mat or which are continuous with the facing mat, use the resistance factor for strip reinforcements.

## 9.9 SSL INDUCED GEOTECHNICAL SEISMIC HAZARDS

Geotechnical Resistance Factors ( $\phi$ ) for SSL and SSL induced geotechnical seismic hazards are provided in Tables 9-10 and 9-11. Resistance factors for other seismic hazards that are not SSL induced (i.e., seismic slope stability, lateral foundation displacements, downdrag on deep foundations, etc.) are addressed under the Extreme Event limit state for each specific structure. These resistance factors apply only to the EE I limit state and either SSL (Table 9-10) or SSL induced geotechnical seismic hazards (Table 9-11).

**Table 9-10, Resistance Factors for Soil Shear Strength Loss**

Seismic Hazard Description	Resistance Factor Symbol $\phi$	Extreme Event I
Sand-Like Soil Shear Strength Loss (Liquefaction) (Triggering)	$\phi_{SL-Sand}$	0.90
Clay-Like Soil Shear Strength Loss (Triggering)	$\phi_{SL-Clay}$	0.90

Flow failure is the global instability induced by SSL beneath an embankment or ERS without the effect of the inertial loading. Seismic instability is the combination of SSL beneath an embankment or ERS with the effect of inertial loading. Both of these checks are for sites that have undergone SSL.

**Table 9-11, Resistance Factors for Soil SSL Induced Seismic Hazards**

Seismic Hazard Description	Resistance Factor Symbol $\phi$	Extreme Event I
Flow Failure (Triggering)	$\phi_{Flow}$	1.00
Seismic Instability	$\phi_{EQ-Stability}$	1.00

## 9.10 REFERENCES

American Association of State Highway and Transportation Officials, (2017), AASHTO LRFD Bridge Design Specifications Customary U.S. Units, 8<sup>th</sup> Edition, American Association of State Highway and Transportation Officials, Washington, D.C.

South Carolina Department of Transportation, (2006), Bridge Design Manual, South Carolina Department of Transportation, <https://www.scdot.org/business/structural-design.aspx>.

South Carolina Department of Transportation, (2008), Seismic Design Specifications for Highway Bridges, South Carolina Department of Transportation, <https://www.scdot.org/business/structural-design.aspx>.

**Chapter 10**  
**GEOTECHNICAL**  
**PERFORMANCE LIMITS**

**GEOTECHNICAL DESIGN MANUAL**

*January 2019*





**Table of Contents**

<b><u>Section</u></b>	<b><u>Page</u></b>
10.1 Introduction.....	10-1
10.2 Performance Objectives.....	10-2
10.2.1 General .....	10-2
10.2.2 Service Limit State Performance Objectives.....	10-3
10.2.3 Extreme Event Limit State Performance Objectives .....	10-3
10.3 Performance Limits.....	10-4
10.4 Deformations .....	10-6
10.5 Global Instability Deformations .....	10-6
10.6 Embankment Deformations .....	10-11
10.6.1 Embankment Terminology and Deformation Notations.....	10-11
10.6.2 Embankment Settlement.....	10-12
10.6.3 Embankment Widening Differential Settlements.....	10-15
10.6.4 Embankment/Bridge Transition Settlement .....	10-17
10.7 Earth Retaining Structure Deformations.....	10-18
10.7.1 Earth Retaining Structure Terminology and Deformation Notations...	10-18
10.7.2 Settlement Deformation – Longitudinal.....	10-20
10.7.3 Settlement Deformation – Transverse .....	10-22
10.7.4 Lateral Displacements.....	10-25
10.8 Performance Limits for Global Instability.....	10-26
10.8.1 Service Limit State .....	10-26
10.8.2 Extreme Event I Limit State.....	10-26
10.8.3 Extreme Event II Limit State.....	10-27
10.9 Performance Limits For Embankments .....	10-27
10.9.1 Service Limit State .....	10-27
10.9.2 Extreme Event I Limit State.....	10-28
10.9.3 Extreme Event II Limit State.....	10-29
10.10 Performance Limits For Earth Retaining Structures .....	10-30
10.10.1 Service Limit State .....	10-30
10.10.2 Extreme Event I Limit State.....	10-33
10.10.3 Extreme Event II Limit State.....	10-33
10.11 References .....	10-34

**List of Tables**

<b><u>Table</u></b>	<b><u>Page</u></b>
Table 10-1, Global Instability Deformations Performance Limits.....	10-7
Table 10-2, Embankment Deformation Notations .....	10-11
Table 10-3, Embankment Settlement Performance Limits .....	10-13
Table 10-4, Embankment Widening Settlement Performance Limits .....	10-16
Table 10-5, Bridge/Embankment Transition Settlement Performance Limits .....	10-17
Table 10-6, Fill – Earth Retaining Structures (ERS) .....	10-19
Table 10-7, Cut – Earth Retaining Structures (ERS).....	10-19
Table 10-8, ERS Deformation Notations.....	10-19
Table 10-9, ERS Settlement (Longitudinal) Performance Limits .....	10-21
Table 10-10, ERS Settlement (Transverse) Performance Limits .....	10-23
Table 10-11, ERS Lateral Performance Limits.....	10-25
Table 10-12, Embankment (Pavement) Performance Limits.....	10-28
Table 10-13, Embankment Widening Performance Limits .....	10-28
Table 10-14, Bridge/Embankment Transition Settlement Performance Limit .....	10-28
Table 10-15, Bridge/Embankment Transition Settlement Performance Limit .....	10-29
Table 10-16, Fill ERS Performance Limits at Service Limit State.....	10-31
Table 10-17, Cut ERS Performance Limits at Service Limit State.....	10-32

**List of Figures**

<b>Figure</b>	<b>Page</b>
Figure 10-1, Front Slope Definition.....	10-7
Figure 10-2, Embankment Circular Instability at Bridge End Bent.....	10-8
Figure 10-3, Embankment Sliding Block Instability at Bridge End Bent .....	10-8
Figure 10-4, Embankment Circular Arc Instability.....	10-9
Figure 10-5, Embankment Sliding Block Instability .....	10-9
Figure 10-6, ERS Global Instability.....	10-10
Figure 10-7, ERS Circular-Arc Instability (Section B-B) .....	10-10
Figure 10-8, ERS Sliding-Wedge Instability (Section B-B).....	10-11
Figure 10-9, Embankment Settlement (Section A–A) .....	10-13
Figure 10-10, Divided Highway (Section A-A).....	10-14
Figure 10-11, Embankment Settlement Profile .....	10-15
Figure 10-12, Embankment Widening Settlement (Section A-A) .....	10-16
Figure 10-13, Bridge-Embankment Transition Settlement with Approach Slab .....	10-17
Figure 10-14, Bridge-Embankment Transition Settlement without Approach Slab ....	10-18
Figure 10-15, ERS Settlement (Section B–B).....	10-21
Figure 10-16, ERS Settlement Profile.....	10-22
Figure 10-17, ERS Reinforced Soils - Transverse Differential Settlement .....	10-24
Figure 10-18, ERS Tieback Anchor - Transverse Differential Settlement.....	10-24
Figure 10-19, ERS Lateral Deformation (Section C-C) .....	10-25
Figure 10-20, ERS Lateral Deformations.....	10-26



# CHAPTER 10

## GEOTECHNICAL PERFORMANCE LIMITS

### 10.1 INTRODUCTION

LRFD incorporates the use of limit states as a condition beyond which a component/member or foundation of a structure ceases to satisfy the provisions for which it was designed. The Strength, Service and Extreme Event limit states have design boundary conditions for structural performance that account for some acceptable measure of structural movement throughout the structure's design life. The performance limits for geotechnical structures such as embankments and ERSs are presented in this Chapter. Although performance limits for bridge foundations are not presented, the determination of the settlement of bridge foundations is required and shall be reported to the SEOR, who will determine if the structure is capable of withstanding these deformations.

The design of embankments shall include consideration for the performance of the pavements as well as any structure located within the embankments (i.e., culverts, pipes, and ERSs). No performance objectives or limits have been established for hydraulic structures (i.e., culverts and pipes). The acceptable performance of a hydraulic structure is based on the integrity of the structure and the ability of the structure to continue to function as designed (i.e., convey water from one side of the embankment to the other). Therefore, the GEOR shall report anticipated deformations (i.e., total and differential settlement, etc.) to both the SEOR as well as the HEOR. It is the responsibility of these designers (i.e., SEOR and HEOR) to determine if the hydraulic structure will perform as designed given the anticipated deformations.

Performance limits are based on the design life of the structure. For bridge structures the design life shall be 75 years, as established by AASHTO LRFD Specifications, and for other non-bridge elements (embankments and ERSs) the design life shall be 100 years. However, it is noted that the typical design life for pavements is 20 years and that this life shall be used in the determining the amount and acceptable rate of deformation for embankments. Structures that cannot be replaced without significant expense or that may be subject to structural distress due to environmental conditions (corrosion, biological degradation, etc.) may have a design life that exceeds the typical design life. The structural performance under Strength, Service and Extreme Event loads are typically expressed in terms of settlement, settlement rate, differential settlement, vertical displacement, lateral displacements, rotations, etc.

The LRFD geotechnical design philosophy and the load factors,  $\gamma$ , for geotechnical engineering are provided in Chapter 8. The geotechnical resistance factors,  $\phi$ , for the Strength, Service, and Extreme Event limit states are provided in Chapter 9. The design methodology to analyze structure performance shall be in accordance with AASHTO design methodology with modifications/deviations as indicated in the appropriate Chapters of this Manual. The load and resistance factors provided in this Manual shall be used. These factors were considered in the selection of the performance limits established in this Chapter.

## 10.2 PERFORMANCE OBJECTIVES

### 10.2.1 General

Transportation structures are typically thought of as being rigid and stationary, but in reality they deform throughout their service life due to various physical (loads) and environmental (temperature, degradation, etc.) conditions exerted on the structures. The deformations range from the elastic range where no permanent deformations remain after unloading, to the plastic range where deformations become permanent even after unloading, and finally to rupture where the material is permanently severed and collapse is imminent. The types of loadings that cause these deformations are discussed in Chapter 8. The deformations experienced by geotechnical structures are typically non-linear, dependent on subsurface site variability, influenced by environmental factors, and are highly dependent on soil-structure interaction due to strain compatibility (stiffness) between soil, aggregates (stone, gravel, etc.), soil reinforcements/anchors (steel or geosynthetic), and reinforced concrete, steel, etc. Soils are considerably more compressible, have essentially no tensile strength, and have shear strengths that occur at considerably larger displacements than occur in most typical structural elements. Unlike concrete and steel, soil properties are highly variable. Soils found in-place may vary significantly over short distances both vertically and horizontally because soil composition and properties are based on geologic mechanisms. When soils are engineered through material selection and construction control, soil variability in composition and density can still occur as a result of the non-uniformity of the material stockpile, weather, and construction.

Performance Limits are the result of first establishing Performance Objectives for typical structures used by SCDOT such as embankments, ERSs, bridge and hydraulic structures. Performance Objectives should be established by the design team based on guidelines established by SCDOT for each limit state the structure is being designed for. Once the Performance Objectives are established, the design team should establish Performance Limits for each structure to meet the level of functionality defined by the objectives. These Performance Objectives and Performance Limits shall have the concurrence and acceptance of the PC/SDS and the PC/GDS. This Chapter provides the Performance Objectives and Performance Limits for embankments and ERSs. The Performance Objectives and Performance Limits for bridge structures at the Strength, Service or Extreme Event limit states shall be developed by the SEOR on a project specific basis. The Performance Objectives and Performance Limits for hydraulic structures including 3-sided culverts, concrete box culverts, pipes, etc. at the Service or Extreme Event limit states shall be developed on a project specific basis by the SEOR and HEOR (see Section 10.1). When evaluating the performance of hydraulic structures, consideration of adjacent structures such as Embankments (Section 10.8) or ERSs (Section 10.9) shall be given since the Performance Objectives and Performance Limits of these geotechnical structures may not be compatible with the requirements for hydraulic structures.

The Performance Objectives define the level of functionality of the structure for the limit state loading condition being evaluated. Performance Objectives are based on:

- Limit State: Service I limit state or Extreme Event limit state load combinations defined in Chapter 8.
- Operational Classification: Bridge OC (see Seismic Specs).

Typically, there is no adjustment for variability in both the load and resistance portions of the analysis. The load ( $\gamma$ ) and resistance ( $\phi$ ) factors generally used in geotechnical analyses are unity (1.0) unless indicated otherwise in Chapters 8 and 9. When load factors greater than unity ( $\gamma > 1.0$ ) or resistance factors less than unity ( $\phi < 1.0$ ) are used, this is typically due to the variability or uncertainty associated with the load or resistance being computed. The design

intent is to analyze the most likely behavior of the structure when subjected to typical loadings for each limit state.

Temporary (i.e., having a life of less than 5 years) embankments and structures (e.g., temporary steepened slope, temporary ERSs, etc.) shall not be designed for the EE I limit state. Project specific Performance Objectives and Performance Limits for temporary embankments and structures at the Service limit state shall be based on whether the structure is critical or is support of excavation only (see Chapters 17 and 18). The design team shall determine whether a temporary embankment or structure is for excavation support only or is critical. In addition, the Performance Objectives and Performance Limits shall be established by the design team.

The Performance Objectives and Performance Limits for both permanent and temporary structures at the EE II (collision/impact loadings only) limit state are developed on a project specific basis by the design team. The Performance Objectives and Performance Limits for this limit state check shall be established by the design team and shall have the concurrence and acceptance of the PC/SDS and the PC/GDS. For the EE II (check flood (500-yr flow event)) limit state, stability shall be maintained (i.e., a resistance factor of 1.0 ( $\phi = 1.0$ ) shall be obtained from the analysis). See Chapters 15 through 18 for analysis procedures.

Development of Performance Objectives and Performance Limits for structures subjected to Service and Extreme Event loadings that are not included in this Chapter shall be developed by the design team on a project specific basis. These Performance Objectives and Performance Limits shall have the concurrence and acceptance of the PC/SDS and the PC/GDS.

### **10.2.2 Service Limit State Performance Objectives**

The Performance Objective for the Service limit state requires that, with standard SCDOT maintenance, the structure remains fully functional to normal traffic for the design life of the structure. The performance of a structure under Service loads is influenced by many factors that may or may not be within the designer's control. Provided in Appendix K is a list of considerations that may influence the performance of the structure over its design life Service limit state.

### **10.2.3 Extreme Event Limit State Performance Objectives**

The Extreme Event limit states (EE I and EE II) are load combinations that are typically in excess of the Service limit state loadings and may also be in excess of the Strength limit state. The loadings from these Extreme Events are typically the result of seismic events or the check flood (500-yr flow event) or collisions from ships, barges, or vehicles. The Extreme Event limit states have the potential to cause damage to a structure and impact the structure's functionality. Even though Extreme Event limit states typically have a low probability of occurring within the design life of the structure, these limit state loadings must be evaluated since the potential for loss of life and loss of service of the structure can be significant. Because the probability of these events occurring is relatively low, a lower safety margin is used and performance limits are less rigid than those for the Service limit state. The damage resulting from these Extreme Event loading conditions may be significant enough to warrant replacement of the structure, but the bridges should have a low probability of collapse due to seismic motions.

The Performance Objectives for the Extreme Event limit state of a structure are defined by selecting an appropriate Service Level and Damage Level for each component/member or foundation element being analyzed. For complex structures such as bridges and ERSs, performance objectives are first given to the overall structure and then component performance

objectives are given to the individual component/members or foundation of the structure. Although this approach is somewhat subjective at this time, it allows for a more methodical way of evaluating each component of the structure to assure that the component meets the overall performance objective of the complete structure. The Performance Objectives for the EE I limit state for bridges are provided in the Seismic Specs. The Performance Objectives and Performance Limits for bridges for the EE II should be established by the design team.

The Performance Objectives for the EE I limit state for bridge embankments and any ERSs located within the bridge embankment are that any movements shall conform to the Performance Objectives established for the bridge in the Seismic Specs and are based on the OC of the bridge as indicated in the Seismic Specs. It should be noted that certain slopes, embankments and ERSs do not require global stability analysis during the EE I limit state, see Chapters 13 (embankments) and 14 (ERSs) for these conditions.

The Service and Damage Level descriptions are provided in the Seismic Specs and are intended to apply to bridges, roadway structures and bridge embankments. Because soils found in-place and within embankments may significantly vary within short distances both vertically and horizontally due to South Carolina geology, it is difficult to associate closure time and degree of collapse along a continuous embankment. Generally, it is not economically feasible to entirely prevent failure of a roadway embankment due to a seismic event; however, a bridge embankment can and will be improved as required to prevent the collapse of the bridge. This should not be taken as to mean that movement of the bridge or embankment is not allowed, but that movement commiserate with the Performance Objective of the bridge is permitted. Observations from past earthquakes around the world indicate that embankment failures are isolated and discontinuous after a seismic event and the accessible area along the top of the embankment has for the most part remained traversable. Based on these observations, roadway embankments that are not designed for seismic events may still be traversable even though they may exhibit significant damage that may require repair.

The EE I limit state is a load combination that is associated with a design seismic event. SCDOT uses the design seismic events listed in the Seismic Specs. Additional information concerning the design seismic events can be found in Chapters 11 and 12. The Performance Objectives and seismic design requirements for bridges are provided in the latest edition of the Seismic Specs. While the Seismic Specs limit the applicability of the 2-level design (i.e., designing using both FEE and SEE) for bridges, all bridge embankments and ERSs located within bridge embankments shall be designed for both seismic events. ERSs located in roadway embankments shall be designed for the SEE only.

The EE II limit state is associated with vehicular or vessel collision/impact and certain hydraulic events including the check flood (500-year flow event). Project specific Performance Objectives and Performance Limits shall be determined by the design team and shall have the concurrence and acceptance of the PC/SDS and the PC/GDS for vehicular or vessel collision/impact as applicable to ERSs. The Performance Objectives for the check flood shall conform to the requirements contained in this Manual. EE II (collision/impact loadings only) limit state loadings shall not be considered in the design of embankments. However, the stability of an embankment shall be determined using the EE II (check flood (500-yr flow event)).

### **10.3 PERFORMANCE LIMITS**

The Performance Limits that are specified in this Manual are for new construction including embankment widenings required during staged bridge replacement, but do not apply to retrofitting or maintaining existing structures or embankments. For road or bridge embankments widened as part of either the widening of a road or the widening of an existing bridge, only the



Service limit state checks will be required. Performance Limits have been developed based on SCDOT design and construction standards of practice contained in this Manual, AASHTO LRFD Specifications, FHWA publications, BDM, Seismic Specs, and in accordance with SCDOT construction specifications and SCDOT experience. SCDOT reserves the right to modify these Performance Limits based on project specific requirements or as new research or additional experience becomes available.

The Performance Limits presented are based on the deformations that occur at the Service and EE limit states. The deformations determined at the Service limit state shall be compared to the Performance Limits contained in this Manual. If the deformations exceed the Performance Limits contained in this Manual, the GEOR shall consult with the design team to determine the impact of the deformations on the Performance Objectives. The design team shall make the determination of whether remediation is required or not. If remediation is not required the GEOR shall report the deformations and shall indicate that the design team has elected to not remediate the limit state as the Performance Objectives are still met. If remediation is required, both the SEOR and GEOR shall consider different remediation options and shall present the various options to the design team along with the anticipated cost of the remediation. The design team will select the most appropriate remediation to achieve the Performance Objectives of the project. This should include the longitudinal and transverse limits of remediation as well as the depth of remediation.

The EE limit state Performance Limits shall be considered a general guide and not a limit. The design team has the ultimate responsibility for determining performance of the project/structure during the design seismic event. The performance must meet the required Performance Objectives as described in the Seismic Specs. The design team has the responsibility to ensure that the Performance Limits are used judiciously so as not to place in jeopardy the Performance Objectives of the structure being designed. It is the GEOR's responsibility to present the geotechnical performance findings to the design team and to assist the design team in evaluating geotechnical and structural solutions for maintaining the structure's performance within the Performance Objectives and Performance Limits previously established by the design team. If the design team makes no comment concerning the geotechnical performance findings; the GEOR may assume the findings are acceptable and no remediation will be required.

The Performance Limits specified in this Chapter are specific to the type of structure being designed. The acceptable deformations specified are based on the structure's intended use as provided in the Service limit Performance Objectives for Embankments (Section 10.8) and Earth Retaining Structures (Section 10.9). Performance Limits may need to be adjusted for these structures based on any adjacent structures such as hydraulic structures, utilities (water, gas, electricity, phone, etc.), pavements, bridges, ERSs, signs, homes, buildings, etc. that may be impacted by the deformations that are deemed acceptable for the structures that are addressed in this Manual. For example, settlements that may be acceptable for an embankment may not be acceptable for an existing building within the influence of a roadway embankment. Another example where the Performance Limits provided may not be acceptable would be during global instability where deformations of an embankment may distress adjacent structures such as bridges, side ramps, or other structures beyond the Right-of-Way.

Performance Objectives and Performance Limits not covered in this Manual shall be determined by the design team and shall have the concurrence and acceptance of the PC/SDS and the PC/GDS. The design team will first establish Performance Objectives for the structure being analyzed. Once the Performance Objectives have been developed and accepted, Performance Limits shall be established that meet the Performance Objectives.

## 10.4 DEFORMATIONS

Deformations are specified in terms of vertical and lateral displacements, whereas Performance Limits are not to exceed deformations (i.e., acceptable displacements). Displacements can be a result of direct movements such as settlement of an embankment or as a result of rotations such as embankment instability or foundation rotations due to lateral loadings. Vertical displacements that occur in a downward direction (into the ground) are referred to as settlement. Specifying a Maximum Vertical Settlement (i.e., a Performance Limit) can help to control total settlements. Damage or poor performance of a structure most often occurs as a result of excessive differential displacements. An example of this would be a bridge with foundations supported by rock and with an approach embankment supported on very compressible soils. While the bridge would remain relatively stationary vertically, the approach embankment would settle substantially relative to the bridge. The vertical differential displacements would affect vehicle rideability and add structural loads to the abutment foundations as a result of downdrag on deep foundations. Specifying a Maximum Vertical Differential Settlement would help to control the differential vertical displacements that occur between the bridge abutment and the bridge approach embankment to an acceptable level of performance. There may be situations where vertical displacements act upward, due to heave or differential movements of a structure. This condition may cause part of the structure to move up when other parts of the structure move downward (settle). The Maximum Vertical Differential Displacement limits also control these upward and downward displacements to an acceptable level of performance.

Lateral displacements (horizontal movements) are identified as occurring in either the longitudinal or transverse directions. On bridges and roadways, the longitudinal direction is parallel to the centerline, while the transverse direction is perpendicular to the centerline. Unless otherwise indicated in the performance limit description, the lateral displacements do not have sign convention and may occur in either direction.

## 10.5 GLOBAL INSTABILITY DEFORMATIONS

Accepted design methodologies for evaluating the global stability of a structure at the Strength limit state are not currently available. Currently, global stability is evaluated at the Service limit state using appropriate resistance factors that provide for designs that are the equivalent of ASD. This method of evaluating global stability assumes that the driving and resisting forces are maintained in equilibrium within an appropriate safety margin and therefore no displacements occur. Embankments and ERSs at the Service limit state shall have global stability checked (Chapter 17); however, a specified resistance factor,  $\phi$  (margin of safety) against instability must be achieved (i.e., deformation of the embankment or ERS is not allowed). Therefore, there are no Performance Limits for global instability at the Service limit state for either embankments or ERSs. If the required resistance factor,  $\phi$ , is not achieved, then either ground improvement (see Chapter 19) will be required to maintain stability or the slope may be made flatter (i.e., decrease slope from 2H:1V to 3H:1V). Embankments and ERSs at the EE II (check flood (500-yr flow event)) limit state are required to just maintain stability (i.e.,  $\phi = 1.0$ ); therefore, just like at the Service limit state there are no Performance Limits.

The Performance Objectives for embankments and ERSs at EE I limit state is that neither the embankments nor the ERSs adversely affect the bridge structure during the design seismic event. Bridge embankments are defined in Chapter 2 and shall include any ERSs. ERSs beyond this longitudinal limit are discussed in the following paragraphs.

Global stability analysis shall be performed to determine the portion of the embankment (i.e., bridge embankment) that will have instability during the EE I limit state and that will directly

affect the bridge (i.e., typically the front slope, see Figure 10-1). Mitigation shall be limited longitudinally from the bridge to the point where the Global Performance Objectives of the Bridge System are met (see Seismic Specs). The embankment beyond this point is a roadway embankment and is not required to be seismically designed. ERSs not located within bridge embankments shall be designed for no collapse. These ERSs shall be designed to account for the surrounding area and shall be allowed to displace as necessary.

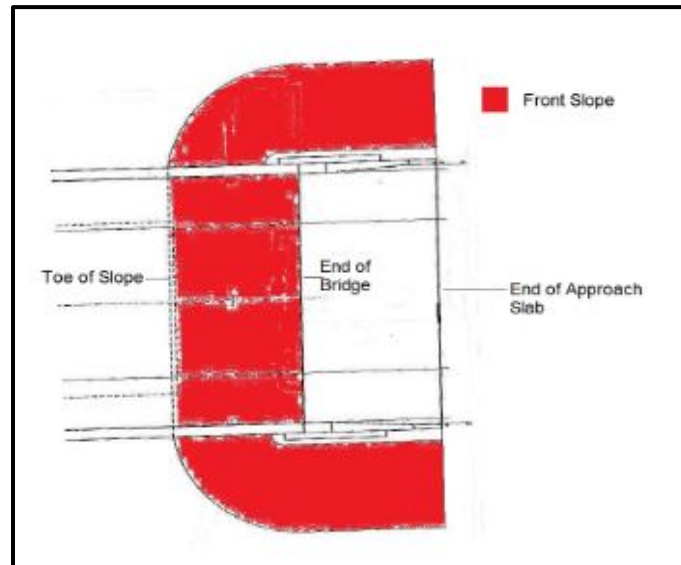


**Figure 10-1, Front Slope Definition**

Deformations can only occur when there is an imbalance of the driving and resisting forces within the earthen mass. Because the Performance Objectives for the EE I limit state permits an acceptable amount of deformation, global instability analyses and the subsequent deformation determination must be made for the EE I limit state. Embankment deformations associated with the EE I limit state (seismic loadings) include flow failure, seismic instability, and seismic settlement. Deformations associated with flow failure are assumed to exceed the Performance Limits for the EE I limit state and must be either mitigated or the bridge protected from the flow failure. In addition, flow failure also requires the presence of SSL at the project site. Methods of analyzing deformations due to seismic instability are provided in Chapter 13. Performance Limits for global instability have been developed that address these types of deformations and are identified in Table 10-1. The Performance Limits for seismic displacement are discussed in the following Section.

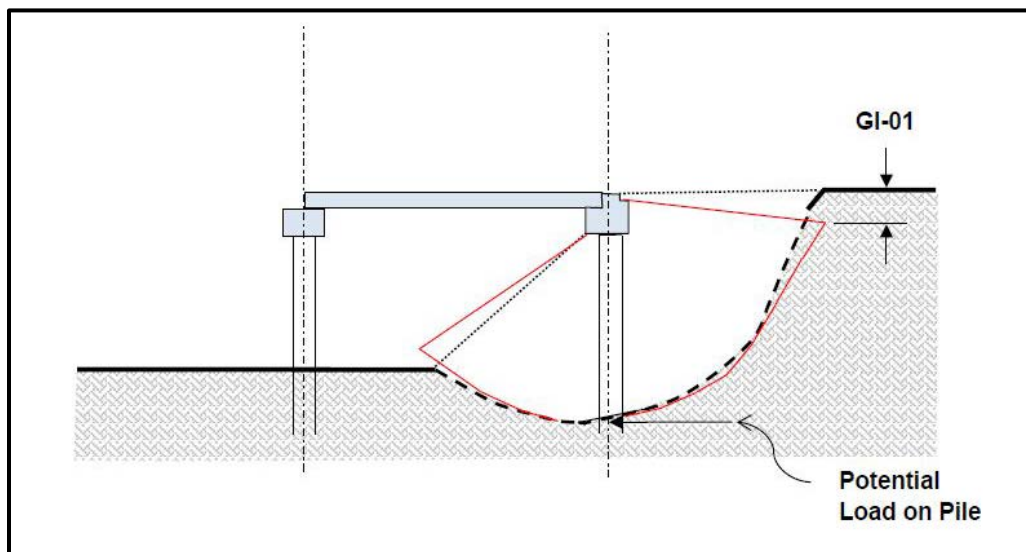
**Table 10-1, Global Instability Deformations Performance Limits**

Notation	Deformation ID No.	Description
Vertical Displacement, $\Delta_V$	GI-01	Maximum Vertical Displacement at top of the failure surface (circular).
Lateral Displacement, $\Delta_L$	GI-02	Maximum Lateral Displacement at either top or bottom of the failure surface (sliding block).

EE I limit state Performance Limits for global instability deformations associated with seismic slope instability are specified along the shear failure surface that results from the imbalance in the driving and resisting forces of the slope. The evaluation of global instability deformations is very complex and the methods (Chapter 13) that have been developed to evaluate deformations

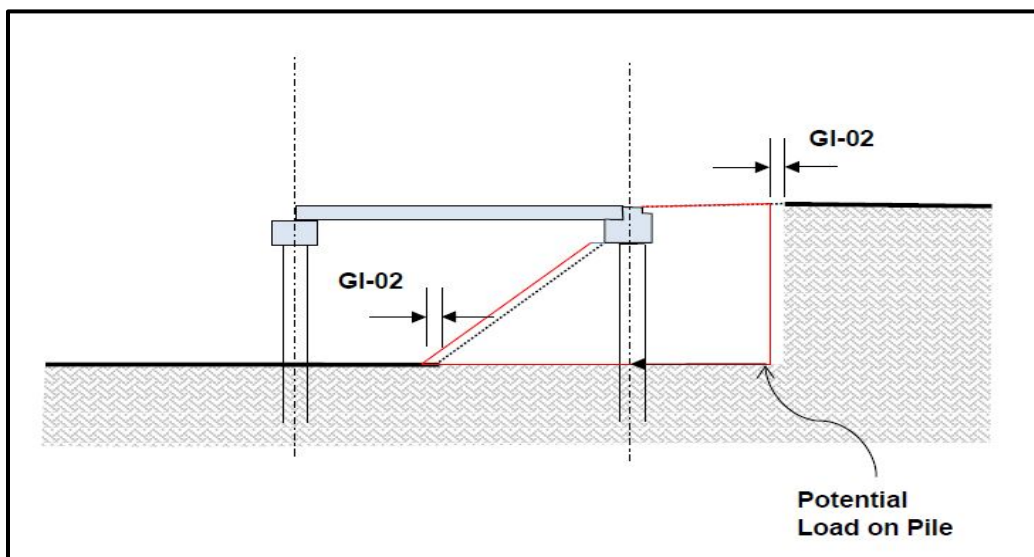
are typically either empirical or are very simplistic models that only provide an approximation of the slope instability deformations. A considerable amount of engineering judgment will be required to evaluate embankment deformations. To simplify this evaluation, it can be assumed that the soil is incompressible, that the deformations occur equally along the critical failure surface and that failing mass, whether embankment or ERS remains as a block during failure. The deformations measured along the failure surface shall be considered to be completely vertical at that top of slope for a circular failure surface (see Figure 10-2), while for a sliding block failure surface the deformation shall be completely horizontal (lateral) regardless of whether the displacement is measured at the top or bottom of the slope (see Figure 10-3).

Figures 10-2 and 10-3 depict the results of global instability at the end bent of a bridge. Figure 10-2 indicates a circular failure surface, while Figure 10-3 indicates a sliding block failure surface. Please note that depending on the stiffness of the piles, the end bent may or may not move. Therefore, it is possible that the end bent could be in “air” with soil having pulled away from the end bent. Similar deformations would happen if instead of a slope, an ERS were located at the end bent.



Not to Scale

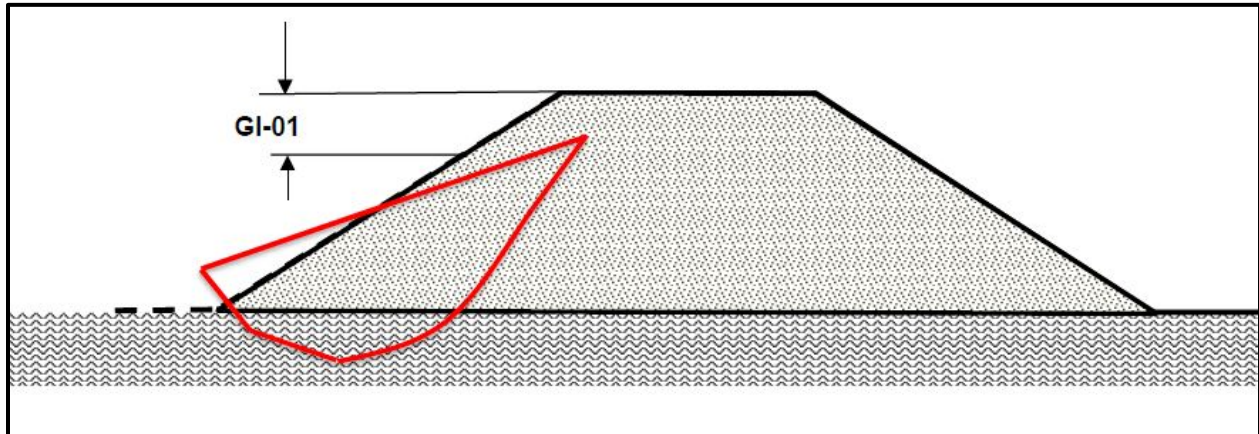
**Figure 10-2, Embankment Circular Instability at Bridge End Bent**



Not to Scale

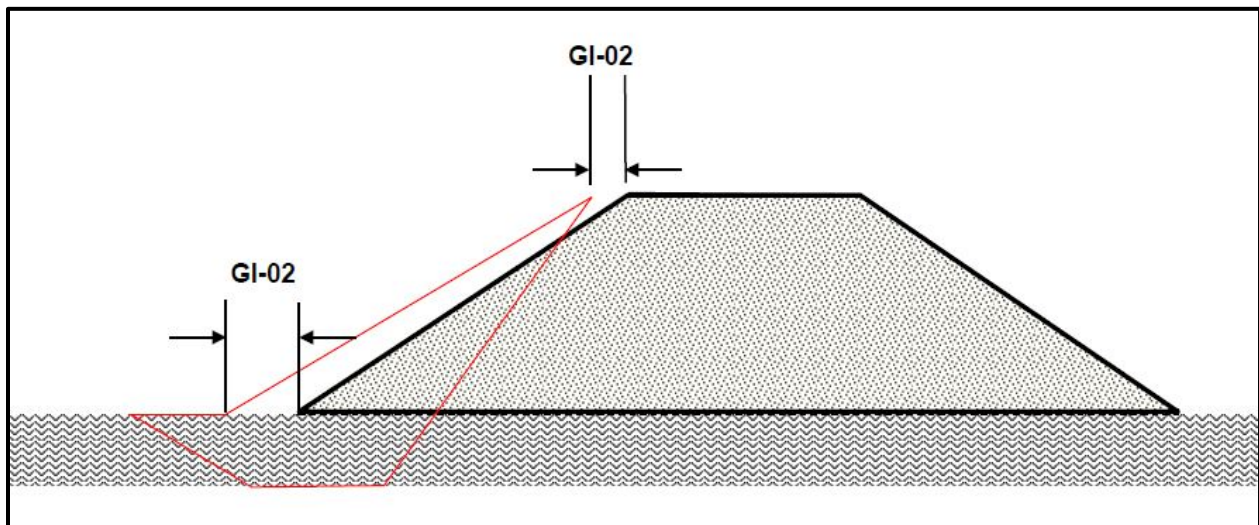
**Figure 10-3, Embankment Sliding Block Instability at Bridge End Bent**

Figures 10-4 and 10-5 indicate the instability of the transverse (side) slope of an embankment located within the “bridge embankment” portion of the approach embankment. If these instabilities affect the end bent of the bridge, then either structural or geotechnical mitigation will be required. The type and amount of mitigation that will be required is based on the Performance Objectives of the bridge, which are based on the OC of the bridge. OC determination and the Performance Objectives are defined in the Seismic Specs.



Not to Scale

**Figure 10-4, Embankment Circular Arc Instability**



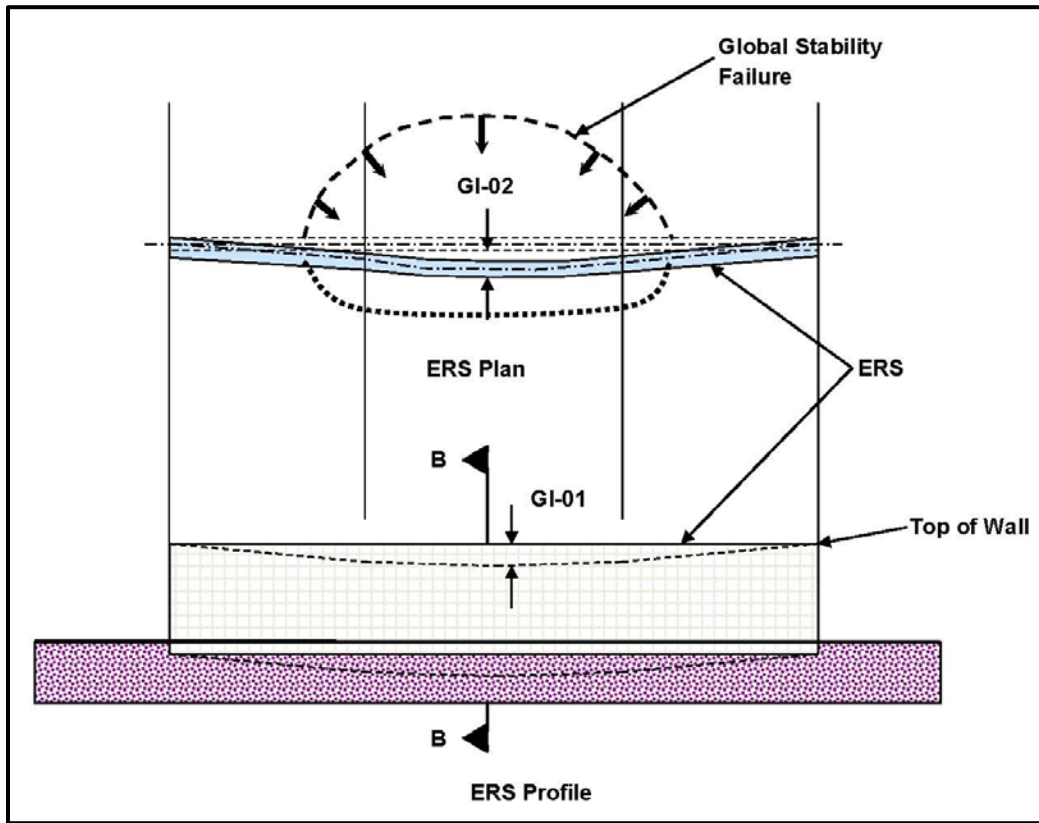
Not to Scale

**Figure 10-5, Embankment Sliding Block Instability**

As indicated previously the global instability assumes that the ERS maintains integrity (i.e., the ERS functions as a unit) during the instability. If the anticipated failure surface passes through the ERS, the ERS will need to be increased in size (i.e., the reinforcement material should be longer for MSE walls or the heel of the wall of a cantilevered gravity retaining wall should be increased). For ERSs located at the end bent of a bridge, global instability will be handled similarly to the embankment instability as discussed previously. ERSs located within the portion of the roadway embankment shall meet the Performance Objectives and Performance Limits established for ERSs. Figure 10-6 depicts the effect of localized global instability that does not affect the full length of the ERS. Section B-B is depicted in Figures 10-7 and 10-8, which indicate the anticipated movements for a circular and sliding block failure surface, respectively. The Performance Limits for global instability presented in this Chapter only apply to Rigid and

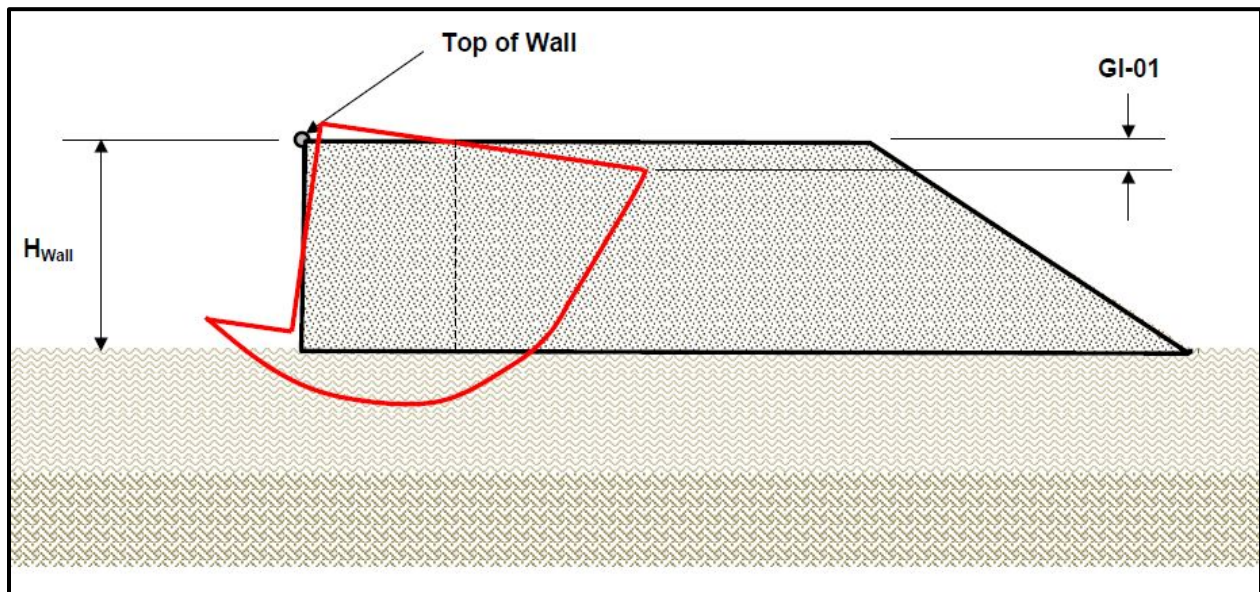


Flexible Gravity ERSs (see Table 10-6). A global stability check is required for all Cantilevered ERSs as discussed in Chapter 18.



Not to Scale

Figure 10-6, ERS Global Instability



Not to Scale

Figure 10-7, ERS Circular-Arc Instability (Section B-B)

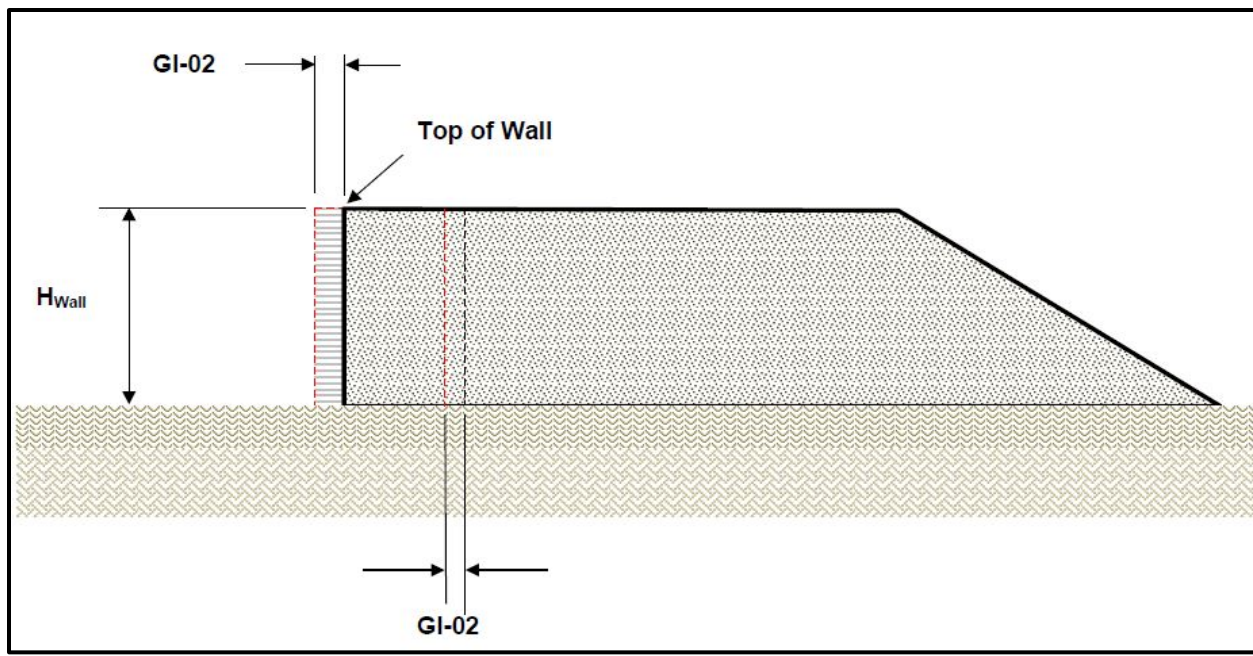


Figure 10-8, ERS Sliding-Wedge Instability (Section B-B)

## 10.6 EMBANKMENT DEFORMATIONS

### 10.6.1 Embankment Terminology and Deformation Notations

Embankment design with respect to global stability and settlements (deformations) is discussed in Chapter 17. Terminology used to specify geotechnical performance limits for embankments along roadways and at bridge approaches is presented in Chapter 2. RSSs as well as reinforced embankments are included with unreinforced embankments.

Embankment deformation notations are listed in Table 10-2. Embankment deformations where Performance Limits are specified can be categorized as follows:

- Embankment Settlement
- Embankment/Bridge Transition Settlement
- Embankment Widening Settlement

Table 10-2, Embankment Deformation Notations

Notation	Description
$\delta_v$	Vertical Differential Settlement
$\Delta_v$	Total Vertical Displacement / Settlement
$\Delta_L$	Lateral Displacement
$L_{SLAB}$	Longitudinal Length of the approach slab
$\Delta L$	Deformation occurring along the critical failure surface due to slope instability
$L_L$	Longitudinal distance of area affected by the compressive soils producing embankment settlements.
$L_T$	Transverse distance that defines the span of maximum differential settlement from the existing embankment (no settlement or minimal settlement) to the location of maximum settlement for the portion of new embankment that has been widened.

## 10.6.2 Embankment Settlement

Embankment vertical settlements are typically due to embankments being constructed over compressible soils that experience soil deformation (elastic compression, primary consolidation, and secondary compression) under constant load. It is anticipated that elastic compression will be completed prior to the placement of pavement; however, the total settlement (elastic compression, primary consolidation, and secondary compression) shall be determined. The total settlement shall be used in the development of static downdrag loads (see Chapter 16), if required. Settlement analysis methods are provided in Chapter 17. The vertical settlements that are evaluated under the Service limit state are as indicated below.

- Maximum Settlement from Elastic compression + Primary consolidation + Secondary Compression (i.e., total settlement occurring during construction)
- Maximum Settlement from Primary consolidation + Secondary Compression (i.e., total settlement after paving)
- Maximum Differential Settlement from Primary Consolidation + Secondary Compression (occurs after paving)

The maximum settlement shall be based on a 20-year design life which is used to match the typical repaving schedule anticipated by SCDOT.

Under the EE I limit state, performance limits for embankment settlement are specifically those caused by geotechnical seismic hazards that may affect the embankment or subgrade during or after a seismic event especially at the transition between the embankment and bridge. Methods of analyzing geotechnical seismic hazards due to soil SSL of the subgrade or seismic settlement of the embankment and subgrade are discussed in Chapter 13. It is noted that there is no limit on the amount of vertical settlement that can occur at the end bent of a bridge during EE I. Instead the vertical movements are converted into downdrag loads that are determined as discussed in Chapter 16. The maximum differential settlement may be determined under the EE I limit state analysis. The differential settlements may be either between the end of the approach slab and the bridge, between a point on the embankment and the end of the approach slab or between 2 points along the embankment. The longitudinal differential settlement of the embankment and the bridge should not be determined if an approach slab is present.

Performance limits for embankment settlements are identified in Table 10-3.



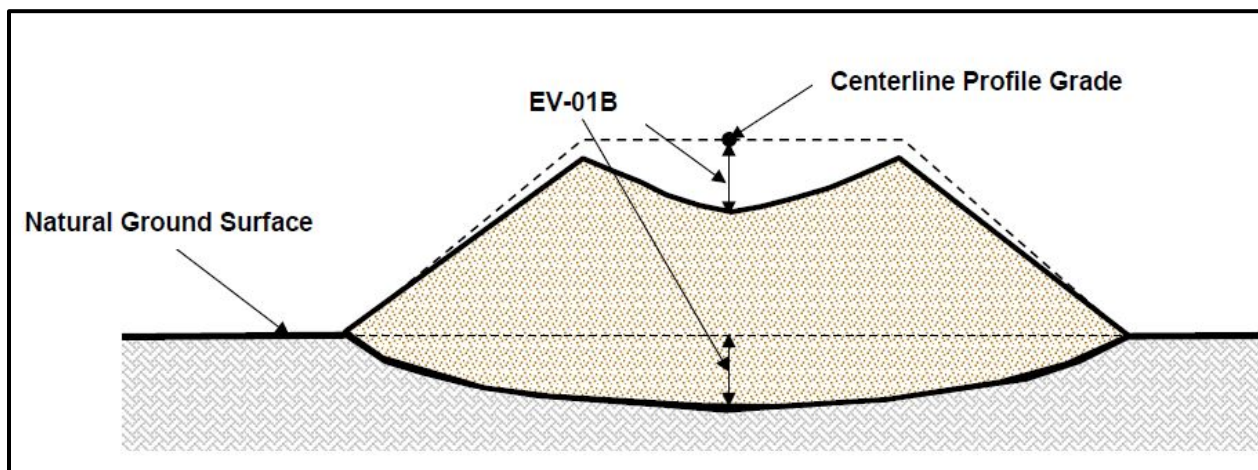
**Table 10-3, Embankment Settlement Performance Limits**

Notation	Deformation ID No.	Description
Vertical Settlement, $\Delta_v$	EV-01A	Maximum Settlement from Elastic Compression + Primary Consolidation + Secondary Compression along the profile grade <sup>1</sup> that occurs during the duration of the construction of the embankment and commences at the start of construction and terminates just prior to paving operations. This deformation is used to adjust borrow requirements, if necessary
	EV-01B	Maximum Settlement from Primary Consolidation + Secondary Compression along the profile grade <sup>1</sup> over the design life <sup>2</sup> of the embankment. The design life begins after the pavement has been placed (i.e., the settlement that occurs after EV-01A).
Vertical Differential Settlement, $\delta_v$	EV-03	Maximum Differential Settlement from Primary Consolidation + Secondary Compression occurring longitudinally along the profile grade after the roadway has been paved. Determined either between the end of the approach slab and a point on the embankment or between 2 points on the embankment that may affect rideability.

<sup>1</sup>The longitudinal location of EV-01(A or B) shall be noted (i.e., at end bent, at end of approach slab, at Sta. XX+XX, etc.)

<sup>2</sup>Design life of 20 years shall be used.

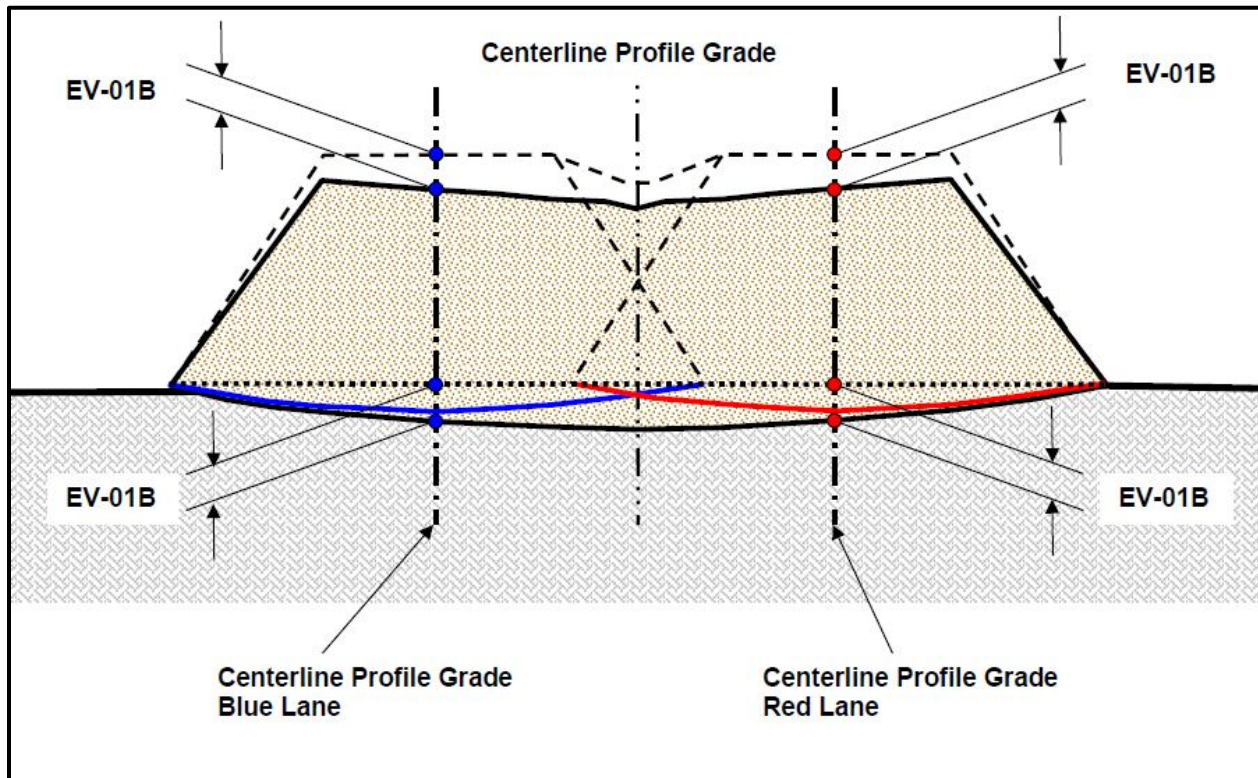
The roadway profile grade (P.G.) for non-divided highways (highways without medians) is typically located at the center of the roadway as indicated in Figure 10-9. Figure 10-9 is designated as Section A-A and corresponds to an embankment cross-section taken transverse to the travel lane as indicated in Figure 10-11. Embankment settlements are evaluated at the center of embankment sections where the maximum settlements are most likely to occur and consequentially also where the maximum differential settlements occur.



Not to Scale

**Figure 10-9, Embankment Settlement (Section A-A)**

Divided highways may have a P.G. elevation for each travel direction as indicated in Figure 10-10. Figure 10-10 is designated as Section A-A and corresponds to an embankment cross-section taken transverse to the travel lane as indicated in Figure 10-11. To differentiate the divided profile grades the color Blue was used to designate the roadway on the left and the color Red was used to designate the roadway on the right. Divided highways should be evaluated separately for each P.G. Settlement analyses must take into account the total embankment cross-section and the construction sequencing.



Not to Scale

**Figure 10-10, Divided Highway (Section A-A)**

The Performance Limit EV-01A is for maximum settlement ( $\Delta_v$ ) that occurs at the profile grade during the construction of the embankment that begins immediately after construction starts and ends immediately prior to paving and may be determined at any specified point along the length of the embankment. Because this deformation also includes elastic compression, EV-01A should be used to adjust borrow quantities as required. The Performance Limit EV-01B is for  $\Delta_v$  that occurs at the profile grade over the design life (20 years) of the embankment that begins after the pavement has been placed and may be determined at any specified point along the length of the embankment.

Performance Limit EV-03 is specified as the maximum differential settlement ( $\delta_v$ ) occurring longitudinally along the profile grade. The differential settlement is specified over a distance of 50 feet, measured longitudinally along the embankment. It is anticipated that Performance Limit EV-03 will be determined only if there is concern about the rideability of the roadway surface. Performance EV-03 should only be determined from end of the approach slab and another point along the profile grade of the roadway or between 2 points located along the profile grade. If vertical displacements are encountered at an isolated location such as shown in Figure 10-11, the differential settlement performance limit EV-03 may be pro-rated so that at any point along the distance,  $L_L$ , the tolerances specified are not exceeded. The distance  $L_L$  shall never exceed 50 feet. There are no Performance Limits for differential settlements ( $\delta_v$ ) that occur perpendicular (transverse) to the alignment for new embankments since these types of displacements are relatively small due to the relatively uniform loading and the assumed low soil variability in the transverse direction (not typically investigated). If excessive transverse differential settlement is anticipated to affect the performance of the roadway, refer to Section 10.6.3.



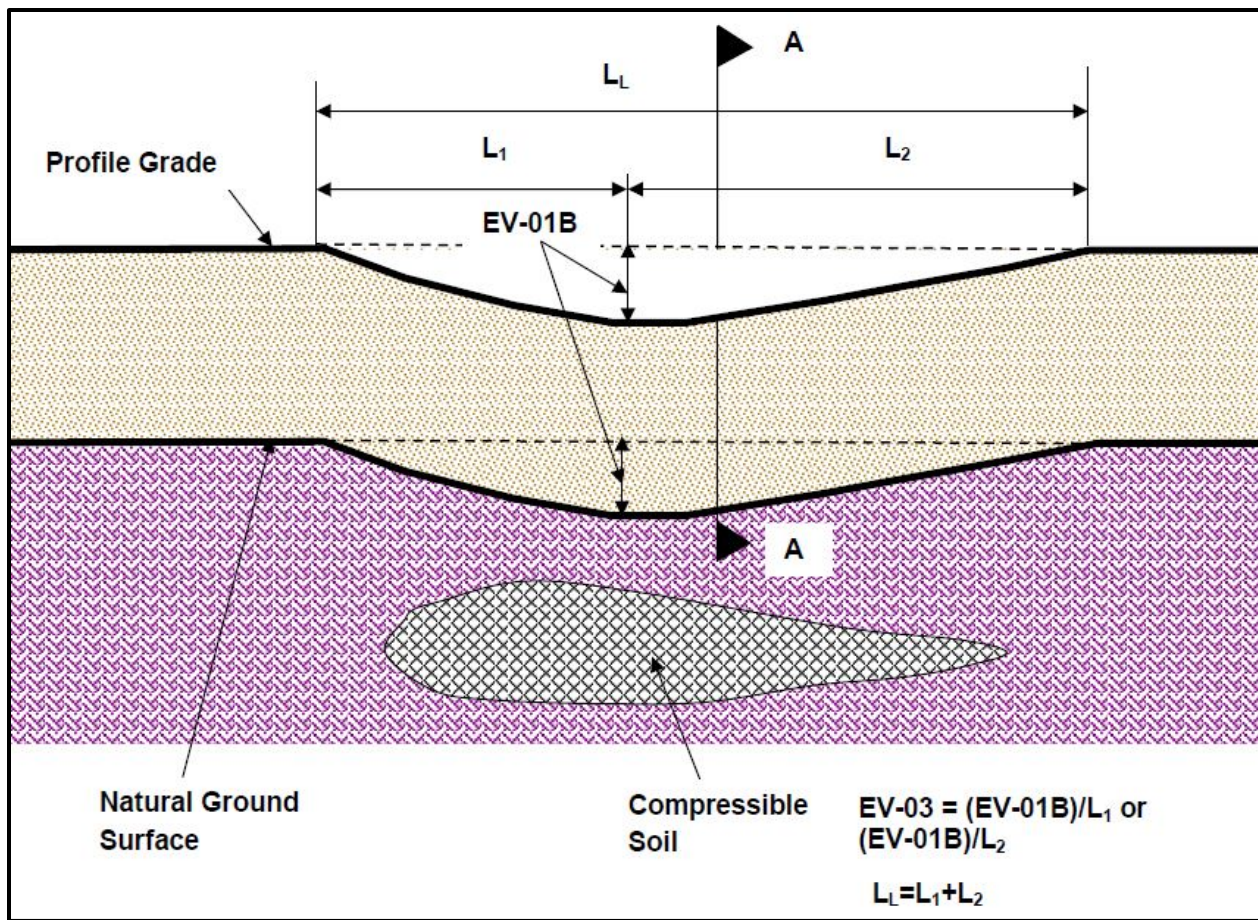


Figure 10-11, Embankment Settlement Profile

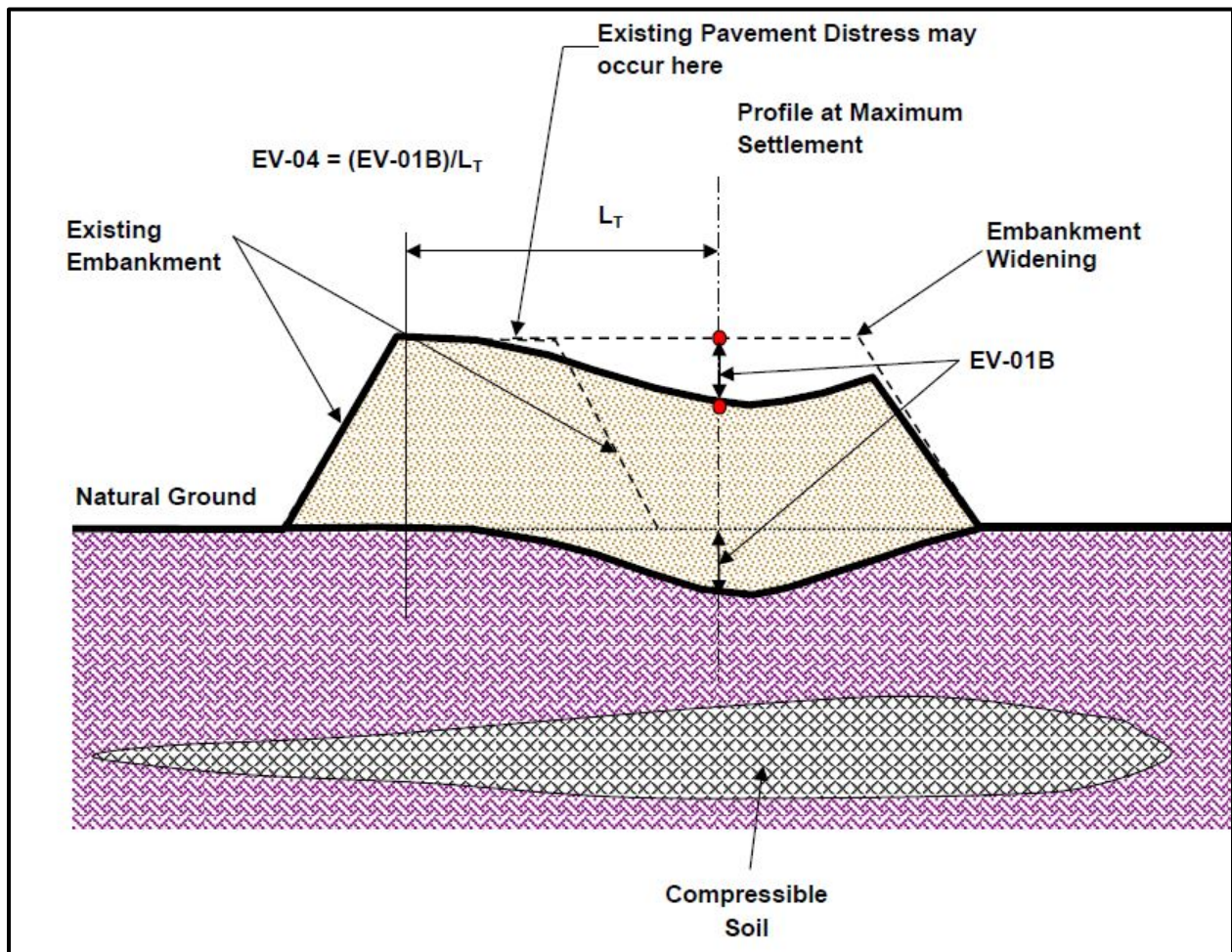
### 10.6.3 Embankment Widening Differential Settlements

Existing embankments are often widened to accommodate additional traffic lanes or are widened in order to accommodate a re-alignment of a new bridge being constructed adjacent to an existing bridge. These Performance Limits are used on roadways where differential settlement due to widening of the roadway or to soil variability could adversely affect the roadway pavement. The embankment subject to transverse differential embankment settlement shall be designed for the Performance Limits indicated in Table 10-3 (EV-01A, EV-01B, and EV-03), and transverse differential embankment settlement Performance Limit (EV-04) provided in Table 10-4. It is noted that transverse differential settlement should be anticipated between a widened portion of the embankment and the existing embankment. The widened embankment will induce loading on the existing embankment that will in turn cause settle of the existing embankment. This settlement may potentially cause damage to the existing embankment. The GEOR should note on the plans that damage is anticipated and that the Contractor is responsible for maintaining the existing travelway. In addition, the GEOR will coordinate with Construction to determine the quantities required to maintain the existing travelway.

**Table 10-4, Embankment Widening Settlement Performance Limits**

Notation	Deformation ID No.	Description
Differential Settlement, $\delta_v$	EV-04	Maximum Vertical Differential Settlement occurring transverse to the adjusted profile grade between the existing embankment and the new widened embankment after the roadway has been paved.

When existing embankments are widened, a parallel profile grade is established at the location of maximum vertical settlement for the embankment widening as shown in Figure 10-12. Figure 10-12 is designated as Section A-A and corresponds to an embankment widening cross-section taken transverse to the travel lane as indicated in Figure 10-11. The performance limits, EV-01A, EV-01B, and EV-03, are computed in the same manner as discussed in Section 10.6.2 except that the settlements are computed along the profile of maximum settlement. The maximum vertical differential settlement (EV-04) limits the differential settlements between the existing embankment and the embankment widening section that may affect the paved roadway surface. The differential settlements transverse to the embankment are computed at distance “ $L_T$ ” between the existing embankment (where zero or minimal settlement occurs) and the new embankment at point of maximum settlement as indicated in Figure 10-12. For RSSs and reinforced embankments the differential settlement between the face of the slope and the end of the reinforcement should be determined. This differential movement should be determined using the procedure to determine RV-06A and RV-06B as indicated in Table 10-10 and depicted in Figure 10-17.



Not to Scale

**Figure 10-12, Embankment Widening Settlement (Section A-A)**



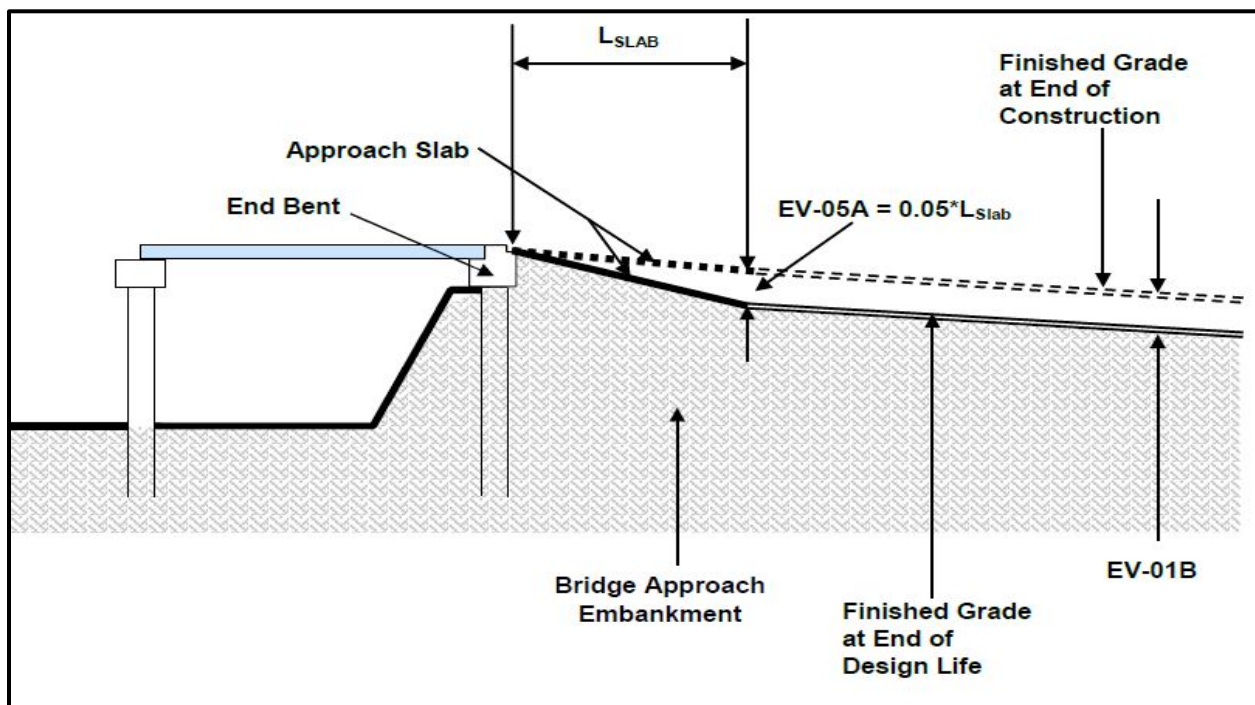
### 10.6.4 Embankment/Bridge Transition Settlement

At the transition between the bridge approach embankments and the bridge ends there is a potential for large differential vertical settlement ( $\delta_v$ ). The vertical differential settlement can be significant in magnitude because the bridge end bents are typically supported on deep foundations that are relatively stationary in the vertical direction as compared to the approach embankment. If the new bridge approach embankments are placed over compressible soils the approach embankments tend to settle significantly more than the bridge ends. Performance Limits for the Embankment/Bridge transition settlement are identified in Table 10-5.

**Table 10-5, Bridge/Embankment Transition Settlement Performance Limits**

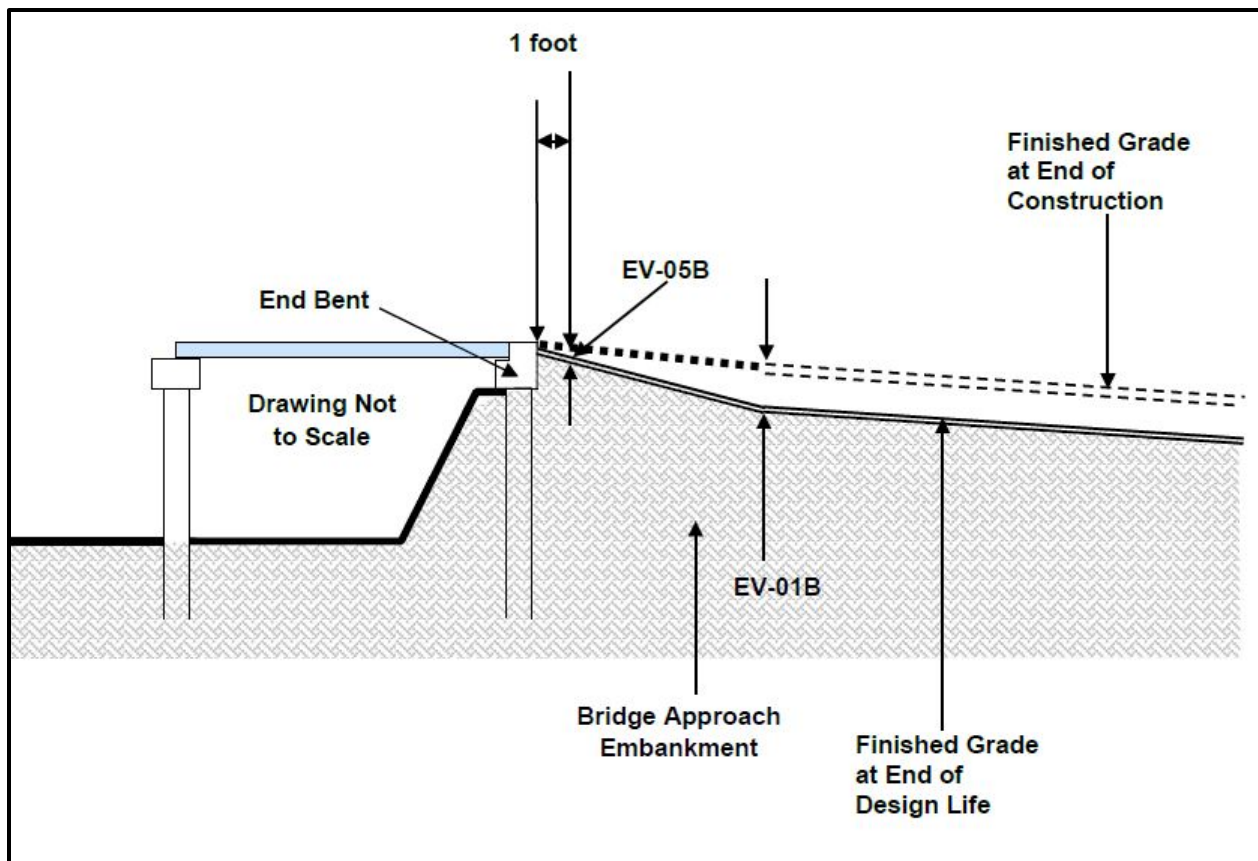
Notation	Deformation ID No.	Description
Vertical Differential Settlement, $\delta_v$	EV-05A	Maximum Differential Settlement ( $\delta_v$ ) between the bridge End Bent and the end of the Approach Slab after the roadway has been paved at the end of the pavement design life (20 yrs).
	EV-05B	Maximum Differential Settlement ( $\delta_v$ ) between the bridge End Bent and a point 1 foot from either the “begin” or “end” of bridge, for bridges without approach slabs after the roadway has been paved at the end of the pavement design life (20 yrs).

Differential vertical settlements between the bridge ends and the approach embankments can significantly affect the roadway rideability at the bridge abutment and at the end of the approach slab as shown in Figures 10–13 and 10-14.



Not to Scale

**Figure 10-13, Bridge-Embankment Transition Settlement with Approach Slab**



Not to Scale

**Figure 10-14, Bridge-Embankment Transition Settlement without Approach Slab**

Performance Limit EV-05A is specified as a percentage of the length of the approach slab ( $L_{SLAB}$ ) in feet. EV-05B shall be used to determine the differential settlement between the end of the bridge and the bridge embankment across a distance of 1 foot from the bridge, for bridges that do not have approach slabs. EV-03 shall not be used to determine the longitudinal differential displacement between the bridge and the bridge embankment. For purposes of the transition from the bridge embankment to the bridge EV-05A or EV-05B shall be used, depending on whether the bridge has an approach slab or not. The differential settlement ( $\delta_v$ ) is the absolute value of the difference between the settlement at the end of the approach slab and the settlement of the End Bent. The vertical settlement at the End Bent shall be used in the development of static downdrag and is discussed in Chapter 16. The Performance Limit at the Service limit state is used to minimize the displacements typically observed at the bridge ends that are typically referred to as the “bump at the end of the bridge.” The EE I limit state Performance Limit is used to obtain the Performance Objectives of the bridge by maintaining the Damage and Service Levels required for the design earthquake.

## 10.7 EARTH RETAINING STRUCTURE DEFORMATIONS

### 10.7.1 Earth Retaining Structure Terminology and Deformation Notations

ERS selection and design methodologies are discussed in Chapter 18. For the purposes of defining Performance Limits, ERSs have been classified based on the construction method. A cut ERS refers to a retaining system that is constructed from the top of the wall to the base of the wall concurrent with excavation operations of the in-place soil in front of the wall. A fill ERS refers to a retaining system that is constructed from the base of the wall to top of the wall with the retained soil being placed during construction. Terminology used to specify geotechnical Performance Limits for ERSs is presented in Chapter 2.

Fill ERSs and Cut ERSs that are commonly used by SCDOT have been grouped by categories as indicated in Tables 10-6 and 10-7, respectively.

**Table 10-6, Fill – Earth Retaining Structures (ERS)**

Wall Type	Category	Type
Rigid Gravity Walls	Rigid Walls	Concrete Barrier Walls, Concrete Retaining Walls
	Semi-Rigid Walls	Concrete Stem Walls
Flexible Gravity Walls	Prefabricated Modular Gravity Wall	Gabion Wall
	Mechanically Stabilized Earth Walls	MSE (Full Height Panel Facing) MSE (Modular Block Facing) MSE (Precast Panel Facing) MSE (Gabion Facing)

**Table 10-7, Cut – Earth Retaining Structures (ERS)**

Category	Type
Cantilever Walls	Sheet Pile Wall, Soldier Pile Wall, Tangent/Secant Pile Wall,
Cantilever Walls with Anchors	Sheet Pile Wall w/ Anchor, Soldier Pile and Lagging Wall w/ Anchor, Tangent/Secant Pile Wall w/ Anchors
In-Situ Reinforced Earth Walls	Soil Nailed Wall

The Performance Limits for Fill and Cut ERSs are based on the intended use and the type of wall being considered. There are many types of walls and each wall has its own limitations, advantages, and disadvantages with respect to economics, construction, and performance. Proper ERS selection (see Chapter 18) is essential for the retaining system to meet the Performance Limits required. Unless otherwise indicated, the deformations that are described in this Section apply to both Fill and Cut type ERSs. ERS deformation notations are listed in Table 10-8.

**Table 10-8, ERS Deformation Notations**

Notation	Description
$\delta_v$	Vertical Differential Settlement
$\Delta_v$	Total Vertical Displacement / Settlement
$\Delta_{VR}$	Maximum Vertical Displacement of soil reinforcement
$\delta_L$	Lateral Differential Displacement along the top of the wall
$\Delta_L$	Lateral Displacement
$L$	Distance used to denote boundaries for differential settlement computations
$L_E$	Distance along the face that an ERS deforms away from the retained soil. Deformations are caused by lateral earth pressures.
$L_L$	Longitudinal distance of area affected by the compressive soils producing ERS settlements.
$L_R$	Transverse distance that defines the length of the reinforcement over which the maximum settlement of the reinforcement is measured and the transverse maximum differential settlement if determined.

ERS vertical settlements are typically due to ERSs being constructed over compressible soils that experience soil deformation (elastic compression, primary consolidation, and secondary compression) under constant load. It is anticipated that elastic compression will be completed prior to the placement of pavement; however, the total settlement (elastic compression, primary

consolidation, and secondary compression) anticipated to occur during construction of the ERS shall be determined (RV-01A). The total settlement (primary consolidation and secondary compression) after paving (RV-01B) shall be used in the determination of the Performance Limit for all ERSs constructed in a single stage. For all ERSs constructed in 2 or more stages, the settlement remaining after completion of the ERS shall be used in determining the Performance Limits. In addition for ERSs located at the end bent of a bridge, the total settlement shall be used in the development of static downdrag loads (see Chapter 16), if required. The vertical settlements that are evaluated under the Service limit state are as indicated below. The Performance Limits for ERSs are specified for the following types of deformations:

- Longitudinal Settlement Deformation
- Transverse Settlement Deformation
- Lateral Displacements

The maximum settlement shall be based on a 20-year design; however, the structural design life (i.e., the structural components) shall be 100 years. The 20-year design life is used to match the anticipated repaving schedule anticipated by SCDOT. Methods to evaluate stability and deformations are provided in Chapters 13, 17 and 18.

### **10.7.2 Settlement Deformation – Longitudinal**

ERS settlements are typically due to fill ERSs being placed over compressible soils. This type of settlement is typically due to elastic compression, primary consolidation and secondary compression of the compressible soils. ERS settlements can also be due to seismic hazards such as soil SSL of the subgrade during or after a seismic event. ERS settlements are evaluated at the top of the wall adjacent to the wall facing where differential settlements are likely to cause the most distress to the wall facing. Performance Limits for settlements occurring longitudinally (along the wall profile) are identified in Table 10-9. As indicated previously, whether the ERS is completed in a single stage or multiple stages will affect how the maximum vertical total and differential settlement will be determined. Methods to evaluate settlements are provided in Chapters 13 and 17.



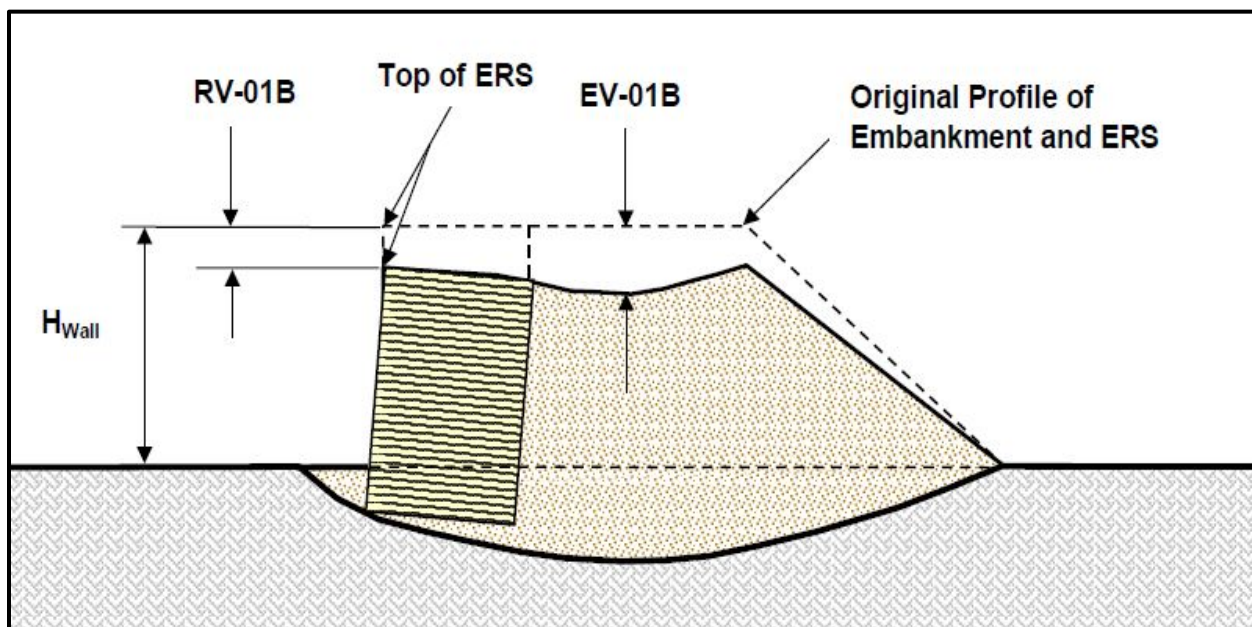
**Table 10-9, ERS Settlement (Longitudinal) Performance Limits**

Notation	Deformation Limit ID No.	Description
Vertical Settlement, $\Delta_v$	RV-01A	Maximum Settlement from Elastic Compression + Primary Consolidation + Secondary Compression along the top of wall profile grade <sup>1</sup> that occurs during the construction of the ERS and commences immediately after construction begins and terminates just prior to paving operations. This deformation is used to adjust borrow and ERS height requirements, if necessary.
	RV-01B	Maximum Settlement from Primary Consolidation + Secondary Compression along the profile grade <sup>1</sup> over the design life <sup>2</sup> of the pavement behind the ERS. The design life begins after the pavement has been placed (i.e., the settlement that occurs after RV-01A).
Vertical Differential Settlement, $\delta_v$	RV-03A	Maximum Differential Settlement from Elastic Compression + Primary Consolidation + Secondary Compression occurring longitudinally along the ERS profile grade (i.e., top of ERS) during construction.
	RV-03B	Maximum Differential Settlement from Primary Consolidation + Secondary Compression occurring longitudinally along the ERS profile grade (i.e., top of ERS) post construction.

<sup>1</sup>The longitudinal location of RV-01 shall be noted (i.e., at ERS Sta. XX+XX)

<sup>2</sup>Design life of 20 years shall be used.

The Performance Limit, RV-01A is the maximum settlement that occurs at the face at the top of the wall profile during construction. RV-01B is the maximum settlement that occurs at the face of the top of the wall over the design life of the pavement on top of the ERS as indicated in Figure 10-15.



Not to Scale

**Figure 10-15, ERS Settlement (Section B-B)**

Wall distress due to settlements along the top of the wall profile, are limited by specifying a Performance Limit, RV-03 for the maximum differential settlement ( $\delta_v$ ) observed longitudinally along the top of the wall profile. The Performance Limit RV-03A is determined from the differential displacements that are anticipated to occur during the construction of the wall and should be used to assist in the determination of whether the wall should be built in more than 1 stage. The Performance Limit RV-03B is differential displacement anticipated to occur after the ERS has been constructed. The differential settlement is specified over a distance of 50 feet, measured longitudinally along the top of the wall profile. If vertical displacements are encountered at an isolated location such as shown in Figure 10–16, the differential settlement Performance Limit, RV-03, may be pro-rated so that at any point along the distance,  $L_L$ , the tolerances specified are not exceeded. The distance  $L_L$  shall never exceed 50 feet.

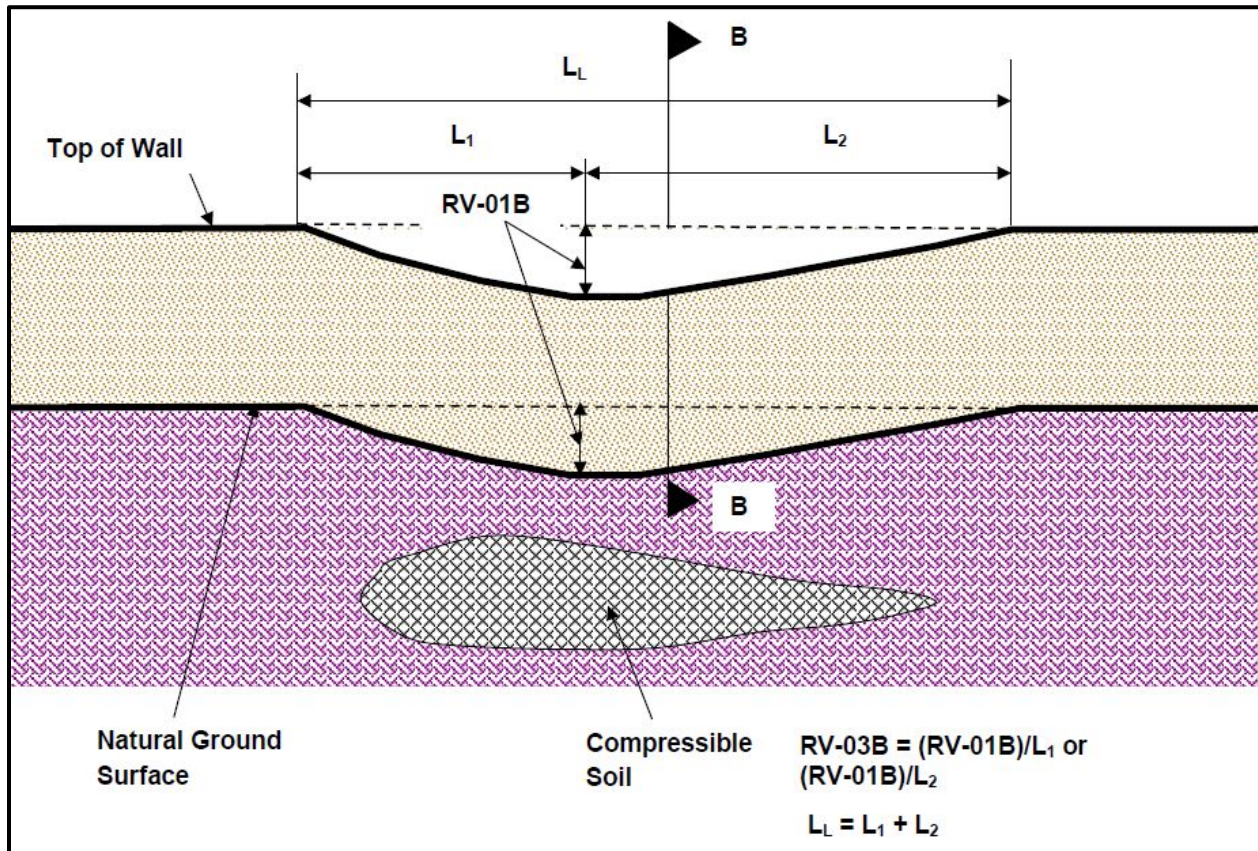


Figure 10-16, ERS Settlement Profile

### 10.7.3 Settlement Deformation – Transverse

This Performance Limit is used for differential settlements ( $\delta_v$ ) that occurs perpendicular to the wall alignment and is only applicable to retaining walls that have discrete soil reinforcements (geosynthetic reinforcement, steel reinforcement, soil anchors, etc.) extending perpendicular to the wall facing to the end of the length of the reinforcement,  $L_R$ . The Performance Limit for settlement occurring perpendicular to the wall profile (transverse direction) is identified in Table 10-10.

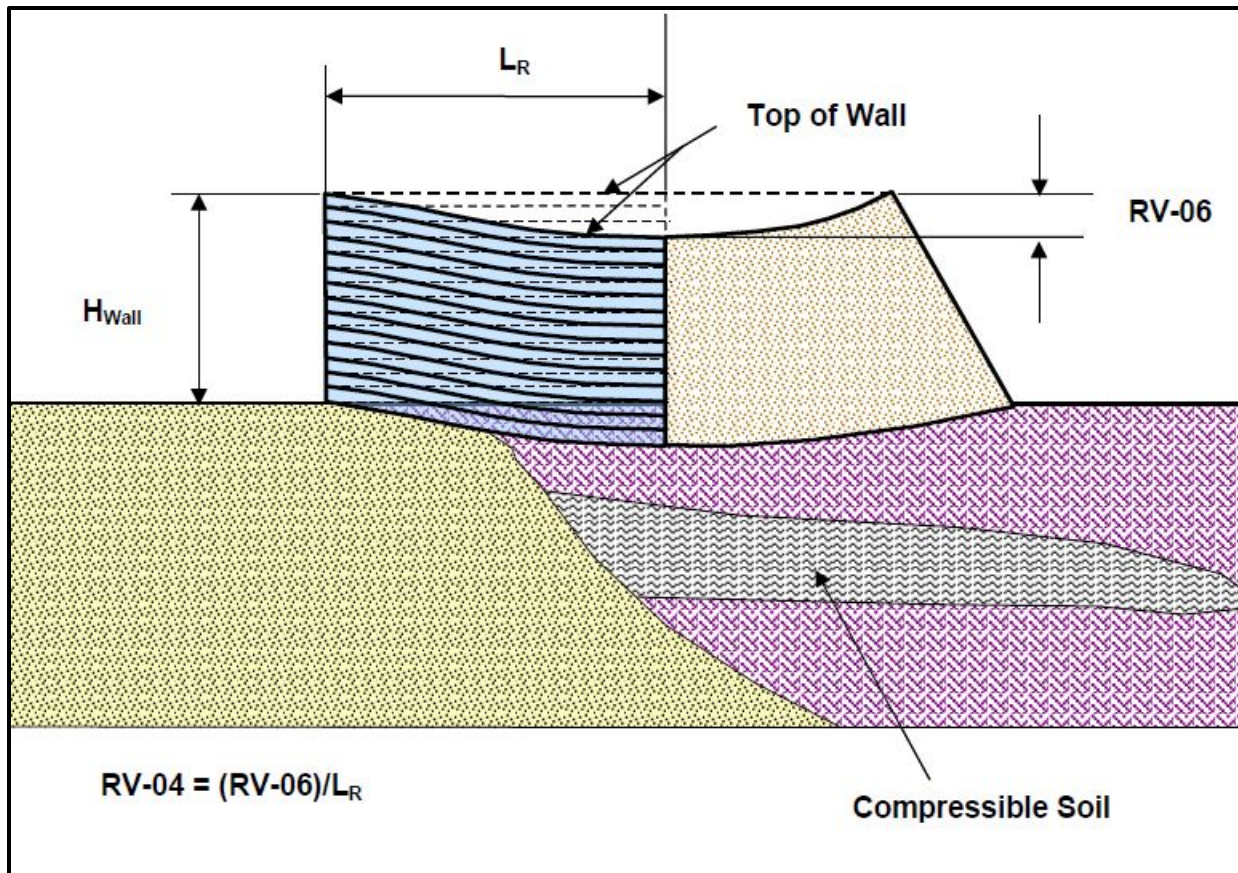
**Table 10-10, ERS Settlement (Transverse) Performance Limits**

Notation	Deformation Limit ID No.	Description
<b>Vertical Differential Settlement, <math>\delta_{VR}</math></b>	<b>RV-04A</b>	The absolute value of the Maximum Differential Settlement observed perpendicular (transverse) to the top of the wall profile during construction of the wall.
	<b>RV-04B</b>	The absolute value of the Maximum Differential Settlement observed perpendicular (transverse) to the top of the wall profile after construction of the wall.
<b>Vertical Settlement, <math>\Delta_{VR}</math></b>	<b>RV-06A</b>	Maximum Settlement from Elastic Compression + Primary Consolidation + Secondary Compression at the termination of the reinforcement that occurs during the construction of the ERS and commences immediately after construction begins and terminates just prior to paving operations.
	<b>RV-06B</b>	Maximum Settlement from Primary Consolidation + Secondary Compression at the termination of the reinforcement that occurs over the design life <sup>1</sup> of the pavement behind the ERS. The design life begins after the pavement has been placed (i.e., the settlement that occurs after RV-06A).

<sup>1</sup>Design life of 20 years shall be used

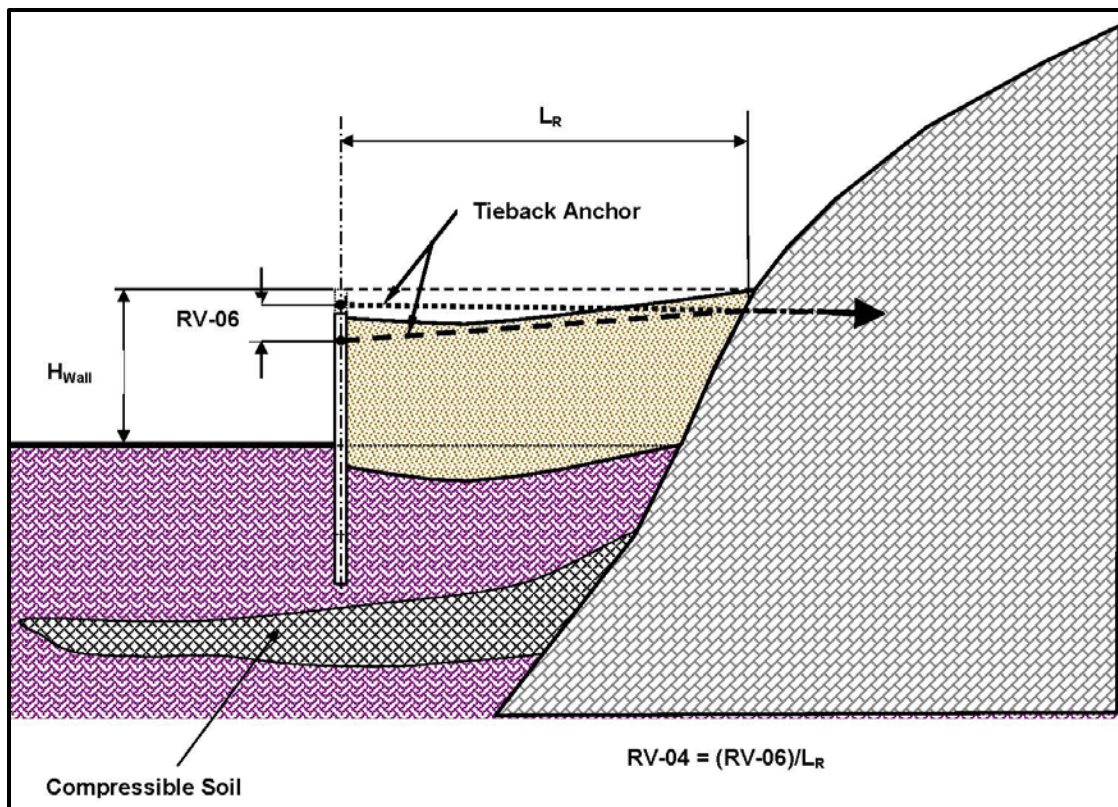
Examples of ERSs with reinforced soil (MSE walls) and ERSs with tieback anchors (cantilever walls w/ tieback anchors) are shown in Figures 10-17 and 10-18, respectively. A cantilevered ERS should not have a tip elevation above a compressible layer as shown in Figure 10-18, unless unavoidable. Contact the PC/GDS prior to designing a cantilevered ERS above a compressible layer. Excessive differential settlements (transverse) may cause distress and even wall collapse from the added load induced to the wall facing and soil reinforcements. The Performance Limit, RV-04(A or B) is the maximum differential settlements perpendicular (transverse) to the adjusted profile over a distance,  $L_R$ , as indicated in Figure 10-17 and 10-18 and is determined both for vertical displacements that occur during construction as well as for post construction displacements. Performance Limit, RV-04(A or B) is computed along maximum increments of 5 feet.





Not to Scale

**Figure 10-17, ERS Reinforced Soils - Transverse Differential Settlement**



Not to Scale

**Figure 10-18, ERS Tieback Anchor - Transverse Differential Settlement**

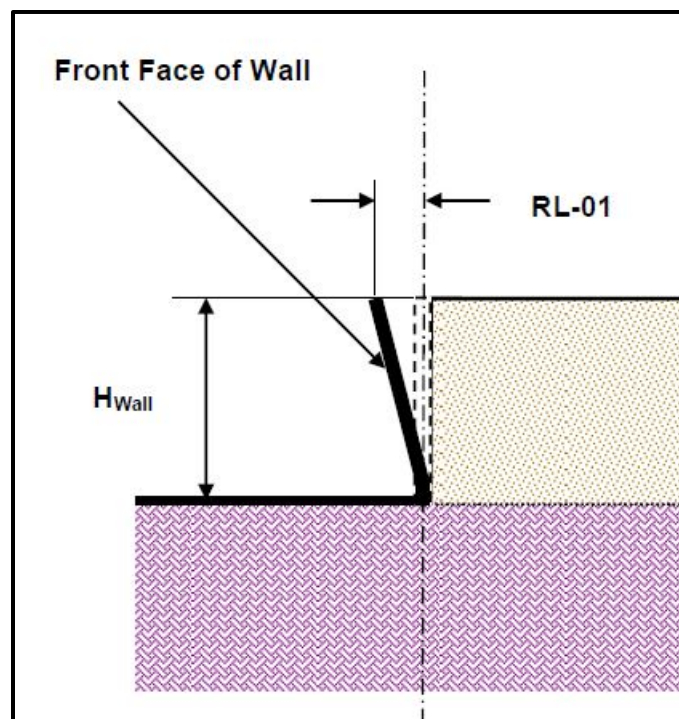
### 10.7.4 Lateral Displacements

ERS lateral displacements are those movements that occur as a result of lateral soil pressures. Lateral soil pressure loadings produce displacements of the structural members of the wall system and also displacements of the soil (soil-structure interaction). ERS lateral displacements can also occur as a result of active seismic loadings that are transmitted laterally to the ERS. These lateral displacements are not the same as those caused by global instabilities as discussed previously. The Performance Limits for lateral displacements occurring perpendicular to the wall profile (transverse direction) are identified in Table 10-11.

**Table 10-11, ERS Lateral Performance Limits**

Notation	Deformation ID No.	Description
Lateral Displacement, $\Delta_L$	RL-01	Maximum Lateral Displacement at the top of the wall.
Lateral Differential Displacement, $\delta_L$	RL-02	Maximum Differential Lateral Displacement longitudinally along the top of the wall. This performance limit is typically referred to as wall "bulging."

The Performance Limit, RL-01 is the maximum lateral displacement that occurs at the top of the wall over the design life of the structure. For this Performance Limit the design life shall be 100 years, since this displacement has more to do with the structural performance of the ERS. ERS Performance Limit, RL-01 is evaluated at the top of the wall as indicated in Figure 10-19.



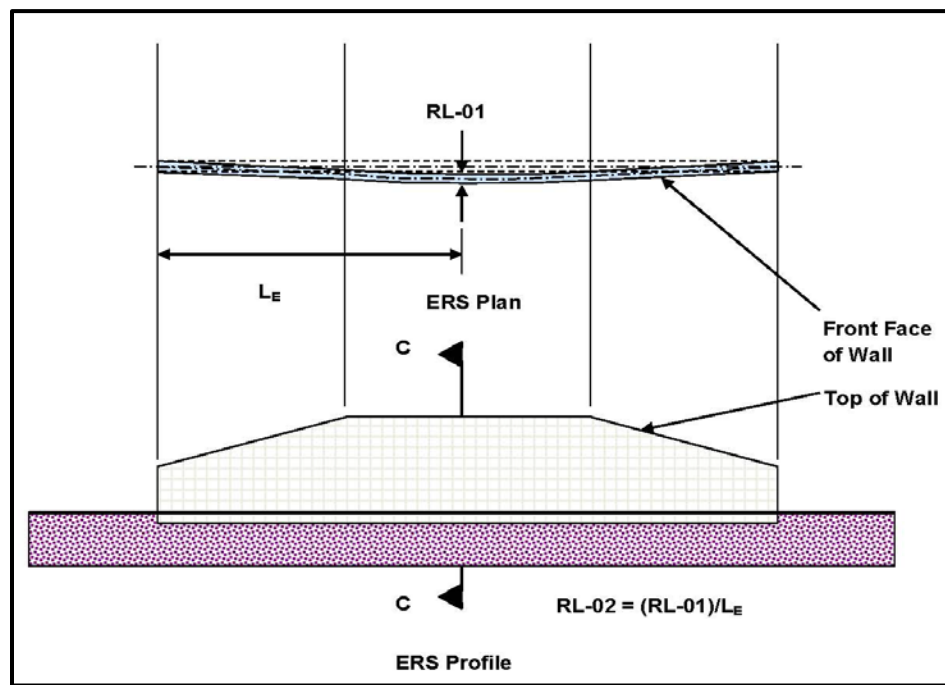
Not to Scale

<sup>1</sup>Front face of wall shown has negative batter, negative batter is not allowed at the SLS.

**Figure 10-19, ERS Lateral Deformation (Section C-C)**

Lateral wall distress (bulging), due to differential lateral displacement along the top of the wall profile, is limited by specifying a Performance Limit, RL-02 for the maximum differential lateral

displacement observed longitudinally along the top of the wall profile after the ERS has been constructed as shown in Figure 10-20. The differential lateral displacement is specified over a distance of 50 feet and measured longitudinally along the top of the wall profile. If lateral displacements are encountered at an isolated location, the differential lateral displacement Performance Limit, RL-02 may be pro-rated so that at any point along the distance,  $L_E$ , the tolerances specified are not exceeded.



Not to Scale

<sup>1</sup>Front face of wall shown has negative batter, negative batter is not allowed at the SLS.

**Figure 10-20, ERS Lateral Deformations**

## 10.8 PERFORMANCE LIMITS FOR GLOBAL INSTABILITY

### 10.8.1 Service Limit State

#### 10.8.1.1 Performance Objective

The embankment and ERS Performance Objectives for global stability at the Service limit state is that instability is not allowed. Therefore, no Performance Limits are established.

### 10.8.2 Extreme Event I Limit State

#### 10.8.2.1 Performance Objective

The Performance Objectives for bridge embankments and ERSs at EE I limit state is that neither the bridge embankments nor ERSs adversely affect the bridge structure during the design seismic event. “Bridge embankments” are defined in Chapter 2. ERSs not located in “bridge embankments” shall not collapse at the EE I limit state. Collapse shall mean adversely affecting either area in front or behind the ERS a distance of 1.1 times the height of the wall. In addition, the seismic design of the ERS shall comply with the requirements of Chapter 14.



### **10.8.2.2 Performance Limits**

The design team has the ultimate responsibility for development of Performance Limits of the structure during the design Extreme Event and for assuring that the Performance Objectives of the structure are met. The Performance Limits established by the design team shall conform to the Deformation ID No. and the Performance Limit description contained in Table 10-1. The design team shall supply this information to and have the concurrence and acceptance of the PC/SDS and the PC/GDS. The GEOR shall provide the anticipated displacements caused by global instability using the Deformation ID No. contained in Table 10-1 to the design team.

### **10.8.3 Extreme Event II Limit State**

#### **10.8.3.1 Performance Objective**

The embankment and ERS Performance Objectives for global stability at the EE II (check flood (500-yr flow event)) limit state is that instability is not allowed. Therefore, there are no Performance Limits established. As indicated previously, EE II (collision/impact loadings only) shall not be used in the design of embankments or ERSs; therefore, no Performance Objectives or Performance Limits are established.

## **10.9 PERFORMANCE LIMITS FOR EMBANKMENTS**

### **10.9.1 Service Limit State**

#### **10.9.1.1 Performance Objective**

The Performance Objectives for permanent embankments at the Service limit state are that the embankment remains fully functional for the design life of the pavement structure (20 years) and that through periodic maintenance any deformations can be adjusted for in order to maintain the serviceability requirements of the roadway pavement. Temporary embankments (i.e., widened embankments) may induce settlements that are in excess of the Performance Limits established for transverse differential settlement for short periods (less than 1 year). If this condition exists on a project site, the GEOR is required to include notes and quantities on the plans that instruct the Contractor to maintain the rideability and safety of the existing pavement section. See Section 10.2.1 for additional requirements that were used to develop the Performance Limits.

#### **10.9.1.2 Performance Limits**

The following embankment Performance Limits have been developed to meet the Performance Objective indicated in Section 10.9.1.1. The embankment Performance Limits at the Service limit state are presented in Tables 10-12 to 10-14. Embankment deformation descriptions are found in Section 10.6.

**Table 10-12, Embankment (Pavement) Performance Limits**

Deformation ID No.	Service Limit State Performance Limit Description	
		Minimum Design Life (Years)
EV-01A	Maximum Settlement from Elastic Compression + Primary Consolidation + Secondary Compression along the profile grade <sup>1</sup> that occurs during the duration of the construction of the embankment commences at the start of construction and terminates just prior to paving operations. This deformation is used to adjust borrow requirements, if necessary	NL
EV-01B	Maximum Settlement from Primary Consolidation + Secondary Compression along the profile grade <sup>1</sup> over the design life <sup>2</sup> of the embankment. The design life begins after the pavement has been placed (i.e., the settlement that occurs after EV-01A).	3"
EV-03	Maximum Differential Settlement from Primary Consolidation + Secondary Compression occurring longitudinally along the profile grade after the roadway has been paved. Differential ratio is shown in parenthesis for informational purposes. (Inches per 50 Feet of Embankment Longitudinally)	1" (1/600)

<sup>1</sup>The longitudinal location of EV-01 shall be noted (i.e., at end of approach slab, at Sta. XX+XX, etc.)

<sup>2</sup>Design life of 20 years shall be used.

NL – No Limit; however EV-01A shall be reported.

**Table 10-13, Embankment Widening Performance Limits**

Deformation ID No.	Service Limit State Performance Limit Description	
		Minimum Design Life (Years)
EV-04	Maximum Vertical Differential Settlement occurring transverse to the adjusted profile grade between the existing embankment and the new widened embankment after the roadway has been paved. (Inches per 5 Feet of Embankment Transverse)	0.2" (1/300)

**Table 10-14, Bridge/Embankment Transition Settlement Performance Limit**

Deformation ID No.	Service Limit State Performance Limit Description	
		Minimum Design Life (Years)
EV-05A	Maximum Differential Settlement ( $\delta_v$ ) between the bridge End Bent and the end of the Approach Slab after the roadway has been paved at the end of the pavement design life (20 yrs). The Approach Slab length ( $L_{Slab}$ ) is measured in feet.	$0.05 \times L_{Slab}$
EV-05B	Maximum Differential Settlement ( $\delta_v$ ) between the bridge End Bent and a point 1 foot from either the "begin" or "end" of bridge after the roadway has been paved at the end of the pavement design life (20 yrs).	0.5"

## 10.9.2 Extreme Event I Limit State

### 10.9.2.1 Performance Objective

The Performance Objective for embankments at the EE I limit state is that bridge embankments do not adversely affect bridge structures during the design seismic event. Mitigation may be required to meet the required Performance Objectives. Mitigation shall be limited longitudinally



to that extent which is required to satisfy the Bridge (Global) Seismic Performance Objectives (Seismic Specs). For a more detailed discussion of Performance Objectives during the design seismic event see Section 10.2.

### 10.9.2.2 Performance Limits

If vertical displacement is the only anticipated movement (i.e., there is no global instability), there are no limits to the amount of settlement that can occur within the embankment; however the amount of settlement induced by the EE I within the bridge embankment shall be reported. The only Performance Limit related to settlement established in this Manual will be at the transition from the embankment to the bridge. It is noted that the settlements provided in Table 10-15 are a guide only and that the actual Performance Limits shall be established by the design team based on the Performance Objectives. All Performance Limits shall be submitted to SCDOT for review and concurrence by the PC/SDS and PC/GDS. The remaining embankment Performance Limits shall be developed by the design team to meet the Performance Objective indicated in Section 10.9.2.1. However, the settlement anticipated at the end bent shall be converted into downdrag loads as described in Chapter 16 and shall be included in the design of the end bent foundations. Embankment deformation descriptions are found in Section 10.6. For a more detailed discussion of Performance Objectives during the design seismic event see Section 10.2.

**Table 10-15, Bridge/Embankment Transition Settlement Performance Limit**

Deformation ID No.	EE I Limit State Performance Limit Description	Design EQ	OC		
			I	II	III
EV-05A	Maximum Vertical Differential Settlement between the bridge End Bent and the End of the Approach Slab (Inches). The Approach Slab length ( $L_{\text{Slab}}$ ) is measured in feet.	FEE	0.200 $L_{\text{Slab}}$	0.400 $L_{\text{Slab}}$	NL
		SEE	0.400 $L_{\text{Slab}}$	NL	NL
EV-05B	Maximum Differential Settlement ( $\delta_v$ ) between the bridge End Bent and a point 1 foot from either the "begin" or "end" of bridge.	FEE	2"	8"	NL
		SEE	8"	NL	NL

NL – No limit; low probability of collapse; anticipated displacement shall be reported and considered by the design team

### 10.9.3 Extreme Event II Limit State

#### 10.9.3.1 Performance Objective

The embankment Performance Objectives at the EE II (check flood (500-yr flow event)) limit state is that settlement is not allowed. Therefore, there are no Performance Limits established. Performance Objectives for the EE II (collision/impact loadings only) is not required since embankments are not typically effected by collision or impact loading. However, Performance Objectives and Performance Limits may be established by the design team, if the necessity is determined by the design team, and shall have the concurrence and acceptance of the PC/SDS and the PC/GDS.

## **10.10 PERFORMANCE LIMITS FOR EARTH RETAINING STRUCTURES**

### **10.10.1 Service Limit State**

#### **10.10.1.1 Performance Objective**

The Performance Objectives for ERSs at the Service limit state are that the ERS remains fully functional for the design life (20 years shall be used for determining movements of the ERS; however 100 years shall be used for the design life of the structural components) and that through periodic maintenance any deformations can be adjusted to maintain the serviceability requirements. See Section 10.2.1 for additional requirements that were used to develop the Performance Limits.

#### **10.10.1.2 Performance Limits**

Geotechnical Performance Limits have been developed for Fill ERSs and Cut ERSs in Tables 10-16 and 10-17, respectively. These Performance Limits have been developed to meet the Performance Objective indicated in Section 10.10.1.1. ERS deformation descriptions are defined in Section 10.7. It should be noted that at no time will negative batter (i.e., the ERS leans outward from plumb) be acceptable under Service limit state conditions. All ERSs shall be designed and constructed with positive batter that shall be large enough to account for any movements required to develop full active earth pressures.

Deformation ID No.		Service Limit State Performance Limit Description		
Settlement	RV-01A	Maximum Settlement from Elastic Compression + Primary Consolidation + Secondary Compression along the top of wall profile grade that occurs during the construction of the ERS and commences immediately after construction begins and terminates just prior to paving operations. This deformation is used to adjust borrow and ERS height requirements, if necessary. (Inches)		NL <sup>1</sup>
	RV-01B	Maximum Settlement from Primary Consolidation + Secondary Compression along the profile grade over the design life <sup>2</sup> of the pavement behind the ERS. The design life begins after the pavement has been placed (i.e. the settlement that occurs after RV-01A). (Inches)		2"
	RV-03A	Longitudinal	Maximum Differential Settlement from Elastic Compression + Primary Consolidation + Secondary Compression occurring longitudinally along the ERS profile grade (i.e. top of ERS) during construction. (Inches/50 feet along the length of ERS regardless of ERS type)	NL
			Maximum Differential Settlement from Primary Consolidation + Secondary Compression occurring longitudinally along the ERS profile grade (i.e. top of ERS) post construction. (Inches/50 feet along the length of ERS) (Maximum settlement ratio indicated in parenthesis for informational purposes only)	1" (1/600) 1" (1/600) 2" (1/300) 2-1/2" (1/240) 6" (1/100)
	RV-03B		Rigid/Semi-Rigid walls MSE w/Full Height Panel Facing MSE Panel Facing Joint Spacing $\geq$ 1/2 inches MSE w/Block or Gabion Facing Gabion Wall	
	RV-04A <sup>3</sup>	Transverse	The absolute value of the Maximum Differential Settlement observed perpendicular (transverse) to the top of the wall profile during construction of the wall. (Inches/5 feet perpendicular to wall or slope face)	NL
	RV-04B <sup>3</sup>		The absolute value of the Maximum Differential Settlement observed perpendicular (transverse) to the top of the wall profile after construction of the wall. <sup>4</sup> (Inches/5 feet perpendicular to wall or slope face)	0.150 L <sub>Reinf</sub>
	RV-06A <sup>3</sup>		Maximum Settlement from Elastic Compression + Primary Consolidation + Secondary Compression at the termination of the reinforcement that occurs during the construction of the ERS and commences immediately after construction begins and terminates just prior to paving operations.	NL
	RV-06B <sup>3</sup>		Maximum Settlement from Primary Consolidation + Secondary Compression at the termination of the reinforcement that occurs over the design life <sup>5</sup> of the pavement behind the ERS. The design life begins after the pavement has been placed (i.e. the settlement that occurs after RV-06A).	14"
	Lateral Displ. <sup>6</sup>	RL-01	Maximum Lateral Displacement at the top of the wall. <sup>6</sup> (Inches)	All Earth Retaining Structures
RL-02		Maximum Differential Lateral Displacement longitudinally along the top of the wall. (Inches/50 feet of wall)	All Earth Retaining Structures	1"

NL – No limit; however, displacements shall be reported; anticipated displacements shall be considered by the design team.  
<sup>1</sup>A limit of 12 inches shall be used for all MSE walls with rigid facing elements as the demarcation between single stage and multi-stage construction.  
<sup>2</sup>The Minimum Design Life is based on an anticipated repaving cycle of 20 years.  
<sup>3</sup>RV-04 and RV-06 apply only to MSE Walls w/Panel, Block or Gabion Facing, and Reinforced Soil Slopes  
<sup>4</sup>The soil reinforcement length (L<sub>Reinf</sub>) is measured in feet.  
<sup>5</sup>At no point in time will negative batter be acceptable.  
<sup>6</sup>The wall height (H<sub>Wall</sub>) is measured in feet. For the reinforced soil slopes the H<sub>Wall</sub> is the vertical distance from the toe of the slope to shoulder edge.

Table 10-16, Fill ERS Performance Limits at Service Limit State

Deformation ID No.		Service Limit State Performance Limit Description	
Settlement	RV-01A	Maximum Settlement from Elastic Compression + Primary Consolidation + Secondary Compression along the top of wall profile grade that occurs during the construction of the ERS and commences immediately after construction begins and terminates just prior to paving operations. This deformation is used to adjust borrow and ERS height requirements, if necessary. (Inches)	NL
	RV-01B	Maximum Settlement from Primary Consolidation + Secondary Compression along the profile grade over the design life <sup>1</sup> of the pavement behind the ERS. The design life begins after the pavement has been placed (i.e. the settlement that occurs after RV-01A). (Inches)	2"
	RV-03A	Maximum Differential Settlement from Elastic Compression + Primary Consolidation + Secondary Compression occurring longitudinally along the ERS profile grade (i.e. top of ERS) during construction. (Inches/50 feet along the length of ERS regardless of ERS type)	NL
			1-1/2" (1/400)
	RV-03B	Maximum Differential Settlement from Primary Consolidation + Secondary Compression occurring longitudinally along the ERS profile grade (i.e. top of ERS) post construction. (Inches/50 feet along the length of ERS) (Maximum settlement ratio indicated in parenthesis for informational purposes only)	
	RV-04A <sup>1</sup>	The absolute value of the Maximum Differential Settlement observed perpendicular (transverse) to the top of the wall profile during construction of the wall. (Inches/5 feet perpendicular to wall or slope face)	NL
	RV-04B <sup>1</sup>	The absolute value of the Maximum Differential Settlement observed perpendicular (transverse) to the top of the wall profile after construction of the wall. <sup>3</sup> (Inches/5 feet perpendicular to wall or slope face)	0.100 L <sub>Anchor</sub>
	RV-06A <sup>1</sup>	Maximum Settlement from Elastic Compression + Primary Consolidation + Secondary Compression at the termination of the reinforcement that occurs during the construction of the ERS and commences immediately after construction begins and terminates just prior to paving operations.	NL
	RV-06B <sup>1</sup>	Maximum Settlement from Primary Consolidation + Secondary Compression at the termination of the reinforcement that occurs over the design life <sup>1</sup> of the pavement behind the ERS. The design life begins after the pavement has been placed (i.e. the settlement that occurs after RV-06A).	14"
	RL-01	Maximum Lateral Displacement at the top of the wall. <sup>5</sup> (Inches)	0.050 H <sub>Wall</sub>
RL-02	Maximum Differential Lateral Displacement longitudinally along the top of the wall. (Inches/50 feet of wall)	1"	

Table 10-17, Cut ERS Performance Limits at Service Limit State

NL – No limit; however, displacements shall be reported; anticipated displacements shall be considered by the design team.  
<sup>1</sup>The Minimum Design Life is based on an anticipated repaving cycle of 20 years.  
<sup>2</sup>RV-04 and RV-06 apply only to walls with In-Situ reinforcement.  
<sup>3</sup>The soil anchor length (L<sub>Anchor</sub>) is measured in feet.  
<sup>4</sup>At no point in time will negative batter be acceptable.  
<sup>5</sup>The wall height (H<sub>Wall</sub>) is measured in feet. For the reinforced soil slopes the H<sub>Wall</sub> is the vertical distance from the toe of the slope to shoulder edge.

## **10.10.2 Extreme Event I Limit State**

### **10.10.2.1 Performance Objective**

The Performance Objective for ERSs at the EE I limit state is that ERSs located at or beneath a bridge do not adversely affect the bridge structure during the design seismic event. Mitigation may be required to meet the required Performance Objectives. Mitigation shall be limited longitudinally to that extent which is required to satisfy the Bridge (Global) Seismic Performance Objectives (Seismic Specs). The exception to this is if the ERS extends beyond bridge embankments then the mitigation may need to be extended. For those ERSs that are located completely beyond the bridge embankment, the ERS should not collapse. For a more detailed discussion of Performance Objectives during the design seismic event see Section 10.2

### **10.10.2.2 Performance Limits**

If there is no global instability, there is no limit to the amount of settlement or lateral displacement that can occur with an ERS during the EE I. However the amount of settlement (RV-01B, RV-03B, RV-04B and RV-06B) and lateral displacement (RL-01 and RL-02) at the face of the ERS induced by the EE I within the bridge embankment shall be reported. It is anticipated that the Performance Limit related to settlement at the transition from the embankment supported by the ERS to the bridge shall govern design. The ERS Performance Limits shall be developed by the design team to meet the Performance Objective indicated in Section 10.10.2.1. However, the settlement anticipated at the end bent shall be converted into downdrag loads as described in Chapter 16 and shall be included in the design of the end bent foundations. Lateral displacements shall be used to determine structural forces on the ERS system to prevent structural failure of the system. In addition, the design team shall consider the area immediately adjacent to the wall when determining the Performance Limits. The area immediately adjacent to the wall shall begin at either the base or the top of the wall and shall extend a minimum of 1.1 times the height of the wall (i.e.,  $1.1H_{Wall}$ ) either in front of the wall or behind the wall. ERS deformation descriptions are found in Section 10.7. For a more detailed discussion of Performance Objectives during the design seismic event see Section 10.2.

## **10.10.3 Extreme Event II Limit State**

### **10.10.3.1 Performance Objective**

The ERS Performance Objectives at the EE II (check flood (500-yr flow event)) limit state is that settlement is not allowed. However, Performance Objectives at the EE II (check flood (500-yr flow event)) limit state shall be established by the design team to conform to the overall requirements of the project. Therefore, the design team shall establish Performance Limits and shall have the concurrence and acceptance of the RPG/SDS and the RPG/GDS. Performance Objectives for the EE II (collision/impact loadings only) are required since an ERS is potentially affected at either the top of the ERS or at the bottom of the ERS by the collision or impact loading. However, Performance Objectives and Performance Limits shall be established by the design team, if the necessity is determined by the design team, and shall have the concurrence and acceptance of the PC/SDS and the PC/GDS. In addition, the design team shall consider the effects of the collision/impact loading on the structural elements that compose the ERS.

## 10.11 REFERENCES

American Association of State Highway and Transportation Officials, (2017), AASHTO LRFD Bridge Design Specifications Customary U.S. Units, 8<sup>th</sup> Edition, American Association of State Highway and Transportation Officials, Washington, D.C.

South Carolina Department of Transportation, (2006), Bridge Design Manual, South Carolina Department of Transportation, <https://www.scdot.org/business/structural-design.aspx>.

South Carolina Department of Transportation, (2008), Seismic Design Specifications for Highway Bridges, South Carolina Department of Transportation, <https://www.scdot.org/business/structural-design.aspx>.

**Chapter 11**

**SOUTH CAROLINA**  
**GEOLOGY AND SEISMICITY**

**GEOTECHNICAL DESIGN MANUAL**

*January 2019*





## Table of Contents

<u>Section</u>	<u>Page</u>
11.1 Introduction.....	11-1
11.2 South Carolina Geology.....	11-1
11.3 Blue Ridge Unit.....	11-5
11.4 Piedmont Unit.....	11-5
11.5 Fall Line.....	11-6
11.6 Coastal Plain Unit.....	11-6
11.6.1 Lower Coastal Plain.....	11-8
11.6.2 Middle Coastal Plain.....	11-8
11.6.3 Upper Coastal Plain.....	11-8
11.7 South Carolina Seismicity.....	11-9
11.7.1 Central and Eastern United States Seismicity.....	11-9
11.7.2 SC Seismic Event Intensity.....	11-10
11.8 South Carolina Seismic Sources.....	11-12
11.8.1 Non-Characteristic Seismic Sources.....	11-12
11.8.2 Characteristic Seismic Sources.....	11-15
11.9 South Carolina Seismic Hazards.....	11-16
11.9.1 Design Seismic Events.....	11-16
11.9.2 Probabilistic Seismic Hazard Maps.....	11-16
11.9.3 Seismic Event Deaggregation Charts.....	11-21
11.9.4 Ground Motions.....	11-22
11.10 References.....	11-24

**List of Tables**

<b><u>Table</u></b>	<b><u>Page</u></b>
Table 11-1, Modified Mercalli Intensity Scale .....	11-10
Table 11-2, Source Areas for Non-Characteristic Background Events.....	11-14
Table 11-3, Coastal Plain Geologically Realistic Model .....	11-17
Table 11-4, Geologically Realistic Model Outside of Coastal Plain .....	11-18
Table 11-5, Site Conditions .....	11-18
Table 11-6, Latitude and Longitude for South Carolina Cities.....	11-19
Table 11-7, Location of Ground Motion .....	11-23

**List of Figures**

<b><u>Figure</u></b>	<b><u>Page</u></b>
Figure 11-1, South Carolina Physiographic Units .....	11-2
Figure 11-2, Generalized Geologic Map of South Carolina.....	11-3
Figure 11-3, Geologic Time Scale for South Carolina.....	11-4
Figure 11-4, South Carolina “Fall Line” .....	11-6
Figure 11-5, Contour Map of Coastal Plain Sediment Thickness.....	11-7
Figure 11-6, U.S. Seismic Events Causing Damage 1750 – 1996.....	11-10
Figure 11-7, Interpreted MMI for the 1886 Charleston Seismic Event.....	11-11
Figure 11-8, Interpreted Seismic Event MMI by County.....	11-12
Figure 11-9, Source Areas for Non-Characteristic Seismic Events.....	11-13
Figure 11-10, Alternative Source Areas for Non-Characteristic Seismic Events .....	11-13
Figure 11-11, Southeastern U.S. Seismic Events ( $M_w > 3.0$ from 1600 to Present) ..	11-14
Figure 11-12, South Carolina Characteristic Seismic Sources.....	11-15
Figure 11-13, SCDOT Site Condition Selection Map .....	11-17
Figure 11-14, Scenario_PC (2006) Sample Output for Columbia, SC .....	11-19
Figure 11-15, SEE Seismic Hazard Curves for Various Periods.....	11-20
Figure 11-16, FEE UHS Curves for Selected South Carolina Cities .....	11-20
Figure 11-17, SEE UHS Curves for Selected South Carolina Cities .....	11-21
Figure 11-18, Scenario_PC (2006) Deaggregation – Columbia, SC.....	11-21



# CHAPTER 11

## SOUTH CAROLINA GEOLOGY AND SEISMICITY

### 11.1 INTRODUCTION

This Chapter describes South Carolina's basic geology and seismicity within the context of performing geotechnical engineering for SCDOT. It is anticipated that the material contained in this Chapter will establish a technical framework by which basic geology and seismicity can be addressed. It is not intended to be an in-depth discussion of all the geologic formations and features found in South Carolina (SC) or a highly technical discussion of the state's seismicity. The GEORs are expected to have sufficient expertise in these technical areas and to have the foresight and resourcefulness to keep up with the latest advancements in these areas.

The State of South Carolina is located in the Southeastern United States and is bounded on the north by the State of North Carolina, on the west and the south by the State of Georgia, and on the east by the Atlantic Ocean. The State is located between Latitudes 32° 4' 30" N and 35° 12' 00" N and between Longitudes 78° 0' 30" W and 83° 20' 00" W. The State is roughly triangular in shape and measures approximately 260 miles East-West and approximately 200 miles North-South at the states widest points. The South Carolina coastline is approximately 187 miles long. South Carolina is ranked 40<sup>th</sup> in size in the United States with an approximate total area of 31,189 square miles.

The geology of South Carolina is similar to that of the neighboring states of Georgia, North Carolina, and Virginia. These states have an interior consisting of the Appalachian Mountains with an average elevation of 3,000 feet. Just east of the Appalachian Mountains is the Piedmont region that typically ranges in elevation from 300 feet to 1000 feet. Continuing eastward from these highlands is a "Fall Line" which serves to transition into the Atlantic Coastal Plain. The Atlantic Coastal Plain gently slopes towards the Atlantic Ocean with few elevations higher than 300 feet.

The 1886 seismic event that occurred in the Coastal Plain near Charleston, South Carolina dominates the seismic history of the southeastern United States. It is the largest historic seismic event in the southeastern United States with an estimated moment magnitude ( $M_w$ ) of 7.3. The damage area with a Modified Mercalli Intensity (MMI) scale of X, is an elliptical shape roughly 20 by 30 miles trending northeast between Charleston and Jedburg and including Summerville and roughly centered at Middleton Place. The intraplate epicenter of this seismic event and its magnitude is not unique in the Central and Eastern United States (CEUS). Other intraplate seismic events include those at Cape Ann, Massachusetts (1755) with an estimated  $M_w$  of 5.9, and New Madrid, Missouri (1811-1812) with an estimated  $M_w$  of at least 7.7.

The following Sections describe the basic geology of South Carolina and the seismicity that will be used to perform geotechnical engineering designs and analyses. The topics discussed in these Sections will be referenced throughout this Manual.

### 11.2 SOUTH CAROLINA GEOLOGY

South Carolina geology can be divided into 3 basic physiographic units: Blue Ridge Unit (Appalachian Mountains), Piedmont Unit, and the Coastal Plain Unit. The generalized locations of these physiographic units are shown in Figure 11-1.

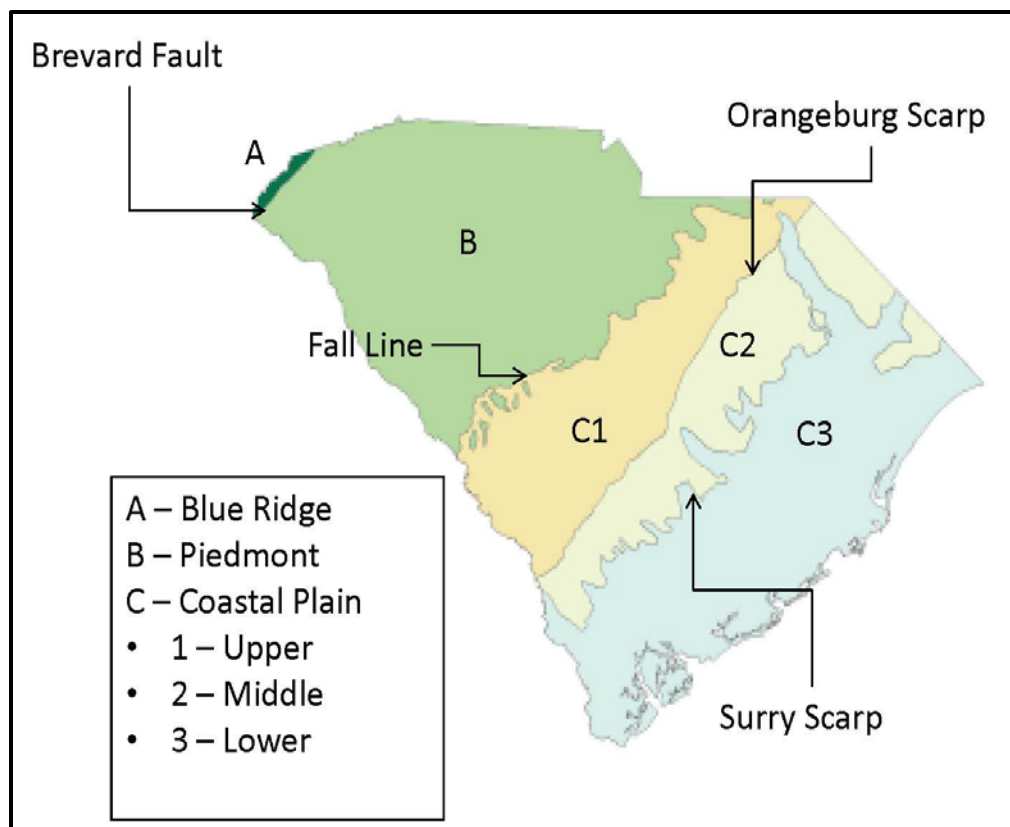


**Figure 11-1, South Carolina Physiographic Units (SCDNR (2013))**

The Blue Ridge Unit (Appalachian Mountains) covers approximately 2 percent of the state and is located in the northwestern corner of the state. The Blue Ridge Unit is separated from the Piedmont Unit by the Brevard Fault. The Piedmont Unit comprises approximately one-third of the state with the Coastal Plain Unit covering the remaining two-thirds of the state. The Piedmont and Coastal Plain Units are separated by the “Fall Line” as indicated in Figure 11-1. The geologic formations are typically aligned from the South-Southwest to the North-Northeast and parallel the South Carolina Atlantic coastline as shown in the generalized geologic map in Figure 11-2. The physiographic units in Figure 11-2 are broken down by the geologic time of the surface formations. South Carolina formations span in age from late Precambrian through the Quaternary period. The descriptions of events that have occurred over geologic time in South Carolina are shown in Figure 11-3. Please note that the term “Tertiary” is used in Figure 11-3; however, the Tertiary Period has been divided into the Paleogene and Neogene Periods by the International Commission on Stratigraphy, a subunit of the International Union of Geological Sciences. For the purposes of the GDM the term Tertiary Period will be deleted and replaced by Paleocene and Neogene Periods.

A description of the geologic formations, age, and geologic features for the Blue Ridge, Piedmont, and Coastal Plain Physiographic Units are provided in the following Sections.

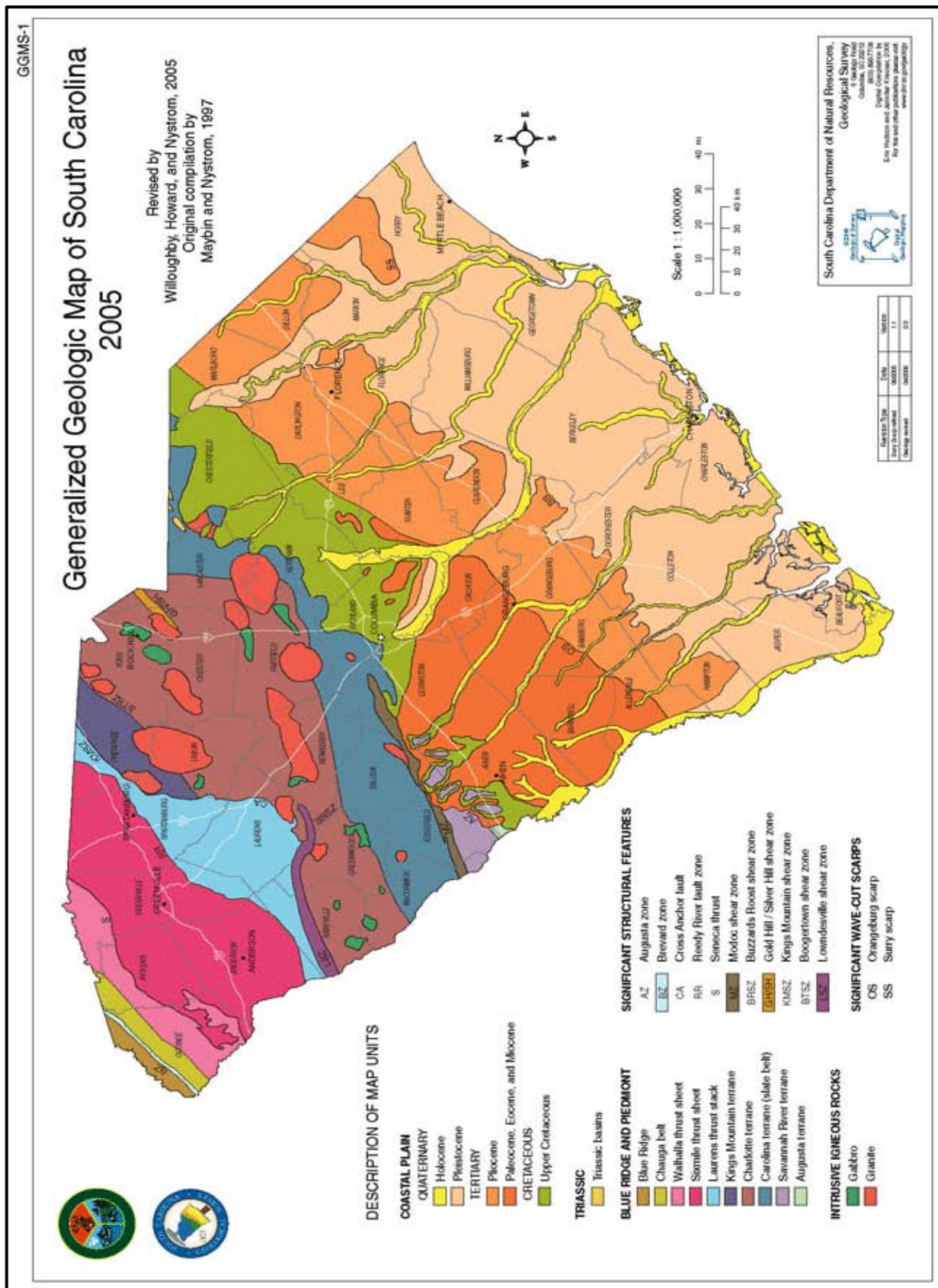


Figure 11-2, Generalized Geologic Map of South Carolina (SCDNR (2005))



**Figure 11-3, Geologic Time Scale for South Carolina (SCDNR (1998))**



### 11.3 BLUE RIDGE UNIT

The Blue Ridge Unit consists of mountains that are part of the Blue Ridge Mountains and is a southern continuation of the Appalachian Mountains. The Brevard Fault zone (depicted as the Brevard zone, BZ, in Figure 11-2) separates the Blue Ridge Unit from the Piedmont Unit. It consists of metamorphic and igneous rocks. The topography is rugged and mountainous and contains the highest elevations in the State of South Carolina with elevations ranging from 1,400 feet to 3,500 feet. Sassafras Mountain is the highest point in South Carolina with an elevation of 3,560 feet. The Appalachian Mountains were formed in the late Paleozoic Era, about 342 MYA. The basement rocks in the Blue Ridge Unit were formed in the late Precambrian time period (570 to 2,500 MYA). The oldest rock dated in South Carolina is 1,200 million years old.

The bedrock in this region is a complex crystalline formation that has been faulted and contorted by past tectonic movements. The rock has weathered to residual soils that form the mantle for the hillsides and hilltops. The typical residual soil profile in areas not disturbed by erosion or the activities of man consists of clayey soils near the surface where weathering is more advanced, underlain by sandy silts and silty sands. There may be colluvial (old land-slide) material on the slopes.

### 11.4 PIEDMONT UNIT

The Piedmont Unit is bounded on the west by the Blue Ridge Unit and on the east by the Coastal Plain Unit. The boundary between the Blue Ridge Unit and the Piedmont Unit is typically assumed to be the Brevard Fault zone (depicted as the Brevard zone, BZ, in Figure 11-2). The common boundary between the Piedmont Unit and the Coastal Plain Unit is the "Fall Line". It is believed that the Piedmont is the remains of an ancient mountain chain that has been heavily eroded with existing elevations ranging from 300 feet to 1,400 feet. The Piedmont is characterized by gently rolling topography, deeply weathered bedrock, and relatively few rock outcrops. It contains monadnocks that are isolated outcrops of bedrock (usually quartzite or granite) that are a result of the erosion of the mountains. The vertical stratigraphic sequence consists of 5 to 70 feet of weathered residual soils at the surface underlain by metamorphic and igneous basement rocks (granite, schist, and gneiss). The weathered soils (saprolites) are physically and chemically weathered rocks that can be soft/loose to very hard and dense, or friable and typically retain the structure of the parent rock. The geology of the Piedmont is complex with numerous rock types that were formed during the Paleozoic Era (250 to 570 MYA).

The typical residual soil profile consists of clayey soils near the surface, where soil weathering is more advanced, underlain by sandy silts and silty sands. The boundary between soil and rock is not sharply defined. This transitional zone termed "partially weathered rock" (PWR) is normally found overlying the parent bedrock. Partially weathered rock is defined, for engineering purposes, as residual material with Standard Penetration Test resistances exceeding 100 blows/foot. The partially weathered rock is considered in geotechnical engineering as an Intermediate Geomaterial (IGM) (see Chapter 6 for more discussion of IGM). Weathering is facilitated by fractures, joints, and by the presence of less resistant rock types. Consequently, the profile of the partially weathered rock and hard rock is quite irregular and erratic, even over short horizontal distances. Also, it is not unusual to find lenses and boulders of hard rock and zones of partially weathered rock within the soil mantle, well above the general bedrock level.

## 11.5 FALL LINE

The Fall Line is an unconformity that marks the boundary between an upland region (bed rock) and a coastal plain region (sediment). In South Carolina the Piedmont Unit is separated from the Coastal Plain Unit by a “Fall Line” that begins near the Edgefield-Aiken County line and traverses to the northeast through Lancaster County. In addition to Columbia, SC many cities were built along the “Fall Line” as it runs up the east coast (Macon, Raleigh, Richmond, Washington D.C., and Philadelphia). The “Fall Line” generally follows the southeastern border of the Savannah River terrane formation and the Carolina terrane (slate belt) formation shown in Figure 11-2. Along the “Fall Line” between elevations 300 to 725 is the Sandhills formations that are the remnants of a prehistoric coastline. The Sandhills are unconnected bands of sand deposits that are remnants of coastal dunes that were formed during the Miocene Epoch (5.3 to 23 MYA). The land to the southeast of the “Fall Line” is characterized by a gently downward sloping elevation (2 to 3 feet per mile) as it approaches the Atlantic coastline as shown in Figure 11-4. Several rivers such as the Pee Dee, Wateree, Lynches, Congaree, N. Fork Edisto, and S. Fork Edisto flow from the “Fall Line” towards the Atlantic coast as they cut through the Coastal Plain sediments.

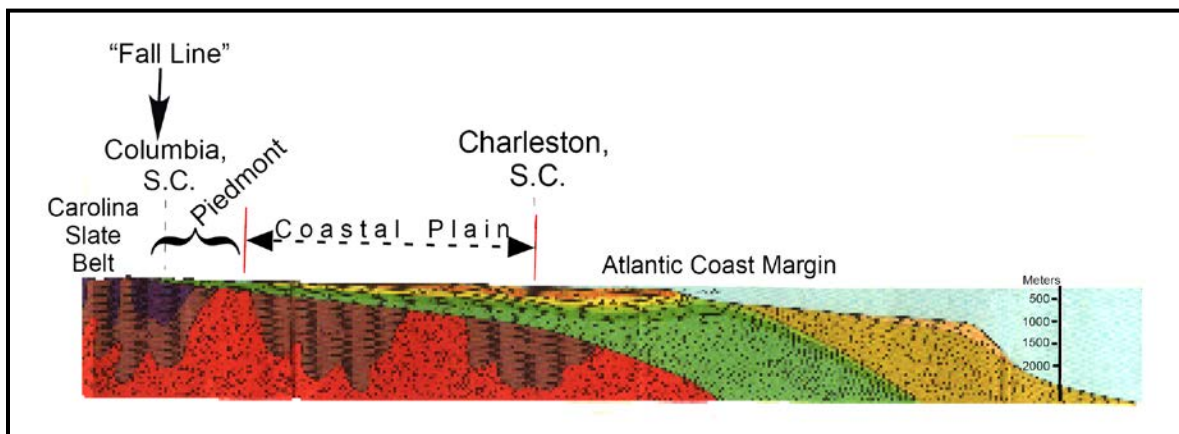


**Figure 11-4, South Carolina “Fall Line”  
(Odum, Williams, Stephenson and Worley (2003))**

## 11.6 COASTAL PLAIN UNIT

The Coastal Plain Unit is a compilation of wedge shaped formations that begin at the “Fall Line” and dip towards the Atlantic Ocean with ground surface elevations typically less than 300 feet. The Coastal Plain is underlain by Mesozoic/Paleozoic basement rock. This wedge of sediment is comprised of numerous geologic formations that range in age from the late Cretaceous Period to Recent. The sedimentary soils of these formations consist of unconsolidated sand, clay, gravel, marl, cemented sands, and limestone that were deposited over the basement rock. The marl and limestone are considered in geotechnical engineering as a cohesive IGM as long as the criteria provided in Chapter 6 is met. The basement rock consists of granite, schist, and gneiss similar to the rocks of the Piedmont Unit. The thickness of the Coastal Plain sediments varies from zero at the “Fall Line” to more than 4,000 feet at the southern tip of South Carolina near Hilton Head Island. The thickness of the Coastal Plain sediments along the Atlantic coast varies from ~1,300 feet at Myrtle Beach to ~4,000 feet at Hilton Head Island. The top of the basement rock beneath the Coastal Plain has been mapped at selected locations where deep wells/borings were performed. The Seismic Hazard Study that was prepared for SCDOT developed contours of the top of the basement rock through interpretation of the available data. Predominantly, sediments lie in nearly horizontal layers; however, erosional episodes occurring between depositions of successive layers are often expressed by undulations in the contacts

between the formations. The contours of the Coastal Plain sediment thickness shown in Figure 11-5 are in meters.

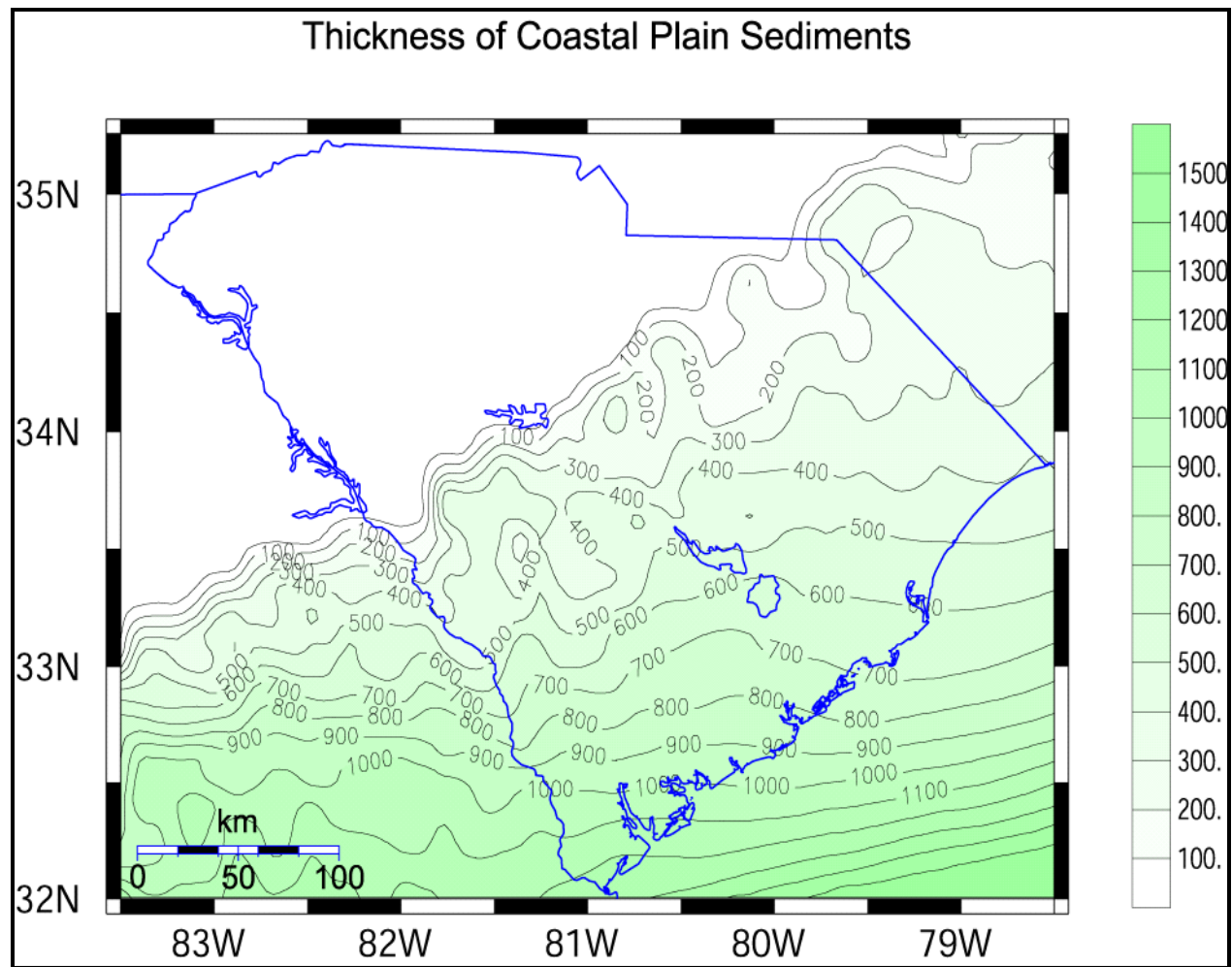


**Figure 11-5, Contour Map of Coastal Plain Sediment Thickness  
(Chapman and Talwani (2002))**

This Coastal Plain Unit was formed during Quaternary, Neogene, Paleogene, and late Cretaceous geologic periods. The Coastal Plain can be divided into the following 3 subunits:

- Lower Coastal Plain
- Middle Coastal Plain
- Upper Coastal Plain

The Lower Coastal Plain comprises approximately one-half of the entire Atlantic Coastal Plain of South Carolina. The Surry Scarp (-SS-) depicted in Figures 11-1 and 11-2 separates the Lower Coastal Plain from the Middle Coastal Plain. The Surry Scarp is a seaward facing scarp with a toe elevation of 90 to 100 feet. The Middle Coastal Plain and the Upper Coastal Plain each compose approximately one fourth of the Coastal Plain area, each. The Orangeburg Scarp (-OS-) depicted in Figures 11-1 and 11-2 separates the Middle Coastal Plain from the Upper Coastal Plain. The Orangeburg Scarp is also a seaward facing scarp with a toe elevation of 250 to 270 feet.

### **11.6.1 Lower Coastal Plain**

The Lower Coastal Plain is typically identified as the area east of the Surry Scarp below elevation 100 feet. However, as seen in Figures 11-1 and 11-2, the Lower Coastal Plain extends beyond both Surry and Orangeburg Scarps along some of the major river valleys in South Carolina. The 2 major river valleys where this occurs are the Pee Dee and Santee River systems. Therefore, Lower Coastal Plain soils may be found west of both scarps in the river valleys. The vertical stratigraphic sequence overlying the basement rock consists of unconsolidated Cretaceous, Paleogene, Neogene, and Quaternary sedimentary deposits. The surface deposits of the Lower Coastal Plain were formed during the Quaternary Period that began approximately 1.6 MYA and extends to present day. The Quaternary Period can be further subdivided into the Pleistocene Epoch (1.6 MYA to 10 thousand years ago) and the Holocene Epoch (10 thousand years ago to present day). The Pleistocene Epoch is marked by the deposition of the surficial soils, the formation of the Carolina Bays and the scarps found throughout the East Coast due to sea level rise and fall. Barrier islands and flood plains along the major rivers were formed during the Holocene Epoch. Preceding the Quaternary Period during the Eocene Epoch (53 to 36.6 MYA) of the Paleogene Period, limestone was deposited in the Lower Coastal Plain.

### **11.6.2 Middle Coastal Plain**

The Middle Coastal Plain is typically identified as the area between the Surry Scarp and the Orangeburg Scarp and falls between elevation 100 feet and 270 feet. The vertical stratigraphic sequence overlying the basement rock consists of unconsolidated Cretaceous, Paleogene and Neogene sedimentary deposits. The surface deposits of the Middle Coastal Plain were formed during the Pliocene Epoch of the Neogene Period. During the Pliocene Epoch (5.3 to 1.6 MYA) of the Neogene Period, the Orangeburg Scarp was formed as a result of scouring from the regressive cycles of the Ocean as it retreated. During the Eocene Epoch (53 to 36.6 MYA) of the Paleogene Period, limestone was deposited in the Middle Coastal Plain.

### **11.6.3 Upper Coastal Plain**

The Upper Coastal Plain is typically identified as the area between the Orangeburg Scarp and the "Fall Line" and has elevations between 270 feet and 300 feet. The Upper Coastal Plain was formed during the Paleogene, Neogene and late Cretaceous Periods. The Paleogene Period began approximately 65 MYA and ended approximately 23 MYA and is subdivided into the Paleocene, Eocene and Oligocene Epochs. The Neogene Period began approximately 23 MYA and ended approximately 1.6 MYA and is subdivided into the Miocene and Pliocene Epochs. The Miocene Epoch (23 to 5.3 MYA) is marked by the formation of the Sandhills dunes as a result of fluvial deposits over the Coastal Plain. During the early Paleogene Period (65 to 23 MYA) fluvial deposits over the Coastal Plain consisted of marine sediments, limestone, and sand. The Upper Coastal Plain is formed of older, generally well-consolidated layers of sands, silts, or clays that were deposited by marine or fluvial action during a period of retreating ocean shoreline. Due to their age, sediments exposed at the ground surface are often heavily eroded. Ridges and hills are either capped by terrace gravels or wind-deposited sands. Younger alluvial soils may mask these sediments in swales or stream valleys.

## 11.7 SOUTH CAROLINA SEISMICITY

### 11.7.1 Central and Eastern United States Seismicity

Even though seismically active areas in the United States are generally considered to be in California and the Western United States (WUS), historical records indicate that there have been major seismic events in the Central and Eastern United States (CEUS) that have not only been of equal or greater magnitude but that have shaken broader areas of the CEUS. The United States Geologic Survey (USGS) map shown in Figure 11-6 indicates seismic events that have caused damage within the United States between 1750 and 1996. Of particular interest to South Carolina is the 1886 seismic event in Charleston, SC that has been estimated to have an  $M_w$  of approximately 7.3. In addition, the upstate of South Carolina underwent a moderate seismic event in 1913 in Union County, SC having an  $M_w$  of approximately 5.5. Also of interest to the northwestern end of South Carolina is the influence of the New Madrid seismic zone, near New Madrid, Missouri, where historical records indicate that between 1811 and 1812 there were several large seismic events with an  $M_w$  of at least 7.7.

The CEUS is located in the approximate middle of the North American tectonic plate. Specifically, Charleston, SC lies along the modern coastline with the Atlantic Ocean. Typically, seismic events occur along the margins of tectonic plates, where the plates either slide past each other; one plate overrides the adjoining plate (subduction); or the plates push apart with new plates being formed by volcanism (e.g., the mid-Atlantic Ridge). As indicated previously, South Carolina is located in the approximate middle of the North American Plate. The source of the seismic events in SC appears to be from partially formed rift valleys that have been infilled; therefore, covering and obscuring the rift valley (Stein, Pozzaglia, Meltzer, Wolin, Kafka and Berti (2013), Fillingim (1999)). The infilling of these ancient rift valleys has erased any evidence of the valley at the existing ground surface. Fillingim (1999) has also identified stress concentrations and high heat flow as possible causes of CEUS seismic events. Further evidence for faulting beneath SC is provided by Durá-Gómez and Talwani (2009) as the Zone of River Anomalies (ZRA) that appears to provide evidence that the faulting is strike-slip in nature. Unfortunately, this is all speculative given the lack of evidence at the existing ground surface.



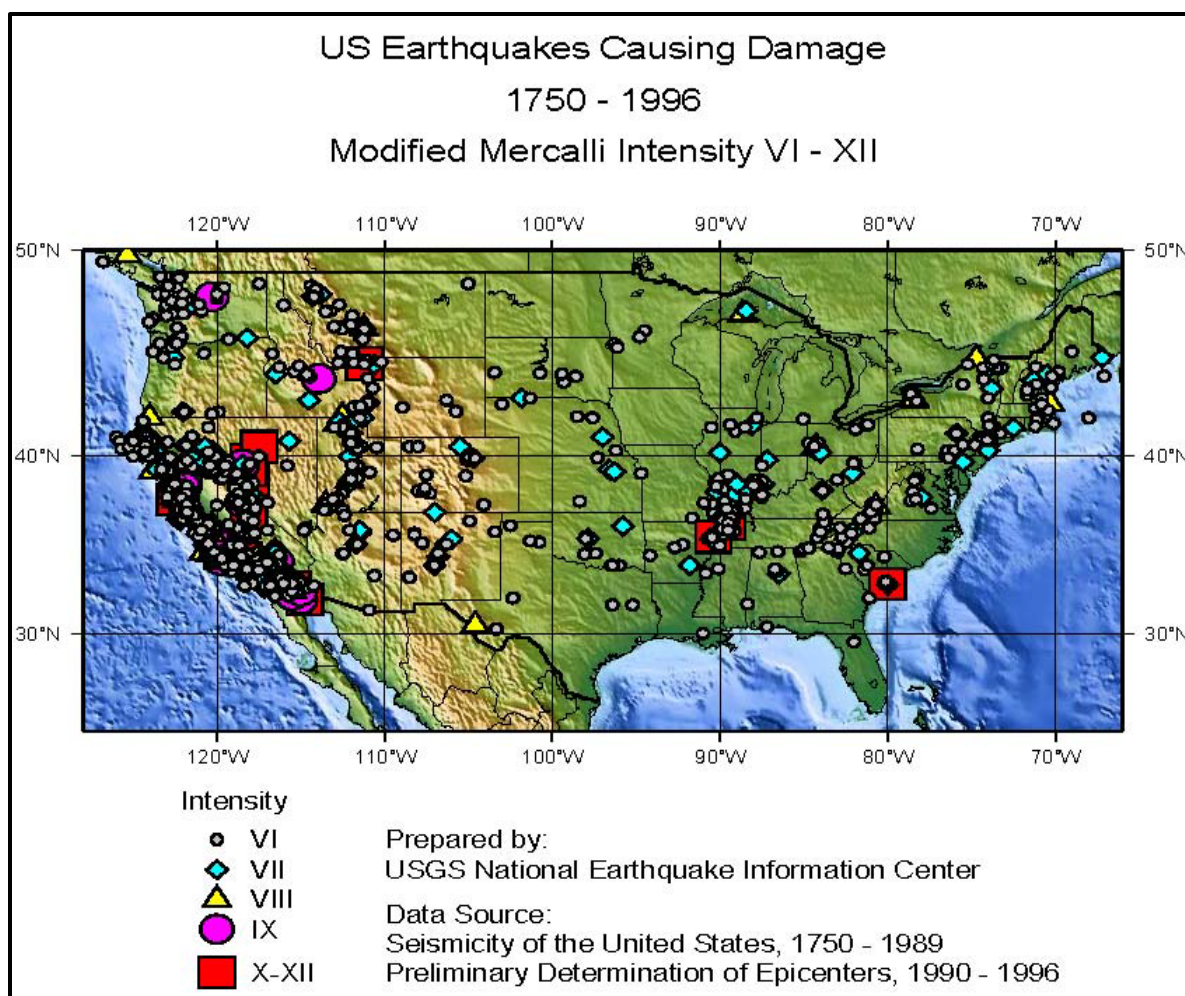


**Figure 11-6, U.S. Seismic Events Causing Damage 1750 – 1996 (USGS Website (2012b))**

### 11.7.2 SC Seismic Event Intensity

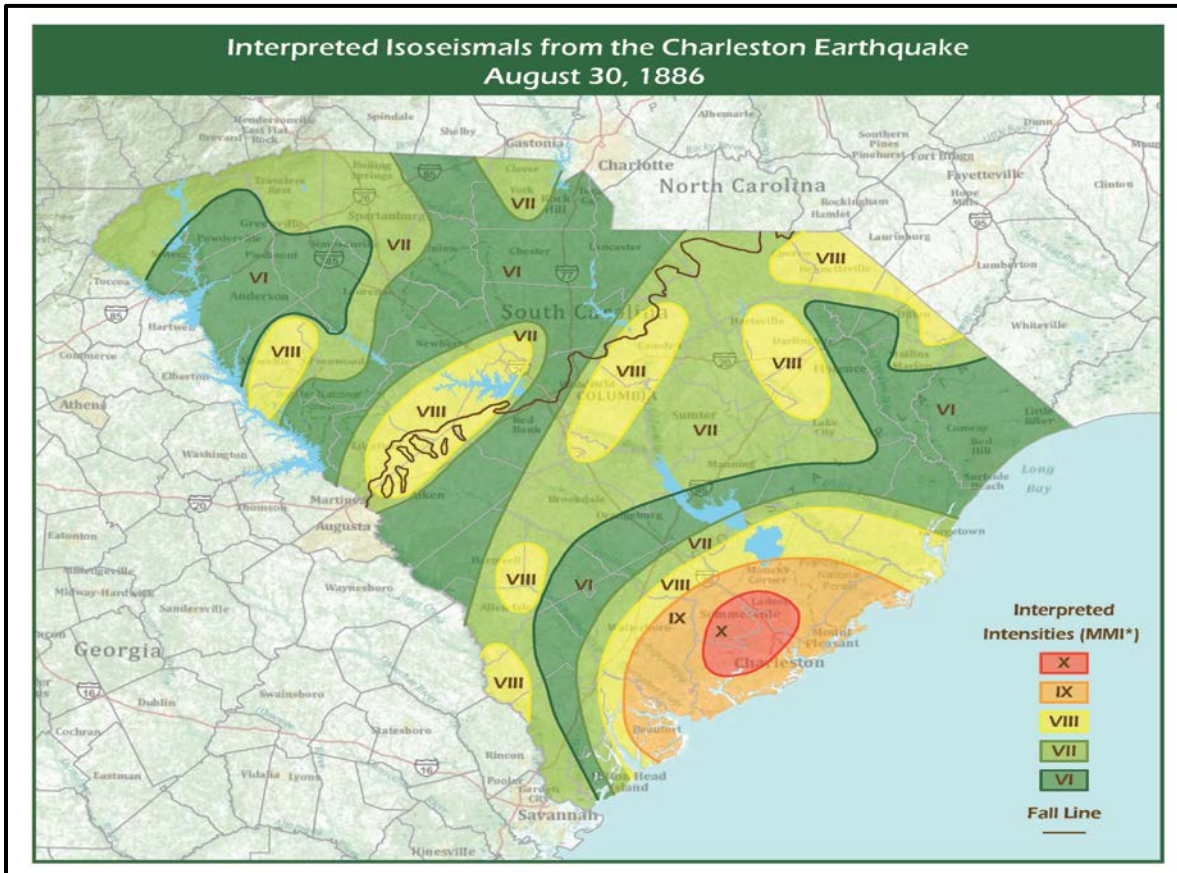
The Modified Mercalli Intensity (MMI) scale is a qualitative measure of the strength of ground shaking at a particular site that is used in the United States. Each seismic event large enough to be felt will have a range of intensities. Typically the highest intensities are measured near the seismic event epicenter and lower intensities are measured farther away. The MMI scale is used to distinguish how the ground shaking is felt at different geographic locations as opposed to the moment magnitude scale that is used to compare the energy released by the seismic event. Roman numerals are used to identify the MMI scale of ground shaking with respect to shaking and damage felt at a geographic location as shown in Table 11-1.

**Table 11-1, Modified Mercalli Intensity Scale**

INTENSITY	I	II – III	IV	V	VI	VII	VIII	IX	X+
<b>SHAKING</b>	Not Felt	Weak	Light	Moderate	Strong	Very Strong	Severe	Violent	Extreme
<b>DAMAGE</b>	None	None	None	Very Light	Light	Moderate	Moderate / Heavy	Heavy	Very Heavy

Figure 11-7 shows a map developed by the South Carolina Geological Survey (SCGS) with interpreted isoseismals of seismic intensities based on the MMI scale. These intensities (MMI) are for the August 31, 1886, Charleston, S.C. seismic event ( $M_w \approx 7.3$ ). Figure 11-8 shows a

map also developed by the SCGS with seismic event intensities, by county, based on the anticipated MMI. The intensities shown on this map are the highest likely under the most adverse geologic conditions that would be produced by a combination of the August 31, 1886, Charleston ( $M_w \approx 7.3$ ) and the January 1, 1913, Union County, S.C., ( $M_w \approx 5.5$ ) seismic events. These maps are for informational purposes only and are not intended as a design tool, but reflect the potential for damage based on seismic events similar to the Charleston seismic event.



See Table 11-1 Modified Mercalli Intensity Scale definitions.

**Figure 11-7, Interpreted MMI for the 1886 Charleston Seismic Event (SCDNR (2012a))**

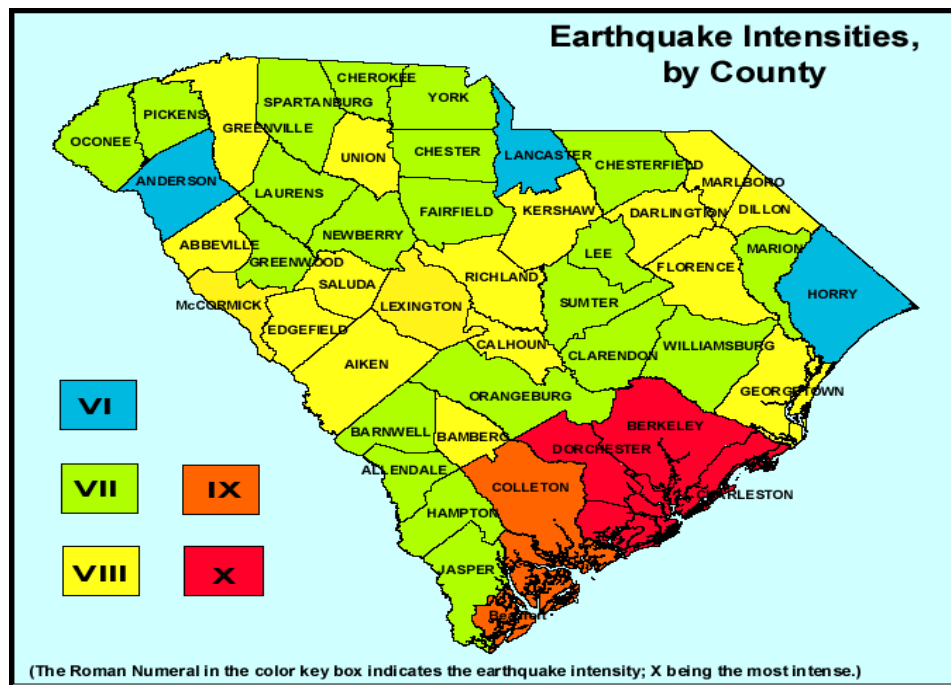


**Figure 11-8, Interpreted Seismic Event MMI by County  
(SCDNR (2012b))**

## 11.8 SOUTH CAROLINA SEISMIC SOURCES

Sources of seismicity are not well defined in much of the CEUS. However, based on recent studies in the geology and seismology of the CEUS, it appears that the source of the seismic events may be infilled rift valleys (Stein, et al. (2013)). It is noted that the rift valleys along the Atlantic seaboard are not fully formed such as the Great Rift Valley in northeast Africa. Since the presence of these rift valleys cannot be accurately confirmed; the South Carolina seismic sources have been defined based on seismic history in the Southeastern United States. The “Seismic Hazard Mapping for Bridge and Highway Design in South Carolina” (Seismic Hazard Mapping) study (Chapman and Talwani, 2002) has identified 2 types of seismic sources: Non-Characteristic Seismic Sources and Characteristic Seismic Sources.

### 11.8.1 Non-Characteristic Seismic Sources

Seismic histories were used to establish seismic area sources for analysis of non-characteristic background events. The study by Chapman and Talwani (2002) modified the Frankel, et al. (1996) source area study to develop the seismic source areas shown in Figures 11-9 and 11-10.



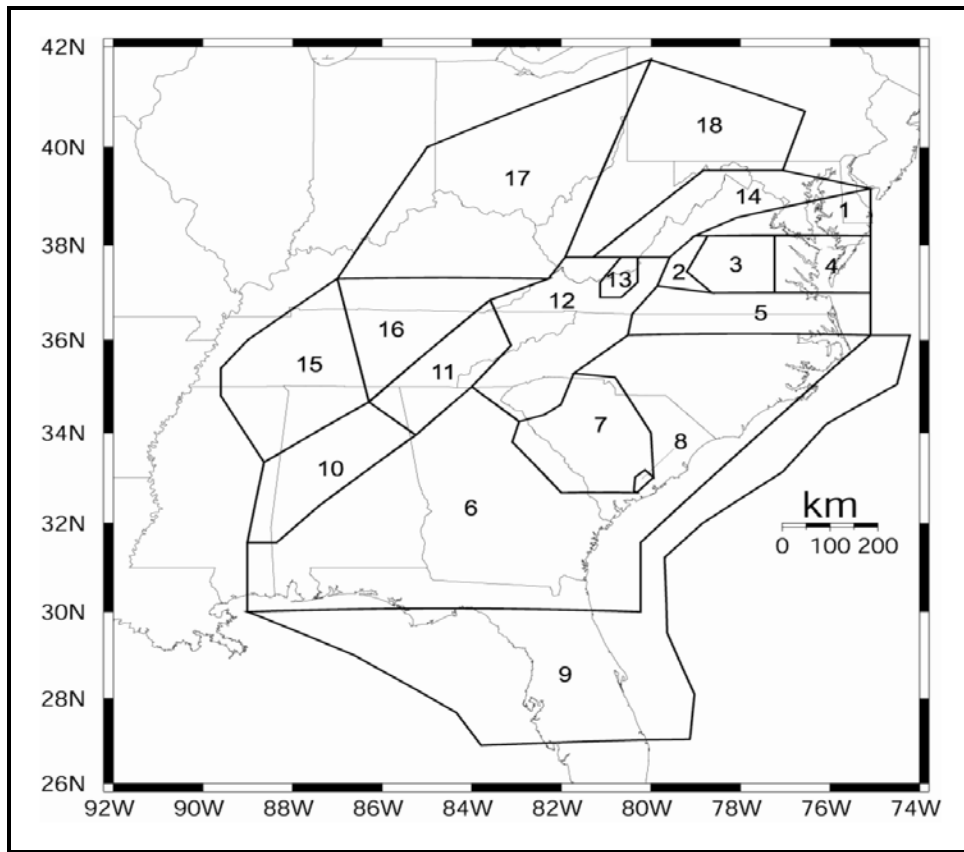


**Figure 11-9, Source Areas for Non-Characteristic Seismic Events (Chapman and Talwani (2002))**

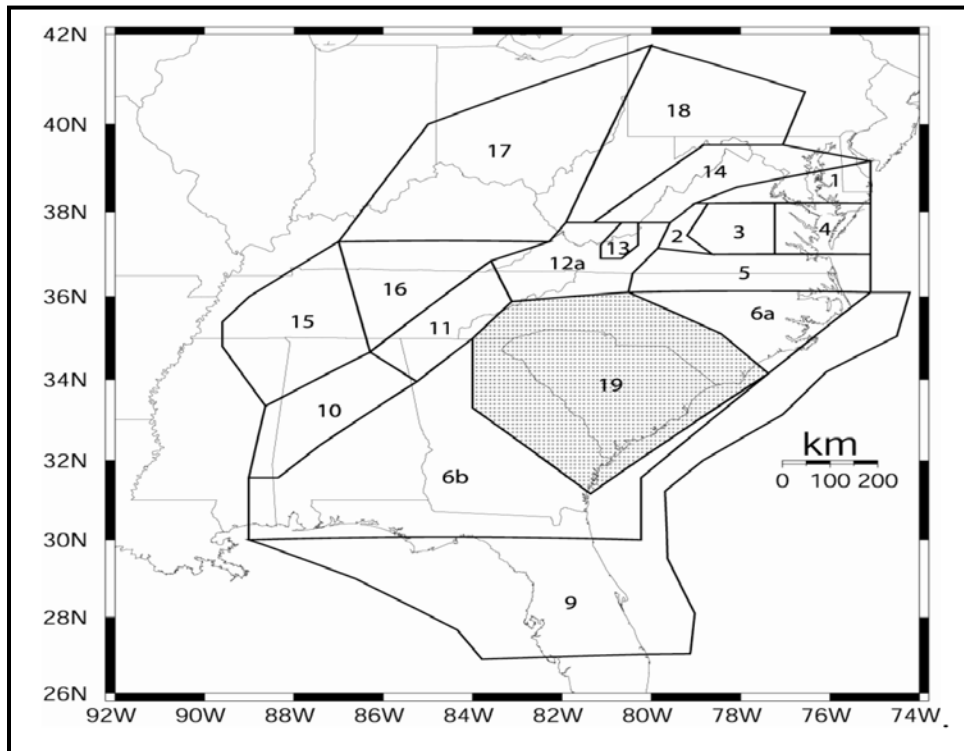


**Figure 11-10, Alternative Source Areas for Non-Characteristic Seismic Events (Chapman and Talwani (2002))**

The source areas listed in Figures 11-9 and 11-10 are described in Table 11-2.

**Table 11-2, Source Areas for Non-Characteristic Background Events  
(Chapman and Talwani (2002))**

Area No.	Description	Area (sq.miles)	Area No.	Description	Area (sq.miles)
1	Zone 1	8,133	10	Alabama	20,257
2	Zone 2	2,475	11	Eastern Tennessee	14,419
3	Central Virginia	7,713	12	Southern Appalachian	29,234
4	Zone 4	9,687	12a	Southern Appalachian N.	17,034
5	Zone 5	18,350	13	Giles County, VA	1,980
6	Piedmont and Coastal Plain	161,110	14	Central Appalachians	16,678
6a	Piedmont & CP NE	18,815	15	West Tennessee	29,667
6b	Piedmont & CP SW	95,854	16	Central Tennessee	20,630
7	SC Piedmont	22,248	17	Ohio – Kentucky	58,485
8	Middleton Place	455	18	West VA-Pennsylvania	34,049
9	Florida/Continental Margin	110,370	19	USGS Gridded Seis.-1996	---

Figure 11-11 shows additional historical seismic information obtained from the Virginia Tech catalog of seismicity in the Southeastern United States from 1600 to present that was used to model the non-characteristic background events in the source areas.

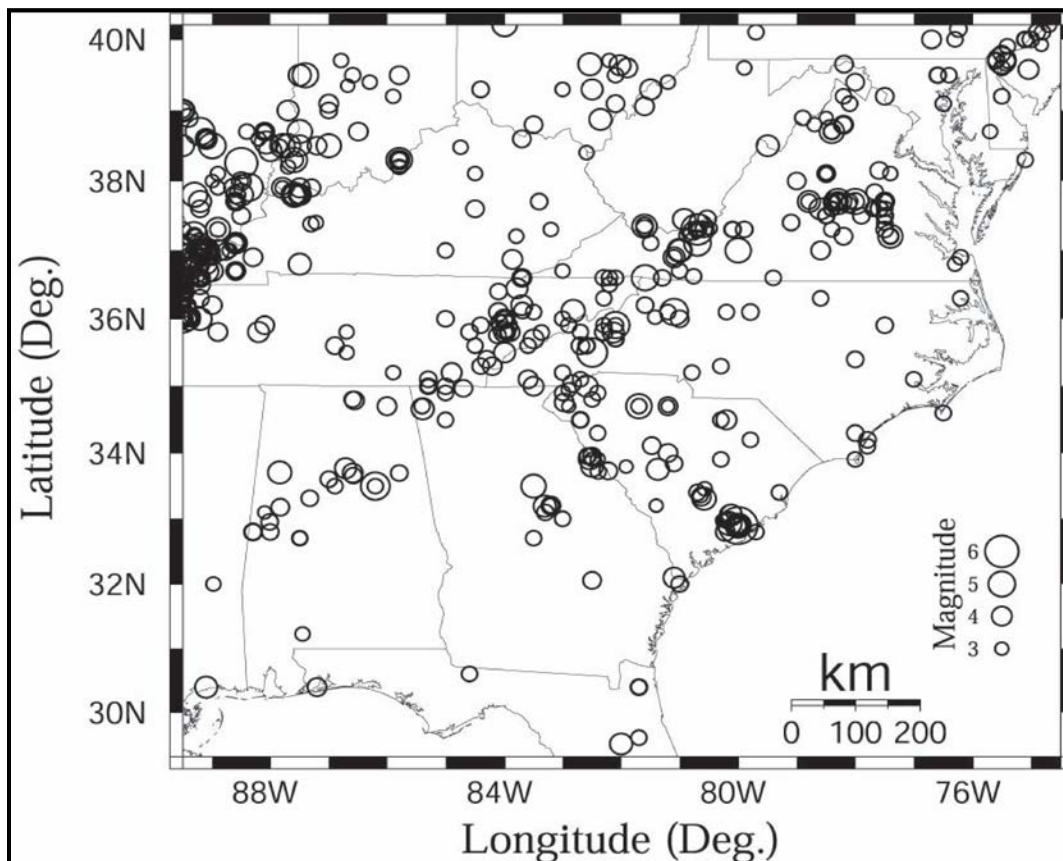


**Figure 11-11, Southeastern U.S. Seismic Events ( $M_w > 3.0$  from 1600 to Present)  
(Chapman and Talwani (2002))**

### 11.8.2 Characteristic Seismic Sources

The single most severe seismic event that has occurred in South Carolina's recorded human history occurred in Charleston, South Carolina, in 1886. It was one of the largest, seismic events to affect the CEUS in historical times. The  $M_w$  of this seismic event has been estimated to range from 7.0 to 7.5. It is typically assigned an  $M_w$  of 7.3. The faulting source that was responsible for the 1886 Charleston seismic event remains uncertain to date.

Large magnitude seismic events with the potential to occur in coastal South Carolina are considered characteristic seismic events. These seismic events are modeled as a combination of fault sources and a seismic Area Source. The Seismic Hazard Mapping study used the 1886 Seismic Event fault source, also known as the Middleton Place seismic zone, and ZRA fault source. For the 1886 Seismic Event fault source it is assumed that rupture occurred on the NE trending "Woodstock" fault and on the NW trending "Ashley River" fault. The 1886 Seismic Event fault source is modeled as 3 independent parallel faults.

Recent studies (Marple and Talwani, (1993, 2000)) suggest that the "Woodstock" fault may be a part of larger NE trending fault system that extends to North Carolina and possibly Virginia, referred to in the literature as the "East Coast Fault System". The ZRA fault source is the term used for the portion of the "East Coast Fault System" that is located within South Carolina. The ZRA fault system is modeled by a 145-mile long fault with a NE trend. The characteristic seismic Area Source is the same as is used in the 1996 National Seismic Hazard Maps. It models a network of individual faults no greater than 46 miles in length within the Lower Coastal Plain. The fault sources and area sources used to model the characteristic seismic sources in the Seismic Hazard Mapping study are shown in Figure 11-12.

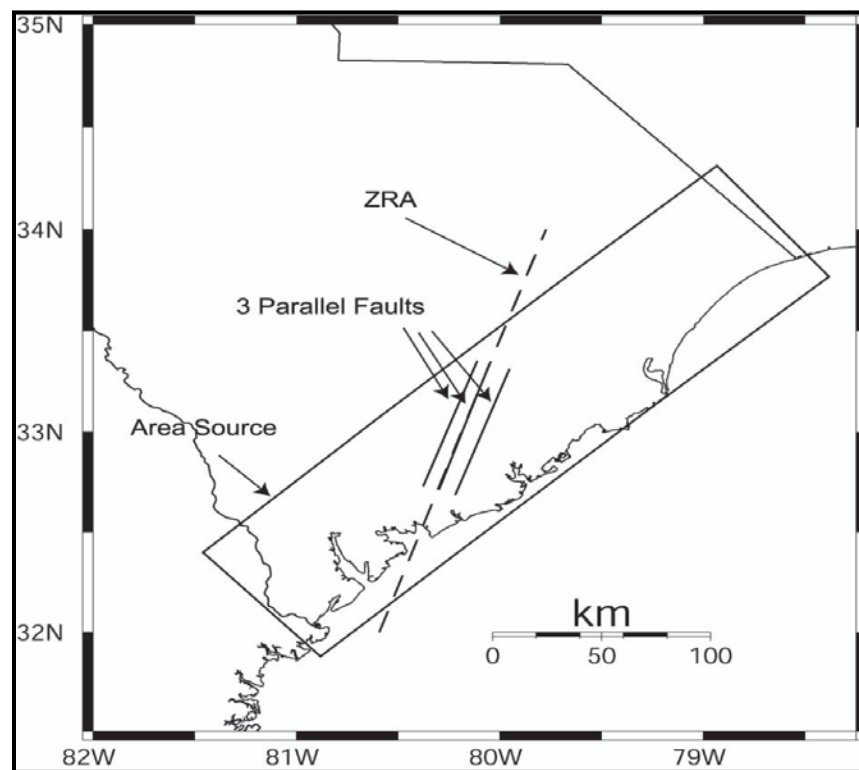


**Figure 11-12, South Carolina Characteristic Seismic Sources (Chapman and Talwani (2002))**

## 11.9 SOUTH CAROLINA SEISMIC HAZARDS

### 11.9.1 Design Seismic Events

SCDOT uses the FEE and the SEE to design transportation infrastructure in South Carolina. The FEE represents a small ground motion that has a likely probability of occurrence within the life of the structure being designed. The SEE represents a large ground motion that has a relatively low probability of occurrence within the life of the structure. The 2 levels of seismic events have been chosen for South Carolina because SEE spectral accelerations can be as much as 3 to 4 times higher than FEE spectral accelerations in the CEUS. In contrast, the California SEE spectral accelerations can be the same or as much as 1.8 times the FEE spectral accelerations. Because of the large variation between FEE and SEE design events it is necessary to perform geotechnical seismic engineering analyses for each event and compare the resulting performance with the SCDOT Performance Limits established in Chapter 10. The design life for transportation infrastructure is typically assumed to be 75 years when evaluating the design seismic events, regardless of the actual design life specified in Chapter 10.

### 11.9.2 Probabilistic Seismic Hazard Maps

The seismic hazard of South Carolina is estimated from the probabilistic pseudo-spectral accelerations (PSA) maps for SCDOT (Chapman and Talwani (2002), Chapman (2006)) assuming a geologically realistic rock model for the State and the 2  $P_E$  conditions. The motions are defined in terms of PSA at frequencies of 0.5, 1.0, 2.0, 3.3, 5.0, 6.67, and 13.0 Hz, for a damping ratio of 0.05 (5%) and the peak horizontal ground acceleration (PGA or PHGA). Please note that period is the inverse of frequency, therefore, the frequencies previously indicated become periods of 2.0, 1.0, 0.50, 0.303, 0.20, 0.15, and 0.077 seconds. The accelerations were developed for the geologically realistic site conditions as well as for the hypothetical hard-rock basement outcrop. The motions are termed the Uniform Hazard Spectrum (UHS) at the respective geologic condition (i.e., geologically realistic or hard-rock). All of the PSAs contained in the UHS have the same  $P_E$ . The geologically realistic site condition is a hypothetical site condition that was developed by using a transfer function of a linear response. South Carolina has been divided into 2 zones as shown in Figure 11-13: Zone I – Physiographic Units Outside of the Coastal Plain and Zone II – Coastal Plain Physiographic Unit. The delineation between these 2 zones has been shown linearly in Figure 11-13 but in reality it should follow the “Fall Line.” Because of the distinct differences between these 2 physiographic units, a geologically realistic model has been developed for each zone.

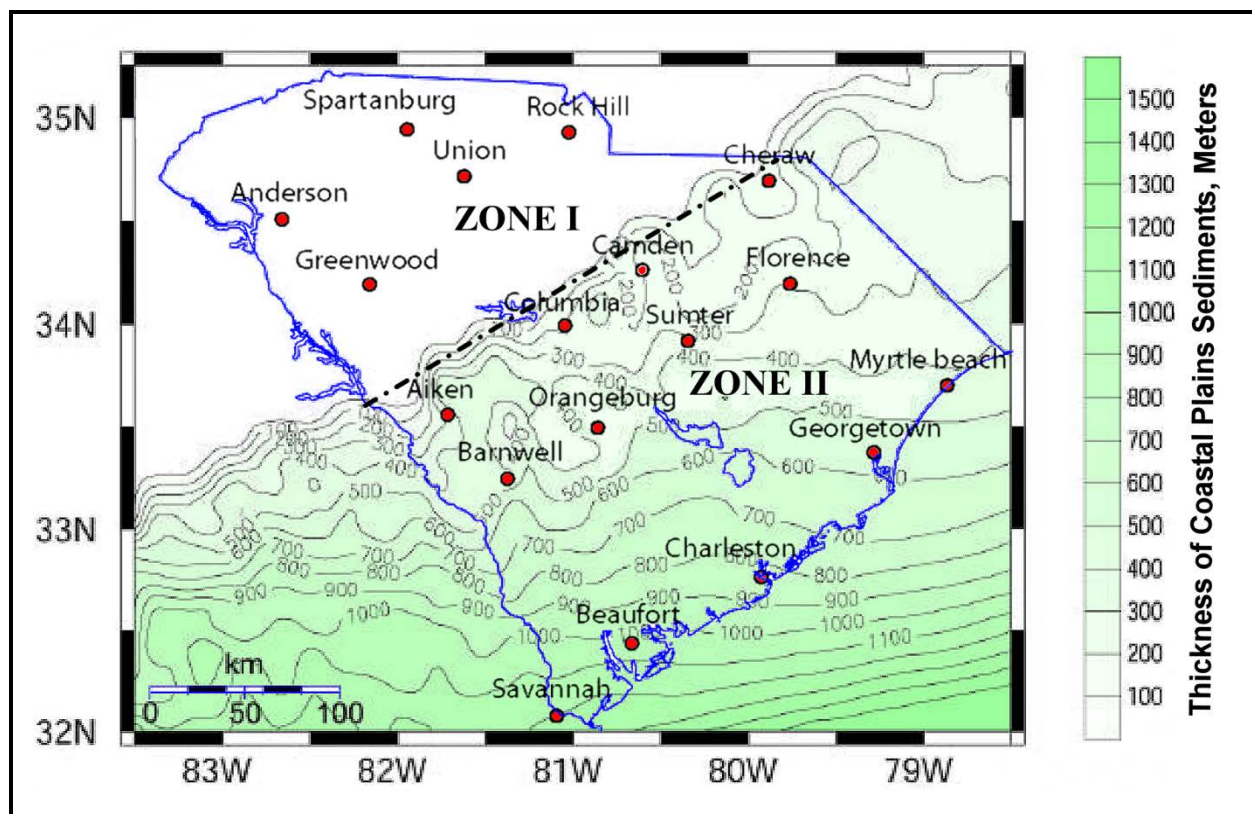


**Figure 11-13, SCDOT Site Condition Selection Map (Modified Chapman and Talwani (2002))**

The Coastal Plain geologically realistic site condition consists of 2 layers, the shallowest layer consists of Coastal Plain sedimentary soil (Q=100) and weathered rock (Q=600), over a half-space of unweathered Mesozoic and Paleozoic sedimentary, and metamorphic/igneous rock, assuming vertical shear wave incidence. The variable Q is called the Quality Factor and is a measure of the energy dissipation during a seismic event due to absorption of the energy by the soil. A higher Q results in lower energy dissipation (i.e., less soil grains bumping into each). The soil/rock properties for the Coastal Plain geologically realistic model are shown in Table 11-3.

The Piedmont geologically realistic site condition consists of 1 layer of weathered rock (Q=600) over a half-space of unweathered Mesozoic and Paleozoic sedimentary, and metamorphic/igneous rock, assuming vertical shear wave incidence. The soil/rock properties for the Piedmont geologically realistic model are shown in Table 11-4.

**Table 11-3, Coastal Plain Geologically Realistic Model**

Soil Layer	Mass Density, $\rho$	Total Unit Weight, $\gamma$	Shear Wave Velocity, $V_s$
	slug <sup>a</sup> /ft <sup>3</sup>	pcf	ft/sec
Layer 1 – Sedimentary Soils	3.88	125	2,300
Layer 2 – Weathered Rock	4.81	155	8,200
Half-Space – Basement Rock	5.12	165	11,200

<sup>a</sup>slug = (lb<sub>r</sub>\*s<sup>2</sup>)/ft

**Table 11-4, Geologically Realistic Model Outside of Coastal Plain**

Soil Layer	Mass Density, $\rho$	Total Unit Weight, $\gamma$	Shear Wave Velocity, $V_s$
	slug <sup>a</sup> /ft <sup>3</sup>	pcf	ft/sec
Layer 1 – Weathered Rock	4.81	155	8,200
Half-Space - Basement Rock	5.12	165	11,200

$$^a\text{slug} = (\text{lb}_f \cdot \text{s}^2) / \text{ft}$$

The transfer functions were computed using the one-quarter wavelength approximation of Boore and Joyner (1991). For more information on the development of the transfer function refer to Chapman and Talwani (2002).

The selection of the appropriate site condition is very important in the generation of probabilistic seismic hazard motions in the form of PSA and (PGA or PHGA). The available site conditions for use in generating probabilistic seismic hazard motions are defined in Table 11-5. The selection of the appropriate site condition should be based on the results of the geotechnical site investigation, geologic maps, and any available geologic or geotechnical information from past projects in the area. Generally speaking the geologically realistic site condition should be used in the Coastal Plain. In areas outside of the Coastal Plain such as the Piedmont / Blue Ridge Physiographic Units and along the “Fall Line” the use of the geologically realistic site condition should be evaluated carefully. The geotechnical investigation in these areas should be sufficiently detailed to determine depth to weathered rock having a shear wave velocity of approximately 8,000 to 8,200 ft/sec or to define the basement rock outcrop having a shear wave velocity greater than 11,000 ft/sec.

**Table 11-5, Site Conditions**

South Carolina Zones	Site Condition	
	Geologically Realistic	Hard-Rock Basement Outcrop
<b>Zone I – Physiographic Units Outside of the Coastal Plain</b>	Hypothetical outcrop of “Weathered Southeastern U.S. Piedmont Rock” that consist of an 820-foot thick weathered formation of shear wave velocity, $V_s = 8,200$ ft/s overlying a hard-rock formation having shear wave velocity, $V_s = 11,500$ ft/s.	A hard-rock basement outcrop formation having shear wave velocity, $V_s = 11,500$ ft/s.
<b>Zone II – Coastal Plain Physiographic Unit</b>	Hypothetical outcrop of “Firm Coastal Plain Sediment” having a shear wave velocity, $V_s = 2,500$ ft/s.	

The seismic hazard computations use the seismic sources listed in Section 11.8, the design seismic event in Section 11.9.1, and the ground motions described in Section 11.9.4.

The PGA and PSA can be obtained for any location in South Carolina by specifying a Latitude and Longitude. The Latitude and Longitude of a project site may be obtained from the plans or by using an Interactive Internet search tool. Typical Latitude and Longitude for select South Carolina cities are provided in Table 11-6 for reference.

**Table 11-6, Latitude and Longitude for South Carolina Cities**

SC City	Latitude	Longitude <sup>a</sup>	SC City	Latitude	Longitude <sup>a</sup>
Anderson, SC	34.50	-82.72	Greenwood, SC	34.17	-82.12
Beaufort, SC	32.48	-80.72	Myrtle Beach, SC	33.68	-78.93
Charleston, SC	32.90	-80.03	Nth Myrtle B, SC	33.82	-78.72
Columbia, SC	33.95	-81.12	Orangeburg, SC	33.50	-80.87
Florence, SC	34.18	-79.72	Rock Hill, SC	34.98	-80.97
Georgetown, SC	33.83	-79.28	Spartanburg, SC	34.92	-81.96
Greenville, SC	34.90	-82.22	Sumter, SC	33.97	-80.47

<sup>a</sup>Longitude is negative indicating west.

The site-specific hazard PGA and PSA are generated by the PC/GDS for every project using Scenario\_PC (2006) (Chapman (2006)). Scenario\_PC (2006) generates seismic hazard data (UHS) in a similar format as that generated by the USGS.

A sample of the Seismic Hazard information generated by Scenario\_PC (2006) for Columbia, SC is shown in Figure 11-14.

```

THIS FILE CONTAINS THE RESULTS FROM ONE EXECUTION
OF PROGRAM scenario_pc (Martin Chapman, 2006).

THE NAME OF THE DIRECTORY CONTAINING THIS FILE
AND ALL ASSOCIATED OUTPUT FILES IS: Columbia_SEE

2% PROBABILITY OF EXCEEDANCE (For 50 year Exposure)
FOR GEOLOGICALLY REALISTIC SITE CONDITION

RESULTS OF INTERPOLATION

Site Location: 33.9500 N 81.1200 W
Nearest Grid Point: 34.0000 N 81.1250 W Distance From Site: 5.56 Km
Thickness of sediments, meters: 262.2

PSA and PGA as Percentage of g
0.5Hz 1.0Hz 2.0Hz 3.3Hz 5Hz 6.7Hz 13Hz PGA
6.44409 19.45698 32.21224 44.23877 52.80246 53.29054 56.02329 30.17862

```

**Figure 11-14, Scenario\_PC (2006) Sample Output for Columbia, SC**

Note: 2% Probability of Exceedance (for 50-year Exposure) is equal to 3% Probability of Exceedance (for 75-year Exposure)

As indicated previously, the PSAs generated by Scenario\_PC (2006) all have the same  $P_E$ . Figure 11-15 shows the seismic hazard curves for Charleston for seismic events having  $P_E$ s of 0.0004 (3%/75yr (2%/50yrs)), 0.0010 (7.5%/75yr (5%/50yr)), 0.0014 (10.5%/75yr (7%/50yr)) and 0.0020 (15%/75yr (10%/50yr)). Also shown is a line indicating a  $P_E$  of 0.0004 (3%/75yr (2%/50yr)), the PGA and PSAs that are indicated by this line are used to create the UHS for the SEE (3%/75yr) depicted in Figure 11-17. In order to provide the designer with an overview of South Carolina's UHS, for the FEE and SEE, the PGA and PSAs (generated by Scenario\_PC (2006)) for selected cities in South Carolina have been plotted at either the geologically realistic (B-C boundary) or hard rock basement outcrop in Figures 11-16 and 11-17. The UHS curves for various cities are provided for information only and shall not be used for design of any structures in South Carolina.



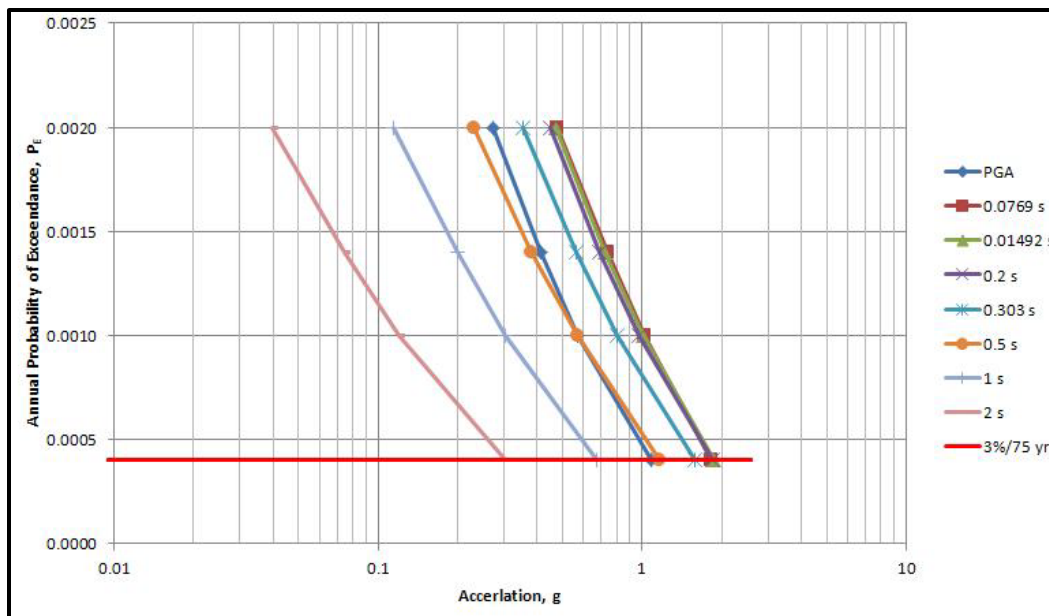


Figure 11-15, SEE Seismic Hazard Curves for Various Periods

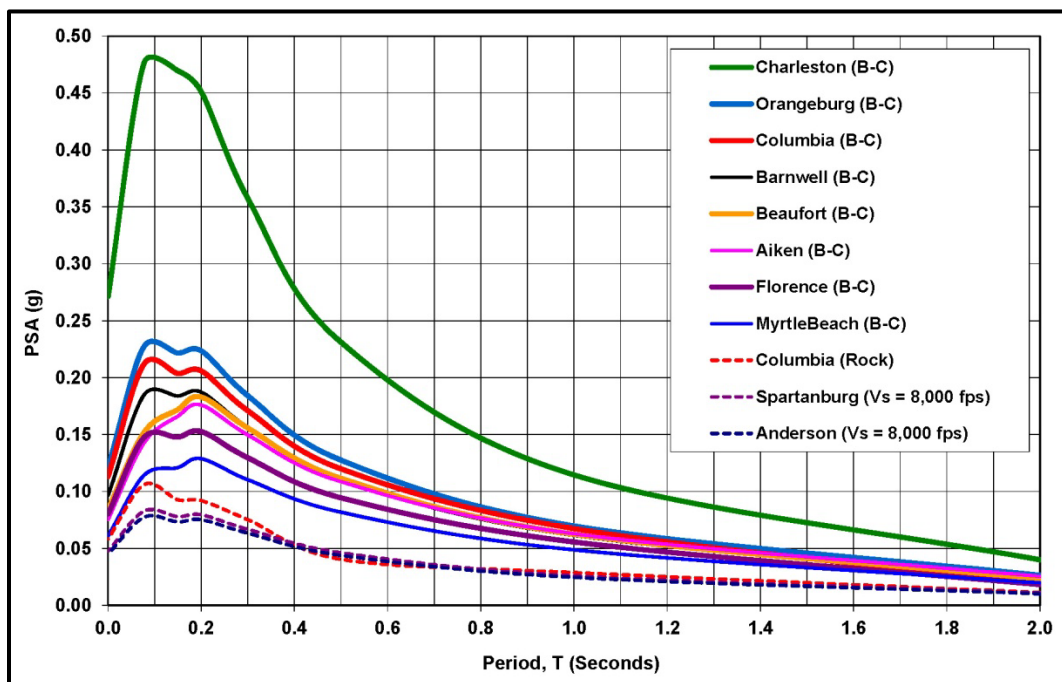


Figure 11-16, FEE UHS Curves for Selected South Carolina Cities



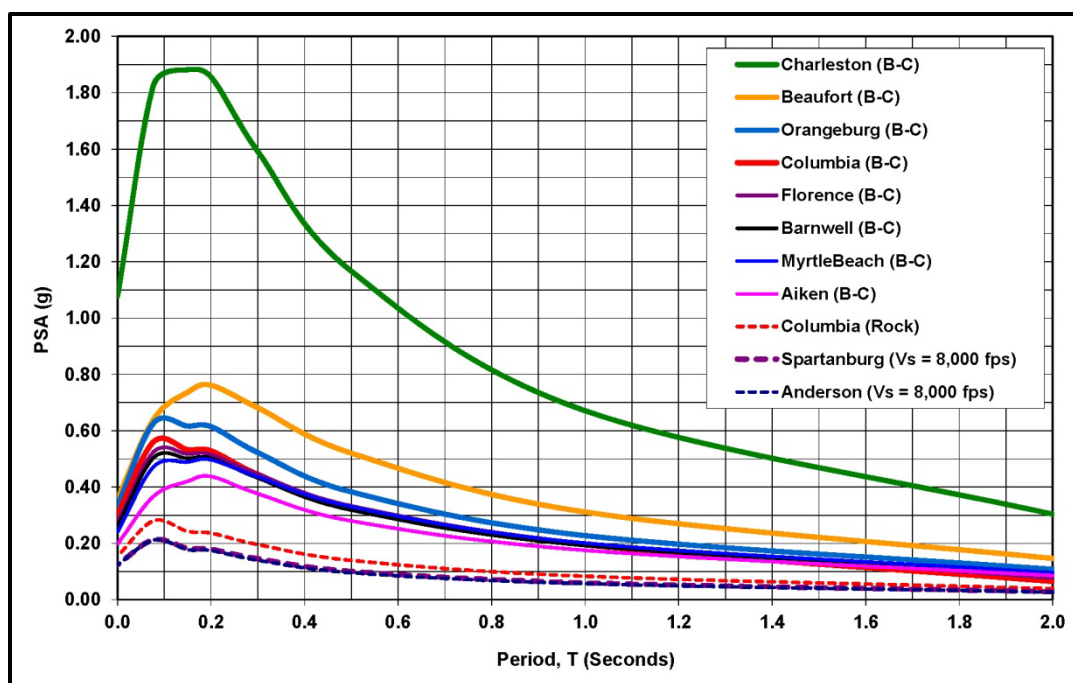


Figure 11-17, SEE UHS Curves for Selected South Carolina Cities

### 11.9.3 Seismic Event Deaggregation Charts

The ground motion hazard from a probabilistic seismic hazard analysis can be deaggregated to determine the predominant seismic event  $M_w$  and distance (R) contributions from a hazard to guide in the selection of seismic event magnitude, site-to-source distance, and in development of appropriate time histories. On March 1, 2017, the USGS Interactive Earthquake Deaggregation program was taken off line by USGS and replaced with the either the 2008 or 2014 deaggregation maps. Scenario\_PC (2006) is based on the 2002 deaggregation maps. The 2002 deaggregation maps were included in Scenario\_PC (2006); therefore, deaggregation shall be based on the results contained in Scenario\_PC (2006). Scenario\_PC (2006) generates the interpolated results from the USGS Deaggregation 2002 data. A sample deaggregation output is provided in Figure 11-18 that was generated along with the SC Seismic Hazard results shown in Figure 11-14.

Interpolated results from USGS Deaggregation 2002						
Freq.	R(mean) km	mag(mean)	eps0(mean)	R(modal) km	mag(modal)	eps0(modal)
PGA	58.6	6.31	.44	125.4	7.31	1.23
5 HZ	77.3	6.64	.68	125.1	7.30	1.05
1 HZ	113.1	7.06	.74	125.0	7.30	.81

Figure 11-18, Scenario\_PC (2006) Deaggregation – Columbia, SC

The seismic event deaggregations typically provide the source category, percent contribution of the source to the hazard, R, mean and modal  $M_w$ , and epsilon ( $\epsilon$ ). Mean  $M_w$  covers several sources that are typically not used and it is an overall average of seismic events from these other seismic sources and does not appropriately reflect magnitude of the hazard contribution within a specific seismic source. Mean  $M_w$  values listed with respect to principal sources can be used. The  $\epsilon$  (eps0 in Figure 11-18) parameter is as important to understanding a ground motion as is the  $M_w$  and the R values for the various sources. The  $\epsilon$  parameter is a measure of how close the ground motion is to the mean value in terms of standard deviation ( $\sigma$ ). The  $\epsilon_0$  parameter is provided for ground motions having a fixed  $P_E$ . If a structure is designed for a seismic event with a magnitude  $M_w$  that occurs a distance R from the site and the  $\epsilon_0 = 0.0$ , then

the structure was designed to resist a median motion from this source. If the  $\varepsilon_0 = 1.0$ , then the structure was designed to resist a motion one standard deviation ( $+1\sigma$ ) greater than the median motion. Consequently, if the  $\varepsilon_0 = -1.0$ , then the structure was designed to resist a motion one standard deviation ( $-1\sigma$ ) less than the median motion. Predominance of a modal seismic source is generally indicated if the  $\varepsilon$  is within  $\pm 1\sigma$ .

#### **11.9.4 Ground Motions**

Ground motions are required when a site-specific seismic response analysis is being performed, see Chapter 12 for requirements, and/or, see the Seismic Specs for when a time history analysis is required. Time histories can be either recorded with seismographs or synthetically developed. Since the Charleston 1886 seismic event occurred, a seismic event with a magnitude of +7 has not occurred in South Carolina and therefore, no seismograph records are available for strong motion seismic events in South Carolina. The following Sections will outline the development of synthetic time histories and the selection of "real" time histories.

##### **11.9.4.1 Synthetic Ground Motions**

SCDOT has chosen to generate synthetic project-specific time histories based on the Seismic Hazard Mapping study completed for SCDOT. The ground motion predictions used in the study are based on the results of work involving both empirical and theoretical modeling of CEUS strong ground motion. Even though the strong motion database for the CEUS is small compared to the WUS, the available data indicate that high frequency ground motions attenuate more slowly in the CEUS than in the WUS. The Seismic Hazard Mapping study computer program Scenario\_PC (2006) shall be used to generate synthetic ground motions.

A minimum of 7 time histories shall be required for either an equivalent-linear or a non-linear one-dimensional site-specific response analysis. See Chapter 12 for the type of site-specific analysis required (i.e., equivalent-linear or non-linear). As indicated previously, additional time histories may be needed based on the deaggregation results. Additional time histories may be required by SCDOT if project and site conditions warrant it. The time histories are generated based on project specific information using Scenario\_PC (2006).

The method of scaling the time series to match a Uniform Hazard Spectrum (UHS), PGA, or a PSA frequency is primarily dependent on the results of the seismic deaggregation described in Section 11.9.3. When the uniform hazard is dominated by a well-defined modal seismic event, the method of scaling the time series should be to match the UHS. The seed number is used to start development of the ground motion process and shall be different for each ground motion required.

Synthetic ground motions are developed using an attenuation model. The ground motions on hard rock produced from the Seismic Hazard Mapping program Scenario\_PC (2006) uses a stochastic model that uses weighted ( $w$ ) attenuation relationships from Toro and McGuire (1987) ( $w=0.143$ ), Frankel, et al. (1996) ( $w=0.143$ ), Atkinson and Boore (1995) ( $w=0.143$ ), Somerville, Collins, Abrahamson, Graves and Saikia (2001) ( $w=0.286$ ), and Campbell (2003) ( $w=0.286$ ) for the characteristic seismic events with magnitudes ranging from 7.0 to 7.5. For the non-characteristic seismic events with magnitudes less than 7.0, the following weighted prediction equations were used, Toro and McGuire (1987) ( $w=0.286$ ), Frankel, et al. (1996) ( $w=0.286$ ), Atkinson and Boore (1995) ( $w=0.286$ ), and Campbell (2003) ( $w=0.143$ ).

The location of the ground motion is dependent on the Site Condition (Geologically Realistic or Hard-Rock Basement Outcrop) selected in Section 11.9.2. Table 11-7 provides the location

where the ground motions are computed based on the Site Condition selected and Geologic Unit.

**Table 11-7, Location of Ground Motion**

Site Condition	Geologic Unit <sup>1</sup>	Location of Ground Motion
Geologically Realistic	Piedmont / Blue Ridge (Zone I)	Generated at a hypothetical outcrop of weathered rock ( $V_s = 8,200 \text{ ft/s}$ )
	Coastal Plain (Zone II)	Generated at a hypothetical outcrop of firm Coastal Plain sediment ( $V_s = 2,500 \text{ ft/s}$ )
Hard-Rock Basement Outcrop	Piedmont / Blue Ridge (Zone I)	Generated at a hard-rock basement outcrop ( $V_s = 11,500 \text{ ft/s}$ )
	Coastal Plain (Zone II)	

<sup>1</sup>For geologic unit locations see Figure 11-1 and 11-2 and for Site Condition locations see Figure 11-13.

#### 11.9.4.2 “Real” Ground Motions

Should a 3-dimensional site-specific response analysis be required, typically on “non-typical” SCDOT bridges, then 7 three-component (orthogonal directions) “real” time histories shall be required. “Real” time histories are recorded time histories from actual seismic events as opposed to the synthetic time histories generated by Scenario\_PC (2006). The use of “real” time histories on “typical” bridges shall be determined by the PC/GDS on a project specific basis.

The “real” time histories shall be selected based on the following criteria:

- Tectonic environment
- Seismic magnitude,  $M_w$
- Type of faulting
- Site-to-seismic source distance, R
- Local site conditions
- Design or expected ground-motion (time history) characteristics (including duration and energy content (Arias Intensity,  $I_A$ ))

As indicated in this Chapter, South Carolina is located in the approximate middle of the North American tectonic plate with the type and distribution of faulting unknown. However, based on recent evidence (Virginia Seismic Event, August 2011), the tectonic environment is probably comprised of infilled rift valleys (Stein, et al. (2013)). These rift valleys appear to be located adjacent to the modern coastline of the CEUS, where the change in density between the overlying rock and the underlying rock is greatest (i.e., granite under the North American continent and basalt under the Atlantic Ocean). In addition, the thickness of the infill materials is also greatest adjacent to the coastline. These infill materials can cause downward pressure on the faults (i.e., similar to the New Madrid Seismic Zone), that can be uneven along the fault causing stress differentials along the rift valley that can lead to seismic shaking. Based on this evidence the tectonic environment used to select the “real” ground motion shall not include ground motions generated by a subduction zone seismic event.

According to Durá-Gómez and Talwani (2009), the faults located in the Charleston, South Carolina area appear to be strike-slip faults. Strike-slip faults are faults where the ground on either side of the fault moves laterally to each other. This type of faulting is evidenced by the ZRA as identified by Chapman and Talwani (2002).

The magnitude and distance shall be determined as previously indicated in this Chapter. The local site conditions shall be identified as either soil (typical of the Lower and Middle Coastal Plain) or rock (typical of the Piedmont). Rock as used here has a  $V_{s,H}^*$  of greater than 11,500 feet per second ( $V_{s,H}^* > 11,500$  ft/sec). The selected seismic event should also match the estimated duration (see Section 12.9.3) as closely as possible. In addition, the selected seismic event should closely match the design UHS.

## 11.10 REFERENCES

- Atkinson, G. A. and Boore, D. M., (1995), "Ground motion relations for Eastern North America", *Bulletin of the Seismological Society of America*, v. 85, pp. 17-30.
- Boore D. M. and Joyner, W. B., (1991), "Ground motion at deep soil sites in eastern North America", *Bulletin of the Seismological Society of America*, v. 81, pp. 2167-2187.
- Campbell, K. W., (2003), "Prediction of strong ground motion using the hybrid empirical method: example application to eastern North America", *Bulletin of the Seismological Society of America*, v. 93, pp. 1012-1033.
- Chapman, M. and Talwani, P., (2002), "Seismic Hazard Mapping for Bridge and Highway Design", Report to SCDOT, Referred to in this manual as SCDOT Seismic Hazard Study.
- Chapman, M., (2006), "User's Guide to SCENARIO\_PC and SCDOTSHAKE", Report to SCDOT.
- Durá-Gómez, I., and Talwani, P., (2009), "Finding Faults in the Charleston Area, South Carolina: 1. Seismological Data", *Seismological Research Letters*, v. 80, no. 5, pp. 883-900.
- Frankel, A., Mueller, C., Barnhard, T., Perkins, D., Leyendecker, E. V., Dickman, N., Hanson, S., and Hopper, M., (1996), "National seismic-hazard maps; documentation", United States Geological Survey Open-File Report 96-532, 110p.
- Fillingim, M., (1999), "Intraplate Earthquakes: Possible Mechanisms for the New Madrid and Charleston Earthquakes", Final Paper for GPHYS 502, University of California at Berkeley.
- Marple, R. T., and Talwani, P., (1993), "Evidence of possible tectonic upwarping along the South Carolina Coastal Plain from an examination of river morphology and elevation data", *Geology*, v. 21, pp. 651-654.
- Marple, R. T., and Talwani, P., (2000), "Evidence for a buried fault system in the Coastal Plain of the Carolinas and Virginia; Implications for neotectonics in the southeastern United States", *Geological Society of America Bulletin*, v. 112, no. 2, pp. 200-220.
- Odum, J .K., Williams, R. A., Stephenson, W. J., and Worley, D. M., (2003), "Near-surface S-wave and P-wave seismic velocities of primary geological formations on the Piedmont and Atlantic Coastal Plain of South Carolina, USA", United States Geological Survey Open-File Report 03-043, 14p.

South Carolina Department of Natural Resources (SCDNR), Geological Survey, (1998), "Geologic Time Scale for South Carolina", OFR-108, <http://www.dnr.sc.gov/geology/images/gifs/OFR108.gif>.

South Carolina Department of Natural Resources, Geological Survey, (2005), "Generalized Geologic Map of South Carolina 2005," GGMS-1, <http://www.dnr.sc.gov/geology/images/gifs/GGMS1.gif>.

South Carolina Department of Natural Resources, Geological Survey, (2012a), personal communication, "Interpreted Isoseismals from the Charleston Earthquake, August 31, 1886".

South Carolina Department of Natural Resources, Geological Survey, (2012b), "Projected Earthquake Intensities for South Carolina", OFR-111, <http://www.dnr.sc.gov/geology/images/gifs/OFR111.gif>.

South Carolina Department of Natural Resources, GIS, (2013), "Generalized Geologic Provinces/Regions", <http://www.dnr.sc.gov/GIS/descgeolrp.html>.

Somerville, P., Collins, N., Abrahamson, N., Graves, R., and Saikia, C., (2001), "Ground motion attenuation relations for the central and eastern United States", final report to the U. S. Geological Survey.

Stein, S., Pozzaglia, F., Meltzer, A., Wolin, E., Kafka, A., and Berti, C., (2013), "Tectonic Setting of the August 2011 Virginia Earthquake", <http://earth.northwestern.edu/people/seth/research/VA2011/>.

Toro, G., and McGuire, R. K., (1987), "An investigation into earthquake ground motion characteristics in eastern North America", Bulletin of the Seismological Society of America, v. 77, pp. 468-489.

United States Geological Service (USGS), (2012a), Earthquake Hazards Program Website, <http://earthquake.usgs.gov/hazards/apps/#deaggint>.

United States Geological Service (USGS), (2012b), "Damaging Earthquakes In the US (1750 – 1996)", [http://earthquake.usgs.gov/earthquakes/states/us\\_damage\\_eq.php](http://earthquake.usgs.gov/earthquakes/states/us_damage_eq.php).

**Chapter 12**

**GEOTECHNICAL  
SEISMIC ANALYSIS**

**GEOTECHNICAL DESIGN MANUAL**

*January 2019*



## Table of Contents

<u>Section</u>	<u>Page</u>	
12.1	Introduction.....	12-1
12.2	Geotechnical Seismic Analysis .....	12-1
12.3	Dynamic Soil Properties.....	12-2
	12.3.1 Soil Properties.....	12-2
	12.3.2 Site Stiffness .....	12-2
	12.3.3 Equivalent Uniform Soil Profile Period and Stiffness .....	12-3
	12.3.4 $V_{s,H}^*$ Variation Along a Project Site.....	12-5
	12.3.5 South Carolina Reference $V_{s,H}^*$ .....	12-6
12.4	Project Site Classification .....	12-7
12.5	Depth-To-Motion Effects On Site Class and Site Factors.....	12-9
12.6	SC Seismic Hazard Analysis .....	12-9
12.7	Acceleration Response Spectrum.....	12-10
	12.7.1 Effects of Rock Stiffness WNA vs. ENA .....	12-11
	12.7.2 Effects of Weathered Rock Zones Near the Ground Surface.....	12-12
	12.7.3 Effects of Soil Softening and Liquefaction on Spectral Acceleration ..	12-13
	12.7.4 Horizontal Ground Motion Response Spectra .....	12-13
	12.7.5 Vertical Ground Motion Response Spectra.....	12-16
12.8	Site Response Analysis Using Seismic Hazard Mapping Study .....	12-17
	12.8.1 ADRS Curves for FEE and SEE .....	12-17
	12.8.2 Local Site Effects – Coastal Plain.....	12-18
	12.8.3 Local Site Effects – Piedmont.....	12-21
	12.8.4 Local Site Effects on Spectral Response Accelerations.....	12-23
	12.8.5 3-Point Acceleration Design Response Spectrum .....	12-24
	12.8.6 Multi-Point Acceleration Design Response Spectrum.....	12-28
	12.8.7 ADRS Evaluation using Seismic Hazard Mapping Study.....	12-30
	12.8.8 Damping Modifications of ADRS Curves .....	12-30
12.9	Site-Specific Response Analysis.....	12-31
	12.9.1 Equivalent-Linear One-Dimensional Site-Specific Response .....	12-31
	12.9.2 One-Dimensional Non-Linear Site-Specific Response .....	12-32
	12.9.3 Site-Specific Response Analysis Methodology .....	12-32
	12.9.4 Site-Specific Horizontal ADRS Curve .....	12-34
12.10	Ground Motion Design Parameters.....	12-38
	12.10.1 Peak Horizontal Ground Acceleration.....	12-38
	12.10.2 Earthquake Magnitude / Site-to-Source Distance .....	12-38
	12.10.3 Seismic Event Predominant Period .....	12-38
	12.10.4 Earthquake Duration .....	12-39
	12.10.5 Energy Content .....	12-42
	12.10.6 Peak Ground Velocity.....	12-43
12.11	References .....	12-43



**List of Tables**

<b><u>Table</u></b>	<b><u>Page</u></b>
Table 12-1, Modified Successive 2-Layer Approach.....	12-5
Table 12-2, USGS Site Stiffness .....	12-6
Table 12-3, USGS Site Stiffness .....	12-7
Table 12-4, Site Stiffness Variability Proposed Procedure.....	12-8
Table 12-5, Site Response Selection Criteria .....	12-15
Table 12-6, Spectral Period Ranges and Designations.....	12-17
Table 12-7, Regression Coefficients for the Coastal Plain .....	12-19
Table 12-8, Typical Normalized Period Values by Region .....	12-19
Table 12-9, Adjustment Factors for $d_{B-C} < 330$ feet for the Coastal Plain .....	12-20
Table 12-10, Regression Coefficients for the Piedmont.....	12-22
Table 12-11, Typical Normalized Period Values by Region .....	12-22
Table 12-12, Adjustment Factors for $d_{HR}$ for the Piedmont .....	12-22
Table 12-13, 3-Point ADRS Construction Procedures .....	12-26
Table 12-14, Multi-Point ADRS Construction Procedure.....	12-29
Table 12-15, Damping Adjustment Factors.....	12-30
Table 12-16, One-Dimensional Soil Column Model .....	12-33
Table 12-17, Site-Specific ADRS Construction Procedures.....	12-35

### List of Figures

<u>Figure</u>	<u>Page</u>
Figure 12-1, Site Stiffness ( $V_{s,H}^*$ ) vs. Site Natural Period ( $T_N$ ).....	12-4
Figure 12-2, Soil Site Effects on Average Normalized Response Spectra .....	12-10
Figure 12-3, Predominant Period ( $T'_o$ ) of Selected SC Cities.....	12-11
Figure 12-4, WNA / ENA Rock Effects on Normalized Response Spectra.....	12-12
Figure 12-5, Vertical/Horizontal Spectral Ratios vs. Period.....	12-16
Figure 12-6, Geologic Map Indicating Sites Used in Ground Response Analysis .....	12-18
Figure 12-7, 3-Point ADRS Curve Construction.....	12-25
Figure 12-8, 3-Point ADRS Curve .....	12-27
Figure 12-9, 3-Point/Multi-Point ADRS .....	12-28
Figure 12-10, Site-Specific Horizontal ADRS Curve Construction .....	12-36
Figure 12-11, Site-Specific Horizontal ADRS Curve .....	12-37
Figure 12-12, Effects of Site Stiffness on Earthquake Duration .....	12-41
Figure 12-13, Effects of Depth-to-Hard Rock on Earthquake Duration .....	12-41



# CHAPTER 12

## GEOTECHNICAL SEISMIC ANALYSIS

### 12.1 INTRODUCTION

Geotechnical seismic analysis consists of evaluating the seismic hazard and the effects of the hazard on the transportation structure being designed. This is accomplished by characterizing the subsurface soils, determining the seismic hazard, evaluating the local site effects on the response spectra, and developing an Acceleration Design Response Spectrum (ADRS) for use in designing bridges and other transportation structures.

SCDOT has made a commitment to design transportation systems in South Carolina so as to minimize the potential for collapse during a seismic event. The latest edition of the SCDOT Seismic Specs establishes the seismic design requirements for the design of bridges on the South Carolina highway transportation system. This Chapter presents geotechnical seismic analysis requirements for evaluating ground shaking using either the Seismic Hazard Mapping study or by performing a site-specific response analysis. Determining the potential for soil strength losses, analyzing the hazard caused by reduced soil strengths, and analyzing seismic lateral loadings are contained in Chapters 13 and 14.

The PC/GDS performs the following types of geotechnical seismic engineering analyses:

1. Determine Seismic Design Parameters – PGA, PSA,  $M_w$ , R, etc. (Chapter 11)
2. Develop Acceleration Design Response Spectrum (ADRS) curves (Chapter 12)
3. Generate Seismic Ground Motions - Time Histories (Chapter 11)
4. Review Consultant Geotechnical Seismic Engineering Reports (Chapter 21)

Based on the information obtained from the above analyses, the GEOR performs the following geotechnical seismic engineering analyses:

1. Perform Seismic Hazard Analyses – SSL, etc. (Chapter 13)
2. Perform Geotechnical Seismic Engineering Design (Chapter 14)

### 12.2 GEOTECHNICAL SEISMIC ANALYSIS

The geotechnical analysis requirements for determining the seismic hazard and associated site response have been developed for the design of “typical” bridges as defined by the Seismic Specs. Bridges not meeting the definition of “Typical SCDOT Bridges” include suspension bridges, cable-stayed bridges, arch type bridges, movable bridges, and bridges with spans exceeding 300 feet. For these “non-typical” bridges, the PC/GDS in conjunction with the PC/SDS will specify and/or approve appropriate geotechnical seismic engineering provisions on a project specific basis. The geotechnical seismic analysis requirements in this Manual shall also apply to the design of bridge embankments, ERSs, and other miscellaneous transportation related structures. The Seismic Specs limit the applicability of the 2-level (i.e., designing using both FEE and SEE) design to select bridges that meet specific criteria contained in the Seismic Specs. All bridge embankments (unreinforced, reinforced and RSS) and ERSs located within bridge embankments are required to be designed using both events. ERSs located within roadway embankments shall only be designed for the SEE. As indicated previously, roadway embankments (unreinforced, reinforced and RSS) will not be designed for the EE I limit state.

The preliminary geotechnical engineering report (PGER) typically contains a geotechnical seismic hazard analysis that includes the ADRS curve to be used for preliminary design of the

bridge structure. The final bridge or roadway geotechnical engineering report (BGER or RGER) contains the results of the final geotechnical subsurface investigation and modifies, if necessary, the ADRS curves.

## 12.3 DYNAMIC SITE PROPERTIES

### 12.3.1 Soil Properties

A project specific subsurface geotechnical investigation shall be performed in accordance with the subsurface investigation guidelines provided in Chapter 4. Basic soil properties will be obtained in accordance with the field and laboratory testing procedures specified in Chapter 5. These basic soil properties can be directly measured by field and laboratory testing results or can be correlated from those results as described in Chapter 7. Dynamic soil properties, specifically shear wave velocity,  $V_s$ , shall be measured in the field (Chapter 5). Correlation as indicated in Chapter 7 may only be used when insufficient field measurements are available for the development of the site factors as indicated in this Chapter. Other dynamic properties such as shear modulus curves, damping ratio curves, and the residual strength of soils that lose shear strength during the seismic event are determined as indicated in Chapter 7.

### 12.3.2 Site Stiffness

Site stiffness ( $V_{s,H}^*$ ), as used in this Manual, is a weighted average of the measured soil stiffness of individual soil layers to a specific depth of interest ( $H$ ). The measured  $V_s$  values shall not be corrected for overburden. The weighted average shall be computed using the measured  $V_s$  obtained during the geotechnical site investigation. As an alternate, when  $V_s$  has not been obtained,  $V_s$  may be correlated using SPT resistances or CPT values as indicated in Chapter 7; however, written approval of the PC/GDS shall be obtained prior to using the correlations in Chapter 7. The SPT or CPT correlated  $V_s$  values will be determined as required for use in Chapter 13.

Site stiffness shall be computed from measured shear wave velocities as indicated in the following equation.

$$V_{s,H}^* = \frac{H}{t_d} \quad \text{Equation 12-1}$$

Where,

- $V_{s,H}^*$  = Weighted, average site stiffness to a specific depth of interests, typically either the B-C Boundary or Hard Rock basement outcrop, ft/sec
- $H$  = Total depth where  $V_s$  is being averaged, typically either the B-C Boundary or Hard Rock basement outcrop, feet
- $t_d$  = Time that it takes for the shear wave to travel from the  $H$  to the ground surface, seconds

For layered profile,  $V_{s,H}^*$  may also be computed by

$$V_{s,H}^* = \frac{H}{\sum_{i=1}^n \left( \frac{H_i}{V_{si}} \right)} \quad \text{Equation 12-2}$$

Where,

- $V_{s,H}^*$  = Weighted, average site stiffness to a specific depth of interest,  $H$ , ft/sec
- $H$  = Total depth where  $V_s$  are being averaged, feet
- $V_{si}$  = Shear wave velocity of layer  $i$ , ft/sec

$H_i$  = Thickness of any layer  $i$  between the ground surface, 0, and  $H$ , feet

Appendix H provides  $V_s$  profiles for various locations in South Carolina. These profiles are included for reference only. Site specific  $V_s$  profiles shall be used for the upper 100 feet (30 meters) of a site profile. Deeper, beyond 100 feet,  $V_s$  profiles are available for select areas of South Carolina, see the SCDOT website for a spreadsheet of available deep, beyond 100 feet, shear wave profiles. Contact the PCS/GDS for the deep  $V_s$  profile data.

### 12.3.3 Equivalent Uniform Soil Profile Period and Stiffness

The thickness of the soil deposit,  $H$ , above the B-C Boundary or Hard Rock and average site stiffness,  $V_{s,H}^*$ , are used to compute the natural period of the site,  $T_N$ , as indicated below.  $H$  typically begins at the ground surface, but may begin at the depth where the ground motion is of interest to the structure being designed (see Section 12.5), and extends to the depth where the motion is being generated, typically either the B-C Boundary or a Hard Rock basement outcrop (see Chapter 11). The B-C Boundary is the depth below which the  $V_s$  remains consistently either equal to or greater than 2,500 feet per second. A comprehensive evaluation of how to determine the fundamental period of the soil profile has been made by Dobry, Oweis, and Urzua (1976). Dobry, et al. (1976) presented 2 methods for determining  $T_N$ . The first is a simplified procedure, typically used for uniform soil conditions, as presented in Equation 12-3. The second is a more complex method but is still relatively simple and more accurate method to determine the fundamental period of the soil profile and consists of using the Successive 2-Layer Approach proposed by Madera (1970). Hadjian (2002) presented a simplification to the Successive 2-Layer Approach by Madera (1970). It should be noted that the simplified procedure could be as much as 20 percent greater than the Successive 2-Layer Approach according to Vijayendra, Parsad, and Nayak (2010). According to Bray and Travasarou (2007),  $T_N$  may degrade as the site softens during the seismic event. During the seismic event  $T_N$  may increase by as much as 50 percent when compared to the  $T_N$  generated prior to the seismic event. Equation 12-3 indicates the unsoftened natural site period, while Equation 12-4 indicates the softened site period.

$$T_{NB-C} = \frac{4 * H_{B-C}}{V_{s,H_{B-C}}^*} \quad \text{Equation 12-3}$$

$$T_{NB-C} = \frac{6 * H_{B-C}}{V_{s,H_{B-C}}^*} \quad \text{Equation 12-4}$$

Where,

$T_{NB-C}$  = Natural site period measured from the B-C Boundary or Hard Rock basement outcrop, sec

$V_{s,H}^*$  = Equivalent uniform soil profile stiffness of thickness ( $H$ ), ft/sec (Section 12.3.2)

$H$  = Thickness of soil deposit above B-C Boundary or Hard Rock basement outcrop depending on the level where ground motion input has been developed, feet

As can be seen by Equations 12-3 and 12-4, the  $T_N$  is influenced by the  $V_{s,H}^*$  and  $H$ . A general trend is observed in Figure 12-1 that  $T_N$  decreases as the site stiffness increases while keeping the soil deposit thickness the same. In addition, as  $H$  increases (keeping the  $V_{s,H}^*$  the same), the  $T_N$  of the site increases. Consequently, a combination of lower  $V_{s,H}^*$  and increased  $H$  will work together to increase the  $T_N$  of the site. At the same time, a reduction in the  $T_N$  of the site is observed primarily when the  $V_{s,H}^*$  increases as  $H$  decreases.

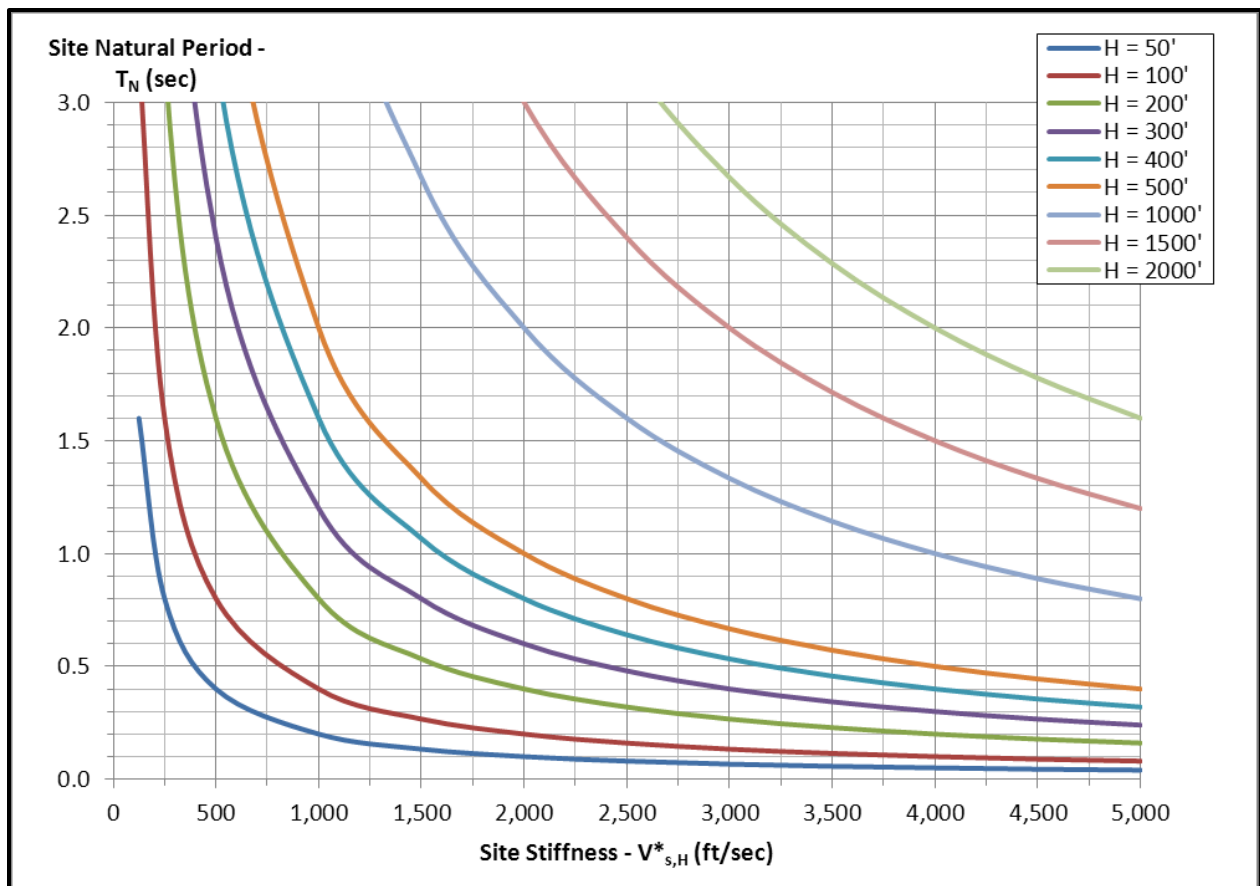


Figure 12-1, Site Stiffness ( $V_{s,H}^*$ ) vs. Site Natural Period ( $T_N$ )

The Successive 2-Layer Approach consists of solving for the fundamental period of 2 soil layers at a time, and then repeating the procedure successively (from the top to bottom of profile) until the entire soil profile is modeled as a single equivalent layer having a fundamental or natural period,  $T_N$ . The Successive 2-Layer Approach as modified by Hadjian (2002) to compute the equivalent uniform soil profile period,  $T_N$ , and stiffness,  $V_{s,H}^*$ , is provided in Table 12-1.

**Table 12-1, Modified Successive 2-Layer Approach  
(Modified Hadjian (2002))**

Step	Procedure Description
1	Begin with the layer at the top (n=1) of the profile under evaluation and continue working to the bottom of the profile (H). Compute the periods, $T_A$ and $T_B$ where A = n (i.e., 1) and B = n+1 (i.e., 2) using Equations 12-3 and 12-4 in order to provide a range of potential site periods.
2	Beginning at the same point in Step 1 determine the following ratio: $\frac{\gamma_A * H_A}{\gamma_B * H_B} \quad \text{Equation 12-5}$ Where: $\gamma_A$ = Unit weight of layer 1, pounds per cubic foot $\gamma_B$ = Unit weight of layer 2, pounds per cubic foot $H_A$ = Thickness of layer 1, feet $H_B$ = Thickness of layer 2, feet
3	Determine the ratio of thickness of consecutive layers: $\frac{H_A}{H_B} \quad \text{Equation 12-6}$ If the ratio is greater than 1 (> 1.0) go to Step 4. If the ratio is less than or equal to 1 ( $\leq 1.0$ ) go to Step 5.
4	Compute the period for combined layers A and B, $T_{A-B}$ , using the following equation: $T_{A-B} = T_B * \sqrt{\frac{\pi^2}{8} * \left[ 0.75 + \left(\frac{T_B}{T_A}\right)^2 * \left(1 + \frac{2 * \gamma_A * H_A}{\gamma_B * H_B}\right) \right]} \quad \text{Equation 12-7}$
5	Compute the period for combined layers A and B, $T_{A-B}$ , using the following equation: $T_{A-B} = T_B * \sqrt[N]{1.0 + \beta * \left(\frac{T_B}{T_A}\right)^N * \left(1 + \frac{\gamma_A * H_A}{\gamma_B * H_B}\right)^N} \quad \text{Equation 12-8}$ Where, $\beta = 1 - 0.2 * \left(\frac{H_A}{H_B}\right)^2 \quad \text{Equation 12-9}$ $N = 4 - \frac{1.8 * H_A}{H_B} \quad \text{Equation 12-10}$
6	Repeat from Step 2 until the entire soil column has been analyzed, substituting ( $\gamma_{A-B} * H_{A-B}$ ) for $\gamma_A * H_A$ , $H_{A-B}$ for $H_A$ , and $T_{A-B}$ for $T_A$ each time.

### 12.3.4 $V_{s,H}^*$ Variation Along a Project Site

If the  $V_{s,H}^*$  varies between the interior bents and abutments of a bridge, the  $V_{s,H}^*$  used in the design of the bridge structure must be evaluated jointly between the SEOR and the GEOR. The motion at the bridge abutment for short bridges with relatively few spans will generally be the primary mechanism by which energy is transferred to the bridge superstructure and therefore



the  $V_{s,H}^*$  at the bridge abutment will govern. The  $V_{s,H}^*$  for longer bridges may differ significantly along the bridge alignment due to variability in soil conditions such as when an abutment is founded on rock ( $V_{s,H}^* > 2,500$  ft/sec), the other abutment is founded on soft soils ( $V_{s,H}^* < 600$  ft/sec), and the interior bents are founded on stiff soils ( $V_{s,H}^* \approx 1,250$  ft/sec). In this circumstance, the primary mechanism by which energy is transferred to the bridge is more difficult to determine. If only a single site response will be used in the analyses, then an envelope could be developed that captures the predominant periods for the entire spectrum using the various ADRS curves developed using the various  $V_{s,H}^*$  values. If the structural analytical method allows the input of several motions at different locations, then several ADRS curves should be used.

The GEOR is responsible for evaluating soil conditions and the extent of site variability (if any) at the bridge location and then determining the  $V_{s,H}^*$  for each individual soil region based on the guidelines provided in this Section. The SEOR and the GEOR will then jointly evaluate the appropriate ADRS curve to be used for the structural design.

### 12.3.5 South Carolina Reference $V_{s,H}^*$

A  $V_{s,H}^*$  was computed for the USGS Shear Wave Velocity Data (Odum, Williams, Stephenson, and Worley (2003) and South Carolina Emergency Management Division (URS (2001)) based on the shear wave reference profiles in Appendix H. The reference  $V_{s,H}^*$  was determined for each shear wave profile using a  $V_{s,H}^*$  computed in accordance with 12.3.2 at the ground surface. The  $V_{s,H}^*$  for the USGS Shear Wave Velocity Data are provided in Tables 12-2 and 12-3.

**Table 12-2, USGS Site Stiffness  
(Modified Odum, et al. (2003))**

Site No.	Site Name	Latitude (degrees)	Longitude (degrees)	Surficial Geology <sup>(1)</sup>	Site Stiffness $V_{s,H}^*$	
					(m/s)	(ft/sec)
1	Lake Murray Spillway	35.052	-81.210	Fill, Pz	661	2,168
2	Fort Jackson	34.028	-90.912	$K_u$	465	1,525
3	Deep Creek School	33.699	-79.351	Q?, $K_u$	246	807
4	Black Mingo	33.551	-79.933	Q, $T_l$	477	1,565
5	Santee Ls	33.235	-80.433	$T_l$	583	1,912
6	The Citadel, Charleston	32.798	-79.958	Q, $T_u$	248	813
7	US Hwy. 17, Charleston	32.785	-79.955	Fill, Q	182	597
8	Isle of Palms	32.795	-79.775	Q, $T_u$	179	587
9	USNSN	33.106	-80.178	Q, $T_u$	464	1,521

<sup>1</sup>Definitions: Q – Quaternary;  $T_u$  – upper Tertiary;  $T_l$  – lower Tertiary;  $K_u$  – upper Cretaceous; Pz – Paleozoic

<sup>2</sup>Longitude is negative indicating west.

The  $V_{s,H}^*$  for the SCEMD Seismic Risk and Vulnerability Study are provided in Table 12-3.

**Table 12-3, USGS Site Stiffness  
(Modified URS Corporation (2001))**

Site No. <sup>(1)</sup>	Site Response Category <sup>(1)</sup>	Geology	Site Stiffness	
			$V_{s,H}^*$ (m/s)	(ft/sec)
1, 2, 4 <sup>(2)</sup>	Piedmont/Blue Ridge, Savannah River, Myrtle Beach <sup>(2)</sup>	Crystalline	3,400	11,152
1	Piedmont/Blue Ridge	Piedmont/Blue Ridge	453	1,486
2	Savannah River	Savannah River	355	1,165
3	Charleston	Charleston	328	1,077
4	Myrtle Beach	Myrtle Beach	239	784

1 Site Response Categories are shown in Appendix H.

2 Various Site Nos. and Site Response Categories are provided for a crystalline geology to account for transition zones between geologies and to allow for any hard-rock basement outcrops located outside of the Piedmont/Blue Ridge Response Category.

## 12.4 PROJECT SITE CLASSIFICATION

In Versions 1.0 (2008) and 1.1 (2010) of the GDM, the Site Class (A through E) was determined using  $V_{s,100}^*$ . The Site Class was used to determine the appropriate site amplification factors ( $F_{PGA}$ ,  $F_a$ , or  $F_v$ ) that were then used to transform the ground motion at the B-C Boundary or Hard Rock basement outcrop to the ground motion at the ground surface. However, according to Andrus, Ravichandran, Aboye, Bhuiyan, and Martin (2014), the requirement for determining Site Class is no longer required, because the site factors will be based directly on the  $V_{s,H}^*$  as measured on the site (see Chapters 4, 5, 6 and Section 12.3). However, the use of the term B-C Boundary will continue even though the Site Classes B and C will no longer be used. B-C Boundary as used in this version of the GDM indicates that the mean (average)  $V_{s,H}^*$  is in excess of 2,500 ft/sec and is no more than 1 standard deviation ( $\sigma$ ) less than this value ( $-1\sigma$ ) from the point where  $V_{s,H}^* = 2,500$  ft/sec is encountered. The B-C Boundary shall be moved to a deeper depth if the shear wave velocity profile is more than  $-1\sigma$  from 2,500 feet per second. The GEOR shall determine the depth to the B-C Boundary based on available data using the spreadsheet previously discussed in Section 12.3.2. In addition, Site Class F (sites requiring site-specific seismic response analyses) shall continue to be used.

The  $V_{s,H}^*$  to be used in the determination of the site amplification factors are different periods ( $F_t$ ) shall be computed in accordance with Section 12.3.2. The H where  $V_s$  will be analyzed should begin at either the existing ground surface if no fill is present or at the estimated original ground surface beneath the embankment, and extend to a depth of at least 100 feet ( $H = 100$  ft.). If the depth-to-motion,  $Z_{DTM}$  concept is to be used, the  $V_{s,H}^*$  profile shall begin at the  $Z_{DTM}$  and extend 100 feet below the  $Z_{DTM}$ . The  $Z_{DTM}$  is the location where the ground shaking is transmitted to the structure being designed. Guidance in selecting the,  $Z_{DTM}$ , is provided in Section 12.5.

When there is a high contrast in  $V_s$  in the soil column, the computed  $V_{s,H}^*$  may not be representative of the site response. The GEOR will need to evaluate the computed  $V_{s,H}^*$  for

high variation in  $V_s$  within the profile that could potentially overestimate the  $V_{s,H}^*$  and in turn miscalculate amplification of the spectral accelerations. The procedure provided in Table 12-4 should be used to evaluate  $V_{s,H}^*$  variability and should be used cautiously as only a guide. The GEOR will be responsible for making all  $V_{s,H}^*$  recommendations, and these recommendations will be submitted to the PC/GDS for review and acceptance. The proposed procedure to evaluate the  $V_{s,H}^*$  variability is based on the potential variability of  $V_s$  testing having a COV of 0.10 to 0.20.

**Table 12-4, Site Stiffness Variability Proposed Procedure**

Step	Description
1	Compute the COV of the $V_s$ values ( $COV_{V_s}$ ) within the soil profile column. If the $COV_{V_s}$ is greater than 0.10 but less than or equal to 0.30 proceed to Step 2. For $COV_{V_s}$ greater than 0.30 proceed to Step 3. If the $COV_{V_s} \leq 0.10$ then compute the $V_{s,H}^*$ using the $V_s$ values in accordance with Section 12.3.
2	<p>If <math>0.10 &lt; COV_{V_s} \leq 0.20</math> adjust <math>V_{s,H}^*</math> using Equation 12-11 then proceed to Step 3.</p> $V_{s,H,\leq 0.2}^* = V_{s,H}^* * (1 - 0.20) \quad \text{Equation 12-11}$ <p>If <math>0.20 &lt; COV_{V_s} \leq 0.30</math> adjust <math>V_{s,H}^*</math> using Equation 12-12 then proceed to Step 3.</p> $V_{s,H,\leq 0.3}^* = V_{s,H}^* * (1 - COV_{V_s}) \quad \text{Equation 12-12}$
3	If $COV_{V_s}$ is greater than 0.30, the GEOR shall submit to the PC/GDS either a recommended (with documentation) $V_{s,H}^*$ to be used for the project or request a site-specific response analysis be performed in accordance with Section 12.9.

When a project site has variable  $V_{s,H}^*$  due to soil spatial variations along the project alignment or when different structural components (bridge abutment, interior bents, embankments, etc.) require differing,  $Z_{DTM}$ , the design team will need to evaluate the  $V_{s,H}^*$  for each structural component being designed. Guidance in selecting the most appropriate  $V_{s,H}^*$  for the structure being designed can be found in Section 12.5.

The following conditions shall be used for determining a Site Class F:

- Peats and/or highly organic clays ( $H > 10$  ft [3 m] of peat and/or highly organic clay where  $H$  = thickness of soil)
- Very high plasticity clays ( $H > 25$  ft [8 m] with  $PI > 75$ )
- Very thick soft/medium stiff clays ( $H > 120$  ft [36 m])
- Soft soil layer ( $H > 10$  ft [3 m]);  $PI > 20$ ;  $w > 40\%$ , and  $\overline{s_u} < 500$  psf (25 kPa) {All conditions must be met.}

If the site meets any of these criteria, classify the project site as Site Class F and perform site-specific seismic site response analysis. In addition, Kavazanjian, et al. (2012) has further identified sites where the use of the 3-Point method may not be appropriate. These sites include sites with a soil column in excess of 500 feet or where a sharp impedance contrast (i.e., a change in soil stiffness or  $V_s$ ) occurs within 150 feet of the ground surface. The recently completed research (Andrus, et al. (2014)) accounts for both of these additional site conditions. Therefore, a site-specific seismic response analysis will typically not be required for either a soil column with a depth greater than 500 feet or for sites with a sharp impedance contrast within 150 feet of the ground surface (see Section 12.8 for guidance). However, the PC/GDS in consultation with the PCS/GDS shall determine whether a site-specific seismic response analysis is required.

## 12.5 DEPTH-TO-MOTION EFFECTS ON SITE CLASS AND SITE FACTORS

For certain types and lengths of bridges it may be more practical to apply the seismic ground motion at a point different from the existing/original ground surface. The types of bridges where changing this depth (depth-to-motion,  $Z_{DTM}$ ) may be practical are those bridges that are not covered by the Seismic Specs. The length of bridge where changing the  $Z_{DTM}$  is beneficial shall be determined by the SEOR with concurrence from the PCS/SDS.

A site-specific response analysis (Section 12.9) shall be required to determine the ADRS curve, when using  $Z_{DTM}$ . It is anticipated that an iterative process will be required between the SEOR and the PC/GDS to determine the  $Z_{DTM}$ . In the cases where the  $Z_{DTM}$  is used, the PC/GDS shall provide to the SEOR the soil models and the critical penetration (Chapter 16). Once the SEOR has determined a  $Z_{DTM}$ , the PC/GDS shall provide the ADRS curve for this depth.

The  $V_{s,H}^*$  shall be determined to 100 feet below the  $Z_{DTM}$ . This  $V_{s,H}^*$  shall be used to determine the 3-point ADRS curve, with this ADRS curve being used for comparison with the ADRS curve from the site-specific seismic response analysis.

## 12.6 SC SEISMIC HAZARD ANALYSIS

The SC Seismic Hazard study shall be used for all “typical” bridges as defined in the Seismic Specs, as well as, bridge embankments and roadway structures. For “non-typical” bridges, the PC/GDS will specify and/or approve appropriate geotechnical seismic analysis provisions on a project specific basis. The Seismic Hazard Mapping study is described in Chapter 11. The seismic hazard information generated from these maps includes the PGA and PSA for 0.5Hz, 1.0Hz, 2.0Hz, 3.3Hz, 5Hz, 6.7Hz, and 13Hz frequencies for the FEE and SEE design earthquakes at hard rock basement outcrop or at geologically realistic site condition. The GEC shall obtain a Seismic Information Request form (GDF 002, see Appendix A) and submit it to the PC/GDS. The most current version of this request form is available on the SCDOT website.

The request form requires that the GEC provide the following information.

- SCDOT Project Name and Project ID
- Latitude and Longitude of Project Site
- OC
- $V_{s,H}^*$
- H – depth for which  $V_s$  was measured
- Site Condition: Geologically Realistic or Hard-Rock Basement Outcrop

The GEC, using the “Site Condition” models contained in Chapter 11, is required to provide documentation for the selection of the Site Condition (Geologically Realistic or Hard-Rock basement outcrop) used. Typically, most sites will be Geologically Realistic unless the  $V_{s,H}^*$  is over 11,000 ft/sec within the 100-foot soil column. Then the “Site Condition” would be considered to be Hard-Rock.

Upon receipt of a completed Seismic Information Request form from the GEC, the PC/GDS shall use the information to develop a 3-Point ADRS curve in accordance with the requirements of this Chapter.

## 12.7 ACCELERATION RESPONSE SPECTRUM

The acceleration response spectrum of a specific seismic motion is a plot of the maximum spectral acceleration,  $S_a$ , response of a series of linear single degree-of-freedom systems with the same damping and mass, but variable stiffness. The Seismic Hazard Mapping study generates a probabilistic UHS consisting of the PGA and PSA at either a Hard-Rock basement outcrop or at Geologically Realistic site conditions (i.e., B-C Boundary). The response spectrum at these locations needs to be adjusted for the local site effects. The local site effects are influenced by the soil stiffness (resonant frequency) of the soil column above the location where ground motion was generated.

The maximum local site amplification occurs when the predominant or maximum period,  $T'_o$  (see Section 12.10.3), of the rock outcrop ground motion, the soil deposit's natural period,  $T_N$ , and the fundamental period of the structure,  $T_0$ , are all in phase. The relationship between rock outcrop and soil surface motions is complex and depends on numerous factors including the fundamental period of the soil profile, strain dependency of soil stiffness and damping, and the characteristics of the rock outcrop motion (Seed and Idriss (1982)).

The effects of local soil site conditions such as rock outcrop, stiff site conditions, soft to medium clay and sand, and deep cohesionless soils on the response spectra shapes (5 percent damped) are shown in Figure 12-2 (Seed, Ugas, and Lysmer (1976)). Normalized spectral shapes were computed by dividing the spectral acceleration by the peak ground acceleration (PGA) at the surface. These spectral shapes were computed from motion records made on rock and soil sites at close distances to earthquakes ( $6 \leq M_w \leq 7$ ). These normalized spectral curves show that spectral response amplification is significantly greater at longer periods ( $\approx 1$  second) with soil site conditions that have decreasing soil site stiffness. The observed variations in spectral response as a function of subsurface site conditions underscore the importance of properly evaluating the project  $V^*_{s,H}$  in accordance with Section 12.3.

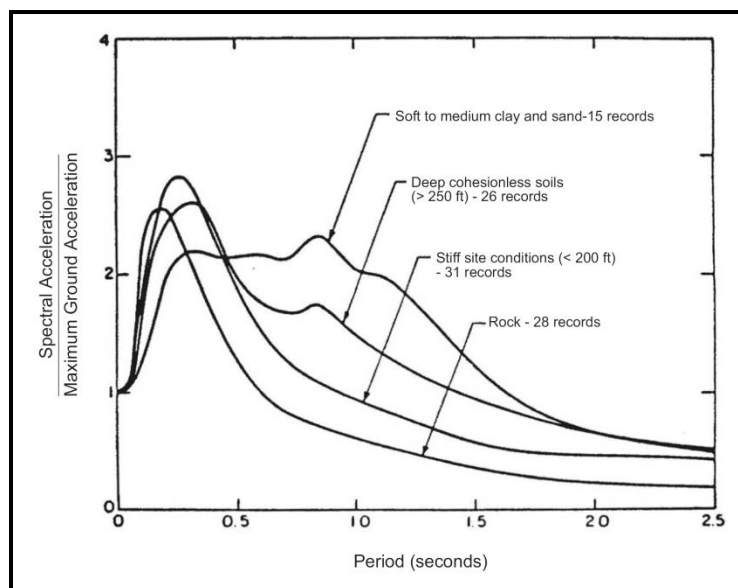
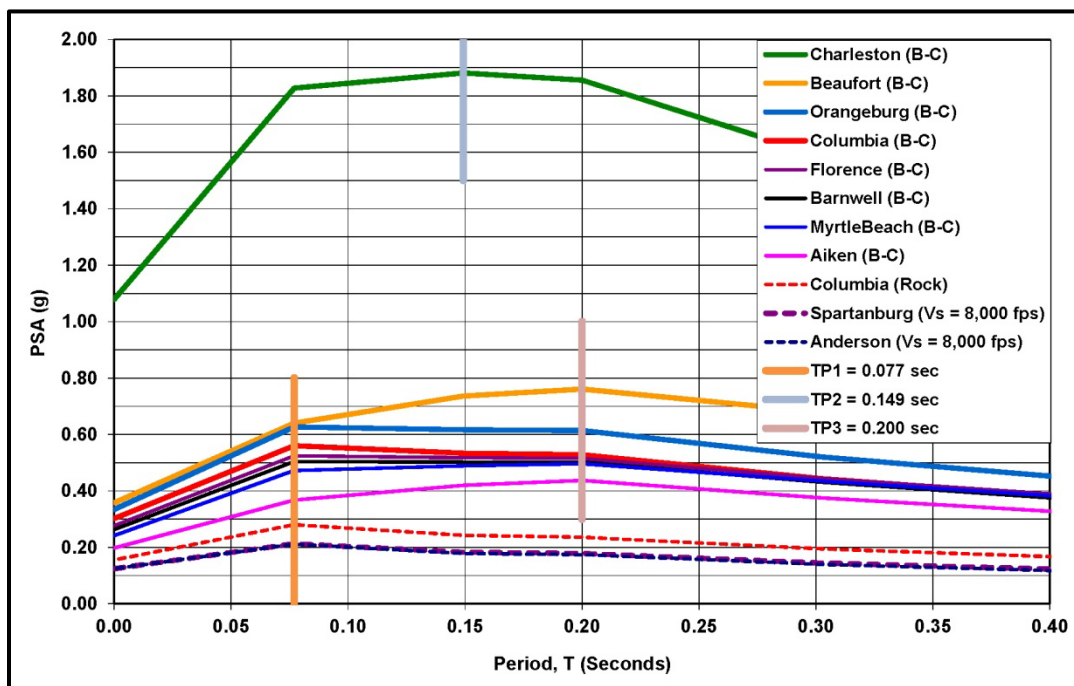


**Figure 12-2, Soil Site Effects on Average Normalized Response Spectra (Seed, et al. (1976))**

It is equally important to know the fundamental period (first order mode) of the structure ( $T_0$ ) (i.e., bridge, ERS, dam, etc.) being designed since structures with periods similar to the period of the ground motion reaching the structure will tend to exert higher seismic loads (demand) and potentially cause significant damage to the structure.  $T_0$  is determined by the SEOR.

A study by Green (2001) reveals that the maximum period,  $T_{max}$ , of the bedrock motion in the Central and Eastern United States (CEUS) varies  $0.05 < T_{max} < 0.10$  sec. as compared to the Western United States (WUS) which varies  $0.15 < T_{max} < 0.25$  sec. The predominant period ( $T'_o$ ) for the SEE seismic motion for select South Carolina cities may be obtained from the UHS, see Figure 12-3. The UHS is determined using the Geologically Realistic model, B-C Boundary in the Coastal Plain or soils outside of the Coastal Plain or at the Hard-Rock basement outcrop (see Chapter 11 for selection of the appropriate geologic conditions). The difference between Green (2001) and Figure 12-3 is  $T_{max}$  was determined for Hard-Rock conditions and did not account for the thickness of the soil deposit on top of the rock.



$T'_o$  = Predominant Period based on the SEE ground motion

$T'_o$ -1 (TP1) – Anderson, Barnwell, Columbia, Florence, Orangeburg, Spartanburg

$T'_o$ -2 (TP2) – Charleston

$T'_o$ -3 (TP3) – Aiken, Beaufort, Myrtle Beach

**Figure 12-3, Predominant Period ( $T'_o$ ) of Selected SC Cities**

$T'_o$ ,  $T_N$  and  $T_0$  should be compared by the SEOR and if these periods coincide then harmonic resonance between the seismic event, the site and the structure should be anticipated. If  $T'_o$  and  $T_N$  coincide then site amplification should be anticipated. The PC/GDS shall determine if a site-specific seismic response analysis is required if  $T'_o$  and  $T_N$  coincide.

The local site effects are taken into account by performing a site response analysis using the Seismic Hazard Mapping Study (Section 12.8) or by performing a site-specific response analysis (Section 12.9). The following Subsections describe special site conditions that may influence the site response that typically cannot be addressed by simplified response methods that use the Seismic Hazard Mapping Study (Section 12.8).

### 12.7.1 Effects of Rock Stiffness WNA vs. ENA

The effects of rock stiffness (shear wave velocity) and damping on normalized response spectra shapes (5 percent damped) on rock sites are shown in Figure 12-4 (Silva and Darragh (1995)). Normalized spectral shapes were computed by dividing the spectral acceleration by the PGA at the surface. Normalized response spectra were computed for Western North America (WNA), representative of soft rock encountered in California and for Eastern North America (ENA),

representative of hard rock encountered in the Eastern United States. The normalized response spectra were computed from motion records made on rock sites at close distances to earthquakes ( $M_w = 4.0$  and  $6.4$ ). These normalized spectral curves show that ENA spectral response amplification is greater at shorter periods or higher frequencies when compared to WNA spectral response. This effect of higher amplification at shorter periods or higher frequencies is more evident for smaller earthquakes because of higher corner frequencies for smaller magnitude earthquakes (Boore (1983); Silva and Green (1989); Silva and Darragh (1995)).

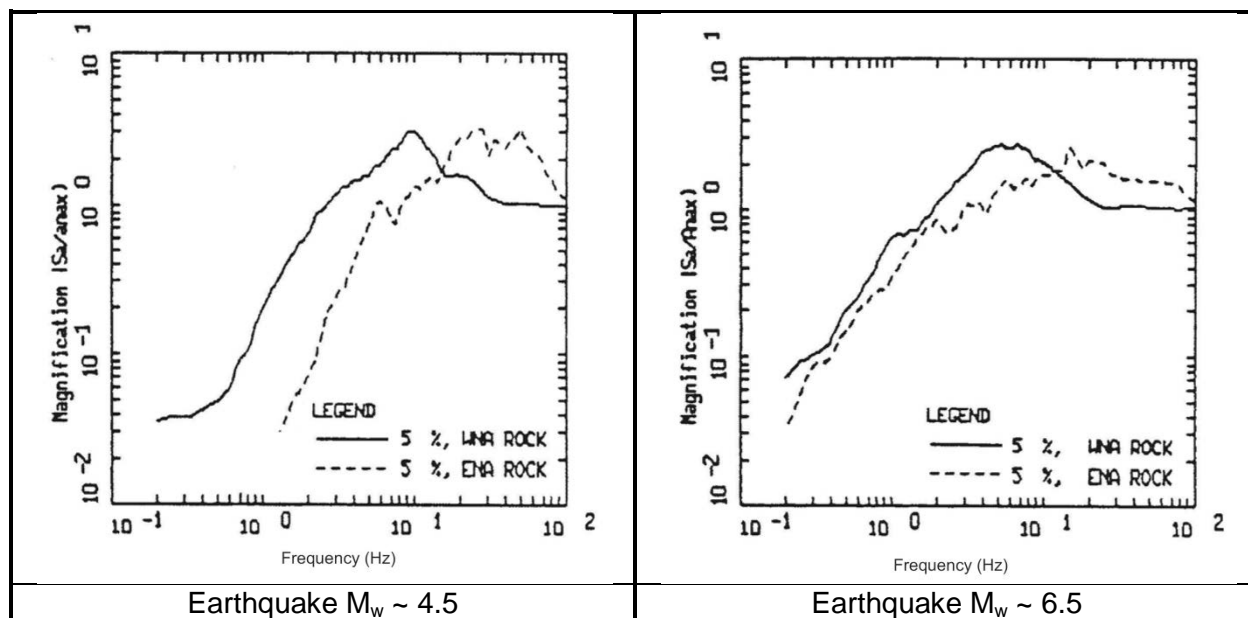


Figure 12-4, WNA / ENA Rock Effects on Normalized Response Spectra (Silva and Darragh, 1995)

### 12.7.2 Effects of Weathered Rock Zones Near the Ground Surface

Some caution should be exercised when evaluating the site response of sites where weathered rock zones are near the surface such as in the Blue Ridge/Piedmont Units and in transition areas between the Piedmont Unit and the Coastal Plain Unit. Transition areas between physiographic units can be found along the "Fall Line" with the Columbia, SC metropolitan area being an example. The Columbia, SC area generally consists of 10 to 30 feet of surficial soils ( $200 \leq V_s \leq 500$  ft/sec), underlain by 30 to 90 feet of a weathered rock zone ( $2,500 < V_s < 8,000$  ft/sec), followed by a Hard-Rock basement outcrop ( $V_s > 11,000$  ft/sec). A site-specific response study (Lester (2005)) of the Columbia, SC area compared spectral accelerations modeled at the B-C Boundary (weathered rock) outcropping conditions and Hard-Rock outcropping conditions with a weathered rock zone modeled by a shear wave velocity gradient from 2,500 to 8,000 ft/sec on 1.5 ft. increments. This study found that the spectral accelerations for the 2 models were similar for frequencies up to 10 Hz. (periods  $> 0.10$  seconds). The spectral accelerations increased for frequency greater than 10 Hz. (periods  $< 0.10$  seconds) for the model extended to the hard-rock outcropping conditions. The magnitude of the increase in spectral acceleration was dependent on the thickness of the graded weathered rock zone.

Based on this study (Lester (2005)) the following preliminary guidelines are provided:

1. **Coastal Plain Unit with sedimentary surface soils:** When ground motions are generated using a geologically realistic site condition using Scenario\_PC (2006) the thickness of the firm Coastal Plain sediment and/or weathered rock zone will be modeled approximately by the transfer function that places the ground motion

at the B-C boundary ( $V_s = 2,500$  ft/sec) and therefore the amplification observed from weathered rock thickness greater than 30 feet will not be as significant.

2. **Blue Ridge/Piedmont Unit with Weathered Rock Zone:** The 3-Point site response method can only be used if the weathered rock thickness ( $2,500 \leq V_s \leq 8,000$  ft/sec) is less than 30 feet thick. When performing site-specific response analyses in the Blue Ridge/Piedmont units with weathered rock zone ( $2,500 \leq V_s \leq 8,000$  ft/sec) thickness greater than 30 feet, this zone must be modeled by a shear wave velocity gradient. If the thickness ( $d_{WR}$ ) of the weathered rock zone is unknown, a sensitivity analysis of the thickness will be required to determine the amplification effects on the spectral accelerations and PGA.

### 12.7.3 **Effects of Soil Softening and Liquefaction on Spectral Acceleration**

Youd and Carter (2005) have studied the effects of soil softening and liquefaction on spectral accelerations of 5 instrumented sites. Three of the sites were in the United States (California) and the other 2 in Japan. Youd and Carter (2005) made the following observations:

1. Soil softening due to increased pore water pressure generally reduces short period spectral accelerations ( $T < 1.0$  sec) as compared to those spectral accelerations that would have occurred without soil softening.
2. Soil softening may have little influence on short period spectral accelerations ( $T < 1.0$  sec) when soil softening occurs late in the strong motion sequence.
3. Soil softening usually amplifies or enhances long period spectral accelerations ( $T > 1.0$  sec) due to lengthening of the  $T_N$  of the site as it softens (See Figure 12-1). When liquefaction-induced ground oscillations continue after earthquake shaking, there may be considerable enhancement of the long-period ( $T > 1.0$  sec) spectral accelerations.

When a site-specific response analysis is not performed and the simplified response methods that use the Seismic Hazard Mapping study (Section 12.8) are used, the effects of soil softening and liquefaction on the design spectral response generated will have the following implications to the structures being designed.

1. For structures with short-fundamental periods ( $T_0 < 1.0$  sec), the design spectral accelerations will conservatively envelope the actual spectral acceleration for sites where soil softening or liquefaction occurs early in the strong motion sequence.
2. For structures with long-fundamental periods ( $T_0 > 1.0$  sec), the design spectral accelerations may be unconservative due to the lengthening of the  $T_N$  of the site. For these types of structures with long-fundamental periods ( $T_0 > 1.0$  sec), a site-specific seismic response analysis should be considered.

### 12.7.4 **Horizontal Ground Motion Response Spectra**

The Seismic Specs require safety and functional evaluations for bridges based on the bridge Operational Classification, OC. All bridges (OC = I, II, or III) require a structural response evaluation using the SEE. Bridges with an OC = I or II also require a structural evaluation using the FEE only if the project site has the potential for SSL or slope instability at bridge abutments and no geotechnical mitigation is performed during the FEE. Seismic structural design shall be



required, as required in the Seismic Specs, even if the displacement criteria established in GDM is met. Therefore, meeting the displacement criteria is not considered as geotechnical mitigation for meeting this design requirement.

The ADRS curves is determined using either the 3-Point method (Section 12.8) or the Site-Specific Seismic Response Analysis (Section 12.9) using the selection criteria in Table 12-5.

ADRS curves described in Sections 12.8 and 12.9 are generated for the design earthquakes (SEE and/or FEE) as needed by the SEOR to perform a structural evaluation. However, a 2-level design approach (SEE and FEE) is required for all bridge embankments and all ERSs located within the limits of the bridge embankments. Therefore, the ADRS curve for both seismic events shall be developed and provided to the design team. ERSs located within the roadway embankment shall be designed for the SEE only; unless in the opinion of the design team a 2-level approach (i.e., designing for both FEE and SEE) should be considered. The ADRS curves are supplied to the SEOR in the form of a curve and tabulated values of spectral accelerations,  $S_a$ , in units of gravity (g) and corresponding time period, T, in units of seconds (see Figure 12-8 for format).

Physiographic Unit <sup>1</sup>	Site Response Method	Site Condition	Weathered Rock Thickness $d_{WR}$ <sup>2</sup> (feet)	Geologic Condition	Outcrop Description	Comments
Coastal Plain Unit	3-Point	$V_{s,H} < 2,500$ ft/sec	$d_{WR}$ Any	Geologically Realistic	$V_{s,H} = 2,500$ ft/sec B-C Boundary	Soil column should consist of soils ( $V_{s,H}^* < 2,500$ ft/sec).
	Site-Specific Response	F or Required by SCDOT	$d_{WR}$ Any	Geologically Realistic	$V_{s,H} = 2,500$ ft/sec B-C Boundary	Soil column model must extend to hypothetical firm Coastal Plain outcrop equivalent of B-C Boundary ( $V_{s,H}^* > 2,500$ ft/sec (see Section 12.4)). Document soil column properties and soil stratification sensitivity.
Outside Coastal Plain Unit (Blue Ridge/Piedmont Units)	3-Point	$2,500$ ft/sec $< V_{s,H} < 8,000$ ft/sec	$0 < d_{WR}$	Hard-Rock Basement Outcrop	$V_{s,H} = 11,500$ ft/sec	Use of ground motions generated at the hard-rock basement outcrop will require written permission by the PC/GDS. The soil column model must extend to hard-rock basement outcrop ( $V_{s,H}^* > 11,500$ ft/sec). The soil column development must be documented thoroughly and extensive soil stratification sensitivity analyses must be performed, particularly below the B-C Boundary.
	3-Point		$d_{WR} = 0$	Geologically Realistic	$V_{s,H} = 8,200$ ft/sec	Soil column should consist of soils ( $V_{s,H}^* < 2,500$ ft/sec).
	Site Specific Response	F or Required by SCDOT	$d_{WR} > 30$	Hard-Rock Basement Outcrop	$V_{s,H} = 11,500$ ft/sec	Note that hard-rock must be verified by shear wave velocity measurements of hard-rock ( $V_{s,H}^* > 11,500$ ft/sec).
	Site Specific Response		$d_{WR} \leq 30$	Geologically Realistic	$V_{s,H} = 8,200$ ft/sec	Soil column model must extend to hypothetical firm Coastal Plain outcrop equivalent of a hypothetical outcrop of Piedmont weathered rock ( $V_{s,H}^* > 8,000$ ft/sec). Document soil column development and soil stratification sensitivity.
				Hard-Rock Basement Outcrop	$V_{s,H} = 11,500$ ft/sec	Soil column model must extend to hard-rock basement outcrop ( $V_{s,H}^* > 11,500$ ft/sec). Document soil column development and soil stratification sensitivity. The weathered rock zone ( $2,500 \leq V_{s,H}^* \leq 11,500$ ft/sec) must be modeled by a shear wave velocity gradient. If thickness ( $d_{WR} > 30$ ft.) of the weathered rock zone is unknown, a sensitivity analysis of the thickness will be required.

<sup>1</sup> If Senario\_PC (2006) indicates a zero sediment thickness ( $d_s = 0$ ) the site is assumed to be outside of the Coastal Plain (Blue Ridge/Piedmont). If the sediment thickness is greater than zero ( $d_s > 0$ ) the site is assumed to be in the Coastal Plain.

<sup>2</sup> Weathered rock zone with shear wave velocities 2,500 – 8,000 ft/sec.

Table 12-5, Site Response Selection Criteria

### 12.7.5 Vertical Ground Motion Response Spectra

Recent studies shown in Figure 12-5 reveal that the ratio of vertical to horizontal ground motion response spectra can vary substantially from the nominal two-thirds ( $2/3$ ) ratio commonly used. Studies show that the  $2/3$  ratio of vertical to horizontal ground motion response spectra may be conservative for  $T_0$  longer than 0.2 seconds. For  $T_0$  shorter than 0.2 seconds the ratio of vertical to horizontal ground motion response spectra may exceed the  $2/3$  value and may be on the order of 1 to 1.5 times the horizontal for earthquakes with close source-to-site distances and  $T_0$  of less than 0.1 seconds. Although the studies shown in Figure 12-5 are from ground motion data from the WUS, Chiou, Silva, and Power (2002) indicates that the ratios for the CEUS are not greatly different from the ratios in the WUS.

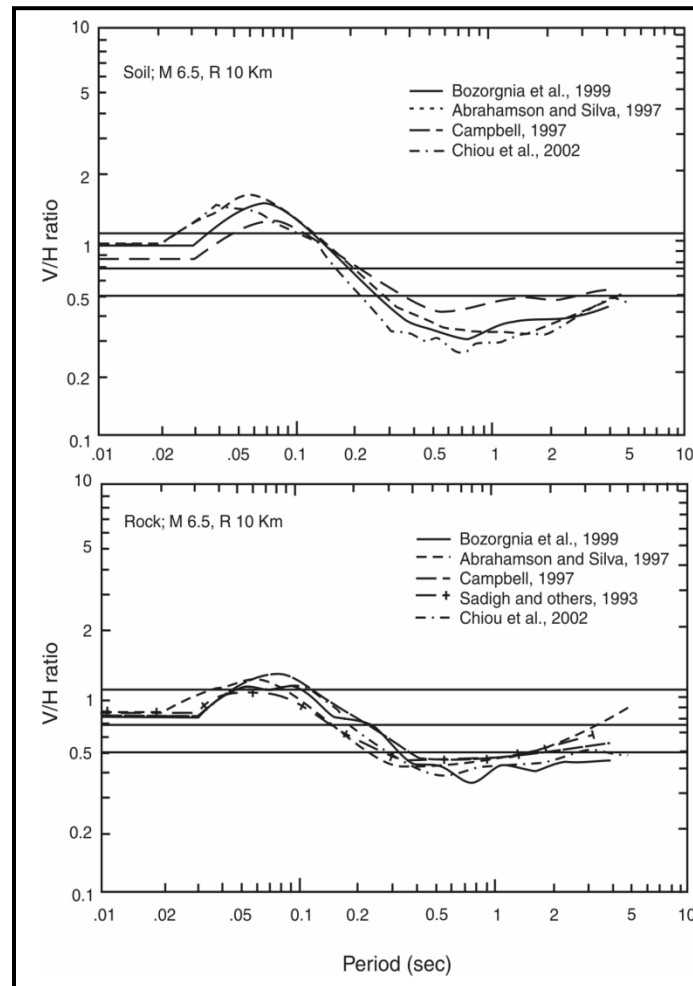


**Figure 12-5, Vertical/Horizontal Spectral Ratios vs. Period (Buckle, et al. (2006))**

Because there are currently no accepted procedures for constructing the vertical response spectra or having an appropriate relationship with the horizontal response spectra constructed using the Seismic Hazard Mapping study, Section 12.8, the  $2/3$  ratio of vertical-to-horizontal response spectra shall be used for bridges with  $T_0$  of 0.2 seconds or longer. When the bridge's  $T_0$  is less than 0.2 seconds, a site-specific vertical response spectrum using the results of recent studies such as those shown in Figure 12-5 should be used to develop the vertical ground motion response spectra.

## 12.8 SITE RESPONSE ANALYSIS USING SEISMIC HAZARD MAPPING STUDY

The results of the Seismic Hazard Mapping study (i.e., SCENARIO\_PC (2006)) shall be used to develop the 3-Point ADRS curve. The 3-Point ADRS curve is anticipated to be used on all typical SCDOT bridges, except those sites meeting the Site Class F criteria provided in Section 12.4 or as determined by SCDOT. Non-typical bridges, sites with Site Class F soils and those bridges selected by SCDOT shall have site-specific seismic response analysis performed in accordance with Section 12.9. The following Sections describe the procedures for developing the site amplification factors,  $F_t$  that are required to develop the 3-Point ADRS curve.

### 12.8.1 ADRS Curves for FEE and SEE

As described in Chapter 11 there are 2 design seismic events used for evaluation of SCDOT structures, the FEE and the SEE. The PGA and spectral response accelerations,  $S_a$ , developed using Sections 12.8.2 and 12.8.3 will depend on which design earthquake is being analyzed and on the local site conditions. Selected locations within South Carolina have been used, where depending on the geology the site amplification factors,  $F_t$ , can be different (Figure 12-6). Figure 12-6, as well as indicated in Chapter 11, depicts South Carolina as divided between the Coastal Plain (SCCP) and the Piedmont ((SCP) areas outside of the Coastal Plain). This is a change from the previous site factors, where a single set of site amplification factors (PGA ( $F_{PGA}$ ), short-period ( $F_a$ ) and long-period ( $F_v$ )) were used for the entirety of South Carolina and with the sites being differentiated by Site Class.

Based on Andrus, et al. (2014),  $F_t$  was determined to vary greatly with the  $V_{s,100}^*$  (the average shear wave velocity for the upper 100 feet of the site), specifically,

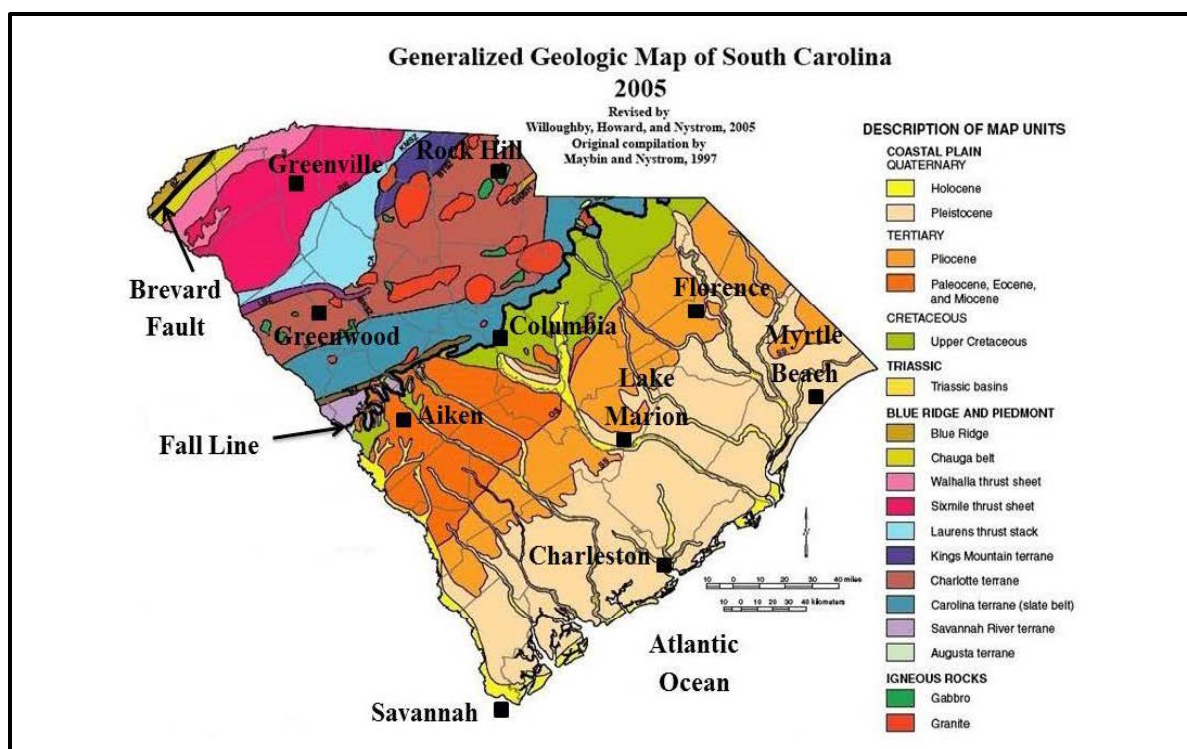
- An increasing trend in  $F_t$  as  $V_{s,100}^*$  increased from a low value
- A zone of peak  $F_t$  values ( $F_{P,t}$ ), depending on  $V_{s,100}^*$  and  $PSA_{B-C}$
- A decreasing trend in  $F_t$  as  $V_{s,100}^*$  increases beyond the zone of  $F_P$  values

These trends are the same for both the Coastal Plain as well as the Piedmont. The  $F_t$  factors were determined for a range of spectral periods ( $t$ ) and are referred to by the middle of the range periods as indicated in Table 12-6.

**Table 12-6, Spectral Period Ranges and Designations**

Spectral Period Range, $t$ (sec)	Spectral Period Designation, $t$ (sec)	Corresponding Pseudo-Acceleration, $PSA_{B-C,t}$ (g)	$F_t$ Factor Designation
$\leq 0.01$	0.0	$PGA_{B-C}$	$F_{PGA}$
0.01 – 0.40	0.2	$S_s$	$F_{0.2}(F_a)$
0.41 – 0.80	0.6	$S_{0.6}$	$F_{0.6}$
0.81 – 1.20	1.0	$S_{1.0}$	$F_{1.0}(F_v)$
1.21 – 2.00	1.6	$S_{1.6}$	$F_{1.6}$
2.01 – 4.00	3.0	$S_{3.0}$	$F_{3.0}$

The ADRS curves generated using the Seismic Hazard Mapping Study will be based on a 5 percent viscous damping ratio since the pseudo spectral accelerations (PSA) have been generated for 5 percent damping.



Note: In the Columbia and Aiken areas, if depth to Weathered Hard Rock < 330 feet, Piedmont Factors shall be used.

**Figure 12-6, Geologic Map Indicating Sites Used in Ground Response Analysis (Andrus, et al. (2014))**

### 12.8.2 Local Site Effects – Coastal Plain

The  $F_t$  factors for the Coastal Plain are based on the soil column (model) beginning at the B-C Boundary (i.e., the depth where  $V_{s,H}^*$  remains consistently more than 2,500 ft/sec (~760 m/sec)). For the reference models developed in Andrus, et al. (2014), the B-C Boundary (termed soft rock half space in Andrus, et al. (2014)) ranged from 450 ft (137 m) to 485 ft (148 m). The peak average shear wave velocity in the top 100 feet,  $V_{s,100,P,t}^*$  and the corresponding peak site coefficient at a specific spectral period,  $F_{P,t}$ , can be determined using:

$$V_{s,100,P,t}^* = x_1 * \left( \frac{PSA_{B-C,t}}{1g} \right)^{x_2} * \left( \frac{T_m}{1s} \right)^{x_3} * K_{H2} \quad \text{Equation 12-13}$$

$$F_{P,t} = \left\{ x_4 * \left[ e^{\left( \frac{x_5 * PSA_{B-C,t}}{1g} \right)} \right] * \left( \frac{T_m}{T_{330}} \right)^{x_6} + 1 \right\} * K_{H1} \quad \text{Equation 12-14}$$

Where,

$V_{s,100,P,t}^*$  = Weighted, average site stiffness in the top 100 feet corresponding to the peak site factor adjusted for  $d_{B-C}$ , ft/sec

$F_{P,t}$  = Peak  $F_t$  factor at a specific spectral period adjusted for  $d_{B-C}$

t = Specific spectral period, second (see Table 12-6)

$x_{1 \text{ to } 6}$  = Regression coefficients (see Table 12-7)

$d_{B-C}$  = Depth to B-C Boundary, ft

$PSA_{B-C,t}$  = Pseudo-acceleration at the B-C Boundary outcrop at a specific spectral period, from SCENARIO\_PC (2006)

$T_m$  = Mean period of input rock motion, sec

$T_{330}$  = Period for the top 330 feet (100 meters) of the site, sec

$K_{H1}$  and  $K_{H2}$  = Adjustment factors for  $d_{B-C} < 330$  feet, see Table 12-9

$T_m$  may be estimated using Equation 12-15 and is applicable for those sites that are dominated by the Charleston seismic hazard zone (i.e., the deaggregation indicates that the dominate source of the seismic hazard is Charleston).  $T_{330}$  may be estimated using Equation 12-16.

$$T_m = 0.031 * \left(\frac{d_{HR}}{1000}\right) + 0.485 * \left(\frac{R}{1000}\right) + 0.233 \quad \text{Equation 12-15}$$

$$T_{330} = \frac{4*330}{V_{s,330}^*} = \frac{1,320}{V_{s,330}^*} \quad \text{Equation 12-16}$$

$$V_{s,330}^* = \frac{330}{\left(\frac{100}{V_{s,100}^*} + \frac{230}{V_{s,100-330}^*}\right)} \quad \text{Equation 12-17}$$

Where,

$d_{HR}$  = Depth to Hard Rock ( $V_s \geq 11,000$  ft/sec) from SCENARIO\_PC (2006), feet

R = Site to source distance (see Chapter 11), miles

$V_{s,100}^*$  = Weighted, average site stiffness in the top 100 feet at a specific site, ft/sec

$V_{s,100-330}^*$  = Weighted, average site stiffness between the depths of 100 and 330 feet estimated on a regional basis, ft/sec

$V_{s,330}^*$  = Weighted, average site stiffness for the top 330 feet combining the site stiffness at a specific site with the regional site stiffness below 100 feet, ft/sec

Typical values of  $V_{s,330}^*$ ,  $V_{s,100-330}^*$ ,  $T_{330}$  and  $T_m$  are provided in Table 12-8. As additional deep shear wave velocities are obtained (i.e.,  $V_{s,330}^*$ ), it may become possible to determine  $V_{s,100-330}^*$ . Until that time use Table 12-8 to determine  $V_{s,330}^*$ ,  $V_{s,100-330}^*$ .

**Table 12-7, Regression Coefficients for the Coastal Plain**

$PSA_{B-C,t}$	$x_1$ (ft/sec)	$x_2$	$x_3$	$x_4$	$x_5$	$x_6$	a
$PGA_{B-C}$	846	0.222	-0.276	7.510	-4.394	1.614	- <sup>1</sup>
$S_s$	804	0.206	-0.141	7.305	-1.980	1.546	0.65
$S_{0.6}$	466	0.181	-0.721	10.691	-3.382	1.487	0.85
$S_{1.0}$	344	0.214	-0.867	4.929	-2.734	0.437	0.90
$S_{1.6}$	420	0.228	-0.647	3.477	-2.555	0.185	0.99
$S_{3.0}$	692	0.208	-0.036	0.720	-5.638	-0.860	0.99

<sup>1</sup>Use Equation 12-18

**Table 12-8, Typical Normalized Period Values by Region**

Site Regions	$V_{s,330}^*$ (ft/sec)	$V_{s,100-330}^*$ (ft/sec)	$T_{330}$ (sec)	$T_m$ (sec)	$T_m/T_{330}$
Charleston	1,237	1,445	1.06	0.29	0.27
Savannah	1,237	1,445	1.06	0.40	0.38
Myrtle Beach	1,555	1,945	0.84	0.37	0.44
Columbia	1,381	1,620	0.95	0.29	0.30
Florence	1,381	1,620	0.95	0.30	0.32
Lake Marion	1,381	1,620	0.95	0.28	0.29
Aiken	1,299	1,370	1.01	0.31	0.31

**Table 12-9, Adjustment Factors for  $d_{B-C} < 330$  feet for the Coastal Plain**

$PSA_{B-C,t}$	Adjustment Factor	Depth to B-C Boundary, $d_{B-C}$ (feet)							
		1.5	5	16.5	33	65	100	165	$\geq 330$
$PGA_{B-C}$	$K_{H1}$	0.96	1.11	1.53	1.40	1.24	1.15	1.02	1.00
	$K_{H2}$	2.71	2.29	2.08	1.67	1.25	1.17	1.04	1.00
$S_s$	$K_{H1}$	0.77	0.90	1.23	1.55	1.35	1.23	1.10	1.00
	$K_{H2}$	2.71	2.29	1.88	1.50	1.25	1.04	1.02	1.00
$S_{0.6}$	$K_{H1}$	0.48	0.70	0.83	0.91	1.00	1.04	1.04	1.00
	$K_{H2}$	2.95	2.27	1.59	1.36	1.36	1.14	1.09	1.00
$S_{1.0}$	$K_{H1}$	0.46	0.73	0.80	0.84	0.88	0.92	0.96	1.00
	$K_{H2}$	2.86	2.14	1.52	1.43	1.29	1.19	1.05	1.00
$S_{1.6}$	$K_{H1}$	0.26	0.29	0.60	0.81	0.83	0.95	0.98	1.00
	$K_{H2}$	3.53	2.65	1.76	1.47	1.29	1.06	1.03	1.00
$S_{3.0}$	$K_{H1}$	0.37	0.41	0.46	0.61	0.69	0.78	0.89	1.00
	$K_{H2}$	5.36	4.02	2.68	1.88	1.52	1.34	1.07	1.00

As indicated previously, the  $F_t$  factor varies based on the shear wave velocity encountered at each site. A linear relationship for determining the  $F_t$  factor was developed by Andrus, et al. (2014) when  $V_{s,100}^* < V_{s,100,P,t}^*$  and is applicable for all values of  $t$ ,

$$F_t = \left( \frac{F_{P,t}}{V_{s,100,P,t}^*} \right) * V_{s,100}^* \quad \text{Equation 12-18}$$

Where,

$F_t$  = Amplification factor at a specific spectral period

$V_{s,100,P,t}^*$  = Weighted, average site stiffness in the top 100 feet corresponding to the peak site factor adjusted for  $d_{B-C}$  (Equation 12-13), ft/sec

$F_{P,t}$  = Peak  $F_t$  factor at a specific spectral period adjusted for  $d_{B-C}$  (Equation 12-14)

$V_{s,100}^*$  = Weighted, average site stiffness in the top 100 feet at a specific site, ft/sec

When  $V_{s,100}^* \geq V_{s,100,P,t}^*$ , the  $F_t$  factor for periods less than 0.2 seconds is expressed as a linear relationship. For periods greater than or equal 0.2 seconds the  $F_t$  factor is expressed as an exponential relationship. Both relationships were developed by Andrus, et al. (2014) and are provided below.

For  $t < 0.2$  sec and  $V_{s,100}^* \geq V_{s,100,P,t}^*$

$$F_t = \left[ \frac{(F_{P,t}-1)*(2,500-V_{s,100}^*)}{2,500-V_{s,100,P,t}^*} \right] + 1 \quad \text{Equation 12-19}$$

For  $t \geq 0.2$  sec and  $V_{s,100}^* \geq V_{s,100,P,t}^*$

$$F_t = a + b * e^{(c*V_{s,100}^*)} \quad \text{Equation 12-20}$$

Where,

$F_t$  = Amplification factor at a specific spectral period

$V_{s,100,P,t}^*$  = Weighted, average site stiffness in the top 100 feet corresponding to the peak site factor adjusted for  $d_{B-C}$  (Equation 12-13), ft/sec

$F_{P,t}$  = Peak  $F_t$  factor at a specific spectral period adjusted for  $d_{B-C}$  (Equation 12-14)

$V_{s,100}^*$  = Weighted, average site stiffness in the top 100 feet at a specific site, ft/sec

$a$  = Regression coefficient from Table 12-7

$b$  = Regression coefficient determined from Equation 12-21

$c$  = Regression coefficient determined from Equation 12-22, sec/ft

$$b = \frac{1-a}{e^{(2500*c)}} \quad \text{Equation 12-21}$$

$$c = \left( \frac{1}{2500 - V_{s,100,P,t}^*} \right) * \ln \left( \frac{1-a}{F_{P,t}-a} \right) \quad \text{Equation 12-22}$$

If the project site is located within one of the Coastal Plain counties near the “Fall Line” (i.e., Aiken, Chesterfield, Kershaw, Lexington, or Richland Counties) and the depth to shallow weathered hard rock ( $V_s^* \geq 8,200$  ft/sec) is less than 330 feet, then the  $F_t$  factors developed in Section 12.8.3 shall be used.

### 12.8.3 Local Site Effects – Piedmont

The  $F_t$  factors for the Piedmont (see Figure 12-6) are based on the soil column (model) beginning at the weathered hard rock boundary (i.e., the depth where  $V_{s,H}^*$  remains consistently greater than 8,200 ft/sec (2500 m/sec)). For the reference models developed in Andrus, et al. (2014), the weathered hard rock boundary ranged from 33 ft (10 m) to 100 ft (30 m). The peak  $F_t$  factor,  $F_P$ , and the peak average shear wave velocity for the top 100 ft,  $V_{s,100,P}^*$ , are determined using the following equations:

$$V_{s,100,P,t}^* = x_7 * \left( \frac{PSA_{HR,t}}{1g} \right)^{x_8} * \left( \frac{T_m}{1s} \right)^{x_9} * K_{H4} \quad \text{Equation 12-23}$$

$$F_{P,t} = \left\{ x_{10} * \left[ e^{\left( \frac{x_{11} * PSA_{HR,t}}{1g} \right)} \right] + 1 \right\} * K_{H3} \quad \text{Equation 12-24}$$

Where,

$V_{s,100,P,t}^*$  = Weighted, average site stiffness in the top 100 feet corresponding to the peak site factor adjusted for  $d_{HR}$ , ft/sec

$F_{P,t}$  = Peak  $F_t$  factor at a specific spectral period adjusted for  $d_{HR}$

$d_{HR}$  = Depth to Hard Rock ( $V_s \geq 11,000$  ft/sec) from SCENARIO\_PC (2006), feet

$t$  = Specific spectral period, second (see Table 12-6)

$x_7$  to  $x_{11}$  = Regression coefficients (see Table 12-10)

$PSA_{HR,t}$  = Pseudo-acceleration at the Hard Rock ( $V_s \geq 11,000$  ft/sec) outcrop at a specific spectral period, from SCENARIO\_PC (2006)

$T_m$  = Mean period of input rock motion, sec

$T_{330}$  = Period for the top 330 feet (100 meters) of the site, sec

$K_{H3}$  and  $K_{H4}$  = Adjustment factors for  $d_{HR}$ , see Table 12-12

$T_m$  may be estimated using Equation 12-15 with  $d_{HR}$  equal to 0 ( $d_{HR} = 0$ ) and is applicable for those sites that are dominated by the Charleston seismic hazard zone (i.e., the deaggregation



indicates that the source of the seismic event is Charleston).  $T_m$  for the SEE in the western Piedmont (Abbeville, Anderson, Greenville, Greenwood, Laurens, McCormick, Oconee and Pickens Counties) cannot be determined using Equation 12-15, since this area is dominated by different seismic hazard zone than the Charleston seismic hazard zone. For the western Piedmont,  $T_m$  shall be set as 0.37 sec ( $T_m = 0.37$  sec) for the SEE condition.

Typical values of  $T_m$  are provided in Table 12-11. As additional deep shear wave velocities are obtained (i.e.,  $V_{s,330}^*$ ), it may become possible to determine  $V_{s,100-330}^*$  and  $T_{330}$  may be estimated using the Equation 12-17.

**Table 12-10, Regression Coefficients for the Piedmont**

$PSA_{HR,t}$	$x_7$ (ft/sec)	$x_8$	$x_9$	$x_{10}$	$x_{11}$	a
$PGA_{HR}$	1,916	0.162	0.198	2.589	-3.772	<sup>-1</sup>
$S_s$	1,765	0.180	0.184	2.420	-0.934	0.70
$S_{0.6}$	1,765	0.162	0.228	2.940	-2.653	0.99
$S_{1.0}$	1,227	0.090	0.333	1.489	-0.896	0.99
$S_{1.6}$	1,230	0.204	0.427	1.159	-1.423	0.99
$S_{3.0}$	695	0.208	-0.036	1.093	-4.480	0.99

<sup>1</sup>Use Equation 12-25

**Table 12-11, Typical Normalized Period Values by Region**

Site Regions	$T_m$ (sec)
Columbia	0.27
Rock Hill	0.28
Greenwood	0.35
Greenville	0.33

**Table 12-12, Adjustment Factors for  $d_{HR}$  for the Piedmont**

$PSA_{HR,t}$	Adjustment Factor	Depth to Weathered Hard Rock Boundary, $d_{HR}$ (feet)						
		16.5	33	66	100	131	165	330
$PGA_{HR}$	$K_{H3}$	0.35	0.37	1.00	1.00	0.96	0.89	0.78
	$K_{H4}$	7.83	7.33	1.67	1.00	0.97	0.93	0.77
$S_s$	$K_{H3}$	0.34	0.37	1.13	1.00	0.94	0.87	0.79
	$K_{H4}$	7.03	6.25	1.41	1.00	0.97	0.94	0.78
$S_{0.6}$	$K_{H3}$	0.30	0.32	0.62	1.00	1.04	1.05	1.18
	$K_{H4}$	9.69	9.39	2.86	1.00	0.97	0.94	0.79
$S_{1.0}$	$K_{H3}$	0.35	0.36	0.45	1.00	1.15	1.19	1.25
	$K_{H4}$	12.63	12.11	3.79	1.00	0.95	0.89	0.63
$S_{1.6}$	$K_{H3}$	0.59	0.61	0.77	1.00	1.03	1.03	1.10
	$K_{H4}$	12.00	11.00	3.60	1.00	0.95	0.90	0.65
$S_{3.0}$	$K_{H3}$	0.78	0.78	0.91	1.00	1.03	1.03	1.11
	$K_{H4}$	13.16	11.58	3.79	1.00	0.89	0.79	0.26

As indicated previously, the  $F_t$  factor varies based on the shear wave velocity encountered at each site. A linear relationship for determining the  $F_t$  factor was developed by Andrus, et al. (2014) when  $V_{s,100}^* < V_{s,100,P,t}^*$  and is applicable for all values of  $t$ ,

$$F_t = \left( \frac{F_{P,t}}{V_{s,100,P,t}^*} \right) * V_{s,100}^* \quad \text{Equation 12-25}$$

Where,

$F_t$  = Amplification factor at a specific spectral period

$V_{s,100,P,t}^*$  = Weighted, average site stiffness in the top 100 feet corresponding to the peak site factor adjusted for  $d_{HR}$  (Equation 12-23), ft/sec

$F_{P,t}$  = Peak  $F_t$  factor at a specific spectral period adjusted for  $d_{HR}$  (Equation 12-24)

$V_{s,100}^*$  = Weighted, average site stiffness in the top 100 feet at a specific site, ft/sec

When  $V_{s,100}^* \geq V_{s,100,P,t}^*$ , the  $F_t$  factor for periods less than 0.2 seconds is expressed as a linear relationship. For periods greater than or equal 0.2 seconds the  $F_t$  factor is expressed as an exponential relationship. Both relationships were developed by Andrus, et al. (2014) and are provided below,

For  $t < 0.2$  sec and  $V_{s,100}^* \geq V_{s,100,P,t}^*$

$$F_t = \left[ \frac{(F_{P,t}-1)*(8,200-V_{s,100}^*)}{8,200-V_{s,100,P,t}^*} \right] + 1 \quad \text{Equation 12-26}$$

For  $t \geq 0.2$  sec and  $V_{s,100}^* \geq V_{s,100,P,t}^*$

$$F_t = a + b * e^{(c*V_{s,100}^*)} \quad \text{Equation 12-27}$$

Where,

$F_t$  = Amplification factor at a specific spectral period

$V_{s,100,P,t}^*$  = Weighted, average site stiffness in the top 100 feet corresponding to the peak site factor adjusted for  $d_{HR}$  (Equation 12-23), ft/sec

$F_{P,t}$  = Peak  $F$  factor at a specific spectral period adjusted for  $d_{HR}$  (Equation 12-24)

$V_{s,100}^*$  = Weighted, average site stiffness in the top 100 feet at a specific site, ft/sec

$a$  = Regression coefficient from Table 12-10

$b$  = Regression coefficient determined from Equation 12-28

$c$  = Regression coefficient determined from Equation 12-29, sec/ft

$$b = \frac{1-a}{e^{(8,200*c)}} \quad \text{Equation 12-28}$$

$$c = \left( \frac{1}{8,200-V_{s,100,P,t}^*} \right) \ln \left( \frac{1-a}{F_{P,t}-a} \right) \quad \text{Equation 12-29}$$

#### 12.8.4 Local Site Effects on Spectral Response Accelerations

The PSA values, generated from the Seismic Hazard Mapping study, as indicated in Section 12.6 and Chapter 11 at the B-C Boundary for the Coastal Plain and the weathered hard rock for the Piedmont, are termed the UHS. The  $PGA_{B-C}$  or  $PGA_{HR}$ ,  $S_S$  and  $S_1$  shall be obtained for the appropriate design earthquake (FEE or SEE) being analyzed. The  $PGA$ ,  $S_{DS}$  and  $S_{D1}$  at the ground surface shall be determined by adjusting the  $PGA_{B-C}$  or  $PGA_{HR}$ ,  $S_S$  and  $S_1$  using the  $F_t$

factors developed in the previous Sections based on the geologic condition of the site (i.e., is the site in the Coastal Plain or the Piedmont) using the following equations.

$$PGA = F_{PGA} * PGA_{B-C} \text{ or } F_{PGA} * PGA_{HR} \quad \text{Equation 12-30}$$

$$S_{DS} = F_a * S_S \quad \text{Equation 12-31}$$

$$S_{D1} = F_v * S_1 \quad \text{Equation 12-32}$$

Where:

$PGA_{B-C}$  = Mapped peak ground acceleration at the B-C boundary outcrop (period,  $t = 0.0$  sec)

$PGA_{HR}$  = Mapped peak ground acceleration at the Hard-Rock outcrop (period,  $t = 0.0$  sec)

$PGA$  = Peak ground acceleration at the original ground surface (period,  $t = 0.0$  sec) adjusted for local site conditions

$S_S$  = The mapped spectral acceleration for the short-period (0.2-second) as determined in Section 12.8 and Chapter 11 at the B-C boundary or Hard-Rock outcrop

$S_{DS}$  = Design short-period (0.2-second = 5 Hz) spectral response acceleration parameter

$S_1$  = The mapped spectral acceleration for the one second period as determined in Section 12.8 and Chapter 11 at the B-C boundary or Hard-Rock outcrop

$S_{D1}$  = Design long-period (1.0 second = 1 Hz) spectral response acceleration parameter

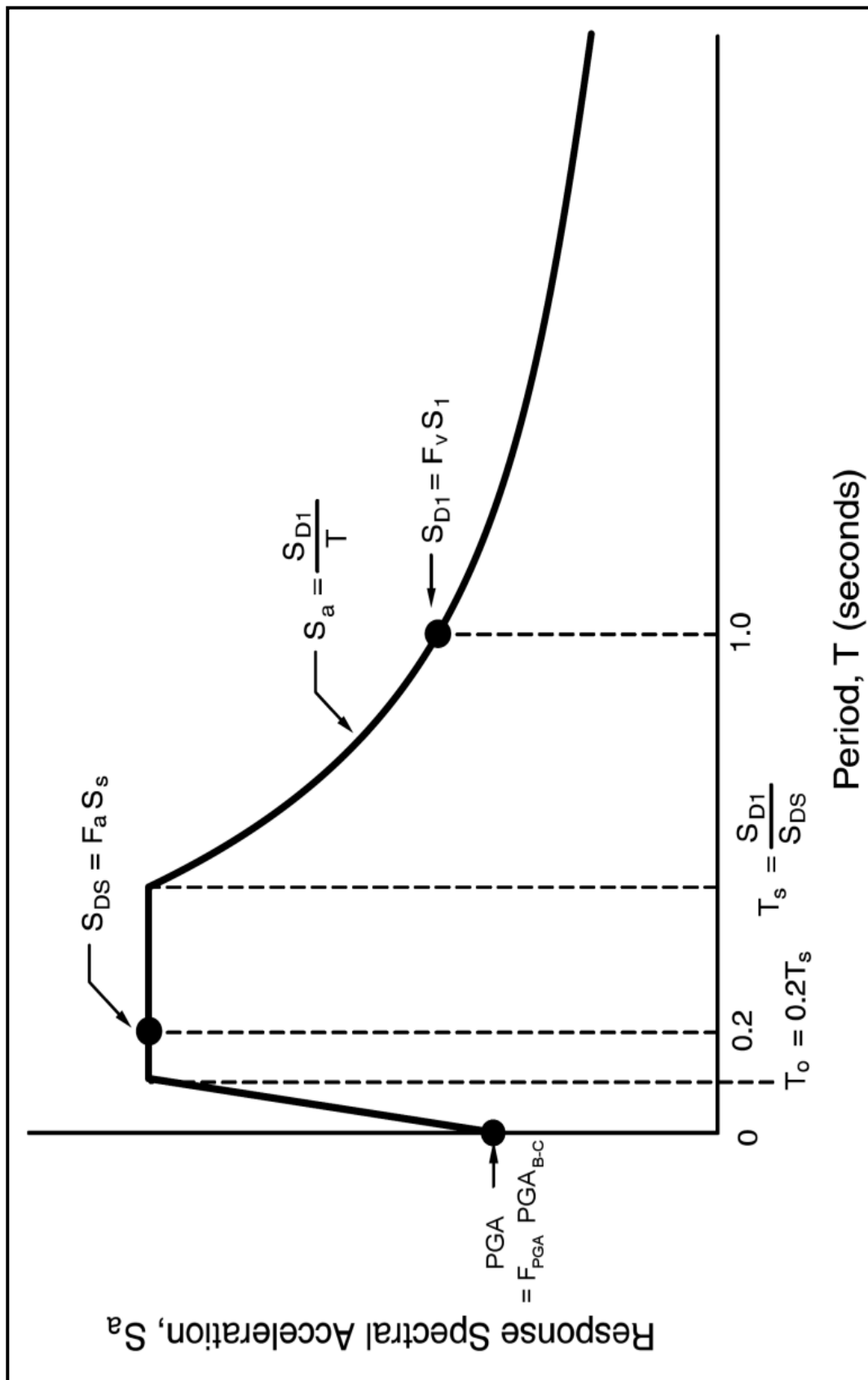
$F_{PGA}$  = Site amplification factors determined in the preceding Sections

$F_a = F_{0.2}$  = Site amplification factors determined in the preceding Sections

$F_v = F_{1.0}$  = Site amplification factors determined in the preceding Sections

### 12.8.5 3-Point Acceleration Design Response Spectrum

The 3-Point method of constructing the horizontal ADRS curve is typically used for structures having natural periods of vibration between 0.2 second and 3.0 second. The 3-Point method has been shown by Power, et al. (1997, 1999) to be unconservative in the CEUS for periods between 1.0 second and 3.0 seconds, and a Site Class B (Rock). When the  $T_0$  is less than 0.2 seconds or greater than 3.0 seconds, a site-specific response analysis as described in Section 12.9 may be required. Therefore, the 3-Point method shall be limited to  $T_0$  equal to or less than 3.0 seconds (i.e.,  $T_0 \leq 3.0$  seconds) as indicated in Step 7 of Table 12-13. The Multi-Point method shall be used to evaluate the reasonableness of the 3-Point ADRS Curve as discussed in Section 12.8.6. Guidelines for constructing the 3-Point ADRS Curve are illustrated in Figure 12-7 and step-by-step instructions are provided in Table 12-13.

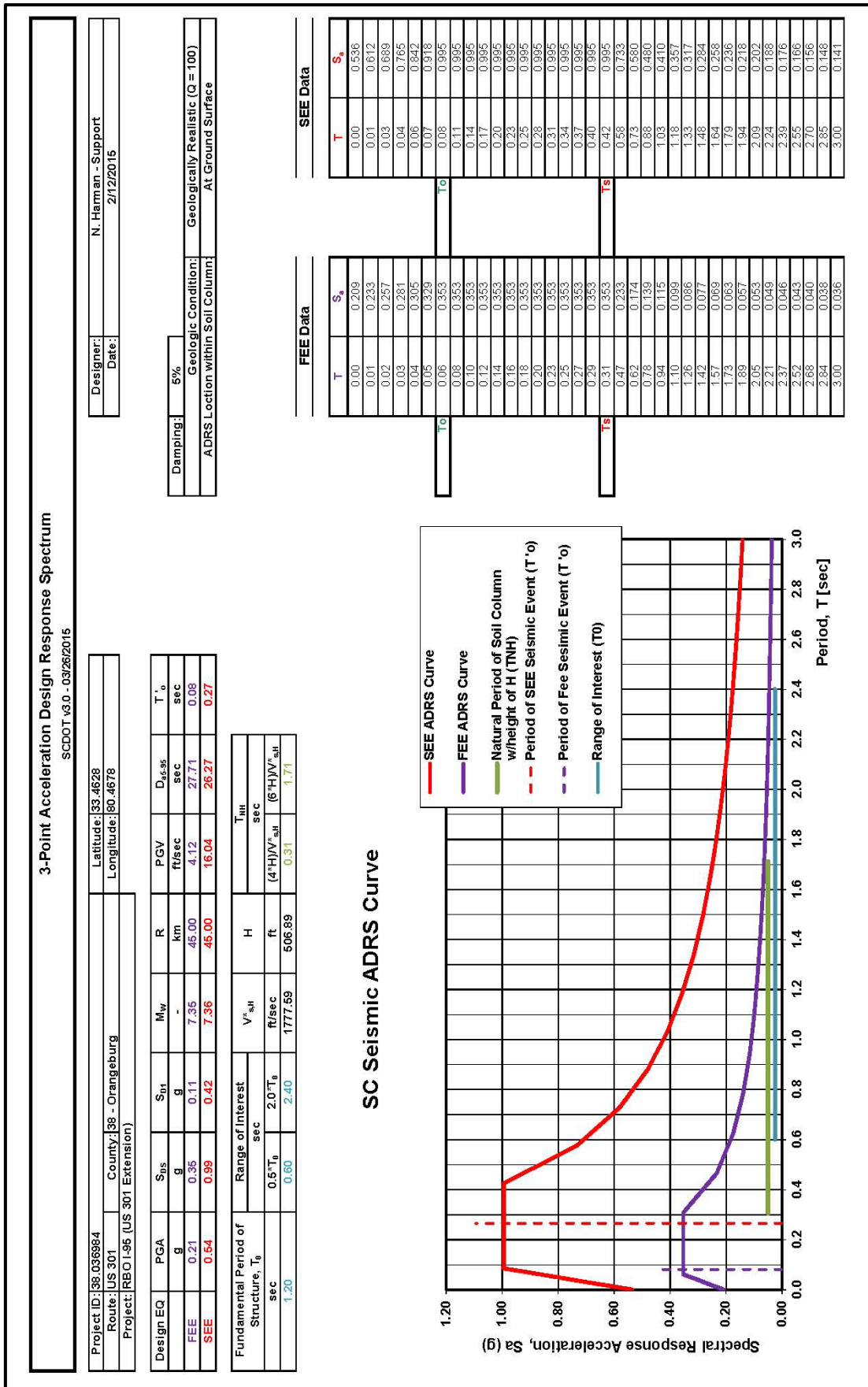


Note:  $PGA_{HR}$  may be substituted for  $PGA_{B-C}$ .

Figure 12-7, 3-Point ADRS Curve Construction

**Table 12-13, 3-Point ADRS Construction Procedures**

Step	Procedure Description
1	The design short-period acceleration, $S_{DS}$ , at period, $T = 0.2$ second and the design long-period acceleration, $S_{D1}$ , at period, $T = 1.0$ second are computed using Section 12.8.4.
2	<p>Period markers <math>T_o</math> and <math>T_s</math> used in constructing the ADRS curves are determined using the following equations.</p> $T_s = \frac{S_{D1}}{S_{DS}} \quad \text{Equation 12-33}$ $T_o = 0.20 * T_s \quad \text{Equation 12-34}$ <p>Where <math>S_{DS}</math> and <math>S_{D1}</math> are obtained in Step 1.</p>
3	The PGA at the original ground surface at period, $T=0.0$ second is computed using Section 12.8.4.
4	<p>The design spectral response acceleration <math>S_a</math> for periods, <math>T \leq T_o</math>, is computed by the following equation.</p> $S_a = PGA + \left[ (S_{DS} - PGA) * \left( \frac{T}{T_o} \right) \right] \quad \text{Equation 12-35}$ <p>Where, <math>S_{DS}</math> is obtained in Step 1, <math>T_o</math> is obtained in Step 2, and PGA is obtained in Step 3.</p>
5	The design spectral response acceleration, $S_a$ , for periods, $T_o \leq T \leq T_s$ , is taken equal to $S_{DS}$ , as obtained in Step 1.
6	<p>The design spectral response acceleration, <math>S_a</math>, for periods, <math>T_s &lt; T \leq 3.0</math> seconds, is computed by the following equation.</p> $S_a = \frac{S_{D1}}{T} \quad \text{Equation 12-36}$ <p>Where, <math>S_{D1}</math> is obtained in Step 1.</p>
7	<p>The 3-Point ADRS curve shall include the following items:</p> <ul style="list-style-type: none"> <li>• 3-Point ADRS curve (both FEE and SEE as required)</li> <li>• Table of smoothed ADRS data values (<math>T</math> and <math>S_a</math>)</li> <li>• Provide the design spectral response parameters PGA, <math>S_{DS}</math>, <math>S_{D1}</math>; period markers <math>T_o</math> and <math>T_s</math>; <math>M_w</math> and <math>R</math>; PGV; <math>D_{a5-95}</math>; PGV; <math>T'_o</math>; <math>T_0</math>; <math>V_{s,H}^*</math>; <math>H</math>; and <math>T_{NH}</math>. An example of the information required is shown in Figure 12-8.</li> </ul>



### 12.8.6 Multi-Point Acceleration Design Response Spectrum

The Multi-point method of constructing an ADRS curve shall be used to check the reasonableness of the 3-Point ADRS curve. This is accomplished by first constructing the 3-Point ADRS curve and then overlaying on the same graph the Multi-point ADRS values as shown in Figure 12-9. The GEOR should be aware that Power, et al. (1999) have found that the Multi-point method may give ambiguous results for structures on sites other than rock ( $V_s > 2,500$  ft/sec). This is due to the Multi-point method using the short period (0.2 seconds) site factor  $F_a$  ( $F_{0.2}$ ) for all the PSA values with periods less than or equal to 0.2 seconds and using long-period (1.0 seconds) site factor,  $F_v$  ( $F_{1.0}$ ), for all periods greater than or equal to 1.0 seconds to compute the acceleration response spectrum. Because of this ambiguous result Andrus et al. (2014) provided a method to develop F factors at other periods. The procedures provided in the previous Sections shall be used to develop the Multi-point curve. Andrus et al. (2014) recommends the use of the Multi-point method when  $V_{s,100}^* < 660$  ft/sec. However, the Multi-point method shall be used for all ranges of  $V_{s,100}^* < 2,500$  ft/sec. Since the Multi-point method is only used to check the reasonableness of the 3-Point ADRS curve for sites with  $V_{s,100}^* < 2,500$  ft/sec this procedure should be adequate. Guidelines for constructing the Multi-Point ADRS curve are provided in Table 12-14.

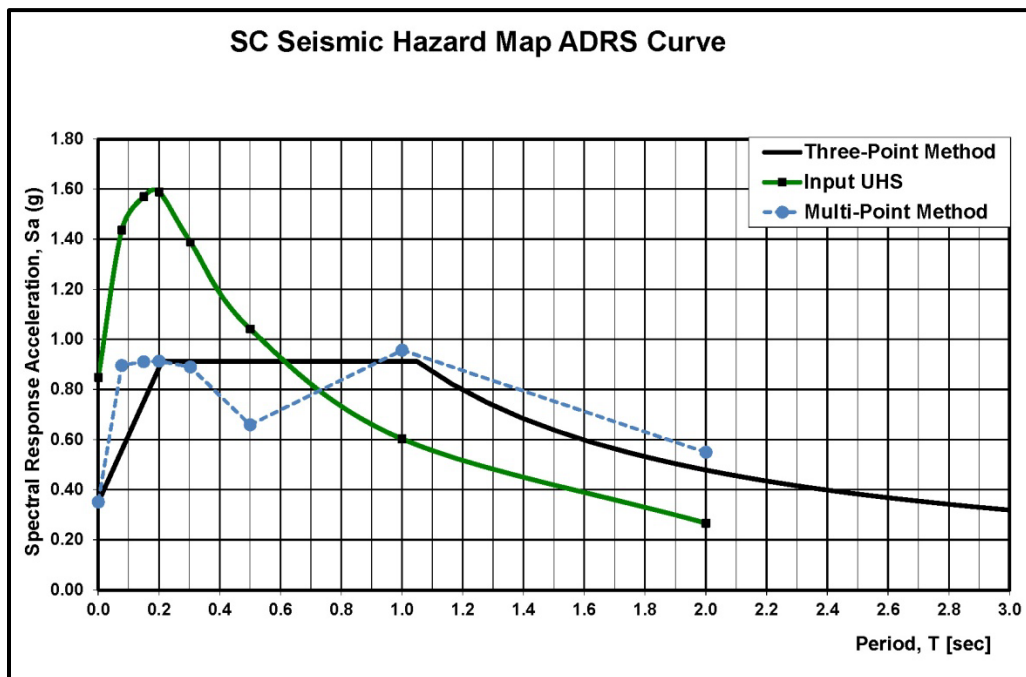


Figure 12-9, 3-Point/Multi-Point ADRS

**Table 12-14, Multi-Point ADRS Construction Procedure**

Step	Procedure Description
1	The FEE or SEE mapped pseudo spectral accelerations at the B-C boundary ( $PSA_{B-C}$ ) for periods, $T = 2.0$ sec (0.5Hz), 1.0 sec (1.0Hz), 0.303 sec (3.3Hz), 0.20 sec (5Hz), 0.15 sec (6.7Hz), 0.08 sec (13Hz) and PGA ( $PGA_{B-C}$ ) are obtained from the SC Seismic Hazard map as indicated in Section 12.6 and Chapter 11.
2	The PGA, $S_{DS}$ , $S_{D1}$ are computed using Section 12.8.4.
3	<p>The design spectral response acceleration, <math>S_a</math>, for periods, <math>0.01 \leq T \leq 0.40</math> second is computed using the following equation.</p> $S_a = F_s * S_s \quad \text{Equation 12-37}$ <p>Where <math>S_s</math> includes <math>PSA_{B-C}</math> for periods, <math>T = 0.08</math> sec (13Hz), 0.15 sec (6.7Hz), 0.20 sec (5Hz) and 0.303 sec (3.3Hz) from Step 1. The site factor <math>F_s</math> is obtained as indicated in Sections 12.8.2 (Coastal Plain) and 12.8.3 (Piedmont).</p>
4	<p>The design spectral response acceleration, <math>S_a</math>, for periods, <math>0.41 \leq T \leq 0.80</math> second is computed using the following equation.</p> $S_a = F_{0.6} * S_{0.6} \quad \text{Equation 12-38}$ <p>Where <math>S_{0.6}</math> is the <math>PSA_{B-C}</math> for periods, <math>T = 0.5</math> sec (2Hz) from Step 1. The site factor <math>F_{0.6}</math> is obtained as indicated in Sections 12.8.2 (Coastal Plain) and 12.8.3 (Piedmont).</p>
5	<p>The design spectral response acceleration, <math>S_a</math>, for periods, <math>0.81 \leq T \leq 1.20</math> second is computed using the following equation.</p> $S_a = F_{1.0} * S_{1.0} \quad \text{Equation 12-39}$ <p>Where <math>S_{1.0}</math> is the <math>PSA_{B-C}</math> for 1.0 sec (1.0Hz). The site factor <math>F_{1.0}</math> is obtained as indicated in Sections 12.8.2 (Coastal Plain) and 12.8.3 (Piedmont).</p>
6	<p>The design spectral response acceleration, <math>S_a</math>, for periods, <math>1.21 \leq T \leq 2.00</math> second is computed using the following equation.</p> $S_a = F_{1.6} * S_{1.6} \quad \text{Equation 12-40}$ <p>Where <math>S_{1.6}</math> is the <math>PSA_{B-C}</math> for 2.0 sec (0.5Hz). The site factor <math>F_{1.6}</math> is obtained as indicated in Sections 12.8.2 (Coastal Plain) and 12.8.3 (Piedmont).</p>
7	<p>The design spectral response acceleration, <math>S_a</math>, for periods, <math>2.01 \leq T \leq 4.00</math> second is computed using the following equation.</p> $S_a = F_{3.0} * S_{3.0} \quad \text{Equation 12-41}$ <p>Currently, <math>S_{3.0}</math> is not determined; however, in the future this value may be added to the ADRS curve development. The site factor <math>F_{3.0}</math> is obtained as indicated in Sections 12.8.2 (Coastal Plain) and 12.8.3 (Piedmont). For periods greater than 4.01 seconds a site-specific response analysis shall be required.</p>

Note: This Table indicates B-C Boundary conditions; however, HR conditions,  $PSA_{HR}$  may be substituted for  $PSA_{B-C}$

After the Multi-point horizontal ADRS curve has been constructed, the following should be checked by both the SEOR and the GEOR to see if the 3-Point ADRS curve is either underestimating spectral accelerations or not representative of the acceleration response spectrum. The SEOR will provide the fundamental periods of vibration that are important to the



structural response and the GEOR will compare this value to the Multi-point spectral acceleration curve.

- If fundamental periods of vibration greater than 1.0 second are important to the structural response, check Multi-point spectral acceleration,  $S_a$ , corresponding to the 2.0 second period to assure that the long-period response is not underestimated.
- If fundamental periods of vibration less than 0.20 seconds are important to the structural response, check Multi-point spectral acceleration,  $S_a$ , corresponding to the 0.10 sec period to assure that the short-period response is not underestimated.
- Check to see if the general trend of the 3-Point ADRS curve is similar to the Multi-point ADRS curve. If the fundamental period of the structure is in the range of longer periods the spectral accelerations will be significantly underestimated using the 3-Point ADRS.

If discrepancies between the 3-Point method and the Multi-point method have the potential to significantly underestimate the spectral response, the PC/GDS must be contacted. The PC/GDS will either approve modifications to the 3-Point ADRS curve or require a site-specific response analysis.

### 12.8.7 ADRS Evaluation using Seismic Hazard Mapping Study

Even though ADRS determination using the Seismic Hazard Mapping study is relatively straight forward, a series of checks are necessary to ensure its appropriateness. This involves using the 3-Point method as the basis of developing the ADRS curve and the Multi-point method to confirm its validity. A decision flow chart is provided in Appendix J to assist the designer with developing the ADRS curve based on the Seismic Hazard Mapping Study.

### 12.8.8 Damping Modifications of ADRS Curves

The ADRS curves developed using the Seismic Hazard Mapping Study is based on a damping ratio of 5 percent. ADRS curves for structural damping ratios other than 5 percent can be obtained by multiplying the 5 percent damped ADRS curve by the period-dependent factors shown in Table 12-15. For spectra constructed using the 3-Point method, the factors for periods of 0.20 sec and 1.0 sec can be used.

**Table 12-15, Damping Adjustment Factors  
(Newmark and Hall (1982) and Idriss (1990))**

Period (seconds)	Ratio of Response Spectral Acceleration for Damping Ratio $\lambda$ to Response Spectral Acceleration for $\xi_{\text{eff}} = 5\%$		
	$\lambda_{\text{eff}} = 2\%$	$\lambda_{\text{eff}} = 7\%$	$\lambda_{\text{eff}} = 10\%$
0.02	1.00	1.00	1.00
0.10	1.26	0.91	0.82
0.20	1.32	0.89	0.78
0.30	1.32	0.89	0.78
0.50	1.32	0.89	0.78
0.70	1.30	0.90	0.79
1.00	1.27	0.90	0.80
2.00	1.23	0.91	0.82
4.00	1.18	0.93	0.86

## 12.9 SITE-SPECIFIC RESPONSE ANALYSIS

The site-specific response analyses requirements in this Section apply only to “typical” bridges as defined by the Seismic Specs. Similarly to the 3-Point method ADRS curve development, all site-specific response analyses shall be performed by the PC/GDS. The site-specific response analysis shall be considered when any of the following conditions are met.

- Structure has a Site Class F (Section 12.4)
- SC Seismic Hazard Maps are not appropriate (Section 12.8.6)
- $T_{NH}$  and  $T'_o$  intersect on the 3-Point ADRS Curve (Figure 12-8)
- As required by SCDOT

In addition, a site-specific response analysis may be required for a structure meeting the following criteria:

- $T_0$  is less than 0.2 seconds or more than 3.0 seconds (i.e.,  $T_0 < 0.2 \text{ sec}$  or  $T_0 > 3.0 \text{ sec}$ )

As required in Chapter 11, a minimum of 7 time histories (synthetic or “real”) shall be required. The synthetic time histories shall be developed as required in Chapter 11. In addition, the “real” time histories shall be selected as required in Chapter 11. It is noted that prior to performing a site-specific response analysis a 3-Point ADRS is required. The 3-Point curve shall be used for comparison purposes with the site-specific response analysis as required in Section 12.9.4.

### 12.9.1 Equivalent-Linear 1-Dimensional Site-Specific Response

An equivalent-linear 1-dimensional site-specific response analysis shall be performed using SHAKE2000 or other computer software that is based on the SHAKE2000 computational model. The SHAKE2000 computer program models a soil column with horizontal layered soil deposits overlying a uniform visco-elastic half space. The SHAKE2000 computer program is based on the original SHAKE program was developed by Schnabel, Lysmer, and Seed (1972), and updated by Idriss and Sun (1992) to SHAKE91. SHAKE91 was updated by Ordóñez (2011) with SHAKEDIT added as a pre- and post-processor to SHAKE91. The computer program DeepSoil (Hashash (2012)) has been developed specifically for the CEUS and performs the equivalent linear analysis similar to SHAKE2000. The PCS/GDS shall approve in writing the use of software other than SHAKE2000 or DeepSoil. The software must be nationally recognized in the United States as SHAKE2000 type software.

For most projects and site conditions, the SHAKE2000 method (or equivalent) of performing a site-specific response analysis will be required. When this method cannot accurately capture or model the site response, a non-linear 1-dimensional site-specific response analysis may be required. Situations where an equivalent-linear 1-dimensional site-specific response analysis (SHAKE2000) method has been shown to be unreliable are listed below:

- When the PGA at the ground surface is greater than 0.4g or if calculated peak shear strains exceed approximately 2 percent.
- When sites have significant liquefaction potential.
- When the non-linear mass participation factor ( $r_d$ ) indicates either very low site stiffness,  $V_{S,40'}^* < 400 \text{ ft/sec}$  (120 m/sec) or very high site stiffness,  $V_{S,40'}^* > 820$

ft/sec (250 m/sec) and the project site has soil layers that have been screened to be potentially liquefiable.

- When seismic slope instability evaluations are required where complex geometries exist such as compound slopes, broken back slopes, or excessively high earth structures (embankments, dams, earth retaining systems).
- When sites have sensitive soils ( $S_t > 8$ ).

### 12.9.2 Non-Linear 1-Dimensional Site-Specific Response

A non-linear 1-dimensional analysis shall be required when a site-specific response analysis is required and the  $PGA_{B-C}$  is greater than 0.3 g ( $PGA_{B-C} > 0.3$  g). Both total and effective stress analyses shall be performed. It is noted that the pore water pressure generation model shall be matched as closely as can be expected to the soils on the project site. Guidance in using non-linear site response analysis procedures can be obtained from Stewart, et al. (2008). One-dimensional non-linear site response analyses shall be performed using approved computer software such as DMOD2000 (Matasović and Ordóñez (2011)) that models the behavior of the soil subjected to cyclic loadings by tracing the evolution of the hysteresis loops generated in a soil by cyclic loading in a sequential manner. A number of other software programs such as DESRA-MUSC (Qiu, (1998)), and DeepSoil (Hashash (2012)) have been developed that modify and improve the accuracy of the constitutive soil models originally developed. Authorized software used to perform 1-dimensional non-linear site-specific response analysis must be based on DMOD2000 (Matasović and Ordóñez (2011)), DeepSoil (Hashash (2012)) or equivalent. The PCS/GDS shall approve in writing the use of software other than DMOD2000 or DeepSoil. The software must be nationally recognized in the United States. Nonlinear site response codes such as DMOD2000 have issues estimating both small and large strain damping (Phillips and Hashash (2009)). DeepSoil has theoretical improvements on this matter and therefore better accuracy in computed responses is expected from this software.

### 12.9.3 Site-Specific Response Analysis Methodology

A 1-dimensional soil column model is needed when performing a site-specific response analysis using either the equivalent-linear or non-linear methods. The soil column extends from either the bedrock or the Geologically Realistic site condition (B-C Boundary) to the location where the ground motion transmits the ground shaking energy to the structure being designed, typically the ground surface.

When performing either an equivalent-linear or non-linear 1-dimensional site-specific response analysis, the soil layers in the 1-dimensional column are characterized by the layer thickness,  $H$ ; soil description including classification testing and geologic age; total unit weight ( $\gamma_T$ ); and, Shear Wave Velocity ( $V_s$ ). The development of the 1-dimensional soil column for a project site may require making several assumptions as to the selection of layer thicknesses and soil properties. Individual layer thicknesses should be no greater than:

$$H_i = \frac{V_{s,i}}{100} \quad \text{Equation 12-42}$$

Where,

$V_{s,i}$  = Shear wave velocity for each layer, ft/sec

$H_i$  = Thickness of each individual layer, feet

100 = Constant representing 4 times the maximum frequency of the individual layer, assuming the maximum frequency is 25 Hz

In addition, a layer shall be placed at the ground water table used in the model; i.e., the ground water table shall be located at the interface between 2 soil layers. The soil parameters required are described in Chapter 7. The soil column model should be prepared in tabular form similar to Table 12-16. An equivalent linear code uses a constant number for both shear modulus and damping ratio for the entire excitation period while a non-linear code picks different numbers for both shear modulus and damping ratio corresponding to the varying shear strain during excitation.

**Table 12-16, One-Dimensional Soil Column Model**

Geologic Time	Layer No.	Layer Thickness, $H_i$	Soil Formation	Soil Description (USCS)	PI	FC	Total Unit Weight, $\gamma_T$	Shear Wave Velocity, $V_{s,i}$
Quaternary	1							
	2							
Neogene	3							
Paleogene	4							
Cretaceous	5							
	6							
Bed Rock	i							

The PC/GDS shall perform a sensitivity analysis on the 1-dimensional soil column model being developed to evaluate the consequences of the following:

- Variation in depth to B-C boundary and/or depth to basement rock
- Variations in soil properties for soils encountered below the maximum depth of the geotechnical investigation.
- Variations in soil properties of soils encountered during the geotechnical investigation across the project site.
- Variation in soil properties to account for effects of ground improvement, specifically, if deep soil mixing or some form of grouting is used to bind the soil grains together.

The sensitivity analysis methodology must be well developed and documented in detail in the report. As a result of the sensitivity analysis performed, a series of site-specific horizontal acceleration response spectra (ARS) curves may be developed. The ARS curve developed from the baseline model (i.e., the base model used in the sensitivity analysis) shall be given no less than 5 percent weight nor more than 10 percent weight over the other ARS curves developed during the sensitivity analyses. A single recommended site-specific horizontal ARS curve should be superimposed on the graph to develop a site-specific ADRS curve. Since 7 ground motions will be used, the arithmetic mean of the ARSs shall be used to develop the site-specific ADRS curve. The method of selecting the recommended site-specific ARS curve shall be documented in the report. The sensitivity analysis will be required for each ground motion developed for the project site.

When performing a non-linear 1-dimensional site-specific response analysis, the soil column model input motions shall be documented to at least the same level of detail as used in the equivalent-linear 1-dimensional site-specific response analysis.

In addition to the site-specific design response report, all electronic input and output files shall be submitted.

#### **12.9.4 Site-Specific Horizontal ADRS Curve**

The development of the recommended site-specific ADRS shall be based on results of the site-specific response analysis (Sections 12.9.1 or 12.9.2) and shall be developed at the existing ground surface unless the requirements of Section 12.5 are met (i.e., the SEOR requests the development of Site-Specific ADRS curve at a different depth than the ground surface). The Site-Specific ADRS curve shall be developed for an equivalent viscous damping ratio of 5 percent. Additional ADRS curves may be required for other damping ratios appropriate to the indicated structural behavior (see Section 12.8.8). When the Site-Specific ADRS curve has spectral accelerations in the period range of greatest significance to the structural response (typically 0.5 to 2.0 seconds; for  $T_0$  equal to 1.0 second, where  $T_0$  is the fundamental period of the bridge or structure) are between the 3-Point ADRS curve and 70 percent of the 3-Point ADRS curve, the Site-Specific ADRS curve shall be used. If any point of the Site-Specific ADRS curve is less than 70 percent of the spectral accelerations computed using the 3-Point method, the PCS/GDS shall be consulted to determine if the 70 percent of the 3-point curve will be used or if the spectral accelerations less than the 70 percent criterion can be used or if an independent third-party review (Peer Review) of the ADRS curve by an individual with the expertise in the evaluation of ground motions is to be undertaken. The Peer Review shall be conducted by an individual who has a minimum of 10 years' experience in geotechnical seismic design and who shall have conducted a minimum of 7 site-specific response analyses as the lead designer. If a non-linear analysis is performed, the PEER Reviewer shall have conducted at least 3 non-linear site response analyses. The 3 non-linear analyses may be included in the 7 site-specific response analyses. In addition, the Peer Reviewer shall be licensed as either an engineer (PE) or geologist (PG) pursuant to the laws of South Carolina.

A smoothed ADRS curve shall be superimposed over the recommended site-specific acceleration response spectrum generated from site-specific response analysis (Sections 12.9.1 or 12.9.2). The steps to develop the smoothed ADRS curve shall be based on Table 12-17 and Figure 12-11.

**Table 12-17, Site-Specific ADRS Construction Procedures**

Step	Procedure Description
1	The design short-period acceleration, $S_{DS}$ , shall be the $S_a$ at $T = 0.20$ seconds but shall not be less than 90 percent of the maximum design spectral response acceleration, $S_{DMax}$ , at any period greater than 0.20 seconds.
2	The design long-period acceleration, $S_{D1}$ , shall be the greater of either the $S_a$ at $T = 1.0$ second or twice the $S_a$ at $T = 2.0$ seconds.
3	<p>Period markers <math>T_o</math> and <math>T_s</math> used in constructing the Site-Specific ADRS curves are determined using the following equations.</p> $T_s = \frac{S_{D1}}{S_{DS}} \quad \text{Equation 12-43}$ $T_o = 0.20 * T_s \quad \text{Equation 12-44}$ <p>Where <math>S_{DS}</math> and <math>S_{D1}</math> are obtained in Steps 1 and 2.</p>
4	The PGA at the original ground surface shall be determined, $T=0.0$ second.
5	<p>The design spectral response acceleration <math>S_a</math> for periods, <math>T \leq T_o</math>, is computed by the following equation.</p> $S_a = PGA + \left[ (S_{DS} - PGA) * \left( \frac{T}{T_o} \right) \right] \quad \text{Equation 12-45}$ <p>Where, <math>S_{DS}</math> is obtained in Step 1, <math>T_o</math> is obtained in Step 3, and PGA is obtained in Step 4.</p>
6	The design spectral response acceleration, $S_a$ , for periods, $T_o \leq T \leq T_s$ , is taken equal to $S_{DS}$ , as obtained in Step 1.
7	<p>The design spectral response acceleration, <math>S_a</math>, for periods, <math>T_s &lt; T \leq 3.0</math> seconds, is computed by the following equation.</p> $S_a = \frac{S_{D1}}{T} \quad \text{Equation 12-46}$ <p>Where, <math>S_{D1}</math> is obtained in Step 2.</p>
8	<p>The Site-Specific ADRS curve shall include the following items:</p> <ul style="list-style-type: none"> <li>• Site-Specific ADRS curve (both FEE and SEE as required)</li> <li>• Table of smoothed ADRS data values (<math>T</math> and <math>S_a</math>)</li> <li>• Provide the design spectral response parameters PGA, <math>S_{DS}</math>, <math>S_{D1}</math>; period markers <math>T_o</math> and <math>T_s</math>; <math>M_w</math> and <math>R</math>; PGV; <math>D_{a5-95}</math>; PGV; <math>T'_o</math>; <math>T_o</math>; <math>V_{s,H}^*</math>; <math>H</math>; and <math>T_{NH}</math>. An example of the information required is shown in Figure 12-11.</li> </ul>



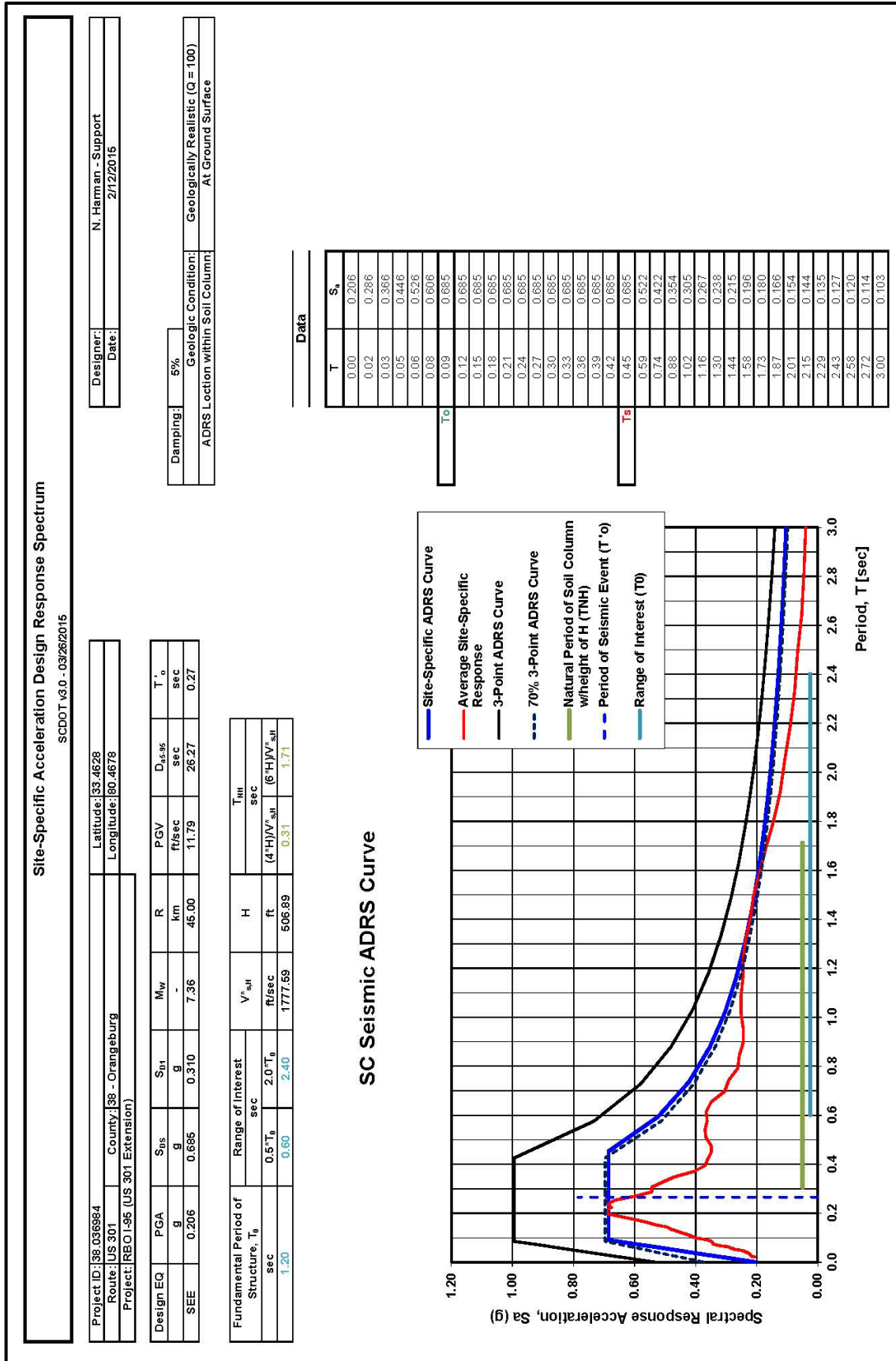


Figure 12-11, Site-Specific Horizontal ADRS Curve



## 12.10 GROUND MOTION DESIGN PARAMETERS

### 12.10.1 Peak Horizontal Ground Acceleration

The PGA at the ground surface is defined as the acceleration in the response spectrum obtained at a period,  $T = 0.0$  seconds. If the 3-Point ADRS curves are used, the PGA obtained from Section 12.8.4 shall be used. If a site-specific response analysis is performed the spectral acceleration at period  $T = 0.0$  second obtained from Site-Specific ADRS curve shall be used.

### 12.10.2 Earthquake Magnitude / Site-to-Source Distance

The  $M_W$  and  $R$  can be obtained from the seismic hazard deaggregations charts discussed in Chapter 11.

### 12.10.3 Seismic Event Predominant Period

The period of a seismic event should be determined in order to determine if the seismic input motion and the soils at a particular site match. If period matching occurs the potential for amplification of the ground motion at the site is possible. Matching of the period of the seismic event and the on-site soils may be termed harmonic resonance. The potential for significant damage may be magnified if the harmonic resonance includes not only the soil and seismic event having the same period but also the structure being designed. Therefore as indicated in Figures 12-8 and 12-11, the periods of the soil column, seismic event and structure should be indicated. The period of the soil column and seismic event are determined by the PC/GDS, with the period of the structure (first or fundamental period) by the SEOR. The period of the soil column is determined using the procedures provided in Section 12.3.3 and are based on actual site conditions.

The period of the seismic event is determined using the procedure provided by Rathje, Faraj, Russell and Bray (2004). In Rathje, et al. (2004) 4 different periods are discussed;  $T_m$ ,  $T_{avg}$ ,  $T_o$  and  $T_p$ . The development of  $T_m$ , the mean period, is discussed in Sections 12.8.2 and 12.8.3.  $T_{avg}$ , the average spectral period is not used.  $T_o$  is the smoothed spectral predominant period, is the period of the seismic event, while according to Rathje, et al. (2004)  $T_p$ , the predominant spectral period, should not be used. Therefore, the smoothed spectral predominant period,  $T_o$ , will be determined for each seismic event using the following equation. However, it should be noted that  $T_o$  is used in the development of the 3-Point ADRS curve as the beginning period of the flattened portion of the ADRS curve. Therefore,  $T'_o$  will be used to represent the smoothed spectral predominant period, not  $T_o$  as indicated in Rathje, et al. (2004).

$$T'_o = \frac{\sum \left[ t * \ln \left( \frac{PSA_{B-C,t}}{PGA_{B-C}} \right) \right]}{\sum \ln \left( \frac{PSA_{B-C,t}}{PGA_{B-C}} \right)} \quad \text{Equation 12-47}$$

For spectral periods,  $t$  as defined in Table 12-6, where the  $PSA_{B-C,t}$  meets the following criteria,

$$PSA_{B-C,t} = 1.2 * PGA_{B-C} \quad \text{Equation 12-48}$$

Substitute  $PSA_{HR,t}$  and  $PGA_{HR}$  into Equations 12-47 and 12-48, if hard rock conditions exist at the site as appropriate. The  $PSA_{B-C,t}$ ,  $PGA_{B-C}$ ,  $PSA_{HR,t}$  and  $PGA_{HR}$  are determined from SCENARIO\_PC.

Where,

$t$  = Specific spectral period, second (see Table 12-6)

$PSA_{B-C,t}$  = Pseudo-acceleration at the B-C Boundary outcrop at a specific spectral period, from SCENARIO\_PC (2006)

$PGA_{B-C}$  = Pseudo Peak Ground Acceleration at the B-C Boundary outcrop at a spectral period of 0.0 seconds, from SCENARIO\_PC (2006)

$PSA_{HR,t}$  = Pseudo-acceleration at the Hard Rock ( $V_s \geq 11,500$  ft/sec) outcrop at a specific spectral period, from SCENARIO\_PC (2006)

$PGA_{HR}$  = Pseudo Peak Ground Acceleration at the Hard Rock ( $V_s \geq 11,500$  ft/sec) outcrop at a spectral period of 0.0 seconds, from SCENARIO\_PC (2006)

#### 12.10.4 Earthquake Duration

The earthquake duration is important when evaluating geotechnical seismic hazards that are influenced by degradation under cyclic loading. The longer the duration of the earthquake, the more damage tends to occur. Geotechnical seismic hazards that would be affected by degradation under cyclic loading would be sites with cyclic liquefaction potential and liquefaction induced hazards such as lateral spreading and seismic instability.

The SCEC (Southern California Earthquake Center) DMG Special Publication 117 recommends using the Abrahamson and Silva (1996) relationship for rock. The Abrahamson and Silva (1996) correlation between  $M_w$ ,  $R$ , and the earthquake significant duration as a function of acceleration ( $D_{a5-95}$ ) can be computed by the following equation.

**$R < 10$  km:**

$$\ln(D_{a5-95}) = \ln \left\{ \frac{\left[ \frac{\exp(5.204 + 0.851 * (M_w - 6))}{10(1.5 * M_w + 16.05)} \right]^{-\left(\frac{1}{3}\right)}}{15.7 * 10^6} \right\} + 0.8664 \quad \text{Equation 12-49}$$

**$R \geq 10$  km:**

$$\ln(D_{a5-95}) = \ln \left\{ \frac{\left[ \frac{\exp(5.204 + 0.851 * (M_w - 6))}{10(1.5 * M_w + 16.05)} \right]^{-\left(\frac{1}{3}\right)}}{15.7 * 10^6} + 0.063 * (R - 10) \right\} + 0.8664 \quad \text{Equation 12-50}$$

Where:

$M_w$  = Moment magnitude of design earthquake (FEE or SEE) Section 12.10.2

$R$  = Site-to-source distance, kilometers, Section 12.10.2

$D_{a5-95}$  = Seismic event significant duration, seconds

Kempton and Stewart (2006) developed a ground motion prediction equation to estimate the earthquake significant duration as a function of acceleration ( $D_{a5-95}$ ) by using a modern database and a random-effects regression procedure. The correlation presented in the following equation uses the earthquake  $M_w$ ,  $R$ ,  $V_{s,H}^* = V_{s,100}$ , and depth-to-hard rock ( $d_{HR}$ ) to estimate the  $D_{a5-95}$ .

$$\ln(D_{a5-95}) = \ln \left\{ \frac{\left[ \frac{\Psi}{\Upsilon} \right]^{-\frac{1}{3}}}{15.68 * 10^6} + K \right\} + \varepsilon \quad \text{Equation 12-51}$$

$$\Psi = \exp(2.79 + 0.82 * (M_w - 6)) \quad \text{Equation 12-52}$$

$$\Upsilon = 10^{(1.5 * M_w + 16.05)} \quad \text{Equation 12-53}$$

$$K = 0.15 * R + 3.00 - 0.0041 * \left( \frac{V_{s,100}^*}{3.2808} \right) + 0.0012 * d_{HR} \quad \text{Equation 12-54}$$

Where:

$V_{s,100}^*$  = Site stiffness with  $Z_{DTM}=0$ , ft/sec (Section 12.3.2)

$M_w$  = Moment magnitude of design earthquake (FEE or SEE) Section 12.9.2

$R$  = Site-to-source distance, kilometers, Section 12.10.2

$d_{HR}$  = Depth from ground surface to hard rock ( $V_s > 5,000$  ft/sec (1,500 m/s)), m

$\varepsilon$  = Near-fault forward directivity correction for earthquakes (dip-slip or strike-slip faults)

**$R < 20$  km:**

$$\varepsilon = 0.015 * (R - 20) \quad \text{Equation 12-55}$$

**$R \geq 20$  km:**

$$\varepsilon = 0 \quad \text{Equation 12-56}$$

The Kempton and Stewart (2006) study confirmed the previous correlations (i.e., Abrahamson and Silva (1996)) that  $D_{a5-95}$  increased with an increase in  $M_w$  and  $R$ . In addition, the study found that the  $D_{a5-95}$  significantly increased with decreasing  $V_{s,H}^*$ . The  $D$  also increased slightly with an increase of depth-to-hard rock ( $d_{HR}$ ).

South Carolina shear wave profiles have indicated that site stiffness  $V_{s,H}^*$  can vary significantly across the state from greater than 5,000 ft/s (1,500 m/s) to less than 600 ft/s (180 m/s). The effects of site stiffness on earthquake duration using Kempton and Stewart (2006) relationship have been plotted on Figure 12-12. An  $M_w = 7.3$  and a  $d_{HR} = 2,600$  feet (800m) have been selected as typical of the lower South Carolina Coastal Plain. The Abrahamson and Silva (1996) relationship for rock has also been plotted for reference.

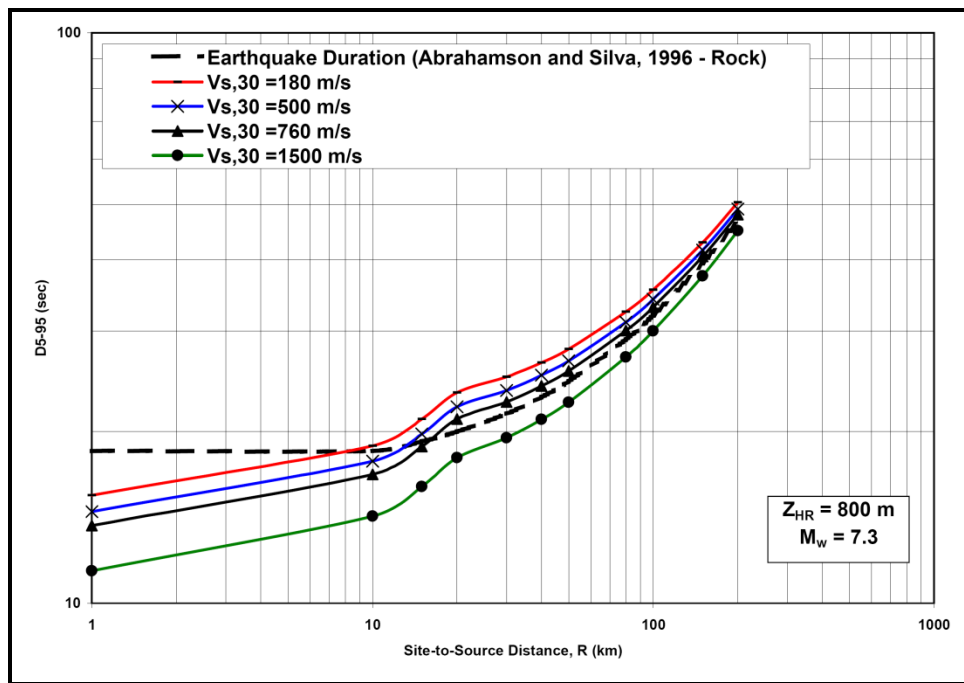


**Figure 12-12, Effects of Site Stiffness on Earthquake Duration**

South Carolina Coastal Plain geology (Chapter 11) indicates that the depth-to-hard rock varies from zero at the “Fall Line” up-to 4,000 feet (1,200 meters) at the southeastern corner of the state. The effects of depth-to-hard rock on earthquake duration using Kempton and Stewart (2006) relationship have been plotted on Figure 12-13. The Abrahamson and Silva (1996) relationship for rock has also been plotted as a reference.

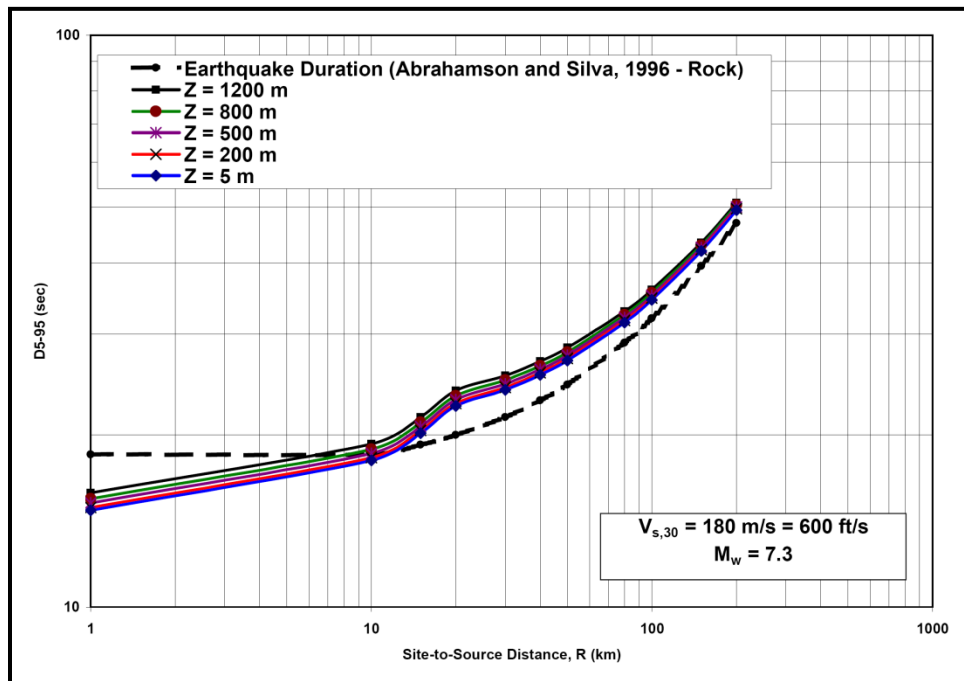


**Figure 12-13, Effects of Depth-to-Hard Rock on Earthquake Duration**

The project site conditions shall be evaluated and the most appropriate earthquake duration model shall be used.

### 12.10.5 Energy Content

According to Kavazanjian, et al. (2012),

The *energy content* of the acceleration time history provides another means of characterizing quantitatively the intensity of strong ground motions. The energy content of a strong ground motion record is proportional to the square of the acceleration. In engineering practice, the energy content of the motion is typically expressed in terms of either the *root-mean-square* and *duration* of the acceleration time history or the *Arias Intensity*,  $I_A$ . The *Arias Intensity*,  $I_A$ , is proportional to the square of the acceleration integrated over the entire acceleration time history:

$$I_A = \frac{\pi}{2g} \int_0^{t_f} [a(t)]^2 dt \quad \text{Equation 12-57}$$

where  $a(t)$  is the time history of acceleration (the accelerogram),  $g$  is the acceleration of gravity and  $t_f$  is the duration of the shaking. Arias (1969) showed that this integral is a measure of the total energy of the accelerogram.

The root-mean-square of the acceleration time history, or *RMSA*, is the square root of the square of the acceleration integrated over the duration of the motion and divided by the duration:

$$RMSA = \sqrt{\frac{1}{t_f} \left\{ \int_0^{t_f} [a(t)]^2 dt \right\}} \quad \text{Equation 12-58}$$

where  $a(t)$  is the acceleration time history, and  $t_f$  is the duration of the strong ground shaking. The RMSA represents an average value of acceleration over the duration of strong shaking. The square of RMSA multiplied by the duration of the motion is directly proportional to the energy content of the motion, i.e., Arias intensity is related to the RMSA as follows:

$$I_A = \frac{\pi}{2g} (RMSA)^2 * t_f \quad \text{Equation 12-59}$$

The value of the Arias Intensity is independent of the duration of strong shaking, while RMSA depends upon the definition of the strong shaking duration. However, as the energy content of the motion is fixed, the product of the RMSA and the squared duration will remain constant as suggested in *Equation 12-59*. The definition of the duration of strong shaking for an acceleration time history can be somewhat arbitrary, as relatively low intensity motions may persist for a long time towards the end of a strong motion record. If the defined duration of strong motion is increased to include these low intensity motions, the Arias Intensity will remain essentially constant but the RMSA will decrease. Therefore, some investigators prefer Arias Intensity to RMSA as a measure of energy content, as the Arias Intensity is essentially a fixed value while the RMSA depends upon the definition of the duration of strong ground motion.

Arias Intensity and/or RMSA and duration are useful parameters in selecting time histories for geotechnical analysis. This is particularly true if a seismic

deformation analysis is to be performed, as the deformation potential of a strong motion records is related to the energy content, which can be expressed as a function of either Arias Intensity or the product of the RMSA and duration of the records.

The duration of shaking ( $t_f$ ) discussed above may be taken as  $D_{a5-95}$  as discussed in Section 12.10.4. The use of  $D_{a5-95}$  as the duration of shaking is only an approximation; the actual  $t_f$  should be obtained from a time series.

### 12.10.6 Peak Ground Velocity

The peak ground velocity, PGV, of the earthquake can be determined from a site-specific response analysis. If the 3-Point ADRS curves are developed, PGV correlations based on the Anderson, Martin, Lam, and Wang (2008) may be used.

The mean PGV, in units of in/sec can be computed by the following equation.

$$PGV = V_{Peak} = 38 * (F_v * S_1) = 38 * S_{D1} \quad \text{Equation 12-60}$$

Anderson, et al. (2008) recommends using the mean plus one standard deviation value for determining the PGV, to provide a margin of conservatism, using the following equation.

$$PGV = V_{Peak} = 55 * (F_v * S_1) = 55 * S_{D1} \quad \text{Equation 12-61}$$

Where,

$F_v$  = Site coefficient defined in Sections 12.8.2 and 12.8.3, based on the Site Class and the mapped spectral acceleration for the long-period,  $S_1$ .

$S_1$  = The mapped spectral acceleration for the one second period as determined in Sections 12.8 and 11.8.2 at the B-C Boundary or Hard Rock outcrop

$S_{D1}$  = Design long-period (1.0 second = 1 Hz) spectral response acceleration parameter

However, Kavazanjian, et al. (2012) recommends the use of Equation 12-60, which is more consistent with LRFD principles, then Equation 12-61.

## 12.11 REFERENCES

Abrahamson, N. A. and Silva, W. J., (1996), "Empirical Ground Motion Models", Report for Brookhaven National Laboratory, New York, NY, May, 144 p.

Anderson, D. G., Martin, G. R., Lam, I., and Wang, J. N., (2008), "Seismic Analysis and Design of Retaining Walls, Buried Structures, Slopes and Embankments". NCHRP Report 611, National Cooperative Highway Research Program, Transportation Research Board, Washington D.C., 137p.

Andrus, R. D., Ravichandran, N., Aboye, S. A., Bhuiyan, A. H., and Martin, J. R., (2014), "Seismic Site Factors and Acceleration Design Response Spectra Based on Conditions in South Carolina", Final Report to SCDOT SPR No. 686.

Arias, A., (1969), "A Measure of Earthquake Intensity", Seismic Design for Nuclear Power Plants, R. Hansen, editor, Massachusetts Institute of Technology Press, Cambridge, Massachusetts, pp 438-483.

- Boore, D. M., (1983), "Stochastic simulation of high-frequency ground motions based on seismological models of the radiated spectra", *Bulletin of the Seismological Society of America*, v. 73, p. 1865-1894.
- Bray, J. D. and Travasarou, T., (2007), "Simplified Procedure for Estimating Earthquake-Induced Deviatoric Slope Displacements", *Journal of Geotechnical and Geoenvironmental Engineering Division*, ASCE, Volume 133, Issue 4, p. 381-392.
- Buckle, I., Friedland, I., Mander, J., Martin, G., Nutt, R., and Power, M. S., (2006), "Seismic Retrofitting Manual for Highway Structures: Part 1 – Bridges", (Publication No. FHWA-HRT-06-032), US Department of Transportation, Office of Infrastructure Research and Development, Federal Highway Administration, Washington, D.C.
- Chiou, B. S.-J., Silva, W. J., and Power, M. S., (2002), "Vertical to Horizontal Spectral Ratios for Seismic Design and Retrofit of Bridges in Western and Eastern United States", Poster Session, Third National Seismic Conference and Workshop on Bridges and Highways, Portland, Oregon.
- Dobry, R., Oweis, I., and Urzua, A., (1976), "Simplified Procedures for Estimating the Fundamental Period of a Soil Profile", *Bulletin of the Seismological Society of America*, 66(4), pp. 1293-1321.
- Green, R. A., (2001), "Energy-Based Evaluation and Remediation of Liquefiable Soils", Ph.D. Dissertation, Virginia Polytechnic Institute and State University, 397 p.
- Hadjian, A. H., (2002), "Fundamental Period and Mode Shape of Layered Soil Profiles", *Soil Dynamics and Earthquake Engineering*, Volume 22, pp. 885 - 891.
- Hashash, Y., (2012), "DEEPSOIL Version 5.1 – User Manual and Tutorial", University of Illinois at Urbana-Champaign, October 3.
- Idriss, I.M., (1990), "Response of soft soil sites during earthquakes," Proc. H. Bolton Seed Memorial Symposium, J. M. Duncan (editor), Vol. 2, pp. 273-290.
- Idriss, I. M. and Sun, J. I., (1992), "User's Manual for SHAKE91", Center for Geotechnical Modeling, Department of Civil and Environmental Engineering, University of California, Davis, California, 13 p. (plus Appendices).
- Kavazanjian, E., Wang, J-N. J., Martin, G. R., Shamsabadi, A., Lam, I., Dickenson, S. E., and Hung, C. E., (2012). LRFD Seismic Analysis and Design of Transportation Geotechnical Features and Structural Foundations, Engineering Circular No. 3, (Publication No. FHWA-NHI-11-032, August (Rev. 1)), US Department of Transportation, National Highway Institute, Federal Highway Administration, Washington, D.C.
- Kempton, J. J. and Stewart, P. S., (2006), "Prediction equations for significant duration of earthquake ground motions considering site and near-source effects", *Earthquake Spectra*, 22(4), pp. 985-1013.
- Lester, A. P., (2005), "An Examination of Site Response in Columbia, South Carolina: Sensitivity of Site Response to "Rock" Input Motion and the Utility of  $V_s(30)$ " MS Thesis, Virginia Polytechnic Institute and State University, 91 p.

Madera, G. A., (1970), "Fundamental Period and Amplification of Peak Acceleration in Layered Systems", Research Report R70-37, Soils Publication No. 260, Department of Civil Engineering, MIT, 77 p.

Matasović, N. and Ordóñez, G. A., (2011), "D-MOD2000 – A Computer Program Package for Seismic Response Analysis of Horizontally Layered Soil Deposits, Earthfill Dams and Solid Waste Landfills", GeoMotions, LLC.

Newmark, N. M. and Hall, W. J., (1982), "Earthquake Spectra and Design", *EERI Monograph*, Earthquake Engineering Research Institute, Berkeley, CA.

Odum, J. K., Williams, R. A., Stephenson, W. J., and Worley, D. M., (2003), "Near-surface S-wave and P-wave seismic velocities of primary geological formations on the Piedmont and Atlantic Coastal Plain of South Carolina, USA", United States Geological Survey Open-File Report 03-043, 14 p.

Ordóñez, G. A., (2011), "SHAKE2000 – A Computer Program for the 1-D Analysis of Geotechnical Earthquake Engineering Programs", GeoMotions, LLC.

Phillips, C. and Hashash, Y. M. A., (2009), "Damping formulation for nonlinear 1D site response analysis", *Soil Dynamics and Earthquake Engineering*, 29(7), pp. 1143-1158.

Power, M. S., Chiou, B. S.-J., and Mayes, R. L., (1999), "National Representation of Seismic Ground Motion for Highway Facilities", Research Progress and Accomplishments 1997 - 1999, Multidisciplinary Center for Earthquake Engineering Research, University at Buffalo.

Power, M. S., Chiou, B. S.-J., Rosidi, D., and Mayes, R. L., (1997), "Background Information for Issue A: Should New USGS Maps Provide a Basis for the National Seismic Hazard Portrayal for Highway Facilities? If So, How Should They be Implemented in Terms of Design Values?", *Proceedings of the FHWA/NCEER Workshop on the National Representation of Seismic Ground Motion for New and Existing Highway Facilities*, Burlingame, California, May 29-30, Technical Report NCEER-97-0010, National Center for Earthquake Engineering Research, University at Buffalo.

Qiu, P., (1998), Earthquake-induced Nonlinear Ground Deformation Analyses, Ph.D. Dissertation, University of Southern California, Los Angeles.

Rathje, E. M., Faraj, F., Russell, S., and Bray, J. D., (2004), "Empirical Relationships for Frequency Content Parameters of Earthquake Ground Motions", *Earthquake Spectra*, 20(1), pp. 119-144.

South Carolina Department of Transportation, (2008), Seismic Design Specifications for Highway Bridges, South Carolina Department of Transportation, <https://www.scdot.org/business/structural-design.aspx>.

Schnabel, P. B., Lysmer, J., and Seed, H. B., (1972), "SHAKE: A Computer Program for Earthquake Response Analysis of Horizontally Layered Sites", Report No. EERC 72-12, Earthquake Engineering Research Center, University of California, Berkeley, California.

Seed, H. B. and Idriss, I. M., (1982), "Ground Motions and Soil Liquefaction During Earthquakes", *EERI Monograph*, Earthquake Engineering Research Institute, Berkeley, CA.



Seed, H. B., Ugas, C., and Lysmer, J., (1976), "Site-dependent spectra for earthquake resistant design", *Bulletin of the Seismological Society of America*, v. 66, pp. 221-243.

Silva, W. J. and Darragh, R., (1995), "Engineering characterization of earthquake strong ground motion recorded at rock sites", Electric Power Research Institute, TR-102262.

Silva, W. J. and Green, R. K., (1989), "Magnitude and distance scaling of response spectral shapes for rock sites with applications to North American tectonic environment", *Earthquake Spectra*, v. 5, pp. 591-624.

Stewart, J. P., Kwok, A. O., Hashash, Y. M. A., Matasović, N., Pyke, R., Wang, Z., and Yang, Z., (2008), "Benchmarking on Nonlinear Geotechnical Ground Response Analysis Procedures", Report No. PEER 2008/04, Pacific Earthquake Engineering Research Center, University of California, Berkeley.

URS Corporation (2001), "Comprehensive Seismic Risk and Vulnerability Study for the State of South Carolina", Report to the South Carolina Emergency Management Division (SCEMD).

Vijayendra, K. V., Prasad, S. K. and Nayak, S., (2010), "Computation of Fundamental Period of Soil Deposit: A Comparative Study", Indian Geotechnical Conference – 2010 (*GEOtrendz*), Mumbai, India.

Youd, T. L. and Carter, B. L., (2005), "Influence of Soil Softening and Liquefaction on Spectral Acceleration", *Journal of Geotechnical and Geoenvironmental Engineering Division*, ASCE, Vol. 131, No. 7, pp. 811-825.

**Chapter 13**

**GEOTECHNICAL  
SEISMIC HAZARDS**

**GEOTECHNICAL DESIGN MANUAL**

*January 2019*



**Table of Contents**

<b><u>Section</u></b>		<b><u>Page</u></b>
13.1	Introduction.....	13-1
13.2	Geotechnical Seismic Hazard Failure Modes.....	13-2
	13.2.1 Seismic Acceleration Hazards.....	13-2
	13.2.2 Global Hazards .....	13-3
13.3	Geotechnical Seismic Hazard Evaluation Process.....	13-3
	13.3.1 Seismic Shaking Evaluation Process .....	13-4
	13.3.2 Soil Shear Strength Loss Hazard Evaluation Process .....	13-4
13.4	Geotechnical Seismic Hazard Analytical Methodologies.....	13-7
13.5	Soil Shear Strength Loss Mechanisms .....	13-7
	13.5.1 Cyclic Liquefaction of Sand-Like Soils.....	13-8
	13.5.2 Cyclic Softening of Clay-Like Soils .....	13-9
	13.5.3 SC Historical Cyclic Liquefaction.....	13-9
13.6	Soil Shear Strength Loss Susceptibility Screening Criteria .....	13-12
	13.6.1 Sand-Like Soil.....	13-14
	13.6.2 Normally Sensitive (NS) Clay-Like Soil.....	13-16
	13.6.3 Highly Sensitive (HS) Clay-Like Soil.....	13-16
13.7	Soil Shear Strength Loss Triggering .....	13-16
13.8	Cyclic Stress Ratio (CSR).....	13-18
	13.8.1 Equivalent Seismic-Induced Stress ( $CSR_{eq}$ ).....	13-19
	13.8.2 Magnitude Scaling Factor.....	13-21
13.9	Cyclic Resistance Ratio (CRR) .....	13-22
	13.9.1 Sand-Like Soil - SPT Based CRR* Curves.....	13-25
	13.9.2 Sand-Like Soil - CPTu Based CRR* Curves .....	13-26
	13.9.3 Clay-Like Soil CRR* Curves.....	13-28
	13.9.4 High Overburden Correction ( $K_G$ ) .....	13-30
	13.9.5 Age Correction Factor ( $K_{DR}$ ) .....	13-32
	13.9.6 Static Shear Stress Ratio Correction Factor ( $K_a$ ).....	13-36
13.10	Soil Shear Strength for Seismic Analyses.....	13-44
	13.10.1 Sand-Like Soil Cyclic Shear Strength Triggering .....	13-44
	13.10.2 Sand-Like Soil Cyclic Liquefaction Shear Strength.....	13-46
	13.10.3 Clay-Like Soil Cyclic Shear Strength Triggering .....	13-52
	13.10.4 Clay-Like Soil Cyclic Softening Shear Strength .....	13-52
	13.10.5 Seismic Soil Shear Strength Selection .....	13-52
13.11	Flow Slide Failure .....	13-53
13.12	Seismic Acceleration Coefficients .....	13-54
13.13	Seismic Global Stability .....	13-56
13.14	Newmark Seismic Displacement Methods .....	13-58
	13.14.1 Newmark Time History Analyses.....	13-59
	13.14.2 Simplified Newmark Charts .....	13-61
13.15	Seismic Soil Settlement .....	13-63
	13.15.1 Soil Characterization .....	13-64
	13.15.2 Saturated Sand Settlement.....	13-64
13.16	References .....	13-69

**List of Tables**

<b><u>Table</u></b>	<b><u>Page</u></b>
Table 13-1, Global Hazard Instability Cases.....	13-2
Table 13-2, CRR Determination Based on Types of In-situ Testing.....	13-23
Table 13-3, Liquefaction Susceptibility of Sedimentary Deposits.....	13-33
Table 13-4, Simplified $K_{\alpha}$ Values for Sand-Like Soils .....	13-41
Table 13-5, Simplified $K_{\alpha}$ Values for Clay-Like Soils .....	13-44
Table 13-6, Sand-Like Shear Strengths.....	13-45
Table 13-7, Values of $\Delta N_{1,60-r1}$ .....	13-47
Table 13-8, Values of $\Delta q_{t,1,N,-r1}$ .....	13-48
Table 13-9, Seismic Soil Shear Strength Selection .....	13-53
Table 13-10, No Slope Stability Analysis Required.....	13-57

### List of Figures

<u>Figure</u>	<u>Page</u>
Figure 13-1, Cyclic Liquefaction-Induced Seismic Geotechnical Hazards.....	13-6
Figure 13-2, Sand Boil Crater - 1886 Charleston, SC Seismic Event.....	13-9
Figure 13-3, 1886 Liquefaction and Ground Deformations Sites .....	13-10
Figure 13-4, Coastal Plain Paleoliquefaction Study Sites .....	13-11
Figure 13-5, SC Quaternary Liquefaction Areas .....	13-12
Figure 13-6, Liquefaction Susceptibility Based on Soil Plasticity .....	13-13
Figure 13-7, Transition from Sand-Like to Clay-Like behavior .....	13-14
Figure 13-8, Plasticity Chart – Sand-Like/Clay-Like Soils .....	13-15
Figure 13-9, Variations of Shear Stress Reduction Coefficient, $r_d$ .....	13-20
Figure 13-10, Magnitude Scaling Factor (MSF) .....	13-22
Figure 13-11, Typical CRR Curve.....	13-23
Figure 13-12, Field CRR- $\xi_R$ Correlations Based on SPT and CPTu .....	13-24
Figure 13-13, Variation in $\Delta N_{1,60}^*$ With Fines Content .....	13-25
Figure 13-14, SPT Liquefaction Triggering Correlation ( $CRR^*$ ) .....	13-26
Figure 13-15, Variation in $\Delta q_{c,1,N}$ With Fines Content.....	13-27
Figure 13-16, CPTu Liquefaction Triggering Correlation ( $CRR^*$ ).....	13-28
Figure 13-17, $CRR^*$ Clay-Like – Shear Strength Correlation.....	13-29
Figure 13-18, $CRR^*$ Clay-Like Soils – OCR Correlation .....	13-30
Figure 13-19, High Overburden Correction ( $K_\sigma$ ) ( $\sigma'_{vo} > 1$ tsf) .....	13-31
Figure 13-20, Sand-Like Soil Strength Gain With Age .....	13-34
Figure 13-21, Relationship Between Strength Gain Factor and Time .....	13-34
Figure 13-22, Variations of $K_\alpha$ with SPT Blow Count ( $N_{1,60}^*$ ) .....	13-39
Figure 13-23, Variations of $K_\alpha$ with CPT Tip Resistance ( $q_{c,1,N}$ ) .....	13-40
Figure 13-24, $K_\alpha$ versus $(\tau_s/S_u)_{\alpha=0}$ For Clay-Like Soil (NC Drammen Clay) .....	13-42
Figure 13-25, $K_\alpha$ versus $(\tau_s/S_u)_{\alpha=0}$ For Clay-Like Soil ( $1 \leq OCR \leq 8$ ) .....	13-43
Figure 13-26, Excess Pore Pressure Ratio - Liquefaction Triggering.....	13-45
Figure 13-27, Liquefied Shear Strength Ratio - SPT.....	13-47
Figure 13-28, Liquefied Shear Strength Ratio - CPTu Tip Resistance .....	13-48
Figure 13-29, Liquefied Shear Strength Ratio - SPT Blow Count.....	13-50
Figure 13-30, Liquefied Shear Strength Ratio - CPT Tip Resistance .....	13-51
Figure 13-31, Simplified Wave Scattering Scaling Factor .....	13-55
Figure 13-32, Pseudo-Static Limit Equilibrium Analysis Slice .....	13-56
Figure 13-33, Newmark Sliding Block Method .....	13-59
Figure 13-34, Newmark Time History Analysis .....	13-60
Figure 13-35, Simplified Newmark Chart (PGV = 30 $k_{max}$ in/sec) .....	13-62
Figure 13-36, Simplified Newmark Chart (PGV = 60 $k_{max}$ in/sec) .....	13-62
Figure 13-37, Volumetric Strain Relationship Comparison - $M_w=7.5$ ; $\sigma'_{vc} = 1$ atm .....	13-65
Figure 13-38, Volumetric Strain Relationship - $M_w=7.5$ ; $\sigma'_{vc} = 1$ atm .....	13-67
Figure 13-39, Liquefiable Soil Layer Thickness in Stratified Soils .....	13-68



# CHAPTER 13

## GEOTECHNICAL SEISMIC HAZARDS

### 13.1 INTRODUCTION

The screening, identification, and evaluation of geotechnical seismic hazards at a project site are integral parts of geotechnical seismic engineering. The effects of these hazards must be taken into consideration during the design of geotechnical structures such as bridge foundations, ERSs, and embankments. Geotechnical seismic hazards can generally be divided into those that are associated with losses in soil shear strength and stiffness; seismic ground shaking (i.e., accelerations and inertial forces); and, seismic induced lateral ground movements and settlement. Losses in the soil shear strength in South Carolina are primarily due to cyclic liquefaction of loose cohesionless soils and secondarily due to cyclic softening of plastic cohesive soils. Seismic accelerations and inertial forces can create instability due to increased driving forces as a result of increased static active soil pressures. Seismic induced lateral ground movement can occur in sloping ground conditions where the increased driving forces can exceed the soil shear strength. Seismic settlement can be either the result of cyclic liquefaction of cohesionless soils or densification/compression of unsaturated soils and compacted fill materials.

The procedures for analyzing soil Shear Strength Loss (SSL) and associated geotechnical seismic hazards such as flow slide failure and seismic slope instability are provided in this Chapter. Methods of computing horizontal seismic accelerations based on peak ground accelerations (PGA) and seismic displacements are also provided in this Chapter. Finally, procedures for evaluating seismic settlement due to either cyclic liquefaction or densification/compression of unsaturated and saturated soils are presented in this Chapter. Methods of computing seismic active and passive soil pressures on ERSs and bridge abutments are provided in Chapter 14.

SCDOT recognizes that the methods presented in this Manual may not be the only methods available, particularly since geotechnical seismic engineering is developing at a very rapid pace as seismic events around the world contribute to the study and enhancement of analytical methods for geotechnical seismic hazard evaluation. Because geotechnical seismic engineering in South Carolina (and CEUS) is at the very early stages of development, the overall goal of this Chapter is to establish a state-of-practice that can evolve and be enhanced as methodologies improve and regional (CEUS) experience develops. Methods other than those indicated in this Manual may be brought to the attention of the PC/GDS for consideration on a specific project or to the PCS/GDS for consideration in future updates of this Manual.

Geotechnical seismic hazards such as fault rupturing and flooding (tsunami, seiche, etc.) are not addressed in this Chapter since current views suggest that the potential for these types of hazards in the CEUS is very low. If there is any evidence of faults traversing a project site that have been active within the Holocene epoch (10 thousand years ago to present day) it should be brought to the attention of the PC/GDS.

South Carolina geology and seismicity, discussed in Chapter 11, will have a major impact on the evaluation of soil SSL and should be well understood when evaluating geotechnical seismic hazards. Seismic shaking parameters will have a direct effect on the amount and extent of the deformations caused by geotechnical seismic hazards. Seismic shaking parameters such as the  $M_w$ ,  $R$ ,  $D_{a5-95}$ , PGV, and PGA must be determined based on the design seismic event (FEE or SEE) under evaluation as described in Chapter 12. Geotechnical seismic hazards that may



affect the design of transportation structures are described in the following Sections and analytical methods are presented to evaluate the potential for, and magnitude of displacement. The effects of geotechnical seismic hazards on the geotechnical design of bridge foundations, abutment walls, ERSs, and other miscellaneous structures are discussed in Chapter 14.

### 13.2 GEOTECHNICAL SEISMIC HAZARD FAILURE MODES

In order to evaluate the potential for the various geotechnical seismic hazards to occur at a project site, it is important to understand the various modes of failure that have been documented through case histories. Geotechnical seismic hazard modes of failure can be generally categorized as: Seismic Acceleration Hazards (seismic stability) or Global Hazards (flow failure). These geotechnical seismic hazard categories are discussed in the following Sections and are also summarized in Table 13-1.

**Seismic Stability** - Instability due to seismic inertial driving forces and static gravitational driving forces either with or without soil SSL.

**Flow Failure** - Instability due to static gravitational driving forces and soil SSL without seismic inertial driving forces.

**Table 13-1, Global Hazard Instability Cases**

Contributors to Instability	Instability Types		
	Seismic Stability		Flow Failure
Seismic Inertial Driving Forces	X	X	N/A
Static Gravitational Driving Forces	X	X	X
Soil SSL	N/A	X	X

#### 13.2.1 Seismic Acceleration Hazards

Seismic Acceleration Hazards consist of seismically-induced global instability and lateral spreading that can occur at bridge abutments, roadway embankments, bridge approach fills, natural cut slopes, and at ERSs. This geotechnical seismic hazard occurs as a coherent sliding soil mass (assumes that soil mass stays together as a block) moves along a critical shear failure surface. The triggering mechanism for slope instabilities is the seismic horizontal acceleration that induces inertial driving forces in addition to the initial static driving stresses that already exist within the slope. Lateral spreading is caused by a combination of seismic inertial driving forces, static gravitational driving stresses and soil SSL. Lateral spreading will typically end once the seismic inertial driving forces cease. Typically seismic instability failures are characterized by translational or rotational slope failure that occurs during seismic shaking and are evaluated using conventional limit-equilibrium pseudo-seismic slope stability methods with appropriate soil shear strengths (accounting for soil SSL) and seismic acceleration coefficients. Deformations are typically evaluated using Newmark's rigid sliding block displacements method. Seismic inertial loads can cause damage as described below:

- Static active earth pressures plus seismic inertial loads can increase lateral earth pressures on ERSs which can result in failure due to deformations that exceed the performance limits or structural capacity of the ERS. Failure may manifest itself in the form of lateral translations, rotations, overturning, or structural failure. Failure of tie-back systems (soil anchors or soil nails) may jeopardize the integrity of the whole structure. Increased bearing loads at the toe of shallow foundations may exceed the bearing capacity of the soil causing rotational displacement or bearing failure.

- Static passive earth pressure resistance to lateral loads can be reduced due to seismic inertial loads that can result in failure of the ERS by allowing forces from either seismic active soil pressures or inertial forces from the structure to cause large translational displacements.
- Global limit-equilibrium instability of the structure resulting in rotational or translational deformations that may exceed the ERS performance limits or structural capacity.
- Volumetric strain and accompanying ground settlement (Section 13.15) that results from the seismic shaking. The settlement can be due to either seismic densification/compression of unsaturated soils or fills and/or seismic densification resulting from excess pore water pressure relief of and rearrangement of cohesionless soils that have undergone cyclic liquefaction. There may be ground surface manifestations in the form of sand-boils as excess pore water pressure dissipates to the ground surface during cyclic liquefaction. Alternatively, water may get trapped under non-liquefiable soil layers above the cyclic liquefiable soils that will affect the rate of soil subsidence and may trigger other hazards due to soil SSL at these interfaces.

### **13.2.2 Global Hazards**

Global hazards are those failures that result in large-scale site instability in the form of translational/rotational instability and/or flow failure sliding. Displacements associated with global hazards (flow failure) are the result of static gravitational driving forces combined with soil SSL.

Flow slide failures are the most catastrophic form of ground failures. Sites susceptible to flow failure typically are continuous over large areas of soils that are contractive and susceptible to cyclic liquefaction (Section 13.6.1 – Sand-Like Soil). These failures result from instability when the resisting force available from soils that undergo soil SSL is less than the static gravitational driving force of the soil mass. Flow slide failure potential is typically characterized by screening for contractive soils that are susceptible to soil SSL, evaluating triggering of soil SSL, and then evaluating instability by using conventional limit-equilibrium static slope stability methods.

## **13.3 GEOTECHNICAL SEISMIC HAZARD EVALUATION PROCESS**

The effects of geotechnical seismic hazards must be considered in the design of all bridges, ERSs, embankments, and other transportation structures where poor performance could endanger the lives and safety of the traveling public. The effectiveness of highways in South Carolina depends on the proper evaluation of the geotechnical seismic hazards and designs to meet the performance requirements established in Chapter 10 for embankments, and ERSs.

The geotechnical seismic hazard evaluation begins with an evaluation of the seismic shaking parameters that are used to define the intensity and duration of the seismic event at the project site. A summary of the seismic shaking parameters that will be used for geotechnical seismic hazard evaluation is presented in Section 13.3.1.

The geotechnical seismic hazard evaluation process then proceeds to screening and identification of the subsurface soils that have the potential to experience soil SSL. The soil SSL evaluation process is presented in Section 13.3.2. Once the potential for soil SSL has been identified, the potential failure modes of the geotechnical seismic hazards presented in Section 13.2 can be evaluated.

The effects of the geotechnical seismic hazards on the stability and performance of embankments and slopes are addressed in this Chapter. The seismic design of bridge foundations, bridge abutments, and ERSs is addressed in Chapter 14.

Provided in Appendix J are a series flow charts of the geotechnical seismic hazard evaluation process upon which this Chapter is based. The processes presented in this Manual are meant to serve as a guide in the evaluation and assessment of geotechnical seismic hazards. It is by no means the only approach that can be used; at a minimum, it should serve as a point of reference to understand the layout of the following Sections in this Chapter.

### **13.3.1 Seismic Shaking Evaluation Process**

Geotechnical seismic hazards are triggered by the intensity and duration of the seismic shaking at the project site. The intensity and duration of the seismic shaking is primarily dependent on the size and location of the seismic events and the characteristics of the site. Chapters 11 and 12 provide the methodology for the assessment of the seismic shaking at a project site. The seismic shaking can be quantitatively assessed by the seismic  $M_w$ ,  $R$ ,  $T'_o$ ,  $T_{NH}$ ,  $PGV$ ,  $D_{a5-95}$ ,  $PGA$ ,  $S_{DS}$  and  $S_{D1}$ . Project sites that are closer to the seismic source experience higher levels of shaking; therefore, more damage can occur from geotechnical seismic hazards when compared to project sites further away.

### **13.3.2 Soil Shear Strength Loss Hazard Evaluation Process**

Soil SSL that is induced by seismic shaking can produce severe damage as a result of the various geotechnical seismic hazard failure mechanisms described in Section 13.2. The soil SSL hazard evaluation process has three components: (1) Evaluating soil SSL susceptibility at the project site; (2) Evaluating soil SSL triggering potential of the seismic shaking; and (3) Evaluating the effects of soil SSL on the design parameters used to evaluate the geotechnical seismic hazard.

The soil SSL evaluation process begins by screening for soils that are susceptible to soil SSL for the design seismic events (FEE or SEE) under evaluation. The screening criteria (Section 13.6) consist of 3 soil categories that are susceptible to soil SSL: Sand-Like soils, Normally Sensitive (NS) Clay-Like soils, and Highly Sensitive (HS) Clay-Like soils. The screening criteria uses site conditions (i.e., water table); in-situ testing; and standard laboratory index testing and soil shear strength testing to determine if soils are susceptible to soil SSL. If the soils are found not to be susceptible to soil SSL during the screening process, then no further analysis is required to determine the triggering of soil SSL and an evaluation of geotechnical seismic hazard evaluation can proceed. Soils found to be susceptible to soil SSL during the screening process shall be further evaluated for soil SSL triggering. An exception to this is, if the  $PGA$  is less than or equal to  $0.2g$  ( $PGA \leq 0.2g$ ); the Seismic Design Category (SDC) is A (see Seismic Specs for definition); and the slope is 2H:1V or flatter, then neither screening nor soil SSL triggering analysis will be required for bridge embankments. However, if the slope is steeper than 2H:1V or an ERS is located within the bridge embankment, then either screening or soil SSL triggering analysis will be required. In addition, the screening or triggering analysis may be required by either SCDOT or if in the opinion of the GEOR it is required. The GEOR shall document why SSL is required in the BGER.

Determining whether soil SSL triggering occurs during the seismic shaking or after the seismic shaking is very complex and beyond the scope of the methodology that will be used in the design of typical bridges and typical roadway structures. Therefore, the effects of cyclic liquefaction and cyclic softening (soil SSL) shall be assumed to occur during the seismic

shaking and will continue into the post-seismic period, to allow for the evaluation of soil SSL-induced geotechnical seismic hazards. Soil SSL shall be assumed to occur instantaneously throughout the full thickness of the soil layer and shall be assumed to occur at the beginning of shaking. These fundamental assumptions must be used when selecting soil shear strengths in accordance with Section 13.10.

The main contributor to catastrophic damage and poor performance of structures has in past case histories been attributed to cyclic liquefaction-induced seismic geotechnical hazards shown in Figure 13-1. Soil SSL due to cyclic liquefaction of Sand-Like soils (Section 13.6.1) has the potential to cause the most damage in the Coastal Plain of South Carolina as evident from the cyclic liquefaction case histories presented in Section 13.5.3.

Soils that are identified as being susceptible to losses in soil shear strength need to be evaluated to determine if the seismic shaking can trigger (or initiate) soil SSL. Soil SSL triggering for Sand-Like soils and Clay-Like soils is dependent on the site conditions (i.e., soil in-situ strength; soil composition including grain-size and moisture-plasticity relationship and location of ground water surface). The soil SSL triggering of Clay-Like soils is applicable to both NS Clay-Like soils and HS Clay-Like soils. The overall method for analyzing soil SSL triggering for Sand-Like soils and Clay-Like soils consists of determining if the cyclic stress ratio (CSR) induced by the design seismic event (FEE or SEE) and any initial static shear stresses ( $\tau_{\text{static}}$ ) in the soil ( $\text{CSR} = \text{Demand, D}$ ) are greater than the soil's cyclic resistance ratio ( $\text{CRR} = \text{Capacity, C}$ ) based on a specified margin of safety (on-set of soil SSL resistance factor,  $\phi_{\text{SL}}$ ), see Equation 13-1. If the soil SSL resistance ratio,  $(\text{D}/\text{C})_{\text{SL}}$ , is greater than  $\phi_{\text{SL}}$ , the soil under evaluation has the potential for soil SSL and a reduced shear strength shall be used in the evaluation of geotechnical seismic hazards.

$$\left(\frac{D}{C}\right)_{\text{SL}} = \frac{\text{CSR}_{\text{eq}}^*}{\text{CRR}_{\text{eq}}^*} \leq \phi_{\text{SL}} \quad \text{Equation 13-1}$$

Where,

$\text{CRR}_{\text{eq}}^*$  = Corrected, magnitude weighted and normalized CRR (Section 13.9).

$\text{CSR}_{\text{eq}}^*$  = Magnitude weighted and equivalent-seismically induced CSR (Section 13.8).

Initial static shear stress ( $\tau_{\text{Static}}$ ) reduces the soil's capacity (C) to resist the soil SSL. If the triggering of soil SSL is indicated at the site, then a flow failure analysis as described in Section 13.11 shall be conducted. If the flow failure resistance ratio,  $(\text{D}/\text{C})_{\text{Flow}}$  is greater than  $\phi_{\text{Flow}}$ , then a displacement analysis is required as described in Section 13.14. The triggering of soil SSL in Clay-Like soils (NS and HS) can also occur due to an increase in static shear stresses similar to that which occurs when Sand-Like soils experience cyclic liquefaction. Soil SSL in NS Clay-Like soils causes the soils to have cyclic softened residual shear strength ( $\tau_{\text{rs}}$ ) and in HS Clay-Like soils causes the soils to have remolded soil shear strength ( $\tau_{\text{remolded}}$ ).

The selection of soil shear strength properties for soils with and without the potential for soil SSL is performed during the geotechnical seismic hazard evaluation. The overall process for evaluating soil SSL is shown in Appendix J.

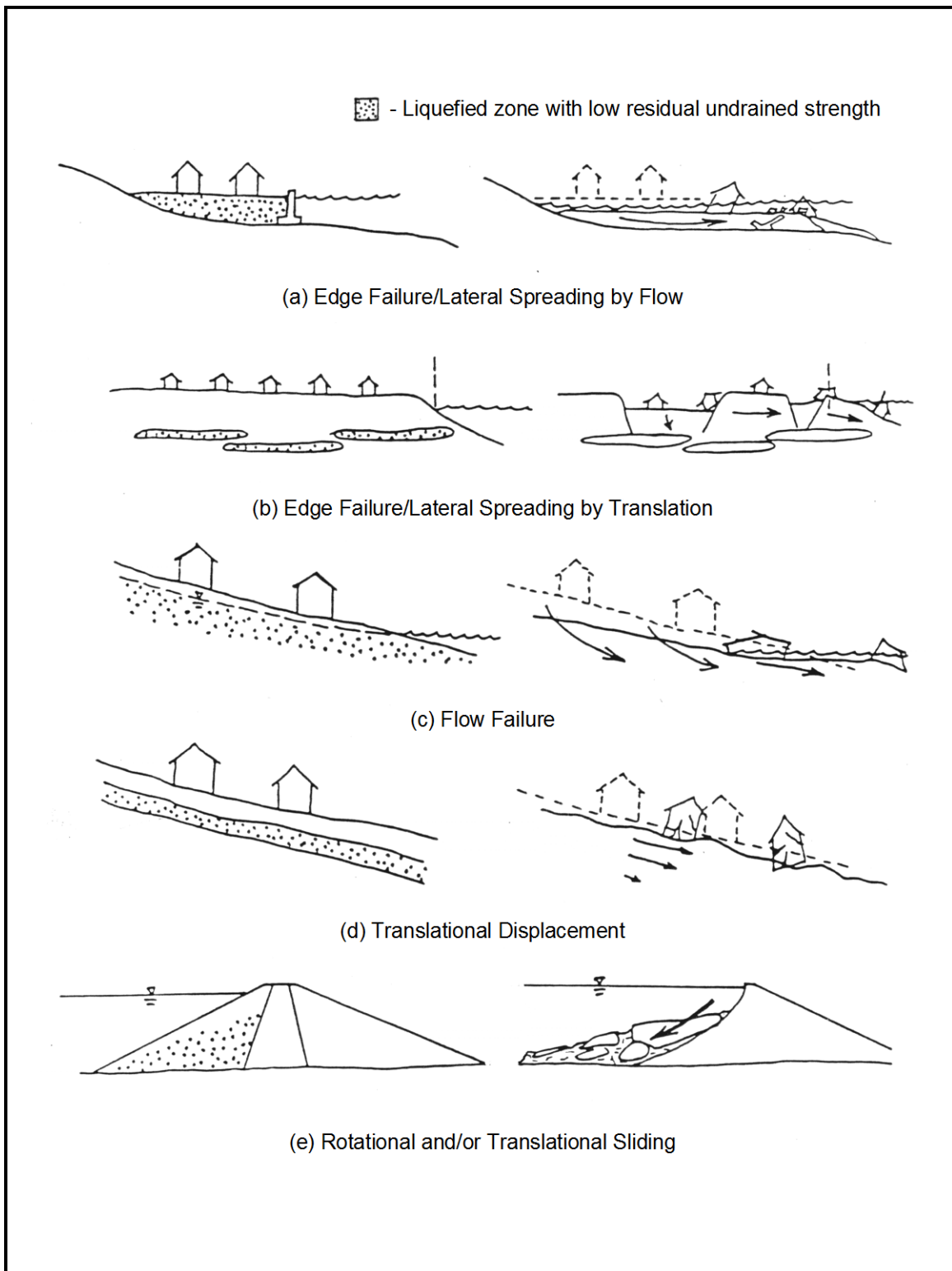


**Figure 13-1, Cyclic Liquefaction-Induced Seismic Geotechnical Hazards (Seed, et al. (2003))**

## 13.4 GEOTECHNICAL SEISMIC HAZARD ANALYTICAL METHODOLOGIES

The methodologies presented in this Chapter for evaluating and assessing the impact of the geotechnical seismic hazards on transportation structures are based primarily on general limit-equilibrium (GLE) (see Chapter 17 for definition) methods of analyses and empirical/semi-empirical analytical methods that are easily performed and are currently within the state-of-practice of geotechnical seismic engineering. References for the design methodologies used in this Manual have been listed to allow the designer the opportunity to become more thoroughly familiar with the methodology, its applicability, and its limitations. Within the scope of this Manual, it is not possible to provide sufficient detail and caveats to preclude any misuse of the methods. When necessary, several methods of analyzing the geotechnical seismic hazard have been provided in order to allow for variance in analytical methodologies and to identify trends in results or performance. Several of the methods presented are empirical/semi-empirical and their applicability to the project site is dependent on the limits of the database used to develop the analytical basis of the method. Therefore, it is the responsibility of the GEOR to know the applicability and limitations of these methods. This Chapter does not address numerical analyses (e.g., finite element, finite difference, etc.), because these methods are typically not performed in the design of typical bridges or typical transportation structures. If numerical analyses are required for a project, contact the PC/GDS for design requirements, review and acceptance of the proposed methods.

## 13.5 SOIL SHEAR STRENGTH LOSS MECHANISMS

The mechanism of soil SSL is very complex and has been the subject of much confusion in literature. This is particularly due to the lack of standardization of terminology and the fact that research efforts are still ongoing. Additional confusion has occurred when the method of soil SSL triggering (static stresses, cyclic loads, etc.) has been used as a means of categorizing the soil SSL mechanism. Current understanding of soil SSL failure mechanisms is based on the study of case histories and laboratory experimentation. One of the problems in the evaluation of field case histories is that more than 1 geotechnical seismic hazard is typically responsible for the observed failures. For example, this problem can occur when lateral spread movements trigger flow failures and the resulting final deformations observed reflect the influence of all geotechnical seismic hazard failure modes (lateral spread, flow failure, and seismic settlement). Laboratory testing has provided much insight into the mechanisms that trigger soil SSL under a controlled laboratory environment. Laboratory experimentation has limitations in that sampling disturbance of the in-situ soil structure (i.e., cementation, layering, etc.) can significantly affect the initial and residual soil shear strength results. Another limitation is that laboratory testing can be very complex and routinely not within the standard-of-practice for design of typical bridge structures. Detailed explanation of the mechanisms of soil SSL based on field and laboratory observations can be obtained from Robertson and Wride (1997), Kramer and Elgamal (2001), and Idriss and Boulanger (2008). Although the term liquefaction has been used widely in literature (Kramer (1996) and Robertson and Wride (1997)) to describe several mechanisms of soil SSL, the term liquefaction as used in this Manual will only be applicable to discussions of Sand-Like soil SSL that results from cyclic loading.

The predominant soil behavior (i.e., cohesionless or cohesive) is used in this Manual to evaluate the soil's SSL susceptibility (Section 13.6) and to determine the most appropriate soil SSL triggering evaluation method for use in geotechnical seismic design. Field case histories and laboratory testing have demonstrated that the predominant soil SSL behavior for the majority of soils can be grouped into either Sand-Like soils (i.e., cohesionless) that are subject to cyclic liquefaction failure mechanisms or Clay-Like soils (i.e., cohesive) that are subject to cyclic

softening failure mechanisms. A description of these soil failure mechanisms is provided in the following Sections.

### **13.5.1 Cyclic Liquefaction of Sand-Like Soils**

Cyclic liquefaction of Sand-Like soils is typically responsible for the most damaging geotechnical seismic hazards that affect transportation infrastructure. Potential damage to transportation facilities due to cyclic liquefaction includes loss of bearing capacity, lateral spread, flow failure, excessive settlements, and reduced lateral and vertical carrying capacity of deep foundations. Even though cyclic liquefaction can be triggered by non-seismic loadings such as low amplitude vibrations produced by rail traffic/construction equipment or by static loads, such as those that might be caused by rapid drawdown, this Manual will focus on liquefaction triggered by seismic shaking. Non-seismic cyclic liquefaction triggers are not covered by this Manual. Cyclic liquefaction occurs in Sand-Like soils that are nonplastic, saturated, and have been deposited during the Quaternary Period (past 1.6 million years) in a loose state and are subject to strain softening. Typically, the more recent soil deposits have the greatest susceptibility for cyclic liquefaction. Cyclic liquefaction typically begins during a seismic event when the in-situ soil pore water pressure ( $u_0$ ) increases ( $+\Delta u$ ). As the increased pore water pressure ( $u = u_0 + \Delta u$ ) approaches the total overburden stress ( $\sigma_{v0}$ ), the effective overburden stress ( $\sigma'_{v0} = \sigma_{v0} - u$ ) will approach zero causing a reduction in grain-to-grain contact and a significant decrease in soil shear strength. The reduction in grain-to-grain contacts cause a redistribution of soil particles resulting in densification. As indicated previously it is assumed that pore pressures increase to the total overburden stress instantaneously within a Sand-Like soil layer at the beginning of the seismic event and continues into the post-seismic period. Further it is assumed that the entire Sand-Like soil layer experiences soil SSL across the full soil layer thickness at the same time.

Significant lateral soil deformation may occur as a result of reduced soil shear strength of the liquefied soil zone combined with the seismic inertial forces and/or initial static driving forces. Other surface manifestations of cyclic liquefaction are often associated with the upward flowing of pore water that generates sand boils at the ground surface. Evidence of sand boils occurring at the ground surface have been found throughout the South Carolina Coastal Plain as indicated in Section 13.5.3. The absence of sand boils is not an indication that cyclic liquefaction has not occurred. Sand boils will not always occur during or after cyclic liquefaction, especially if the drainage paths are restricted due to overlying less permeable layers, i.e., the sand is immediately beneath a less permeable soil. Seismic settlement at the ground surface may occur from cyclic liquefaction induced volumetric strain that develops as seismically induced pore water pressures dissipate.

The determination of the onset of cyclic liquefaction either during shaking or post-seismic is a very complex analytical problem and beyond the scope of typical SCDOT projects. Several case histories have documented that liquefaction can both occur during shaking or after shaking has occurred (Seed (1986), Kramer and Elgamal (2001)). The onset and manifestation of cyclic liquefaction is primarily dependent on the magnitude, duration, and proximity of the seismic event, the depth of the liquefied soil zone, stratification and relative permeability of the soil layers above and below the liquefied soil zone, and the susceptibility of the soils to liquefy. Consequently liquefaction will conservatively be assumed to occur at the beginning of the seismic shaking and continues into the post-seismic time.

### 13.5.2 Cyclic Softening of Clay-Like Soils

Cyclic softening refers to soil SSL and deformations in Clay-Like soils. Clay-Like soils are typically moist, plastic clays. Cyclic softening occurs when the seismic-induced cyclic shear stresses exceed the soil's cyclic shear resistance, causing an accumulation of deformations that result in soil SSL in cohesive soils that exhibit strain softening. Cyclic softening of Clay-Like soils typically results in soil SSL that is dependent on the soil's sensitivity (Chapter 7). Soil deformations may occur as a result of reduced soil shear strength of Clay-Like soils combined with the inertial forces and/or initial static driving forces. The limited case histories in South Carolina have not documented cyclic softening of Clay-Like soils. Field evidence of cyclic softening of Clay-Like soils is difficult to document because it does not manifest itself as sand boils at the ground surface as has been documented for cyclic liquefaction of Sand-Like soils. As with Sand-Like soils, it will be conservatively assumed that cyclic softening occurs at the beginning of the shaking and that the entire layer softens at the same time.

### 13.5.3 SC Historical Cyclic Liquefaction

There is significant evidence that cyclic liquefaction has historically occurred in the CEUS. Soil liquefaction has been found to have occurred as a result of seismic events in New Madrid, Missouri 1811–1812 and in Charleston, South Carolina 1886. The 1886 Charleston seismic event caused the manifestation of large sand boils as a result of cyclic liquefaction. Sand boils were created as the soil pore water, carrying soil particles, was expelled from the ground, collapsing the surface and forming craters at the ground surface. Figure 13-2 shows a sand boil crater that appeared during the 1886 Charleston seismic event.



**Figure 13-2, Sand Boil Crater - 1886 Charleston, SC Seismic Event (McGee, et al. (1986))**

Hayati and Andrus (2008) developed a liquefaction potential map of Charleston, South Carolina based on the 1886 seismic event. The geologic map of the Charleston Peninsula and Drum Island originally developed by Weems, et al. (1997) was used by Hayati and Andrus (2008) to



indicate locations of liquefaction and ground deformations as shown in Figure 13-3. For a description of the near surface geologic units and a description of the Cases (indicated on the map as 1 – 27) of cyclic liquefaction evidence and permanent ground deformation see Hayati and Andrus (2008).

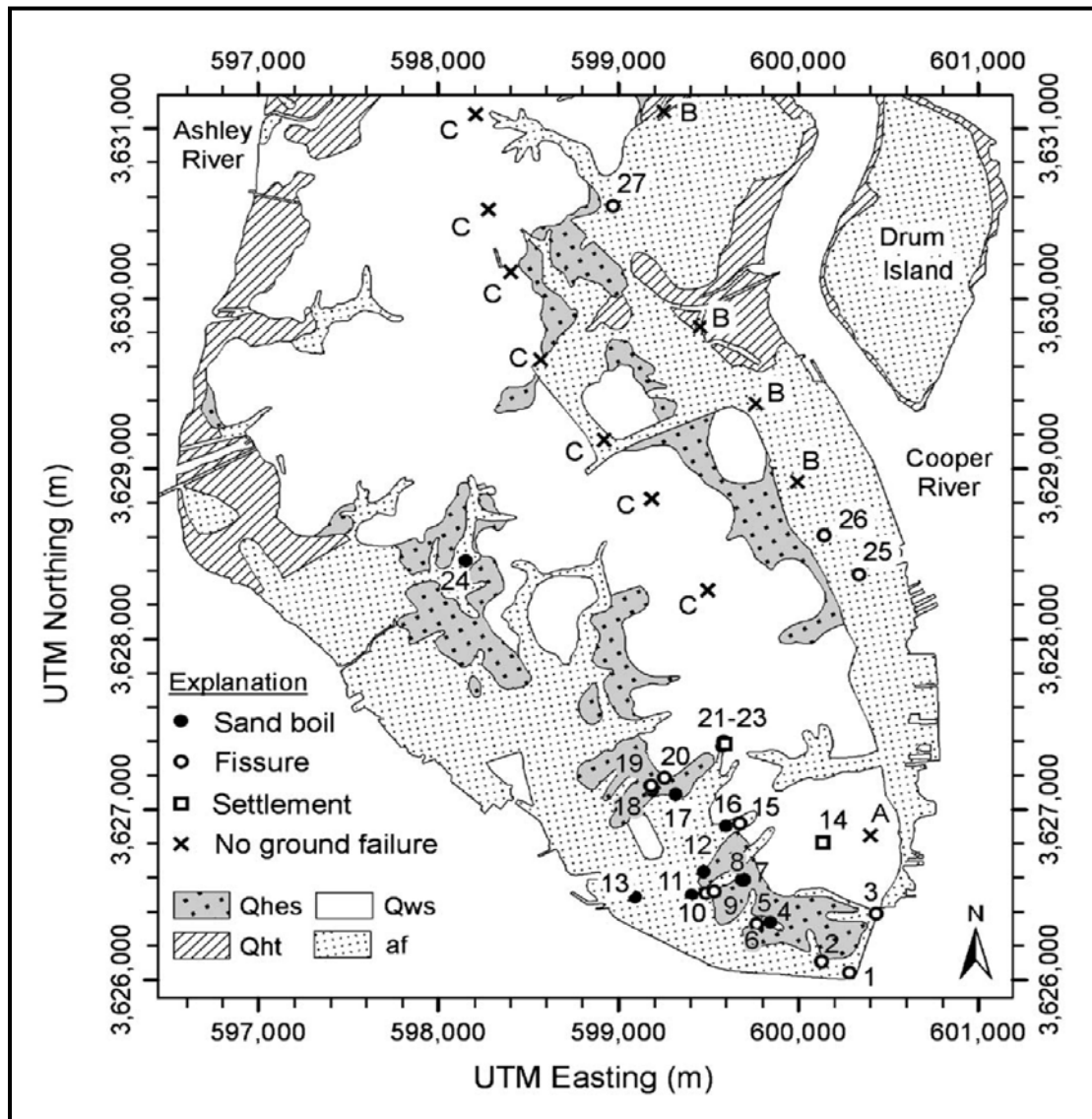


**Figure 13-3, 1886 Liquefaction and Ground Deformations Sites (Weems, et al. (1997), Hayati and Andrus (2008) with permission from ASCE)**

Paleoliquefaction studies in South Carolina conducted since the mid-1980s have indicated that at least 7 episodes of paleoliquefaction have occurred in the past 6,000 years. The seismic events in the Charleston, SC area appear to have magnitudes greater than 7 and the seismic event cycle suggests a recurrence interval of 500-600 years (Talwani and Schaffer, 2001). Paleoliquefaction study site locations in the South Carolina Coastal Plain are shown in Figure 13-4.

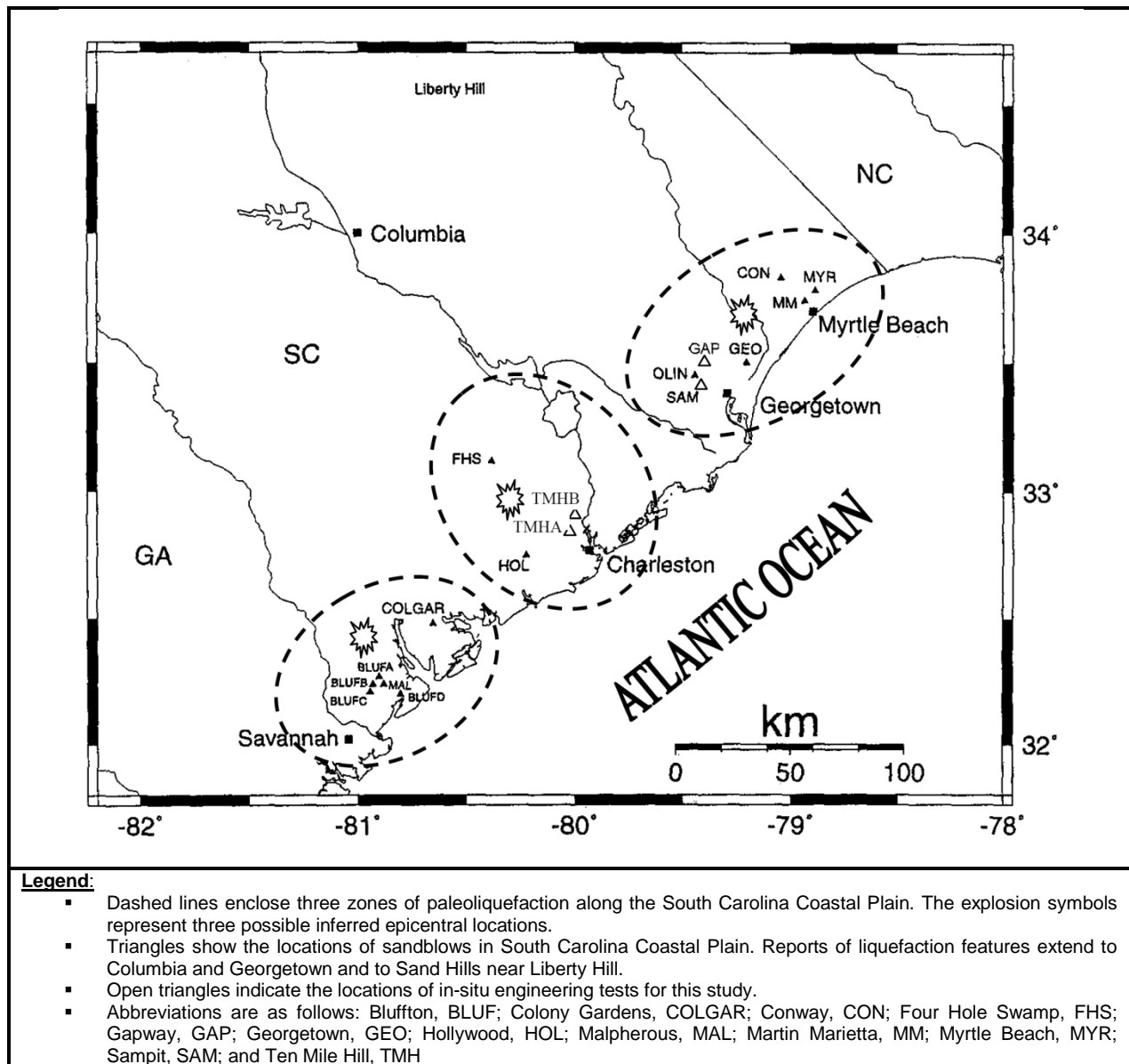


**Figure 13-4, Coastal Plain Paleoliquefaction Study Sites (adapted from Talwani and Schaffer (2001)).**

Figure 13-5 shows a map, prepared by the USGS, of the liquefaction features in South Carolina. The shaded area on the map indicates areas of potential Quaternary and historic liquefaction. The USGS maintains a database of published reports of Quaternary faults, liquefaction and tectonic features in the CEUS. The USGS database for South Carolina contains the following 3 sites with liquefaction features: 2657, Charleston, SC; 2658, Bluffton, SC; and 2659, Georgetown, SC. Liquefaction feature 2657 has geologic evidence of the 1886 Charleston seismic event. Liquefaction features 2658 and 2659 have geologic evidence of prehistoric liquefaction that occurred during the late Quaternary Period (Holocene, <10,000 years ago).

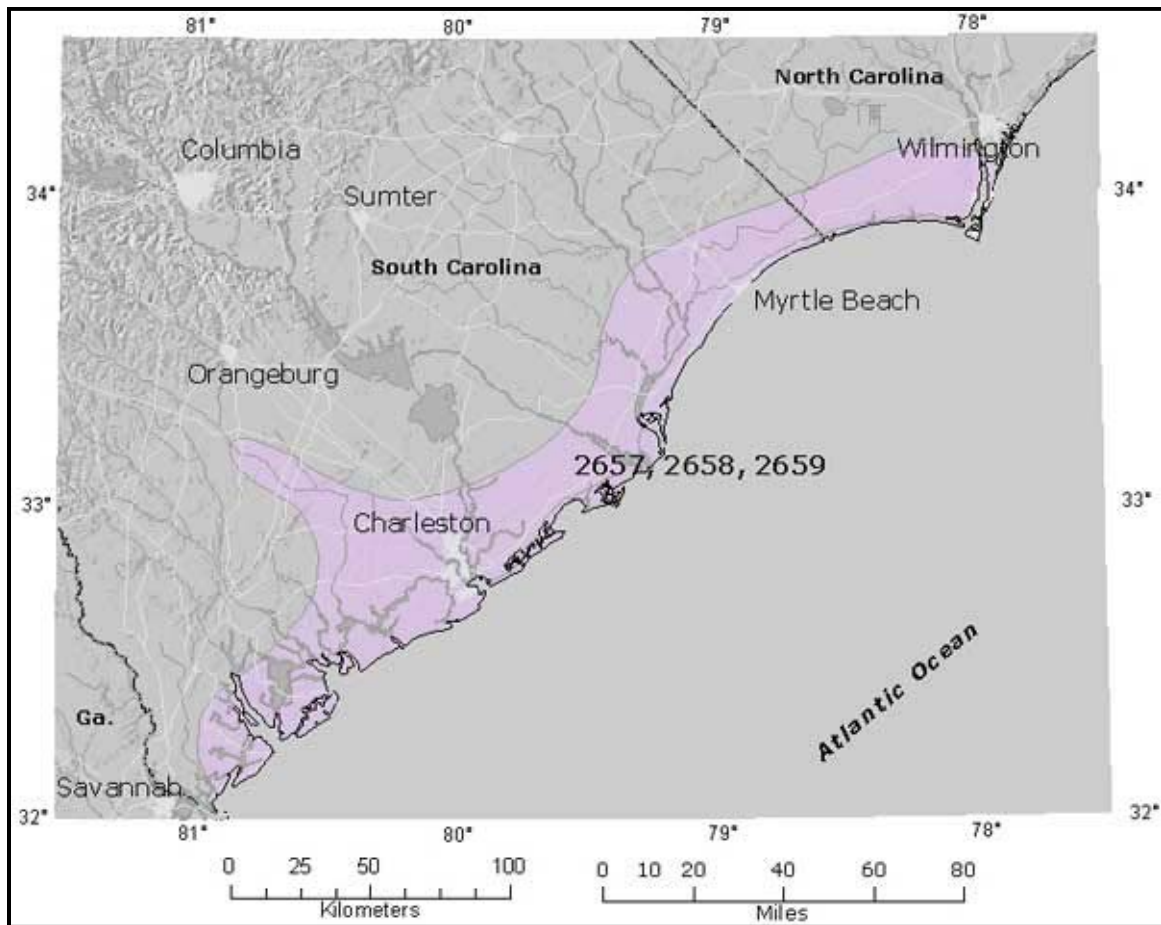


**Figure 13-5, SC Quaternary Liquefaction Areas  
(USGS Website)**

Even though liquefaction has occurred in the CEUS, a limited number of the liquefaction case histories have been evaluated, since most seismic events with moment magnitudes,  $M_w$ , greater than 6.5 occurred more than 100 years ago. Liquefaction evaluation in the CEUS and consequently in South Carolina, is relatively more complex than in other areas where liquefaction has occurred in the more recent past. The deep vertical soil column (up to 4,000 feet) encountered in the Atlantic Coastal plain, lack of recorded large seismic events, and uncertainty of the mechanisms and subsequent motions resulting from intraplate seismic events make liquefaction evaluation difficult (Schneider and Mayne (1999)). Nevertheless, historical soil liquefaction studies in the CEUS (Schneider and Mayne (1999)) indicate that current methods to evaluate cyclic liquefaction are in general agreement with predictions of cyclic liquefaction.

### 13.6 SOIL SHEAR STRENGTH LOSS SUSCEPTIBILITY SCREENING CRITERIA

Screening criteria is based on laboratory and in-situ test properties of soils that experience soil SSL in seismic hazard case histories. It has been observed that the potential for cyclic liquefaction decreases as FC and PI of the soils increase and as the  $w$  decreases below the LL.

Screening for seismic-induced soil SSL has traditionally been focused on cyclic liquefaction of cohesionless soils. Recent studies (Seed, et al. (2003), Boulanger and Idriss (2004 and 2007); Bray and Sancio (2006), Idriss and Boulanger (2008)) have stressed the need to evaluate soil SSL in other soil types, such as cyclic liquefaction of low plasticity silts and cyclic softening of

plastic clays. Seed, et al. (2003) proposed the liquefaction susceptibility chart for fine grained soils shown in Figure 13-6 that is based on soil plasticity. The chart is divided into 3 zones of varying soil SSL susceptibility. Zone A has the highest potential for loss in shear strength resulting from cyclic liquefaction. Zone B was considered a transition area where soils could be subject to soil SSL and would require laboratory cyclic load testing for confirmation of soil shear strength susceptibility. Soils located in Zone C (the Zone not covered by Zones A or B) were not susceptible to cyclic liquefaction induced soil SSL but can be susceptible to soil SSL due to cyclic softening of sensitive cohesive soils.

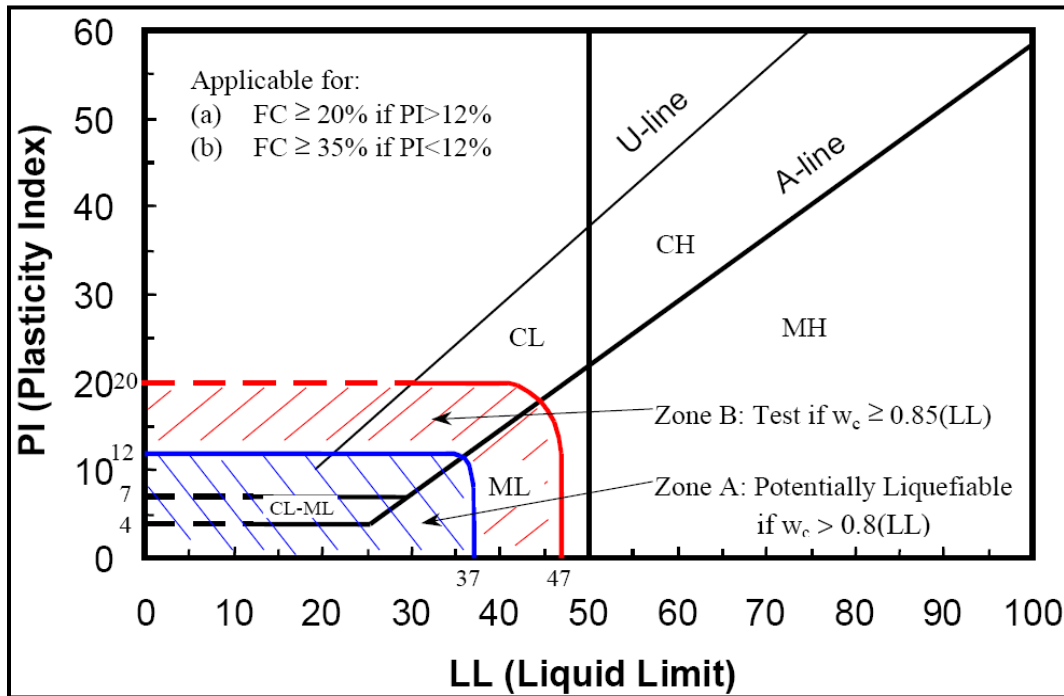
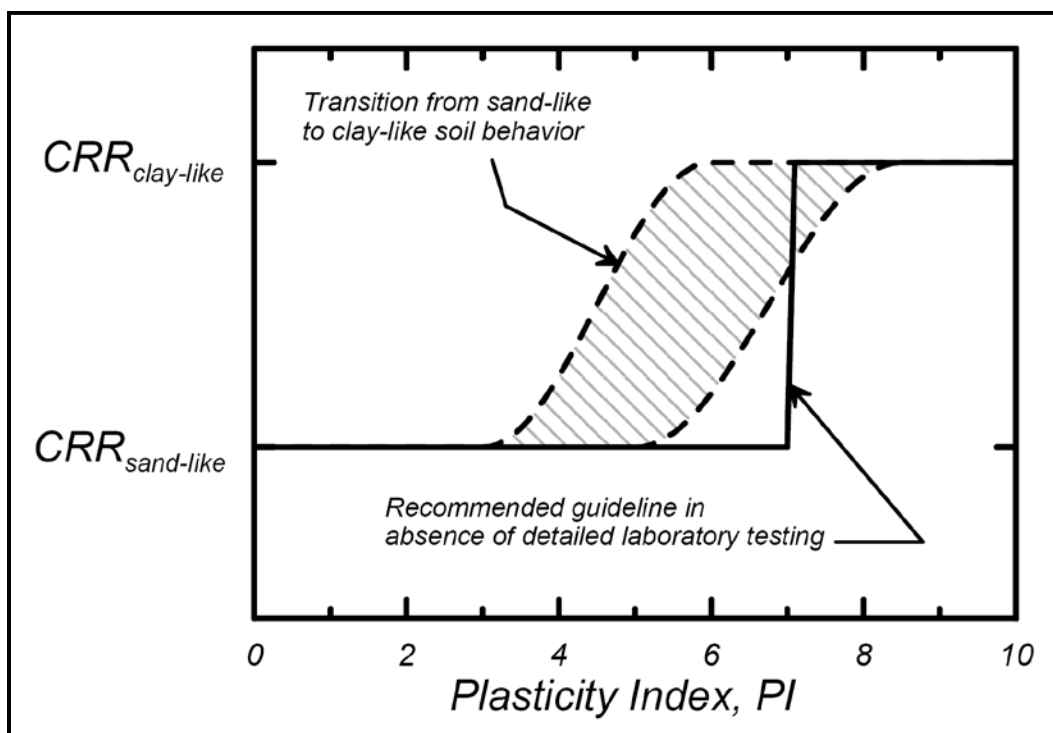


Figure 13-6, Liquefaction Susceptibility Based on Soil Plasticity (Seed, et al. (2003))

The liquefaction guidelines described by Seed, et al. (2003) are best considered as envelopes of fine-grained soils that have been observed to experience significant strains or strength loss during seismic events (Boulanger and Idriss (2004, 2006, and 2007)). Boulanger and Idriss (2004, 2006, and 2007) recommend that the fine-grained cyclic soil behavior would be best described as either Sand-Like or Clay-Like based on the Plasticity Index (PI). Boulanger and Idriss (2004, 2006, and 2007) suggested that there is a narrow soil SSL behavior transition zone between Sand-Like and Clay-Like that ranges from about a PI of 3 to 8 as indicated in Figure 13-7.



**Figure 13-7, Transition from Sand-Like to Clay-Like behavior (Boulanger and Idriss (2004, 2006, and 2007); Idriss and Boulanger (2008)) (With Permission from ASCE)**

The soil SSL behavior screening adopted by SCDOT in the following Sections is consistent with not only Idriss and Boulanger (2008) but also the soil behavior discussed in Chapter 7 and has been expanded to distinguish between NS and HS Clay-like soils as indicated below (see Figure J-2, Appendix J). The soil SSL susceptibility criteria shall be based on the following 3 categories:

- 1 Sand-Like soils
- 2 NS Clay-Like soils
- 3 HS Clay-Like soils

Laboratory cyclic load testing of Sand-Like or Clay-Like soils is typically not required for typical bridges or typical transportation structures but may be required by the PC/GDS on a project specific basis depending on the risk associated with the geotechnical seismic hazards under evaluation or may be requested by the GEOR with concurrence from the PC/GDS.

### 13.6.1 Sand-Like Soil

SSL in Sand-Like soils is caused by cyclic liquefaction as described in Section 13.5.1. Sand-Like soils will be screened to a minimum depth of 80 feet below the existing ground surface or 20 feet beyond the lowest deep foundation element; whichever extent of screening is deeper.

The following steps shall be used to determine if a soil is Sand-Like and whether a full soil SSL analysis is required:

1. Sand-Like soils susceptible to cyclic liquefaction must be below the water table. The water table selection for this evaluation must take into account the seasonal fluctuation of the ground water and the historic and/or possible

future rise of the ground water level with respect to the soils being analyzed for liquefaction susceptibility. To determine the depth that soils are adequately saturated for liquefaction to occur, seasonally averaged groundwater elevations shall be used. The Natural Resources Conservation Service (NRCS) website (<http://websoilsurvey.nrcs.usda.gov/app/>) may be consulted for determining the seasonal fluctuation of groundwater. Groundwater fluctuations caused by tidal action or seasonal variations will cause a portion of the soil to be saturated only during a limited period of time, significantly reducing the risk that liquefaction could occur within the zone.

2. Sand-Like soils have less than or equal to 20 percent passing the No. 200 sieve (i.e.,  $\%200 \leq 20\%$ ) regardless of the plasticity or an  $I_c$  of less than or equal to 2.05 ( $I_c \leq 2.05$ ). If these soils are below the water table (see Step 1 for determining the depth to the water table) go to Step 4. If these Sand-Like soils are above the water table (see Step 1), then soil SSL cannot occur. For soils with fines contents greater than 20 percent (i.e.,  $\%200 > 20\%$ ), go to Step 3 and check PI.
3. For soils with fines contents greater than 20 percent (i.e.,  $\%200 > 20\%$ ), check the PI to determine if these soils are Sand-Like. Soils with PI less than or equal to 10 ( $PI \leq 10$ ) will be treated as Sand-Like (see Figure 13-8). Proceed to Step 4 to complete the screening process.
4. Soils characterized as Sand-Like that have normalized corrected SPT blow counts,  $N_{1,60,CS}^*$  less than 30 blows/foot ( $N_{1,60,CS}^* < 30$  bpf) or normalized corrected CPTu tip resistances,  $q_{C,1,N,CS}$  less than 170 unitless ( $q_{C,1,N,CS} < 170$ ) are susceptible to cyclic liquefaction; therefore a full soil SSL analysis shall be conducted.

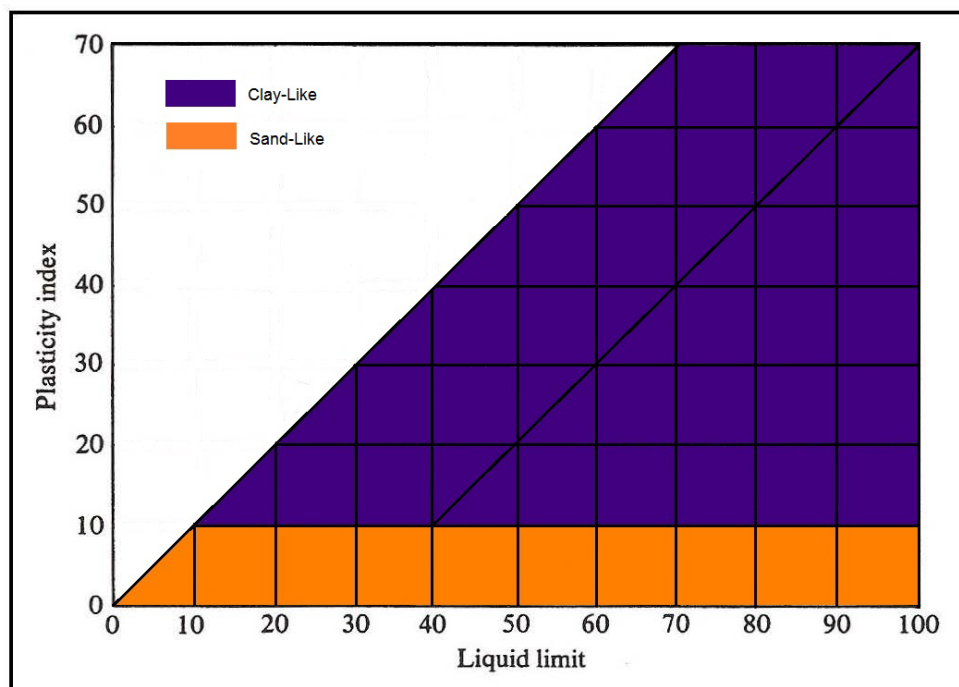


**Figure 13-8, Plasticity Chart – Sand-Like/Clay-Like Soils**

### 13.6.2 Normally Sensitive (NS) Clay-Like Soil

SSL in NS Clay-Like soils is caused by cyclic softening as described in Section 13.5.2. Clay-Like soils will be screened to a minimum depth of 80 feet below the existing ground surface or 20 feet beyond the lowest deep foundation element; whichever extent of screening is deeper.

The following steps shall be used to determine if a soil is NS Clay-Like and whether the soil is susceptible to cyclic softening:

1. Soils with fines contents greater than 20 percent (i.e., %200 > 20%), check PI to determine if these soils are Clay-Like. Soils with PI more than 10 ( $PI > 10$  (see Figure 13-8)) or an  $I_c$  of greater than or equal to 2.6 ( $I_c \geq 2.6$ ) will be treated as Clay-Like.
2. Soils with  $I_c$  greater than 2.05, but less than 2.6 ( $2.05 < I_c < 2.6$ ) may require pore pressure dissipation testing during CPTu testing to determine whether the soil will behave Sand-Like or Clay-Like. The GEOR shall document how the soil behavior determination was made.
3. Soils with a sensitivity less than 5,  $S_t < 5$  (Chapter 7), are NS Clay-Like.
4. Soils that meet these criteria shall have a full soil SSL analysis conducted.

### 13.6.3 Highly Sensitive (HS) Clay-Like Soil

SSL in HS Clay-Like soils is caused by cyclic softening as described in Section 13.5.2. Clay-Like soils will be screened to a minimum depth of 80 feet below the existing ground surface or 20 feet beyond the lowest deep foundation element; whichever extent of screening is deeper.

The following steps shall be used to determine if a soil is HS Clay-Like and whether the soil is susceptible to cyclic softening:

1. Soils with fines contents greater than 20 percent (i.e., %200 > 20%), check PI to determine if these soils are Clay-Like. Soils with PI more than 10 ( $PI > 10$  (see Figure 13-8)) or an  $I_c$  of greater than or equal to 2.6 ( $I_c \geq 2.6$ ) will be treated as Clay-Like.
2. Soils with  $I_c$  greater than 2.05, but less than 2.6 ( $2.05 < I_c < 2.6$ ) may require pore pressure dissipation testing during CPTu testing to determine whether the soil will behave Sand-Like or Clay-Like. The GEOR shall document how the soil behavior determination was made.
3. Soils with a sensitivity equal to or greater than 5,  $S_t \geq 5$  (Chapter 7), are HS Clay-Like.
4. Soils that meet these criteria shall have a full soil SSL analysis conducted.

## 13.7 SOIL SHEAR STRENGTH LOSS TRIGGERING

The soil SSL triggering analyses will include an evaluation of Sand-Like and Clay-Like soils that were identified to be susceptible to cyclic liquefaction or cyclic softening during the screening

process described in Section 13.6. The ground conditions and any surcharges or surface loads that will induce static shear stresses in the underlying soils must be accounted for when evaluating soil SSL triggering for both Sand-Like and Clay-Like soils.

The *Simplified Procedure* for determining liquefaction triggering of Sand-Like soils shall be based on SPT in-situ testing or on CPT in-situ testing using the methods described in the Earthquake Engineering Research Institute (EERI) Monograph MNO-12, Soil Liquefaction During Earthquakes (Idriss and Boulanger (2008)).

The *Simplified Procedure* for determination of cyclic liquefaction triggering is an empirical method based on field investigations of sites with Sand-Like soils. The *Simplified Procedure* for Sand-Like soils cannot differentiate between the types of liquefaction (flow liquefaction or cyclic softening). The *Simplified Procedure* for determining the onset/trigging of cyclic softening of Clay-Like soils during seismic events is based on laboratory investigations. The PC/GDS may require on a project specific basis, more rigorous analytical methods such as non-linear effective stress site response methods and advanced laboratory testing, which are not included in this Manual.

The *Simplified Procedure* compares the ratio of the seismic-induced stresses plus the static shear stresses ( $D$ ) to the soils resistance to soil SSL ( $C$ ), thus defining the strength loss ratio  $(D/C)_{SL}$ . The Demand,  $D$ , is expressed in terms of the equivalent uniform cyclic stress ratio that has been magnitude-weighted ( $CSR_{eq}^* = CSR_{eq,M=7.5}$ ), while the Capacity,  $C$ , is the soil's resistance to soil SSL expressed in terms of corrected cyclic resistance ratio that also has been magnitude-weighted and normalized to an effective overburden stress of 1 tsf ( $CRR_{eq}^* = CRR_{M=7.5,1\text{ tsf}}$ ). The LRFD equation that is to be used to evaluate the onset of strength loss (SL) is provided below:

$$\left(\frac{D}{C}\right)_{SL} = \frac{CSR_{eq}^*}{CRR_{eq}^*} \leq \phi_{SL} \quad \text{Equation 13-2}$$

The onset of cyclic liquefaction (Sand-Like soils) or cyclic softening (Clay-Like soils) occurs when the SL ratio  $(D/C)_{SL}$  is greater than the SL resistance factor ( $\phi_{SL}$ ) provided in Chapter 9.

Alternate methods of evaluating liquefaction triggering of Sand-Like soils such as those described in the 1996 NCEER and 1998 NCEER/NSF workshop (Youd, et al. (2001)) may be required on a project specific basis.

Since the *Simplified Procedure* is a deterministic procedure, a load factor,  $\gamma$ , of unity (1.0) is used and the resistance factor,  $\phi$ , accounts for the site variability and the level of acceptable risk to triggering soil SSL. As research advances and soil SSL analytical models are calibrated for LRFD design methodology, adjustments will be made in the implementation of the LRFD design methodology.

The overall process for conducting a soil SSL triggering analysis using the *Simplified Procedure* for level project site conditions is presented in a flow chart in Figure J-2 in Appendix J. The analytical procedures for computing cyclic stress ratio (CSR) and cyclic resistance ratio (CRR) of Sand-Like soils and Clay-like soils are provided in Section 13.8 and Section 13.9, respectively.

Soils that are susceptible to cyclic liquefaction or cyclic softening will require additional analyses to evaluate the effects of the soil shear strength degradation as discussed in Section 13.10. Project sites that have subsurface soils with the potential for soil SSL will require the evaluation



for soil SSL-induced geotechnical seismic hazards such as flow slide failure, global instability, and soil settlements. The analytical procedures to determine the magnitude and extent of these SSL-induced hazards are provided in Sections 13.11 – 13.15 of this Chapter.

The effects of initial static shear stress must be included in the evaluation of soil SSL triggering by the methods indicated below:

1. **Static Shear Stress Ratio Correction Factor,  $K_{\alpha}$ , Method:** The static shear stress ratio (SSSR) correction factor ( $K_{\alpha}$ ) method (Section 13.9.6) is presented by Idriss and Boulanger (2008) to account for static shear stresses in the *Simplified Procedure* method of evaluating soil SSL triggering. The SSSR correction factor,  $K_{\alpha}$ , method is further explained in Section 13.9.6, and shall be used.
2. **Shear Strength Ratio Method:** The shear strength ratio (SSR) triggering method computes the ratio of shear stress demand on the soil layer susceptible to soil SSL with the soil's yield strength. This method, developed by Olson and Stark (2003), uses the yield shear strength ratio and soil SSL ratio to evaluate the triggering of soil SSL. The SSR method is further explained in Appendix I.

The  $K_{\alpha}$  method presented above should be used to evaluate soil SSL triggering evaluation when the initial static stress ratio ( $\alpha$ ) is less than or equal to 0.35 ( $\alpha \leq 0.35$ ). When the maximum initial static stress ratio ( $\alpha$ ) is greater than 0.35 ( $\alpha > 0.35$ ), or when complex geometries and loadings need to be evaluated, the shear strength ratio (SSR) method presented in Appendix I shall be used. Soils that are susceptible to cyclic liquefaction or cyclic softening will require additional analyses to evaluate the soil shear strength degradation (Section 13.10).

### 13.8 CYCLIC STRESS RATIO (CSR)

The seismic-induced cyclic stresses in the soil are quantified by CSR. The equivalent uniform cyclic stress ratio,  $CSR_{eq}^*$ , is the equivalent uniform seismic-induced stress that has been magnitude-weighted ( $M_w = 7.5$ ) as shown in the following equation:

$$CSR_{eq}^* = CSR_{eq,7.5} = \frac{CSR_{eq}}{MSF} \quad \text{Equation 13-3}$$

Where,

$CSR_{eq}$  = Equivalent seismic-induced stress (Section 13.8.1)

MSF = Magnitude Scaling Factor (Section 13.8.2)

### 13.8.1 Equivalent Seismic-Induced Stress ( $CSR_{eq}$ )

The equivalent seismic-induced stress,  $CSR_{eq}$ , sometimes referred to as the average seismic-induced stress, is defined as shown in the following equation:

$$CSR_{eq} = 0.65 * CSR_{Peak} \quad \text{Equation 13-4}$$

Where,

$CSR_{Peak}$  = Maximum seismic-induced CSR (Section 13.8.1.1)

Note that a factor of 0.65 is included in Equation 13-4 to obtain an “average” or equivalent  $CSR_{eq}$  value. The method of computing the maximum seismic-induced stress ratio,  $CSR_{Peak}$ , depends on the method of performing the site response analysis discussed in Chapter 12.

#### 13.8.1.1 Simplified Procedure Determination of $CSR_{Peak}$

The *Simplified Procedure* for determination of the  $CSR_{Peak}$  should typically be used for evaluation of soil SSL. The *Simplified Procedure* for computing  $CSR_{Peak}$  is shown in the following equation:

$$CSR_{Peak} = \frac{\tau_{max}}{\sigma'_{vo}} = \left( \frac{a_{max}}{g} \right) * \left( \frac{\sigma_v}{\sigma'_{vo}} \right) * r_d \quad \text{Equation 13-5}$$

Where,

$a_{max}$  = PGA, gravity (g). The PGA is determined from the 3-Point ADRS curve developed according to Chapter 12.

$\sigma_v$  = Total overburden stress

$\sigma'_{vo}$  = Effective overburden stress

$r_d$  = Shear stress reduction coefficient (dimensionless)

$\tau_{max}$  = Maximum seismic induced stress with depth. In the *Simplified Procedure* the maximum seismic induced stress ( $\tau_{max}$ ) is approximated by the following equation.

$$\tau_{max} = \left( \frac{a_{max}}{g} \right) * \sigma_v * r_d \quad \text{Equation 13-6}$$

The shear stress reduction coefficient,  $r_d$ , is a parameter that describes the ratio of cyclic stresses for a flexible column to the cyclic stresses of a rigid column ( $r_d = \tau_{flexible}/\tau_{rigid}$ ). For an  $r_d = 1$ , the flexibility of the soil column would correspond to rigid body behavior. One-dimensional dynamic site response studies (Seed and Idriss (1971), Golesorkhi (1989), Idriss (1999), and Cetin, et al. (2004)) have shown that the shear stress reduction factor is dependent on the ground motion characteristics (i.e., intensity and frequency content), shear wave velocity profile of the site (i.e., site stiffness), and nonlinear dynamic soil properties. Idriss (1999) performed several hundred parametric site response analyses and developed a shear stress reduction coefficient,  $r_d$  that was expressed as a function of depth and seismic moment magnitude ( $M_w$ ) as indicated in Figure 13-9.

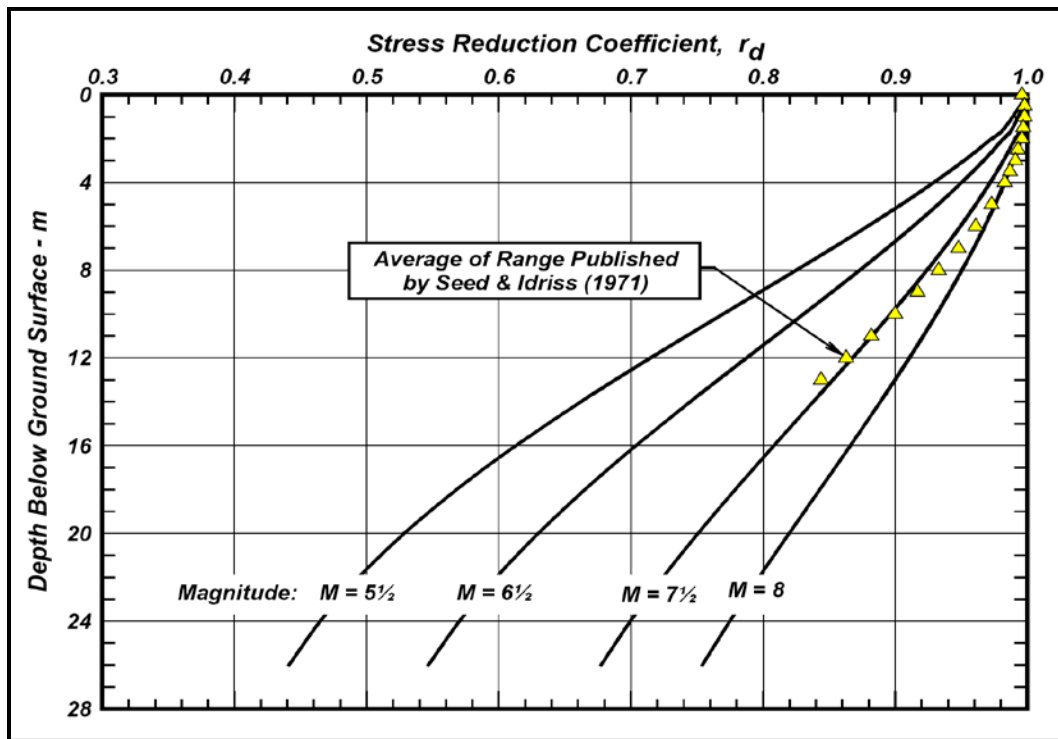


Figure 13-9, Variations of Shear Stress Reduction Coefficient,  $r_d$  (Idriss (1999))

Shear stress reduction coefficient ( $r_d$ ) equations for US customary units were modified from SI equations proposed by Idriss (1999) as indicated below.

$$r_d = \exp[\alpha + (\beta + M_w)] \quad \text{Equation 13-7}$$

$$\alpha = -1.012 - 1.126 \sin \left[ \left( \frac{\left( \frac{z}{3.28} \right)}{11.73} \right) + 5.133 \right] \quad \text{Equation 13-8}$$

$$\beta = 0.106 + 0.118 \sin \left[ \left( \frac{\left( \frac{z}{3.28} \right)}{11.28} \right) + 5.142 \right] \quad \text{Equation 13-9}$$

Where,

$z$  = Depth below ground surface, feet

$M_w$  = Seismic moment magnitude

Note that the arguments inside the “sin” terms above are in radians. For the purposes of evaluating soil SSL, the  $CSR_{Peak}$  should not be evaluated using this method for depths greater than 80 feet (24 m). The uncertainty increases for shear stress reduction coefficients ( $r_d$ ) at depths greater than  $z > 65$  feet (20 m). When the maximum seismic-induced stress ratio,  $CSR_{Peak}$ , is required for depths greater than 80 feet, a site-specific response analysis (Section 13.8.1.2) may be warranted with approval of the PC/GDS.

### 13.8.1.2 Site Specific Response Determination of $CSR_{Peak}$

When approved by the PC/GDS, the maximum seismic-induced stress ratio,  $CSR_{Peak}$ , can be computed for depths greater than 80 feet (24 m) by using the results of a site-specific seismic response analysis (Chapter 12) as indicated by the following equation.

$$CSR_{Peak} = \frac{\tau_{max}}{\sigma'_{vo}} \quad \text{Equation 13-10}$$

Where,

$\tau_{max}$  = Maximum seismic-induced cyclic shear stress obtained from the site-specific response analysis of the ground motions

$\sigma'_{vo}$  = Effective overburden stress at the depth being evaluated

Site-specific seismic response analyses referenced in Chapter 12 are typically 1-dimensional equivalent linear analyses. Because the 1-dimensional equivalent linear analyses have a reduced reliability as ground shaking levels (PGA) increase above 0.40g in softer soils or where the maximum shearing strain amplitudes exceed 1 to 2 percent, a comparison with the *Simplified Procedure* should be performed for depths greater than 80 feet (24 m) and the more conservative values should be used. In lieu of using the more conservative analytical results, the PC/GDS should be consulted to determine if a nonlinear effective stress site response method should be used to determine the maximum seismic-induced shear stress,  $\tau_{max}$ .

### 13.8.2 Magnitude Scaling Factor

The Magnitude Scaling Factor (MSF) is used to scale the equivalent uniform seismic-induced stresses,  $CSR_{eq}$ , to the number of uniform cycles that is typical of an average seismic event of magnitude  $M_w = 7.5$ . A large amount of scatter in the MSF is observed from various studies presented in Youd, et al. (2001), particularly at the lower range of seismic moment magnitudes ( $5.5 < M_w < 6.5$ ). Boulanger and Idriss (2007) have recommended MSF for Sand-Like soils ( $MSF_{Sand}$ ) and for Clay-Like soils ( $MSF_{Clay}$ ) as indicated in Figure 13-10. Because the predominant seismic event in South Carolina had an approximate seismic magnitude of 7.3 and the target scaling seismic is a 7.5, the variability observed in the magnitude scaling factor studies should have minimal impact on the liquefaction analyses.

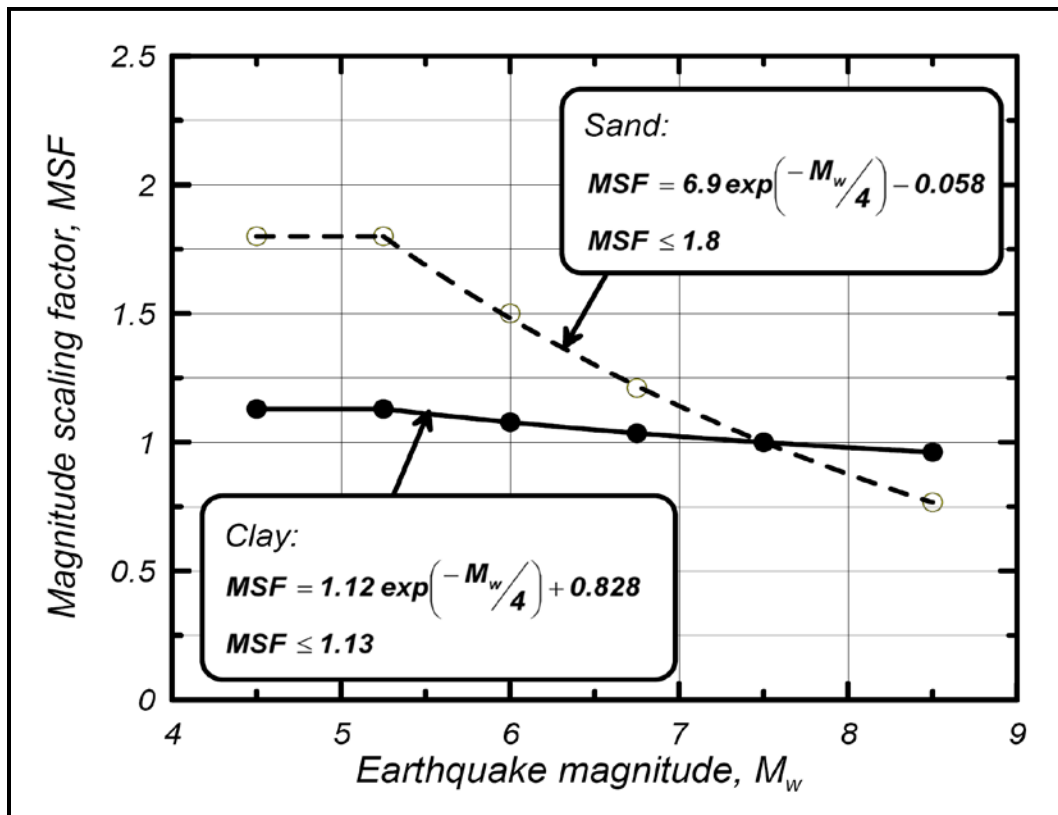


Figure 13-10, Magnitude Scaling Factor (MSF)  
(Boulanger and Idriss (2007) with permission from ASCE)

In lieu of using Figure 13-10, the following equations may be used to compute the  $MSF_{Sand}$  and  $MSF_{Clay}$ .

$$MSF_{Sand} = 6.9 * \exp(-0.25 * M_w) - 0.058 \leq 1.80 \quad \text{Equation 13-11}$$

$$MSF_{Clay} = 1.12 * \exp(-0.25 * M_w) + 0.828 \leq 1.13 \quad \text{Equation 13-12}$$

Where,

$M_w$  = Moment magnitude of the design seismic event being evaluated for soil SSL triggering.

### 13.9 CYCLIC RESISTANCE RATIO (CRR)

The soil's resistance to SSL is quantified by the CRR. The CRR for Sand-Like soils is typically characterized as a curvilinear boundary that indicates the relationship between CSR and in-situ testing results from SPT or CPTu. The CRR for Clay-Like soils is typically characterized as a linear reduction of the undrained shear strength that indicates the relationship between CSR and in-situ testing results from SPT or CPTu. A typical CRR curve for Sand-Like soils is shown in Figure 13-11(A) and for Clay-Like soils is shown in Figure 13-11(B).

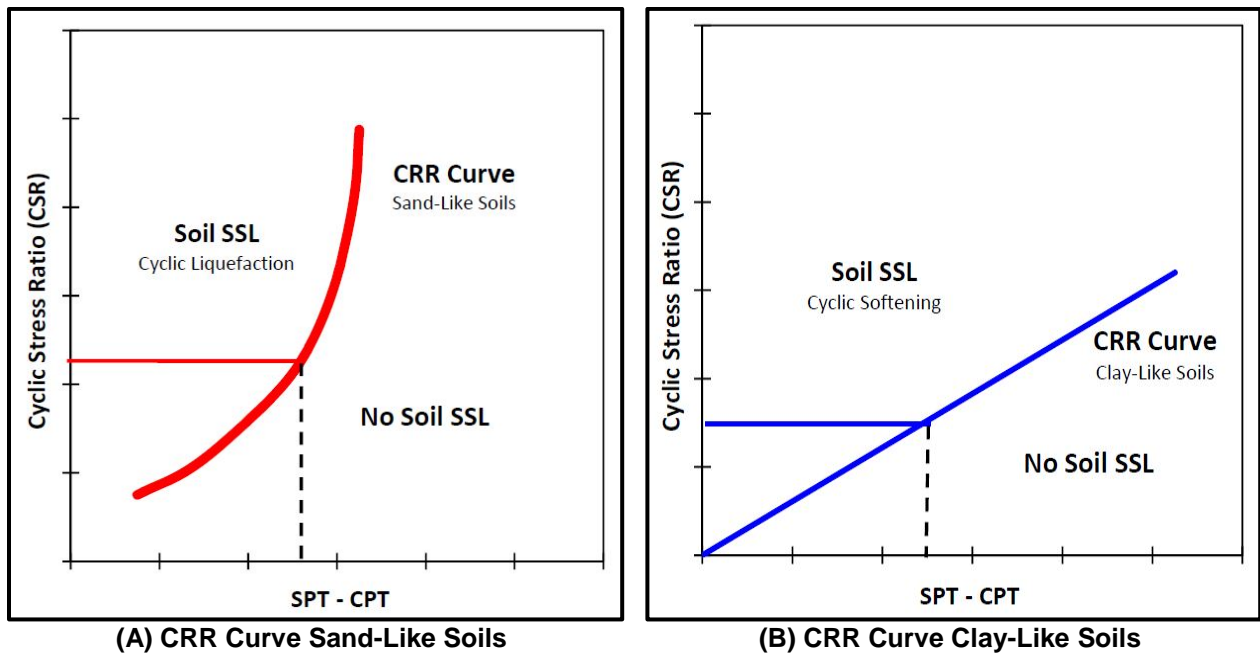


Figure 13-11, Typical CRR Curve

For a specific seismic-induced CSR value, the value located on the CRR boundary establishes a threshold in-situ testing value whereas in-situ testing results greater than the threshold value will not be susceptible to soil SSL and values less than the threshold value are subject to soil SSL.

Several empirical procedures have been developed to determine the CRR of Holocene (< 10,000 years) Sand-Like soils based on in-situ testing. In-situ tests acceptable to be used on SCDOT projects are SPT and CPTu. A comparison of advantages and disadvantages of these in-situ tests for determination of CRR are presented in Table 13-2. SPT and CPTu measured results must be adjusted in accordance with subsequent Sections of this Chapter.

Table 13-2, CRR Determination Based on Types of In-situ Testing (Modified after Youd and Idriss (1997))

Feature	Type of In-situ Testing	
	SPT	CPT
Number of test measurements at liquefaction sites	Substantial	Several
Type of stress-strain behavior influencing test	Partially Drained, Large strain	Drained, Large Strain
Quality control and repeatability	Poor to Good	Very Good
Detection of variability of soil deposits	Good	Very Good
Soil types in which test is recommended	Non-Gravel	Non-Gravel
Test provides sample of soil	Yes	No
Test measures index or engineering property	Index	Index

The normalized CRR curves ( $CRR^* = CRR_{M=7.5, 1 \text{ tsf}}$ ) for Sand-Like soils presented in Sections 13.9.1 and 13.9.2 are magnitude weighted ( $M_w=7.5$ ) and normalized to a reference effective overburden stress of  $\sigma'_v = 1 \text{ tsf}$ . These correlations were derived based on the relative state parameter index ( $\xi_R$ ) by Idriss and Boulanger (2006). The  $\xi_R$  is the difference between the  $D_R$  and the  $D_{R,CS}$  (the critical state  $D_R$ ) at the same mean effective normal stress. The corresponding  $CRR-\xi_R$  relationships derived from these 2 liquefaction correlations are shown in Figure 13-12 to illustrate the consistency between the SPT and CPTu methods to predict field

cyclic resistance ratio. It is noted that the agreement in Figure 13-12 is for soils meeting the condition depicted in the Figure and that direct relationship between the correlated SPT and correlated CPT  $\xi_R$  should not be anticipated for other soil conditions.

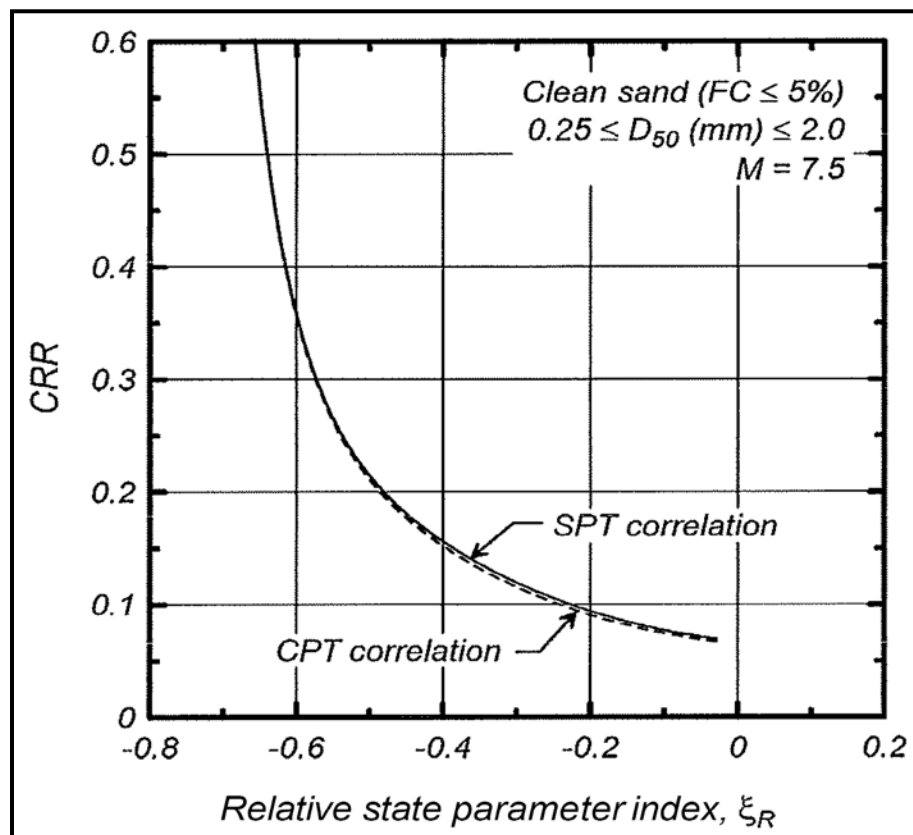


Figure 13-12, Field CRR- $\xi_R$  Correlations Based on SPT and CPTu (Idriss and Boulanger (2006))

The normalized  $CRR^* = CRR_{M=7.5, 1 \text{ tsf}}$  for Clay-Like soil presented in Section 13.9.3 is magnitude weighted ( $M_w = 7.5$ ).

Shear wave velocities ( $V_s$ ) and the Becker Penetration Tests (BPT) methods for determination of the soil's resistance for liquefaction shall not be used for routine SCDOT soil SSL evaluations unless approved in writing by the PC/GDS.

The  $CRR^*$  correlations must be further corrected to account for the effects of high overburden stress on Sand-Like soils ( $K_\sigma$ ), effects of soil aging in Sand-Like soils ( $K_{DR}$ ), and effects of initial static shear stress on Sand-Like Soils and Clay-Like Soils ( $K_\alpha$ ). The  $CRR_{eq}^*$  curves are computed as indicated in the following general equation:

$$CRR_{eq}^* = CRR^* * (K_\sigma) * (K_{DR}) * (K_\alpha) \quad \text{Equation 13-13}$$

Where,

$CRR^* = CRR_{M=7.5, 1 \text{ tsf}}$  = Magnitude weighted ( $M_w = 7.5$ ) and normalized ( $\sigma'_v = 1 \text{ tsf}$ ) cyclic resistance ratio. (Sand-Like Soil: Sections 13.9.1 and 13.9.2; Clay-Like Soil: Section 13.9.3)

$K_\sigma$  = High overburden stress correction factor for Sand-Like Soils (Section 13.9.4)

$K_{DR}$  = Age and cementation correction factor for Sand-Like Soils (Section 13.9.5)

$K_{\alpha}$  = Static shear stress ratio correction factor for Sand-Like and Clay-Like soils (Section 13.9.6)

### 13.9.1 Sand-Like Soil - SPT Based CRR\* Curves

The CRR correlations for SPT in-situ testing presented by Idriss and Boulanger (2008) shall be used to evaluate Sand-Like soils. Deterministic CRR\* curves are  $M_w$  weighted, adjusted to a reference effective overburden stress of  $\sigma'_v = 1$  tsf, and adjusted for fines content. Similar to the CSR, a reference seismic event of  $M_w$  equal to 7.5 is used. The corrected SPT blow count ( $N_{1,60}^*$ ) is adjusted to an equivalent clean sand (CS) blow count based on the FC as indicated by the following equation.

$$N_{1,60,CS}^* = N_{1,60}^* + \Delta N_{1,60}^* \quad \text{Equation 13-14}$$

Where,

$N_{1,60}^*$  = SPT blow count normalized to a reference effective overburden stress of  $\sigma'_v = 1$  tsf, corrected for energy (60%) (see Chapter 7). Units of blows/foot

$\Delta N_{1,60}^*$  = Fines content correction for  $5\% < FC < 35\%$ . The variation in  $\Delta N_{1,60}^*$  with fines content is shown in Figure 13-13

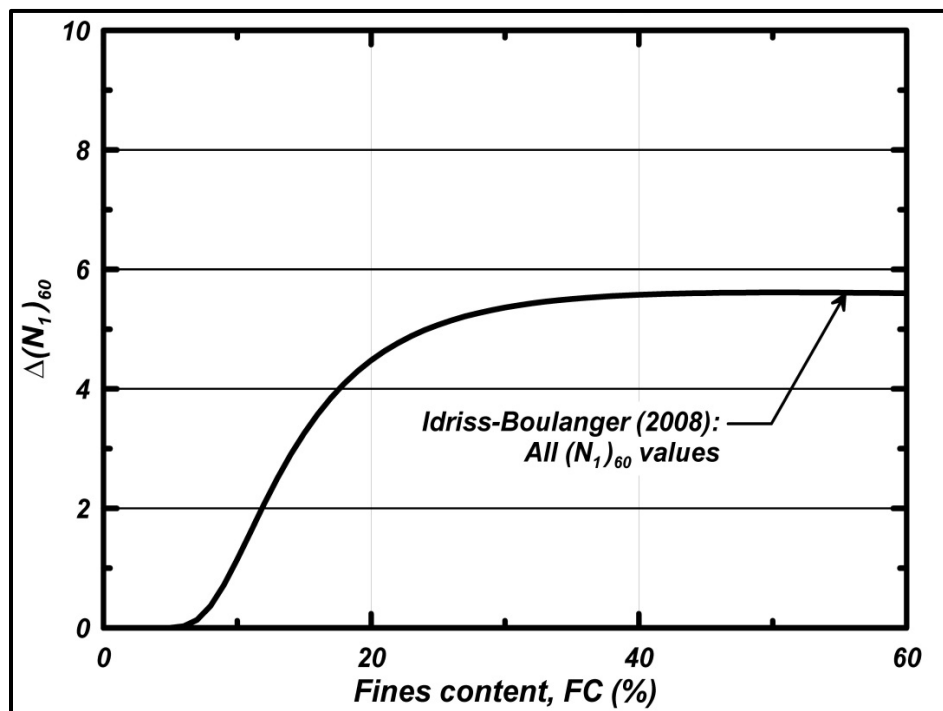


Figure 13-13, Variation in  $\Delta N_{1,60}^*$  With Fines Content (Idriss and Boulanger (2014))

In lieu of using Figure 13-13 the following equation may be used.

$$\Delta N_{1,60}^* = \exp \left[ 1.63 + \left( \frac{9.7}{FC+0.01} \right) - \left( \frac{15.7}{FC+0.01} \right)^2 \right] \leq 5.5 \quad \text{Equation 13-15}$$

Where,

FC = Fines content of the soil fraction passing the No. 200 sieve, percent



The Idriss and Boulanger (2006) recommended deterministic  $CRR^*$  curve (Curve 5 in Figure 13-14) for SPT in-situ testing based on a seismic moment magnitude,  $M_w = 7.5$ , effective overburden reference stress,  $\sigma'_v = 1.0$  tsf, and fines content  $FC < 5\%$ .

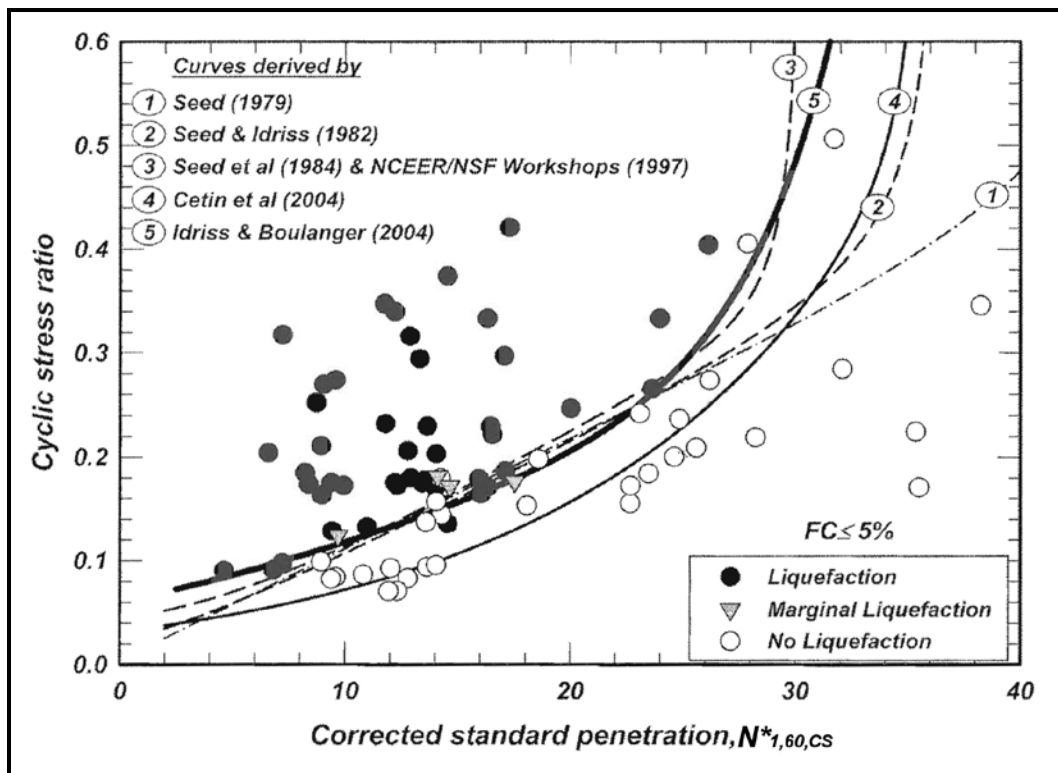


Figure 13-14, SPT Liquefaction Triggering Correlation ( $CRR^*$ )  
 $M_w = 7.5$ ;  $\sigma'_{vo} = 1.0$  tsf;  $FC \leq 5\%$   
 (Idriss and Boulanger (2006))

In lieu of using Curve 5 in Figure 13-14, the following equation may be used.

$$CRR^* = \exp \left[ \left( \frac{N^*_{1,60,CS}}{14.1} \right) + \left( \frac{N^*_{1,60,CS}}{126} \right)^2 - \left( \frac{N^*_{1,60,CS}}{23.6} \right)^3 + \left( \frac{N^*_{1,60,CS}}{25.4} \right)^4 - 2.8 \right] \text{ Equation 13-16}$$

Where,

$CRR^*$  = CRR for a  $M_w$  of 7.5 and normalized to 1 tsf overburden pressure

$N^*_{1,60,CS}$  = Normalized corrected SPT blow count (see Chapter 7) including FC correction (see Equation 13-14), blows/foot

### 13.9.2 Sand-Like Soil - CPTu Based $CRR^*$ Curves

The  $CRR$  correlations for CPTu in-situ testing presented by Idriss and Boulanger (2008) shall be used to evaluate Sand-Like soils. Deterministic  $CRR^*$  curves are  $M_w$  weighted, adjusted to a reference effective overburden stress of  $\sigma'_v = 1$  tsf, and adjusted for fines content. Similarly to the CSR, a reference seismic event of  $M_w$  equal to 7.5 is used. The normalized corrected CPTu tip resistance ( $q_{t,1,N}$ ) is adjusted to an equivalent CS tip resistance based on the FC as indicated by the following equation.

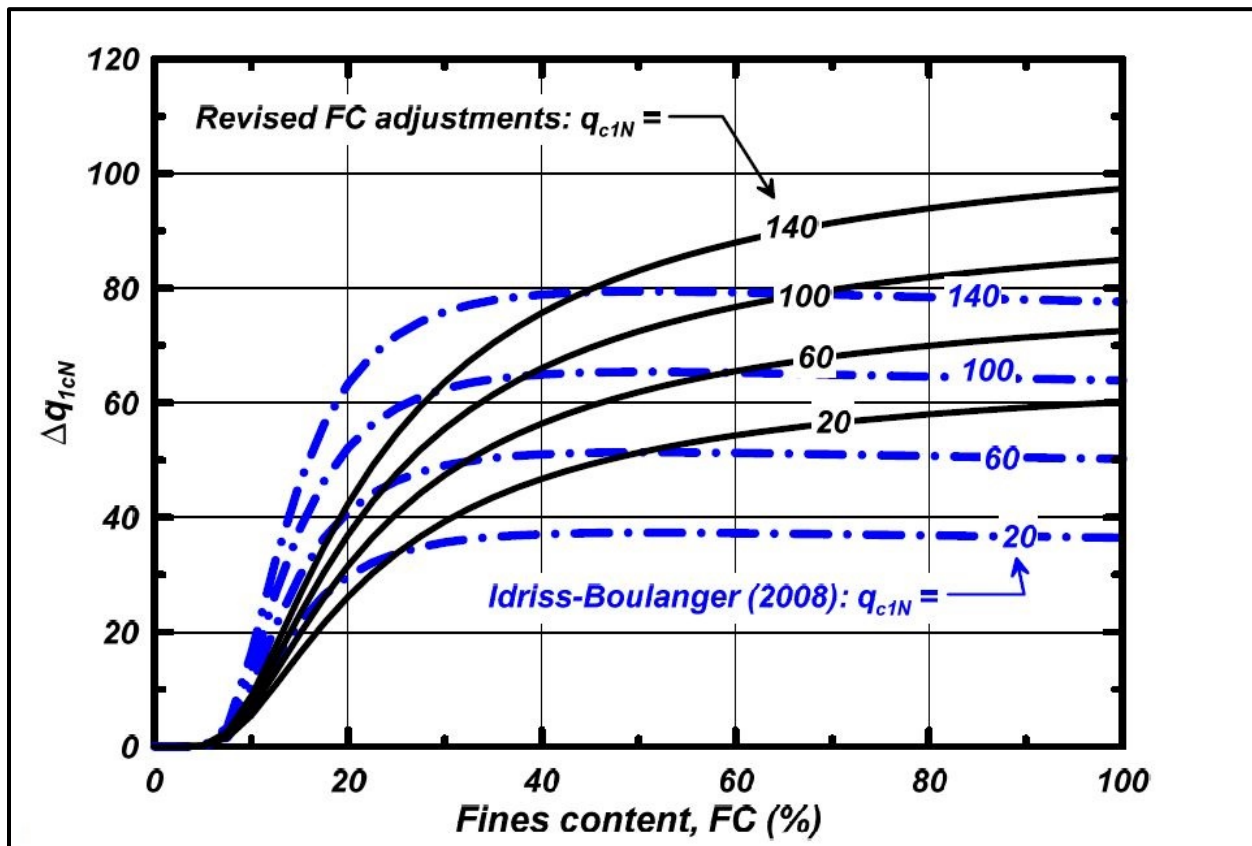
$$q_{t,1,N,CS} = q_{t,1,N} + \Delta q_{t,1,N} \quad \text{Equation 13-17}$$

Where,

$q_{t,1,N}$  = Normalized corrected CPT tip resistance (see Chapter 7) (unitless)

$\Delta q_{t,1,N}$  = Fines content correction for FC > 5%

The variation in  $\Delta q_{t,1,N}$  with fines content (FC) based on Boulanger and Idriss (2014) can be obtained from Figure 13-15 for FC > 5%.



Note:  $\Delta q_{c,1,N} = \Delta q_{t,1,N}$  in this Figure

**Figure 13-15, Variation in  $\Delta q_{c,1,N}$  With Fines Content (Boulanger and Idriss (2014))**

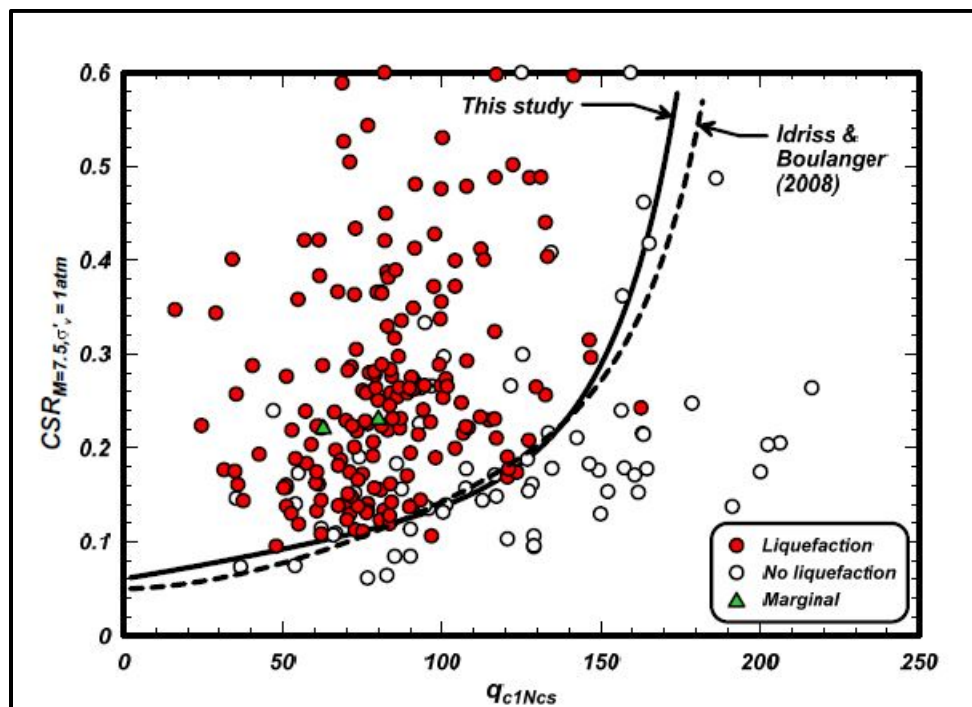
In lieu of using Figure 13-15 the following equation may be used.

$$\Delta q_{t,1,N} = \left[ 11.9 + \left( \frac{q_{t,1,N}}{14.6} \right) \right] * \exp \left[ 1.63 + \left( \frac{9.7}{FC+2} \right) - \left( \frac{15.7}{FC+2} \right)^2 \right] \quad \text{Equation 13-18}$$

Where,

FC = Fines content of the soil fraction passing the No. 200 sieve, percent

Figure 13-16 shows the Boulanger and Idriss (2014) recommended deterministic CRR<sup>\*</sup> curve for CPTu in-situ testing based on a seismic moment magnitude,  $M_w = 7.5$ , effective overburden reference stress,  $\sigma'_{v0} = 1.0$  tsf, and fines content FC < 5%.



Note:  $q_{c,1,N,CS} = q_{t,1,N,CS}$  in this Figure

**Figure 13-16, CPTu Liquefaction Triggering Correlation ( $CRR^*$ )**  
 $M_w = 7.5$ ;  $\sigma'_{vo} = 1.0$  tsf;  $FC \leq 5\%$   
**(Boulanger and Idriss (2014))**

In lieu of using Figure 13-16 the following equation may be used.

$$CRR^* = \exp \left[ \left( \frac{q_{t,1,N,CS}}{14.1} \right) + \left( \frac{q_{t,1,N,CS}}{126} \right)^2 - \left( \frac{q_{t,1,N,CS}}{23.6} \right)^3 + \left( \frac{q_{t,1,N,CS}}{25.4} \right)^4 - 2.8 \right] \text{ Equation 13-19}$$

Where,

$CRR^*$  = CRR for a  $M_w$  of 7.5 and normalized to 1 tsf overburden pressure

$q_{t,1,N,CS}$  = Normalized corrected CPT tip resistance (see Chapter 7) including FC correction (see Equation 13-17). (unitless)

### 13.9.3 Clay-Like Soil $CRR^*$ Curves

The  $CRR$  correlations presented by Idriss and Boulanger (2008) shall be used to evaluate Clay-Like soils. Deterministic  $CRR^*$  curves are  $M_w$  weighted. Similar to the CSR, a reference seismic event  $M_w$  equal to 7.5 is used. The  $CRR$  of Clay-Like soils will typically be determined by using empirical correlations.  $CRR$  of Clay-Like soils can also be determined by cyclic laboratory testing with approval from the PC/GDS. Boulanger and Idriss (2007) developed empirical correlations based on the undrained shear strength profile and the consolidation stress history profile.

The preferred empirical correlation for determining the  $CRR^*$  curves for Clay-Like soils is based on the undrained shear strength profile using the relationship shown in Figure 13-17, where undrained shear strengths have been obtained from laboratory testing. If in-situ testing methods (SPT or CPTu) are used to estimate undrained shear strengths then  $CRR^*$  correlations using the consolidation stress history profile presented in Figure 13-17 should be used as a check on the in-situ testing shear strength correlations.

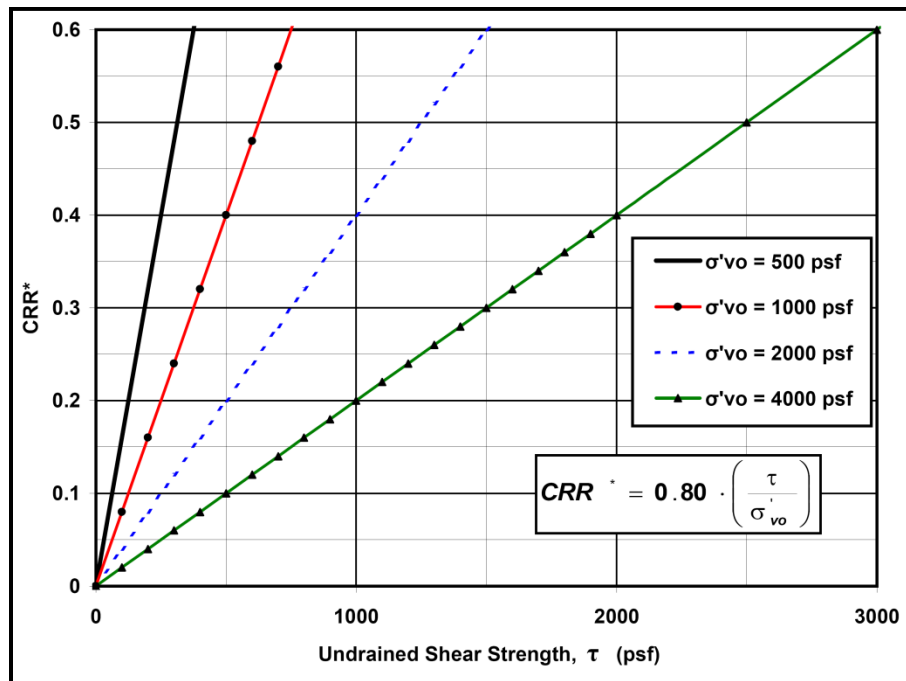


**Figure 13-17, CRR\* Clay-Like – Shear Strength Correlation  
(Modified from Boulanger and Idriss (2007) with permission from ASCE)**

In lieu of using Figure 13-17, the following equation may be used to determine the CRR\* curves for Clay-Like soils.

$$CRR^* = CRR_{Mw=7.5} = 0.80 * \left( \frac{\tau}{\sigma'_{vo}} \right) \quad \text{Equation 13-20}$$

Where,

$\tau$  = Undrained shear strength ( $S_u$ )

$\sigma'_{vo}$  = Effective overburden stress

Boulanger and Idriss (2007) have suggested using the empirical correlations developed from SHANSHEP laboratory testing (Ladd, et al. (1977)) shown in Figure 13-18. These correlations are based on a relationship between the undrained shear strength ratio and the consolidation stress history. The overconsolidation ratio (OCR) provides a measure of the consolidation stress history. These correlations require a consolidation stress history profile that is sometimes difficult to accurately evaluate without performing consolidation tests on undisturbed samples from representative depths. It has also been observed that the undrained shear strength ratio can vary based on the type of clay formation used as shown in Chapter 7 and in Figure 13-18. Estimating CRR solely from OCR should only be used for preliminary analyses or to compare with the CRR\* determined by the undrained shear strength ratio, particularly if in-situ testing is used to estimate the undrained shear strength of Clay-Like soils.

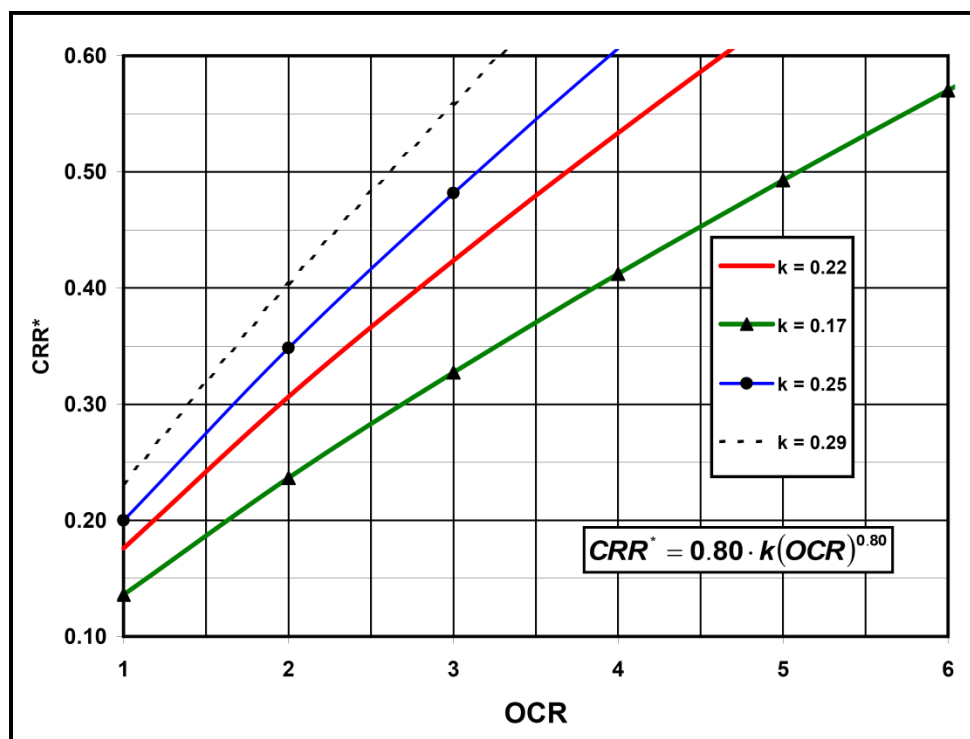


Figure 13-18,  $CRR^*$  Clay-Like Soils – OCR Correlation

In lieu of using Figure 13-18, the following equation may be used to compute the  $CRR^*$  curves for Clay-Like soils based on OCR.

$$CRR^* = 0.80 * k * (OCR)^n \quad \text{Equation 13-21}$$

Where,

$k$  = Shear strength ratio for normally consolidated soils ( $OCR = 1$ ) typically ranges between 0.17 and 0.29. Use  $k = 0.22$  (DSS testing) as recommended by Boulanger and Idriss (2007) unless laboratory testing and local correlations indicate otherwise.

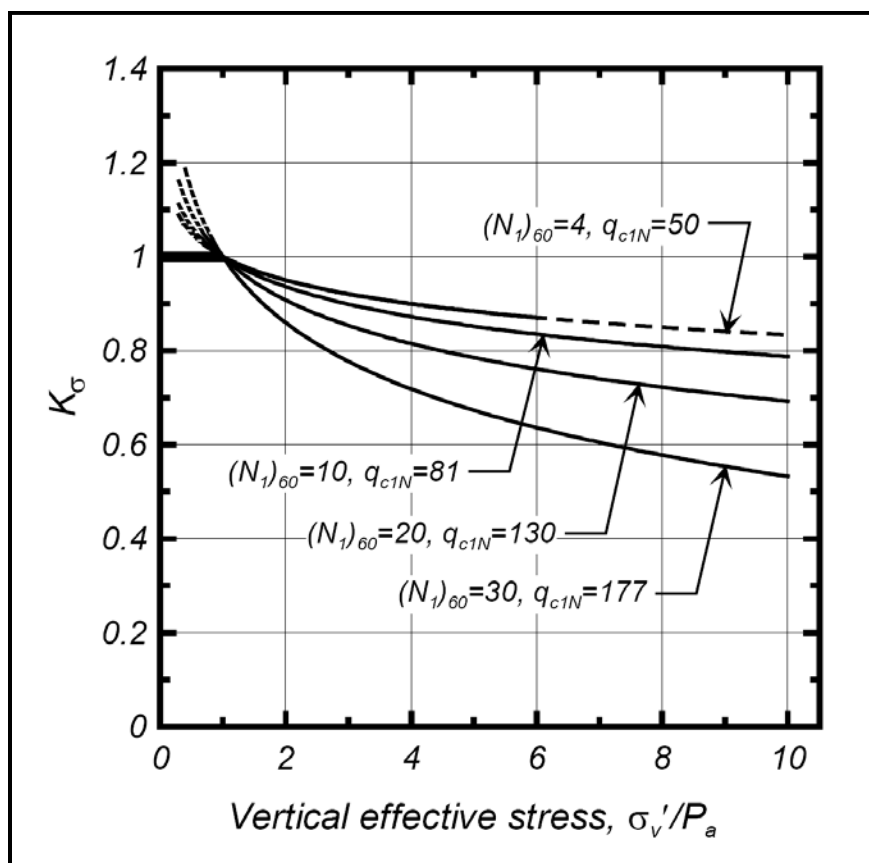
$OCR$  = Overconsolidation ratio ( $\sigma'_p / \sigma'_{v0}$ ) (See Chapter 7)

$n$  = Soil constant typically taken as 0.80 for unstructured and uncemented soils.

#### 13.9.4 High Overburden Correction ( $K_\sigma$ )

The high overburden correction,  $K_\sigma$ , accounts for the increased susceptibility of Sand-Like soils to cyclic liquefaction, at the same CSR, under large effective overburden stresses. For Clay-Like soils there is no increased susceptibility, therefore,  $K_\sigma = 1.0$  shall be used.

The high overburden correction factors for Sand-Like soils presented by Idriss and Boulanger (2008) shall be used. These high overburden correction factors are based on the relative state parameter index ( $\xi_R$ ), and were correlated with corrected SPT blow counts ( $N^*_{1,60}$  – Section 13.9.1) and normalized corrected CPTu tip resistance ( $q_{t,1,N}$  – Section 13.9.2). The high overburden corrections,  $K_\sigma$ , for effective overburden  $\sigma'_{v0} > 1$  tsf, are plotted for selected values of  $N^*_{1,60}$  and  $q_{t,1,N}$  in Figure 13-19.



Note:  $q_{c,1,N} = q_{t,1,N}$  in this Figure

**Figure 13-19, High Overburden Correction ( $K_\sigma$ ) ( $\sigma'_{vo} > 1$  tsf) (Boulanger (2003a) with permission from ASCE)**

In lieu of using Figure 13-19, the following equation may be used to compute the  $K_\sigma$  of Sand-Like soils. These correlations are based on  $Q \approx 10$ ,  $K_o \approx 0.45$ ,  $D_R \leq 0.9$ , and  $(\sigma'_{vo}/P_a) \leq 10$ .

$$K_\sigma = 1 - C_\sigma * \ln\left(\frac{\sigma'_{vo}}{P_a}\right) \leq 1.1 \quad \text{Equation 13-22}$$

Where,

$\sigma'_{vo}$  = Effective overburden stress (or  $\sigma'_v$ ), tsf.

$P_a$  = Atmospheric pressure, taken as 1 tsf

$C_\sigma$  = Coefficient used to correlate  $D_R$ ,  $N^*_{1,60}$ , and  $q_{c,1,N}$  to  $K_\sigma$

$D_R$  = Relative density, where  $D_R \leq 0.90$  (90%)

$N^*_{1,60}$  = Corrected SPT blow count, where  $N^*_{1,60} \leq 37$  blows/foot

$q_{c,1,N}$  = Corrected and normalized CPTu tip resistance, where  $q_{c,1,N} \leq 211$  unitless

The coefficient  $C_\sigma$  can be expressed in terms of relative density ( $D_R$ ), corrected SPT blow count ( $N^*_{1,60}$ ), and corrected and normalized CPTu tip resistance ( $q_{c,1,N}$ ) based on Boulanger and Idriss (2004) as indicated by the following equations.

$$C_\sigma = \frac{1}{18.9 - 17.3 * D_R} \leq 0.3 \quad \text{Equation 13-23}$$

$$C_{\sigma} = \frac{1}{18.9 - 2.55(N_{1,60}^*)^{0.5}} \leq 0.3 \quad \text{Equation 13-24}$$

$$C_{\sigma} = \frac{1}{37.3 - 8.27*(q_{t,1,N})^{0.264}} \leq 0.3 \quad \text{Equation 13-25}$$

### 13.9.5 Age Correction Factor ( $K_{DR}$ )

The susceptibility of Sand-Like soils to cyclic liquefaction has been found to be a function of geologic age and origin; therefore an age correction factor ( $K_{DR}$ ) shall be applied to Sand-Like soils. Currently there is no research indicating the influence of age on the susceptibility or non-susceptibility of Clay-Like soils to undergo soil SSL, therefore, a  $K_{DR} = 1.0$  shall be used. Soils that were formed during the Quaternary period (past 1.6 million years ago - MYA), including the Holocene and Pleistocene Epochs, shall be considered to have a moderate to very high potential for liquefaction. Pre-Pleistocene age (more than 1.6 MYA) deposits shall be considered to have a lower susceptibility to liquefaction. Youd and Perkins (1978) proposed a geologic susceptibility chart for cyclic liquefaction of sedimentary cohesionless soil deposits that was based on soil deposition and geologic age as indicated in Table 13-3. The soil resistance to cyclic liquefaction tends to increase with increase in age as observed in Table 13-3. Table 13-3 shall only be used as a guide and shall not be used to determine the susceptibility of a Sand-Like soil for liquefaction.

Soil formations that are Pre-Pleistocene (>1.6 MYA) potentially will have a lower susceptibility to experience cyclic liquefaction unless the soils are found in areas where there is evidence of the soils having experienced cyclic liquefaction. Soils found in Pre-Pleistocene areas that have been subjected to cyclic liquefaction will have the same susceptibility to cyclic liquefaction as soils formed during the Holocene period. Figure 13-4 provides the location of paleoliquefaction sites that have been studied and Figure 13-5 provides a map developed by the USGS that identifies areas in South Carolina that potentially have experienced Quaternary liquefaction.

Simplified liquefaction-triggering methods used to compute the CRR for Sand-Like soils such as those proposed by Youd and Idriss (1997) and Idriss and Boulanger (2008) were developed from case histories of relatively young Holocene (< 10,000 years ago) soils. A study by Leon, et al. (2006) has demonstrated that Pleistocene Sand-Like soils in the upper 20 feet of several locations within the South Carolina Coastal Plain may have increased resistance to liquefaction due to aging. The location of paleoliquefaction sites in the Coastal Plain that were used by Leon, et al. (2006) are shown in Figure 13-4.

**Table 13-3, Liquefaction Susceptibility of Sedimentary Deposits  
(Modified after Youd and Perkins (1978) with permission from ASCE)**

Type of Deposit <sup>(1)</sup>	General Distribution of Cohesionless Sediments in Deposits	Likelihood that Cohesionless Sediments, When Saturated, Will be Susceptible to Liquefaction (By Age of Deposit)			
		Modern < 500 yr	Holocene 500 yr to 10 ka	Pleistocene 10ka – 1.6 MYA	Pre-Pleistocene > 1.6 MYA
<b>(a) Continental Deposits</b>					
River Channel	Locally Variable	Very High	High	Low	Very Low
Floodplain	Locally Variable	High	Moderate	Low	Very Low
Alluvial Fan & Plain	Widespread	Moderate	Low	Low	Very Low
Marine Terraces & Plains	Widespread	---	Low	Very Low	Very Low
Delta and Fan-delta	Widespread	High	Moderate	Low	Very Low
Lacustrine and Playa	Variable	High	Moderate	Low	Very Low
Colluvium	Variable	High	Moderate	Low	Very Low
Talus	Widespread	Low	Low	Very Low	Very Low
Dunes	Widespread	High	Moderate	Low	Very Low
Loess	Variable	High	High	High	Unknown
Glacial Till	Variable	Low	Low	Very Low	Very Low
Tuff	Rare	Low	Low	Very Low	Very Low
Tephra	Widespread	High	High	Unknown	Unknown
Residual Soils	Rare	Low	Low	Very Low	Very Low
Sebka	Locally Variable	High	Moderate	Low	Very Low
<b>(b) Coastal Zone</b>					
Delta	Widespread	Very High	High	Low	Very Low
Estuarine	Locally Variable	High	Moderate	Low	Very Low
Beach - High Wave-energy	Widespread	Moderate	Low	Very Low	Very Low
Beach - Low Wave-energy	Widespread	High	Moderate	Low	Very Low
Lagoonal	Locally Variable	High	Moderate	Low	Very Low
Fore Shore	Locally Variable	High	Moderate	Low	Very Low
<b>(c) Artificial</b>					
Uncompacted Fill	Variable	Very High	---	---	---
Compacted Fill	Variable	Low	---	---	---
<b>Definitions:</b> ka = thousands of years ago Mya = millions of years ago		<b>(1) Notes:</b> The above types of soil deposits may or may not exist in South Carolina. All of the soil deposits included by the original authors have been kept for completeness.			

A study was recently conducted at the Savannah River Site (SRS) by Lewis, et al. (2007) to re-evaluate the soil aging effects on the liquefaction resistance of Sand-Like soils that were encountered within shallow subsurface Tertiary soils from the Eocene (53 MYA) and Miocene (23 MYA) Epochs. The results of these and other studies indicate that there is a significant increase in the CRR of sand with time as indicated by Figure 13-20.



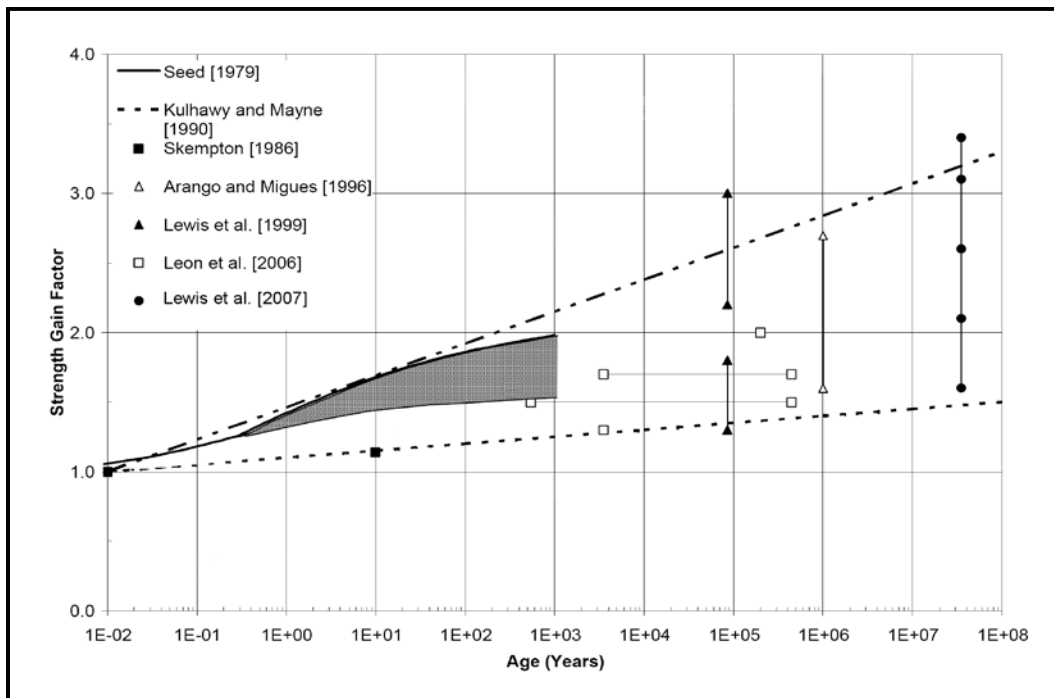


**Figure 13-20, Sand-Like Soil Strength Gain With Age (Adapted from Lewis, et al. (2007))**

Hayati and Andrus (2008 and 2009) reviewed the results of 16 published studies on the effects of aging on liquefaction resistance of soils and developed a regression line (Solid Line) shown in Figure 13-21 that represents the average variation in liquefaction  $K_{DR}$  with time ( $t$ ). The  $K_{DR}$  is the ratio of resistance-corrected cyclic resistance ratio of the aged soil ( $CRR_{DR}$ ) to the cyclic resistance ratio of recently deposited soil ( $CRR_{Holocene}$ ) as indicated by the following equation.

$$K_{DR} = \frac{CRR_{DR}}{CRR_{Holocene}} \quad \text{Equation 13-26}$$

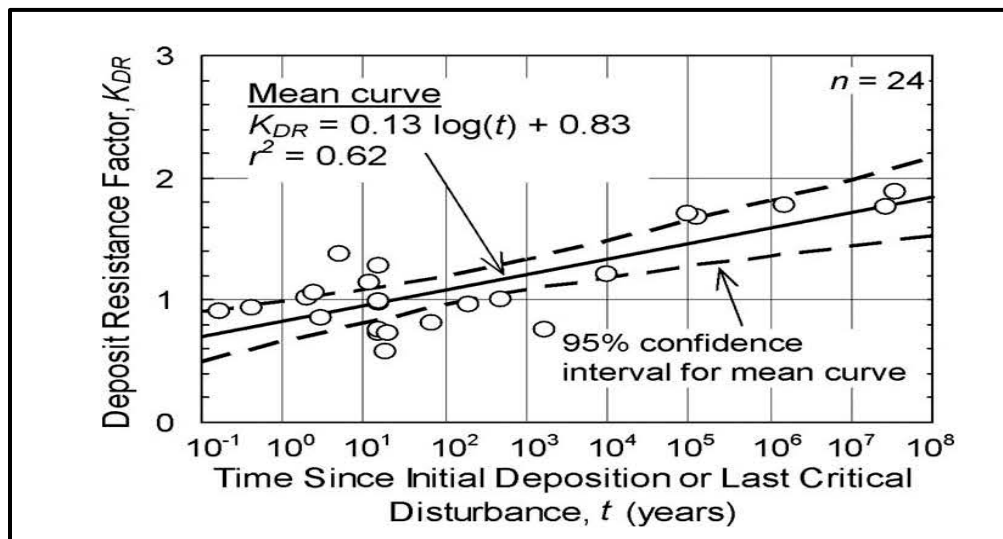


**Figure 13-21, Relationship Between Strength Gain Factor and Time (Hayati and Andrus, 2009 with permission from ASCE)**

There are 2 methods that may be used to develop  $K_{DR}$ . The first is the measured to estimated  $V_s$  ratio (MEVR). The second uses the actual age of the formation. It should be noted that the use of age is limited to non-cemented soils and those soils that have a good prediction of age. Both methods are discussed in the following Sections.

### 13.9.5.1 $K_{DR}$ using MEVR

The use of MEVR is the preferred method for determining  $K_{DR}$ . MEVR is an index that quantifies the aging processes during the time since deposition or last critical disturbance (e.g., liquefaction or excavation and placement). In addition,  $K_{DR}$  also accounts for cementation and stress history. The measured  $V_s$  shall conform to the requirements contained in other Chapters of the GDM.

MEVR may be determined using either SPT or CPTu data Hayati and Andrus (2008 and 2009) as indicated in the following equations.

$$MEVR = \frac{(V_{s,1,CS})_{meas}}{(V_{s,1,CS})_{SPT}} \quad \text{Equation 13-27}$$

$$MEVR = \frac{(V_{s,1,CS})_{meas}}{(V_{s,1,CS})_{CPT}} \quad \text{Equation 13-28}$$

Where,

$(V_{s,1,CS})_{meas}$  = Measured shear wave velocity corrected for overburden and fines content, ft/sec

$(V_{s,1,CS})_{SPT}$  = Estimated shear wave velocity based on SPT N-values corrected for overburden and fines content (see Chapter 7), ft/sec

$(V_{s,1,CS})_{CPT}$  = Estimated shear wave velocity based CPTu data corrected for overburden and fines content (see Chapter 7), ft/sec

Hayati and Andrus (2009) recommend the following  $K_{DR}$  and MEVR relationship be used.

$$K_{DR} = (1.08 * MEVR) - 0.08 \quad \text{Equation 13-29}$$

### 13.9.5.2 $K_{DR}$ Based on Deposit Age

As an alternate to determining  $K_{DR}$  using MEVR the actual age of the soil may be used. The age determination shall be from either first deposition or from the last critical disturbance (e.g., liquefaction or excavation and placement), whichever is most recent. In addition, these soils cannot be cemented for this procedure to be used. Therefore, because of the critical nature of the age determination, the age and time since liquefaction event for a specific soil formation shall be determined either by a Professional Geologist (PG) or Professional Engineer (PE). The PG or PE shall be registered in South Carolina and shall be required to provide a minimum of 3 years of experience in determining the age of a soil formation. A separate letter signed and sealed by the professional making the age and time since last liquefaction event determination shall be required and shall be included in the geotechnical engineering reports.

A liquefaction age correction factor of  $K_{DR} = 1.0$  corresponds to a soil deposit with an age of approximately 23 years. The  $t$  is the time since initial deposition ( $K_{DR} = 1.0$ ) or critical disturbance in years, whichever is most recent. Critical disturbance occurs when the effects of soil aging are removed as a result of grain-to-grain contacts being broken and reformed such as has been observed when Sand-Like soils experience cyclic liquefaction.

The  $K_{DR}$  shown in Figure 13-20 can be computed using the following equation.

$$K_{DR} = (0.13 * \log_{10} t) + 0.83 \leq 2.09 \quad \text{Equation 13-30}$$

Where,

$t$  = Time since initial soil deposition or last critical disturbance (e.g., liquefaction), whichever is most recent, years

### 13.9.6 Static Shear Stress Ratio Correction Factor ( $K_\alpha$ )

The static shear stress ratio correction factor,  $K_\alpha$ , accounts for the effects of initial static shear stresses on cyclic resistance of the soils beneath sloping ground. Sloping ground for SCDOT projects is any site that contains an embankment or free-face.

The static shear stresses are typically expressed as the static shear stress ratio ( $\alpha$ ) that is defined as the initial static shear stress ( $\tau_{static}$ ) divided by the effective vertical (normal) consolidation stress ( $\sigma'_{vc}$ ) as indicated by the following equation.

$$\alpha = \frac{\tau_{static}}{\sigma'_{vc}} = \frac{\tau_{static}}{\sigma'_{v0}} \quad \text{Equation 13-31}$$

The initial static shear stress ( $\tau_{static}$ ) is the static soil shear stress that exists prior to the seismic shaking onset and can be computed as indicated in Section 13.9.6.1. The effective normal consolidation stress is typically assumed to be equal to the effective overburden stress ( $\sigma'_{vc} = \sigma'_{v0}$ ) because most design situations assume enough time has elapsed that the soils have been fully consolidated under sustained loading. For under consolidated soils, the existing effective consolidation stress ( $\sigma'_{vc}$ ) shall be used.  $K_\alpha$  is defined by the following equation.

$$K_\alpha = \frac{(CRR)_\alpha}{(CRR)_{\alpha=0}} \quad \text{Equation 13-32}$$

Where,

$CRR_\alpha$  = CRR at some value of  $\alpha$

$CRR_{\alpha=0}$  = CRR at a value of  $\alpha = 0$

$K_\alpha$  for Sand-Like soils and Clay-Like soils can be computed in accordance with Sections 13.9.6.2 and 13.9.6.3, respectively.

The static shear stress ratio (SSSR)  $K_\alpha$  can be used with the *Simplified Procedure* to evaluate the effects of initial static shear stresses for sites containing embankments or ERSs. This is accomplished by multiplying the SSSR  $K_\alpha$  by the soil's  $CRR^*$  as indicated in this Section. The SSSR  $K_\alpha$  proposed by Idriss and Boulanger (2008) is computed as indicated in Section 13.9.6. The SSSR  $K_\alpha$  method is limited to a maximum initial static stress ratio  $\alpha$  less than or equal to 0.35 ( $\alpha \leq 0.35$ ). Because of the difficulty in determining  $K_\alpha$ ,  $K_\alpha$  can be assumed to be 1.0 for

either Sand-Like soils or Clay-Like soils. However,  $K_\alpha$  may be determined as indicated in the following Sections.

### 13.9.6.1 Initial Static Shear Stress ( $\tau_{static}$ ) of Soils

The  $\tau_{static}$  for each soil layer (Sand-Like soils and Clay-Like soils) can be computed by performing a slope stability analysis of the pre-failure geometry with reduced soil shear strengths that achieves a condition of the slope just being stable (i.e.,  $FS = 1$  or  $\phi = 1$ ). The slope stability analysis shall be performed in accordance with Chapter 17 with Spencer's method (Spencer (1967)). The slope stability analysis should be evaluated using both circular and sliding wedge potential failure surfaces. Determine the slope stability ratio,  $(D/C)_{SSSR}$  using the following equation.

$$\left(\frac{D}{C}\right)_{SSSR} = \frac{1}{FS_{SSSR}} = \phi_{SSSR} = 1 \quad \text{Equation 13-33}$$

The  $\tau_{static}$  is defined as the soil shear stress along the failure surface that corresponds to slope stability ratio of  $(D/C)_{Stability} = 1$ . The  $\tau_{static}$  along the critical failure surface can be computed by reducing soil shear strengths based on the computed slope stability ratio,  $(D/C)_{Stability}$  for the pre-failure geometry. The reduced undrained shear strengths for cohesive soil layers,  $c_{static}$ , can be computed using the following equation.

$$c_{static} = c * \left(\frac{D}{C}\right)_{SSSR} = \frac{c}{FS_{SSSR}} = c * \phi_{SSSR} \quad \text{Equation 13-34}$$

Where,

$c_{static}$  = Reduced undrained shear strength required to just maintain stability (i.e.,  $\phi_{SSSR} = 1$ )

$c$  = Undrained shear strength,  $S_u = c$

$\left(\frac{D}{C}\right)_{SSSR}$  = Demand to capacity ratio for the pre-failure geometry where the Demand equals the Capacity

$FS_{SSSR}$  = Factor of Safety for the pre-failure geometry where the Factor of Safety equals 1

$\phi_{SSSR}$  = Resistance Factor for the pre-failure geometry where the soil resistance is equal to the soil loading

The  $\tau_{static}$  along the critical failure surface for cohesionless soils is computed by the following equation.

$$\tau_{static} = c_{static} \quad \text{Equation 13-35}$$

The reduced drained shear strength for a cohesionless soil layer is computed by reducing the internal friction angle,  $\phi_{static}$ , and can be computed using the following equation.

$$\phi_{static} = \tan^{-1} \left[ \tan \phi * \left(\frac{D}{C}\right)_{SSSR} \right] = \tan^{-1} [\tan \phi * (\phi_{SSSR})] \quad \text{Equation 13-36}$$

Where,

$\phi_{static}$  = Reduced internal friction angle required to just maintain stability (i.e.,  $\phi_{SSSR} = 1$ )

$\phi$  = Internal friction angle

$\left(\frac{D}{C}\right)_{SSSR}$  = Demand to capacity ratio for the pre-failure geometry where the Demand equals the Capacity

$\varphi_{SSSR}$  = Resistance Factor for the pre-failure geometry where the soil resistance is equal to the soil loading

The  $\tau_{static}$  along the critical failure surface for cohesionless soils is computed by the following equation.

$$\tau_{static} = \sigma'_{vo} * \tan \phi_{static} \quad \text{Equation 13-37}$$

Alternatively, some slope stability software allows the input of the shear strength ratio directly ( $\tau/\sigma'_{vo}$ ). The  $\alpha$  for Clay-Like soils can be computed using the following equation:

$$\alpha = \left(\frac{\tau_{static}}{\sigma'_{vo}}\right) = \left(\frac{\tau}{\sigma'_{vo}}\right) * \left(\frac{D}{C}\right)_{SSSR} = \frac{\tau}{\sigma'_{vo} * FS_{SSSR}} = \varphi_{SSSR} * \left(\frac{\tau}{\sigma'_{vo}}\right) \quad \text{Equation 13-38}$$

The  $\alpha$  for Sand-Like soils can be computed using the following equation:

$$\alpha = \left(\frac{\tau_{static}}{\sigma'_{vo}}\right) = (\tan \phi) * \left(\frac{D}{C}\right)_{SSSR} = \frac{\tan \phi}{FS_{SSSR}} = \varphi_{SSSR} * \tan \phi \quad \text{Equation 13-39}$$

The computed  $\tau_{static}$  should be checked by using the reduced soil shear strengths ( $\tau_{static}$  or  $\alpha$ ) to perform a slope stability analysis and to determine if the slope stability ratio,  $(D/C)_{SSSR}$ , for the critical failure surface corresponds to a slope stability ratio of  $(D/C)_{SSSR} = \varphi_{SSSR} = 1$ .

If the slope stability ratio of  $(D/C)_{SSSR} \neq 1$ , the soil shear strength should be further adjusted until a slope stability ratio of  $(D/C)_{SSSR} = 1$  is achieved.

The  $\tau_{static}$  ( $(D/C)_{SSSR} = 1$ ) for each soil layer (Sand-Like soils and Clay-Like soils) can be computed by performing a slope stability back analysis of the pre-failure geometry using reduced soil shear strengths. The slope stability search should evaluate both circular and sliding wedge potential failure surfaces in accordance with Chapter 17 with Spencer's method being required. Slope stability back analysis of the static shear stress ( $\tau_{static}$ ) for a single soil layer is relatively straight forward when compared to slope failure surfaces that have multiple soil layers.

The soil layers that intersect the failure surface are initially assigned reduced "trial" soil shear strengths ( $\tau$ ). The soil shear strength ( $\tau$ ) for the layer is varied iteratively until the slope stability ratio,  $(D/C)_{SSSR} = 1$  that is equivalent to the static driving stress ( $\tau_{static}$ ) induced by the slope on the subgrade soils. Alternatively, some slope stability software programs allow the input of the static shear strength ratio directly ( $\alpha = \tau_{static}/\sigma'_{vo}$ ). For this software option, the static shear strength ratio ( $\alpha$ ) is varied iteratively until the slope stability ratio,  $(D/C)_{SSSR} = 1$  is obtained.

### 13.9.6.2 $K_\alpha$ For Sand-Like Soils

Harder and Boulanger (1997) observed variations in cyclic shear stresses as a function of  $D_R$  and  $\sigma'_{vo}$  when they summarized available cyclic laboratory test data. It was observed that cyclic resistance of dense sands can increase significantly as  $\alpha$  increases and that cyclic resistance of loose sands decreases as  $\alpha$  increases.

Boulanger (2003b) developed  $K_\alpha$  for Sand-Like soils based on  $\xi_{SR}$ . These correction factors were then correlated for use with normalized SPT N-values ( $N^*_{1,60}$  – Section 13.9.1) normalized and effective overburden corrected CPT tip resistance ( $q_{c,1,N}$  – Section 13.9.2). The  $K_\alpha$  for selected effective overburden stresses of  $\sigma'_{vo} = 1$  tsf and  $\sigma'_{vo} = 4$  tsf,  $K_o = 0.45$  and  $Q = 10$  (Sand), are provided for SPT values of  $N^*_{1,60}$  in Figure 13-22 and CPT values of  $q_{c,1,N}$  in Figure 13-23.

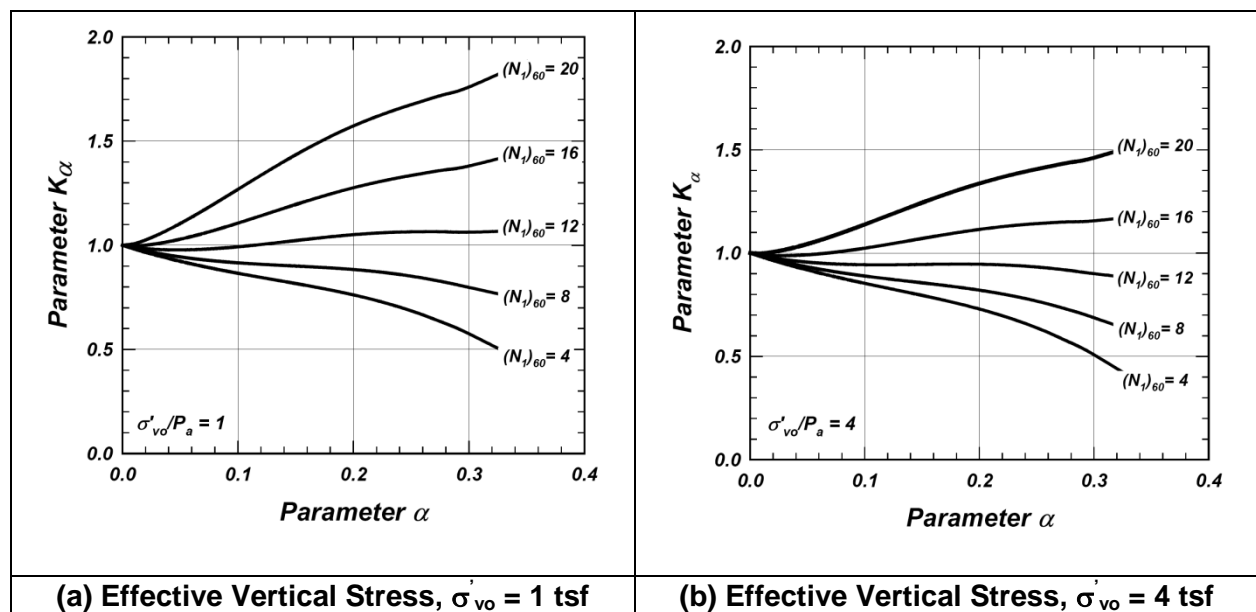


Figure 13-22, Variations of  $K_\alpha$  with SPT Blow Count ( $N^*_{1,60}$ ) (Idriss and Boulanger (2003))

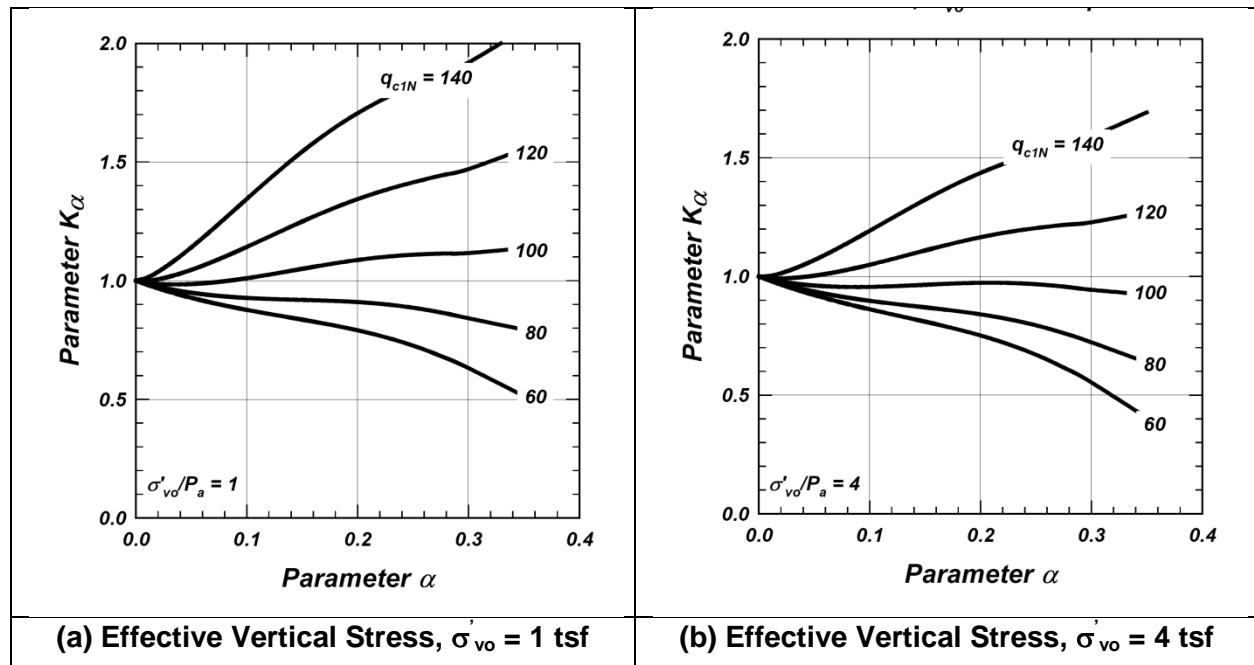


Figure 13-23, Variations of  $K_\alpha$  with CPT Tip Resistance ( $q_{c,1,N}$ ) (Idriss and Boulanger (2003))

In lieu of using Figures 13-22 and 13-23, the following equation may be used to compute  $K_\alpha$ . The following equations were developed from data that limit the static shear stress ratio to  $\alpha \leq 0.35$  and relative state parameter index to  $-0.6 \leq \xi_R \leq 0.1$ .

$$K_\alpha = a + b * \left[ \exp\left(\frac{-\xi_R}{c}\right) \right] \quad \text{Equation 13-40}$$

Where,

$$a = 1267 + 636\alpha^2 - (634 \cdot \exp(\alpha)) - (632 \cdot \exp(-\alpha))$$

$$b = \exp(-1.11 + 12.3\alpha^2 + (1.31 \cdot \ln(\alpha + 0.0001)))$$

$$c = 0.138 + 0.126\alpha + 2.52\alpha^3$$

$\alpha$  = Static shear stress ratio as per Equation 13-39 and Section 13.9.6.1 (limited to  $\alpha \leq 0.35$ )

$\xi_R$  = Relative state parameter index used to correlate  $D_r$ ,  $N_{1,60}^*$ , and  $q_{c,1,N}$  to  $K_\alpha$  (Limited to:  $-0.6 \leq \xi_R \leq 0.1$ )

$$\xi_R = \frac{1}{Q-\psi} - D_r \quad \text{Equation 13-41}$$

$$\xi_R = \frac{1}{Q-\psi} - \left(\frac{N_{1,60}^*}{46}\right)^{0.5} \quad \text{Equation 13-42}$$

$$\xi_R = \frac{1}{Q-\psi} - \left[0.478 * (q_{c,1,N})^{0.264} - 1.063\right] \quad \text{Equation 13-43}$$

$$\psi = \ln \left[ \frac{100 * (1 + 2 * K_\alpha) * \sigma'_{vo}}{3 * P_a} \right] \quad \text{Equation 13-44}$$

Where,

$D_r$  = Relative density, where  $D_r \leq 0.90$  (90%)

$N_{1,60}^*$  = Standardized and normalized SPT blow count, where  $N_{1,60}^* \leq 37$  blows/foot

$q_{c,1,N}$  = Normalized CPT tip resistance, where  $q_{c,1,N} \leq 211$  (unitless)

$Q$  = Empirical Constant:  $Q=10$  for Quartz and feldspar (Sand),  $Q=8$  for limestone,  $Q=7$  for anthracite, and  $Q=5.5$  for chalk.

$K_o$  = At-rest lateral earth pressure coefficient

$\sigma'_{vo}$  = Effective vertical overburden stress, tsf

$P_a$  = Atmospheric Pressure, tsf

The procedure provided in the preceding paragraphs is complex. Therefore, the  $K_\alpha$  provided in Table 13-4 may be used. Note that values provided are based on an  $\alpha$  less than or equal to 0.35 ( $\alpha \leq 0.35$ ) and an overburden stress of less than 4 tsf (approximately 50 feet of fill). These values are anticipated to be conservative. The GEOR may elect to use the preceding equations to determine  $K_\alpha$ . The GEOR shall provide the necessary computations used to determine  $K_\alpha$ . For  $N_{1,60}^*$  and  $q_{c,1,N}$  that between the values indicated linear interpolation may be used.

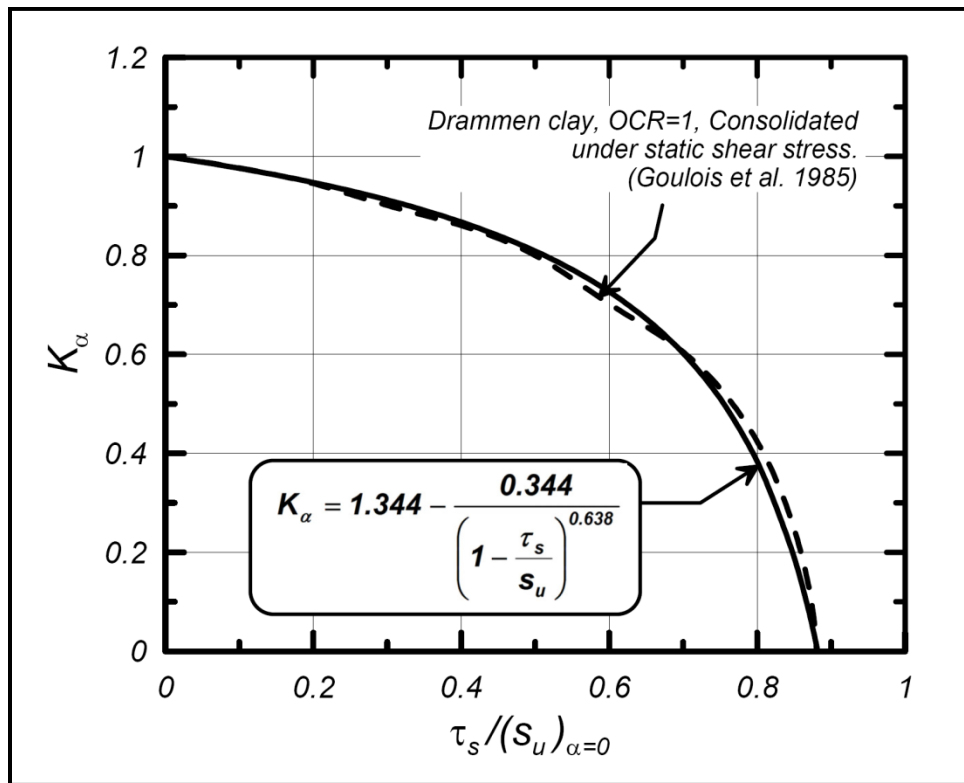
**Table 13-4, Simplified  $K_\alpha$  Values for Sand-Like Soils**

$N_{1,60}^*$	$K_\alpha$	$q_{c,1,N}$	$K_\alpha$
$\leq 4$	0.50	$\leq 60$	0.50
8	0.75	80	0.75
$\geq 12$	1.00	$\geq 100$	1.00

### 13.9.6.3 $K_\alpha$ For Clay-Like Soils

Boulangier and Idriss (2004 and 2007) developed  $K_\alpha$  for Clay-Like soils based on laboratory testing of Drammen clay (Goulois, et al. (1985)) that was consolidated under a sustained static shear stress. The relationship developed from these laboratory tests for  $K_\alpha$  versus  $(\tau_{static}/S_U)_{\alpha=0}$  for Clay-Like soils are shown in Figure 13-24.





$\tau_s = \tau_{static}$

**Figure 13-24,  $K_\alpha$  versus  $(\tau_s/S_u)_{\alpha=0}$  For Clay-Like Soil (NC Drammen Clay) (Boulanger and Idriss (2004))**

The  $K_\alpha$  relationship shown in Figures 13-24 is presented in the following equation as a function of  $(\tau_{static}/S_u)$  and  $(\alpha = \tau_{static}/\sigma'_{vc})$ .

$$K_\alpha = 1.344 - \frac{0.344}{\left(1 - \frac{\tau_{static}}{S_u}\right)^{0.638}} = 1.344 - \frac{0.344}{\left[1 - \left(\frac{\alpha}{S_u/\sigma'_{vc}}\right)\right]^{0.638}} \quad \text{Equation 13-45}$$

Where,

$\tau_{static}$  = Initial static shear stress

$S_u$  = Undrained shear strength

$\sigma'_{vc}$  = Effective vertical consolidating stress

$S_u/\sigma'_{vc}$  = Undrained shear strength ratio (See Chapter 7)

$\alpha$  = Static shear stress ratio as per Equation 13-38 and Section 13.9.6.1 (limited to  $\alpha \leq 0.35$ )

Boulanger and Idriss (2007) recommended using an empirical shear strength ratio relationship  $(S_u/\sigma'_{vc})$  such as those developed by Ladd and Foot (1974) that take the form of the following equation:

$$\left(\frac{S_u}{\sigma'_{vc}}\right) = k * (OCR)^n \quad \text{Equation 13-46}$$

Where,

k = Shear strength ratio for normally consolidated soils (OCR=1). Typically range between 0.17 and 0.29. Use k=0.22 (DSS testing) as recommended by Boulanger and Idriss (2007) unless laboratory testing available.

OCR = Overconsolidation ratio ( $\sigma'_p / \sigma'_{vo}$ ) (See Chapter 7)

n = Soil constant typically taken as 0.80 for unstructured and uncemented soils.

The  $K_\alpha$  presented in Equation 13-45 can be combined with the empirical shear strength ratio shown in Equation 13-46 to develop  $K_\alpha$  as a function of the consolidation stress history as shown in Figure 13-25 and Equation 13-47.

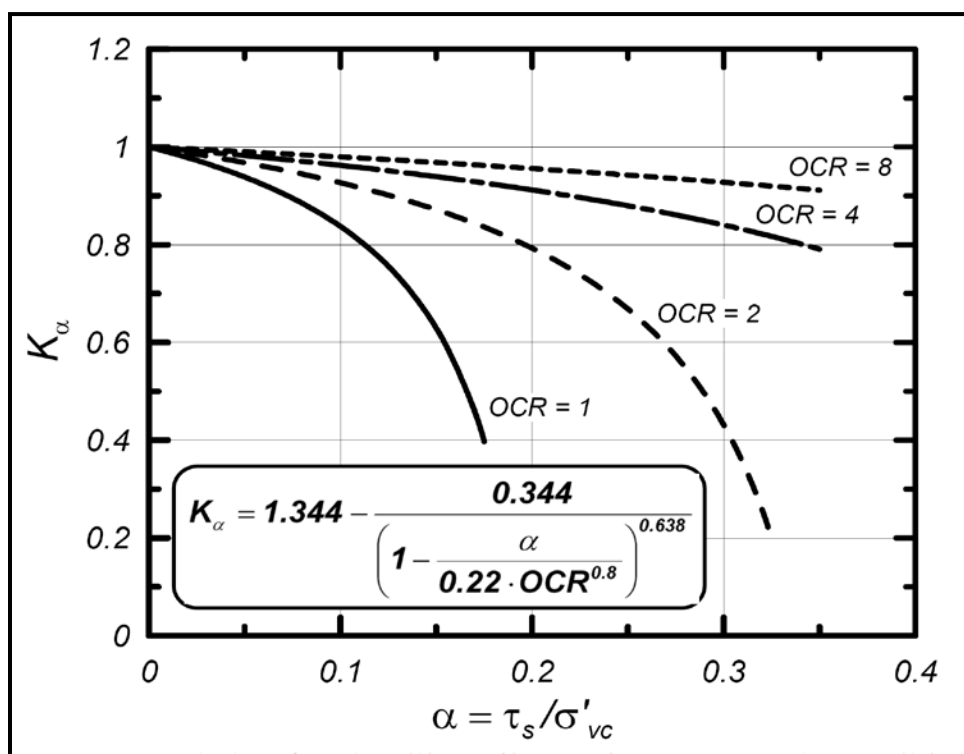


Figure 13-25,  $K_\alpha$  versus  $(\tau_s/S_u)_{\alpha=0}$  For Clay-Like Soil ( $1 \leq OCR \leq 8$ ) (Boulanger and Idriss (2004 and 2007))

$$K_\alpha = 1.344 - \frac{0.344}{\left\{1 - \left[\frac{\alpha}{k \cdot (OCR)^n}\right]\right\}^{0.638}} = 1.344 - \frac{0.344}{\left\{1 - \left[\frac{\alpha}{0.22 \cdot (OCR)^{0.8}}\right]\right\}^{0.638}} \quad \text{Equation 13-47}$$

The procedure provided in the preceding paragraphs is complex. Therefore, similarly to Sand-Like soils, the  $K_\alpha$  provided in Table 13-5 may be used. Note that values provided are based on the OCR value to the soil. For OCR values ranging from 4 to 8, the  $\alpha$ -value is less than or equal to 0.35 ( $\alpha \leq 0.35$ ). These values are anticipated to be conservative. The GEOR may elect to use the preceding equations to determine  $K_\alpha$ . The GEOR shall provide the necessary computations used to determine  $K_\alpha$ . For  $N_{1,60}^*$  and  $q_{c,1,N}$  that between the values indicated linear interpolation may be used.

**Table 13-5, Simplified  $K_\alpha$  Values for Clay-Like Soils**

OCR	$K_\alpha$
$\leq 1$	0.10
2	0.20
4	0.80
$\geq 8$	1.00

### 13.10 SOIL SHEAR STRENGTH FOR SEISMIC ANALYSES

When performing seismic analyses, for soils that are not subject to losses in shear strength, the appropriate undrained shear ( $\tau$ ) or drained shear ( $\tau'$ ) strengths should be used, in accordance with Chapter 7. Soils that are subject to cyclic strain-softening should use residual soil shear strengths. Undrained/drained soil shear strengths can be evaluated in accordance with the field and laboratory testing procedures specified in Chapter 5.

During strong seismic shaking, cyclic liquefaction of Sand-Like soils or cyclic softening of Clay-Like soils may result in a sudden loss of strength and stiffness. Laboratory testing to determine residual shear strength of soils that have been subject to cyclic liquefaction or cyclic softening is difficult and not typically performed. The standard-of-practice is to use correlated residual undrained shear strengths of cohesionless soils as indicated in Sections 13.10.1 and 13.10.2 and to use correlated cyclic shear strength of cohesive soils as indicated in Sections 13.10.3 and 13.10.4. Guidance in selection of soil shear strengths for seismic analyses is presented in Section 13.10.5.

#### 13.10.1 Sand-Like Soil Cyclic Shear Strength Triggering

The shear strength of Sand-Like soils that should be used in seismic analyses is dependent on the results of the liquefaction triggering and on pore pressure generation. The liquefaction triggering resistance ratio  $(D/C)_{SL}$  is presented in Section 13.7. Figure 13-26 shows a relationship between liquefaction triggering resistance ratio  $(D/C)_{SL}$  and the excess pore pressure ratio,  $R_u$ , that was proposed by Marcuson, et al. (1990).

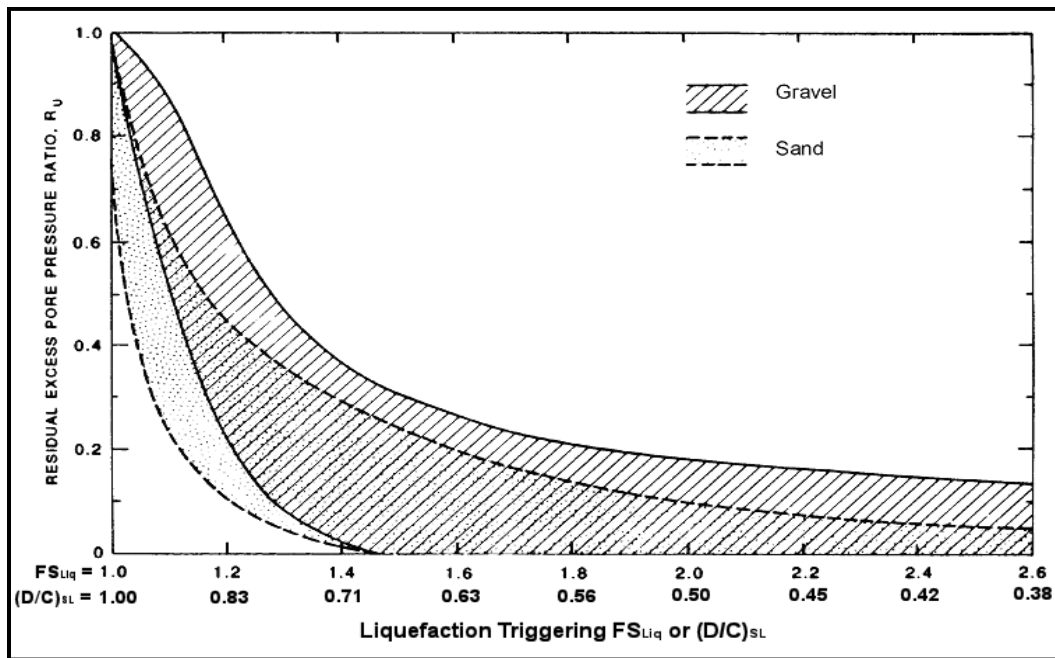


**Figure 13-26, Excess Pore Pressure Ratio - Liquefaction Triggering (Modified Marcuson, et al. (1990))**

The excess pore pressure ratio,  $R_u = \Delta u / \sigma'_{vo}$  is the ratio of excess pore water pressure ( $\Delta u$ ) to effective overburden stress ( $\sigma'_{vo}$ ). The liquefaction triggering resistance ratio  $(D/C)_{SL}$  of Sand-Like soils can be defined based on the excess pore pressure ratio generated as either Cyclic Liquefaction or No Liquefaction. Resistance factors used for design shall be those presented in Chapter 9.

Guidelines for determining the shear strength of Sand-Like soils are provided in Table 13-6.

**Table 13-6, Sand-Like Shear Strengths**

Liquefaction Potential	Liquefaction Triggering Criteria	Soil Shear Strength
Cyclic Liquefaction	$(D/C)_{SL-Sand} > \phi_{SL-Sand}$ $(0.7 \leq R_u \approx 1.0)$	Use Idriss and Boulanger (2008) or Olson and Johnson (2008) residual shear strength of liquefied soils ( $\tau_{rl}$ ) correlations. Sections 13.10.2.1 and 13.10.2.2  $\phi_{rl} = \tan^{-1} \left( \frac{\tau_{rl}}{\sigma'_{vo}} \right) \quad \text{Equation 13-48}$ or  $\tau_{rl} = \sigma'_{vo} * \tan \phi_{rl} \quad \text{Equation 13-49}$
No Liquefaction	$(D/C)_{SL-Sand} \leq \phi_{SL-Sand}$ $(R_u < 0.70)$	Drained shear strength ( $\tau$ ) or residual shear strength ( $\tau_r$ ) based on strain level. See Chapter 7.

### 13.10.2 Sand-Like Soil Cyclic Liquefaction Shear Strength

The following methods are currently used to estimate the residual shear strength of liquefied Sand-Like soils.

1. SPT and CPT – Idriss and Boulanger (2008)
2. SPT and CPT - Olson and Johnson (2008)
3. SPT – Kramer and Wang (2015)

The Idriss and Boulanger (2008) method is the preferred method because it incorporates case histories from Olson and Johnson (2008). The Idriss and Boulanger (2008) method is also more advanced in that it uses residual shear strength ratios, permits adjustment for fines content, and allows residual shear strengths to be evaluated for void redistribution effects. Both methods are presented below to provide the designer with the appropriate background to evaluate the appropriate residual shear strength for liquefied Sand-Like soils. Kramer and Wang (2015) discuss some discrepancies that occur in both Idriss and Boulanger (2008) and Olson and Johnson (2008) with relating normalization of  $\tau_{rl}$  using  $\sigma'_{vo}$ , which can indicate very low  $\tau_{rl}$  at low  $\sigma'_{vo}$ . These discrepancies and the recommended procedure to eliminate these discrepancies are provided in the following Sections.

#### 13.10.2.1 Idriss and Boulanger (2008) – Liquefied Residual Shear Strength

The Idriss and Boulanger (2008) method allows for the computation of the liquefaction residual shear strength ratio ( $\tau_{rl}/\sigma'_{vo}$ ), which is the ratio of liquefied residual shear strength ( $\tau_{rl} = S_{rl}$ ) to effective overburden stress ( $\sigma'_{vo}$ ). Both SPT-based and CPTu-based relationships with  $\tau_{rl}/\sigma'_{vo}$  were proposed by Idriss and Boulanger (2008). Furthermore, the Idriss and Boulanger (2008) relationships distinguish between 2 types of cases:

- Case 1:** Condition in which the effects of void redistribution can be confidently judged to be negligible. This condition occurs at sites where the site stratigraphy would not impede dissipation of excess pore water pressure and the dissipation of excess pore water pressure would be accompanied by densification of the soils.
- Case 2:** Condition in which the effects of void redistribution can be significant. This condition occurs at sites where the site stratigraphy would impede dissipation of excess pore water pressure. Sites that meet this condition include sites with relatively thick layers of liquefiable soils that are overlain by lower permeability soils that would impede the dissipation of excess pore water pressure by trapping the upwardly seeping pore water beneath the lower permeability soil. This condition would lead to localized loosening, strength loss, and possibly even the formation of water film beneath the lower permeability soil.

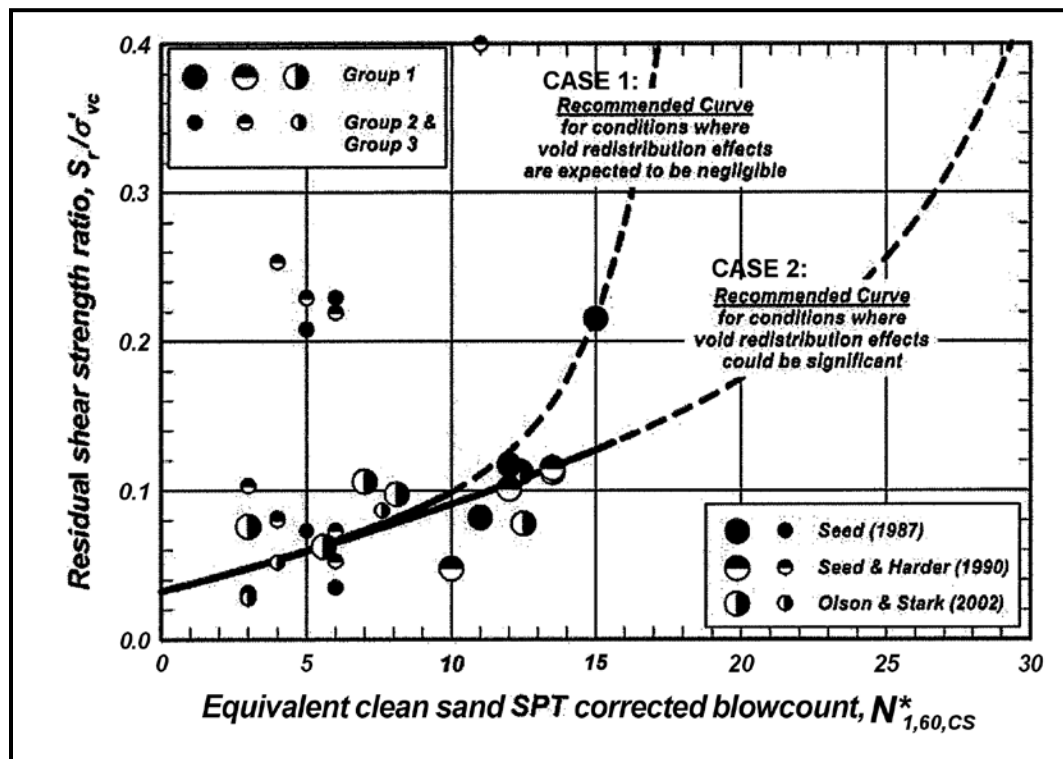
The SPT correlation uses a corrected fines content SPT blow count,  $N_{1,60,cs}^*$ , computed as shown in Equation 13-50. Corrected and normalized SPT blow counts,  $N_{1,60}$ , should be computed in accordance with Chapter 7. Values for  $\Delta N_{1,60-rl}$  can be found in Table 13-7.

$$N_{1,60,cs}^* = N_{1,60}^* + \Delta N_{1,60-rl} \quad \text{Equation 13-50}$$

Table 13-7, Values of  $\Delta N_{1,60-rl}$   
(Seed, 1987)

Fines Content, FC (% passing No. 200 sieve)	$\Delta N_{1,60-rl}$
10	1
25	2
50	4
75	5

The  $\tau_{rl}/\sigma'_{vo}$  for SPT can be determined for Case 1 and Case 2 using Figure 13-27.



Note:  $\tau_{rl} = S_r$

Figure 13-27, Liquefied Shear Strength Ratio - SPT  
(Idriss and Boulanger (2008))

In lieu of using Figure 13-27,  $\tau_{rl}/\sigma'_{vo}$  for SPT can be determined for Case 1 and Case 2 by using the following equations.

**Case 1:**

$$\left(\frac{\tau_{rl}}{\sigma'_{vo}}\right) = (\psi) * \left[1 + \exp\left(\frac{N_{1,60,CS}^*}{2.4} - 6.6\right)\right] \leq \tan \phi'_{rl} \quad \text{Equation 13-51}$$

for,  $N_{1,60,CS}^* \leq 17$  blows per foot

**Case 2:**

$$\left(\frac{\tau_{rl}}{\sigma'_{vo}}\right) = (\psi) \leq \tan \phi'_{rl} \quad \text{Equation 13-52}$$

Where,

$$\psi = \exp \left[ \frac{N_{1,60,CS}^*}{16} + \left( \frac{N_{1,60,CS}^* - 16}{21.2} \right)^3 - 3.0 \right] \quad \text{Equation 13-53}$$

for,  $N_{1,60,CS}^* \leq 30$  blows per foot

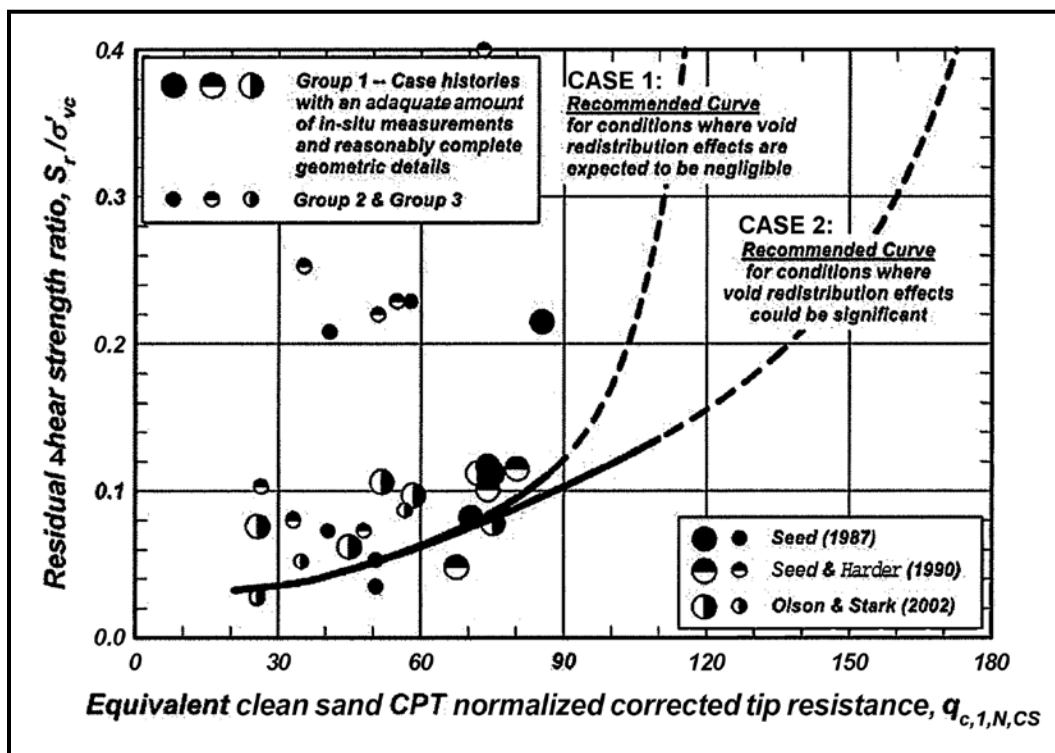
The CPTu correlation uses a corrected, normalized CPTu tip resistance adjusted for fines content,  $q_{t,1,N,CS}$ , computed as shown in Equation 13-54. Corrected and normalized tip resistances,  $q_{t,1,N}$ , should be computed in accordance with Chapter 5. Values for  $\Delta q_{t,1,N-rl}$  can be found in Table 13-8.

$$q_{t,1,N,CS} = q_{t,1,N} + \Delta q_{t,1,N-rl} \quad \text{Equation 13-54}$$

Table 13-8, Values of  $\Delta q_{t,1,N-rl}$   
(Idriss and Boulanger (2008))

Fines Content, FC (% passing No. 200 sieve)	$\Delta q_{t,1,N-rl}$
10	10
25	25
50	45
75	55

The  $\tau_{rl}/\sigma'_{vo}$  for CPTu can be determined for Case 1 and Case 2 using Figure 13-28.



Note:  $\tau_{rl} = S_r; q_{c,1,N,CS} = q_{t,1,N,CS}$

Figure 13-28, Liquefied Shear Strength Ratio - CPTu Tip Resistance  
(Idriss and Boulanger (2008))

In lieu of using Figure 13-28,  $\tau_{rl}/\sigma'_{vo}$  for CPTu can be determined for Case 1 and Case 2 by using the following equations.

**Case 1:**

$$\left(\frac{\tau_{rl}}{\sigma'_{vo}}\right) = (\psi) \leq \tan \phi'_{rl} \quad \text{Equation 13-55}$$

for,  $q_{t,1,N,CS} \leq \sim 115$

**Case 2:**

$$\left(\frac{\tau_{rl}}{\sigma'_{vo}}\right) = (\psi) * \left\{1 + \exp \left[ \left( \frac{q_{c,1,N,CS}}{11.1} \right) - 9.82 \right] \right\} \leq \tan \phi'_{rl} \quad \text{Equation 13-56}$$

for,  $q_{t,1,N,CS} \leq \sim 170$

Where,

$$\psi = \exp \left[ \left( \frac{q_{c,1,N,CS}}{24.5} \right) - \left( \frac{q_{c,1,N,CS}}{61.7} \right)^2 + \left( \frac{q_{c,1,N,CS}}{106} \right)^3 - 4.42 \right] \quad \text{Equation 13-57}$$

### 13.10.2.2 Olson and Johnson (2008) – Liquefied Residual Shear Strength

The Olson and Johnson (2008) methods also allow for the computation of the  $\tau_{rl}/\sigma'_{vo}$ . The relationship between liquefaction shear strength ratio and the normalized SPT blow count ( $N^*_{1,60}$ ) is provided in Figure 13-29. The average trend line for Figure 13-29 can be computed using the following equation.

$$\left(\frac{\tau_{rl}}{\sigma'_{vo}}\right) = 0.03 + 0.0075 * (N^*_{1,60}) \pm 0.03 \quad \text{Equation 13-58}$$

Where,

$N^*_{1,60}$  = Normalized SPT blow count and values of  $N^*_{1,60} \leq 16$  blows per foot.



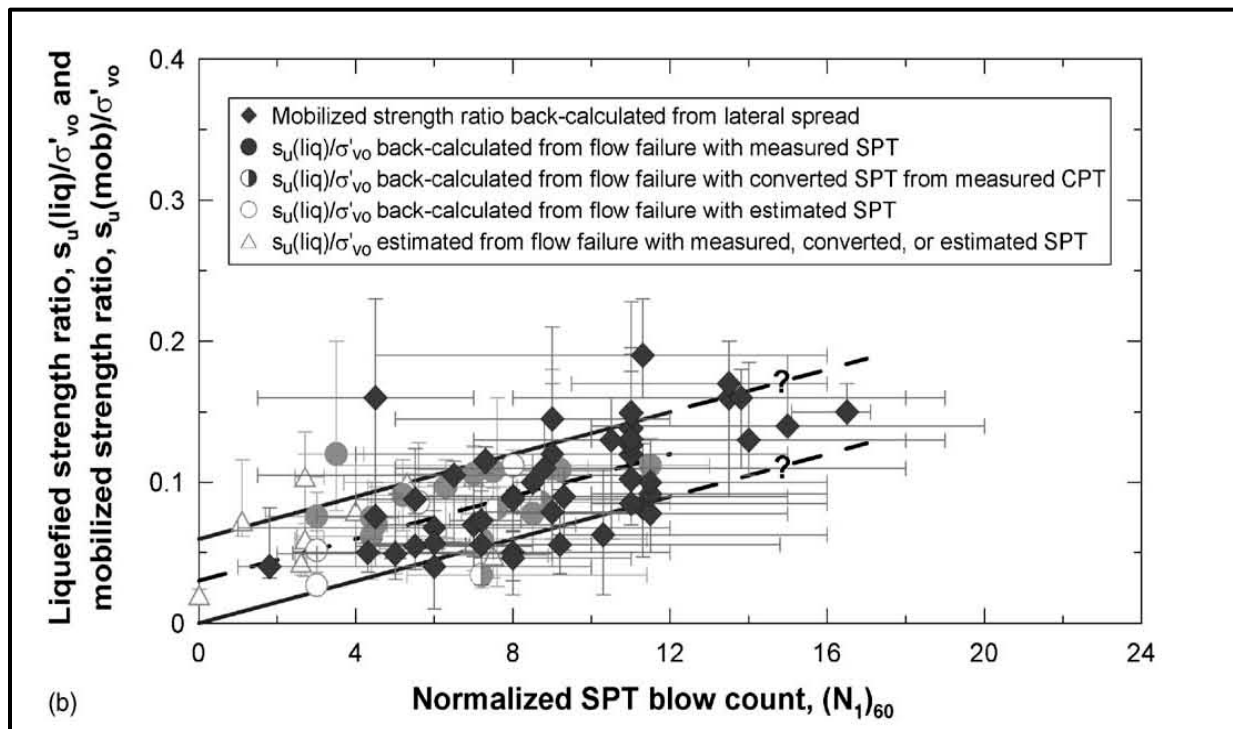


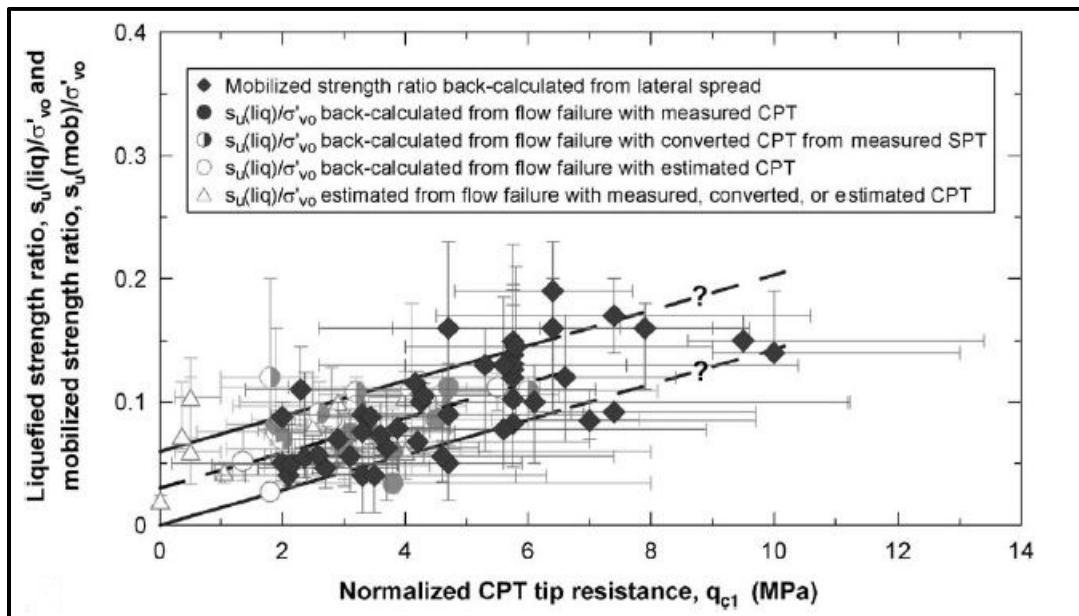
**Figure 13-29, Liquefied Shear Strength Ratio - SPT Blow Count (Olson and Johnson (2008) with permission from ASCE)**

The relationship between liquefaction shear strength ratio and the normalized CPTu tip resistance ( $q_{t,1}$ ) is provided in Figure 13-30. The average trend line for Figure 13-30 can be computed using the following equation.

$$\left(\frac{\tau_{rl}}{\sigma'_{vo}}\right) = 0.03 + 0.0143 * (q_{t,1}) \pm 0.03 \quad \text{Equation 13-59}$$

Where,

$q_{t,1}$  = Normalized CPT tip resistance (MPa) for values  $q_{t,1} \leq 10$  MPa (approximately 104 tsf)



Note:  $q_{c,1} = q_{t,1}$

**Figure 13-30, Liquefied Shear Strength Ratio - CPT Tip Resistance (Olson and Johnson (2008) with permission from ASCE)**

### 13.10.2.3 Kramer and Wang (2015) – Liquefied Residual Shear Strength

The previously discussed Idriss and Boulanger (2008) and Olson and Johnson (2008) procedures both rely on normalized shear strength (i.e.,  $\tau_{rl}/\sigma'_{vo}$ ) to determine the liquefied shear strength ( $\tau_{rl}$ ); however, according to Kramer and Wang (2015) this can lead to extremely low residual strength values at low initial vertical stresses. The normalized shear strength approach assumes the liquefied shear strength is affected by both the corrected N-values as well as being proportional to the effective overburden pressure. Kramer and Wang (2015) also point that the direct method (Seed (1987) and Seed and Harder (1990)) assumes the liquefied shear strength only varies with corrected N-values. The direct method tends to predict high liquefied shear strengths at shallow depths and low liquefied shear strengths at deeper depths. Kramer and Wang (2015) have developed a procedure to determine the liquefied shear strength that accounts for both the direct and normalized shear strength approaches. The equation is provided below:

$$\tau_{rl} = e^Z \tag{Equation 13-60}$$

$$Z = -8.444 + 0.109(N_{1,60}^*) + 5.379(\sigma'_{vo})^{0.1} \tag{Equation 13-61}$$

Where,

$N_{1,60}^*$  = Standardized and normalized SPT blow count

$\sigma'_{vo}$  = Effective vertical overburden stress, atmospheres (atm) (1 atm = 2,116.22 psf)

If is noted that  $\tau_{rl}$  provided in Equation 13-60 is in atm.

### 13.10.3 Clay-Like Soil Cyclic Shear Strength Triggering

Clay-Like soils with soil SSL triggering resistance ratio  $(D/C)_{SL}$  greater than the Clay-Like soil SSL triggering resistance factor  $(\phi_{SL-Clay})$  will be subject to soil SSL approximately equal to the cyclic softening residual shear strength,  $\tau_{rs}$ . Resistance factors used for design shall be those presented in Chapter 9.

### 13.10.4 Clay-Like Soil Cyclic Softening Shear Strength

Saturated NS Clay-Like soils having low sensitivity ( $S_t < 5$ ) and subjected to modest cyclic shear stresses can produce significant permanent strains that can lead to stresses near the soil's yield stress. The degree of saturation of the NS Clay-Like soils should be determined using appropriate laboratory testing. It is noted that the groundwater table may be used as a general indicator of saturation with soils below the groundwater table being considered saturated. Alternatively, all Clay-Like soils may be considered saturated regardless of the depth of the groundwater table. The residual cyclic softening shear strength,  $\tau_{rs}$ , of cohesive soils can be estimated by reducing the soil's undrained shear strength ( $\tau_{Peak} = S_u$ ) using the following equation.

$$\tau_{rs} = 0.8 * \tau_{Peak} \quad \text{Equation 13-62}$$

HS Clay-Like soils having sensitivity ratio,  $S_t \geq 5$  that are subject to modest cyclic shear stresses can experience moderate to significant loss in soil shear strengths. The reduced shear strength can be estimated with the remolded soil shear strength ( $\tau_{remolded}$ ) as indicated in Chapter 7.

### 13.10.5 Seismic Soil Shear Strength Selection

The use of drained/undrained soil shear strengths is dependent on the type of soil and the shear strain level the soil is experiencing. Large variations in shear strain levels can occur during a seismic event from small strains during cyclic loadings to large strains during soil failures. The EE I limit state is used to perform geotechnical analyses for seismic loadings (Design Seismic Events FEE and SEE). Because performance limits for the EE I limit state allow for deformations, the selected shear strength will depend on the strain level that the soil will experience and its potential for soil SSL.

Soil shear strength selection for seismic analyses should be made based on laboratory testing and soil strain level anticipated from analyses. Table 13-7 provides a summary of "general" soil behavior (shear stress vs. strain) observed from published soil stress-strain curves from Holtz and Kovacs (1981), Terzaghi, Peck, and Mesri (1996), and Duncan and Wright (2005). Table 13-9 should be used for "general" guidance on the selection of seismic shear strengths based on soil type and soil strain level anticipated from analyses.

**Table 13-9, Seismic Soil Shear Strength Selection**

Sand-Like Soils (Undrained)	Strain Level at Failure <sup>(1)</sup>			
	Cyclic Strains	±5% Strains	15–20% Strains	Large Strains >20%
Med. To Dense Sand	$\tau_{Peak}$	$\tau_{Peak}$	$\tau_r$	$\tau_r$
Non-Liquefying Loose Sands	$\tau_{Peak}$	$\tau_{Peak}$	$\tau_{Peak}$	$\tau_{Peak}$
Liquefied Soils	$\tau_{rl}$	$\tau_{rl}$	$\tau_{rl}$	$\tau_{rl}$
NS Clay-Like Soils (Undrained)	Strain Level at Failure <sup>(1)</sup>			
	Cyclic Strains	±2% Strains	10–15% Strains	Large Strains >15%
OCR =1, $S_t < 5$	$\tau_{rs}$	$\tau_{Peak}$	$\tau_{Peak}$	$\tau_{Peak}$
OCR >1, $S_t < 5$	$\tau_{rs}$	$\tau_{Peak}$	$\tau_r$	$\tau_r$
HS Clay-Like Soils (Undrained)	Strain Level at Failure <sup>(1)</sup>			
	Typically Failure < 3%			
Highly Sensitive ( $S_t \geq 5$ )	$\tau_{remolded}$			
<b>Shear Strength Nomenclature:</b>				
$\tau_{Peak}$ = Peak Soil Shear Strength		$\tau_{rl}$ = Cyclic Liquefaction Residual Shear Strength		
$\tau_r$ = Residual Soil Shear Strength		$\tau_{rs}$ = Cyclic Softening Residual Shear Strength		
$\tau_{remolded}$ = Remolded Soil Shear Strength				
<sup>(1)</sup> Strain levels indicated are generalizations and are dependent on the stress-strain characteristics of the soil and should be verified by laboratory testing.				

### 13.11 FLOW SLIDE FAILURE

Flow failure occurs when the soils exhibit strain softening and have static gravitational shear stresses larger than the soil shear strengths after soil SSL has occurred. The strain softening can be a result of monotonic or cyclic undrained loading. Flow liquefaction failures typically occur rapidly and are usually catastrophic. Seismic-induced flow failure tends to occur after the cyclic loading ceases due to the progressive nature of the load redistribution; however, if the soils are sufficiently loose and the static shear stresses are sufficiently large, the seismic loading may trigger essentially “spontaneous liquefaction” within the first few cycles of loading leading to flow failure during seismic shaking.

Flow failure is characterized by substantial masses of surficial soils undergoing large translational or rotational deformations that typically occur after the seismic shaking has ceased. The surficial soils undergo deformations when static gravitational driving forces exceed the average soil shear strength after soil SSL has occurred, where the critical failure surface passes through the soil layers that have undergone soil SSL. Because flow liquefaction is driven by the imbalance of  $\tau_{static}$  versus  $\tau_{rl}$ ,  $\tau_{rs}$ , or  $\tau_{remolded}$ , the effects of seismic ground motions (inertial forces due to the seismic shaking) are not included in the analyses.

The evaluation of flow failure proceeds as follows:

1. Perform a soil SSL Triggering analysis to determine which soils are susceptible to soil SSL.
2. Assign appropriate soil shear strengths to Sand-Like, NS Clay-Like, and HS Clay-Like soils susceptible to soil SSL and undrained/drained shear strengths to soils not susceptible to soil SSL.

3. Perform a conventional static slope stability analysis using Spencer's method (no seismic acceleration coefficient). Determine the static resistance to flow failure  $(D/C)_{Flow}$  and the required resistance factor against flow failure,  $\phi_{Flow}$ . If the static resistance to flow failure  $(D/C)_{Flow} > \phi_{Flow}$ , flow failure potential exists at the site. The LRFD equation for use in determining the onset of flow failure is shown below.

$$\left(\frac{D}{C}\right)_{Flow} \leq \phi_{Flow} \quad \text{Equation 13-63}$$

The magnitude of flow failure deformations is typically in excess of 25 feet, depending on the geometry of the flowing ground, the extent of strain softening of the subsurface soils, and the soil stratification. Estimation of lateral flow deformation is very complex and there are currently no accepted methods for evaluating this type of deformation. Since flow failure deformations cannot be reliably estimated, it is assumed that the soils will undergo unlimited deformation and as a result will exert soil pressure loadings on any structures that are affected by the flow failure movements.

### 13.12 SEISMIC ACCELERATION COEFFICIENTS

The magnitude of seismic inertial forces and seismic loading (active / passive pressures) that are used in pseudo-static stability analyses or limit-equilibrium analyses of ERSs are based on computing average horizontal acceleration coefficients adjusted for wave scattering ( $k_h$ ). The  $k_h$  is computed using the PGA at the ground surface with adjustments that typically reduce the acceleration by taking into account wave scattering of the horizontal ground accelerations and displacements of a yielding structure. The wave scattering scaling factor ( $\alpha_w$ ) is dependent on the design pseudo-spectral acceleration at 1 second ( $S_{D1}$ ) from the ADRS curve and the height of the embankment, slope, or ERS.

Seismic inertial loadings are typically estimated by pseudo-static analytical methods that consist of multiplying the average  $k_h$  and average vertical seismic coefficient ( $k_v$ ) by the mass of the soil or structure that is being accelerated due to the seismic shaking. The  $k_v$  is typically neglected ( $k_v = 0$ ) by the fact that the vertical accelerations will be out of phase with the horizontal accelerations. According to AASHTO LRFD Specifications,  $k_v$  is usually very small when  $k_h$  approaches its maximum value. The  $k_h$  is used to compute a constant horizontal force in global seismic stability of slopes and ERSs. The  $k_h$  has typically been assigned some fraction (0.3 to 0.7) of the PGA. Reductions in PGA are typically attributable to either wave scattering or stress relief associated with displacements. The displacement dependent stress relief reduction of the horizontal seismic coefficient is computed using the Newmark displacement method as shown in Section 13.14.

Wave scattering is a term used to account for the seismic wave incoherence or variations behind a wall or slope. Kavazanjian, et al. (2012) provides a relationship utilizing a scale factor,  $\alpha_w$ , (reduction factor) to account for wave scattering as indicated by the following equation.

$$k_h = k_{avg} = \alpha_w * PGA \quad \text{Equation 13-64}$$

Where,

- $k_h$  = Average seismic horizontal coefficient due to wave scattering
- $\alpha_w$  = Wave scattering scaling factor (reduction factor)
- PGA = Peak ground acceleration coefficient for the design event ( $k_{max}$ )

The  $\alpha_w$  was found to be dependent on the ground motion and the height of the wall or slope as shown in Figure 13-31. For wall or slope heights greater than 100 feet a  $\alpha_w$  of 0.5 shall be used.

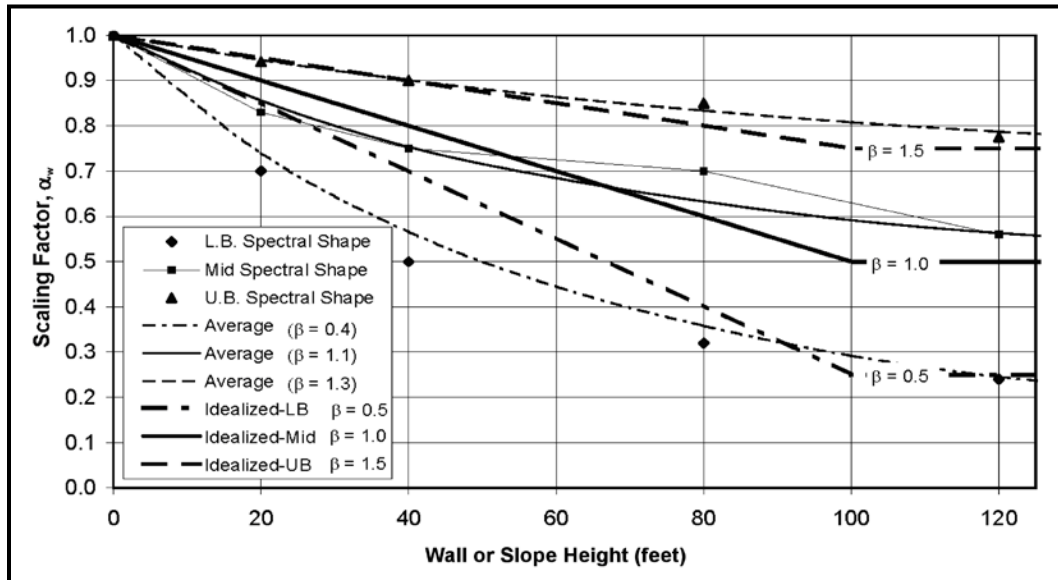


**Figure 13-31, Simplified Wave Scattering Scaling Factor (Kavazanjan, et al. (2012))**

For wall or slope heights less than or equal to 100 feet,  $\alpha_w$  shall be determined by the following equation.

$$\alpha_w = 1.0 + 0.01 * H * [(0.5 * \beta) - 1] \leq 1.0 \quad \text{Equation 13-65}$$

Where,

H = Height of slope or ERS above the natural ground surface,  $H \leq 100$  feet, feet

$\beta$  = Ground motion index that is used to characterized shape of the ADRS.

The ground motion index ( $\beta$ ), is computed using the following equation and typically has a lower bound of 0.5 and an upper bound 1.5. The lower bound value is typically associated with seismic conditions in the eastern United States, ground conditions with average  $V_s$  greater than or equal to 2,500 feet per second ( $\overline{V_s} \geq 2,500$  ft/sec) and low acceleration levels. The upper bound is typically associated with seismic conditions in the Western United States, ground conditions with average  $V_s$  less than 2,500 feet per second ( $\overline{V_s} < 2,500$  ft/sec) and high acceleration levels.

$$\beta = \frac{S_{D1}}{PGA} \quad \text{Equation 13-66}$$

Where,

$S_{D1}$  = Peak ADRS spectral acceleration at 1 second (Chapter 12)

PGA = Peak horizontal acceleration at ground surface (Chapter 12)

The  $\alpha_w$  determined above is applicable to soil sites, for sites founded on rock,  $\alpha_w$  should be increased by 20 percent.

### 13.13 SEISMIC GLOBAL STABILITY

The standard-of-practice for evaluating seismic global instabilities consists of performing pseudo-static limit equilibrium slope stability analyses. Global instability shall be checked when  $(D/C)_{\text{flow}} \leq \phi_{\text{flow}}$  (Section 13.11). The pseudo-static limit equilibrium slope stability analysis is a modified conventional slope stability analysis that allows the inclusion of inertial driving forces generated by the seismic event as an equivalent static horizontal force acting on the potential sliding mass (see Figure 13-32) or includes both the inertial driving forces as well as the reduced shear strength of any soil that has experienced soil SSL. The inclusion of both the inertial driving forces and the reduced shear strengths caused by soil SSL is called lateral spread. As required in Chapter 17 both circular and non-circular potential failure surfaces shall be checked. The pseudo-static slope stability method uses the average horizontal acceleration coefficients adjusted for wave scattering ( $k_h$ ) as indicated in Section 13.12 to compute the inertial loadings in the seismic global stability analysis. If the seismic slope stability ratio  $(D/C)_{\text{EQ-Stability}} \leq \phi_{\text{EQ-Stability}}$ , then the EE I limit state stability requirements and performance criteria have been satisfied. If the seismic slope stability ratio  $(D/C)_{\text{EQ-Stability}} > \phi_{\text{EQ-Stability}}$ , then a Newmark sliding block analysis (Section 13.14) is performed to estimate the displacements and determine if they meet the performance criteria. If the failure surface is circular all displacements at the top of the slope shall be considered to be vertical. All displacements at the top of the slope for a non-circular failure surface shall be considered horizontal.

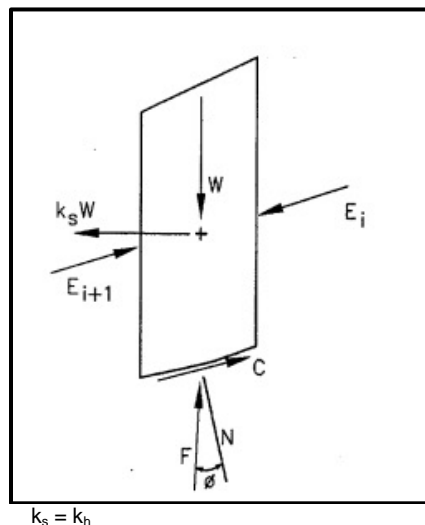


**Figure 13-32, Pseudo-Static Limit Equilibrium Analysis Slice (Kavazanjian, et al. (2012))**

No pseudo-static slope stability analysis is needed for bridge embankments meeting the requirements of Table 13-10 and the conditions established in this paragraph. No analysis is required when soil SSL is not predicted in the bridge embankment soil slope profile or the criteria for no soil SSL analysis is met (see Section 13.3.2); the water table is not located within the bridge embankment; and the soils that compose the bridge embankment are homogenous (i.e., there are no thin layers of soft soil within the slope model). In addition, it is assumed either less than 2 inches of horizontal movement occurs at the top of the slope (assumes non-circular failure surface) or less than 2 inches of vertical settlement occurs at the top of the slope (assumes circular failure surface).

**Table 13-10, No Slope Stability Analysis Required**

<b>Slope Angle</b>	<b>Total Embankment Height</b>	<b>PGA</b>
2H:1V	≤ 10 ft	≤ 0.2g
3H:1V and flatter	≤ 15 ft	≤ 0.3g

The overall seismic global slope stability evaluation process is shown as follows:

1. Determine seismic parameters (PGA,  $S_{D1}$ , and PGV) from Chapter 12.
2. Determine wave scattering scaling factor ( $\alpha_w$ ) from Section 13.12.
3. Compute average horizontal seismic coefficient,  $k_h$ , in accordance with Section 13.12.
4. Perform a conventional pseudo-static slope stability analysis (using Spencer's method) conforming to the requirements of Chapter 17 with average horizontal acceleration coefficient adjusted for wave scattering ( $k_h$ ). The vertical acceleration coefficient ( $k_v$ ) is assumed to equal zero. Assign appropriate soil shear strengths based on soil SSL triggering to Sand-Like soils, NS Clay-Like soils, and HS Clay-Like soils that are susceptible to soil SSL. Use peak undrained/drained shear strengths for soils not susceptible to soil SSL.
5. Determine the seismic stability resistance ratio  $(D/C)_{EQ-Stability}$ . Obtain the required seismic slope instability resistance factor ( $\phi_{EQ-Stability}$ ) from Chapter 9. The LRFD equation shown below is used to determine if the slope is seismically unstable.

$$\left(\frac{D}{C}\right)_{EQ-Stability} \leq \phi_{EQ-Stability} \quad \text{Equation 13-67}$$

If the seismic instability ratio  $(D/C)_{EQ-Stability} \leq \phi_{EQ-Stability}$ , then there is no potential for seismic slope instability. If the seismic instability ratio  $(D/C)_{EQ-Stability} > \phi_{EQ-Stability}$ , seismic instability potential exists at the site and the evaluation process should continue to Step 6 to evaluate the displacements.

6. Compute the horizontal yield acceleration ( $k_y$ ) by varying the horizontal acceleration until the seismic instability ratio  $(D/C)_{EQ-Stability} = 1.0$ . If the ratio of  $k_y$  to  $k_h$  is more than 0.5 ( $k_y/k_h \geq 0.5$ ), then a displacement ( $\Delta L$ ) of 2 inches shall be assumed and reported. As indicated previously, if the failure surface is circular all displacements at the top of the slope shall be considered to be vertical, while all displacements at the top of the slope for a non-circular failure surface shall be considered horizontal.
7. If  $k_y/k_h$  is less than 0.5 ( $k_y/k_h < 0.5$ ), compute the deformations ( $\Delta L$ ) induced by seismic slope instability using the Newmark sliding block method described in Section 13.14.
8. If the displacements are within the acceptable performance criteria established by the design team, then the seismic slope stability hazard is acceptable with respect to the EE I limit state. If the deformations computed exceed the performance criteria established by the design team then develop methods to



mitigate this hazard as indicated in Chapter 14 and then evaluate the seismic global stability hazard again (Step 4).

### 13.14 NEWMARK SEISMIC DISPLACEMENT METHODS

The Newmark sliding block model is used to evaluate displacements that occur as a result of an imbalance between driving forces (static and seismic) and loss in resisting forces (strain softening of soils) acting on the displaced soil mass. The models that have been developed based on Newmark rigid sliding block assume that the deformation takes place on a well-defined failure surface, the yield acceleration remains constant during shaking, and the soil is perfectly plastic. The displacements are computed based on the cumulative displacements of the sliding mass generated when accelerations exceed the yield acceleration that defines the point of impending displacement. Newmark type methods for computing deformations are typically associated with an improved reliability when compared to the empirical methods because it is a numerical method that permits modeling of the site response for the design seismic event being investigated.

The state-of-practice is that the assumptions used in the Newmark sliding block model provide reasonable results when the shear failure surface as a whole has not lost more than 50% of the shear resistance prior to the soil's SSL. These assumptions are applicable to seismic slope instability and to lateral seismic deformation of gravity ERSs that are not significantly affected by cyclic liquefaction. Bardet, et al. (1999) observed that when cyclic liquefaction occurs in a lateral spread, the assumptions of the Newmark sliding block model requirements are not met because (1) the shear strain in liquefied soil does not concentrate within a well-defined surface, (2) the shear strength and yield acceleration of saturated soils varies during cyclic loading as pore pressure varies, and (3) soils are generally not perfectly plastic materials, but commonly harden and/or soften.

Several analytical methods based on the Newmark sliding block model have been developed to estimate deformations induced by seismic cyclic loadings. The Newmark type methods typically fall into one of the following categories:

- Newmark Time History Analyses
- Simplified Newmark Charts

The Newmark Time History Analyses method can be performed using the design seismic time history acceleration record if a Site-specific Seismic Response Analysis is performed in accordance with Chapter 12. Alternatively, Simplified Newmark charts can be used when a site-specific seismic response is not performed. The Simplified Newmark charts are based on a large database of seismic records and the Newmark Time History Analysis method to develop charts that relate the ratio of acceleration to yield acceleration occurring at the base of the sliding mass to ground displacement.

If a Site-specific Seismic Response Analysis is performed in accordance with Chapter 12, then the Newmark Time History Analyses should be performed in combination with the Simplified Newmark evaluation to validate deformation analyses performed using the Newmark Time History Analyses. If a simplified site response method is used (i.e., 3-Point ADRS curves) to evaluate the local response site effects, then the Simplified Newmark charts should be used. The Newmark time history method and the Simplified Newmark charts are described in the following Sections.

### 13.14.1 Newmark Time History Analyses

The Newmark “sliding block” method for analyzing ground displacements along a shear plane was developed by Newmark (1965). Newmark’s method has been applied to seismic slope stability performance of dams, embankments, natural slopes, and retaining walls (Newmark (1965), Makdisi and Seed (1978), Yegian, et al. (1991), Jibson (1994), and Richards and Elms (1979)). This method is typically incorporated into computer programs as described by Houston, Houston, and Padilla (1987).

Randall W. Jibson, Ellen M. Rathje, Matthew W. Jibson and Yong W. Lee have developed a computer program, SLAMMER, to model slope performance during seismic events. The Java program uses a modification of Newmark’s method where a decoupled analysis is performed that allows modeling landslides that are not assumed to be rigid blocks. The software and more information can be obtained at the USGS website <https://pubs.usgs.gov/tm/12b1/>.

Ebeling, et al. (2007) have developed a computer program for the US Army Corps of Engineers that estimates the translational response of retaining walls to seismic ground motions called  $C_{\text{orps}}W_{\text{allSlip}}$  (CWSlip) that could be used to estimate lateral displacements for gravity ERSs.

In the Newmark method, the deformations are assumed to occur along a well-defined plane and the sliding mass is assumed to be a rigid block as shown in Figure 13-33. When the seismic accelerations exceed a yield acceleration threshold, the sliding mass displaces as indicated in Figure 13-34. The displacement accumulates over a time span ( $t_3 - t_1$ ) where the acceleration exceeds the  $k_y$  at time  $t_1$  to when the induced velocity drops to zero at time  $t_3$ . The displacements are computed by double integrating the accelerogram over the time span ( $t_3 - t_1$ ). Displacement is cumulative over each cycle for the duration of the seismic event as indicated in Figure 13-34. The total displacement is computed as the cumulative displacement that occurs during the seismic shaking.

Note that the  $k_y$  in Figure 13-34 varies with the level of acceleration as a result of the cyclic soil strength degradation or liquefaction. Soils that are subject to significant strain softening will develop lower  $k_y$  thresholds as the seismic-induced cyclic soil strength degradation progresses. The  $k_y$  generally remains constant because of the conservative approach used to determine its value.

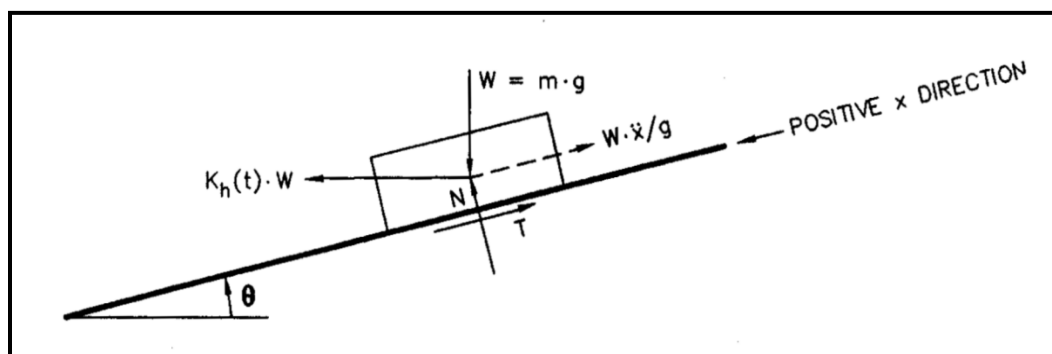


**Figure 13-33, Newmark Sliding Block Method (Matasovic, Kavazanjian, and Giroud (1998))**

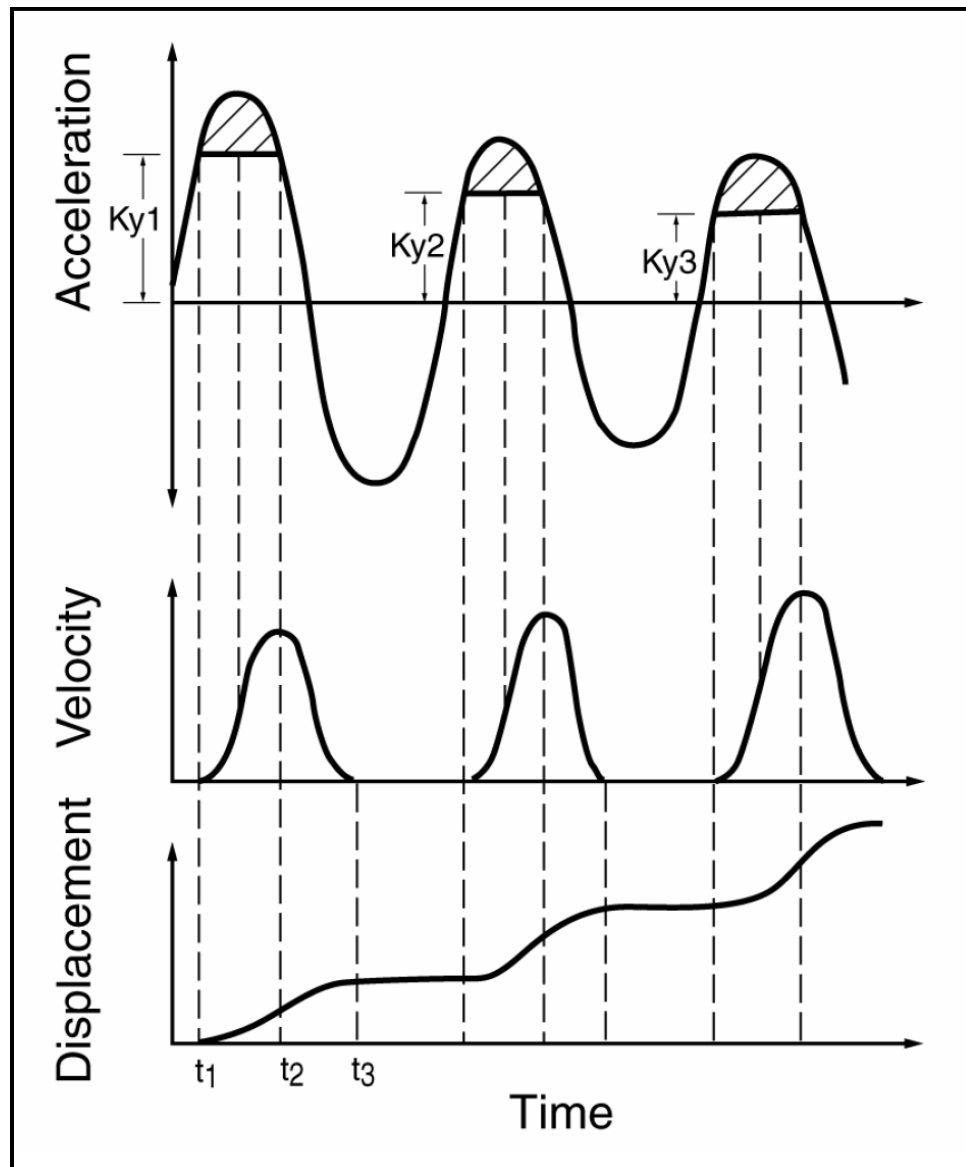


**Figure 13-34, Newmark Time History Analysis  
(Goodman and Seed (1966) with permission from ASCE)**

The seismic shaking that triggers the displacement is characterized by an acceleration record at the base of the sliding mass for the design seismic event being evaluated. A minimum of 12 independent seismic records should be selected from a catalogue of seismic records that are representative of the source mechanism,  $M_w$ , and  $R$ . A sensitivity analysis of the input parameters used in the site-specific response analysis should be performed to evaluate its effect on the magnitude of the displacement computed.

A pseudo-static slope stability analysis is performed to determine the threshold  $k_y$  where displacements begin to occur for a specific critical failure surface. The pseudo-static slope stability analysis should be performed with cyclic residual shear strength (Section 13.10) assigned to soils with the potential for soil SSL. The  $k_y$  is the acceleration that corresponds to a pseudo-static slope stability analysis for a critical failure surface with a seismic stability resistance ratio of  $(D/C)_{EQ-Stability} = 1.0$  ( $1/FS = 1.0$ ).

The following are sources of uncertainty that are inherent when using the Newmark Time History Analysis method to compute displacements in the CEUS:

- Lack of strong motion time history records in the CEUS
- Seismic source mechanism is not well understood
- $R$  is not well defined in the CEUS
- Infrequency of seismic events in the last 10,000 years (Holocene Period)
- Point in the time history when cyclic strength degradation or liquefaction is triggered
- Magnitude of the apparent post-liquefaction residual resistance
- Influence of the thickness of liquefied soil on displacement
- Changes in values of  $k_y$  as deformation accumulates
- Influence of non-rigid sliding mass
- Influence of ground motion incoherence over the length of the sliding mass

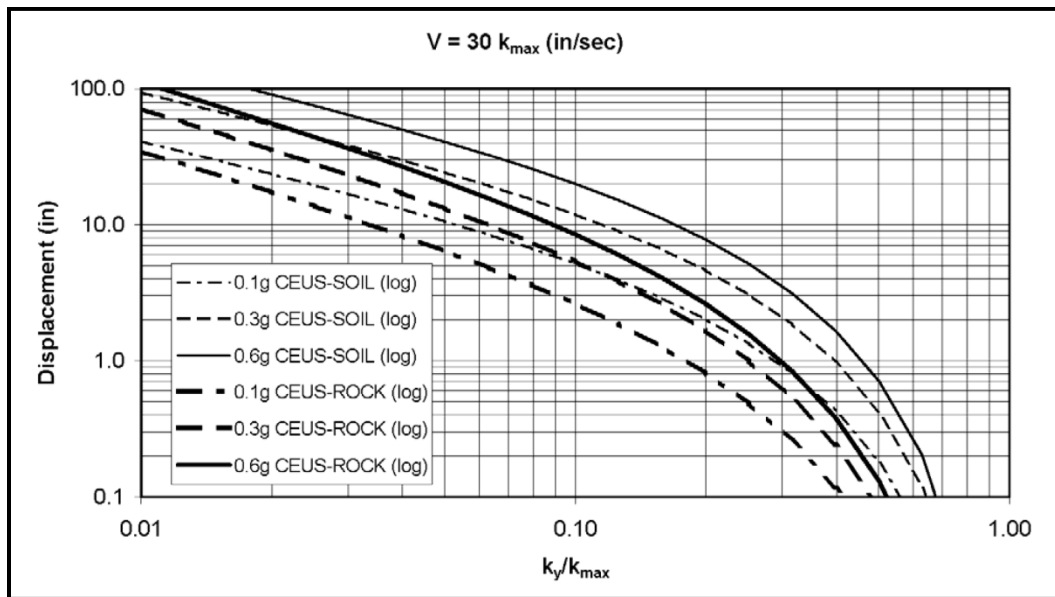
Because of the uncertainties involved in the selection of the time history acceleration records in the CEUS, results of the Newmark Time History Analyses must be compared with the results obtained using Simplified Newmark Charts discussed in Section 13.14.2.

### **13.14.2 Simplified Newmark Charts**

Simplified Newmark displacement charts were developed as a result of the Anderson, Martin, Lam, and Wang (2008) study based on Newmark's Time History Analyses discussed in Section 13.14.1. These Simplified Newmark displacement charts are based on the seismic database published by Hynes and Franklin (1984). The database of seismic records used for this study was limited to seismic events with moment magnitudes of  $6.0 \leq M_w \leq 7.5$ .

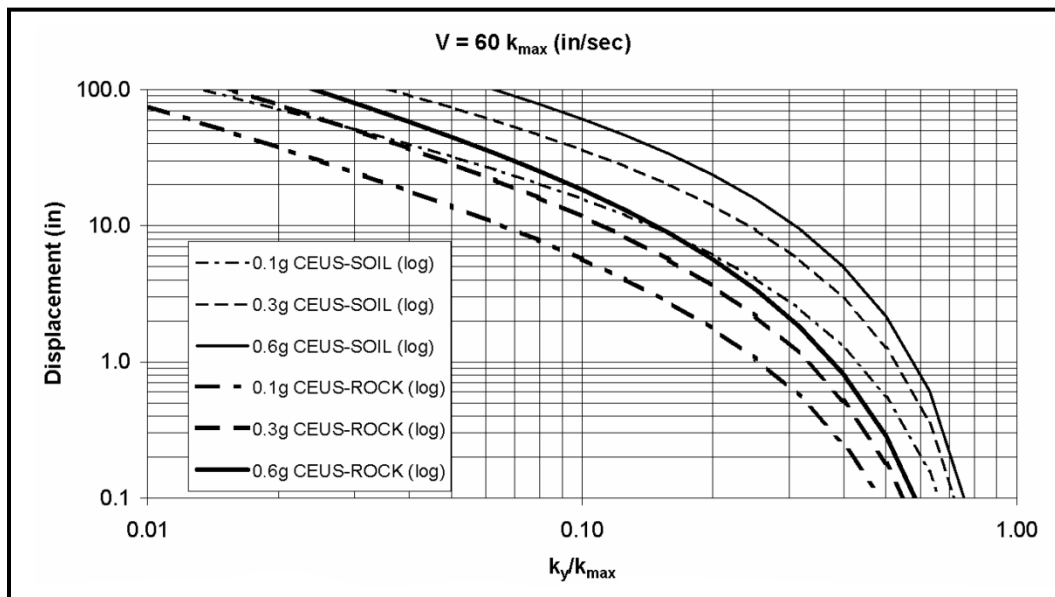
These charts have been developed as a function of a ratio ( $k_y / k_{max}$ ) or  $k_y$  to  $k_{max}$  ratio,  $PGV = V_{Peak}$ ,  $PGA$ , and by region of the United States (WUS and CEUS) for either rock or soil site conditions. The charts shown in Figures 13-35 and 13-36 are based on a seismic moment magnitude of  $6.0 \leq M_w \leq 7.5$  in the CEUS. Figure 13-35 is appropriate for a stiff site with a peak ground velocity of  $PGV = 30 k_{max}$  in/sec ( $PGV = 760 k_{max}$  mm/sec). Figure 13-36 is appropriate for a soft soil site with a peak ground velocity of  $PGV = 60 k_{max}$  in/sec ( $PGV = 1520 k_{max}$  mm/sec).

The computed displacements should be compared with the required Performance Limits as required in Chapter 10 that have been previously established by the design team.



V=PGV; k<sub>max</sub> = PGA

**Figure 13-35, Simplified Newmark Chart (PGV = 30 k<sub>max</sub> in/sec)  
(Anderson, et al. (2008))**



V=PGV; k<sub>max</sub> = PGA

**Figure 13-36, Simplified Newmark Chart (PGV = 60 k<sub>max</sub> in/sec)  
(Anderson, et al. (2008))**

In lieu of using charts in Figures 13-35 and 13-36 to compute the residual displacement, *d*, for predetermined site factors (PGA and PGV), the following may be used for design specific site factors.

**CEUS-Rock (Standard Error of 0.31 log<sub>10</sub> units):**

$$\begin{aligned}
 \log d = & -1.31 - 0.93 * \log \left( \frac{k_y}{PGA} \right) + 4.52 * \log \left[ 1 - \left( \frac{k_y}{PGA} \right) \right] - 0.46 \\
 & * \log PGA + 1.12 \log PGV
 \end{aligned}$$

**Equation 13-68**

**CEUS-Soil (Standard Error of 0.23 log<sub>10</sub> units):**

$$\log d = -1.49 - 0.75 * \log \left( \frac{k_y}{PGA} \right) + 3.62 * \log \left[ 1 - \left( \frac{k_y}{PGA} \right) \right] - 0.85 * \log PGA + 1.61 * \log PGV \quad \text{Equation 13-69}$$

Where,

$k_y$  = Yield Acceleration, g (Sections 13.14 and 13.15.1)

PGV = Peak Ground Velocity, inches/sec. Correlations of peak ground velocity are found in Chapter 12.

**13.15 SEISMIC SOIL SETTLEMENT**

Seismically-induced ground settlements are one of the potential geotechnical seismic hazards that must be evaluated. Seismically induced ground settlements that are not due to flow failure or global instability are typically caused by densification of the underlying soils during shaking. Densification or seismic compression of soils has been observed in unsaturated sands, silts, and clayey sands above the water table. Densification of saturated loose sands subject to cyclic liquefaction has also been observed below the water table. Seismic settlements for depths greater than 80 feet, do not need to be computed unless the settlements are being computed to evaluate the effects of downdrag on deep foundations.

Soil settlements computed for unsaturated soils and saturated soils are additive as indicated by the following equation.

$$S_{TS} = S_{us} + S_{sat} \quad \text{Equation 13-70}$$

Where,

$S_{TS}$  = Total seismic settlement, inches.

$S_{us}$  = Total seismic settlement of unsaturated soils, inches (Section 13.15.3)

$S_{sat}$  = Total seismic settlement of saturated soils, inches (Section 13.15.4)

Given the relative shallow depth of groundwater throughout most of the South Carolina Coastal Plain, the unsaturated seismic settlement is anticipated to be small (less than 1 inch) and therefore, will not need to be determined. The procedures presented in the following Section for computing settlements are only applicable in the absence of flow failure and/or global instability. Soils susceptible to ground settlements that are located below sloping ground or adjacent to a free-face may be subject to static driving shear stresses oriented towards down-slope or free-face direction. The presence of static driving shear stresses for these site conditions will tend to increase vertical settlements and lateral displacements. Since the simplified methods presented to analyze settlements do not account for static driving shear stresses, the GEOR should be aware that settlements may be on the order of 10 percent to 20 percent greater (Wu (2002)).

### 13.15.1 Soil Characterization

The corrected SPT driving resistance ( $N_{1,60}^*$ ) will be computed in accordance with Chapter 7. For soils with FC greater than 5 percent, the SPT driving resistance must be adjusted for fines content to obtain an equivalent corrected clean sand SPT resistance ( $N_{1,60,cs}^*$ ) in accordance with Section 13.9.1.

The normalized corrected CPTu tip resistance ( $q_{c,1,N}$ ) will be computed in accordance with Chapter 7. For soils with FC greater than 5 percent, the normalized corrected CPTu tip resistance must be adjusted for fines content to obtain an equivalent normalized corrected clean sand tip resistance ( $q_{c,1,N,CS}$ ) in accordance with Section 13.9.2.

When seismic settlement methods require an equivalent normalized corrected clean sand SPT resistance ( $N_{1,60,cs}^*$ ) and only CPTu in-situ testing data are available to compute seismic settlements, the normalized cone tip resistance,  $q_{c,1,N}$ , (Chapter 7) will be correlated to corrected SPT  $N_{1,60}^*$  values in accordance with Chapter 7. The correlated SPT blow count ( $N_{1,60}^*$ ) should then be adjusted for FC greater than 5 percent, in accordance with Section 13.9.1.

### 13.15.2 Saturated Sand Settlement

Settlement of saturated sands can occur when Sand-Like soils have the potential to experience cyclic liquefaction due to dissipation of excess pore water pressure generated during the seismic shaking. These soils reconsolidate as the pore water pressure dissipates and the sand particles rearrange into a more compact state, causing settlement. Seismically induced settlements of Sand-Like soils that have the potential to experience cyclic liquefaction are typically larger than compaction settlements that result from unsaturated sands (these settlements are ignored). Several methods to evaluate the magnitude of seismic settlement of saturated sands have been proposed by Tokimatsu and Seed (1987), Ishihara and Yoshimine (1992), Shamoto, et al. (1998), and Wu (2002). These methods all use the reconsolidation volumetric strain due to cyclic liquefaction ( $\varepsilon_v$ ). The total settlement,  $S_{sat}$ , of Sand-Like Soils with the potential to experience cyclic liquefaction is computed using the following equation.

$$S_{sat} = \sum_{n=1}^{i_{sat}} \delta_{sat} = \sum_{n=1}^{i_{sat}} \varepsilon_v * H_{sat} \quad \text{Equation 13-71}$$

Where,

- $\delta_{sat}$  = Post-Liquefaction Settlement of Saturated Sand layer, inches
- $\varepsilon_v$  = Reconsolidation Volumetric Strain due to Liquefaction, percent (%)
- $H_{sat}$  = Layer Thickness of Saturated Sand layer, inches
- $i_{sat}$  = Total number (n) of Potentially Liquefiable sand layers

The most referenced method used to compute the settlement potential of saturated liquefiable clean sands was proposed by Tokimatsu and Seed (1987). Several other methods (Ishihara and Yoshimine (1992), Shamoto, et al. (1998), and Wu (2002)) have been proposed that address some of the deficiencies found with Tokimatsu and Seed (1987) with respect to soils that have higher fines content. Idriss and Boulanger (2008) compared these 3 alternate methods as shown in Figure 13-37.

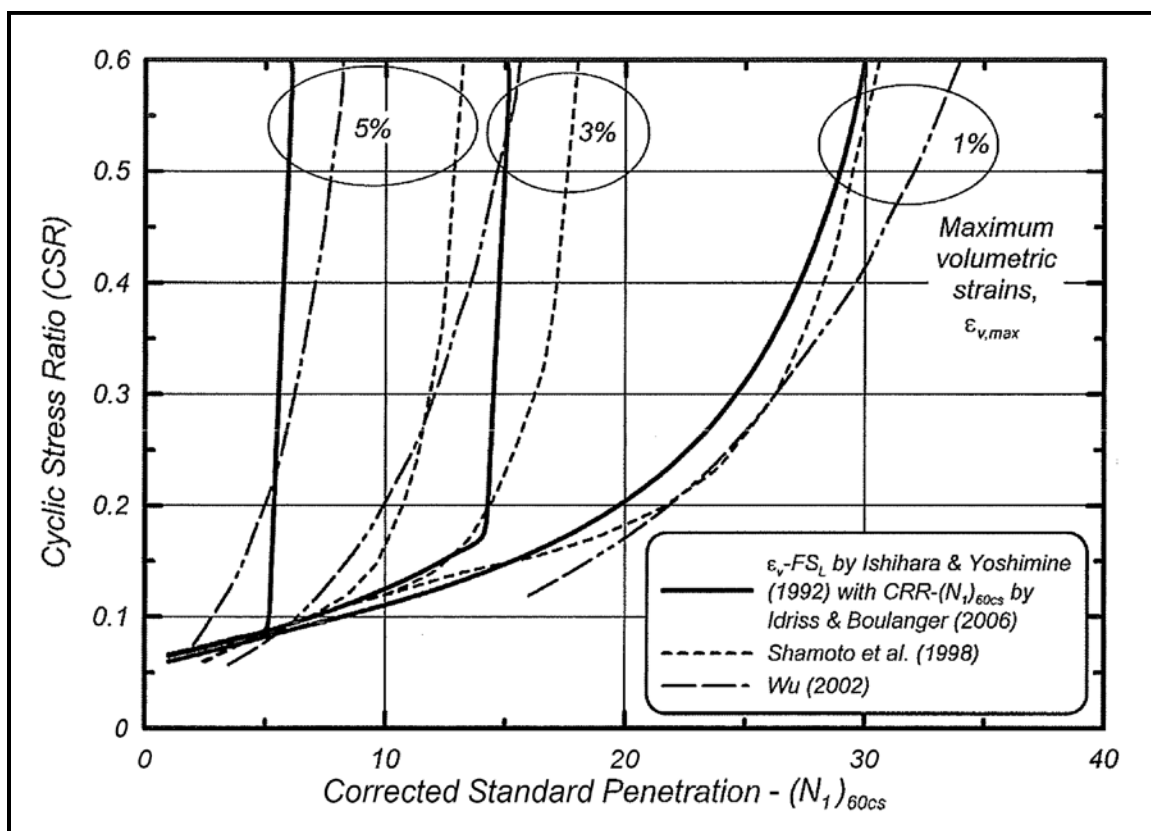


Figure 13-37, Volumetric Strain Relationship Comparison -  $M_w=7.5$ ;  $\sigma'_{vc} = 1 \text{ atm}$  (Idriss and Boulanger (2008))

The settlement of saturated sands that are potentially liquefiable shall be computed based on Idriss and Boulanger (2008) recommended reconsolidation volumetric strain,  $\epsilon_v$ , relationship based on Ishihara and Yoshimine (1992) shown in Figure 13-38. The  $\epsilon_v$  from Ishihara and Yoshimine (1992) has been approximated by Yoshimine, Nishizaki, Amano, and Hosono (2006) using the following equations for SPT N-values and CPT tip resistances.

$$\epsilon_v = 1.5 * e^{(-0.3698 \sqrt{N_{1,60,CS}^*})} * \min(0.08 \text{ or } \gamma_{max}) \quad \text{Equation 13-72}$$

$$\epsilon_v = 1.5 * e^{(2.551 - 1.147(q_{c,1,N,CS})^{0.264})} * \min(0.08 \text{ or } \gamma_{max}) \quad \text{Equation 13-73}$$

Where,

- $N_{1,60,CS}^*$  = Normalized and corrected SPT N-values (Section 13.9.1)
- $q_{c,1,N,CS}$  = Normalized and corrected CPT tip resistance (Section 13.9.2)
- $\gamma_{max}$  = Maximum cyclic shear strain

Idriss and Boulanger (2008) recommend placing a limit on  $\gamma_{max}$  ( $\gamma_{lim}$ ) depending on the resistance factor for Sand-Like soil  $SSL (D/C)_{SL}$ . The limitations for  $\gamma_{max}$  are listed as follows

$$\text{If } \left(\frac{D}{C}\right)_{SL} \leq 0.5 \text{ then } \gamma_{max} = 0 \quad \text{Equation 13-74}$$



$$\text{If } 0.5 < \left(\frac{D}{C}\right)_{SL} < \frac{1}{F_\alpha} \text{ then ...} \quad \text{Equation 13-75}$$

$$\gamma_{max} = \min \left\{ 0.08 \text{ or } \left[ 0.035 * (2 - \Phi_{SL}) * \left( \frac{1-F_\alpha}{\Phi_{SL}-F_\alpha} \right) \right] \right\} \quad \text{Equation 13-76}$$

$$\text{If } \left(\frac{D}{C}\right)_{SL} \geq \frac{1}{F_\alpha} \text{ then } \gamma_{max} = \gamma_{lim} \quad \text{Equation 13-77}$$

Where,

$$\Phi_{SL} = \frac{1}{\left(\frac{D}{C}\right)_{SL}} \quad \text{Equation 13-78}$$

$$F_\alpha = 0.032 + 0.69 * \sqrt{N_{1,60,CS}^*} - 0.13 * N_{1,60,CS}^* \quad \text{Equation 13-79}$$

For  $N_{1,60,CS}^* \geq 7$  blows per foot

$$F_\alpha = -11.74 + 8.34 * (q_{t,1,N,CS})^{0.264} - 1.371 * (q_{t,1,N,CS})^{0.528} \quad \text{Equation 13-80}$$

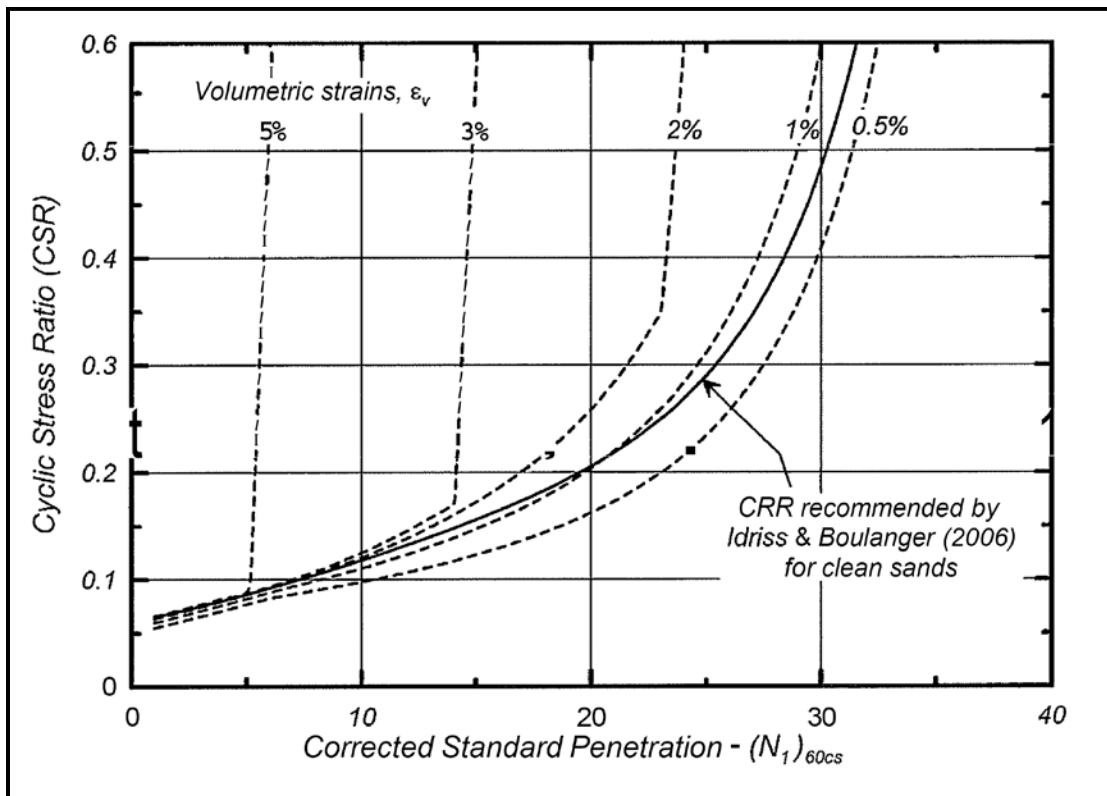
For  $q_{t,1,N,CS} \geq 69$  unitless

$$\gamma_{lim} = 1.859 * \left( 1.1 - \sqrt{\frac{N_{1,60,CS}^*}{46}} \right)^3 \geq 0 \quad \text{Equation 13-81}$$

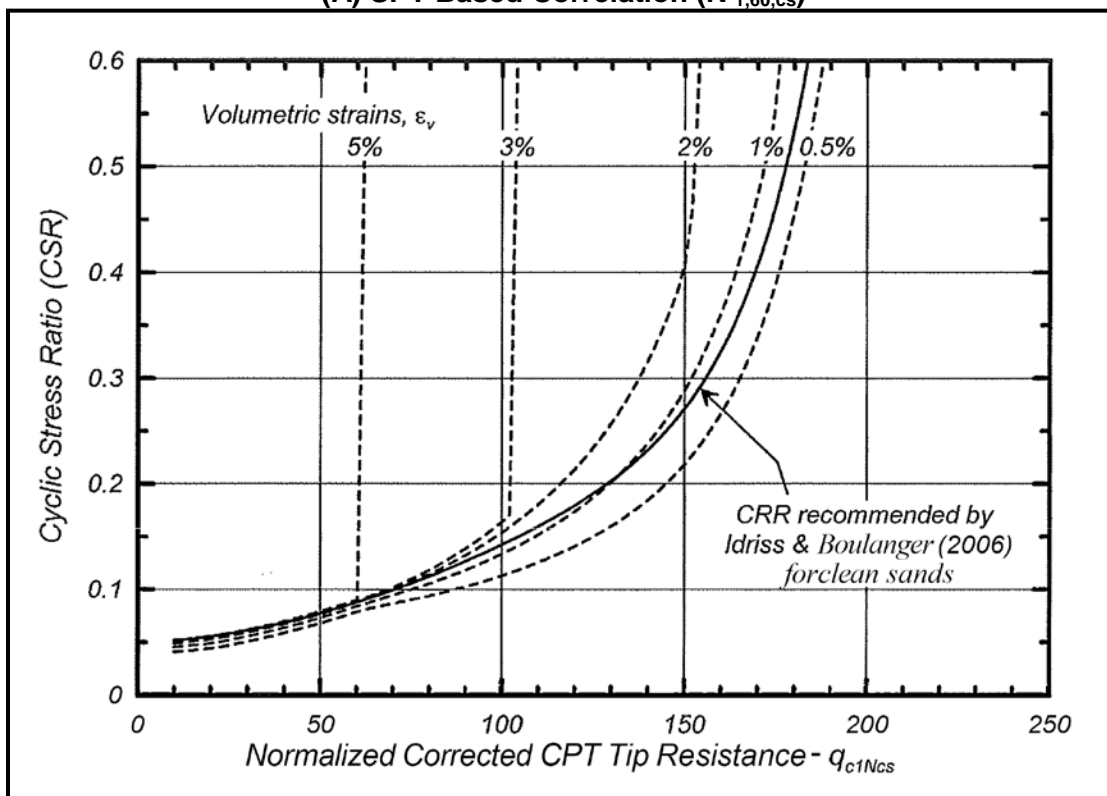
$$\gamma_{lim} = 1.859 * \left( 2.163 - 0.478 * (q_{t,1,N,CS})^{0.264} \right)^3 \geq 0 \quad \text{Equation 13-82}$$

Reconsolidation volumetric strain,  $\varepsilon_v$ , relationships for SPT and CPTu results in Figure 13-38 have been developed to be compatible by using the correlations for relative density from SPT and CPTu in Chapter 7. The  $CSR_{eq}^*$  is computed based on Section 13.8.

The use of reconsolidation volumetric strain,  $\varepsilon_v$ , relationship based on Shamoto, et al. (1998), or Wu (2002) will require approval from the PC/GDS. If CPTu testing data are used with these relationships, the correlations for relative density from SPT and CPTu in Chapter 7 shall be used in order to maintain compatibility between testing methods.



(A) SPT Based Correlation ( $N_{1,60,cs}^*$ )



Note:  $q_{c,1,N,CS} = q_{t,1,N,CS}$

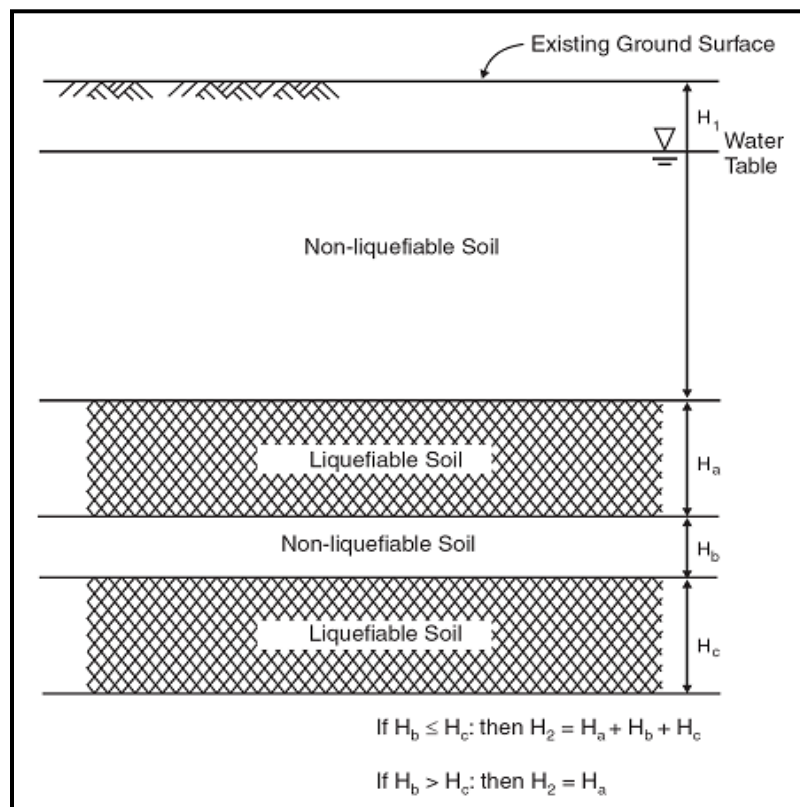
(B) CPT Based Correlation ( $q_{t,1,N,cs}$ )

Figure 13-38, Volumetric Strain Relationship -  $M_w=7.5$ ;  $\sigma'_{vc} = 1$  atm (Ishihara and Yoshimine (1992); modified by Idriss and Boulanger (2008))

When soils are stratified and potentially cyclic liquefiable layers are located between non-liquefiable soil layers, there is a possibility of under-predicting or over-predicting excess pore water developed depending on the location of the soil layers within the stratified system (Polito and Martin (2001)). Polito and Martin (2001) have shown that thin layers of dense sand (non-liquefiable soil) could liquefy if sandwiched between liquefiable soil layers. Ishihara (1985) proposed the method shown in Figure 13-39 to determine the thickness,  $H_2$ , of the liquefiable soil layer.  $H_1$  is the thickness of the non-liquefiable soil layer above the liquefiable soil layer,  $H_2$ . The thickness of the liquefiable soil layer,  $H_2$ , is dependent on criteria indicated in Figure 13-39. In addition to the criteria indicated in Figure 13-39, the following criteria must also be satisfied:

1. Thickness of the non-liquefiable layer ( $H_b$ ) is less than or equal to 5 feet ( $H_b \leq 5$  feet).
2. Non-liquefiable soil layer "B" has a normalized and corrected SPT  $N_{1,60,cs}^* < 30$  blows/foot or a normalized corrected CPT tip resistance  $q_{1,c,N,cs} < 170$ .
3. Non-liquefiable soil layer "B" is a sand or silty sand with  $FC \leq 35$ .
4. Moment magnitude of design seismic,  $M_w \geq 7.0$ .

This procedure to evaluate thickness,  $H_2$ , of liquefiable soil layers is used for all subsequent soil layers that have the potential to liquefy in the stratified soil system.



**Figure 13-39, Liquefiable Soil Layer Thickness in Stratified Soils (Ishihara (1985))**

## 13.16 REFERENCES

American Association of State Highway and Transportation Officials, (2017), AASHTO LRFD Bridge Design Specifications Customary U.S. Units, 8<sup>th</sup> Edition, American Association of State Highway and Transportation Officials, Washington, D.C.

Anderson, D. G., Martin, G. R., Lam, I. and Wang, J. N., (2008), "Seismic Analysis and Design of Retaining Walls, Buried Structures, Slopes and Embankments", NCHRP Report 611, Volumes 1 and 2, Transportation Research Board.

Bardet, J. P., Mace, N. and Tobita, T. (1999), "Liquefaction-induced Ground Deformation and Failure." Report to PEER/PG&E, Task 4A - Phase 1, University of Southern California, Los Angeles.

*as of Geotechnical and Geoenvironmental Engineering*, ASCE, v. 129, Issue 12, pp. 1071 - 1082.

Boulanger, R. W. (2003b), "Relating  $K_a$  to a Relative State Parameter Index", *Journal of Geotechnical and Geoenvironmental Engineering*, ASCE, v. 129, Issue 8, pp. 770 - 773.

Boulanger, R. W., and Idriss, I. M. (2004), "Evaluating the Potential for Liquefaction or Cyclic Failure of Silts and Clays", Report UCD/CGM-04/01, Center for Geotechnical Modeling, University of California, Davis, California.

Boulanger, R. W., and Idriss, I. M. (2006), "Liquefaction Susceptibility Criteria for Silts and Clays", *Journal of Geotechnical and Geoenvironmental Engineering*, ASCE, v. 132, Issue 11, pp. 1413 - 1426.

Boulanger, R. W., and Idriss, I. M. (2007), "Evaluation of Cyclic Softening in Silts and Clays", *Journal of Geotechnical and Geoenvironmental Engineering*, ASCE, v. 133, Issue 6, pp. 641 - 652.

Boulanger, R. W., and Idriss, I. M., (2014), "CPT and SPT Based Liquefaction Triggering Procedures", Report UCD/CGM-14/01, Center for Geotechnical Modeling, University of California, Davis, California.

Bray, J. D., and Sancio R. B. (2006), "Assessment of the Liquefaction Susceptibility of Fine-Grained Soils", *Journal of Geotechnical and Geoenvironmental Engineering*, ASCE, v. 132, Issue 9 pp. 1165 - 1177.

Cetin, K. O., Seed, R. B., Der Kiureghian, A., Tokimatsu, K., Harder, L. F. Jr, Kayen, R. E., and Moss, R. E. S. (2004), "Standard Penetration Test-Based Probabilistic and Deterministic Assessment of Seismic Soil Liquefaction Potential", *Journal of Geotechnical and Geoenvironmental Engineering*, ASCE, v. 130, Issue 12, pp. 1314 - 1340.

Darendeli M. B., (2001). "Development of a New Family of Normalized Modulus Reduction and Material Damping Curves", PhD Dissertation, Department of Civil Engineering, University of Texas, Austin, Texas.

Duncan, J. M., and Wright, S. G., (2005), Soil Strength and Slope Stability, John Wiley & Sons, Inc., Hoboken, New Jersey.

Ebeling, R. M., Chase, A., White, B. C., (2007), "Translational Response of Toe-Restrained Retaining Walls to Earthquake Ground Motions Using  $C_{corps}W_{allSlip}$  (CWSLIP)", Technical Report ERDC/ITL TR-07-01. Vicksburg, Mississippi: Corps of Engineers Waterways Experiment Station, June 2007.

Golesorkhi, R. (1989), "Factors Influencing the Computational Determination of Earthquake-Induced Shear Stresses in Sandy Soils", Ph. D. Thesis, University of California, Berkeley.

Goodman, R. E., and Seed, H. B. (1966), "Earthquake-induced Displacements in Sand Embankments", *Journal of the Soil Mechanics and Foundations Division*, ASCE, v. 92, Issue 2, pp. 125 - 146.

Goulois, A. M., Whitman, R. V. and Hoeg, K., (1985), "Effects of Sustained Shear Stresses on the Cyclic Degradation of Clay", Strength Testing of Marine Sediments: Laboratory and In-Situ Strength Measurements, ASTM STP 883, R. C. Chaney and K. R. Demars, eds., ASTM, Philadelphia, pp. 336-351.

Harder, L. F., and Boulanger, R. W. (1997), "Application of K-alpha and K-sigma Correction Factors", Proceedings of the NCEER Workshop on Evaluation of Liquefaction Resistance of Soils, T. L. Youd and I. M. Idriss, editors, Technical Report NCEER-97-0022, pp. 167 – 190.

Hayati, H. and Andrus, R. D., (2008), "Liquefaction Potential Map of Charleston, South Carolina Based on the 1886 Earthquake", *Journal of Geotechnical and Geoenvironmental Engineering*, ASCE, v. 134, Issue 6, pp. 815 - 828.

Hayati, H. and Andrus, R. D., (2009), "Updated Liquefaction Resistance Correction Factors for Aged Sands", *Journal of Geotechnical and Geoenvironmental Engineering*, ASCE, v. 135, Issue 11, pp. 1683 - 1692.

Holtz, R. D., and Kovacs, W.D., (1981), An Introduction to Geotechnical Engineering, Prentice-Hall, Inc., Englewood Cliffs, New Jersey.

Houston, S. L., Houston, W. N., and Padilla, J. M. (1987), "Microcomputer-aided Evaluation of Earthquake-induced Permanent Slope Deformations", *Microcomputers in Civil Engineering*, Vol. 2, p. 207 - 222.

Hynes, M. E. and Franklin, A. G., (1984), "Rationalizing the Seismic Coefficient Method," Miscellaneous Paper GL-84-13, U.S. Army Waterways Experiment Station, Vicksburg, MS, July.

Idriss, I. M. (1999), "An Update to the Seed-Idriss Simplified Procedure for Evaluating Liquefaction Potential", Proceedings, TRB Workshop on New Approaches to Liquefaction, (Publication No. FHWA-RD-99-165), FHWA, U.S. Department of Transportation.

Idriss, I. M. and Boulanger, R. W. (2003), "Estimating  $K_{\alpha}$  for use in Evaluating Cyclic Resistance of Sloping Ground", Proceedings, 8<sup>th</sup> U.S. – Japan Workshop on Earthquake Resistant Design of Lifeline Facilities and Countermeasures Against Liquefaction, M. Hamada, J.-P. Bardet and T. D. O'Rourke editors, MCEER.

Idriss, I. M. and Boulanger, R. W. (2006), "Semi-empirical Procedures for Evaluating Liquefaction Potential During Earthquakes," Proceedings, 11<sup>th</sup> International Conference on Soil Dynamics and Earthquake Engineering and 3<sup>rd</sup> International Conference on Earthquake Geotechnical Engineering, D. Doolin et. al., eds., Stallion Press, Vol. 1.

Idriss, I. M. and Boulanger, R. W., (2008), Soil Liquefaction During Earthquakes, Earthquake Engineering Research Institute (EERI), EERI Monograph MNO-12.

Ishihara, K., (1985), "Stability of Natural Deposits During Earthquakes", Proceedings, 11th International Conference on Soil Mechanics and Foundation Engineering, San Francisco, CA, Volume 1.

Ishihara, K. and Yoshimine, M. (1992), "Evaluation of Settlements in Sand Deposits Following Liquefaction During Earthquakes", *Soils and Foundations*, 32 (1).

Iwasaki, T., Tatsuoka, F., and Takagi, Y. (1978), "Shear Moduli of Sands Under Cyclic Torsional Shear Loading", *Soils and Foundations*, 18 (1).

Jibson, R., (1994), "Predicting Earthquake-induced Landslide Displacement Using Newmark's Sliding Block Analysis", *Transportation Research Record 1411*, Transportation Research Board, Washington, D.C.

Kavazanjian, E., Wang, J-N. J., Martin, G. R., Shamsabadi, A., Lam, I., Dickenson, S. E., and Hung, C. E., (2012), LRFD Seismic Analysis and Design of Transportation Geotechnical Features and Structural Foundations, Engineering Circular No. 3, (Publication No. FHWA-NHI-11-032, August (Rev. 1)), US Department of Transportation, National Highway Institute, Federal Highway Administration, Washington, DC.

Kramer, S. L. (1996), Geotechnical Earthquake Engineering, Prentice-Hall, Upper Saddle River, NJ

Kramer, S. L. and Elgamal, A.-W. (2001), "Modeling Soil Liquefaction Hazards for Performance-Based Earthquake Engineering," State-of-the-Art Report, Pacific Earthquake Engineering Research Center, in preparation.

Kramer, S. L. and Wang, C.-H., (2015), "Empirical Model for Estimation of the Residual Strength of Liquefied Soil", *Journal of Geotechnical and Geoenvironmental Engineering*, ASCE, published online May 6, 2015, ISSN 1090-0241/04015038(15).

Ladd, C., and Foot, R. ,(1974), "New Design Procedure for Stability of Soft Clays", *Journal of the Geotechnical Engineering Division*, ASCE, v. 100, Issue 7, pp. 763 - 786.

Ladd, C. C., Foot, R., Ishihara, K., Schlosser, F., and Poulos, H. G. (1977), "Stress Deformation and Strength Characteristics", Proceedings of 9th Int. Conf. on Soil Mech. and Found. Engrg., Vol. 2, Tokyo, Japan.

Leon, E., Gassman, S. L., and Talwani, P., (2006), "Accounting for Soil Aging When Assessing Liquefaction Potential", *Journal of Geotechnical and Geoenvironmental Engineering*, ASCE, v. 132, Issue 3, pp. 363 - 377.

Lewis, M. R., Arango, I., and McHood, M. D., (2007), "Geotechnical Engineering at the Savannah River Site and Bechtel", Report No. WSRC-STI-2007-00373, Contract No. DE-AC09-96SR18500, U. S. Department of Energy, July 17, 2007.

Makdisi, F. T., and Seed, H. B., (1978), "Simplified Procedure for Estimating Dam and Embankment Earthquake-Induced Deformations", *Journal of Geotechnical Engineering*, ASCE, v. 104, Issue 7, 849 - 867.

Marcuson, W. F. III, Hynes, M. E., and Franklin, A. G. (1990), "Evaluation and Use of Residual Strength in Seismic Safety Analysis of Embankments", *Earthquake Spectra*, Vol 6, No. 3, pp. 529 - 572.

Matasovic, N., Kavazanjian, E., and Giroud, J. P. (1998), "Newmark Seismic Deformation Analysis for Geosynthetic Covers", Geosynthetics International, International Geosynthetics Society.

McGee W. J. , Sloan E., Manigault, G. E., Newcomb, S., Peters, K. E., and Herrmann, R. B. eds., (1986), "First-hand Observations of the Charleston Earthquake of August 31, 1886, and Other Earthquake Materials", Reports of Bulletin 41, South Carolina Geological Survey.

Newmark, N. M. (1965), "Effects of Earthquakes on Dams and Embankments", *Geotechnique*, v.5, no.2 London, England.

Olson, S. M., and Johnson, C. I., (2008), "Analyzing Liquefaction-Induced Lateral Spreads Using Strength Ratios," *Journal of Geotechnical and Geoenvironmental Engineering*, ASCE, Volume 134, Issue 8, pp. 1035-1049.

Olson, S. M., and Stark, T. D., (2003), "Yield Strength Ratio and Liquefaction Analysis of Slopes and Embankments", *Journal of Geotechnical and Geoenvironmental Engineering*, ASCE v. 129, Issue 8, pp. 727 - 737.

Polito, C. P., and Martin, J. R. (2001), "Effects of Nonplastic Fines on the Liquefaction Resistance of Sands", *Journal of Geotechnical and Geoenvironmental Engineering*, ASCE, v. 127, Issue 5, pp. 408 - 415.

Pyke, R., Seed, H.B., Chan, C.K. (1975), "Settlement of Sands Under Multi-directional Shearing", *Journal of Geotechnical Engineering*, ASCE, v. 101, Issue 4, pp. 379 - 398.

Richards, R. and Elms, D. G., (1979), "Seismic Behavior of Gravity Retaining Walls", *Journal of Geotechnical Engineering*, ASCE, v.105, Issue 4, pp. 449 - 464.

Robertson, P. K., and Wride, C. E. (1997), "Cyclic Liquefaction and its Evaluation Based on SPT and CPT", Proceedings NCEER Workshop on Evaluation of Liquefaction Resistance of Soils.

Schneider, J. A., and Mayne, P. W. (1999), "Soil Liquefaction Response in Mid-America Evaluated by Seismic Piezocone Tests", Report MAE-GT-3A, Mid America Earthquake Center, October, 253 pp.

Seed, H. B. (1986), "Design Problems in Soil Liquefaction", University of California, Earthquake Engineering Research Center (UCB/EERC), UBC/EERC-86/02, February.

Seed, H. B. (1987), "Design Problems in Soil Liquefaction", *Journal of Geotechnical Engineering*, ASCE, v.113, Issue 8, pp. 827 - 845.

Seed, R. B., Cetin, K. O., Moss, R. E. S., Kammerer, A., Wu, J., Pestana, J. and Riemer, M., Sancio, R. B., Bray, J. D., Kayen, R. E., and Faris, A. (2003), "Recent Advances in Soil Liquefaction Engineering: A Unified and Consistent Framework", EERC-2003-06, Earthquake Engineering Research Institute, Berkeley, Calif.

Seed, R. B. and Harder, L. F., Jr., (1990), "SPT-Based Analysis of Cyclic Pore Pressure Generation and Undrained Residual Strength", Proceedings, H. Bolton Seed Memorial Symposium, BiTech Publishers, Ltd.

Seed, H. B., and Idriss, I. M., (1971), "Simplified Procedure or Evaluating Soil Liquefaction Potential", *Journal of the Soil Mechanics and Foundations Division*, ASCE, v. 97, Number SM9, pp. 1249 - 1271.

Shamoto, Y., Zhang, J., and Tokimatsu, K. (1998), "New charts for predicting large residual post-liquefaction ground deformations", *Soil dynamics and earthquake engineering*, Vol. 17, Elsevier, New York.

Spencer, E. (1967), "A Method of Analysis of the Stability of Embankments Assuming Parallel Inter-Slice Forces," *Geotechnique*, v.17, no.12 London, England.

Stewart, J. P., Whang, D. H., Moyneur, M., and Duku, P. (2004), "Seismic Compaction of As-Compacted Fill Soils With Variable Levels of Fines Content and Fines Plasticity", Department of Civil and Environmental Engineering, University of California, Los Angeles, Consortium of Universities for Research in Earthquake Engineering (CUREE), CUREE Publication No. EDA-05, July 2004.

Talwani, P., and Schaeffer, W. T. (2001), "Recurrence rates of large earthquakes in the South Carolina Coastal Plain based on paleoliquefaction data", *Journal of Geophysical Research*, 106(B4), 6621–6642.

Terzaghi, K., Peck, R. B., and Mesri, G., (1996), Soil Mechanics in Engineering Practice, John Wiley & Sons, Inc., 605 Third Avenue, New York, NY.

Tokimatsu, K., and H. B. Seed. (1987), "Evaluation of Settlements in Sands Due to Earthquake Shaking", *Journal of Geotechnical Engineering*, ASCE, v. 113 Issue 8, pp. 861 - 878.

U.S. Geological Survey, <http://earthquake.usgs.gov/hazards/qfaults/eusa/char.php>.

Vucetic, M. and Dobry, R. (1991), "Effect of Soil Plasticity on Cyclic Response", *Journal of Geotechnical Engineering*, ASCE, v. 117 Issue 1, pp. 89 - 107.

Weems, R. E., Lemon, E. M., Jr., and Chirico, P. (1997), "Digital Geology and Topography of the Charleston Quadrangle, Charleston and Berkeley Counties, South Carolina", USGS Open-File Report Number 97-531, U.S. Geological Survey, Reston, Va.

Willoughby, R. H., Nystrom, P. J., Campbell, L. D., Katuna, M. P. (1999), "Cenozoic Stratigraphic Column of the Coastal Plain of South Carolina", South Carolina Department of Natural Resources, Geological Survey, Columbia, SC.

Wu, J. (2002), "Liquefaction triggering and Post-liquefaction Deformations of Monterey 0/30 Sand Under Uni-directional Cyclic Simple Shear Loading", Ph.D. Dissertation, University of California, Berkeley.

Yegian, M. K. Marciano, E., and Ghahraman, V.G. (1991), "Earthquake-Induced Permanent Deformations: Probabilistic Approach", *Journal of Geotechnical Engineering*, ASCE, v. 117 Issue 1, pp. 35 - 50.



Yoshimine, M., Nishizaki, H., Amano, K., and Hosono, Y., (2006), "Flow Deformation of Liquefied Sand under Constant Shear Load and its Application to Analysis of Flow Slide in Infinite Slope", Geomechanics, Geotechnical Special Publication (GSP) 143, ASCE.

Youd, T. L., and Idriss, I. M., eds. (1997), Technical Report NCEER-97-0022 Proceedings, *NCEER Workshop on Evaluation of Liquefaction Resistance of Soils*, National Center for Earthquake Engineering Research, State Univ. of New York at Buffalo.

Youd, T. L., Idriss, I. M., Andrus, R. D., Arango, I., Castro, G., Christian, J. T., Dobry, R., Finn, W. D. L., Harder, L. F., Jr., Hynes, M. E., Ishihara, K., Koester, J. P., Liao, S. S. C., Marcuson, W. F., III, Martin, G. R. Mitchell, J. K., Moriwaki, Y., Power, M. S., Robertson, P. K., Seed, R. B., and Stokoe, K. H., II, (2001), "Liquefaction resistance of soils: Summary Report from the 1996 NCEER and 1998 NCEER/NSF Workshops on Evaluation of Liquefaction Resistance of Soils," *Journal of Geotechnical and Geoenvironmental Engineering*, ASCE, v. 127, Issue 10, pp. 817 - 833.

Youd, T. L. and Perkins, D. M., (1978), "Mapping of Liquefaction-Induced Ground Failure Potential", *Journal of the Geotechnical Engineering Division*, ASCE, v. 104, Issue 4, pp. 433 - 446.

**Chapter 14**  
**GEOTECHNICAL**  
**SEISMIC DESIGN**

**GEOTECHNICAL DESIGN MANUAL**

*January 2019*



## Table of Contents

<u>Section</u>	<u>Page</u>
14.1 Introduction.....	14-1
14.2 Geotechnical Seismic Design Approach .....	14-1
14.2.1 No Soil SSL Condition .....	14-2
14.2.2 Soil SSL Condition.....	14-2
14.3 Seismic Lateral Loadings.....	14-2
14.4 Seismic Active Soil Pressures.....	14-3
14.4.1 Mononobe-Okabe Method .....	14-4
14.4.2 Trial Wedge Method.....	14-6
14.4.3 Modification to MO Method to Consider Cohesion .....	14-6
14.4.4 LSR Method.....	14-8
14.4.5 GLE Method .....	14-16
14.4.6 Unyielding Structures.....	14-16
14.5 Seismic Passive Soil Pressures.....	14-17
14.6 Geotechnical Seismic Design of Bridges.....	14-26
14.6.1 ADRS Curves .....	14-26
14.6.2 Bridge Abutments .....	14-27
14.6.3 Bridge Approach Embankment .....	14-27
14.6.4 Bridge Foundations.....	14-27
14.7 Shallow Foundation Design .....	14-28
14.8 Deep Foundation Design .....	14-28
14.8.1 Axial Loads .....	14-29
14.8.2 Downdrag Loads.....	14-29
14.8.3 Lateral Soil Response of Liquefied Soils (p-y Curves).....	14-29
14.8.4 Effects of Seismic Soil Instability on Deep Foundations .....	14-31
14.8.5 Evaluation of Soil Loading on Substructures.....	14-32
14.8.6 Soil Load Contribution on a Single Deep Foundation .....	14-33
14.8.7 Load Transfer Between Pile Group and Lateral Spreading Crust.....	14-34
14.8.8 Lateral Soil Loads Due to Seismic Hazard Displacements .....	14-36
14.9 Bridge Abutment Back Wall Passive Resistance.....	14-39
14.9.1 Development of Passive Resistance.....	14-39
14.9.2 Effective Width of Abutment Wall.....	14-47
14.10 Geotechnical Seismic Design of Embankments .....	14-50
14.11 Rigid Gravity Earth Retaining Structure Design.....	14-50
14.12 Flexible Gravity Earth Retaining Structure Design.....	14-56
14.13 Cantilever Earth Retaining System Design .....	14-62
14.13.1 Unanchored Cantilever ERSs .....	14-62
14.13.2 Anchored Cantilever ERSs .....	14-63
14.14 In-situ Reinforced Retaining System Design .....	14-64
14.15 Seismic Hazard Mitigation.....	14-64
14.15.1 Structural Mitigation .....	14-65
14.15.2 Geotechnical Mitigation.....	14-65
14.15.3 Selection of Mitigation Method .....	14-65
14.16 References .....	14-65

**List of Tables**

<b><u>Table</u></b>	<b><u>Page</u></b>
Table 14-1, Effective Pile Width Coefficient ( $\lambda$ ) .....	14-34
Table 14-2, Relative Movements Required to Reach Passive Earth Pressures.....	14-41
Table 14-3, Cohesionless Soil Parameters Used to Create Figure 14-46.....	14-43
Table 14-4, Cohesive Soil Parameters Used to Create Figure 14-47 .....	14-43
Table 14-5, $c$ - $\phi$ Soil Parameters Used to Create Figure 14-48 .....	14-43

**List of Figures**

<b>Figure</b>	<b>Page</b>
Figure 14-1, Pseudo-Static Method – Inertial Forces and Seismic Loadings .....	14-4
Figure 14-2, Mononobe-Okabe Method .....	14-5
Figure 14-3, Trial Wedge Method.....	14-6
Figure 14-4, MO Active Seismic Wedge.....	14-7
Figure 14-5, LSR Active Seismic Wedge .....	14-8
Figure 14-6, Seismic Active Earth Pressure Coefficient ( $\delta = 0$ ; $C/\gamma H = 0.0$ ) .....	14-9
Figure 14-7, Seismic Active Earth Pressure Coefficient ( $\delta = 0$ ; $C/\gamma H = 0.025$ ) .....	14-9
Figure 14-8, Seismic Active Earth Pressure Coefficient ( $\delta = 0$ ; $C/\gamma H = 0.05$ ) .....	14-10
Figure 14-9, Seismic Active Earth Pressure Coefficient ( $\delta = 0$ ; $C/\gamma H = 0.075$ ) .....	14-10
Figure 14-10, Seismic Active Earth Pressure Coefficient ( $\delta = 0$ ; $C/\gamma H = 0.1$ ) .....	14-11
Figure 14-11, Seismic Active Earth Pressure Coefficient ( $\delta = 1/2\phi$ ; $C/\gamma H = 0.0$ ) .....	14-11
Figure 14-12, Seismic Active Earth Pressure Coefficient ( $\delta = 1/2\phi$ ; $C/\gamma H = 0.025$ ) .....	14-12
Figure 14-13, Seismic Active Earth Pressure Coefficient ( $\delta = 1/2\phi$ ; $C/\gamma H = 0.05$ ) .....	14-12
Figure 14-14, Seismic Active Earth Pressure Coefficient ( $\delta = 1/2\phi$ ; $C/\gamma H = 0.075$ ) .....	14-13
Figure 14-15, Seismic Active Earth Pressure Coefficient ( $\delta = 1/2\phi$ ; $C/\gamma H = 0.1$ ) .....	14-13
Figure 14-16, Seismic Active Earth Pressure Coefficient ( $\delta = 2/3\phi$ ; $C/\gamma H = 0.0$ ) .....	14-14
Figure 14-17, Seismic Active Earth Pressure Coefficient ( $\delta = 2/3\phi$ ; $C/\gamma H = 0.025$ ) .....	14-14
Figure 14-18, Seismic Active Earth Pressure Coefficient ( $\delta = 2/3\phi$ ; $C/\gamma H = 0.05$ ) .....	14-15
Figure 14-19, Seismic Active Earth Pressure Coefficient ( $\delta = 2/3\phi$ ; $C/\gamma H = 0.075$ ) .....	14-15
Figure 14-20, Seismic Active Earth Pressure Coefficient ( $\delta = 2/3\phi$ ; $C/\gamma H = 0.01$ ) .....	14-16
Figure 14-21, LSR Passive Seismic Wedge.....	14-17
Figure 14-22, Seismic Passive Earth Pressure Coefficient ( $\delta = 0$ ; $C/\gamma H = 0.0$ ) .....	14-18
Figure 14-23, Seismic Passive Earth Pressure Coefficient ( $\delta = 0$ ; $C/\gamma H = 0.025$ ) .....	14-19
Figure 14-24, Seismic Passive Earth Pressure Coefficient ( $\delta = 0$ ; $C/\gamma H = 0.05$ ) .....	14-19
Figure 14-25, Seismic Passive Earth Pressure Coefficient ( $\delta = 0$ ; $C/\gamma H = 0.075$ ) .....	14-20
Figure 14-26, Seismic Passive Earth Pressure Coefficient ( $\delta = 0$ ; $C/\gamma H = 0.1$ ) .....	14-20
Figure 14-27, Seismic Passive Earth Pressure Coefficient ( $\delta = 1/2\phi$ ; $C/\gamma H = 0.0$ ) .....	14-21
Figure 14-28, Seismic Passive Earth Pressure Coefficient ( $\delta = 1/2\phi$ ; $C/\gamma H = 0.025$ ).....	14-21
Figure 14-29, Seismic Passive Earth Pressure Coefficient ( $\delta = 1/2\phi$ ; $C/\gamma H = 0.05$ ) .....	14-22
Figure 14-30, Seismic Passive Earth Pressure Coefficient ( $\delta = 1/2\phi$ ; $C/\gamma H = 0.075$ ).....	14-22
Figure 14-31, Seismic Passive Earth Pressure Coefficient ( $\delta = 1/2\phi$ ; $C/\gamma H = 0.1$ ) .....	14-23
Figure 14-32, Seismic Passive Earth Pressure Coefficient ( $\delta = 2/3\phi$ ; $C/\gamma H = 0.0$ ) .....	14-23
Figure 14-33, Seismic Passive Earth Pressure Coefficient ( $\delta = 2/3\phi$ ; $C/\gamma H = 0.025$ ).....	14-24
Figure 14-34, Seismic Passive Earth Pressure Coefficient ( $\delta = 2/3\phi$ ; $C/\gamma H = 0.05$ ) .....	14-24
Figure 14-35, Seismic Passive Earth Pressure Coefficient ( $\delta = 2/3\phi$ ; $C/\gamma H = 0.075$ ).....	14-25
Figure 14-36, Seismic Passive Earth Pressure Coefficient ( $\delta = 2/3\phi$ ; $C/\gamma H = 0.1$ ) .....	14-25
Figure 14-37, Pile Damage Mechanisms in Liquefied Ground.....	14-28
Figure 14-38, P-Multipliers ( $m_p$ ) for Sand-Like Soils Subject to Cyclic Liquefaction.....	14-31
Figure 14-39, Flow of Soil Around Deep Foundation (Case 1) .....	14-32
Figure 14-40, Movement of Soil and Deep Foundation (Case 2).....	14-33
Figure 14-41, Load Transfer Between Pile Group and Lateral Spreading Crust .....	14-35
Figure 14-42, BNWF Methods for Evaluating Seismic Hazard Displacements .....	14-37
Figure 14-43, Methods for Imposing Kinematic Loads on Deep Foundations.....	14-38
Figure 14-44, End-Bent Schematic Plan View.....	14-39
Figure 14-45, Hyperbolic Force-Displacement Formulation.....	14-40

Figure 14-46, Bridge Abutment Wall Passive Pressure, Cohesionless Backfill Example.....	14-44
Figure 14-47, Bridge Abutment Wall Passive Pressure, Cohesive Backfill Example .....	14-45
Figure 14-48, Bridge Abutment Wall Passive Pressure, $c-\phi$ Backfill Example .....	14-46
Figure 14-49, Skewed Bridge Abutment Wall Seismic Passive Resistance.....	14-49
Figure 14-50, Skewed Bridge Abutment Wall Seismic Sliding Resistance .....	14-50
Figure 14-51, Rigid Gravity ERS Seismic Force Diagram – Level Backfill.....	14-53
Figure 14-52, Rigid Gravity ERS Seismic Force Diagram – Sloping Backfill.....	14-54
Figure 14-53, Determination of Yield Acceleration ( $k_y$ ) .....	14-56
Figure 14-54, Flexible Gravity ERS Seismic Force Diagram – Level Backfill.....	14-59
Figure 14-55, Flexible Gravity ERS Seismic Force Diagram – Sloping Backfill .....	14-60
Figure 14-56, Determination of Yield Acceleration ( $k_y$ ) .....	14-62

# CHAPTER 14

## GEOTECHNICAL SEISMIC DESIGN

### 14.1 INTRODUCTION

This Chapter provides guidance for the geotechnical seismic design of bridges, embankments, ERSs, and miscellaneous structures. Geotechnical seismic design consists of evaluating the EE I limit state of transportation structures owned and maintained by the State of South Carolina for performance under seismic hazards (Chapter 13) and seismic lateral loadings (Chapter 14). Seismic lateral loadings (inertial accelerations) affect soil pressures by increasing static active soil pressures and decreasing static passive soil pressures. Methods for computing seismic active and passive soil pressures are included in this Chapter. The geotechnical seismic design will typically be evaluated using performance based design methodologies to evaluate if the structure's performance meets the geotechnical performance criteria established in Chapter 10. Force based design methodologies are included where appropriate for evaluating boundary conditions. If the performance limits are exceeded, seismic hazard mitigation methods will be discussed that can be used to meet the required performance limits.

The procedures for seismic geotechnical design are consistent with those procedures presented for static geotechnical design in this Manual. The seismic geotechnical design guidelines presented in this Manual may not be the only methods available particularly since geotechnical seismic design is constantly evolving and developing. The overall goal of this Chapter is to establish a state-of-practice that can and will evolve and be enhanced as methodologies improve and regional (CEUS) experience develops. Methods other than those indicated in this Manual may be brought to the attention of the PC/GDS or the PCS/GDS for consideration on a specific project or for consideration in future updates of this Manual, respectively.

### 14.2 GEOTECHNICAL SEISMIC DESIGN APPROACH

Geotechnical seismic design is typically performed using either a Force Based Design or Performance Based Design methodology. SCDOT LRFD geotechnical seismic design of transportation structures typically consists of using Performance Based Design methodologies. The EE I limit state performance criteria established in Chapter 10 should be used as a starting point with significant collaboration between the SEOR and the GEOR. The geotechnical seismic design approach will be consistent with design philosophy for structural design. It will be the responsibility of the design team to define the performance of bridges, roadway embankments, and ERSs within the frame work of SCDOT policy of maximizing the safety of the motoring public and minimizing the susceptibility of a bridge structure to collapse during strong earthquake shaking.

The design approach typically begins by designing the transportation structure for the Strength and Service limit states. The resulting structure is then evaluated for the EE I limit state.

For sites where bridges and bridge foundations are located within soils that are susceptible to SSL in accordance with Chapter 13 due to either cyclic liquefaction of Sand-Like soils or cyclic softening of Clay-Like soils, the design methodology shall include the evaluation of the following 2 conditions:



### **14.2.1 No Soil SSL Condition**

The structure should first be analyzed and designed for the inertial forces induced by the EE I limit state without the soil SSL condition. This will allow the design team to understand the effect of just the inertial loading on the structures. The site response developed should not include any effects of the soil SSL.

### **14.2.2 Soil SSL Condition**

The structure, as designed for the No Soil SSL condition, is reanalyzed assuming that the Sand-Like and Clay-Like soils have experienced soil SSL. The soils susceptible to SSL are assigned appropriate residual shear strengths in accordance with Chapter 13. The design spectrum for the No Soil SSL is used unless the period of the structure is greater than 1.0 second and the site response is susceptible to increase for the soil SSL condition in accordance with Chapter 12. The geotechnical seismic design is then performed using these soil and site response parameters.

If the structure meets the performance objectives (resistance factors and performance criteria) for the EE I limit state, the design is complete. Otherwise, measures to mitigate the effects of the seismic hazard are developed. The full horizontal acceleration ( $k_h = k_{avg}$ ) shall be used in design. However,  $k_y$  shall be determined and if the ratio of  $k_y$  to  $k_h$  is greater than or equal to 0.5 (i.e.,  $k_y/k_h \geq 0.5$ ) and displacement of approximately 2.0 inches can be tolerated then the design is complete. If 2.0 inches of displacement cannot be tolerated or if the ratio of  $k_y$  to  $k_h$  is less than 0.5 (i.e.,  $k_y/k_h < 0.5$ ), then the actual displacement shall be determined using the procedures described in Chapter 13. Displacements shall be computed in accordance with Chapter 13 when instability is determined. Mitigation can be accomplished by redesign of the structure to resist the seismic hazards (structural mitigation), reducing the effects of the seismic hazard by performing geotechnical mitigation measures, or by developing a mitigation approach that consists of both structural and geotechnical mitigation procedures.

The evaluation of the EE I limit state typically requires a geotechnical evaluation of the Geology and Seismicity (Chapter 11), and the Site Response (Chapter 12) and the evaluation of the effects of the Seismic Hazards (Chapter 13) on the transportation structures being designed. For transportation structures (bridges, ERSs, etc.) that require structural design of concrete or steel components, the GEOR typically provides the SEOR with site response analyses, soil-structure interaction modeling of foundations, seismic loadings (active and passive), and the effects of seismic hazards. When mitigation of seismic hazards is required, the GEOR provides geotechnical mitigation options and assists in the evaluation of structural mitigation options. When evaluating certain structural mitigation options, the GEOR may require input from the SEOR for the design of piles/shafts for providing slope stability of a roadway embankment or river/channel bank at a bridge crossing.

It should be noted that the procedures outlined in this Chapter are to be used with new construction. The seismic design or retrofit of existing structures is currently performed on a case-by-case basis. At the discretion of the Regional Production Engineer (RPE), the Regional Program Manager (PM), or the Regional Design Manager (DM), existing structures may be required to have seismic retrofit design performed.

## **14.3 SEISMIC LATERAL LOADINGS**

Seismic lateral loadings are those seismic hazards that are induced by the acceleration of a soil mass or structure during earthquake shaking. The average seismic horizontal acceleration

( $k_{avg}$ ) that is generated by the earthquake is computed by using seismic acceleration coefficients as indicated in Chapter 13. The seismic lateral loadings are exhibited as either seismic active soil pressures or seismic passive soil pressures. Seismic active soil pressures are generated when seismic accelerations mobilize the active soil driving wedge behind an ERS or bridge abutments. Seismic passive soil pressures are generated when an earthquake load is applied from a structure to the soil. When passive soil pressures are generated as a result of seismic loadings, the earthquake's inertial acceleration forces also affect the passive soil wedge. The mechanism of this hazard is dependent on the type of structure being analyzed. Because a performance based design is used in the design of transportation structures, the effects of seismic lateral loadings must take into account the added force on the structure and any deformations caused by shearing of the soils. Examples of how this hazard can affect typical transportation structures are provided below:

- ERSs must not only resist static active soil pressure but also seismic active pressures as a result of the average earthquake accelerations acting on the active soil wedge. Additional lateral loads are generated as a result of the acceleration acting on the mass of the retaining structure and any soil that is contained in the structure.
- While a bridge abutment on one end of a bridge may experience the same seismic lateral loadings as ERSs, the abutment at the other end of the bridge may experience seismic induced lateral loads from the bridge and mass of the abutment that places a lateral seismic load on the soils behind the abutment, resulting in passive pressure resistance. Soils retained by bridge abutments will cycle between active and passive soil pressures throughout the earthquake shaking.
- Bridge approach and roadway embankments not only must resist static driving forces, but also seismic driving forces. Seismic driving forces result from peak ground accelerations acting on the soil mass contained within the bridge embankment failure surface.

#### 14.4 SEISMIC ACTIVE SOIL PRESSURES

Earthquake-induced lateral loadings addressed in this Section are limited to those loadings (seismic active earth pressures) that are the result of soil-structure interaction between soils and ERSs. Seismic active soil pressures are generally analyzed using pseudo-static methods. The pseudo-static method is a force-equilibrium method that is used to analyze external forces and the effects (i.e., sliding, overturning, bearing capacity, etc.) on the structure being designed. The pseudo-static method used to analyze seismic active soil pressures uses the average horizontal acceleration coefficients that has been adjusted for wave scattering, ( $k_h = k_{avg}$ ), multiplied by the weight of the structural wedge (weight of the structure and any soil above the structure) and the weight of the active driving wedge,  $W_{DW}$ . The seismic active earth loadings in the pseudo-static method are illustrated in Figure 14-1.

The limit-equilibrium method is based on the following assumptions:

- The retaining wall yields sufficiently to produce active soil pressures during an earthquake.
- The backfill is a dry cohesionless soil (Mononobe-Okabe method).
- Active failure wedge behaves as a rigid body so that the accelerations are uniform throughout the soil mass.
- The soils behind the wall are not saturated and liquefaction does not occur.

The following methods can be used to evaluate the seismic active pressures:

1. Mononobe-Okabe (MO) Method
2. Trial Wedge Method
3. Modification to MO Method to Consider Cohesion
4. Log-Spiral-Rankine (LSR) Method – Shamsabadi, Xu, and Taciroglu (2013a and 2013b)
5. Generalized Limit Equilibrium (GLE) Method

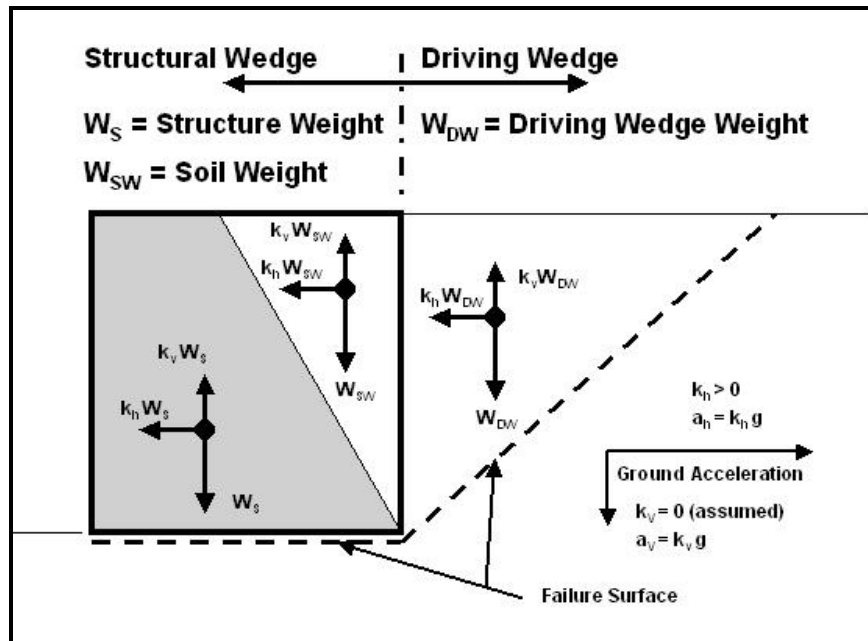


Figure 14-1, Pseudo-Static Method – Inertial Forces and Seismic Loadings (Modified Ebeling, et al. (2007))

#### 14.4.1 Mononobe-Okabe Method

One of the most frequent methods used to evaluate seismic active loadings is the Mononobe-Okabe (MO) method shown in Figure 14-2. The total dynamic active earth thrust,  $P_{ae}$ , is determined by the following equation:

$$P_{ae} = \frac{1}{2} * \gamma * H^2 * (1 - k_v) * K_{ae} \quad \text{Equation 14-1}$$

Where the seismic active earth pressure coefficient,  $K_{ae}$ , is determined as follows:

$$K_{ae} = \frac{\cos^2(\phi - \Psi - \theta)}{\cos \Psi * \cos^2 \theta * \cos(\Psi + \theta + \delta) * \left[ 1 + \sqrt{\frac{\sin(\phi + \delta) * \sin(\phi - \Psi - \beta)}{\cos(\delta + \Psi + \theta) * \cos(\beta - \theta)}} \right]^2} \quad \text{Equation 14-2}$$

Where,

- $\gamma$  = Unit weight of soil, pounds per cubic foot
- $H$  = Height of wall or effective height of wall ( $h_{eff}$ ), feet
- $\phi$  = Angle of internal friction of soil, degrees
- $\Psi$  =  $\tan^{-1}[k_h/(1-k_v)]$ , degrees
- $\delta$  = Angle of friction between soil and wall, degrees
- $k_h$  = Horizontal acceleration coefficient, g
- $k_v$  = Vertical acceleration coefficient, typically set to 0.0, g

- $\beta$  = Backfill slope angle, degrees  
 $\theta$  = Angle of backface of the wall with the vertical, degrees

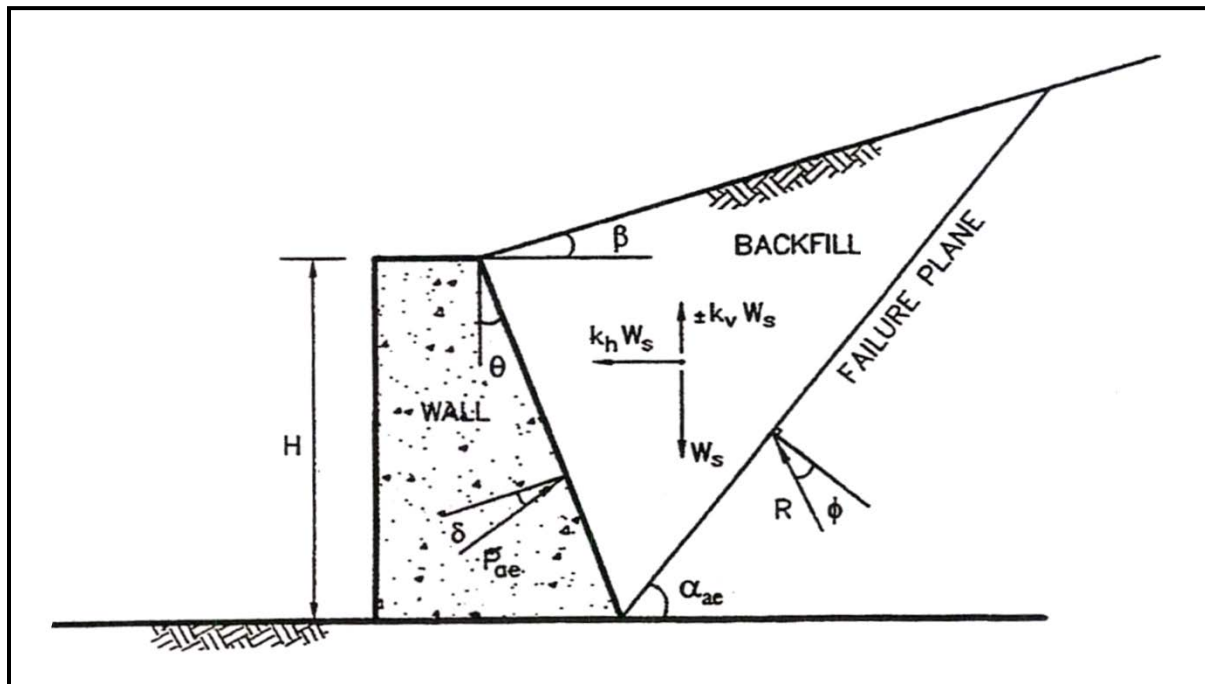


**Figure 14-2, Mononobe-Okabe Method  
(Munfakh, et al. (1998))**

Although the MO method is often used to compute seismic active soil pressures, this method has been found to produce very high pressures that tend to approach infinity when high accelerations and/or steep backslopes are analyzed. Richards and Elms (1979) indicates that when  $(\phi - \Psi - \beta)$  becomes negative no real solution to Equation 14-2 is possible. When this term is equal to 0, that maximum thrust is developed, thus establishing a limiting condition. Alternately, a limiting acceleration can be developed from Equation 14-4. This situation occurs when either of the following limiting conditions are met:

$$\beta \geq \phi - \Psi \quad \text{Equation 14-3}$$

$$k_h \leq (1 - k_v) * \tan(\phi - \beta) \quad \text{Equation 14-4}$$

Because the MO equation is limited to backfills consisting of dry cohesionless soils that may not typically be found at very large distances behind the wall, the MO method may not be the most appropriate analytical method.

Because of the various limitations associated with the MO method, the use of this method should be limited to the following criteria provided that the limiting conditions of Equations 14-3 and 14-4 are met:

- Backfill slopes,  $\beta \leq 18.4$  degrees (3H:1V or flatter)
- Limited to  $K_{ae} \leq 0.60$
- Free draining backfill materials (cohesionless soils) behind the wall should extend throughout the seismic active wedge.

### 14.4.2 Trial Wedge Method

The Trial Wedge method can be used to determine critical earthquake-induced active forces when the MO method is not the appropriate method. The trial wedge method is more adaptable and can accommodate various types of soil behind the wall and relatively complex surface geometries. The Trial Wedge method is illustrated in Figure 14-3.

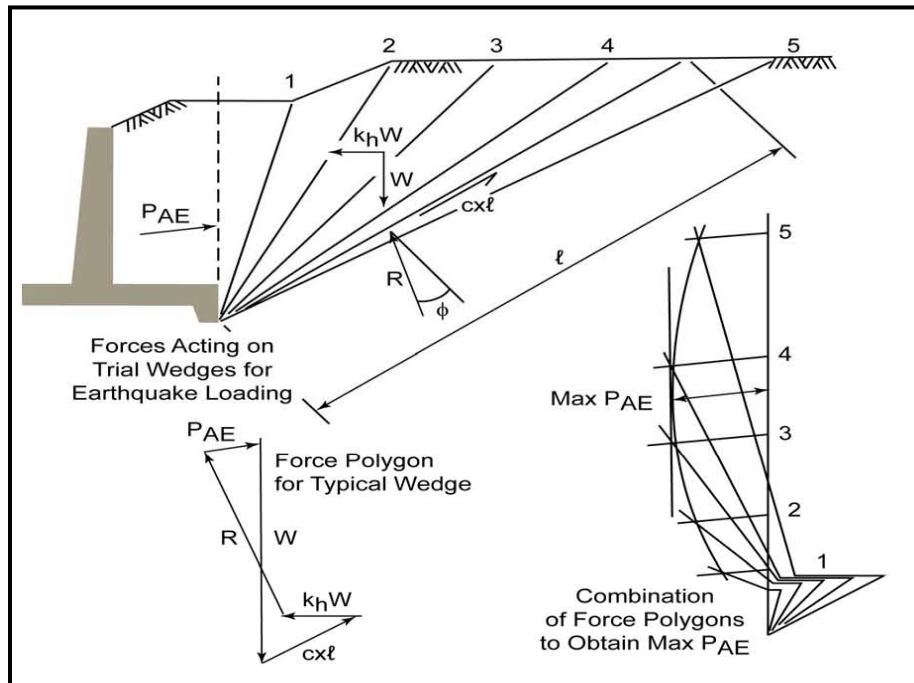


**Figure 14-3, Trial Wedge Method  
(Anderson, et al. (2008))**

Details on conducting the trial wedge method of analysis can be found in Ebeling, et al. (2007) and Bowles (1982). It should be noted that the seismic-induced inertial forces resulting from the structural wedge (retaining structure or soil mass contained within the structural wedge), as indicated in Figure 14-1, are not included in the MO method or the Trial Wedge method and that the structural wedge must also be included in the analysis.

When the horizontal acceleration,  $k_h$ , is equal to the peak horizontal ground acceleration (PGA), the seismic active loadings can become very large resulting in the design of the retaining structure becoming increasingly large and uneconomical. Designing for  $k_h = \text{PGA}$  will limit the deformations to 0.0. If deformations can be tolerated within the performance limits of the structure, then the horizontal acceleration,  $k_h$ , can be reduced. The method of reducing the horizontal acceleration,  $k_h$ , consists of allowing displacements to occur as provided in the Chapter 13.

### 14.4.3 Modification to MO Method to Consider Cohesion

Anderson, et al. (2008) has developed the following Coulomb-type wedge analysis that is based on the trial wedge method as shown in Figure 14-4. The following equation allows the input of cohesion into developing the seismic active earth pressure ( $P_{ae}$ ):

Equation 14-5

$$P_{nae} = \frac{W[(1 - k_v) \tan(\Xi) + k_h] - cL_n[\sin \alpha \tan(\Xi) + \cos \alpha] - c_a H[\tan(\Xi) \cos \omega + \sin \omega]}{[1 + \tan(\delta + \omega) \tan \Xi] * [\cos(\delta + \omega)]}$$

Where,

- $P_{nae}$  = Active earth pressure on each wedge (see Figure 14-4)
- $\alpha$  = Failure plane angle (Variable), degrees
- $\phi$  = Angle of internal friction of soil, degrees
- $\Xi$  =  $\alpha - \phi$ , degrees
- $k_h$  = Average horizontal acceleration coefficient adjusted for wave scattering, g
- $k_v$  = Vertical acceleration coefficient, typically set to 0.0, g
- $c$  = Soil cohesion, pounds per square foot
- $c_a$  = Soil wall adhesion, pounds per square foot
- $\delta$  = Angle of friction between soil and wall ( $\delta = 0.67\phi$ ), degrees
- $\omega$  = Angle of backface of the wall with the vertical, degrees
- $H$  = Height of wall, feet
- $L_n$  = Length of failure surface AH located along failure plan angle ( $\alpha$ ), feet
- $W_1$  = Weight of wedge ABCDEF +  $q_1$  +  $f$ , pounds per foot of wall width
- $W_n$  = Weight of wedge ABCDEGH +  $q_1$  +  $q_2$  +  $f$ , pounds per foot of wall width
- $W_{n+1}$  = Weight of wedge ABCDEGI +  $q_1$  +  $q_2$  +  $f$ , pounds per foot of wall width
- $q_1$  = Uniform strip surcharge located between DE, pounds per foot per foot of wall width
- $q_2$  = Uniform strip surcharge located between GI, pounds per foot per foot of wall width
- $f$  = Line load located between BC, pounds per foot of wall width

The design parameters should be selected based on site conditions. The only parameter that must be determined on a trial basis is the failure plane angle ( $\alpha_n$ ). The failure plane angle ( $\alpha_n$ ) is determined by varying the failure plane angle ( $\alpha_n$ ) until the maximum  $P_{an} = P_{ae}$  is computed.

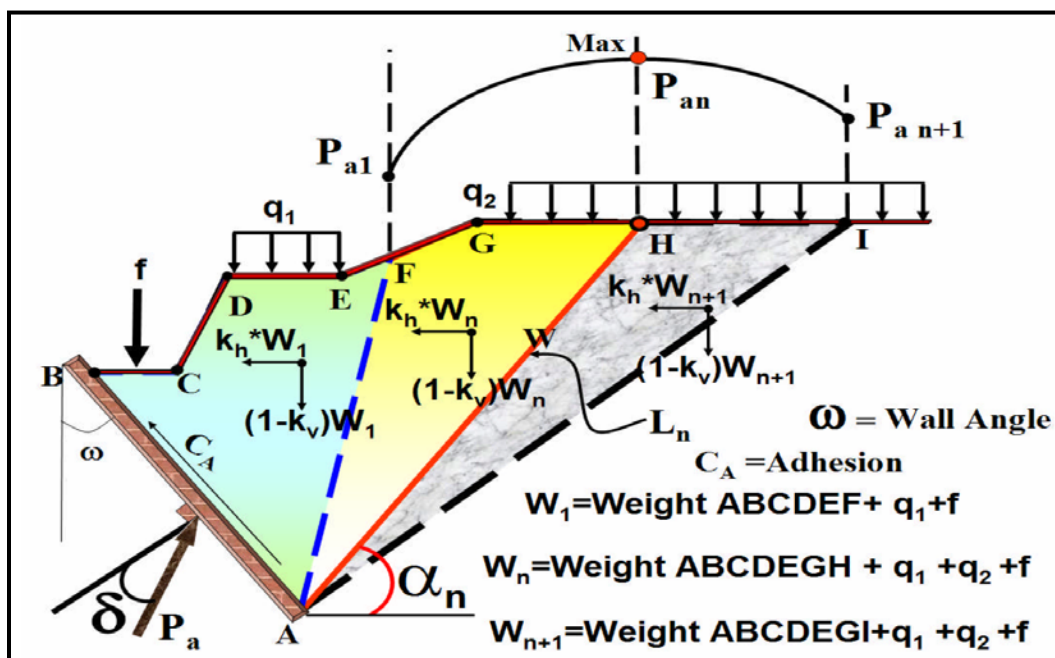
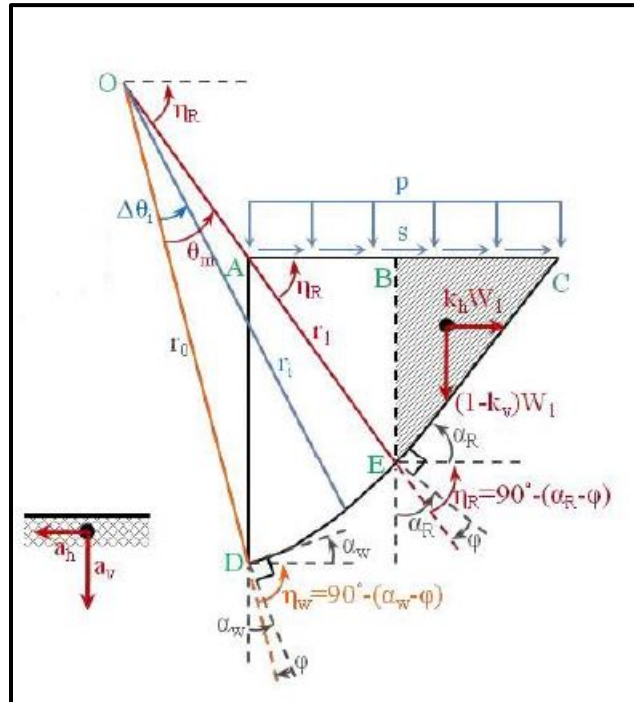


Figure 14-4, MO Active Seismic Wedge (Anderson, et al. (2008))

#### 14.4.4 LSR Method

The Log-Spiral-Rankine (LSR) Method uses a both a log-spiral portion of the soil wedge behind the wall as well as a Rankine portion (see Figure 14-5). The LSR Method uses procedures that account for internal friction and cohesion as well as wall-soil interface friction and adhesion. The LSR Method can be used to determine both active and passive earth pressures; however, it is more advantageous to passive earth pressures. The triangular (shaded) area in Figure 14-5 is a Rankine Zone, because the shear stress ( $\tau$ ) in this region is induced only by the horizontal seismic body forces without any contribution from friction or cohesion.



**Figure 14-5, LSR Active Seismic Wedge  
(Shamsabadi, et al. (2013b))**

For a detailed explanation of the LSR Method please refer to Shamsabadi, Xu, and Taciroglu (2013a), Shamsabadi, Xu, and Taciroglu (2013b), and Xu, Shamsabadi and Taciroglu (2015). Because of the complexity of this method, design charts have been developed for the LSR Method based on the following site conditions:

1. Level ground behind the wall
2.  $k_v = 0g$
3. Wall friction angles of  $\delta = 0.0, 1/2(\phi), 2/3(\phi)$
4. Shear strength friction ratios of  $C/\gamma \cdot H = 0.0, 0.025, 0.05, 0.075, \text{ and } 0.10$

Where:

- |          |   |  |
|----------|---|--|
| c        | = | Cohesion, pounds per square foot           |
| $\gamma$ | = | Unit weight of soil, pounds per cubic foot |
| H        | = | Wall height, feet                          |



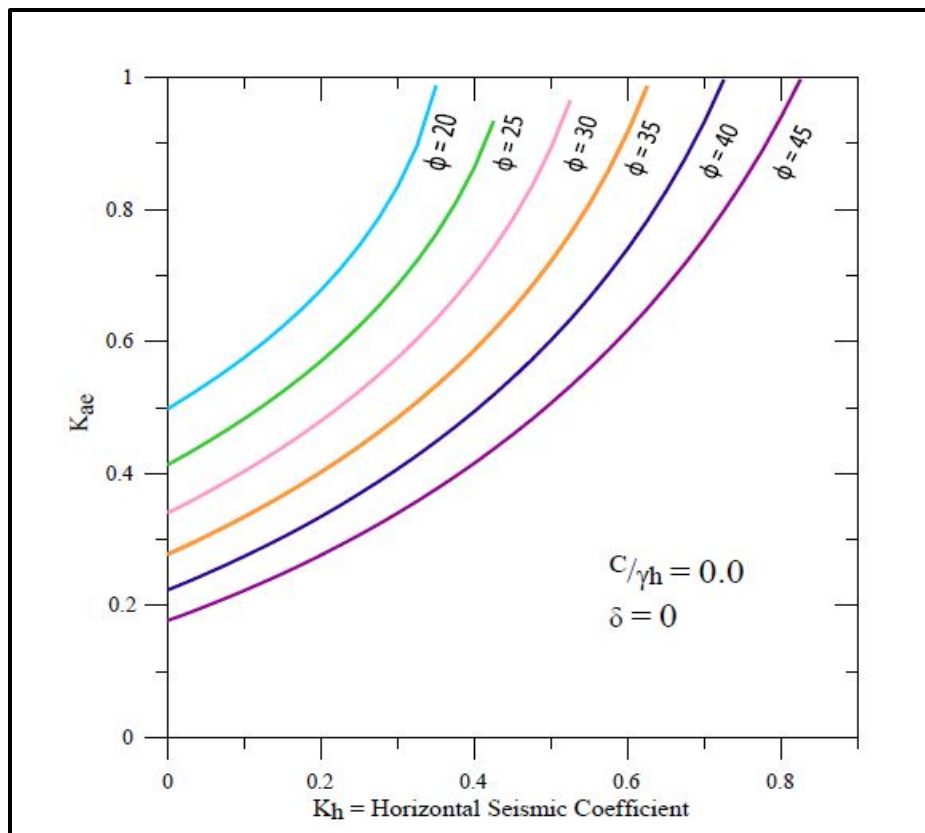


Figure 14-6, Seismic Active Earth Pressure Coefficient ( $\delta = 0$ ;  $C/\gamma_h = 0.0$ ) (modified Shamsabadi, et al. (2013b))

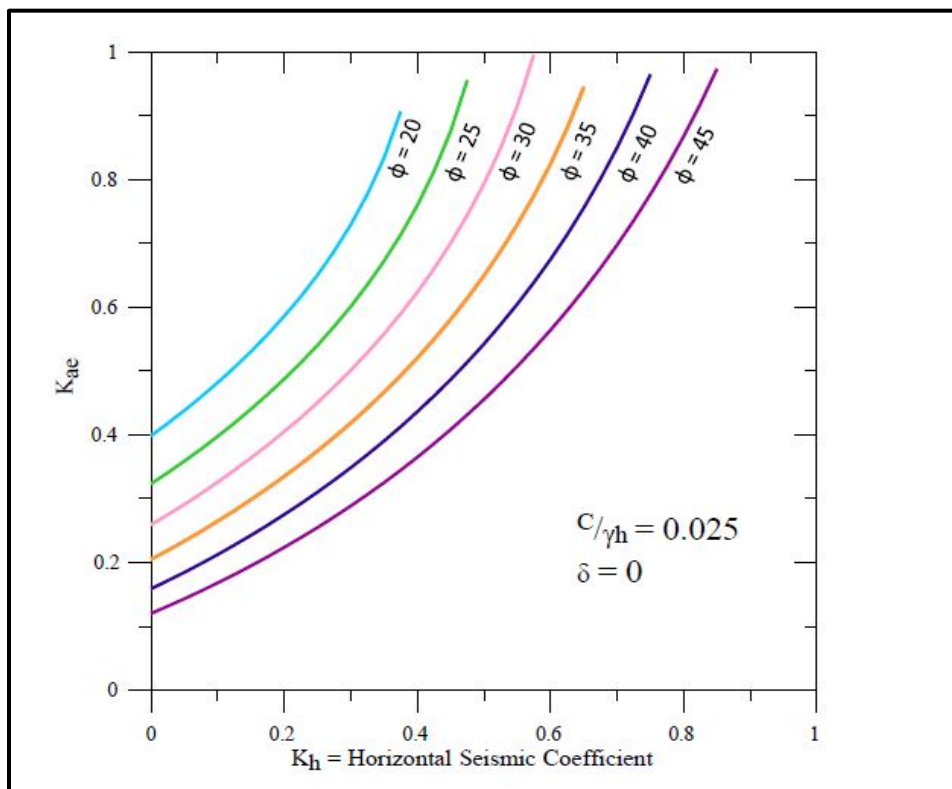


Figure 14-7, Seismic Active Earth Pressure Coefficient ( $\delta = 0$ ;  $C/\gamma_h = 0.025$ ) (modified Shamsabadi, et al. (2013b))



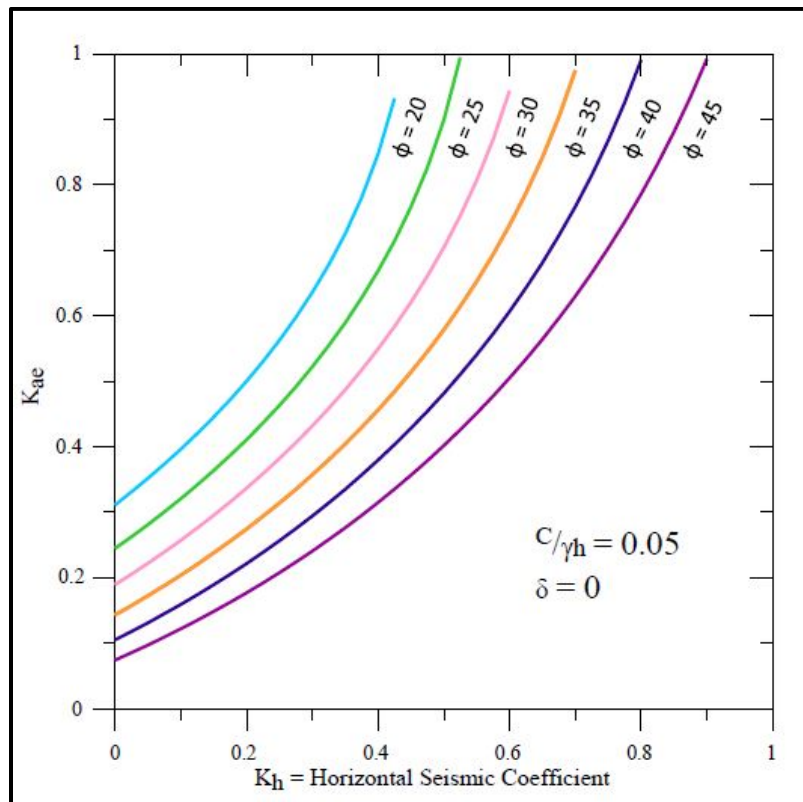


Figure 14-8, Seismic Active Earth Pressure Coefficient ( $\delta = 0$ ;  $C/\gamma H = 0.05$ ) (modified Shamsabadi, et al. (2013b))

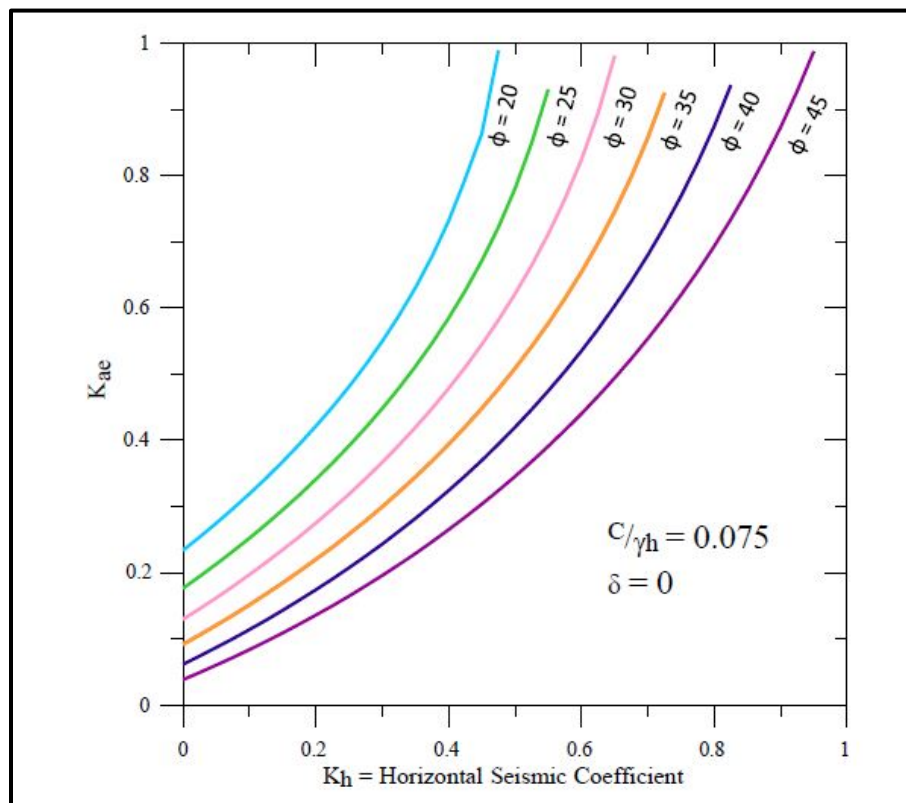


Figure 14-9, Seismic Active Earth Pressure Coefficient ( $\delta = 0$ ;  $C/\gamma H = 0.075$ ) (modified Shamsabadi, et al. (2013b))

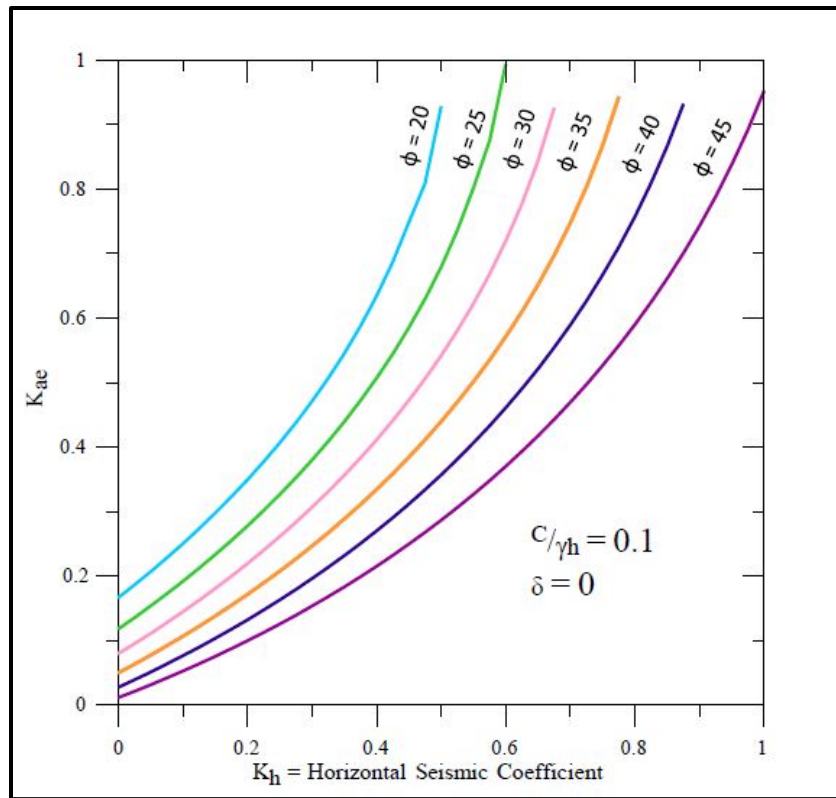


Figure 14-10, Seismic Active Earth Pressure Coefficient ( $\delta = 0$ ;  $C/\gamma_h = 0.1$ ) (modified Shamsabadi, et al. (2013b))

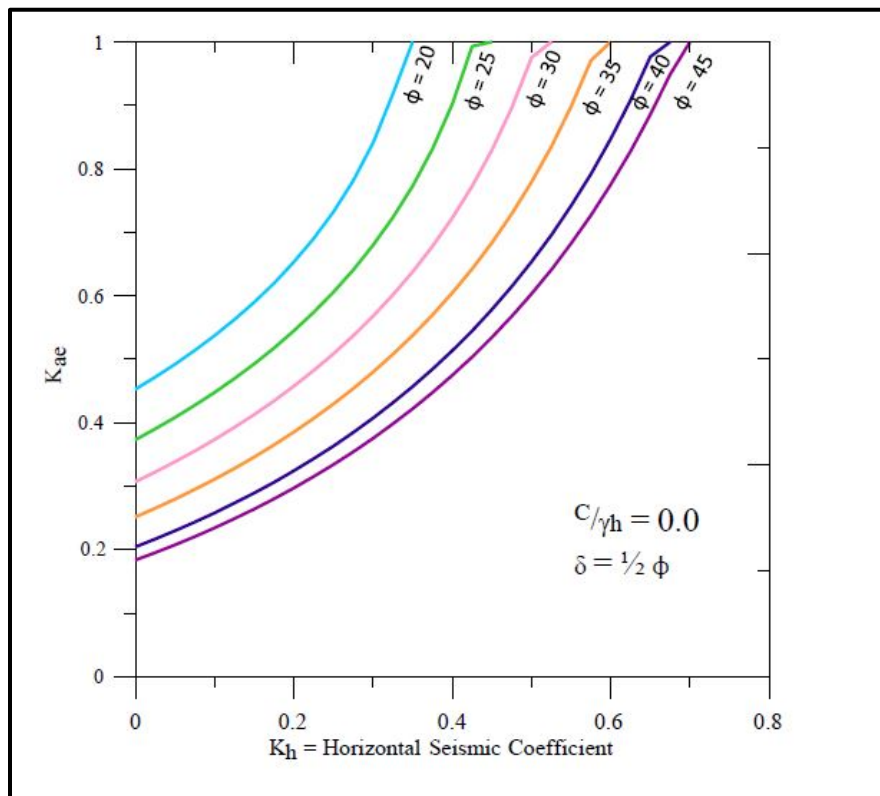


Figure 14-11, Seismic Active Earth Pressure Coefficient ( $\delta = 1/2\phi$ ;  $C/\gamma_h = 0.0$ ) (modified Shamsabadi, et al. (2013b))

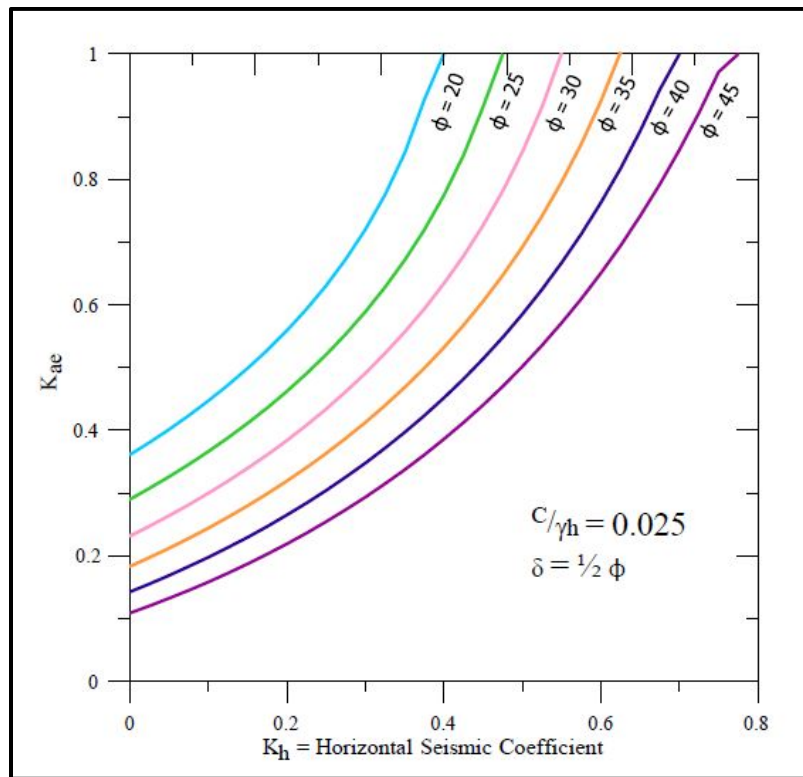


Figure 14-12, Seismic Active Earth Pressure Coefficient ( $\delta = 1/2\phi$ ;  $C/\gamma H = 0.025$ ) (modified Shamsabadi, et al. (2013b))

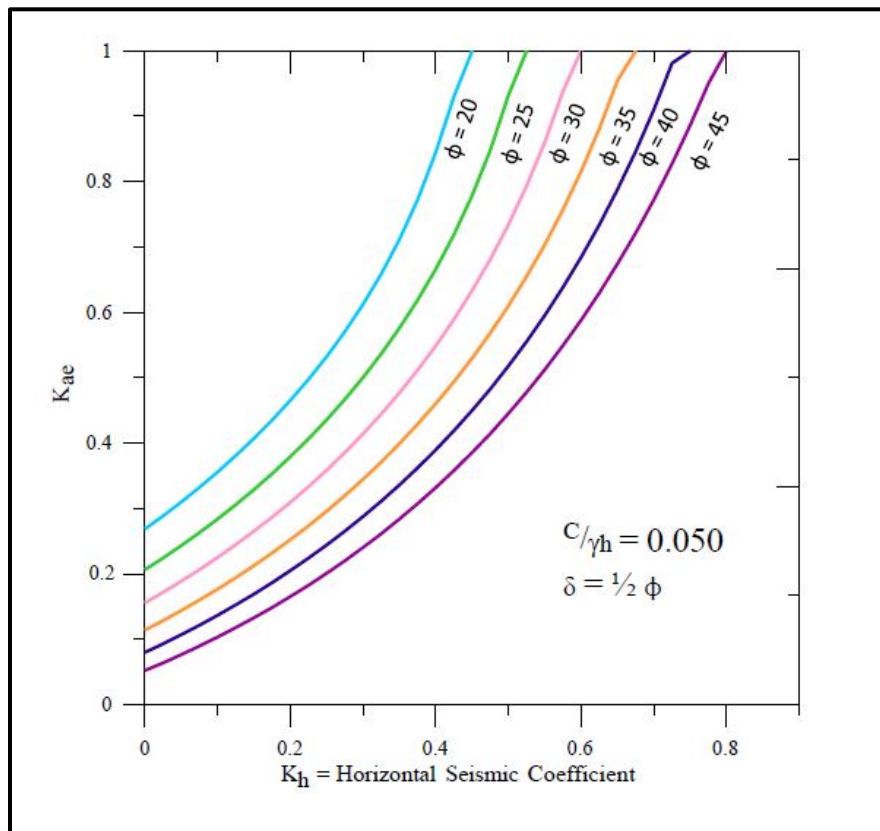


Figure 14-13, Seismic Active Earth Pressure Coefficient ( $\delta = 1/2\phi$ ;  $C/\gamma H = 0.05$ ) (modified Shamsabadi, et al. (2013b))

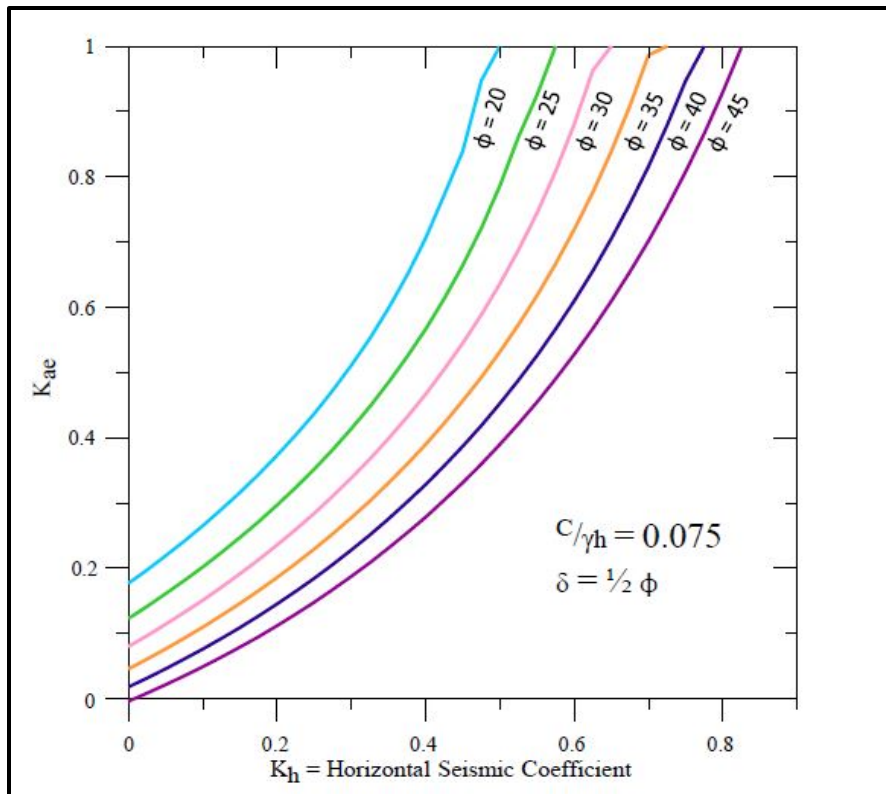


Figure 14-14, Seismic Active Earth Pressure Coefficient ( $\delta = 1/2\phi$ ;  $C/\gamma h = 0.075$ ) (modified Shamsabadi, et al. (2013b))

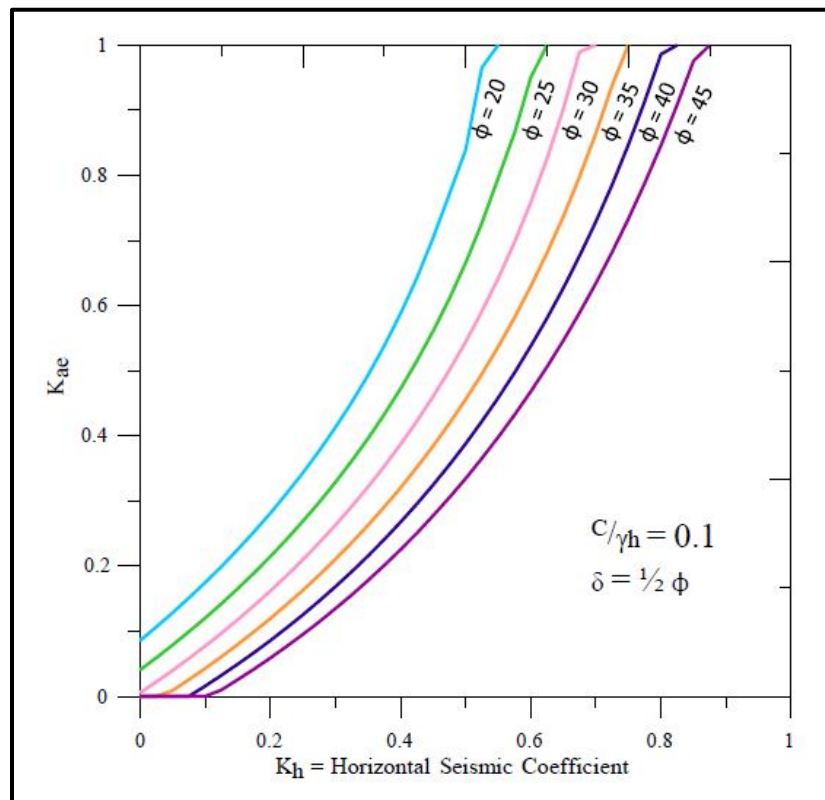


Figure 14-15, Seismic Active Earth Pressure Coefficient ( $\delta = 1/2\phi$ ;  $C/\gamma h = 0.1$ ) (modified Shamsabadi, et al. (2013b))

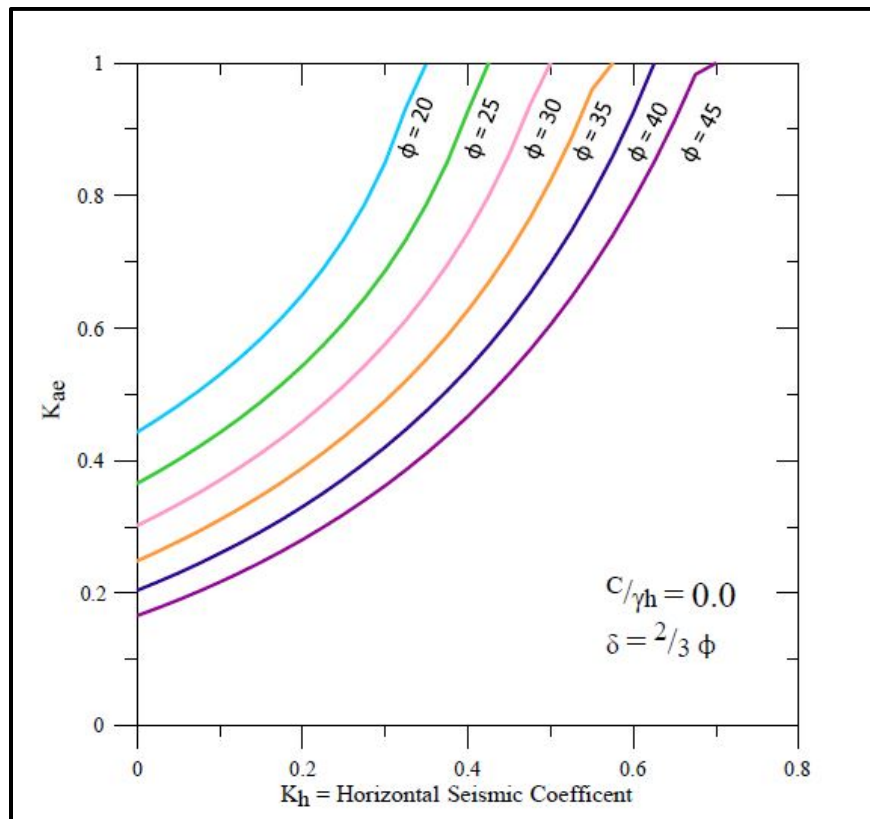


Figure 14-16, Seismic Active Earth Pressure Coefficient ( $\delta = 2/3\phi$ ;  $C/\gamma h = 0.0$ ) (modified Shamsabadi, et al. (2013b))

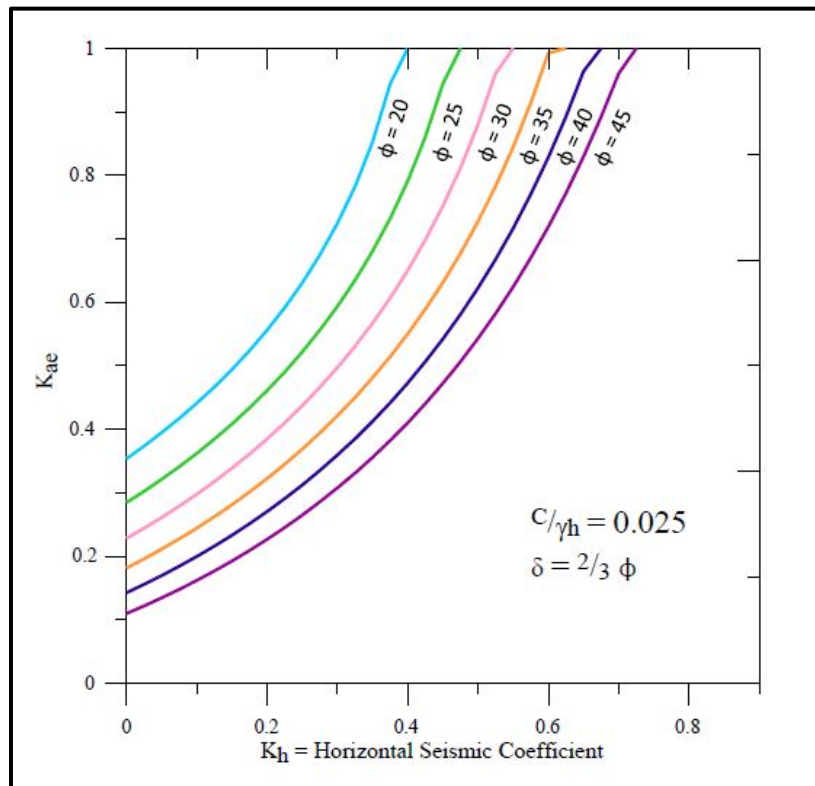


Figure 14-17, Seismic Active Earth Pressure Coefficient ( $\delta = 2/3\phi$ ;  $C/\gamma h = 0.025$ ) (modified Shamsabadi, et al. (2013b))



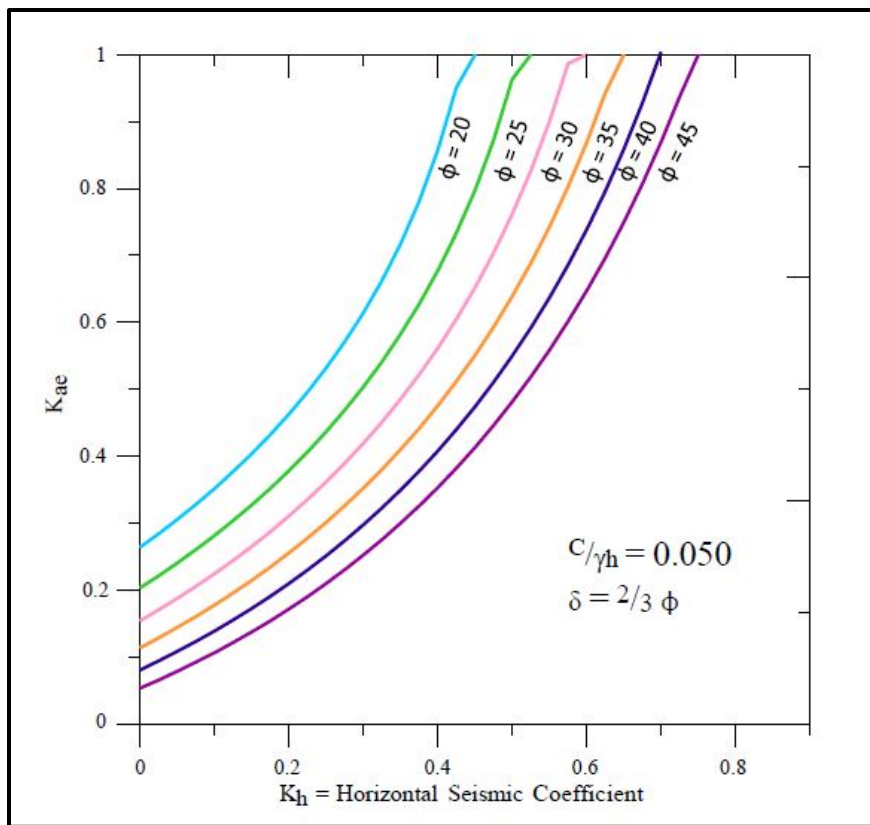


Figure 14-18, Seismic Active Earth Pressure Coefficient ( $\delta = 2/3\phi$ ;  $C/\gamma H = 0.05$ ) (modified Shamsabadi, et al. (2013b))

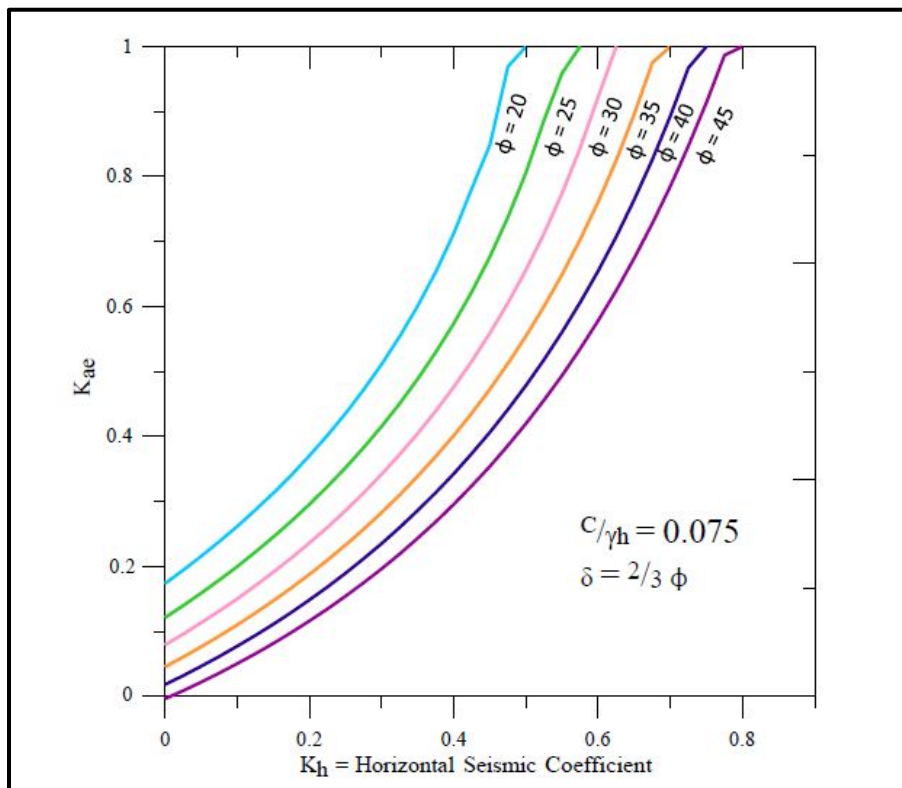


Figure 14-19, Seismic Active Earth Pressure Coefficient ( $\delta = 2/3\phi$ ;  $C/\gamma H = 0.075$ ) (modified Shamsabadi, et al. (2013b))

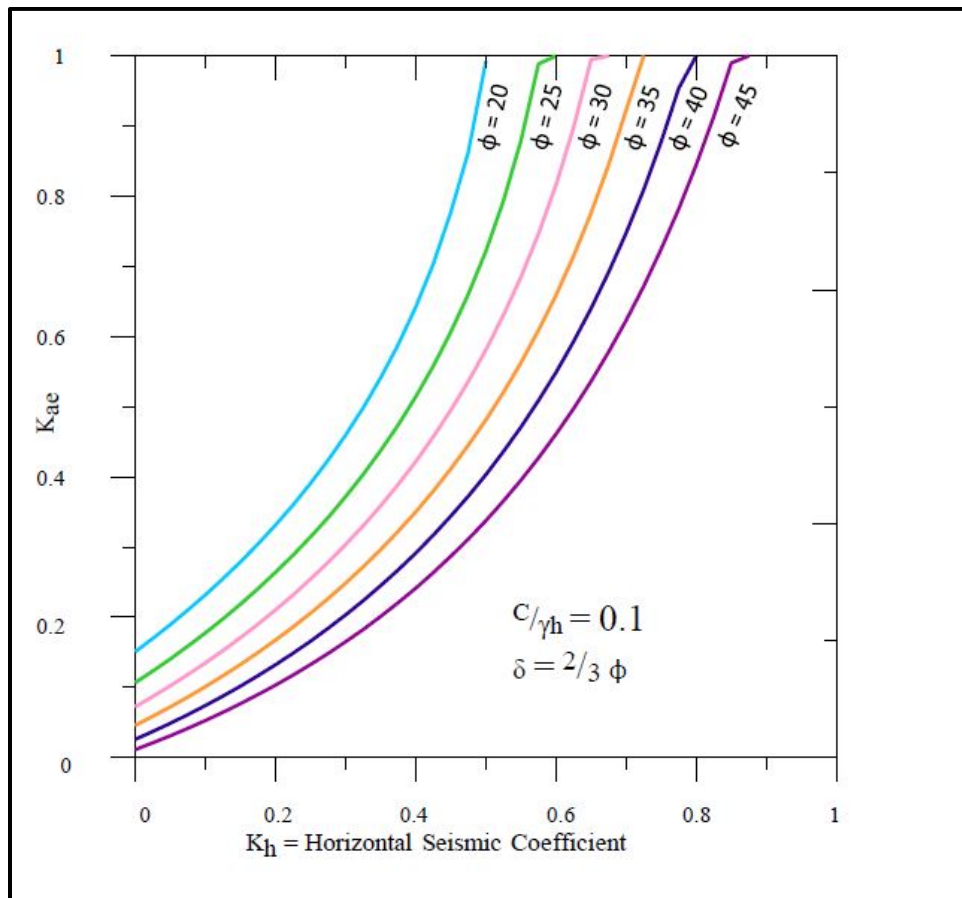


Figure 14-20, Seismic Active Earth Pressure Coefficient ( $\delta = 2/3\phi$ ;  $C/\gamma H = 0.01$ ) (modified Shamsabadi, et al. (2013b))

#### 14.4.5 GLE Method

The GLE method can also be used to evaluate critical seismically-induced active forces when the MO method is not the appropriate method. This method has been included in several conventional limit-equilibrium slope stability computer programs. This method is the most robust of the limit equilibrium methods because it can handle complex geometries, it incorporates various soil layers, and it allows the user to explore unlimited failure surfaces and soil combinations without sacrificing time or accuracy.

The slope stability method that shall be used in this analysis is Spencer's method because it satisfies the equilibrium of forces and moments. Circular, linear, multi-linear, or random failure surfaces should be investigated. Additional guidance on using this method can be obtained from NCHRP Report 611 by Anderson, et al. (2008) and Chugh (1995).

#### 14.4.6 Unyielding Structures

Seismic active soil pressures require that the wall yield sufficiently to mobilize minimum active soil pressures. Approximate values of relative movement required to reach active earth pressure conditions are provided in Chapter 18.

If the retaining structure is rigidly fixed or restrained from movement, the earthquake-induced forces will be much higher than those predicted by the seismic active pressures. Analytical methods to evaluate these types of loads on unyielding structures are not within the state of

practice for this type of structure. AASHTO requires that walls and abutments that are rigidly fixed or restrained from movements be designed using horizontal acceleration coefficients that are 1.5 times the horizontal acceleration coefficient ( $k_h$ ). The average horizontal acceleration coefficient ( $k_h$ ) that has been adjusted for wave scattering should be used when computing seismic lateral loadings on unyielding structures. The vertical accelerations shall be set to 0.0.

## 14.5 SEISMIC PASSIVE SOIL PRESSURES

Seismically-induced lateral loadings can mobilize passive soil pressure resistance such as those that occur when an ERS resists sliding by either shear keys or when an abutment backwall is displaced into the backfill. The passive resistance versus displacement behind bridge abutment wall is provided in Section 14.9.

For retaining wall components subject to passive resistance that are less than 5 feet in height, the passive resisting forces shall be computed using static passive forces. Static passive forces for wall heights or foundation thicknesses less than 5 feet shall be used because it is anticipated that the inertial effects from earthquake loadings will be small (see Chapter 18). For retaining wall components subject to passive resistance that are 5 feet or greater in height, the passive resisting forces must take into account the inertial effects from the earthquake. The MO method of determining passive pressure coefficients shall not be used due to the various limitations of the method.

The Log-Spiral-Rankine (LSR) Method uses a both a log-spiral portion of the soil wedge behind the wall as well as a Rankine portion (see Figure 14-21). The LSR Method uses procedures that account for internal friction and cohesion as well as wall-soil interface friction and adhesion. The LSR Method can be used to determine the passive earth pressures and is more advantageous to passive earth pressures. The triangular (shaded) area in Figure 14-21 is a Rankine Zone, because the shear stress ( $\tau$ ) in this region is induced only by the horizontal seismic body forces without any contribution from friction or cohesion.

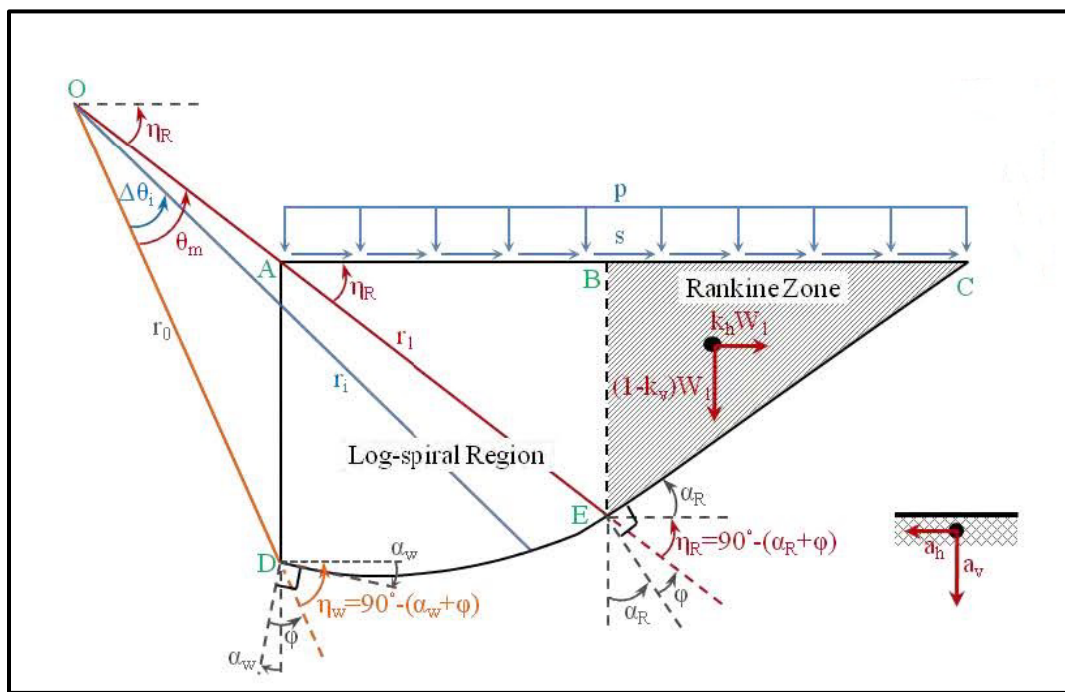


Figure 14-21, LSR Passive Seismic Wedge  
(Shamsabadi, et al. (2013b))



For a detailed explanation of the LSR Method please refer to Shamsabadi, Xu, and Taciroglu (2013a), Shamsabadi, Xu, and Taciroglu (2013b), and Xu, Shamsabadi and Taciroglu (2015). Because of the complexity of this method, design charts have been developed for the LSR Method based on the following site conditions:

1. Level ground behind the wall
2.  $k_v = 0g$
3. Wall friction angles of  $\delta = 0.0, 1/2(\phi), 2/3(\phi)$
4. Shear strength friction ratios of  $C/\gamma \cdot H = 0.0, 0.025, 0.05, 0.075, \text{ and } 0.10$

Where:

- $c$  = Cohesion, pounds per square foot  
 $\gamma$  = Unit weight of soil, pounds per cubic foot  
 $H$  = Wall height, feet

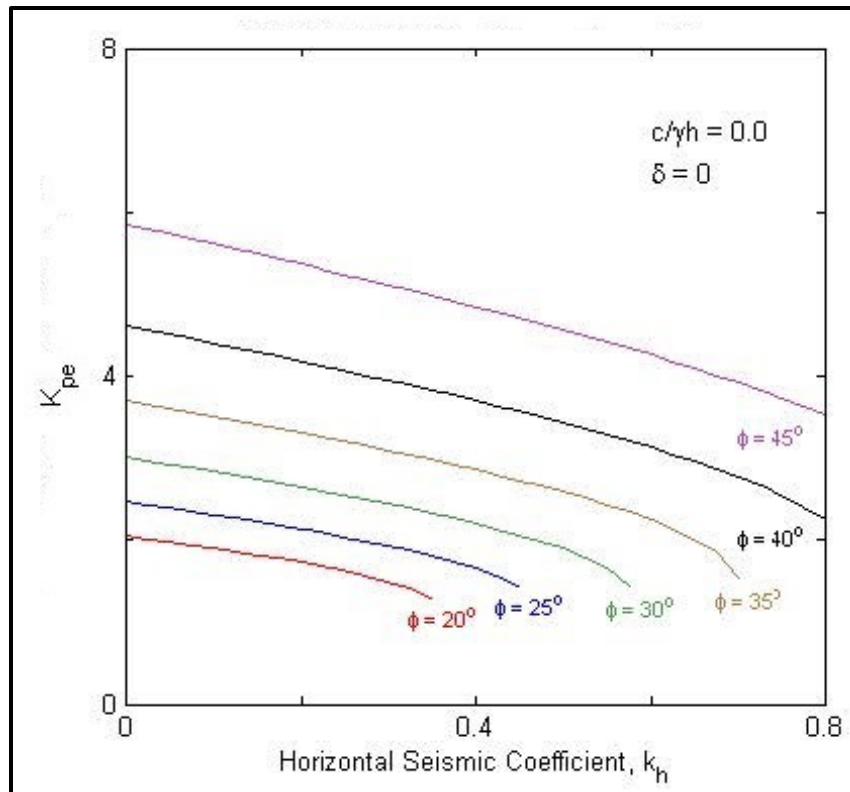


**Figure 14-22, Seismic Passive Earth Pressure Coefficient ( $\delta = 0$ ;  $C/\gamma H = 0.0$ ) (modified Shamsabadi, et al. (2013b))**

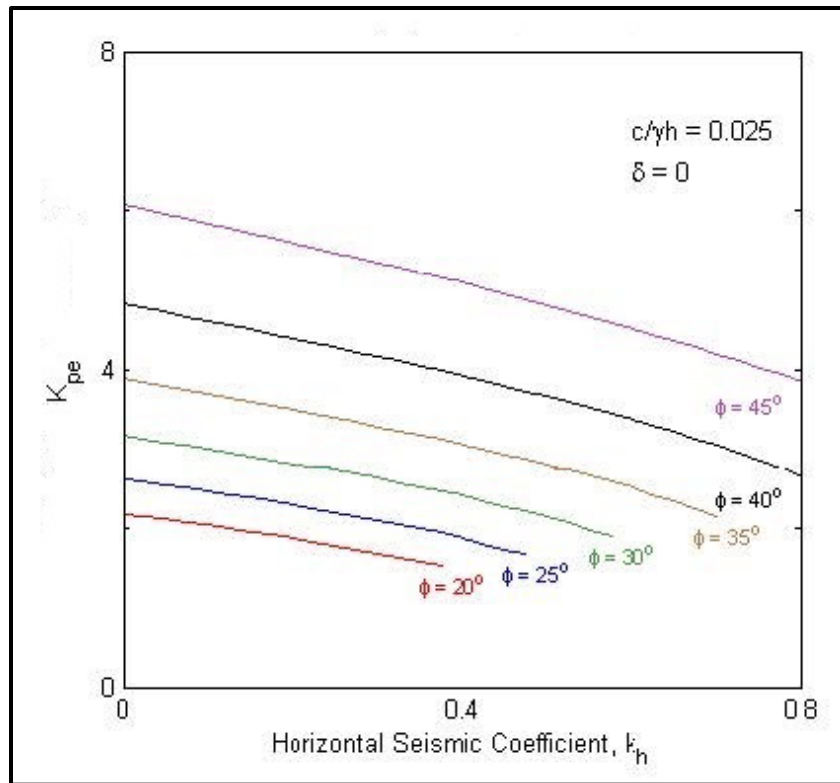


Figure 14-23, Seismic Passive Earth Pressure Coefficient ( $\delta = 0$ ;  $C/\gamma H = 0.025$ ) (modified Shamsabadi, et al. (2013b))

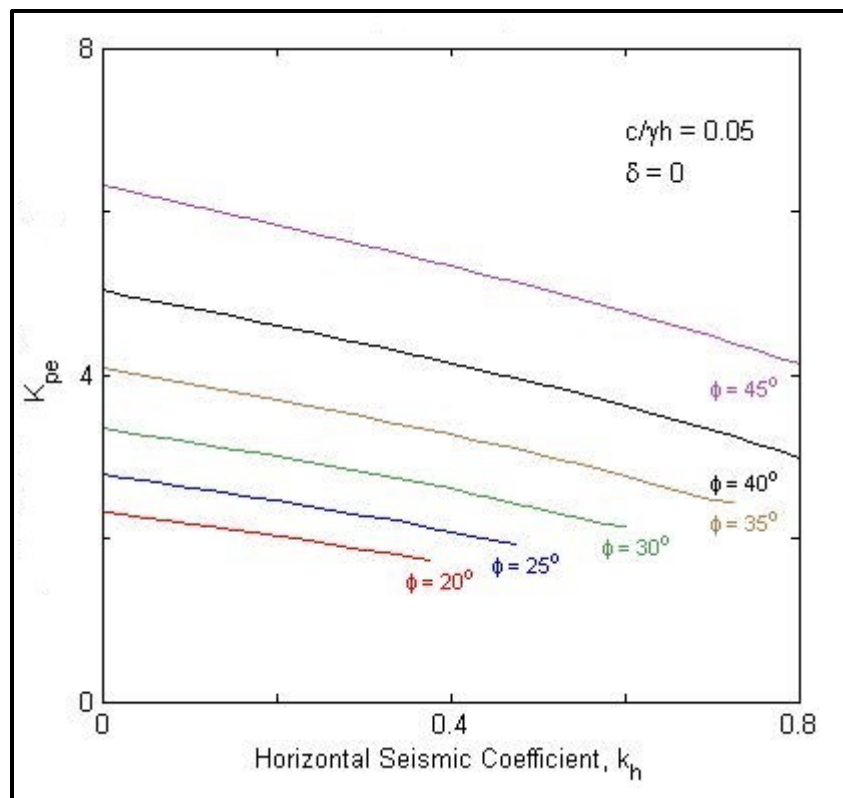


Figure 14-24, Seismic Passive Earth Pressure Coefficient ( $\delta = 0$ ;  $C/\gamma H = 0.05$ ) (modified Shamsabadi, et al. (2013b))

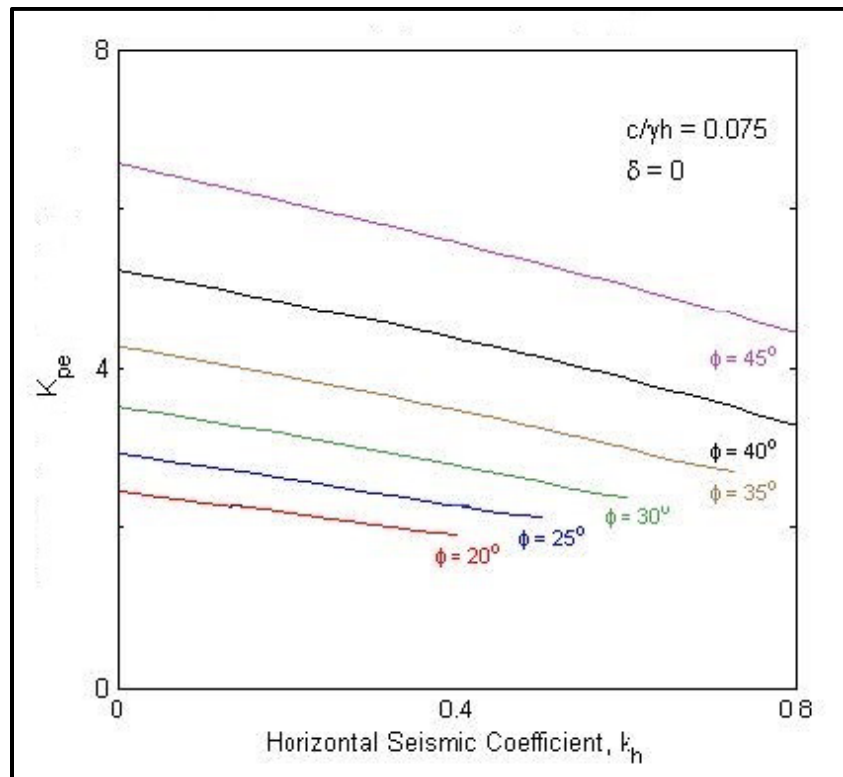


Figure 14-25, Seismic Passive Earth Pressure Coefficient ( $\delta = 0$ ;  $C/\gamma H = 0.075$ ) (modified Shamsabadi, et al. (2013b))

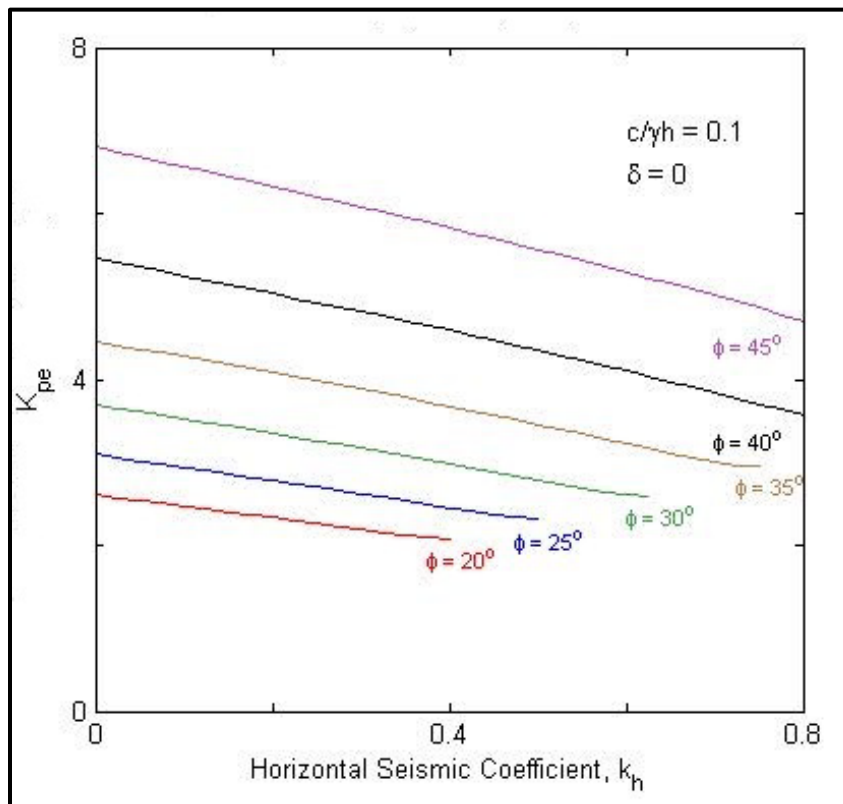


Figure 14-26, Seismic Passive Earth Pressure Coefficient ( $\delta = 0$ ;  $C/\gamma H = 0.1$ ) (modified Shamsabadi, et al. (2013b))

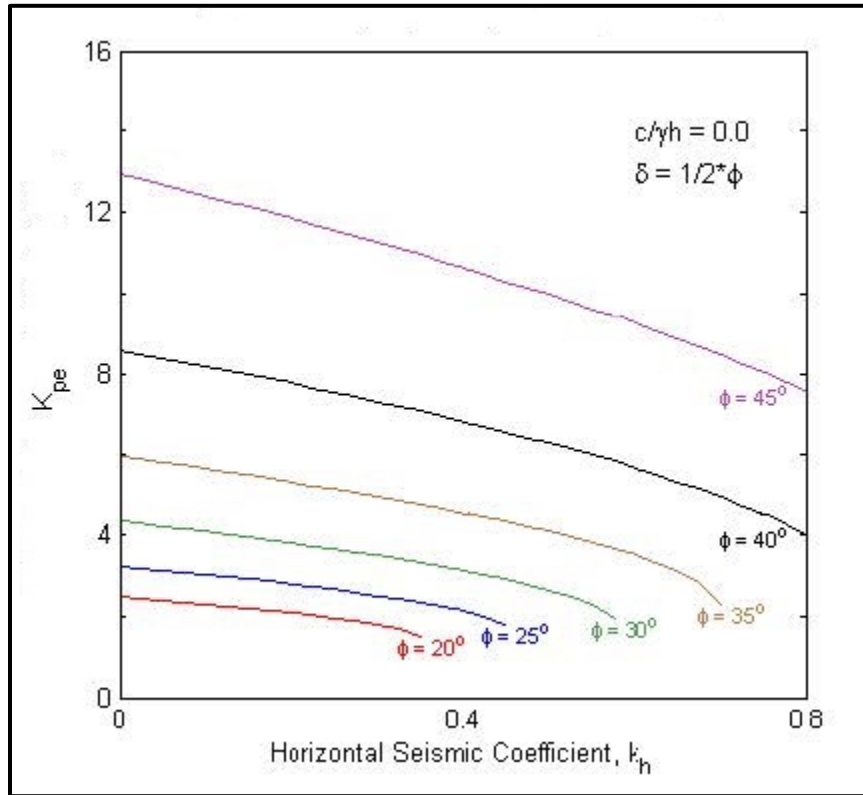


Figure 14-27, Seismic Passive Earth Pressure Coefficient ( $\delta = 1/2\phi$ ;  $C/\gamma H = 0.0$ ) (modified Shamsabadi, et al. (2013b))

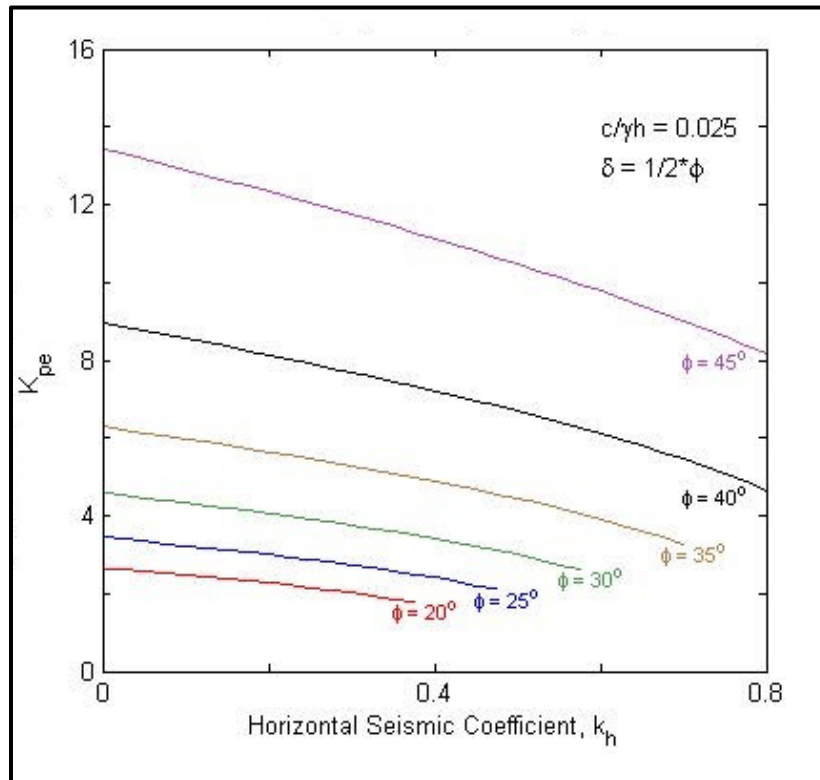


Figure 14-28, Seismic Passive Earth Pressure Coefficient ( $\delta = 1/2\phi$ ;  $C/\gamma H = 0.025$ ) (modified Shamsabadi, et al. (2013b))

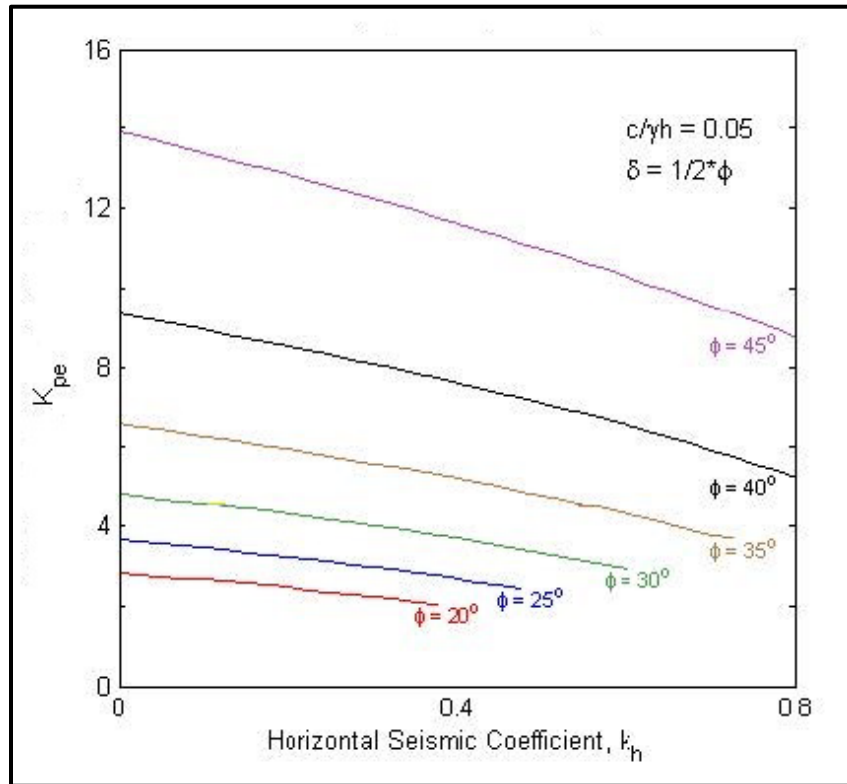


Figure 14-29, Seismic Passive Earth Pressure Coefficient ( $\delta = 1/2\phi$ ;  $C/\gamma H = 0.05$ ) (modified Shamsabadi, et al. (2013b))

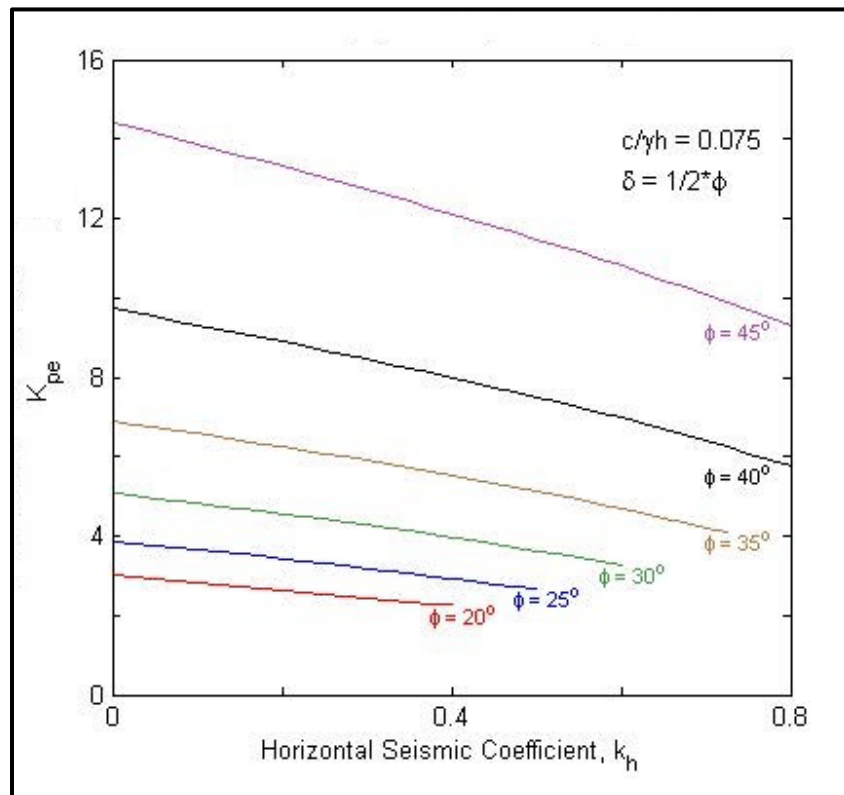
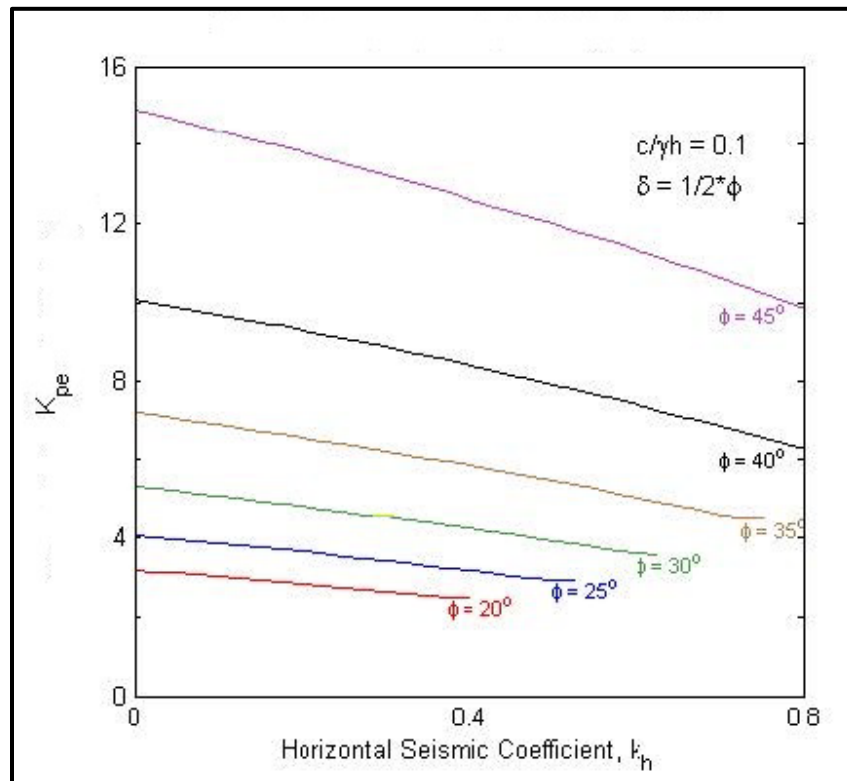
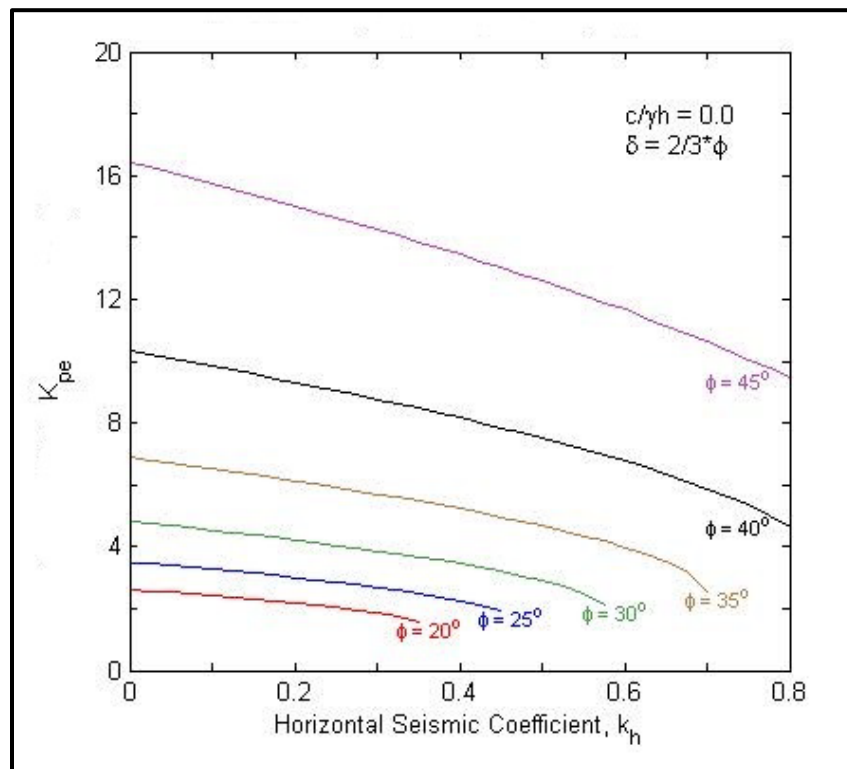


Figure 14-30, Seismic Passive Earth Pressure Coefficient ( $\delta = 1/2\phi$ ;  $C/\gamma H = 0.075$ ) (modified Shamsabadi, et al. (2013b))



**Figure 14-31, Seismic Passive Earth Pressure Coefficient ( $\delta = 1/2\phi$ ;  $C/\gamma H = 0.1$ ) (modified Shamsabadi, et al. (2013b))**



**Figure 14-32, Seismic Passive Earth Pressure Coefficient ( $\delta = 2/3\phi$ ;  $C/\gamma H = 0.0$ ) (modified Shamsabadi, et al. (2013b))**

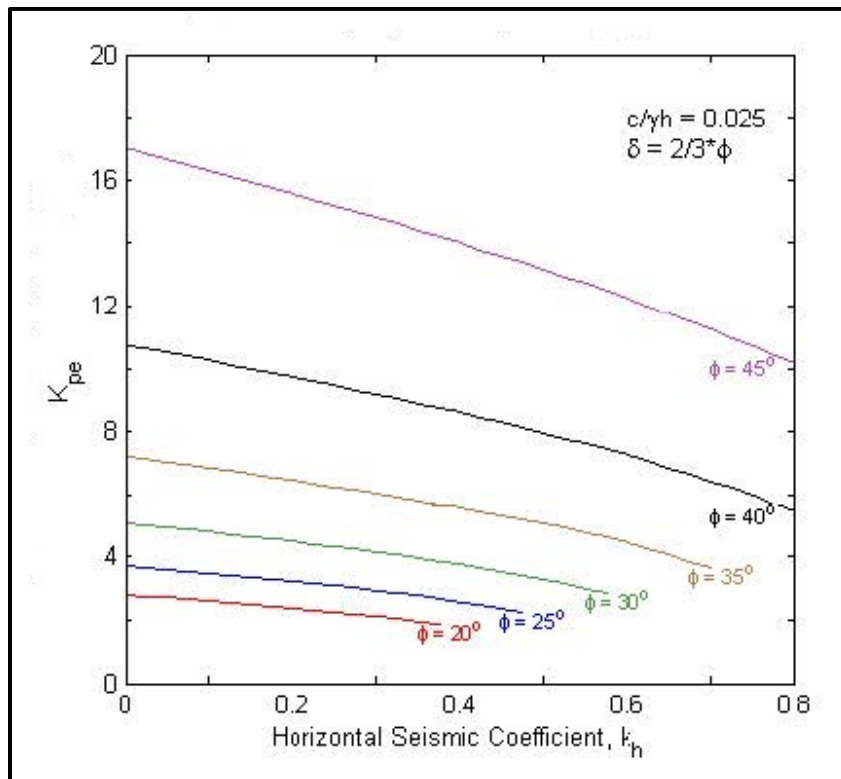


Figure 14-33, Seismic Passive Earth Pressure Coefficient ( $\delta = 2/3\phi$ ;  $C/\gamma H = 0.025$ ) (modified Shamsabadi, et al. (2013b))

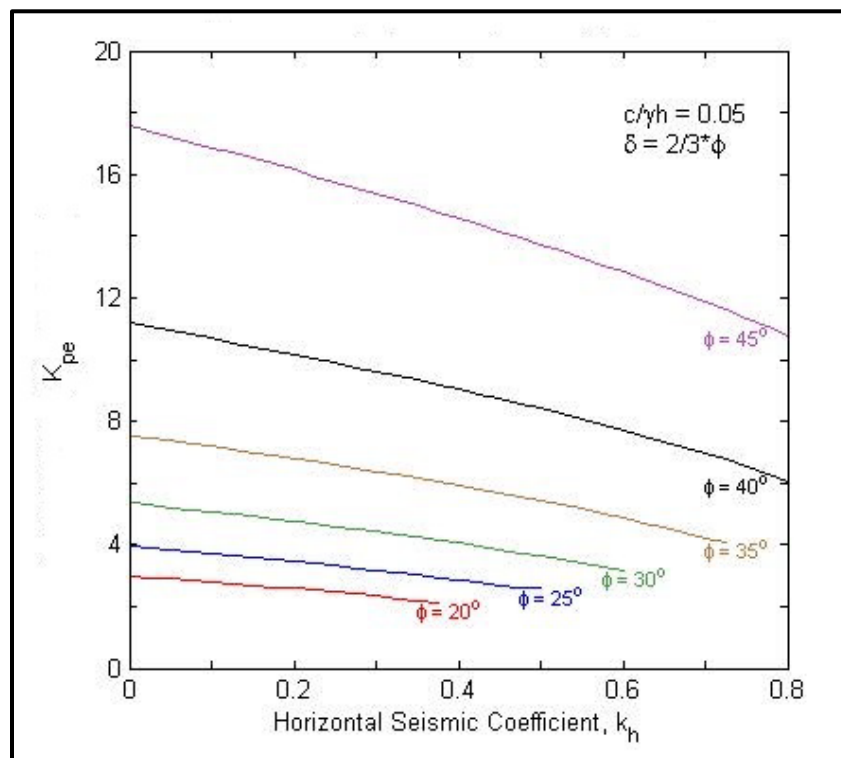


Figure 14-34, Seismic Passive Earth Pressure Coefficient ( $\delta = 2/3\phi$ ;  $C/\gamma H = 0.05$ ) (modified Shamsabadi, et al. (2013b))

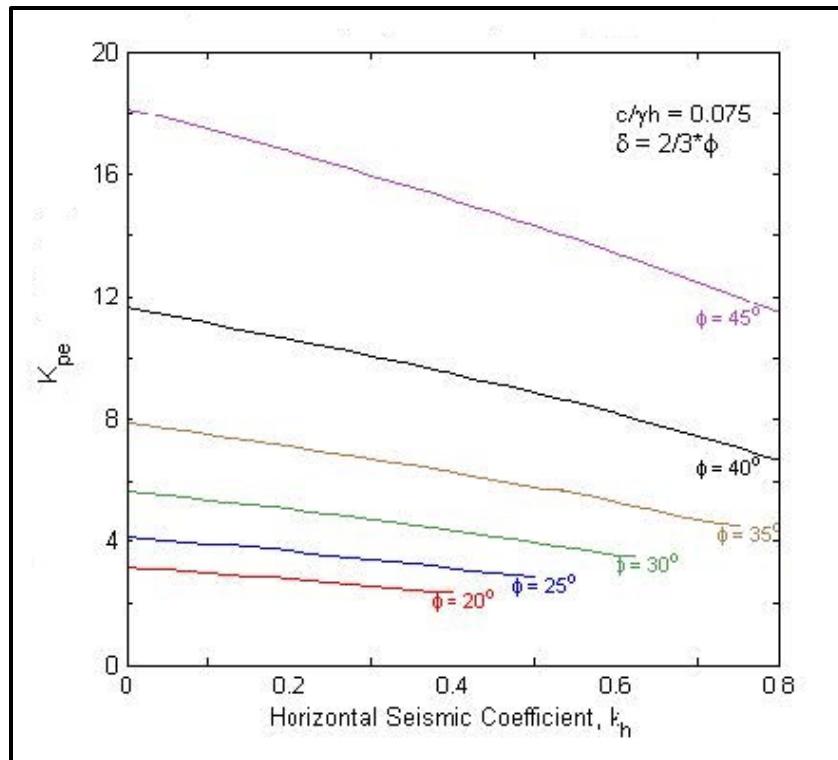


Figure 14-35, Seismic Passive Earth Pressure Coefficient ( $\delta = 2/3\phi$ ;  $C/\gamma H = 0.075$ ) (modified Shamsabadi, et al. (2013b))

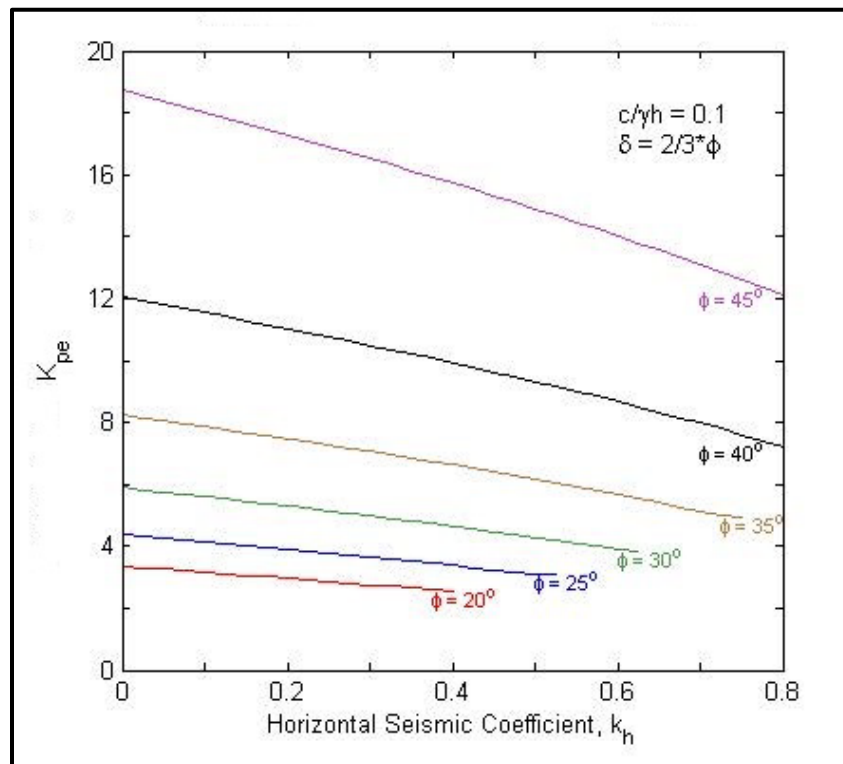


Figure 14-36, Seismic Passive Earth Pressure Coefficient ( $\delta = 2/3\phi$ ;  $C/\gamma H = 0.1$ ) (modified Shamsabadi, et al. (2013b))



## 14.6 GEOTECHNICAL SEISMIC DESIGN OF BRIDGES

The geotechnical seismic design of bridges is a collaborative effort between the SEOR and the GEOR. In order to provide the appropriate geotechnical seismic design information, the GEOR will need to develop an understanding of the bridge design and behavior under seismic loading. The GEOR will need to become familiar with:

- Bridge Characteristics: structural fundamental period ( $T_0$ ), structure type, bridge damping (i.e., 5%), and bridge plans.
- Structural analysis method to be used by the SEOR to model the bridge foundations and abutments.
- Performance Criteria: Geotechnical seismic design for the EE I limit state design uses a Performance Based Design methodology. It is, therefore, necessary to establish performance criteria that are specific to the bridge being designed. The performance criteria provided in Chapter 10 should be used as a guide. Performance limits may need to be revised as the bridge design is modified to accommodate bridge movements.

The GEOR typically provides the SEOR the following:

- ADRS Curves
- Bridge Abutment Soil-Structure Interaction Boundaries
- Foundation Soil-Structure Interaction Boundaries
- Effects of Seismic Hazards on the Bridge
- Geotechnical mitigation options to eliminate or reduce the effects of seismic hazards

### 14.6.1 ADRS Curves

The site response for the design earthquake (FEE or SEE) is represented by a horizontal ADRS curve that represents the pseudo-spectral accelerations for the uniform hazard at different frequencies or periods. The PC/GDS develops ADRS curves at either the ground surface or the depth-to-motion location of the bridge element being evaluated as presented in Chapter 12. The site response is evaluated by either using the 3-Point method or performing a Site-Specific Seismic Response Analysis.

Site-Specific Seismic Response Analysis shall be performed in accordance with Chapters 11 and 12. The Site-Specific Response Analysis is typically performed using 1-dimensional equivalent linear site response software (i.e., SHAKE2000). When the subsurface site conditions and earthquake motion input exceed the limitations of the 1-dimensional equivalent linear site response methodology as indicated in Chapter 12, a non-linear site response analysis using appropriate non-linear site response software (i.e., DMOD2000) must be used to develop the ADRS.

All earthquake input motions must be scaled to match the uniform hazard spectral accelerations. SCDOT typically provides the earthquake input motion by developing synthetic earthquake time histories. The software used to develop the synthetic earthquake input motions can vary the frequency content by using different seeds. The use of real strong motion earthquakes will follow the procedures developed in Chapters 11 and 12.

A bridge site can have multiple site response curves depending on the subsurface soils, depth-to-motion of the foundations (i.e., interior bents vs. bridge abutments), fundamental period of the bridge, and the number and locations of joints on the bridge (i.e., is the bridge jointless, regardless of length or does the bridge have a number of joints that have ability to absorb

deflections). The development of a single ADRS curve for use in bridge seismic analyses will require input from the SEOR. The SEOR will provide input as to the site response curve that will have the largest effect on the behavior of the bridge during a seismic event. The SEOR is responsible for determining the Seismic Design Category (SDC) using  $S_{D1}$  and the requirements of the Seismic Specs. The GEOR's determination of the SDC does not relieve the SEOR of the responsibility for confirming that the correct SDC has been selected. For jointless bridges and those bridges without sufficient ability to absorb deflections, the site response curve generated at the bridge abutment typically has the largest impact on the seismic design of a bridge and may be used as the ADRS curve with concurrence from the SEOR. For bridges with sufficient ability to absorb deflections, it may be necessary to develop an ADRS curve that envelopes all of the site-response curves for the bridge site. This necessitates that the GEOR, PC/GDS and SEOR work together to evaluate the anticipated structure performance.

### **14.6.2 Bridge Abutments**

The GEOR needs to be familiar with the different types of bridge abutments that are currently being used by SCDOT and the effect of the seismic demand on the performance of the bridge abutment. See the BDM for a detailed explanation of each abutment type. Listed below are the 3 abutment types, typically used by SCDOT:

- Free-Standing End Bent
- Semi-Integral End Bent
- Integral End Bent

The GEOR will provide the soil component of the soil-structure design parameters for the bridge abutment to the SEOR. Soil-structure design parameters will be developed based on the SEOR's modeling requirements and anticipated abutment performance. Soil-structure parameters typically require either a single lateral linear spring to be used for the entire bridge abutment or a matrix of linear and rotational springs in all principal directions (i.e., x, y, and z). Because soil-structure interaction is typically non-linear, the secant modulus of linear springs must be provided to be compatible with the displacements. An analysis using the secant modulus typically requires several iterations on spring stiffness and displacement until the parameters converge.

### **14.6.3 Bridge Approach Embankment**

The bridge approach embankment (see Chapter 2 for definition) is designed to meet performance objectives of the bridge abutment by using performance limits that are based on the bridge OC. The bridge approach embankments are, therefore, designed for more stringent performance limits than are typically used for roadway embankments.

### **14.6.4 Bridge Foundations**

The performance of a bridge structure that is subjected to earthquake shaking is dependent on the superstructure and substructure (bridge foundations). Bridge foundations are typically driven piles or drilled shafts.

The GEOR is responsible for providing the soil component of the bridge foundation's soil-structure interaction model in order for the SEOR to be able to evaluate the performance of the bridge due to the seismic demand. Additional seismic design requirements are presented for shallow foundations in Section 14.7 and for deep foundations in Section 14.8.

## 14.7 SHALLOW FOUNDATION DESIGN

Shallow foundations shall be designed for EE I loads using the procedures outlined in Chapter 15. Shallow foundations should not be considered when the subsurface soils are susceptible to SSL as defined in Chapter 13. If shallow foundations are to be considered at sites that are susceptible to SSL contact the PC/GDS for further guidance. In addition, shallow foundations shall not be used within any slope that becomes unstable during the EE I unless prior written approval is obtained from the PC/GDS. All of the limitations provided in Chapter 15 for shallow foundations shall apply to the use of shallow foundations during EE I. Any settlement induced by the EE I shall be determined in accordance with procedures indicated in Chapter 13.

## 14.8 DEEP FOUNDATION DESIGN

The GEOR typically assists the SEOR in modeling the foundation performance. The performance of deep foundations is typically modeled by evaluating the soil-structure interaction between the deep foundation (i.e., driven piles, drilled shafts, etc.) and the subsurface soils. The soil-structure interaction is dependent on maintaining compatibility between the response of the deep foundation and the response of the soil when evaluating axial and lateral loads.

Geotechnical seismic hazards (Chapter 13) can significantly impact deep foundations and consequently, the performance of the bridge. The failure mechanism of these geotechnical hazards needs to be thoroughly evaluated and understood in order to consider the effects of the geotechnical seismic hazard on deep foundations supporting a bridge. Deep foundation failure mechanisms are presented in Figure 14-37.

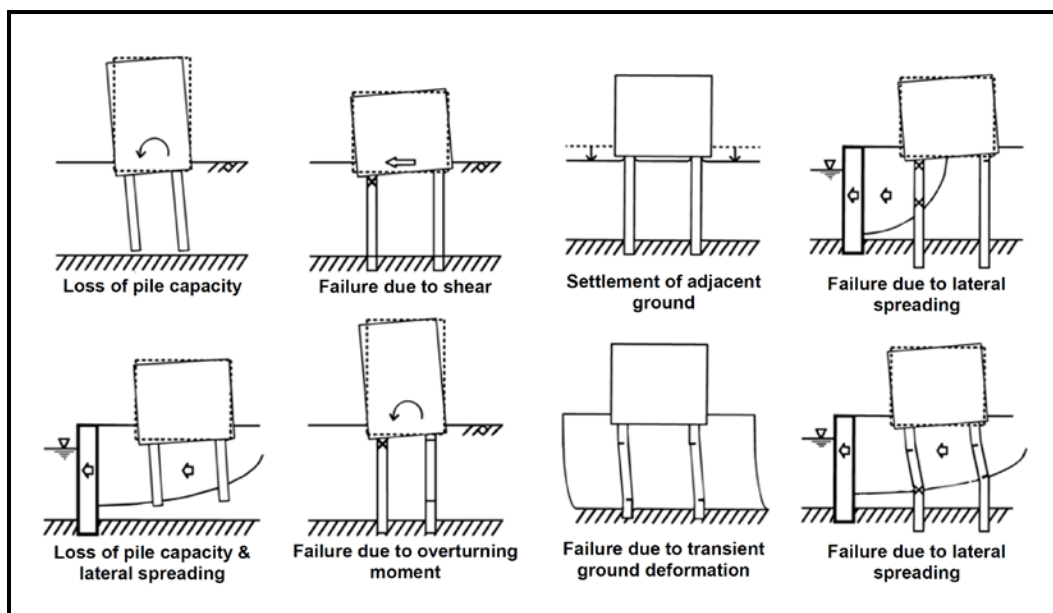


**Figure 14-37, Pile Damage Mechanisms in Liquefied Ground  
(Boulanger, et al. (2003))**

Geotechnical seismic hazards such as SSL and the resulting seismic settlement can reduce the axial bearing capacity of the deep foundation (Section 14.8.1) and the lateral soil resistance (Section 14.8.3). Deep foundation axial bearing capacity can be further reduced by downdrag loads (Section 14.8.2) induced during seismic settlement of the subsurface soils. Seismic hazard displacements due to flow slide failure and seismic global instability may impose lateral

soil loads on the deep foundations (Section 14.8.4). The lateral soil loads on the deep foundations will increase the complexity of the soil-structure interaction. The effects of the lateral soil loads on soil-structure interaction between the substructure (i.e., footings, single deep foundations, deep foundation groups, etc.) are discussed in Section 14.8.5. The effects of geotechnical seismic hazards may significantly impact the performance of the bridge and may require mitigation as discussed in Section 14.15.

### **14.8.1 Axial Loads**

When soil SSL is anticipated based on Chapter 13, the axial capacity of deep foundations for the EE I limit state shall be evaluated by adjusting the soil shear strength properties to residual soil shear strength in accordance with Chapter 13 and Section 14.8.2; and computing the axial capacity using the methods presented in Chapter 16. If the subsurface soils are susceptible to seismic settlement (Chapter 13), the axial capacity shall be evaluated using downdrag loads as indicated in Section 14.8.2.

### **14.8.2 Downdrag Loads**

Geotechnical seismic hazards such as seismic soil settlement can induce downdrag loads on deep foundations similarly to downdrag loads that result from soil consolidation. Seismic soil settlements in unsaturated soils can occur as a result of densification or seismic compression. Seismic settlement of saturated soils is typically due to densification of Sand-Like soils that are subject to cyclic liquefaction.

Soils experiencing seismic settlement and those soils above the depth of seismic settlement will induce downdrag loads on deep foundations. Analytical methods for evaluating downdrag on deep foundations are provided in Chapter 16. Downdrag loads induced from unsaturated soils and soils not subject to seismic settlement should be based on soil-pile adhesion developed from total peak soil shear strengths. The shear strength of Sand-Like soils during cyclic liquefaction will initially be reduced to liquefied shear strength ( $\tau_{fl}$ ) as the soil reaches full liquefaction (excess pore pressure ratio  $R_u \approx 1.0$ ). As the pore pressure dissipates ( $R_u < 1.0$ ), seismic soil settlement occurs and at some point, the soil shear strength will begin to increase and the soils will be in a state of limited liquefaction. The soil-pile adhesion of Sand-Like soils during cyclic liquefaction is, therefore, greater than the liquefied shear strength ( $\tau_{fl}$ ), but considerably less than the undrained peak soil shear strengths ( $\tau_{Peak}$ ). Therefore, the selection of the soil shear strength of Sand-Like soils during cyclic liquefaction should be based on using the soil shear strength occurring during limited liquefaction (i.e.,  $R_u \leq 0.7$ ) in accordance with Chapter 13.

### **14.8.3 Lateral Soil Response of Liquefied Soils (p-y Curves)**

Lateral resistance of deep foundations and cantilever retaining wall systems are typically modeled by “non-linear springs” that represent the lateral soil resistance and deflection response (P-y curves). The lateral response of liquefied soils consists of estimating the lateral resistance of the liquefied soils ( $P_{Liq}$ ) and the corresponding displacements ( $y$ ). These P-y curves of liquefied soils are used to model the non-linear soil response of applied load vs. displacement. Rollins, et al. (2005) has shown that P-y curves of liquefied soils have the following characteristics:

1. P-y curves of liquefied soils are characterized by a concave-up shape load-displacement curve. This shape appears to be due to dilative behavior of the soil during shearing.

2. P-y curves of liquefied sand transition from a concave-up shape to a concave-down shape as pore water pressure ( $u$ ) dissipates after full liquefaction ( $R_u = 1.0$ ).
3. P-y curves of liquefied sand stiffen with depth. Smaller displacements are required to develop significant resistance.
4. P-y curves of liquefied sand become progressively stiffer after liquefaction due to pore water pressure dissipation.
5. P-y curves of liquefied sand exhibit almost no lateral resistance (zone of no lateral resistance) followed by a stiffening response occurring after a certain relative displacement.
6. P-y curve zone of no lateral resistance is smaller for larger piles when compared to smaller piles.

The computer program, LPile Plus (Reese, et al. (2004)), is typically used to evaluate lateral loads on piles using P-y curves. The P-y curves for liquefied soils (Rollins, et al. (2005)) that are included in LPile Plus attempt to model the strain hardening behavior of liquefied soils, but tends to predict a response that is too soft. Since the Rollins, et al. (2005) model (Liquefied Sand in LPile Plus) has several limitations and response is very soft, it shall not be used to develop P-y curves of liquefied soils.

The P-y curves for Sand-Like soils subject to cyclic liquefaction should be estimated by either of the following two options:

1. The method recommended by Brandenburg, et al. (2007b) to develop P-y curves for fully liquefied Sand-Like soils (excess pore pressure ratio =  $R_u = u/\sigma'_v \approx 1.0$ ) consists of using static P-y curves for sands with a P-multiplier ( $m_p$ ). The  $m_p$  values developed by Brandenburg, et al. (2007b) are shown in Figure 14-38. The  $m_p$  should be selected using the thick red line shown in Figure 14-38 that is consistent with the range recommended by Brandenburg, et al. (2007b) of 0.05 for loose sand to 0.30 for dense sand. The  $m_p$  is selected based on corrected SPT blow counts ( $(N_1)_{60CS} = N_{1,60,CS}$  for Figure 14-38 only) which is consistent with the effects of relative density on undrained shear strength of sand. When limited liquefaction occurs ( $0.20 \leq R_u = u/\sigma'_v < 1.0$ ), the  $m'_p$  can be estimated by the following equation:

$$m'_p = 1 - [R_u * (1 - m_p)] \quad \text{Equation 14-6}$$

2. Alternatively, the static P-y curves for sands may be used to develop P-y curves for fully liquefied soils ( $R_u \approx 1.0$ ) by using the liquefaction shear strength ratio ( $\tau_{rl}/\sigma'_{vo}$ ) to compute a reduced soil friction angle ( $\phi_{rl}$ ). The liquefaction shear strength ratio ( $\tau_{rl}/\sigma'_{vo}$ ) can be estimated from Chapter 13. The reduced soil friction angle due to cyclic liquefaction ( $\phi_{rl}$ ) can be computed by the following equation:

$$\phi_{rl} = \tan^{-1} \frac{\tau_{rl}}{\sigma'_{vo}} \quad \text{Equation 14-7}$$

The reduced soil friction angle for limited liquefaction ( $\phi_{rl-lim}$ ) can be computed by the following equation:

Equation 14-8

$$\phi_{rl-lim} = \tan^{-1} \left[ (1 - R_u) * \left( \frac{\tau_{rl}}{\sigma'_{vo}} \right) \right] = \tan^{-1} [(1 - R_u) * \tan \phi_{rl}]$$

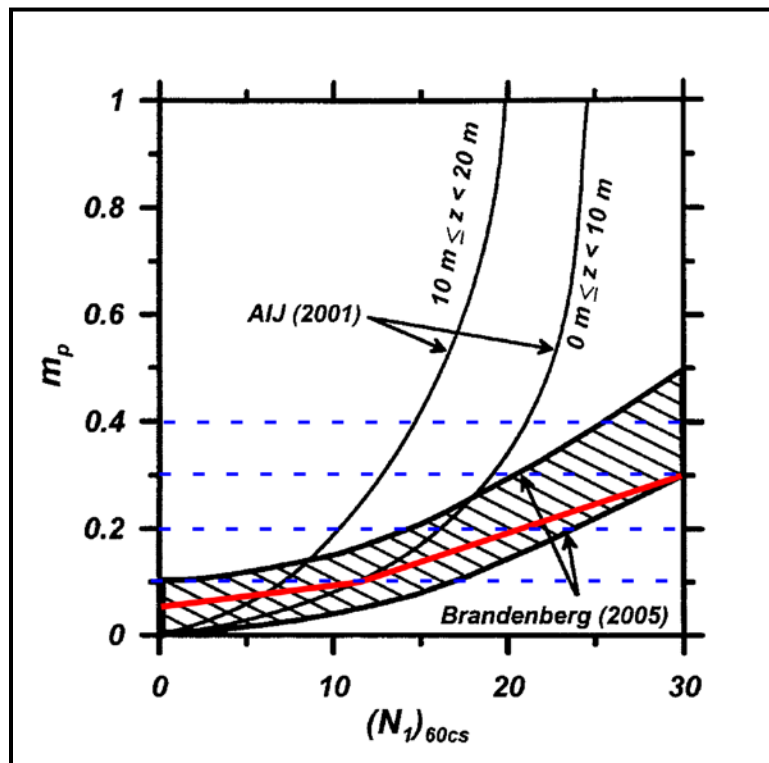


Figure 14-38, P-Multipliers ( $m_p$ ) for Sand-Like Soils Subject to Cyclic Liquefaction (Modified Brandenberg, et al. (2007b) with permission from ASCE)

Lateral loadings of pile groups that are in fully liquefied soils (excess pore pressure ratio =  $R_u = u/\sigma'_v > 1.0$ ) are not influenced by  $m_p$  when group effects are considered (even if closely spaced). During partial liquefaction ( $0.20 \leq R_u < 0.7$ ), prior to full liquefaction or after excess pore water pressures begin to dissipate, the group effects become increasingly apparent.

The preferred method to model lateral soil response is to use non-linear P-y curves. Because some structural software packages can only use linear springs to model lateral soil response, the secant modulus spring constant ( $K$ ) can be computed for the corresponding displacement of a non-linear soil response model. The use of linear springs makes it necessary to adjust the linear spring constant ( $K$ ) and it becomes an iterative process until displacements of the foundations match the displacement assumed in the development of the secant modulus spring constant.

#### 14.8.4 Effects of Seismic Soil Instability on Deep Foundations

Seismic soil instability resulting from geotechnical seismic hazards can produce soil movements that can affect the performance of the bridge substructure (i.e., caps, single or group deep foundations, etc.). The soil-structure interaction can be very complex and will require a thorough understanding of the failure mechanism (Chapter 13). The proposed methodology for evaluating and modeling the soil-structure interaction is presented as guidance in evaluating the effects of seismic soil instability on deep foundations:

- Step 1:** Evaluate potential for instability due to geotechnical seismic hazard – Seismic hazard evaluation procedures are presented in Chapter 13.
- Step 2:** Evaluate potential for free field soil displacements – After the potential for instability has been confirmed, the maximum amount of the free-field displacements needs to be estimated. The preferred method for computing displacements is to use methods that are based on the sliding block displacement model proposed by Newmark (1965) that are presented in Chapter 13.
- Step 3:** Evaluate soil loadings and displacements of substructures – This consists of determining if soil flows around the substructure or if substructures are loaded, thereby, causing movement of the substructure. Evaluation procedures are presented in Section 14.8.5.
- Step 4:** Evaluate substructure performance and structural adequacy – The GEOR will need to provide the estimated displacements and loadings to the SEOR for evaluation of the performance and structural adequacy of the substructures. If the substructures cannot be effectively designed to meet the required performance and structural strength, mitigation as discussed in Step 5 may be necessary.
- Step 5:** Evaluate mitigation of geotechnical seismic hazard – The GEOR and the SEOR will work together to evaluate the best mitigation strategy that will meet the EE I limit state performance objectives in the most safe and cost efficient manner as discussed in Section 14.15.

### 14.8.5 Evaluation of Soil Loading on Substructures

An evaluation of the soil loading on the substructures consists of evaluating which of the following 2 cases is occurring:

- Case 1:** The soil flows around the substructure with limited movement of the substructure. (See Figure 14-39)
- Case 2:** The soil and substructure move together. (See Figure 14-40)

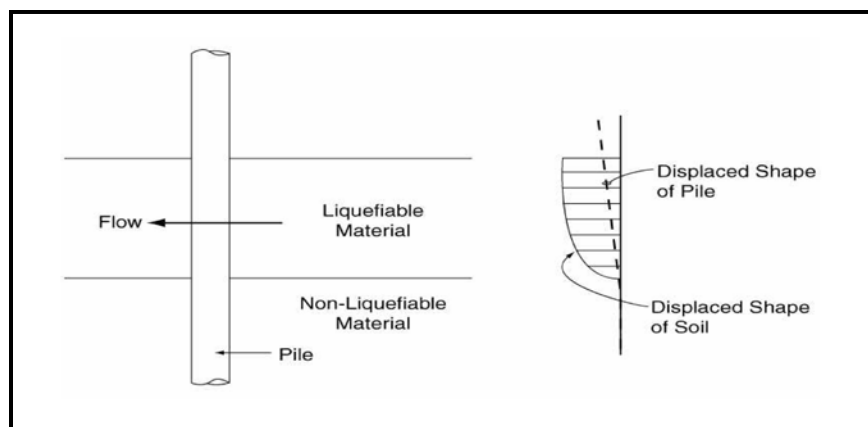
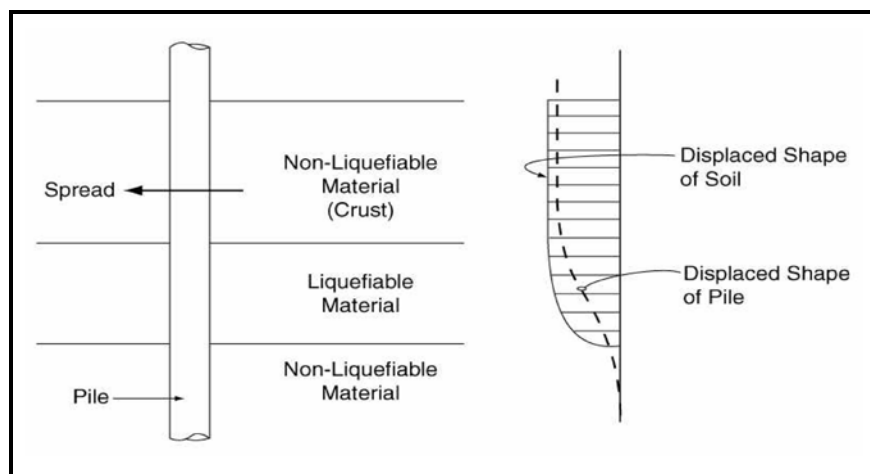


Figure 14-39, Flow of Soil Around Deep Foundation (Case 1)  
(NCHRP 12-49 (2001))



**Figure 14-40, Movement of Soil and Deep Foundation (Case 2)  
(NCHRP 12-49 (2001))**

The method to evaluate loading Case 1 on deep foundations is the displacement method presented in Section 14.8.7. If the free field soil displacements (Section 14.8.4, Step 2) are greater than deep foundation displacements and there is no crust, then the liquefied soil will flow around the substructure. When it is established that the soil will flow around the substructure, the substructure should be designed to withstand passive pressures computed by the force based methods presented in Sections 14.8.7.1 or 14.8.7.2. This site condition is anticipated occurring at interior bents only.

If a crust of non-liquefied material is present on site (e.g., at bridge end bents), then it is anticipated that the substructure movements are similar in magnitude as the free field soil movements; therefore, the substructure will need to be evaluated for structural (i.e., yield strength) and performance (i.e., displacement, rotation, etc.) adequacy. This is represented as Case 2. Typically, when the soil does not flow around the substructure, the displacements of the substructure are relatively large and cause plastic deformations of the deep foundation and/or induce significant forces on the superstructure. When there is a crust of non-liquefied soils above the liquefied soils as shown in Figure 14-40, the passive forces tend to be significantly higher in the zone of non-liquefied material and the substructure will tend to move along with the free-field displacements. When a substructure includes a pile group within the crust of non-liquefied soils, the passive force load transfer can be evaluated as indicated in Section 14.8.7.

### **14.8.6 Soil Load Contribution on a Single Deep Foundation**

The soil loading contribution from soil displacement on a single deep foundation (i.e., driven pile or drilled shaft) is very complex and generally depends on the soil shear strength, soil stiffness, spacing of piles, pile size (i.e., diameter or side dimension), arching effects, and construction method used to install the deep foundation. Although, there is no accepted method to evaluate the soil loading contribution, typical practice is that the contribution area of the soil loading or the effective pile width ( $B_{eff}$ ) can be estimated as some multiple ( $\lambda$ ) of pile size ( $B$ ) where the soil loading contribution would be defined as ( $\lambda B$ ) for different soil shear strengths. It is accepted AASHTO LRFD practice that, if loading a single row of piles in the perpendicular direction and the pile spacing is less than  $5B$ , there should be a reduction in resistance of the soil when using Beam on Nonlinear Winkler Foundation (BNWF) methods (i.e., Com624, LPile). Conversely, it can be estimated that the effective pile width ( $B_{eff} = \lambda B$ ) on a single pile will range somewhere between 1 pile diameter up to 5 pile diameters ( $B \leq \lambda B < 5B$ ). Until further research in this area



becomes available, the effective pile width ( $B_{eff}$ ) to be used for loading contribution shall be determined using the following equation:

$$B_{eff} = \lambda * B \quad \text{Equation 14-9}$$

Where,

- $B$  = Pile size (i.e., diameter or side dimension), inches  
 $\lambda$  = Effective pile width coefficient (Table 14-1)  
 $\phi$  = Angle of internal friction of soil (backwall fill materials), degrees

The effective pile width coefficient is determined as follows:

**Table 14-1, Effective Pile Width Coefficient ( $\lambda$ )**  
 (Adapted from Anderson, et al. (2008))

Pile Spacing	$\lambda$			
	Cohesive Soils		Cohesionless Soils	SSL of Sand-Like Soils
	$S_u < 1000$ psf & SSL of Clay-Like Soils	$S_u \geq 1000$ psf		
1B (side-by-side)	1	1	1	1
2B	1	2	$0.08\phi \leq 3$	1
3B	1	2	3	1
>3B	1	2	3	1

#### **14.8.7 Load Transfer Between Pile Group and Lateral Spreading Crust**

Brandenberg, et al. (2007a) proposed the Structural Model and the Lateral Spreading Model to evaluate the load transfer between pile groups and laterally spreading crusts. In the Structural Model, the pile cap moves horizontally into a stationary soil mass. In the Lateral Spreading Model, the crust of non-liquefied soil moves laterally towards the stationary pile group. Brandenberg, et al. (2007a) suggests that the actual loading condition would likely include some combination of ground displacement and pile cap displacement. The 2 load transfer models suggested by Brandenberg, et al. (2007a) are to be used as an envelope of field loading behavior and do not capture the hysteretic dynamic behavior that actually occurs during shaking. A schematic to the pile group and block of stress influence in the non-liquefied crust is presented in Figure 14-41. A brief description of the Structural Model is presented in Section 14.8.7.1 and the Lateral Spreading Model discussed in Section 14.8.7.2. The GEOR is strongly encouraged to review and thoroughly understand the procedures presented in the Brandenberg, et al. (2007a) original publication.

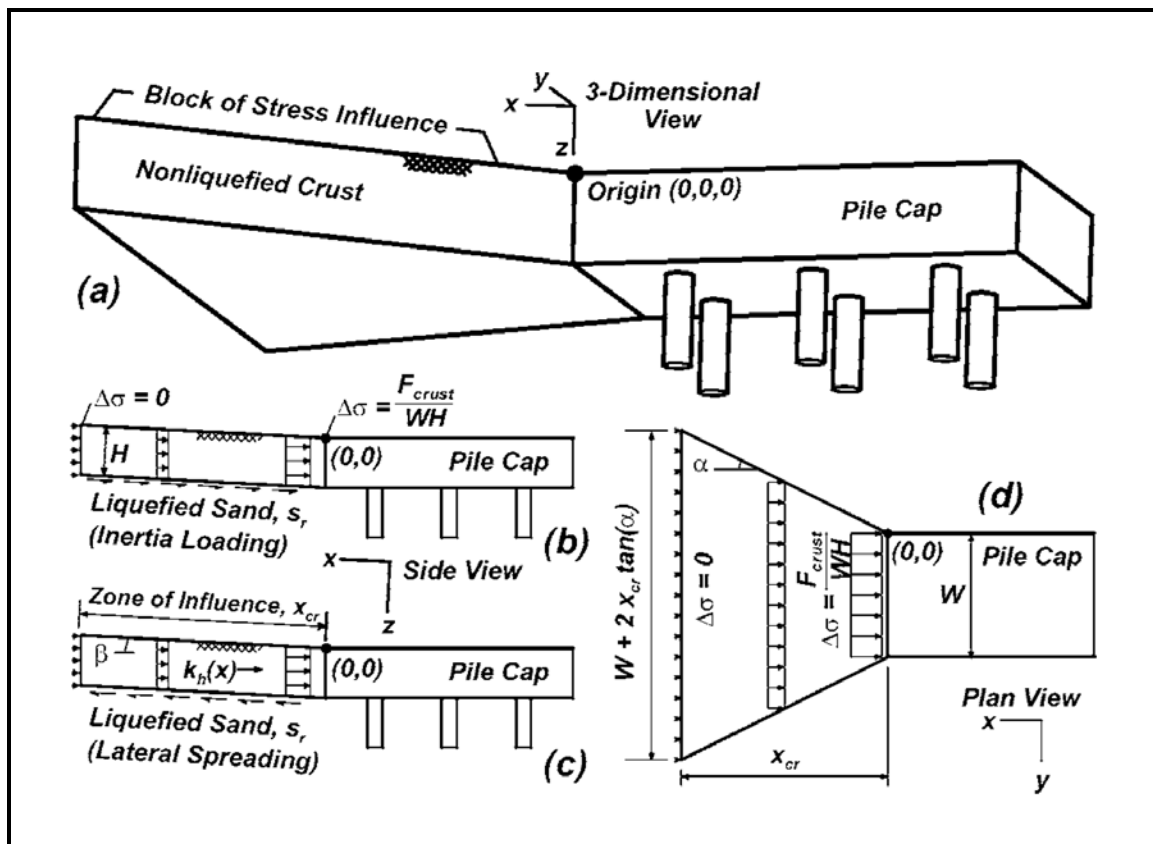


Figure 14-41, Load Transfer Between Pile Group and Lateral Spreading Crust (Brandenberg, et al. (2007a) with permission from ASCE)

#### 14.8.7.1 Structural Model

The pile cap moves horizontally into a stationary soil mass in the Structural Model. This model represents the superstructure and/or pile cap inertia loading cycle and transient ground displacements are small. The assumptions of the Structural model are as follows:

1. Inertia of non-liquefied crust is neglected since the ground is assumed stationary.
2. The residual strength of the liquefied sand is fully mobilized along the base of the non-liquefied crust and acts in the downslope direction against the force imposed by the pile group (Figure 14-41(b)).
3. Stresses attenuate within a 3D block of stress influence that geometrically extends at an angle  $\alpha$  from the backface of the pile cap in plan view (Figure 14-41(d)).

#### 14.8.7.2 Lateral Spreading Model

The crust of non-liquefied soil moves laterally towards the stationary pile group in the Lateral Spreading Model. This may occur when the lateral spreading soil fails in passive pressure mode and flows around a laterally stiff pile foundation that exhibits little cap displacement. The assumptions of the Lateral Spreading model are as follows:

1. Pile cap displacement is 0.0.

2. The residual strength of the liquefied sand is fully mobilized along the base of the non-liquefied crust and acts in the upslope direction to resist lateral spreading of the crust (Figure 14-41(c)).
3. Stresses attenuate within a block of stress influence that geometrically extends at an angle  $\alpha$  from the backface of the pile cap in plan view (Figure 14-41(d)).
4. Horizontal acceleration and downslope displacement at a given location in the nonliquefied crust layer must be compatible with the acceleration versus displacement relation obtained from sliding block solutions based on Newmark (1965) for a given ground motion.

### **14.8.8 Lateral Soil Loads Due to Seismic Hazard Displacements**

Lateral loads on deep foundations resulting from seismic hazards can be evaluated by either displacement methods or force based methods. It may be necessary to use both methods to evaluate boundary conditions and reasonableness of the results.

Boulanger, et al. (2003) and Brandenberg, et al. (2007a and 2007b) have suggested modeling the effects of seismic hazard displacements using BNWF methods (i.e., Com624, LPile) that either use free-field soil displacement (Displacement Based Method: BNWF-SD) or limit pressures (Force Based Method: BNWF-LP) that are presented in Figures 14-42(a) and 14-42(b), respectively. The BNWF-SD method is a more general approach that consists of applying the Demand from seismic hazard free-field soil displacements (SD) on the free-end of the p-y soil springs. The BNWF-LP method consists of applying the limit pressures (LP) directly on the pile foundation and is therefore, a more restrictive approach, because it assumes that soil displacements are large enough to mobilize the ultimate loads from the spreading crust and liquefiable layer against the deep foundations. Application of the displacement boundary condition on the BNWF-SD method is typically more difficult than applying the force boundary condition on the BNWF-LP method. The BNWF-SD and the BNWF-LP methods are described in Sections 14.8.8.1 and 14.8.8.2, respectively. An alternate force based method that consists of using a limit equilibrium slope stability program is described in Section 14.8.8.3.

For either the displacement or force based method presented, the inertial forces should be included as static forces applied concurrently with the seismic hazard displacement demands.

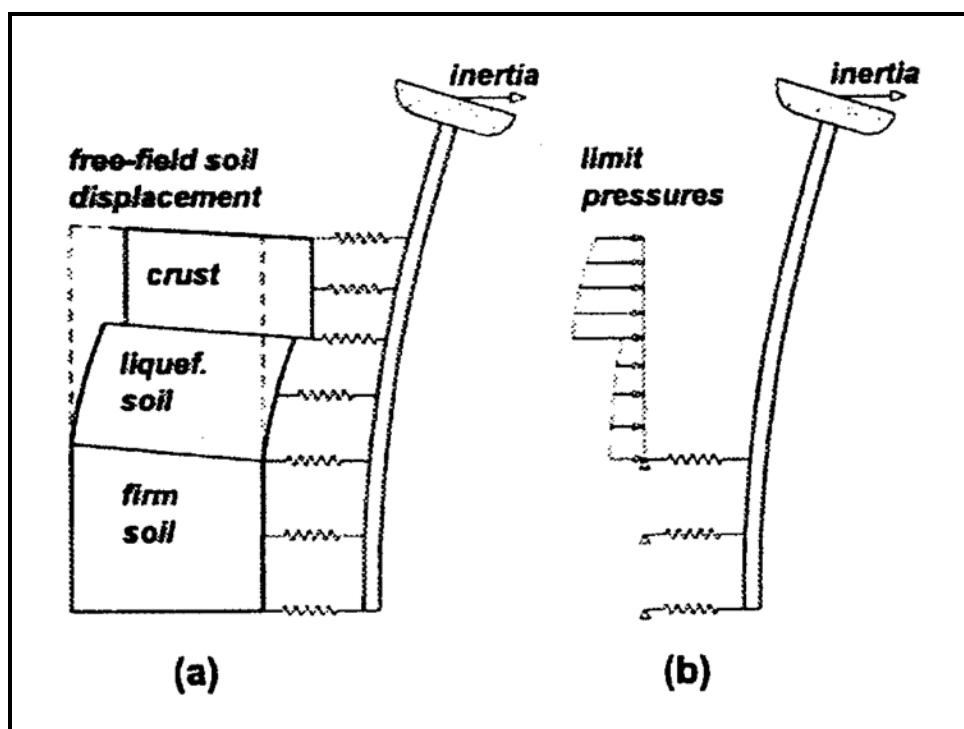


Figure 14-42, BNWF Methods for Evaluating Seismic Hazard Displacements (Brandenberg, et al. (2007b) with permission from ASCE)

#### 14.8.8.1 Displacement Based Methods (BNWF-SD)

The displacement based method for evaluating the effects of lateral loads on deep foundations is based on procedures developed by Boulanger, et al. (2003) and Brandenberg, et al. (2007a and 2007b). This method uses LPILE Plus or a similar computer program to perform the analysis. This performance based method is summarized below:

1. Estimate the free-field ground surface displacements of slope instability in accordance with Chapter 13.
2. Estimate the lateral displacements as a function of depth. The shear strain profile approach described in Zhang, et al. (2004) and illustrated by Idriss and Boulanger (2008) may be used. Another method would be to assume a constant displacement at the ground surface and crust; and then vary the displacements linearly with depth to the failure surface.
3. Model the free-field displacement and its displacement distribution with depth into LPILE Plus computer program to compute the mobilized soil reaction vs. depth.  $P_{Liq}$  is modeled in accordance with Section 14.8.3 and should be limited to:

$$P_{Liq} \leq 0.6 * \sigma'_{vo} * B \quad \text{Equation 14-10}$$

Where,

$\sigma'_{vo}$  = Effective overburden stress before seismic loading, pounds per square foot (psf)

B = Pile width, feet.

The lateral load analysis using LPILE Plus should consider the structural resistance of the foundation and the lateral resistance of the soil in front of the foundation as shown in Figure 14-43 (Imposed soil displacements).

4. Estimate the kinematic lateral loading effects on the deep foundation by using mobilized soil reaction vs. depth (Step 3) to evaluate deep foundation response using LPile Plus as shown in Figure 14-43 (Imposed pressure from spreading soil) to evaluate deflections, moments, shear, etc. Deep foundations should be evaluated for sufficient penetration below spreading soil to maintain lateral stability, location of plastic hinges, etc. If foundation resistance is greater than the applied pressures from the spreading soil, the soil will flow around the foundation. If the applied pressures from the spreading soil are greater than the deep foundation resistance, the foundation is likely to move along with the spreading soil. When pile caps are in contact with the spreading soil (or crust) passive pressures and side friction should be considered in the total loads applied to the foundation.

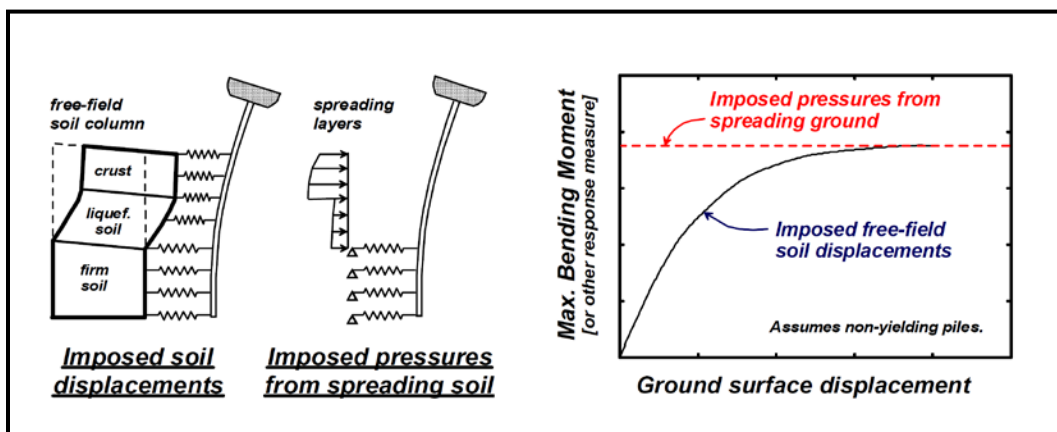


Figure 14-43, Methods for Imposing Kinematic Loads on Deep Foundations (Boulanger, et al. (2003))

#### 14.8.8.2 Force Based Methods (BNWF-LP)

This force based method for evaluating the effects of lateral loads on deep foundations is based on using limit pressures and BNWF modeling to evaluate lateral spreading induced loads on deep foundations. This method is based on back calculation from pile foundation failures caused by lateral spreading. Limit pressures assume that sufficient displacement occurs to fully mobilize lateral earth pressures. The LP for non-liquefied soils is computed based on full passive pressures acting on the foundation. For liquefied soils, the LP is computed as 30 percent of the total overburden pressure. The LP are then imposed on the deep foundation using LPILE Plus or a similar computer program to perform the analysis.

#### 14.8.8.3 Force Based Methods (Slope Stability-LP)

This force based method uses a limit equilibrium slope stability program to estimate the shear load the foundation must resist to achieve the target resistance factor,  $\phi$ , (Chapter 9). The shear loads are then distributed as a limit uniform pressure within the liquefiable zone on the deep foundation using LPILE Plus or similar computer program to perform the analysis.

## 14.9 BRIDGE ABUTMENT BACK WALL PASSIVE RESISTANCE

Earthquake-induced lateral loadings addressed in this Section are limited to the loads that are a result of soil-structure interaction between soils and abutment walls. The abutment walls are used to provide seismic passive resistance (Capacity) to earthquake-induced lateral loadings (Demand). Abutment walls discussed in this Section include the bridge back or end, wing, and shear walls, see Figure 14-44. The term “abutment wall” is used generically for this Section; however, the designer (both GEOR and SEOR) is required to know the specific location of the wall that is being analyzed. The bridge back wall and/or end wall are defined in the BDM. Shear walls are placed perpendicular to the abutment to resist transverse seismic loads. Wing walls are placed to retain sloping fills and can be used as shear walls. However, only the passive resistance developed by a fully embedded wing wall shall be used (i.e., no passive resistance will be allowed to be developed on the exterior face of the wing wall). In addition, only the passive resistance developed by the wing and/or shear walls in the transverse direction shall be used. When multiple shear walls are used, the walls shall be placed with sufficient spacing to avoid overlap of the passive resistance wedges. The development of the seismic passive resistance is discussed in detail in the following Sections. Limitations on the development of full seismic passive pressures due to wall skews are also discussed.

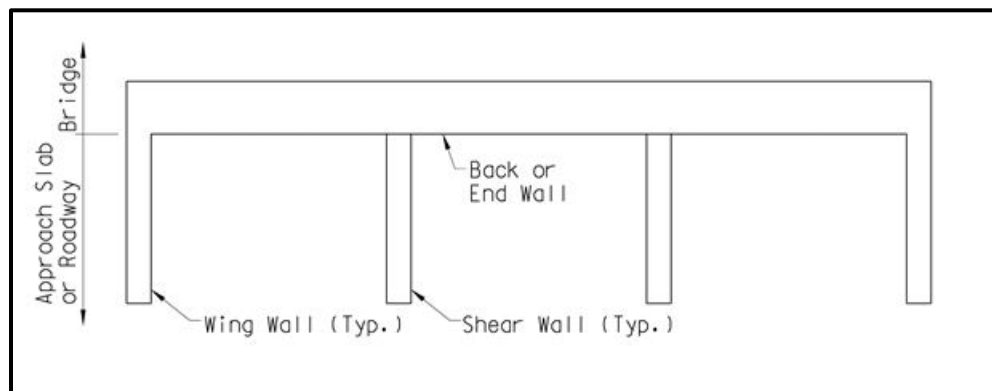
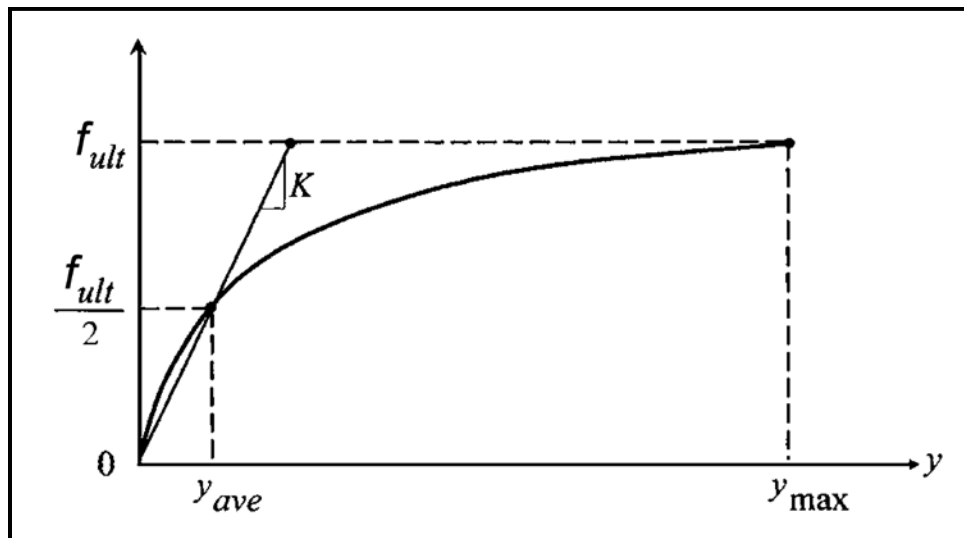


Figure 14-44, End-Bent Schematic Plan View

### 14.9.1 Development of Passive Resistance

Seismic lateral loadings can mobilize seismic passive soil pressures (resistances) such as those that occur at bridge abutments (in both the longitudinal and transverse directions) during a seismic event. Because the design methodologies presented in this Manual are performance-based, a nonlinear soil-abutment-bridge structure interaction model is used to compute the mobilized passive resistance as a function of displacement. The method to develop this model is based on the work by Shamsabadi (2006) and Shamsabadi, et al. (2007 and 2010). The basic framework of the model is a logarithmic spiral passive failure wedge coupled with a modified hyperbolic abutment-backfill stress-strain behavior (LSH). A hyperbolic force-displacement (HFD) curve is calculated by using the LSH relationship. The HFD curve is defined as shown in Figure 14-45. The HFD model is based on the assumption that the bridge superstructure is in direct contact with the back wall (i.e., the expansion joint is completely closed for free-standing end bents).



**Figure 14-45, Hyperbolic Force-Displacement Formulation (Modified Shamsabadi, et al. (2007) with permission from ASCE)**

The total maximum abutment passive resistance for the entire wall,  $F_{ult}$ , is developed at the maximum deflection ( $y_{max}$ ) considering the effective width of the wall.  $F_{ult}$  is determined as indicated below:

$$F_{ult} = f_{ult} * b_{wall} \quad \text{Equation 14-11}$$

The maximum abutment passive resistance per unit width of wall is computed as follows:

$$f_{ult} = p_{wall} * h_{wall} \quad \text{Equation 14-12}$$

Where,

- $f_{ult}$  = Maximum abutment passive resistance developed at a maximum displacement ( $y_{max}$ ), kips per foot of wall width
- $y_{max}$  = Maximum displacement where the maximum abutment passive resistance per unit width ( $f_{ult}$ ) is developed, inches
- $b_{wall}$  = Width of abutment wall or the effective width of the abutment depending on the skew angle, feet
- $p_{wall}$  = Maximum average uniform wall pressure developed at a maximum displacement ( $y_{max}$ ), kips per square foot
- $h_{wall}$  = Height of abutment wall, feet

The maximum abutment passive resistance ( $f_{ult}$ ) is estimated to occur when the ratio of the wall movement ( $y_{max}$ ) to wall height ( $h_{wall}$ ) is equal to the values in Table 14-2. This ratio ( $y_{max}/h_{wall}$ ) is also dependent on the type of backfill (Sand-Like or Clay-Like soils). These values are recommended by Shamsabadi, et al. (2007) and Shamsabadi, et al. (2010). These values are in general agreement with those  $y_{max}/h_{wall}$  values observed by Clough and Duncan (1991) for passive earth pressures.

**Table 14-2, Relative Movements Required to Reach Passive Earth Pressures  
(Modified Clough and Duncan (1991))**

Type of Backfill		$y_{max}^{(1)}$
<b>Sand-Like (Cohesionless)</b>	Dense Sand	$0.05 * h_{wall}^{(2)}$
	Medium Dense Sand	
	Loose Sand	
	Compacted Silt	
<b>Clay-Like (Cohesive - <math>c-\phi</math> Soils)</b>	Compacted Lean Clay	$0.10 * h_{wall}^{(2)}$
	Compacted Fat Clay	

<sup>(1)</sup> $y_{max}$  = maximum movement at top of wall (feet)

<sup>(2)</sup> $h_{wall}$  = height of wall (feet)

Shamsabadi, et al. (2010) indicates a maximum uniform wall passive resistance ( $p_{wall}$ ) of 1.0 ksf for a 5-1/2-foot high wall as a result of full-scale tests that were primarily conducted in California using select backfill properties that are not representative of the backfill materials that are typically used on SCDOT projects. Therefore, the maximum uniform wall passive resistance ( $p_{wall}$ ) shall be computed as indicated in Equation 14-13. The method presented to compute the maximum uniform wall passive resistance ( $p_{wall}$ ) allows for the variation in abutment wall height, backfill type and soil properties, and the effect of the seismic inertial forces on the passive wedge.

$$p_{wall} = 2 * c * \sqrt{K_{pe}} + 0.5 * \gamma_{backfill} * h_{wall} * K_{PE} \quad \text{Equation 14-13}$$

Where,

- $c$  = Soil cohesion (total stress condition), pounds per square foot
- $K_{pe}$  = Seismic passive earth pressure coefficient determined in accordance with Section 14.5.
- $\gamma_{backfill}$  = Backfill unit weight, pounds per cubic foot
- $h_{wall}$  = Height of abutment wall, feet

Seismic passive resistance shall be computed using total stress soil parameters since the rate of loading in a seismic event is not sufficient to allow dissipation of pore pressures. The actual shear strength parameters used to design the embankments shall be used unless the designer can provide a technical explanation for using different shear strength parameters.

The height of the abutment wall ( $h_{wall}$ ) depends on the type of bridge abutment (see BDM for abutment types) used and how the abutment is expected to perform. For example in an integral abutment the back wall and pile cap are typically rigidly connected so that abutment and pile cap act as a single unit. Therefore,  $h_{wall}$  is the sum of back wall plus the pile cap. However, in a free-standing abutment (seat-type), the back wall may be designed to “break off”. Therefore,  $h_{wall}$  is the height of the back wall of the abutment that “breaks off”. The GEOR is required to fully understand the anticipated abutment type and how the abutment is expected to perform. In addition,  $h_{wall}$  affects the length,  $\overline{AC}$ , (see Figure 14-21) of the passive wedge. The passive wedge distance  $\overline{AC}$  is determined using the following equation, which is based on Shamsabadi, et al. (2010):

$$\overline{AC} = 3.25 * h_{wall} \quad \text{Equation 14-14}$$

The average soil stiffness,  $K_{avg}$ , of the HFD curve shall be assumed to be  $K_{avg}=50k/in/ft$  and  $K_{avg}=25k/in/ft$  as default values for Sand-Like and Clay-Like and/or  $c-\phi$  soils, respectively, unless



site-specific soil information is available. The stiffness of the aggregate drain shall not be included in the average soil stiffness. The average soil stiffness,  $K_{avg}$  (slope  $K$  in Figure 14-45), is defined as indicated below:

$$K_{avg} = \frac{0.5 * f_{ult}}{y_{avg}} \quad \text{Equation 14-15}$$

Where,

- $f_{ult}$  = Maximum abutment passive resistance developed at a maximum displacement ( $y_{max}$ ), kips per foot of wall width
- $y_{avg}$  = Average displacement where the abutment passive resistance is equal to half of the abutment passive resistance ( $0.5f_{ult}$ ) [ $y_{ave}$  in Figure 14-45], inches

The development of the HFD curve is based on the following three boundary conditions:

- Condition I:  $f=0$  at  $y_i=0$
- Condition II:  $f=0.5f_{ult}$  at  $y_i=y_{ave}=y_{avg}$
- Condition III:  $f=f_{ult}$  at  $y_i=y_{max}$

The force-relationship is a function of displacement ( $f\{y_i\}$ ) in the general hyperbolic form as defined by the following equation:

$$f\{y_i\} = \frac{C * y_i}{1 + D * y_i} \quad \text{Equation 14-16}$$

Where,

- $y_i$  = Displacement, inches
- $C$  and  $D$  = Constants as defined below:

$$C = \left( 2 * K_{avg} - \frac{f_{ult}}{y_{max}} \right) \quad \text{Equation 14-17}$$

$$D = 2 * \left( \frac{K_{avg}}{f_{ult}} - \frac{1}{y_{max}} \right) \quad \text{Equation 14-18}$$

Where,

- $f_{ult}$  = Maximum abutment passive resistance developed at a maximum displacement ( $y_{max}$ ) (see Equation 14-12), kips per foot of wall width
- $y_{max}$  = Maximum displacement where the maximum abutment passive resistance per unit width ( $f_{ult}$ ) is developed (see Table 14-2), inches
- $K_{avg}$  = Average soil stiffness, either 50 k/in/ft for Sand-Like soils or 25 k/in/ft for Clay-Like and/or  $c-\phi$  soils

The GEOR shall provide the SEOR the appropriate HFD curves ( $f$  vs.  $y$ ) and wall secant modulus stiffness-displacement curves ( $K$  vs.  $y$ ) similar to those shown in Figure 14-46 for Sand-Like Soils, Figure 14-47 for Clay-Like Soils, and Figure 14-48 for  $c-\phi$  soils. The soil parameters indicated in Tables 14-3, 14-4, and 14-5 were used to develop the examples depicted in Figures 14-46, 14-47, and 14-48, respectively. However for bridges that have a SDC of "A", the determination of the seismic passive pressure is not required.

**Table 14-3, Sand-Like Soil Parameters Used to Create Figure 14-46**

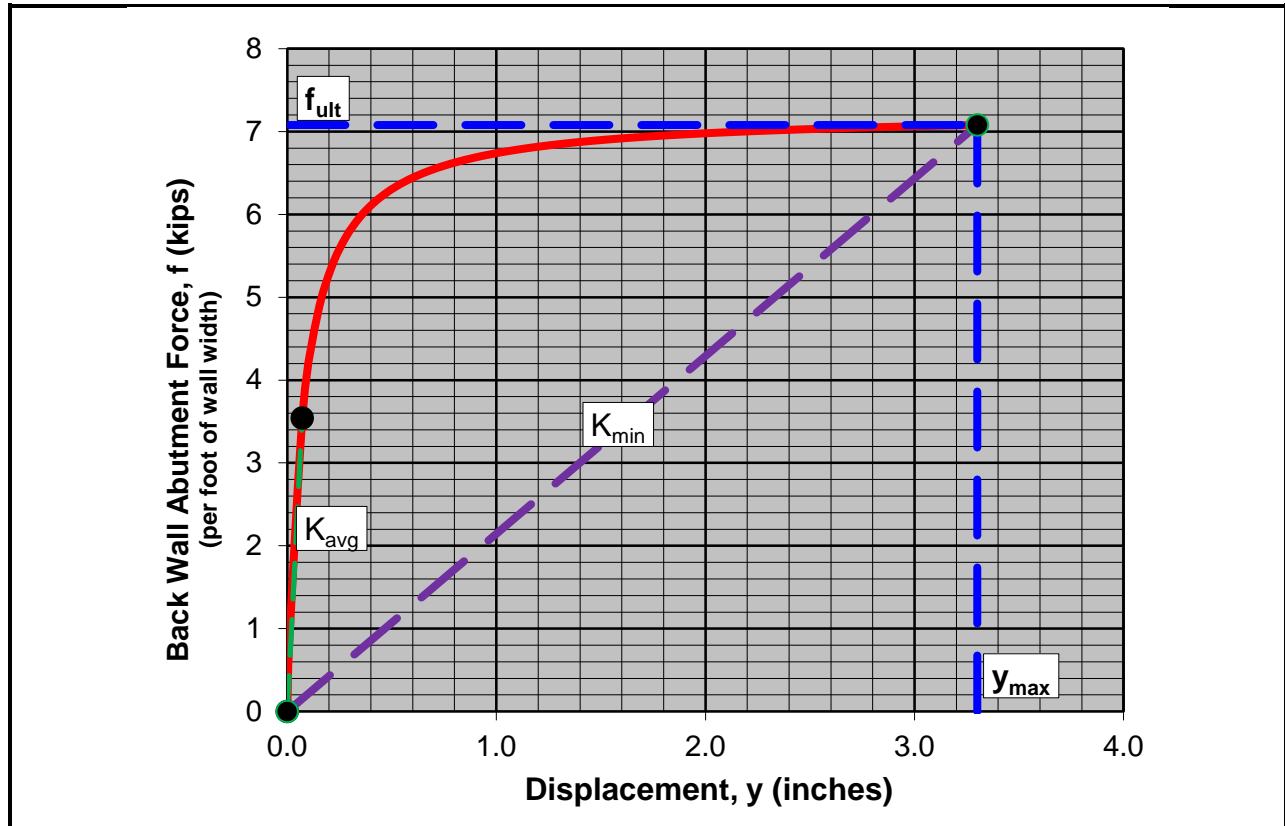
Wall Type:	Free-standing abutment back wall				
$h_{wall} =$	5.5 ft	$b_{wall} =$	50 ft	$\alpha =$	0°
Earthquake:	SEE	$S_{D1} =$	0.20	$k_{max} =$	0.30
$\beta =$	0.67	$\alpha_w =$	1.0	$k_h =$	0.30
Soil Type:	Sand-Like	$\phi =$	30°	$c =$	0 psf
$\gamma =$	120 pcf	$c/\gamma * H$	0	$K_{PE} =$	3.9
$\overline{AE}$	17.9 ft	$p_{wall} =$	1.29 ksf	$f_{ult} =$	7.08 k/ft
$y_{max}/h_{wall}$	0.05	$y_{max} =$	3.3 in.	$K_{avg} =$	50 k/in/ft
$y_{avg} =$	0.07 in.	$C =$	97.86	$D =$	13.52

**Table 14-4, Clay-Like Soil Parameters Used to Create Figure 14-47**

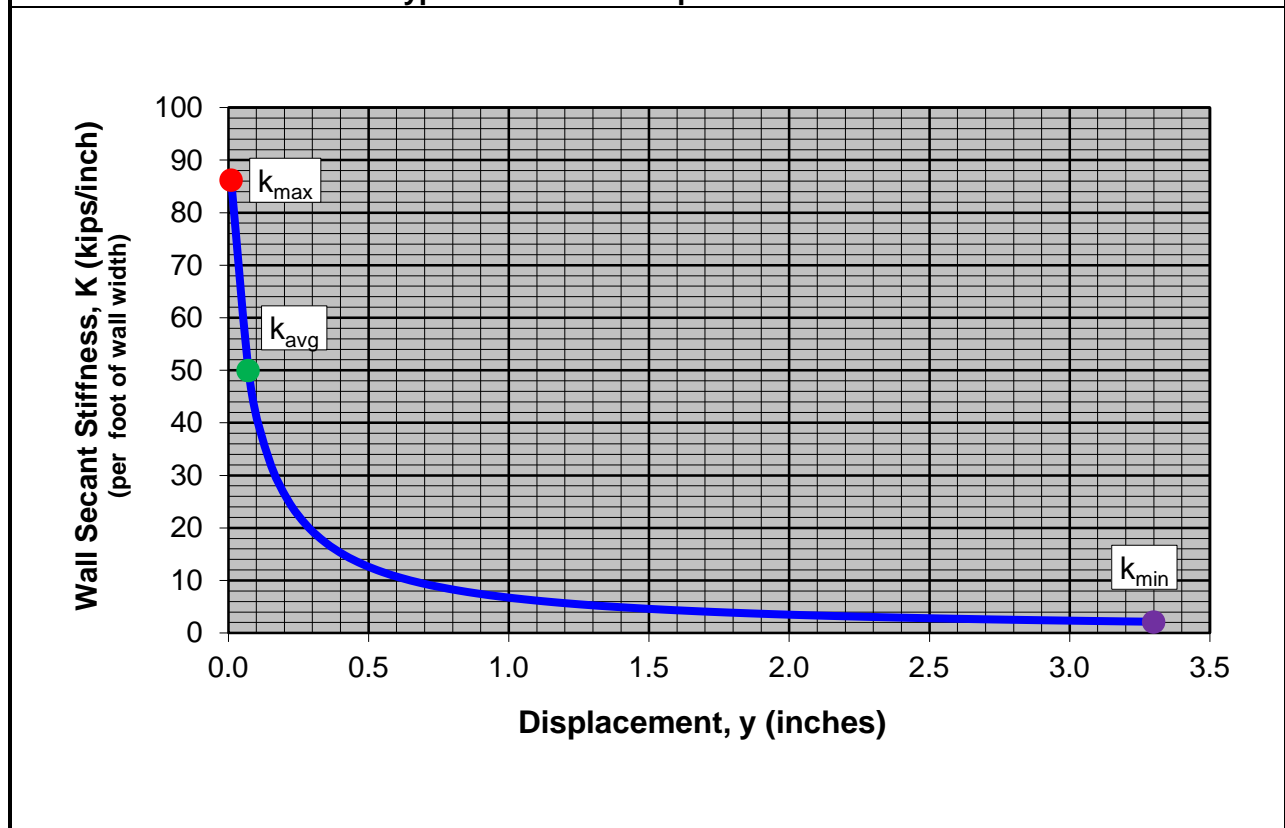
Wall Type:	Free-standing abutment back wall				
$h_{wall} =$	5.5 ft	$b_{wall} =$	50 ft	$\alpha =$	0°
Earthquake:	SEE	$S_{D1} =$	0.20	$k_{Max} =$	0.30
$\beta =$	0.67	$\alpha_w =$	1.0	$k_h =$	0.30
Soil Type:	Clay-Like	$\phi =$	0°	$c =$	2,500 psf
$\gamma =$	115 pcf	$c/\gamma * H$	3.95	$K_{PE} =$	1.0
$\overline{AE}$	17.9 ft	$p_{wall} =$	5.32 ksf	$f_{ult} =$	29.24 k/ft
$y_{max}/h_{wall}$	0.10	$y_{max} =$	6.6 in.	$K_{avg} =$	25 k/in/ft
$y_{avg} =$	0.58 in.	$C =$	45.57	$D =$	1.41

**Table 14-5, c- $\phi$  Soil Parameters Used to Create Figure 14-48**

Wall Type:	Free-standing abutment back wall				
$h_{wall} =$	5.5 ft	$b_{wall} =$	50 ft	$\alpha =$	0°
Earthquake:	SEE	$S_{D1} =$	0.20	$k_{Max} =$	0.30
$\beta =$	0.67	$\alpha_w =$	1.0	$k_h =$	0.30
Soil Type:	c- $\phi$	$\phi =$	20°	$c =$	150 psf
$\gamma =$	110 pcf	$c/\gamma * H$	0.25	$K_{PE} =$	4.0
$\overline{AE}$	17.9 ft	$p_{wall} =$	1.81 ksf	$f_{ult} =$	9.96 k/ft
$y_{max}/h_{wall}$	0.10	$y_{max} =$	6.6 in.	$K_{avg} =$	25 /in/ft
$y_{avg} =$	0.20 in.	$C =$	58.49	$D =$	5.72

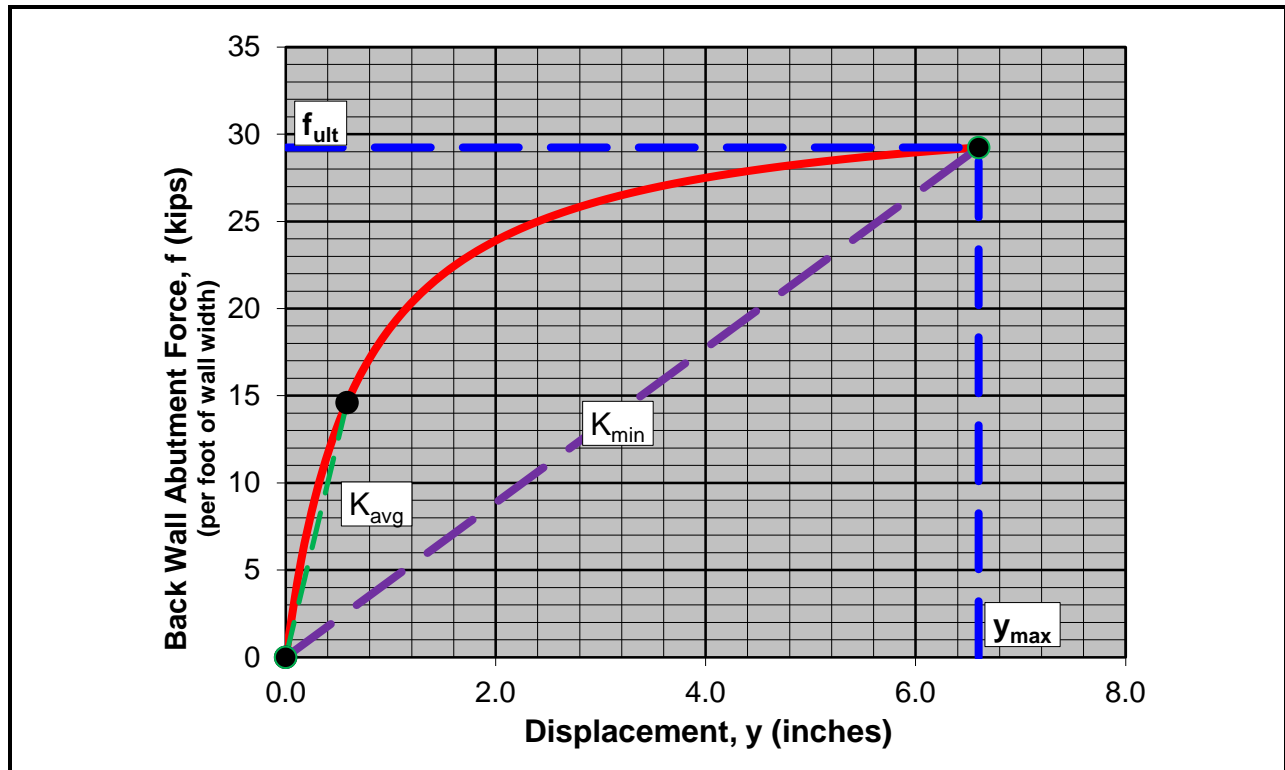


Hyperbolic Force-Displacement Curve

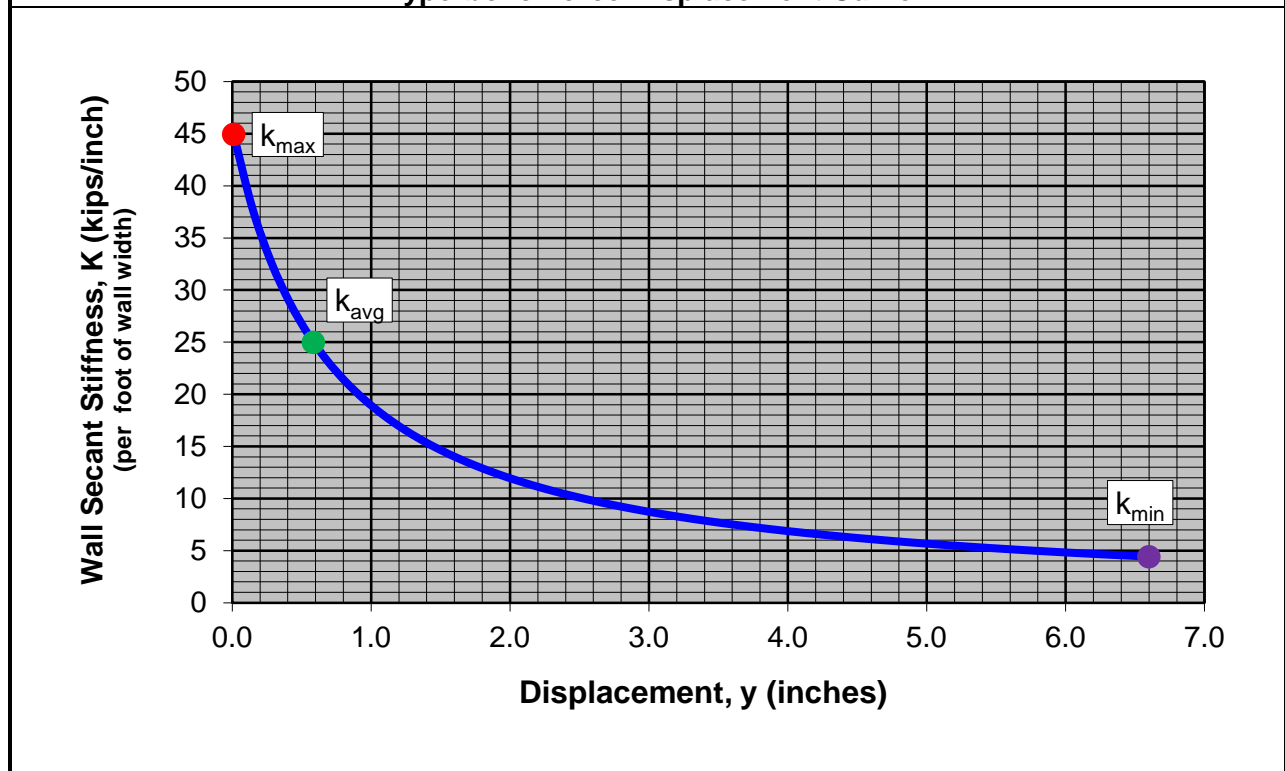


Wall Secant Stiffness-Displacement Curve

Figure 14-46, Bridge Abutment Wall Passive Pressure, Sand-Like Backfill Example

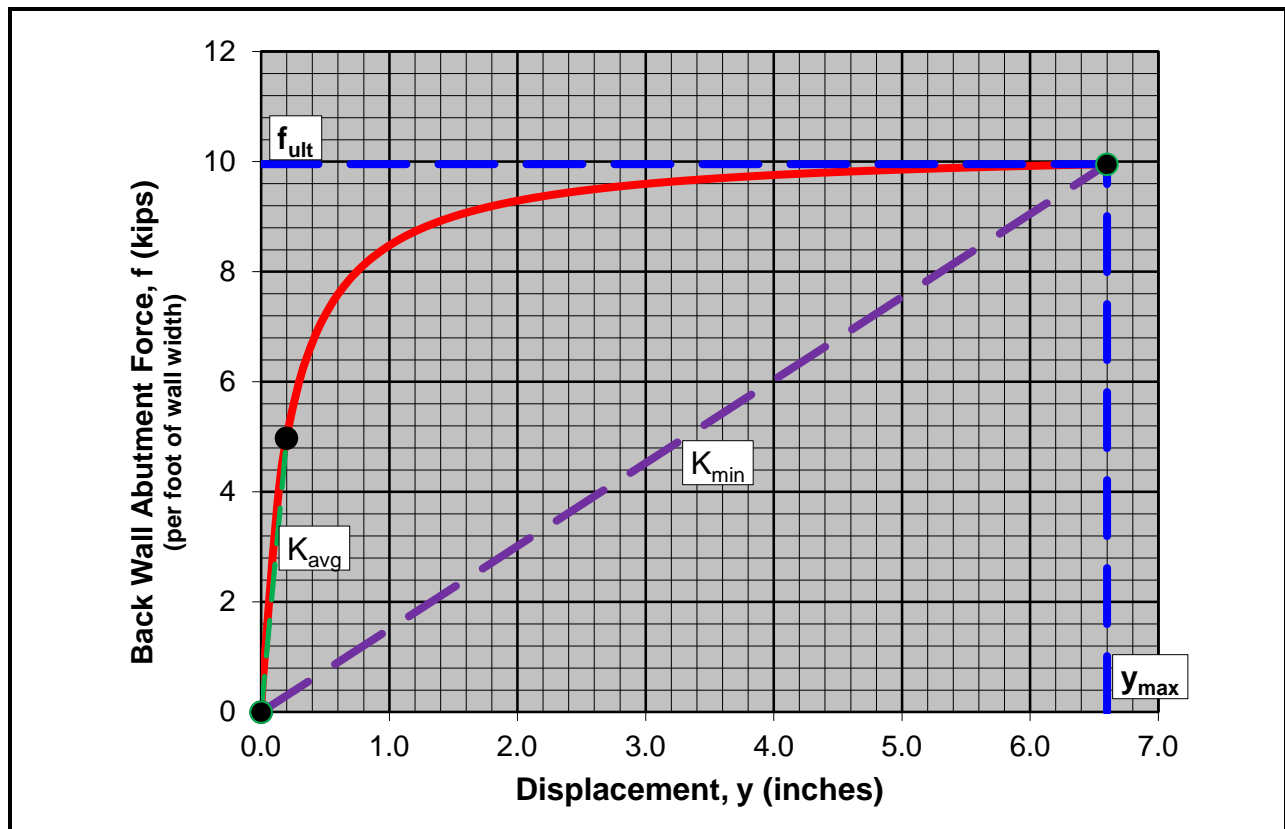


Hyperbolic Force-Displacement Curve

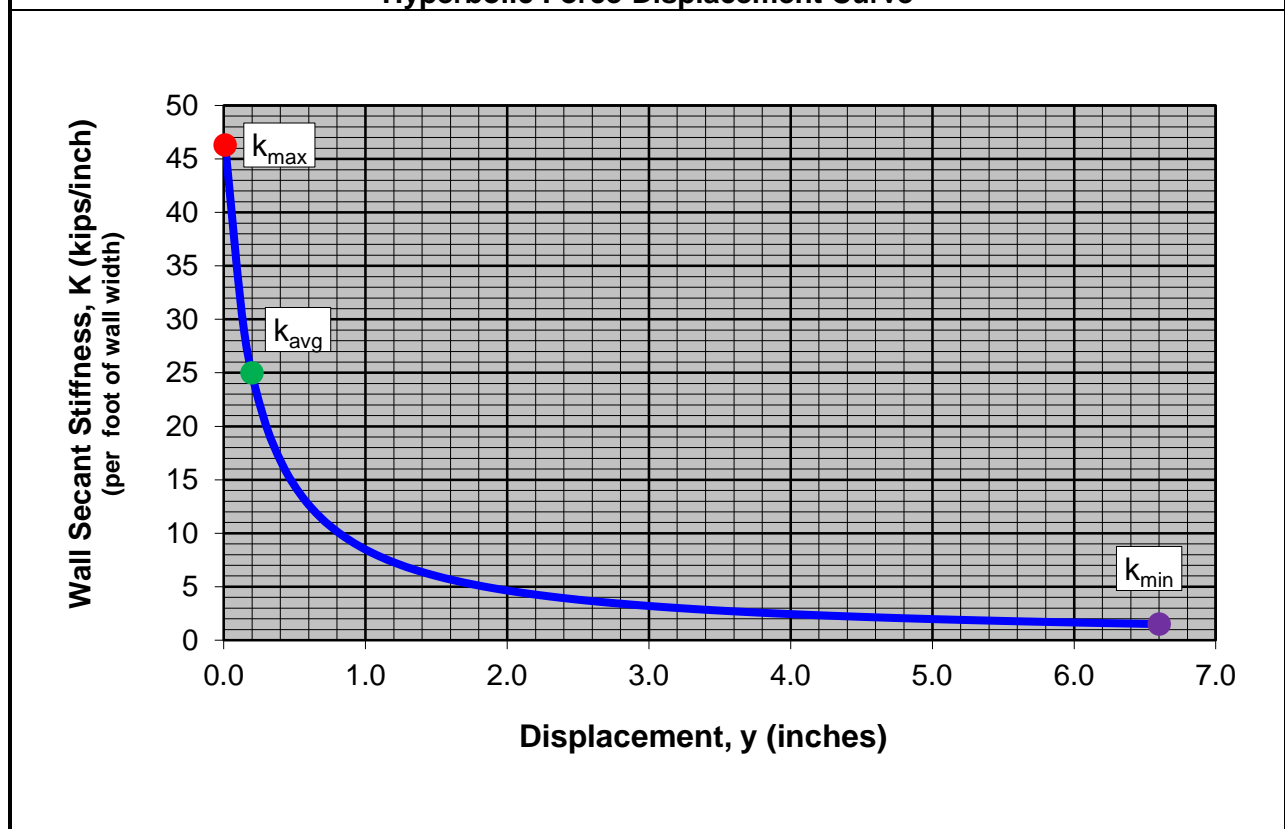


Wall Secant Stiffness-Displacement Curve

Figure 14-47, Bridge Abutment Wall Passive Pressure, Clay-Like Backfill Example



Hyperbolic Force-Displacement Curve



Wall Secant Stiffness-Displacement Curve

Figure 14-48, Bridge Abutment Wall Passive Pressure,  $c-\phi$  Backfill Example

### 14.9.2 Effective Width of Abutment Wall

The development of the total seismic passive resistance ( $F_{ult}$ ) is dependent on the effective width ( $B_{eff}$ ) of the wall being analyzed (see Figure 14-49). The effective wall width ( $B_{eff}$ ) is equal to the wall width ( $b_{wall}$ ) when the bridge skew angle,  $\alpha$ , is zero degrees or when the ground surface adjacent to the abutment is level or sloping upward away from the finished grade of the roadway. The effective abutment width,  $B_{eff}$ , is typically less than the wall width ( $b_{wall}$ ) when the bridge skew angle,  $\alpha$ , is greater than zero degrees and when the ground surface adjacent to the abutment is sloping downward or is vertical (i.e., MSE wall). For skew angles ( $\alpha$ ) greater than 60 degrees, contact the PC/GDS for additional information.

The effective abutment width,  $B_{eff}$ , is computed based on the distance,  $L_{min}$ , perpendicular to the abutment wall (See Figures 14-49 and 14-50).  $L_{min}$  is the distance required to develop the full seismic passive pressure. The distance,  $L_{min}$ , is the critical distance (longest distance) as determined by evaluating the following 2 passive resistance failure mechanisms:

1. Ground surface projection of the passive failure wedge designated as distance  $\overline{AC}$  (see Figures 14-21 and 14-49). As indicated in Equation 14-14, this distance is approximately 3.25 times the height of the abutment wall,  $h_{wall}$ .
2. Length of the sliding soil wedge (trapezoid CEFHGC – see Figure 14-50) along  $\overline{EH}$  ( $L_{Slide}$ ) located behind the passive failure wedge (log spiral shape ABCEDA) required to allow full development of the maximum abutment passive resistance ( $f_{ult}$ ). The length of the sliding soil wedge along  $\overline{EH}$  ( $L_{Slide}$ ) is computed as presented below.

Limiting mechanism No. 2 is related to the shearing resistance of the soil at the base of the wall and the skew angle ( $\alpha$ ). The sliding resistance ( $f_{Slide}$ ) along the horizontal distance  $\overline{EH}$  ( $L_{Slide}$ ) is equal to the sum of sliding resistances  $f_{Skew}$  along the skew horizontal distance ( $\overline{EF}$ ) plus the sliding resistance  $f_{Slope}$  along the side slope horizontal distance ( $\overline{FH}$ ). In order to develop the maximum abutment passive resistance ( $f_{ult}$ ) determined in accordance with Section 14.9.1, the sliding resistance ( $f_{Slide}$ ) along the horizontal distance  $\overline{EH}$  must be equal to or greater than  $f_{ult}$  as indicated in the following equation:

$$f_{ult} \leq f_{Slide} = f_{Skew} + f_{Slope} \quad \text{Equation 14-19}$$

$$f_{Slide} = \frac{f_{ult}}{\phi_{Slide}} \quad \text{Equation 14-20}$$

Where the resistance factor against sliding soil on soil ( $\phi_{Slide}$ ) shall be equal to 1.0 for the EE I limit state.

The minimum sliding resistance ( $f_{Slide}$ ) required to prevent failure of this soil wedge during full seismic passive loading is computed as follows:

$$f_{Slide} = \frac{f_{ult}}{\phi_{Slide}} = (L_{Skew-ult} * \tau_{Skew}) + (L_{Slope} * \tau_{Slope}) \quad \text{Equation 14-21}$$

$$\tau_{Skew} = c + \gamma * h_{wall} * \tan \phi \quad \text{Equation 14-22}$$

$$\tau_{Slope} = c + 0.5 * \gamma * h_{wall} * \tan \phi \quad \text{Equation 14-23}$$

The soil parameters above the base of the wall at  $\overline{DH}$  may be different from those below this shear plane. Whichever set of soil parameters develops the minimum  $\tau_{Skew}$  and  $\tau_{Slope}$  shall be used in evaluating the minimum horizontal distance  $\overline{EH}$  ( $L_{Slide}$ ).

The distance  $L_{Slope}$  extends from the shoulder break, point G, to where the slope intersects  $\overline{DH}$  and is determined using the following equation.

$$L_{Slope} = (X_1^2 + X_2^2)^{0.5} \quad \text{Equation 14-24}$$

Where,

$$X_1 = h_{wall} * Slope_H \quad \text{Equation 14-25}$$

$Slope_H$  = Slope along  $\overline{FH}$  of horizontal (H) distance to one vertical (V).

$$X_2 = X_1 * \sin \alpha \quad \text{Equation 14-26}$$

As shown in Figure 14-50, distance  $L_{Skew}$  ( $\overline{EF}$ ) extends from where the base of the Rankine passive failure wedge intersects  $\overline{DH}$  and extends to directly below the shoulder break. Equation 14-24 should be rearranged to solve for  $L_{Skew}$  as follows:

$$L_{Skew} = \frac{\left[ \left( \frac{f_{ult}}{\phi_{Slide}} \right) - (L_{Slope} * \tau_{Slope}) \right]}{\tau_{Skew}} \quad \text{Equation 14-27}$$

The minimum length ( $L_{min}$ ) required to mobilize full seismic passive resistance (See Figures 14-49 and 14-50) is the lesser of the following:

$$\overline{AC} = 3.25 * h_{wall} \quad (\text{Failure Mechanism No. 1}) \quad \text{Equation 14-28}$$

or

$$\overline{DE} + L_{Skew} \quad (\text{Failure Mechanism No. 2}) \quad \text{Equation 14-29}$$

Where,

$$\overline{DE} = 0.5 * \overline{AC} \quad \text{Equation 14-30}$$

The effective width ( $B_{eff}$ ) for skewed bridge abutments will typically be less than the width of the abutment wall ( $b_{wall}$ ). The effective abutment width ( $B_{eff}$ ) is determined using the following equation.

$$B_{eff} = b_{wall} - b_x \quad \text{Equation 14-31}$$

Where,

$$b_x = L_{min} * \tan \alpha \tag{Equation 14-32}$$

The effective abutment width ( $B_{eff}$ ) will be capable of providing fully mobilized seismic passive resistance and displacements perpendicular to the back of the abutment wall as indicated in Section 14.9.1. The resultant of the seismic demand acting perpendicular to the abutment wall face shall be used to evaluate displacements (perpendicular to the back of the wall) resulting from seismic passive resistance. Similar evaluations as those presented above will be required when evaluating shear walls to resist transverse seismic demand parallel to the bridge abutment wall.

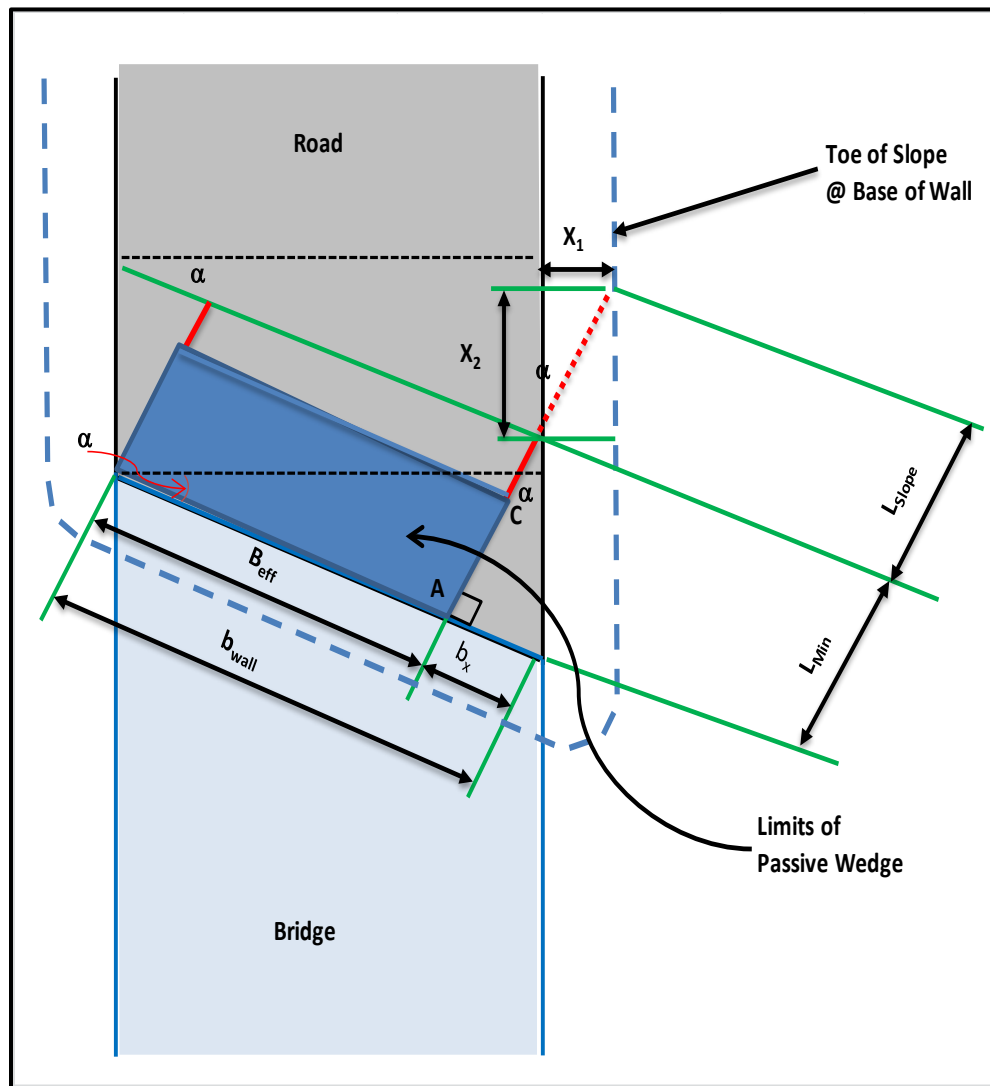


Figure 14-49, Skewed Bridge Abutment Wall Seismic Passive Resistance



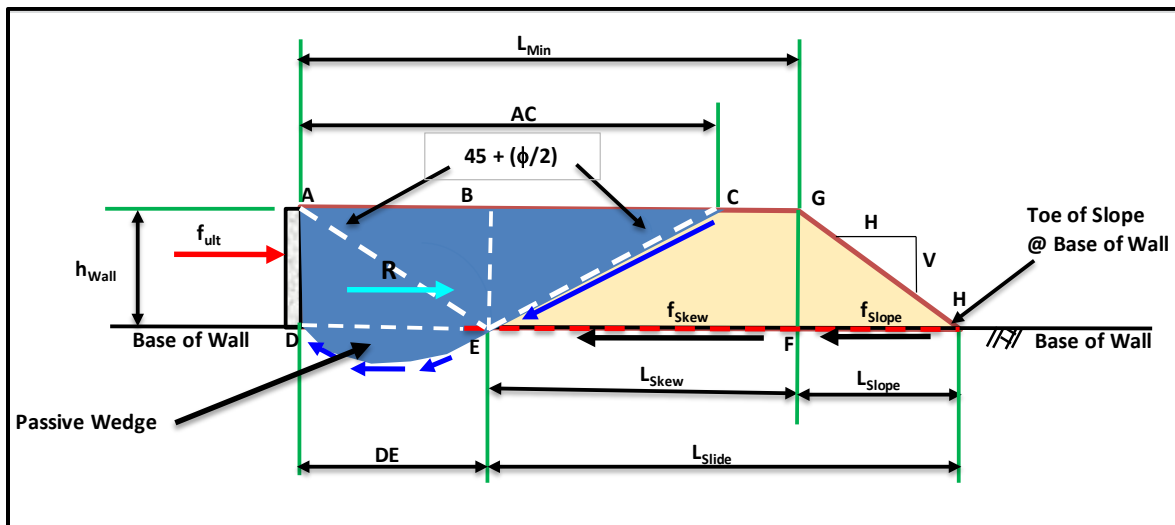


Figure 14-50, Skewed Bridge Abutment Wall Seismic Sliding Resistance

## 14.10 GEOTECHNICAL SEISMIC DESIGN OF EMBANKMENTS

As discussed in Chapter 17, slopes comprise 2 basic categories: natural and man-made (engineered). Typically man-made slopes are comprised of relatively uniform imported soils, thus allowing for more predictable performance and analysis during a seismic event. The design of these slopes becomes problematic when the embankment is placed on soft cohesive soils or loose cohesionless soils that can undergo SSL as described in Chapter 13. Natural slopes present greater difficulties than man-made slopes, because of the potentially wide variation in soil type and shear strength that may be present in these slopes. As indicated in Chapter 17, natural slopes are those slopes that are formed from natural processes. Natural slopes are harder to analyze given the potential variability of not only material type and shear strength, but also thickness as well. Low shear strength layers that are thin may not be indicated in the geotechnical exploration and therefore could have potential consequences in not only seismic design, but also static design. Natural slopes are also hard to investigate because the terrain of most natural slopes is steep (1H:1V) making access extremely difficult. Natural slopes tend to fail during seismic events more frequently than man-made slopes. If the potential for SSL is present beneath the slope, the procedures discussed in Chapter 13 shall be followed.

The seismic design of the embankments shall conform to the procedures discussed in Chapter 13. Settlement induced by the seismic event shall be determined using the procedures discussed in Chapter 13. If seismic instability is determined to occur, all displacements determined shall conform to the performance limits discussed in Chapter 10. For displacements that exceed the limits of Chapter 10, see Section 14.15 for mitigation methods.

## 14.11 RIGID GRAVITY EARTH RETAINING STRUCTURE DESIGN

Rigid gravity ERSs are comprised of gravity, semi-gravity and modular gravity ERSs as defined in Chapter 18. Gravity retaining structures use the weight of mass concrete and retained soil to resist the driving forces placed on the structure. A rigid gravity earth wall is analyzed using the pseudo-static method as shown in Figure 14-1. Discussed in the following paragraphs are the requirements for determining the external stability of a rigid gravity ERS during a seismic event (EE I). The seismic internal stability calculations shall conform to the requirements contained in the AASHTO LRFD Specifications, except all accelerations used shall conform to the

requirements of this Manual (i.e.,  $k_{avg}$ ). Additionally, all load and resistance factors shall conform to Chapters 8 and 9 and all displacements shall conform to Chapter 10.

Similarly to embankments as discussed in Chapter 13, there are conditions for which no seismic analysis of rigid gravity ERSs is required. For rigid gravity ERSs located within bridge embankments, no seismic analysis is required when the PGA is less than or equal to 0.4g ( $PGA \leq 0.4g$ ), the wall height ( $H_{wall}$  in Figures 14-51 and 14-52) is less than or equal to 35 feet ( $H_{wall} \leq 35$  feet) and the subsurface soils do not have the potential for SSL. The no seismic analysis may be extended beyond a PGA of 0.4g provided all of the previous criteria are met; PGA ( $k_{max}$ ) is less than or equal to 0.8g ( $PGA \leq 0.8g$ ); the  $k_y$  to  $k_{max}$  (0.8g) ratio is more than 0.5 (i.e.,  $k_y/k_{max} \geq 0.5$ ); and 2.0 inches of displacement can be tolerated. A seismic analysis for a rigid gravity ERS located within a bridge embankment will be required if any of the previous criteria are not met or if the ERS is located within a larger slope (i.e., the ground slopes upward from the top of the ERS or downward from the bottom of the ERS).

Rigid gravity ERSs located within roadway embankments will not require seismic analysis if the PGA is less than or equal to 0.4g ( $PGA \leq 0.4g$ ), the wall height ( $H_{wall}$  in Figures 14-51 and 14-52) is less than or equal to 10 feet ( $H_{wall} \leq 10$  feet) regardless of the potential for the subsurface soils susceptibility for SSL. If the subsurface soils do not have the potential for SSL, then the criteria established for rigid gravity ERSs in bridge embankments may be applied. A seismic analysis for a rigid gravity ERS located within a roadway embankment will be required if any of the previous criteria are not met or if the ERS is located within a larger slope (i.e., the ground slopes upward from the top of the ERS or downward from the bottom of the ERS) or the ERS supports another structure that could be impacted by the instability of the ERS.

The external stability shall be determined using the following procedure:

- Step 1:** The first step in designing a rigid gravity ERS is to establish the initial ERS design using the procedures indicated in Chapter 18. This establishes the dimensions and weights of the rigid gravity ERS.
- Step 2:** Determine the PGA and  $S_{D1}$  using the procedures outlined in Chapter 12 regardless of whether the 3-Point method or a Site-Specific Seismic Response Analysis is performed. All ERSs are required to be designed for both EE I events (FEE and SEE).
- Step 3:** Determine the PGV using the correlation provided in Chapter 12.
- Step 4:** Compute the average seismic horizontal acceleration coefficient ( $k_h = k_{avg}$ ) due to wave scattering as indicated in Chapter 13.
- Step 5:** Determine  $K_{ae}$  in accordance with the procedures described in Section 14.4.
- Step 6:** Compute the seismic active earth pressure force ( $P_{ae}$ ), horizontal inertial force of the structural soil wedge ( $P_{IR}$ ), and the horizontal inertial force of the slope surcharge above the structural soil wedge ( $P_{IS}$ ) if the wall has a sloped backfill. The seismic force diagrams and appropriate variables are shown in Figure 14-51 for the level backfill surface case and Figure 14-52 for the sloped backfill surface case. For broken back backfill surface case, convert to a sloped backfill surface case using an effective backfill  $\beta$  angle in accordance with AASHTO LRFD Section 11 and then evaluate as shown in Figure 14-52. The width of the structural soil wedge ( $B_{SSW}$ ) is the distance from the back of the wall to the heel of the footing as

shown in Figures 14-51 and 14-52. The height ( $H_2$ ) is the height where the seismic earth pressures are exerted on the structural wedge as is computed using the following equations:

Level Backfill Case (Figure 14-51):

$$H_2 = H_{wall} + H_{ftg} \quad \text{Equation 14-33}$$

Sloped Backfill Case (Figure 14-52):

$$H_2 = H_{wall} + H_{ftg} + B_{ssw} * \tan \beta \quad \text{Equation 14-34}$$

Where,

- $H_{wall}$  = Height of wall stem, feet  
 $H_{ftg}$  = Height of wall footing, feet

Once the effective wall height ( $H_2$ ) and the width of the structural soil wedge ( $B_{ssw}$ ) have been determined, compute the seismic active earth force ( $P_{ae}$ ) that is distributed as a uniform pressure over a height equal to  $H_2$ , the horizontal inertial force of the structural soil wedge ( $P_{IR}$ ), and the horizontal inertial force of the soil surcharge above the structural soil wedge ( $P_{IS}$ ) assumed to be triangular as shown in Figure 14-52. The horizontal seismic forces are computed as indicated below:

Level Backfill Case (Figure 14-51):

$$P_{ae} = 0.5 * \gamma_P * K_{ae} * \gamma_{Backfill} * (H_2)^2 \quad \text{Equation 14-35}$$

$$P_{IR} = \gamma_P * k_{avg} * \gamma_{Backfill} * B_{ssw} * H_{wall} \quad \text{Equation 14-36}$$

Where,

- $\gamma_P$  = Permanent load factor, use 1.0 for ERS in EEI  
 $K_{ae}$  = Seismic active earth pressure coefficient from Section 14.4  
 $\gamma_{Backfill}$  = Backfill wet unit weight, pounds per cubic foot  
 $H_2$  = Height over which the seismic earth pressures are exerted on the structural wedge from Equation 14-33, feet  
 $k_{avg}$  = Average horizontal acceleration that accounts for wave scattering in accordance with Chapter 13, g  
 $B_{ssw}$  = Width of the structural soil wedge, feet  
 $H_{wall}$  = Height of wall stem, feet

Sloped Backfill Case (Figure 14-52):

$$P_{ae} = 0.5 * \gamma_P * K_{ae} * \gamma_{Backfill} * (H_2)^2 \quad \text{Equation 14-37}$$

$$P_{IR} = \gamma_P * k_{avg} * \gamma_{Backfill} * B_{ssw} * H_{wall} \quad \text{Equation 14-38}$$

$$P_{IS} = 0.5 * \gamma_P * k_{avg} * \gamma_{Backfill} * \tan \beta * (B_{ssw})^2 \quad \text{Equation 14-39}$$

Where,

- $\gamma_P$  = Permanent load factor, use 1.0 for ERS in EE I
- $K_{ae}$  = Seismic active earth pressure coefficient from Section 14.4
- $\gamma_{Backfill}$  = Backfill wet unit weight, pounds per cubic foot
- $H_2$  = Height over which the seismic earth pressures are exerted on the structural wedge from Equation 14-34, feet
- $k_{avg}$  = Average horizontal acceleration that accounts for wave scattering in accordance with Chapter 13, g
- $B_{SSW}$  = Width of the structural soil wedge, feet
- $H_{wall}$  = Height of wall stem, feet
- $\beta$  = Backslope angle, degrees

Compute the horizontal inertial force of the weight of wall stem ( $F_{IW}$ ) and horizontal inertial force of the weight of the wall footing ( $F_{IF}$ ), as indicated by the following equations:

$$F_{IW} = W_{Stem} * k_{avg} \quad \text{Equation 14-40}$$

$$F_{IF} = W_{Ftg} * k_{avg} \quad \text{Equation 14-41}$$

Where,

- $W_{Stem}$  = Weight of wall stem, pounds per foot of wall width
- $W_{Ftg}$  = Weight of wall footing, pounds per foot of wall width
- $k_{avg}$  = Average horizontal acceleration that accounts for wave scattering in accordance with Chapter 13, g

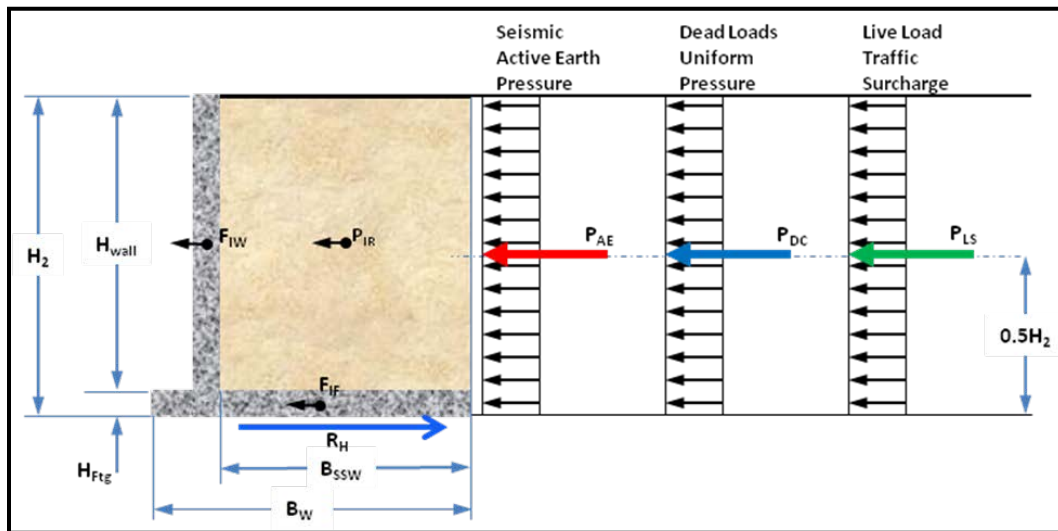


Figure 14-51, Rigid Gravity ERS Seismic Force Diagram – Level Backfill

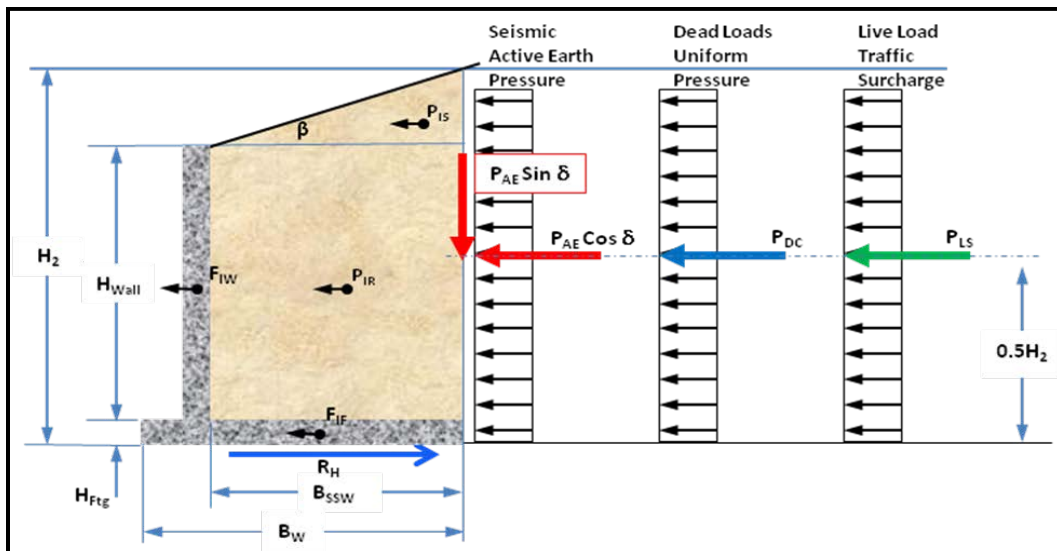


Figure 14-52, Rigid Gravity ERS Seismic Force Diagram – Sloping Backfill

**Step 7:** Compute dead load uniform pressure ( $P_{DC}$ ), and live load traffic surcharge ( $P_{LS}$ ) as indicated below:

$$P_{DC} = \gamma_P * K_{ae} * q_{DC} * H_2 \quad \text{Equation 14-42}$$

$$P_{LS} = \gamma_{EQ} * K_{ae} * q_{LS} * H_2 \quad \text{Equation 14-43}$$

Where,

- $\gamma_P$  = Permanent load factor, use 1.0 for ERS in EE I
- $K_{ae}$  = Seismic active earth pressure coefficient from Section 14.4
- $q_{DC}$  = Dead load uniform pressure, pounds per square foot
- $H_2$  = Height over which the seismic earth pressures are exerted on the structural wedge. For level backfill surface use Equation 14-33 and for sloped backfill surface use Equation 14-34, feet
- $\gamma_{EQ}$  = EE I load factor, See Chapter 8
- $q_{LS}$  = Live load traffic surcharge pressure, pounds per square foot

**Step 8:** Compute the horizontal driving forces ( $F_H$ ). The passive earth pressure force shall only be included for shear keys that are located below the footing (see Section 14.5). The horizontal driving force ( $F_H$ ) is determined by the following equation:

$$F_H = P_{ae} * \cos \beta + P_{IR} + P_{IS} + P_{DC} + P_{LS} + F_{IW} + F_{IF} \quad \text{Equation 14-44}$$

**Step 9:** The frictional resistance of the foundation soils ( $R_{HF}$ ) is computed using the following equations:

$$R_{HF} = \phi * \tau * B_w = \phi * (c * B_w + N * \tan \delta_f) \quad \text{Equation 14-45}$$

Where,

- $\phi$  = Resistance factor, See Chapter 9
- $\tau$  = Foundation soil shear strength, pounds per square foot
- $B_w$  = Base width of the wall footing, feet
- $c$  = Cohesion of foundation soils, pounds per square foot

$\delta_F$  = Foundation-soil interface friction angle (AASHTO LRFD), degrees

$\tan(\delta_F)$  = Foundation-soil interface friction coefficient,  $\mu$  (AASHTO LRFD)

$N$  = Normal force that is the sum of the vertical loads over the base width ( $B_W$ ) of the reinforced soil mass, pounds per foot of wall width. The normal force is computed by the following equation:

**Equation 14-46**

$$N = (B_{ssw}H_{wall}\gamma_{Backfill}) + P_{ae} \sin \beta + 0.5[B_{ssw}(H_2 - H_{wall} - H_{ftg})\gamma_{Backfill}] + W_{Stem} + W_{Ftg}$$

Where,

$B_{ssw}$  = Width of the structural soil wedge, feet

$H_{wall}$  = Height of wall stem, feet

$\gamma_{Backfill}$  = Backfill wet unit weight, pounds per cubic foot

$P_{ae}$  = Seismic active earth force, pounds per foot of wall width

$\beta$  =  $0^\circ$  - level backfill or  
backslope angle, degrees

$\gamma_P$  = Permanent load factor, use 1.0 for ERS in EE I

$K_{ae}$  = Seismic Active Earth Pressure Coefficient from Section 14.4

$H_2$  = Height over which the seismic earth pressures are exerted on the structural wedge. For level backfill surface use Equation 14-33 and for sloped backfill surface use Equation 14-34, feet

$k_{avg}$  = Average horizontal acceleration that accounts for wave scattering in accordance with Chapter 13, g

$B_{ssw}$  = Width of the structural soil wedge, feet

$\beta$  = Backslope angle, degrees

$W_{Stem}$  = Weight of wall stem, pounds per foot of wall width

$W_{Ftg}$  = Weight of wall footing, pounds per foot of wall width

Evaluate the ERS Wall bearing pressure, limiting eccentricity for overturning, sliding and global stability for the maximum seismic design load in accordance with the appropriate Chapters of the GDM. For determination of bearing capacity, see Chapter 15. If deep foundations are to be used to support rigid gravity ERSs, see Chapter 16 for deep foundation design methodology. It should be noted that all EE I resistance factors ( $\phi$ ) are provided in Chapter 9. If all of the resistance factors are met, the static design is satisfactory and the seismic design is complete. It is reasonable to assume that if the demand/capacity ratio (D/C) for rigid gravity ERS meets the required resistance factors for the SEE design earthquake, the required resistance factors for the FEE design earthquake will be met. If bearing pressure and limiting eccentricity for overturning are not met, then the rigid gravity wall requires redesign to meet these resistances. If the sliding or global stability resistance factor criterion is not met, the ERS is unstable; therefore, continue to Step 10 and evaluate the displacements caused by both the FEE and SEE design earthquakes.

**Step 10:** Determine the yield acceleration ( $k_y$ ) for the global stability of the ERS in accordance with Chapter 13. The  $k_y$  is the acceleration at which the ERS becomes just stable (i.e.,  $\phi = 1.0 = 1/FS = 1.0$ ). If the ratio of  $k_y$  to  $k_h$  is more than 0.5 ( $k_y/k_h \geq 0.5$ ), then a displacement ( $\Delta L$ ) of 2 inches shall be assumed and reported (Elms and Martin (1979)). As indicated previously, if the failure surface is circular all displacements at the top of the slope shall be considered to be vertical, while all

displacements at the top of the slope for a non-circular failure surface shall be considered horizontal.

For evaluating the yield acceleration ( $k_y$ ) for sliding of the ERS, first determine the driving forces ( $F_H$ ) as a function of horizontal acceleration ( $k = k_h$ ) and the resisting forces ( $R_H$ ) as a function of horizontal acceleration ( $k = k_h$ ) as depicted in Figure 14-53. The passive earth pressure force shall only be included for shear keys that are located below the footing (see Section 14.5); otherwise, no passive earth pressure force shall be used to resist lateral seismic forces. The yield acceleration ( $k_y$ ) will be the location where the driving forces ( $F_H$ ) and resisting forces ( $R_H$ ) are equal.

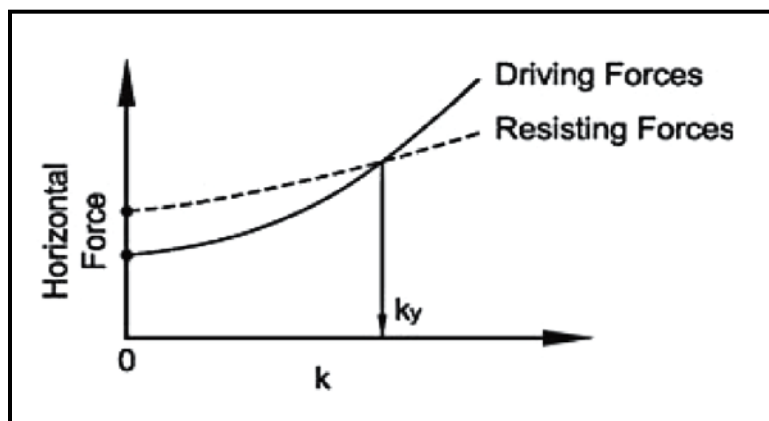


**Figure 14-53, Determination of Yield Acceleration ( $k_y$ ) (Anderson, et al. (2008))**

After determining  $k_y$ , determine the amount of displacement ( $d$ ) using the procedures in Chapter 13. If the displacement is within the performance limits, as indicated in Chapter 10, then design is complete. If the displacement exceeds the performance limits in Chapter 10, redesign the ERS to achieve acceptable performance limits or determine if the amount of anticipated movement is acceptable to both the design team as well as SCDOT.

## 14.12 FLEXIBLE GRAVITY EARTH RETAINING STRUCTURE DESIGN

Flexible gravity earth retaining systems are comprised of gabion and Mechanically Stabilized Earth (MSE) ERSs as defined in Chapter 18. Flexible gravity retaining structures use the reinforced soil mass for MSE walls and the stone for gabion ERSs, and the foundation soils to resist the driving forces placed on the structure. Discussed in the following paragraphs are the requirements for determining the external stability of a flexible gravity ERS during an EE I event. The seismic internal stability calculations shall conform to the requirements contained in the AASHTO LRFD Specifications (Section 11.10 – Mechanically Stabilized Earth Walls), except all accelerations used shall conform to the requirements of this Manual (i.e.,  $A_s = k_{avg}$  as determined in Chapter 13). Additionally, all load and resistance factors shall conform to Chapters 8 and 9 and all displacements shall conform to Chapter 10.

Similarly to embankments as discussed in Chapter 13, there are conditions for which no seismic analysis of flexible gravity ERSs is required. For flexible gravity ERSs located within bridge embankments, no seismic analysis is required when the PGA is less than or equal to 0.4g ( $PGA \leq 0.4g$ ), the wall height ( $H_{wall}$  in Figures 14-54 and 14-55) is less than or equal to 35 feet ( $H_{wall} \leq 35$  feet) and the subsurface soils do not have the potential for SSL. The no seismic analysis

may be extended beyond a PGA of 0.4g provided all of the previous criteria are met; PGA ( $k_{max}$ ) is less than or equal to 0.8g ( $PGA \leq 0.8g$ ); the  $k_y$  to  $k_{max}$  (0.8g) ratio is more than 0.5 (i.e.,  $k_y/k_{max} \geq 0.5$ ); and 2.0 inches of displacement can be tolerated. A seismic analysis for a flexible gravity ERS located within a bridge embankment will be required if any of the previous criteria are not met or if the ERS is located within a larger slope (i.e., the ground slopes upward from the top of the ERS or downward from the bottom of the ERS).

Flexible gravity ERSs located within roadway embankments will not require seismic analysis if the PGA is less than or equal to 0.4g ( $PGA \leq 0.4g$ ), the wall height ( $H_{wall}$  in Figures 14-54 and 14-55) is less than or equal to 10 feet ( $H_{wall} \leq 10$  feet) regardless of potential for the subsurface soils having the susceptibility for SSL. If the subsurface soils do not have the potential for SSL, then the criteria established for flexible gravity ERSs in bridge embankments may be applied. A seismic analysis for a flexible gravity ERS located within a roadway embankment will be required if any of the previous criteria are not met or if the ERS is located within a larger slope (i.e., the ground slopes upward from the top of the ERS or downward from the bottom of the ERS) or the ERS supports another structure that could be impacted by the instability of the ERS.

The external stability shall be determined using the following procedure:

- Step 1:** The first step in designing a flexible gravity ERS is to establish the initial ERS design using the procedures indicated in Chapter 18 and Appendix C (MSE walls). This establishes the dimensions and weights of the flexible gravity ERS.
- Step 2:** Determine the PGA and  $S_{D1}$  using the procedures outlined in Chapter 12 regardless of whether the 3-Point method or a Site-Specific Seismic Response Analysis is performed. All ERSs are required to be designed for both EE I events (FEE and SEE).
- Step 3:** Determine the PGV using the correlation provided in Chapter 12.
- Step 4:** Compute the average seismic horizontal acceleration coefficient ( $k_h = k_{avg}$ ) due to wave scattering as indicated in Chapter 13.
- Step 5:** Determine  $K_{ae}$  in accordance with the procedures described in Section 14.4.
- Step 6:** Compute the seismic active earth pressure force ( $P_{ae}$ ), the horizontal inertial force of the reinforced soil mass ( $P_{IR}$ ) and the horizontal inertial force of the slope surcharge above the reinforced soil mass ( $P_{IS}$ ) if wall has a sloped backfill. The seismic force diagrams and appropriate variables are shown in Figure 14-54 for the level backfill surface case and Figure 14-55 for the sloped backfill surface case. For broken back backfill surface case, convert to sloped backfill surface case using an effective backfill  $\beta$  angle in accordance with AASHTO LRFD Section 11 and then evaluate as shown in Figure 14-55. The height ( $H_2$ ) is the height where the seismic earth pressures and effective inertial wall width ( $B_{Inertial}$ ) are computed as indicated below:

Level Backfill Case (Figure 14-54):

$$H_2 = H_{wall} \quad \text{Equation 14-47}$$

$$B_{Inertial} = \omega * H_2 \quad \text{Equation 14-48}$$



Where,

- $H_{wall}$  = Height of MSE wall facing, feet  
 $\omega$  = Coefficient equal to 0.50

Sloped Backfill Case (Figure 14-55):

$$H_2 = H_{wall} + \left( \frac{\omega * H_{wall} * \tan \beta}{1 - \omega * \tan \beta} \right) \quad \text{Equation 14-49}$$

$$B_{Inertial} = \omega * H_2 \quad \text{Equation 14-50}$$

Where,

- $H_{wall}$  = Height of MSE wall facing, feet  
 $\beta$  = Backslope angle, degrees  
 $\omega$  = Coefficient equal to 0.50 provided that

$$B_w \geq \omega * H_{wall} \quad \text{Equation 14-51}$$

If  $\omega H_{wall} > B_w$  then,

$$\omega = \frac{B_w}{H_{wall}} \quad \text{Equation 14-52}$$

Where  $B_w$  is the base width of the wall as determined in Step 1. For MSE walls with concrete panel facing, the base width of the wall is taken from the back of the wall facing and for MSE walls with concrete block facing, the base width of the wall is taken from the front of the block facing.

Once the effective wall height ( $H_2$ ) and the  $B_{Inertial}$  variables have been determined, compute the seismic active pressures ( $P_{ae}$ ). The seismic active earth pressure is distributed as a uniform pressure over a height equal to  $H_2$ . The horizontal inertial force of the reinforced soil mass ( $P_{IR}$ ) and the horizontal inertial force of soil surcharge above the reinforced soil mass ( $P_{IS}$ ), assumed to be triangular as shown in Figure 14-55, as indicated below:

Level Backfill Case (Figure 14-54):

$$P_{ae} = 0.5 \gamma_P K_{ae} \gamma_{Backfill} (H_2)^2 = 0.5 \gamma_P K_{ae} \gamma_{Backfill} (H_{wall})^2 \quad \text{Equation 14-53}$$

$$P_{IR} = \gamma_P k_{avg} \gamma_R B_{Inertial} H_2 = \gamma_P k_{avg} \gamma_R B_{Inertial} H_{wall} \quad \text{Equation 14-54}$$

Where,

- $\gamma_P$  = Permanent load factor, use 1.0 for ERS in EE I  
 $K_{ae}$  = Seismic active earth pressure coefficient from Section 14.4  
 $\gamma_{Backfill}$  = Backfill wet unit weight, pounds per cubic foot  
 $\gamma_R$  = Reinforced fill wet unit weight, pounds cubic foot  
 $H_2$  = Equal to the wall height,  $H_{wall}$ , feet  
 $k_{avg}$  = Average horizontal acceleration that accounts for wave scattering in accordance with Chapter 13, g

$B_{inertial}$  = Effective inertial wall width from Equation 14-50, feet

Sloped Backfill Case (Figure 14-55):

$$P_{ae} = 0.5\gamma_P K_{ae} \gamma_{Backfill} (H_2)^2 \quad \text{Equation 14-55}$$

$$P_{IR} = \gamma_P k_{avg} \gamma_R B_{inertial} H_2 \quad \text{Equation 14-56}$$

$$P_{IS} = 0.5\gamma_P K_{avg} \gamma_{Backfill} \tan \beta (B_{inertial})^2 \quad \text{Equation 14-57}$$

Where,

- $\gamma_P$  = Permanent load factor, use 1.0 for ERS in EE I
- $K_{ae}$  = Seismic active earth pressure coefficient from Section 14.4
- $\gamma_{Backfill}$  = Backfill wet unit weight, pounds per cubic foot
- $\gamma_R$  = Reinforced fill wet unit weight, pounds per cubic foot
- $H_2$  = Equal to the wall height,  $H_{wall}$  from Equation 14-49, feet
- $k_{avg}$  = Average horizontal acceleration that accounts for wave scattering in accordance with Chapter 13, g
- $B_{inertial}$  = Effective inertial wall width from Equation 14-50, feet
- $\beta$  = Backslope angle, degrees

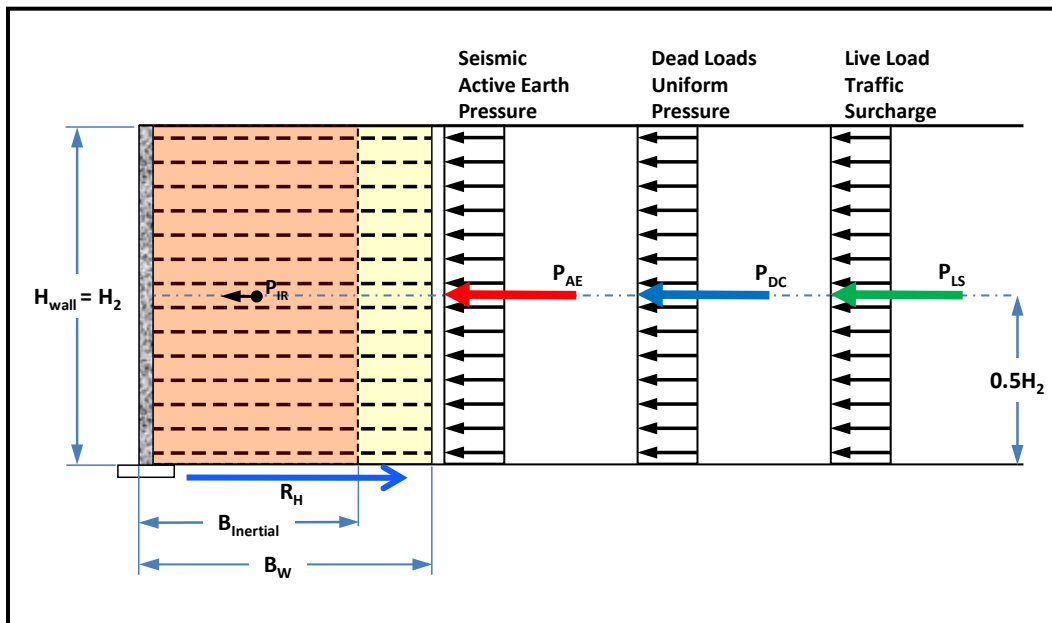


Figure 14-54, Flexible Gravity ERS Seismic Force Diagram – Level Backfill

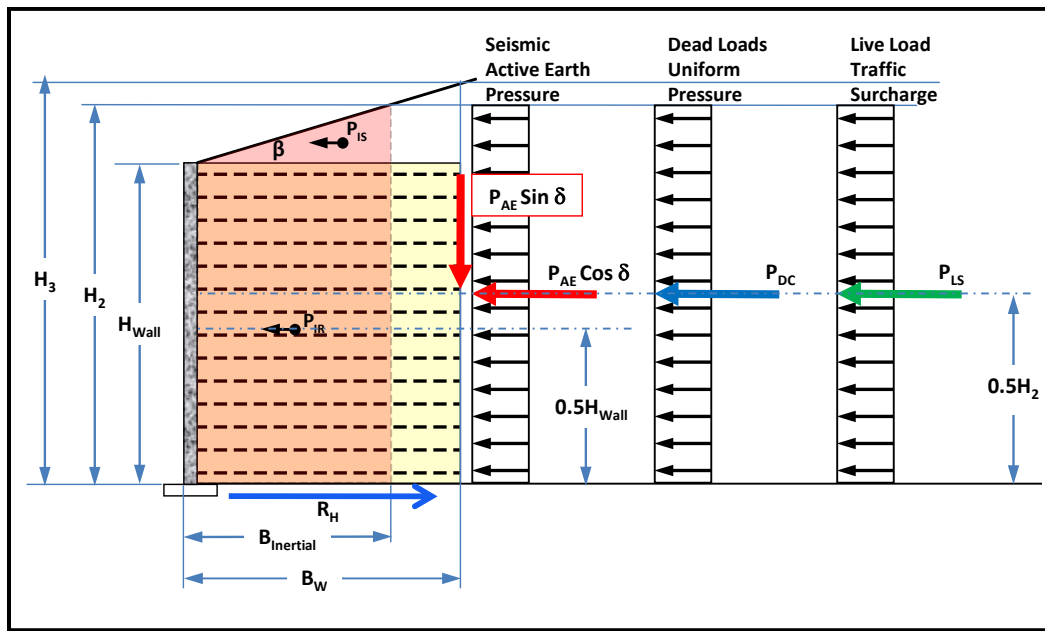


Figure 14-55, Flexible Gravity ERS Seismic Force Diagram – Sloping Backfill

**Step 7:** Compute dead load uniform pressure ( $P_{DC}$ ), and live load traffic surcharge ( $P_{LS}$ ) as indicated below:

$$P_{DC} = \gamma_P K_{ae} q_{DC} H_2 \quad \text{Equation 14-58}$$

$$P_{LS} = \gamma_{EQ} K_{ae} q_{LS} H_2 \quad \text{Equation 14-59}$$

Where,

- $\gamma_P$  = Permanent load factor, use 1.0 for ERS in EE I
- $\gamma_{EQ}$  = EE I load factor, See Chapter 8
- $K_{ae}$  = Seismic active earth pressure coefficient from Section 14.4
- $q_{DC}$  = Dead load uniform pressure, pounds per square foot
- $q_{LS}$  = Live load traffic surcharge pressure, pounds per square foot
- $H_2$  = Equal to the wall height,  $H_{Wall}$ . For level backfill surface use Equation 14-47 and for sloped backfill surface use Equation 14-49, feet
- $K_{avg}$  = Average horizontal acceleration that accounts for wave scattering in accordance with Chapter 13, g

**Step 8:** Compute the horizontal driving forces ( $F_H$ ) and the horizontal resisting forces ( $R_H$ ). No passive earth pressure force shall be used to resist horizontal driving forces on MSE walls. The horizontal driving force ( $F_H$ ) is determined by the following equation:

$$F_H = P_{ae} \cos \beta + P_{IR} + P_{IS} + P_{DC} + P_{LS} \quad \text{Equation 14-60}$$

The resisting force ( $R_H$ ) is determined using the lesser of soil-soil frictional resistance within the reinforced soil mass ( $R_{HSoil-Soil}$ ), soil-reinforcement frictional resistance within the reinforced soil mass ( $R_{HSoil-Reinf}$ ), or the frictional resistance in the foundation soils ( $R_{HF}$ ).

$$R_H = \text{Lesser of } R_{H\text{Soil-Soil}} \text{ or } R_{H\text{Soil-Reinf}} \text{ or } R_{HF} \quad \text{Equation 14-61}$$

Where the frictional resistance forces are computed using the following equations:

$$R_{H\text{Soil-Soil}} = \varphi N \tan \phi_R \quad \text{Equation 14-62}$$

$$R_{H\text{Soil-Reinf}} = \varphi N \tan \rho \quad \text{Equation 14-63}$$

$$R_{HF} = \varphi \tau B_w = \varphi (c B_w + N \tan \phi_R) \quad \text{Equation 14-64}$$

Where,

- $\varphi$  = Resistance factor, See Chapter 9.
- $\phi_R$  = Internal friction angle of the reinforced fill
- $\rho$  = Friction angle between the soil reinforcement and the reinforced fill material. For continuous reinforcement (sheet type)  $\rho = 0.67\phi_R$ . For all other non-continuous reinforcement (strip type)  $\rho = \phi_R$ .
- $B_w$  = Base width to the wall as defined in Step 6, feet
- $N$  = Normal force that is the sum of the vertical loads over the base width ( $B_w$ ) of the reinforced soil mass, pounds per foot of wall width. The normal force is computed by the following equation:

$$N = (\gamma_R B_w H_{wall}) + P_{ae} \sin \beta + [0.5 \gamma_{Backfill} B_w (H_3 - H_{wall})] \quad \text{Equation 14-65}$$

Where,

- $H_3$  = The height where the projection of the rear of the reinforced zone intersects the slope, feet
- $\beta$  =  $0^\circ$  - level backfill or backslope angle, degrees

**Step 9:** Evaluate the MSE Wall bearing pressure, limiting eccentricity for overturning, sliding, and global stability for the maximum seismic design load in accordance with the appropriate Chapters of the GDM and Appendix C. For determination of bearing capacity see Chapter 15. If deep foundations are to be used to support flexible gravity ERSs, please contact the PCS/GDS. It should be noted that all EEI resistance factors ( $\varphi$ ) are provided in Chapter 9. If all of the resistance factors are met, the static design is satisfactory and the seismic design is complete. It is reasonable to assume that if the demand/capacity ratio (D/C) for flexible gravity ERS meets the required resistance factors for the SEE design earthquake, the required resistance factors for the FEE design earthquake will be met. If bearing pressure and limiting eccentricity for overturning are not met, then MSE Wall requires redesign to meet these resistances. If the sliding or global stability resistance factor criterion is not met, the ERS is unstable; therefore, continue to Step 10 and evaluate the displacements caused by both the FEE and SEE design earthquakes.

**Step 10:** Determine the yield acceleration ( $k_y$ ) for the global stability of the ERS in accordance with Chapter 13. The  $k_y$  is the acceleration at which the ERS becomes

just stable (i.e.,  $\phi = 1.0 = 1/FS = 1.0$ ). If the ratio of  $k_y$  to  $k_h$  is more than 0.5 ( $k_y/k_h \geq 0.5$ ), then a displacement ( $\Delta L$ ) of 2 inches shall be assumed and reported (Elms and Martin (1979)). As indicated previously, if the failure surface is circular all displacements at the top of the slope shall be considered to be vertical, while all displacements at the top of the slope for a non-circular failure surface shall be considered horizontal.

For evaluating the yield acceleration ( $k_y$ ) for sliding of the ERS, first determine the driving forces ( $F_H$ ) as a function of horizontal acceleration ( $k = k_h$ ) and the resisting forces ( $R_H$ ) as a function of horizontal acceleration ( $k = k_h$ ) as depicted in Figure 14-56. No passive earth pressure force shall be used to resist lateral seismic forces. The yield acceleration ( $k_y$ ) will be the location where the driving forces ( $F_H$ ) and resisting forces ( $R_H$ ) are equal.

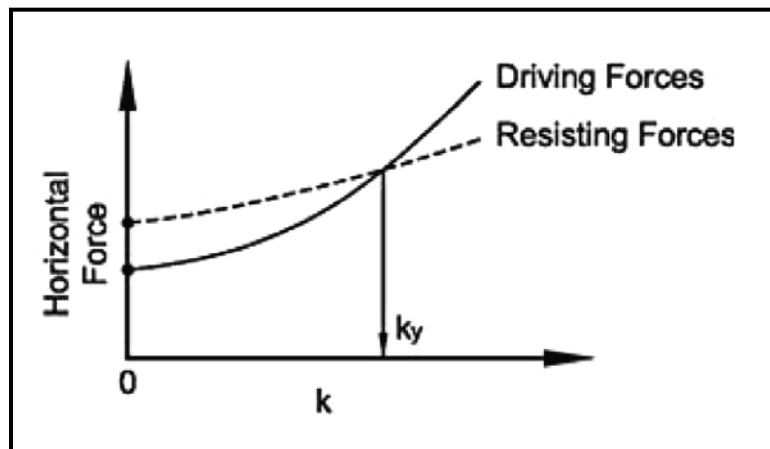


Figure 14-56, Determination of Yield Acceleration ( $k_y$ ) (Anderson, et al. (2008))

After determining  $k_y$  determine the amount of displacement ( $d$ ) using the procedures in Chapter 13. If the displacement is within the performance limits as indicated in Chapter 10, then design is complete. If the displacement exceeds the performance limits in Chapter 10, redesign the ERS to achieve acceptable performance limits or determine if the amount of anticipated movement is acceptable to both the design team as well as SCDOT.

## 14.13 CANTILEVER EARTH RETAINING SYSTEM DESIGN

Cantilevered earth retaining systems are comprised of unanchored sheet-pile and soldier pile and lagging and anchored sheet-pile and soldier pile and lagging ERSs as defined in Chapter 18 (see Table 18-1). Unanchored cantilevered walls will be discussed first and then anchored cantilevered walls.

### 14.13.1 Unanchored Cantilever ERSs

Design unanchored cantilever ERSs to establish the initial ERS design using the procedures indicated in Chapter 18. This establishes the dimensions of the cantilever ERS. Typically unanchored cantilevered ERSs are limited to a height of less than 16 feet. It should be noted that it is customary to ignore the inertial loadings of the structure members.

- Step 1:** Determine the PGA and  $S_{D1}$  using the procedures outlined in Chapter 12 of this Manual regardless of whether the 3-Point method or a Site-Specific Seismic Response Analysis is performed. All ERSs are required to be designed for both EEI events (FEE and SEE). It is reasonable to assume that if an unanchored cantilever ERS satisfies the required resistance factors for the SEE, the required resistance factors for the FEE will be met.
- Step 2:** Determine the PGV as described in Chapter 12.
- Step 3:** Compute the average seismic horizontal acceleration coefficient ( $k_h = k_{avg}$ ) due to wave scattering as indicated in Chapter 13.
- Step 4:** Determine  $K_{ae}$  and  $P_{ae}$  in accordance with the procedures described in Section 14.4 of this Chapter. The passive earth pressure coefficient  $K_{pe}$  and the passive earth pressure,  $P_{pe}$ , shall be determined as indicated in Section 14.5.
- Step 5:** Evaluate the structural requirements using either a suitable software package or by hand calculation (i.e., using something similar to the free earth support method). Confirm that the displacements predicted to achieve active earth pressure conform to the performance limits provided in Chapter 10.
- Step 6:** Check the global stability using the procedures outlined in Chapter 17. The acceleration used in the global stability analysis shall be the  $k_{avg}$  as determined in Step 4. If the resistance factor ( $\phi$ ) is greater than 1.0, determine displacements and compare to Chapter 10. If the displacements are within limits, design is complete. If the displacements exceed the limits, redesign the wall and begin again at Step 1.

### 14.13.2 Anchored Cantilever ERSs

Design anchored cantilever ERSs to establish the initial ERS design using the procedures indicated in Chapter 18. This establishes the dimensions of the cantilever ERS. Typically anchored cantilevered ERSs have heights in excess of 15 feet, but typically no more than 70 feet. It should be noted that it is customary to ignore the inertial loadings of the structure members.

- Step 1:** Determine the PGA and  $S_{D1}$  using the procedures outlined in Chapter 12 of this Manual regardless of whether the 3-Point method or a Site-Specific Seismic Response Analysis is performed. All ERSs are required to be designed for both EEI events (FEE and SEE). It is reasonable to assume that if an anchored cantilever ERS satisfies the required resistance factors for the SEE, the required resistance factors for the FEE will be met.
- Step 2:** Determine the PGV as described in Chapter 12.
- Step 3:** Compute the average seismic horizontal acceleration coefficient ( $k_h = k_{avg}$ ) due to wave scattering as indicated in Chapter 13.
- Step 4:** Determine  $K_{ae}$  and  $P_{ae}$  in accordance with the procedures described in Section 14.4 of this Chapter. The passive earth pressure coefficient  $K_{pe}$  and the passive earth pressure,  $P_{pe}$ , shall be determined as indicated in Section 14.5.

- Step 5:** Evaluate the structural requirements using the same pressure distribution from the static analysis. From the resulting loading diagram, check the loads on the tendons and grouted anchors to confirm that seismic loads do not exceed the loads applied during proof testing of each anchor. Confirm that the grouted anchors are located outside of the active seismic pressure failure wedge.
- Step 6:** Check the global stability using the procedures outlined in Chapter 17. The acceleration used in the global stability shall be the  $k_{avg}$  as determined in Step 4. If the resistance factor ( $\phi$ ) is greater than 1.0, determine displacements and compare to Chapter 10. If the displacements are within limits, design is complete. If the displacements exceed the limits, redesign the wall and begin again at Step 1.

## 14.14 IN-SITU REINFORCED RETAINING SYSTEM DESIGN

In-situ reinforced earth retaining systems are comprised of soil nail wall ERSs as defined in Chapter 18 (see Table 18-1).

Design in-situ reinforced ERSs to establish the initial ERS design using the procedures indicated in Chapter 18. This establishes the dimensions of the soil nail ERS. Typically soil nail ERSs have heights in excess of 10 feet but typically no more than 70 feet.

- Step 1:** Determine the PGA and  $S_{D1}$  using the procedures outlined in Chapter 12 of this Manual regardless of whether the 3-Point method or a Site-Specific Seismic Response Analysis is performed. All ERSs are required to be designed for both EEI events (FEE and SEE). It is reasonable to assume that if a soil nail ERS satisfies the required resistance factors for the SEE, the required resistance factors for the FEE will be met.
- Step 2:** Determine the PGV as described in Chapter 12.
- Step 3:** Compute the average seismic horizontal acceleration coefficient ( $k_h = k_{avg}$ ) due to wave scattering as indicated in Chapter 13.
- Step 4:** Use the  $k_{avg}$  determined previously in a pseudo-static analysis of the soil nail ERS, using a commercially available software (i.e., SNAIL<sup>®</sup> or GOLDNAIL<sup>®</sup>). If the resistance factor ( $\phi$ ) is less than 1.0, the design is acceptable. However, if the resistance factor ( $\phi$ ) is greater than 1.0, determine displacements and compare to Chapter 10. First, determine the yield acceleration ( $k_y$ ) corresponding to the point where the horizontal driving and resisting forces are equal (i.e.,  $\phi = 1.0$  or FS = 1.0). After determining  $k_y$ , determine the amount of displacement ( $d$ ) using the procedures in Chapter 13. If the displacement is within the performance limits as indicated in Chapter 10, then design is complete. If the displacement exceeds the performance limits in Chapter 10 either redesign the ERS to achieve acceptable performance limits or determine if the amount of anticipated movement is acceptable to both the design team as well as SCDOT.

## 14.15 SEISMIC HAZARD MITIGATION

If the performance limits established in Chapter 10 are exceeded, then the design team must decide if mitigation is practical or not (i.e., do nothing). “Doing nothing” is a decision that must be made by the entire design team. In some cases, this may be the most viable option. For instance, if flow failure is anticipated, the cost of mitigation would be excessively prohibitive;

therefore, it would be less expensive to accept the movement. If mitigation is practical, there are 2 categories, either structural mitigation or geotechnical mitigation.

#### **14.15.1 Structural Mitigation**

Structural mitigation is where the structure is designed to handle the displacements anticipated during the seismic event. Structural mitigation of displacements should be attempted first before using geotechnical mitigation methods. Typically, structural mitigation efforts are more economical than geotechnical mitigation methods. The decision to use structural mitigation should be made by the entire design team.

#### **14.15.2 Geotechnical Mitigation**

Geotechnical mitigation is where the soil beneath and around the structure is modified to prevent displacements occurring during a seismic event from exceeding the limits contained in Chapter 10. Additional guidance on geotechnical mitigation methods may be found in Idriss and Boulanger (2008). Geotechnical mitigation efforts are limited to those indicated in Chapter 19 or those approved by the PC/GDS on a project specific basis.

#### **14.15.3 Selection of Mitigation Method**

The selection of the appropriate mitigation strategy should be based on the cost of the mitigation method, the anticipated results of the mitigation method and the amount of post-seismic displacement that is anticipated to occur. The need for mitigation should be identified as early as possible in the design process to allow for time to consider all mitigation alternatives.

### **14.16 REFERENCES**

American Association of State Highway and Transportation Officials, (2017), AASHTO LRFD Bridge Design Specifications Customary U.S. Units, 8<sup>th</sup> Edition, American Association of State Highway and Transportation Officials, Washington, D.C.

Anderson, D. G., Martin, G. R., Lam, I. and Wang, J. N., (2008), "Seismic Analysis and Design of Retaining Walls, Buried Structures, Slopes and Embankments", NCHRP Report 611, Volumes 1 and 2, Transportation Research Board.

Boulanger, R. W., Kutter, B. L., Brandenburg, S. J., Singh, P., and Chang, D., (2003), "Pile Foundations in Liquefied and Laterally Spreading Ground During Earthquakes: Centrifuge Experiments & Analyses", College of Engineering, University of California at Davis, 205 pp.

Bowles, J. E., (1982), Foundation Analysis and Design, 3rd ed., McGraw-Hill, New York.

Brandenburg, S.J., Boulanger, R.W., Kutter, B.L., and Chang, D., (2007a), "Liquefaction Induced Softening of Load Transfer Between Pile Groups and Laterally Spreading Crusts", *ASCE Journal of Geotechnical and Geoenvironmental Engineering*, Vol. 133, No. 1, pp. 91 - 103.

Brandenburg, S. J., Boulanger, R. W., Kutter, B. L., and Chang, D., (2007b), "Static Pushover Analyses of Pile Groups in Liquefied and Laterally Spreading Ground in Centrifuge Tests", *ASCE Journal of Geotechnical and Geoenvironmental Engineering*, Vol. 133, No. 9, pp. 1055 - 1066.



Chugh, A. K. (1995), "A Unified Procedure for Earth Pressure Calculations," Proceedings: Third International Conference on Recent Advances in Geotechnical Earthquake Engineering and Soil Dynamics, Volume III, St. Louis, Missouri.

Clough, G. W. and Duncan, J. M. (1991), "Earth Pressures," Foundation Engineering Handbook, 2nd edition, edited by Hsai-Yang Fang, van Nostrand Reinhold, New York, NY, pp. 223 - 235.

Ebeling, R. M., Chase, A., White, B. C., (2007), "Translational Response of Toe-Restrained Retaining Walls to Earthquake Ground Motions Using  $C_{\text{orps}}W_{\text{allSlip}}$  (CWSLIP)", Technical Report ERDC/ITL TR-07-01. Vicksburg, Mississippi: Corps of Engineers Waterways Experiment Station, June 2007.

Elms, D. G. and Martin, G. R. (1979), "Factors Involved in the Seismic Design of Bridge Abutments", Proceedings of a Workshop on Earthquake Resistance of Highway Bridges, pp 229-252, Applied Technology Council, Palo Alto, California.

Idriss, I. M. and Boulanger, R. W., (2008), Soil Liquefaction During Earthquakes, Earthquake Engineering Research Institute (EERI), EERI Monograph MNO-12.

Munfakh, G., Kavazanjian, E., Matasović, N., Hadj-Hamou, T. and Wang, J. N., (1998), Geotechnical Earthquake Engineering Reference Manual, (Publication Number FHWA-HI-99-012), US Department of Transportation, Federal Highway Administration, National Highway Institute, Arlington, Virginia.

NCHRP 12-49 (2001), "Comprehensive Specification for the Seismic Design of Bridges – Revised LRFD Design Specifications (Seismic Provisions)," National Cooperative Highway Research Program (NCHRP), Transportation Research Board, Washington, D.C.

Newmark, N.M. (1965), "Effects of Earthquakes on Dams and Embankments", *Geotechnique*, v.5, no.2 London, England.

Reese, L. C., Wang, S. T., Isenhower, W. M., and Arrellaga, J. A., (2004), "Computer Program L-Pile Plus," Version 5.0, Technical Manual, ENSOFT, Inc., Austin, Texas.

Richards, R. and Elms, D. G., (1979), "Seismic Behavior of Gravity Retaining Walls." *ASCE Journal of the Geotechnical Engineering Division*, Vol. 105, No. GT4, pp. 449 - 464.

Rollins, K. M., Gerber, T. M., Lane, J. D., and Ashford, S., (2005), "Lateral Resistance of a Full-Scale Pile Group in Liquefied Sand." *ASCE Journal of Geotechnical and Geoenvironmental Engineering*, Vol. 131, No. 1, pp. 115 - 125.

Shamsabadi, A. (2006). CT-FLEX – Computer Manual, Office of Earthquake Engineering, California Department of Transportation.

Shamsabadi, A. Rollins, K.M., and M. Kapuskar (2007), "Nonlinear Soil-Abutment-Bridge Structure Interaction for Seismic Performance-Based Design", *ASCE Journal of Geotechnical and Geoenvironmental Engineering*, Vol. 133, No. 6, pp. 707 - 720.

Shamsabadi, A., Khalili-Tehrani, P., Stewart, J. P., and Taciroglu, E. (2010), "Validated Simulation Models for Lateral Response of Bridge Abutments with Typical Backfills", *ASCE Journal of Bridge Engineering*, Vol. 15, No. 3, May 2010, pp. 302 - 311.

Shamsabadi, A., Xu, S.-Y., and Taciroglu, E. (2013a), "A Generalized Log-Spiral-Rankine Limit Equilibrium Model for Seismic Earth Pressure Analysis", *Soil Dynamics and Earthquake Engineering*, Vol. 49, June 2013, pp. 197-209.

Shamsabadi, A., Xu, S.-Y., and Taciroglu, E. (2013b), "Development of Improved Guidelines for Analysis and Design of Earth Retaining Structures", Report UCLA-SGEL Report 2013/02, Structural & Geotechnical Engineering Laboratory, University of California, Los Angeles, California

South Carolina Department of Transportation, (2006), Bridge Design Manual, South Carolina Department of Transportation, [http://www.scdot.org/doing/structural\\_Bridge.aspx](http://www.scdot.org/doing/structural_Bridge.aspx).

South Carolina Department of Transportation, (2008), Seismic Design Specifications for Highway Bridges, South Carolina Department of Transportation, <https://www.scdot.org/business/structural-design.aspx>.

Xu, S.-Y., Shamsabadi, A., and Taciroglu, E. (2015), "Evaluation of Active and Passive Seismic Earth Pressures Considering Internal Friction and Cohesion", *Soil Dynamics and Earthquake Engineering*, Vol. 70, March 2015, pp. 30-47.

Zhang, G., Roberson, P. K., and Brachman, R. W. I. (2004). "Estimating Liquefaction-Induced Lateral Displacements Using the Standard Penetration Test or Cone Penetration Test." *ASCE Journal of Geotechnical and Geoenvironmental Engineering*, v. 130, Issue 8, pp. 861 - 871

**Chapter 15**  
**SHALLOW FOUNDATIONS**

**GEOTECHNICAL DESIGN MANUAL**

*January 2019*



**Table of Contents**

<b><u>Section</u></b>	<b><u>Page</u></b>
15.1 Introduction .....	15-1
15.2 Design Considerations .....	15-1
15.2.1 Bearing Depth – Bridge Foundations .....	15-3
15.2.2 Bearing Depth – Other Structures .....	15-3
15.2.3 Bearing Depth – Embankments and MSE Walls .....	15-3
15.3 Bearing Capacity Determination .....	15-3
15.4 Sliding Resistance .....	15-4
15.5 Eccentricity .....	15-4
15.6 Settlement .....	15-4
15.7 References .....	15-7
15.8 Resources .....	15-7

**List of Figures**

<b><u>Figure</u></b>	<b><u>Page</u></b>
Figure 15-1, Footing Width vs Bearing Capacity on What Controls Footing Size.....	15-2
Figure 15-2, Depth of Significant Influence (DOSI).....	15-2
Figure 15-3, Construction-Point Concept .....	15-5
Figure 15-4, Three-Dimensional Reduction Factors .....	15-6

# CHAPTER 15

## SHALLOW FOUNDATIONS

### 15.1 INTRODUCTION

This Chapter presents the design and analysis requirements for shallow foundations that will be used to support SCDOT structures. According to the BDM a shallow foundation “distributes the loads...to suitable soil strata or rock at relatively shallow depths (less than 10 feet)”. Shallow foundations are used not only to support bridges, but also to support building structures, ERSs (see Chapter 18), box and floorless culverts and other ancillary structures. Shallow foundations are not limited to spread footings, but may also include strip footings, mat foundations and thickened (turned-down) edge slabs. The type of shallow foundation to be used will be based on the structure to be supported. The BDM includes the use of pile/drilled shaft supported footings; however, since the footing (shallow foundation) is supported by deep foundations see Chapter 16 for the design and analysis of the deep foundation. For these types of foundations the footing is not anticipated to transmit any load directly to the soil beneath the footing.

The use of shallow foundations shall conform to the requirements of Chapter 14. In addition, shallow foundations shall not be used at any location where scour beneath the bottom of the shallow foundation (i.e., the bearing stratum) is anticipated. The exception to this is if scour prevention measures are used to mitigate scour. This exception shall be approved in writing by the PCS/GDS, PCS/HDS, and PCS/SDS.

Samtani and Nowatzki (2006) indicate that a strip footing has a length dimension ( $L_f$ ) at least 10 times larger than the width dimension ( $B_f$ ). Spread footings have a ratio of  $L_f/B_f$  less than 10. Mat foundations according to Bowles (1996) are very large spread footings that have thicknesses ranging from 2-1/2 to 6-1/2 feet and have negative moment steel. A mat foundation should be used in a pile/drilled shaft supported footing. A thickened edge slab is a variation of a mat foundation, where the interior of the slab is typically thin, 4 to 6 inches in thickness, while at the locations of columns and at the edge the thickness is at least 18 inches. Thickened edge slabs are typically used to support buildings and shall not be used to support bridges, ERSs, culverts or other ancillary structures (i.e., signal mast arms or light poles).

### 15.2 DESIGN CONSIDERATIONS

The design of shallow foundations consists of 2 components, the bearing (resistance to shear) capacity and settlement (performance limits). According to Samtani and Nowatzki (2006) most shallow foundation problems occur because of settlement, while true bearing failure is limited. Typically, the factored resistance ( $R_f$ ) will be dictated by the settlement (performance limits, see Chapter 10). Therefore, the initial footing dimensions ( $B_{fi}$  and  $L_{fi}$ ) should be based on the results of the settlement analysis. The effect of footing width on bearing capacity and settlement is shown conceptually in Figure 15-1. For narrow footings with high bearing capacity shear will typically control. However, structural considerations usually limit tolerable settlements. As the footing width increases, the bearing capacity is limited by the settlement of the soil within the Depth of Significant Influence (DOSI). Using elastic theory, the DOSI is the finite depth below which there are no significant strains in the soil mass due to the loads imposed at the surface (bearing pressure induced by structure). At stress reductions of 10 to 15 percent of the applied bearing pressure (stress), the strains induced in the soil column become insignificant. For strip footings the DOSI is 4 to 6 times the footing width (i.e.,  $4B_f$  to  $6B_f$ ), while for spread footings the DOSI is 1-1/2 to 2 times the footing width (i.e.,  $1-1/2B_f$  to  $2B_f$ ) (see Figure 15-2).

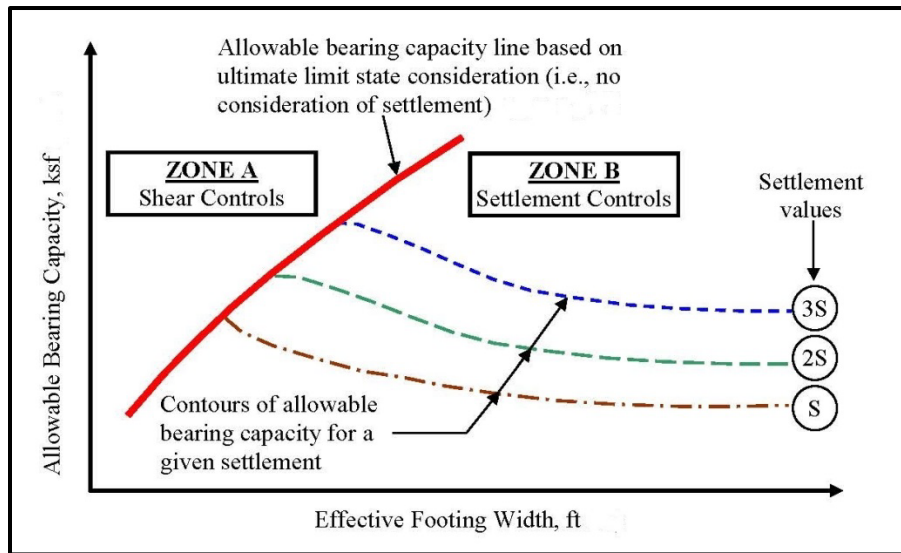


**Figure 15-1, Footing Width vs Bearing Capacity on What Controls Footing Size (Samtani and Nowatzki (2006))**

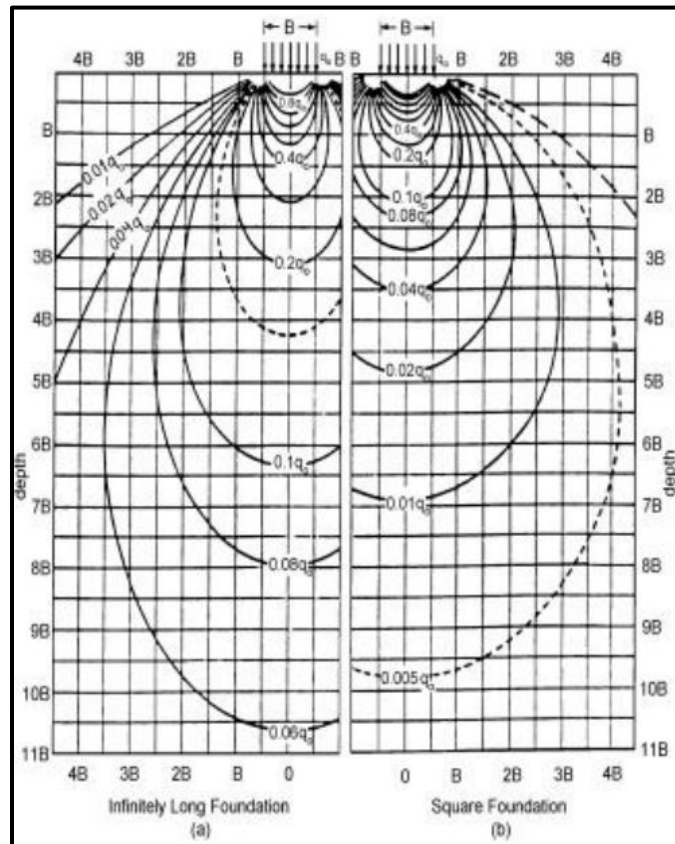


**Figure 15-2, Depth of Significant Influence (DOSI) (FHWA-NHI-132084 (2014))**

Roadway embankments do not typically have a structural foundation element; however, either settlement or global stability (Chapter 17) will govern the design and acceptability of the embankment. Therefore, it is not required or necessary to determine the bearing capacity of the soil beneath embankments, unless there is a question of localized (punching) shearing failure. Shallow foundations shall be designed for Service (displacement), Strength (bearing capacity),



EE I and EE II (bearing capacity and displacement) limit states as required by LRFD. All shallow foundation designs will be governed by the basic LRFD equation:

$$Q = \sum \eta_i \gamma_i Q_i \leq \phi R_n = R_r \quad \text{Equation 15-1}$$

Where,

Q	=	Factored load
Q <sub>i</sub>	=	Force effect
η <sub>i</sub>	=	Load modifier
γ <sub>i</sub>	=	Load factor
R <sub>r</sub>	=	Factored Resistance (i.e., allowable capacity)
R <sub>n</sub>	=	Nominal Resistance (i.e., ultimate capacity)
φ	=	Resistance Factor

Shallow foundations shall be proportioned so that the factored resistance is not exceeded when the factored (nominal) loading is applied to the foundation and the performance limit (e.g., settlements at the Service limit state loading) of the foundation is not exceeded. Further, the effect of inclined loads that cause the reduction of the net bearing area shall also be considered. The bearing depth of shallow foundations depends on the type of structure being built. The bearing depths for shallow foundations are discussed in greater detail in the following sections.

### **15.2.1 Bearing Depth – Bridge Foundations**

The bearing depth of shallow foundations, referred to as Spread Footings in the BDM, used to support bridges shall be determined in accordance with the latest edition of the BDM.

### **15.2.2 Bearing Depth – Other Structures**

The bearing depth of shallow foundations used to support structures (i.e., buildings, signs, ERSs other than MSE walls, etc.) shall account for the presence of groundwater and frost penetration. Shallow foundations should not be placed beneath the groundwater table since this will require additional effort in construction, unless approved in writing by the PC/GDS. To prevent frost from affecting shallow foundations, shallow foundations shall be placed beneath the frost penetration depth, which according to the Building Code Council for South Carolina is between 1 and 2 inches. The bottom of shallow foundations shall be placed no shallower than 18 inches unless the depth to the groundwater table is shallower than this depth. If the depth to the groundwater table is shallower than 12 inches, contact the PC/GDS with recommendations for installing the shallow foundations prior to completing foundation design plans.

### **15.2.3 Bearing Depth – Embankments and MSE Walls**

The bearing capacity for embankments (if necessary) shall be determined from the existing ground surface (i.e., d = 0). The bearing depth of an MSE wall is the top of the leveling pad and shall meet the requirements contained in Chapter 18 and Appendix C for the leveling pad depth. The leveling pad of an MSE wall is not a shallow foundation and does not have to meet the requirements of this Chapter.

## **15.3 BEARING CAPACITY DETERMINATION**

The nominal bearing capacity of a shallow foundation shall be determined using the procedures published in the AASHTO LRFD Specifications (Section 10.6 – Spread Footings). The size of the foundation shall be determined using the factored resistance. This proportionally sized

foundation shall be compared to the initial footing dimensions to determine which footing is larger (i.e., does settlement or bearing control footing design). The nominal bearing capacity of foundations placed on top of or within slopes shall also be determined in accordance with the AASHTO LRFD Specifications (Section 10.6 – Spread Footings). Further, the proportionally sized foundation shall be checked for the EE I and II limit states. Both bearing and settlement shall be determined for the EE I and II limit states. The bearing determined for the EE I and II limit states shall be compared to and not exceed the nominal resistance. The settlement determined (Chapter 13) for the EE I and II limit states shall be compared to the performance limits provided in Chapter 10. The resistance factors provided in Chapter 9 are for shallow foundations with vertical loads. The AASHTO LRFD Specifications allow for the use of plate load tests to determine the bearing capacity of soil; however, the use of plate load tests to determine bearing capacity is not allowed by SCDOT.

#### **15.4 SLIDING RESISTANCE**

The nominal sliding resistance of a shallow foundation shall be determined using the appropriate limit state in accordance with the procedures published in the AASHTO LRFD Specifications (Section 10.6 – Spread Footings). In addition, the proportionally sized foundation shall also be used to check for sliding due to inclined and shear loads. The effect of inclined loads on the resistance factor is not well known or understood; therefore caution should be used when applying the resistance factors of Chapter 9 to shallow foundations with inclined loads.

#### **15.5 ECCENTRICITY**

The eccentricity of a shallow foundation shall be determined using the appropriate limit state in accordance with the procedures published in the AASHTO LRFD Specifications (Section 10.6 – Spread Footings). In addition, the proportionally sized foundation shall also be used to check for eccentricity due to inclined and shear loads. The effect of inclined loads on the resistance factor is not well known or understood; therefore caution should be used when applying the resistance factors of Chapter 9 to shallow foundations with inclined loads.

#### **15.6 SETTLEMENT**

As indicated previously, settlement normally governs the size and capacity for shallow foundations. The total settlement as well as the differential settlement (the difference in settlement between 2 points) shall be considered when sizing a shallow foundation. Further, the time for settlement to occur as well as the rate of settlement (amount per unit of time) shall also be considered in shallow foundation design. The amount and time for settlement to occur shall be determined using the methods described in Chapter 17. Settlement shall be determined for the Service limit state. The amount (total and differential) and the rate of settlement at the Service limit state shall conform to the limits presented in Chapter 10. Depending on the requirements of the particular project, the use of the Construction-Point Concept may be used. Unlike traditional settlement calculations which assume the bridge is instantaneously placed, the Construction-Point Concept determines the settlement at specific critical construction points (see Figure 15-3).

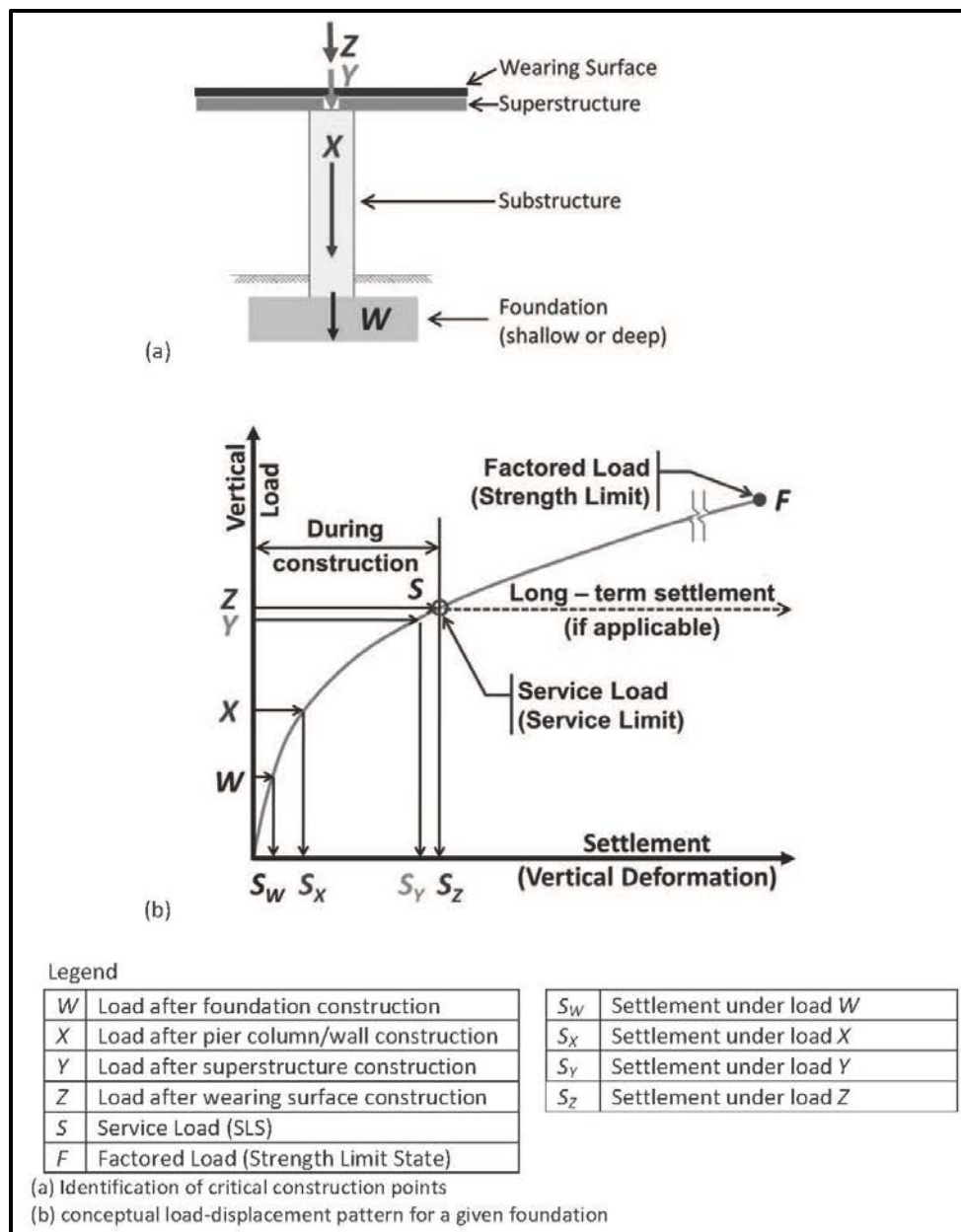


**Figure 15-3, Construction-Point Concept (DeMarco, Bush, Samtani, Kulicki and Severns (2015))**

If the differential settlement is, according to the AASHTO LRFD Specifications determined to be “...extreme values...” then the settlement determination should be determined using the procedure recommend by Abu-Hejleh, Alzamora, Mohamed, Saad, and Anderson (2014). This procedure determines settlement to account for construction sequencing, since the amount of settlement determined at various stages of construction will affect the overall performance of the bridge. Settlement should be determined upon completion of the footing, pier and cap for interior bents and footing, abutment and wing walls and any earth fill behind the abutment for end bents prior to the installation of the superstructure. Typically, live loads are not included in the loads for determining this settlement. This settlement is termed  $S_{t-1}$  for use in this Manual. The next settlement to be determined is after the placement of girders on to the caps and is termed  $S_{t-2}$ . These settlements will not affect the bridge deck since these settlements will occur prior to the placement of the bridge deck.  $S_{t-1}$  and  $S_{t-2}$  include immediate settlement as well as any consolidated settlement that may occur during construction. The final settlement to be determined is  $S_{t-3}$  which account for the loads induced by placement of the bridge deck as well

as the appropriate live loads used to determine the Service limit states. Both immediate settlement, induced by application of the bridge deck, and any consolidation settlement that will occur after the completion of construction should be included in  $S_{t-3}$ .  $S_{t-3}$  settlement should be used to determine the performance of the bridge. The acceptable performance of the bridge shall be determined by the SEOR. These settlements should be determined not only in the longitudinal direction but also in the transverse direction if the conditions indicate the potential for differential settlement in the transverse direction.

Typically for shallow foundations founded on dense cohesionless materials the amount of settlement will be relatively small and will typically occur during construction. For cohesive soils the amount of settlement can be quite large and can take a long time to occur. Therefore, preloading may be used to reduce or remove the anticipated settlement amount prior to installation of the shallow foundations. If preloading is performed, the pressure applied by the preload should achieve at least 1/2 of the factored bearing resistance required. Under this condition additional settlement will occur after preloading and shall be determined, as well as the time for this settlement to occur. According to AASHTO LRFD Specifications 3-dimensional effects should be considered if the following criterion is met.

$$\frac{B_f}{H_o} \leq 4 \quad \text{Equation 15-2}$$

Where,

$B_f = B =$  Foundation width

$H_o = H =$  Total thickness of consolidating layer

Then the settlement should be reduced using the following equation

$$S_{c(3D)} = \lambda S_{c(1D)} \quad \text{Equation 15-3}$$

Where,

$S_{c(1D)} =$  Total primary consolidation

$\lambda =$  3-dimensional reduction factor (see Figure 15-4)

$S_{c(3D)} =$  Reduced total primary consolidation accounting for 3-dimensional effects

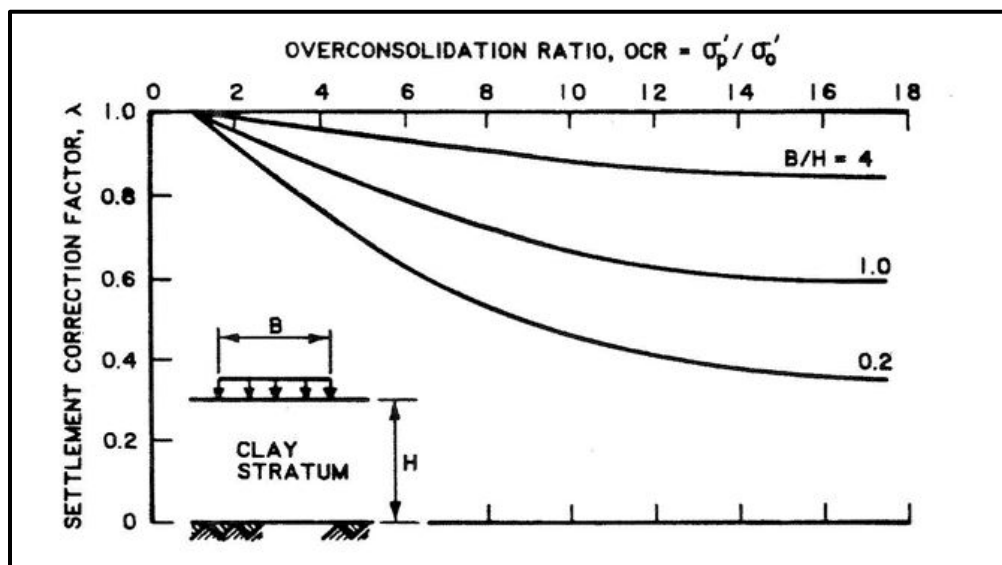


Figure 15-4, Three-Dimensional Reduction Factors  
(EM 1110-1-1904 (1990))

## 15.7 REFERENCES

Abu-Hejleh, N. M., Alzamora, D., Mohamed, K., Saad, T., and Anderson, S., (2014), Implementation Guidance for Using Spread Footings on Soils to Support Highway Bridges, (Publication No. FHWA-RC-14-001), US Department of Transportation, Resource Center, Federal Highway Administration, Matteson, IL.

American Association of State Highway and Transportation Officials, (2017), AASHTO LRFD Bridge Design Specifications Customary U.S. Units, 8<sup>th</sup> Edition, American Association of State Highway and Transportation Officials, Washington, D.C.

Bowles, J. E., (1996), Foundation Analysis and Design, 5<sup>th</sup> Edition, The McGraw-Hill Companies, Inc.

DeMarco, M., Bush, P., Samtani, N. C., Kulicki, J. M., and Severns, K., (2015), Draft - Incorporation of Foundation Deformations in AASHTO LRFD Bridge Design Process, 2<sup>nd</sup> Strategic Highway Research Program (SHRP2), Transportation Research Board, The National Academies of Sciences, Engineering, and Medicine, Washington, D.C.

Department of Defense, Department of the Army, Army Corps of Engineers, (1990), Settlement Analysis, EM 1110-1-1904, Washington, D.C.

FHWA-NHI-132084, (2014), Subsurface Exploration, Design and Construction Considerations, Depth of Significant Influence (DOSI), Slide 13, Module 1: Transportation Projects and Geotechnical Engineering, Retrieved March 6, 2014, from course FHWA-NHI-132084.

Kimmerling, R. E., (2002), Geotechnical Engineering Circular No. 6 – Shallow Foundations, (Publication No. FHWA-SA-02-054), US Department of Transportation, Office of Bridge Technology, Federal Highway Administration, Washington, D.C.

Samtani, N. C., and Nowatzki, E. A., (2006), Soils and Foundations Reference Manual – Volume II, NHI Course No. FHWA-NHI-132012 (Publication No. FHWA-NHI-06-089), U.S. Department of Transportation, National Highway Institute, Federal Highway Administration, Arlington, Virginia.

South Carolina Department of Transportation, (2006), Bridge Design Manual, South Carolina Department of Transportation, <https://www.scdot.org/business/structural-design.aspx>.

## 15.8 RESOURCES

Arneson, L. A., Zevenbergen, L. W., Lagasse, P. F., and Clooper, P. E., (2012), Evaluating Scour at Bridges, Hydraulic Engineering Circular 18, (Publication No. FHWA-HIF-12-003), 5<sup>th</sup> Edition, US Department of Transportation, Office of Bridge Technology, Federal Highway Administration, Washington, D.C.

Lagasse, P. F., Zevenbergen, L. W., Spitz, W. J., and Arneson, L. A., (2012), Stream Stability at Highway Structures, Hydraulic Engineering Circular 20 (Publication No. FHWA-HIF-12-004), 4<sup>th</sup> Edition, US Department of Transportation, Office of Bridge Technology, Federal Highway Administration, Washington, D.C.

Lagasse, P. F., Clooper, P. E., Pagán-Oritz, J. E., Zevenbergen, L. W., Arneson, L. A., Schall, J. D., and Girard, L. G., (2009), Bridge Scour and Stream Instability Countermeasures, Hydraulic Engineering Circular 23 - Volumes 1 and 2, (Publication No. FHWA-NHI-09-111 and FHWA-NHI-09-112), 3<sup>rd</sup> Edition, US Department of Transportation, Office of Bridge Technology, Federal Highway Administration, Washington, D.C.

Samtani, N. C., Nowatzki, E. A., and Mertz, D. R., (2010), Selection of Spread Footings on Soils to Support Highway Bridge Structures, (Publication No. FHWA-RC/TD-10-001), U.S. Department of Transportation, Resource Center, Federal Highway Administration, Matteson, IL.

**Chapter 16**  
**DEEP FOUNDATIONS**

**GEOTECHNICAL DESIGN MANUAL**

*January 2019*





### Table of Contents

<u>Section</u>		<u>Page</u>
16.1	Introduction.....	16-1
16.2	Design Considerations.....	16-3
	16.2.1 Axial Load .....	16-4
	16.2.2 Lateral Load.....	16-4
	16.2.3 Settlement.....	16-5
	16.2.4 Scour .....	16-6
	16.2.5 Downdrag.....	16-7
16.3	Driven Piles .....	16-7
	16.3.1 Axial Compressive Resistance .....	16-8
	16.3.2 Axial Uplift Resistance.....	16-11
	16.3.3 Group Effects .....	16-11
	16.3.4 Settlement.....	16-12
	16.3.5 Pile Driveability .....	16-13
16.4	Drilled Shafts .....	16-15
	16.4.1 Axial Compressive Resistance .....	16-16
	16.4.2 Uplift Resistance .....	16-19
	16.4.3 Group Effects .....	16-19
	16.4.4 Settlement.....	16-21
	16.4.5 Constructability .....	16-22
16.5	Drilled Piles.....	16-23
16.6	Continuous Flight Auger Piles.....	16-23
16.7	Micropiles .....	16-24
16.8	Lateral Resistance .....	16-24
	16.8.1 Lateral Stability – Geotechnical Check .....	16-26
	16.8.2 Lateral Stability – Structural Check.....	16-27
	16.8.3 Lateral Stability – Serviceability Check.....	16-27
	16.8.4 Lateral Resistance – Groups .....	16-27
16.9	Downdrag .....	16-27
	16.9.1 Traditional Approach .....	16-28
	16.9.2 Alternative Approach.....	16-29
	16.9.3 Downdrag Mitigation .....	16-30
16.10	Foundation Length.....	16-30
16.11	References .....	16-33

**List of Tables**

<b><u>Table</u></b>	<b><u>Page</u></b>
Table 16-1, Deep Foundation Limit States .....	16-3
Table 16-2, Typical Pile Types and Sizes.....	16-7
Table 16-3, Driveability Analysis.....	16-14
Table 16-4, Group Reduction Factor Values, $\eta$ .....	16-21
Table 16-5, k Factor .....	16-22
Table 16-6, Governing Conditions .....	16-32
Table 16-7, Pile Resistance.....	16-32
Table 16-8, Drilled Shaft Resistance .....	16-33

**List of Figures**

<b><u>Figure</u></b>	<b><u>Page</u></b>
Figure 16-1, Reasons for Deep Foundations .....	16-2
Figure 16-3, Typical Wave Equation Model .....	16-14
Figure 16-4, Block Failure Model.....	16-20
Figure 16-5, Typical LPILE Pile-Soil Model .....	16-25
Figure 16-6, Downdrag Scenarios due to Compressible Soils .....	16-28
Figure 16-7, Neutral Point Determination .....	16-30



# CHAPTER 16

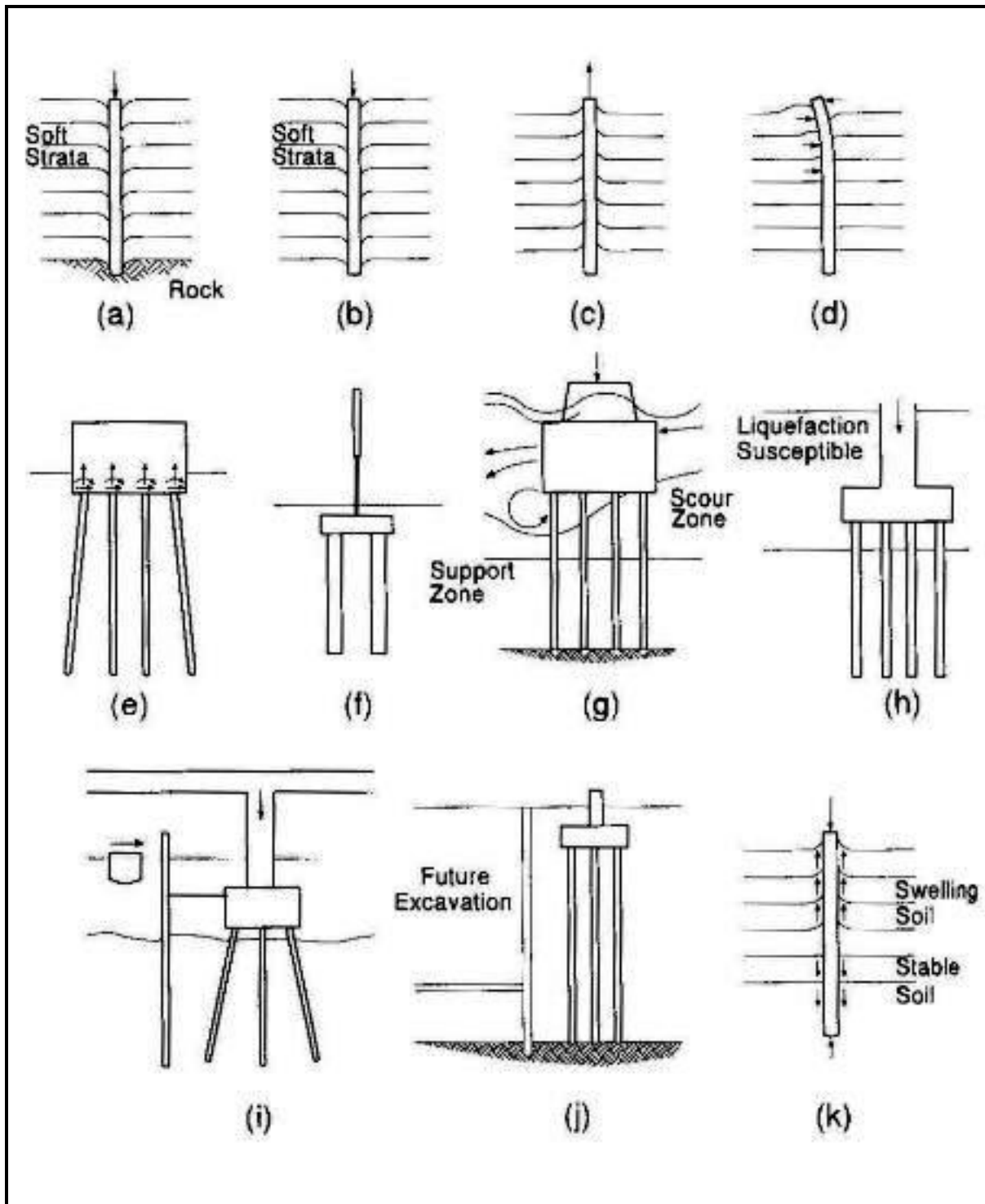
## DEEP FOUNDATIONS

### 16.1 INTRODUCTION

This Chapter provides general guidance in the design and analysis of deep foundations used to support highway structures. Deep foundations consist of driven piles, drilled shafts or piers, drilled piles, auger cast-in-place (continuous flight auger, CFA) piles, micro-piles and pile or drilled shaft supported footings. Each foundation type has specific advantages and disadvantages that will be discussed in subsequent Sections. The design of deep foundations is comprised of 2 components, the axial and lateral capacity (resistance to shear) and settlement (performance); however, in the design of deep foundations axial resistance typically governs.

According to NAVFAC DM-7.2 (1986) deep foundations are defined as developing resistance at depths ( $D_f$ ) greater than 5 times the size (diameter) ( $B_f$ ) of the foundation (i.e.,  $D_f \geq 5B_f$ ). As indicated previously, axial resistance typically governs the design of deep foundations not settlement. The resistance of deep foundations is based on either the end resistance ( $R_t$ ) or side resistance ( $R_s$ ) along the shaft of the foundation acting independently of the other component or a combination of the 2 components acting together. Deep foundations need to be considered for several reasons:

- When the upper soil strata are too weak or compressible to support the required vertical loads (a), (b), (c) (letters refer to Figure 16-1);
- When shallow foundations cannot adequately support inclined, lateral, or uplift loads, and overturning moments (d), (e), (f);
- When scour around foundations could cause loss of bearing capacity at shallow depths (g);
- When soils around foundations are subjected to SSL during seismic events (h);
- When fender systems are required to protect bridge piers from vessel impact (i);
- When future excavations are planned which would require underpinning of shallow foundations (j), and;
- When expansive or collapsible soils are present, this could cause undesirable seasonal movements of the foundations (k).



Note: Illustrations (e) and (i) above shows battered piles, please note that SCODT prefers vertical piles.

**Figure 16-1, Reasons for Deep Foundations  
(Hannigan, et al. (2006))**

All deep foundation designs will be governed by the basic LRFD equation.

$$Q = \sum \eta_i \gamma_i Q_i \leq \phi R_n = R_r = \phi R_t + \phi R_s \quad \text{Equation 16-1}$$

Where,

- Q = Factored Load
- Q<sub>i</sub> = Force Effect
- η<sub>i</sub> = Load modifier
- γ<sub>i</sub> = Load factor
- R<sub>r</sub> = Factored Resistance (i.e., allowable capacity)
- R<sub>n</sub> = Nominal Resistance (i.e., ultimate capacity)
- R<sub>t</sub> = Nominal End or Tip Resistance
- R<sub>s</sub> = Nominal Side Resistance
- φ = Resistance Factor

The selection of φ will be discussed in greater detail in the following Sections. Typically, φ is based on the method of construction control for piles and on the type of material and where (i.e., end or side) the capacity is developed. SCDOT does not use design method specific resistance factors (see Chapter 9) for the design of pile foundations but instead uses resistance factors based on load resistance construction verification. Drilled shafts are designed using either design method specific or construction verification resistance factors, with construction verification resistance factors taking precedence over the design method resistance factors if construction verification is used. The factored load is provided by the SEOR.

## 16.2 DESIGN CONSIDERATIONS

The design of deep foundations supporting bridge piers, abutments, or walls should consider all limit state loading conditions applicable to the structure being designed. A discussion of the load combination limit states that are used in deep foundation design is discussed in Chapter 8 and the deep foundation corresponding limit state is reproduced below in Table 16-1. Most substructure designs will require the evaluation of foundation and structure performance at the Strength and Service limit states; however there are instances where the EE limit state may control design. These limit states are generally similar to evaluations of ultimate capacity and deformation behavior in ASD, respectively.

**Table 16-1, Deep Foundation Limit States**

Performance Limit	Limit States		
	Strength	Service	Extreme Event
Axial Compression Load	√		√
Axial Uplift Load	√		√
Structural Capacity <sup>1</sup>	√		√
Lateral Displacements		√	√
Settlement		√	√

<sup>1</sup>Determined by SEOR

In addition, the environment (corrosive or non-corrosive) into which the deep foundations are installed should be evaluated as a part of design. As required in Chapters 4 and 7, the GEOR shall conduct electro-chemical tests and shall indicate whether the soils at the project site are Aggressive or Non-aggressive. This information shall be provided to the design team, specifically the SEOR. The SEOR and the design team shall evaluate the results of the electro-chemical tests and shall determine if the subsurface environment has the potential for foundation material deterioration and what measures need to be taken to avoid deterioration of the foundations.

### 16.2.1 Axial Load

Axial loadings should include both compressive and uplift forces in evaluation of deep foundations. Forces generated from the Strength limit state and EE limit state are used to determine nominal axial pile resistances from the axial design process. The Strength limit state is a design boundary condition considered to ensure that strength and stability are provided to resist specified load combinations, and avoid the total or partial collapse of the structure. The Service limit state is the design boundary condition for structure performance under the intended service loads. This boundary condition accounts for some acceptable level of deflection over the life of the structure. The Service limit state is checked to determine foundation movements. If the foundations excessively deflect, the performance of the structure could be compromised. All deflections determined by the GEOR shall be reported to the design team. The design team shall evaluate the foundation deflections and determine the impact of the deflections on the Performance Objective of the structure. The EE limit states are design boundary conditions considered to represent an excessive or improbable loading combination. Such conditions may include vessel or vehicular impacts, scour (check flood), and seismic events. Because the probability of these events occurring during the life of the structure is relatively small, a smaller safety margin (higher  $\phi$ ) is appropriate when evaluating this limit state.

The static resistance of a pile/shaft can be defined as the sum of soil/rock resistances along the pile/shaft surface and at the pile/shaft toe (tip) available to support the imposed loads on the pile. A static analysis is performed to determine the nominal bearing resistance ( $R_n$ ) of an individual pile/shaft and of a pile/shaft group as well as the deformation response of a pile and/or group to the applied loads. The nominal bearing resistance ( $R_n$ ) of an individual pile and of a pile group is the smaller of:

- (1) The resistance of surrounding soil/rock medium to support the loads transferred from the pile/shaft or,
- (2) The structural capacity of the pile/shaft.

The static pile/shaft resistance from the sum of the soil/rock resistances along the pile/shaft surface and at the pile/shaft toe can be estimated from geotechnical engineering analysis using:

- (1) Laboratory determined shear strength parameters of the soil and rock surrounding the pile;
- (2) Standard Penetration Test (SPT) data;
- (3) In-Situ Test data (i.e., CPT); or
- (4) Full scale load test data.

### 16.2.2 Lateral Load

Lateral loadings applied in foundation design shall consider foundation members placed through embankments, locations on, near or within a slope, loss of support due to erosion or scour, and the bearing strata significantly inclined. Forces generated from the Service and EE limit states are used to determine the horizontal and vertical movements of the foundation system. The Service limit state is a design boundary condition for structure performance under intended service loads, and accounts for some acceptable measure of structure movement throughout its performance life. The EE limit states are design boundary conditions considered to represent an excessive or improbable loading combination. Such conditions may include vessel or vehicular impacts, scour (check flood), and seismic events. Because the probability of these events occurring during the life of the structure is relatively small, a smaller safety margin is appropriate when evaluating this limit state.



### 16.2.3 Settlement

The amount of settlement is normally limited to the amount required to develop the resistance of the deep foundation element. Settlements are determined for the Service and Extreme Event limit states. The appropriate loads shall be used in the determination of settlement. The procedures discussed in the following Sections shall be used to determine the amount of settlement of the foundation elements. Typically settlement along shafts is limited to the amount required to develop side resistance which in turn limits the amount of displacement of the shaft tip thus reducing the amount of load carried by the tip. For deep foundations, the settlement of the group is normally determined. In addition, the elastic shortening of the deep foundation elements due to the load should be included in the overall settlement. The inclusion of elastic shortening is required, since the performance of the structure will be affected by this movement. Static analysis calculations of the deformation response to lateral loads and of pile/shaft groups' settlement are compared to the performance criteria established for the structure. All settlements shall be reported to the SEOR. It is the responsibility of the SEOR to determine if the settlement causes excessive deformation of the structure or induces additional stress on a particular element. Depending on the requirements of the particular project, the use of the Construction-Point Concept may be used. Unlike traditional settlement calculations which assume the bridge is instantaneously placed, the Construction-Point Concept determines the settlement at specific critical construction points (see Figure 16-2).

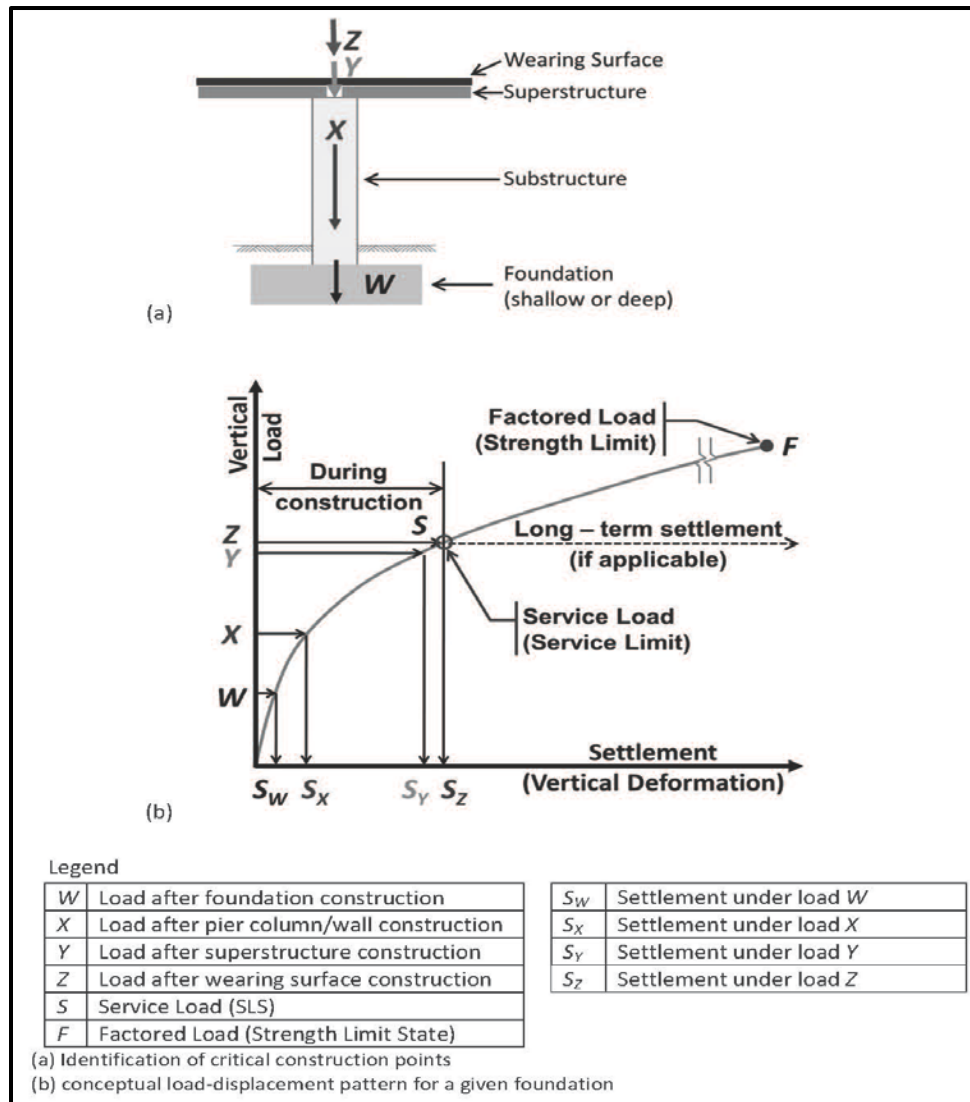


**Figure 16-2, Construction-Point Concept (DeMarco, Bush, Samtani, Kulicki and Severns (2015))**

**16.2.4 Scour**

The design of deep foundations shall consider the effects of scour (design flood) on the capacity and length requirements of the foundation as part of the Strength and Service limit state design. The nominal resistance of deep foundations shall be determined for the soils beneath the scourable soils. The depth of scour shall be determined by the HEOR. The capacity of the scourable soils shall be added to the nominal capacity of driven piles when developing driving criteria, but no increase in capacity is required for the drilled shafts, CFAs and micro-piles because they are not driven. The following Sections will provide additional details for handling scour for each foundation type. In addition, the design of deep foundations shall include the effects of scour induced by the check flood. The check flood is part of the EE II limit state. All deep foundations shall be checked to ascertain that the soils beneath the check flood scour have sufficient capacity to resist the EE II loads. Similar to the Strength and Service limit state designs, all resistance shall be determined utilizing the soils beneath the check flood scour.

### 16.2.5 Downdrag

Downdrag on deep foundations is caused by 2 distinct phenomena, settlement of subgrade soils and seismically induced SSL, specifically liquefaction of Sand-Like soils. Settlement is normally anticipated to occur at the end bent of bridges where the bridge meets the embankment. As part of the settlement analysis the potential for lateral squeeze should be considered. Lateral squeeze of compressible soils may induce lateral loads on the deep foundations. Downdrag induced settlements are applied to the Strength limit state of the deep foundation. Downdrag loads will be discussed in the following Sections, while the settlement of the embankments is discussed in Chapter 17. The other phenomenon that may induce downdrag is seismically induced SSL. This downdrag load is applied to the EE I limit state and will be discussed in the following Sections in greater detail. The amount of seismically induced SSL settlement is determined using the procedures outlined in Chapter 13.

### 16.3 DRIVEN PILES

Driven piles typically used by SCDOT include prestressed concrete, steel H-piles, steel pipe piles and combination piles consisting of prestressed concrete and steel H-pile sections. In addition, SCDOT has used timber piles in the past; however, timber piles are typically only used for pedestrian bridge structures. The use of concrete cylinder piles shall be approved in writing by the PC/SDS and PC/GDS prior to commencing design. Piling is further categorized as either displacement or non-displacement. Displacement piles increase lateral ground stresses, densify Sand-Like soils, can weaken Clay-Like soils (temporarily), have large set up times for Clay-Like soils, and primarily get their capacity from skin resistance. Typically, prestressed concrete and closed-ended steel pipe piles are considered displacement piles. Non-displacement piles usually cause minimal disturbance to surrounding soil and primarily get their capacity from end bearing and are typically driven to dense/hard soils or rock. Steel H-piles and opened steel pipe piles are considered non-displacement piles. The BDM provides typical sizes for driven piles. Table 16-2 provides a summary of these pile types and sizes.

**Table 16-2, Typical Pile Types and Sizes**

Pile Type	Size
Steel H-piles	HP 12x53 HP 14x73 HP14x89 HP 14x117 <sup>1</sup>
Steel Pipe Piles	16-inch <sup>2</sup> 18-inch <sup>2</sup> 20-inch <sup>2</sup> 24-inch <sup>2</sup>
Prestressed Concrete Piles (PSC) <sup>3</sup>	18-inch 20-inch 24-inch 30-inch <sup>4</sup> 36-inch <sup>4</sup>
Combination Piles	18-inch PSC <sup>3</sup> with W 8x58 stinger 20-inch PSC <sup>3</sup> with HP 10x57 stinger 24-inch PSC <sup>3</sup> with HP 12x53 stinger

<sup>1</sup>Used where penetration is minimal and nominal capacity is large

<sup>2</sup>Wall thickness is ½ inch, minimum, for all pipe pile sizes

<sup>3</sup>Prestressed concrete piles are solid and square in section

<sup>4</sup>These sizes are only allowed with the written approval of SCDOT

As required in the AASHTO LRFD Specifications, driven pile analyses and design should address the following:

- Nominal axial resistance, pile type, size of pile group, and how the nominal axial pile resistance will be determined in the field;
- Pile group interaction;
- Pile penetration required to meet nominal axial resistance and other design requirements;
- Minimum pile penetration necessary to satisfy the requirements caused by uplift, scour, downdrag, settlement, lateral loads, SSL, and seismic conditions;
- Foundation deflection should meet the established movement and associated structure performance criteria;
- Pile foundation nominal structural resistance;
- Verification of pile driveability to confirm acceptable driving stresses and blow counts can be achieved, and;
- Long-term durability of the pile in service (i.e., corrosion and deterioration).

A thorough reference on pile foundations is presented in the FHWA publication Design and Construction of Driven Pile Foundations – Volume I and II (Hannigan, et al. (2006)).

### 16.3.1 Axial Compressive Resistance

There are numerous static analysis methods available for calculating the bearing resistance of a single pile. The axial compressive capacity for driven piles shall follow the procedures provided in the AASHTO LRFD Specifications (Section 10.7 - Driven Piles). The methods found in the AASHTO LRFD Specifications are used to satisfy the Strength, Service and EE limit states.

The basic LRFD equation presented previously and in Chapter 8 is expanded on the resistance side of the equation to account for the factored resistance of piles ( $R_r$ ), and may be taken as:

$$Q \leq \phi R_n = R_r = (R_t + R_s)\phi \quad \text{Equation 16-2}$$

$$R_t = q_t * A_t \quad \text{Equation 16-3}$$

$$R_s = q_s * A_s \quad \text{Equation 16-4}$$

Where,

- Q = Factored Load (demand)
- $R_r$  = Factored Resistance (i.e., allowable capacity)
- $R_n$  = Nominal Resistance (i.e., ultimate capacity)
- $R_t$  = Nominal End or Tip Resistance
- $q_t$  = Unit End or Tip Resistance of pile (force/area)
- $A_t$  = Area of pile tip (area)
- $R_s$  = Nominal Side Resistance
- $q_s$  = Unit Side Resistance of pile (force/area)
- $A_s$  = Surface area of pile side (area)
- $\phi$  = Resistance Factor based on construction control (see Chapter 9)

The nominal resistance of driven pile at the Strength limit state shall include the effects of scour (design flood). The nominal resistance shall be developed beneath the scour elevation or depth; however, the resistance developed in the scourable soils shall be determined and added

to the nominal resistance to obtain the required driving resistance ( $R_{nDR}$ ) for use during pile installation.

The axial compressive design methodologies can be separated based on either total or effective stress methods or whether the soils are cohesionless (Sand-Like) or cohesive (Clay-Like) in nature. As indicated in the above equations the total axial compressive resistance of a deep foundation is based on the combination of unit side resistance and unit tip resistance values. Another factor that affects the axial compressive resistance of driven piles is the type of pile being installed (i.e., non-displacement vs. displacement). The followings methods shall be used to determine the resistance of driven piles:

- (1) Nordlund Method: This method is an effective stress method and is used for sands and non-plastic silts (cohesionless soils (Sand-Like)). Further this method is based on field observations and considers the pile shape, and its soil displacement properties in calculating the shaft resistance. The unit side resistance is a function of: friction angle of the soil, the friction angle of the sliding soils, pile taper, the effective unit weight of the soil, pile length, the minimum pile perimeter, and the volume of soil displaced. The friction angle of the soil shall be determined in accordance with the procedures outlined in Chapter 7. While there is no limiting value for the side resistance, the effective overburden pressure shall be limited to 3 kips per square foot (ksf) for determining the tip resistance. For pile sizes greater than 24 inches, this method tends to overpredict the pile resistance.
- (2)  $\alpha$ -Method: A total stress analysis used where the ultimate resistance is calculated from the undrained shear strength of the soil and is applicable for clays and plastic silts (cohesive soils (Clay-Like)). The undrained shear strength shall be determined in accordance with the procedures provided in Chapter 7. This method assumes that side resistance is independent of the effective overburden pressure and that the unit side resistance can be expressed in terms of an empirical adhesion factor times the undrained shear strength. The coefficient  $\alpha$  depends on the nature and strength of the clay, pile dimension, method of pile installation, and time effects. The unit tip resistance is expressed as a dimensionless bearing capacity factor times the undrained shear strength. The dimensionless bearing capacity factor ( $N_c$ ) depends on the pile diameter and the depth of embedment, and is usually assumed to be 9.
- (3) SPT 97 Method: A total stress method originally developed by the Florida Department of Transportation (FDOT). The method uses uncorrected  $N_{60}$ -values to determine the nominal resistance of driven piles. The method is based on the results of numerous load tests conducted by FDOT. The soils of the South Carolina Coastal Plain are similar to the soils in Florida. This is applicable to both cohesionless (Sand-Like) and cohesive (Clay-Like) soil.
- (4) Historical Load Test Data: The nominal resistance for driven piles may be developed based on the results of historical load test data from the anticipated load bearing stratum (i.e., the same geologic formation). The use of this type of data for development of resistance shall be reviewed by the PC/GDS. The results of more than 5 load tests shall be used to develop the resistance. Load testing shall include static load tests, dynamic load tests and rapid load tests. A comparison to the soils at the load test site to the soils at the new location shall be performed.

For driven piles that will develop resistance in a layered subsurface profile consisting of both cohesionless (Sand-Like) and cohesive (Clay-Like) soils; the appropriate method will be used for each soil type and the nominal resistance determined by adding the results of the various

layers together. For soil layers that are comprised of  $\phi - c$  soils, the axial resistance for the layer should be determined using the Nordlund, SPT 97 and  $\alpha$  methods with the actual resistance of the layer being the more conservative resistance.

The AASHTO LRFD Specifications provide additional methods for determining the axial compressive resistance of driven piles. These additional methods shall be used only as a check to the Nordlund, SPT 97 and  $\alpha$  methods discussed previously. These additional methods include:

- (1)  $\beta$ -Method: An effective stress analysis used in cohesionless (Sand-Like), cohesive (Clay-Like), and layered soils.
- (2)  $\lambda$ -Method: An effective stress method that relates undrained shear strength and effective overburden to the shaft resistance.
- (3) Meyerhof SPT data Method: This method was derived by empirical correlations between Standard Penetration Test (SPT) results and static pile load tests for cohesionless (Sand-Like) soils.
- (4) Nottingham and Schmertmann CPT Methods: The method uses Cone Penetrometer Test data relating pile shaft resistance to CPT sleeve friction.

In addition, Hannigan, et al. (2006) provides additional procedures for determining the axial compressive resistance of driven piles.

- (1) Brown Method: An empirical method using SPT data for cohesionless (Sand-Like) materials.
- (2) Elsami and Fellenius Method: A CPT based method that correlates the effective tip resistance to the unit shaft resistance.
- (3) Laboratoire des Ponts et Chaussées (LPC) Method: A CPT based method that correlates the tip resistance, soil type, pile type and installation method to the unit shaft resistance.

As with the other methods listed in the AASHTO LRFD Specifications, these methods shall only be used to check the resistances determined by the Nordlund, SPT 97 and  $\alpha$  methods.

For driven piles bearing in rock with an RQD greater than 10 percent (see Chapter 6), the nominal resistance of the pile is typically limited by the structural capacity of the foundation element itself. This is especially true with prestressed concrete piles driven into rock, and why prestressed concrete piles typically have pile points when driven to bearing in rock. In many cases steel piles are fitted with “reinforced tips” to avoid damage to the foundation element. If the depth to rock with RQD greater than 10 percent is less than 10 feet, then the pile should be installed as a drilled pile. Therefore piles should be driven to rock when the depth to top of rock is greater than 10 feet. For rock with RQD less than 10 percent and soils with 100 or more blows per foot of penetration, it has been the experience of SCDOT that piles can be driven into these materials. Penetrations typically range from 5 to 10 feet.

There are numerous computer software packages available for performing the axial compressive resistance of driven pile foundations. The preferred software packages are APILE v2014<sup>®</sup> as produced by ENSOFT, Inc. or SPT 97 as developed by the University of Florida for

FDOT. The latest version of SPT 97 is contained within FB-Deep<sup>®</sup> as developed by the University of Florida, Bridge Software Institute (<http://bsi-web.ce.ufl.edu/>). APILE v2015<sup>®</sup> uses the Norlund method for determining axial resistance for cohesionless (Sand-Like) soils (tip and skin friction). While for cohesive (Clay-Like) soils the  $\alpha$  method is used for determining the tip and side resistance. In APILE v2015<sup>®</sup> these methods are collectively called the “FHWA Method”. FB-Deep<sup>®</sup> can be applied to both cohesionless (Sand-Like) and cohesive (Clay-Like) soils. Other computer software packages may be used to determine axial compressive resistance of driven piles; however, prior to being used, the designer must submit copies of the output, the method used for design, a set of hand calculations performed using the procedure and evidence of applicability and acceptability using load testing information. This information shall be submitted to the PC/GDS for technical review prior to being approved and is in addition to the requirements of Chapter 26. It is incumbent upon the GEOR, that prior to using any software, that the methodologies used by the software are fully understood.

### 16.3.2 Axial Uplift Resistance

The axial uplift resistance should be evaluated when tensile forces may be present. The side resistance of the driven pile shall be determined using either the Norlund or  $\alpha$  methods. All resistance losses due to scour shall not be included in the determination of the axial uplift resistance. In addition, static settlement induced downdrag loads shall not be included, since it is anticipated that at some point in time settlement will cease. The factored uplift resistance ( $R_r$ ) may be evaluated by:

$$Q \leq \phi R_n = \phi_{up} R_s = R_r \quad \text{Equation 16-5}$$

Where,

- Q = Factored Load (demand)
- $R_r$  = Factored Resistance (i.e., allowable capacity)
- $R_n$  = Nominal Resistance (i.e., ultimate capacity)
- $R_s$  = Nominal Side Resistance
- $\phi$  and  $\phi_{up}$  = Uplift Resistance Factors (see Chapter 9)

### 16.3.3 Group Effects

The analysis procedures discussed in the preceding paragraphs are for single driven piles. For most structures, driven piles are installed in groups. Typically SCDOT uses trestle bents (i.e., a single row of piles). Trestle bents shall be considered to be groups for the purpose of determining group efficiency. The nominal axial (compressive or tensile) resistance of a pile group is the lesser of:

- The sum of individual nominal pile resistances, or
- The nominal resistance of the pile group considered as a block.

The minimum center-to-center spacing in a trestle bent is 2-1/2 times the nominal pile size; therefore, the group efficiency shall be taken as 1.0. For pile groups having 2 or more rows of piles, the group efficiency shall be determined following the procedures outlined in Section 10.7 of the AASHTO LRFD Specifications. The spacing between piles shall not be less than a center-to-center spacing of 2-1/2 times the nominal pile size in either the longitudinal or transverse directions. The procedures for determining the dimensions of the block are presented in the following section.

### 16.3.4 Settlement

Typically, the settlement of deep foundations is comprised of immediate and primary consolidation settlement and elastic compression (shortening). Secondary compression is not normally considered as part of the settlement of deep foundations. In many cases primary consolidation settlement is not a concern, since most deep foundations are founded in cohesionless soils (Sand-Like), overconsolidated ( $OCR \geq 4$ ) (Clay-Like) soils, or rock. Elastic compression is included since the deep foundation will elastically deform when a load is applied. Pile groups are used in determining the amount of settlement instead of single piles, since very rarely are single piles used to support a structure. The total settlement is defined by the following equation.

$$\Delta_v = S_t = S_i + S_c + S_s + \Delta_E \quad \text{Equation 16-6}$$

Where,

- $S_t = \Delta_v =$  Total Settlement
- $S_i =$  Immediate Settlement
- $S_c =$  Primary Consolidation Settlement
- $S_s =$  Secondary Compression Settlement
- $\Delta_E =$  Elastic Compression

Elastic compression is the compression (deflection or shortening) of a single pile caused by the application of load at the top of the pile. The elastic compression of combination piles is complex and difficult to determine. Therefore, engineering judgment should be used in determining if the concrete or steel portion of the combination pile contributes more to the settlement of the pile group. Elastic compression should be determined using the following equation.

$$\Delta_E = \frac{Q_a * L}{A * E} \quad \text{Equation 16-7}$$

Where,

- $Q_a =$  Applied load
- $L =$  Pile length (embedment)
- $A =$  Cross sectional area of pile
- $E =$  Elastic modulus of pile material

For piles founded in cohesionless (Sand-Like) soils and in overconsolidated ( $OCR \geq 4$ ) cohesive (Clay-Like) soils, the settlement shall be determined using elastic theory as presented in Chapter 17. An equivalent foundation is used to determine the dimensions required. The width of the foundation ( $B_f$ ) is either the pile diameter or face dimension for pile bents or the center to center dimension of the outside piles along the shortest side of a pile footing (group). The length ( $L_f$ ) is the center to center dimension of the outside piles along the length of the pile bent or pile footing. The depth of the equivalent foundation shall be 2/3 of the pile embedment depth into the primary bearing resistance layer. The applied bearing pressure ( $q_o$ ) shall be taken as the sum of the pile loads at the limit state being checked divided by the area of the equivalent footing. For each subsequent layer, the equivalent foundation is enlarged 1 horizontal to 2 vertical (1H:2V) proportion until the settlement for all subsequent layers is determined.

The settlements for pile foundations placed in NC to slightly OC ( $1 < OCR < 4$ ) plastic cohesive (Clay-Like) soils shall be determined using consolidation theory as presented in Chapter 17. Similar to the elastic settlement determination an equivalent foundation shall be placed 2/3 of the pile embedment depth into the primary bearing resistance layer and the applied bearing



pressures and changes in stress determined according. The applied bearing pressure ( $q_o$ ) shall be taken as the sum of the pile loads at the limit state being checked divided by the area of the equivalent footing. For each subsequent layer, the equivalent foundation is enlarged 1 horizontal to 2 vertical (1H:2V) proportion until the settlement for all subsequent layers is determined.

As indicated previously, settlement is determined at the Service and Extreme Event limit state loading. All settlements will be reported to the SEOR to determine if the structure can tolerate the displacement (Service and Extreme Event).

### **16.3.5 Pile Driveability**

Pile driveability refers to the ability of a pile to be driven to a desired penetration depth and/or resistance. Pile driveability shall be performed as part of the design process. When evaluating driveability, the soil disturbance during installation and the time dependent soil strength changes should be considered.

There are 3 methods available for predicting and/or checking pile driveability.

- Wave Equation Analysis
- Dynamic Testing and Analysis
- Static Load Tests

Geotechnical Resistance factors for each of these 3 methods for analysis and level of resistance determination are provided in Chapter 9.

Wave equation analysis is required during design and again during construction. The following graphic illustrates some of the variables involved with the model. The most widely accepted program is GRLWEAP, and is available at <http://pile.com/pdi/>. It is incumbent upon the GEOR, that prior to using any software, that the methodologies used by the software are fully understood.

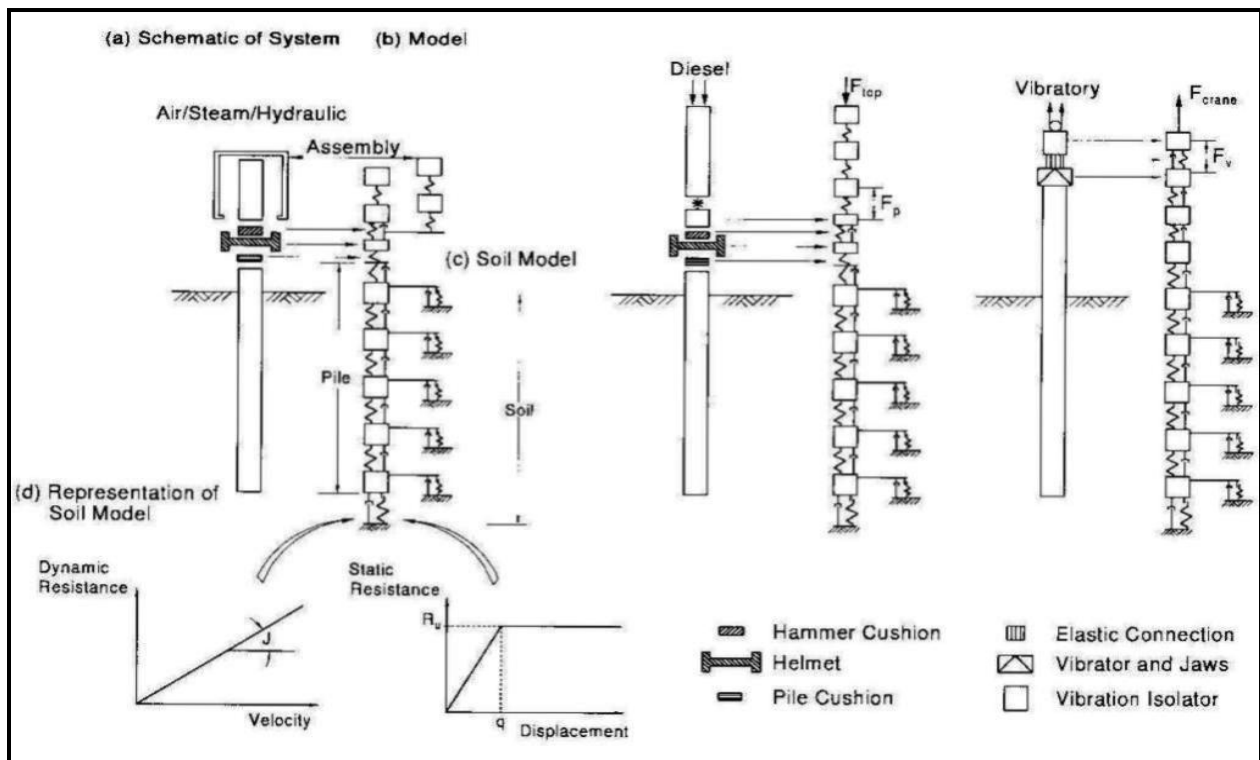


**Figure 16-3, Typical Wave Equation Model  
(Hannigan, et al. (2006))**

Some of the parameters that must be considered are hammer type, cushion material, pile properties and sizes, soil resistance distributions, soil quake and damping parameters. Some of these parameters are placed on the drawings (see Table 16-3). The wave equation is a computer simulation of the pile driving process that models wave propagation through the hammer-pile-soil system. The wave equation analysis should be used to establish the range of hammer energies, based on achieving a penetration between 36 and 180 blows per foot. The  $R_{nDR}$  (see Foundation Length) shall be used in wave equation analyses.

**Table 16-3, Driveability Analysis**

Skin Quake (QS)	0.10 in
Toe Quake (QT)	0.08 in
Skin Damping (SD)	0.20 s/ft
Toe Damping (TD)	0.15 s/ft
% Skin Friction	80%
Distribution Shape No. <sup>1</sup>	1
Resistance Distribution Model	Proportional <sup>2</sup>
Toe No. 2 Quake	0.15 in
Toe No. 2 Damping	0.15 s/ft
End Bearing Fraction (Toe No. 2)	0.95
Pile Penetration	80%
Hammer Energy Range <sup>3</sup>	25 – 60 ft-kips

<sup>1</sup>Distribution Shape No. varies with depth: 0 at the ground surface (creek bottom); 1 at a depth of 5ft; and 1 to a depth beyond driving depth below the ground surface.

<sup>2</sup>Bearing Graph options – proportional, constant skin friction, constant end bearing  
Note: GRLWEAP (XXXX) was used to perform the wave equation analysis.

<sup>3</sup>Based on achieving a penetration rate ranging from 80 to 120 bpf; however, the SCDOT Standard Specifications for Highway Construction requires a penetration rate ranging from 36 to 180 bpf

During construction, additional wave equation analysis should be performed on the actual driving system and cushions to be used. The model should be used for checking for adequate hammer energy, establishing fuel settings, for checking compressive and tensile stresses, and to see if the penetration rate falls within a certain range. The required number of blows shall range from 36 to 180 blows per foot for the driving system to be acceptable. Practical refusal is defined as 5 blows per quarter (1/4) inch or 20 blows per inch.

Dynamic Testing and Analysis shall be in accordance with ASTM D4945. This test consists of measuring strain and acceleration near the pile top during driving, or restrike using a Pile Driving Analyzer (PDA). The PDA is used to calculate valuable information such as pile driving stresses, energy transfer, damping and quake values, and the nominal pile resistance. Additional analysis of the data collected in the field can be performed by using signal matching methods such as CAPWAP. Unlike static load testing which typically requires the cessation of pile driving, PDA testing is performed during initial pile installation as well as at some point later in time (i.e., restrike) to determine pile setup. During initial pile installation PDA testing only requires time to install the monitoring equipment. Restrikes will require some additional time to perform, but are anticipated to require less than a day for testing. PDA testing further allows for the capacity of the pile to be determined relatively quickly and allows for a determination of the stresses induced on the pile by the pile driving equipment. Additional information on the dynamic testing is provided in Chapter 24.

Static load tests are the most accurate method of determining the nominal resistance of a pile (if carried to failure). While this method accurately determines the obtained resistance and the penetration required to achieve the nominal resistance, it does not determine if there is any damage to the pile during installation. If static load testing is recommended for a project with driven piles, then dynamic testing and Wave Equation analysis will also be required. This procedure has limited applicability since static load testing requires several days to setup and perform the testing. Static load testing can add several weeks to a construction project. Optimally, static load testing should be performed as a part of the design phase of a project, when the results can more readily be used to affect the design. A comprehensive report by the FHWA on this topic is Static Testing of Deep Foundations (Kyfor, Schnore, Carlo, and Bailey (1992)).

## 16.4 DRILLED SHAFTS

A drilled shaft (also called drilled caisson or caisson) is a deep foundation element that is constructed by excavating a hole with power auger equipment. Reinforcing steel and concrete are then placed within the excavation. In unstable soils, casing and drilling slurry is used to maintain the stability of the hole. Drilling slurry typically consists of natural materials (i.e., bentonite); the use of polymer materials is not allowed. For certain geologic conditions (i.e., sound rock) the use of plain water (potable) as a drilling fluid is allowed; however, permission to use plain water must be obtained from SCDOT. Drilled shafts should be considered when large loads are anticipated (compressive, uplift or lateral) and where the amount of allowable deformation is small. Additionally, drilled shafts should be considered in locations where the losses due to scour are large, seismically induced downdrag loads are large or where the instability of slope cannot be maintained using conventional methods. Further drilled shafts should be considered when there is a limitation on water crossing work.

Drilled shaft sizes (diameters) can typically range from 30 inches (2-1/2 feet) to 144 inches (12 feet). Drilled shaft sizes typically used by SCDOT range from 42 inches (3-1/2 feet) to 84 inches (7 feet) in diameter. Drilled shaft diameters should be a minimum of 6 inches larger than the column above the shaft. Unless approved otherwise by the PC/GDS, all shafts shall be detailed with construction casing. The portion of the shaft below the bottom of the casing, in rock, shall be detailed with a diameter that is 6 inches smaller than the diameter of construction

casing. According to the BDM drilled shafts are typically used when the span length of a bridge is greater than 50 feet.

As required by the AASHTO LRFD Specifications, the drilled shaft analyses and design should address the following:

- Nominal axial resistance of a single shaft and of a group of shafts.
- The resistance of the underlying strata to support the load of the shaft group.
- The effects of constructing the shaft(s) on adjacent structures.
- Minimum shaft penetration necessary to satisfy the requirements caused by uplift, scour, downdrag, settlement, lateral loads, SSL, and seismic conditions.
- Drilled shaft nominal structural resistance
- Satisfactory behavior under service loads
- Long-term durability of the shaft in service (i.e., corrosion and deterioration)

A thorough reference on shaft foundations is presented in the FHWA publication Drilled Shafts: Construction Procedures and LRFD Design Methods (Brown, Turner, Castelli, and Loehr (2018)).

#### 16.4.1 Axial Compressive Resistance

There are numerous static analysis methods available for calculating the bearing resistance of a single drilled shaft. The axial compressive resistance for drilled shafts shall follow the procedures provided in the AASHTO LRFD Specifications (Section 10.8 – Drilled Shafts). The methods found in the AASHTO LRFD Specifications are used to satisfy the Strength, Service and EE limit states.

The basic LRFD equation presented previously and in Chapter 8 is expanded on the resistance side of the equation to account for the factored resistance of drilled shafts ( $R_r$ ), and may be taken as:

$$Q \leq \phi R_n = R_r = \phi_t R_t + \phi_s R_s \quad \text{Equation 16-8}$$

$$R_t = q_t * A_t \quad \text{Equation 16-9}$$

$$R_s = q_s * A_s \quad \text{Equation 16-10}$$

Where,

- Q = Factored Load (demand)
- $R_r$  = Factored Resistance (i.e., allowable capacity)
- $R_n$  = Nominal Resistance (i.e., ultimate capacity)
- $R_t$  = Nominal End or Tip Resistance
- $q_t$  = Unit tip resistance of drilled shaft (force/area)
- $A_t$  = Area of drilled shaft tip (area)
- $R_s$  = Nominal Side Resistance
- $q_s$  = Unit side resistance of drilled shaft (force/area)
- $A_s$  = Surface area of drilled shaft side (area)
- $\phi$ ,  $\phi_t$  and  $\phi_s$  = Resistance Factors (see Chapter 9)

Where construction (permanent) casing is used, the side resistance along the length of the casing shall not be included in the nominal or factored resistances for axial compression or tension. However, any downdrag developed along the length of the cased section shall be

added to the Strength, Service and EE limit state axial loads. Construction casing should normally be used on all drilled shafts in order to facilitate column construction above the shaft. If the nominal loads provided by the SEOR are located at the top of the column, then the GEOR shall add the weight of the column to the axial compressive load in order to develop the appropriate nominal resistance. However, if the SEOR provides the nominal loads at the top of the drilled shaft, then the GEOR shall not include the weight of the column.

The axial compressive design methodologies can be separated based on either total or effective stress methods or whether the soils are cohesionless (Sand-Like) or cohesive (Clay-Like) in nature. As indicated in the above equations the total axial compressive resistance of a deep foundation is based on the combination of unit side resistance and unit tip resistance values. The combination of side and tip resistance shall be settlement compatible (i.e., the settlement required to achieve side friction shall be used to develop tip resistance). The factored tip resistance shall be reduced to limit the amount of settlement of the drilled shaft; therefore, satisfying the Service limit state for the drilled shaft. See Chapter 17 for settlement analysis methods.

The following methods shall be used to determine unit side resistances in soils:

- (1)  $\alpha$ -Method: A total stress analysis used where ultimate capacity is calculated from the undrained shear strength of the soil (clay or plastic silt (Clay-Like)). This approach assumes that side resistance is independent of the effective overburden pressure and that the unit shaft resistance can be expressed in terms of an empirical adhesion factor times the undrained shear strength. The coefficient  $\alpha$  is related to the undrained shear strength and is derived from the results of full-scale pile and drilled shaft load tests. The top 5 feet should be ignored in estimating the nominal shaft side resistance. If a construction casing is used, the shaft resistance shall be determined from the bottom of the casing to the bottom of the shaft. The maximum unit shaft resistance shall not exceed 5 ksf unless supported by load test data.
- (2)  $\beta$ -Method: An effective stress analysis used in cohesionless (Sand-Like) soils. The unit shaft resistance is expressed as the average effective overburden pressure along the shaft times the  $\beta$  coefficient. This load transfer coefficient ( $\beta$ ) is based on the effective preconsolidation pressure as determined using  $N_{60}$ -values in the design zones under consideration.
- (3) Shafts in Rock: The side-wall resistance of drilled shafts in rock is based upon the uniaxial compressive strength of rock and “normal” rock sockets. “Normal” rock sockets are defined as sockets constructed using conventional equipment resulting in clean, smooth side-walls where the rock does not decompose nor is artificial roughing required. If the side-wall is roughened, then the side-wall shear will be greater. This increased side-wall resistance shall be confirmed by load testing. If the uniaxial compressive strength of the rock is greater than the concrete strength, the concrete strength shall be used in design. Factors that should be considered when applying an engineering judgement to neglect either side or tip resistance component from the total shaft resistance include but are not limited to: the presence of a rock socket, is the shaft bearing a karstic formation or if the rock strength is greater than the shaft concrete strength.
- (4) Shafts in IGM: IGM is material that is transitional between soil and rock in terms of strength and compressibility and is defined in Chapter 6. Drilled shafts bearing in cohesive IGM should follow the modified  $\alpha$ -Method contained in Brown, et al. (2018). Drilled shafts bearing in cohesionless IGM shall use the  $\beta$ -method.

The following methods shall be used to determine unit tip resistances in soils:

- (1)  $\alpha$ -Method: A total stress analysis method is used to determine the ultimate unit tip resistance capacity and is calculated from the undrained shear strength of a cohesive soil (clay or plastic silt (Clay-Like)). The unit tip resistance is expressed as a dimensionless bearing capacity factor times the undrained shear strength. The dimensionless bearing capacity factor ( $N_c$ ) depends on the shaft diameter and the depth of embedment, and is usually assumed to be less than 9. This method limits the unit tip resistance to 80 ksf and is based on the undrained shear strength of the soil located within 2 diameters of the tip of the shaft.
- (2)  $\beta$ -Method: The unit tip resistance is based on the average SPT  $N_{60}$  blow counts being less than or equal to 50 blows per foot (bpf). The ultimate unit tip resistance of cohesionless soils is determined using a total stress analysis method. The method is based on the  $N_{60}$  and is limited to 60 ksf.
- (3) Shafts in Rock: The ultimate unit tip resistance for rock is based on the quality and strength of the rock within 2 diameters of the tip.
- (4) Shafts in IGM: IGM is material that is transitional between soil and rock in terms of strength and compressibility and is defined in Chapter 6. Drilled shafts bearing in cohesive IGM should follow the modified  $\alpha$ -Method contained in Brown, et al. (2018). Drilled shafts bearing in cohesionless IGM shall use the  $\beta$ -method.

As an alternate to the procedures provided for development of side and tip resistances of drilled shafts, the GEOR may elect to use historical load test data. The nominal resistance for drilled shafts may be developed based on the results of historical load test data from the anticipated load bearing stratum (i.e., the same geologic formation). The use of this type of data for development of nominal resistance shall be reviewed by the PC/GDS and the PCS/GDS. The results of more than 5 load tests shall be used to develop the resistance. Load testing shall include static, rapid and dynamic load tests. A comparison to the soils at the load test site to the soils at the new location shall be performed.

The analysis procedures discussed in the preceding paragraphs are for single drilled shafts. For some structures, drilled shafts are sometimes installed in groups. Drilled shaft groups installed in cohesive (Clay-Like) and cohesionless (Sand-Like) soils will typically have group efficiencies less than 1 with spacing's less than 6 and 4 diameters, respectively. The efficiencies of shaft groups are typically less than 1 due to overlapping zones of shear deformation and because the construction process tends to relax the effective stresses.

SCDOT recommends the  $\phi$  provided in Chapter 9 for analysis for drilled shaft group capacity in Clay-Like soils. This  $\phi$  is based on block failure of the Clay-Like soils, which is more due to settlement of the group. There is no group resistance factor for Sand-Like soils other than reduction required for group spacing. For additional information on the analysis of drilled shaft groups please refer to Section 10.8 in the AASHTO LRFD Specifications or the FHWA publication Drilled Shafts: Construction Procedures and LRFD Design Methods (Brown, et al. (2018)).

SHAFT v2012 (Ensoft, Inc. at <http://www.ensoftinc.com/>) is a windows-based program used to compute the axial resistance and the short-term, load versus settlement curves of drilled shafts in various types of soils. SHAFT v2012 can analyze drilled shaft response in 9 types of strata:

- i) Sand (FHWA)
- ii) Clay (FHWA)
- iii) Shale (Aurora and Reese (1976))
- iv) Strong Rock (FHWA,  $q_u > 1,000$  psi)
- v) Decomposed Rock/Gravel (FHWA)
- vi) Weak Rock (FHWA)
- vii) Strong Rock (Side friction and Tip resistance)
- viii) Gravelly Sand (Rollins, Clayton, Mikesell and Bradford (2005))
- ix) Gravel (Rollins, Clayton, Mikesell and Bradford (2005))

The program allows for any combination of soil layers to be placed in a layered profile. Most of the analytical methods used by SHAFT v2012 are based on suggestions from the FHWA manual Drilled Shafts: Construction Procedures and LRFD Design Methods (Brown, et al. (2010)). It is incumbent upon the GEOR, that prior to using any software, that the methodologies used by the software are fully understood.

### 16.4.2 Uplift Resistance

The uplift resistance should be evaluated when there are chances that upward forces may be present. The shaft side resistance should be determined from 1 of the methods presented above. The factored uplift resistance ( $R_r$ ) may be evaluated by:

$$Q \leq \phi R_n = R_r = \phi_{up} R_s = \phi_{up} q_s A_s \quad \text{Equation 16-11}$$

Where,

- Q = Factored Load (demand)
- $R_r$  = Factored Resistance (i.e., allowable capacity)
- $R_n$  = Nominal Resistance (i.e., ultimate capacity)
- $R_s$  = Nominal Side Resistance
- $q_s$  = Unit side resistance of drilled shaft (force/area)
- $A_s$  = Surface area of drilled shaft side (area)
- $\phi$  and  $\phi_{up}$  = Resistance Factors (see Chapter 9)

Shaft group uplift resistance is the lesser of:

- The sum of the individual shaft uplift resistance, or
- The uplift resistance of the shaft group considered as a block.

### 16.4.3 Group Effects

The analysis procedures discussed in the preceding paragraphs are for single drilled shafts. For most structures, drilled shafts are installed in groups. Typically SCDOT uses frame bents (i.e., a single row of drilled shafts with a column on top of each shaft); these types of bents shall be considered to be groups for the purpose of determining group efficiency. Group effects are affected by the soil the drilled shaft is founded in; therefore, discussed below are the group effects for cohesive and cohesionless soils.

According to Brown, et al. (2018):

For cohesive (*Clay-Like*) geomaterials in which installation of the foundations is not considered to have a significant effect on the in-situ soil and state of stress, the resistance for the geotechnical strength limit state should be determined from

the lesser of a block failure mode or the sum of the individual shaft resistances. That is, the efficiency cannot exceed 1.0 as shown in *Equation 16-12*. The nominal resistance of the block ( $R_{Block}$ ) is estimated as described *below*, while the individual drilled shaft nominal resistance ( $R_{n,i}$ ) is estimated as *discussed previously*.

$$\eta_g = \frac{R_{Block}}{\sum_{i=1}^n R_{n,i}} \leq 1 \quad \text{Equation 16-12}$$

Where,

$R_{Block}$  = Nominal resistance of block (see Figure 16-4) formed by drilled shafts

$R_{n,i}$  = Nominal resistance of individual drilled shafts

$R_{Block}$  can be estimated as the sum of the side shear resistance determined from the surface area of the block and the bearing capacity resistance determined from the block footprint area.

$$R_{Block} = f_{max} * [2D * (Z + B)] + q_{max} * (Z * B) \quad \text{Equation 16-13}$$

Where,

$f_{max}$  = Nominal unit side resistance of the block

$q_{max}$  = Nominal base resistance of the block

$D$  = Depth of the block (see Figure 16-4)

$Z$  = Length of the block (see Figure 16-4)

$B$  = Width of the block (see Figure 16-4)

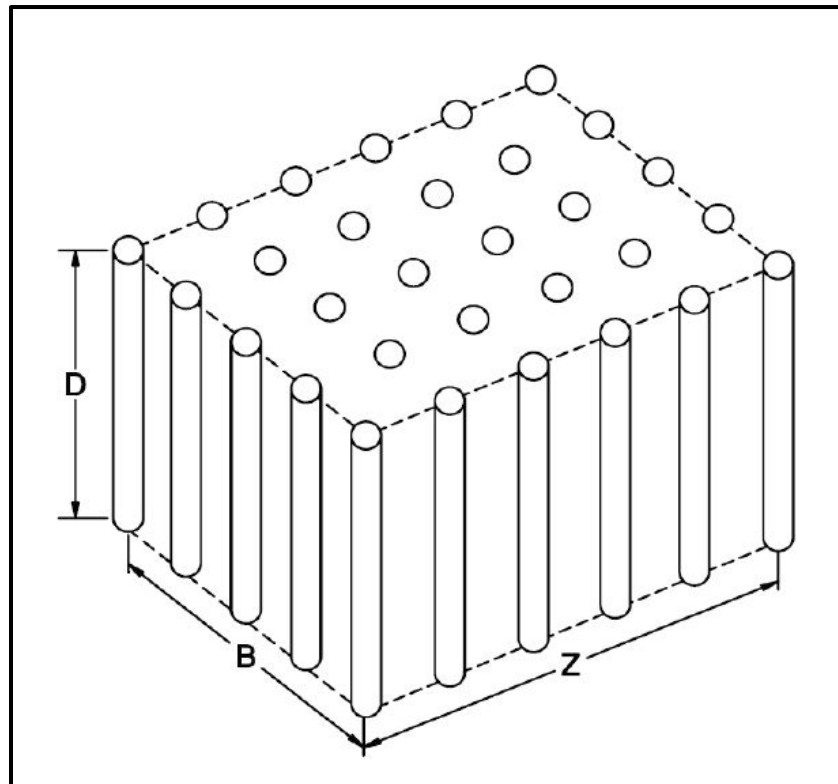


Figure 16-4, Block Failure Model  
(Brown, et al. (2018))



The nominal base resistance,  $q_{\max}$ , must take into account a zone of influence deeper for the block failure model than for a single drilled shaft. The DOSI from conventional shallow foundation design (see Chapter 15) will be used to determine the zone of influence of the block as well as the  $q_{\max}$ .

For drilled shafts founded in Sand-Like soils the individual nominal shaft resistances of each shaft in the group is reduced by a group efficiency factor,  $\eta$  (i.e., the group reduction factor). Provided in the following table are the  $\eta$ -values to be used.

**Table 16-4, Group Reduction Factor Values,  $\eta$**

Shaft Group Configuration	Drilled Shaft Center-to-Center Spacing	Group Reduction Factor, $\eta$
Single Row	2D	0.90
	3D or more	1.00
Multiple Row	2.5D	0.67
	3D	0.80
	4D or more	1.00

For drilled shafts founded in rock use an  $\eta$  of 1.0 regardless of the spacing.

#### 16.4.4 Settlement

Settlements of single drilled shafts under axial compression loadings (Service limit state) shall be determined. Settlements determine the distribution of load carrying capacity between side and tip resistances. Determine the distribution of load between the side and tip using the procedures outlined in Section 10.8 of the AASHTO LRFD Specifications.

Typically, the settlement of deep foundations is comprised of immediate and primary consolidation settlement and elastic compression (shortening). Secondary compression is not normally considered as part of the settlement of deep foundation. In many cases primary consolidation settlement is not a concern, since most deep foundations are founded in Sand-Like, overconsolidated ( $OCR \geq 4$ ) Clay-Like soils, or rock. Elastic compression is included since the deep foundation will elastically deform when a load is applied. The settlement of drilled shaft groups shall be used instead of the using the settlement for single drilled shafts. However, in some cases (i.e., hammer heads) single drilled shafts are used to support a structure. The total settlement is defined by the following equation.

$$\Delta_v = S_t = S_i + S_c + S_s + \Delta_E \quad \text{Equation 16-14}$$

Where,

- $S_t$  =  $\Delta_v$  = Total Settlement
- $S_i$  = Immediate Settlement
- $S_c$  = Primary Consolidation Settlement
- $S_s$  = Secondary Compression Settlement
- $\Delta_E$  = Elastic Compression

Elastic compression is the compression (deflection or shortening) of a drilled shaft caused by the application of load at the top of the drilled shaft. The elastic compression of drilled shafts is complex or difficult to determine; therefore, engineering judgment should be used in determining the elastic properties of a drilled shaft. Elastic compression should be determined using the following equation.

$$\Delta_E = k * \left( \frac{Q_a L}{AE} \right) \quad \text{Equation 16-15}$$

Where,

- Q<sub>a</sub> = Applied load
- L = Drilled shaft length (embedment)
- A = Cross sectional area of drilled shaft
- E = Elastic modulus of drilled shaft material
- k = Factor that accounts for load distribution along drilled shaft (see Table 16-5)

**Table 16-5, k Factor**

Loading Condition	k Factor
All End Bearing <sup>1</sup>	1.00
All Side Resistance	0.50
Combination of End and Side	0.67

<sup>1</sup>Drilled shafts founded in rock are included in this category

For drilled shafts founded in Sand-Like soils and in overconsolidated (OCR ≥ 4) Clay-Like soils, the settlement shall be determined using elastic theory as presented in Chapter 17. An equivalent foundation is used to determine the dimensions required. The width of the foundation (B in Figure 16-4) is either the drilled shaft diameter or the center to center of the outside shafts along the shortest side of a shaft footing (group). The length (Z in Figure 16-4) is measured from the center to center of the outside shafts along the length of the shaft frame or shaft footing. The depth of the equivalent foundation shall be 2/3 of the drilled shaft embedment depth into the primary bearing resistance layer. The applied bearing pressure (q<sub>o</sub>) shall be taken as the sum of the drilled shaft service loads divided by the area of the equivalent footing. For each subsequent layer, the equivalent foundation is enlarged 1 horizontal to 2 vertical (1H:2V) portion until the settlement for all subsequent layers is determined.

The settlements for drilled shaft foundations placed in NC to slightly OC (1 < OCR < 4) plastic Clay-Like soils shall be determined using consolidation theory as presented in Chapter 17. Similar to the elastic settlement determination an equivalent foundation shall be placed 2/3 of the drilled shaft embedment depth into the primary bearing resistance layer and the applied bearing pressures and changes in stress are determined accordingly. The applied bearing pressure (q<sub>o</sub>) shall be taken as the sum of the drilled shaft service loads divided by the area of the equivalent footing. For each subsequent layer, the equivalent foundation is enlarged 1 horizontal to 2 vertical (1H:2V) portion until the settlement for all subsequent layers is determined.

Once the total settlement (S<sub>t</sub> or Δ<sub>v</sub>) is determined, then the distribution of the load between side and end should be determined as indicated previously.

### **16.4.5 Constructability**

The constructability of drilled shafts consists of estimating the soil and rock excavation quantities as well as estimation of the elevation of the top and bottom of the construction casing. The quantity for soil excavation should be estimated to include all materials that have an N<sub>meas</sub> less than 50 blows for 6 inches of penetration (50/6") (N<sub>meas</sub> < 50/6"). Note that N<sub>meas</sub> is being used as opposed to N<sub>60</sub> or N<sub>1,60</sub>, since N<sub>meas</sub> is the value that the contractor will have access to on the Soil Test Logs. Materials with an N<sub>meas</sub> greater than or equal to 50/6" (N<sub>meas</sub> ≥ 50/6")

should be for the purposes of estimating drilled shaft rock excavation quantities. Report estimated quantities for soil and rock excavation as required in Chapter 22.

Typically the top elevation of the construction casing is estimated by the SEOR in consultation with the GEOR and is typically indicated on the construction plans. In dry environments, the top of casing elevation should be set at the ground line. In wet or fluctuating water environments, the top of casing elevation should be set 5 feet above the water elevation expected during construction. If the column supported on a drilled shaft would be less than 5 feet tall, the Contractor should be given the option, at no additional cost to SCDOT, of extending the shaft to the bottom of the bent cap. It should be noted that the estimated quantity for soil (wet and dry) excavation includes the length from the groundline to the top of the casing for this case.

The GEOR typically estimates the bottom elevation of the casing. The bottom elevation of the casing is governed by several factors including the soils encountered at the site, the anticipated loading conditions (i.e., lateral loads, scour, downdrag, etc.) and other factors determined by the project team. All construction casings should extend approximately a minimum of 20 feet beneath the original ground surface or 20 feet beneath any cut excavations required to achieve the proposed finished grade of the project, whichever is deeper. In Clay-Like soils the construction casing should extend to an  $N_{1,60}$  of approximately 20 blows per foot ( $N_{1,60} \sim 20$  bpf) or 20 feet as previously described, whichever is deeper. In Sand-Like soils the construction casing should extend to an  $N_{1,60}$  of approximately 35 blows per foot ( $N_{1,60} \sim 35$  bpf) or 20 feet as previously described, whichever is deeper. If materials with  $N_{meas}$  greater than 50/6" ( $N_{meas} > 50/6"$ ) occur within the top 20 feet, then the casing tip can be estimated to extend 1 foot into this material.

## 16.5 DRILLED PILES

Drilled piles are constructed normally at end bents where the depth to rock is less than 10 to 15 feet. Drilled piles can be a subset of drilled shafts or driven piles depending on the strength of the rock. An RQD of less than 10 percent indicates that the pile may be driven; however, refusal criteria still apply (i.e., 5 blows in 1/4 inch). The capacity of the drilled pile is determined based on whether the pile is driven or not after being placed in the bore hole. Piles placed in the bore hole and not driven shall be designed using drilled shaft design procedures. This design methodology requires coordination with the SEOR to ensure that adequate load transfer from the steel to the concrete occurs. Drilled piles typically consist of steel H-piles having sizes of HP12x53 and HP14x73. The borehole should have a diameter that measures the diagonal dimension of the pile plus 6 inches to allow for the insertion of the pile and the placement of concrete. The use of concrete and combination piles is allowed only with the prior written permission of the PC/GDS. The GEOR should be prepared to adequately explain how the resistance of the pile will be evaluated and how the pile will be constructed. Drilled piles are typically used only at end bents. Prior approval of both the PC/GDS and PC/SDS shall be required prior to using drilled piles at interior bents.

## 16.6 CONTINUOUS FLIGHT AUGER PILES

Continuous flight auger piles (CFAs) also known as Auger Cast Piles are a new technology being considered by FHWA for transportation projects. CFAs may be used on SCDOT projects; however, CFAs should not be used to support bridges without prior approval. The use of CFAs on any SCDOT project must be approved prior to completion of preliminary design. Approval shall be in writing from either the RPE or the Preconstruction Support Engineer (PSE). In addition, the designer shall contact the PC/GDS for instructions on analytical methods for determining capacity. CFAs will range in size from 18 to 30 inches (1-1/2 to 2-1/2 feet, respectively) in diameter for SCDOT projects.

## 16.7 MICROPILES

The AASHTO LRFD Specifications allows for the use of micropiles to support structures. Section 10.9 of the AASHTO LRFD Specifications provides a list of when micropiles would be acceptable; however, approval by both the PC/GDS and PC/SDS shall be obtained prior to designing micropiles. The design of micropiles when allowed shall follow Section 10.9 of the AASHTO LRFD Specifications.

## 16.8 LATERAL RESISTANCE

Deep foundations are subjected to lateral loads from wind, traffic loading, bridge curvature, vessel or vehicular impact or seismic loadings. The lateral capacity for deep foundations may be designed using either lateral load tests or analytical methods. Full scale load tests are typically not performed and will therefore not be discussed in this Chapter. Analytical methods will be presented only as an overview. More detailed information and the theory can be found in the FHWA publication Handbook on Design of Piles and Drilled Shafts Under Lateral Load (Reese (1984)). According to Hannigan, Goble, Likins, and Rauschce (2006),

The design of laterally loaded piles requires the combined skills of the geotechnical (*GEOR*) and structural (*SEOR*) engineer. It is inappropriate for the geotechnical engineer to analyze a laterally loaded pile without a full understanding of pile-structure interaction. Likewise it is inappropriate for the structural engineer to complete a laterally loaded pile design without a full understanding of how pile section or spacing changes may alter soil response. Because of the interaction of pile structural and geotechnical considerations, the economical solution of lateral pile loading problems requires communication between the structural and geotechnical engineer. (Underline added for emphasis.)

It is therefore anticipated by SCDOT that the proper development of lateral loads and resistances will require an iterative process between the GEOR and the SEOR.

The movements or deflections associated with lateral loadings should be within Performance Limits from Service and EE limit state loadings established by the design team. These movements should account for soil parameters, pile parameters and lateral load parameters. The soil parameters consist of soil type, appropriate shear strength parameters, moisture-density relationship (unit weight), moisture content, moisture-plasticity relationship, groundwater level and the Coefficient of Horizontal Subgrade Reaction ( $k_s$ ).  $k_s$  is the ratio of horizontal pressure ( $\sigma_h$ ) per unit of vertical surface area and the corresponding horizontal displacement ( $\Delta_h$ ). The pile parameters consist of the physical properties of the pile (shape, material and dimensions), pile head condition (fixed or free), method of pile placement and any group action. The lateral load parameters consist of whether the load is applied statically or seismically and if the loads are applied eccentrically (i.e., moment coupled with shear forces).

Methods of analysis that use manual computation include Broms' Method which should only be used for preliminary analysis only. Reese (1984) developed a nonlinear response analysis method that models the horizontal soil resistance using P-y curves. The soil is represented as nonlinear springs distributed over the length of the pile (see Figure 16-3).

The horizontal movements determined during the foundation design stage may be analyzed using computer applications that consider soil-structure interactions. Computer programs are available for analyzing single piles and pile groups. The computer program LPILE (Ensoft, Inc.

at <http://www.ensoftinc.com/>) is typically used by SCDOT to determine the lateral capacity of deep foundations.

The design team performs the lateral soil-structure interaction analysis with computer programs such as LPILE or FB-Pier. The design team uses this information to compute lateral displacements and to analyze the structural adequacy of the columns and foundations. The lateral soil-structure interaction analysis is also used to select the appropriate method (point-of-fixity, stiffness matrix, linear stiffness springs, or P-y nonlinear springs) to model the bridge foundation in the structural design software. If lateral design controls the minimum point of penetration for a deep foundation, the BGER should indicate this fact. In addition, for driven piles, the nominal capacity should be increased to account for the additional installation depth required to achieve the tip elevation governed by lateral design.

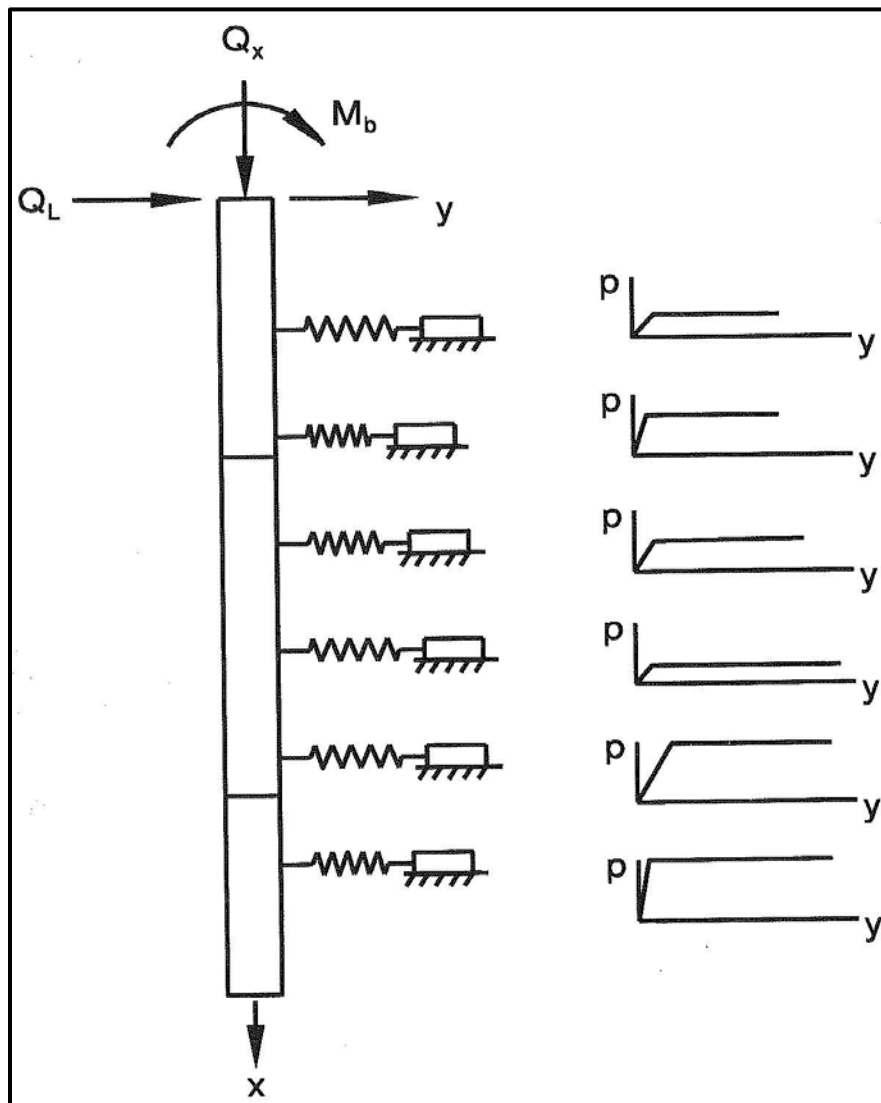


**Figure 16-5, Typical LPILE Pile-Soil Model  
(Hannigan, et al. (2006))**

According to Brown, et al. (2018) lateral designs are controlled by either geotechnical or structural strength requirements or by serviceability requirements. Each of these controlling limit states are discussed in greater detail in the following Sections.

### 16.8.1 Lateral Stability – Geotechnical Check

The deep foundation must be of sufficient size and depth to support the nominal design loads for each limit state (Strength and EE) checked without the potential for geotechnical failure (i.e., lateral stability is maintained). It is anticipated that the GEOR will perform this lateral stability check. For these geotechnical limit state checks deflections are not the controlling consideration. The geotechnical limit state checks shall be determined using a P-y analysis method as described by Brown, et al. (2018). The modified steps recommended by Brown, et al. (2018) are presented below:

1. Model the deep foundations as a simple linear elastic beam with the elastic modulus of concrete ( $E_c$ ) (use  $E_s$  for steel deep foundations) determined as indicated in the following equation and the moment of inertia ( $I$ ) equal to the uncracked cross section;

$$E_c = 33,000 * K_1 * w_c^{1.5} * \sqrt{f'_c} \quad \text{Equation 16-16}$$

$$0.090 \leq w_c \leq 0.155 \quad \text{Equation 16-17}$$

$$f'_c \leq 15.0 \quad \text{Equation 16-18}$$

Where,

- $E_c$  = Elastic modulus of concrete, ksi
  - $E_s$  = Elastic modulus of steel, 29,000 ksi
  - $K_1$  = Correction factor for aggregate source, use 1.0 unless determine by physical tests and value is provided
  - $w_c$  = Unit weight of concrete (see Chapter 8), kcf
  - $f'_c$  = 28-day cylinder strength of concrete, ksi
2. The soil is modeled using the appropriate soil parameters of each limit state (use the procedures in Chapter 7 to develop a composite profile of the site);
  3. Apply various lateral loads up to and exceeding the nominal design load for the appropriate limit state thus performing a “pushover” type of analysis. For the Strength limit state exceed the nominal by at least 20 percent; no increase is required for the EE I limit state;
  4. “Although deflection is not the controlling consideration for stability, the computed deflection must be a reasonable value (e.g., 10 percent of the nominal foundation size) at and slightly larger than the factored design loads...” (Brown, et al. (2018)), the reasonable value shall be determined by the design team;
  5. The use of larger than nominal design loads at the appropriate limit state is necessary to ensure that a ductile load response exists and there is adequate reserve to account for site variability and variation in construction methods.

The deflection determined in Step 4 above is determined at the design ground line (i.e., not the top of the deep foundation and shall include the scour caused by the design flood) and is anticipated to prevent the collapse of other portions of the structure. Should this limit, as determined by the design team, be exceeded, the design team shall be informed and the design team shall decide if the deflections are tolerable. If the deflections are intolerable then the size and/or the embedment depth of the foundation should be increased and the analysis performed again. This methodology assumes that the deep foundation is free to rotate at the head. This geotechnical check may be used to determine the critical penetration depth. This is the depth at which the soil has sufficient strength to resist overturning of the foundation element.

### **16.8.2 Lateral Stability – Structural Check**

The structural check is used to determine the resistance of the foundation element to axial, flexure (bending) and shear for all appropriate limit states. It is anticipated that the lateral capacity structural checks will be conducted by the SEOR. As with LRFD, the resistances should be greater than the nominal loads. If the resistances aren't then redesign may be required.

### **16.8.3 Lateral Stability – Serviceability Check**

According to Brown, et al. (2018), "Deformation limits should be chosen based upon actual serviceability requirements for the structure rather than "rule of thumb" criteria." Therefore, acceptable deflections shall be determined by the design team, based on the anticipated Performance Objectives (Service and EE) of the structure. The serviceability check is conducted at the Service and EE limit state conditions and limits the deflections of the foundation element under Service and EE loads to an acceptable deflection. The deflections should be determined at the top of the column or bent cap, since deflections at this location typically exceed the deflections at the ground line. It will take the combined effort of both the SEOR and the GEOR to determine the deflections.

### **16.8.4 Lateral Resistance – Groups**

The design method presented in the preceding Sections is for a single pile or drilled shafts. Pile bents and drilled shaft frames are typical SCDOT practice and both bents and frames are considered to be groups. Group loadings used in the P-y method of analysis require reduction to account for the "shadowing effect" of adjacent piles or shafts. Therefore, P-multipliers shall be used and determined in accordance with AASHTO LRFD Specifications Section 10.7 – Driven Piles.

## **16.9 DOWNDRAG**

Downdrag loads (also known as Negative Skin Resistance) can be imposed on piles and shafts where:

- Sites are underlain by compressible material such as clays, silts, or organic soils,
- Fill will be or has recently been placed adjacent to the piles or shafts, such as is frequently the case for bridge approach fills,
- The groundwater is substantially lowered, or,
- Liquefaction of loose sandy soils can occur.

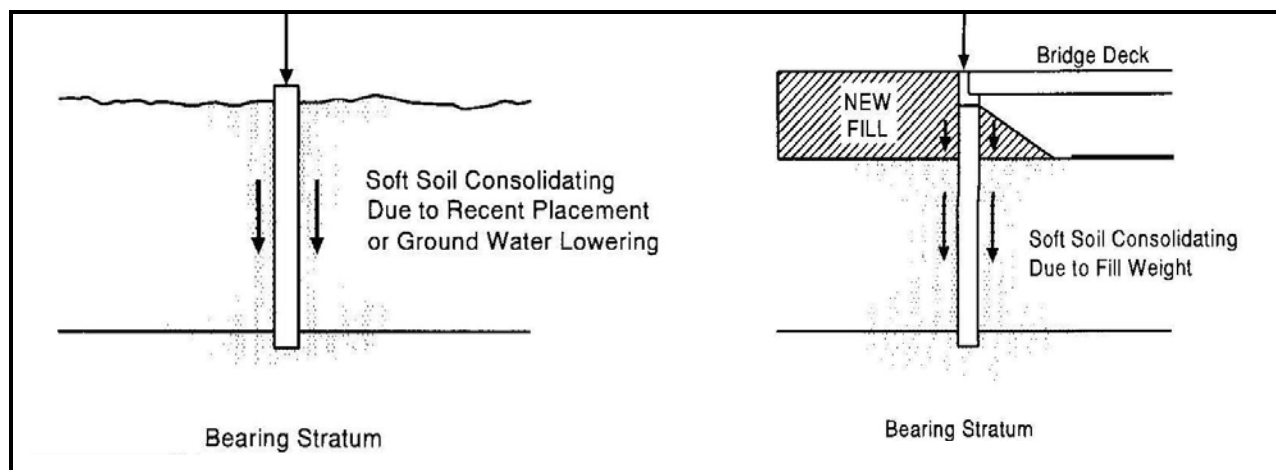


**Figure 16-6, Downdrag Scenarios due to Compressible Soils  
(Hannigan, et al. (2006))**

According to Briaud and Tucker (1997) if any of the following criteria are met, then downdrag on the deep foundation should be considered:

- Total settlement of ground surface ( $\Delta_v$ ) is more than 4 inches
- Settlement of ground surface after installation of foundation is more than 0.4 inches
- Embankment height exceeds 6-1/2 feet (assumed to be additional embankment height)
- Thickness of compressible layer is more than 10 feet
- The groundwater table will be permanently lowered more than 13 feet

Downdrag is typically caused by static movements (i.e., settlements) and is termed DD in the GDM. Further, downdrag may also be caused by seismic settlement resulting from SSL, specifically liquefaction of Sand-Like soils, and is termed  $DD_{SL}$  in the GDM. The AASHTO LRFD Specifications indicate that DD and  $DD_{SL}$  are not to be combined. According to the AASHTO LRFD Specifications static downdrag is considered to be a permanent load and therefore has a permanent load factor,  $\gamma_p$ , applied to the downdrag load. While this is appropriate for static DD, SCDOT has determined that  $DD_{SL}$  is more closely related to live loads than dead loads will therefore, apply a seismic load factor  $\gamma_{EQ}$  of 1.0 to  $DD_{SL}$ . It is noted that Chapter 8 indicates that  $\gamma_{EQ}$  is typically 0.0; however, SSL induced downdrag is the exception. Deep foundations that are anticipated having uplift loads and that experience downdrag shall use the minimum  $\gamma_p$  indicated in Chapter 8 for the static design method selected. There are 2 methods for determining downdrag that can be applied to both static and seismic conditions. The first method is the Traditional Approach and the second method is the Alternative Approach. Each approach is discussed in more detail in Hannigan, et al. (2006).

### 16.9.1 Traditional Approach

The Traditional Approach assumes that the deep foundation does not move relative to the soil column (i.e.,  $\Delta_v$  of the deep foundation is equal to or less than 0.4 inches). Therefore all settlement is used to develop drag loads on the deep foundation. The appropriate static method and  $\gamma_p$  corresponding to the individual soil layers are used to develop the downdrag. DD is added to both the Strength and Service limit state loads as indicated in the following equations:

$$R_{nST} = \frac{\sum_1^i \gamma_{pi} * Q_{STi}}{\phi_{dyn}} + \frac{\gamma_p * DD}{\phi_{dyn}} \quad \text{Equation 16-19}$$



$$R_{nSV} = \frac{\sum_1^i \gamma_{pi} * Q_{SVi}}{\phi_{dyn}} + \frac{\gamma_p * DD}{\phi_{dyn}} \quad \text{Equation 16-20}$$

Where,

- $R_{nST}$  = Nominal resistance at the Strength limit state
- $\gamma_{pi}$  = Permanent load factor for each force effect
- $Q_{STi}$  = Force effect at the Strength limit state
- $\gamma_p$  = Permanent load factor applied to downdrag load, DD
- DD = Downdrag load
- $\phi_{dyn}$  = Resistance factor based on the use of dynamic construction control
- $R_{nSV}$  = Nominal resistance of the Service limit state
- $Q_{SVi}$  = Force effect at the Service limit state

Typically  $R_{nST}$  and  $R_{nSV}$  are provided by the SEOR after the GEOR has provided the factored downdrag load ( $\gamma_p * DD$ ). It is noted that  $R_{nSV}$  is used to determine if the deep foundation settles.

Similarly to the statically induced DD loads,  $DD_{SL}$  is caused by settlement induced by liquefaction of Sand-Like soils. It is not anticipated that  $DD_{SL}$  will be caused by the loss of shear strength in Clay-Like soils. As with the DD, it is assumed that the deep foundation does not settle. For those soil layers that undergo SSL, residual shear strengths shall be used to determine  $DD_{SL}$  while for those soils not affected by SSL peak shear strength shall be used in the determination  $DD_{SL}$ . The nominal resistance for the EE I limit state is determined using the following equation.

$$R_{nEEI} = \frac{\sum_1^i \gamma_{pi} * Q_{EEIi}}{\phi_{EQ}} + \frac{\gamma_{EQ} * DD_{SL}}{\phi_{EQ}} \quad \text{Equation 16-21}$$

Where,

- $R_{nEEI}$  = Nominal resistance at the EE I limit state
- $\gamma_{pi}$  = Permanent load factor for each force effect
- $Q_{EEIi}$  = Force effect at the EE I limit state
- $\gamma_{EQ}$  = Seismic load factor applied to downdrag load,  $DD_{SL}$
- $DD_{SL}$  = Downdrag load induced by SSL
- $\phi_{EQ}$  = Seismic resistance factor

Typically the SEOR will provide the summation of  $\gamma_{pi}$  and  $Q_{EEIi}$  as the EE I load and the GEOR will add the factored  $DD_{SL}$  to determine the EE I limit state nominal resistance ( $R_{nEEI}$ ).

### 16.9.2 Alternative Approach

As indicated previously, Hannigan, et al. (2006) provides an Alternative Approach to developing downdrag loads on deep foundations. Briaud and Tucker (1997) presented the Alternative Approach in NCHRP Report 393 – Design and Construction Guidelines for Downdrag on Uncoated and Bitumen-Coated Piles. The basic concept is that since both the soil and deep foundation are moving in the same direction no downdrag loads are developed along the shaft of the deep foundation. This approach is also called the Neutral Point or Neutral Plane method, since a neutral plane is developed where the settlement of the deep foundation exceeds the settlement of the soil (see Figure 16-5). For a detailed procedure of how to use the Alternative Approach see Hannigan, et al. (2006). Please note that in order to use the Alternative

Approach, the deep foundation must settle into the subsurface soils. It is anticipated that piles with appreciable end bearing will not settle sufficiently; therefore, the Alternative Approach should only be used for friction piles. The amount of settlement required to develop tip resistance in drilled shafts may allow for the use of the Alternative Approach; however, the Service limit state check of the structure may not allow this approach.

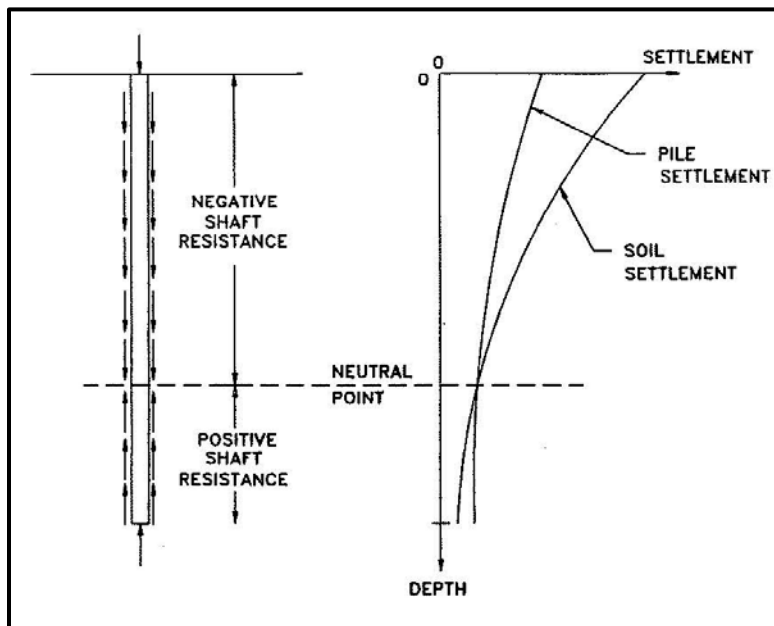


**Figure 16-7, Neutral Point Determination  
(Briaud and Tucker (1997))**

If during the EE I event SSL occurs in soil layers above the location of the Neutral Point before the EE I event, then SSL will have limited effect on the deep foundation. If SSL occurs in soil layers below the pre-EE I event Neutral Point, it will increase the axial compression load (i.e., downdrag will occur) in the deep foundation as well as result in additional deep foundation settlement.

Each of the downdrag loads discussed previously are used to determine the length of deep foundation required to resist the respective nominal load (i.e.,  $R_{nST}$ ,  $R_{nSV}$  or  $R_{nEQ}$ ).

### **16.9.3 Downdrag Mitigation**

The effect of DD and  $DD_{SL}$  can be mitigated through the use of embankment surcharge loads, ground improvement techniques, and/or vertical drainage and settlement monitoring measurements. In addition, either coatings or sleeves/jackets may be applied to the piles allowing the soil to slide adjacent to the piles.

## **16.10 FOUNDATION LENGTH**

The BGER is used to report the geotechnical resistances that should be used in the design of foundations for bridges and bridge related structures. For drilled shaft/pile bents and drilled shaft/pile group footings, the BGER provides estimated pile/shaft tip elevations, the minimum pile/shaft tip elevations required to maintain lateral stability (critical penetration), and the necessary soil parameters to develop a P-y soil model of the subsurface that is used in performing foundation lateral soil-structure interaction analyses. The estimated tip elevations shall be established using  $R_{nDR(ST)}$ ,  $R_{nDR(SV)}$  (not anticipated to control),  $R_{nDR(EEI)}$  or  $R_{nDR(EEII)}$ .

$R_{nDR(ST)}$  and  $R_{nDR(SV)}$  shall account for the effects of scour caused by the design flood, while  $R_{nDR(EEI)}$  shall account for any losses due to liquefaction of Sand-Like soils and  $R_{nDR(EEII)}$  shall account for the effects caused by the check flood or impact (vehicular or vessel) loadings. Soil layers that are anticipated to scour or undergo SSL shall not be included in the determination of resistance; however, these soils shall be included in the determination of nominal required driving resistance,  $R_{nDR}$  as indicated in the following equations:

$$R_{nDR(ST)} = \frac{\sum_1^i \gamma_{pi} * Q_{STi}}{\phi_{dyn}} + \frac{\gamma_p * DD}{\phi_{dyn}} + R_{designfldscr} + R_{DD} \quad \text{Equation 16-22}$$

$$R_{nDR(SV)} = \frac{\sum_1^i \gamma_{pi} * Q_{SVi}}{\phi_{dyn}} + \frac{\gamma_p * DD}{\phi_{dyn}} + R_{designfldscr} + R_{DD} \quad \text{Equation 16-23}$$

$$R_{nDR(EEI)} = \frac{\sum_1^i \gamma_{pi} * Q_{EEIi}}{\phi_{dyn}} + \frac{\gamma_{EQ} * DD_{SL}}{\phi_{dyn}} + R_{DD(SL)} \quad \text{Equation 16-24}$$

$$R_{nDR(EEII)} = \frac{\sum_1^i \gamma_{pi} * Q_{EEIIi}}{\phi_{dyn}} + R_{checkfldscr} \quad \text{Equation 16-25}$$

Where,

$R_{nDR(ST)}$	=	Required driving resistance at the Strength limit state
$R_{nDR(SV)}$	=	Required driving resistance of the Service limit state
$R_{nDR(EEI)}$	=	Required driving resistance at the EE I limit state
$R_{nDR(EEII)}$	=	Required driving resistance at the EE II limit state
$\gamma_{pi}$	=	Permanent load factor for each force effect
$\gamma_p$	=	Permanent load factor applied to downdrag load, DD
$\gamma_{EQ}$	=	Seismic load factor applied to downdrag load, DD <sub>SL</sub>
$Q_{STi}$	=	Force effect at the Strength limit state
$Q_{SVi}$	=	Force effect at the Service limit state
$Q_{EEIi}$	=	Force effect at the EE I limit state
$Q_{EEIIi}$	=	Force effect at the EE II limit state
DD	=	Downdrag load
DD <sub>SL</sub>	=	Downdrag load induced by SSL
$\phi_{dyn}$	=	Resistance factor based on the use of dynamic construction control
$R_{designfldscr}$	=	Unfactored soil resistance from soils scoured by the design flood
$R_{checkfldscr}$	=	Unfactored soil resistance from soils scoured by the check flood
$R_{DD}$	=	Unfactored soil resistance from soils that undergo static settlements
$R_{DD(SL)}$	=	Unfactored soil resistance from soils that undergo SSL induced settlement at the EE I limit state

As part of the design process the GEOR shall determine the anticipated minimum tip elevation required to achieve the required driving capacity (i.e.,  $R_{nDR(ST)}$ ,  $R_{nDR(SV)}$ ,  $R_{nDR(EEI)}$  or  $R_{nDR(EEII)}$ ). The report shall clearly indicate the governing conditions for development of the tip elevation using the words depicted in Table 16-6.

**Table 16-6, Governing Conditions**

Limit State	Loading Direction
Strength or Service	Axial (Compression or Tensile)
Extreme Event I or II	Lateral

Each governing condition shall consist of a loading type and a loading direction (i.e., Extreme Event I Lateral or Strength Axial). In addition to indicating which governing condition was used to develop the minimum tip elevation, the report shall also include a loading table that will provide the information depicted in Table 16-7, Pile Resistance or Table 16-8, Drilled Shaft Resistance.

**Table 16-7, Pile Resistance**

	Strength or Service Limit State <sup>1,2</sup>	EE I or EE II Limit State <sup>1,3</sup>
Factored Design Load	112 kips <sup>4</sup>	152 kips <sup>4</sup>
Geotechnical Resistance Factor <sup>5</sup>	0.40	1.00
Nominal Resistance	280 kips	152 kips
Resistance from:		
Design Flood Scourable Soils <sup>6</sup>	40 kips	NA
Soils undergoing static downdrag <sup>6</sup>	0 kips	
Resistance from Liquefiable Soils <sup>7</sup>	NA	220 kips
Required Driving Resistance	320 kips	372 kips

<sup>1</sup>Use only 1 column; middle column represents static resistance while last column represents Extreme Event resistance. Use the column that governs driving resistance.

<sup>2</sup>Indicate whether Strength or Service limit state controls resistance

<sup>3</sup>Indicate whether EE I or EE II limit state controls resistance

<sup>4</sup>Factored design loads include DD or DD<sub>SL</sub>. Note that in this example the Strength limit state DD = 0.0 kips

<sup>5</sup>Use appropriate construction control resistance factor

<sup>6</sup>Design flood scour and static downdrag are not included with Extreme Event limit state loading conditions

<sup>7</sup>Full resistance that is developed by soils within the liquefiable zone during pile installation

The  $R_{nDR}$  is used to determine the driving resistance (see Pile Driveability above) and acceptability of the driving equipment. Depending on the controlling condition, the piles will be driven to a higher capacity than required to achieve the Nominal Resistance and the Pile Driveability analysis shall account for this higher required resistance. Alternatively the driving resistance could be the Resistance required to achieve a minimum tip elevation. The minimum tip elevation is typically governed by the geotechnical lateral stability of the pile, but may also be the tip required to limit the amount of settlement of the pile. If settlement controls the minimum tip elevation, contact the design team to discuss the effects of the settlement. In addition, this may affect the pile driving equipment that a contractor selects.

**Table 16-8, Drilled Shaft Resistance**

	<b>Strength or Service Limit State<sup>1,2</sup></b>	<b>EE I or EE II Limit State<sup>1,3</sup></b>
Factored Design Load	1400 kips <sup>4</sup>	1400 kips <sup>4</sup>
Factored Resistance – Side	1130 kips	1130 kips
Factored Resistance – End	270 kips	270 kips
Geotechnical Resistance Factor – Side <sup>5</sup>	0.50	1.0
Geotechnical Resistance Factor – End <sup>5</sup>	0.50	1.0
Total Nominal Resistance	2800 kips	1400 kips

<sup>1</sup>Use only 1 column; middle column represents static resistance while last column represents Extreme Event resistance, use the column that governs resistance

<sup>2</sup>Indicate whether Strength or Service limit state controls resistance

<sup>3</sup>Indicate whether EE I or EE II limit state controls resistance

<sup>4</sup>Factored design loads include DD or DD<sub>SL</sub>. Note that in this example the Strength limit state DD = 0.0 kips

<sup>5</sup>Use appropriate construction control resistance factor for static and  $\phi_{EQ}$  equal to 1.0 for seismic

Please note that the weight of a drilled shaft is not subtracted from the nominal capacity, since the geotechnical resistance factors were obtained from static load tests. Therefore the resistance factors already account for the weight of the shaft in both compression and tension. However, depending on where the loads are applied, the weight of the column above the drilled shaft shall be added to the axial load. The column weight is added if the loads are applied at the top of the column, however, if the loads are applied at the top of the shaft, the column weight is not added. The factored column weight shall be determined by the SEOR and provided to the GEOR. In addition, the SEOR shall indicate where the loads are applied on the load data sheet.

If the Downdrag loads exceed the Nominal Resistance of the deep foundation, then additional length will be required. For driven piles this additional length shall be accounted for in the  $R_{nDR}$ . For drilled shafts the tip elevation shall be changed to reflect this increase and a Total Nominal Resistance shall be indicated on the plans.

## 16.11 REFERENCES

American Association of State Highway and Transportation Officials, (2017), AASHTO LRFD Bridge Design Specifications Customary U.S. Units, 8<sup>th</sup> Edition, American Association of State Highway and Transportation Officials, Washington, D.C.

Aurora, R. P., and Reese, L. C., (1976), Behavior of Axially Loaded Drilled Shafts in Clay-Shales, CFHR 3-5-72-176-4, Texas Department of Highways and Public Transportation, Austin, Texas.

Briaud, J.-L., and Tucker, L., (1997), “Design and Construction Guidelines for Downdrag on Uncoated and Bitumen-Coated Piles”, NCHRP Report 393, Transportation Research Board.

Brown, D. A., Turner, J. P., and Castelli, R. J., (2010), Drilled Shafts: Construction Procedures and LRFD Design Methods, (Publication No. FHWA NHI-10-016), National Highway Institute, U.S. Department of Transportation, Federal Highway Administration, Washington D.C.

Brown, D. A., Turner, J. P., Castelli, R. J., and Loehr, E. J., (90% DRAFT 2018), Drilled Shafts: Construction Procedures and LRFD Design Methods, (Publication No. FHWA NHI-18-XX), National Highway Institute, U.S. Department of Transportation, Federal Highway Administration, Washington D.C.

DeMarco, M., Bush, P., Samtani, N. C., Kulicki, J. M., and Severns, K., (2015), Draft - Incorporation of Foundation Deformations in AASHTO LRFD Bridge Design Process, 2<sup>nd</sup> Strategic Highway Research Program (SHRP2), Transportation Research Board, The National Academies of Sciences, Engineering, and Medicine, Washington, D.C.

Department of Defense, Department of the Navy, Naval Facilities Engineering Command, (1986), Foundations & Earth Structures – Design Manual 7.2, (Publication No. NAVFAC DM-7.02), Alexandria, Virginia.

Hannigan, P. J., Goble, G. G., Likins, G. E., and Rausche, F., (2006), Design and Construction of Driven Pile Foundations – Reference Manual - Volume I and II, (FHWA Publication Nos. FHWA-NHI-05-042 and FHWA-NHI-05-043). U.S. Department of Transportation, National Highway Institute, Federal Highway Administration, Washington D.C.

Kyfor, Z. G., Schnore, A. R., Carlo, T. A. and Bailey, P. F., (1992), Static Testing of Deep Foundations, (Publication No. FHWA-SA-091-042), U.S. Department of Transportation, Office of Technology Applications, Federal Highway Administration, Washington D.C.

Reese, L. C., (1984), *Handbook on Design of Piles and Drilled Shafts Under Lateral Loads*, (FHWA Publication No. FHWA-IP-84-11). U.S. Department of Transportation, Federal Highway Administration, Washington D.C.

Rollins, K. M., Clayton, R. J., Mikesell, R. C., and Bradford, B. C., (2005), “Drilled Shaft Side Friction in Gravelly Soils.” *Journal of Geotechnical and Geoenvironmental Engineering*, ASCE, Volume 131, Issue 8, pp. 987-1003.

South Carolina Department of Transportation, (2006), Bridge Design Manual, South Carolina Department of Transportation, <https://www.scdot.org/business/structural-design.aspx>.

# **Chapter 17**

## **EMBANKMENTS**

**GEOTECHNICAL DESIGN MANUAL**

*January 2019*





**Table of Contents**

<b><u>Section</u></b>	<b><u>Page</u></b>
17.1 Introduction.....	17-1
17.2 LRFD Slope Stability.....	17-2
17.3 Failure Mechanisms.....	17-3
17.3.1 Creep.....	17-3
17.3.2 Slide.....	17-4
17.3.3 Flow.....	17-6
17.3.4 Spread.....	17-7
17.3.5 Fall and Topple.....	17-8
17.4 Loading Conditions.....	17-9
17.4.1 End-of-Construction Condition.....	17-11
17.4.2 Long-term Condition.....	17-11
17.4.3 Seismic Event Condition.....	17-11
17.4.4 Vertically Staged Construction Condition.....	17-12
17.4.5 Rapid Drawdown Condition.....	17-12
17.4.6 Surcharge Loading Condition.....	17-12
17.4.7 Partial Submergence Condition.....	17-12
17.5 Slope Stability Analysis.....	17-12
17.5.1 Ordinary Method of Slices.....	17-13
17.5.2 Simplified Bishop.....	17-14
17.5.3 Force Equilibrium.....	17-14
17.5.4 Spencer's Method.....	17-14
17.5.5 Morgenstern and Price Method.....	17-14
17.6 Settlement – General.....	17-14
17.7 Change In Stress.....	17-15
17.7.1 Shallow Foundations.....	17-15
17.7.2 Embankments.....	17-19
17.7.3 Buried Structures.....	17-25
17.8 Immediate Settlement.....	17-25
17.8.1 Cohesionless Soils.....	17-25
17.8.2 Cohesive Soils.....	17-32
17.9 Primary Consolidation Settlement.....	17-33
17.9.1 Amount of Settlement.....	17-34
17.9.2 Time for Settlement.....	17-35
17.10 Secondary Compression Settlement.....	17-37
17.11 Settlement in Rock.....	17-38
17.12 Lateral Squeeze.....	17-41
17.13 Embankment Design.....	17-43
17.13.1 Unreinforced Embankments.....	17-45
17.13.2 Reinforced Embankments.....	17-47
17.13.3 Reinforced Soil Slopes.....	17-55
17.13.4 Vertical Stage Construction.....	17-57
17.14 Plans.....	17-59
17.15 References.....	17-59

**List of Tables**

<b><u>Table</u></b>	<b><u>Page</u></b>
Table 17-1, No External Slope Stability Analysis <sup>1</sup> .....	17-1
Table 17-2, Width Correction Factor, $C_B$ .....	17-28
Table 17-3, Time Rate Factors.....	17-28
Table 17-4, Correlation Factor, $F_s$ .....	17-31
Table 17-5, Vertical Strain Influence Factor Equations .....	17-31
Table 17-6, Footing Shape and Rigidity Factors.....	17-32
Table 17-7, Primary Consolidation Settlement Steps.....	17-34
Table 17-8, Primary Consolidation Settlement Equations.....	17-35
Table 17-9, Secondary Compression Settlement Equations.....	17-37
Table 17-10, Rock Settlements on various Geological Conditions.....	17-39
Table 17-11, Shape Factors, $C_d$ .....	17-40
Table 17-12, Shape Factors, $C'_d$ .....	17-41
Table 17-13, Elastic Distortion Settlement Correction Factor, $\alpha$ .....	17-41
Table 17-14, RSS Design Steps.....	17-56

**List of Figures**

<b><u>Figure</u></b>	<b><u>Page</u></b>
Figure 17-1, Signs of Creep .....	17-4
Figure 17-2, Translational Slide.....	17-4
Figure 17-3, Rotational Slide .....	17-5
Figure 17-4, Compound Slide.....	17-6
Figure 17-5, Flow Failures.....	17-7
Figure 17-6, Spread Failure.....	17-8
Figure 17-7, Fall Failure .....	17-8
Figure 17-8, Topple Failure .....	17-9
Figure 17-9, Stress Isobars .....	17-16
Figure 17-10, Influence Factor Chart.....	17-18
Figure 17-11, Principle of Superposition.....	17-19
Figure 17-12, Influence Factor Chart – Infinitely Long Embankments.....	17-20
Figure 17-13, Influence Chart Beneath Crest of Slope .....	17-21
Figure 17-14, Influence Chart Beneath Toe of Slope.....	17-22
Figure 17-15, Pressure Coefficients Beneath the End of a Fill.....	17-24
Figure 17-16, Bearing Capacity Index Chart.....	17-26
Figure 17-17, Vertical Strain Influence Factor Chart.....	17-30
Figure 17-18, Janbu Influence Factor Chart .....	17-33
Figure 17-19, Secondary Compression .....	17-37
Figure 17-20, Schematic of Lateral Squeeze.....	17-42
Figure 17-21, Lateral Squeeze Model .....	17-42
Figure 17-22, ERS vs Slope Diagram.....	17-44
Figure 17-23, Construction-Point Concept.....	17-45
Figure 17-24, Reinforced Embankment Failure Modes.....	17-48
Figure 17-25, Reinforced Embankment Applications .....	17-49
Figure 17-26, Rotational Failure Model.....	17-50
Figure 17-27, Sliding Failure – Rupture of Reinforcement .....	17-50
Figure 17-28, Sliding Failure of Embankment over Reinforcement .....	17-51
Figure 17-29, Reinforced Embankment Construction Sequence over Soft Ground ..	17-52
Figure 17-30, Fill Placement over Soft Ground.....	17-53
Figure 17-31, Fill Placement over Firm Ground.....	17-54
Figure 17-32, Geosynthetic Reinforcement Placement for Widened Embankments .	17-55
Figure 17-33, Reinforced Soil Slope .....	17-56
Figure 17-34, Reinforced Soil Slope Failure Modes .....	17-57
Figure 17-35, Staged Construction Schematic .....	17-58



# CHAPTER 17

## EMBANKMENTS

### 17.1 INTRODUCTION

This Chapter provides general guidance in stability and settlement design and analysis of embankments. Embankments typically consist of unreinforced soil slopes, reinforced embankments and Reinforced Soil Slopes (RSSs) and may also include ERSs (see Chapter 18) constructed within the SCDOT ROW or belonging to SCDOT. This Chapter is concerned with the external stability of embankments and ERSs. The internal stability of ERSs, depending on the type, is the responsibility of the SEOR. The settlement of earthen embankments, ERSs, and foundations (shallow and deep) is also discussed in this Chapter. The amount of settlement is for the Service limit state. Settlements induced by the EE I limit state are discussed in Chapter 13 and are applicable only to bridge embankments and ERSs. Neither stability nor settlement need to be checked for roadway embankments including RSSs and reinforced embankments at the EE I limit state. The amount of total and differential settlement shall be determined. All settlements shall be determined for a 20-year period, unless specifically directed by the PC/GDS to use another time period. However, the design life of all embankments is 100 years. The 20-year period is used to coincide with the anticipated pavement replacement/rehabilitation cycle.

Stability and settlement should be determined on the critical section. The selection of the critical section or sections is left to the GEOR. The following are suggested guidelines for use in this selection process:

1. Highest slope or ERS
2. Steepest slope
3. Soft underlying soils
4. Slope or ERS critical to performance of a structure (i.e., bridge, culvert, etc.)

There are 2 applications of embankments used by SCDOT: bridge and roadway (defined in Chapter 2). All embankments regardless of type of embankment (i.e., unreinforced slope, RSS, etc.) shall have slope stability and settlement checked at the appropriate limit state. However, embankments meeting the criteria presented in Table 17-1 are not required to have external slope stability analyses. All ERSs shall have slope stability and settlement checked for all limit states (see Chapter 8).

**Table 17-1, No External Slope Stability Analysis**

Embankment Slope	Total Embankment/Slope Height <sup>1</sup>
2H:1V	≤ 10 ft
3H:1V or flatter	≤ 15 ft

<sup>1</sup>Includes the design scour depth

The exception to the No External Slope Stability Analysis concept is if in the opinion of the GEOR that the analysis is required. In addition, a stability analysis for slopes flatter than 3H:1V may be performed if in the opinion of the GEOR it is required. Additionally, if structural reinforcement is required to limit settlement then an analysis will be required. If reinforcement is placed within the embankment as an aide to construction (see Chapter 19) then the No External Analysis concept may be used provided the criteria provided in Table 17-1 is met.

Embankments can be divided into 2 main categories: natural and man-made. Natural embankments are those slopes formed by natural processes and are composed of natural

materials. Natural embankments may include river banks to the valleys passing through or parallel to mountain ridges. Man-made embankments are those slopes and ERSs that are constructed by man. Man-made embankments may be subdivided into 2 types of embankments: fill (bottom up construction) and cut (top down construction). Fill slopes, including ERSs, are constructed by placing soil materials to elevate the grade above the natural or existing grade. Fill slopes may be unreinforced or reinforced. Cut slopes, including ERSs, are constructed by excavating material from either a natural or man-made fill slopes in order to reduce the grade. The stability and settlement procedures discussed in this Chapter exclusively apply to slopes constructed of soil and founded on either soil or rock materials. For the design of slopes in rock see FHWA-HI-99-007 – *Rock Slopes* (Munfakh, Wylie, and Mah (1998)) for design procedures.

## 17.2 LRFD SLOPE STABILITY

FHWA/AASHTO has recommended that the stability of an embankment be determined using the Service limit state instead of the Strength limit state. The use of Service instead of Strength limit state accounts for 2 design issues; the first is that current slope stability analysis software does not allow for the input of load and resistance factors. Second is that most of the strength parameters, required in stability analysis, are derived from correlations (see Chapter 7). Further, the research is incomplete for the determination of resistance factors, since relatively few embankment or ERS failures occur, where the strength of the soil can be accurately determined and applied across a broad spectrum of soils. Therefore, the basic ASD calculation methods will continue to be used. After completion of the analysis using ASD, the calculated Safety Factor (SF) is inversed to convert from ASD to LRFD.

$$\mathbf{Driving\ Forces\ (\sum q_i) \leq Resistance\ Forces\ (\sum r_i)} \quad \mathbf{Equation\ 17-1}$$

In other words:

$$\mathbf{SF = \frac{\sum r_i}{\sum q_i}} \quad \mathbf{Equation\ 17-2}$$

As indicated in Chapter 8, the basic LRFD equation is

$$\mathbf{Q = \sum \eta_i \gamma_i Q_i \leq \phi R_n = R_r} \quad \mathbf{Equation\ 17-3}$$

Where,

Q = Factored Load

Q<sub>i</sub> = Force Effect

η<sub>i</sub> = Load modifier

γ<sub>i</sub> = Load factor

R<sub>r</sub> = Factored Resistance (i.e., allowable capacity)

R<sub>n</sub> = Nominal Resistance (i.e., ultimate capacity)

φ = Resistance Factor

In using the Service limit state versus the Strength limit state, the stability analysis reverts to the typical way of performing stability analysis since the various Service limit states (I, II, III, and IV) all use a load factor (γ<sub>i</sub>) of 1.0. Therefore, Equation 17-3 can be rewritten:

$$\mathbf{Q = \sum Q \leq \phi \sum R_n} \quad \mathbf{Equation\ 17-4}$$

Rearranging Equation 17-4:

$$\frac{1}{\varphi} = \frac{R_n}{Q} = \frac{\sum r_i}{\sum q_i} \quad \text{Equation 17-5}$$

Equating Equation 17-2 with Equation 17-5 produces

$$SF = \frac{\sum r_i}{\sum q_i} = \frac{1}{\varphi} \quad \text{Equation 17-6}$$

Equation 17-6 may be rearranged and written as,

$$\varphi = \frac{1}{SF} \quad \text{Equation 17-7}$$

Therefore, to obtain the required  $\varphi$  from typical slope stability software packages, the SF obtained is simply inverted. The lower the resistance factor the higher the Safety Factor.

### 17.3 FAILURE MECHANISMS

There are several failure mechanisms that affect embankments. The mechanisms of failure may dictate the required analysis method to be used to determine stability or instability. Further, the types of soil that the embankment is comprised of will also affect the failure mechanism. The different failure mechanisms are listed below:

- |                    |                               |
|--------------------|-------------------------------|
| 1. Creep           | 4. Slide                      |
| 2. Flow            | 5. Spread                     |
| 3. Fall and Topple | 6. Deformation and settlement |

#### 17.3.1 Creep

Creep is the very slow movement of slopes, either natural or man-made, toward the toe and a more stable configuration. This movement can range up to approximately 1 inch per year. Slopes that creep can remain stable for extended periods of time. However, once the limit of the soil shear strength has been reached, the amount of movement may increase and the time for movement may decrease resulting in a rapid or sudden failure of the slope. Creep movements can be divided into 2 general types: seasonal and massive. Seasonal creep is the creep that occurs during successive seasons, such as freezing and thawing, or wetting and drying. The amount of seasonal creep can vary from year to year, but is always present. Seasonal creep extends to the depth limit of seasonal variations of moisture and temperature. Massive creep causes almost constant movement within the slope and is not affected by seasonal variations. Massive creep typically occurs in clay-rich soils. While the actual mechanism of massive creep is not fully understood, this type of creep can be attributed to exceeding some threshold shear strength that is below peak shear strength. This threshold shear strength may be a very small portion of the peak shear strength. If the stresses in the slope remain below the threshold level, then movement will not occur; however, if the stresses exceed the threshold, then movements will occur. If enough stresses accumulate to exceed the peak shear strength, then a more rapid failure is possible. In general, once creep has started it is difficult or impossible to stop. However, the rate of creep may be reduced by placement of drainage. During the Geoscopying of the project site, the trees should be observed for any convex curvature with the convex part pointing down slope (see Figure 17-1).

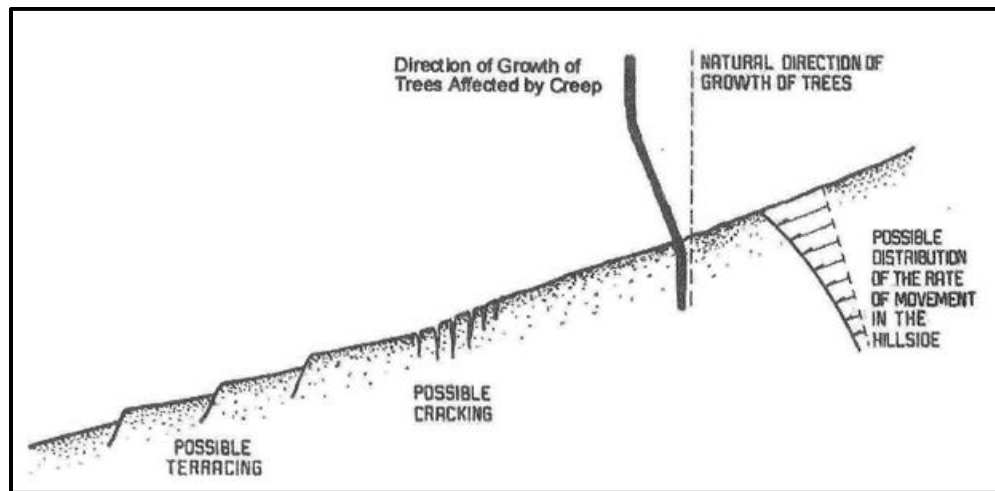


**Figure 17-1, Signs of Creep**  
(Collin, Leshchinsky, and Hung (2005))

### 17.3.2 Slide

Slides are downward slope movements that occur along definite slip or sliding surfaces. Slides may be translational, rotational, or a composite of rotation and translation. Translational slides are typically shallow and linear in nature. Translational slides typically occur along thin weak layers or along the boundary between a firm overlying layer and weaker underlying layer (see Figure 17-2).

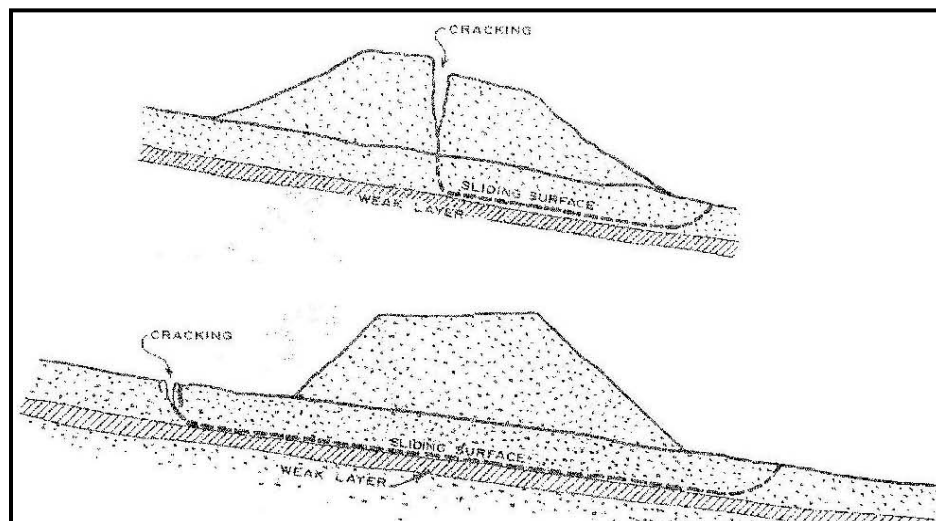


**Figure 17-2, Translational Slide**  
(Collin, Leshchinsky, and Hung (2005))

Rotational slides are slides that form an arc along the shearing surface. This is the most common type of failure analyzed. In soft, relatively homogenous Clay-Like materials, the rotational slide forms a deep seated arc, while in Sand-Like materials the rotational slide failure surface tends to be relatively shallow. Examples of different types of rotational slides are depicted in Figure 17-3.



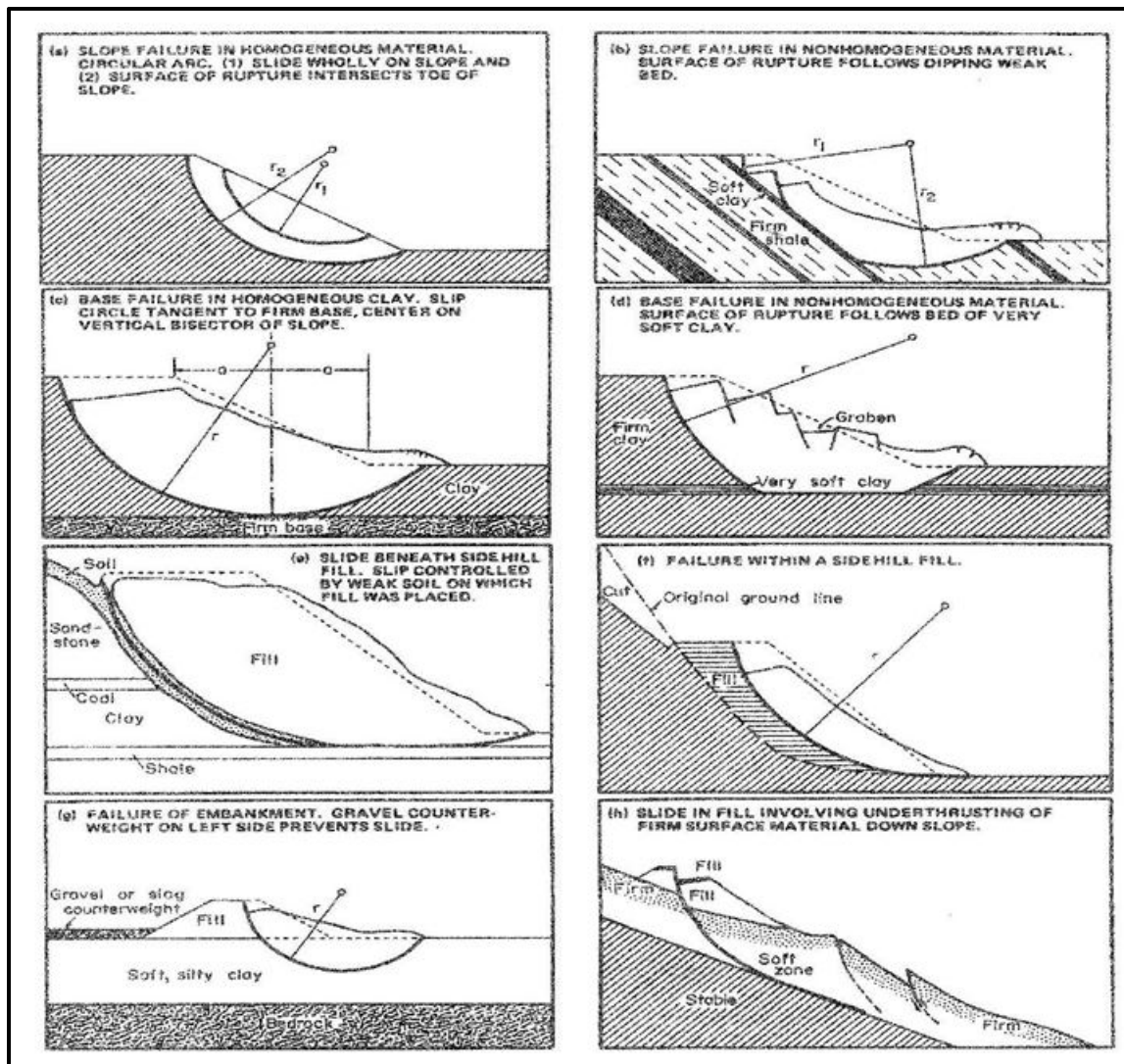


**Figure 17-3, Rotational Slide  
(Collin, Leshchinsky, and Hung (2005))**

Compound slides are a composite of translational and rotational slides. This type of slide tends to have a complex structure and can be difficult to analyze. Compound slides can have 2 general forms: retrogressive and progressive. Retrogressive compound slides continue to cut into the existing slope. After initial failure, the new slope that is formed is unstable and fails, developing another new unstable slope face that fails. This slide type may result in a series of slides that tend to converge on 1 extended slope. Progressive slides occur when an existing slope surface is loaded with either new fill or debris from a slope failure, resulting in failure of the slope toward the toe. Compound slide types are depicted in Figure 17-4.

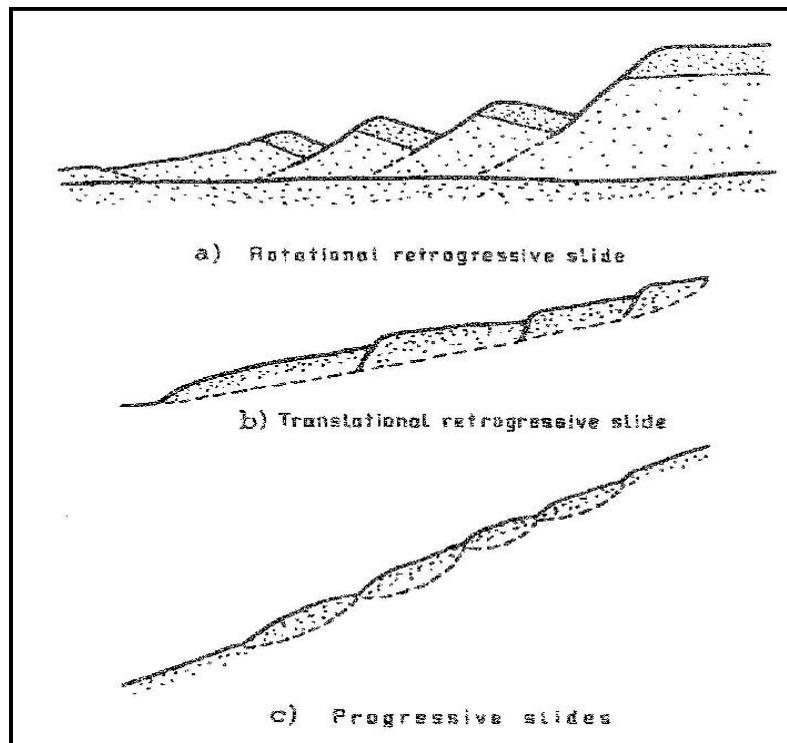


**Figure 17-4, Compound Slide**  
(Collin, Leshchinsky, and Hung (2005))

### 17.3.3 Flow

Flow failures can occur in both dry, as well as wet soils, depending on the materials and the relative density. Flows are defined as mass soil movements that have greater internal deformations than slides. In a slide, the soil block will maintain some definition during sliding, whereas in flows, the definition of the block is completely lost. Flow failures, depending on the moisture condition of the soil, may behave similar to a fluid. In dry flow failures of fine-grained Sand-Like soils, the movements are caused by a combination of sliding and individual particle movements. These types of failures may be caused by soils being cut on steep slopes that are stable when first constructed, but become unstable with time. Dry flow failures are also termed earthflows. Moist flows occur in soils that have higher moisture contents than the soils in a dry flow. In Clay-Like soils, moist flows occur when the moisture content exceeds the liquid limit of the material. In Sand-Like soils, moist flows may occur when water becomes trapped in the soils by an impermeable barrier. Liquefaction is a form of moist flow that is caused by high moisture content and a seismic shock (see Chapter 13). Wet flows are also termed mudflows. See Figure 17-5 for dry and moist flow failure examples.

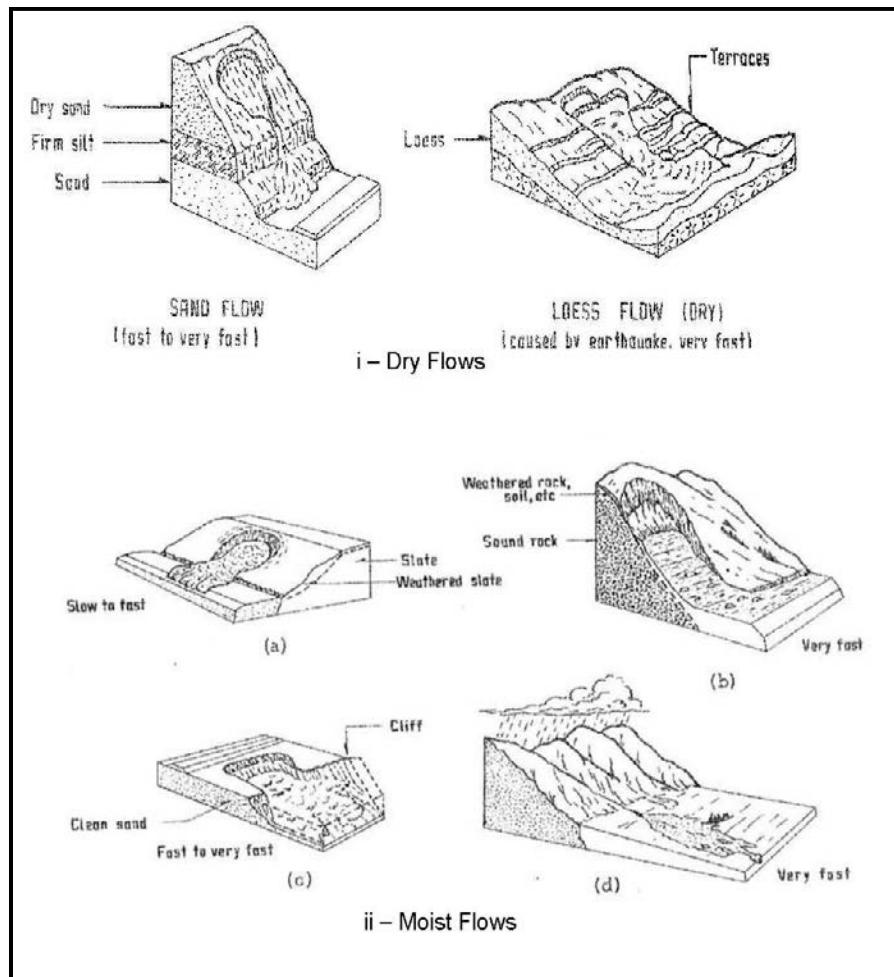


**Figure 17-5, Flow Failures  
(Collin, Leshchinsky, and Hung (2005))**

**17.3.4 Spread**

Spread was originally defined by Terzaghi and Peck in 1948 to describe sudden movements of water bearing seams of Sand-Like materials overlain by homogeneous Clay-Like soils or fills. Spreads occur on very gentle slopes (< 5 percent) or flat terrain. Spreads can occur in Sand-Like soils (liquefaction) or in Clay-Like soils (quick clays) that are externally loaded. In the case of liquefaction, the load is the seismic shock, and in quick clays, that load may be applied by the placement of fill materials. Figure 17-6 illustrates a typical soil spread.

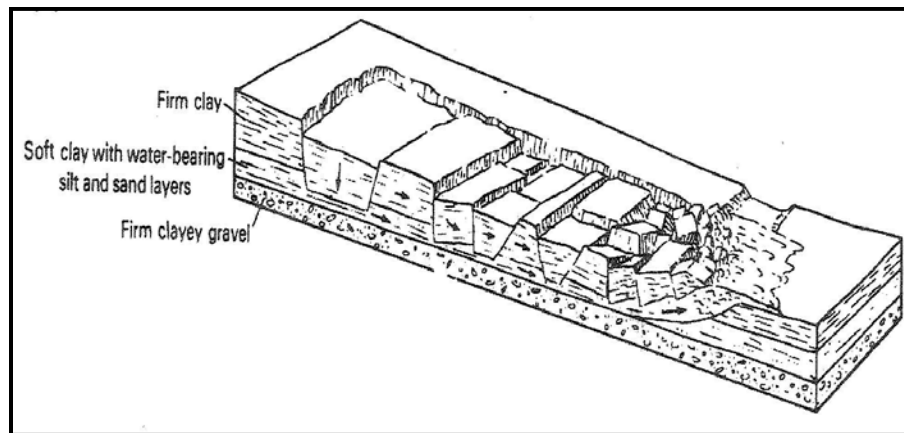


**Figure 17-6, Spread Failure  
(Collin, Leshchinsky, and Hung (2005))**

### 17.3.5 Fall and Topple

Fall and topple failures typically occur on rock slopes, although, topples can occur in steeply cut or constructed soil slopes. Falls are sudden movements of rocks and boulders that have become detached from steep slopes or cliffs (see Figure 17-7). Cracks can form at the top of the steep slope that may fill with water that will exert pressure on the rock mass causing it to fall. The water may freeze during colder weather exerting pressure on the rock mass as well. A topple is the forward rotation of rock or soil mass around a pivot point in the mass (see Figure 17-8). The steepness of the slope affects the formation of the topple, the slope can be constructed too steep or can be eroded to a steep configuration.

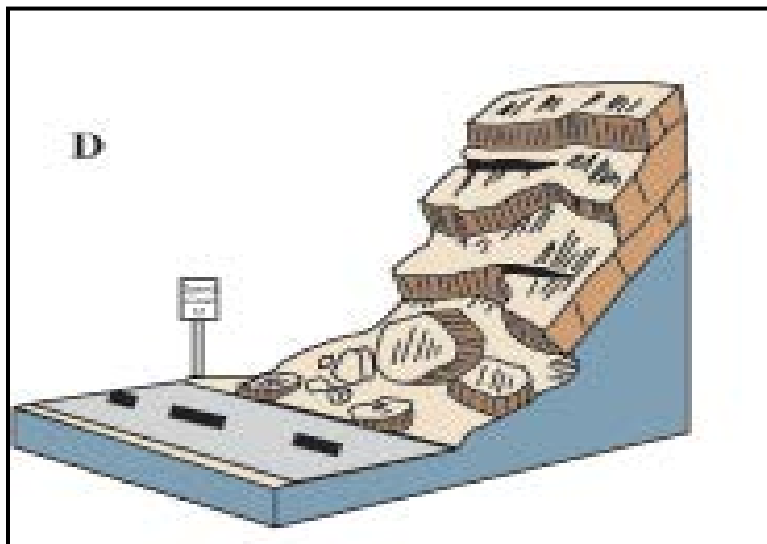


**Figure 17-7, Fall Failure  
(USGS (2004))**

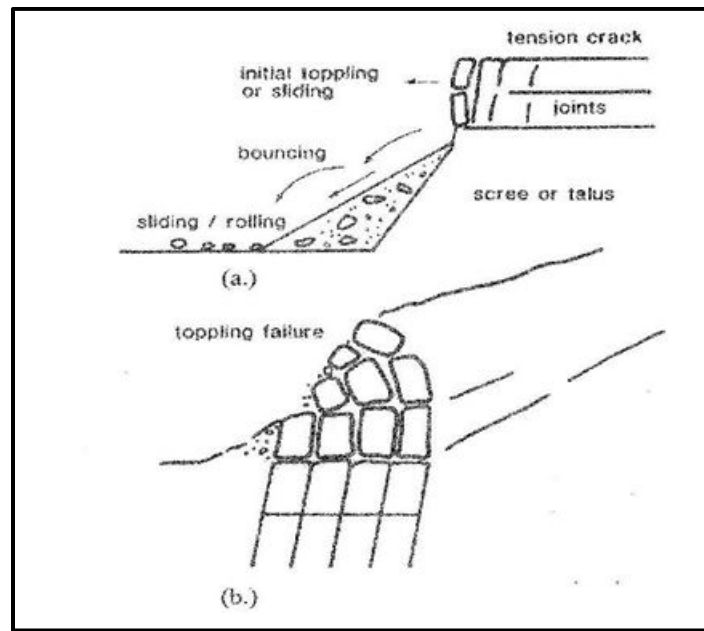


**Figure 17-8, Topples Failure**  
(Collin, Leshchinsky, and Hung (2005))

## 17.4 LOADING CONDITIONS

The stability of embankments is based on the height of the slope or ERS (i.e., the load) and the resistance of the subsurface soils (i.e., shear strength) to that loading. Increasing the height and steepness of the embankment increases the potential for instability. It is incumbent upon the GEOR to know and understand the loading conditions for which the stability analysis is being performed to evaluate. All of these loading conditions apply to both natural and man-made fill and cut embankments, but each condition does not have to be analyzed in every case. These loading conditions are listed below:

1. End-of-Construction (Short-term)
2. Long-term
3. Seismic (EE I)
4. Vertically Staged Construction
5. Rapid Drawdown
6. Surcharge Loading
7. Partial Submergence

Each of these loading conditions requires the selection of the appropriate soil strength parameters. Chapter 7 provides a more detailed discussion on the selection of drained and undrained soil shear strength parameters and the differences in total and effective stress. Once the rate of loading (i.e., loading condition) is determined, the soil response should be determined (i.e., drained or undrained). The drained response of soil is determined by loading the soil slowly enough to allow for the dissipation of pore pressures ( $\Delta u = 0$ ). Conversely, the undrained response of a soil is determined by loading the soil faster than the pore pressures can dissipate ( $\Delta u \neq 0$ ). This change in pore pressure can be either positive or negative depending on whether the soil compresses ( $\Delta u > 0$ ) or dilates ( $\Delta u < 0$ ). After determining the soil response (either drained or undrained), the type of analysis is selected based on the dissipation of pore pressures and the rate of loading. If the pore pressure increases with the application of load, i.e., during fast loading on a fine-grained soil, then a total stress analysis is

conducted. If the loading does not produce a change in pore pressure, i.e., during slow loading of a fine-grained soil or the loading is placed on coarse-grained material, then an effective stress analysis is conducted.

According to Duncan, Wright and Brandon (2014), “Whether slope stability analyses are performed for drained conditions or undrained conditions, the most basic requirement is that equilibrium must be satisfied in terms of total stress.” In other words, all forces, including water that act on the embankment, need to be accounted for in the stability analysis. The development of these forces allows for the determination of the total normal stress acting on the shear surface and the shear strength required to maintain equilibrium. Normal stresses are required to develop the soil shear strength ( $\phi > 0^\circ$ ). The shear strength of cohesive, fine-grained ( $\phi = 0^\circ$ ) is independent of the normal stress acting on the shear surface.

To develop effective stress shear strength parameters, the pore pressures along the shear surface need to be known and need to be subtracted from the total shear strength. For drained conditions, the pore pressures can be estimated using either hydrostatic or steady seepage boundary conditions. However, for undrained conditions, the pore pressures are a function of the response of the soil to shearing, therefore, the evaluation of the pore pressures is difficult. The development of total stress shear strength parameters does not require determination of pore pressures. Total stress analyses therefore can only be applied to undrained conditions. In total stress analyses, the pore pressures are determined as a function of the behavior of the soil during shear.

In drained soil response, the load is applied slow enough to allow for the dissipation of excess pore pressures ( $\Delta u = 0$ ). An effective stress analysis is performed using:

- Total unit weights
- Effective stress shear strength parameters
- Pore pressures determined from hydrostatic water levels or steady seepage analysis

Total unit weights are required in drained soil response. Since the majority of the analytical software packages account for the location of the groundwater table, it is incumbent on the GEOR to know the requirements of the analytical software package and provide the correct input parameters.

In undrained soil response, the load is applied rapidly and excess pore pressures ( $\Delta u > 0$ ) are allowed to build up. The pore pressures are controlled by the response of the soil to the application of the external load. A total stress analysis is performed using:

- Total unit weights
- Total stress shear strength parameters

The previous discussion dealt with the selection of total or effective stress strength parameters; however, these strength parameters are for peak shear strength. The use of peak shear strengths is appropriate for fill type slopes. However, the use of peak shear strength parameters in cut slopes should be considered questionable. Therefore, the use of residual shear strength shall be used in the design of cut slopes. Residual shear strength should be either determined from laboratory testing or using the procedures outlined in Chapter 7. The location of the water surface in cut slopes should be accounted for during design. The use of steady state seepage may be required, particularly, if the slopes intercepts the water table well above the toe of the slope. In addition, surface drainage features may be required to control the flow of groundwater as it exits the slope.

### **17.4.1 End-of-Construction Condition**

The End-of-Construction condition also termed Short-term can have either drained or undrained soil response depending on the time for excess pore pressure ( $\Delta u \neq 0$ ) dissipation. The time for excess pore pressure dissipation shall be determined using the method described in Chapter 7 or from consolidation testing of the embankment materials. If the time for pore pressure dissipation is determined to be days or weeks (typically Sand-Like soils), then drained soil response should be used. Conversely, if the time for pore pressure dissipation is months to years (typically, Clay-Like soils), then undrained soil response should be used. Engineering judgment should be used for the soils that have a time for pore pressure dissipation of weeks to months. The selection on the use of drained or undrained soil response should be based on the time for the completion of construction. In addition, the slope being analyzed may consist of materials that have both drained and undrained soil responses (i.e., the slope contains Sand-Like and Clay-Like materials). The soil response of each layer should be determined based on the time for dissipation of pore pressures in each layer.

For the End-of-Construction loading condition (Service limit state) for embankments, the weight of the pavement and live load surcharges shall be applied. However the thickness of the pavement, and therefore the weight of the pavement, is ignored during this analysis (i.e., soil unit weights are used to finish grade). In addition, it is typical to assume that the live load is 250 pounds per square foot (psf). The loads should be determined as specified in Chapter 8. The load factor ( $\gamma_i$ ) shall be taken as 1.0.

### **17.4.2 Long-term Condition**

The Long-term condition should use a drained soil response model. The use of the drained soil response is based on the assumption that excess pore pressures have dissipated ( $\Delta u = 0$ ). The time for dissipation of pore pressures should be determined, if the GEOR suspects that not enough time has passed to allow for the dissipation. The appropriate soil response should be selected (i.e., drained if  $\Delta u = 0$  or undrained if  $\Delta u \neq 0$ ).

During Long-term analysis, the live load surcharge (see Chapter 8) and the dead load induced by the existing pavement section and any asphalt overlays (see Chapter 8 for asphalt unit weight) should be included. The thickness of the overlay shall be based on a 20-year repaving cycle (i.e., 4 repaving cycles in an embankment life of 100 years). The total thickness of the asphalt overlay shall be a minimum of 8 inches (i.e., 2 inches of overlay for each repaving cycle). Similarly to the End-of-Construction loading condition, it is typical to assume that the live load is 250 psf. The load factor ( $\gamma_i$ ) shall be 1.0.

### **17.4.3 Seismic (EE I) Event Condition**

According to Duncan, Wright and Brandon (2014), the stability of embankments is affected by earthquakes in 2 ways; first the earthquake subjects the soils to cyclically varying loads and secondly, cyclic strains induced by these loads may lead to a reduction in the shear strength of the soil. The soil response during cyclic loading is undrained (i.e.,  $\Delta u \neq 0$ ), since the load is applied rapidly and excess pore pressures do not have time to dissipate. In soils where the shear strength reduction is less than 15 percent, a pseudo-static analysis is normally conducted. If the soil shear strength is reduced more than 15 percent, then a dynamic analysis should be performed. However, due to the complexity of performing dynamic analysis, the pseudo-static analysis may be performed for soils with shear strength reductions greater than 15 percent. If a dynamic analysis is warranted by the GEOR, contact the PC/GDS to explain the reasoning for a dynamic analysis and how the dynamic analysis will be performed. See Chapter 7 for aid in

determining the reduced shear strengths that should be used. The seismic event condition is discussed in greater detail in Chapter 13.

In the EE I limit state check stability analysis, include the dead load induced by the addition of asphalt to the pavement section, but do not include the live load surcharges.

#### **17.4.4 Vertically Staged Construction Condition**

If very soft to soft soils are located within the subgrade beneath an embankment, vertical stage construction may be required. Vertical stage construction consists of placement of a portion of the total embankment height and allowing settlement to occur. It is during the process of settlement that soil shear strength increases. A more detailed design procedure is provided in later Sections.

#### **17.4.5 Rapid Drawdown Condition**

The Rapid Drawdown Condition occurs when an embankment (i.e., a dam) that is used to retain water experiences a rapid (sudden) lowering of the water level and the internal pore pressures in the embankment cannot reduce fast enough creating unbalanced forces along the outer face of the embankment. These unbalanced forces may lead to slope instability because the internal pore pressures are “pushing” on the outer surface of the embankment. For SCDOT projects, this is not a normal condition since SCDOT embankments are typically not designed to retain water. However, in some situations water may build up against an embankment. Where this occurs Rapid Drawdown should be considered. For procedures on how to conduct rapid drawdown analysis, see Duncan, Wright and Brandon (2014).

#### **17.4.6 Surcharge Loading Condition**

Surcharge loads can be either temporary or permanent. Temporary surcharge loads can include construction equipment or additional fill materials placed on an embankment to increase the rate of settlement. Temporary soil surcharges are typically used in conjunction with staged constructed embankments. Therefore, the effects of the surcharge will need to be accounted for in staged construction. Typically, for temporary surcharges like equipment, the undrained shear strength of the soil should be used. Permanent surcharges consist of asphalt overlays and live load surcharges caused by traffic, the use of these surcharges has been discussed previously.

#### **17.4.7 Partial Submergence Condition**

The partial submergence condition occurs when an embankment experiences the flood stage of a river or stream. When these conditions occur, water can penetrate the embankment and affect the shear strength of the soil. The amount of water that actually penetrates the embankment is a function of the permeability of the material used in the construction of the embankment. The permeability of the embankment material or retained backfill can be estimated as indicated in Chapter 7. Further, the duration of the flood event will also determine the effect of the flood on the embankment. The longer the flood lasts, the more the potential effect on the embankment.

### **17.5 SLOPE STABILITY ANALYSIS**

Stability analysis is based on the concept of limit equilibrium (see Equation 17-1). The Driving Forces include the weight of the soil wedge (i.e., dead load), any live load surcharges and any other external loads (i.e., impact loads on ERSs). The Resisting Force is composed entirely of



the shearing resistance of the soil. Limit equilibrium is defined as the state where the resisting force is just larger than the driving force (i.e.,  $SF = 1.01$  or  $\phi = 0.99$ ). According to Duncan, Wright and Brandon (2014), the equilibrium can be determined for either “single free body or for individual vertical slices.” Regardless of how equilibrium is determined, 3 static equilibrium conditions must be satisfied.

- Moment equilibrium
- Vertical equilibrium
- Horizontal equilibrium

Not all methods resolve all of the equilibrium conditions; some just resolve 1 condition while others solve 2 conditions and assume the third condition is 0.0. Other methods solve all 3 equilibrium conditions.

The single free body looks at the driving forces and the resisting forces along an assumed failure surface. These solutions tend to be relatively simple and are more conducive to the use of design charts. The second method of solving equilibrium is dividing the slope into individual vertical slices. There are numerous procedures that resolve equilibrium using vertical slices. Listed below are some of the more common types.

- Ordinary Method of Slices
- Simplified (Modified) Bishop
- Force Equilibrium
- Spencer
- Morgenstern and Price

The Ordinary Method of Slices and Simplified Bishop assume a circular failure surface. The Spencer and Morgenstern and Price both provide a solution for all 3 equilibrium conditions. In addition, both Spencer and Morgenstern and Price can assume a circular as well as non-circular failure surface. The vast majority of slope stability software packages are capable of using more than 1 method to determine the stability of an embankment, and changing the method will affect the resistance factor ( $\phi = 1/SF$ ). Therefore, SCDOT has elected to select a single analysis method, Spencer’s method, for determining stability. Spencer’s method uses not only both circular and non-circular failure (i.e., sliding block) surfaces but also solves all 3 equilibrium equations. In addition, this method may be used in determining seismic stability/instability. The use of Factor of Safety recognizes the fact that virtually all software currently in use to determine the stability of slopes utilizes Allowable Strength Design (ASD) as opposed to LRFD. The following Subsections provide a brief discussion of all of the slope stability analysis methods listed above. The inclusion of other methods beside Spencer is for completeness of the discussion as well as to partially present SCDOT’s reason for selecting the Spencer method.

The use of computer generated solutions for slope stability is required for both preliminary as well as final design. The GEOR should discuss with the PC/GDS the number and location of slope stability analyses for preliminary design. At a minimum perform End-of-Construction, Long-term and Seismic Event conditions for preliminary design. The Seismic Event condition should include the preliminary SSL results.

### **17.5.1 Ordinary Method of Slices**

The Ordinary Method of Slices (OMS) is 1 of the earliest methods for determining the stability of a slope and was developed by Fellenius in 1936. This method solves moment equilibrium conditions only and is applicable only to circular failure surfaces. This method does not solve

either vertical or horizontal equilibrium conditions. This method is relatively simplistic and can be solved by hand easily. This method should not be used during final design. Its inclusion here is for completeness of the various slope stability methods.

### **17.5.2 Simplified Bishop**

The Simplified Bishop method was developed by Bishop in 1955 and can also be called the Modified Bishop method. The Simplified Bishop method solves 2 of the equilibrium equations, moment and vertical. This method assumes that horizontal forces are not only perpendicular to the vertical sides of the slice, but are equal and opposite; therefore, the horizontal forces cancel out. Since horizontal equilibrium is not satisfied, the use of the Simplified Bishop method in pseudo-static seismic design is questionable and should therefore not be used. As with the OMS, Simplified Bishop can only be used on circular failure surfaces.

### **17.5.3 Force Equilibrium**

For the Force Equilibrium method of determining slope stability, depending on the method selected (Lowe and Karafiath (1959); Simplified Janbu (1973); Modified Swedish (1970)), moment equilibrium is either ignored or assumed to be 0.0. Duncan, Wright and Brandon (2014) and the Department of Defense (DOD) [US Army Corps of Engineers (2003)] contain a detailed description of each of these Force Equilibrium methods. The Force Equilibrium method solves both the horizontal and vertical forces. The main assumption required using this method is the inclination of the horizontal forces on the given slice. The inclination of the horizontal forces acting on slice may be either the slope angle or the average slope angle if multiple slopes are involved (i.e., a broken back slope). In addition, the Force Equilibrium methods solve non-circular failure surfaces and therefore, may be solved graphically.

### **17.5.4 Spencer's Method**

Spencer's Method (Spencer (1967)) solves all 3 conditions of equilibrium and is therefore termed a complete limit equilibrium method. Spencer's Method was originally developed to determine the stability of circular failure surfaces; however, Wright (1969) determined that the Spencer Method could also be used on non-circular failure surfaces as well. This method assumes that the interslice forces are parallel and act on an angle ( $\theta$ ) above the horizontal. This angle is one of the unknowns in this method. Therefore, a first approximation of the angle should be the slope angle. The other unknown is the Factor of Safety. Because the method solves for Factor of Safety, an iterative process is required; therefore, this method lends well to the use of computers.

### **17.5.5 Morgenstern and Price Method**

The Morgenstern and Price Method is very similar to the Spencer Method. The main difference between the 2 methods is that Spencer solves for the interslice angle, while the Morgenstern and Price Method solves for the scaling parameter that is used on a function that describes the slice boundary conditions. The Morgenstern and Price Method provides added flexibility using the interslice angle assumptions.

## **17.6 SETTLEMENT – GENERAL**

Regardless of the type of structure, embankments, ERSs, bridges or buildings are all placed on geomaterials (i.e., soil and rock) and will therefore potentially undergo settlement. According to Collin, Leshchinsky, and Hung (2005), settlement is comprised of 3 components: immediate (elastic or instantaneous), primary consolidation and secondary compression. Settlements

(strains) are caused by an increase in the overburden stress (i.e., increase in load or demand). In many cases, the amount of settlement (strain) determines the capacity (resistance) to a load (demand).

$$\Delta_v = S_t = S_i + S_c + S_s \quad \text{Equation 17-8}$$

Where,

$S_t = \Delta_v$  = Total Settlement

$S_i$  = Immediate Settlement

$S_c$  = Primary Consolidation Settlement

$S_s$  = Secondary Compression Settlement

Immediate settlement ( $S_i$ ) is typically built out during construction; however, this amount of settlement shall be reported since it can affect the quantity of borrow required. The total settlement (post construction, i.e., after paving) shall be reported as the amount of primary consolidation ( $S_c$ ) and secondary compression ( $S_s$ ) settlement for use in comparing to the Performance Limits established in Chapter 10. In addition, to determine the total amount of settlement that geomaterials will undergo, the time for the settlement shall also be determined. It is anticipated that immediate settlement will occur over a period of days to months, while primary consolidation and secondary compression settlement will typically occur over months to years. Another phenomenon that occurs in very soft fine-grained soils is lateral squeeze. Lateral squeeze can cause both vertical as well as lateral displacements. These displacements may induce loadings on structures that have foundations located in the layer susceptible to squeeze.

## 17.7 CHANGE IN STRESS

As indicated previously, in order for settlement to occur there must be an increase in stress placed on the geomaterials, especially in the case of soil. The increase in stress can be caused by placement of an embankment, shallow or deep foundation or dewatering. The effects of dewatering will not be described in this Manual; however, should dewatering be required, an expert in dewatering shall be consulted. There are various methods for determining the change in stress at different depths within the soil profile. The method used in this Manual is the Boussinesq method. Discussed below is the change in stress caused by shallow foundations and by the placement of an embankment. In addition, the increased stress on buried structures caused by the placement of fill is also discussed.

### 17.7.1 Shallow Foundations

Shallow foundations, as indicated in Chapter 15, are used to support bridges, ERSs and other ancillary transportation facilities. Earthen embankments are theoretically supported by shallow foundations; however, the change in stress caused by embankments is discussed in the following Section. According to Chapter 15, a spread footing has a length to width ( $L_f/B_f$ ) ratio of less than 5. Shallow foundations having a length to width ratio greater than 5 are termed strip or continuous footings. Figure 17-9 depicts the approximate distribution of stresses beneath spread (square) and continuous footings.

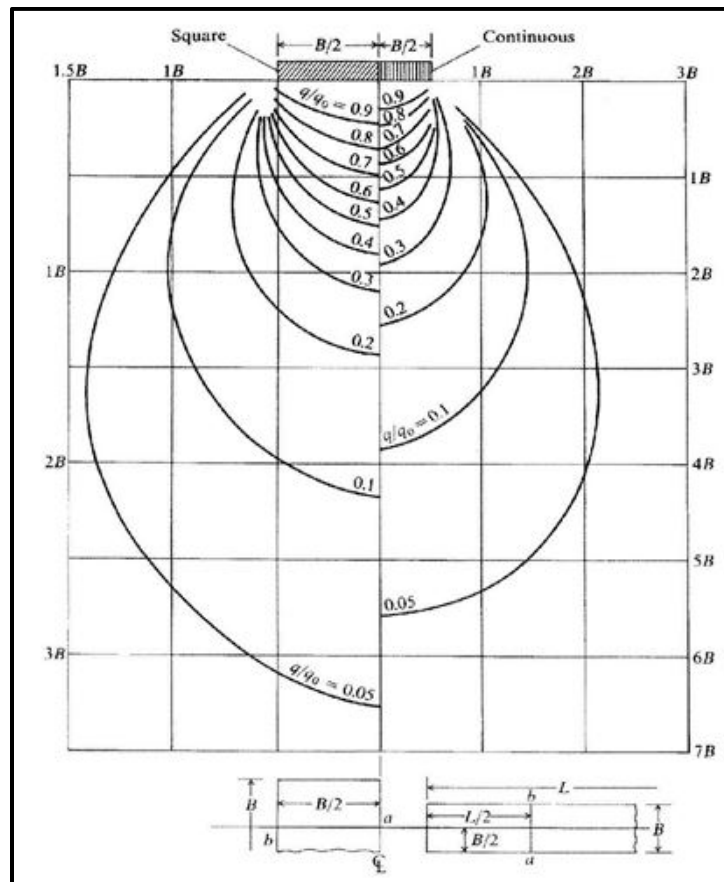


**Figure 17-9, Stress Isobars (Bowles (1986))**

Where,

- B = Foundation width
- L = Foundation length
- q = Stress at depth indicated
- q<sub>0</sub> = Applied vertical stress

Figure 17-9 should only be used as an approximate estimate of the increase in stress on a soil layer. To more accurately determine the increase in stress caused by a shallow foundation, the following equation should be used.

$$\Delta\sigma_v = \int_0^r \left[ \left( \frac{3q_0}{2\pi Z^2} \right) * \left\{ \frac{1}{\left[ 1 + \left( \frac{r}{Z} \right)^2 \right]^{\frac{5}{2}}} \right\} * 2\pi dr \right] \quad \text{Equation 17-9}$$

Where,

- q<sub>0</sub> = Applied vertical stress
- Z = Vertical depth below load
- r = Horizontal distance between the load application and the point where the vertical pressure is being determined

Newmark (1935) performed the integration of this equation and derived an equation for the increase in vertical stress beneath a corner of a uniformly loaded area.

$$\Delta\sigma_v = I * q_o$$

**Equation 17-10**

Where,

I = Influence factor which depends on m and n

m = x/z

n = y/z

x = Width of the loaded area

y = Length of loaded area

z = Depth below the loaded surface to the point of interest

q<sub>o</sub> = Applied vertical stress

The influence factor, I, can be obtained from Figure 17-10.

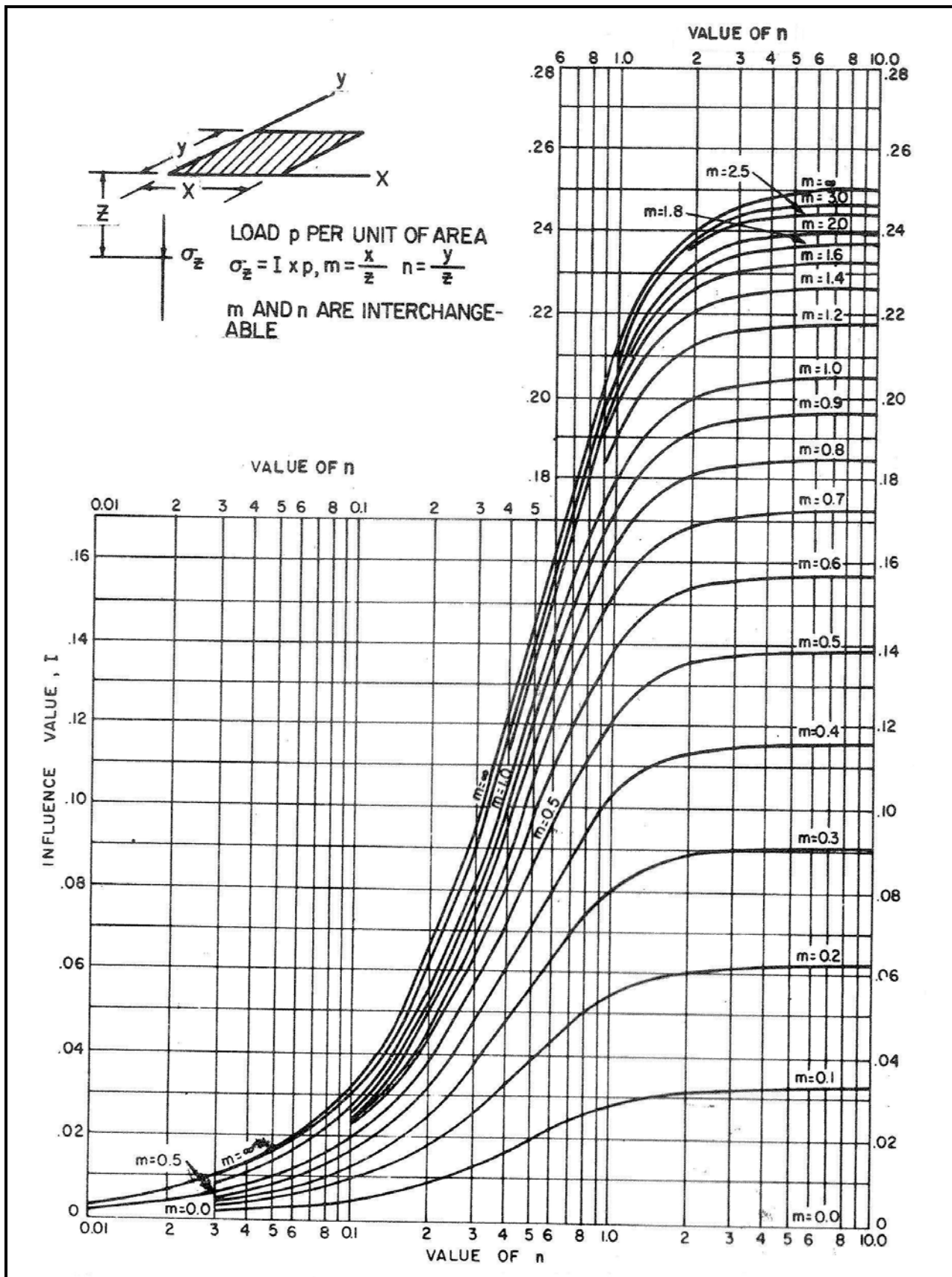
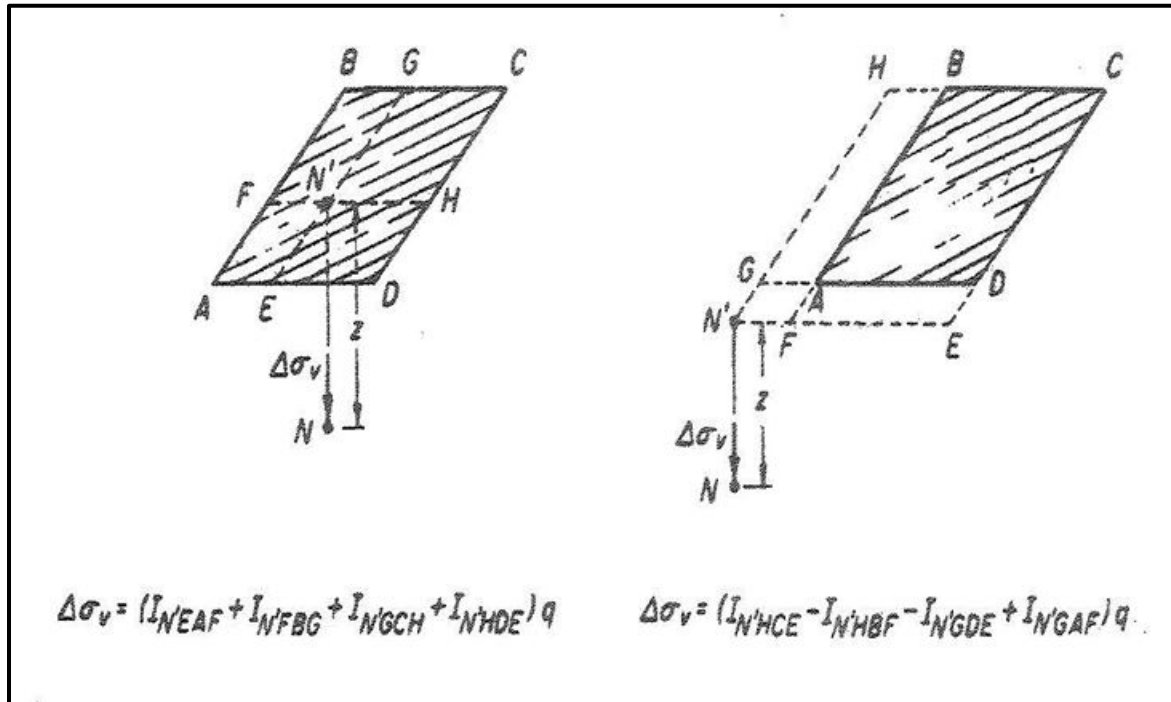


Figure 17-10, Influence Factor Chart (DOD (NAVFAC DM 7.1) (1982))

The change in stress determined using Equation 17-10 is for a point underneath the corner of a loaded area. Therefore, the change in stress at a depth underneath the center of the footing is 4 times the amount determined from Equation 17-10. The change in stress at the mid-point of an edge of a footing is twice the amount determined from Equation 17-10. To find the change in stress at points other than the middle, middle of the edge or a corner of a footing, the Principle of Superposition is used. The Principle of Superposition states that the change in stress at any point is sum of the stresses of the corners over the point (see Figure 17-11).



**Figure 17-11, Principle of Superposition  
(Collins, Leshchinsky, and Hung (2005))**

### 17.7.2 Embankments

The change in stress beneath embankments is determined differently than for shallow foundations, because the area loaded by an embankment is larger than for a shallow foundation. Further the change in stress beneath an embankment is complicated by the geometry of the embankment, i.e., the sides slope downward. Embankments comprise 2 groups; those with infinite length (i.e., side slopes) and those with finite length (i.e., end slopes). The first group is generally longitudinal to the direction of travel, while the other is generally transverse to the direction of travel. For infinite slope embankments, the loading can be represented as a trapezoid. The change in stress beneath an embankment is determined using Equation 17-10. Osterberg (1957) integrated the Boussinesq equations to develop the influence factors (I). Figure 17-12 provides the chart for determining the influence factors (I) for use in Equation 17-10.

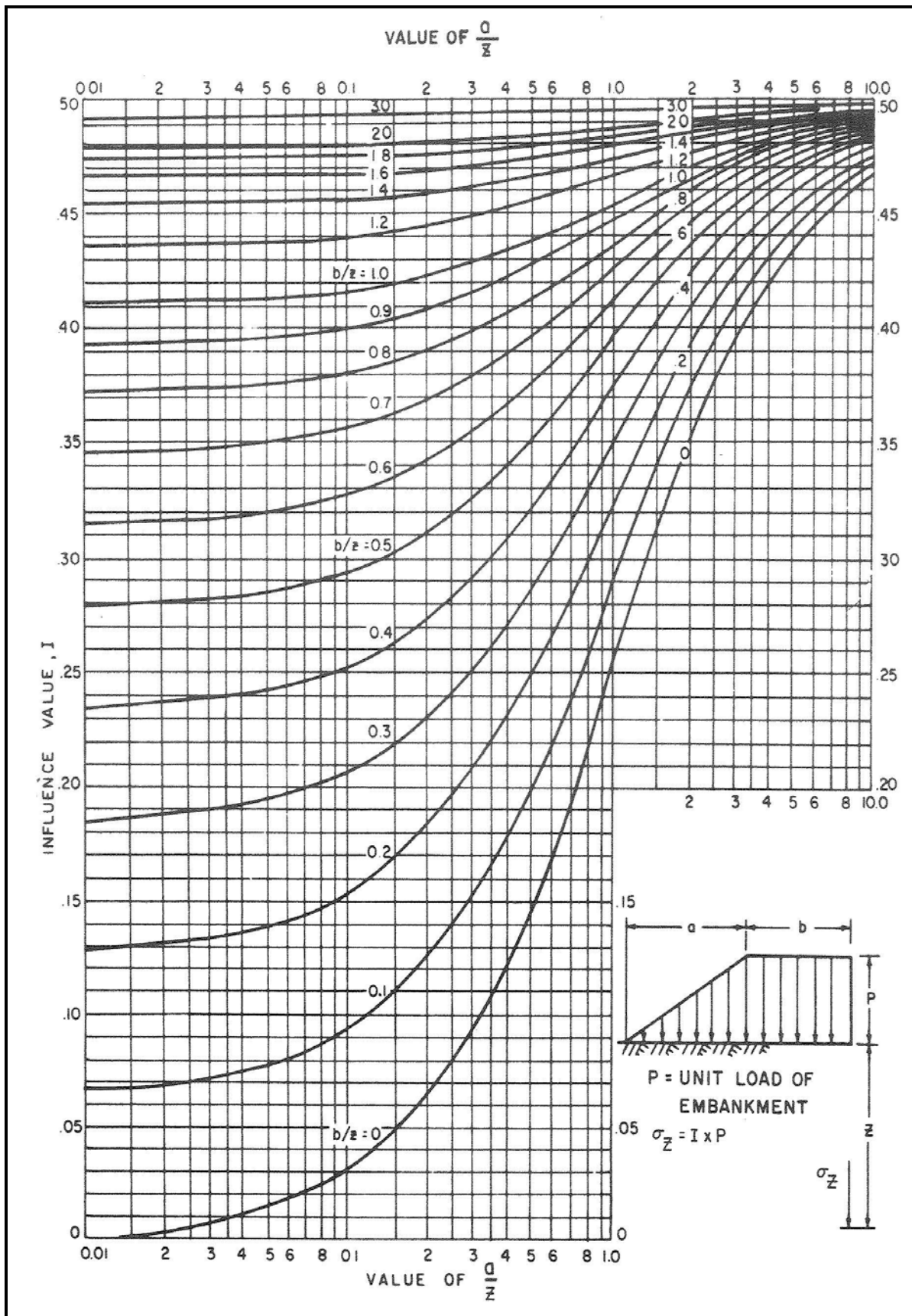


Figure 17-12, Influence Factor Chart – Infinitely Long Embankments (DOD (NAVFAC DM 7.1) (1982))



For finite slopes, Equation 17-10 is used to determine the change in stress. However, the development of the influence factor ( $I$ ) is complicated by the geometric requirements of the slope. The loading consists of 2 components; first the areal load of the embankment and second the load of the sloping section. The influence factor for the area load is determined using Figure 17-10. Note that the stress is doubled, because the stress is determined at a corner of the loaded area. The influence factor for the sloping portion is determined from Figures 17-13 and 17-14.

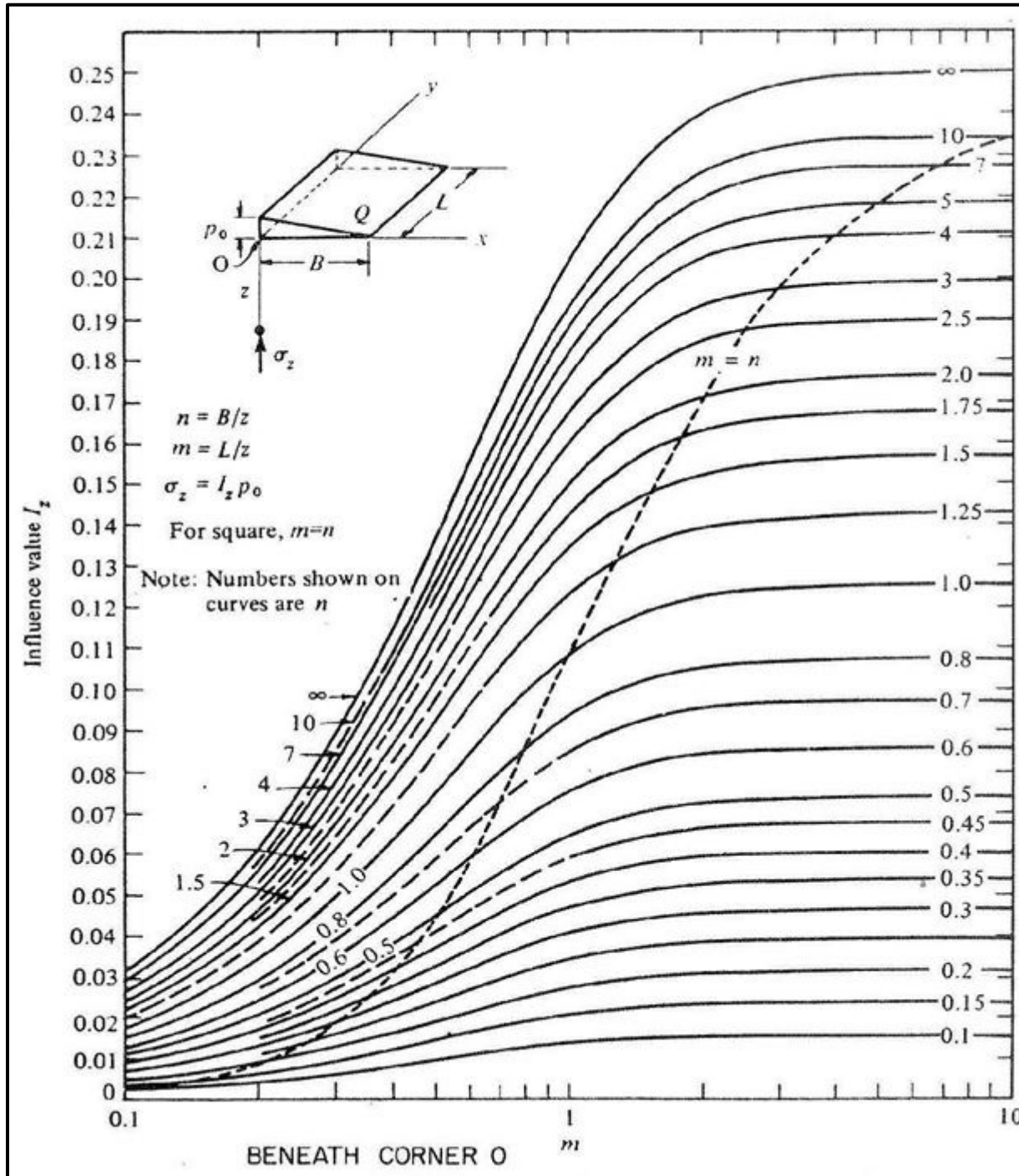
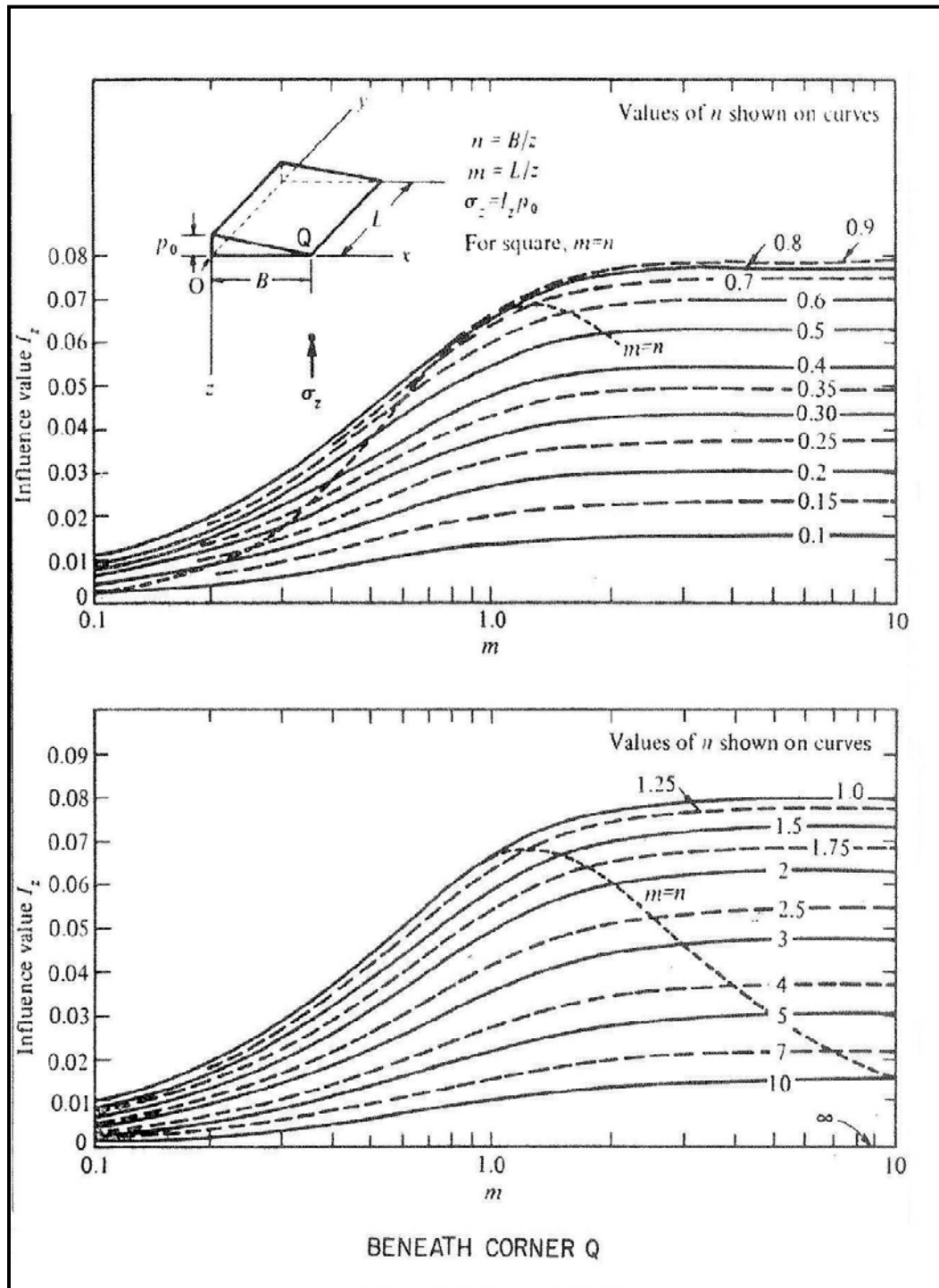


Figure 17-13, Influence Chart Beneath Crest of Slope (DOD (NAVFAC DM 7.1) (1982))



**Figure 17-14, Influence Chart Beneath Toe of Slope (DOD (NAVFAC DM 7.1) (1982))**

An alternate to the procedures indicated above for finding the change in stress beneath a sloped embankment, the procedure described in the Samtani and Nowatzki (2006) may be used. This method was originally developed by the New York State Department of Transportation. This method uses the following equation.

$$\rho = K * \gamma_f * h$$

**Equation 17-11**

Where,

$\rho$  = Change in vertical stress caused by the embankment ( $\Delta\sigma_v$ )

K = Influence factor from Figure 17-15

$\gamma_f$  = Unit Weight of fill Material

h = Height of embankment (see Figure 17-15)

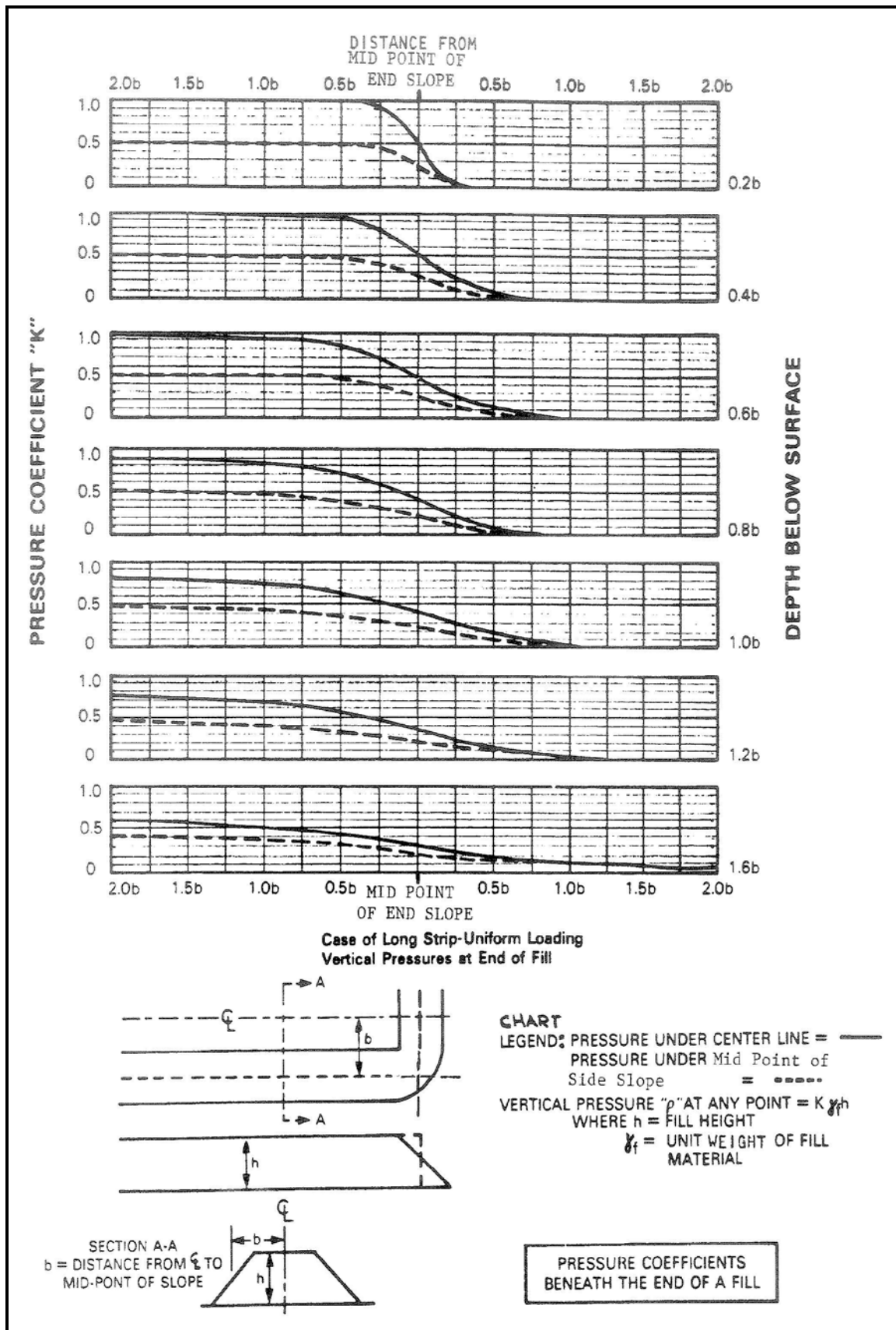


Figure 17-15, Pressure Coefficients Beneath the End of a Fill (Samtani and Nowatzki (2006))

### 17.7.3 Buried Structures

Buried structures consist of culverts, pipes, boxes, etc. and are required to be designed to handle the loads imposed by embankments. The structural design of these structures is beyond the scope of this Manual; however, the design of buried structures is handled in AASHTO LRFD Specifications (Section 12 – Buried Structures and Tunnel Liners). These structures shall be designed to handle horizontal and vertical earth pressures, pavement dead load, live load and vehicular dynamic loads. In addition, these structures may be required to accommodate earth and live load surcharges, downdrag loads, external hydrostatic pressure and buoyancy effects. These last 2 loads are caused by the structure being placed below the water table. Please note that any structure placed below the water table will require additional construction effort. It should be anticipated that dewatering will be required and that an expert in dewatering shall be retained by the Contractor during construction. Because most of these structures are placed within or below embankments, the GEOR shall determine the settlement of the structure as required in Chapter 10 and will report the results to both the SEOR and HEOR who will determine the impact of the settlement to the performance of the structure.

## 17.8 IMMEDIATE SETTLEMENT

Immediate settlement ( $S_i$ ), also termed elastic or instantaneous, occurs upon initial loading of the subgrade soils. This type of settlement occurs in both Sand-Like and Clay-Like soils. The amount of settlement is based on elastic compression of the soils and the time for settlement to occur typically ranges from days to months (1 to 3) or typically during construction. The settlement consists of the compression of air filled voids (Clay-Like soils) and the rearrangement of soil particles (Sand-Like soils). This settlement is anticipated to comprise EV-01A or RV-01A (see Chapter 10) depending on whether the embankment contains an ERS or not. As indicated in Chapter 10 the results of the  $S_i$  determination shall be reported; since this settlement can affect the amount of borrow material required for a project.

### 17.8.1 Sand-Like Soils

Sand-Like soils as defined in Chapter 7 consist of sands, gravels, low plasticity silts and residual soils. In Sand-Like soils, the  $S_i$  (elastic) typically comprises the total amount of settlement anticipated. This Section provides several different methods for determining the  $S_i$  of Sand-Like soils. All of the methods should be used and the largest settlement shall be used to compare to the performance limits provided in Chapter 10. The methods are based on the SPT, on the CPTu and on the DMT.

#### 17.8.1.1 SPT Method

There are 3 SPT methods for determining immediate settlement of Sand-Like soils. The first method is the Hough (1959) method and is used in AASHTO LRFD Specifications (Section 10.6 – Spread Footings). The amount of  $S_i$  is determined using the following equation.

Equation 17-12

$$S_i = \sum_{i=1}^n \left( \frac{1}{C'} \right) * H_i * \left[ \log \left( \frac{\sigma'_{vo} + \Delta\sigma'_v}{\sigma'_{vo}} \right) \right]$$

Where,

$C'$  = Bearing Capacity Index (from Figure 17 -16)

$H_i$  = Thickness of the  $i^{\text{th}}$  layer

$\sigma'_{vo}$  = Effective overburden pressure at the mid-point of  $i^{\text{th}}$  layer

$\Delta\sigma'_v$  = Change in effective vertical stress at the mid-point of  $i^{\text{th}}$  layer

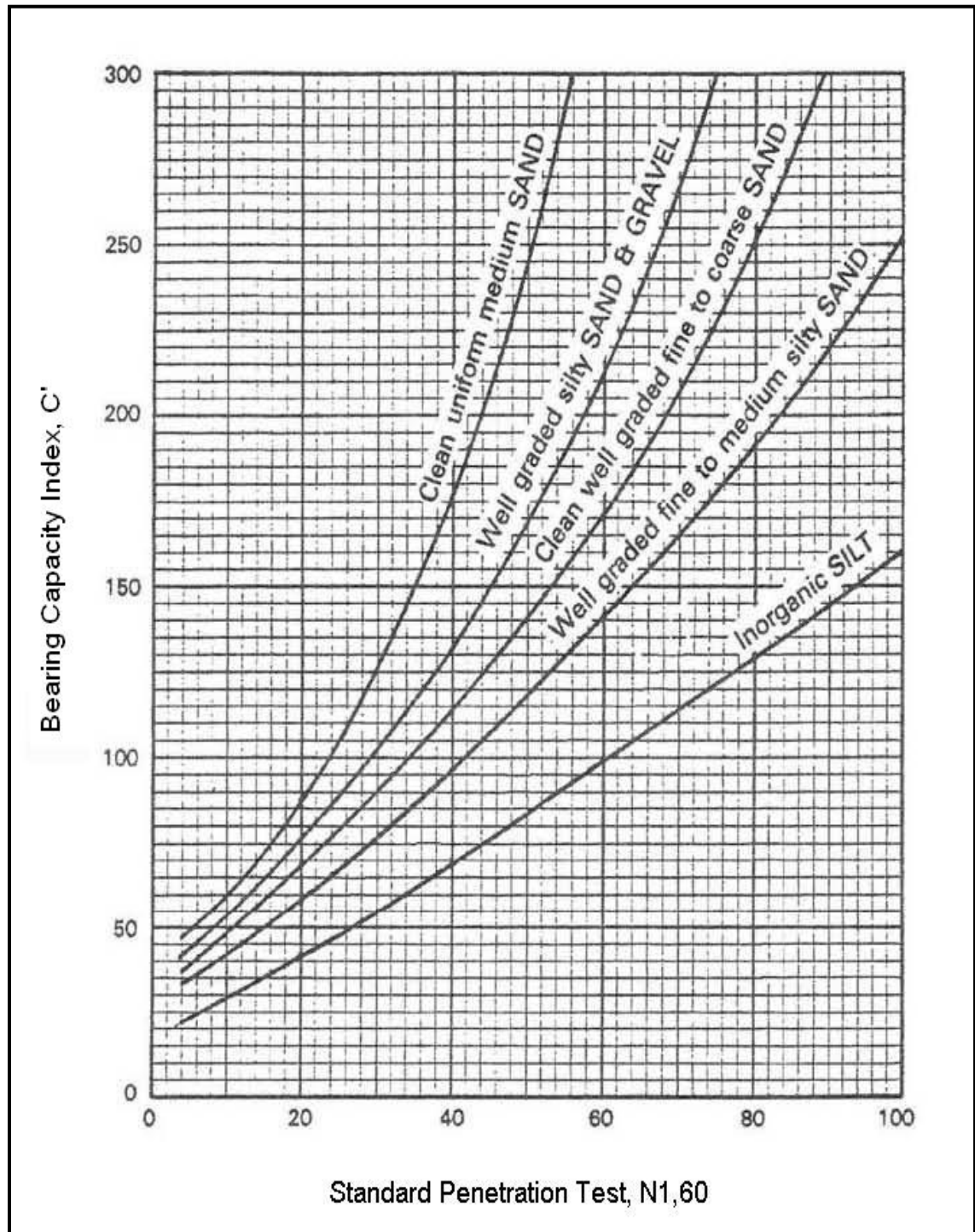


**Figure 17-16, Bearing Capacity Index Chart  
(Collin, Leshchinsky, and Hung (2005),  
Modified from Hough (1959))**

The  $N_{1,60}$  is determined using the methodology discussed in Chapter 7.

The second SPT method of determining elastic settlement is the Peck and Bazaraa Method (Munfakh, Arman, Collin, Hung, and Brouillette (2001)). This method is a modification of the method described by Terzaghi and Peck (1967). It should be noted the equation used to determine the settlement is in SI units. The Peck and Bazaraa Method equation is listed below.

$$S_i = 0.265 * C_W * C_D * \left[ \left( \frac{2q_o}{(N_{1,60})_{ave}} \right) * \left( \frac{2B_f}{B_f + 0.3} \right)^2 \right] \quad \text{Equation 17-13}$$

$$C_W = \frac{\sigma_{vo}}{\sigma'_{vo}} \quad \text{Equation 17-14}$$

$$C_D = 1 - 0.4 * \sqrt{\frac{\gamma * D_f}{q_o}} \quad \text{Equation 17-15}$$

Where,

$S_i$  = Immediate settlement, millimeters (mm) [1 mm = 0.03937 in]

$C_W$  = Water table correction factor, at a depth of 1/2 of  $B_f$

$C_D$  = Embedment correction factor, use 1.0 when filling above original grade

$B_f$  = Footing width, meters (m) [1 m = 3.28084 ft]

$D_f$  = Depth of footing base embedment from ground surface, meters

$\gamma$  = Total unit weight of soil, kiloNewtons per cubic meter ( $\text{kN/m}^3$ )

[1  $\text{kN/m}^3$  = 6.3656  $\text{lbs/ft}^3$ ]

$q_o$  = Applied vertical stress or bearing pressure, kiloPascals (kPa) [1 kPa = 0.0209  $\text{ksf}$ ]

$\sigma_{vo}$  = Total overburden pressure

$\sigma'_{vo}$  = Effective overburden pressure

$(N_{1,60})_{ave}$  = Average  $N_{1,60}$ -value from base of footing to a depth of  $B_f$  below footing, blows per 0.3 meters

1N = 1\*[( $\text{kg}\cdot\text{m}$ )/ $\text{s}^2$ ]

1Pa = 1\*( $\text{N}/\text{m}^2$ ) = 1\*[ $\text{kg}/(\text{m}\cdot\text{s}^2)$ ]

The third SPT method was developed by Duncan and Buchignani (1976) based on Meyerhof (1965). The immediate settlement equation is provided below.

$$S_i = \frac{5q_o}{(N_{60} - 1.5) * C_B} \quad \text{Equation 17-16}$$

Where,

$S_i$  = Immediate settlement, inches

$q_o$  = Applied vertical stress, tsf

$N_{60}$  = Standard Penetration value corrected only for energy (see Chapter 7)

$C_B$  = Width Correction (see Table 17-2)

The  $N_{60}$ -value is an average value from the base of the footing to a depth of  $B_f$ .

**Table 17-2, Width Correction Factor,  $C_B$   
(Duncan and Buchignani (1976))**

Footing Width, B (feet)	$C_B$
$\leq 4$	1.00
6	0.95
8	0.90
10	0.85
$\geq 12$	0.80

Duncan and Buchignani (1976) indicate that immediate (elastic) settlement will continue to increase over time (i.e., creep). The total amount of elastic settlement over time is determined using the following equation.

$$S_{iet} = S_i * C_t \quad \text{Equation 17-17}$$

Where

$S_{iet}$  = Elastic settlement after a period of time

$S_i$  = Immediate or elastic settlement

$C_t$  = Time rate factor (see Table 17-3)

**Table 17-3, Time Rate Factors  
(Duncan and Buchignani (1976))**

Time	$C_t$
1 month	1.0
4 months	1.1
1 year	1.2
3 years	1.3
10 years	1.4
30 years	1.5

For times other than those depicted in Table 17-3, the following equation may be used.

$$C_t = [0.0858 * \ln(t)] + 0.9907 \quad \text{Equation 17-18}$$

Where,

$C_t$  = Time rate factor

t = Time period over which settlement occurs, months

### 17.8.1.2 CPT Method

There is 1 CPT method available for determining the immediate settlement of Sand-Like soils. It was developed by Schmertmann (1970) and is applicable only to shallow foundations (i.e., a rigid structure is required). Similarly to the Peck and Bazaraa Method, the Schmertmann Method uses SI units. The Schmertmann Method uses the following equations.

$$S_i = C_D * C_t * q_{net} * \left[ \sum_{i=1}^n \left( \frac{H_i}{E_{si}} \right) * I_{azi} \right] \quad \text{Equation 17-19}$$

$$C_D = 1 - 0.5 \left( \frac{\sigma'_D}{q_{net}} \right) \geq 0.5 \quad \text{Equation 17-20}$$



$$C_t = 1 + 0.2 \left[ \log \left( \frac{t}{0.1} \right) \right] \quad \text{Equation 17-21}$$

$$q_{net} = q_o - \sigma'_D \quad \text{Equation 17-22}$$

$$I_p = 0.5 + 0.1 * \sqrt{\frac{q_{net}}{\sigma'_{Ip}}} \quad \text{Equation 17-23}$$

Where,

$C_D$  = Depth correction factor

$C_t$  = Creep correction factor ( $t > 0.1$  years)

$q_{net}$  = Net total average bearing pressure, kPa

$H_i$  = Thickness of the  $i^{\text{th}}$  layer, meters

$E_{si}$  = Modulus of Elasticity of the  $i^{\text{th}}$  layer, kPa

$I_{azi}$  = Average vertical strain influence factor of the  $i^{\text{th}}$  layer (from Figure 17-17)

$q_o$  = Applied bearing pressure, kPa

$\sigma'_D$  = Vertical effective stress at the base of the footing, kPa

$t$  = Time, years

$I_p$  = Peak influence factor value

$\sigma'_{Ip}$  = Vertical effective stress at the depth of the peak influence factor ( $I_p$ ), kPa

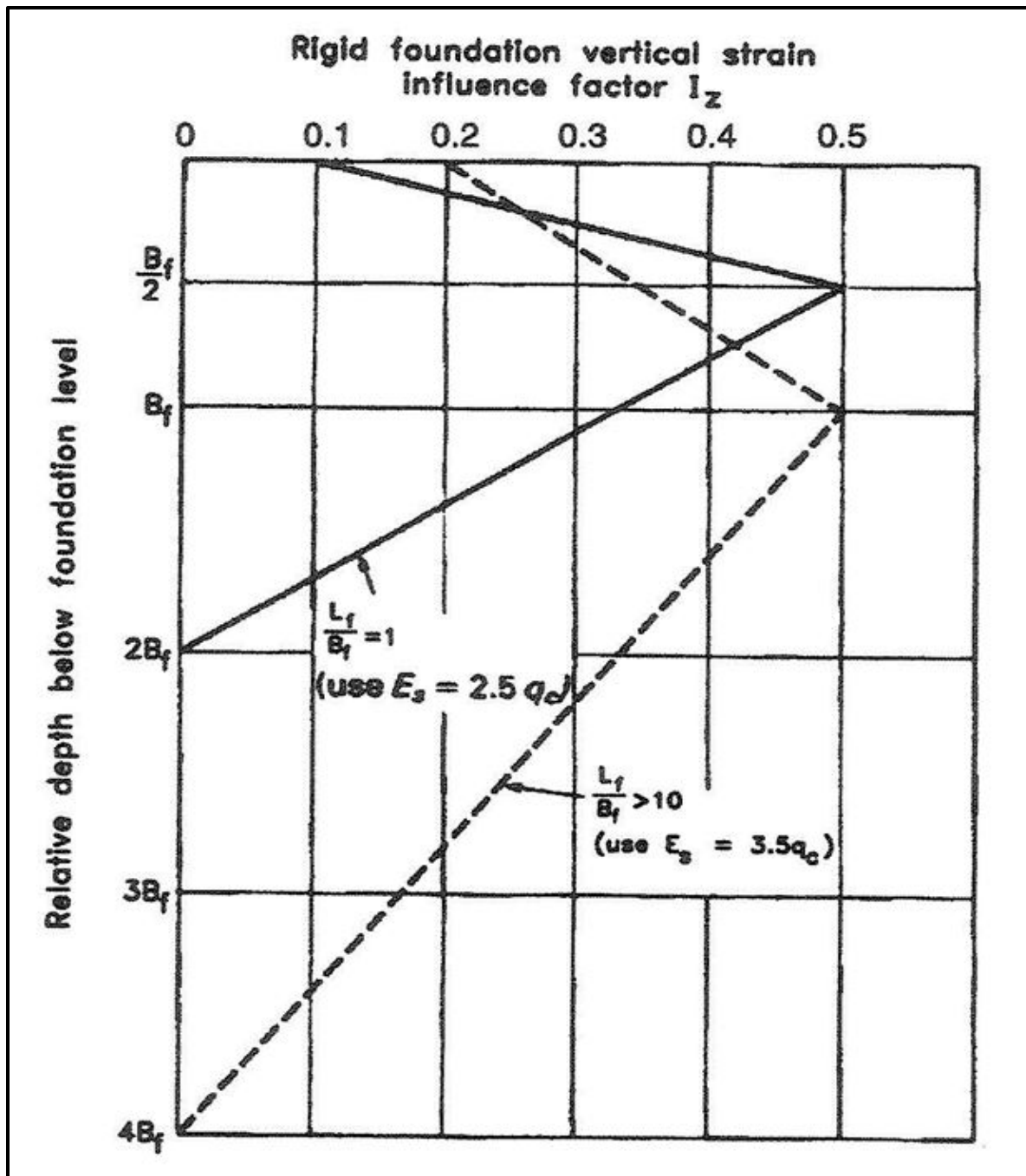


**Figure 17-17, Vertical Strain Influence Factor Chart  
(Munfakh, et al. (2001))**

The Modulus of Elasticity ( $E_s$ ) can be developed directly from laboratory testing, from Chapter 7 or from the following equation. This equation applies only to determining the  $E_s$  from CPT data.

$$E_s = F_s * q_c \tag{Equation 17-24}$$

Where,

$F_s$  = Correlation factor depending on cone and soil type, stress level and footing shape (see Table 17-4)

$q_c$  = Uncorrected cone penetration tip resistance, kPa

**Table 17-4, Correlation Factor,  $F_s$   
(Munfakh, et al. (2001))**

Case	$F_s$
$L_f/B_f = 1$	2.5
$L_f/B_f > 10$	3.5

Where,

$B_f$  = Footing width

$L_f$  = Footing length

As an alternate to Figure 17-17, the vertical strain influence factor may be determined using the equations in Table 17-5.

**Table 17-5, Vertical Strain Influence Factor Equations  
(Munfakh, et al. (2001))**

Footing Shape	I Terms	$H_i$	$I_{azi}$ Equations
$L_f/B_f < 1$ (square)	$I_{zsq}$	0 to $B_f/2$	$0.1 + \left(\frac{H_i}{B_f}\right) * (2I_p - 0.2)$
		$B_f/2$ to $2B_f$	$0.667I_p * \left(2 - \frac{H_i}{B_f}\right)$
$L_f/B_f > 10$ (continuous)	$I_{zc}$	0 to $B_f$	$0.2 + \left(\frac{H_i}{B_f}\right) * (I_p - 0.2)$
		$B_f$ to $4B_f$	$0.333I_p * \left(4 - \frac{H_i}{B_f}\right)$
$1 < L_f/B_f < 10$ (rectangular)	$I_{zr}$	N/A	$I_{zsq} + 0.111(I_{zc} - I_{zsq}) * \left[\left(\frac{L_f}{B_f}\right) - 1\right]$

### 17.8.1.3 DMT Method

Immediate settlement can be determined from Dilatometer Test data. The method is described in detail by Briaud and Miran (1992). The equation for determining immediate settlement is provided below.

**Equation 17-25**

$$S_i = \sum_{i=1}^n \left(\frac{\Delta\sigma_v}{M_i}\right) * H_i$$

Where,

$\Delta\sigma_v$  = Change in vertical stress at the mid-point of  $i^{\text{th}}$  layer

$M_i$  = Averaged constrained modulus of the  $i^{\text{th}}$  layer

$H_i$  = Thickness of the  $i^{\text{th}}$  layer

## 17.8.2 Clay-Like Soils

There is some immediate settlement in Clay-Like (clays and plastic silts) soils with most settlement occurring within a relatively short period after loading is applied. Most of this immediate settlement is from distortion and compression of air filled voids. It is anticipated that very little immediate settlement would occur in saturated Clay-Like soils. However, for unsaturated and/or highly overconsolidated ( $OCR \geq 4$ ) Clay-Like soils, immediate settlement can be a predominant portion of the total settlement ( $S_i$ ). These immediate settlements can be determined using the Theory of Elasticity (Timoshenko and Goodier (1951)) and are determined using the following equation.

$$S_i = \frac{[q_o * (1 - \nu^2) * \sqrt{A}]}{(E_s * \beta_z)} \quad \text{Equation 17-26}$$

Where,

$q_o$  = Applied bearing pressure at the bottom of loaded area

$\nu$  = Poisson's ratio (see Chapter 7)

A = Contact area of the load

$E_s$  = Modulus of elasticity for the soil (see Chapter 7)

$\beta_z$  = Footing shape and rigidity factor (see Table 17-6)

**Table 17-6, Footing Shape and Rigidity Factors  
(Munfakh, et al. (2001))**

$L_f/B_f$	$\beta_z$ Flexible	$\beta_z$ Rigid
1	1.06	1.08
2	1.09	1.10
3	1.13	1.15
5	1.22	1.24
10	1.41	1.41

Where  $B_f$  and  $L_f$  are the same as in the CPT Method described previously. If  $L_f/B_f$  is between 5 and 10, use linear interpretation. For  $L_f/B_f$  greater than 10, use the  $\beta_z$  for 1.5. The elastic parameters, Poisson's ratio ( $\nu$ ) and modulus of elasticity ( $E_s$ ), are provided in Chapter 7 for Clay-Like soils.

Christian and Carrier (1978) developed an improved Janbu approximation for determining immediate settlement in Clay-Like soils. The improved Janbu approximation is provided below and assumes that the Poisson's ratio ( $\nu$ ) of the soil is 0.5.

$$S_i = \mu_0 * \mu_1 * \left( \frac{q_o * B_f}{E_s} \right) \quad \text{Equation 17-27}$$

Where,

$\mu_0$  = Influence factor for depth (see Figure 17-18)

$\mu_1$  = Influence factor for foundation shape (see Figure 17-18)

$q_o$  = Applied vertical stress at the bottom of loaded area

$B_f$  = Foundation width

$L_f$  = Foundation length

D = Foundation depth below ground surface

H = Distance between bottom of foundation and a firm (non-compressible) layer

$E_s$  = Modulus of elasticity for the soil (see Chapter 7)

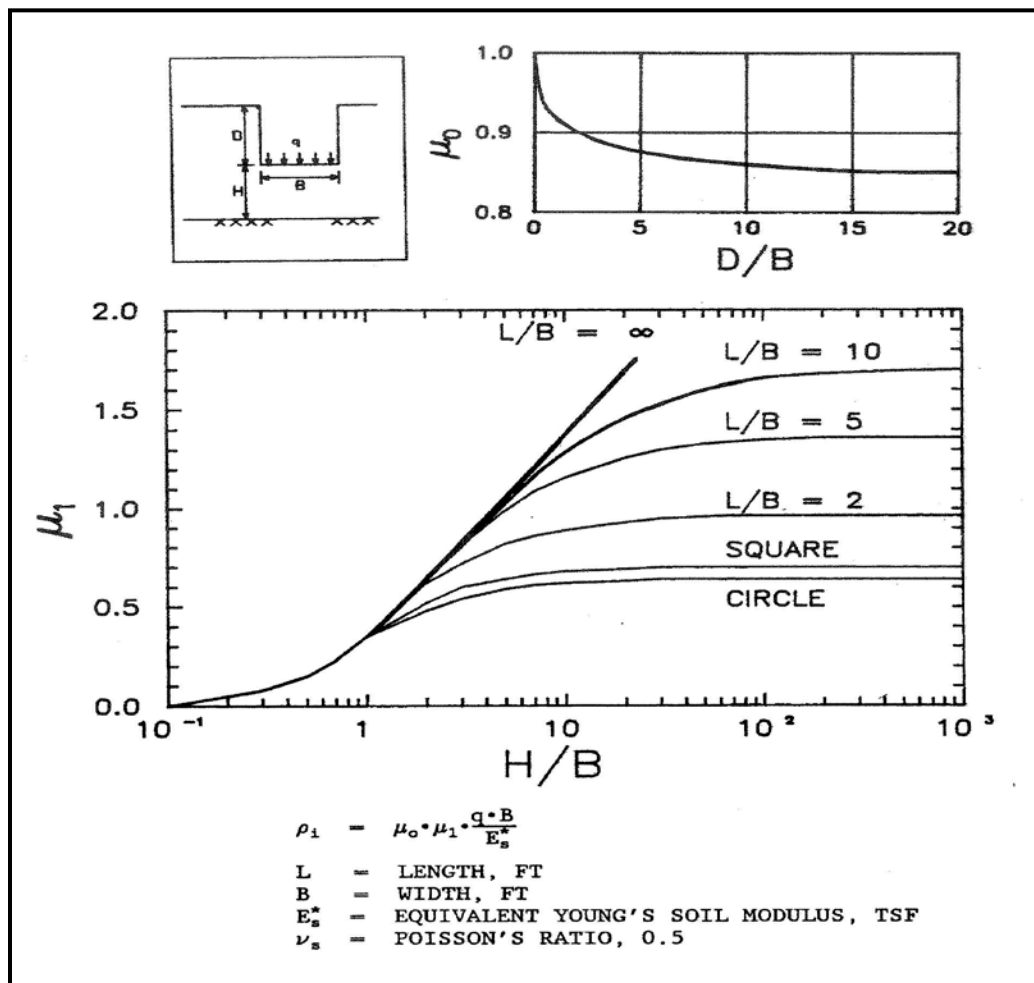


Figure 17-18, Janbu Influence Factor Chart  
(DOD (USACE EM 1110-1-1904) (1990))

## 17.9 PRIMARY CONSOLIDATION SETTLEMENT

Primary consolidation settlement ( $S_c$ ) occurs when the increase in load on a soil results in the generation of excess pore pressures within the soil voids. Depending on the type of soil, the time to reduce the excess pore pressures to some steady state level may be rapid (Sand-Like soils) or may require long periods of time (Clay-Like soils). Therefore, primary consolidation settlement is comprised of 2 components: the amount of settlement and the time for settlement to occur. The amount of time required for Sand-Like soil to settle is relatively short, typically occurring during construction, and the amount of settlement can be determined using immediate or elastic settlement theory. Therefore, the remainder of this Section will exclusively look at Clay-Like soils. Typically, normally consolidated ( $OCR = 1$ ) soils undergo primary consolidation settlement. For the purpose of this Chapter, all plastic Clay-Like soils that have an OCR of less than 4 shall have the primary consolidation settlement determined. Primary consolidation is considered to begin at the end of elastic settlement. For Clay-Like soils, elastic settlement should occur relatively quickly and as indicated previously is comprised of the closing of air filled voids. With the completion of elastic settlement it should be assumed that the Clay-Like soils are saturated.

The determination of primary consolidation settlement is based on 6 steps as presented in Table 17-7.

**Table 17-7, Primary Consolidation Settlement Steps  
(Modified from Munfakh, et al. (2001))**

Step	Item
1	Computation of the initial vertical effective stress ( $\sigma'_{vo}$ ) [total vertical stress ( $\sigma_{vo}$ ) and pore water pressure ( $u_o$ )] of the layer(s) midpoint
2	Determination of preconsolidation stresses ( $\sigma'_p$ or $p'_c$ )
3	Computation of changes in vertical effective stress ( $\Delta\sigma'_v$ ) [associated with changes in both total stress ( $\Delta\sigma_v$ ) and pore water pressures ( $\Delta u$ )] due to the construction
4	Determination of compressibility of the clay or plastic silt
5	Computation of layer compressions ( $S_c$ )
6	Computation of time for compressions

### 17.9.1 Amount of Settlement

In Clay-Like soils, loads are carried first by the pore water located in the interstitial space between the soil grains and then by the soil grains. The pore water pressure increases proportional to the load applied at that depth. As the excess pore water pressures reduce through drainage, the load is transferred to the soil grains. This drainage causes the settlement of Clay-Like soils. Therefore, the settlement is directly proportional to the volume of water drained from the soil layer. Typically, the area loaded is large, resulting in the flow of water vertically (either up or down) and not horizontally. Therefore, 1-dimensional consolidation theory may be used to determine settlements of Clay-Like soils.

The determination of the amount of settlement is dependent on whether the soil is normally consolidated, overconsolidated or a combination of both. The amount of settlement for under consolidated soils is determined the same as normally consolidated soil. In addition, the way the data is presented, either  $e$ -log  $p$  or  $\varepsilon$ -log  $p$  curves, will also determine which equation is used. Presented in Table 17-8 are the equations for determining the total primary consolidation settlement ( $S_c$ ).

Table 17-8, Primary Consolidation Settlement Equations

e-log p		
$\sigma'_{vo} = \sigma'_p$	$S_c = \sum_1^i H_o * \left( \frac{C_c}{1 + e_o} \right) * \left( \log \frac{\sigma'_f}{\sigma'_{vo}} \right)$	Equation 17-28
$\sigma'_f < \sigma'_p$	$S_c = \sum_1^i H_o * \left( \frac{C_r}{1 + e_o} \right) * \left( \log \frac{\sigma'_f}{\sigma'_{vo}} \right)$	Equation 17-29
$\sigma'_{vo} < \sigma'_p$ < $\sigma'_f$	$S_c = \sum_1^i H_o * \left[ \left( \frac{C_c}{1 + e_o} \right) * \left( \log \frac{\sigma'_f}{\sigma'_p} \right) + \left( \frac{C_r}{1 + e_o} \right) * \left( \log \frac{\sigma'_p}{\sigma'_{vo}} \right) \right]$	Equation 17-30
ε-log p		
$\sigma'_{vo} = \sigma'_p$	$S_c = \sum_1^i H_o * (C_{\varepsilon c}) * \left( \log \frac{\sigma'_f}{\sigma'_{vo}} \right)$	Equation 17-31
$\sigma'_f < \sigma'_p$	$S_c = \sum_1^i H_o * (C_{\varepsilon r}) * \left( \log \frac{\sigma'_f}{\sigma'_{vo}} \right)$	Equation 17-32
$\sigma'_{vo} < \sigma'_p$ < $\sigma'_f$	$S_c = \sum_1^i H_o * \left[ (C_{\varepsilon c}) * \left( \log \frac{\sigma'_f}{\sigma'_p} \right) + (C_{\varepsilon r}) * \left( \log \frac{\sigma'_p}{\sigma'_{vo}} \right) \right]$	Equation 17-33

Where,

- $H_o$  = Thickness of  $i^{\text{th}}$  layer
- $e_o$  = Initial void ratio of  $i^{\text{th}}$  layer
- $\sigma'_f$  = Final pressure on the  $i^{\text{th}}$  layer

$$\sigma'_f = \sigma'_{vo} + \Delta\sigma_v \quad \text{Equation 17-34}$$

Where,

- $\sigma'_{vo}$  = initial vertical effective stress on the  $i^{\text{th}}$  layer
- $\Delta\sigma_v$  = change in stress on the  $i^{\text{th}}$  layer

### 17.9.2 Time for Settlement

As indicated previously, consolidation settlement occurs when a load is applied to a saturated Clay-Like soil squeezing water out from between the soil grains. The length of time for primary consolidation settlement to occur is a function of compressibility and permeability of the soil. The Coefficient of Consolidation ( $c_v$ ) is related to the permeability ( $k$ ) and the Coefficient of Vertical Compression ( $m_v$ ) as indicated in the following equations

$$c_v = \frac{1}{\gamma_w} * \left( \frac{k}{m_v} \right) \quad \text{Equation 17-35}$$

$$m_v = \frac{\Delta \varepsilon_v}{\Delta \sigma'_v} = \frac{\Delta e}{\Delta \sigma'_v * (1 + e_{av})} \quad \text{Equation 17-36}$$

Where,

$\gamma_w$  = Unit weight of water

$\Delta \varepsilon_v$  = Change in sample height

$\Delta \sigma'$  = Change in effective stress

$\Delta e$  = Change in void ratio

$e_{av}$  = Average void ratio during consolidation

The  $c_v$  is typically provided as part of the results of consolidation testing. A  $c_v$  is provided for each load increment applied during the test. The  $c_v$  used to determine the time for primary consolidation settlement should be at the stress (load increment) closest to the anticipated field conditions. If  $c_v$  is not provided, it should be determined using the procedures outlined in Munfakh, et al. (2001).

The time (t) for primary consolidation settlement is determined using the equation listed below.

$$t = \frac{T(H_o)^2}{c_v} \quad \text{Equation 17-37}$$

Where,

t = time for settlement

T = Time Factor from Equation 17-38

$H_o$  = Maximum distance pore water must flow through

$c_v$  = Coefficient of Consolidation

The distance the pore water must flow through is affected by the permeability of the materials above and below the Clay-Like material. If the Clay-Like material is between 2 Sand-Like materials (i.e., highly permeable materials) then the thickness of the Clay-Like material is cut in half. This is also known as 2-way or double drainage. If the Clay-Like material is bordered by an impermeable material, then the drainage path is the full thickness of the layer. This is called 1-way or single drainage. According to Das (1990), the time factor (T) is related to the degree of consolidation (U) in the following equations.

$$T = \frac{\left( \frac{\pi}{4} \right) * \left( \frac{U\%}{100} \right)^2}{\left[ 1 - \left( \frac{U\%}{100} \right)^{5.6} \right]^{0.357}} \leq 2.5 \quad \text{Equation 17-38}$$

for

$$0 \leq U\% < 100\% \quad \text{Equation 17-39}$$

Where,

U% = Degree of Consolidation in percent



When U equals 100 percent, T approaches infinity ( $\infty$ ). The limit of T indicated in Equation 17-38 results in a U of 99.3%.

### 17.10 SECONDARY COMPRESSION SETTLEMENT

Secondary compression settlement occurs after the completion of primary consolidation settlement (i.e., U = 95%). This type of compression settlement occurs when the soil continues to vertically displace despite the fact that the excess pore pressures have essentially dissipated. Secondary compression typically occurs in highly plastic (PI > 21) or organic (percent organics > 30 percent) Clay-Like soils. Secondary compression settlement is evident on both the e-log p and the  $\epsilon$ -log p curves (see Figure 17-19).

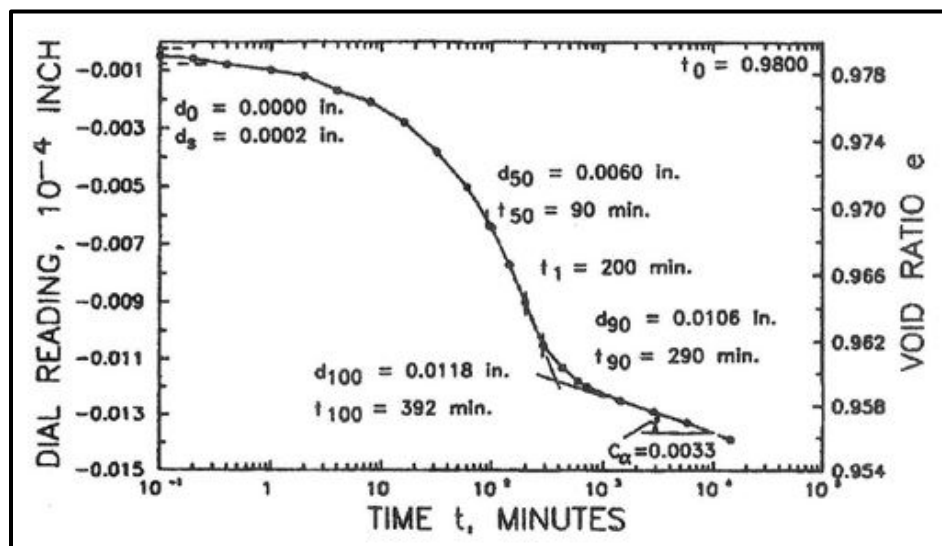


Figure 17-19, Secondary Compression (Munfakh, et al. (2001))

The Coefficient of Secondary Compression ( $C_{\alpha}$ ) can be determined using the slope of the corrected curve over 1 full logarithmic cycle. As with primary consolidation settlement, the amount of secondary compression settlement can be determined using either the e-log p or  $\epsilon$ -log p curves. Presented in Table 17-9 are the equations for determining secondary compression settlement.

Table 17-9, Secondary Compression Settlement Equations

e-log p	$S_s = \sum_1^i H_o * \left( \frac{C_{\alpha}}{1 + e_o} \right) * \left( \log \frac{t_2}{t_1} \right)$	Equation 17-40
$\epsilon$ -log p	$S_s = \sum_1^i H_o * (C_{\epsilon\alpha}) * \left( \log \frac{t_2}{t_1} \right)$	Equation 17-41

Where,  
 $H_o$  = Thickness of  $i^{th}$  layer

$e_o$  = Initial void ratio of  $i^{\text{th}}$  layer

$t_1$  = Time when secondary compression begins (i.e.,  $U = 95\%$ )

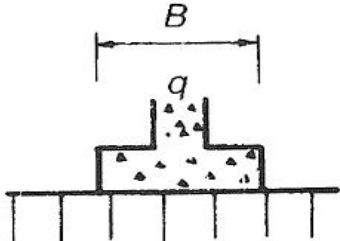
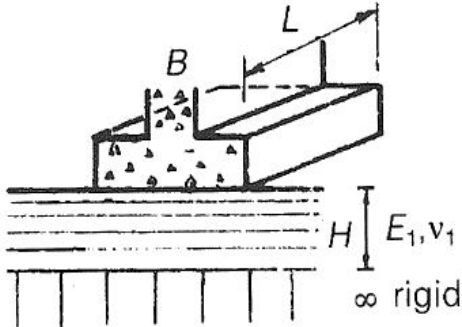
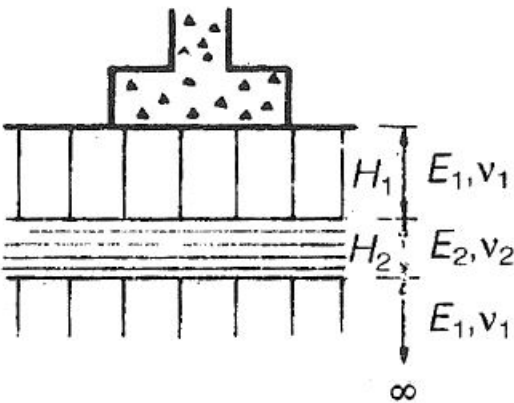
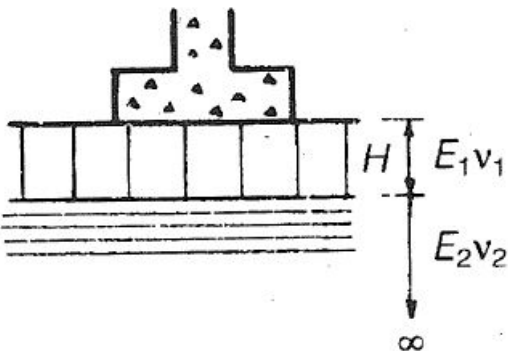
$t_2$  = Time when secondary compression is desired, usually the service life of structure

Secondary compression settlement is sometimes confused with creep. As indicated previously, secondary compression settlement occurs after the pore pressures have achieved a steady state condition and the settlement is the result of particle movement or realignment. Creep occurs after the pore pressures have achieved a steady state condition and there is no volume change. Creep is related to loss of shear strength with time rather than compressibility. In many cases, it is not possible to distinguish between creep and secondary compression settlement.

### **17.11 SETTLEMENT IN ROCK**

The settlement procedures discussed previously are for soil. Rock is normally considered incompressible; however, the potential for settlement on rock does exist. The settlement of foundations on rock can be determined using elastic theory. The settlement determinations provided in this Section cover 4 combinations of rock (incompressible) and compressible layers (see Table 17-10).

**Table 17-10, Rock Settlements on various Geological Conditions  
(Munfakh, et al. (2001))**

Geological Condition	Graph of Geological Condition	Settlement Calculations
Incompressible Layer		<ol style="list-style-type: none"> <li>Determine shape factor <math>C_d</math> from Table 17-11;</li> <li>Calculate <math>S_r</math> using Equation 17-42</li> </ol>
Compressible Layer on Incompressible Layer		<ol style="list-style-type: none"> <li>Determine ratio of <math>H/B_f</math> &amp; <math>L_f/B_f</math>;</li> <li>Determine shape factor <math>C_d</math> from Table 17-11;</li> <li>Calculate <math>S_r</math> using Equation 17-42</li> </ol>
Compressible Layer between Incompressible Layers		<ol style="list-style-type: none"> <li>Determine ratios <math>(H_1 + H_2)/B_f</math> &amp; <math>L_f/B_f</math>;</li> <li>Calculate weighted modulus (E) for upper two layers using Equation 17-43;</li> <li>Determine shape factor <math>C'_d</math> for ratio <math>(H_1 + H_2)/B_f</math> from Table 17-12;</li> <li>Calculate <math>S_r</math> using Equation 17-42</li> </ol>
Incompressible Layer on Compressible Layer		<ol style="list-style-type: none"> <li>Determine ratios <math>H/B_f</math> &amp; <math>E_1/E_2</math>;</li> <li>Determine factor <math>\alpha</math> from Table 17-13;</li> <li>Determine shape factor <math>C_d</math> from Table 17-11;</li> <li>Calculate <math>S_{r\infty}</math> using Equation 17-42 using elastic parameters <math>E_2</math> &amp; <math>v_2</math> for overall foundation;</li> <li>Calculate <math>S_r</math> by reducing calculated <math>S_{r\infty}</math> by <math>\alpha</math> (see Equation 17-44)</li> </ol>

$$S_r = \frac{C_d q B_f^*(1-\nu^2)}{E_m} \quad \text{Equation 17-42}$$

$$\bar{E} = \frac{(E_1 H_1 + E_2 H_2)}{(H_1 + H_2)} \quad \text{Equation 17-43}$$

$$S_r = \alpha S_{r\infty} \quad \text{Equation 17-44}$$

Where,

$S_r$  = Rock Settlement

$S_{r\infty}$  = Settlement of incompressible layer underlain by a compressible layer

$C_d$  = Shape Factor from Table 17-11

$C'_d$  = Shape Factor from Table 17-12

$q_0$  = Applied vertical stress at the bottom of loaded area

$B_f$  = Foundation width

$\nu$  = Poisson's ratio

$E_m$  = Modulus of elasticity of rock mass (see Chapter 7)

$E_1$  = Modulus of elasticity of incompressible layer

$E_2$  = Modulus of elasticity of compressible layer

$\alpha$  = Elastic distortion settlement correction factor from Table 17-13

**Table 17-11, Shape Factors,  $C_d$   
(Munfakh, et al. (2001))**

Shape	Center	Corner	Middle of Short Side	Middle of Long Side	Average
Circle	1.00	0.64	0.64	0.64	0.85
Circle (rigid)	0.79	0.79	0.79	0.79	0.79
Square	1.12	0.56	0.76	0.76	0.95
Square (rigid)	0.99	0.99	0.99	0.99	0.99
<b>Rectangle: Length/Width</b>					
1.5	1.36	0.67	0.89	0.97	1.15
2	1.52	0.76	0.98	1.12	1.30
3	1.78	0.88	1.11	1.35	1.52
5	2.10	1.05	1.27	1.68	1.83
10	2.53	1.26	1.49	2.212	2.25
100	4.00	2.00	2.20	3.60	3.70
1000	5.47	2.75	2.94	5.03	5.15
10000	6.90	3.50	3.70	6.50	6.60

**Table 17-12, Shape Factors,  $C'_d$**   
(Munfakh, et al. (2001))

H/B <sub>f</sub>	Circle Dia. (B <sub>f</sub> )	Rectangle Shape Foundation (L <sub>f</sub> /B <sub>f</sub> )						
		1	1.5	2	3	5	10	∞
0.10	0.09	0.09	0.09	0.09	0.09	0.09	0.09	0.09
0.25	0.24	0.24	0.23	0.23	0.23	0.23	0.23	0.23
0.50	0.48	0.48	0.47	0.47	0.47	0.47	0.47	0.47
1.00	0.70	0.75	0.81	0.83	0.83	0.83	0.83	0.83
1.50	0.80	0.86	0.97	1.03	1.07	1.08	1.08	1.08
2.50	0.88	0.97	1.12	1.22	1.33	1.39	1.40	1.40
3.50	0.91	1.01	1.19	1.31	1.45	1.56	1.59	1.60
5.00	0.94	1.05	1.24	1.38	1.55	1.72	1.82	1.83
∞	1.00	1.12	1.36	1.52	1.78	2.10	2.53	∞

**Table 17-13, Elastic Distortion Settlement Correction Factor,  $\alpha$**   
(Munfakh, et al. (2001))

H/B <sub>f</sub>	E <sub>1</sub> /E <sub>2</sub>				
	1	2	5	10	100
0.00	1.000	1.000	1.000	1.000	1.000
0.10	1.000	0.972	0.943	0.923	0.760
0.25	1.000	0.885	0.779	0.699	0.431
0.50	1.000	0.747	0.566	0.463	0.228
1.00	1.000	0.627	0.399	0.287	0.121
2.5	1.000	0.550	0.274	0.175	0.058
5.0	1.000	0.525	0.238	0.136	0.036
∞	1.000	0.500	0.200	0.100	0.010

## 17.12 LATERAL SQUEEZE

Lateral squeeze is a phenomenon that occurs when a soft Clay-Like soil deforms and displaces when subjected to embankment loadings and is primarily a concern at the end bents where the deep foundations may be installed through thick layers of soft Clay-Like soils. In addition, if the thickness of the soft Clay-Like soil is finite and is less than the width of the sloped portion of the embankment ( $b_e$ ) then the potential for lateral squeeze is present (Figure 17-20). This phenomenon can cause rotation and horizontal displacement of the end bent and can induce excessive loadings in the deep foundations. The following equation is used to determine if the potential for lateral squeeze exists at a site.

$$\gamma_f H_f > 3\tau \quad \text{Equation 17-45}$$

Where,

- $\gamma_f$  = Total unit weight of fill material
- $H_f$  = Height of fill
- $\tau$  = Undrained shear strength (see Chapter 7)

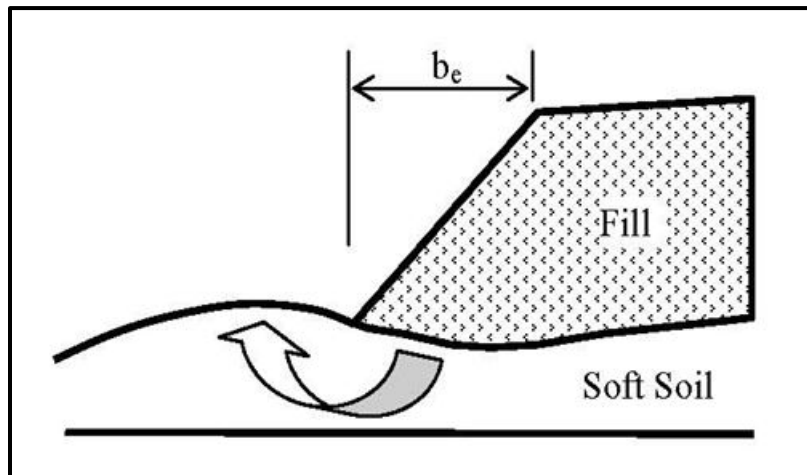


**Figure 17-20, Schematic of Lateral Squeeze (Samtani and Nowatzki (2006))**

If the load applied by the soil (fill height times fill unit weight) exceeds 3 times the undrained shear strength the potential for lateral squeeze is present; therefore, check the resistance against lateral squeeze using the following equation.

$$\phi = \left( \frac{\gamma_f D_s \tan \theta}{2\tau} \right) + \left( \frac{\gamma_f H_f}{4.14\tau} \right) \quad \text{Equation 17-46}$$

Where,

- $D_s$  = Depth of soft soil (see Figure 17-21)
- $\theta$  = Slope angle

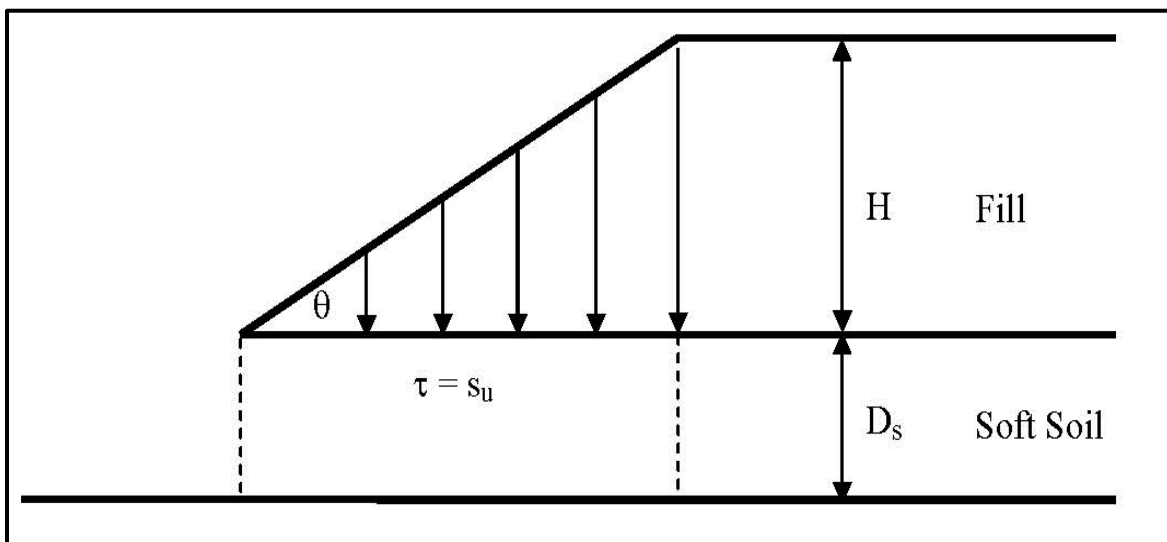


**Figure 17-21, Lateral Squeeze Model (modified Samtani and Nowatzki (2006))**

When  $D_s$  is greater than the width of the embankment, global stability of the embankment and the bearing resistance of the soft subgrade soils will typically govern design. If the  $\phi$  is exceeded lateral movements of the soil may occur. These lateral movements may be estimated using the following equation.

$$\Delta_L = 0.25S_t \quad \text{Equation 17-47}$$

Where,

$\Delta_L$  = Horizontal displacement

$S_t$  = Total settlement of fill

### 17.13 EMBANKMENT DESIGN

Embankments may be comprised of slopes and ERSs with unreinforced slopes and RSSs as a subset of slopes (see Figure 17-22 and Chapter 2). As indicated in Figure 17-22 all ERSs, RSSs, and slopes with angles greater than or equal to 1H:1V, require facing elements. Typically facing elements are comprised of panels, blocks, geotextile wrap, and wire baskets with geosynthetics. The purpose of the facing elements is to prevent the erosion of the soil material either behind or within the structure. Reinforced embankments and unreinforced slopes do not typically require facing elements. However, the design team may add facing elements if the site conditions warrant the use of these elements. Figure 17-22 is provided as a general guide and actual site conditions should dictate which type of embankment should be used. All proposed reinforced embankments and RSSs shall be evaluated using the ERS Selection Philosophy contained in Chapter 18. The use of this selection process will aid in the determination of whether the use of reinforced embankments or RSSs is justified. Discussed in the following Sections are limited design procedures and issues that should be considered in the design of embankments.

Short-term (end-of-construction) and long-term loading conditions are typically used. The short-term condition loads should be comprised of the self-weight of the embankment and any live loads (i.e., traffic loads) applied at the top of the embankment. The long-term condition loads are similar to the short-term but should also include an additional dead load for the addition of pavement. As indicated previously, it is anticipated that the thickness of the addition pavement is estimated to be approximately 8 inches. Bridge embankment design shall include seismic loading and shall therefore, include the effects of the seismic event (i.e., SSL).

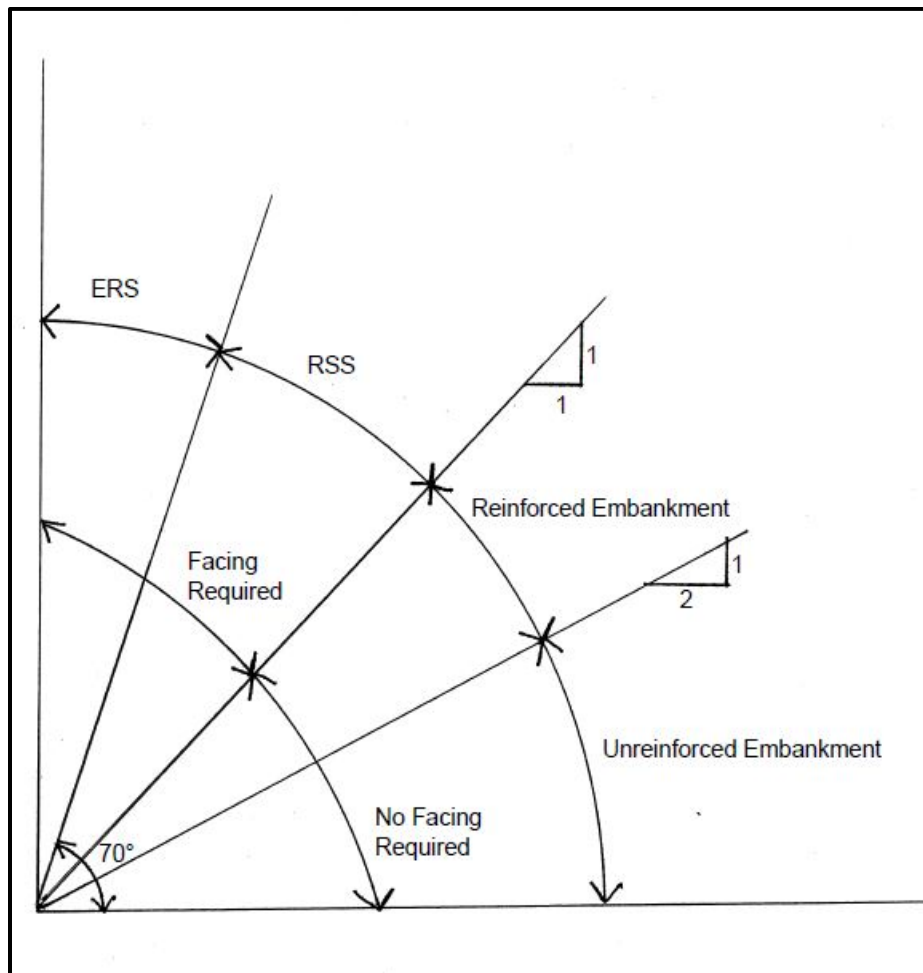


**Figure 17-22, ERS vs Slope Diagram**

The total settlement as well as the differential settlement (the difference in settlement between 2 points) should be considered in embankment design. Further, the time for settlement to occur as well as the rate of settlement (amount per unit of time) should also be considered in embankment design. The amount and time for settlement to occur shall be determined using the methods described earlier in this Chapter. Settlement shall be determined for the Service limit state. The amount (total and differential) and the rate of settlement at the Service limit state should conform to the limits presented in Chapter 10. Depending on the requirements of particular project the use of the Construction-Point Concept may be used. Unlike traditional settlement calculations which assume the bridge is instantaneously placed, the Construction-Point Concept determines the settlement at specific critical construction points (see Figure 17-23).

Temporary embankments whether unreinforced, reinforced embankments or RSSs shall follow the design procedures of this Section; however the  $\phi$  indicated in Chapter 9 will be for temporary embankments. Temporary embankments are not designed for the EE limit state.



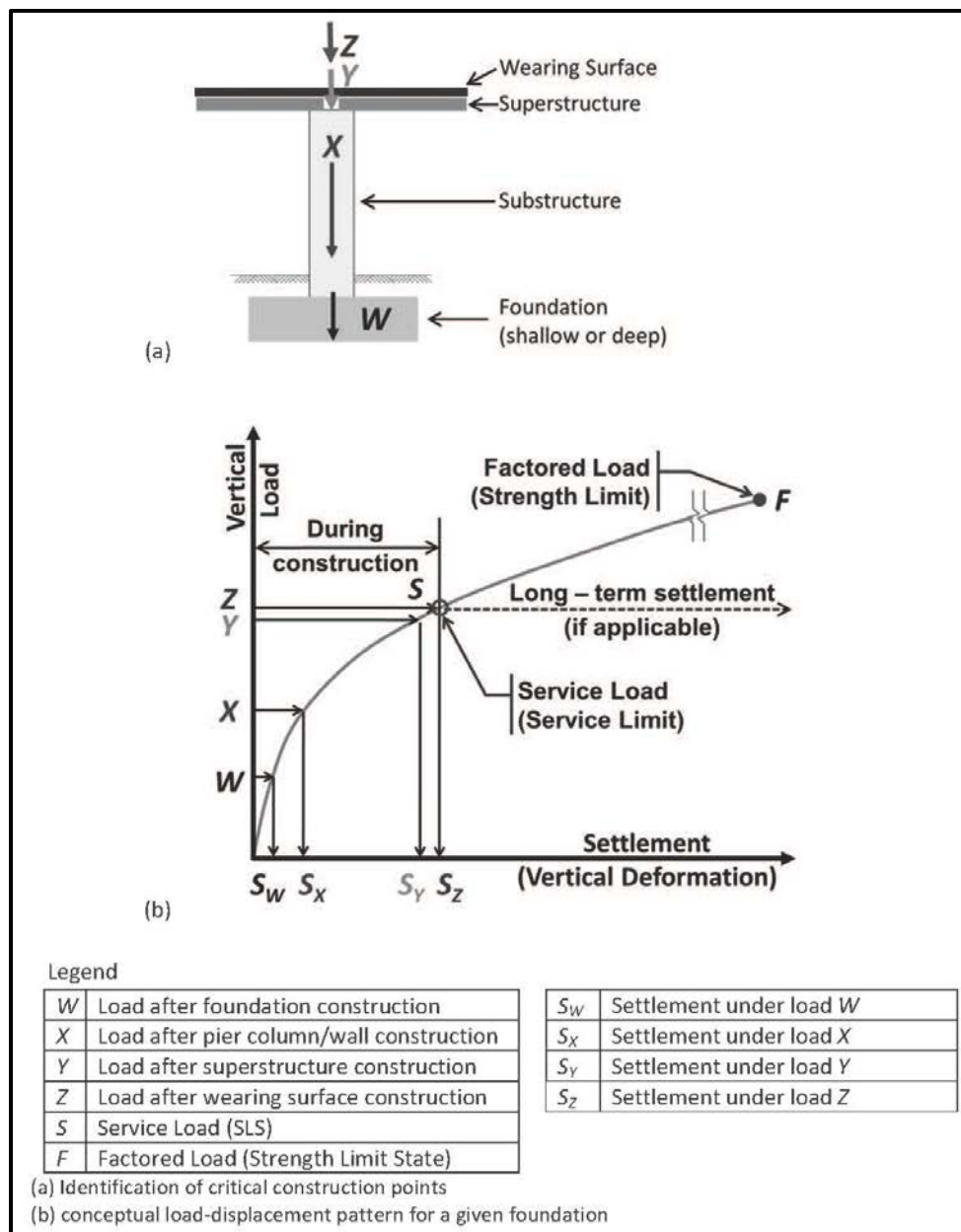


**Figure 17-23, Construction-Point Concept (DeMarco, Bush, Samtani, Kulicki and Severns (2015))**

### 17.13.1 Unreinforced Embankments

Unreinforced embankments typically have slopes equal to 2H:1V or flatter, are constructed of borrow materials and may comprise either bridge or roadway embankments. Roadway embankments as defined in Chapter 2 begin at the termination of the bridge embankment and shall be designed for the Service limit state as indicated in Chapter 8. In addition, according to Table 17-1, there are conditions when slope stability analysis may not be required. While slope stability may not be required for certain roadway embankments, settlement shall be determined and reported to the design team for all roadway embankments. Bridge embankments shall be designed for Service/Strength as well as the EE limit state (see Chapter 8). Bridge embankments, regardless of height, shall always have slope stability analyses, except as note in Section 17.1, as well as settlement analyses performed. All embankments should meet the

Performance Objectives and Performance Limits as established in Chapter 10 for the appropriate limit state.

The following design procedure is adopted from the design steps presented in the Holtz, et al. (2008) and is applicable to both unreinforced as well as reinforced embankments.

1. Geometry and Loading Conditions – The geometric parameters required are the height and length of the embankment, the width of the crest (shoulder break-to-shoulder break), and the slide slope angle. The loading conditions include any surcharges and any temporary or dynamic loads. The construction rate should also be included, because the gain in shear strength is directly affected by the placement of the embankments.
2. Soil Profile and Engineering Properties – The subsurface stratigraphy should be determined, including soil layering and groundwater table location for the foundation soils. The testing should include basic classification testing (see Chapter 4 for testing classification requirements). The shear strength and consolidation properties should be determined either from correlations with field testing or from laboratory testing. The spatial variation (length and depth) of the soil properties should also be determined.
3. Embankment Fill Engineering Properties – The engineering properties of the fill (borrow) material should be determined, including basic classification testing (see Chapter 4 for testing classification requirements), moisture-density relationship, shear strength, and chemical properties. A drainage media (e.g., free draining granular materials, non-woven geotextiles, etc.) should be placed at the interface between the existing subgrade and the embankment fill to permit drainage of water. Above this drainage media, normal backfill materials may be placed.
4. Establish Resistance Factors and Performance Limits – The Resistance Factors and Performance Limits shall meet the requirements contained in Chapters 9 and 10, respectively. The stability analyses performed in the following steps are for the Service/Strength limit state at the end of construction. The end of construction is the most critical condition. The EE will be checked using the shear strength anticipated from the increase with time as well as any affects from SSL.
5. Bearing Capacity Check – The bearing capacity of the subgrade soils can be checked using the procedures indicated in Chapter 15, using limit equilibrium analyses for strip footings and assuming a logarithmic spiral failure surface on an infinitely deep soil. When the thickness of soft foundation soil is much greater than the width of the embankment, the following equation may be used to determine the ultimate bearing capacity:

$$q_{ult} = \gamma_{fill} * H = c_u * N_c \quad \text{Equation 17-48}$$

Where,

$q_{ult}$  = Ultimate bearing capacity

$N_c$  = 5.14

$c_u$  = Undrained shear strength of foundation soil

$\gamma_{fill}$  = Unit weight of fill material

H = Height of embankment

If the thickness of the soft soil is less than the width of the embankment, check lateral squeeze using the procedure provided in Section 17.12.

6. Rotational Shear Stability Check – Perform a rotational slip surface analysis on the unreinforced embankment and foundation to determine the critical failure surface and the resistance factor against local shear instability. If the calculated resistance factor is less than required, then, reinforcement is not required. A resistance factor greater than required indicates slope instability and that reinforcement is required (see Section 17.13.2).
7. Sliding Block Stability Check – Perform a sliding block analysis. If the calculated resistance factor is less than required, then reinforcement is not required. If the resistance factor is inadequate, then reinforcement is required (see Section 17.13.2).
8. Estimate Magnitude and Rate of Embankment Settlement – The magnitude and rate of embankment settlement should be determined using the procedures outlined previously in this Chapter.
9. Establish Construction Sequence and Procedures – The construction sequence and procedures should be established. Proper placement and performance of the geosynthetic is highly influenced by the construction sequence and procedure. The sequence and procedure should be as clear and concise as possible to prevent misunderstandings during construction.
10. Establish Construction Observation Requirements – Since implemented construction procedures are crucial to the success of reinforced embankments on very soft foundations, competent and professional construction inspection is absolutely essential. Field personnel must be properly trained to observe every phase of the construction and to ensure that:
  - a. The specified material is delivered to the project
  - b. The specified construction sequence is explicitly followed

Instrumentation requirements should also be established. As typical instruments include piezometers, settlement points, surface survey points and slope inclinometers. Part of the instrumentation requirements is establishing who will obtain the measurements and how often the measurements will be obtained.

### **17.13.1.1 Unreinforced Embankments in Deep Water**

If the depth of water is more than 5 feet, place riprap as defined by Section 804 of the Standard Specifications. The riprap may be placed to a depth ranging from 5 feet below the water level surface to approximately 6 inches above the water level surface. A geosynthetic material acting as soil separator and meeting the requirements of STS for *Geosynthetic Materials for Separation and Stabilization* (SC-M-203-1) shall be placed between the riprap and the overlying materials to prevent the loss of fill materials into the voids of the riprap. The portion of the embankment constructed of riprap is an unreinforced embankment, a reinforced embankment or RSS may be placed on top of this portion.

### **17.13.2 Reinforced Embankments**

Reinforced embankments are those embankments that require reinforcement to maintain stability, have slopes between 2H:1V and 1H:1V, and are constructed of borrow material as specified in the Standard Specifications. Geosynthetic reinforcement (either geogrids or

geotextiles) is included in the stability analysis (see Section 17.5) unlike separation and stabilization geosynthetics which are not included in the stability analysis.

The design approach for the reinforced embankment is to prevent failure. Figure 17-24 provides depictions of potential modes of failure. These potential modes of failure indicate the type of analyses that will be required. However, reinforcement will not increase the bearing resistance of the foundation soil. Further, reinforcement will not reduce the magnitude of consolidation settlement or secondary compression of the embankment. Settlement of the embankment and the resulting creep of the reinforcement, need to be considered in design as well. Creep of the reinforcement only becomes an issue if the creep rate of the reinforcement is greater than the increase in shear strength of the subgrade soils. The most critical condition for embankment stability is typically at the end-of-construction. Therefore, a total stress analysis should be performed.

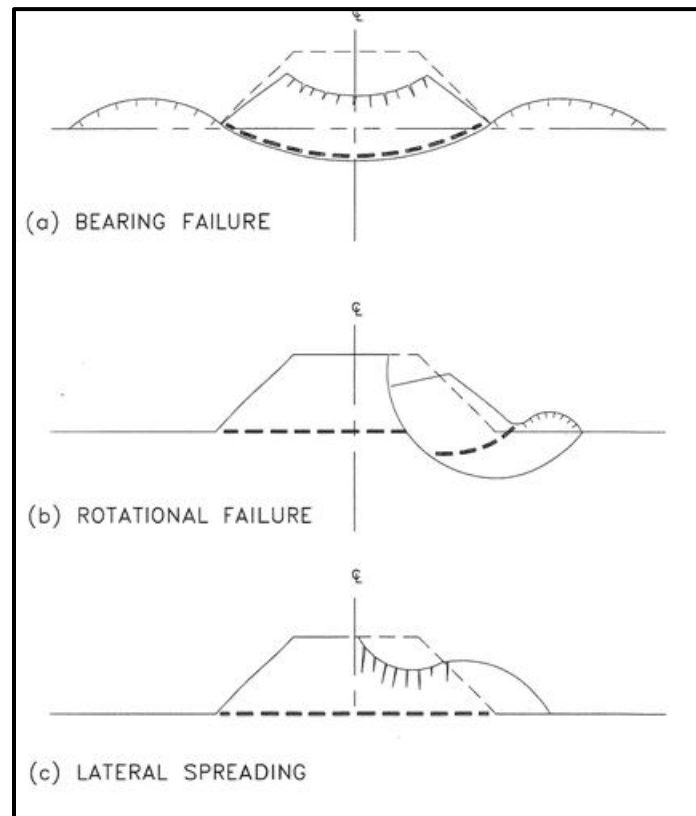


**Figure 17-24, Reinforced Embankment Failure Modes (Holtz, et al. (2008))**

In addition, reinforced embankments are also used over soft foundation soils that typically fall into 2 situations: first, construction over uniform deposits, and second, construction over localized anomalies (Figure 17-25). The most common application in transportation construction is the placement of embankments over uniform soft soil foundations. Typically, the reinforcement is placed perpendicular to the centerline of the embankment to prevent long joints parallel to the centerline and the potential for sliding of the outer most reinforcement. As the end of the embankment is approached, the turning of the reinforcement may be required.

The reinforcement normally used consists of biaxial and uniaxial geogrids; however, geotextiles may also be used. The design using geotextiles is based upon constructability, survivability, and the amount of strain required to achieve the desired strength. In some cases the geotextile may require sewn seams. Sewn seams shall comply with the requirements of Chapter 20.

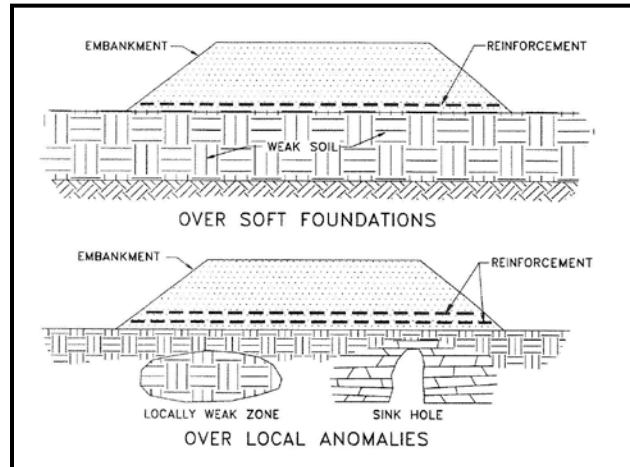


**Figure 17-25, Reinforced Embankment Applications  
(Holtz, et al. (2008))**

The procedure provided in Section 17.13.1 is used for the design of Reinforced Embankments except as modified. Specifically Steps 6 and 7 are modified by the following.

6. Rotational Shear Stability Check – If the determined resistance factor is greater than required (see Figure 17-24(b)), then, calculate the required reinforcement strength ( $T_g$ ) to provide an adequate resistance factor using the Figure 17-26 and the following equation:

$$T_g = \frac{\Delta M_r}{y} \quad \text{Equation 17-49}$$

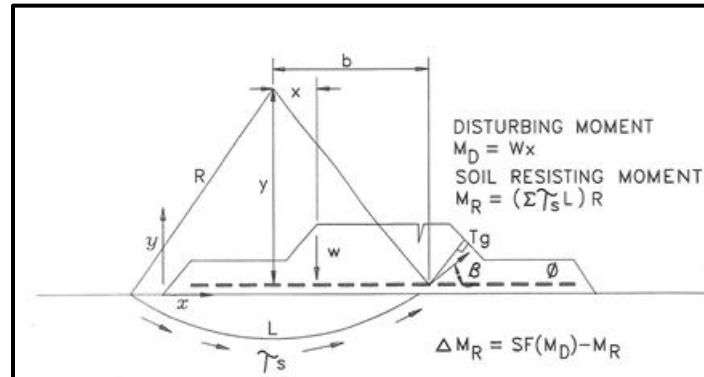


**Figure 17-26, Rotational Failure Model (Holtz, et al. (2008))**

Note:  $SF = 1/\phi$

Alternatively, instead of determining the required reinforcement strength, a suitable reinforcement strength from the available STSs may be used in the Rotational Shear Stability Check.

7. Sliding Block Stability Check – If the sliding block analysis indicates a resistance factor greater than required, reinforcement of the slope is required (see Figure 17-24(c)). The embankment can fail in 2 ways, either rupture of the reinforcement or sliding of the embankment over the reinforcement. Determining the tensile strength of reinforcement ( $T_{1s}$ ) is required (Figure 17-27). The soil/geosynthetic adhesion,  $c_a$ , should be assumed to be 0.0 for extremely soft soils and low embankments. An adhesion value should be included with placement of all subsequent fills in staged embankment construction. In addition to checking for rupture, sliding of the embankment and the sliding of the embankment on top of the reinforcement should be checked (Figure 17-28).

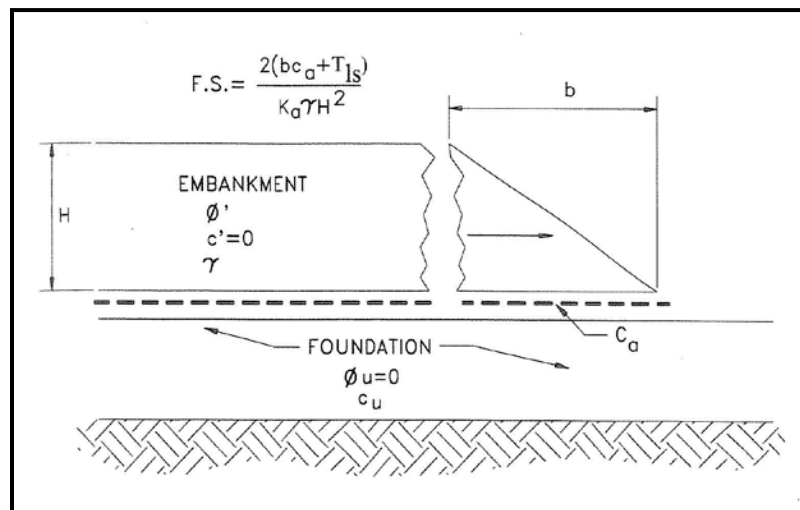


**Figure 17-27, Sliding Failure – Rupture of Reinforcement (Holtz, et al. (2008))**

Note:  $FS = 1/\phi$

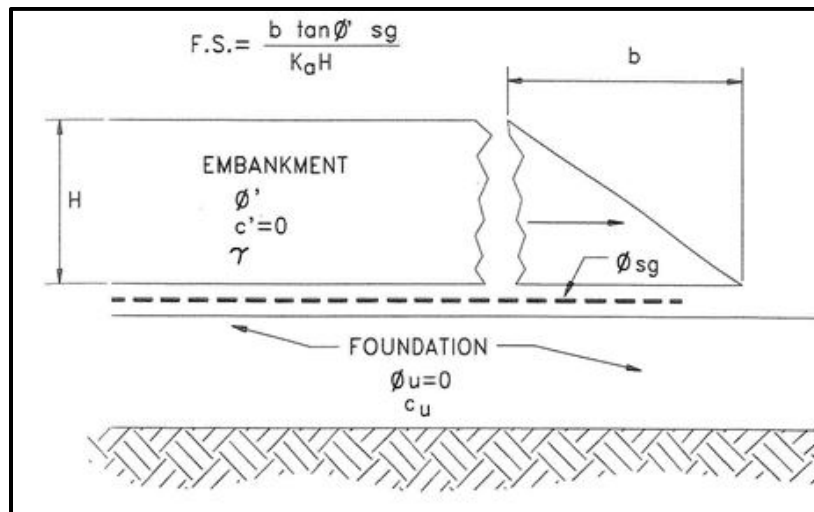


**Figure 17-28, Sliding Failure of Embankment over Reinforcement (Holtz, et al. (2008))**

Note: FS = 1/φ

Alternatively, instead of determining the required reinforcement strength, a suitable reinforcement strength from the available STSs may be used in the Sliding Block Stability Check.

The following steps are to be inserted between Steps 7 and 8 of the design methodology provided in Unreinforced Embankments, Section 17.13.1.

8. Establish Tolerable Geosynthetic Deformation – The deformation of the geosynthetic reinforcement is required to develop the tensile capacity required to prevent failure. The strain in the geosynthetic reinforcement is provided in the following equation.

$$\epsilon_{geosyn} = \frac{T_{ls}}{J} \quad \text{Equation 17-50}$$

Where,

$\epsilon_{geosyn}$  = Strain in the geosynthetic

Sand-Like Soils:  $\epsilon_{geosyn} = 5$  to 10 percent

Clay-Like Soils:  $\epsilon_{geosyn} = 2$  percent

Peats:  $\epsilon_{geosyn} = 2$  to 10 percent

$T_{ls}$  = Lateral spreading strength of reinforcement (required; not ultimate)

$J$  = Reinforcement Modulus

The maximum strain in the geosynthetic reinforcement will be approximately twice the average strain in the embankment. The  $\epsilon_{geosyn}$  shall be limited to 5 percent strain, since the available strength information for both geotextiles and geogrids is provided at 5 percent strain as well as at ultimate. Therefore,  $T_5$  shall be provided on the plans, where  $T_5$  is defined as the tension strength of a geosynthetic material at 5 percent strain. It is noted that  $T_5$  is not reduced using the Reduction Factors for Installation Damage, Creep nor Durability.

9. Establish Geosynthetic Strength Requirements – Most embankments are relatively long and narrow in shape. Thus, during construction, stresses are imposed on the geosynthetic in the longitudinal direction (i.e., along the direction of the centerline).

Reinforcement may also be required for loadings that occur at bridge abutments, and due to differential settlements and embankment bending, especially over nonuniform foundation conditions and at the edges of soft soil deposits, because both rotational and sliding block failures are possible in the direction along the alignment of the embankment. This determines the longitudinal strength requirements of the geosynthetic. Because the usual placement of the geosynthetic is in strips perpendicular to the centerline, the longitudinal stability will be controlled by the strength of the transverse seams.

10. Selection of Geosynthetic Reinforcement – Once the geosynthetic strength requirements are established, the geosynthetic reinforcement should be selected that meets the required strength and deformation (strain) requirements.
12. Establish Construction Sequence and Procedures – An example of the construction sequence of a reinforced embankment over soft ground is provided in Figure 17-29. In addition, Figures 17-30 and 17-31 depict the placement of fill over soft ground and over firmer ground, respectively. Figure 17-32 provides an example of reinforcement placement for a widened embankment.
13. Establish Construction Observation Requirements – Modify Item 10 of Section 17.13.1, Establish Construction Observation Requirements presented previously by adding the following:
  - a. The geosynthetic is not damaged during construction

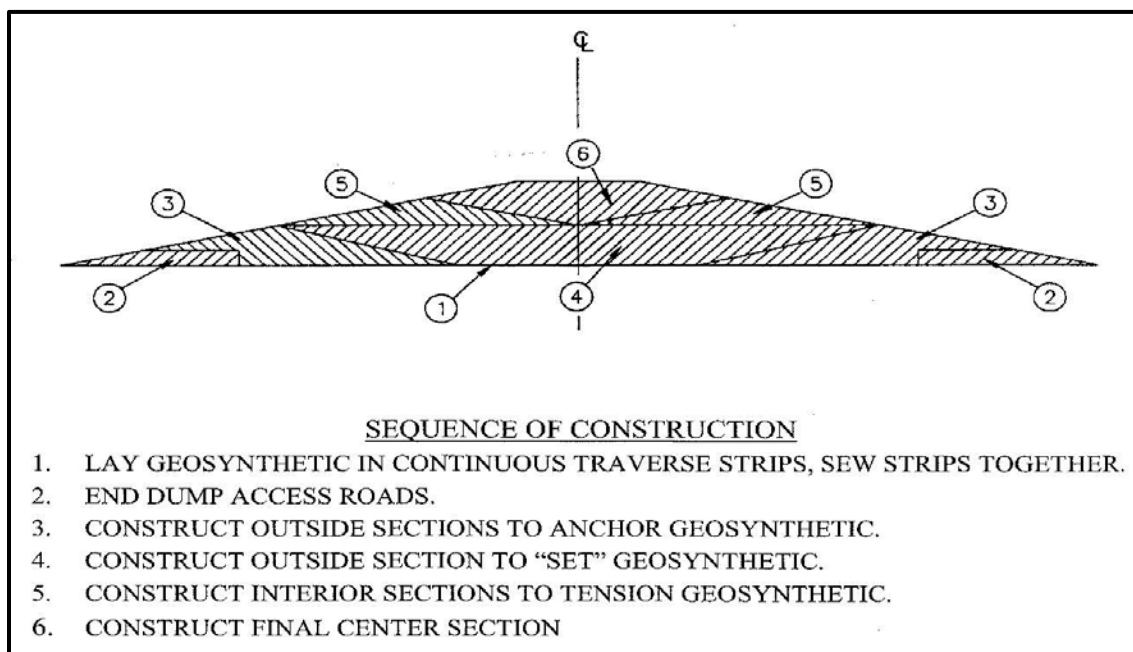


**Figure 17-29, Reinforced Embankment Construction Sequence over Soft Ground (Holtz, et al. (2008))**



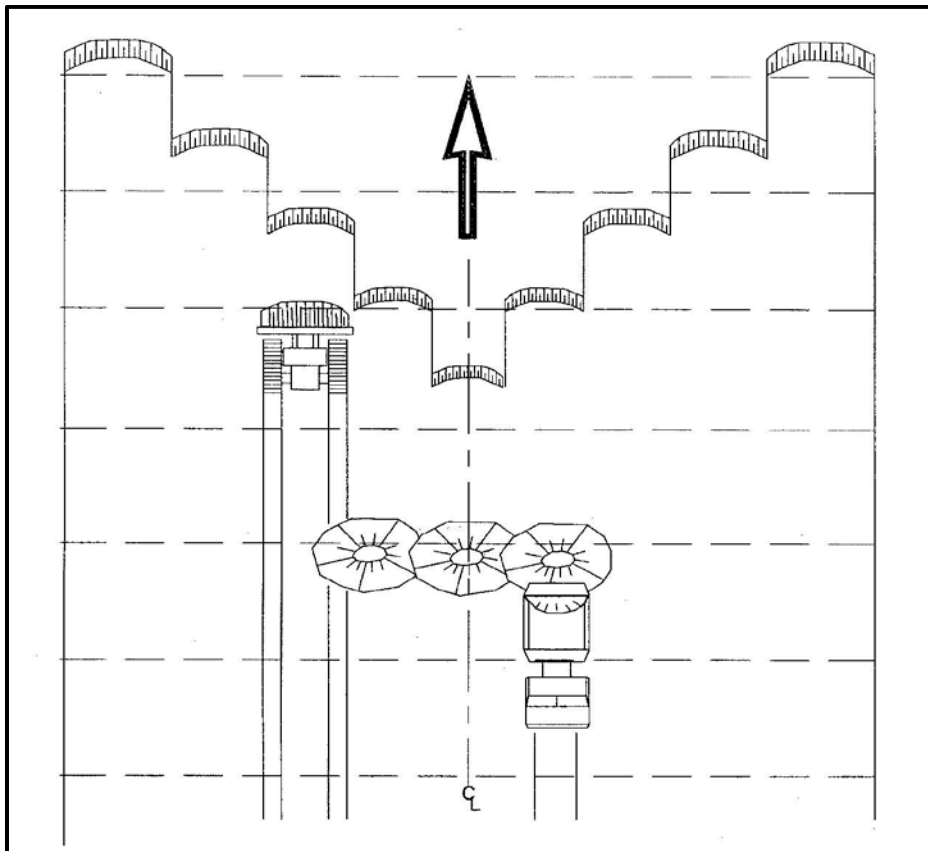


**Figure 17-30, Fill Placement over Soft Ground  
(Holtz, et al. (2008))**

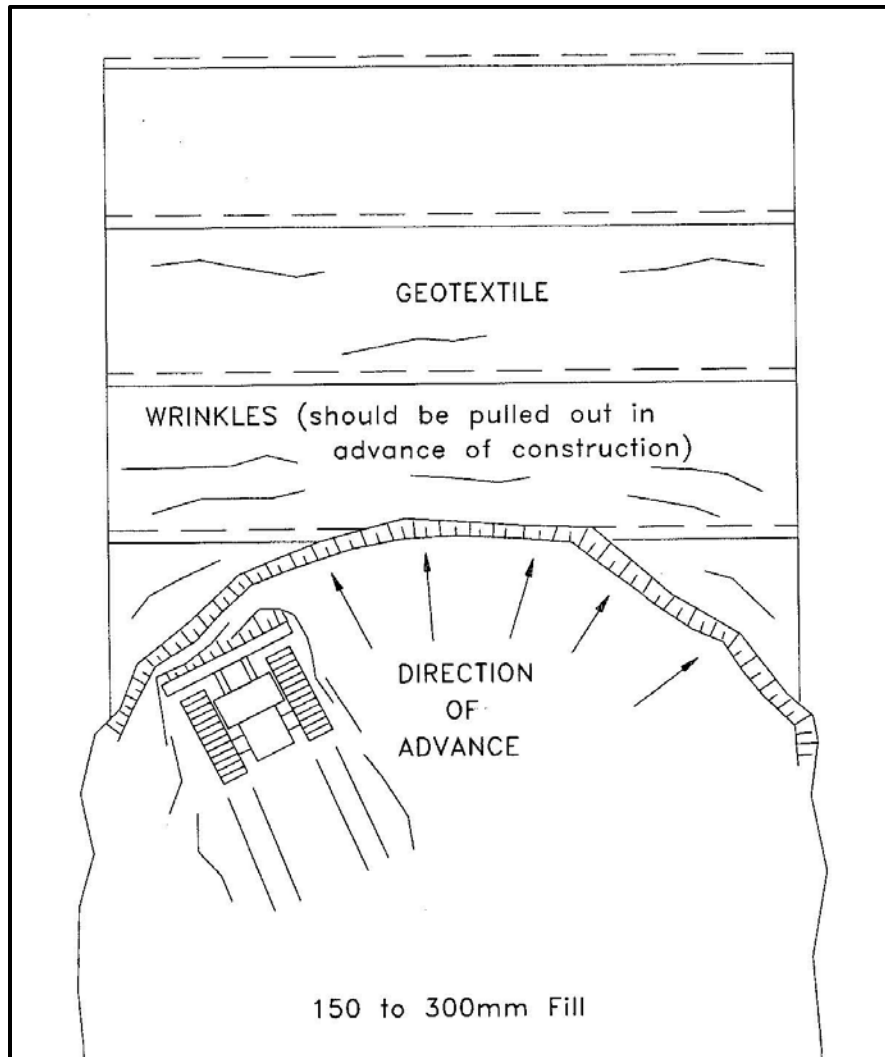


**Figure 17-31, Fill Placement over Firm Ground (Holtz, et al. (2008))**

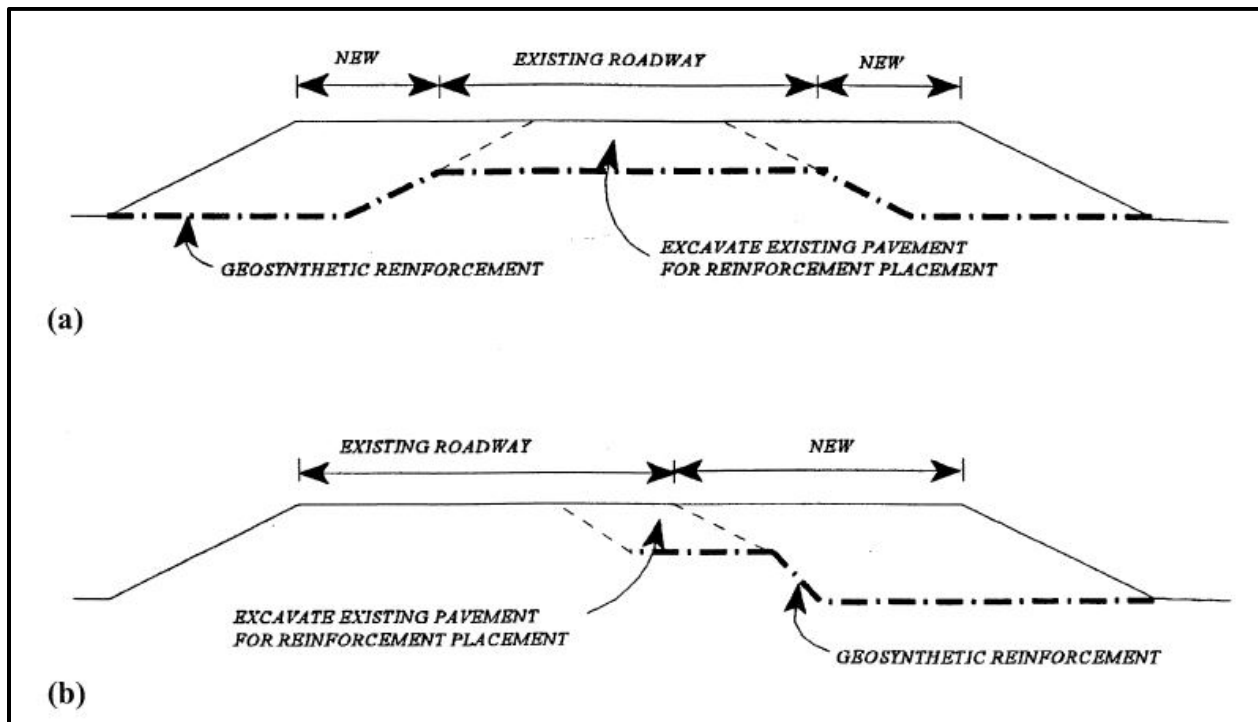
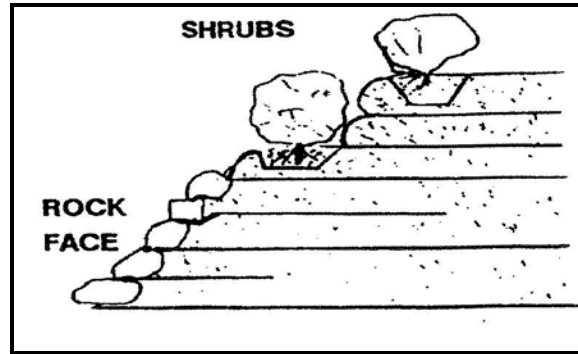


Figure 17-32, Geosynthetic Reinforcement Placement for Widened Embankments (Holtz, et al. (2008))

### 17.13.3 Reinforced Soil Slopes

RSSs have slopes ranging from equal to 1H:1V to 70°, require reinforcement to maintain stability and require select backfill materials for construction. Appendix D and the SCDOT STS entitled *Reinforced Soil Slopes* (SC-M-206-1) shall be consulted for the gradation requirements of the select backfill materials. RSSs consist of reinforcement arranged in horizontal planes in the reinforced mass to resist the outward movement of this mass. The reinforcement allows the reinforced mass to act more rigidly than in an unreinforced soil slope. Facing treatments can range from vegetated to flexible armor systems that are applied to prevent unraveling and sloughing off of the face (see Figure 17-33). Roadway embankment RSSs shall only be designed for the Service/Strength limit state condition and shall have both slope stability analyses as well as settlement analyses performed. Bridge embankment RSSs shall be designed for both the Service/Strength and EE limit states. All RSS embankments shall meet the Performance Objectives and Performance Limits as established in Chapter 10 for the appropriate limit state. Appendix D contains detailed design methodologies for RSSs. Table 17-14 provides the design steps that are used in the design of RSS.



**Figure 17-33, Reinforced Soil Slope  
(Berg, Christopher, and Samtani (2009))**

**Table 17-14, RSS Design Steps  
(modified from Berg, Christopher, and Samtani (2009))**

Step	Action
1	Establish project requirements including all geometry, external loading conditions (transient and/or permanent, seismic, etc.), performance criteria and construction constraints.
2	Evaluate existing topography, site subsurface conditions, and in-situ soil/rock parameters.
3	Determine properties of available fill materials.
4	Evaluate design parameters for the reinforcement.
5	Check unreinforced stability.
6	Design reinforcement to provide stable slope.
7	Determine type of reinforcement.
8	Check external stability (static and seismic): <ul style="list-style-type: none"> <li>• Bearing capacity</li> <li>• Settlement</li> <li>• Rotational slope stability</li> <li>• Sliding slope stability</li> </ul>
9	Evaluate requirements for subsurface and surface water control.
10	Establish construction: <ul style="list-style-type: none"> <li>• Sequence and procedures</li> <li>• Observation requirements</li> </ul>

The overall design of RSSs is similar to unreinforced slopes. However, there are 3 possible modes of slope failure (see Figure 17-34):

- I. Internal – failure plane passes through reinforced soil mass
- II. External – failure plane passes behind and underneath reinforced soil mass
- III. Compound – failure plane passes behind and through reinforced soil mass

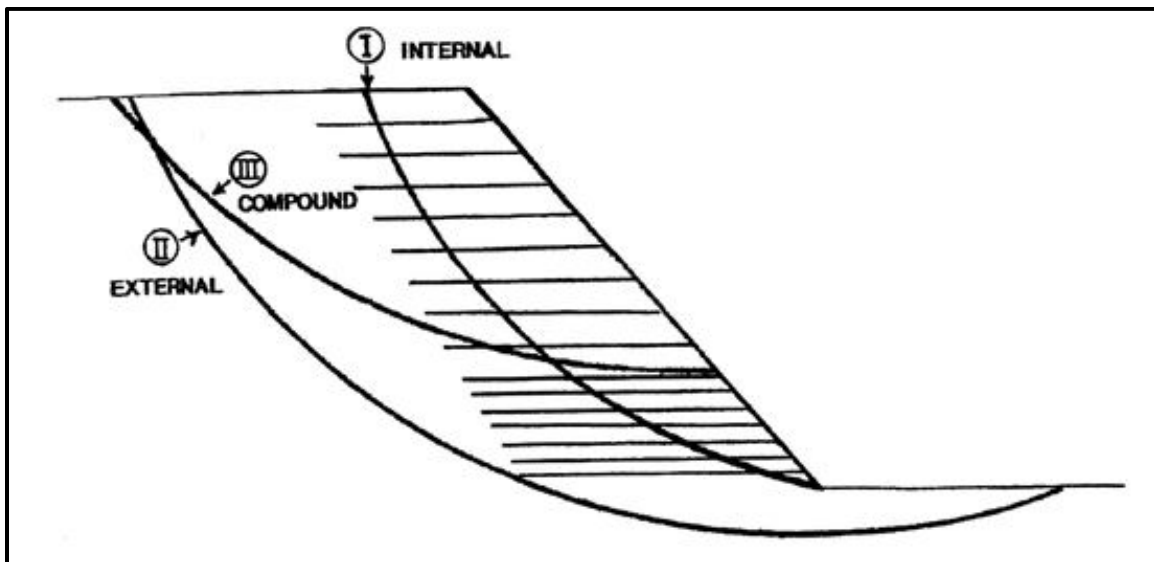
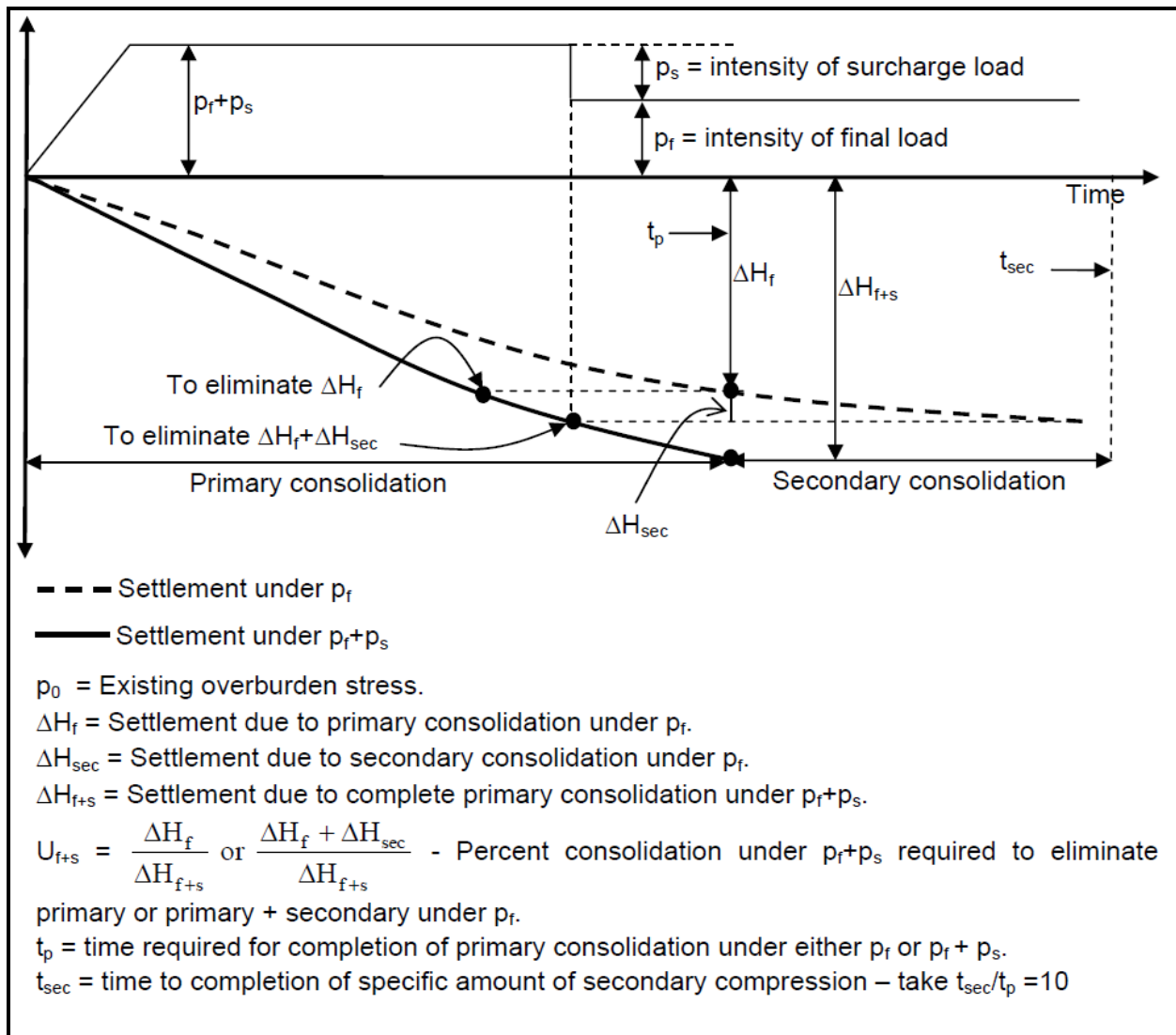


Figure 17-34, Reinforced Soil Slope Failure Modes  
(Berg, Christopher, and Samtani (2009))

#### 17.13.4 Vertical Stage Construction

As indicated previously, the placement of embankments over very soft to soft Clay-Like soils may require vertical staging of the construction to prevent instability. The instability is caused by the low shear strength of the Clay-Like soil and the increase in excess pore pressures. The increase in pore pressures lowers the undrained shear strength of the soil; however, with the dissipation of the excess pore pressures, the effective strength of the soil will increase. Therefore, vertical staging can be used to increase the soil shear strength by placing a stage (thickness) of soil over the soft Clay-Like soil and allowing the excess pore pressures to dissipate (waiting period). Determine  $\phi_{temp}$  at the end of each vertical stage (i.e., immediately after the completion of fill placement, but prior to the dissipation of any pore pressures) for both lateral squeeze and for slope stability using a total stress approach. The completion of placement of each stage is critical; since this is when instability is most likely to occur (i.e., the soil shear strength has not increased). Determine  $\phi_{final}$  again at the completion of waiting period (i.e., once the excess pore pressures have dissipated), but prior to the placement of any additional fill materials, for both lateral squeeze and slope stability. Then the next stage can be placed. This process can be repeated until the final height of the embankment is achieved. Further additional soil materials (i.e., surcharge) may be added to the embankment height to increase the loading and thus reducing the time to achieve the required settlement. Settlement at each stage will also occur as the excess pore pressures dissipate (see Figure 17-35). Therefore, consolidation testing is required to determine the time rate of settlement, as well as the magnitude of total settlement, that is anticipated for each stage as well as the full embankment. If the time rate of settlement indicates that the waiting periods are too long, then prefabricated vertical (wick) drains may be used to increase the time to complete settlement. The increase in shear strength is a function of the Degree of Consolidation ( $U$ ). Provided below are equations based on Ladd (1991) and Ladd and Foott (1974) relating the increase in undrained shear strength to  $U$ .



**Figure 17-35, Staged Construction Schematic (McVay and Nguyen (2004))**

$$\Delta c_u = U_t * [\Delta \sigma * \tan(\phi_{cu})] \quad \text{Equation 17-51}$$

Alternately,

$$\Delta c_u = U_t * \left[ \Delta \sigma * \left( \frac{\tau}{\sigma'_{vo}} \right) \right] \quad \text{Equation 17-52}$$

Where,

$$\tan(\phi_{cu}) = \frac{\tau}{\sigma'_{vo}} = 0.23 * (OCR)^{0.8} \quad \text{Equation 17-53}$$

Where,

- $\Delta c_u$  = Increase in undrained cohesion
- $U_t$  = Degree of consolidation at a specific time (enter as decimal)
- $\Delta \sigma$  = Increase in applied vertical stress
- $\phi_{cu}$  = Consolidated undrained internal friction angle

- $\tau$  = Undrained Shear Strength  
 $\sigma'_{vo}$  = Vertical effective overburden stress  
OCR = Overconsolidation Ratio (see Chapter 7)

The soil shear strength and consolidation parameters should be determined in accordance with the procedures outlined in Chapter 7. See Chapter 19 for information concerning prefabricated vertical drain design. The stability of the embankment should be monitored using the instrumentation described in Chapter 25.

## 17.14 PLANS

This Section details the information that should be placed on construction drawings related to embankment construction. For an unreinforced embankment, no information is required in the construction drawings. If project specific shear strength is required for the borrow materials that exceeds both the on-site shear strength parameters and the county maximum shear strength value, then a Special Provision shall be prepared (see Chapter 7). The GEOR is reminded that the use of a Special Provision will require a 60-day advertisement for construction. The requirements for plans for reinforced embankments and RSSs are contained in Chapter 22 and Appendix D.

## 17.15 REFERENCES

American Association of State Highway and Transportation Officials, (2017), AASHTO LRFD Bridge Design Specifications Customary U.S. Units, 8<sup>th</sup> Edition, American Association of State Highway and Transportation Officials, Washington, D.C.

Berg, R. R., Christopher, B. R., and Samtani, N. C., (2009), Design of Mechanically Stabilized Earth Walls and Reinforced Soil Slopes – Volume II, (Publication No. FHWA NHI-10-025; FHWA GEC 11 – Volume II), National Highway Institute, Federal Highway Administration, U.S. Department of Transportation, Washington D.C.

Bowles, J. E., (1986), Foundation Analysis and Design, Fifth Edition, The McGraw-Hill Companies, Inc.

Briaud, J.-L. and Miran, J., (1992), The Flat Dilatometer Test, (Publication No. FHWA-SA-91-044), Office of Technology Applications, Federal Highway Administration, U.S. Department of Transportation, Washington D.C.

Christian, J. T. and Carrier III, W. D., (1978), “Janbu, Bjerrum and Kjaernsli’s Chart Reinterpreted,” Canadian Geotechnical Journal, Volume 15, Issue No. 1, pp 123 - 128.

Collin, J. G., Leshchinsky, D., and Hung, C.-J. J., (2005), Soil Slope and Embankment Design – Reference Manual, (Publication No. FHWA NHI-05-123), National Highway Institute, Federal Highway Administration, U.S. Department of Transportation, Washington D.C.

Das, B. M., (1990), Principles of Foundation Engineering, 2<sup>nd</sup> Edition, PWS-Kent Publishing Company, Boston, Massachusetts.

DeMarco, M., Bush, P., Samtani, N. C., Kulicki, J. M., and Severns, K., (2015), Draft - Incorporation of Foundation Deformations in AASHTO LRFD Bridge Design Process, 2<sup>nd</sup> Strategic Highway Research Program (SHRP2), Transportation Research Board, The National Academies of Sciences, Engineering, and Medicine, Washington, D.C.

Department of Defense, Department of the Army, Army Corps of Engineers (USACE), (1990), Settlement Analysis, EM 1110-1-1904, Washington D.C.

Department of Defense, Department of the Army, Army Corps of Engineers (USACE), (2003), Slope Stability, EM 1110-2-1902, Washington D.C.

Department of Defense, Department of the Navy, Naval Facilities Engineering Command (NACFAC), (1982), Soil Mechanics – Design Manual 7.1, Publication No. NAVFAC DM-7.1, Alexandria, Virginia.

Duncan, J. M. and Buchignani, A. L., (1976), *An Engineering Manual for Settlement Studies*, University of California at Berkeley, Berkeley, California.

Duncan, J. M., Wright, S. G., and Brandon, T. L., (2014), Soil Strength and Slope Stability, 2<sup>nd</sup> Edition, John Wiley & Sons, Inc., New Jersey

Hough, B. K., (1959), "Compressibility as the Basis for Soil Bearing Values," Journal of Soil Mechanics and Foundations Division, ASCE, Vol. 84, No. SM 4, August, pp 10 - 39.

Ladd, C. C., (1991), "Stability Evaluation During Staged Construction," Journal of Geotechnical Engineering, ASCE, Vol. 117, No. 4, April, pp 540 - 615.

Ladd, C. C. and Foott, R., (1974), "New Design Procedure for Stability of Soft Clays," Journal of the Geotechnical Engineering Division, ASCE, Vol. 100, No. GT7, July, pp 763 - 786.

McVay, M. C. and Nugyen, D., (2004), Evaluation of Embankment Distress at Sander's Creek – SR20, BC 354, RPWO# 17, Department of Civil and Coastal Engineering, University of Florida, Gainesville, FL.

Meyerhof, G. G. (1965), "Shallow Foundations," Journal of the Soil Mechanics and Foundations Division, ASCE, Vol. 91, No. SM 2.

Munfakh, G., Arman, A., Collin, J. G., Hung, C.-J. J., and Brouillette, R. P., (2001), Shallow Foundations – Reference Manual, (Publication No. FHWA NHI-01-023), National Highway Institute, Federal Highway Administration, U.S. Department of Transportation, Washington D.C.

Munfakh, G., Wylie, D., and May, C. W., (1998), Rock Slopes – Reference Manual, (Publication No. FHWA-HI-99-007), National Highway Institute, Federal Highway Administration, U.S. Department of Transportation, Washington D.C.

Newmark, N. M., (1935), "Simplified Computation of Vertical Pressures in Elastic Foundations", *University of Illinois Engineering Experiment Station Circular 24*, University of Illinois, Urbana, Illinois, <http://hdl.handle.net/2142/49868>.

Osterberg, J. O. (1957), "Influence Values for Vertical Stresses in a Semi-infinite Mass Due to an Embankment Loading," *Proceedings of the Fourth International Conference on Soil Mechanics and Foundation Engineering*, London, England.

Samtani, N. C. and Nowatzki, E. A., (2006), Soils and Foundations Reference Manual – Volume I, (FHWA Publication No. FHWA-NHI-06-088), National Highway Institute, Federal Highway Administration, U.S. Department of Transportation, Washington D.C.



Schmertmann, J. H. (1970), "Static Cone to Compute Static Settlement Over Sand," Journal of Soil Mechanics and Foundations Division, ASCE, Vol. 96, No. SM 3, May, pp 1011 - 1043.

Spencer, E. (1967), "A Method of Analysis of the Stability of Embankments Assuming Parallel Inter-Slice Forces", *Geotechnique*, Vol. 17, Issue 1, pp. 11-26.

Terzaghi, K. and Peck, R., (1967), Soil Mechanics in Engineering Practice, 2<sup>nd</sup> Edition, John Wiley & Sons.

Timoshenko, M. J. and Goodier, J. N., (1951), Theory of Elasticity, 2<sup>nd</sup> Edition, McGraw-Hill Book Company, Inc.

USGS (United States Geologic Survey), (2004), Landslide Types and Processes, Fact Sheet 2004-3072, <http://pubs.usgs.gov/fs/2004/3072/pdf/fs2004-3072.pdf>, U.S. Department of the Interior, Washington, D.C.

Wright, S. G. (1969), "A Study of Slope Stability and the Undrained Shear Strength of Clay Shales," thesis presented to the University of California at Berkeley, California, in partial fulfillment of requirements for degree of Doctor of Philosophy.

**Chapter 18**  
**EARTH RETAINING  
STRUCTURES**

**GEOTECHNICAL DESIGN MANUAL**

*January 2019*



## Table of Contents

<u>Section</u>	<u>Page</u>
18.1 Introduction.....	18-1
18.2 Earth Retaining Structure Classification.....	18-2
18.2.1 Load Support Mechanism Classification.....	18-2
18.2.2 Construction Concept Classification.....	18-3
18.2.3 System Rigidity Classification.....	18-3
18.2.4 Service Life Classification.....	18-3
18.3 LRFD ERS Design.....	18-3
18.4 ERS Selection Philosophy.....	18-5
18.4.1 Necessity for ERS.....	18-6
18.4.2 Site Constraints and Project Requirements.....	18-7
18.4.3 Factors Affecting ERS Selection.....	18-8
18.4.4 Evaluate ERS Alternates.....	18-9
18.4.5 Selection of Acceptable ERS Type.....	18-12
18.5 Earth Pressure Theory.....	18-13
18.5.1 Active Earth Pressure.....	18-15
18.5.2 At-Rest Earth Pressure.....	18-18
18.5.3 Passive Earth Pressure.....	18-18
18.5.4 Determination of Earth Pressures.....	18-19
18.6 Rigid Gravity Earth Retaining Structures.....	18-21
18.6.1 Gravity Retaining Walls.....	18-21
18.6.2 Semi-Gravity Retaining Walls.....	18-22
18.6.3 Modular Gravity Walls.....	18-23
18.6.4 Rigid Gravity Wall Design.....	18-23
18.7 Flexible Gravity Earth Retaining Structures.....	18-24
18.8 Cantilever Earth Retaining Structures.....	18-25
18.9 In-Situ Reinforced Earth Retaining Structures.....	18-28
18.10 Hybrid Walls.....	18-29
18.11 Temporary Walls.....	18-30
18.12 References.....	18-31

**List of Tables**

<b><u>Table</u></b>	<b><u>Page</u></b>
Table 18-1, Cut Wall Evaluation Factors .....	18-6
Table 18-2, Fill Wall Evaluation Factors .....	18-7
Table 18-3, ERS Importance Selection Factors (ISF) .....	18-8
Table 18-4, Weighted ERS Selection Factors.....	18-9
Table 18-5, Wall Selection Matrix .....	18-13
Table 18-6, Required Relative Movements To Reach $P_A$ or $P_P$ .....	18-15
Table 18-7, Gravity Wall Types .....	18-21
Table 18-8, Rigid Gravity Wall Design Steps.....	18-24
Table 18-9, MSE Wall Design Steps .....	18-25
Table 18-10, Cantilevered Wall Design Steps .....	18-26
Table 18-11, Anchored Cantilevered Wall Design Steps .....	18-27
Table 18-12, Soil Nail Wall Design Steps .....	18-29

**List of Figures**

<b><u>Figure</u></b>	<b><u>Page</u></b>
Figure 18-1, Retaining Wall Schematic.....	18-1
Figure 18-2, ERS Classification Chart .....	18-2
Figure 18-3, Construction-Point Concept.....	18-4
Figure 18-4, Wall Selection Flow Chart .....	18-6
Figure 18-5, Relative Magnitude of Displace. Required to Develop Earth Pressures	18-14
Figure 18-6, Effects of Wall Movement on Static Horizontal Earth Pressures .....	18-15
Figure 18-7, Coulomb Active Earth Pressures.....	18-17
Figure 18-8, Coulomb Active Earth Pressures.....	18-17
Figure 18-9, Coulomb Passive Earth Pressures .....	18-19
Figure 18-10, Gravity Retaining Wall.....	18-22
Figure 18-11, Semi-Gravity Retaining Wall.....	18-22
Figure 18-12, Gabion Retaining Wall.....	18-23
Figure 18-13, In-Situ Structural Walls.....	18-26
Figure 18-14, Wall Support Systems .....	18-27
Figure 18-15, MSE Wall .....	18-24
Figure 18-16, In-Situ Reinforced (Soil Nail) Walls.....	18-28
Figure 18-17, Hybrid Wall – Cantilever Concrete under MSE Wall .....	18-30
Figure 18-18, Compound Slope – Slope Above and Below ERS .....	18-30



# CHAPTER 18

## EARTH RETAINING STRUCTURES

### 18.1 INTRODUCTION

ERSs are used to retain earth materials while maintaining a grade change between the front and rear of the wall (see Figure 18-1). ERSs transmit the loads ( $Q_1$ ,  $Q_2$ , and  $p_1$ ) to the base and to a possible internal stability reinforcement element ( $p_2$  and  $p_3$ ) to maintain stability. Typically, ERSs are expensive when compared to embankments; therefore, the need for an ERS should be carefully considered in preliminary design. An effort should be made to keep the retained soil height to a minimum. ERSs are used to support cut and fill slopes where space is not available for construction of flatter more stable slopes (see Chapter 17). Bridge abutments and foundation walls are designed as ERSs since these structures are used to support earth fills.

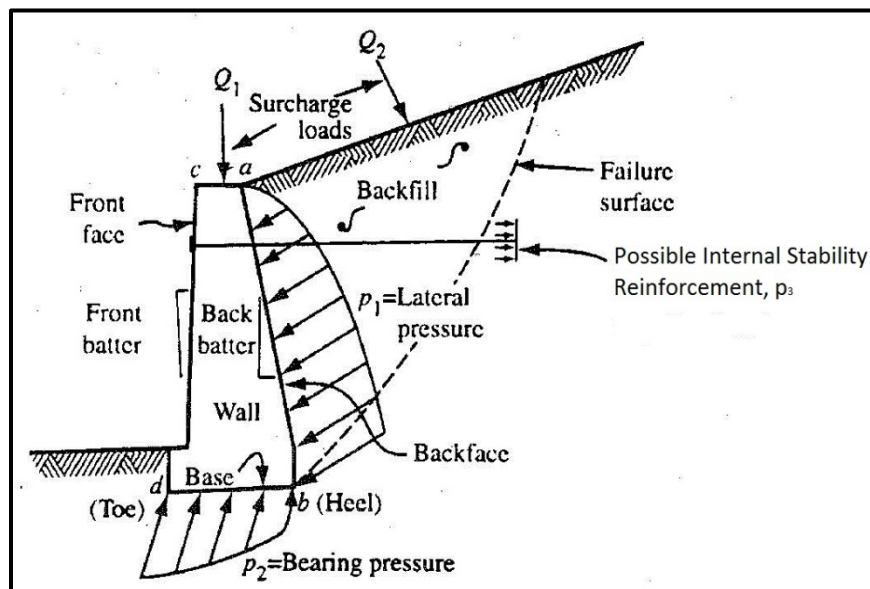


**Figure 18-1, Retaining Wall Schematic  
(modified Tanyu, Sabatini, and Berg (2008))**

According to Tanyu, et al. (2008), ERSs are typically used in highway construction for the following applications:

- New or widened highways in developed areas
- New or widened highways at mountains or steep slopes
- Grade separations
- Bridge abutments, wing walls and approach embankments
- Culvert walls
- Tunnel portals and approaches
- Flood walls, bulkheads and waterfront structures
- Cofferdams for construction of bridge foundations
- Stabilization of new or existing slopes and protection against rockfalls
- Groundwater cut-off barriers for excavations or depressed roadways



## 18.2 EARTH RETAINING STRUCTURE CLASSIFICATION

There are 4 criteria for classifying an ERS:

- Load support mechanism (externally or internally stabilized walls)
- Construction concept (fill or cut)
- System rigidity (rigid or flexible)
- Service life (permanent or temporary)

All ERSs are classified using all 4 of the criteria listed above; however, the service life is not normally used since most ERSs are designed as permanent and are expected to have a minimum service life of 100 years. For example, a soldier pile and lagging wall is classified as an externally stabilized flexible cut wall, while a soil nail wall is an internally stabilized flexible cut wall. The design of temporary ERSs is discussed at the end of this Chapter. Therefore, the intermediate Sections are concerned with the design of permanent ERSs. Figure 18-2 provides a partial representation of the classification of permanent ERSs; this Figure is partial in that it does not include all of the possible types of walls available.

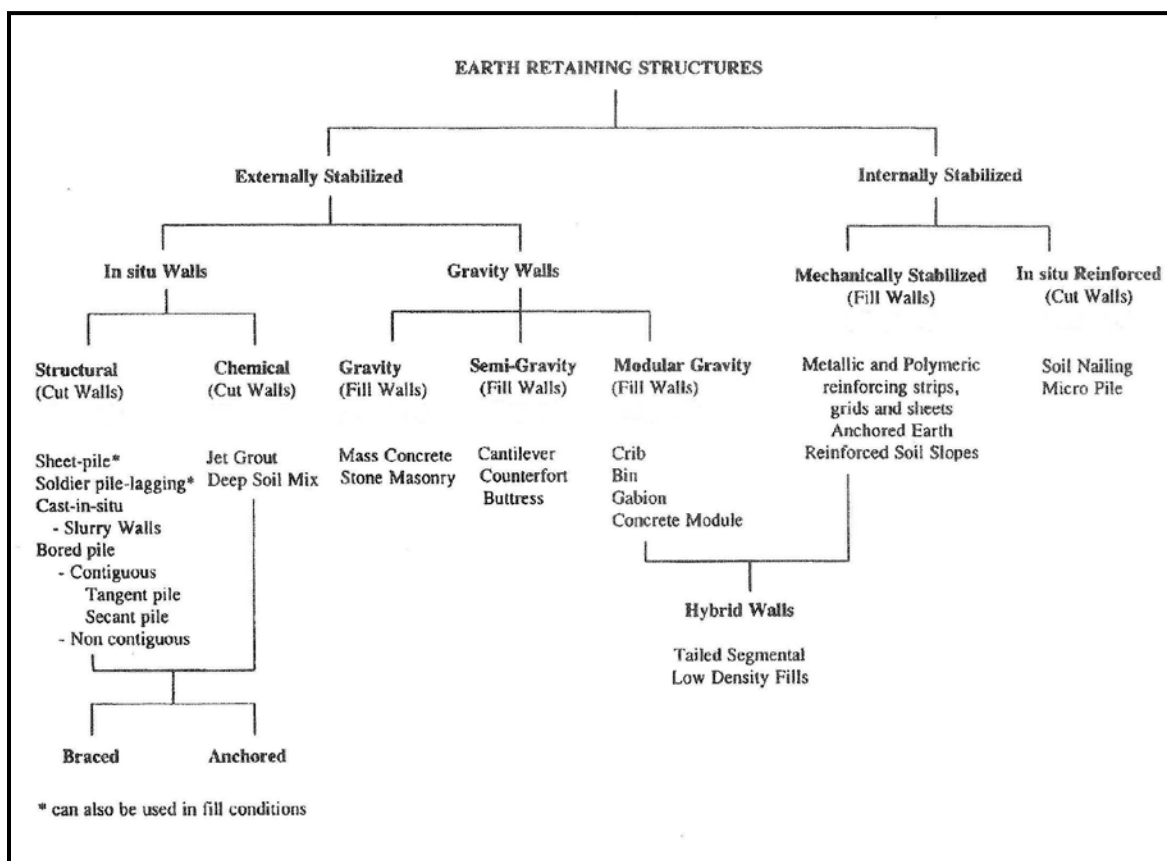


Figure 18-2, ERS Classification Chart  
(modified from Tanyu, et al. (2008))

### 18.2.1 Load Support Mechanism Classification

The load support mechanism classification is based on whether the ERS is stabilized externally or internally. Externally stabilized ERSs use an external structure against which the stabilizing forces are mobilized. Internally stabilized ERSs use reinforcements that are installed within the soil mass and extend beyond a potential failure surface to mobilize the stabilizing forces. A hybrid ERS may use both external and internal support mechanisms to achieve external stability. See Section 18.10 for more information regarding hybrid ERSs.

### **18.2.2 Construction Concept Classification**

ERSs are also classified based on the construction method used. The construction methods consist of fill or cut. Fill construction refers to an ERS that is constructed from the base to the top of the ERS (i.e., bottom-up construction). Conversely, cut construction refers to an ERS that is constructed from the top to the base of the ERS (i.e., top-down construction). It is very important to realize the cut or fill designations refer to how the ERS is constructed, not the nature of the earthwork. For example, a prefabricated bin wall could be placed in front of a “cut” slope, but the wall would be classified as a “fill” wall since the construction is from the bottom-up.

### **18.2.3 System Rigidity Classification**

The rigidity of the ERS is fundamental to understanding the development of the earth pressures that develop behind and act on the ERS. A rigid ERS moves as a unit (i.e., rigid body rotation and/or translation) and does not experience bending deformations. A flexible ERS undergoes not only rigid body rotation and/or translation, but also experiences bending deformations. In flexible ERSs, the deformations allow for the redistribution of the lateral (earth) pressures from the more flexible portion of the wall to the more rigid portion of the wall. Most gravity type ERSs would be considered an example of a rigid wall. Almost all of the remaining ERS systems would be considered flexible.

### **18.2.4 Service Life Classification**

The focus of this Chapter is on permanent ERS construction. According to Chapter 10, all geotechnical structures including ERS shall have a design life of 100 years. Temporary ERSs shall have a service life less than 5 years. Temporary ERSs that are to remain in service more than 5 years shall be designed as a permanent ERS. A more detailed explanation of temporary ERSs is provided at the end of this Chapter.

## **18.3 LRFD ERS DESIGN**

The design of ERSs is comprised of 2 basic components: external and internal. External design handles stability, sliding, eccentricity, and bearing; while internal design handles pullout failure of soil anchors or reinforcement and structural failure of the ERS. The external stability of an ERS is checked using the procedures outlined in Chapter 17. For ERSs supported by shallow foundations, sliding, eccentricity, and bearing are checked using Chapter 15, while those ERSs supported by deep foundations are checked using Chapter 16. All loads that affect the external stability of an ERS shall be developed using Chapter 8, as well as the procedures outlined in AASHTO LRFD Specifications (Section 11.5 – Limit States and Resistance Factors). Where there is conflict, this Manual takes precedence over the AASHTO LRFD Specifications. According to Tanyu, et al. (2008); “In general, use minimum load factors if permanent loads increase stability and use maximum load factors if permanent loads reduce stability.” The resistance factors shall be developed using Chapter 9 for Strength, Service, and Extreme Event limit states. Chapter 9 divides ERSs into three types of walls; Rigid Gravity, Flexible Gravity and Cantilever ERSs and provides examples of different types of common walls that fit within each group. In accordance with Chapter 8, the Service limit state is the boundary condition for performance of the structure under Service load conditions. The Service limit state is evaluated for the movements induced by the Service load combinations (see Chapter 8). The movements induced by the Service loads are compared to the Performance Objectives established in Chapter 10. Depending on the requirements of a particular project, the use of the Construction-

Point Concept may be used. Unlike traditional settlement calculations which assume the bridge or embankment is instantaneously placed, the Construction-Point Concept determines the settlement at specific critical construction points (see Figure 18-3). At the end of construction, the ERS shall have a front batter that either meets the Performance Objectives indicated in Chapter 10 or is vertically plumb.

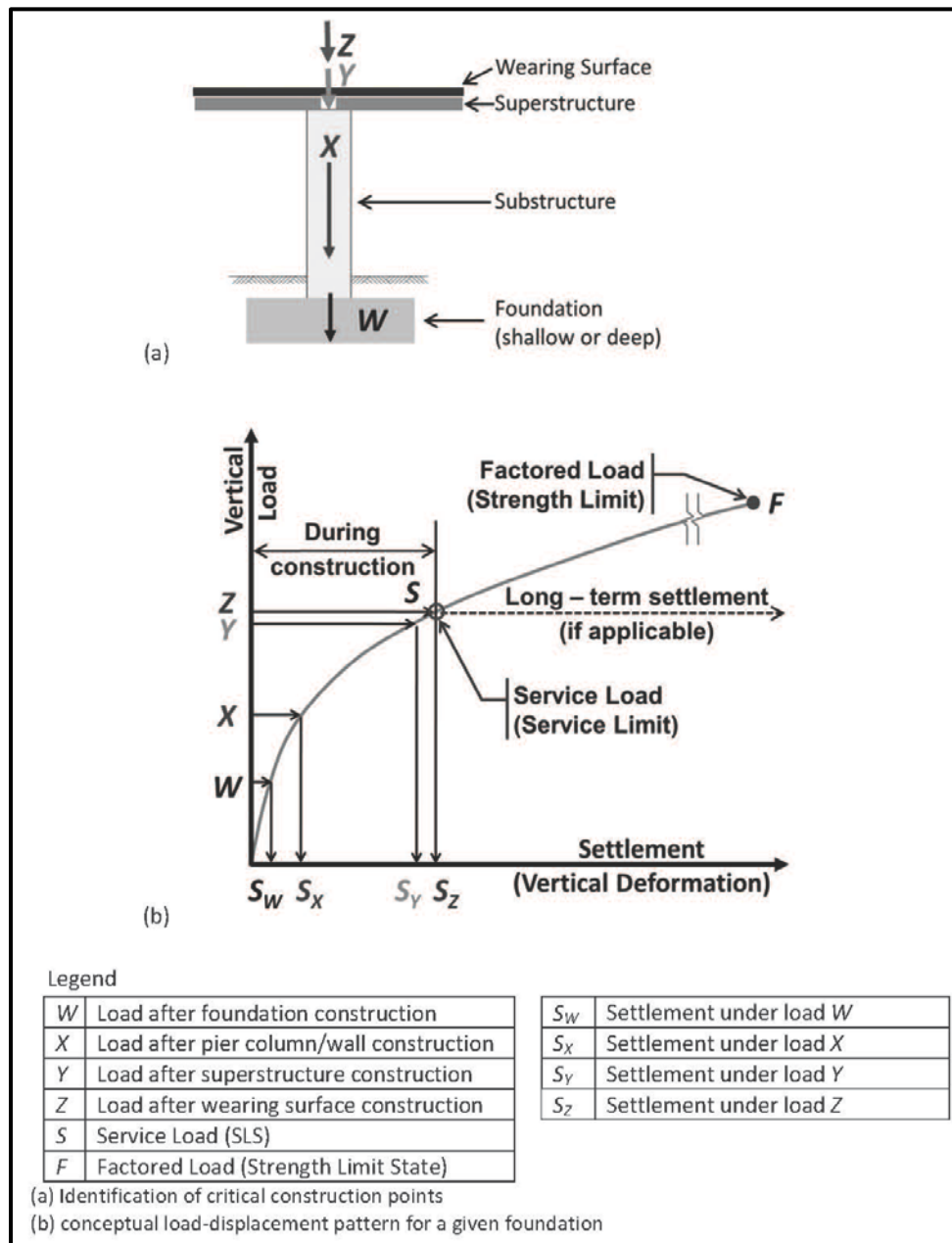


**Figure 18-3, Construction-Point Concept (DeMarco, Bush, Samtani, Kulicki and Severns (2015))**

All permanent ERSs shall have the external design performed by the GEOR regardless of the contracting method. If Procedural Based Construction is used, then the internal design shall be performed by the SEOR; however, if Performance-Based Construction is used, then the internal design shall be performed by the Contractor. According to Lazarte, et al. (2015),

Procedural Based Construction – "...includes the development of a detailed set of plans and specifications to be provided in the bidding documents. In this approach, complete

design details and specifications are developed so that each Contractor submitting a bid has a defined product to price, making it more straightforward ... to compare pricing.”

Performance-Based Construction – “...*SCDOT*: (i) prepares drawings defining the geometric and aesthetic requirements for the structure, and material specifications for the components, (ii) defines performance requirements including LRFD resistance factors (*Chapter 9*), ... and deformation limits (*Chapter 10*), and (iii) indicates the range of acceptable design and construction methods.”

ERSs comprised of internal support elements use the internal resistance factors as presented in Chapter 9.

Temporary ERSs shall use the Performance Based Construction method, with the Contractor performing both the internal as well as external design. The GEOR is required to determine the feasibility (i.e., proof of concept) of particular temporary wall. The GEOR should consult the Standard Specifications to determine the types of temporary ERSs allowed.

All ERS designs must meet the requirements of the basic LRFD equation,

$$Q = \sum \gamma_i * Q_i \leq \phi_n * R_n = R_r \quad \text{Equation 18-1}$$

Where,

Q = Factored Load

Q<sub>i</sub> = Force Effect

γ<sub>i</sub> = Load factor

R<sub>r</sub> = Factored Resistance

R<sub>n</sub> = Nominal Resistance (i.e., ultimate capacity)

φ<sub>n</sub> = Resistance Factor

#### 18.4 ERS SELECTION PHILOSOPHY

The selection of the type of ERS is based on numerous factors. It is possible for more than 1 ERS type to be applicable to a given site. Figure 18-4 provides a flow chart for determining the most appropriate type of wall for a specific location. Further, Tables 18-1 and 18-2 provide the most common cut and fill walls (see discussion above on ERS classification). The ERSs listed in Tables 18-1 and 18-2 contain walls that are typically used by *SCDOT* and walls that would be allowed. Written permission to use walls other than those indicated in these tables shall be obtained from the PC/GDS prior to designing the ERS. As indicated in Chapter 17 this same process shall be used to evaluate the applicability of reinforced embankments and RSSs at specific project site. Reinforced embankment or RSS may be substituted for ERS in following Subsections of this Section.

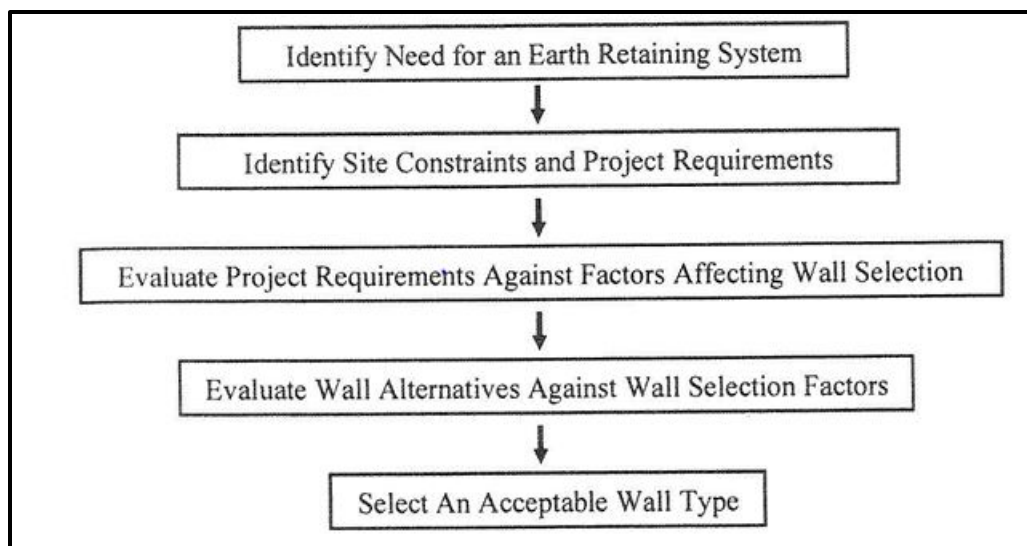


**Figure 18-4, Wall Selection Flow Chart (Tanyu, et al. (2008))**

**18.4.1 Necessity for ERS**

As indicated in Figure 18-4, the first step in selecting an ERS type is to determine if a wall is needed. According to the SCDOT Roadway Design Manual (RDM) (2017), the need for ERSs is determined jointly by the design team which includes an experienced geo-structural engineer. Typically, ERSs are required in areas where additional ROW cannot be obtained or there are other factors (i.e., other roads, major utilities, etc.) that limit the development of stable slopes. The need for ERSs can often be determined during the DFR. It is critical to identify the need for an ERS early on in the project development process.

**Table 18-1, Cut Wall Evaluation Factors (Tanyu, et al. (2008))**

	Wall Type	Application <sup>1</sup>	Height Range <sup>2</sup>	Required ROW <sup>2</sup>	Lateral Movements	Advantages	Disadvantages
CANTILEVERED	Sheet-pile	P/T	<16 ft	None	Large	- Rapid construction - Readily Available	- Difficult to construct in hard ground or penetrate obstructions
	Soldier Pile/Lagging	P/T	<16 ft	None	Medium	- Rapid construction - Soldier piles can be drilled or driven	- Difficult to maintain vertical tolerances in hard ground - Potential for ground loss at excavated face
	Anchored	P/T	15 - 70 ft	0.6H + abl <sup>3</sup>	Small-medium	- Can resist large horizontal pressures - Adaptable to varying site conditions	- Requires skilled labor and specialized equipment - Anchors may require permanent easements
IN-SITU REINFORCED	Soil-nailed	P/T	10 – 70 ft	1.0H	Small-medium	- Rapid construction - Adaptable to irregular wall alignment	- Nails may require permanent easements - Difficult to construct and design below water table
	Micropile	P	N/A	Varies	N/A	- Does not require excavation	- Requires specialty contractor

<sup>1</sup>P/T – Permanent and Temporary  
<sup>2</sup>Height range based on cost effectiveness  
<sup>3</sup>abl – Anchor Bond Length  
<sup>4</sup>ROW requirements expressed as the distance (as a fraction of wall height, H) behind the wall face where anchorage components are installed

**Table 18-2, Fill Wall Evaluation Factors  
(Tanyu, et al. (2008))**

	Wall Type	Application <sup>1</sup>	Height Range <sup>2</sup>	Required ROW <sup>3</sup>	Differential Settlement Tolerance	Advantages	Disadvantages
RIGID GRAVITY	Gravity <sup>4</sup>	P	3 – 10 ft	0.7H	1/500	- Durable - Requires smaller quantity of select backfill as compared to MSE walls - Can meet aesthetic requirements	- Deep foundation support may be necessary - Relatively long construction time
	Cantilever <sup>4</sup>	P	6 – 30 ft	0.7H	1/500	- Durable - Requires smaller quantity of select backfill as compared to MSE walls - Can meet aesthetic requirements	- Deep foundation support may be necessary - Relatively long construction time
	Counterfort <sup>4</sup>	P	30 – 60 ft	0.7H	1/500	- Durable - Requires smaller quantity of select backfill as compared to MSE walls - Can meet aesthetic requirements	- Deep foundation support may be necessary - Relatively long construction time
FLEXIBLE GRAVITY	Gabion	P/T	6 – 30 ft	0.7H	1/50	- Does not require skilled labor or equipment	- Need adequate source of stone - Construction of wall requires significant labor
	MSE Wall – precast facing	P/T	10 - 100 ft	1.0H	1/100	- Does not require skilled labor or equipment - Flexibility in choice of facing	- Requires use of select backfill - Subject to corrosion in aggressive environments (metallic reinforcement)
	MSE Wall – modular block facing	P/T	6 – 60 ft	1.0H	1/200	- Does not require skilled labor or equipment - Flexibility in choice of facing - Blocks are easily handled	- Requires use of select backfill - Subject to corrosion in aggressive environments (metallic reinforcement) - Positive reinforcement connection to blocks is difficult to achieve
	MSE Wall – geotextile / geogrid / welded wire facing	P/T	6 – 50 ft	1.0H	1/60	- Does not require skilled labor or equipment - Flexibility in choice of facing	- Facing may be unaesthetically pleasing - Geosynthetic reinforcement is subject to degradation in some environments
	MSE Wall – vegetated soil face	P/T	10 – 100 ft	1.0H	1/60	- Does not require skilled labor or equipment - Flexibility in choice of facing - Vegetation provides ultraviolet light protection to geosynthetic reinforcement	- Facing may be unaesthetically pleasing - Geosynthetic reinforcement is subject to degradation in some environments - Vegetated soil face requires significant maintenance

<sup>1</sup>P/T – Permanent and Temporary  
<sup>2</sup>Height range based on cost effectiveness  
<sup>3</sup>ROW requirements expressed as the distance (as a fraction of wall height, H) behind the wall face where anchorage components are installed  
<sup>4</sup>These walls are all constructed of cast-in-place concrete and/or standard brick and mortar

### 18.4.2 Site Constraints and Project Requirements

Once the need for an ERS is identified, then specific site constraints and project requirements need to be identified. Listed below are some items that will affect ERS selection. This list is not all inclusive.

1. Site accessibility and space restrictions
  - a. Limited ROW
  - b. Limited headroom
  - c. On-site material storage areas
  - d. Access for specialized construction equipment
  - e. Traffic disruption restrictions
2. Utility locations, both above and underground
3. Nearby structures
4. Aesthetic requirements
5. Environmental concerns
  - a. Construction noise
  - b. Construction vibration
  - c. Construction dust
  - d. On-site stockpiling, transport and disposal of excavated materials
  - e. Discharge of large volumes of water
  - f. Encroachment on existing waterways
6. Exposed wall face height

The relative importance of each of these items should be assessed by the design team for the specific project under consideration. This assessment should identify those items that should be given priority in the selection process.

### **18.4.3 Factors Affecting ERS Selection**

Step 3 from Figure 18-4 establishes the process for evaluating project requirements against fairly common factors that affect the selection of an ERS. Twelve importance selection factors (ISFs) have been identified and indicated in Table 18-3. The ISFs are listed in no particular order. Additional factors may be considered based on the requirements of the design team. Each factor is evaluated based on its relevancy and importance to the project requirements and site constraints. Each ISF is assigned an importance rating (IR) from 1, the least important, to 3, the most important. The GEOR shall provide a written justification for the selection of the IRs by the project team. Table 18-4 depicts an example of the ISFs and IR for each factor.

**Table 18-3, ERS Importance Selection Factors (ISF)  
(modified from Tanyu, et al. (2008))**

1	Ground type	7	Environmental concerns
2	Groundwater	8	Durability and maintenance
3	Construction considerations	9	Tradition
4	Speed of construction	10	Contracting practices
5	ROW	11	Cost
6	Aesthetics	12	Displacements (lateral and vertical)

**Table 18-4, Weighted ERS Selection Factors  
(modified from Tanyu, et al. (2008))**

Displace.	3
Cost	3
Contracting Practice	1
Tradition	3
Durability and Maintenance	2
Environmental Concerns	2
Aesthetics	1
ROW	1
Speed of Construction	3
Construction Considerations	2
Groundwater	2
Ground Type	3
ISF <sup>1</sup>	IR <sup>2</sup>

<sup>1</sup>Importance selection factor (ISF)  
<sup>2</sup>Importance rating of each ERS selection factor based on project requirements and site constraints. Each factor should be rated between 1, least importance factor, and 3, most important factor.

**18.4.4 Evaluate ERS Alternates**

The fourth step in selecting an ERS type consists of reviewing specific ERS types versus the Weighted ERS ISFs presented in the previous Section. A logical first step in this process is the elimination of ERS types that would be inappropriate for the specific project site. This elimination process should focus on project constraints such as ERS geometry and performance; however, the project constraints related to costs should not be included as a reason to eliminate an ERS type. In addition, the factors affecting cut (top-down construction) or fill (bottom-up construction) ERS selection should also be evaluated.



The selection issues discussed in this Section apply to permanent ERSs, selection issues for temporary cut walls are discussed later in this Chapter. Typically, permanent cut walls are designed with greater corrosion protection or with higher strength materials. In addition, these types of ERSs have permanent facing elements that consist of either cast-in-place concrete or precast concrete panels. Cut ERSs are typically either cut or drilled into the existing geomaterials at a site and require specialty contractors. If ground anchors are not required, then little or no ROW is required. However, if anchors or soil nails are used, then either additional ROW or permanent easements will be required. The taller a cut ERS becomes, the higher the unit cost of the ERS becomes. Depending on the geotechnical conditions, for ERS heights ranging from 15 to 30 feet or greater, either anchors or soil nails will be required. Cut ERSs typically used by SCDOT are provided in Table 18-1.

Fill ERSs are constructed from the bottom-up and are typically used for permanent construction. However, temporary MSE walls can also be constructed using flexible facing elements. Fill ERSs typically require more ROW than cut ERSs. Typically, the soil used for fill ERSs is comprised of Sand-Like geomaterials. The requirements for high quality fill materials typically increase the cost of fill ERSs. Fill ERSs typically used by SCDOT are provided in Table 18-2.

Those ERS systems not eliminated earlier in this step should be evaluated using the ERS ISFs and IRs previously established (see Table 18-3). Each ISF is assigned a suitability factor (SF). The SF is based on how suitable a particular wall type is considering the ISF and the importance of each ISF. SF ranges from 4, most suitable, to 1, least suitable. The determination of SF is very subjective; every effort should be made to avoid making a specific type of ERS appear suitable. Any cost associated with a selection factor should be considered when developing the rating. A brief description of each selection factor is provided in the following sections.

#### **18.4.4.1 Ground Type**

According to Tanyu, et al. (2008), “An *ERS* is influenced by the earth it is designed to retain, and the one on which it rests.” For example, ERSs that are internally supported (MSE walls and soil nail walls, etc.), the quality of the retained soil in which the reinforcement is placed is of great influence. For MSE walls, the pull-out force of the reinforcement is developed by the friction along the soil-reinforcement interface and any passive resistance that develops along transverse members of the reinforcement, if any are present. Typically, MSE walls require high quality granular fill materials with relatively high friction angles. Clay-Like soils are not used in MSE wall design or construction. For soil nail walls used to support excavations, the possible saturation and creep associated with Clay-Like soils can have a negative impact on the performance of the structure. For externally supported ERSs (gravity, semi-gravity, modular gravity and in-situ walls, etc.), the influence of the retained soil is less important. However, for soils that undergo large vertical and horizontal displacements, a flexible ERS (i.e., gabion) should be used in lieu of a more rigid ERS. A rigid ERS will attempt to resist the movements, thereby placing more stress on the structural members.

#### **18.4.4.2 Groundwater**

The groundwater table behind ERSs should be lowered for the following reasons:

1. To reduce the hydrostatic pressures on the structure
2. To reduce the potential for corrosion of metal reinforcing in the retained soil
3. To reduce the potential for corrosion of metal reinforcing in facing elements
4. To prevent saturation of the soil
5. To limit displacements that can be caused by saturated soils
6. To reduce the potential for soil migration through or from the ERS

Typically, fill ERSs are constructed with free-draining backfill, while the ERS face contains numerous weep holes or other means for water to be removed from behind the structure. Drainage media is also installed in cut walls. An SCDOT ERS shall never be designed to retain water/hydraulic forces. If the necessity for water/hydraulic forces retention is mandated on a project, the PC/GDS shall be contacted for instructions and guidance.

#### **18.4.4.3 Construction Considerations**

Construction considerations that need to be accounted for in the selection of an ERS are material availability, site accessibility, equipment availability and labor considerations. The availability of construction materials can affect selection of an ERS. For example, the use of a gabion wall in Charleston would be expensive since all stone for the gabion would have to be imported, while on the other hand a gabion wall in Cherokee County could be efficiently used. Limited site accessibility could limit the type of ERS that could be constructed. Another construction consideration is the requirement for specialized equipment and is the equipment locally or at least regionally available. The final construction consideration is the labor force to be used to build the wall (i.e., does the labor force require specialized training?).

#### **18.4.4.4 Speed of Construction**

Another factor to be considered is the speed at which the ERS can be constructed. The more rapidly an ERS can be constructed, the more rapidly the project can be completed.

#### **18.4.4.5 Right-of-Way**

The amount or need for additional ROW should be considered when selecting an ERS wall type. The question that needs to be asked is whether the ERS is being used to support the transportation facility or to support an adjacent owner. ERSs supporting the transportation facility should require limited to no additional ROW, while ERSs supporting an adjacent owner may require either additional ROW or an easement to install internally stabilizing reinforcements.

#### **18.4.4.6 Aesthetics**

Depending on the location of the ERS, the aesthetics of the wall can be of great importance in final selection. Typically, the aesthetics of wall is more important in populated areas than in non-, or limited, populated areas. In more environmentally sensitive areas, the ERS may need to blend in with the surrounding environment. This need for blending should be accounted for in ERS selection.

#### **18.4.4.7 Environmental Concerns**

ERSs can both cause, as well as alleviate, environmental concerns. ERSs cause environmental concerns if contaminated soil must be removed prior to or during the construction of the structure. In addition, noise and vibration from certain ERS wall installations can have a negative impact on the environment around the project. In addition, the fascia of some ERSs may allow for the bouncing or echoing of traffic noise; therefore, in cases where this may become a concern, an alternate fascia material may need to be selected. ERSs may alleviate environmental concerns by allowing for smaller footprints in environmentally sensitive areas; therefore, eliminating the need for environmental permits.

### 18.4.4.8 Durability and Maintenance

Depending on the environmental conditions (corrosiveness) of materials the ERS is founded on or is constructed of, certain ERS types may not be satisfactory. The ERS must meet design requirements and be durable for the life of the structure (100 years) or must have definitive maintenance procedures that will need to be identified. These maintenance procedures should also clearly indicate the time periods that maintenance should be performed.

### 18.4.4.9 Tradition

Tradition (i.e., what is normally done) can impact what type of ERS is selected. Traditionally, SCDOT uses the following wall types:

1. MSE
2. Cantilever (concrete)
3. Soil Nail
4. Sheetpile (cantilever or anchored)
5. Soldier pile and lagging (cantilever or anchored)
6. Gabion
7. Gravity

### 18.4.4.10 Contracting Practices

The use of sole source or patented ERSs should be avoided at all times. If sole source or patented ERSs cannot be avoided, a written justification is required. The written justification shall be maintained in the project file and shall include the endorsement (approval) of the RPE.

### 18.4.4.11 Cost

The total cost of the ERS should include the structure (structural elements; incidentals, including drainage items; and backfill materials, if any), ROW (acquisition or easement), excavation and disposal of unsuitable or contaminated materials, mitigation costs of environmental impacts (such as additional noise abatement) and the time value of construction delays. Credits for eliminating environmental permits or speeding up construction should also be factored into the decision.

### 18.4.4.12 Displacements

The amount of displacement (horizontal and vertical) that an ERS may be required to handle also affects the selection process. Some walls are more flexible than others. An idea of the amount of displacement that an ERS is anticipated to endure should also be known prior to making the final ERS selection.

## 18.4.5 Selection of Acceptable ERS Type

The final step in selecting an ERS is to determine the most acceptable type. This determination is made based on the IR and SF for each ISF. A weighted rating (WR) is developed as the product of IR and SF. A total weighted rating ( $WR_T$ ) is determined. The ERS type with the highest  $WR_T$  should be selected for the specific project site. Other highly scored walls may be included in the Contract Documents as acceptable alternatives. Table 18-5 provides an example of this process. The Wall Selection Matrix is available on the Geotechnical page of the SCDOT website; <https://www.scdot.org/business/geotech.aspx>.

$$WR_T = \sum_{i=1}^n (IR_i * SF_i) = \sum_{i=1}^n WR_i \quad \text{Equation 18-2}$$

**Table 18-5, Wall Selection Matrix  
(modified Tanyu, et al. (2008))**

ISF ERS Type		Total Weighted Rating (WR <sub>T</sub> )															
		IR	SF	WR	SF	WR	SF	WR	SF	WR	SF	WR					
MSE Wall – Precast Facing <sup>1</sup>		3	4	12	2	3	4	1	2	3	4	6	9	2	3	6	77
Gabion Wall <sup>1</sup>		3	4	9	2	3	4	1	2	3	4	6	9	2	3	6	62
Cast-in-place Concrete Gravity Wall <sup>1</sup>		3	4	12	2	3	4	1	2	3	4	6	9	2	3	6	58
RSS <sup>1</sup>		3	4	12	2	3	4	1	2	3	4	6	9	2	3	6	68

<sup>1</sup>SF for each ERS, RSS or reinforced embankment are based on project requirements and site constraints. Each SF should be rated between 1, least suitable, and 4, most suitable.

### 18.5 EARTH PRESSURE THEORY

Earth pressures act on the rear face of an ERS or an abutment wall, (ERS will used generically for the remainder of the Chapter and will include abutment walls as well as ERSs) and are caused by the weight of the soil (backfill or retained fill), seismic loads and various surcharge loads. The ERS is designed to resist these loads, as well as, any water (pore) pressures that may build up on the rear of the wall. There are 3 different lateral pressures used in the design of ERSs: active, at-rest and passive (see Chapter 2 for definitions).

The general horizontal earth pressure is expressed by the following equation.

$$\sigma_h = K * \sigma_v \quad \text{Equation 18-3}$$

Where,

$\sigma_h$  = Horizontal earth pressure at a specific depth on an ERS

K = Earth pressure coefficient

$\sigma_v$  = Vertical earth pressure (overburden stress) at a specific depth on an ERS

The active and passive earth pressure coefficients ( $K_a$  and  $K_p$ , respectively) are a function of the soil shear strength, backfill geometry, the geometry of the rear face of the ERS and friction and cohesion that develop along the rear face as the wall moves relative to the retained backfill. The active earth pressure condition is developed by a relatively small movement of the ERS away from the retained backfill, while the movements required to develop the passive earth pressure condition are on the order to approximately 10 times larger than the movements required to develop active conditions (see Figure 18-5).

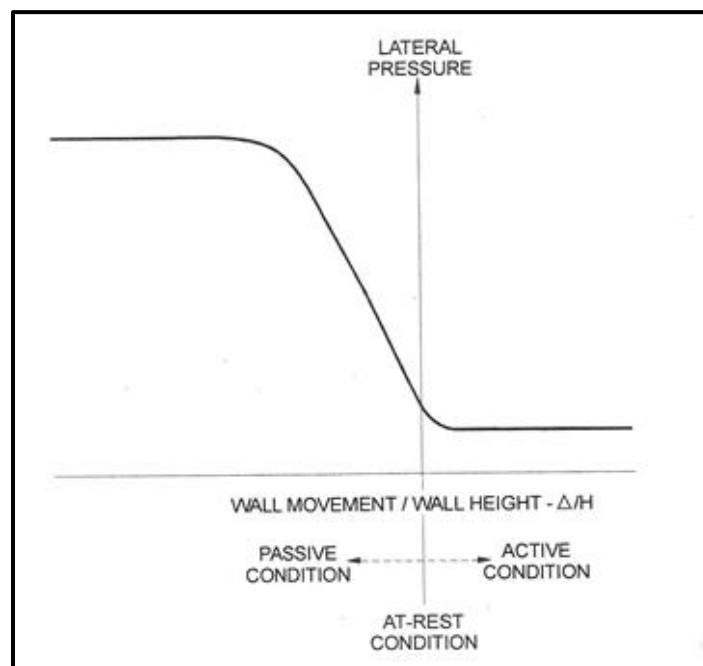


**Figure 18-5, Relative Magnitude of Displace. Required to Develop Earth Pressures (Tanyu, et al. (2008))**

Figure 18-6 presents a graphical relationship between displacement at the top of the wall and the earth pressure developed on the wall. Clough and Duncan (1991) developed a relationship between movement of the top of the wall and the wall height (Table 18-6).

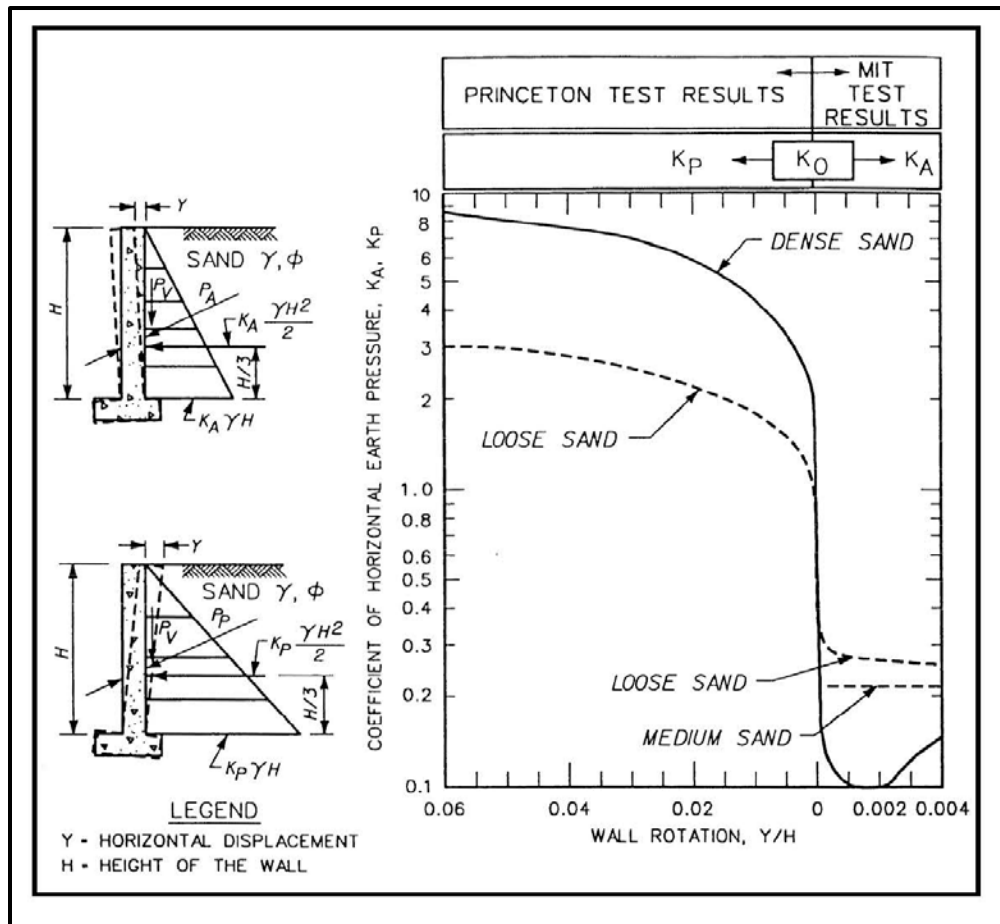


Figure 18-6, Effects of Wall Movement on Static Horizontal Earth Pressures (DOD (NAVFAC DM 7.2) (1986))

Table 18-6, Required Relative Movements To Reach  $P_A$  or  $P_P$  (Clough and Duncan, 1991)

Type of Backfill	$\Delta / H$	
	Active <sup>1</sup>	Passive <sup>2</sup>
Dense Sand	0.001	0.010
Medium Dense Sand	0.002	0.020
Loose Sand	0.004	0.040
Compacted Silt	0.002	0.020
Compacted Lean Clay	0.010	0.050

Note:  $\Delta$  = movement of top of wall (feet);  $H$  = height of wall (feet)  
<sup>1</sup>At minimum active earth pressure  
<sup>2</sup>At maximum passive earth pressure

### 18.5.1 Active Earth Pressure

The active earth pressure condition exists when an ERS is free to rotate or displace away from the retained backfill. There are 2 earth pressure theories available for determining the earth pressure coefficients; Rankine and Coulomb earth pressure theories. Rankine earth pressure makes several assumptions concerning the wall and the backfill. The first assumption is that the retained soil has a horizontal surface, secondly, that the failure surface is a plane and finally that the wall is smooth (i.e., no friction). Unlike Rankine earth pressure theory Coulomb earth

pressure theory accounts for the friction between the wall and the soil,  $\delta$  and allows for both a sloping backfill as well as a sloping back face of an ERS. Therefore, the use of Coulomb earth pressure theory is a better fit to most ERSs; however, the determination of the  $K_a$  is more rigorous.

### 18.5.1.1 Rankine Earth Pressure Coefficient

The use of Rankine earth pressure theory will cause a slight over estimation of  $K_a$ , therefore, increasing the pressure on the wall. The equations for developing the active earth pressure coefficients for Sand-Like soils ( $\leq 20$  percent fines) and Sand-Like ( $> 20$  percent fines,  $PI \leq 10$ ) (see Chapter 7) are indicated below. For Clay-Like soils ( $> 20$  percent fines,  $PI > 10$ ) contact the PC/GDS to discuss how to handle these soils.

Sand-Like ( $\leq 20$  percent fines)

$$K_a = \tan^2 \left( 45 - \frac{\phi'}{2} \right) \quad \text{Equation 18-4}$$

Sand-Like ( $> 20$  percent fines,  $PI \leq 10$ )

$$K_a = \tan^2 \left( 45 - \frac{\phi'}{2} \right) - \frac{2c'}{\sigma'_v} * \left[ \tan^2 \left( 45 - \frac{\phi'}{2} \right) \right] \quad \text{Equation 18-5}$$

Where,

$\phi'$  = Effective friction angle

$c'$  = Effective cohesion

$\sigma'_v$  = Effective overburden pressure at bottom of wall

### 18.5.1.2 Coulomb Earth Pressure Coefficient

As indicated previously, the development of the Coulomb earth pressure coefficient is a more rigorous methodology that depends more on the geometry of the ERS and backfill. Unlike the Rankine earth pressure coefficient, Coulomb earth pressure theory is based on Sand-Like materials with cohesion being used to develop the pressures and resultants (see Section 18.5.4).

$$K_a = \frac{\cos^2(\theta - \phi)}{\cos^2\theta * \cos(\theta + \delta) * [1 + \Gamma]^2} \quad \text{Equation 18-6}$$

$$\Gamma = \sqrt{\frac{\sin(\phi + \delta) * \sin(\phi - \beta)}{\cos(\theta + \delta) * \cos(\theta - \beta)}} \quad \text{Equation 18-7}$$

Where,

$\phi$  = Friction angle

$\delta$  = Wall friction (see Figure 18-8)

$\theta$  = Slope of back of ERS (see Figure 18-7)

$\beta$  = Slope of backfill above horizontal (see Figure 18-7)

H = Height of ERS





### 18.5.2 At-Rest Earth Pressure

In the at-rest earth pressure ( $K_o$ ) condition, the top of the ERS is not allowed to deflect or rotate; therefore, requiring the wall to support the full pressure of the soil behind the wall. The  $K_o$  coefficient is related to the OCR (Chapter 7) of the soil. The following equation is used to determine the at-rest earth pressure coefficient:

$$K_o = (1 - \sin \phi')(\text{OCR})^\Omega \quad \text{Equation 18-8}$$

$$\Omega = \sin \phi' \quad \text{Equation 18-9}$$

While all soils can be overconsolidated, the ability to accurately determine the OCR for Sand-Like soil is not cost effective; therefore, the OCR for all Sand-Like materials shall be taken as 1.0. Therefore for Sand-Like materials, Equation 18-8 may be rewritten as:

$$K_o = 1 - \sin \phi' \quad \text{Equation 18-10}$$

Flexible cantilevered ERSs are not typically designed to withstand the at-rest earth pressure condition.

### 18.5.3 Passive Earth Pressure

The development of passive earth pressure requires the ERS to move into or toward the soil. As with the active earth pressure, there are 2 earth pressure theories available for determining the earth pressure coefficients; Rankine and Coulomb earth pressure theories. Rankine earth pressure makes several assumptions concerning the wall and the backfill. The first assumption is that the retained soil has a horizontal surface, secondly, that the failure surface is a plane and finally that the wall is smooth (i.e., no friction). Unlike Rankine earth pressure theory Coulomb earth pressure theory accounts for the friction between the wall and the soil,  $\delta$  and allows for both a sloping backfill as well as a sloping back face of an ERS. Therefore, the use of Coulomb earth pressure theory is a better fit to most ERSs; however, the determination of the  $K_p$  is more rigorous.

#### 18.5.3.1 Rankine Earth Pressure Coefficient

The use of Rankine earth pressure theory will cause an under estimation of  $K_p$ , therefore, decreasing the pressure on the wall. The equations for developing the passive earth pressure coefficients for Sand-Like soils ( $\leq 20$  percent fines) and Sand-Like ( $> 20$  percent fines,  $PI \leq 10$ ) (see Chapter 7) are indicated below. For Clay-Like soils ( $> 20$  percent fines,  $PI > 10$ ) contact the PC/GDS to discuss how to handle these soils.

Sand-Like ( $\leq 20$  percent fines)

$$K_p = \tan^2 \left( 45 + \frac{\phi'}{2} \right) \quad \text{Equation 18-11}$$

Sand-Like ( $> 20$  percent fines,  $PI \leq 10$ )

$$K_p = \tan^2 \left( 45 + \frac{\phi'}{2} \right) + \frac{2c'}{\sigma'_v} * \left[ \tan^2 \left( 45 + \frac{\phi'}{2} \right) \right] \quad \text{Equation 18-12}$$

Where,

$\phi'$  = Effective friction angle

$c'$  = Effective cohesion

$\sigma'_v$  = Effective overburden pressure at bottom of wall

### 18.5.3.2 Coulomb Earth Pressure Coefficient

As indicated previously, the development of the Coulomb earth pressure coefficient is a more rigorous methodology that depends more on the geometry of the ERS and backfill. Unlike the Rankine earth pressure coefficient, Coulomb earth pressure theory is based on cohesionless materials with cohesion being used to develop the pressures and resultants (see Section 18.5.4).

$$K_p = \frac{\cos^2(\theta + \phi)}{\cos^2\theta * \cos(\theta - \delta) * [1 - \Gamma]^2} \quad \text{Equation 18-13}$$

$$\Gamma = \sqrt{\frac{\sin(\phi + \delta) * \sin(\phi + \beta)}{\cos(\theta - \delta) * \cos(\theta - \beta)}} \quad \text{Equation 18-14}$$

Where,

$\phi$  = Friction angle

$\delta$  = Wall friction

$\theta$  = Slope of back of ERS (see Figure 18-9)

$\beta$  = Slope of backfill above horizontal (see Figure 18-9)

H = Height of ERS

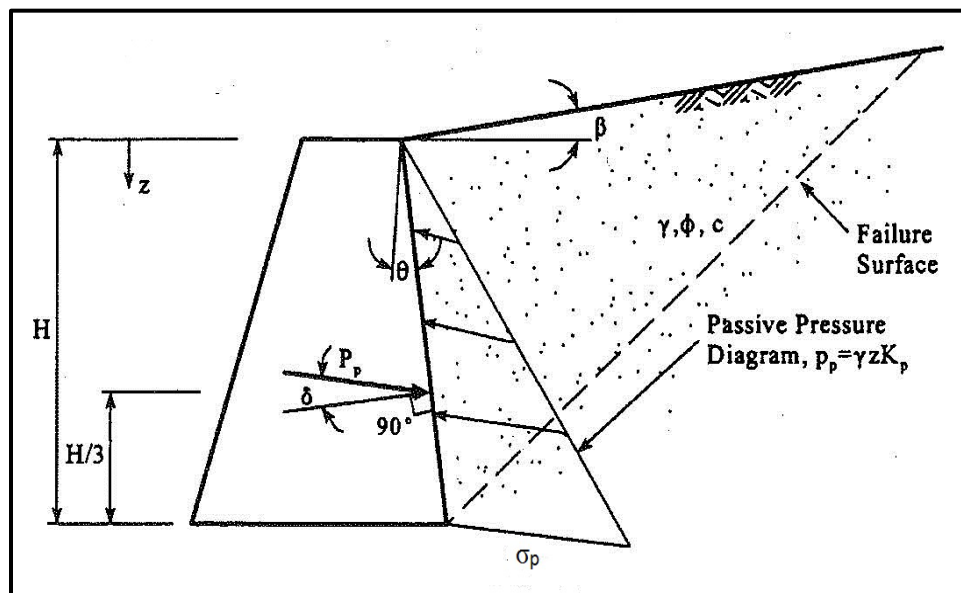


Figure 18-9, Coulomb Passive Earth Pressures  
(Tanyu, et al. (2008))

### 18.5.4 Determination of Earth Pressures

The active and passive earth stresses and pressures may be determined using either Rankine or Coulomb earth pressure theory. As indicated previously, ERSs used on SCDOT projects shall be designed to prevent the buildup of pore water pressures behind the wall. The effective earth stress at any depth along the ERS shall be determined using the following equations for

Sand-Like soils ( $\leq 20$  percent fines) and Sand-Like ( $> 20$  percent fines,  $PI \leq 10$ ) (see Chapter 7) are indicated below. For Clay-Like soils ( $> 20$  percent fines,  $PI > 10$ ) contact the PC/GDS to discuss how to handle these soils.

Sand-Like ( $\leq 20$  percent fines)

Active

$$\sigma'_a = K_a * [(\gamma_T * z) - u] \quad \text{Equation 18-15}$$

At-Rest

$$\sigma'_o = K_o * [(\gamma_T * z) - u] \quad \text{Equation 18-16}$$

Passive

$$\sigma'_p = K_p * [(\gamma_T * z) - u] \quad \text{Equation 18-17}$$

Sand-Like ( $> 20$  percent fines,  $PI \leq 10$ )

Active

$$\sigma'_a = K_a * [(\gamma_T * z) - u] - 2c' * \sqrt{K_a} \quad \text{Equation 18-18}$$

Passive

$$\sigma'_p = K_p * [(\gamma_T * z) - u] + 2c' * \sqrt{K_p} \quad \text{Equation 18-19}$$

$$u = \gamma_w * z \quad \text{Equation 18-20}$$

Where,

$\gamma_T$  = Total unit weight of soil, pcf

$\gamma_w$  = Unit weight of water, pcf

$z$  = Depth of interest (see Figures 18-6 and 18-8), ft

$u$  = Static pore water pressure (see Equation 18-9), psf

$K_a$  = Active earth pressure coefficient, Rankine or Coulomb

$K_o$  = At-Rest earth pressure coefficient

$K_p$  = Passive earth pressure coefficient, Rankine or Coulomb

$c'$  = Effective cohesion, psf

The resultant load,  $P_a$  or  $P_p$ , shown in Figures 18-7 or 18-9, respectively, are determined using the following equations.

Sand-Like ( $\leq 20$  percent fines)

Active

$$P_a = \frac{\sigma'_a * H}{2} \quad \text{Equation 18-21}$$

At-Rest

$$P_o = \frac{\sigma'_o * H}{2} \quad \text{Equation 18-22}$$

Passive

$$P_p = \frac{\sigma'_p * H}{2} \quad \text{Equation 18-23}$$

Where,

$\sigma'_a$  = Effective active earth pressure at the base of the wall (i.e.,  $z = H$ ), psf

$\sigma'_o$  = Effective at-rest earth pressure at the base of the wall (i.e.,  $z = H$ ), psf

$\sigma'_p$  = Effective passive earth pressure at the base of the wall (i.e.,  $z = H$ ), psf

$H$  = Height of wall, ft

$P_a$  = Active resultant force per foot of wall width, pounds per foot of wall width

$P_o$  = At-Rest resultant force per foot of wall width, pounds per foot of wall width

$P_p$  = Passive resultant force per foot of wall width, pounds per foot of wall width

Sand-Like (> 20 percent fines,  $PI \leq 10$ )

Active

$$P_a = \frac{\sigma'_a * H}{2} - 2c' * H * \sqrt{K_a} + \frac{2(c')^2}{[(\gamma_t * H) - u]} \quad \text{Equation 18-24}$$

Passive

$$P_p = \frac{\sigma'_p * H}{2} + 2c' * H * \sqrt{K_p} \quad \text{Equation 18-25}$$

For Clay-Like soils (> 20 percent fines,  $PI > 10$ ) contact the PC/GDS to discuss how to handle these soils.

## 18.6 RIGID GRAVITY EARTH RETAINING STRUCTURES

Gravity ERSs are externally stabilized fill walls and consist of the wall types provided in Table 18-7. Gravity wall types can be subdivided into 3 categories; gravity, semi-gravity and modular gravity. The limited details of each wall type are discussed in the following Sections. The design of gravity retaining walls is also discussed.

**Table 18-7, Gravity Wall Types**

<b>Gravity</b>	<b>Semi-Gravity</b>	<b>Modular Gravity</b>
Mass Concrete	Cantilever	Gabion
Stone	Counterfort	Crib
Masonry	Buttress	Bin

### 18.6.1 Gravity Retaining Walls

Gravity walls are typically trapezoidal in shape; although for shorter walls, the walls are more rectangular (see Figure 18-10). Gravity walls are constructed of either mass concrete with little or no reinforcement or masonry or stone walls. These types of walls tend to behave rigidly and depend on the weight (mass) of concrete to resist eccentricity (overturning) and sliding.

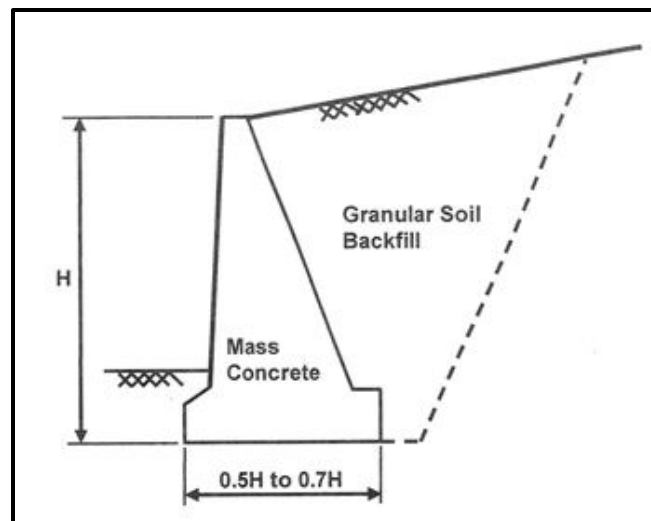


**Figure 18-10, Gravity Retaining Wall (Tanyu, et al. (2008))**

### 18.6.2 Semi-Gravity Retaining Walls

Semi-gravity walls are comprised of cantilevered, counterfort or buttress walls (see Figure 18-11). Semi-gravity walls are constructed of reinforced concrete, with the reinforcing in the stem designed to withstand the moments induced by the retained soil. Typically, cantilevered walls are limited to heights less than 30 feet. The counterforts (buttress within the retained soil mass) or buttresses (buttress on exposed face of the wall) are used when the moments are too large requiring a thicker stem and more reinforcing. Typically, these types of walls are used when the cantilevered wall height exceeds 30 feet.

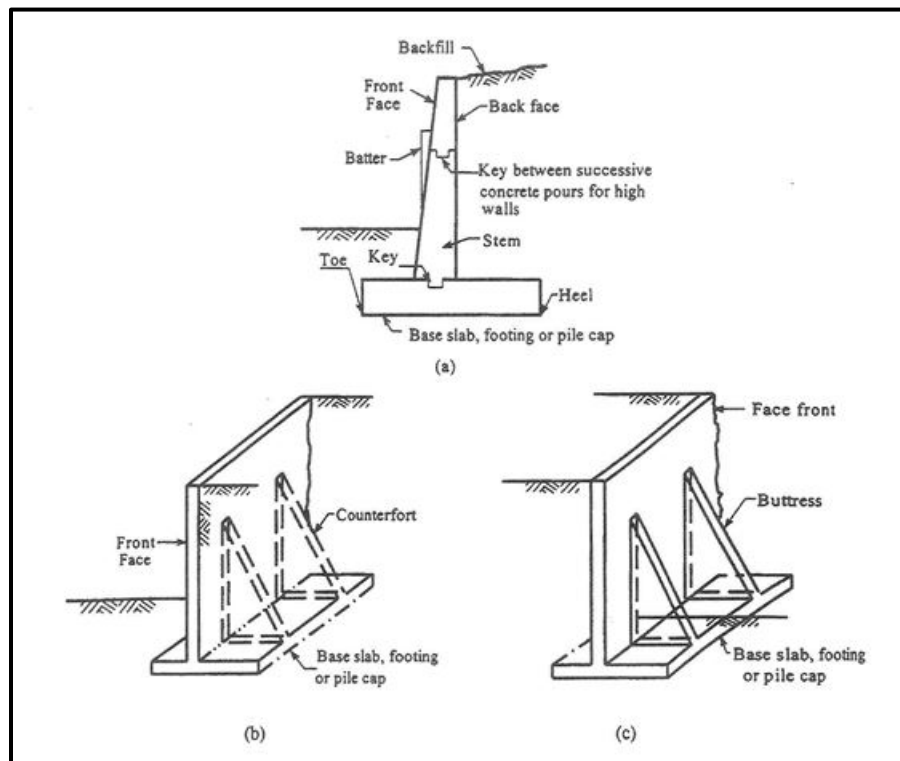


**Figure 18-11, Semi-Gravity Retaining Wall (Tanyu, et al. (2008))**

(a) Cantilever; (b) Counterfort; (c) Buttress

### 18.6.3 Modular Gravity Walls

Modular gravity walls are comprised of gabion, crib or bin walls (see Figure 18-12). Gabion walls are rock filled wire baskets. Gabion walls are used in locations where rock is plentiful. These types of walls are labor intensive to construct. Gabion walls are often used in applications that will experience cycles of inundation from streams. Currently SCDOT does not use crib or bin walls. The use of crib or bin walls must be approved in writing by the PC/GDS prior to commencing design.

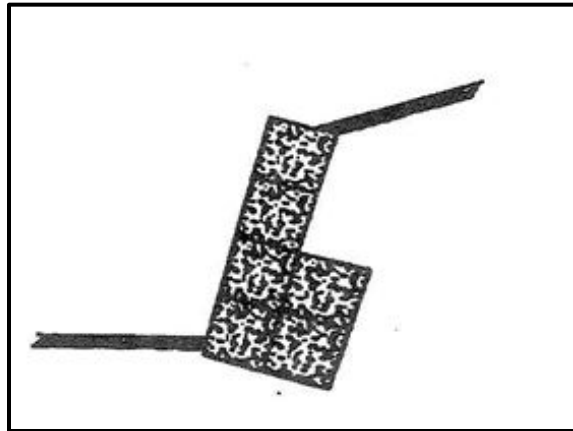


**Figure 18-12, Gabion Retaining Wall  
(Tanyu, et al. (2008))**

### 18.6.4 Rigid Gravity Wall Design

The design of gravity ERSs includes the overall (global) stability, bearing and deformation, sliding and eccentricity (overturning). The overall (global) stability and deformation analyses are performed using the procedures presented in Chapter 17. The bearing, sliding and eccentricity (overturning) analyses are performed using the procedures discussed in Chapter 15, if shallow foundations are used. If deep foundations are required, then the procedures presented in Chapter 16 should be used. Table 18-8 provides the design steps for gravity walls. For additional details on the design of gravity walls refer to Tanyu, et al. (2008). The loads placed on gravity retaining walls should be developed in accordance with the AASHTO LRFD Specifications (Section 11 – Abutments, Piers and Walls) and Chapter 8 of this Manual. Resistance Factors and Performance Limits shall be developed in accordance with Chapters 9 and 10 of this Manual.

**Table 18-8, Rigid Gravity Wall Design Steps  
(Tanyu, et al. (2008))**

Step	Action
1	Establish project requirements including all geometry, external loading conditions (transient and/or permanent, seismic, etc.), performance criteria and construction constraints.
2	Evaluate site subsurface conditions and relevant properties of in-situ soil and rock parameters and wall backfill parameters.
3	Evaluate soil and rock parameters for design and establish resistance factors.
4	Select initial base dimension of wall for Strength limit state (external stability) evaluation.
5	Select lateral earth pressure distribution. Evaluate water, surcharge, compaction and seismic pressures.
6	Evaluate factored loads for all appropriate loading groups and limit states.
7	Evaluate bearing resistance (Chapter 15).
8	Check eccentricity (see AASHTO LRFD Specification Section 11.6 – Abutments and Conventional Retaining Walls).
9	Check sliding (Chapter 15).
10	Check overall stability at the Service limit state and revise wall design if necessary (Chapter 17).
11	Estimate maximum lateral wall movement, tilt (rotation), and wall settlement at the Service limit state. Revise design if necessary.
12	Design wall drainage systems.

## 18.7 FLEXIBLE GRAVITY EARTH RETAINING STRUCTURES

Flexible gravity earth retaining structures consist of either Mechanically Stabilized Earth (MSE) Walls or gabion walls and are internally stabilized fill walls that are constructed using alternating layers of compacted soil and reinforcement (i.e., geosynthetics, metallic strips or metallic grids) (see Figure 18-13). As indicated in Table 18-2, there are 4 MSE Wall face alternatives that may be used. MSE Wall with precast panel facing shall be used at bridge end bent locations. However, other face options may be used with written permission of the PC/GDS. Table 18-9 provides the design steps that are used in the design of MSE Walls. Appendix C provides a detailed design procedure. The loads placed on in-situ structural retaining walls should be developed in accordance with the AASHTO LRFD Specifications (Section 11 – Abutments, Piers and Walls) and Chapter 8 of this Manual. Resistance Factors and Performance Limits shall be developed in accordance with Chapters 9 and 10 of this Manual. The external stability of the MSE Wall is the responsibility of the GEOR. The internal stability of the MSE Wall is the responsibility of the MSE Wall supplier.

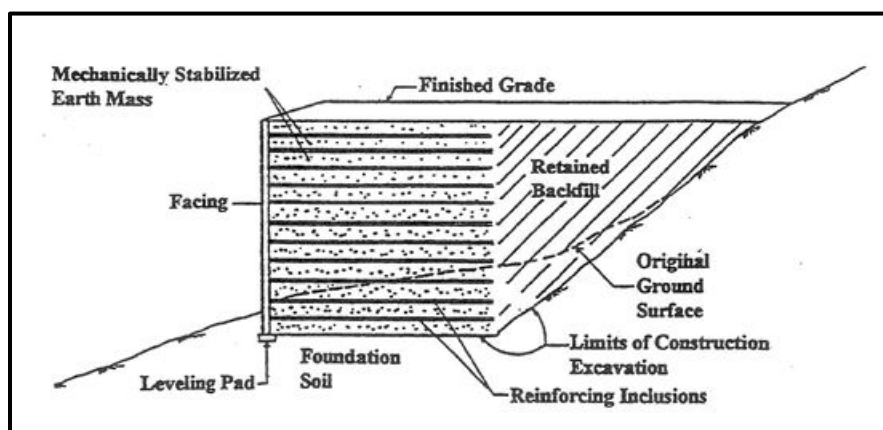


**Figure 18-13, MSE Wall  
(Tanyu, et al. (2008))**

**Table 18-9, MSE Wall Design Steps  
(modified Berg, Christopher, and Samtani – Volume I (2009))**

Step	Action
1	Establish project requirements including all geometry, external loading conditions (transient and/or permanent, seismic, etc.), performance criteria and construction constraints.
2	Evaluate existing topography, site subsurface conditions, in-situ soil/rock parameters and wall backfill parameters.
3	Based on initial wall geometry (including wall height), estimate wall embedment depth and length of reinforcement.
4	Define nominal loads
5	Summarize load combinations, load factors ( $\gamma$ ), and resistance factors ( $\phi$ )
6	Evaluate external stability
	a Check eccentricity (Appendix C).
	b Check sliding resistance (Appendix C).
	c Check bearing resistance of foundation soil (Appendix C).
7	d Estimate vertical wall movements at the Service limit state
	Evaluate Internal Stability
	a Select type of soil reinforcement
	b Estimate critical failure surface based on reinforcement type (i.e., extensible or inextensible) for internal stability design at all appropriate Strength limit states.
	c Define unfactored loads
	d Establish vertical layout of soil reinforcements
	e Calculate factored horizontal stress and maximum tension at each reinforcement level.
	f Calculate nominal and factored long-term tensile resistance of soil reinforcements.
	g Select grade (strength) of soil reinforcement and/or number of soil reinforcements, and check established layout.
	h Calculate nominal and factored pullout resistance of soil reinforcements and check established layout
	i Check connection resistance requirements at facing
	j Estimate lateral wall movements at the Service limit state. Revise design if necessary.
	k Check vertical movement and compression of pads
8	Design of facing elements.
9	Check overall stability at the Service limit state (Chapter 17). Revise design if necessary.
10	Assess Compound stability.
11	Design wall drainage systems.
	a Subsurface drainage
	b Surface drainage

## 18.8 CANTILEVER EARTH RETAINING STRUCTURES

Cantilever earth retaining structures have structural elements (i.e., sheetpile or soldier pile and lagging) installed to provide resistance of the applied lateral loads (see Figure 18-14). These types of walls are externally stabilized cut (top-down construction) walls. Cantilever earth retaining structures may develop resistance to the applied lateral loads through cantilever action, anchors or internal bracing (see Figure 18-15). In typical SCDOT applications, the use of exterior bracing is not normally used for permanent applications and will therefore not be discussed. Two different design methods are required for these walls depending if the wall is



cantilevered or supported by anchors. Typically, cantilevered in-situ structural walls can have exposed heights of up to 15 feet. Cantilevered in-situ structural walls taller than this will require anchors to resist the bending moments induced by the soil on the structural elements. The anchors may be either deadman or tendon type, depending on the method of construction, the amount of ROW available, etc. Table 18-10 provides the design steps for a cantilevered in-situ structural wall. Anchored in-situ structural walls are designed using the steps provided in Table 18-11. For additional details on the design of in-situ structural walls refer to Tanyu, et al. (2008). The loads placed on in-situ structural retaining walls should be developed in accordance with the AASHTO LRFD Specifications (Section 11 – Abutments, Piers and Walls) and Chapter 8 of this Manual. Resistance Factors and Performance Limits shall be developed in accordance with Chapters 9 and 10 of this Manual.

**Table 18-10, Cantilevered Wall Design Steps  
(Tanyu, et al. (2008))**

Step	Action
1	Establish project requirements including all geometry, external loading conditions (transient and/or permanent, seismic, etc.), performance criteria and construction constraints.
2	Evaluate site subsurface conditions and profile, water profile, and relevant properties of in-situ soil and rock parameters.
3	Evaluate soil and rock parameters for design and establish resistance factors.
4	Select lateral earth pressure distribution. Evaluate water, surcharge, compaction and seismic pressures.
5	Evaluate factored total lateral pressure diagram for all appropriate limit states.
6	Evaluate embedment depth of vertical wall element and factored bending moment in the wall.
7	Check flexural resistance of vertical wall elements. Check combined flexural and axial resistance (if necessary).
8	Select temporary lagging (for soldier pile and lagging wall). For permanent lagging, lagging must be designed to resist earth pressures.
9	Design permanent facing (if required).
10	Estimate maximum lateral wall movements and ground surface settlement at the Service limit state. Revise design if necessary.

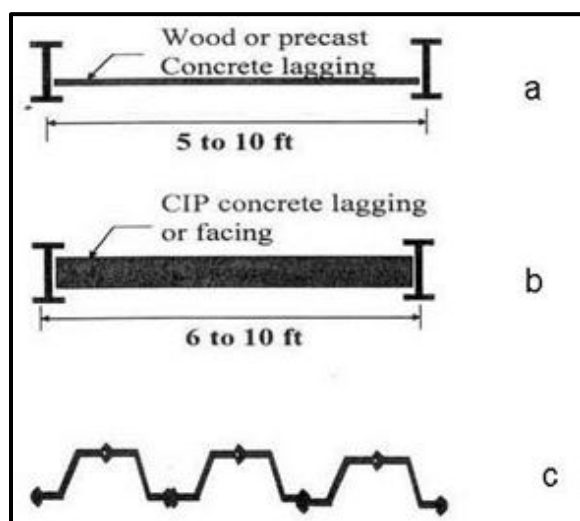


**Figure 18-14, In-Situ Structural Walls  
(Modified from Tanyu, et al. (2008))**

a and b Soldier pile and lagging; c Sheetpile

**Table 18-11, Anchored Cantilevered Wall Design Steps  
(Tanyu, et al. (2008))**

Step	Action
1	Establish project requirements including all geometry, external loading conditions (transient and/or permanent, seismic, etc.), performance criteria and construction constraints.
2	Evaluate site subsurface conditions and relevant properties of in-situ soil and rock parameters.
3	Evaluate soil and rock parameters for design and establish resistance factors and select level of corrosion project for the anchor.
4	Select lateral earth pressure distribution acting on back of wall for the final wall height. Evaluate water, surcharge, and seismic pressures.
5	Evaluate factored total loads for all appropriate limit states.
6	Calculate horizontal ground anchor loads and subgrade reaction force. Resolve each horizontal anchor load into a vertical force component and a force along the anchor. Evaluate horizontal spacing of anchors based on wall type and calculate individual factored anchor loads.
7	Evaluate required anchor inclination based on right-of-way limitations, location of appropriate anchoring strata, and location of underground structures.
8	Select tendon type and check tensile resistance.
9	Evaluate anchor bond length.
10	Evaluate factored bending moments and flexural resistance of wall.
11	Evaluate bearing resistance of wall below excavation subgrade. Revise wall section if necessary.

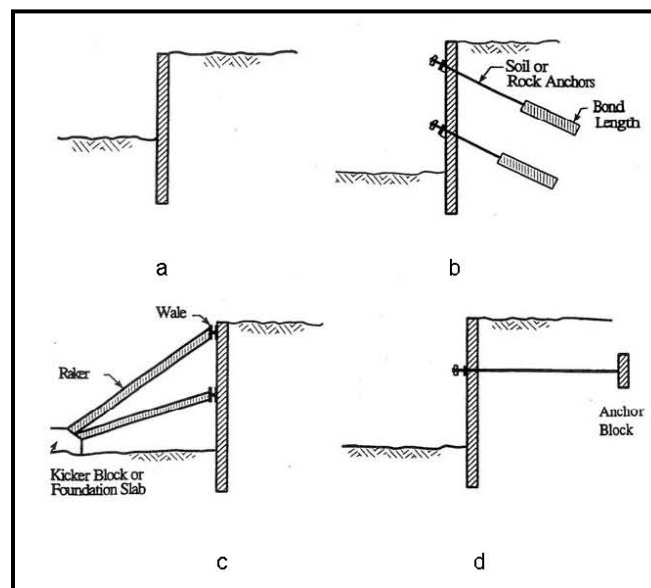


**Figure 18-15, Wall Support Systems  
(Modified from Tanyu, et al. (2008))**

a Cantilever; b Anchored; c Braced; d Deadman Anchored

### 18.9 IN-SITU REINFORCED EARTH RETAINING STRUCTURES

In-situ reinforced ERSs are internally stabilized cut walls that involve the insertion of reinforcing elements into the in-situ soils to create a composite ERS (see Figure 18-16).

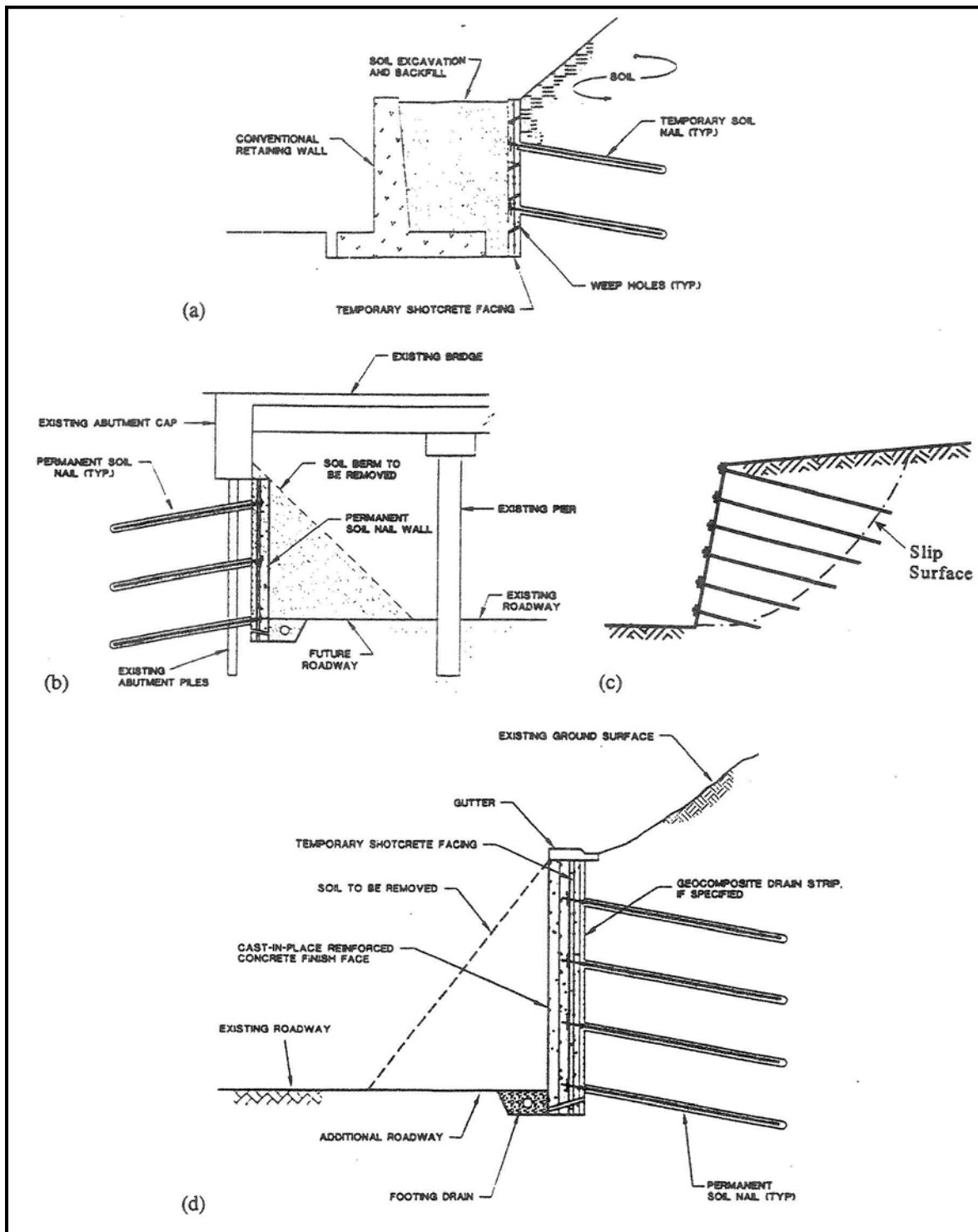


**Figure 18-16, In-Situ Reinforced (Soil Nail) Walls (Tanyu, et al. (2008))**

a Temporary shoring; b Roadway widening under existing bridge; c Slope stabilization; d Roadway cut

The design steps for a soil nail wall are provided in Table 18-12. For detailed requirements of design, please refer to Tanyu, et al. (2008). An alternate detailed design source is Lazarte, et al. (2015). The loads placed on in-situ structural retaining walls should be developed in accordance with the AASHTO LRFD Specifications (Section 11 – Abutments, Piers and Walls) and Chapter 8 of this Manual. Resistance Factors and Performance Limits shall be developed in accordance with Chapters 9 and 10 of this Manual. The external stability of the soil nail wall is the responsibility of the GEOR. The internal stability of the soil nail wall is the responsibility of either the SEOR or the soil nail wall contractor.

**Table 18-12, Soil Nail Wall Design Steps  
(Tanyu, et al. (2008))**

Step	Action
1	Establish project requirements including all geometry, external loading conditions (transient and/or permanent, seismic, etc.), performance criteria, aesthetic requirements, and construction constraints.
2	Evaluate site subsurface conditions and relevant properties of in-situ soil and rock.
3	Develop initial soil nail wall design criteria.
4	Perform preliminary design using simplified design chart solutions.
5	Evaluate external stability including global stability (Chapter 17), sliding and bearing capacity (Chapter 15).
6	Evaluate internal stability including nail pullout resistance and tensile resistance.
7	Perform facing design including: <ul style="list-style-type: none"> <li>a) evaluation of nail head load;</li> <li>b) selection of temporary and permanent facing materials and thicknesses;</li> <li>c) evaluation of facing flexural resistance;</li> <li>d) evaluation of facing punching shear resistance; and,</li> <li>e) evaluation of facing stud tensile resistance.</li> </ul>
8	Estimate maximum lateral wall movements.
9	Design wall subsurface and surface drainage systems

## 18.10 HYBRID WALLS

Hybrid walls are composed of 2 or more different types of walls (see Figure 18-17) or a combination of ERS and slope (see Figure 18-18) regardless of the slope angle or slope height. These kinds of walls allow a reduction in the ROW required for the construction of a project. The use of hybrid walls will require special attention from the design team. The various components of the hybrid wall may require different deformations to develop adequate resistance to the external loads. These differences can lead to incompatible deformations at the face of wall. The continuity of the drainage system must be maintained in both components of the hybrid wall. Finally, while the performance and design information for each component is known, the performance of the hybrid wall system is typically not known.

The combining of cut and fill walls should be performed with extreme care, since most cut walls require small strains to develop resistance, while most fill walls require larger strains to develop the same resistance. If the walls move (displace) different amounts to develop the required resistances, the face of the wall may display unaesthetic differential movements, even if the wall is structurally sound. The fact that the face shows displacement can cause the general public to consider the wall failing. In addition, the higher strains required to develop the resistance of 1 portion of the wall can induce higher loads in another portion of the wall causing failure of the wall.

In most cases, the hybrid wall consists of a stacked system (see Figure 18-17) with 1 wall or slope on top of another. The overall stability of the entire system must be checked in accordance with Chapter 17. Then, each individual wall component should be checked for stability. The lower wall should include the weight of the upper wall as a surcharge load. The design of the upper wall should include the movements (vertical and lateral) of the lower wall in design (see Chapter 17). The design engineer should have a clear understanding of how each different wall component will perform prior to selecting the use of a hybrid wall.

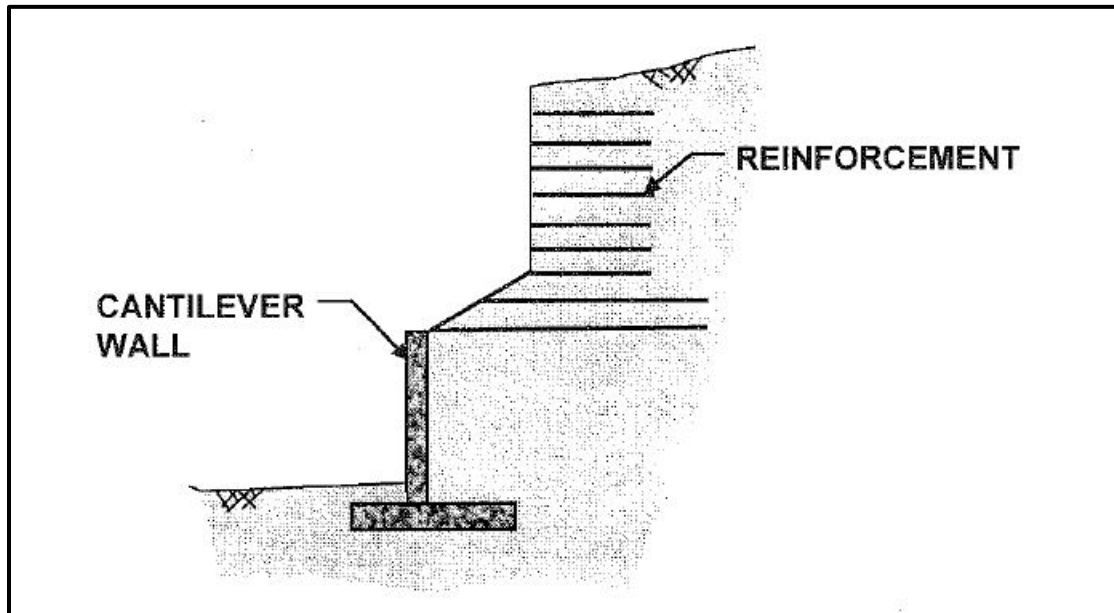


Figure 18-17, Hybrid Wall – Cantilever Concrete under MSE Wall

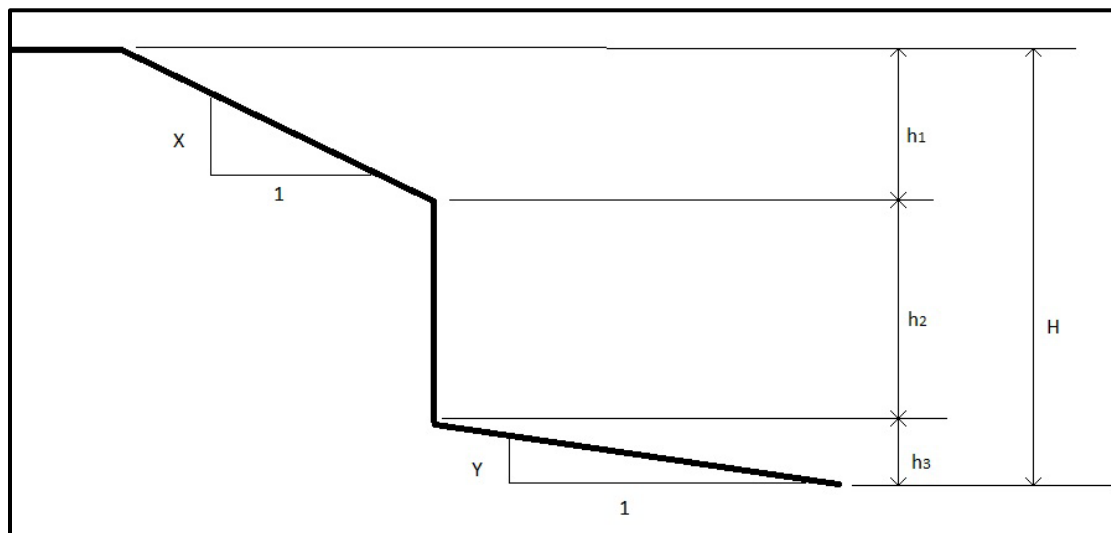


Figure 18-18, Compound Slope – Slope Above and Below ERS

## 18.11 TEMPORARY WALLS

Temporary shoring walls are used to support a temporary excavation that is required to allow construction to proceed. Temporary shoring walls have a service of less than 5 years. Any shoring wall with a service life of greater than 5 years shall be designed as a permanent ERS. Another major distinction between permanent and temporary ERSs is an increase in the resistance factor allowed in design. Temporary walls may be subdivided into 2 classes “support of excavation” (SOE) and “critical.” SOE walls typically support just the excavation while the

critical temporary walls support critical structures (i.e., existing roadway and traffic, bridge end bent fill, utilities, etc.). The resistance factors and performance limits established (see Chapters 9 and 10) are for critical temporary walls. The PC/GDS should be contacted for the resistance factors and performance limits for SOE temporary walls. The design of temporary walls uses the same methodologies as the permanent walls.

## 18.12 REFERENCES

American Association of State Highway and Transportation Officials, (2017), AASHTO LRFD Bridge Design Specifications Customary U.S. Units, 8<sup>th</sup> Edition, American Association of State Highway and Transportation Officials, Washington, D.C.

Berg, R. R., Christopher, B. R., and Samtani, N. C., (2009), Design of Mechanically Stabilized Earth Walls and Reinforced Soil Slopes - Volume I, Geotechnical Engineering Circular No. 11 – Volume I, (Publication No. FHWA-NHI-10-024), U.S. Department of Transportation, National Highway Institute, Federal Highway Administration, Washington D.C.

Clough, G. W. and Duncan, J. M., (1991), “Earth Pressures”, Foundation Engineering Handbook, Second Edition, H.-Y. Fang (editor), Van Nostrand Reinhold, New York, pp. 223 - 235.

DeMarco, M., Bush, P., Samtani, N. C., Kulicki, J. M., and Severns, K., (2015), Draft - Incorporation of Foundation Deformations in AASHTO LRFD Bridge Design Process, 2<sup>nd</sup> Strategic Highway Research Program (SHRP2), Transportation Research Board, The National Academies of Sciences, Engineering, and Medicine, Washington, D.C.

Department of Defense, Department of the Navy, Naval Facilities Engineering Command, (1986), Foundations & Earth Structures – Design Manual 7.2, (Publication No. NAVFAC DM-7.02), Alexandria, Virginia.

Lazarte, C. A., Robinson, H., Gómez, J. E., Baxter, A., Cadden, A., and Berg, R. R., (2003), Soil Nail Walls, Geotechnical Engineering Circular No. 7, (Publication No. FHWA-NHI-14-007), U.S. Department of Transportation, National Highway Institute, Federal Highway Administration, Washington D.C.

Tanyu, B. F., Sabatini, P. J., and Berg, R. R., (2008), Earth Retaining Structures, (Publication No. FHWA-NHI-07-071), U.S. Department of Transportation, National Highway Institute, Federal Highway Administration, Washington D.C.

South Carolina Department of Transportation, Highway Design Manual, (2017), <https://www.scdot.org/business/road-design.aspx>.

South Carolina Department of Transportation, Standard Specifications for Highway Construction, (2007), [https://www.scdot.org/business/pdf/2007\\_full\\_specbook.pdf](https://www.scdot.org/business/pdf/2007_full_specbook.pdf).

**Chapter 19**  
**GROUND IMPROVEMENT**

**GEOTECHNICAL DESIGN MANUAL**

*January 2019*





## Table of Contents

<u>Section</u>		<u>Page</u>
19.1	Introduction.....	19-1
19.2	Prefabricated Vertical Drains .....	19-7
	19.2.1 Design Concepts.....	19-8
	19.2.2 Earthquake Drains .....	19-12
	19.2.3 Construction Considerations .....	19-12
19.3	Lightweight Fill Materials.....	19-15
	19.3.1 General Applications and Limitations .....	19-15
	19.3.2 Geofoam .....	19-17
	19.3.3 Foamed Concrete .....	19-20
	19.3.4 Expanded Shale, Clay & Slate .....	19-21
	19.3.5 Glass Aggregate .....	19-22
19.4	Vibro-Compaction.....	19-23
19.5	Aggregate Columns.....	19-23
	19.5.1 Vibro-Replacement .....	19-24
	19.5.2 Vibro-Displacement.....	19-25
	19.5.3 Vibro-Concrete Columns .....	19-26
	19.5.4 Geotextile-Encased Columns.....	19-26
	19.5.5 Geopier® Rammed Aggregate Pier™ .....	19-27
	19.5.6 General Considerations.....	19-27
	19.5.7 Feasibility .....	19-28
	19.5.8 Environmental Considerations.....	19-30
	19.5.9 Design Considerations .....	19-30
	19.5.10 Geopiers.....	19-34
	19.5.11 Design Verification .....	19-34
19.6	Dynamic Compaction.....	19-35
	19.6.1 Analysis .....	19-35
	19.6.2 Design.....	19-39
19.7	Deep Mixing Methods .....	19-42
	19.7.1 Analysis .....	19-43
	19.7.2 DMM Advantages and Disadvantages/Limitations.....	19-46
	19.7.3 Feasibility .....	19-47
	19.7.4 Design.....	19-50
	19.7.5 Verification .....	19-52
	19.7.6 Construction Considerations .....	19-52
19.8	Grouting.....	19-53
	19.8.1 Grout Materials .....	19-54
	19.8.2 Rock Grouting.....	19-57
	19.8.3 Soil Grouting .....	19-59
19.9	Column Supported Embankment.....	19-66
	19.9.1 Analysis and Feasibility .....	19-67
	19.9.2 Design Approach.....	19-68
	19.9.3 Reinforcement Total Design Load.....	19-82
19.10	Construction Working Platform .....	19-83
	19.10.1 US Forest Service (Steward, et al. (1977)) Method .....	19-84
	19.10.2 Giroud-Han Method.....	19-86

19.11 References ..... 19-88

### List of Tables

<u>Table</u>	<u>Page</u>
Table 19-1, Ground Improvement Design Process.....	19-2
Table 19-2, Ground Improvement Categories, Functions and Methods.....	19-3
Table 19-3, Ground Improvement Importance Selection Factors (ISF).....	19-3
Table 19-4, Weighted Geotechnology Selection Factors.....	19-4
Table 19-5, Geotechnology Selection Matrix.....	19-6
Table 19-6, Lightweight Fill Materials.....	19-15
Table 19-7, Physical Properties of RCPS Geofoam.....	19-19
Table 19-8, Equivalent Soil Subgrade Values of EPS Geofoam.....	19-19
Table 19-9, EPS Geofoam Design Guidelines.....	19-20
Table 19-10, Foamed Concrete Design Guidelines.....	19-21
Table 19-11, ESCS Design Guidelines.....	19-22
Table 19-12, Glass Aggregate Design Guidelines.....	19-23
Table 19-13, Vibro-replacement and Vibro-displacement Definitions.....	19-24
Table 19-14, Upper Bound Test Values after Dynamic Compaction.....	19-41
Table 19-15, Applied Energy Guidelines.....	19-41
Table 19-16, Deep Mixing Generic Terms.....	19-42
Table 19-17, DMM Groups.....	19-43
Table 19-18, Favorable Soil-Chemistry Factors.....	19-48
Table 19-19, Typical DMM Improved Engineering Properties.....	19-49
Table 19-20, Mixing Guidelines.....	19-49
Table 19-21, DMM Required Geometric Parameters.....	19-51
Table 19-22, Types of Grouting Method.....	19-53
Table 19-23, Types, Use, and Applications of Resin Grouts.....	19-57
Table 19-24, Polyurethane Types.....	19-57
Table 19-25, Rock Grouting Categories.....	19-58
Table 19-26, Groutability Guidelines.....	19-61
Table 19-27, Guide to Permeation Grout Potential.....	19-62
Table 19-28, Values of $\Omega$ .....	19-76
Table 19-29, Bearing Capacity Factors for USFS Method.....	19-85
Table 19-30, Bearing Capacity Factor and Aperture Stability Modulus.....	19-87
Table 19-31, Minimum Undrained Shear Strength versus Rut Depth.....	19-87

### List of Figures

<u>Figure</u>	<u>Page</u>
Figure 19-1, PVD Installation for a Highway Embankment .....	19-8
Figure 19-2, PVD Dimensions .....	19-10
Figure 19-3, Crane Mounted Installation Rig .....	19-14
Figure 19-4, Applicable Grain-Size Distributions for Stone Columns .....	19-24
Figure 19-5, Top Feed Construction Method .....	19-25
Figure 19-6, Bottom Feed Construction Method .....	19-25
Figure 19-7, Vibro-Concrete Column .....	19-26
Figure 19-8, Geopier® Rammed Aggregate Pier™ .....	19-27
Figure 19-9, Stone Column Equilateral Triangular Pattern .....	19-32
Figure 19-10, Unit Cell Idealization.....	19-32
Figure 19-11, Dynamic Compaction Schematic.....	19-35
Figure 19-12, Soil Grouping for Dynamic Compaction.....	19-36
Figure 19-13, Dynamic Compaction Phase Diagram .....	19-37
Figure 19-14, Dynamic Compaction Improvements vs. Depth .....	19-40
Figure 19-15, Generic Classification of Deep Mixing Techniques .....	19-42
Figure 19-16, DMM Project Flowchart .....	19-44
Figure 19-17, DMM Grid Treatment Pattern .....	19-44
Figure 19-18, DMM Treatment Pattern Beneath Embankment.....	19-45
Figure 19-19, DMM-MMM Load-Transfer Platform .....	19-45
Figure 19-20, T vs Strength Magnitude and Variability .....	19-50
Figure 19-21, DMM Shear Wall Geometric Detail.....	19-52
Figure 19-22, Types of Grouting Schematic .....	19-54
Figure 19-23, Viscosity versus Time.....	19-55
Figure 19-24, Grain-Size Distribution of Cements .....	19-55
Figure 19-25, Range of Applicability of Soil Grouting Techniques .....	19-60
Figure 19-26, Penetrability of Various Grouts versus Soil Type.....	19-61
Figure 19-27, Grain-Size Distribution for Permeation Grouting.....	19-62
Figure 19-28, Jet Grouting Process Schematic .....	19-64
Figure 19-29, Jet Grouting Systems.....	19-65
Figure 19-30, CSE with Geosynthetic LTP .....	19-67
Figure 19-31, Strength Limit State Failure Modes .....	19-68
Figure 19-32, Service Limit State .....	19-69
Figure 19-33, Area and Perimeter Determination of Round and Square Columns....	19-70
Figure 19-34, Effective Column Diameter Determination .....	19-71
Figure 19-35, Unit Cell Area Determination .....	19-71
Figure 19-36, CSE Edge Stability.....	19-72
Figure 19-37, Load Transfer Platform.....	19-74
Figure 19-38, Collin Method Load Transfer Platform Design .....	19-75
Figure 19-39, Modified Collin Method Reinforcement.....	19-76
Figure 19-40, Definition Sketch for LDC Method .....	19-79
Figure 19-41, CSE Lateral Spreading.....	19-82
Figure 19-42, USFS Method Bridge Lift Thickness – Single Wheel Loads.....	19-85
Figure 19-43, USFS Method Bridge Lift Thickness – Dual Wheel Loads .....	19-86

# CHAPTER 19

## GROUND IMPROVEMENT

### 19.1 INTRODUCTION

According to Charles (2002), the process of altering the ground is ground treatment, while the purpose of the process is ground improvement, and the result of the process is ground modification. The term “ground improvement” is used generically to mean ground treatment, ground improvement, and ground modification throughout the GDM. The “Preface” to Schaefer, et al. – Volumes I and II (2017) states:

One of the major functions of geotechnical engineering is to design, implement, and evaluate ground improvement schemes for infrastructure projects. During the last 40 years significant new technologies and methods have been developed and implemented to assist the geotechnical specialist in providing cost-effective solutions for construction on marginal or difficult sites.

The ground improvement methods discussed in this Chapter are based on the contents of Schaefer, et al. - Volumes I and II (2017), but should not be considered the complete discussion of ground improvement methods. The GEOR should consult each volume as required for more details concerning a specific ground improvement method.

The GEOR should also consult the software package developed by the Strategic Highway Research Program (SHRP2) of the Transportation Research Board (TRB). The software package is called *GeoTech Tools – Geo-Construction Information and Technology Selection Guidance for Geotechnical, Structural & Pavement Engineers*, (GeoTech Tools). GeoTech Tools is located at: <http://www.geotechtools.org/> and requires user registration prior to use.

In keeping with the geotechnical philosophy described in Chapter 7, it is incumbent on the GEOR to be aware of new and innovative ground improvement ideas. If a new or innovative ground improvement method is to be used on an SCDOT project, approval must be first obtained from the PC/GDS with concurrence from the PCS/GDS. The approval process will consist of a minimum of engineering design, the desired outcome, construction methodology, and availability of construction experience/contractors to perform the specified type of work.

Ground improvement construction methods are used to improve poor/unsuitable subsurface soils and/or to improve the performance of embankments or structures. These methods are used when replacement of the in-situ soils is impractical because of physical limitations, environmental concerns, or is too costly. Ground improvement methodologies have the primary functions to:

- Increase bearing capacity, shear, or frictional strength
- Increase density
- Control deformations
- Accelerate consolidation
- Decrease imposed loads
- Provide/increase lateral stability
- Form seepage cutoffs or fill voids
- Increase resistance to SSL
- Transfer embankment and/or ERS loads to more competent layers

There are 3 general strategies available to accomplish the above functions representing different approaches.

1. Increase shear strength, density, and/or decrease compressibility of foundation soil
2. Use lightweight fills to significantly reduce the applied load on the foundation soil
3. Transfer the load to a more competent (deeper) foundation soil

The “Introduction” to Schaefer, et al. – Volumes I and II (2017), recommends a sequential design process that includes a sequence of evaluations that proceed from simple to more detailed. This process identifies the best method and is defined in Table 19-1.

**Table 19-1, Ground Improvement Design Process  
(modified from Schaefer, et al. - Volumes I and II (2017))**

Step	Process
1	Identify potential poor ground conditions, including extent and type of negative impact
2	Identify or establish performance requirements (see Chapter 10)
3	Identify and assess general site conditions including any space or environmental constraints
4	Assessment of subsurface conditions – type, depth and extent of poor soil as well as groundwater table depth and assessment of shear strength and compressibility
5	Develop a short-list of geotechnologies applicable to site conditions (Table 19-2 should be used in this selection process)
6	Identify project constraints
7	Identify project risks
8	Preliminary design
9	Identify alternative solutions (i.e., bridge, re-route, deep foundations, etc.)
10	Evaluate project requirements, constraints, and risks against factors affecting geotechnology selection (Tables 19-3 and 19-4)
11	Compare short-list of geotechnology alternatives with geotechnology selection factors
12	Select a preferred geotechnology (see Table 19-5)

**Table 19-2, Ground Improvement Categories, Functions and Methods  
(modified from Schaefer, et al. - Volumes I and II (2017))**

Category	Function	Method
Consolidation	Accelerate consolidation and increase shear strength	1.) Prefabricated Vertical Drains 2.) Surcharge
Load Reduction	Reduce load on foundation and reduce settlement	1.) Lightweight fill 2.) Geofoam 3.) Foamed Concrete
Densification	Increase density, bearing capacity, and frictional strength of granular soils. Decrease settlement and increase resistance to liquefaction	1.) Vibro-Compaction 2.) Dynamic Compaction by falling weight impact 3.) Stone Columns
Reinforcement	In soft foundation soils, increases shear strength, resistance to liquefaction, and decreases compressibility	1.) Stone Columns 2.) Piles or Drilled Shafts
Soil Mixing	Physio-chemical alteration of foundation soils to increase their tensile, compressive, and shear strength; to decrease settlement; and/or provide lateral stability and/or confinement	1.) Deep mixing methods 2.) Mass mixing methods
Grouting	To fill voids, increase density, increase tensile, and compressive strength	1.) Permeation Grouting 2.) Compaction Grouting 3.) Jet Grouting
Load Transfer	Transfer load to deeper bearing layer	1.) Column Supported Embankment (CSE)

Step 10 from Table 19-1 establishes the process for evaluating project requirements against fairly common factors that affect the selection of an appropriate geotechnology for ground improvement. Eighteen Importance Selection Factors (ISFs) have been identified and indicated in Table 19-3. The ISFs are listed in no particular order. Additional factors may be considered based on the requirements of the design team. Each factor is evaluated based on its relevancy and importance to the project requirements and site constraints. Each ISF is assigned an importance rating (IR) from 1, the least important, to 3, the most important. Table 19-4 depicts an example table of the ISFs and IR for each factor.

**Table 19-3, Ground Improvement Importance Selection Factors (ISF)  
(modified from Schaefer, et al. - Volumes I and II (2017))**

Speed of construction	Familiarity with geotechnology
Minimize construction disturbance	Design procedure
Longevity of constructed works	Contracting
Cost of construction	Life-cycle cost
Constructability	Project constraint – construction season
ROW requirements or restrictions	Additional project constraint
Aesthetics	Project risk – delay due to settlement time
Environmental	Project risk – quality assurance
Degree of establishment	Additional project risk

**Table 19-4, Weighted Geotechnology Selection Factors**

Addition Project Risk (if required)	
Project Risk – Quality Assurance	
Project Risk – Delay Due to Settlement Time	
Additional Project Constraint (if required)	
Project Constraint – Construction Season	
Life-cycle Cost	
Contracting	
Design Procedure	
Familiarity with Geotechnology	
Degree of Establishment	
Environmental Concerns	
Aesthetics	
ROW Requirements or Restrictions	
Constructability	
Cost of Construction	
Longevity of Constructed Works	
Minimize Construction Disturbance	
Speed of Construction	
ISF <sup>1</sup>	IR <sup>2</sup>

<sup>1</sup>Importance selection factor (ISF)  
<sup>2</sup>Importance rating of each Geotechnology selection factor based on project requirements and site constraints. Each factor should be rated between 0, least importance factor, and 3, most important factor.



The final step in selecting an appropriate geotechnology for ground improvement is to determine the most acceptable type. Each ISF is assigned a suitability factor (SF). The SF is based on how suitable a particular geotechnology will achieve the required ground improvement considering the ISF and the importance of each ISF. SF ranges from 4, most suitable, to 1, least suitable. The determination of SF is very subjective; every effort should be made to avoid making a specific type of geotechnology appear suitable. Any cost associated with a selection factor should be considered when developing the rating. This determination is made based on the IR and SF for each ISF. A weighted rating (WR) is developed as the product of IR and SF. A total weighted rating ( $WR_T$ ) is determined (see Equation 19-1). The geotechnology with the highest  $WR_T$  should be selected for the specific project site. Other highly scored geotechnologies may be included in the Contract Documents as acceptable alternatives. Table 19-5 provides an example of this process. The Geotechnology Selection Matrix is available on the Geotechnical page of the SCDOT website; <https://www.scdot.org/business/geotech.aspx>.

$$WR_T = \sum_{i=1}^n (IR_i * SF_i) = \sum_{i=1}^n WR_i \quad \text{Equation 19-1}$$

**Table 19-5, Geotechnology Selection Matrix**

ISF Geotechnology		Total Weighted Rating (WR <sub>T</sub> )	
		IR	WR
Geotechnology A <sup>1</sup>	IR	0	89
	SF	2	
	WR	0	
Geotechnology B <sup>1</sup>	SF	4	57
	WR	0	
Geotechnology C <sup>1</sup>	SF	2	67
	WR	0	
Addition Project Risk (if required)		0	0
Project Risk – Quality Assurance		3	9
Project Risk – Delay Due to Settlement Time		2	8
Additional Project Constraint (if required)		0	0
Project Constraint – Construction Season		0	0
Life-cycle Cost		1	2
Contracting		2	4
Design Procedure		2	8
Familiarity with Geotechnology		1	2
Degree of Establishment		3	12
Environmental Concerns		2	6
Aesthetics		2	8
ROW Requirements or Restrictions		0	0
Constructability		1	1
Cost of Construction		2	9
Longevity of Constructed Works		2	6
Minimize Construction Disturbance		2	2
Speed of Construction		3	12

<sup>1</sup>SF for each geotechnology are based on project requirements and site constraints. Each SF should be rated between 1, least suitable, and 4, most suitable.

Schaefer, et al. – Volumes I and II (2017) also indicate pavement support stabilization as well as reinforced soil structures as ground improvement categories. Pavement support stabilization will not be discussed in the GDM. In addition, the use of reinforced soil structures (i.e., RSSs and MSE walls) is discussed in Chapters 17 and 18, respectively, and therefore, will not be discussed in this Chapter.

The cost of the ground improvement geotechnology must be considered in the selection process. Contact the PC/GDS for cost information for ground improvement methods previously used by SCDOT. For ground improvement geotechnologies not previously used, every effort should be made to contact at least 3 contractors to obtain approximate pricing information.

According to the “Introduction” to Schaefer, et al. – Volumes I and II (2017):

For many years the term QC/QA was used to describe quality activities associated with construction where Quality Control (QC) referred to the quality activities conducted by the contractor and Quality Assurance (QA) referred to quality activities conducted by the owner. More recently, the term Quality Assurance is being used as the umbrella term that includes the contractor’s QC activities and the acceptance functions of the owner-agency. AASHTO (2006), FHWA (2008) and Code of Federal Regulations (23 CFR 637) all define the core elements of a construction Quality Assurance Program to include:

1. Contractor Quality Control (QC)
2. Agency Acceptance
3. Agency Independent Assurance (IA)
4. Dispute Resolution
5. Laboratory Accreditation and Qualification
6. Personnel Qualification/Certification

All 6 elements are deemed necessary to have a complete and effective QA Program. A QA program missing any one or more of the elements is not sufficient and should not be construed as being “substantially complete” with the intent of the AASHTO guidelines or the federal regulation.

The costs for the Quality Assurance Program need to be added to the total cost of the soil and site improvement method.

## **19.2 PREFABRICATED VERTICAL DRAINS**

Prefabricated vertical drains (PVDs), also commonly called wick drains, are used to accelerate consolidation of compressible cohesive soils to speed settlement and strength gain. The use of the term wick drains is a misnomer since water is not wicked out of the ground by the drains under capillary tension, but rather water flows from compressible clays under a pressure gradient induced by excess pore pressures associated with the placement of permanent fill and/or surcharge fill (see Figure 19-1).

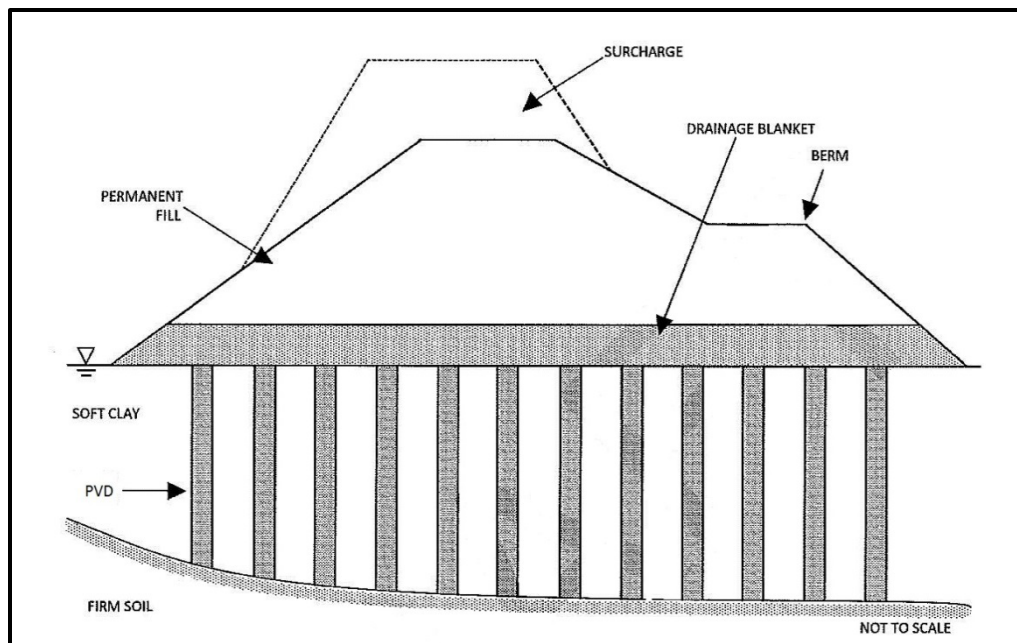


**Figure 19-1, PVD Installation for a Highway Embankment  
(modified Schaefer, et al. – Vol. I (2017))**

PVDs have numerous advantages some of which include economy, installation speed, continuity of drain, and minimal displacement. Additional advantages are presented in Schaefer, et al. – Vol. I (2017), which should be consulted for greater details on this method. There are also some disadvantages to the PVDs which include greater quantities, no compressive strength, headroom limitations, and material must be properly handled and stored. It is noted that these disadvantages are in relation to the use of sand drains. The subsurface soils must be evaluated to determine the feasibility of using PVDs. The evaluation factors are provided below:

- Moderate to high compressibility
- Low permeability
- Full saturation
- Final embankment loads must exceed maximum preconsolidation stress ( $\sigma'_p$  or  $p'_c$ )
- Secondary compression must not be a major concern
- Low-to-moderate shear strength
- Soils normally to slightly overconsolidated ( $OCR < 1.5$ )
- Installation problems through dense subsurface obstructions

PVDs are thin strips (about 1/8 inch thick by 4 inches wide) consisting of a rigid core sheathed in filter fabric. PVDs have generally replaced sand drains. However, the PVD design theories were adapted from sand drain design. To accelerate the rate of settlement, PVDs are typically installed on a regular grid pattern, either triangular or rectangular, to reduce the flow distance for dissipation of excess pore water pressures associated with the placement of fill. Stone columns discussed later in this Chapter can also provide vertical drainage and similar methods can be applied to evaluate their effect on settlement rates.

### **19.2.1 Design Concepts**

The primary purpose of PVDs is to reduce the length of the drainage path, thereby decreasing the time for settlement and strength gain to occur. Prior to selecting the use of PVDs, predictions of the amount and rate of settlement (see Chapter 17) both during and after construction are required. The amount of settlement should meet the performance criteria

provided in Chapter 10. In addition, the stability of the embankment during the placement of the fill materials should also be ascertained. If the stability becomes questionable during construction, then vertical staging may be required. Chapter 17 discusses the stability of the embankment and vertical staging if required. Field testing (SPT, CPT and/or DMT) is required to determine if pre-drilling is necessary to penetrate dense materials and obstructions. The principle of PVD design is the selection of the type, spacing, and length of the drains to accomplish the required Performance Limit (degree of consolidation) within a specified time.

According to Schaefer, et al. – Vol. I (2017), “The assumptions used in developing one dimensional consolidation theory were applied to the development of radial drainage theory related to vertical drains, which resulted in the following relationship between time, drain diameter, spacing, coefficient of consolidation, and the average degree of desired consolidation.”

$$t = \frac{D^2}{8c_h} (F(n) + F_s + F_r) \ln \left( \frac{1}{1-\bar{U}_h} \right) \quad \text{Equation 19-2}$$

$$F(n) = \ln \left( \frac{D}{d} \right) - 0.75 \quad \text{Equation 19-3}$$

Where,

t = Time required to achieve desired average degree of consolidation

$\bar{U}_h$  = Average degree of consolidation due to horizontal drainage

D = Diameter of the cylinder of influence of the drain (drain influence zone)

$c_h$  = Consolidation Coefficient for horizontal drainage

F(n) = Drain spacing factor (see Equation 19-2)

d = Equivalent circular drain diameter

$F_s$  = Factor for soil disturbance

$F_r$  = Factor for well resistance

This equation does not include any consolidation due to vertical drainage. It is noted that the predicted settlement amounts and rates (discussed in Chapter 17) are based on vertical drainage. The following sections contain a discussion of each of these components.

### 19.2.1.1 Determination of $F_s$

Soil disturbance is typically ignored except for highly plastic ( $PI > 21$ ), sensitive ( $S_t > 5$ ) soils, and where the Consolidation Coefficient for vertical drainage ( $c_v$ ) has been accurately determined. For these soils an  $F_s \approx 2$  should be used, otherwise use  $F_s = 0$ . Soil disturbance is more pronounced at drain spacings of less than 5 feet or by the use of large, thick anchor plates.

### 19.2.1.2 Determination of $F_r$

The well resistance factor is normally assumed to be negligible (i.e.,  $F_r = 0$ ), provided the PVD has sufficient discharge capacity. The well resistance is only a factor for very deep PVDs (i.e., greater 150 feet deep). For very deep PVDs, please refer to Chu, Bo, and Choa (2004) for guidance in determining  $F_r$ .

### 19.2.1.3 Determination of $c_h$

The horizontal Consolidation Coefficient ( $c_h$ ) can be obtained only through laboratory consolidation testing of high quality samples. Even with high quality samples and testing, the results of the testing can be off by as much as 50 percent of the actual values. Normally  $c_h$  is greater than  $c_v$ . A conservative approach is set  $c_h$  equal to  $c_v$ , without direct measurements of  $c_h$ . However, for design,  $c_h$  can be taken as 1.2 to 1.5  $c_v$ , if no or only slight evidence of layering is evident in partially dried clay samples. If layering of silt and sand in discontinuous lenses is evident,  $c_h$  may be 2 to 4  $c_v$ . The horizontal Consolidation Coefficient may be assessed in the field using CPTu instrumentation and allowing for pore pressure dissipation.

### 19.2.1.4 Determination of $d$

The equivalent circular drain diameter ( $d$ ) of a PVD has been determined using various methods. Diameters ranging from 1.6 to 5.5 inches have been used for the equivalent circular drain diameter, with the most common being 2.4 inches. According to Chu, et al. (2004), a mandrel having a rhombic shape as shown in Figure 19-2 causes the least disturbance on the in-situ soils during installation of the PVD. Alternatively,  $d$  may be determined using the following equation:

$$d = \frac{[2*(a+b)]}{\pi} \quad \text{Equation 19-4}$$

Where,

$a$  = Width of PVD, inches (see Figure 19-2)

$b$  = Thickness of PVD, inches (see Figure 19-2)

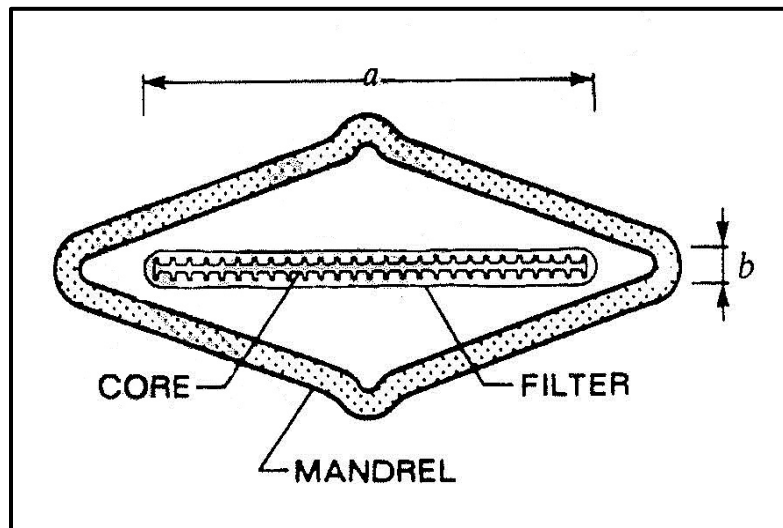


Figure 19-2, PVD Dimensions  
(modified Schaefer, et al. – Vol. I (2017))

### 19.2.1.5 Determination of $\overline{U}_h$

The average degree of consolidation ( $\overline{U}_h$ ) should develop the required settlement to meet the performance limit requirements of Chapter 10. Vertical consolidation can contribute significantly to the total amount of vertical movement and should be considered in the development of the degree of consolidation required.

### 19.2.1.6 Determination of D

According to Schaefer, et al. – Vol. I (2017):

When using an equilateral triangular pattern, *the diameter of the cylinder of influence (D)*, is 1.05 times the spacing between each drain. In a square pattern, *D* is 1.13 times the spacing between drains. Typically, to achieve approximately 90 percent consolidation in 3 to 4 months, designers often choose drain spacing between 3 to 5 feet in homogeneous clays, 4 to 6 feet in silty clays and 5 to 6-1/2 feet in coarser soils.

### 19.2.1.7 Determination of t

The time (t) is the duration required to achieve the desired  $\bar{U}_h$  for a cylinder of diameter (D) and drain diameter (d). According to Schaefer, et al. – Vol. I (2017), “There are 3 basic variables that can be manipulated in order to achieve a desired result from Equation 19-2. These variables are time, PVD spacing, and surcharge.” In order to increase the PVD spacing and reduce the number of PVDs installed, the surcharge can be increased to provide the same amount of consolidation over the same time period. The addition of surcharge and keeping the PVD spacing the same has the effect of reducing the time for consolidation to occur. Typically, time is used as a constant (normally set to meet a specific construction schedule) and the amount of surcharge and the PVD spacing are used as variables.

### 19.2.1.8 Computer Software

Simple applications can be analyzed with hand calculations or with the use of a spreadsheet program to facilitate sensitivity studies. The computer program, FoSSA 2.0, can be used for analyses where the rate of loading becomes more complex and hand solutions become impractical.

A complete set of the design calculations prepared in accordance with this Chapter should be provided. The determination of surcharge amounts and PVD spacing shall be fully documented with all design calculations. Submitted calculations (including computer input and output) shall include all assumptions used in the analysis. Computer generated designs made by software other than FHWA’s FoSSA computer program shall require verification (as required in Chapter 26) that the computer program’s design methodology meets the requirements provided herein; this shall be accomplished by either:

1. Provide complete, legible, calculations that show the design procedure step-by-step for the surcharge and PVD spacing. Calculations may be computer generated provided that all input, equations, and assumptions used are shown clearly.
2. Provide a diskette with the input files and the full computer output of the FHWA sponsored computer program FoSSA (latest version). This software may be obtained at:

**ADAMA Engineering, Inc.**  
33 The Horseshoe, Covered Bridge Farms  
Newark, Delaware 19711, USA  
Tel. (302) 368-3197, Fax (302) 731-1001

### 19.2.2 Earthquake Drains

Earthquake (EQ) drains are a subset of PVDs that are used to mitigate/limit the effects of seismically induced liquefaction. While PVDs are relatively thin strips consisting of a rigid core sheathed in filter fabric; EQ drains are perforated, corrugated plastic pipe placed in a filter fabric sock. Earthquake drains can range in size from 1-1/2 to 10 inches in diameter, but SCDOT typically uses 4 inches in diameter. Earthquake drains are used to reduce the excess pore pressures generated by a seismic event that can lead to liquefaction in loose granular soils (see Chapter 13 for a discussion of liquefaction). The theoretical background for earthquake drains is presented in FEQDrain: A Finite Element Computer Program for the Analysis of the Earthquake Generation and Dissipation of Pore Water Pressure in Layered Sand Deposits with Vertical Drains by Pestana, Hunt, and Goughnour (1997). Because of the uncertainty in how the settlements are determined in FEQDrain and based on field experiment test results (see Rollins, Anderson, McCain and Goughnour (2003)), settlements shall be assumed to reduce to approximately 60 percent of the unmitigated settlement instead of those determined by FEQDrain.

EQ drains work by reducing the pore pressure ratio ( $r_u$ ), to a level that prevents or limits the potential for liquefaction. Recent research on the applicability of EQ drains has indicated that some liquefaction induced settlement will still occur. Typically a  $r_u$  of 0.65 is used to determine the spacing of the drains. However, because of the uncertainties in the amount of liquefaction induced settlement, the effect of high fines content (i.e., percent passing the No. 200 greater than 5 percent), and the effect of high accelerations anticipated from earthquakes in South Carolina, the  $r_u$  shall be limited to 0.50. Using a  $r_u$  of this magnitude will cause the drain spacing to become smaller and potentially increasing the drain size.

$$r_u = \frac{\Delta u}{\sigma'_v} \quad \text{Equation 19-5}$$

Where,

$r_u$  = Pore pressure ratio

$\Delta u$  = Change in pore pressure

$\sigma'_v$  = Effective overburden pressure

### 19.2.3 Construction Considerations

PVDs are installed using equipment similar in size and appearance to pile driving equipment and/or foundation drilling equipment. A typical installation rig for PVDs is shown in Figure 19-3. The contractor is required to submit an installation plan, shop drawings, material samples, and anchorage details. A minimum 12-inch thick layer of drainage material is necessary at the top of the PVDs to provide a drainage path for release of the excess pore pressures. In some applications it will be appropriate to install strip drains across the ground surface to provide horizontal drainage at the top of the PVDs. The drainage layer many times can be installed as a part of the working platform necessary to make the site accessible to PVD installation equipment.

PVDs shall conform to the requirements of STS SC-M-801-1 (latest version) for *Prefabricated Vertical Drain with Fabric*. The drainage material shall conform to the requirements of Supplement Specification *Bridge Lift Materials* (latest version) and shall consist of stone, granular, or man-made (i.e., lightweight) bridge lift materials. The use of borrow excavation materials as the drainage material is not allowed.

EQ drains are installed in a manner similar to PVDs. The EQ drains shall conform to the requirements of STS SC-M-205-1 (latest version) for *Earthquake Drains*. Similar to PVDs the



drainage materials used for EQ drains shall conform to the requirements of Supplemental Specifications *Bridge Lift Materials*, latest version, and shall consist of stone, granular, or man-made (i.e., lightweight) bridge lift materials. The use of borrow excavation materials as the drainage material is typically not sufficient.

The latest version of the Supplemental Specifications and STSs are available on the SCDOT website:

<https://www.scdot.org/business/business-landing.aspx>.

In addition, “go-by” drawings are available to assist the GEOR. The GEOR is reminded that the provided “go-by” must be modified for the specific project. The latest version of the “go-by” is available on the SCDOT website:

<https://www.scdot.org/business/geotech.aspx>.

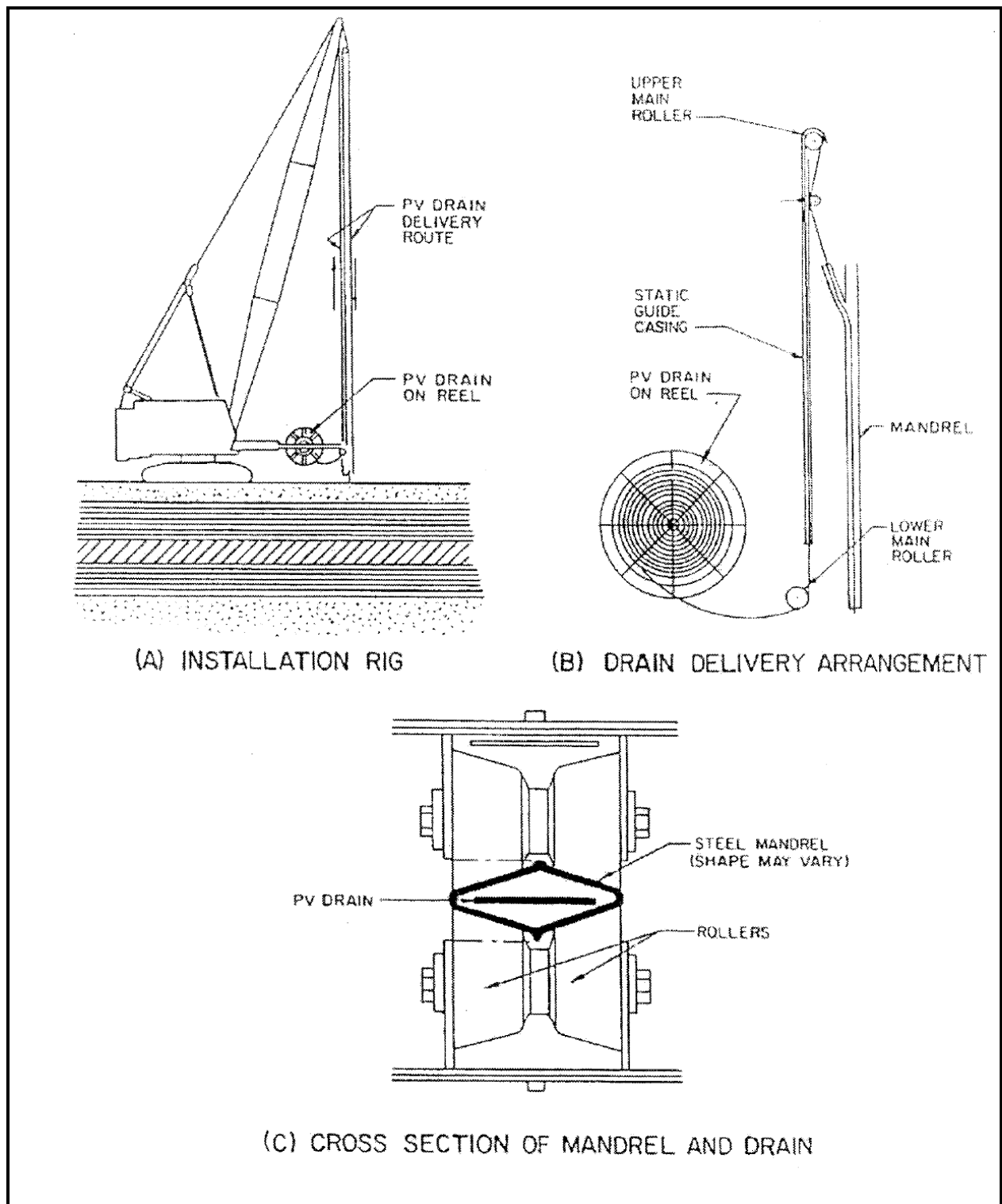


**Figure 19-3, Crane Mounted Installation Rig  
(Schaefer, et al. – Vol. I (2017))**

## 19.3 LIGHTWEIGHT FILL MATERIALS

Lightweight fill materials are used to limit settlement and increase stability through the use of materials with lower densities than conventional fill materials. Conventional fill materials (i.e., sand, silt, and gravel) have densities that range from 115 to 140 pounds per cubic foot (pcf). Lightweight fill materials can have densities ranging from 1 pcf for geofoam (expanded polystyrene (EPS)) to 65 pcf for expanded shale, clay, and slate (ESCS). Geofoam and lightweight cellular concrete will typically behave like materials that have an inherent compressive strength similar to Clay-Like soils in undrained loading. ESCS and glass aggregate will typically behave and have properties similar to Sand-Like soils. In addition to reducing settlement and increasing stability, lightweight fill materials reduce the load applied to ERSs and increase an embankment's resistance to seismic loads by reducing the seismic inertial forces. Table 19-6 provides a list of lightweight fill materials used by SCDOT. Schaefer, et al. – Vol. I (2017) provides additional lightweight materials; however, the use of these other lightweight fill materials (i.e., wood fiber, blast furnace slag, fly ash, shredded tires, or boiler slag), must be approved in writing by SCDOT (including the RPG/GDS and the Office of Materials and Research (OMR)). Lightweight fill materials shall conform to the requirements of STS SC-M-203-5 (latest version) for *Lightweight Aggregates*. If other lightweight materials have been approved for use, the GEOR is required to prepare a Special Provision for that material. The latest version of the STS is available on the SCDOT website:

<https://www.scdot.org/business/business-landing.aspx>.

**Table 19-6, Lightweight Fill Materials  
(modified from Schaefer, et al. – Vol. I (2017))**

Fill Material	Range of Density (pcf)	Range of Specific Gravity
Geofoam (EPS)	0.75 – 2.00	0.01 – 0.03
Foamed Concrete	20 – 60	0.3 – 0.8
Expanded Shale, Clay & Slate (ESCS)	37 – 65	0.6 – 1.0
Glass Aggregate	9.50 – 12.50	0.15 – 0.20

### 19.3.1 General Applications and Limitations

#### 19.3.1.1 Load Reduction

As indicated previously, one of the primary uses of lightweight fill is to reduce the load imposed on soft soils by normal weight fill materials. The use of lightweight fill materials reduces the driving forces, thereby increasing the overall global stability of the embankment or structure. A secondary effect of using lightweight fills is the reduction of the settlement under the imposed load. The amount of settlement reduction is directly proportional to the reduction in the load.

#### 19.3.1.2 Shear Strength

According to Schaefer, et al. – Vol. I (2017):

Granular lightweight fills have an angle of shearing resistance similar to natural soils, while cemented lightweight fills are characterized by a compressive strength. These properties result in internal stability within the lightweight fills. In the case of an embankment over a weak foundation, the shearing surface will

penetrate through the lightweight fill, and the shear strength developed within the lightweight fill deposits will tend to increase the overall global stability.

### 19.3.1.3 Compressibility

According to Schaefer, et al. – Vol. I (2017):

Many lightweight fill materials, such as foamed concrete and ESCS have a compressibility and elasticity similar to natural soils and rock. Under static loading, the amount of internal compression within the fill will often be similar to that for conventional earth fill materials. Under dynamic loading, the resiliency of the lightweight materials will often be similar to the natural soils. Geofoam compressibility or stress strain behavior is generally linear to stress levels of about 0.5 percent. Beyond that, yielding occurs and the material is subject to time-dependent creep.

### 19.3.1.4 Lateral Pressures

According to Schaefer, et al. – Vol. I (2017):

The lateral earth pressure at any depth is a function of the vertical overburden pressure multiplied by the coefficient of earth pressure and then reduced by the cohesion of the deposit. In the case of lightweight fills such as foamed concrete or geofoam, the cohesion of the material is high and the densities are low. *Each* of these factors tend to *significantly* reduce the amount of lateral earth pressure that is transmitted to adjacent structures such as retaining walls, tunnels or pile foundations below bridge abutments.

### 19.3.1.5 Drainage

ESCS and glass aggregate materials, like most of the granular lightweight fill materials, have good drainage characteristics. Good drainage is beneficial behind a retaining wall to eliminate hydrostatic pressures.

### 19.3.1.6 Construction in Adverse Weather

According to Schaefer, et al. – Vol. I (2017):

It is difficult, if not impossible, to place and compact conventional soils during extremely cold or wet weather. However, geofoam, ESCS and foam concrete, have been successfully installed in *inclement* weather.

### 19.3.1.7 Seismic Considerations

According to Schaefer, et al. – Vol. I (2017):

In Japan, there have been case histories where a highway embankment constructed of geofoam did not fail in a severe earthquake, even though adjacent sections of a soil embankment did. The lower unit weight of the material results in lower inertial forces under seismic loading.

### 19.3.1.8 Limitations

Lightweight fill materials have limitations for use; however, these limitations can be overcome by proper evaluation, design, and construction techniques. The following list of limitations is obtained from Schaefer, et al. – Vol. I (2017):

- *Availability of the materials.* Certain geographic areas may have an abundance of 1 type of lightweight fill material, but not of another. Unless the lightweight fill material is available *locally*, the transportation costs raise the price considerably, and make these materials non-competitive.
- *Construction Methods.* In general, all lightweight fill materials involve some special procedures with regard to handling, transportation, placement and compaction. Some lightweight fill materials could be difficult to place and handle. Foam concrete requires the use of specialized equipment at the site to introduce air and other additives into the mixture before placement.
- *Durability of the fill deposits.* Some lightweight fill materials (e.g., geof foam) must be protected to ensure longevity. Because geof foam is subject to deterioration from hydrocarbon spills, a concrete slab or geomembranes are generally placed over the surface of the blocks.
- *Environmental concerns.* Some lightweight fill materials generate leachate as water passes through these deposits. Fortunately, design methods have been developed to minimize the amount of leachate, and, to date, these measures have worked satisfactorily. However, the additional costs of these measures should be considered during design.
- *Geothermal properties.* Most lightweight fill materials possess geothermal properties that are different than soil. This can lead to accelerated deterioration of flexible pavements and/or problems with differential icing of pavement surfaces due to an alteration of the heat balance at the earth's surface. Essentially, most lightweight fill materials act as thermal insulation, even though this is not an intended or desirable function. However, this can be effectively controlled by placing a suitable thickness (20-inch, minimum) of soil and/or paving materials over the surface of the lightweight fill material.

### 19.3.2 Geofoam

According to Schaefer, et al. – Vol. I (2017), “Geofoam is a generic term used to describe any cellular material used as a lightweight fill, *such as* block molded expanded polystyrene (EPS) and extruded polystyrene (XPS), both plant manufactured.” Geofoam materials have the advantage of being not only lightweight, but also may be cut to any size or shape to fit the requirements of the project. Stark, Arellano, Horvarth and Leschinsky (2004), “Guideline and Recommended Standard for Geofoam Applications in Highway Embankments”, contains detailed design guidelines for the use of EPS geof foam in roadway and bridge embankments. Geofoam is a lightweight fill material that has a specific compressive strength.

According to Schaefer, et al. – Vol. I (2017):

The overall design process when using EPS geof foam is divided into 3 phases in order to consider the interaction between the 3 major components in the embankment.

1. Design to preclude external (global) *instability* of the embankment. This should include considerations for settlement, bearing capacity, and slope stability/*instability* under the projected loading conditions.

2. Design for internal stability within the embankment mass. The design must ensure that the geofoam mass can support the overlying pavement system without immediate and time dependent creep compression.
3. Design of an appropriate pavement system for the subgrade provided by the underlying geofoam blocks.

Stability analyses require the modeling and quantifying of both internal shear strength of the geofoam and the shear strength of the geofoam interfaces. The internal shear strength of EPS geofoam correlates to its compressive strength. The interfaces typically include geofoam to geofoam, geofoam to soils and geofoam to geosynthetic material. Interface friction is an important stability design consideration, particularly under horizontal wind, water, and/or seismic loading conditions.

The range of densities and compressive resistance for *Rigid Cellular Polystyrene (RCPS) Geofoam* are listed in ASTM D6817 - *Standard Specification for Rigid Cellular Polystyrene Geofoam*. There are 7 grades of EPS that range in density from 0.70 to 2.85 *pounds per cubic foot (pcf)*, with compressive resistance values of 2.2 to 18.6 *pounds per square inch (psi) at 1 percent strain*, respectively. Six grades of XPS are listed in ASTM D6817. *Table 19-7 provides the density; compressive resistance at 1, 5, and 10 percent strains; and the flexural strength as described in ASTM D6817. The latest version of ASTM D6817 should be consulted to ascertain the relevant properties of the geofoam.* Densities and compressive strengths range from 1.2 to 3.0 pcf and 2.9 to 40.6 psi.

Geofoam embankments often support an overlying roadway pavement. The objective in the design of an appropriate pavement system is to select the most economical arrangement and thickness of pavement materials for the subgrade provided by the supporting EPS blocks. Equivalent soil subgrade strengths for the EPS blocks can be used with traditional pavement design procedures. Subgrade properties as a function of EPS block density are listed in *Table 19-8*.

External stability analyses generally follow traditional geotechnical procedures, although stress distribution must consider a non-homogeneous embankment. Stability analyses require modeling of undrained shear strength of geofoam, which presents some uncertainties.

**Table 19-7, Physical Properties of RCPS Geofoam  
(modified from ASTM (2015))**

Material Designation	Density (pcf)	Compressive Resistance (psi)			Flexural Strength (psi)
		1% Strain	5% Strain	10% Strain	
EPS12	0.70	2.2	5.1	5.8	10.0
EPS15	0.90	3.6	8.0	10.2	25.0
EPS19	1.15	5.8	13.1	16.0	30.0
EPS22	1.35	7.3	16.7	19.6	35.0
EPS29	1.80	10.9	24.7	29.0	50.0
EPS39	2.40	15.0	35.0	40.0	60.0
EPS46	2.85	18.6	43.5	50.0	75.0
XPS20	1.20	2.9	12.3	15.0	40.0
XPS21	1.30	5.1	16.0	15.0	40.0
XPS26	1.60	10.9	26.8	25.0	50.0
XPS29	1.80	15.2	34.1	40.0	60.0
XPS36	2.20	23.2	46.6	60.0	75.0
XPS48	3.00	40.6	77.6	100.0	100.0

**Table 19-8, Equivalent Soil Subgrade Values of EPS Geofoam  
(modified from Schaefer, et al. – Vol. I (2017))**

EPS Block Density (pcf)	CBR (%)	Young's Modulus (psi)	Resilient Modulus (psi)
1.25	2	725	725
1.5	3	1015	1015
2.0	4	1450	1450

Table 19-9 summarizes the design parameters associated with the use of EPS geofoam.

**Table 19-9, EPS Geofam Design Guidelines  
(modified from Schaefer, et al. – Vol. I (2017))**

Design Parameters			
Density, dry	0.75 – 2 pcf	CBR	2 – 4
Compressive and Flexural Strength	6 – 14 psi <sup>1</sup>	Coefficient of Lateral Earth Pressure	Lateral pressures from adjacent soil mass may be reduced to a ratio of 0.1 of horizontal to vertical pressure
Modulus of Elasticity	580 – 1450 psi		
Environmental Considerations			
There are no known environmental concerns. No decay of the material occurs when placed in the ground.			
Design Considerations			
<p>EPS blocks will absorb water when placed in the ground. Blocks placed below water have resulted in densities of 4.8 – 6.4 pcf after 10 years, while blocks above the water had densities of 1.9 – 3.2 pcf for the same period. For settlement and stability analyses, use the highest densities to account for water absorption.</p> <p>Buoyancy forces must be considered for blocks situated below the water table. Adequate cover should be provided to result in <math>\phi = 0.75</math> against uplift.</p> <p>Because petroleum products will dissolve geofam, a geomembrane or a reinforced concrete slab is used to cover blocks in roadways in case of accidental spills.</p> <p>Differential icing potential of pavement, due to a cooler pavement surface above the EPS versus pavement above a soil only subgrade. Differential icing can be minimized by providing a sufficient thickness of soil between the EPS and top of the pavement surface.</p> <p>Use side slopes flatter than or equal to 2H:1V and a minimum cover thickness of 1 foot. If a vertical face is needed, cover exposed face blocks with shotcrete or other material to provide long-term UV protection.</p>			

<sup>1</sup>Varies with density

### 19.3.3 Foamed Concrete

Foamed concrete (lightweight cellular concrete) is created by introducing preformed foam into cement water slurry. The preformed foam is designed for concrete and creates a network of discrete air cells within the cement/water matrix. Sand and fly ash may be added to the mixture with the fly ash partially replacing a portion of the cement. After blending these materials to the specified density, the resulting slurry is pumped into place. Foamed concrete is unique for each application and is normally mixed on site. The quality of foamed concrete is monitored through the cast density. The compressive strength is directly related to the cast density of the mixture. Like geofam, foamed concrete has a specific shear strength that is used in design.

According to Schaefer, et al. – Vol. I (2017):

*Lightweight cellular* concrete (a.k.a. foamed concrete) is a liquid product that is practically self-leveling, and can be pumped over a distance as great as 3,300 feet. The *lightweight cellular* concrete will begin to harden between 2 to 6 hours after placement, and generally solidifies in 24 hours. Design with this product is analogous to design with conventional concrete. The maximum cast unit weight and related minimum compressive strength should be specified as dictated by design and with considerations of local suppliers of *lightweight cellular* concrete. The range of wet cast density and compressive strength that can be specified generally can range from 24 to 80 pcf and 10 to 300 psi, respectively.

Table 19-10 summarizes key design considerations.



**Table 19-10, Foamed Concrete Design Guidelines  
(modified from Schaefer, et al. – Vol. I (2017))**

<b>Design Parameters</b>			
Wet Density Range	24 - 80 pcf	Freeze-thaw Resistance, 100 cycles	92 – 98 % <sup>1</sup>
Compressive Strength	10 - 300 psi <sup>1</sup>	Coefficient of Lateral Earth Pressure	Negligible for vertical loads applied directly over the foamed concrete. Lateral pressures from adjacent soil mass may be transmitted undiminished.
Water Absorption	1.4 – 15 psf <sup>1</sup>		
<b>Environmental Considerations</b>			
There are no known environmental concerns.			
<b>Design Considerations</b>			
<p>Dry density values will be lower than wet density values.</p> <p>Buoyancy could be a problem if foamed concrete is placed below the water table and there is not sufficient vertical confinement.</p> <p>The lower compressive strength mixes are affected by freeze-thaw cycles. The product should be used below the zone of freezing or a higher compressive strength used. Densities greater than 37 pcf have reported excellent freeze-thaw resistance.</p> <p>There is some absorption of water into the voids, which could affect the density and compressive strength. Saturation by water should be prevented by construction of a drainage blanket and drains.</p>			

<sup>1</sup>Varies with density

### **19.3.4 Expanded Shale, Clay & Slate**

ESCS is a granular lightweight fill material. In other words, the strength of these materials is based on the interlock between individual particles, similar to sands and gravels. ESCS is a synthetic aggregate created from heating certain shales, clays, and slates in a rotary kiln to temperatures ranging from 1,800° F to 2,200° F. During this process the clay minerals montmorillonite, illite, and kaolinite become completely dehydrated and expand. Once completely dehydrated, these materials will not re-hydrate under atmospheric conditions; therefore, retaining the expanded shape. The materials are graded through a screening process and may have rounded, cubical, or sub-angular particle shapes. These particles are durable, chemically inert, and relatively insensitive to moisture; however, the particles will absorb and retain some water. ESCS materials can be expensive to manufacture, which has led to the use of these materials primarily as lightweight aggregate in structural concrete.

The design procedures using ESCS use conventional geotechnical methods associated with granular soils. Table 19-11 summarizes key design considerations.

**Table 19-11, ESCS Design Guidelines  
(modified from Schaefer, et al. – Vol. I (2017))**

<b>Design Parameters</b>				
Dry Density	Compacted	50 – 65 pcf	Permeability	High
	Loose	40 – 54 pcf		
Angle of Shearing Resistance	Compacted	37° – 44°	Grain Size Gradation	5 – 25 mm
	Loose	35°		
Coefficient of Subgrade Reaction	Compacted	140 – 155 pci		
	Loose	33 – 37 pci		
<b>Environmental Considerations</b>				
There are no known environmental concerns.				
<b>Design Considerations</b>				
<p>The material will absorb some water after placement, when continually submerged. Samples compacted at a water content of 8.5 percent have been found after 1 year to have a water content of 28 percent. Over a longer period of time, the estimated long-term water content would be about 34 percent.</p> <p>Side slopes of embankments should be covered with a minimum of 3 feet of soil cover. Use side slopes of 1.5H:1V or flatter to confine the material and provide internal stability. For calculating lateral earth pressures, use an angle of shearing resistance of 35° (<i>assumes the soil is placed loose</i>).</p>				

### **19.3.5 Glass Aggregate**

Glass aggregate is made from 99 percent recycled glass with a foaming agent added prior to the aggregate being baked in a kiln at approximately 1,650° F. The first step in the manufacturing process is crushing the glass into small pieces and then grinding the small pieces into a powder. A foaming agent is added to the glass powder. At the temperature previously indicated the blend of foaming agent and glass powder melts forming a solid sheet or “cake”. The cake expands as it is heated in the kiln. Bubbles of gas form inside the cake during the heating and follow a torturous path toward the surface of the cake. As the cake cools naturally to room temperature the cake cracks into glass fragments which are then sieved to form glass aggregate.

The design procedures using glass aggregate use conventional geotechnical methods associated with granular soils. Table 19-12 summarizes key design considerations.

**Table 19-12, Glass Aggregate Design Guidelines**

<b>Design Parameters</b>						
Dry Density	Compacted	50 – 65 pcf	Permeability	High		
	Loose	40 – 54 pcf				
Angle of Shearing Resistance	Compacted	37° – 44°	Grain Size Gradation	5 – 25 mm		
	Loose	35°				
Coefficient of Subgrade Reaction	Compacted	140 – 155 pci				
	Loose	33 – 37 pci				
<b>Environmental Considerations</b>						
There are no known environmental concerns.						
<b>Design Considerations</b>						
<p>The material will absorb some water after placement, when continually submerged. Samples compacted at a water content of 8.5 percent have been found after 1 year to have a water content of 28 percent. Over a longer period of time, the estimated long-term water content would be about 34 percent.</p> <p>Side slopes of embankments should be covered with a minimum of 3 feet of soil cover. Use side slopes of 1.5H:1V or flatter to confine the material and provide internal stability. For calculating lateral earth pressures, use an angle of shearing resistance of 35° (<i>assumes the soil is placed loose</i>).</p>						

## 19.4 VIBRO-COMPACTION

This Section of the GDM has been removed from version 2.0, since vibro-compaction is not typically performed for SCDOT projects. Instead SCDOT typically uses stone as a backfill material (i.e., stone columns are created). If vibro-compaction is required at a project site, the GEOR should consult Ground Modification Methods, FHWA-NI-16-027, Volume I, GEC 13 and obtain acceptance of the PC/GDS and the PCS/GDS.

## 19.5 AGGREGATE COLUMNS

Aggregate (i.e., stone) columns are constructed using a vibratory probe to increase the density of loose sands at depths beyond which surface compaction equipment is inadequate by using stone as a replacement/displacement material. The vibrations in the immediate vicinity of the vibrator induce liquefaction of saturated loose Sand-Like soils. The vibrator densifies loose Sand-Like soils as well as allowing for the insertion of stone into matrix through displacement of the in-situ materials. The mechanical vibrations and water to overcome the in-situ effective stresses between the soil grains allowing the sand grains to rearrange under the action of gravity into a denser state as well as be displaced by the stone. Included in this Section along with stone columns are vibro-concrete columns (VCCs), geotextile-encased columns (GECs), and Geopier<sup>®</sup> Rammed Aggregate Pier<sup>™</sup> (Geopiers). Stone columns are constructed using either vibro-replacement or vibro-displacement. Table 19-13 provides definitions for both terms. Stone columns shall conform to the requirements of STS SC-M-205-2 (latest version) for *Stone Columns*. Prior to specifying the use of Geopiers or VCCs the GEOR shall obtain the acceptance of both the PC/GDS and the PCS/GDS. If Geopiers or VCCs have been approved for use, the GEOR is required to prepare a Special Provision for the Geopier or the VCC. The latest version of the Stone Column STS is available on the SCDOT website:

<https://www.scdot.org/business/business-landing.aspx>.

**Table 19-13, Vibro-replacement and Vibro-displacement Definitions (modified Schaefer, et al. – Vol. I (2017))**

<b>Vibro-replacement</b>	Refers to the wet, top feed process in which jetting water is used to aid the penetration of the ground by the vibrator. Due to the jetting action, part of the in-situ soil is washed to the surface. This soil is then replaced by the backfill material.
<b>Vibro-displacement</b>	Refers to the dry, top or bottom feed process; almost no in-situ soil appears at the surface, but is displaced by the backfill material.

Stone columns are a natural progression from vibro-compaction and extended vibro-system applications beyond the relatively narrow application of densification of clean, granular soils as shown in Figure 19-4.

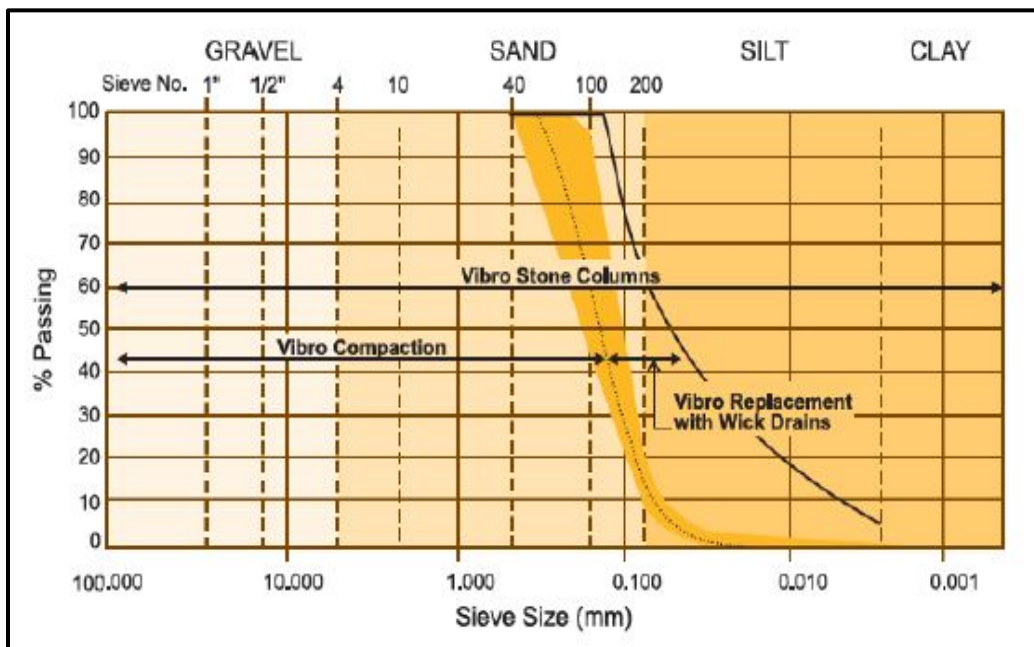


**Figure 19-4, Applicable Grain-Size Distributions for Stone Columns (Schaefer, et al. – Vol. I (2017))**

**19.5.1 Vibro-Replacement**

The top feed method is a wet method and replaces the in-situ soil (i.e., vibro-replacement) with the stone column (see Figure 19-5). In this method a high-pressure water jet is used to open a hole for the vibro-probe to follow into. Once the tip elevation is obtained the vibro-probe is retracted and stone is then placed into the hole from the top. The vibro-probe is then turned on and inserted into the stone to densify the stone, then the vibro-probe is retracted again and the process repeated until the stone column is formed. This method is used at sites with soft to firm soils with undrained shear strengths of 200 to 1,000 psf and a high groundwater table.

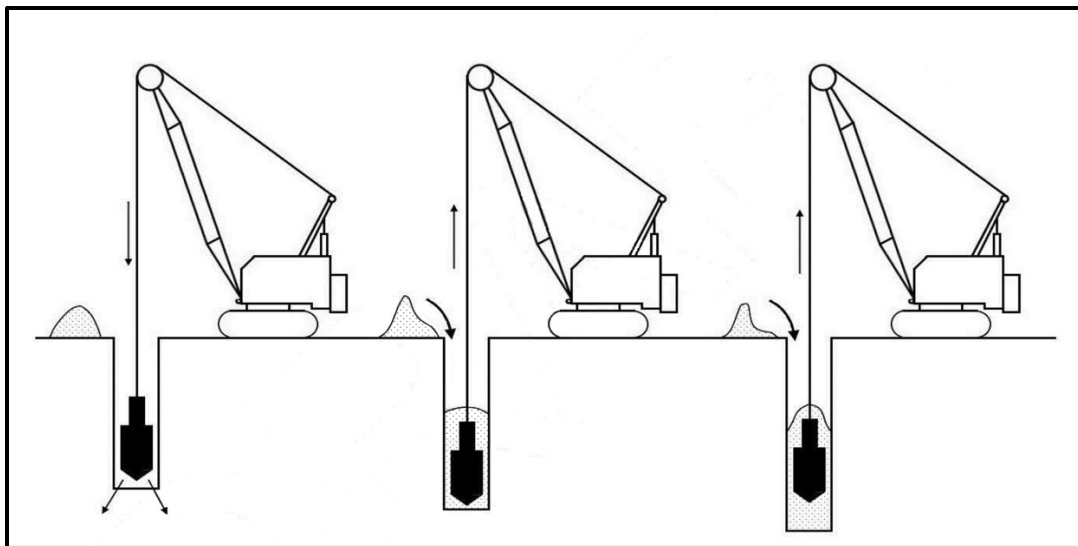


**Figure 19-5, Top Feed Construction Method  
(Schaefer, et al. – Vol. I (2017))**

### 19.5.2 Vibro-Displacement

When environmental impacts are anticipated, stone columns should be constructed using the vibro-displacement method (see Figure 19-6). The vibro-displacement is a dry method that is either top or bottom feed. Using the oscillations of the vibrator in conjunction with the deadweight of the vibrator, air jetting, and/or pre-augering, the vibrator is inserted into the ground without the use of jetting water. The top feed method can be used for short stone columns; however, for deeper columns and where the potential for hole collapse exists, the bottom feed method is used.

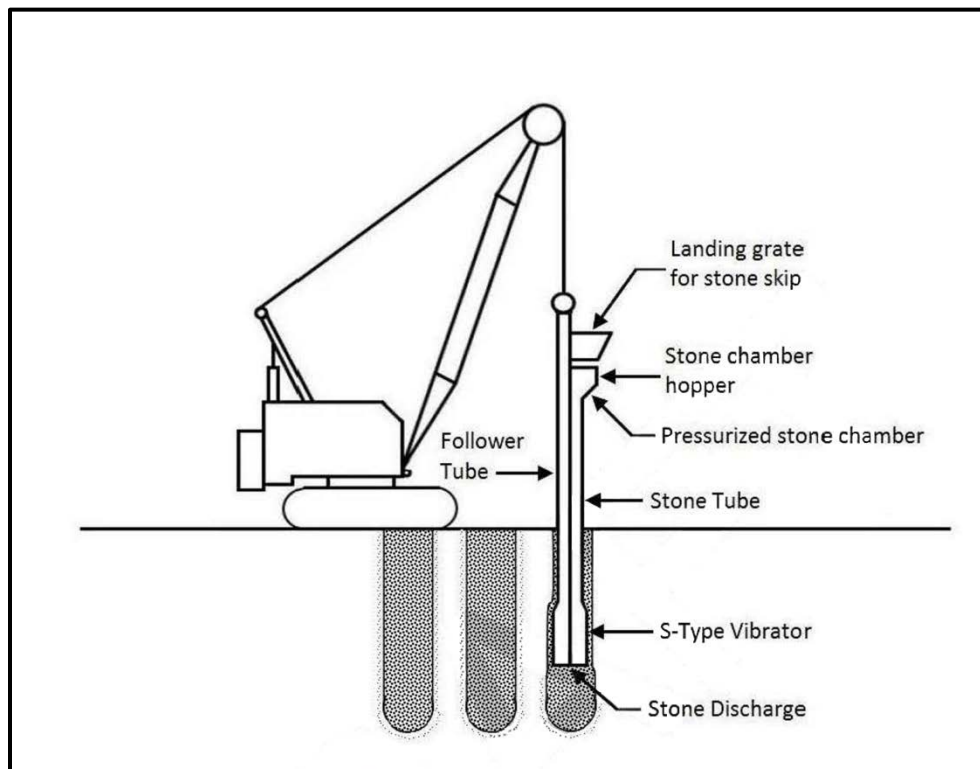


**Figure 19-6, Bottom Feed Construction Method  
(Schaefer, et al. – Vol. I (2017))**

### 19.5.3 Vibro-Concrete Columns

According to Schaefer, et al. – Vol. I (2017)):

Since stone columns derive their strength and settlement characteristics from the surrounding soil, they do not perform well in very soft clay or peat with a thickness greater than the diameter of the column. VCCs were developed to treat these soils. Instead of feeding stone to the tip of the vibrator, concrete is pumped through an auxiliary tube to the bottom of the hole. This method can offer ground improvement advantages of the vibro-systems, with the load carrying characteristics of a deep foundation.

The VCC process employs a bottom feed vibrator that can penetrate the soils to a level suitable for bearing. Concrete is pumped through the vibrator assembly during initial withdrawal. The vibrator then repenetrates the concrete, displacing it into the surrounding soil to form a high-capacity, enlarged column base. The vibrator is then slowly withdrawn as concrete is pumped *and* maintained at a pressure to form a continuous shaft of concrete up to the ground level. At ground level, a slight mushrooming of the concrete column is constructed to assist the transfer of the applied loading into the VCC (see Figure 19-7).

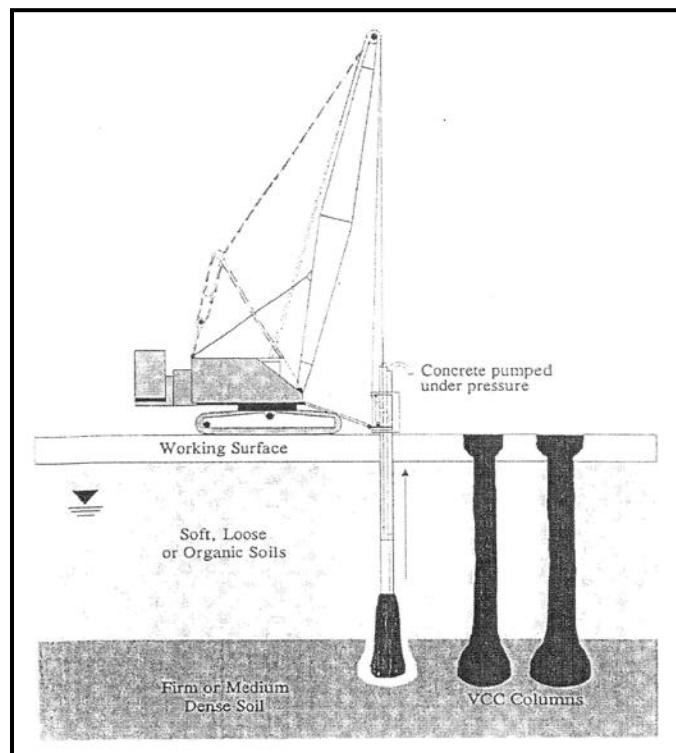


**Figure 19-7, Vibro-Concrete Column  
(Elias, et al. – Vol. I (2006))**

### 19.5.4 Geotextile-Encased Columns

GECs consist of inserting continuous, seamless, high strength geotextile tubes into soft soil with a mandrel. The tube is then filled with either sand or fine gravel to form a column with a high bearing capacity. GECs typically have a diameter of 30 inches. GECs can be installed using either the replacement or the displacement methods. The replacement method consists of driving an open ended steel pipe pile to the bearing stratum. The soil within the pile is removed

with an auger and a tube is inserted into the void and then the tube is filled with sand or fine gravel. The displacement method uses a steel pipe with 2 base flaps (the flaps close on contact with the ground surface) is vibrated to the bearing layer, displacing the soft soil. The geotextile casing is installed and filled with sand or fine gravel and the steel pipe pile is vibration extracted. During this process the sand or gravel within the geotextile is densified. For additional information about GECs please see GeoTech Tools at: <http://www.geotechtools.org/>.

### 19.5.5 Geopier® Rammed Aggregate Pier™

Geopiers are a variant of stone columns, in that a 2- to 3-foot diameter hole is drilled into the foundation soil and gravel is added and then rammed into the foundation soils (see Figure 19-8). Geopiers typically extend to depths of 7 to 35 feet.

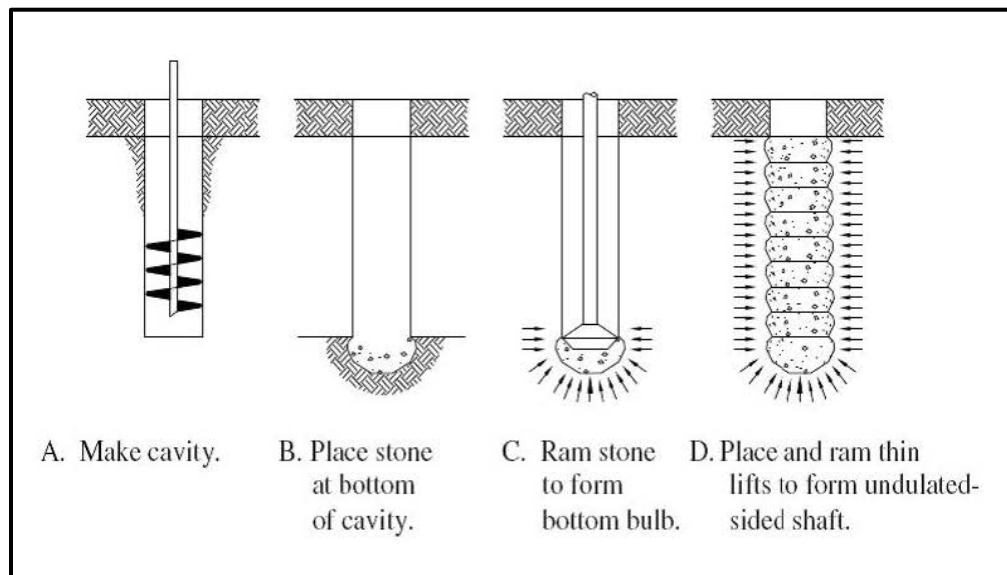


**Figure 19-8, Geopier® Rammed Aggregate Pier™ (Geotech Tools (2012))**

Geopiers are most applicable in soft to stiff cohesive soils with undrained shear strengths ranging from 300 to 4,000 psf and in loose to medium dense silty and clayey sands. The soil must be stable without the need for external support (i.e., casing). Shallow groundwater may require the use of temporary casing; however, a specialist contractor should be consulted prior to designing Geopiers with a temporary casing. The gravel is placed in relatively thin lifts with the first lift of gravel forming a bulb at the bottom of the pier, thus pre-stressing and pre-straining the soil beneath and around the bottom of the pier. The ramming process use a high-energy (250 to 650 kip-foot per foot) beveled tamper that both densifies the gravel and forces the gravel laterally into the sidewalls of the hole. The tamper should have an area at least 85 percent of the area of the pre-bored hole. This action increases the lateral stress in the surrounding soil, further stiffening the stabilized composite soil mass.

### 19.5.6 General Considerations

Stone columns can be used to improve the stability of slopes, increase bearing capacity, reduce total and differential settlements, decrease the time for these settlements to occur, and to mitigate potential for liquefaction. Stone columns can be used to improve the stability of a slope by creating discrete zones of high strength material that will provide more resisting force along the potential failure surface. Stone columns can also increase the bearing capacity by transferring the load to a deeper, stronger layer and by densification of the in-situ soils through the use of vibro-displacement methods of installation. Further, stone columns can be used to

reduce the amount of total and differential settlement that a new embankment or a widened embankment would undergo without the improvement. The stone columns will also provide a conduit for the flow of ground water, thus decreasing the time for settlement to occur similarly to PVDs. Lastly, stone columns are used to mitigate the potential for liquefaction through densification of the in-situ materials and by providing pore pressure relief zones, because the stone column will have a greater hydraulic conductivity than the in-situ sands.

Some of the advantages of stone columns are economy and the technical feasibility to replace deep foundations with shallow foundations. Stone columns also provide a less expensive option to cut and replace, particularly on large sites with shallow groundwater. In developed areas where high-vibration methods such as dynamic compaction, deep blasting, or pile driving would have an impact on adjacent properties, low-vibration stone columns may provide a viable alternative to other ground improvement options. The use of stone columns could decrease the time required for construction by allowing construction to proceed immediately instead of waiting for the placement of surcharge. In areas that have a potential for liquefaction, the installation of stone columns can improve the cyclic resistance ratio (see Chapter 13). In addition, stone columns can provide vertical drainage and storage capacity to dissipate excess pore pressures induced by a seismic event. Geopiers have similar advantages to stone columns.

VCCs have the advantage of transferring loads similar to piles, while mobilizing the full soil and site improvement potential of a vibro-system. The installation of VCCs is a quiet process and induces minimal vibrations into the in-situ soils allowing for installation immediately adjacent to existing structures. Since this is a dry displacement process, there is no spoil to remove and no water requiring detention. VCCs have the additional advantage of being able to extend through thick very soft clays and organic materials.

According to Elias, et al. – Vol. I (2006)):

The major advantage of GECs over stone columns is that they may be used in soft soils with undrained shear strengths as low as 25 psf. The geotextile provides the lateral constraint that the surrounding soils must provide for stone columns. GECs provide excellent vertical drainage, which may result in very rapid construction, due to the dissipation of pore water pressure.

The major disadvantage of stone columns is that stone columns are not effective in soils having thick layers of soft clays and organic materials. If the thickness is more than the diameter of the stone column, then stone columns may not be appropriate because the soft soils will not provide adequate lateral support of the stone column. In addition, stone column construction can be hampered by the presence of dense overburden, boulders, cobbles, or other obstructions that may require pre-drilling prior to installation of the stone column. The major disadvantage of GECs and Geopiers is both methods rely on proprietary, patented technologies.

### **19.5.7 Feasibility**

According to Schaefer, et al. – Vol. I (2017)):

The degree of densification resulting from the installation of vibro-systems is a function of soil type, silt and clay content, soil plasticity, pre-densification relative densities, vibrator type, stone shape and durability, aggregate column area, column spacing, and energy applied. Experience has shown that soils with less than 15 percent passing the #200 (<0.074 mm) sieve, and clay contents less than 2 percent will densify due to the vibrations. Clayey soils do not react favorably to the vibrations, and the improvement in these soils is measured by



the percent soil replaced and/or displaced by the aggregate columns. In the case of clayey soils, the ground improvement is achieved by reinforcing the soil.

A generalized summary of the factors affecting the feasibility of stabilizing soft ground with stone columns is as follows:

1. The allowable design loading of a stone column should be relatively uniform and limited to a maximum of 110 kips per column, provided sufficient lateral support by the in-situ soil can be developed.
2. The most significant improvement is likely to be obtained in compressible *Clay-Like soils* ranging in shear strength from 300 to 1000 psf.
3. Aggregate columns should not be used in highly sensitive soils (see *Chapter 7*). Special care must be taken when using stone columns in soils containing organics and peat lenses or layers with undrained shear strength less than 300 psf. Because of the high compressibility and low strength of these materials, little lateral support may be developed and large vertical deflections of the columns may result. When the thickness of the organic layer is greater than 1 to 2 stone column diameters, the ability to develop consistent column diameters becomes questionable.
4. Ground improvement with stone columns reduce settlements typically from 50 to 70 percent of the unimproved ground response and differential settlement from 5 to 15 percent of unimproved soil response. Ground improvement with rammed aggregate piers can reduce settlement to less than 1 inch.
5. Due to the development of excessive resistance to penetration of the vibrator a practical upper limit is in the range of undrained shear strength of 1,000 to 2,000 psf for stone columns. If stone columns are used in these stiff soils or through stiff lenses, the column hole is commonly pre-bored, which is often the case in landslide projects. This will result in significant additional cost.
6. The installation of rammed aggregate piers in soils that do not stand open during drilling (loose *Sand-Like* soils, very soft *Clay-Like* soils) often requires the use of temporary casing, which reduces the installation rate and increases the cost of the piers.
7. The ultimate capacity of a group of aggregate columns is predicted by estimating the ultimate capacity of a single column and multiplying that capacity by the number of columns in the group.
8. The maximum practical depth of stone columns and rammed aggregate piers is 100 feet and 35 feet, respectively.
9. *Stone columns have been used effectively to improve stability of slopes and embankments. The design is usually based on conventional slip circle or wedge analyses utilizing composite shear strengths.*
10. *The following relationship is recommended to prevent piping of the soil surrounding the stone column:*

$$20D_{S15} < D_{G15} < 9D_{S85} \quad \text{Equation 19-6}$$

Where,

$D_{S15}$  = Diameter of the surrounding soil passing 15 percent

$D_{G15}$  = Diameter of stone (gravel) passing 15 percent

$D_{S85}$  = Diameter of the surrounding soil passing 85 percent

VCCs use the load transferring characteristics of piles, while mobilizing the full ground improvement potential of aggregate columns. In *Sand-Like* soils, VCCs also densify the surrounding soils by the displacement process, in *Clay-Like* soil this densification does not occur. Construction of the columns is a quiet process, with minimal surface vibration, allowing work close to structures. As VCC installation involves a dry process, limited spoil removal is required. Due to enlarged-base construction with VCCs, column lengths are shorter than would be required for conventional piles. Where thick strata of very soft clay or organic material such as peat are present, they can also be technically feasible and economic solution.

A generalized summary of the factors affecting the feasibility of stabilizing soft ground with VCC follows:

1. The allowable design load for VCCs is a function of the diameter of the column, the allowable strength of the concrete, and the strength of the bearing layer. Typical column diameters range from 18 to 24 inches. Typical allowable design loads for VCC range from 150 to 250 kips.
2. VCC are typically used in very soft clay and organic soils.
3. Typical VCC lengths vary from 20 to 75 feet.

### **19.5.8 Environmental Considerations**

Vibro-replacement methods use water jets to create a hole for the vibro-probe. The jetted water can cause the fine portions of the in-situ soils to come to the ground surface. The fines laden water has to be contained temporarily to allow for sediment deposition. The resulting deposited material has to be disposed of properly. Further, this method may also bring other contaminants to the ground surface, causing the treatment and proper disposal of not only the sediments, but also the water used for jetting. For these reasons, the use of dry vibro-displacement methods is preferred for the installation of stone columns.

### **19.5.9 Design Considerations**

The design of stone columns is still an empirical process; however, general design guidelines have been developed and are provided below. Additional information may be obtained from the following references.

1. Design and Construction of Stone Columns - Volume I, Barksdale and Bachus, (1983)
2. "The Design of Vibro Replacement," Priebe, (1995)
3. See Aggregate Columns on GeoTech Tools at: <http://www.geotechtools.org/>

For stone columns to adequately perform, the soils surrounding the columns must provide sufficient lateral support to prevent bulging failures. In addition, the columns should terminate in a dense formation to prevent bearing failures. Stone columns are typically stiffer than the

materials that surround the columns; therefore, the columns will settle less and will carry a larger portion of the applied load. The applied load is transferred between columns through soil arching. Ultimately equilibrium is reached when sufficient load has been transferred to the columns to prevent further settlement of the surrounding soils. In stability and bearing analyses, composite shear strength of the soil-stone column matrix is used. The composite shear strength is based on the shear strength of the in-situ soils, the shear strength of the stone materials, and the area replacement and stress ratios.

According to Schaefer, et al. – Vol. I (2017):

The generalized design process for embankment support is as follows:

1. Perform embankment design without stone columns to determine the overall settlement and global stability and to determine if stone columns or another form of ground modification are required. If yes proceed to Step 2.
2. Assume an area replacement ratio and column diameter.
3. Determine the spacing based on the assumed area replacement ratio and column diameter.
4. Check the load bearing capacity of the stone column to see if it meets the project requirements. If not revise the column diameter and re-check.
5. Determine the total settlement of the embankment supported on the stone columns.
6. Check the time rate of settlement. If the time for settlement is too large consider changing the column spacing.
7. Check global stability.

For the design procedure of Geopiers, the GEOR should review Schaefer, et al. Vol. I (2017). In addition, prior to the use of Geopiers, the GEOR shall obtain concurrence for both the use of Geopiers as well as the design methodology from the PC/GDS and the PCS/GDS.

#### **19.5.9.1 Unit Cell Concept**

According to Schaefer, et al. – Vol. I (2017):

For purposes of settlement and stability analyses, it is convenient to associate the tributary area of soil surrounding each stone column with the column illustrated in Figures 19-9 and 19-10. Although the tributary area forms a regular hexagon about the stone column, it can be closely approximated as an equivalent circle having the same total area. The resulting equivalent cylinder of material having an effective diameter ( $D_e$ ) enclosing the tributary soil and 1 stone column is known as the “unit cell”. The stone column is concentric to the exterior boundary of the unit cell.

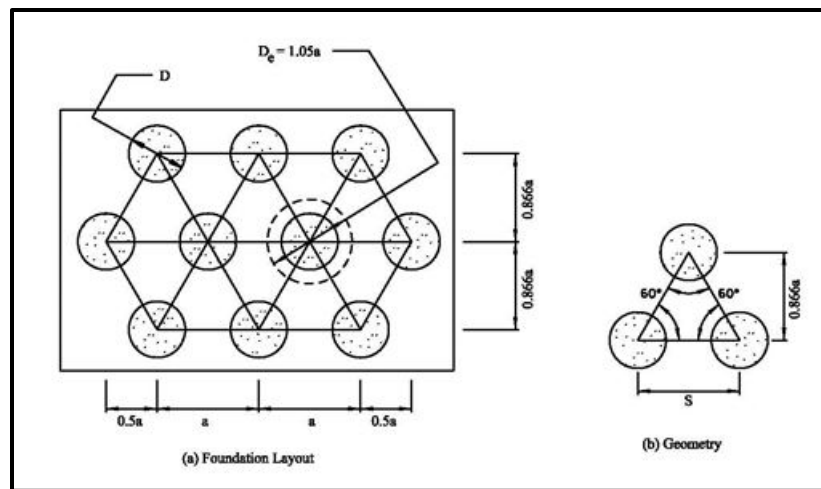


**Figure 19-9, Stone Column Equilateral Triangular Pattern (Schaefer, et al. – Vol. I (2017))**

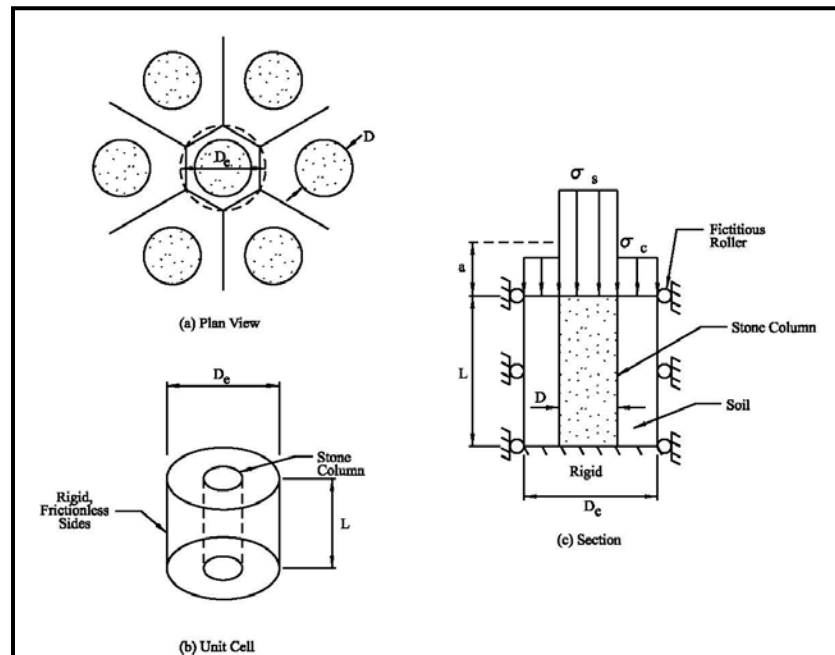


**Figure 19-10, Unit Cell Idealization (Schaefer, et al. – Vol. I (2017))**

### 19.5.9.2 Area Replacement Ratio

The Area Replacement Ratio ( $\alpha_s$ ) defines the area of the soil replaced by the stone column as a function of the tributary area of the unit cell to the area of the stone column. The more soil replaced by the stone column, the greater the effect on performance. Typical values of  $\alpha_s$  range from 0.10 to 0.40.

$$\alpha_s = \frac{A_s}{A} = \frac{D^2}{D_e^2} \tag{Equation 19-7}$$

$$a_{ir} = \frac{1}{\alpha_s} = \frac{A}{A_s} = \frac{D_e^2}{D^2} \tag{Equation 19-8}$$

Where,

$\alpha_s$  = Area replacement ratio  
 $A_s$  = Area of the stone column  
 $A$  = Total area within the unit cell  
 $a_{ir}$  = Area improvement ratio  
 $D$  = Diameter of stone column (see Figure 19-10)  
 $D_e$  = Effective diameter of unit cell (see Figure 19-10)

### 19.5.9.3 Spacing and Diameter

According to Schaefer, et al. – Vol. I (2017):

Stone column diameters vary between 1.5 and 4.0 feet, but are typically in the range of 3.0 to 3.5 feet for the dry method of *installation*, and somewhat larger for the wet method of *installation*.

Triangular, square, or rectangular grid patterns are used with center-to-center column spacing of 5.0 to 12.0 feet. For footing support, *the stone columns* are installed in rows or clusters. For *either* footing or wide area support, *the stone columns* may extend beyond the loaded area.

### 19.5.9.4 Stress Ratio

The transfer of the applied load to the stone columns from the in-situ soils depends on the relative stiffness of the stone column to the in-situ soils, as well as the spacing and diameter of the stone columns. Because the stone columns and the in-situ soils deflect (strain) approximately equally, the stone columns must be carrying a greater portion of the load (stress) than the in-situ soils. This concept has also been called the equal strain assumption. This concept has been proven by both field measurements, as well as finite element analysis. The relationship between the stress in the stone column and the stress in the in-situ soil is defined in the following equation:

$$n = \frac{\sigma_{sc}}{\sigma_c} \quad \text{Equation 19-9}$$

Where,

$n$  = Stress ratio or stress concentration  
 $\sigma_{sc}$  = Stress in the stone column  
 $\sigma_c$  = Stress in the surrounding soil

Measured values of  $n$  have generally been between 2.0 and 5.0. The theory indicates that  $n$  should increase with time. A high  $n$ -value (3.0 to 4.0) may be required in very weak soils and when the column spacing is tight. Lower values of  $n$  (2.0 to 2.5) are required when the surrounding soil is stronger and the column spacing is wider. For preliminary design, a conservative  $n$ -value of 2.5 should be assumed.

Equilibrium of vertical forces for a given  $\alpha_s$  is provided by the following equation.

$$q = (\sigma_{sc} * \alpha_s) + \sigma_c * (1 - \alpha_s) \quad \text{Equation 19-10}$$

Where,

$q$  = Average stress on the unit cell

The stresses in the stone column and the surrounding soil in the unit cell can be determined by rearranging the above equation.

$$\sigma_c = \frac{q}{[1 + \alpha_s(n-1)]} \quad \text{Equation 19-11}$$

$$\sigma_{sc} = \frac{(n \cdot q)}{[1 + \alpha_s(n-1)]} \quad \text{Equation 19-12}$$

### 19.5.9.5 Additional Design Considerations

The procedures indicated in the previous Sections concern the design of stone columns as affected by the diameter, spacing, and distribution of stresses between stone columns and the surrounding soil. See Schaefer, et al. (2017) for the vertical capacity of stone columns, settlement, rate of settlement, shear strength increase caused by the installation of stone columns, and affect the installation of stone columns have on the seismic response of a site.

### 19.5.10 Geopiers<sup>®</sup>

Geopiers<sup>®</sup> shall be designed in accordance with the procedures detailed in Schafer, et al. (2017). In addition, prior to the use of Geopiers<sup>®</sup> on a SCDOT project, the acceptance of both the PC/GDS and the PCS/GDS is required.

### 19.5.11 Design Verification

According to Schaefer, et al. – Vol. I (2017)):

A combination of load tests on aggregate columns constructed before, during and after production should be specified to verify the design assumptions and the performance specification. There are 3 types of load tests: (1) short-term tests, which are used to evaluate ultimate stone column bearing capacity, (2) long-term tests, which are used to measure the consolidation settlement characteristics; and (3) horizontal or composite shear tests, which are used to evaluate the composite aggregate-soil shear strength for use in stability analyses. The most common of these tests is the short-term load test on a single column.

In-situ testing to evaluate the effect of the stone column construction on the native cohesive soil can be also specified. However, the specified test method should be selected on the basis of its ability to measure changes in lateral pressure in cohesive soils. The *electro-piezcone* penetrometer test (*CPTu*), the flat plate dilatometer test (DMT) and the pressuremeter test (PMT) appear to provide the best means for measuring the change, if any, in lateral stress due to stone column construction.

## 19.6 DYNAMIC COMPACTION

Dynamic compaction is the process of ground improvement using weights dropped from a height resulting in the application of high energy levels to the in-situ soil resulting in improvement of the soil. Typically, the weight (called a tamper) ranges from 11 to 40 kips and is dropped from heights of 30 to 100 feet. Dynamic compaction can typically be performed using conventional construction equipment as long as the crane has a free spool attached to allow the cable to unwind with minimal friction. The depth of improvement generally ranges from 10 to 36 feet for light- and heavy-energy applications, respectively. The light-energy applications consist of low weights and low drop heights, while heavy-energy applications consist of heavy weights dropped from high heights. Figure 19-11 provides a schematic of dynamic compaction.

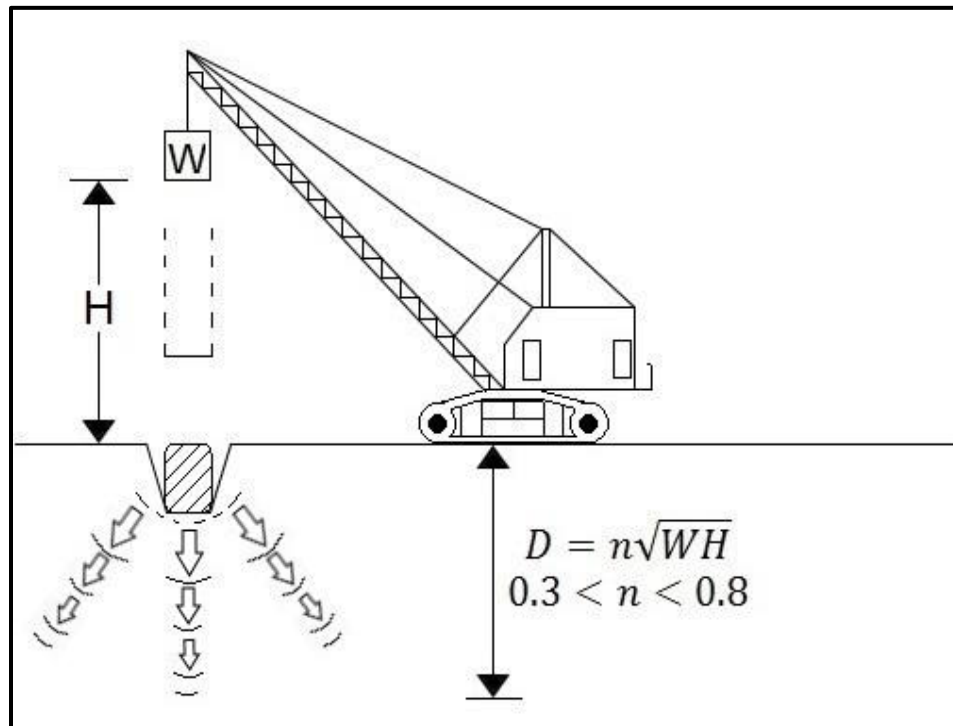


**Figure 19-11, Dynamic Compaction Schematic  
(Schaefer, et al. – Vol. I (2017))**

### 19.6.1 Analysis

Dynamic compaction is used to densify natural and fill deposits to improve the soil properties and performance of the subgrade soils. The primary uses of dynamic compaction are:

- Densification of loose deposits
- Collapse of large voids
- Related applications

Dynamic compaction is used to densify loose deposits of soil by reducing the void ratio. This ground improvement method is used for pervious, Sand-Like soils (Zone 1 - sands, gravels, and non-plastic silts) that meet the gradation, permeability (hydraulic conductivity), and plasticity shown in Figure 19-12. For saturated Zone 1 soils, the induced excess pore pressures from dynamic compaction can cause the soil particles to lose point-to-point contact (i.e., liquefy). Following dissipation of these excess pore pressures, the soil grains settle into a more dense structure. Besides permeability, the degree of saturation, length of the drainage path, and the soil stratigraphy also affect the effectiveness of dynamic compaction. The degree of saturation

is related to the position of the groundwater table. For soils located above the groundwater table, the results of dynamic compaction are immediate, while time is required to allow pore pressure dissipation of soils below the water table. Dense or hard layers near the ground surface can limit the effect of dynamic compaction on deeper soils.

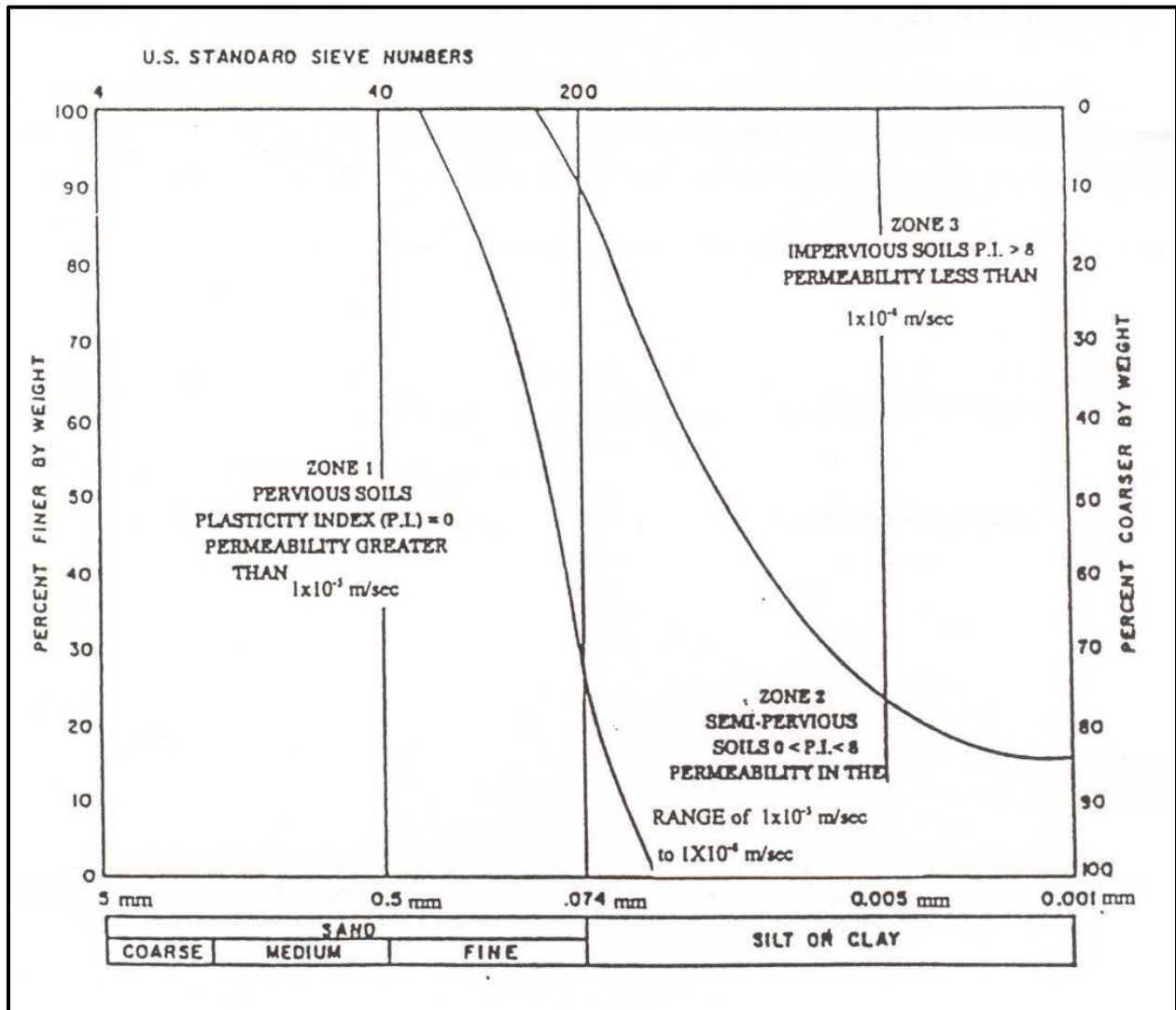
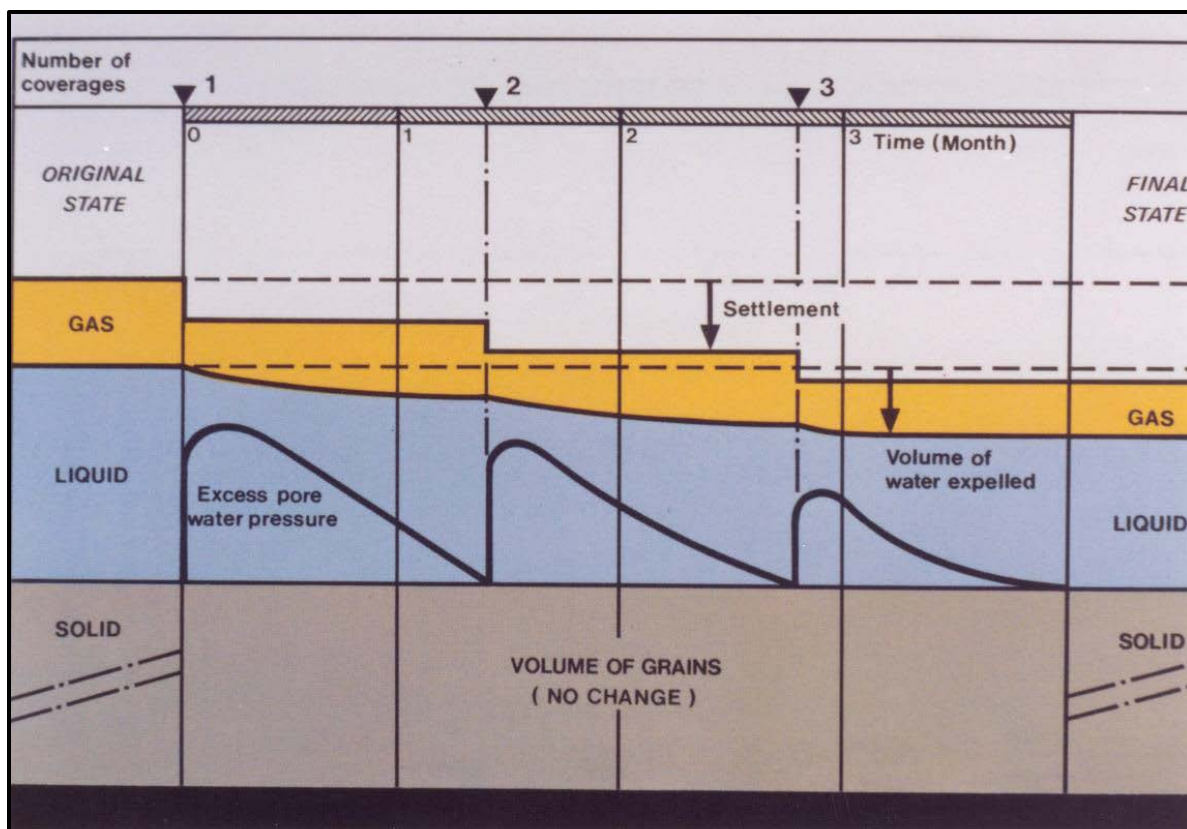


Figure 19-12, Soil Grouping for Dynamic Compaction (Schaefer, et al. – Vol. I (2017))

Using a phase diagram, the results of multiple dynamic compaction passes verify the reduction in void ratio and the resulting densification of the subgrade soils (see Figure 19-13). It should be noted that while the void ratio decreases, the volume of the solids does not change.





**Figure 19-13, Dynamic Compaction Phase Diagram  
(Schaefer, et al. – Vol. I (2017))**

The soils indicated in Zone 3 (Figure 19-12) are typically impervious, Clay-Like soils. The use of dynamic compaction is not recommended for these soils. The soils located in Zone 2 may be improved using dynamic compaction; however, multiple passes of the tamper will be required. Further, additional time will be required between each pass to allow for the dissipation of excess pore pressures.

Large voids in natural or fill deposits can be collapsed using dynamic compaction depending on the depth to the void and the weight and drop of the tamper. Dynamic compaction can be used to improve fill materials of unknown compactive effort. In addition, dynamic compaction is also used to compact construction debris and solid waste materials that may be located within the Right-of-Way. Using dynamic compaction on construction debris and solid waste materials will improve the density of the material and may result in not having to remove and properly dispose of these materials.

According to Schaefer, et al. – Vol. I (2017):

In weak saturated soils relatively deep craters (> 5 feet) can develop. If these craters are filled with coarse granular materials and supplemental energy applied, the granular material will be driven into the weak deposit. This type of improvement is strictly speaking not dynamic compaction and is called dynamic replacement. Dynamic compaction equipment is used to produce the improvement, so this procedure is a related form of ground improvement. The depth of improvement is generally less than about 10 to 13 feet.

### 19.6.1.1 Advantages

Dynamic compaction has many advantages which are listed below:

- The tamper can be used as a probing, as well as a correcting, tool. Dropping the tamper can identify areas of loose soil or voids (deeper crater). This identification allows real time adjustments to the dynamic compaction program.
- Densification of soils can be observed as compaction proceeds. After several passes, the depth of the craters should become shallower indicating densification of the underlying soils.
- Dynamic compaction can be used on sites that have heterogeneous deposits (i.e., boulders, loose fills, construction debris, and solid waste).
- Dynamic compaction results in a bearing stratum that is more uniform after compaction, resulting in uniform compressibility, minimizing differential settlements.
- Densification can be achieved below the water table, eliminating costly dewatering.
- Standard construction equipment can be used for dynamic compaction with the exception of very heavy tampers and high drop heights. Very heavy tampers and high drop heights will require specialty contractors.
- Dynamic compaction can be performed in inclement weather, provided precautions are taken to avoid water accumulation in the craters.

### 19.6.1.2 Disadvantages

Dynamic compaction has the following disadvantages:

- Ground vibrations induced by dynamic compaction can travel significant distances from the point of impact, thus limiting the use of dynamic compaction to light weight tampers and low drop heights in urban environments.
- The groundwater table should be more than 6 feet below the existing ground surface to prevent softening of the surface soils and to limit the potential of the tamper sticking in the soft ground.
- A working platform may be required above very loose deposits. The working platform also functions to reduce the penetration of the tamper. The cost of the working platform can add significant costs to the project.
- Large lateral displacements (1 to 3 inches) have been measured at distances of 20 feet from the point of impact by tampers weighing 33 to 66 kips. Any buried structures or utilities within this zone of influence could be damaged or displaced.

### 19.6.1.3 Environmental Considerations

As indicated previously the vibrations created by dynamic compaction can have an adverse effect on adjoining properties. Therefore determine the potential impact of vibrations caused by Dynamic Compaction using the procedures provided in Chapter 24.

If the estimated particle velocity exceeds the project requirements, then, either the weight of the tamper is reduced or the drop height is lowered. Ground vibrations on the order of  $\frac{1}{2}$  to  $\frac{3}{4}$  inches per second are perceptible to humans. Even though these vibrations should not cause damage, vibrations of this magnitude can lead to complaints. Educating the adjacent property owners to the potential impacts of the ground vibrations should be performed.

Dynamic compaction can lead to lateral soil movement. Measurements and observations from other projects has indicated tampers ranging from 33 to 66 kips should not be used within 20 to 30 feet of any buried structure, if movements can cause damage to the structure. In addition, flying debris can occur following impact of the tamper. To avoid flying debris, a safe working distance should be established from the point of impact. Dynamic compaction has an effective depth limitation of approximately 36 feet.

## 19.6.2 Design

After determining if dynamic compaction is a viable ground improvement method, the next step is to develop a more specific ground improvement plan including the following:

- Determining the project performance requirements for the completed structure.
- Selecting the tamper mass (weight) and drop height to correspond to the required depth of improvement.
- Estimating the degree of improvement that will result from dynamic compaction.
- Determining the applied energy to be used over the project site to produce the improvement.

If additional design guidance or information, is needed see Lukas (1995).

### 19.6.2.1 Performance Requirements

Dynamic compaction densifies in-situ soils and thus improves the shear strength and reduces the compressibility of the in-situ soils. A baseline of in-situ properties should be established prior to commencing dynamic compaction using either SPT or CPTu methods. The approximate required level of improvement should be determined for the specific baseline testing procedure. Verification testing shall be conducted during the dynamic compaction operations to determine if the required amount of densification is being achieved.

### 19.6.2.2 Depth of Improvement

The depth of improvement is based on a number of variables including weight (mass) of the tamper, drop height, soil type, and average applied energy. The maximum depth of improvement is determined from the following equation.

$$D_{max} = n\sqrt{W * H} \quad \text{Equation 19-13}$$

Where,

$D_{max}$  = Maximum depth of improvement (meters) (1 m = 0.3048 ft)

$n$  = Empirical coefficient ranging from 0.3 to 0.8, but normally used as 0.5 for most soils and 0.4 is used for landfills

$W$  = Mass of tamper (metric tonnes) (1 metric tonne = 2,205 pounds)

$H$  = Drop height (meters)

The depth of improvement is also affected by the presence of soft or hard layers. Both types of layers absorb the energy imparted by the tamper and can therefore reduce the depth of improvement.

### 19.6.2.3 Degree of Improvement

As indicated above, the degree of improvement is typically measured using either SPT or CPTu measurements, which are performed prior to and after dynamic compaction to monitor the amount of improvement imparted on the soil. The confirmation testing should be performed after the dissipation of pore pressures induced by dynamic compaction. Figure 19-16 provides a general indication of the amount of improvement from dynamic compaction.

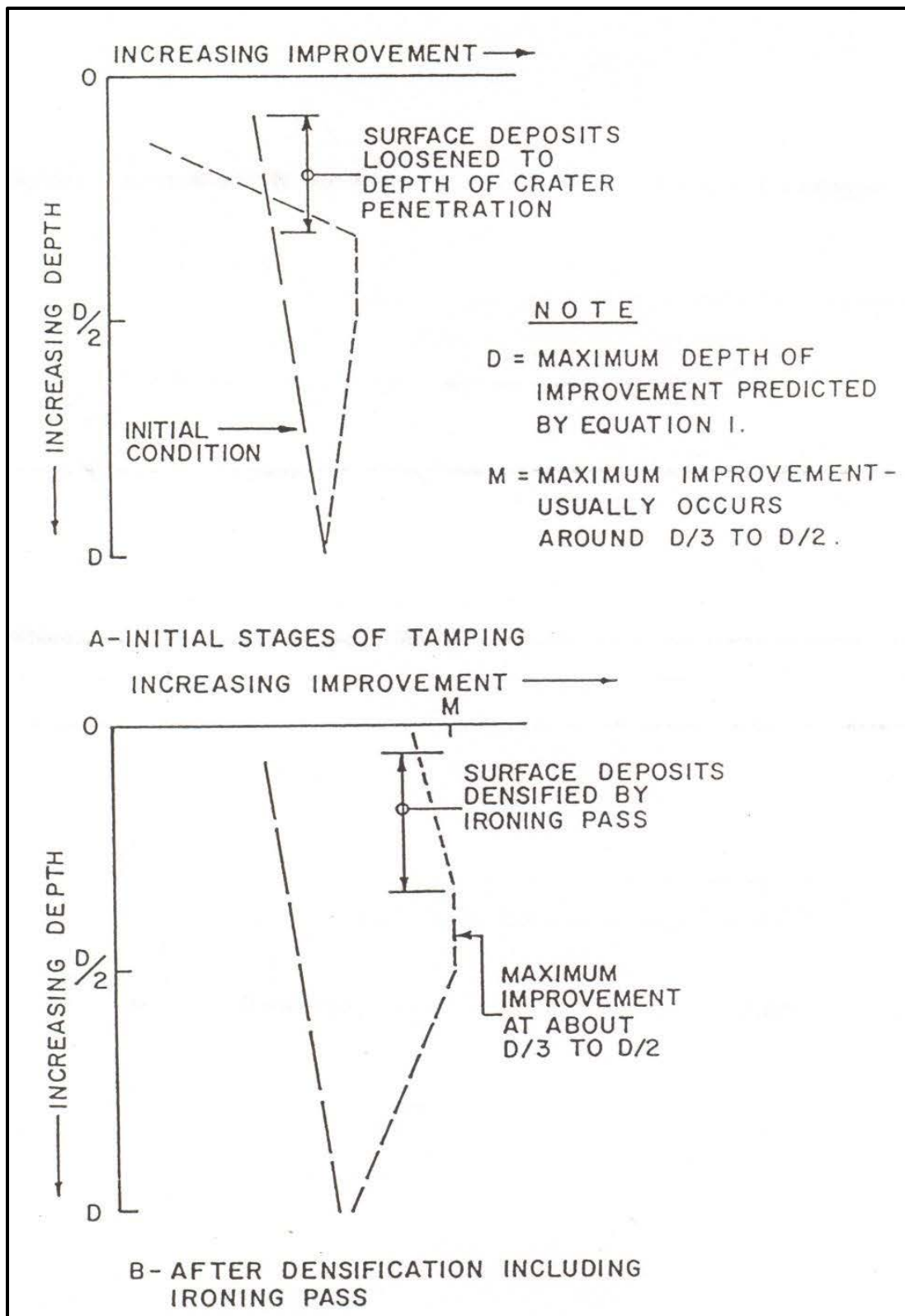


**Figure 19-14, Dynamic Compaction Improvements vs. Depth (Schaefer, et al. – Vol. I (2017))**

The degree of improvement achieved is primarily a function of the average energy applied at the ground surface. Generally, the greater the amount of energy, the greater the degree of improvement; however, there are limitations to the maximum SPT or CPTu values that can be achieved. These maximum values are listed in Table 19-14. These maximum values occur at

improvement depth ranges of D/3 to D/2, above or below this range the test values would be less. These maximum values should only be used as a guide. The actual degree of improvement should be determined during and after the completion of dynamic compaction. The degree of improvement can continue to increase for months or, in some cases, years following the complete dissipation of excess pore pressures.

**Table 19-14, Upper Bound Test Values after Dynamic Compaction  
(Schaefer, et al. – Vol. I (2017))**

Soil Type	Maximum Test Values	
	N-values (bpf)	Cone Tip Resistance (tsf)
Sand & Gravel	30 – 50	200 – 300
Sandy Silts	25 – 35	135 – 175
Silts & Clayey Silts	20 – 35	105 - 135
Clay fill & Mine spoil	20 – 40 <sup>1</sup>	N/A
Landfills	15 – 40 <sup>1</sup>	N/A

<sup>1</sup>Higher test values may occur because of large particles in the soil mass.

### 19.6.2.4 Energy Requirements

According to Schaefer, et al. – Vol. I (2017), “Deep dynamic compaction is generally undertaken in a grid pattern throughout the area. For this reason, it is convenient to express the applied energy in terms of average values. This average applied energy can be calculated on the basis of the following formula:”

$$AE = \frac{W*H*N*P}{G^2} \quad \text{Equation 19-14}$$

Where,

AE = Applied energy

W = Tamper weight

H = Drop height

N = Number of drops at each specific drop point location

P = Number of passes

G = Grid spacing

The average applied energy is the sum of all different size tampers and drop heights. Normally, high energy is achieved using a heavy tamper dropped from a high height. This is frequently followed by the ironing pass (low level energy). The ironing pass is conducted using smaller sized tampers being dropped from lower heights. For planning purposes, the estimated required energy can be obtained from Table 19-15.

**Table 19-15, Applied Energy Guidelines  
(Elias, et al. – Vol. I (2006))**

Soil Deposit	Unit Applied Energy (ft-lb/ft <sup>2</sup> )	Percent Standard Proctor Energy <sup>1</sup>
Zone 1 Soils <sup>2</sup>	4,100 – 5,200	33 - 41
Zones 2 and 3 <sup>2</sup>	5,200 – 7,200	41 - 60
Landfills	12,400 – 22,700	100 - 180

<sup>1</sup>Standard Proctor energy equals 12,400 ft-lb/ft<sup>2</sup>

<sup>2</sup>Refer to Figure19-12

### 19.7 DEEP MIXING METHODS

Deep mixing methods (DMM) are a ground improvement technique that mixes binders (i.e., cement, gypsum, blast furnace slag, fly ash, lime, or other hardening reagents) into the soil at a specific depth to improve the in-situ soil properties without requiring excavation or removal. DMM mixes the soil and binder (reagent) together, whereas grouting injects cementitious materials into the in-situ soil matrix to improve the soil. Grouting is discussed in a subsequent Section. Mass mixing methods (MMM) are a subset of the DMM technology and can be used for a variety of applications including excavation support, soil stabilization, settlement reduction, foundation support, and mitigation of liquefaction potential. There are however differences between DMM and MMM, those differences are indicated below:

1. The percentage area coverage for MMM is 100 or nearly 100 percent.
2. The design strength of the MMM soil is less than the DMM soil.
3. The depth of treatment for MMM soil is limited to approximately 30 feet beneath the existing ground surface.

Because of the similarities between DMM and MMM, other than as indicated previously, DMM will be used generically for the remainder of this Section unless specifically indicated. Detailed design guidance for DMM is available from Bruce, et al. (2013). DMM is performed under many proprietary names, acronyms and processes worldwide. However, the basic concepts and procedures are similar for all techniques. The mixed soil product and the objectives of the mixing program can be divided into standard generic terms as presented in the table below:

**Table 19-16, Deep Mixing Generic Terms  
(Bruce, et al. (2013))**

Method of binder injection	Wet (W) or Dry (D)
Method of binder mixing	Rotary energy (R); High-pressure jet (J) or Vertical (V)
Location of mixing action	End of drilling tool (E); Along shaft (S) or Panel (P)

These generic terms can be combined into 5 distinct processes of deep soil mixing (see Figure 19-17), WRS, WRE, WJE, WVP, and DRE. Some of the possible combinations of deep soil mixing methods do not exist. For example DJE (dry, jet, end) does not exist.

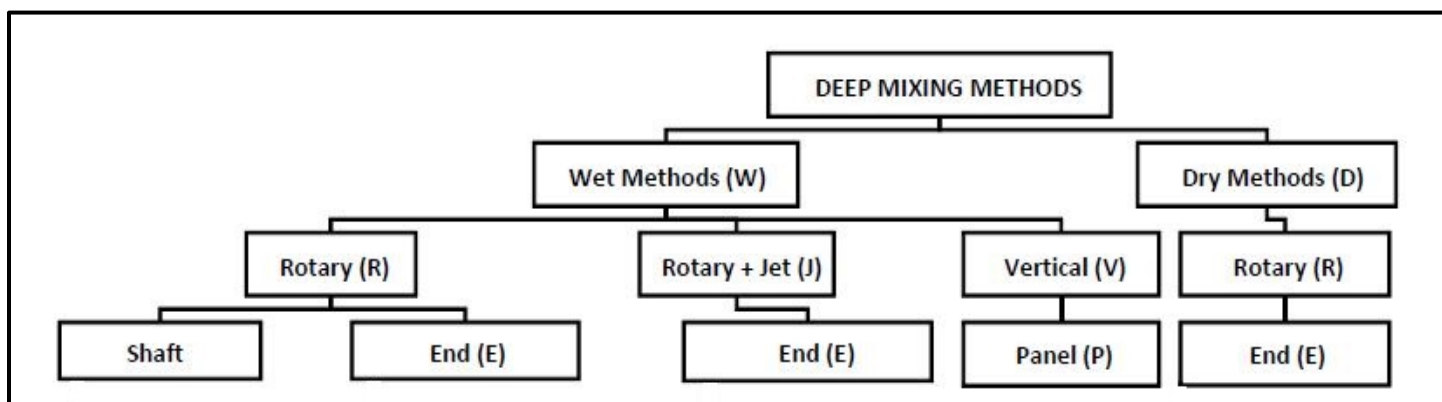


**Figure 19-15, Generic Classification of Deep Mixing Techniques  
(modified from Bruce, et al. (2013))**

The 5 processes discussed previously can be divided into 2 groups as indicated in Table 19-17.

**Table 19-17, DMM Groups**

Wet DMM	WRS – Wet Rotary Shaft	Single or multiple shaft equipment with blades over a length of the shaft that mechanically mix injected slurry with surrounding soil.
	WRE – Wet Rotary End	Single shaft equipment with single mixing tool.
	WJE – Wet Jet End	Single (uncommon) or multiple shaft equipment tipped with blades and assisted by jetting of slurry through high-pressure ports
	WVP – Wet Vertical Panel	Chainsaw-type vertical cutting tool mounted on a central cutter post.
Dry DMM	DRE – Dry Rotary End	Single-auger column technique developed for soil stabilization and reinforcement of cohesive soils. Binder is inserted into the soil via compressed air (jet).

DMM can be performed wet or dry and is generally done using large-diameter, single-axis, vertical-shaft mixing equipment for the wet method. In the dry method the binder is delivered to the mixing/cutting head via compressed air. Dry DMM is typically performed in soft, saturated, or nearly saturated soil. Wet DMM can be applied to soils with any degree of saturation.

### **19.7.1 Analysis**

Regardless of whether wet or dry DMM or MMM is used, all DMM projects should follow the flowchart provided in Figure 19-18. Wet construction DMMs are typically used for large-scale structural support improvement using individual elements, shear walls, or grid type arrangements (see Figures 19-19 and 19-20), while dry DMMs are used primarily for soil stabilization/reinforcement and settlement reduction (i.e., MMM). While DMM provide vertical (compressive) capacity, reduce settlement, increase stiffness, there is limited to no tensile resistance from these materials. Therefore, there is no tensile resistance allowed for DMM by itself. Like any other soil material DMM will provide axial resistance to other structural elements. DMM and MMM can be combined to create load-transfer type platform similar to those used for column supported embankments (see Figure 19-21). Discussed in the following paragraphs are applications, of wet and dry deep soil mixing that are typical for transportation related projects.



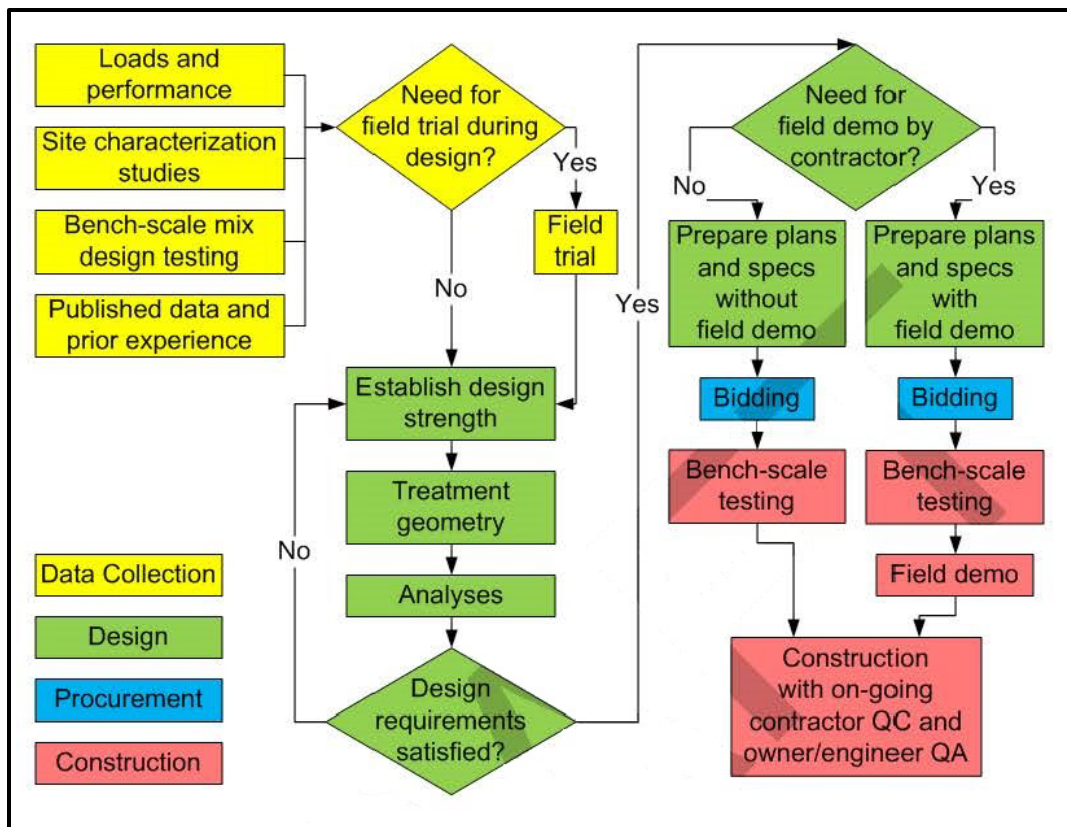


Figure 19-16, DMM Project Flowchart (Schaefer, et al. – Vol. II (2017))

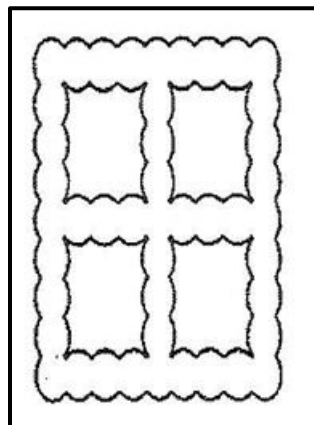


Figure 19-17, DMM Grid Treatment Pattern (Elias, et al. – Vol. I (2006))



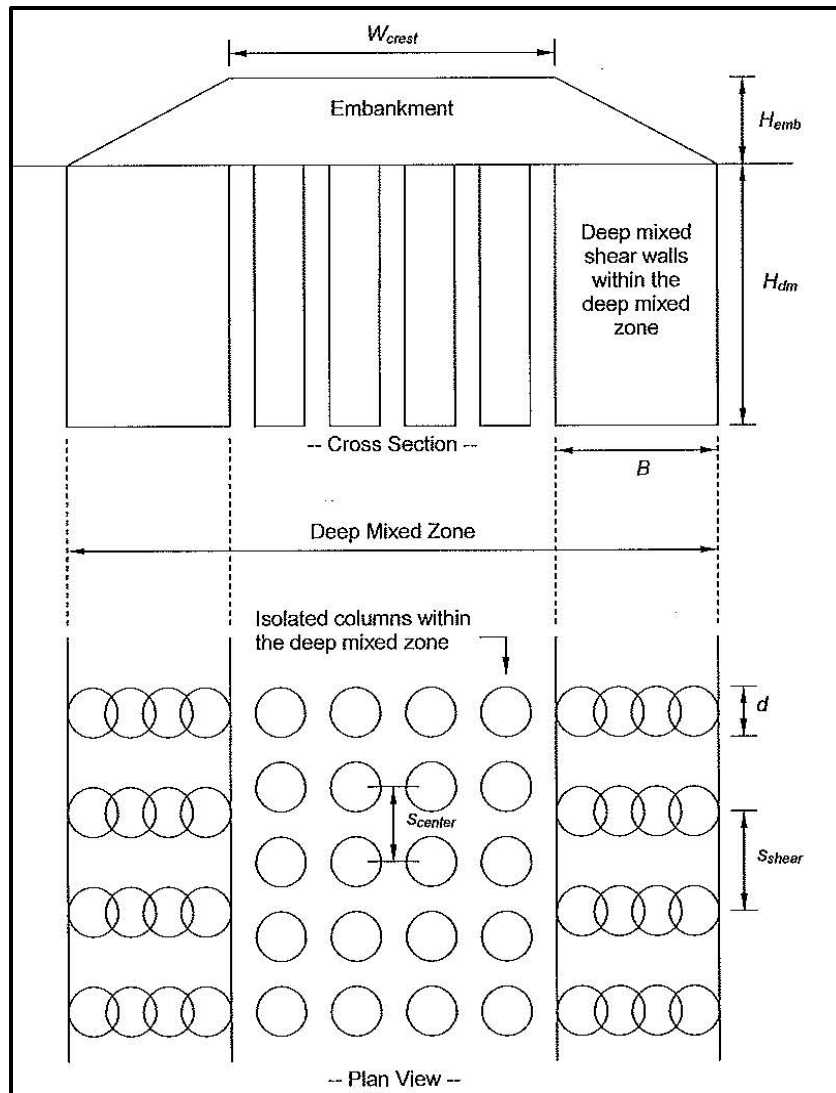


Figure 19-18, DMM Treatment Pattern Beneath Embankment (Bruce, et al. (2013))

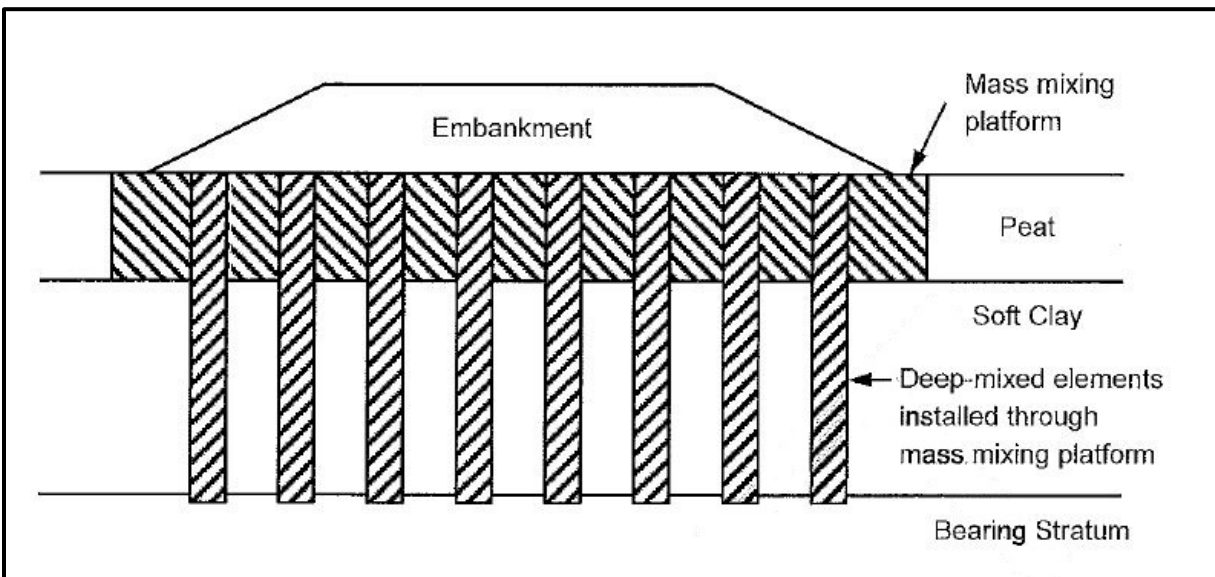


Figure 19-19, DMM-MMM Load-Transfer Platform (Schaefer, et al. – Vol. II (2017))

Wet DMM can be single- or multi-shaft processes that use cement-based slurries to create isolated elements, continuous walls, or blocks. Dry DMM typically use single-auger techniques that use lime, cement, lime-cement, or slag mixtures to create isolated columns, walls, or blocks for soil stabilization and reinforcement.

## **19.7.2 DMM Advantages and Disadvantages/Limitations**

### **19.7.2.1 DMM Advantages**

According to Schaefer, et al. – Vol II (2017) DMM has the following advantages:

- Increases the strength and decreases the compressibility of soft silts, clays and organic soils, and peat.
- Prevents liquefaction of loose sand deposits.
- Wet-mixing equipment can penetrate layers of dense and strong material to treat underlying weak, loose, or compressible layers.
- Improves soft clay deposits more quickly than using *PVDs* with preloads and surcharge.
- Permits reduced embankment footprint and fill volume through use of steeper side slopes or vertical walls.
- The plan view arrangement of treatment, the treatment depth, and the degree of improvement to strength and stiffness can be easily adjusted to satisfy design requirements and subsurface conditions.
- Carries new loads placed adjacent to existing facilities so the new loads do not cause settlement of the existing facilities.
- High production capacity with large equipment.
- Materials are treated in-situ, which can reduce disposal problems:
  - The dry method produces very little to no spoils.
  - Spoils from the wet *DMM* make excellent fill material.
- Stabilizes many types of contaminants (*typically not a reason why DMMs are constructed for SCDOT projects*).
- Can be used for dry land and marine projects.
- Economical on large projects.
- Dewatering is not necessary.
- Less noise and vibrations than from some other technologies.
- *Specific advantages to MMM:*
  - *MMM is typically less expensive than traditional DMM techniques on a unit volume basis, although the treatment per foot of depth is larger because of the larger area replacement ratio.*
  - *MMM can be done rapidly.*

### **19.7.2.2 DMM Disadvantages/Limitations**

According to Schaefer, et al. – Vol II (2017) DMM has the following disadvantages/limitations:

- The mobilization and unit costs can be higher than for other technologies, such as *PVDs* with preloading.
- *DMM* requires familiarity of the *GEOR* with specialized design, construction, specifications, and QC/QA practices.
- Cobbles, boulders, dense sand deposits, buried logs, and other obstructions can interfere with penetration of mixing equipment.

- Buried utilities and structures must be avoided. If buried features cannot be spanned and if treatment immediately adjacent to them is necessary, another technology, such as jet grouting, may be required.
- The wet *DMM* generally uses heavy equipment, which can require timber mats or other techniques to enable equipment to operate on soft ground.
- For the wet *DMM*, if there is not an opportunity for on-site use of the good quality fills generated by the spoils, the spoils may have to be transported off site for use on another project or to be disposed.
- *DMM* elements can only be installed vertically.
- Treatment depths are typically limited to about 130 feet.
- *Specific disadvantages/limitations to MMM:*
  - Treatment depths are typically limited to about 50 feet for shallow soil mixing equipment and to about 30 feet for *MMM* equipment (*i.e.*, *mixing drum attached to backhoe stick*).
  - *MMM* equipment typically cannot penetrate dense or stiff soils, cobbles, boulders, obstructions, and buried utilities or structures.
  - Quality control operations for *MMM* are not usually as sophisticated as for modern *DMM*. The quality and uniformity of the finished product is more operator dependent for *MMM* than for *DMM*.

### 19.7.3 Feasibility

The feasibility of using *DMM* shall be determined prior to recommending this ground improvement method. The feasibility evaluation includes, but is not limited to; a site investigation, a feasibility assessment and a bench-scale treatability study. Typically *DMM* is performed on very soft to firm clays, very loose to medium dense sands, very soft to firm organic soils and peats. Wet *DMM* equipment tends to be more powerful than dry *DMM* equipment; therefore, wet *DMM* equipment is more likely to penetrate layers of stiff clay and dense sands to reach underlying soft/loose soil layers or organics. *DMM* may be used to treat contaminated soils in-situ by immobilizing the contaminants. Wet *DMM* requires more space than does dry *DMM* for an equipment yard, slurry batch plant, and equipment maneuvering. If the near surface soils are soft then a working platform may be required to support not only the *DMM* equipment, but also the slurry batch plant for wet *DMM* as well as storage for the binder.

#### 19.7.3.1 Site Investigation

The site investigation required for *DMM* exceeds the requirements previously indicated in this Manual. If deep soil mixing is selected or proposed as an alternate ground improvement method, then, additional site-specific information will be required. The proposed site investigation plan shall be submitted to the RPG/GDS for concurrence prior to execution. Prior to commencing the site investigation, observations of the proposed construction area should be made to include ground surface condition, the presence of overhead or underground utilities, site access, and any other observations that could affect the ability to use this method. It should be noted that typically the equipment used for *DMM* is relatively large and will require more space to operate in. In addition, use of the wet methods may generate large amounts of spoil, and it should be determined if there is adequate space on site to store this material. Further, the proposed site investigation plan shall include the methodology for obtaining the required amount of material for bench-scale treatability study. The site investigation should include the following items:

- Evaluation of the subsurface: predominant soil type; existence of any obstructions; existence and percentage of organic matter
- Natural moisture content
- Engineering properties: strength and compressibility

- Classification properties: moisture-plasticity relationship and grain-size distribution
- Organic content and loss on ignition
- Chemical and mineralogical properties to include assessment for the presence of pozzolanic materials, including soluble silica and alumina, which can affect lime reactivity only
- Ground water levels

### 19.7.3.2 Feasibility Assessment

DMM is best used when the subsurface conditions are soft to loose, with no obstructions, to depths no greater than 130 feet. There should be unrestricted overhead clearance and a need for relatively vibration free ground improvement methods. DMM will cause the temporary loss of in-situ soil strength, which may affect adjacent structures. The assessment should review the information obtained from the site investigation. Selected soil chemical properties are provided in the table below.

**Table 19-18, Favorable Soil-Chemistry Factors  
(Bruce, et al. (2013))**

Property	Favorable Soil Chemistry
Near surface temperature	$\geq 39^{\circ}$ F
pH	$> 5$
Natural moisture content	$< 200$ % (dry DMM) $< 60$ % (wet DMM)
Organic content	$< 6$ % (wet DMM)
Loss on Ignition	$< 10$ %
Humus Content	$< 1$ %
Electrical conductivity	$\geq 1.2$ m $\Omega$ /cm

### 19.7.3.3 Bench-Scale Treatability Study

After assessing the viability of soil for DMM, samples should be prepared to determine the water, soil, binder (reagent) ratios as well as determining the time required for mixing. A bench-scale treatability study shall be performed during the additional exploration phase. Enough of the targeted material for DMM should be obtained, ranging from a minimum of 35 to more than 70 pounds. A minimum of 5 sets of 8 2- by 4-inch cubes shall be required to determine shear strength for each mix design proposed. The samples should then be tested for unconfined compressive strength at various curing times to determine strength gains with time. The bench-scale treatability study results will assist in narrowing the potential improvements levels that can be achieved in the field. These results should be compared to the typical results presented in the table below. It is important to note that very important variables associated with equipment mixing capabilities, such as rate of penetration and withdrawal, mixing energy, and vertical circulation of materials, cannot be modeled by the laboratory testing program. A more detailed discussion of the bench-scale treatability study is provided in Bruce, et al. (2013).

**Table 19-19, Typical DMM Improved Engineering Properties  
(Bruce, et al. (2013))**

Property	Typical Range
Unconfined Compressive Strength, $q_u$	Dry DMM – 2 – 400 psi Wet DMM – 20 – 4,000 psi
Hydraulic Conductivity, $k$	Wet DMM – $10^{-5}$ – $10^{-6}$ cm/s
Young's Modulus ( $E_{50}$ ) [Secant Modulus at 50% $q_u$ ]	Dry DMM – 150 $q_u$ Wet DMM – 300 $q_u$
Poisson's Ratio	0.19 – 0.45 typically 0.26

Provided in the table below are guidelines related to the penetration, mixing speed, water cement ratio, and reagent content typically used in practice.

**Table 19-20, Mixing Guidelines  
(Elias, et al. – Vol. I (2006))**

Reagent Content	9-1/2 – 22-1/2 pcf
Mixing Rotational Speed	20 – 45 rpm
Penetration Rate	~ 1 yd/min
Water Cement Ratio	0.6 – 1.3 but 1.0 is normal

Bruce, et al., (2013)) have developed an “simplified index” factor, BRN, that quantifies the number of mixing cycles per meter which relates the penetration and retrieval speed (velocity) and the rotation speed during penetration and retrieval. BRN is defined as the total number of rotations during 1 meter of penetration (downstroke) or withdrawal (upstroke) after the binder (reagent) has been added into the ground. Use Equation 19-14 to determine the BRN.

$$BRN = \Sigma M * \left[ \frac{N_p}{V_p} + \frac{N_w}{V_w} \right] \quad \text{Equation 19-15}$$

Where,

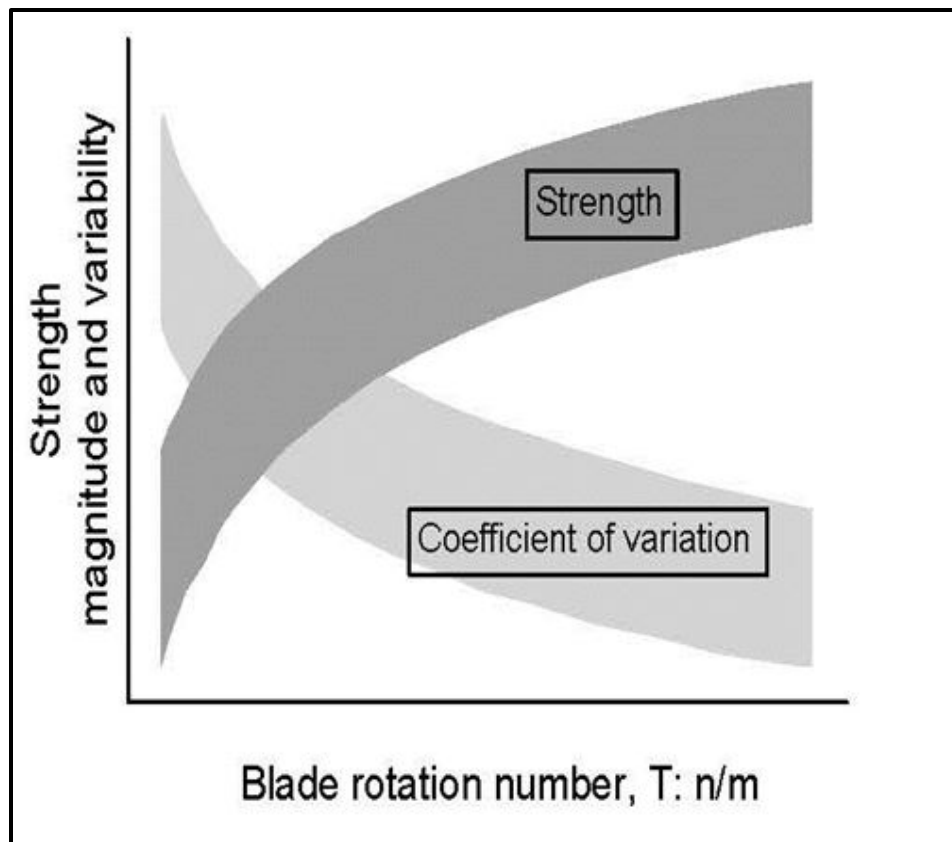
$\Sigma M$  = Total number of mixing blades

$V_p, V_w$  = Penetration and Withdrawal mixing blade velocity (meters/min)

$N_p, N_w$  = Blade rotation speed during penetration and withdrawal (rpm)

1 meter = 3.2808 ft

BRN greater than 360 for wet DMM tend to have a smaller coefficient of variation. In addition Larsson, (2005), indicates that “...the retrieval rate and the number of blades have a significant influence on the strength magnitude and variation.” An approximate logarithmic relationship appears to exist between the strength of the DMM and the mixing energy (see Figure 19-22). However, the strength magnitude cannot be based solely on the mixing energy, but also depends on the reagent, soil, and in-situ condition during curing.



BRN = T

**Figure 19-20, T vs Strength Magnitude and Variability  
(Larsson (2005))**

#### **19.7.4 Design**

DMM shall be designed following the procedures indicated in Bruce, et al. (2013). The GEOR shall determine the required DMM strength based on the needs of the project and the bench-scale treatability study. Strength as used here typically refers to shear strength, while during QC/QA strength typically refers to unconfined compressive strength. The GEOR shall indicate on the plans which strength is being required for the project. The geometric parameters listed in Table 19-21 shall be determined by the GEOR and provided on the DMM plan sheet.

**Table 19-21, DMM Required Geometric Parameters  
(modified Bruce, et al. – Vol. I (2013))**

<b>Common to both Isolated Columns and Shear Walls</b>		
<b>Parameter</b>		<b>Maximum and/or Minimum</b>
Top elevation of DMM element		Minimum
Bottom elevation of DMM element		Maximum
d	Column diameter or shear wall thickness (see Figure 19-19 and Figure 19-23)	Minimum and maximum
<b>Isolated Columns</b>		
<b>Parameter</b>		<b>Maximum and/or Minimum</b>
$s_{center}$	Center-to-center spacing of isolated columns (see Figure 19-19)	Maximum
$s_{center} - d$	Edge-to-edge spacing of isolated columns	Maximum
$\alpha_{s, center}$	Area replacement ratio beneath central portion of embankment (see Figure 19-19)	Minimum
<b>Shear Walls</b>		
<b>Parameter</b>		<b>Maximum and/or Minimum</b>
B	Length of shear wall (see Figures 19-19 and 19-23)	Minimum
b	Average shear wall width (see Figure 19-23)	Minimum
e	Overlap distance (see figure 19-23)	Maximum
e/d	Ratio of overlap distance to column diameter	Minimum
$s_{shear}$	Center-to-center spacing of shear walls (see Figures 19-19 and 19-23)	Maximum
$s_{shear} - d$	Edge-to-edge spacing of shear walls	Maximum
$\alpha_{s, shear}$	Area replacement ratio beneath side slopes embankment (see Figure 19-19)	Minimum
c	Chord length (see Figure 19-23)	Maximum
$c/s_{shear}$	Ratio of chord length to Edge-to-edge spacing of shear walls	Minimum

The area replacement ratio central portion of an embankment (see Figure 19-19) or for isolated columns is determined using the following equation,

$$\alpha_{s, center} = \frac{\pi * d^2}{4 * (s_{center})^2} \quad \text{Equation 19-16}$$

The area replacement ratio for shear walls beneath an embankment (see Figure 19-23) is determined using the following equation,

$$\alpha_{s, shear} = \frac{b}{s_{shear}} \quad \text{Equation 19-17}$$

The area replacement ratio for overlapping columns is influenced by the extent of the overlap between the columns and is determined using the following equation,

$$\alpha_{s, shear} = \frac{\pi * d * (1 - a_e)}{4 * s_{shear} * (1 - \frac{e}{d})} \quad \text{Equation 19-18}$$

$$a_e = \frac{\beta - \sin \beta}{\pi} \quad \text{Equation 19-19}$$

$$\beta = 2 * \arcsin \left( 1 - \frac{e}{d} \right) \quad \text{Equation 19-20}$$

Note that  $a_e$  is the overlap area ratio and  $\beta$  is the chord angle expressed in radians ( $1^\circ = (\pi/180)$ ). The chord length,  $c$ , is determined using the following equation,

$$c = d * \sin \left( \frac{\beta}{2} \right) \quad \text{Equation 19-21}$$

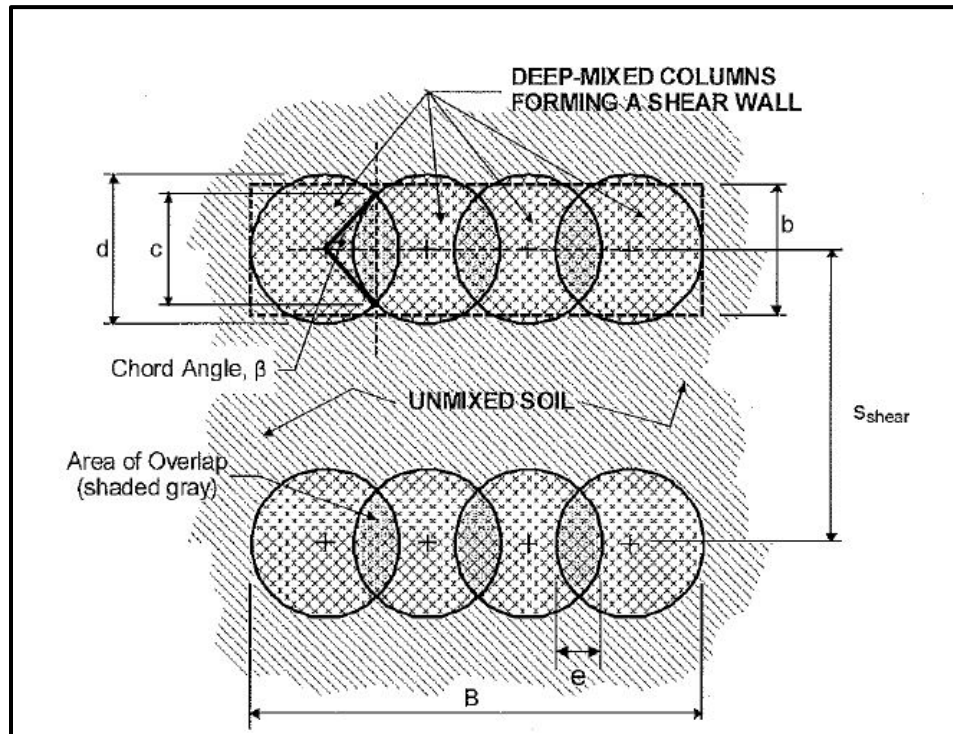


Figure 19-21, DMM Shear Wall Geometric Detail  
(Bruce, et al. (2013))

### 19.7.5 Verification

The properties of the improved ground require verification to ascertain whether the requirements of the project are being met. The contractor shall be required to conduct laboratory (bench-scale) testing to verify that proposed construction methods and mixes will achieve the requirements of the contract. After completion of the mixing, either in-situ testing or obtaining cores for laboratory testing should be performed. The in-situ testing can consist of electro-piezcone penetrometer testing (CPTu), dilatometer testing (DMT), standard penetration testing (SPT), or pressuremeter testing (PMT).

### 19.7.6 Construction Considerations

DMMs shall conform to the requirements of STS SC-M-205-3 (latest version) for *Deep Mixing Methods*. The GEOR should be aware that this STS contains definitions for terms used in both the STS as well as the drawings. The GEOR is required to review this STS to ascertain the meanings of the terms used for DMM. The latest version of the Supplemental Specifications and STSs are available on the SCDOT website:



<https://www.scdot.org/business/business-landing.aspx>.

In addition, “go-by” drawings are available to assist the GEOR. The GEOR is reminded that the provided “go-by” must be modified for the specific project. The latest version of the “go-by” is available on the SCDOT website:

<https://www.scdot.org/business/geotech.aspx>.

## 19.8 GROUTING

According to Schaefer, et al. – Vol. II (2017);

Grouting comprises a variety of techniques that employ injection of a range of materials into soil or rock formations, via boreholes, to improve their engineering properties. More specifically, grouting can be used to fill fissures and voids in rock, to fill voids between the ground and overlying structures, and to treat soils to enhance strength, density, permeability, and/or homogeneity.

The type of grouting used is based on the anticipated/required results and the soil/rock that the grouting is being used in. A successful grouting program consists of a detailed geotechnical investigation, active monitoring during construction, and verification that the grouting program is meeting the project requirements.

The geotechnical investigation is more detailed than is normally performed to identify in-situ conditions that could affect the effectiveness of the grouting program. The results of this detailed investigation are used to select the type of grouting, as well as the grouting materials. In addition, the investigation will aid in determining the potential effectiveness of the grouting program. To improve effectiveness, a real time monitoring plan is required, which allows for field adjustments to the grouting program to account for changes in subsurface conditions. Finally, a comprehensive grouting program shall include a means of verifying that the required results are being achieved.

The definitions contained in the Schaefer, et al. – Vol. II (2017) are used in this Manual. Schaefer, et al. – Vol. II (2017) identifies 2 principle types of grouting which are listed in the table below. Figure 19-24 provides schematics of the various types of grouting.

**Table 19-22, Types of Grouting Method  
(Schaefer, et al. – Vol. II (2017))**

<b>Principle Type of Grouting</b>	<b>Specific Type of Grouting</b>
Rock Grouting	Fissures (using High Mobility Grouts (HMG))
	Voids (natural and artificial, using Low Mobility Grouts (LMG))
Soil Grouting	Permeation (using HMG and solution grouts)
	Low mobility grouting - Compaction or displacement and bulk void filling
	Jet (or replacement)
	Fracture (including compensation grouting)
	Slabjacking

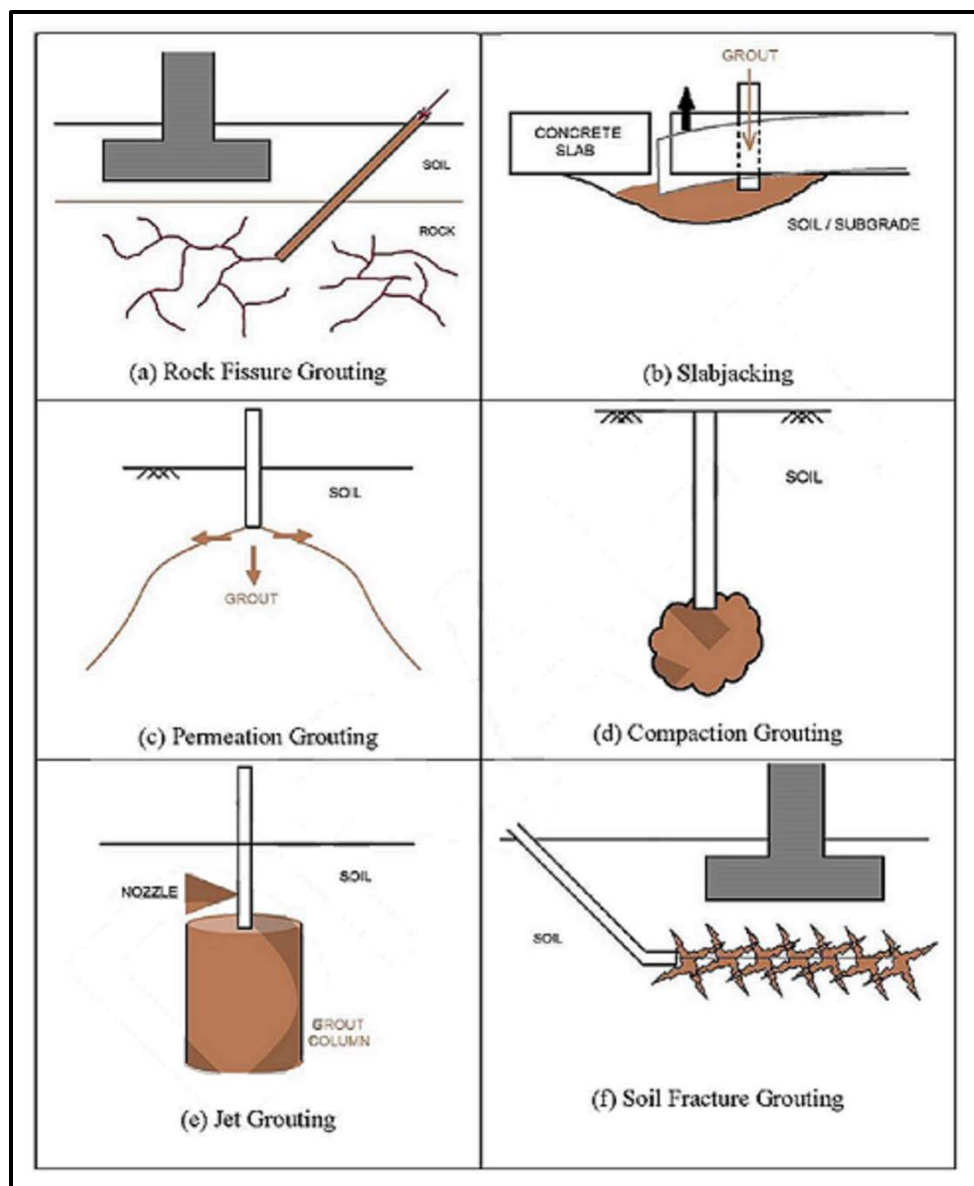


Figure 19-22, Types of Grouting Schematic  
(Schaefer, et al. – Vol. II (2017))

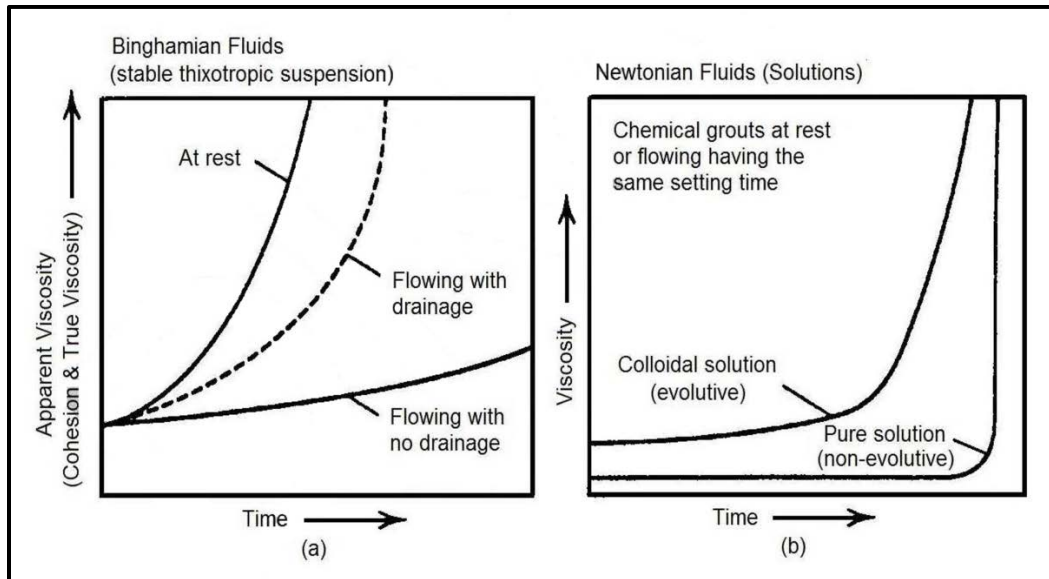
### 19.8.1 Grout Materials

There are 4 categories of grouting materials, which are listed below:

1. Particulate (suspension or cementitious) grout
2. Colloidal solutions
3. Pure solutions
4. Miscellaneous materials

Category 1 grouts are comprised of mixtures of water and particulate solids. The particulate solids may consist of cement, fly ash, clays, or sands. These mixtures are stable and have cohesion and plastic viscosity increasing with time. Due to their basic characteristics and relative economy, these grouts remain the most commonly used for both routine waterproofing and ground strengthening. The water to solids ratio is the prime determinant of their properties and basic characteristics such as stability, fluidity, viscosity, and strength durability. Neat cement or clay/bentonite-cement grouts are comprised of Portland cement or microfine cement

depending on the size requirements of the grout. Figure 19-25(a) shows the increase in apparent viscosity with time for these grouts and Figure 19-26 shows grain-size distribution of various cements.



(a) Category 1 Grouts; (b) Categories 2 and 3 Grouts

**Figure 19-23, Viscosity versus Time  
(Schaefer, et al. – Vol. II (2017))**

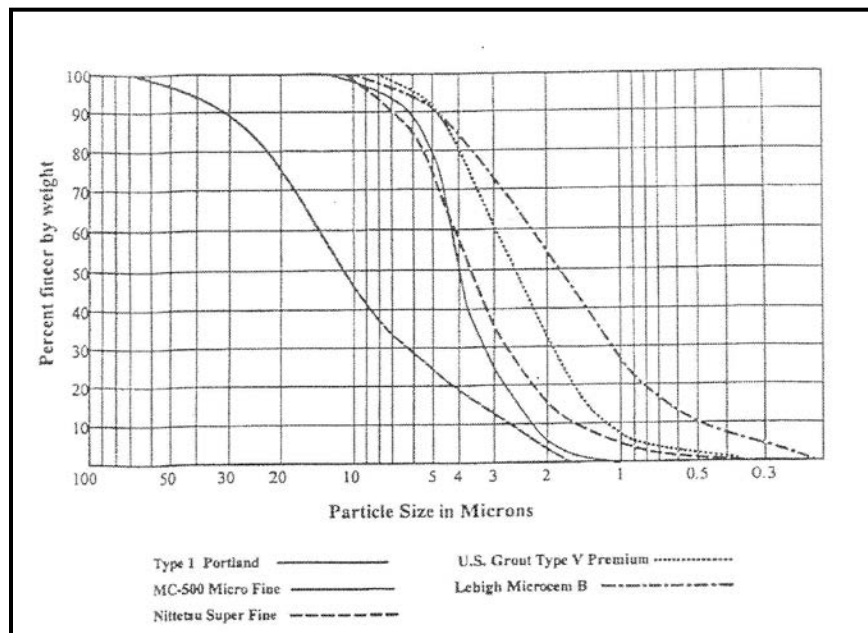


**Figure 19-24, Grain-Size Distribution of Cements  
(Elias, et al. – Vol. II (2006))**

Category 2 and 3 grouts, commonly called solution or chemical grouts, are typically subdivided based on component chemistries; for example, silicate based (Category 2) (colloidal) or resin based (Category 3) (pure solution). Figure 19-25(b) provides an indication of the change of viscosity with time for these grouts. Category 2 grouts are colloidal solutions that are comprised of mixtures of sodium silicate and a reagent, which when mixed, change viscosity over time to a gel. Sodium silicate is an alkaline, colloidal aqueous solution, while the reagents may be organic or inorganic (mineral). The common types of organic reagents are monoesters, diesters, triesters, and aldehydes. These reagents react with the sodium silicate to produce

acid as a by-product and can produce either a soft or hard gel depending on the concentration of each compound. The inorganic reagents contain cations that are capable of neutralizing the silicate alkalinity. Typical inorganic reagents are sodium bicarbonate and sodium aluminate. The relative proportions of silicate and reagent will be determined by their own chemistry and concentration, the desired short- and long-term properties, such as gel setting time, viscosity, strength, synæresis and durability, as well as cost and environment acceptability.

Category 3 grouts are known as pure solutions since these grouts consist of resins. The resins are solutions of organic products in water or a nonaqueous solvent that are capable of causing the formation of a gel with specific mechanical properties under normal temperature conditions and in a closed environment. These grouts exist in the following forms, characterized by the mode of reaction or hardening:

- Polymerization – Activated by the addition of a catalyzing agent (polyacrylamide resins)
- Polymerization and Polycondensation – Arising from the combination of 2 components (epoxies or aminoplasts)

The setting times for these grouts is adjusted by varying the proportions of the reagents or components. According to Schaefer, et al. – Vol. II (2017)):

Resins are used when particulate grouts or colloidal solutions prove inadequate, for example when the following grout properties are needed:

- Particularly low viscosity
- Very fast gain in strength (a few hours)
- Variable setting time (few seconds to several hours)
- Superior chemical resistance
- Special rheological (psuedoplastic)
- Resistance to high groundwater flows

In applications where the durability of the grout is important, resins are typically used for both strength and waterproofing. Resins may be divided into 4 subcategories as indicated in Table 19-23.

**Table 19-23, Types, Use, and Applications of Resin Grouts  
(Schaefer, et al. – Vol. II (2017))**

Type of Resin	Applicable Ground Type	Use/Application
Acrylic	Granular, very fine soils Finely fissured rock	Waterproofing by mass treatment Gas tightening (mines, storage) Strengthening up to 220 psi Strengthening of a granular medium subjected to vibrations
Phenol	Granular, very fine soils	Strengthening
Aminoplastic	Schists and coals	Strengthening (by adherence to materials of organic origin)
Polyurethane	Large Voids	Formation of a foam that forms a barrier against running water (using water-reactive resins) Stabilization or localized filling (using 2-component resins)

There are only 2 types of polyurethanes that are appropriate for grouting. These types are listed in Table 19-24.

**Table 19-24, Polyurethane Types  
(modified Schaefer, et al. – Vol. II (2017))**

Polyurethane Type	Properties
Water Reactive	Liquid resin reacts with groundwater to form either flexible (elastomeric) or rigid foam These resins take 2 forms: <ul style="list-style-type: none"> <li>Hydrophobic – react with water, but repel it after the final (cured) product has formed</li> <li>Hydrophilic – react with water, but continue to physically absorb it after the chemical reaction has been completed</li> </ul>
2-Component	Two compounds in liquid form react to provide either a rigid foam or an elastic

Category 4 grouts (Miscellaneous grouts) are composed of organic compounds or resins. These grouts are used primarily for strengthening and waterproofing, but may also have very specific qualities such as resistance to erosion or corrosion, and flexibility. The use of Category 4 grouts may be limited by specific concerns such as toxicity, injection, handling difficulties, and cost. In addition, many of these grouts are proprietary in nature, which can make their use difficult at best. Category 4 grouts are composed of hot melts, latex, polyesters, epoxies, furanic resins, silicones, and silacols. Some of these types have limited use in ground improvement. Category 4 grouts should only be used if there are either no other options or if the grouting system (grout and application of the grout) is fully understood by both the designer and the contractor.

### **19.8.2 Rock Grouting**

There are 2 types of rock grouting: rock fissure grouting and void filling. Both types of grouting are discussed briefly in the following sections.

### 19.8.2.1 Rock Fissure Grouting

The grouting of rock fissures is primarily used to provide hydraulic cut-offs and has the added benefit of binding the rock mass together thus improving the load bearing capability. Rock fissure grouting typically has limited applications on transportation projects. However, rock fissure grouting can be used to stabilize rock slopes, remediate road tunnels, repair drilled shafts, and seal drilled shaft boreholes from the in-flow of ground water. The variability of the rock mass can make this ground improvement technique extremely difficult to predict the results of. Because of the variability in the rock mass, often a design phase test program is conducted to determine the effectiveness of the rock fissure grouting program. Using the results of the test program, the final design can be completed and a program cost can be estimated.

The use of rock fissure grouting has the advantage of being less expensive when compared to other repair options of weak rock, such as removal, replacement, or abandoning the site. However, the actual cost of rock fissure grouting can vary considerably because of potential variation of the rock mass within the site boundaries. Further, poor field practices can lead to unsatisfactory performance of the rock grouting. These poor field practices include inducing uplift that results from excessive pressures, premature plugging of fissures, unsuitable injection methods or formulations or by inappropriate drilling and flushing methods and improper hole spacing or improper orientation of the grout holes.

The primary purpose of this form of rock grouting is the sealing of cracks and fissures within the rock mass. The main consideration in rock grouting is the grain-size of the particulate grout compared to the width of the rock fracture to be grouted.

$$N_R = \frac{f_w}{(D_{95})_{Grout}} \quad \text{Equation 19-22}$$

Where,

$N_R$  = Groutability ratio of rock

$f_w$  = Fissure width

$(D_{95})_{Grout}$  = Grout diameter at 95 percent finer

$N_R > 5$  – Grouting consistently possible

$N_R < 2$  – Grouting not possible

While the fissure width cannot be changed, the fineness of the grout can be controlled, thus producing a groutability ratio that can be increased to greater than 2. Rock grouting with particulate materials normally falls into 1 of the categories indicated in Table 19-25.

**Table 19-25, Rock Grouting Categories  
(Elias, et al. – Vol. II (2006))**

Rock Grouting Category	Description
Curtain	Drilling and grouting of 2 or more lines of grout holes to an impermeable material to produce a barrier to seepage.
Area	Grouting a shallow zone in a particular area by utilizing grout holes arranged in a pattern or grid to mechanically improve fractured or jointed rock.
Tunnel	Used to fill voids behind tunnel liners, treatment of material surrounding the bore or seepage control. Pre-excavation grouting from the surface or the face may be required for ground strengthening and water control.
Backfilling	Filling subsurface exploration boreholes and grout holes is important to maximize structural stability, to control water, or to prevent passage of contaminants to underlying strata.

### **19.8.2.2 Rock Void Grouting**

Rock void grouting is used to fill natural (karstic limestone features or salt solution cavities) voids or man-made (mining activities) voids. Typically, neither of these features occurs in South Carolina. However, there are some localized areas of karstic limestone features caused by localized dewatering for mining activities. Rock void grouting can also be used for the remediation of some scour issues. However, it will not be discussed in this Manual. Contact the PC/GDS for guidance in the use of this method for remediation of scour.

### **19.8.3 Soil Grouting**

Soil grouting programs are used to achieve a variety of ground improvement objectives. The 2 main objectives of a grouting program are, first, water control and waterproofing, and second, structural improvement. Waterproofing is used mainly in conjunction with new construction and water control is used mainly in conjunction with remedial applications. Structural grouting is used to improve the density of a soil, raise settled structures, control settlement, underpin, mitigate liquefaction, and control water. There are 5 different types of grouting that can be used on soil:

1. Permeation
2. Compaction
3. Jet
4. Soil Fracture
5. Slabjacking

All 5 of these types of grouting can be used for water control, waterproofing, and structural enhancement and are discussed in greater detail in the following Sections. Soil grouting has a distinct economic advantage over removal and replacement. Grouting is also generally less disruptive to the surrounding work area. Soil grouting also has some disadvantages, such as compaction grouting in fine saturated soils. Instead of squeezing the pore water out, the soil may simply displace and not consolidate or densify. Permeation grouting using certain chemical grouts may represent toxicity dangers to the groundwater and underground environment. Low toxicity chemical grouts are now available and should be specified except for unusual circumstances. Each grouting method can cause ground movement and structural distress.

The general limitation of soil grouting is the soil type to be treated. Although the range of soil grouting available encompasses most soil types, individual methods are limited to specific soils as shown in Figure 19-27.

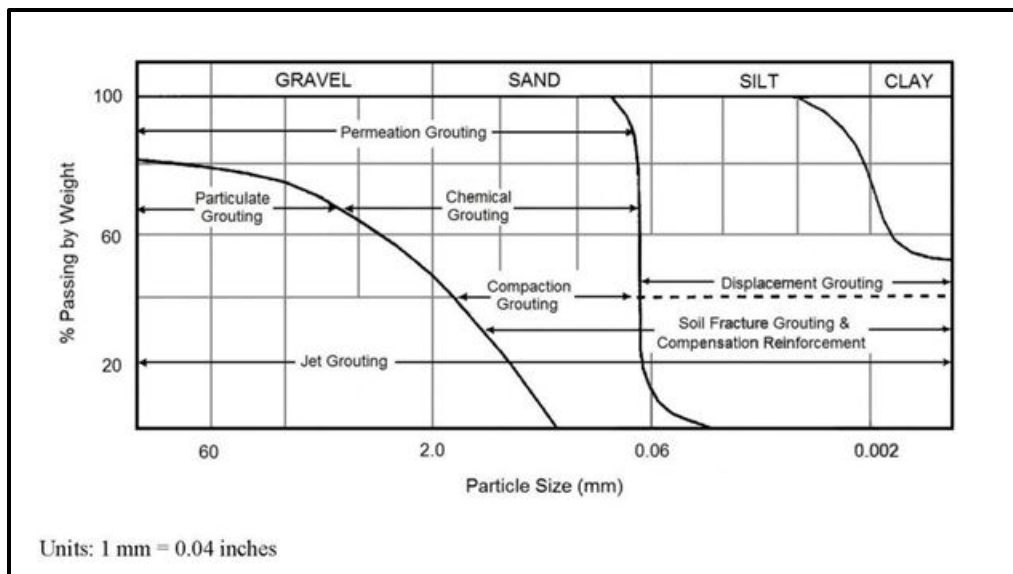


**Figure 19-25, Range of Applicability of Soil Grouting Techniques (Schaefer, et al. – Vol. II (2017))**

Grouting is normally used to solve construction problems related to geological anomalies or environmental conditions. Soil grouting uses the existing soils, improving these soils, by grouting to correct deficiencies in the soil. According to Elias, et al. – Vol. II (2006):

Grouting of a soil involves the following sequential steps:

- Establishing specific objectives for the grouting program (designer)
- Defining the geometric and geotechnical project conditions (designer)
- Developing an appropriate grouting program design and compaction specifications and contract documents (designer)
- Planning the grouting equipment needs and procedural approach (contractor)
- Monitoring and evaluation of the grouting program (designer and contractor)

### 19.8.3.1 Site Investigation

The pregrouting subsurface exploration is more detailed than is normally required and should include continuous sample and laboratory tests. These tests should include grain-size analysis, density, permeability, pH, and other soil index properties.

The subsurface exploration should identify the extent that grouting can be utilized and areas or site conditions where grouting cannot be utilized. Subsurface stratigraphy can be well defined by continuous sampling. Small, fine-grained lenses should be noted, since these layers can retard the progression of some types of grouting. Considerably more descriptive detail is required on the boring log to be used by a grouting specialist than is typically shown on a standard boring log. Past uses of the site should be identified, such as the presence of abandoned wells, cisterns, cesspits, etc. These items can absorb the grout and either increase the grout take or cause no ground improvement. In addition, the presence of utilities should be noted, since the bedding materials of some utilities can cause a loss of grout as well. The grouting contractor should record every anomaly encountered in the drilling and grouting operations. These anomalies should be explained and evaluated prior to continuing drilling and grouting operations. Finally, the groundwater should be well understood. Samples of the groundwater should be tested for compatibility with the grouts to be used. Different levels of pH



will determine which types of grout can be used at a site. In addition, grout specimens should be prepared in the laboratory using samples of groundwater to determine if there will be any interaction between the grout and the groundwater. Further, additional samples should also be prepared using water from the actual source. The direction and rate of groundwater flow should also be established during the subsurface investigation.

### 19.8.3.2 Permeation Grouting

Permeation grouting uses a variety of grout materials, particulate, colloidal, and solution, to permeate the soils. The choice of which grout material to use is based on the grain-size distribution of the soil to be grouted (see Figure 19-28). Permeation grouting is an option in appropriate soils for the following applications:

- Waterproofing, typically for remedial purposes
- Settlement control
- Liquefaction retrofit mitigation by increasing density and displacing pore water

For permeation grouting to be successful, the soils must be “groutable”. Groutability should be based on the permeability of the soil. A first estimate of permeability, and thus groutability, is based on the fines content (i.e., the percentage of material passing the #200 sieve). Table 19-26 and Figure 19-29 provide the approximate percentage of material passing the #200 sieve and the groutability of a soil.

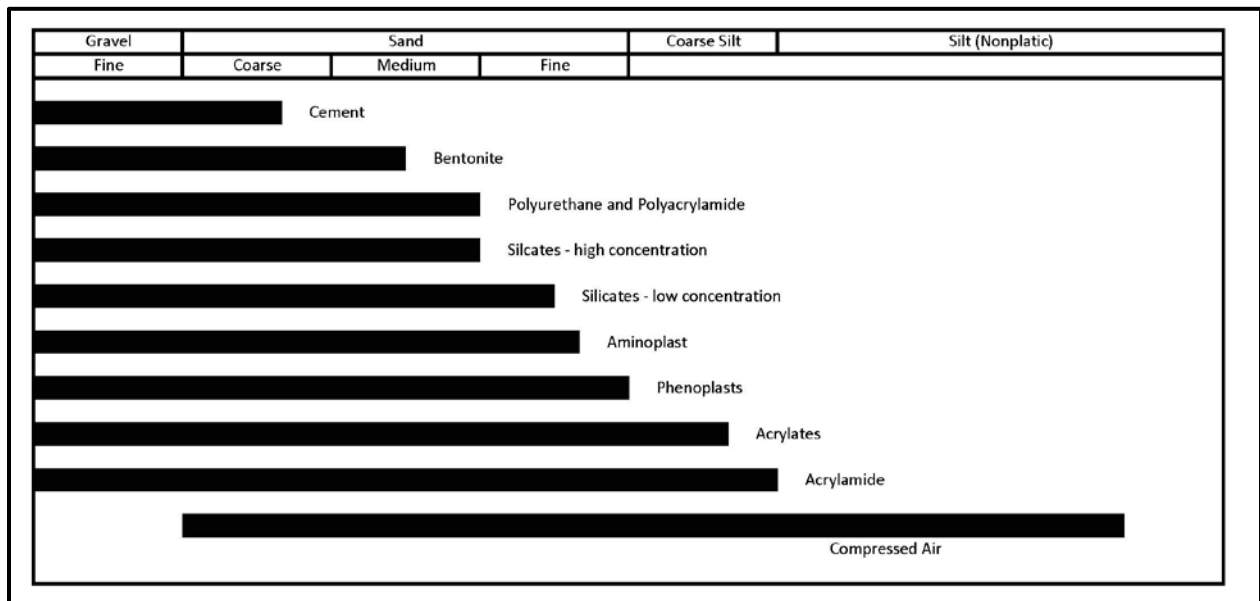


**Figure 19-26, Penetrability of Various Grouts versus Soil Type (modified Elias, et al. – Vol. II (2006))**

**Table 19-26, Groutability Guidelines**

Percent Passing #200 Sieve	Description
<12	Readily groutable
12 – 15	Moderately groutable
15 – 20	Marginally groutable
> 20	Non-groutable

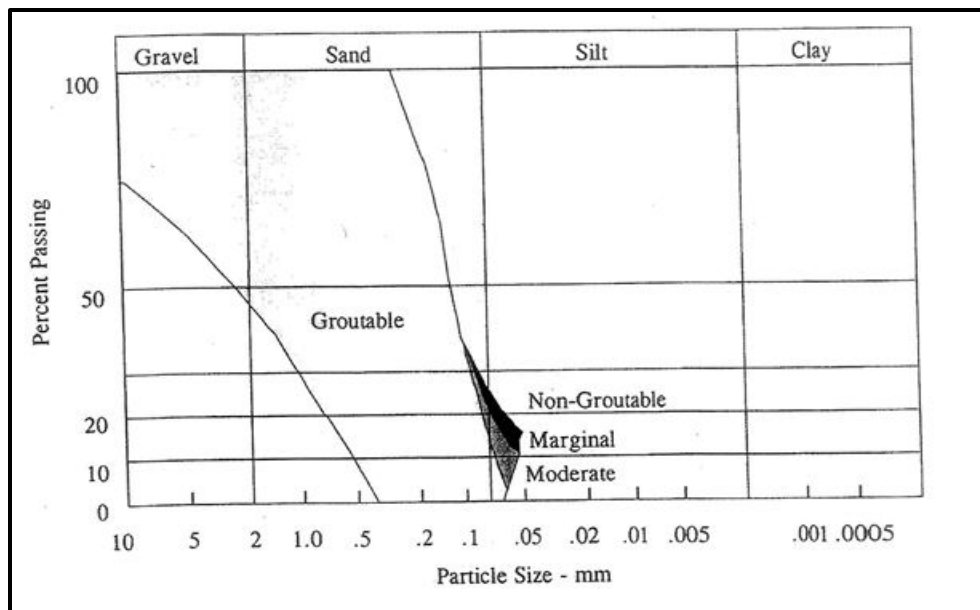


**Figure 19-27, Grain-Size Distribution for Permeation Grouting (Elias, et al. – Vol. II (2006))**

These guidelines provide an indication of permeability; however, the actual permeability of a soil should be determined, either in the laboratory or in field pumping tests or injection tests. It should be noted that environmental permitting will be required for both pumping and injection testing. The following equations provide further guidance for the potential for permeation grouting using particulate grouts.

$$\frac{(D_{15})_{soil}}{(D_{85})_{grout}} = \Psi \quad \text{Equation 19-23}$$

$$\frac{(D_{10})_{soil}}{(D_{95})_{grout}} = \Theta \quad \text{Equation 19-24}$$

Where,

- ( $D_{15}$ )<sub>soil</sub> = Diameter of the fifteen percent passing for soil
- ( $D_{85}$ )<sub>grout</sub> = Diameter of the eighty-five percent passing for the grout material
- ( $D_{10}$ )<sub>soil</sub> = Diameter of the ten percent passing for soil
- ( $D_{95}$ )<sub>grout</sub> = Diameter of the ninety-five percent passing for the grout material

**Table 19-27, Guide to Permeation Grout Potential**

Groutability	$\Psi$	$\Theta$
Impossible	< 11	< 6
Possible	11 – 24	6 – 11
Easy	> 24	>11

After a preliminary determination that permeation grouting is feasible; an expert in the design of permeation grouting should be consulted to complete the final design.

### 19.8.3.3 Compaction Grouting

According to Elias, et al. – Vol. II (2006):

*Compaction grouting* consists of the injection of low slump (*usually 1 inch or less*), low mobility grout into loose or loosened soils of appropriate grain-size distribution. ...compaction grouting can be used in a wide variety of applications, including soil densification (for static and seismic enhancement), raising of surficial structures settlement control over...sinkholes and for structural underpinning. Compaction grout can also be used to seal off major water ingresses through open channel systems.

*Figure 19-29* indicates the range of soils where densification by compaction grouting may be expected to be effective, i.e., in all relatively free-draining soils, including gravels, sands, and coarser silts. In fine-grained soils, pore pressures may not be able to dissipate and improvement may not be economically achievable. Grout mix design is also critical, in that the grout must have internal friction to ensure that the bulbs preserve their “spheroidal” shape in the soil. Otherwise, fracturing and lensing will occur, leading to ineffective densification.

There are no mathematical models for use in compaction grouting (i.e., establishing the spacing, rate of injection, limiting volumes, etc.). Therefore, either an engineer or contractor that specializes in compaction grouting should be retained to assist in the final design of compaction grouting. Typically compaction grout pipes are spaced at 6-1/2 to 16-1/2 feet intervals. The amount of grout required for soil densification ranges from 3 to 12 percent of the soil volume being treated. Normally, compaction grouts use particulate grouts such as Portland Cement Types I or II. The slump of the compaction grout should be around 1 inch.

### 19.8.3.4 Jet Grouting

Jet grouting is a grouting process that uses high pressure, high velocity erosive jets of water and/or grout to remove some of the soil and replacing the removed soil with cement based grout. The combination soil and grout is called “Soilcrete<sup>®</sup>”. Jet grouting can be used in soils ranging from clays to gravels with varying degrees of effectiveness. Jet grouting can be used for a variety of applications:

- Water Control
- Settlement Control
- Underpinning
- Scour Protection
- Excavation Support
- Liquefaction Mitigation
- Treatment of Karst

Jet grouting permits the shape, size, and properties of treated soil, usually a circular column, to be engineered in advance. Figure 19-30 provides a schematic of the jet grouting procedure.

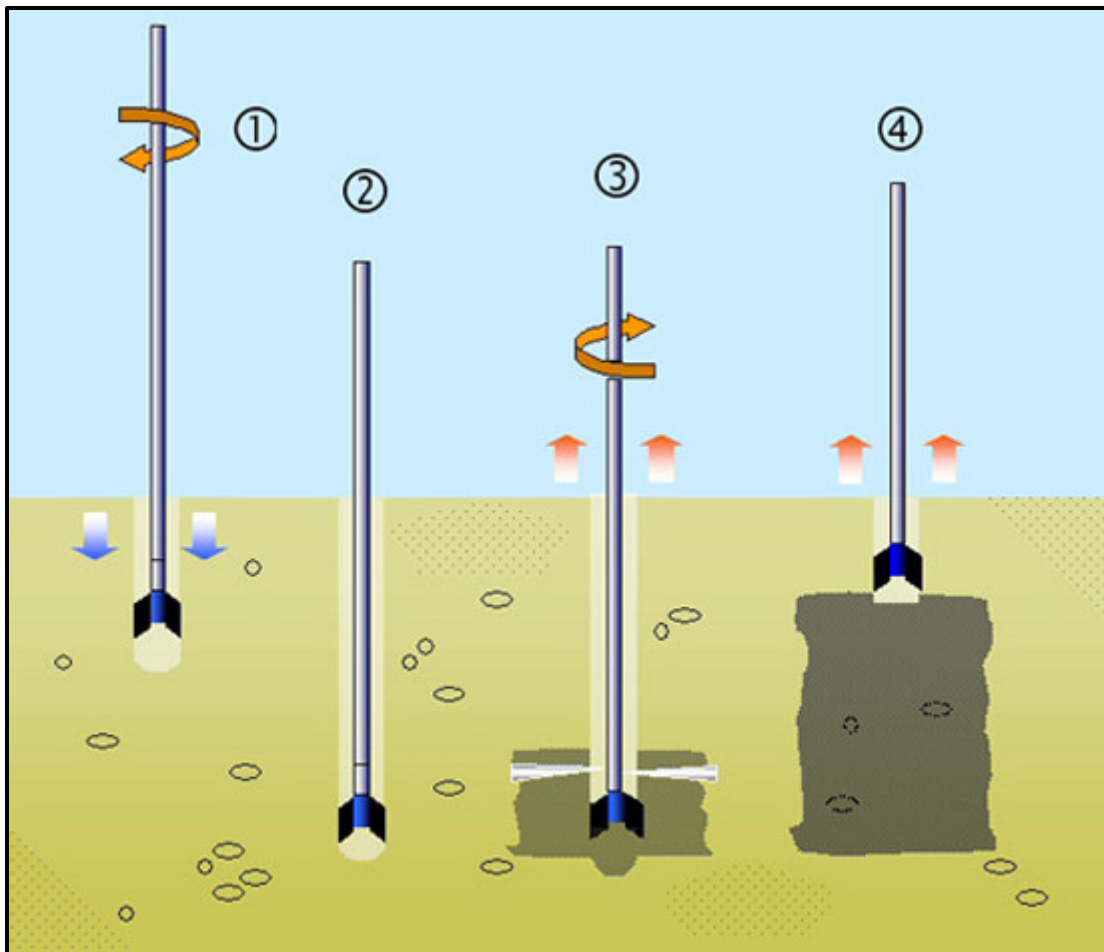


**Figure 19-28, Jet Grouting Process Schematic  
(Altem İnşaat Ind. ve Trd. Ltd. Corp. (2009))**

Jet grouting can be accomplished using 3 different types of jetting procedures as discussed below and depicted in Figure 19-31.

- Single Fluid System – The fluid is the grout and uses a high-pressure (7,200 psi) jet to simultaneously erode the in-situ soil and inject the grout. This system only partially replaces the soil.
- Double Fluid System – A high-pressure grout jet is contained within a compressed air cone. This system produces a larger column diameter, provides a higher degree of soil replacement, although a lower strength “Soilcrete®” is created.
- Triple Fluid System – An upper jet of high-pressure (4,400 to 7,200 psi) water contained inside a cone of compressed air is used for excavation, with a lower jet injecting grout, at a lower pressure, to replace the slurried soil.

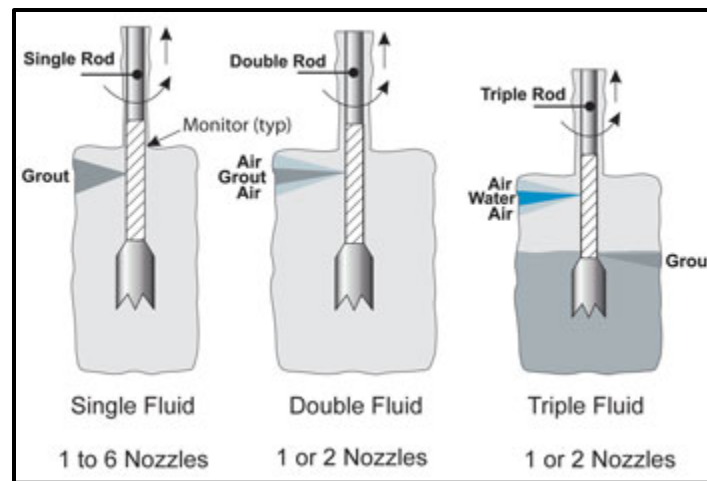


**Figure 19-29, Jet Grouting Systems  
(Burke (Wind Systems) (2010))**

### 19.8.3.5 Soil Fracture Grouting

Soil fracture grouting is the process of injecting grouts in a highly controlled manner that does not permit permeation of the grout in the soil matrix or compaction of the soil matrix. Instead the soil matrix is ruptured and the grout forms a reinforcing “skeleton” within the matrix. Soil fracture grouting can be used to raise settled structures, control settlement, and soil reinforcement. Sophisticated measuring equipment is required when conducting this type of grouting operation. Similar to compaction grouting, designs using soil fracture grouting should be performed by an engineer or contractor specializing in this method.

### 19.8.3.6 Slabjacking

Slabjacking is the process of injecting grout under pressure to raise and relevel concrete paving (typically bridge approach slabs) that have settled. Slabjacking is used to correct the settlement of concrete slabs placed over compressible soils or to replace soils that have eroded away from beneath the slab. Typically, this method is used to correct problems associated with the vertical displacement of bridge approach slabs. According to Elias, et al. – Vol. II (2006):

Slabjacking procedures include raising or leveling, under-slab void filling (no raising), grouting slab joints, and asphalt subsealing. Most slabjacking uses a suite of cementitious grouts, incorporating bentonite, sand, ash and/or other fillers, as dictated by local preference and the project conditions and goals. Certain proprietary methods use expanding chemical foams to create uplift pressures. Best results (when no cracking is caused to the slabs) are obtained when the slabjacking is uniformly and gradually conducted. Slabjacking can also be used to “pump” *sections of rigid pavements* that have sunk below the adjoining section so that the expansion joint may be repaired and have its functionality restored.

Slabjacking has the following advantages:

- Frequently, the most economical repair method
- Usually faster than other solutions, especially compared to removal and replacement
- Planned so that there is little disruption to the existing facility, and can be performed at times of light or no traffic
- The equipment needed to perform the slabjacking operation can be removed from the repair location, providing for maximum accessibility

- Increased load capacity of the slab is provided
- The useful life of the concrete pavement is extended
- A smoother riding surface is established

Following are the disadvantages of slabjacking:

- Cracks already present may tend to open up when the slab is treated, unless great care is taken with the process
- Slabjacking may not be cost-effective on small projects
- The original cause of the settlement is not addressed

The feasibility of using slabjacking should be based on the cost of slabjacking versus the cost of removal and replacement of the slab. Included in this evaluation should be the time required for both operations and if a roadway must be closed to perform this operation. In addition, slabjacking should not be considered when the slab is severely cracked.

After determining that slabjacking is feasible, the design should begin with understanding the underlying problem and determining the desired results of the slabjacking. If the underlying problem is settlement of soft or organic soils, then, future slabjacking may be required. Regardless of the cause of the problem, the GEOR should accurately specify the required performance and tolerances for the project. Another consideration is the appearance of the finished surface. Most slabs that have settled contain some cracks. The cracks will remain visible even if the slabjacking process does not create new cracks. Further, the restored slab will also contain patches from the injection holes. The injection holes are usually on 5- to 6-foot grid spacing. The objectives of slabjacking are to fill voids and raise the slab approximately to its original elevation, without causing additional damage to the slab. Instrumentation as simple as a string line can provide this, although the use of lasers is more accurate.

## 19.9 COLUMN SUPPORTED EMBANKMENT

Constructing embankments over soft, compressible soils creates numerous problems (i.e., excessive settlements, embankment instability, and long periods over which the settlements occur). These problems have led to the development of the ground improvement methods discussed previously in this Chapter; however, in certain cases, time constraints are critical to the success of the project. Therefore, an alternative ground improvement method has been developed: Column Supported Embankment (CSE) (see Figure 19-32). CSEs consist of 2 primary components; first, a column system to transfer loads to a more suitable bearing stratum and second, a load transfer platform (LTP). The LTP can consist of either structural concrete or a geosynthetic reinforced soil layer.

In the previous version of the GDM, the Beam Design Approach based on the Modified Collin Method was recommended for use on SCDOT projects regardless of whether rigid (i.e., prestressed concrete, steel H- or pipe piles, or timber) or flexible (i.e., stone, VCCs, DMM, soil mixed or auger cast-in-place piles) columns will be used to transfer the load to the bearing formation. However, because of advances in the design methodology, the Load and Displacement Compatibility (LDC) method will be used for the design of CSEs supported by flexible columns and is described in Schaefer, et al. – Vol. II (2017). Flexible columns require more movement to engage the capacity of the column and therefore, will transfer some of the induced load to the soils located between the columns. The Modified Collin Method will be used for the design of CSEs supported by rigid columns. Rigid columns will not require the amount of movement required to engage the soil as in the flexible columns; therefore, minimal to no load will be transferred to the soil between the columns. The LTP above the rigid columns will act more like a beam or rigid platform than the LTP above flexible columns.

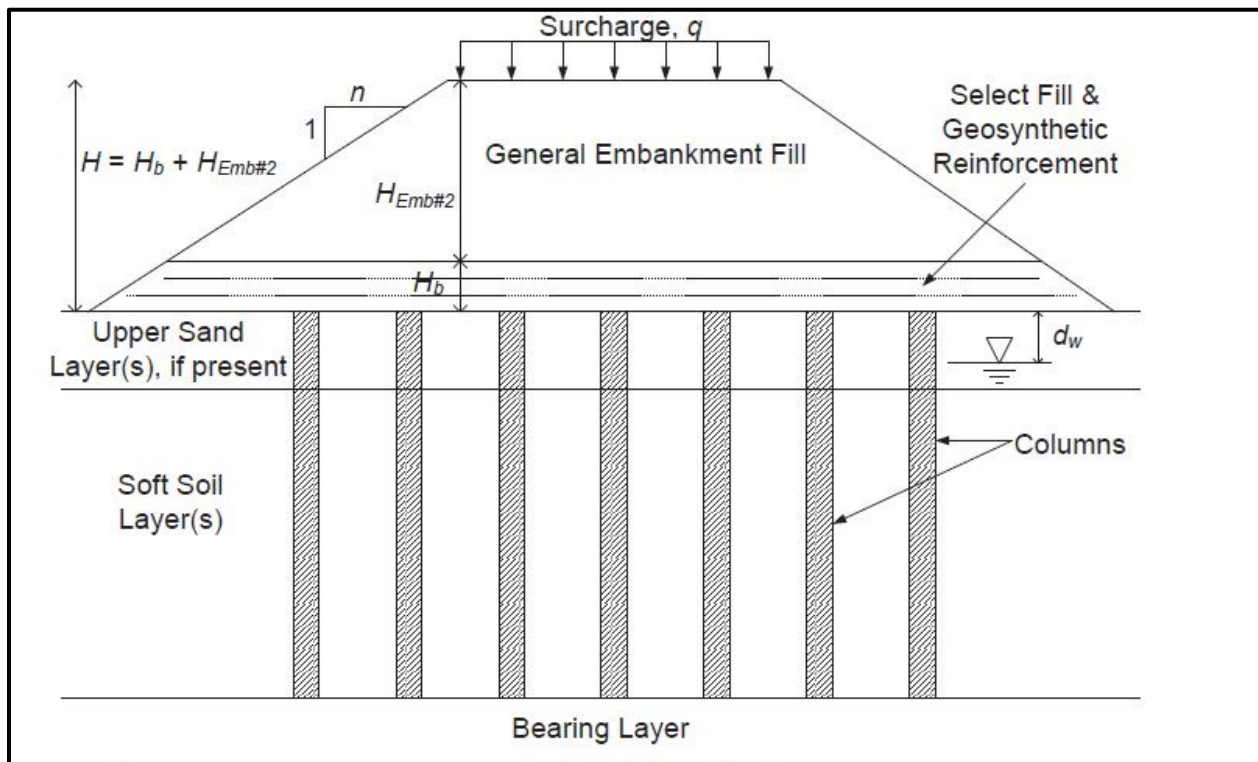


**Figure 19-30, CSE with Geosynthetic LTP  
(Geotech Tools (2012))**

The LTP transfers the embankment load to the columns. The LTP may consist of a rigid structural element or a geosynthetic reinforced soil layer. The rigid LTP is typically economically cost prohibitive and will therefore, not be discussed in this Chapter. If a rigid transfer platform is required for a project, contact the RPG/SDS and RPG/GDS for guidance. The design of a rigid LTP is the responsibility of the SEOR. The GEOR will provide the nominal resistance of the deep foundation system to be used to support the rigid LTP. The geosynthetic reinforced LTP is discussed in subsequent Sub-sections of this Chapter. The GEOR is responsible for not only designing the columns but also the geosynthetic reinforced LTP.

### **19.9.1 Analysis and Feasibility**

As indicated previously, CSEs have traditionally been used to support embankments over soft soils when time constraints are such that consolidation of the soft soils is not practical. CSEs have the advantage of being constructed in a single stage. There is no waiting period for the dissipation of pore water pressures. CSEs are more economical than removing and replacing the soil, especially when the groundwater is close to the ground surface. Where infrastructure precludes high-vibration techniques, the type of column used for the CSE system may be selected to minimize or eliminate the potential for vibrations. Total and differential settlement of the embankment may be drastically reduced when using CSEs over other conventional approaches. Another benefit of using CSEs is that a variety of columns are available for support of the embankment depending on the stiffness of the subsurface soils. CSEs have the major disadvantage of having high initial costs; however, the savings in time can offset these costs.

The thickness of the soft soil is not a critical component in the determination of the feasibility of using CSEs because there are a variety of columns that can be used for support. The selection of the column should also consider the potential environmental impact of the installation of the column.

### 19.9.2 Design Approach

The design of CSEs is a complicated soil-structure interaction problem that requires the engineer to have a good understanding of the Strength and Service limit states of the structure. The Strength limit state failure modes include the following (see Figure 19-33):

- Failure of the columns to carry the full embankment load
- The lateral extent of the columns must be sufficient to prevent slope instability
- The load transfer platform must be designed to transfer the vertical load to the columns
- Lateral sliding of the embankment on top of the columns
- The global (overall) stability must be checked

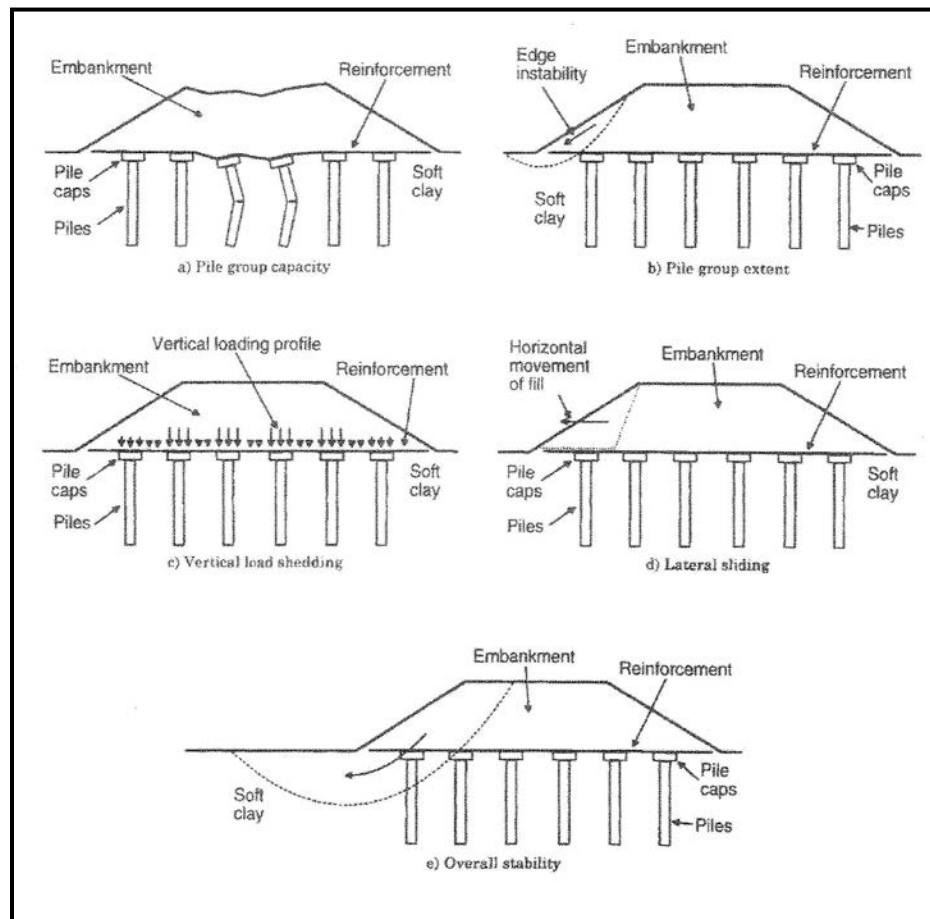


**Figure 19-31, Strength Limit State Failure Modes  
(Schaefer, et al. – Vol. II (2017))**

The Service limit state of the CSE must also be checked. The strain in the geosynthetic reinforcement used to create the LTP should be kept below some maximum threshold to preclude unacceptable deformation reflection (see Figure 19-34, Detail a) at the top of the embankment. In addition, the settlement of the columns should also be analyzed to ascertain whether the CSE will develop unacceptable settlements (see Figure 19-34, Detail b).



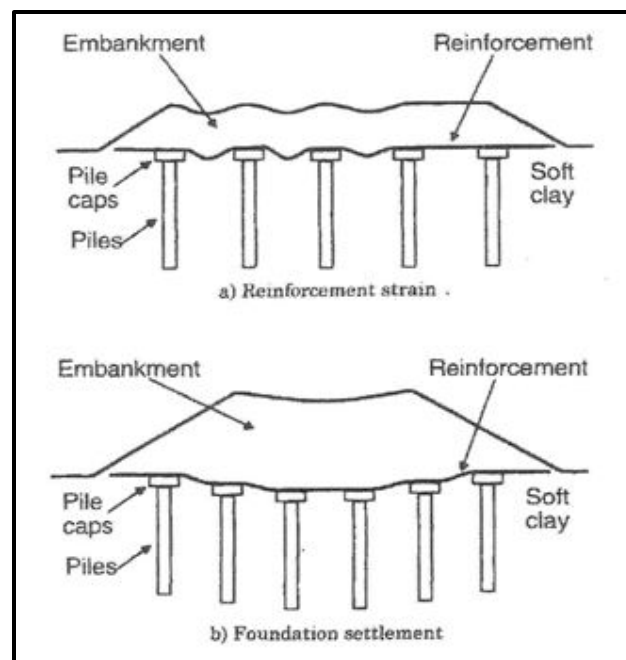


**Figure 19-32, Service Limit State  
(Schaefer, et al. – Vol. II (2017))**

The general design procedure for CSEs is provided below:

1. Estimate preliminary column spacing.
2. Determine required column load.
3. Select preliminary column type based on required column load and site geotechnical requirements.
4. Determine capacity of column to satisfy Strength and Service limit state design requirements.
5. Determine extent of columns required across embankment width.
6. Check critical embankment height criteria and adjust column spacing as required.
7. Determine LTP reinforcement requirements based on estimated column spacing. Revise column spacing as required.
8. Determine reinforcement requirements for lateral spreading.
9. Determine overall reinforcement requirements based on LTP and lateral spreading.
10. Check global stability.
11. Prepare construction drawings and specifications.
12. Observe construction.

### 19.9.2.1 Preliminary Design

The preliminary design of CSEs should consider the following factors:

- The preliminary spacing of the columns should be limited so that the area replacement ratio is between 10 and 20 percent.
- The clear span between columns should be less than the embankment height and should not exceed approximately 10 feet. In addition, the clear span plus twice the column diameter should not exceed the width of the geosynthetic roll, i.e., the geosynthetic should cover 2 rows of columns. Wider clear spans may lead to unacceptable differential settlement between columns.
- The fill required to create the LTP shall be select structural fill with an effective friction angle greater than or equal to  $35^\circ$ .
- The columns shall be designed to carry the entire load of the embankment.

- The CSE reduces post construction settlements of the embankment surface to typically less than 2 to 4 inches for correctly designed and constructed CSEs.

### 19.9.2.2 Column Design

The selection of the type of column should be based on the constructability, load capacity, and cost of the various column types (Steps 2 and 3 of the general CSE design procedure). The load carrying capacity of each column is based on the tributary area of each column (see Figure 19-35). In CSE design, it is assumed that the weight of the embankment and any surcharge loads are carried by the rigid columns and that the surrounding soil carries no load. For CSEs supported by flexible columns it is assumed that the weight of the embankment and any surcharge loads are carried by both the columns and the surrounding soil. The tributary area for a single column is geometrically a hexagon and is termed a unit cell; however, for simplification a circle having the same tributary area is used. Figure 19-36 provides the effective diameter ( $D_e$ ) for both equilateral triangular and square spacing. Prior to using rectangular ( $s_1 \neq s_2$  in Figure 19-37a) or isosceles triangular column layout contact the PC/GDS for permission. Figure 19-37 provides the determination of the area of the unit cell around each column. The typical center-to-center column spacing is 5 to 10 feet. The required design vertical load ( $Q_r$ ) in the column is determined by the following equation:

$$Q_r = \pi * \left(\frac{D_e}{2}\right)^2 * (\gamma * H + q) \quad \text{Equation 19-25}$$

Where,

$Q_r$  = Unfactored or nominal column load

$D_e$  = Effective diameter of the tributary area of column or unit cell

$H$  = Height of embankment

$\gamma$  = Unit weight of embankment soil

$q$  = Live and dead load surcharge (determined similar to long-term stability analysis)

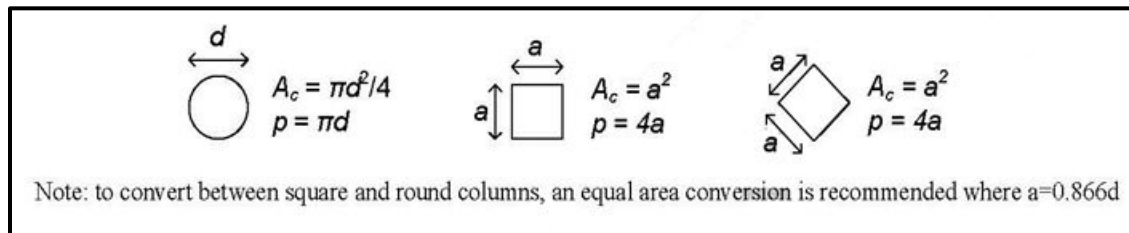


**Figure 19-33, Area and Perimeter Determination of Round and Square Columns (Schaefer, et al. – Vol. II (2017))**

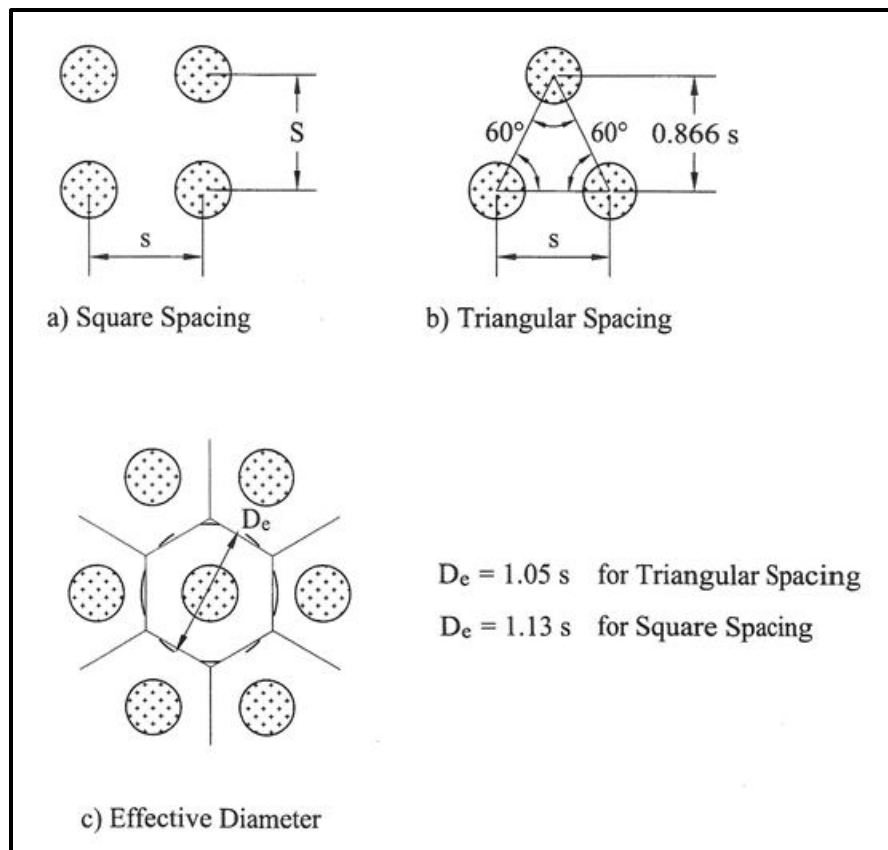


**Figure 19-34, Effective Column Diameter Determination (Elias, et al. – Vol. II (2006))**

Select the appropriate type of column (i.e., rigid or flexible) based on the  $Q_r$  determined previously. For the determination of the resistance of driven concrete, steel, or timber piles, all examples of rigid columns see Chapter 16. For DMM and stone columns (including rammed aggregate piers and VCCs), examples of flexible columns, see previous Sections of this Chapter for the appropriate design methodologies.

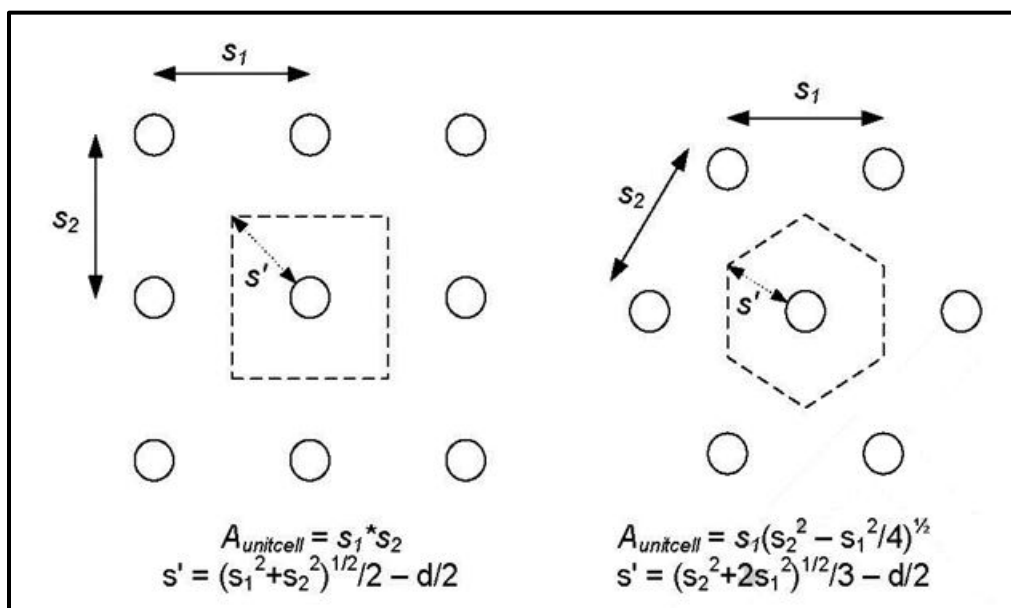


**Figure 19-35, Unit Cell Area Determination (Geotech Tools (2012))**

### 19.9.2.3 Lateral Extent of Columns

Step 4 of the general CSE design procedure establishes the lateral extent of the columns. The columns should extend a sufficient distance beyond the crest of the embankment to ensure that any instability or differential settlement that occurs beyond the limits of the columns will not affect the crest of the embankment. The British Standard (BS8006) requires that the columns extend to at least a minimum distance from the proposed toe of slope,  $L_p$ , to prevent settlement of the unsupported edge of the embankment from affecting the embankment crest.  $L_p$  is determined using the following equations:

$$L_p = H * (n - \tan \theta_p) \quad \text{Equation 19-26}$$

$$\theta_p = \left( 45 - \frac{\phi'_{emb}}{2} \right) \quad \text{Equation 19-27}$$

Where,

$L_p$  = Horizontal distance from the toe of the embankment to the edge of first column

$n$  = Side slope of embankment (see Figure 19-38)

$\theta_p$  = Angle from vertical between the outer-most column and the crest of the embankment (see Figure 19-38)

$\phi'_{emb}$  = Effective friction angle of embankment fill

It is typical SCDOT practice for the columns to extend to at least the toe of slope if not 1 row outside of the toe of slope, but within the SCDOT ROW.

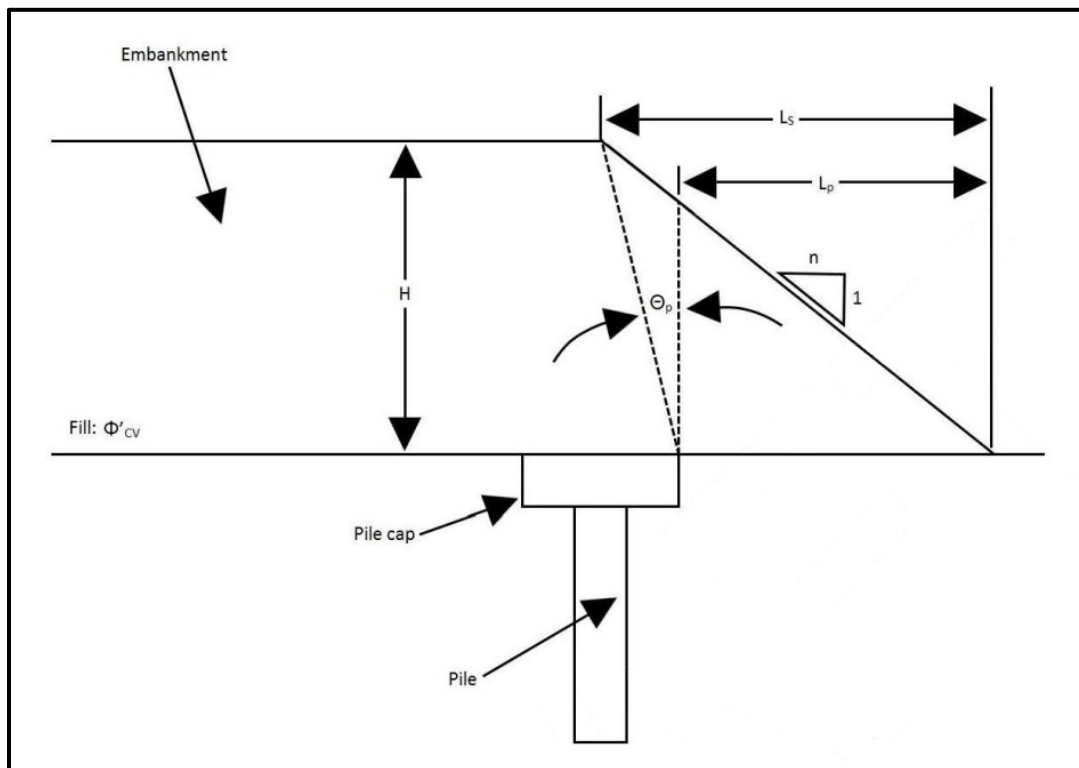


Figure 19-36, CSE Edge Stability  
(Schaefer, et al. – Vol. II (2017))

### 19.9.2.4 Critical Height

According to Schaefer, et al. – Vol. II (2017),

Avoiding differential settlement at the surface of a CSE is often important, for example, to provide good ride quality and to prevent distress to overlying structures. Factors that influence differential surface settlements include column spacing, column diameter, embankment height, quality of subgrade support relative to column stiffness, and loading acting on the embankment surface. For example, differential surface settlement is likely for a relatively low embankment with wide column spacing and poor subgrade support. Differential surface settlement is unlikely for a high embankment with close column spacing and good subgrade support. In this Chapter, the term *critical height* is defined as the embankment height above which differential settlements at the base of the CSE do not produce measurable differential settlement at the embankment surface.

For CSEs without subgrade support, McGuire (2011) found that the critical embankment height,  $H_{crit}$ , depends on the column diameter and spacing, and it is not significantly affected by the relative density of the embankment fill or the use of geosynthetic reinforcement in the load transfer platform.... The approach recommended on [www.GeoTechTools.org](http://www.GeoTechTools.org) design document is to use the larger value of  $H_{crit}$  estimated...as provided below....

$$H > H_{crit} = \max \left\{ \begin{array}{l} 1.5 * (s - a) \\ 1.15 * s' + 1.44d \end{array} \right\} \quad \text{Equation 19-28}$$

Where,

s = Center-to-center distance between columns (see Figure 19-36)

a = Face dimension for a square column (see Figure 19-35)

s' = Determined in Figure 19-37

d = Diameter for a round column (see Figure 19-35)

In cases where a square array of *either square pile caps or square piles without caps* is used and the embankment height is fixed by the difference between the embankment subgrade elevation and roadway elevation, the minimum center-to-center spacing can be estimated by Equation 19-29. If a *square array of round pile caps or round piles without caps* is used, 0.866d can be substituted for a pile cap width, a, resulted in Equation 19-30.

$$s \leq 1.2 * (H - a) \quad \text{Equation 19-29}$$

$$s \leq 1.2 * (H - 0.866d) \quad \text{Equation 19-30}$$

If an equilateral triangular spacing is used for either square pile caps or square piles without caps use Equation 19-31. If round pile caps or round piles without caps are placed in an equilateral triangular array use Equation 19-32 to determine the required spacing.

$$s \leq 1.5 * (H - a) \quad \text{Equation 19-31}$$

$$s \leq 1.5 * (H - 0.866d) \quad \text{Equation 19-32}$$

### 19.9.2.5 Load Transfer Platform

The design of the LTP shall be based on whether rigid or flexible columns are being used to support the LTP. If rigid columns are being used to support the CSE, then the LTP shall be designed using the beam method, specifically the Modified Collin Method. For flexible columns used to support the CSE, the LTP shall be designed using the LDC method.

#### 19.9.2.5.1 Modified Collin Method

The Modified Collin Method or the beam design approach shall be used when rigid columns and a geosynthetic reinforced LTP are used together. As indicated previously the rigid columns may be prestressed concrete piles, steel H-piles, pipe piles, or timber piles. The beam design approach is based on the premise that the reinforcement creates a stiffened beam of reinforced soil to distribute the load imposed by the embankment to the columns. The stiffened beam of reinforced soil should contain a minimum of 3 layers of reinforcement (Figure 19-39). In addition, in the Modified Collin Method, a catenary reinforcement is added at the base of the beam to support the soil beneath the arch.

The Modified Collin Method is based on the following assumptions:

- The thickness ( $h$ ) of the LTP is equal to or greater than  $\frac{1}{2}$  of the clear span between the columns (i.e.,  $0.5(s-d)$ )
- A minimum of 3 layers of geosynthetic reinforcement is used to create the LTP
- A minimum distance of 8 inches is maintained between the layers of reinforcement
- Select fill is used to construct the LTP with an effective friction angle greater than or equal to  $35^\circ$
- The primary function of the reinforcement is to provide lateral confinement of the select fill to facilitate soil arching within the thickness ( $h$ ) of the LTP
- The secondary function of the reinforcement is to support the wedge of the soil below the arch
- All of the vertical load from the embankment above the load transfer platform is transferred to the columns below the platform
- The initial strain in the reinforcement is limited to 5 percent

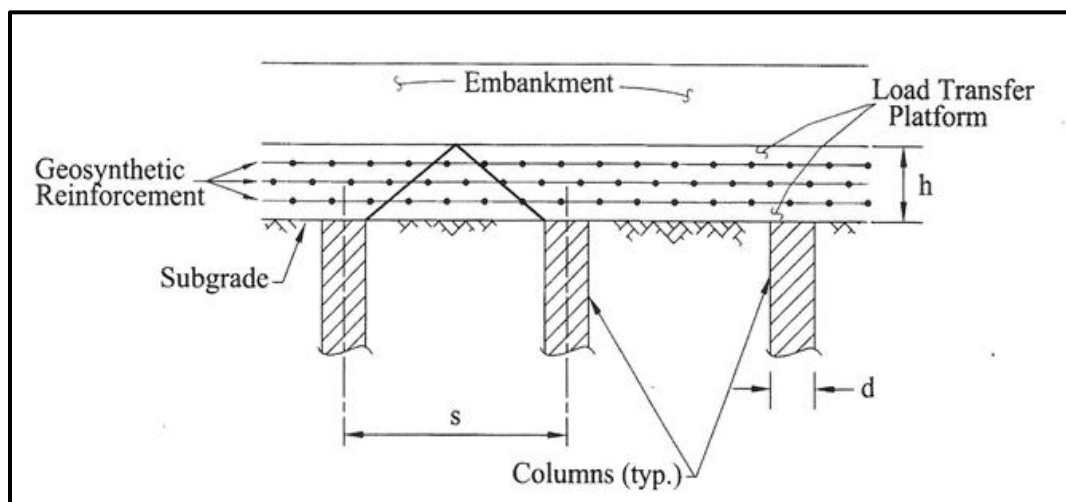


**Figure 19-37, Load Transfer Platform  
(Elias, et al. – Vol. II (2006))**

The fill load attributed to each layer of reinforcement is the material located between the layer of reinforcement and the next layer above (Figure 19-40). The uniform vertical load on any layer

(n) of reinforcement ( $W_{Tn}$ ) may be determined using the following equations for a triangular pattern and a square pattern, respectively.

$$W_{Tn} = \frac{[(s-d)_n^2 + (s-d)_{n+1}^2] * \sin 60^\circ * h_n * \gamma_{emb}}{(s-d)_n^2 * \sin 60^\circ} \quad \text{Equation 19-33}$$

$$W_{Tn} = \frac{[(s-d)_n^2 + (s-d)_{n+1}^2] * h_n * \gamma_{emb}}{(s-d)_n^2} \quad \text{Equation 19-34}$$

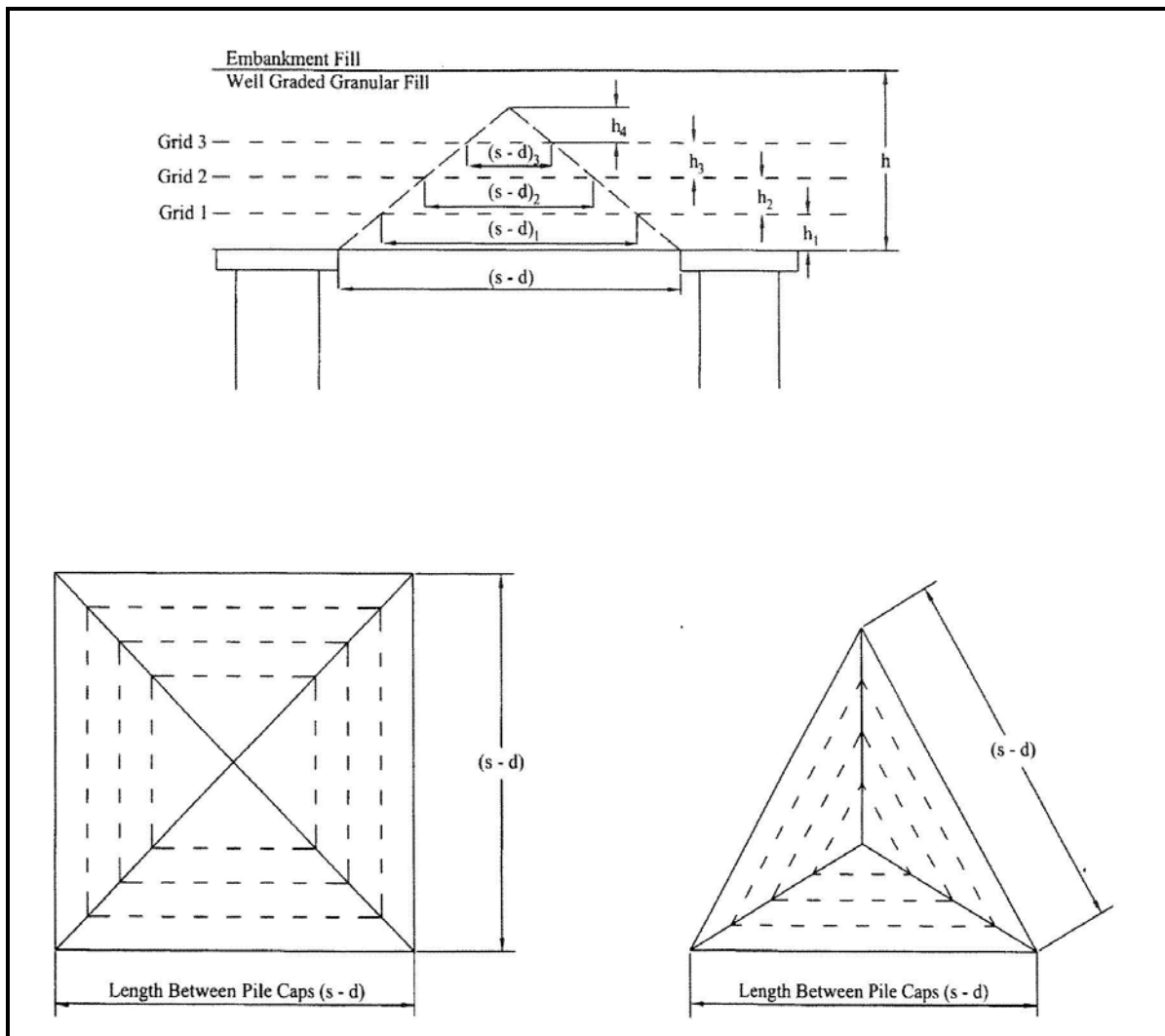


**Figure 19-38, Collin Method Load Transfer Platform Design (Schaefer, et al. – Vol. II (2017))**

The tensile load on any layer of reinforcement ( $T_{RPn}$ ) is determined based on tension membrane theory and is a function of the amount of strain in the reinforcement.  $T_{RPn}$  is determined using the following equation:

$$T_{RPn} = \frac{W_{Tn} * \Omega * D}{2} \quad \text{Equation 19-35}$$

Where,

$D = (s-d)_n$  for square column spacing





$\gamma = \text{Unit weight of LTP (beam) material}$

The tensile load in the reinforcement is determined based on tension membrane theory and is a function of the amount of strain in the reinforcement. The tension in the reinforcement is determined from the following equation:

$$T_{RPC} = \frac{W_{TC} * \Omega * D}{2} \quad \text{Equation 19-37}$$

Where,

D = Design span for tensioned membrane  
Square column layout

$$D = 1.41 * \left[ (s - d) - 2 * \left( \frac{\sum \text{Vertical Spacing}}{\tan 45^\circ} \right) \right] \quad \text{Equation 19-38}$$

Triangular column layout

$$D = 10.867 * \left[ (s - d) - 2 * \left( \frac{\sum \text{Vertical Spacing}}{\tan 45^\circ} \right) \right] \quad \text{Equation 19-39}$$

$\Omega$  = Dimensionless factor from tensioned membrane theory (*Table 19-28*)

### 19.9.2.5.2 Load and Displacement Compatibility Method

The Load and Displacement Compatibility (LDC) Method shall be used if flexible columns will be used to support the CSE. Flexible columns consist of stone columns, VCCs, DMM columns, soil mixed columns, or auger cast-in-place piles. Schaefer, et al. – Vol. II (2017) recommends using the LDC method, stating:

In order for the CSE design to be effective, the embankment load must be transferred to the columns without excessive deformations occurring at the surface of the embankment. ... A practical method that models the actual load transfer mechanisms is the LDC method.

Smith (2005) and Filz and Smith (2006, 2007) developed a LDC method for analyzing the net vertical load that acts on the geosynthetic reinforcement in the LTP....Essential features of the LDC method include:

- Vertical load equilibrium and displacement compatibility are assumed at the level of the geosynthetic reinforcement to calculate the load distribution amount the columns, the soft soil between columns, the geosynthetic, and the base of the embankment above columns and between columns.
- An axisymmetric approximation of a unit cell is employed for calculating the vertical load acting on the geosynthetic reinforcement.
- A 3D representation of the geosynthetic-reinforced CSE system and a parabolic deformation pattern of the geosynthetic between adjacent columns is assumed for the purpose of calculating the tension in the geosynthetic (*i.e., Generalized Parabolic Method*).
- The LDC method was developed for round columns or square pile caps in a square array.
- Nonlinear response of the embankment is incorporated by providing linear response up to a limit state, at which point additional base settlement produces no further load concentration on the columns. The limit state is determined using the Adapted Terzaghi Method described below.

- Linear stress-strain response of the geosynthetic is assumed, but because large displacements of the geosynthetic are involved, the load-displacement relationship for the geosynthetic is nonlinear. Iterations can be performed to approximate nonlinear response of the geosynthetic material.
- Nonlinear compressibility of *Clay-Like* soil between columns is represented using the compression ratio ( $C_c$  or  $C_{ec}$ ), recompression ratio ( $C_r$  or  $C_{er}$ ), and preconsolidation pressure ( $\sigma'_p$  or  $p'_c$ ).
- Slippage is allowed between the soil and the column when the interface shear strength is exceeded.

An exploded profile view of a unit cell, including the vertical stresses at the contacts above and below the geosynthetic reinforcement is shown in *Figure 19-42*. Vertical equilibrium of the system shown in *Figure 19-42* is satisfied when:

$$\gamma * H + q = \bar{\Xi}_{geotop} = \bar{\Xi}_{geobot} \quad \text{Equation 19-40}$$

$$\bar{\Xi}_{geotop} = a_s * \sigma_{col,geotop} + (1 - a_s) * \sigma_{soil,geotop} \quad \text{Equation 19-41}$$

$$\bar{\Xi}_{geobot} = a_s * \sigma_{col,geobot} + (1 - a_s) * \sigma_{soil,geobot} \quad \text{Equation 19-42}$$

$$a_s = \frac{A_c}{A_{unitcell}} \quad \text{Equation 19-43}$$

Where,

$\gamma$  = Unit weight of embankment soil

H = Height of embankment

q = Surcharge pressure

$a_s$  = Area replacement ratio

$A_c$  = Area of column or pile cap

$A_{unitcell}$  = Area of unit cell (see *Figure 19-37*)

$\sigma_{col,geotop}$  = Average vertical stress acting downward at the top of geosynthetic in the area underlain by the column (see *Figure 19-42*)

$\sigma_{soil,geotop}$  = Average vertical stress acting downward at the top of geosynthetic in the area underlain by the soil foundation (see *Figure 19-42*)

$\sigma_{col,geobot}$  = Average vertical stress acting downward at the bottom of geosynthetic in the area underlain by the column (see *Figure 19-42*)

$\sigma_{soil,geobot}$  = Average vertical stress acting downward at the bottom of geosynthetic in the area underlain by the soil foundation (see *Figure 19-42*)

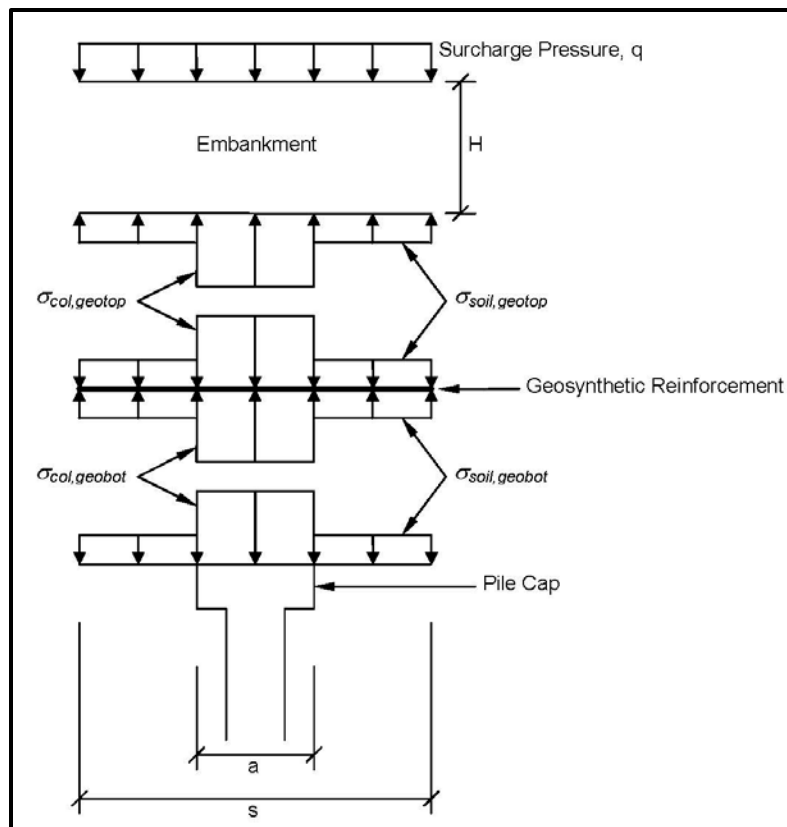


**Figure 19-40, Definition Sketch for LDC Method  
(Schaefer, et al. – Vol. II (2017))**

Load-deflection relationships were developed for:

- i. The embankment settling down around the column or pile cap;
- ii. The geosynthetic deflecting down under the net vertical load acting on the area underlain by soil; and
- iii. The soil settling down between the columns.

The relationships are only described in conceptual terms here; however, supporting equations and additional details are presented by Filz and Smith (2006). The composite foundation system consisting of columns and the soil between the columns is discretized, and the simultaneous nonlinear equations can be solved numerically using a spreadsheet program.

The load-deflection relationship for the embankment settling down around the column or pile cap (*i above*) is assumed to be linear up to the maximum load condition. The linear part is approximated using a linear solution for displacement of a circular loaded area on a semi-infinite mass. As indicated previously, square pile caps of width,  $a$ , can be approximated as circular pile caps with diameter,  $d$ , such that the pile cap areas are the same ( $a = 0.866d$ ). The limiting stress condition in the embankment above the geosynthetic reinforcement is established using the Adapted Terzaghi Method with a lateral earth pressure coefficient,  $K$ , of 0.75, which is between the values of 1.0 used by Russell and Pierpoint (1997) and 0.5 used by Russell, Naughton and Kempton (2003).

The geosynthetic deflects down under the net vertical load applied over the area underlain by soil (*ii above*). The geosynthetic load-deflection relationship was

developed based on analyses of a uniformly loaded annulus of linear elastic membrane material with the inner boundary pinned, which represents the support provided by the column, and with the out boundary free to move vertically but not laterally, which represents the axisymmetric approximation of lines of symmetry in the actual 3-dimensional configuration of a column-supported embankment. The details of the analyses and the results are presented by Smith (2005) and Filz and Smith (2006).

The settlements of the column and the subgrade soil are determined based on the vertical stress applied to the top of the column or pile,  $\sigma_{\text{col,geobot}}$ , and the vertical stress applied to the subgrade soil,  $\sigma_{\text{soil,geobot}}$  (*iii above*). The column compression is calculated based on a constant value of the column modulus. One-dimensional compression of *Clay-Like* soil located between columns is calculated using the compression ratio ( $C_c$  or  $C_{ec}$ ), recompression ratio ( $C_r$  or  $C_{er}$ ), and preconsolidation pressure ( $\sigma'_p$  or  $p'_c$ ) of the soil. If an upper layer of *Sand-Like soil* is located between the columns, the *Sand-Like soil* compression is calculated using a constant value modulus for the *Sand-Like soil*. If voids are anticipated between the LTP and subgrade soil the support from the foundation should be ignored.

As the compressible soil settles down with respect to the stiffer column, the soil sheds load to the column through shear stresses at the contact between the soil and the column along the column perimeter. The magnitude of the shear stress is determined using an effective stress analysis and a value of interface friction angle between the soil and column. The vertical stress increment in the soil from the embankment, and surcharge loads, decreases with depth due to the load shedding process until the depth at which the column settlement and soil settlement are equal. An important detail is that the settlement profile of the subgrade soil at the level of the top of the columns is likely to be dish-shaped between the columns. The difference between the column compression and the average soil compression is the average differential settlement at the subgrade level. To account for the dish-shaped settlement profile between the columns, the suggestion by Russell, et al. (2003) that the maximum differential settlement at subgrade level may be as much as twice the average differential settlement was adopted.

The computational method described above is solved by satisfying vertical equilibrium using *Equations 19-40 to 19-43* and requiring that the calculated values of the differential settlement at subgrade level must be the same for the base of the embankments, the geosynthetics if utilized, and the underlying foundation soil. If there is reason to believe that the soft soil between the columns will settle more than the geosynthetic deforms, e.g., due to groundwater lowering, then the subgrade soil can be assigned a very high compressibility value to essentially eliminate subgrade support of the geosynthetic. The simultaneous nonlinear equations that describe this computational method have been implemented in a spreadsheet **Geogrid Bridge 2.0** (Filz and Smith (2006)) *that is available for purchase (see CGPR #77) at the following website:* [http://www.cgpr.cee.vt.edu/index.php?do=searchpublication&keyword=\\*](http://www.cgpr.cee.vt.edu/index.php?do=searchpublication&keyword=).

**GeogridBridge 2.0** has the following features:

- Two different types of embankment fill are allowed so that lower quality fill can be used above the bridging layer.

- Analyses without geosynthetic reinforcement can be performed by setting the value of the geosynthetic stiffness,  $J$ , equal to 0.
- The column area and properties can vary with depth so that embankments supported on piles with pile caps can be analyzed.
- The subsurface profile can include 2 upper sand layers and 2 underlying clay layers. The preconsolidation stress for the clay can vary linearly within each clay layer.
- The simultaneous nonlinear equations are solved automatically, and the input and output are arranged so that design alternatives can be evaluated easily.

The LDC method was validated by comparison with numerical analyses that were previously validated by comparison with instrumented case histories and pilot-scale experiments performed by others.

### 19.9.2.6 Lateral Spreading

The potential for lateral spreading of the embankment must be analyzed (Figure 19-43). The geosynthetic reinforcement must be designed to prevent lateral spreading of the embankment. This is a critical aspect of the design, because many columns used to support CSEs are not capable of developing adequate lateral resistance to prevent the spreading of the embankment. The geosynthetic reinforcement must be designed to resist the horizontal force caused by the lateral spreading of the embankment. The required tensile force to prevent lateral spreading ( $P_{Lat}$ ) is determined using the following equations.

$$P_{Lat} = K_a * \left( \frac{\gamma * H^2}{2} + q * H \right) \quad \text{Equation 19-44}$$

Sand-Like ( $\leq 20$  percent fines)

$$K_a = \tan^2 \left( 45 - \frac{\phi_{emb}'}{2} \right) \quad \text{Equation 19-45}$$

Sand-Like ( $> 20$  percent fines,  $PI \leq 10$ )

$$K_a = \tan^2 \left( 45 - \frac{\phi_{emb}'}{2} \right) - \frac{2c_{emb}'}{\sigma'_v} * \left[ \tan^2 \left( 45 - \frac{\phi_{emb}'}{2} \right) \right] \quad \text{Equation 19-46}$$

Where,

$\phi'_{emb}$  = Effective friction angle of embankment fill

$c'_{emb}$  = Effective cohesion of embankment fill

$\sigma'_v$  = Effective overburden pressure at bottom of embankment fill

The resistance to lateral spread without geosynthetic reinforcement is determined by:

$$R_{Ls} = (L_s) * S_u \quad \text{Equation 19-47}$$

Where,

$L_s$  = Length of side slope of the embankment

$S_u$  = Undrained shear strength of foundation soil

$P_{Lat}$  is compared to  $R_{Is}$  and shall have an  $\phi$  less than or equal to 0.66 as indicated in the following equation:

$$\left(\frac{P_{Lat}}{R_{Is}}\right) \leq 0.66 \tag{Equation 19-48}$$

If an adequate  $\phi$  cannot be achieved, geosynthetic reinforcement shall be added. The reinforcement shall be able to resist all of  $P_{Lat}$ . The reinforcement long-term design strength ( $T_{al}$ ) shall be greater than  $P_{Lat}$ . Multiple layers of reinforcement may be used to resist the lateral spreading force. The geosynthetic reinforcement materials to be used to resist lateral spreading shall meet the criteria provided in the latest version of the STSs for *Geogrid Soil Reinforcement*, SC-M-203-2 or *Geotextile Soil Reinforcement*, SC-M-203-3.

$$T_{al} \geq P_{Lat} \tag{Equation 19-49}$$

The minimum length of reinforcement ( $L_e$ ) required to prevent the sliding of the embankment across the reinforcement is determined using the following equation.

$$L_e = \frac{T_{al}}{[0.5\gamma * H * (c_{iemb} * \tan \phi'_{emb})]} \tag{Equation 19-50}$$

Where,

$c_{iemb}$  = Coefficient of interaction for sliding between the geosynthetic reinforcement and the embankment fill

$\phi'_{emb}$  = Friction angle of embankment fill material

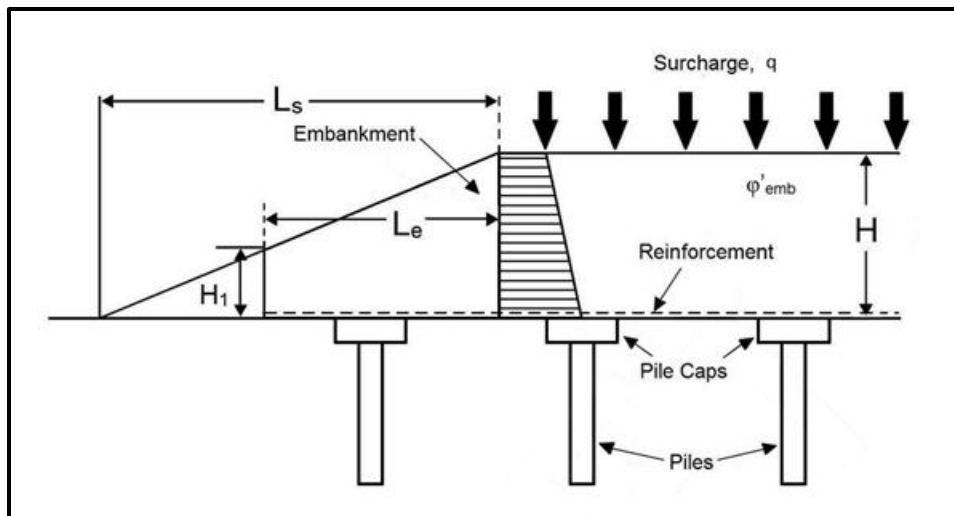


Figure 19-41, CSE Lateral Spreading (modified Schaefer, et al. – Vol. II (2017))

### 19.9.3 Reinforcement Total Design Load

Regardless of the method used to design the LTP, the maximum design load ( $T_{max}$ ) on the geosynthetic reinforcement is determined using the following equations:

Reinforcement along the length of the embankment (longitudinal direction of road)

$$T_{max} = T_{RP} \tag{Equation 19-51}$$

Reinforcement across the width of the embankment (transverse direction of road)

$$T_{max} = T_{RP} + T_{ls} \quad \text{Equation 19-52}$$

## 19.10 CONSTRUCTION WORKING PLATFORM

Embankments constructed on soft soil foundations have a tendency to move both in the vertical as well as the horizontal directions. The vertical settlements are dealt with using ground improvement methods discussed previously in this Chapter. The horizontal movements can consist of either a general sliding of the embankment (block type failure) or from lateral squeeze (see Chapter 17). As indicated in Chapter 17, the soft soils will gain strength with time due to the settlement, however, some reinforcement of the subgrade may be required to prevent lateral movements or slope instabilities while the subgrade soils are gaining strength. The design requirements for reinforced embankments and RSSs are provided in Chapter 17. This Section handles the design of construction working platforms that are intended as an aide to construction.

Please note that the following information is obtained from Holtz, Christopher and Berg (2008) instead of Elias, et al. – Vol. II (2006). The Elias, et al. – Vol. II (2006) Chapter that covers this topic is actually a draft Chapter from Holtz, et al. (2008). Therefore, SCDOT has elected to use the Holtz, et al. (2008) instead.

The use of a combination of stone or granular materials and geosynthetic reinforcement beneath an embankment as subgrade stabilization is also called “bridging”. Bridging is only required if the in-situ soil has an undrained shear strength ( $\tau = c_u$ ) less than 500 pounds per square foot or 3.5 pounds per square inch. A bridge lift should be considered if the exposed subgrade soils are susceptible to deterioration (i.e., contains plastic fines) from inclement weather and exposure to vehicular traffic. Basically, the reinforcement is not considered as part of the design of the embankment, but is placed exclusively to permit construction to proceed, by stabilizing the subgrade materials to permit the placement of bridging materials. Further, the use of reinforcement and bridge lift materials will not prevent or mitigate settlement or slope instability; other ground improvement methods are required to mitigate settlement or slope instability. The reinforcement typically consists of either a geogrid or a geotextile. The reinforcement used in subgrade stabilization is not included in the stability analysis. The use of the reinforcement is to limit the amount of excavation (undercutting or mucking) required. The standard construction practice using reinforcement to aide construction is presented below.

1. Muck excavation to required depth (if necessary)
2. Placement of reinforcement and/or soil separator (if necessary)
3. Placement of bridge lift
4. Placement of soil separator (if necessary)
5. Placement and compaction of backfill materials

Muck excavation or undercut should be limited to no more than 5 feet. If a suitable bearing soil is not encountered within this depth or unless otherwise specified by the GEOR, a geosynthetic material meeting the requirements of Supplement Technical Specification (STS) *Geosynthetic Materials for Separation and Stabilization* (SC-M-203-1) shall be placed beneath the bridge lift material. The use of a geogrid separator should be considered for Sand-Like subsoils and a geotextile separator should be considered for Clay-Like subsoils. Place the geosynthetic material in the bottom of the excavation and up the excavation side slopes. In areas that require muck excavation or undercutting, replace with bridge lift material.

Borrow excavation materials and man-made (lightweight aggregates) may be placed as bridge lift materials as long as the grade on which the material is being placed is at least 6 inches

above ground water level. Borrow excavation materials bridge lift materials shall have a maximum lift thickness of 1 foot. In the event that groundwater does not allow backfilling with a borrow excavation material, place either a stone or granular material as the bridge lift material that meets the Supplemental Specification *Bridge Lift Materials*. Bridge lift materials placed in water shall consist of either stone or coarse granular materials (A-1-a).

Stone bridge lift materials shall have maximum lift thicknesses of 2 feet and shall extend a minimum of 6 inches above the water level surface. Stone bridge lift materials shall not be placed through more than 5 feet of water. For placement of materials through water depths greater than 5 feet see Chapter 17. Granular lift materials shall also have a lift thickness of 1-1/2 feet and shall not be placed in more than 2 feet of water. Granular bridge lift materials shall extend a minimum of 2 feet above water level surface. Individual bridge lifts shall have some type of limited compactive/tamping effort. If additional compacted borrow excavation soil is needed to reach grade, a geosynthetic material meeting the requirements of STS *Geosynthetic Materials for Separation and Stabilization* (SC-M-203-1) shall be placed between any stone bridge lift material and the overlying compacted soil. Bridge lifts consisting of either borrow excavation or granular bridge lift material shall not be placed within 3 feet of the base of the pavement section. Only compacted borrow excavation soil or stone bridge lift material shall be placed within this zone.

The thickness of the bridge lift is determined using both the US Forest Service (Steward, Williamson and Mohny (1977)) and the Giroud and Han (2004a and b) (also called Giroud-Han) methods as presented in Holtz, et al. (2008). The thickest bridge lift shall be used in design. The top of the bridge lift shall not be closer than 3 feet beneath the bottom of the pavement structure, unless the bridge lift is constructed of stone. If the US Forest Service method is used to determine the depth of undercutting and the thickness of the bridge lift, then the maximum size of construction equipment shall be indicated on the plans (see Figures 19-44 and 19-45).

### **19.10.1 US Forest Service (Steward, et al. (1977)) Method**

The US Forest Service (USFS) Method is a chart based solution that requires knowledge of not only the soil conditions, but the methods of fill placement and sizes of construction equipment. Since it will be practically impossible to ascertain the type and size of construction equipment to be used, the type and size of construction equipment should be indicated on the drawings as a limitation until at least 3 feet of embankment fill has been placed. This method is applicable to both geotextiles and geogrids.

The first step in using the USFS Method is determining the subgrade strength. The undrained shear strength ( $c_u$ ,  $\tau$  (psi)) should be determined from either CPT or DMT soundings or from FVSTs. Undrained shear strength, in psi, may also be estimated from field CBR values using the following equation.

$$c_u = 4.3 * (CBR) \quad \text{Equation 19-53}$$

The second and third steps handle the anticipated traffic configuration. The type of construction equipment anticipated should be indicated as well as the amount of traffic passes. It should be noted that the minimum number of traffic passes is 100, while the maximum is 1,000. It should be noted that the traffic estimate is based on the vehicles having a tire pressure of 80 psi. In the fourth step the depth of the tolerable rut is determined. The depth of the tolerable rut ranges from 2 to 4 inches.



The fifth step is determining the bearing capacity factor ( $N_c$ ) for both conditions: without reinforcement and with reinforcement. The table below provides the bearing capacity factor based on the reinforcement condition, tolerable rut depth, and traffic.

**Table 19-29, Bearing Capacity Factors for USFS Method  
(adopted from Holtz, et al. (2008))**

Reinforcement	Tolerable Rut (inches)	Traffic (18 kip ESALs)	Bearing Capacity Factor ( $N_c$ )
Without	< 2	> 1,000	2.8
	2 to 4	100 – 1,000	3.0
	> 4	< 100	3.3
Geotextiles	< 2	> 1,000	5.0
	2 to 4	100 – 1,000	5.5
	> 4	< 100	6.0
Geogrids	< 2	> 1,000	5.8

Step 6 consists of determining the amount of bridge lift material required for both the unreinforced as well as the reinforced subgrade. The material thicknesses are determined from Figures 19-44 for single wheel loads and 19-45 for dual wheel loads depending on the vehicular configuration assumed in the third step.

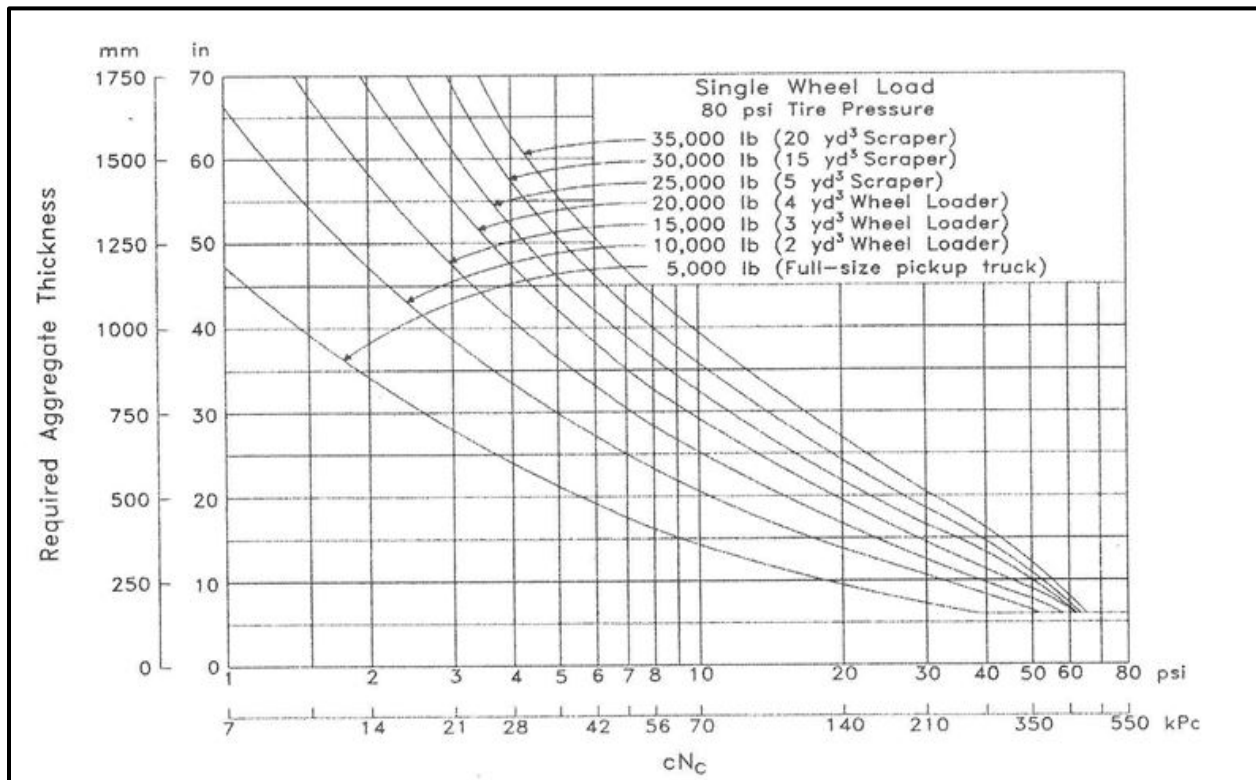


**Figure 19-42, USFS Method Bridge Lift Thickness – Single Wheel Loads  
(adopted from Holtz, et al. (2008))**

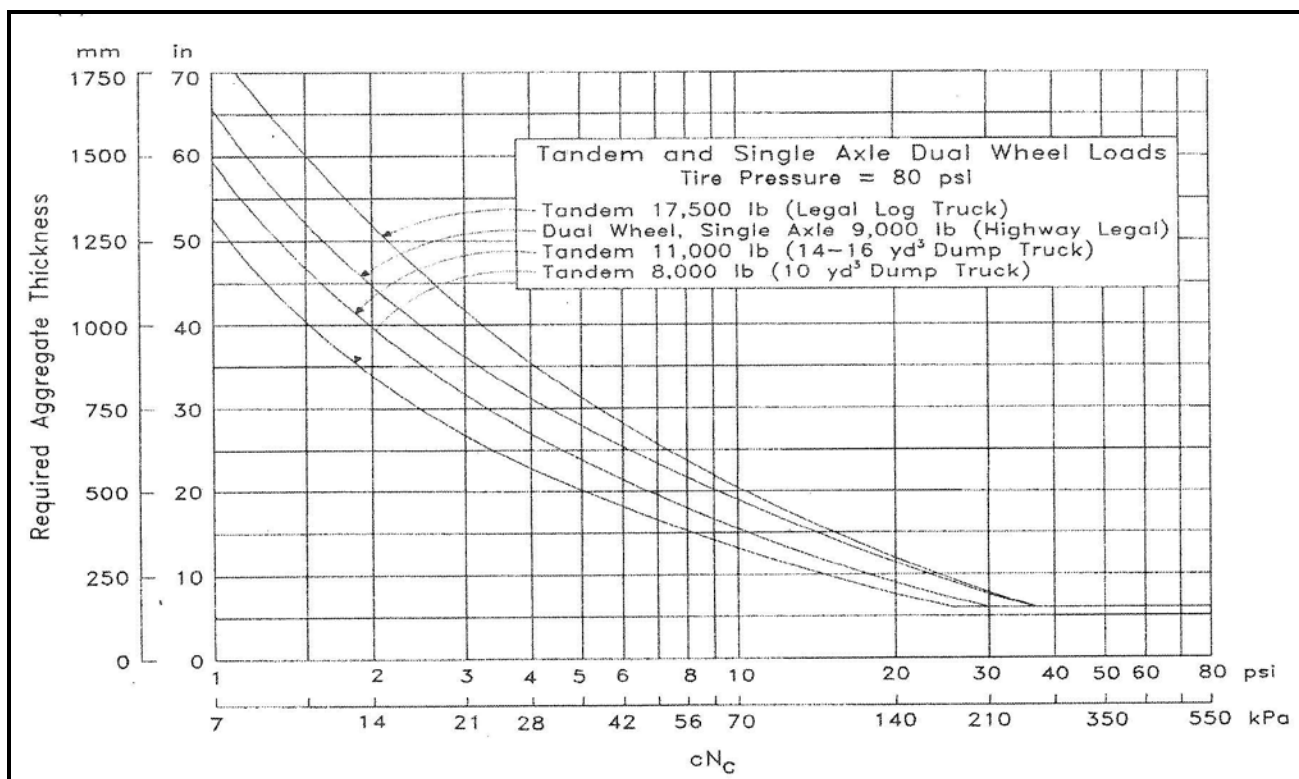


**Figure 19-43, USFS Method Bridge Lift Thickness – Dual Wheel Loads (adopted from Holtz, et al. (2008))**

The seventh step is the selection on the design thickness of the bridge lift as well as material for the bridge lift. The thickness of the bridge lift should be rounded to the next higher thickness divisible by 3. The USFS Method is also based on the bridge lift having an in-place CBR of 80, while the stone will obtain this CBR with little effort, the use of granular backfill, having a CBR much lower than 80, requires that the thickness of the bridge lift be increased. Increase the thickness of the bridge lift 3 inches for the use of granular bridge lift materials.

The eighth step is to determine the survivability of the geotextile materials for the given soil conditions. Given the anticipated conditions that bridge lifts and reinforcement will be used on, a high survivability is required.

The final step in the USFS Method is developing any plan notes required.

**19.10.2 Giroud-Han Method**

As indicated previously, the Giroud-Han method is based on Giroud and Han (2004a and b). The Giroud-Han method is an iterative process since the required thickness of bridging material is on both sides of the following equation:

$$h = \frac{0.868 + 4 * (\gamma) * (X)^{1.5}}{1.816} * \left( \sqrt{\frac{80}{\frac{5}{3} * (1 - 0.9e^{-X^2}) * N_c * c_u}} - 1 \right) * 6.3 \quad \text{Equation 19-54}$$

Where,

$$\gamma = (0.661 - 1.006 * J^2) > 0.0 \quad \text{Equation 19-55}$$

$$X = \frac{r}{h} = \frac{6.3}{h} \quad \text{Equation 19-56}$$

Where,

- h = Required bridge lift thickness (inches)
- J = Aperture stability modulus
- $\tau = c_u$  = Undrained shear strength (psi)
- s = Maximum rut depth (inches)
- $N_c$  = Bearing Capacity Factor (see Table 19-30)

**Table 19-30, Bearing Capacity Factor and Aperture Stability Modulus  
(adopted from Holtz, et al. (2008))**

	Bearing Capacity Factor ( $N_c$ )	Aperture Stability Modulus ( $J^{1,2}$ )
Unreinforced	3.14	0
Geotextile Reinforced	5.17	0
Geogrid Reinforced	5.71	$J^{1,2}$

<sup>1</sup>Aperture Stability Modulus determined by geogrid manufacturer/supplier

<sup>2</sup>(dimensionless in Equation 19-55, but reported in N-m/degree)

The following assumptions and limitations are placed on the Giroud-Han method.

- Rut depth (s) is limited to 2 to 4 inches
- CBR of stone is greater than 30
- CBR of granular material (A-1 through A-2-6) is greater than 10
- The number Equivalent Single Axle Loads (ESALs) is 10,000
- The tension membrane effect was not taken into account, since it is negligible for rut depths less than 4 inches
- The radius of tire contact (r) is 6.3 inches
- Tire pressure (p) is 80 pounds per square inch
- The wheel load (P) is 10.0 kips
- The minimum thickness of bridge lift is 6 inches

The capacity of the existing subgrade soils should be determined to check whether reinforcement is needed or not using the following equation.

$$P_{h=0,unrein} = \left(\frac{s}{3}\right) * 391.53 * c_u \quad \text{Equation 19-57}$$

Where,

$P_{h=0, unreinf}$  = Unreinforced subgrade support capacity with no bridge lift, pounds

If  $P_{h=0, unreinf}$  is greater than P, no reinforcement is required; however, a 6-inch bridge lift is recommended to prevent disturbance of the existing subgrade. If P is greater than  $P_{h=0, unreinf}$ , then reinforcement is required and Equation 19-54 should be used to determine the required thickness of bridge lift. Utilizing a P of 10,000 pounds in Equation 19-57, the minimum undrained shear strength with corresponding rut depth is shown in the following table.

**Table 19-31, Minimum Undrained Shear Strength versus Rut Depth**

Rut Depth (s) (inches)	Undrained Shear Strength ( $c_u, \tau$ ) (psf)
2	5520
3	3675
4	2750

## 19.11 REFERENCES

AASHTO, (2006), Standard Recommended Practice for Definition of Terms Related to Quality and Statistics As Used in Highway Construction, American Association of State Highway and Transportation Officials, Washington, DC.

Altem İnşaat Industry and Trade Limited Company, (2009), retrieved December 8, 2014, from <http://en.alteminsaat.net/jetgrout.html>.

ASTM International, (2015), Annual Book of ASTM Standards, Section 4 – Construction, Volume 04.13 – Geosynthetics.

Barksdale, R. D. and Bachus, R. C., (1983), Design and Construction of Stone Columns – Volume I, (FHWA/RD-83/026), U.S. Department of Transportation, Office of Engineering and Highway Operations, Federal Highway Administration, Washington, D.C.

British Standards Institution, (2010), Code of Practice for Strengthened/Reinforced Soils and Other Fills, BS8006, London, U.K.

Bruce, M. E. C., Berg, R. R., Collin, J. G., Filz, G. M., Terashi, M., and Yang, D. S., (2013), Federal Highway Administration Design Manual: Deep Mixing for Embankment and Foundation Support, (FHWA-HRT-13-046), U.S. Department of Transportation, Office of Transportation Management, Federal Highway Administration, Washington, D.C.

Burke, G. K., (2010), “When conducting site remediation, jet grouting is one technique to consider for improving poor soils without removing the existing structure.” Retrieved December 8, 2014, from Wind Systems web site: <http://www.windsystemsmag.com/article/detail/77/construction>.

Chu, j., Bo, M. W., and Choa, V., (2004), “Practical Considerations for Using Vertical Drains in Soil Improvement Projects”, *Geotextiles and Geomembranes Special Issue on Prefabricated Vertical Drains*, International Geosynthetics Society, Volume 22, Issues 1 and 2, pp. 110-117.

*Column-Supported Embankments (CSE) – Design Guidance*, Geotech Tools, Retrieved August 29, 2106, From: [http://www.geotechtools.org/documents/cse\\_design\\_r1.pdf](http://www.geotechtools.org/documents/cse_design_r1.pdf).

Collin, J. G., Han, J., and Huang, J., (2005), Design Recommendations for Column-Supported Embankments, unpublished report, Federal Highway Administration, Washington, D.C.

Elias, V., Welsh, J., Warren, J., Lukas, R., Collin, J. G., and Berg, R. R., (2006), Ground Improvement Methods – Volume I, (FHWA NHI-06-019), U.S. Department of Transportation, National Highway Institute, Federal Highway Administration, Washington, D.C.

Elias, V., Welsh, J., Warren, J., Lukas, R., Collin, J. G., and Berg, R. R., (2006), Ground Improvement Methods – Volume II, (FHWA NHI-06-020), U.S. Department of Transportation, National Highway Institute, Federal Highway Administration, Washington, D.C.

Federal Highway Administration, (2008), Transportation Construction Quality Assurance Reference Manual, (FHWA-NHI-08-067), Arlington, VA.

Filz, G. M., and Smith, M. E., (2006), Design of Bridging Layers in Geosynthetic-Reinforced, Column-Supported Embankments, (VTRC 06-CR12), Virginia Transportation Research Council, Charlottesville, VA, p. 48.

Filz, G. M., and Smith, M. E., (2007), "Net Vertical Loads on Geosynthetics Reinforcement in Column-Supported Embankments," Proceedings of Geo-Denver 2007, Soil Improvement, Geotechnical Special Publication No. 172, Denver, Colorado.

*Geopier® Rammed Aggregate Pier™*, Geotech Tools, Retrieved June 1, 2016, From: [http://www.geotechtools.org/documents/ac\\_factsheet\\_r1.pdf](http://www.geotechtools.org/documents/ac_factsheet_r1.pdf).

Giroud J. P. and Han J., (2004a), "Design Method for Geogird-Reinforced Unpaved Roads. I. Development of Design Method", *Journal of Geotechnical and Geoenvironmental Engineering*, ASCE, Volume 130, Issue 8, pp. 775-786.

Giroud J. P. and Han J., (2004b), "Design Method for Geogird-Reinforced Unpaved Roads. II. Calibration and Applications", *Journal of Geotechnical and Geoenvironmental Engineering*, ASCE, Volume 130, Issue 8, pp. 787-797.

Holtz, R. D., Christopher, B. R., and Berg, R.R., (2008), Geosynthetic Design and Construction Guidelines, (FHWA NHI-07-092), U.S. Department of Transportation, National Highway Institute, Federal Highway Administration, Washington, D.C.

Johnsen, L. F., Bruce, D. A., and Byle, M. J., (Editors), (2012), Grouting and Deep Mixing 2012, Volumes 1 and 2, Proceedings of the Fourth International Conference on Grouting and Deep Mixing, Geotechnical Special Publication No. 228, New Orleans, Louisiana, USA.

Larsson, S., (2005), "State of Practice Report – Execution, Monitoring and Quality Control", Proceedings of the International Conference on Deep Mixing: Best Practices and Recent Advances 2005, (Deep Mixing '05), Stockholm, Sweden, pp 732-785.

Liu, S.-Y., Du, Y.-J., Yi, Y.-L., and Puppala, A. J., (2012), "Field Investigations on Performance of T-Shaped Deep Mixed Soil Cement Column-Supported Embankments over Soft Ground", *Journal of Geotechnical and Geoenvironmental Engineering*, ASCE, Volume 138, Issue 6, pp. 718-727.

Lukas, R. G., (1995), Geotechnical Engineering Circular No. 1 – Dynamic Compaction, (FHWA-SA-95-037), U.S. Department of Transportation, Office of Technology Applications, Federal Highway Administration, Washington, D.C.

Pestana, J. M., Hunt, C. E., and Goughour, R. R., (1997), FEQDrain: A Finite Element Computer Program for the Analysis of the Earthquake Generation and Dissipation of Pore Water Pressure in Layered Sand Deposits with Vertical Drains, EERC-97/15, Earthquake Engineering Research Institute, University of California at Berkeley, Berkeley, California.

Priebe, H. J. (1995), "The Design of Vibro Replacement." *Ground Engineering*, Volume 28, No. 10, London, U.K., pp 31-37.

Rogbeck, Y., Alén, C., Franzén, G., Kjeld, A., Odén, K., Rathmayer, H., Want, A., and Øiseth, E., (2004), Nordic Guidelines for Reinforced Soils and Fills, May 2003, Revision A – February 2004, Nordic Geosynthetic Group, A Section of Nordic Geotechnical Societies, Nordic Industrial Fund.

Rollins, K. M., Anderson, J. K. S., McCain, A. K., and Goughour, R. R., (2003), "Vertical Composite Drains for Mitigating Liquefaction Hazard", Proceedings of the Thirteenth (2003) International Offshore and Polar Engineering Conference, Honolulu, Hawaii.

SCDOT Standard Specifications for Highway Construction (2007), South Carolina Department of Transportation, [https://www.scdot.org/business/pdf/2007\\_full\\_specbook.pdf](https://www.scdot.org/business/pdf/2007_full_specbook.pdf).

Schaefer, V. R., Berg, R. R., Collins, J. G., Christopher, B. R., DiMaggio, J. A., Filz, G. M., Bruce, D. A., and Ayala, D., (2017), Ground Improvement Methods – Volume I, (FHWA NHI-16-027), U.S. Department of Transportation, National Highway Institute, Federal Highway Administration, Washington, D.C.

Schaefer, V. R., Berg, R. R., Collins, J. G., Christopher, B. R., DiMaggio, J. A., Filz, G. M., Bruce, D. A., and Ayala, D., (2017), Ground Improvement Methods – Volume II, (FHWA NHI-16-028), U.S. Department of Transportation, National Highway Institute, Federal Highway Administration, Washington, D.C.

Smith, M. E., (2005), Design of Bridging Layers in Geosynthetic-Reinforced Column-Supported Embankments.” Doctoral Dissertation, Virginia Tech, Blacksburg, Virginia.

Stark, T. D., Arellano, D., Horvath, J. S., and Leshchinsky, D., (2004), “Guideline and Recommended Standard for Geofoam Applications in Highway Embankments”. NCHRP Report 529, National Cooperative Highway Research Program, Transportation Research Board, Washington, D.C.

Steward, J., Williamson, R. and Mohny, J. (1977), Guidelines for Use of Fabrics in Construction and Maintenance of Low-Volume Roads, USDA, Forest Service, Portland, OR. Also reprinted as Report No. FHWA-TS-78-205, U.S. Department of Transportation, Federal Highway Administration, Washington, D.C.

Title 23 Code of Federal Regulations (CFR), (2011), *Part 637 – Construction Inspection and Approval – Subpart B – Quality Assurance Procedures for Construction*, U.S Government Publishing Office, Washington, D.C.

**Chapter 20**  
**GEOSYNTHETIC DESIGN**

**GEOTECHNICAL DESIGN MANUAL**

*January 2019*





**Table of Contents**

<b><u>Section</u></b>		<b><u>Page</u></b>
20.1	Introduction.....	20-1
20.2	Geotextiles .....	20-3
20.3	Geogrids.....	20-5
20.4	Geomembranes.....	20-6
20.5	Geocomposites.....	20-7
20.6	Functions and Applications .....	20-7
	20.6.1 Filtration .....	20-8
	20.6.2 Drainage .....	20-10
	20.6.3 Separators .....	20-11
	20.6.4 Reinforcement.....	20-11
	20.6.5 Fluid Barriers.....	20-12
	20.6.6 Protection.....	20-12
	20.6.7 Secondary Applications.....	20-12
20.7	Design Approach .....	20-13
20.8	Evaluation of Properties.....	20-13
20.9	References .....	20-15

**List of Tables**

<b><u>Table</u></b>	<b><u>Page</u></b>
Table 20-1, Geosynthetic Generic Identifiers.....	20-3
Table 20-2, Guidelines for Evaluating Critical/Severe Nature .....	20-9
Table 20-3, Permittivity Requirements.....	20-10
Table 20-4, Primary and Secondary Functions.....	20-13
Table 20-5, Important Criteria and Principal Properties .....	20-14
Table 20-6, Evaluation of Geosynthetic Property Requirements.....	20-15

**List of Figures**

<b><u>Figure</u></b>	<b><u>Page</u></b>
Figure 20-1, Geosynthetic Classification Scheme .....	20-2
Figure 20-2, Stitch Type .....	20-4
Figure 20-3, Seam Type.....	20-4
Figure 20-4, Proper Seam Placement .....	20-5
Figure 20-5, Improper Seam Placement.....	20-5
Figure 20-6, Geogrid Mechanical Connection .....	20-6
Figure 20-7, Geomembrane Use Above ERS.....	20-7
Figure 20-8, Permittivity .....	20-9
Figure 20-9, Transmissivity .....	20-10
Figure 20-10, Geogrid Soil Separator.....	20-11



# CHAPTER 20

## GEOSYNTHETIC DESIGN

### 20.1 INTRODUCTION

According to Holtz, Christopher, and Berg (2008),

ASTM (2006) D4439 defines a geosynthetic as a planar product manufactured from a polymeric material used with soil, rock, earth or other geotechnical-related material as an integral part of a civil engineering project, structure, or system.

Geosynthetic materials are comprised of 4 basic groups: geotextiles, geogrids, geomembranes, and geocomposites. Each of these basic groups is discussed in greater detail below. The materials making up the geosynthetics may be either man-made or natural. The most common man-made materials consist of synthetic polymers such as polypropylene (PP), polyester (PET) and high density polyethylene (HDPE). It should be noted that these polymers are highly resistant to biological and chemical degradation. Other man-made polymers used less frequently are polyamides, polyvinyl chloride (PVC) and glass fibers. The polyamides (e.g., nylon) are not very durable in the soil since they tend to soften in the presence of water. Natural materials consist of cotton, jute, etc.; however, natural materials are biodegradable and, therefore, should be used for temporary (< 1 year) applications only. Figure 20-1 provides a classification scheme for geosynthetics. Chapter 2 provides a glossary of selected geosynthetic terms which are based on ASTM (2006) D4439 *Standard Terminology for Geosynthetics*.

SCDOT has prepared STSs for various geosynthetic materials depending on the use of the material. Geosynthetic materials used for separation and stabilization shall conform to the requirements of SC-M-203-1 (latest version) for *Geosynthetic Materials for Separation and Stabilization*. Two STSs have been developed for soil reinforcement, SC-M-203-2 and SC-M-203-3 (latest version) for *Geogrid Soil Reinforcement* and *Geotextile Soil Reinforcement*, respectively. Either geosynthetic group (i.e. geogrids or geotextiles) can be used for reinforced embankments or RSSs as defined in Chapter 17. Reinforcement geosynthetics should not be used for stabilization or separation even though the materials may be the same. The difference in use is that geosynthetics used in slope stability analysis are reinforcement. If the geosynthetic is not used in slope stability analysis then it is a separation and stabilization material. The latest version of the STSs is available on the SCDOT website:

<https://www.scdot.org/business/business-landing.aspx>.

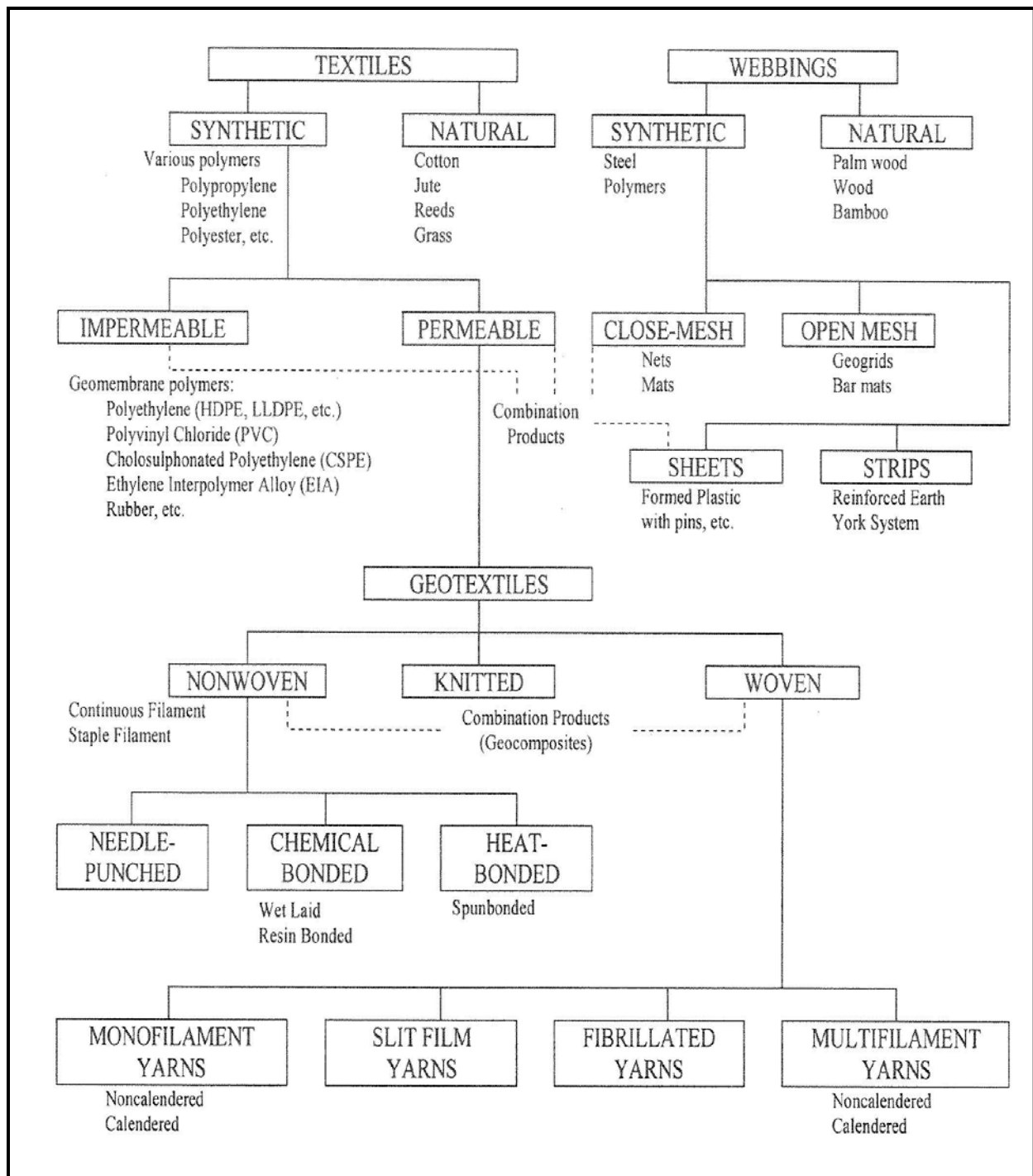


**Figure 20-1, Geosynthetic Classification Scheme (Holtz, et al. (2008))**

Geosynthetics are identified using the information contained in Table 20-1.

**Table 20-1, Geosynthetic Generic Identifiers  
(adopted from Holtz, et al. (2008))**

Identifier	Descriptive Term	Example
Polymer	High density, low density, etc.	<b>High density polyethylene geomembrane</b>
Type of Element	Filament, yarn, type, strand, rib, coated rib, etc.	Polypropylene staple <b>filament</b> needlepunched nonwoven geotextile, 10 oz/yd <sup>2</sup>
Manufacturing Process	Woven, needlepunched nonwoven, heatbonded nonwoven, stitchbonded, extruded, knitted, welded, uniaxial, biaxial, roughened sheet, smooth sheet, etc.	Polypropylene staple filament <b>needlepunched nonwoven</b> geotextile, 10 oz/yd <sup>2</sup>
Primary Geosynthetic Type	Geotextile, geogrid, geomembrane, etc.	High density polyethylene <b>geomembrane</b>
Mass per Unit Area or Thickness <sup>1</sup>	Mass per unit area – geotextiles Thickness – geomembranes	Polypropylene staple filament needlepunched nonwoven geotextile, <b>10 oz/yd<sup>2</sup></b>
Additional Information	As required	Polypropylene extruded biaxial geogrid, <b>with 1 in x 1 in openings</b>

<sup>1</sup>As appropriate

## 20.2 GEOTEXTILES

Geotextiles are subdivided into 2 categories: woven and nonwoven. Both categories are comprised of fibers or yarns that are combined into a planar textile structure. The fibers can be either continuous filaments or staple fibers. The continuous filaments are very long thin polymeric strands, whereas, the staple fibers are short (3/4 to 6 inches) filaments. Both filament types can be manufactured from an extruded plastic sheet that is slit to form thin, flat tapes. The extrusion or drawing process elongates the polymers in the direction of the draw causing an increase in the strength of the filament. After the drawing process, filaments may also be fibrillated, a process in which the filaments are split into finer filaments by crimping, twisting, cutting, or nipping with a pinned roller. Fibrillation provides pliable, multifilament yarns with a more open structure that are easier to weave.

Woven geotextiles are made of monofilament, multifilament, or fibrillated yarns or of slit film tapes. This category of geotextiles is manufactured similarly to cloth or other textiles, using traditional weaving techniques. In nonwoven geotextile manufacturing, the polymeric fibers or filaments are continuously extruded and spun, blown or otherwise, placed onto a moving conveyor belt. The mass of fibers or filaments are then either needlepunched or heat bonded. Needle-punch is the process of mechanically entangling the fibers or filaments using a series of small needles. Heat bonding is the process in which individual fibers or filaments are welded together by heat and pressure at contact points to create a nonwoven mass.

Overlapping of the geotextiles in the strong axis direction is not permitted. The use of sewn seams may be permitted in the strong axis direction; however, the strength of the geotextile will be reduced to the strength of the sewn seam. The sewn seam strength (whether field or factory sewn) shall be at least 25 percent of  $T_{ult}$  (ASTM D4884 – *Standard Test Method for Strength of Sewn or Bonded Seams of Geotextiles*). Prior to using sewn seams obtain written permission

from the PC/GDS. For sewn seams use thread that consists of either polypropylene or polyester polymers and which has a strength matching the strength of the geotextile being seamed. Do not use nylon thread. Use thread that is of contrasting color to that of the geotextile itself. Use a double row of double-thread chain stitch, Type 401 as defined by ASTM D6193 – *Standard Practice for Stitches and Seams* (see Figure 20-2). Use 150 to 400 stitches per yard depending on the weight of the geotextile. The GEOR should consult with a geotextile manufacturer or supplier to determine the appropriate stitch density. Use either a “butterfly” seam (Type SSd) or “J” seam (Type SSn) as defined in ASTM D6193 (see Figure 20-3). Geotextiles may be overlapped in the weak axis direction. The minimum overlap shall be 12 inches. If a sewn seam is allowed in the strong axis direction, the GEOR is reminded that the location of the sewn seam, the type of thread, the color contrast of the thread, the type and density of stitching, and the seam type shall be shown on the plans. In addition, the sewn seam should be easily visible during construction (see Figure 20-4) and the placement of the seam should be indicated on the plans. The seam should not be placed as indicated in Figure 20-5. Further, the plans should also include a requirement for the Contractor to provide the results of sewn seam testing.

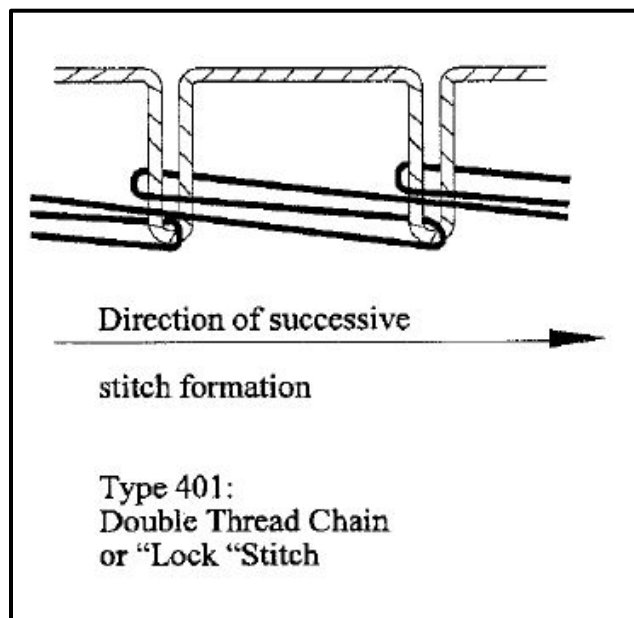


Figure 20-2, Stitch Type  
(Holtz, et al. (2008))

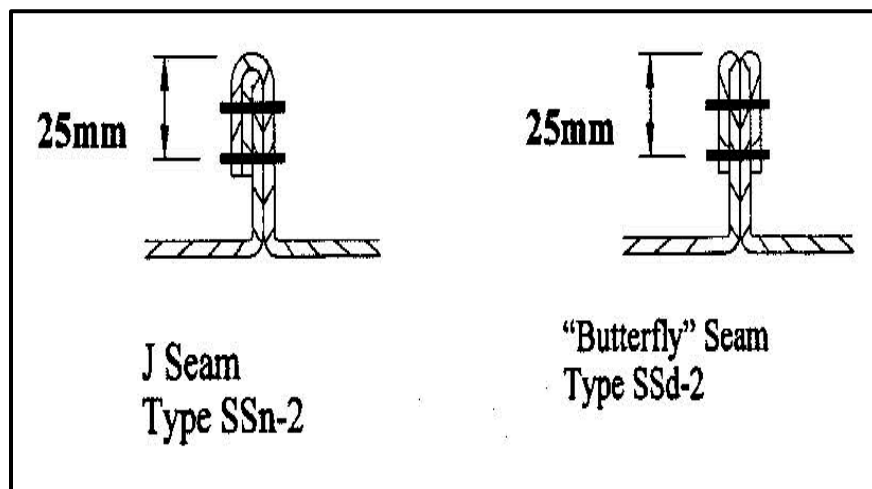
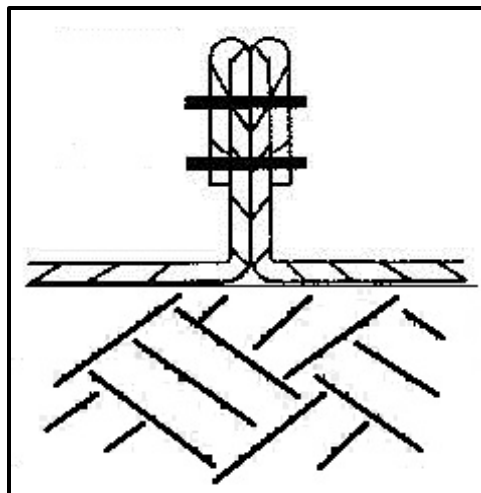
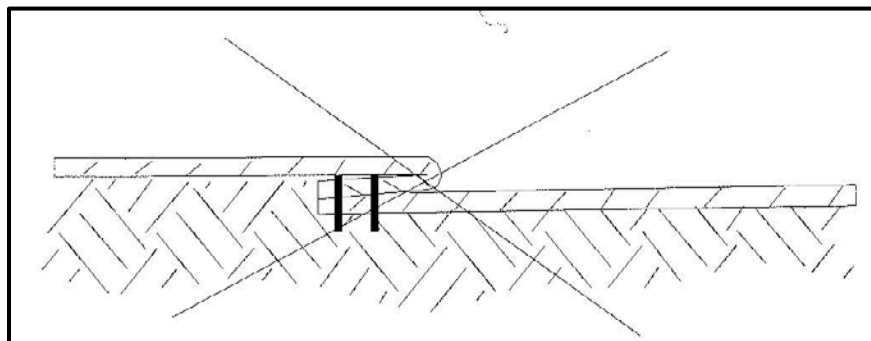


Figure 20-3, Seam Type  
(Holtz, et al. (2008))





**Figure 20-4, Proper Seam Placement**  
(Holtz, et al. (2008))



**Figure 20-5, Improper Seam Placement**  
(Holtz, et al. (2008))

### 20.3 GEOGRIDS

Geogrids are formed by a regular network of tensile elements with openings of sufficient size to allow interlock with the surrounding fill materials. The primary purpose of geogrids is reinforcement. Geogrids can be manufactured in 3 ways: extrusion, knitting or weaving, and welding. Extruded geogrids, also called integral geogrids, are manufactured with integral junctions by extruding and orienting polymeric (polyethylene or polypropylene) materials. Geogrids may also be manufactured of multifilament polyester yarns, joined at the crossover points by knitting or weaving processes and then encased with a polymer-based, plasticized coating. Welded geogrids are manufactured by welding polymeric strips together at the crossover points. All of these manufacturing techniques allow geogrids to be oriented such that the principal strength is in a single direction (uniaxial geogrids) or in both directions (biaxial geogrids). In biaxial geogrids, the strength is typically not the same in both directions.

Overlapping of geogrids in the strong axis direction is not permitted. The use of a mechanical connection (i.e., a bodkin connector (see Figure 20-6)) will be permitted, provided the strength of the connection is equal to the required geogrid strength or if reduced geogrid strength equal to the connection is used. Prior to using a mechanical connection obtain written permission from the PC/GDS. Geogrids may be overlapped in the transverse (i.e., perpendicular to the slope face) direction. The minimum overlap shall be 12 inches. If a mechanical connection is allowed in the strong axis direction, the GEOR is reminded that the location, type and material for the connection, shall be shown on the plans. In addition, the plans should also include a requirement for the Contractor to provide the results of testing of the mechanical connection.

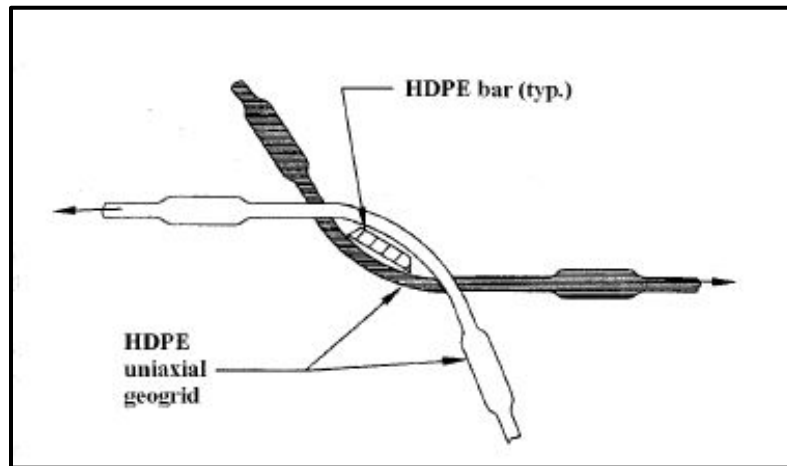


**Figure 20-6, Geogrid Mechanical Connection  
(Holtz, et al. (2008))**

## 20.4 GEOMEMBRANES

Geomembranes, unlike geotextiles and geogrids, are manufactured with a single, solid sheet of geosynthetic material. Geomembranes are used as either a low-permeability or impermeable boundary to prevent the movement of fluids (either liquid or gas). The primary use of geomembranes is in the design and construction of landfills; however, geomembranes have selected uses on transportation projects, such as being used as an impermeable barrier above structural backfill behind an ERS or above lightweight EPS materials (see Figure 20-7). Because there are limited requirements for the use of geomembranes in transportation projects, geomembranes will not be discussed in the remainder of this Chapter.

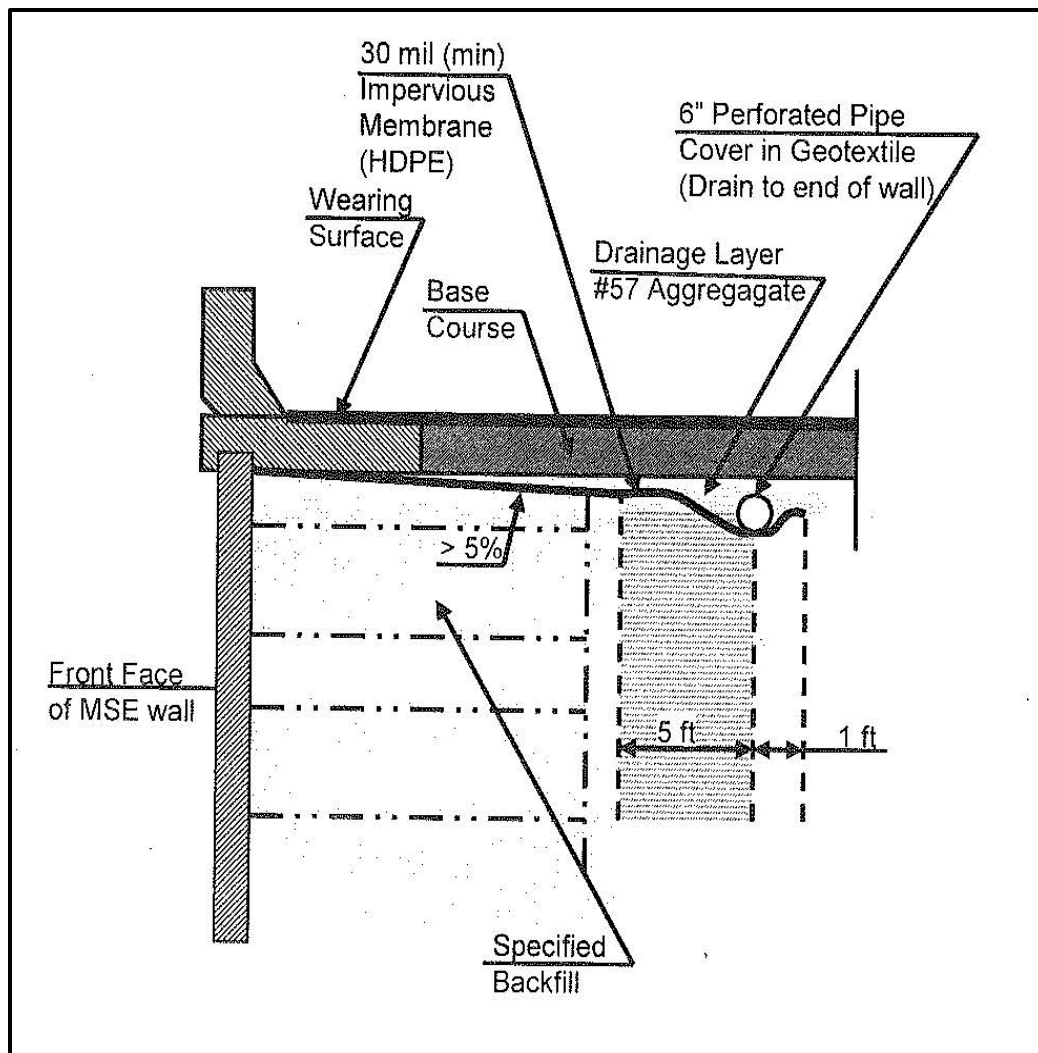


Figure 20-7, Geomembrane Use Above ERS  
(Tanyu, Sabatini, and Berg (2008))

## 20.5 GEOCOMPOSITES

Geocomposites are the combination of 2 or more geosynthetic materials combined together, such as geotextiles and geogrids. Most geocomposites are used in either drainage applications or waste-containment. Prefabricated vertical drains (PVDs) are an example of geocomposites. Included in geocomposites are the 3-dimensional polymeric cell structures.

## 20.6 FUNCTIONS AND APPLICATIONS

Geosynthetics have 6 primary functions as listed below:

- Filtration
- Drainage
- Separation
- Reinforcement
- Fluid Barrier
- Protection

### 20.6.1 Filtration

Geotextiles (woven and nonwoven) are used as filters to prevent soils from migrating into drainage aggregate or pipes, while maintaining water flow through the system. These materials are also used below riprap and other armor materials to prevent erosion of the soils from the stream bank. For a geotextile to function as a filter, the Apparent Opening Size (AOS) must be smaller than the smallest size particle to be retained and still allow for the flow of water through the geotextile material. To provide good filtration, a geotextile should meet the criteria provided in the following equation.

$$AOS \leq B * D_{85(soil)} \quad \text{Equation 20-1}$$

Where,

AOS = Apparent Opening Size (see Chapter 2), millimeter (mm)

$D_{85(soil)}$  = Diameter of soil particle for which 85 percent are smaller, mm

B = Dimensionless coefficient related to  $C_u$

For Sand-Like soils B, for both woven and nonwoven geotextiles, is determined from the following equations.

For  $C_u \leq 2$  or  $C_u \geq 8$ , then

$$B = 1.0 \quad \text{Equation 20-2}$$

For  $2 \leq C_u \leq 4$ , then

$$B = 0.5C_u \quad \text{Equation 20-3}$$

For  $4 \leq C_u \leq 8$ , then

$$B = \frac{8}{C_u} \quad \text{Equation 20-4}$$

For Clay-Like soils, B is a function of the type of geotextile.

Woven geotextiles

$$B = 1.0 \quad \text{Equation 20-5}$$

Nonwoven geotextiles

$$B = 1.8 \quad \text{Equation 20-6}$$

In addition to the AOS, the permeability and permittivity of the geotextile requires consideration. The selection of the correct filter is based on the critical/severe nature of the project. The criteria for critical/severe projects are provided in the following table.

**Table 20-2, Guidelines for Evaluating Critical/Severe Nature**  
(adopted from Holtz, et al. (2008))

<b>A. Critical Nature of Project</b>		
<b>Item</b>	<b>Critical</b>	<b>Less Critical</b>
Risk of loss of life and/or structural damage due to drain failure	High	None
Repair cost versus installation costs of drain	>>>	= or <
Evidence of drain clogging before potential catastrophic failure	None	Yes
<b>B. Severity of Conditions</b>		
<b>Item</b>	<b>Severe</b>	<b>Less Severe</b>
Soil to be drained	Gap-graded, pipable, or dispersible	Well-graded or uniform
Hydraulic gradient	High	Low
Flow conditions	Dynamic, cyclic, or pulsating	Steady state

For less critical applications and less severe conditions,

$$k_{geotextile} \geq k_{soil} \quad \text{Equation 20-7}$$

For critical applications and severe conditions,

$$k_{geotextile} \geq 10k_{soil} \quad \text{Equation 20-8}$$

Where,

$k_{geotextile}$  = Coefficient of permeability of geotextile

$k_{soil}$  = Coefficient of permeability of soil

Permittivity is the coefficient of permeability normal to the plane of the geotextile divided by the thickness of the geotextile material (see Figure 20-8)

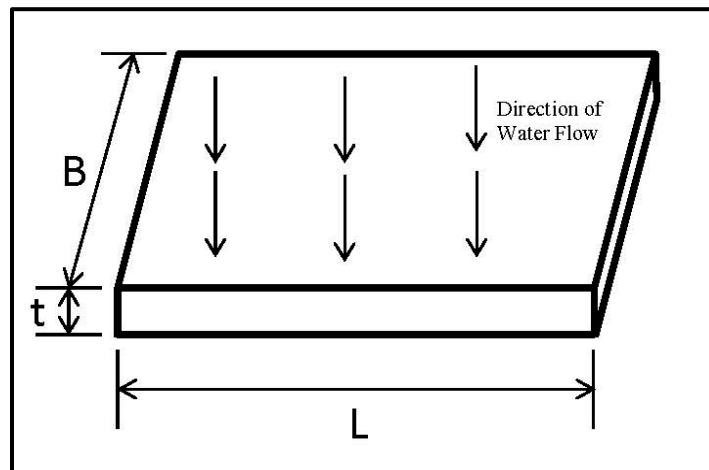


**Figure 20-8, Permittivity**

$$Q_n = \Psi * \Delta h * A_n \quad \text{Equation 20-9}$$

$$\Psi = \frac{k_n}{t} \quad \text{Equation 20-10}$$

$$A_n = L * B \quad \text{Equation 20-11}$$

Where,

- $Q_n$  = Normal volumetric flow
- $\Delta h$  = Head causing flow
- $k_n$  = Coefficient of permeability normal to geotextile
- $t$  = Thickness of geotextile
- $\Psi$  = Permittivity of geotextile
- $L$  = Length of geotextile
- $B$  = Width of geotextile

The permittivity requirements depend on the fines content of the soil to be filtered. The more fines in the soil, the greater the permittivity required. The following table contains approximate fines content and recommended permittivity requirements based on previous experience.

**Table 20-3, Permittivity Requirements  
(adopted from Holtz, et al. (2008))**

Percent Passing No. 200 Sieve	$\Psi$ ( $\text{sec}^{-1}$ )
< 15	$\geq 0.5$
15 – 50	$\geq 0.2$
> 50	$\geq 0.1$

### 20.6.2 Drainage

Nonwoven needlepunched geotextiles and geocomposites can also provide drainage by allowing water to drain from or through low permeability soils. The primary application of the use of geotextiles for drainage is in dissipation of excess pore pressures. In some cases, the nonwoven geotextile is thick and will allow the flow of water through geotextile material itself. This flow of water through (within) the geotextile material is called transmissivity. Transmissivity is the product of the permeability of the geotextile for in plane water flow and the thickness of the geotextile (see figure below).

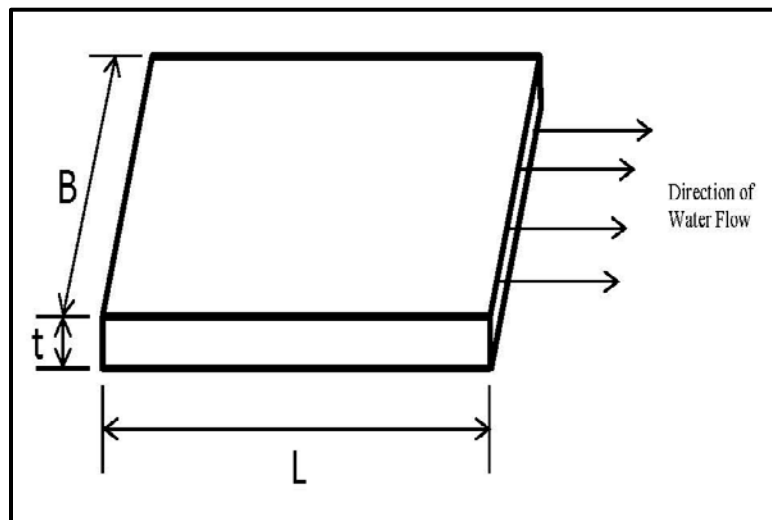


**Figure 20-9, Transmissivity**

$$Q_p = \Theta * i * B \quad \text{Equation 20-12}$$

$$\Theta = k_p * t \quad \text{Equation 20-13}$$

$$i = \frac{\Delta h}{L} \quad \text{Equation 20-14}$$

Where,

$Q_p$  = In-plane volumetric flow

$\Delta h$  = Head causing flow

$i$  = Hydraulic gradient

$k_p$  = Coefficient of permeability in plane to geotextile

$t$  = Thickness of geotextile

$\Theta$  = Transmissivity of geotextile

$L$  = Length of geotextile

$B$  = Width of geotextile

### 20.6.3 Separators

Geosynthetic materials, primarily geotextiles, are used to prevent the migration of fines from subgrade soils into granular bases. The AOS of the geotextile should be sized to prevent the migration of fines. In addition, geogrids may also be used as a separator to prevent the migration of granular materials (aggregate) into fine-grained, soft subgrade soils (see Figure 20-10). However, this application will not prevent the migration of fines from the subgrade soil into the aggregate. The separator materials to be used shall meet the criteria provided in the latest version of the STS for *Geosynthetic Materials for Separation and Stabilization*, SC-M-203-1.

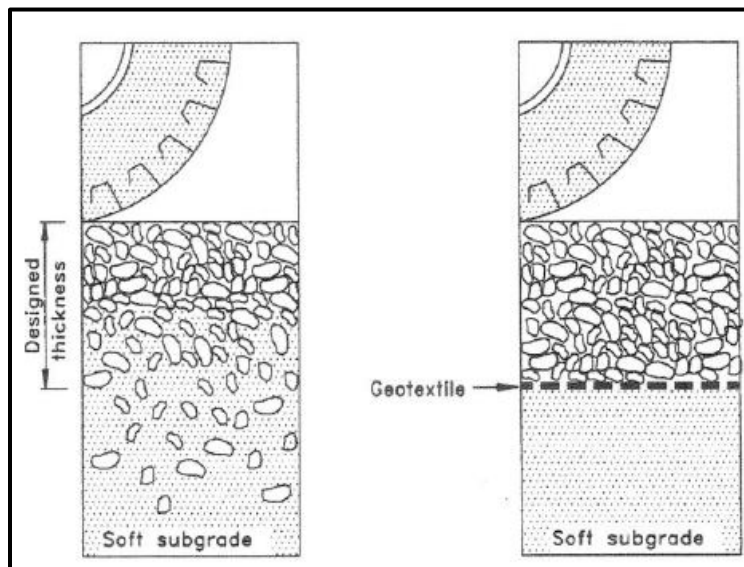


**Figure 20-10, Geogrid Soil Separator  
(Holtz, et al. (2008))**

### 20.6.4 Reinforcement

Both geotextiles and geogrids are used as reinforcement. These materials add tensile strength to a soil matrix, thus providing a more competent and stable material. Reinforcement enables embankments to be constructed over very soft foundation soils (see Chapter 17) and permits the construction of steep slopes and ERs (see Chapters 17 and 18 and Appendices C and D).

The reinforcement materials to be used shall meet the criteria provided in the latest version of the STSs for *Geogrid Soil Reinforcement*, SC-M-203-2 or *Geotextile Soil Reinforcement*, SC-M-203-3.

Geosynthetic materials used for stabilization shall meet the criteria provided in the latest version of the STS for *Geosynthetic Materials for Separation and Stabilization*, SC-M-203-1. Geosynthetic stabilization is a subset of reinforcement and is used to stabilize a subgrade to allow construction to proceed. The geosynthetic stabilization materials are not included in slope stability analysis; however, geosynthetic reinforcement materials are included in slope stability analysis.

### **20.6.5 Fluid Barriers**

Geomembranes, geotextile composites, and geosynthetic clay liners are used as fluid barriers to impede the flow of a liquid or a gas from 1 location to another. As indicated previously, fluid barriers (geomembranes) are used in lightweight (EPS) fill applications for transportation projects. Fluid barriers have limited applications in transportation projects; therefore, there will be no detailed discussion of fluid barriers. If a fluid barrier is required, please refer to Holtz, et al. (2008) for additional details.

### **20.6.6 Protection**

Geosynthetics provide protection by providing a stress relief layer. Temporary geosynthetic blankets and permanent geosynthetic mats are placed over the soil to reduce erosion caused by rainfall impact and water flow shear stress. Geosynthetics are also used to retard the development of reflection cracks in pavement overlays.

### **20.6.7 Secondary Applications**

The previous Sections indicated the various primary functions of geosynthetics; however, geosynthetics can provide several secondary functions while providing the primary function. Provided in Table 20-4 are the primary function and some of the secondary functions. According to Holtz, et al. (2008),

Design for the compaction improvement applications is simple. Place a *geosynthetic reinforcement* that will survive construction at every lift or every other lift in a continuous plane along the edge of the slopes. Only narrow strips, about 4 to 6 *feet* in width, at 2 to 20 *inches* vertical spacing are required. No reinforcement design is required if the overall slope is found to be safe without reinforcement.



**Table 20-4, Primary and Secondary Functions  
(adopted from Holtz, et al. (2008))**

Primary Function	Secondary Function	Selected Applications <sup>1</sup>
Filtration	Separation, drainage, protection, reinforcement, stabilization	Trench drains, pipe wrapping, base course drains
Drainage	Separation, filtration	Retaining walls, vertical and horizontal drains
Separation	Filtration, drainage, reinforcement	Working platforms, embankment construction
Reinforcement	Filtration, drainage, separation, stabilization	Base reinforcement, fill reinforcement, load redistribution
Fluid Barrier	Protection	Asphalt overlays <sup>2</sup>
Protection	Reinforcement, fluid barrier	Permanent and temporary erosion control

<sup>1</sup>More applications are possible; this is not a complete list

<sup>2</sup>Not currently allowed by SCDOT, presented here only for information

## 20.7 DESIGN APPROACH

Holtz, et al. (2008) recommends the following design procedure for geosynthetics:

1. Define the purpose and establish the scope of the project.
2. Investigate and establish the geotechnical conditions at the site (geology, subsurface exploration, laboratory and field testing, etc.)
3. Establish application criticality, severity, and performance criteria. Determine external factors that may influence geosynthetic performance.
4. Formulate trial designs and compare several alternatives.
5. Establish the models to be analyzed, determine the parameters, and carry out the analysis.
6. Compare results and select the most appropriate design; consider alternatives versus cost, construction feasibility, etc. Modify design if necessary.
7. Prepare detailed plans and specifications including:
  - a) specific property requirements for the geosynthetic;
  - b) detailed installation procedures.
8. Hold preconstruction meeting with contractor and inspectors.
9. Approve geosynthetic on the basis of specimens' laboratory test results and/or manufacturer's certification.
10. Monitor construction.
11. Inspect after major events (e.g., 100-year rainfall or an earthquake) that may compromise system performance.

## 20.8 EVALUATION OF PROPERTIES

The required geosynthetic design properties depend on the specific application and associated function the geosynthetic is to provide. Table 20-5 provides a list of properties that cover the range of important criteria that are required to evaluate a geosynthetic for most applications. It should be noted that not all of the listed requirements will be necessary for all applications. Typically 6 to 8 properties are required for a specific application. The properties required for mechanical or hydraulic design are different from those required for constructability (survivability) and durability. Table 20-6 provides typical SCDOT applications along with the associated function. Tables 20-4, 20-5 and 20-6 should be used in conjunction to determine the

appropriate properties for each application. All geosynthetic material properties can be placed into 3 basic categories: general, index, and performance. General properties are usually provided by the manufacturer or distributor or from publically available literature. Index properties were originally developed by manufacturers for quality control purposes and only provide an indication or qualitative assessment of the property of interest. Performance tests are an attempt to model the soil-geosynthetic interaction and, therefore, require the geosynthetic to be tested together with on-site soils. This type of testing provides a direct measure of specific properties of interest.

**Table 20-5, Important Criteria and Principal Properties  
(adopted from Holtz, et al. (2008))**

Criteria and Parameter	Property <sup>1</sup>	Function					
		Filtration	Drainage	Separation	Reinforcement	Fluid Barrier	Protection
<u>Design Requirements:</u>							
<i>Mechanical Strength</i>							
Tensile Strength	Wide Width Strength	-	-	-	✓	✓	-
Tensile Modulus	Wide Width Modulus	-	-	-	✓	✓	-
Seam Strength	Wide Width Strength	-	-	-	✓	✓	-
Tension Creep	Creep Resistance	-	-	-	✓	✓	-
Compression Creep	Creep Resistance	-	✓ <sup>2</sup>	-	-	-	-
Soil-Geosynthetic Friction	Shear Strength	-	-	-	✓	✓	✓
<i>Hydraulic</i>							
Flow Capacity	Permeability	✓	✓	✓	✓	✓	-
	Transmissivity	-	✓	-	-	-	✓
Piping Resistance	AOS	✓	-	✓	✓	-	✓
	Porimetry	✓	-	-	-	-	✓
Clogging Resistance	Gradient Ratio or Long-Term Flow	✓	-	-	-	-	✓
<u>Constructability Requirements:</u>							
Tensile Strength	Grab Strength	✓	✓	✓	✓	✓	✓
Seam Strength	Grab Strength	✓	✓	✓	-	✓	-
Bursting Resistance	Burst Strength	✓	✓	✓	✓	✓	✓
Puncture Resistance	Rod or Pyramid Puncture	✓	✓	✓	✓	✓	✓
Tear Resistance	Trapezoidal Tear	✓	✓	✓	✓	✓	✓
<u>Durability:</u>							
Abrasion Resistance <sup>3</sup>	Reciprocating Block Abrasion	✓	-	-	-	-	-
UV Stability <sup>4</sup>	UV Resistance	✓	-	-	✓	✓	✓
	Chemical	✓	✓	?	✓	✓	?
Soil Environment <sup>5</sup>	Biological	✓	✓	?	✓	✓	?
	Wet-Dry	✓	✓	-	-	-	✓
	Freeze-Thaw	✓	✓	-	-	✓	-
Notes:							
1. See Table 1-4 of Holtz, et al. (2008) for specific procedures.							
2. Compression creep is applicable to some geocomposites.							
3. Erosion control applications where armor stone may move.							
4. Exposed geosynthetics only.							
5. Where required.							

**Table 20-6, Evaluation of Geosynthetic Property Requirements  
(adopted from Holtz, et al. (2008))**

Application	Function			
	Filtration	Drainage	Separation	Reinforcement
Subsurface Drainage	☑		✓	
Prefabricated Drains	✓	☑	✓	
Hard Armor Erosion Control			✓	
Silt Fence			✓	
Subgrade Separation	✓		☑	
Subgrade Stabilization	☑	✓	☑	✓
Base/Subbase Reinforcement			✓	☑
Embankments over Soft Subgrade	☑	✓	✓	☑
Reinforced Slopes		✓		☑
Reinforced Soil Walls	☑			
✓ indicates Primary Function				
☑ indicates Secondary Function				

## 20.9 REFERENCES

ASTM International, (2014), Annual Book of ASTM Standards, Section 4 – Construction, Volume 04.13 – Geosynthetics.

Holtz, R. D., Christopher, B. R., and Berg, R.R., (2008), Geosynthetic Design and Construction Guidelines, (FHWA NHI-07-092), U.S. Department of Transportation, National Highway Institute, Federal Highway Administration, Washington D.C.

Tanyu, B. F., Sabatini, P. J., and Berg, R. R., (2008), Earth Retaining Structures, (Publication No. FHWA-NHI-07-071), U.S. Department of Transportation, National Highway Institute, Federal Highway Administration, Washington D.C.

**Chapter 21**  
**GEOTECHNICAL REPORTS**

**GEOTECHNICAL DESIGN MANUAL**

*January 2019*



**Table of Contents**

<b><u>Section</u></b>		<b><u>Page</u></b>
21.1	Introduction.....	21-1
21.2	Geotechnical Information Reports.....	21-1
	21.2.1 Geotechnical Subsurface Data Report .....	21-1
	21.2.2 Geotechnical Base Line Report.....	21-2
21.3	Bridge Geotechnical Engineering Reports .....	21-2
	21.3.1 Preliminary Bridge Geotechnical Engineering Report (PBGER) .....	21-2
	21.3.2 Final Bridge Geotechnical Engineering Report (BGER).....	21-4
21.4	Roadway Geotechnical Engineering Reports.....	21-9
	21.4.1 Preliminary Roadway Geotechnical Engineering Report (PRGER).....	21-9
	21.4.2 Final Roadway Geotechnical Engineering Report (RGER).....	21-10
21.5	Site-Specific Seismic Response Analysis Report.....	21-12
21.6	Submission Requirements .....	21-13

**List of Tables**

<b><u>Table</u></b>	<b><u>Page</u></b>
Table 21-1, Soil Testing Location Table .....	21-5
Table 21-2, Laboratory Testing Table.....	21-5
Table 21-3, Soil Stratification Table.....	21-5
Table 21-4, Footing Resistance.....	21-6
Table 21-5, Pile Resistance.....	21-7
Table 21-6, Drilled Shaft Resistance .....	21-7
Table 21-7, Governing Conditions .....	21-7
Table 21-8, Drivability Analysis .....	21-8
Table 21-9, Temporary Shoring Wall Soil Design Parameters .....	21-8
Table 21-10, Fill Material Properties Table .....	21-11
Table 21-11, Temporary Shoring Wall Soil Design Parameters .....	21-11
Table 21-12, One-Dimensional Soil Column Model .....	21-13

# CHAPTER 21

## GEOTECHNICAL REPORTS

### 21.1 INTRODUCTION

This Chapter presents the requirements for the preparation of geotechnical reports that will be used to design projects both by and for SCDOT. Geotechnical reports are prepared to convey information concerning subsurface conditions, foundations and construction considerations (plan notes) to other members of the project team. SCDOT uses 5 basic types of reports to convey geotechnical and site-specific seismic response information.

- Geotechnical Subsurface Data Report
- Geotechnical Base Line Report
- Preliminary Geotechnical Engineering Report
- Final Geotechnical Engineering Report
- Site-Specific Seismic Response Analysis Report

The Geotechnical Subsurface Data Report (GSDR) is used to convey geotechnical information on traditional (design-bid-build (DBB)) projects. The Geotechnical Base Line Report (GBLR) is primarily issued in conjunction with Design/Build (D/B) projects. Typically a bridge replacement project will have both Bridge and Roadway Geotechnical Engineering Reports (Preliminary and Final) prepared. However, some bridge replacement projects may not require a Roadway Geotechnical Engineering Report (RGER), while some road projects may not require a Bridge Geotechnical Engineering Report (BGER). The PC/GDS should be contacted if there is a question concerning whether a report (Roadway or Bridge) is required. Typically, Preliminary Bridge and Roadway Geotechnical Engineering Reports (PBGER and PRGER, respectively) will be issued for the project prior to the Design Field Review (DFR). Final Bridge and Roadway Geotechnical Engineering Reports (BGER and RGER, respectively) are issued at the completion of final field operations and generally after the DFR. In some circumstances a Site-Specific Seismic Response Analysis Report (Site-Specific) is prepared to provide an in-depth discussion of the seismic response of a specific site. The following Sections discuss each of the types of reports used by SCDOT.

### 21.2 GEOTECHNICAL INFORMATION REPORTS

#### 21.2.1 Geotechnical Subsurface Data Report

The GSDR is used to convey only factual geotechnical subsurface information to the SEOR as well as for use by a contractor and is typically used with traditional DBB projects. A GSDR does not provide any engineering analysis (preliminary or final). Engineering interpretation in the GSDR shall be limited to the determination, by the GEOR, and placement of geologic formation names on the soil test boring records. In addition, subsurface profiles may be included in the GSDR. These subsurface profiles may contain stratigraphic lines, provided the lines have been developed by the GEOR. If stratigraphic lines are included with the profile, a statement indicating that the lines are the interpretation of the GEOR should be included. However for GSDRs used on D/B projects neither the geologic formation names nor the stratigraphic lines on the subsurface profile shall be provided. A GSDR shall include an introduction, a project description and any procedural variations from the field or laboratory testing methods as described in this Manual. The Appendices should at a minimum contain project and testing location plans, the completed GeoScoping form (also called a Site Reconnaissance form), field



exploration records (soil test boring logs, cone penetrometer and dilatometer records, etc.), and the results of all laboratory testing. Each field exploration record should contain the testing location and should correspond to the testing location plan. The laboratory testing results should indicate the location and depth of each sample clearly on the test result. In addition, all laboratory testing results should be presented in a tabularized format as a summary prior to the results of individual testing being presented. All field and laboratory testing records shall conform to the requirements of this Manual. A draft GSDR will be submitted to the Department for review. Upon completion of review and editing the final GSDR will be submitted in accordance with the submission requirements of this Chapter.

### **21.2.2 Geotechnical Base Line Report**

The GBLR is used to provide limited (preliminary) geotechnical information on a D/B project, thus permitting the contractor to bid on the project with a certain degree of knowledge and acceptable risk. A GBLR provides limited engineering interpretations or very preliminary engineering recommendations. The GBLR should be used in conjunction with project specific D/B criteria. The GBLR should contain at a minimum an introduction, project description, objective and scope of the geotechnical exploration and general recommendations concerning foundations and/or ground improvement requirements. In addition, the GBLR should include the final ADRS curve to be used on the project if possible. Further the GBLR should also indicate if soils having the potential for SSL are present on site and if any ground improvement may be required. Any procedural variations from the field testing methods as described in this Manual should be discussed or mentioned. The narrative portion of this type of report is anticipated to be relatively short, with the Appendices of the report being large. The Appendices should at a minimum contain project and testing location plans, the completed GeoScoping form (also called a Site Reconnaissance form), field exploration records (soil test boring logs, cone penetrometer and dilatometer records, etc.), and the results of all laboratory testing. All field and laboratory testing records shall conform to the requirements of this Manual. Each field exploration record should contain the location of the testing and should correspond to the testing location plan. Any guides used to interpret the data should also be included. The laboratory testing results should indicate the location and depth of each sample clearly on the test result. Any procedural variations from the laboratory testing methods described in this Manual should be indicated. A draft GBLR shall be submitted to the Department for review. Upon completion of review and editing the final GBLR should be submitted in accordance with the submission requirements of this Chapter.

## **21.3 BRIDGE GEOTECHNICAL ENGINEERING REPORTS**

The Bridge Geotechnical Engineering Reports provide geotechnical information related specifically to the design of the bridge and shall include a discussion of the foundations and the bridge embankment. The contents of both preliminary (PBGER) and final (BGER) geotechnical engineering reports are described in the following Sections.

### **21.3.1 Preliminary Bridge Geotechnical Engineering Report (PBGER)**

The purpose of the PBGER is to provide the SEOR and the design team with preliminary information that may be used in the preliminary design of the bridge project. Typically, the preliminary report is issued prior to the DFR so that the information can be used during the field review and in development of preliminary bridge plans. The preliminary report should include, at a minimum, the following items:

- a. General Project Information
- b. General Geology
- c. Soils Encountered

- d. Seismic
  - + Acceleration Design Response Spectrum (ADRS)
  - + SSL Results
- e. Bridge Embankment
  - + Preliminary slope stability analysis
  - + Preliminary settlement analysis
  - + Construction Difficulties
  - + Temporary Shoring
- f. Bridge Foundations
  - + Type and Size
  - + Preliminary input files for LPILE
  - + Construction Difficulties
  - + Vibration Monitoring Assessment
  - + Corrosion Potential Results
- g. Geohazards
  - + Mucking requirements
  - + Potential for long waiting periods for settlement
  - + ERS requirements
  - + Karst voids/sink holes
  - + Artesian conditions

Items a through c above should be used to provide a general description of the project and the soils encountered; in depth details are not required. The preliminary seismic information consists of the ADRS curve and the results of SSL analysis. The ADRS and SSL analysis are conducted in accordance with the procedures provided in Chapters 12 and 13. The ADRS may be either preliminary or final depending on the number of testing locations, depth of testing and type of geotechnical exploration. The design seismic event for bridges is based on the classification of the bridge. Typically the SEE is the primary design seismic event for most bridges in South Carolina. However, certain classifications of bridges require both the SEE and the FEE as the design seismic event (refer to the Seismic Specs). The SSL analysis will be based on the available ADRS curve, design seismic event and the available soil information.

Preliminary slope stability analysis of the end slopes at the bridge location is based on the slopes indicated on the preliminary bridge plans. The preliminary stability analysis is performed in accordance with the procedures outlined in Chapter 17. The purpose of this analysis is to determine if the designed embankment slope will achieve the required stability or if a flatter slope or reinforcement is required. A flatter slope may cause the bridge to become longer. The settlement analysis should provide an indication of the amount and time anticipated for settlement to occur, because these factors may have an impact on the construction of the project. Further any settlement located at the end slopes will induce downdrag on the end bent piles. The results of the preliminary settlement analysis and any impacts to the bridge should be discussed in the PBGER. Any potential construction difficulties, such as mucking/undercutting, should be identified and preliminarily discussed in the PBGER. In addition, the impact of the preliminary SSL analysis shall be discussed including any impacts to the bridge foundation system including but not limited to downdrag, slope instability, the requirement for ground improvement to mitigate SSL, etc.

The bridge foundations provided in the preliminary report are limited to type and size. Actual capacity determinations are not made until the completion of all field work. If there are limitations in the foundation type, the limitations should be defined as part of the preliminary report; therefore, aiding the SEOR and the design team in the final selection of foundations. The preliminary LPILE input files should be a first estimate based on the results of the preliminary subsurface exploration. The preliminary LPILE input files may require revision based on the results of the final exploration. Any potential construction difficulties, such as

anticipated hard driving or the requirement for ground improvement, should be reported. In addition, a preliminary evaluation of the potential need for vibration monitoring should be reported. The corrosion potential of soils, groundwater and surface water, as applicable, should also be provided in the PBGER for use by the SEOR.

The PBGER shall also include a preliminary discussion of potential construction issues, which include, but are not limited to, mucking requirements, anticipated waiting periods to allow for settlement to occur and if ERSs (temporary or permanent) should be anticipated. The mucking requirements should identify the need for mucking and an approximate area and depth. The mucking requirements may be based on visual observation of the project site.

The Appendix should include the results of field testing related to the bridge, any laboratory work, and the ADRS curve. In addition, a field testing location plan and the completed GeoScoping form (also called a Site Reconnaissance form) should be provided. In addition, the results from preliminary SSL and slope stability analyses shall also be provided. For in-house projects, the locations of field tests are typically presented on the Bridge Plan and Profile sheet. In addition, during the preparation of the PBGER, results of hydrometer and grain-size tests are forwarded to the PC/HDS for use in scour studies for the bridge project.

### **21.3.2 Final Bridge Geotechnical Engineering Report (BGER)**

The BGER is produced after completion of all field work and receipt of loading information from the SEOR (see GDF 001 in Appendix A). The BGER should contain detailed information about the project. This report will be used by the project design team to develop the final design for the bridge project.

The BGER should include a detailed description of the project to include bridge length, structure type, foundation type and size proposed by the SEOR and loading information. In addition to the bridge information, information describing the bridge embankments should also be provided including slope height, the length of the bridge embankment and approximate slope angle. Included with the project information should also be a discussion of the existing site conditions at the time of field work. This description should include items such as surface water, exposed rock, vegetation, etc. This is not meant to be a complete list of items describing the actual site conditions. The report should include any items that, in the opinion of the GEOR may affect design or construction. The field and laboratory testing procedures should also be discussed, but this discussion should be limited to deviations from the standard test methods (see Chapter 5). In addition, any non-standard testing procedures shall be discussed. Additionally, any corrections to in-situ testing should also be discussed as well as the results of any calibrations to the field testing equipment. The location of each testing location should also be indicated (see Table 21-1) as well as the type and number of laboratory tests (see Table 21-2). Testing procedures for non-standard tests should be included in the Appendix of the report.

**Table 21-1, Soil Testing Location Table**

Test Number	Test Hole Local	Station*	Offset*	Elevation (msl)	Depth (ft)
STB-1	Road	24+99.94	16.84-R	7.24	30
STB-2	Road/Bridge	26+25.52	21.41-R	8.29	80
STB-3	Road	27+27.36	29.23-R	7.07	30
HA-1	Road	23+50.60	17.36-R	6.88	7
HA-2	Road	24+50.18	24.28-R	4.60	1.5
HA-3	Road	25+45.66	23.52-R	9.68	7
HA-4	Road	26+68.55	25.96-R	6.85	7
SCPT-1	Road/Bridge	25+45.03	14.03-R	9.00	14**
DMT-1	Road/Bridge	26+29.19	12.38-R	8.98	16**
MASW/MAM	Road/Bridge	23+75***	13-R***		210

\*Indicate where station and offset are measured from (i.e., existing centerline, proposed centerline, etc.)

\*\*Depth of refusal.

\*\*\*Array centered at this station and offset.

**Table 21-2, Laboratory Testing Table**

Test Type	Quantity
Atterberg Limits	15
Full Sieve Analysis	15
Moisture Content	15
Organic Loss	3
Laboratory Compaction	1
Consolidation	1
Direct Shear	1
Triaxial	1
Corrosion Series	2

The next section of the BGER should consist of discussions of the area geology as it pertains to the overall project, followed by a specific discussion of the soils located at the project site. The overall geologic discussion should include geologic stratigraphic province (see Chapter 11) and geologic formations that will affect the design of the bridge foundations. This discussion should be followed by a detailed discussion of the soils encountered along the bridge alignment including the bridge embankment. The subsurface conditions should be described as to the type of soil; thickness; and strength of each soil layer as represented by the field work (see Table 21-3). The soil type should be defined based on the field work as corrected with laboratory testing results. Soils that will behave mechanically similarly should be grouped together as a subsurface unit. The thickness may be based on the depth below existing grade or based on elevation. The use of elevations is the preferable way of indicating soil thickness. The soil strength may be represented as blow count or other measured indices from the field testing.

**Table 21-3, Soil Stratification Table**

Geologic Formation	Elevation of Top of Layer (ft msl)	Depth to Top of Layer (ft)	USCS Soil Type	SPT-N Values (bpf)	Average CPT Tip Resistance (tsf)	Average DMT $p_1$ Pressure (tsf)	Comments
Fill	+20	0	SM	3 to 6	73.9	3.8	Existing embankment
Holocene Sediment	+14	6	SM	0 to 1	22.4	3.2	Original ground surface
Cooper	+10	10	SM/ML	12 to 25	138.5	43.7	

After detailing the project information, site conditions and subsurface conditions, the next section of the BGER is the seismic design section. The seismic design section should detail the effects of the design seismic event (see Chapter 12) on the proposed bridge project. A final ADRS should be developed based on the subsurface conditions encountered. The final ADRS will be developed in accordance with Chapter 12. If SSL is indicated during the preliminary investigation, a more detailed SSL analysis is required. The SSL analysis will be conducted in accordance with Chapter 13. The detailed SSL analysis should include the extent, both horizontally and vertically, and determination of the amount of induced potential settlement. The potential settlement is accounted for in the determination of downdrag load on interior bent foundations. End bent foundations have more considerations than just downdrag of the fill materials. The stability of the bridge embankment shall be determined and discussed. The effect of the stability of the bridge embankment and its effect on the lateral stability of the end bent piles must also be addressed. Both the lateral and vertical stability of the bridge embankment will be addressed in this report along with the effects of the stability on the end bent foundations.

After discussing the geology and seismicity of the project, the next sections of the BGER should address the bridge embankments and any ERSs if present. The results of the stability analyses performed in accordance with Chapters 17 and 18 are discussed. The discussion should include both the static (Service limit state) and seismic (EE I limit state) performance of the bridge embankment and any ERSs. The results of the analysis should be compared to the performance criteria contained in Chapter 10. If the criteria are exceeded, then site remediation will be required (see Chapter 19). Further discuss the impacts of the movements induced by the EE I limit state on the bridge. In addition, this section of the report should provide the results of settlement analysis (see Chapter 17). The effects of the settlement should be explained and any measures required to decrease the time for settlement to occur should be provided.

After discussing the bridge embankments, the next sections of the BGER should address the foundations required to support the structure. The foundation section should include a discussion of resistance factors, including not only the resistance factors, but also how the factors were selected. Both the factored design load and nominal capacities should be provided (see Tables 21-4, 21-5 and 21-6). The notes below Tables 21-5 and 21-6 are not to be included in the BGER. The type of foundation (shallow footings, piles or drilled shafts) should be provided next, along with the size of the foundations. The depth required to achieve the nominal resistance should be provided along with the minimum depth required to achieve lateral stability. Also to be included in this section of the report are any displacements associated with Service or EE I limit state loads. This section of the report shall also indicate which limit state (Strength, Service, Extreme Event I or Extreme Event II) and which stability condition (axial – compression, axial – tension or lateral) governs the selection of foundation size and bearing depth (see Table 21-7).

**Table 21-4, Footing Resistance**

Factored Design Load (includes 3 feet of backfill)	295 kips
Factored Net Bearing Resistance	4.6 ksf
Geotechnical Resistance Factor	0.45
Required Net Nominal Bearing Resistance	10.2 ksf

**Table 21-5, Pile Resistance**

	<b>Strength or Service Limit State<sup>1,2</sup></b>	<b>EE I or EE II Limit State<sup>1,3</sup></b>
Factored Design Load	112 kips <sup>4</sup>	152 kips <sup>4</sup>
Geotechnical Resistance Factor <sup>5</sup>	0.40	1.00
Nominal Resistance	280 kips	152 kips
Resistance from:		
Design Flood Scourable Soils <sup>6</sup>	40 kips	NA
Soils undergoing static downdrag <sup>6</sup>	0 kips	
Resistance from Liquefiable Soils <sup>7</sup>	NA	220 kips
Required Driving Resistance	320 kips	372 kips

<sup>1</sup>Use only 1 column; middle column represents static resistance while last column represents Extreme Event resistance. Use the column that governs driving resistance.

<sup>2</sup>Indicate whether Strength or Service limit state controls resistance

<sup>3</sup>Indicate whether EE I or EE II limit state controls resistance

<sup>4</sup>Factored design loads include DD or DD<sub>SL</sub>. Note that in this example the Strength limit state DD = 0.0 kips

<sup>5</sup>Use appropriate construction control resistance factor

<sup>6</sup>Design flood scour and static downdrag are not included with Extreme Event limit state loading conditions

<sup>7</sup>Full resistance that is developed by soils within the liquefiable zone during pile installation

**Table 21-6, Drilled Shaft Resistance**

	<b>Strength or Service Limit State<sup>1,2</sup></b>	<b>EE I or EE II Limit State<sup>1,3</sup></b>
Factored Design Load	1400 kips <sup>4</sup>	1800 kips <sup>4</sup>
Factored Resistance – Side	1130 kips	1430 kips
Factored Resistance – End	270 kips	370 kips
Geotechnical Resistance Factor – Side <sup>5</sup>	0.50	1.0
Geotechnical Resistance Factor – End <sup>5</sup>	0.50	1.0
Total Nominal Resistance	2800 kips	1800 kips

<sup>1</sup>Use only 1 column; middle column represents static resistance while last column represents Extreme Event resistance, use the column that governs resistance

<sup>2</sup>Indicate whether Strength or Service limit state controls resistance

<sup>3</sup>Indicate whether EE I or EE II limit state controls resistance

<sup>4</sup>Factored design loads include DD or DD<sub>SL</sub>. Note that in this example the Strength limit state DD = 0.0 kips

<sup>5</sup>Use appropriate construction control resistance factor for static and  $\phi_{EQ}$  equal to 1.0 for seismic

**Table 21-7, Governing Conditions**

<b>Limit State</b>	<b>Loading Direction</b>
Strength	Axial – Compression
Service	Axial – Tension
Extreme Event I	Lateral
Extreme Event II <sup>1</sup>	-

<sup>1</sup>Indicate whether EE II is induced by scour, vehicular, or vessel impact

Construction considerations should follow the discussion of the bridge embankment and bridge foundations. This section shall address the installation of the foundation and the confirmation of foundation capacity. For driven piles, this section shall include preliminary wave equation parameters that were used to confirm drivability of the piles. The range of hammer energies should be provided (see Table 21-8). For drilled shafts, any special construction considerations, such as Crosshole Sonic Logging (CSL) tubes, shall be included in this section. If shallow foundations are the recommended foundation type to support the structure, this section shall include the procedures for verifying bearing capacity.

**Table 21-8, Drivability Analysis**

Skin Quake (QS)	0.10 in
Toe Quake (QT)	0.08 in
Skin Damping (SD)	0.20 s/ft
Toe Damping (TD)	0.15 s/ft
% Skin Friction	80%
Distribution Shape No.	1
Resistance Distribution Model	Proportional <sup>1</sup>
Toe No. 2 Quake	0.15 in
Toe No. 2 Damping	0.15 s/ft
End Bearing Fraction (Toe No. 2)	0.95
Pile Penetration	80%
Hammer Energy Range	25 – 60 ft-kips

<sup>1</sup>Resistance Distribution Model options – proportional, constant skin friction, constant end bearing

Included in the construction considerations is a discussion of and requirements for temporary shoring as required for stage construction of either the bridge or the bridge embankment. The discussion should also include which type of shoring is or is not permitted (i.e., temporary MSE walls should not be used in a cut condition). The parameters to be used in temporary shoring design should be provided as indicated in Table 21-9.

**Table 21-9, Temporary Shoring Wall Soil Design Parameters**

Depth <sup>1</sup> (ft)	c (psf)	Phi ( $\phi$ ) (degrees)	Saturated Unit Weight ( $\gamma_{sat}$ ) (pcf)	$K_o$	$K_a$	$K_p$
0-7	-	32	100	0.47	0.31	3.25
7-14	343	-	86	1.0	1.0	1.0
14-19	-	30	109	0.50	0.33	3.0
> 19	550	35	120	0.43	0.27	3.69

<sup>1</sup>Elevation may be substituted for Depth, if Elevation is used include appropriate units

The final section of the report consists of notes that are required to be placed on the plans. The plan notes are project specific but should include foundation capacity tables consisting of factored design loads, nominal resistances, and resistance factors. The required depth to achieve axial or lateral capacity and minimum depth if capacity is achieved prior to required depth shall be provided. This section of the report shall be tailored to the requirements of the specific project and shall provide the information required in Chapter 22. However, in GEC prepared reports, an additional report section is added that consists of any limitations to the report. This section is not required in reports prepared by the PC/GDS.

The Appendix of BGER should include the locations of the soil tests, a subsurface profile and the completed GeoScoping form (also called a Site Reconnaissance form). The soil testing reports should be followed by the report of laboratory testing. Only the testing reports that pertain to the bridge and bridge embankment should be included in the Appendix. The BGER Appendix should include the final ADRS curve and the results of the detailed liquefaction study, if performed. The results of lateral pile analyses should also be included in the Appendix of the report. For projects performed by the PC/GDS, the lateral pile analysis input screens will be provided and the SEOR will perform the actual lateral pile analysis. For GEC prepared reports, the GEC may provide a complete analysis or may provide the input for the analysis depending on the contractual relationship between the GEC and the SEOR. In addition, the Appendix of the BGER shall include any Special Provisions pertaining to geotechnical issues that are required for the project. Included in this section of the Appendix are those Special Provisions

previously prepared by SCDOT as well as any Special Provisions written by the GEC. Contact the PC/GDS to determine which Special Provisions are currently available.

## 21.4 ROADWAY GEOTECHNICAL ENGINEERING REPORTS

The Roadway Geotechnical Engineering Reports provide geotechnical information related specifically to the design of roadway embankments and any structures other than bridges and bridge embankments. The contents of both preliminary (PRGER) and final (RGER) geotechnical engineering reports are described in the following sections.

### 21.4.1 Preliminary Roadway Geotechnical Engineering Report (PRGER)

The purpose of the PRGER is to provide the designers with preliminary information that may be used in the preliminary design of the roadway embankment and roadway structures. Typically, the preliminary report is issued prior to the DFR so that the information can be used during the field review and in development of preliminary road plans. The preliminary report should include, at a minimum, the following items:

- a. General Project Information
- b. General Geology
- c. Soils Encountered
- d. Embankment
  - + Preliminary slope stability analysis
  - + Preliminary settlement analysis
  - + Construction Difficulties
  - + Temporary Shoring
- e. Roadway Structure Foundations
  - + Seismic
    - Acceleration Design Response Spectrum (ADRS)
    - SSL Results
  - + Type and Size
  - + Construction Difficulties
  - + Corrosion Potential Results
- f. Geohazards
  - + Mucking requirements
  - + Potential for long waiting periods for settlement
  - + ERS requirements
  - + Karst voids/sink holes

Items a through c above should be used to provide a general description of the project and the soils encountered; in depth details are not required. Preliminary slope stability analysis is based on preliminary road plans and is performed in accordance with the procedures outlined in Chapter 17. The purpose of this analysis is to determine if the designed embankment slope will achieve the required stability or if a flatter slope or reinforcement is required. The settlement analysis should provide an indication of the amount and time anticipated for settlement to occur, because these factors may have an impact on the construction schedule of the project. Any potential construction difficulties, such as mucking/undercutting, should be identified and preliminarily discussed in the PRGER.

For some roadway structures, the preliminary seismic information consists of the ADRS curve and the results of SSL analysis. The ADRS and SSL analysis are conducted in accordance with the procedures provided in Chapter 12 and Chapter 13. The ADRS may be either preliminary or final depending on the number of testing locations, depth and type of geotechnical exploration.



In addition, the ADRS shall be provided for both the SEE and the FEE. The SSL analysis will be based on the available ADRS curve and the available soil information.

The need for temporary shoring to allow for staged construction of the roadway embankment should also be identified in the PRGER. The Appendix should include the results of field testing related to the road embankments, roadway structures and bridge (if present on the project), and any laboratory work. In addition, a field testing location plan, the completed GeoScoping form (also called a Site Reconnaissance form) and the ADRS curve, if required, should be provided.

#### **21.4.2 Final Roadway Geotechnical Engineering Report (RGER)**

The RGER is produced after completion of all field work and receipt of revised roadway plans from the project designers based on the results of the DFR. The RGER should contain detailed information about the project. This report will be used by the project designers to develop the final design for the roadway project.

The RGER should include a detailed description of the project to include the roadway length and any roadway structures that may be required to complete the project. Included with the project information should also be a discussion of the existing site conditions at the time of field work. This description should include items such as surface water, exposed rock, vegetation, etc. This is not meant to be a complete list of items describing the actual site conditions. The report should include any items that in the opinion of the GEOR may affect design or construction. The field and laboratory testing procedures should also be discussed, but this discussion should be limited to the standard test methods used (see Chapter 5). The location of each test should also be indicated (see Table 21-1) as well as the type and number of laboratory tests (see Table 21-2). Testing procedures for non-standard tests should be included in the Appendix of the report.

The next section of the RGER should consist of discussions of the area geology as it pertains to the overall project, followed by a specific discussion of the soils located at the project site. The overall geologic discussion should include geologic stratigraphic province (see Chapter 11) and geologic formations that will affect the design of the roadway embankments and structures. This discussion should be followed by a detailed discussion of the soils encountered along the roadway alignment. The subsurface conditions should be described as to the type of soil, thickness of each soil type, and soil strength as represented by the field work. The soil type should be defined based on the field work (see Table 21-3). Soils that will behave mechanically similarly should be grouped together as a subsurface unit. The layer thickness may be based on the depth below existing grade or based on the elevation. The use of elevations is the preferable way of indicating soil layer thickness. The soil strength may be represented as blow count or other measured indices from the field testing. In addition, the longitudinal extent of each soil layer should be indicated, since longitudinal changes in soil types may affect construction.

After detailing the project information, site conditions and subsurface conditions, the next section of the RGER is the seismic design section, this section of the report only applies to roadway structures, specifically ERSs. The seismic design section should detail the effects of the design seismic event (see Chapter 12) on the proposed road project. A final ADRS should be developed based on the subsurface conditions encountered. The final ADRS will be developed in accordance with Chapter 12. The ADRS shall be based on both the SEE and FEE seismic events. If the site screens for SSL during the PRGER, a detailed SSL study is required. The SSL study will be conducted in accordance with Chapter 13. The detailed SSL study should include the extent, both horizontally and vertically, and determination of the amount of induced potential settlement. In addition, the potential for slope instability of roadway structure should also be determined.

After discussing the geology and seismicity of the project, the next sections of the RGER shall address the roadway embankments (fills and cuts) and other (i.e., culverts, overhead signs, retaining walls, etc.) roadway structures. Other roadway structures here are typically retaining walls, but may also include culverts (pipe, box or floorless), sound barrier walls and other miscellaneous structures. The GEOR is required to provide engineering recommendations for pipes and culverts with diameters equal to or greater than 48 inches. For pipes and culverts with diameters less than 48 inches the GEOR will provide the estimated SPT N-value based on the closest boring to allow for the determination of undercutting and reinforcement requirements detailed on the SCDOT Standard Drawings. The results of the stability analyses performed in accordance with Chapters 17 and 18 are discussed. The discussion shall include both the static (Service limit state) and seismic (EE I limit state) performance of the roadway structure. The results of the analysis should be compared to the performance criteria contained in Chapter 10. If the criteria are exceeded, then site remediation will be required (see Chapter 19). In addition, this section of the report should provide the results of settlement analysis (see Chapter 17). The effects of the settlement should be explained and any measures required to decrease the time for settlement to occur should be provided.

Construction considerations should follow the discussion of the slope stability and settlement analyses. The material properties used during slope stability analysis should be provided in this section (see Table 21-10), because the embankment design is based on these properties being achieved during construction. If the material properties do not exceed those allowed for the specific county the project is located in, no additional information is required. Chapter 7 should be consulted for the allowable shear strengths by county. If the shear strengths must exceed those allowed in the project county, then "Borrow Material – Controlled Fill" shall be used and the notes provided in Chapter 22 shall be used. If ground improvements are required to achieve satisfactory performance of the embankments or roadway structures, the improvements should be discussed in this section. This discussion shall include the ground improvement method, the expected result of the improvement and the procedures required for verification of the improvement.

**Table 21-10, Fill Material Properties Table**

Soil Property	Required Property	
	Total	Effective
Internal Friction, $\phi$	32°	18°
Cohesion, $c$	150 psf	500 psf
Total Unit Weight, $\gamma$	120 pcf	

A more in-depth discussion of the requirements for temporary shoring should be included, if the temporary shoring is required for staged construction or the installation of ground improvement. The discussion shall also include what type of shoring is or is not permitted (i.e., temporary MSE walls shouldn't be used in a cut condition). The parameters to be used in temporary shoring design shall be provided as indicated in Table 21-11.

**Table 21-11, Temporary Shoring Wall Soil Design Parameters**

Depth <sup>1</sup> (ft)	$c$ (psf)	Phi ( $\phi$ ) (degrees)	Saturated Unit Weight ( $\gamma_{sat}$ ) (pcf)	$K_o$	$K_a$	$K_p$
0-7	-	32	100	0.47	0.31	3.25
7-14	343	-	86	1.0	1.0	1.0
14-19	-	30	109	0.50	0.33	3.0
> 19	550	35	120	0.43	0.27	3.69

<sup>1</sup>Elevation may be substituted for Depth, if Elevation is used include appropriate units

The final section of the RGER consists of notes that are required to be placed on the plans. This section of the report shall be tailored to the requirements of the specific project and shall provide the information required in Chapter 22. However, in GEC prepared reports, an additional report section is added that consists of any limitations to the report. This section is not required in reports prepared by the PC/GDS.

The Appendix of RGER should include the locations of the soil tests, a subsurface profile and the completed GeoScoping form (also called a Site Reconnaissance form). The soil testing reports should be followed by the report of laboratory testing. Only the testing reports that pertain to the embankment and roadway structures should be included in the Appendix. The RGER Appendix should include the final ADRS curves and the results of the detailed liquefaction study, if performed. The results of slope stability analyses should also be included in the Appendix of the report. In addition, the Appendix of the RGER shall include any Special Provisions pertaining to geotechnical issues that are required for the project. Included in this section of the Appendix are those Special Provisions previously prepared by SCDOT as well as any Special Provisions written by the GEC. Contact the PC/GDS to determine which Special Provisions are currently available.

## **21.5 SITE-SPECIFIC SEISMIC RESPONSE ANALYSIS REPORT**

The purpose of the Site-Specific Seismic Response Analysis Report (Site-Specific) is to provide the results of a site-specific response analysis. The requirements for conducting a site-specific response analysis are contained in Chapter 12. The Site-Specific should include a detailed description of the project to include bridge length, structure type, foundation type and size proposed by the SEOR and loading information. The results of shear wave testing should be discussed, and included in this discussion should be the testing procedure used to obtain the shear wave velocities.

The next section of the Site-Specific should consist of a discussion of the area geology as it pertains to the overall project, followed by a specific discussion of the soils located at the project site. The overall geologic discussion should include geologic stratigraphic province (see Chapter 11) and geologic formations that will affect the design of the bridge foundations. This discussion should be followed by a detailed discussion of the soils encountered along the project alignment. Also included in this section of the report should be discussion of the project seismicity to include the approximate magnitude and distance from the project site to the anticipated seismic source (M and R, respectively). Included in this section of the report is a discussion of the time histories. Most time histories (synthesized due to a lack of actual time history records in South Carolina) will be developed using SCENARIO\_PC (latest edition); however, actual time histories may also be used. A detailed explanation of the selection of an actual time history shall be provided and should include at a minimum, the M and R and geologic condition where the time history was obtained, along with any scaling required to match the Uniform Hazard Spectrum (UHS) at the project site. The use of actual time histories requires the prior approval of the PCS/GDS.

A detailed SSL study and analysis shall not be reported in the Site-Specific, but shall be reported in the BGER or the RGER, if required. The exception to this is if the amount of liquefaction is significant (see Chapter 12), which may cause a non-linear analysis to be required. The report shall clearly indicate whether a linear or non-linear site response analysis was performed. If a non-linear analysis is required, a discussion of the calibration of the non-linear model with the linear model shall be included. Included in the report shall be a table indicating the geologic profile to the B-C boundary that was used in the modeling (see Table 21-12). In addition, the sensitivity analysis shall be discussed in detail in this section. The discussion should include which soil parameters were varied and how the variation was

determined. In addition, multiple seismic events (minimum of 7) shall be used. As a result of the sensitivity analysis performed, a series of site-specific horizontal acceleration response spectra (ARS) curves may be developed. A single recommended site-specific horizontal ARS curve should be superimposed on the graph. The method of selecting the recommended site-specific ARS curve should be documented in the report. The selection of the recommended site-specific ARS curve may be based on the sum of the squares (SRSS), the arithmetic mean, critical boundary method, or other method deemed appropriate. Use of other methods beyond those included here to develop the ARS curve, requires the prior approval of the PCS/GDS. However, if less than 7 seismic events are used an envelope of all ARS curves is required to develop the final ARS curve.

The Site Class and the 3-point ADRS curve shall be determined as if the site-specific analysis was not performed. The 3-point ADRS curve and the selected site-specific ARS curve shall be superimposed on each other and the final ADRS curve shall be determined in accordance with Chapter 12.

**Table 21-12, One-Dimensional Soil Column Model**

Geologic Time	Layer No.	Layer Thickness, $H$	Soil Formation	Soil Description (USCS)	PI	FC	Total Unit Weight, $\gamma_{TW}$	Shear Wave Velocity, $V_s$	Shear <sup>(1)</sup> Modulus Reduction Curve	Equivalent <sup>(1)</sup> Viscous Damping Ratio Curve
Quaternary	1									
	2									
Tertiary	3									
	4									
Cretaceous	5									
	6									
Bed Rock	i									

**Note:** PI = Plasticity Index; FC=% Passing the #200 sieve

(1) Indicate the cyclic stress-strain behavior method used by indicating reference (i.e., Andrus et al. (2003)).

## 21.6 SUBMISSION REQUIREMENTS

All reports submitted to SCDOT shall bear the stamp of the Professional Engineer in charge as required by South Carolina law. Submit electronically 1 complete color copy in .PDF format of each revised final report including all Appendices. In addition, submit electronically all preliminary and draft reports.

**Chapter 22**  
**PLAN PREPARATION**

**GEOTECHNICAL DESIGN MANUAL**

*January 2019*



**Table of Contents**

<b><u>Section</u></b>		<b><u>Page</u></b>
22.1	Introduction.....	22-1
22.2	Plan Notes.....	22-1
22.2.1	Bridge Plan Notes.....	22-1
22.2.2	Road Plan Notes.....	22-11
22.2.3	Ground Improvement.....	22-14
22.2.4	Earth Retaining Structures.....	22-15
22.3	Plans.....	22-15

**List of Tables**

<b><u>Table</u></b>	<b><u>Page</u></b>
Table 22-1, Pile Resistance.....	22-2
Table 22-2, Drivability Analysis .....	22-3
Table 22-3, Drivability Analysis .....	22-4
Table 22-4, Drilled Shaft Resistance .....	22-5
Table 22-5, Drilled Shaft Elevations .....	22-6
Table 22-6, Drilled Shaft Elevations .....	22-7
Table 22-7, Summary of Rock Core Compressive Strength Testing.....	22-7
Table 22-8, Drilled Pile Resistance .....	22-8
Table 22-9, Drilled Pile Drivability Table .....	22-9
Table 22-10, Temporary Shoring Wall Soil Design Parameters.....	22-10
Table 22-11, Geotechnical Bid Items and Quantities .....	22-11
Table 22-12, Temporary Shoring Wall Soil Design Parameters.....	22-14



# CHAPTER 22

## PLAN PREPARATION

### 22.1 INTRODUCTION

This Chapter presents the requirements for the Plan Notes that are required to be included in the final geotechnical reports (BGER and RGER, see Chapter 21) and the preparation of plans specific to geotechnical engineering efforts (i.e., ground improvement). Plan Notes specific to geotechnical items are prepared by the GEOR and included in the Plan Note section of the geotechnical report. The Plan Notes provided in the geotechnical report are required to be placed on the final construction plans.

### 22.2 PLAN NOTES

Plan Notes are required for bridges, road, ground improvements, geotechnical instrumentation, and ERSs. The list included herein is not meant to be comprehensive of the Plan Notes required. If in the opinion of the GEOR additional plan notes are required, the additional Plan Notes shall be provided in the geotechnical report. It is incumbent on the GEOR to select and modify the notes presented in this Chapter as appropriate for the specific project. Any Plan Notes that modify or replace a Standard Specification, Supplemental Specification or Supplemental Specification should indicate which specification is being modified or replaced.

#### 22.2.1 Bridge Plan Notes

The Plan Notes required on bridge plans have traditionally been the most complete and comprehensive notes prepared by the GEOR. These Plan Notes cover installation of the foundation (typically, driven piles, drilled shafts or drilled piles). Plan Notes shall be developed on a project specific basis. The RPG/GDS along with the PCS/GDS shall be consulted in the development of shallow foundation Plan Notes.

##### 22.2.1.1 Driven Piles

The following Plan Notes apply to driven piles. Provided first are notes that are general to all driven pile foundations, with the subsequent Sections covering notes specific to particular types of driven piles. It should be noted that Plan Notes are required for both end and interior bents and the general notes should be used accordingly. The notes and tables included herein are generic in nature and should be made project specific. Underlined capital letters are used to indicate areas where project specific information is required. Instructions to the GEOR are indicated in *Italics* after the note and shall not be included in the plans. In addition, when the tables presented herein include numbers, these numbers shall be changed to the requirements of specific projects.

The plan quantities for Index piles should include an additional 2 feet, minimum, to allow for PDA testing, when testing is required. In addition, an additional 2 feet, minimum, of production piling should be included in the plan quantities when PDA testing of the production piling is required.

**22.2.1.1.1 General**

Place the following notes on the plans for end (interior) bents X and Y: *(THE NUMBERED FOOTNOTES BENEATH TABLE 22-1 SHALL NOT BE INCLUDED ON THE PLANS.)*

**Table 22-1, Pile Resistance**

	<b>Strength or Service Limit State<sup>1,2</sup></b>	<b>EE I or EE II Limit State<sup>1,3</sup></b>
Factored Design Load	112 kips <sup>4</sup>	152 kips <sup>4</sup>
Geotechnical Resistance Factor <sup>5</sup>	0.40	1.00
Nominal Resistance	280 kips	152 kips
Resistance from: Design Flood Scourable Soils <sup>6</sup> Soils undergoing static downdrag <sup>6</sup>	40 kips 0 kips	NA
Resistance from Liquefiable Soils <sup>7</sup>	NA	220 kips
Required Driving Resistance	320 kips	372 kips

<sup>1</sup>Use only 1 column; middle column represents static resistance while last column represents Extreme Event resistance. Use the column that governs driving resistance.

<sup>2</sup>Indicate whether Strength or Service limit state controls resistance

<sup>3</sup>Indicate whether EE I or EE II limit state controls resistance

<sup>4</sup>Factored design loads include DD or DD<sub>SL</sub>. Note that in this example the Strength limit state DD = 0.0 kips

<sup>5</sup>Use appropriate construction control resistance factor

<sup>6</sup>Design flood scour and static downdrag are not included with Extreme Event limit state loading conditions

<sup>7</sup>Full resistance that is developed by soils within the liquefiable zone during pile installation

The GEOR shall determine the method of controlling pile installation. If however, the wave equation without stress measurements is to be used, use the first note listed below. If the resistance is to be verified by the Pile Driving Analyzer and CAsE Pile Wave Analysis Program (CAPWAP) analysis of index piles use the appropriate PDA notes following the first note below.

Method of controlling installation of piles and verifying their resistance: Pile Installation Chart from wave equation analysis without stress measurements during driving.

Method of controlling installation of piles and verifying their resistance: Resistance and stresses will be verified by Pile Driving Analyzer (PDA) and CAPWAP analysis of index pile(s) during driving. A Pile Installation Chart developed from the analysis will be used to verify the resistance of production piles.

The required minimum tip elevation to achieve critical penetration for the (PILE TYPE HERE) at end (interior) bent X is M feet MSL.

Perform Pile Driving Analyzer (PDA) testing on the first production pile driven at the end (interior) bent X. If a CAPWAP analysis determines that resistance has not been achieved, restrike 1 of the production piles. Perform the restrike on the production pile exhibiting the least blows per foot. On initial drive, piles shall be stopped at the highest allowable finished grade on the plans to accommodate a restrike while still remaining within an allowable plan finished grade elevation. Perform PDA testing during the restrike. The time between initial drive and restrike is estimated at D days. Payment for the restrike will be as indicated in the Standard Specifications.

An additional 2 feet, minimum, of (*PROJECT SPECIFIC PILE TYPE HERE*) has been included in order to accommodate the initial PDA testing. (*DO NOT INCLUDE THIS NOTE IF THE EXTRA 2 FEET IS NOT INCLUDED.*)

Perform Pile Driving Analyzer (PDA) testing on the index pile(s) driven at end (interior) bent X. Drive index pile to grade or to practical refusal, whichever occurs first. If a CAPWAP analysis determines that resistance has not been achieved, restrike the index pile(s). Perform PDA testing during the restrike. The time between initial drive and restrike is estimated at D days. Payment for the restrike will be as indicated in the Standard Specifications.

Each pile is to be installed in one continuous operation. Include details of any anticipated temporary driving discontinuances including anticipated time intervals in the Pile Installation Plan.

Reference the Standard Specifications for Highway Construction for Driven Pile Foundations, Section 711. Notes included in these plans are in addition to the requirements of the Standard Specifications.

In addition the GEOR shall select 1 of the following notes to be placed on the plans depending on the required Earth-borne Vibration Monitoring level required (see Chapter 24 for level determination).

Level 1 – SCDOT has elected to not monitor the site; therefore, no Earth-borne Vibration Monitoring is required. SCDOT assumes all risk for any potential damage

Level 2 – Earth-borne Vibration Monitoring is required. Earth-borne Vibration Monitoring will be performed by the Department. The RCE or his/her designated representative will coordinate with the Contractor for site access, the schedule of vibration inducing activities and the placement of the required equipment. The Contractor is required to provide at least 48 hours' notice prior to commencing any vibration inducing activity to the RCE. Any damage caused by vibrations in excess of permitted levels will be the responsibility of the Contractor.

### 22.2.1.1.2 Uniform Section Piles

The following notes apply to piles that have a uniform cross section for the entire length of the pile. Included in this group are prestressed concrete piles with a steel H-pile (typically) pile point extending no more than 2-1/2 feet out of the concrete.

The following estimated parameters were used for performing a drivability analysis for end (interior) bents X & Y: *(THE NUMBERED FOOTNOTES BENEATH TABLE 22-2 SHALL NOT BE INCLUDED ON THE PLANS.)*

**Table 22-2, Drivability Analysis**

Skin Quake (QS)	0.10 in
Toe Quake (QT)	0.08 in
Skin Damping (SD)	0.20 s/ft
Toe Damping (TD)	0.15 s/ft
% Skin Friction	80%
Distribution Shape No. <sup>1</sup>	1
Resistance Distribution Model	Proportional <sup>2</sup>
Pile Penetration	80%
Hammer Energy Range	25 – 60 ft-kips

Note: GRLWEAP (XXXX) was used to perform the wave equation analysis.

<sup>1</sup>Distribution Shape No. varies with depth: 0 at the ground surface (creek bottom); 1 at a depth of 5 ft; and 1 to a depth beyond driving depth below the ground surface.

<sup>2</sup>Pile Installation Chart options – proportional, constant skin friction, constant end bearing

A pile hammer having the rated energy as indicated above is considered suitable for driven pile installation. However, final hammer approval is based on a wave equation analysis that accurately reflects the Contractor's proposed driving system.

The required minimum tip elevation to achieve critical penetration for the (PILE TYPE HERE) at end (interior) bent X is M feet MSL.

### 22.2.1.1.3 Non-Uniform Section Piles

The following notes apply to combination (composite, non-uniform) piles (i.e., piles that consist of a prestressed concrete pile with a steel H-pile (typically) pile point extending greater than 2-1/2 feet out of the concrete).

The following estimated parameters were used for performing a drivability analysis for end (interior) bents X & Y: *(THE NUMBERED FOOTNOTES BENEATH TABLE 22-3 SHALL NOT BE INCLUDED ON THE PLANS.)*

**Table 22-3, Drivability Analysis**

Skin Quake (QS)	0.10 in
Toe Quake (QT)	0.08 in
Skin Damping (SD)	0.20 s/ft
Toe Damping (TD)	0.15 s/ft
% Skin Friction	80%
Distribution Shape No. <sup>1</sup>	1
Resistance Distribution Model	Proportional <sup>2</sup>
Toe No. 2 Quake	0.15 in
Toe No. 2 Damping	0.15 s/ft
End Bearing Fraction (Toe No. 2)	0.95
Pile Penetration	80%
Hammer Energy Range	25 – 60 ft-kips

Note: GRLWEAP (XXXX) was used to perform the wave equation analysis.

<sup>1</sup>Distribution Shape No. varies with depth: 0 at the ground surface (creek bottom); 1 at a depth of 5 ft; and 1 to a depth beyond driving depth below the ground surface.

<sup>2</sup>Pile Installation Chart options – proportional, constant skin friction, constant end bearing

The required minimum tip elevation (to achieve critical penetration) for the X-inch prestressed concrete piles is M feet MSL. This equates to a minimum tip elevation of the steel pile points of M feet MSL. Fabricate and deliver piles to the job site with either a 2.5-foot length of HP Y pile point or the full length of HP Y pile point extending from the tip of the prestressed concrete pile.

A pile hammer having the rated energy as indicated above is considered suitable for driven pile installation. However, final hammer acceptance is based on a wave equation analysis that accurately reflects the Contractor's proposed driving system.

The Contractor may elect to drive a portion of the HP Y steel piling extension prior to attaching the remaining prestressed portion. If the Contractor elects to attach the additional extension to the piling prior to picking up the pile, it is expressly understood

that the Department is not responsible for any piles damaged during pick-up. Damaged piles are to be replaced at the Contractor's expense.

#### 22.2.1.1.4 Driven Piles – Rock

The previous notes apply to piles driven into soil materials. The following notes should be used for piles driven into intermediate geomaterials (IGM) (i.e., partially weathered rock (PWR)) or to rock. Only 1 of these notes should be used, it is incumbent upon the GEOR to determine if reinforced pile tips with teeth are required.

Reinforced pile tips are required to penetrate partially weathered rock. Install the reinforced pile tips in accordance with the manufacturer's installation recommendations.

Reinforced pile tips with teeth are required to penetrate partially weathered rock. Install the reinforced pile tips with teeth in accordance with the manufacturer's installation recommendations. Include the cost of providing teeth on the reinforced pile tips in the price bid for Reinforced Pile Tips.

#### 22.2.1.2 Drilled Shafts

The following Plan Notes apply to drilled shafts. Drilled shafts are typically used at interior bents only, but Plan Notes are also required if drilled shafts are used at end bents. If the column supported on a drilled shaft would be less than 5 feet tall, the Contractor should be given the option, at no additional cost to SCDOT, of extending the shaft to the bottom of the bent cap. The SEOR shall also provide for permissible construction joints in casings to facilitate construction on projects with large water fluctuations. The notes and tables included are generic in nature and should be made project specific. Underlined capital letters are used to indicate areas where project specific information is required. Instructions to the GEOR are indicated in *Italics* after the note and shall not be included in the plans. In addition, when the tables presented herein include numbers, these numbers shall be changed to the requirements of specific projects.

Add the following notes to the plans for Interior Bents X, Y, and Z: *(THE NUMBERED FOOTNOTES BENEATH TABLE 22-4 SHALL NOT BE INCLUDED ON THE PLANS.)*

**Table 22-4, Drilled Shaft Resistance**

	<b>Strength or Service Limit State<sup>1,2</sup></b>	<b>EE I or EE II Limit State<sup>1,3</sup></b>
Factored Design Load	1400 kips <sup>4</sup>	1800 kips <sup>4</sup>
Factored Resistance – Side	1130 kips	1430 kips
Factored Resistance – End	270 kips	370 kips
Geotechnical Resistance Factor – Side <sup>5</sup>	0.50	1.0
Geotechnical Resistance Factor – End <sup>5</sup>	0.50	1.0
Total Nominal Resistance	2800 kips	1800 kips

<sup>1</sup>Use only 1 column; middle column represents static resistance while last column represents Extreme Event resistance, use the column that governs resistance

<sup>2</sup>Indicate whether Strength or Service limit state controls resistance

<sup>3</sup>Indicate whether EE I or EE II limit state controls resistance

<sup>4</sup>Factored design loads include DD or DD<sub>SL</sub>. Note that in this example the Strength limit state DD = 0.0 kips

<sup>5</sup>Use appropriate construction control resistance factor for static and  $\phi_{EQ}$  equal to 1.0 for seismic

Assess the actual ground and/or water level conditions and determine the required top of casing elevation and casing length before ordering. Prior to installing any proposed top

of casing or top of drilled shaft elevation different from that shown in the plans, obtain approval in writing from the Bridge Construction Office. Support the top of casing to maintain construction tolerances during construction. To extend oversized temporary casing larger in diameter than the construction casing below the scour elevation that is shown on the bridge plan and profile, obtain approval from the Bridge Construction Office.

If a dry hole is attempted and the hole becomes a wet hole with no slurry equipment on site, immediately backfill the hole with spoils 3 feet up inside the casing or to the top of hole until slurry and desanding equipment are ready on site.

Include the details for anticipated or contingency temporary cessation of work in the Drilled Foundation Installation Plan. Such details shall include shaft maintenance during the temporary cessation.

The estimated bottom of casing elevation and the minimum tip elevation of the drilled shaft are indicated in the table below. The minimum diameter of the drilled shafts is A inches.

**Table 22-5, Drilled Shaft Elevations**

<b>Interior Bent No.</b>	<b>Estimated Bottom of Casing Elevation</b>	<b>Minimum Shaft Tip Elevation</b>
2	+125 ft msl	+57 ft msl
3	+121 ft msl	+57 ft msl
4	+125 ft msl	+55 ft msl

Shaft lengths shown below the bottom elevation of the casing shall be uncased.

Reference the Standard Specifications for Highway Construction for Drilled Shafts and Drilled Pile Foundations (Section 712) and for Crosshole Sonic Logging of Drilled Shafts (Section 727). Notes included in these plans are in addition to the requirements of the Standard Specifications.

The following notes shall be used if the wet method using mineral slurry is required by the GEOR.

Wet construction method for drilled shafts is required. Use mineral slurry throughout the excavation and construction of the shafts. The tolerances for testing (including time intervals) and maintaining the mineral slurries are indicated in the Standard Specifications for Highway Construction, Section 712. Do not use plain water, salt water, and/or polymer slurries.

The following notes shall be used as applicable for drilled shafts where a seal is required.

Casing shall be extended into the Cooper Marl (*USE APPROPRIATE FORMATION*) a sufficient distance to obtain an effective water seal (approximately 1 foot).

Extend casing until the full circumference of the casing penetrates the rock sufficient enough to produce an effective seal against overburden material falling into the shaft. Water may still enter the shaft through seams in the rock.

The following note shall be used for drilled shafts cased to rock where water is an acceptable drilling fluid.

Extend casing until the full circumference of the casing penetrates the rock sufficient enough to produce an effective seal against overburden material falling into the shaft. Water may still enter the shaft through seams in the rock. If the wet method is used, either mineral slurry or potable water may be used during excavation and construction of the shafts. The tolerance for testing (including time intervals) and maintaining the mineral slurry are indicated in the Standard Specifications for Highway Construction, Section 712. *(INCLUDE ANY REQUIRED WATER TESTS HERE.)* Do not use salt water and/or polymer slurries.

The following notes shall be used for drilled shafts placed into intermediate geomaterials (IGM) (i.e., partially weathered rock (PWR)) or to rock.

The estimated bottom of casing and estimated tip elevations for the rock sockets are indicated in the table below. The referenced rock socket penetration depths for Bents X through Y are uncased lengths and the depths indicated are required to be obtained below the top of continuous rock. The minimum diameter for the rock sockets is A inches and the minimum diameter of the drilled shafts is B inches. Support the top of casing to maintain construction tolerances during construction.

**Table 22-6, Drilled Shaft Elevations**

<b>Int. Bent No.</b>	<b>Estimated Bottom of Casing Elevation</b>	<b><u>A</u>" Wet &amp; Dry Excavation Per Shaft</b>	<b><u>B</u>" Rock Excavation Per Shaft</b>	<b>Estimated Shaft Tip Elevation</b>
2	+789 ft msl	31 ft	12 ft	+777 ft msl
3	+794 ft msl	25.5 ft	12 ft	+782 ft msl
4	+803 ft msl	15 ft	20 ft	+784 ft msl

During construction, the bottom elevation of the shaft may vary if rock is encountered at a different elevation than shown in the plans. If rock is encountered less than 2 feet higher than the elevation shown, extend the socket to the tip elevation shown. If rock is encountered less than 2 feet lower than the elevations shown, lower the tip elevation as needed to maintain the required depth of rock excavation. If rock is encountered more than 2 feet higher or lower than the elevation shown, immediately notify the Resident Construction Engineer (RCE). The RCE will then immediately notify the Bridge Construction Office.

Provide equipment capable of drilling through rock at the site that may be twenty-five percent (25%) greater than the strength indicated in the Table below.

**Table 22-7, Summary of Rock Core Compressive Strength Testing**

<b>Boring No.</b>	<b>Recovery</b>	<b>RQD (%)</b>	<b>Core Number</b>	<b>Depth (ft)</b>	<b>Compressive Strength (psi)</b>
B-1	100	41	NQ-2	3 – 4	6,920
B-1	100	68	NQ-4	10 – 10-1/2	5,150
B-3	100	91	NQ-2	31 – 32	6,030
B-4	90	90	NQ-2	57-1/2 - 59	6,840
B-5	100	61	NQ-1	49 - 50	15,620

### 22.2.1.3 Drilled Piles

The following Plan Notes apply to drilled piles. It should be noted that drilled piles are typically used when the subsurface conditions consist of either IGM or rock at the foundation locations. This type of foundation is used primarily at end bents; but may be used at interior bents with the approval of PC/SDS and PC/GDS (see Chapter 16 for details). The notes and tables included herein are generic in nature and should be made project specific. Underlined capital letters are used to indicate areas where project specific information is required. Instructions to the GEOR are indicated in *Italics* after the note and shall not be included in the plans. In addition, the tables presented herein include numbers; these numbers shall be changed to the requirements of specific projects.

Place the following notes on the plans for end (interior) bents X and Y: (*THE NUMBERED FOOTNOTES BENEATH TABLE 22-8 SHALL NOT BE INCLUDED ON THE PLANS*)

**Table 22-8, Drilled Pile Resistance**

	<b>Strength or Service Limit State<sup>1,2</sup></b>	<b>EE I or EE II Limit State<sup>1,3</sup></b>
Factored Design Load	112 kips <sup>4</sup>	152 kips <sup>4</sup>
Geotechnical Resistance Factor <sup>5</sup>	0.40	1.00
Nominal Resistance	280 kips	152 kips
Resistance from Design Flood Scourable Soils <sup>6</sup>	40 kips	NA
Resistance from Liquefiable Soils <sup>7</sup>	NA	220 kips
Required Driving Resistance <sup>8</sup>	320 kips	372 kips

<sup>1</sup> Use only 1 column; middle column represents static resistance while last column represents Extreme Event resistance. Use the column governs driving resistance.

<sup>2</sup> Indicate whether Strength or Service limit state controls resistance

<sup>3</sup> Indicate whether EE I or EE II limit state controls resistance

<sup>4</sup> Factored design loads include DD or DD<sub>SL</sub>. Note that in this example the Strength limit state DD = 0.0 kips

<sup>5</sup> Use appropriate construction control resistance factor

<sup>6</sup> Design flood scour is not included with seismic loading conditions

<sup>7</sup> Full resistance that is developed by soils within the liquefiable zone during pile installation

<sup>8</sup> Delete the word "Driving" if the piles are not driven.

The estimated drilled pile tip elevation for End Bent X is M feet below existing grade based on partially weathered rock (*CHANGE TO "rock" AS REQUIRED*) at A feet below existing grade (*reference soil boring PUT ACTUAL BORING NUMBER HERE*). Extend the drilled piles into partially weathered rock a minimum of M feet from top of partially weathered rock. The top of partially weathered rock elevation may be variable across bent location and may result in varying pile lengths. Regardless of the pile lengths, extend the drilled piles M feet into partially weathered rock.

Do not extend the temporary casing for the drilled pile foundations below the top of rock elevation. Prior to concreting and backfilling, remove (pump) any accumulation of water from the excavation. If the hole is a wet hole, concreting using wet construction method may be required as specified in Section 712 (Drilled Shafts and Drilled Pile Foundations) of the Standard Specifications for Highway Construction. After installation of the pile, concrete the HP Y piling at End Bent X in the bottom M feet of the rock socket using Class 4000DS concrete. Wait at least 24 hours after concrete has been placed and then backfill the space between the pile and the excavation with clean sand and tamp in an approved manner. Remove temporary casing used for drilled pile construction.



Payment for concrete in the drilled pile foundations is determined using the contract unit bid price for the pay item.

Concrete, backfill and remove temporary casing prior to drilling any adjacent piles within a 20-foot radius.

Reference the Standard Specifications for Highway Construction for Driven Pile Foundations (Section 711) and Drilled Shafts and Drilled Pile Foundations (Section 712). Notes included in these plans are in addition to the requirements of the Standard Specifications.

The following notes shall be used if the pile is to be driven after placement in the drilled hole.

The following estimated parameters were used for performing a drivability analysis for End Bents X and Y: (*THE NUMBERED FOOTNOTES BENEATH TABLE 22-9 SHALL NOT BE INCLUDED ON THE PLANS.*)

**Table 22-9, Drilled Pile Drivability Table**

Skin Quake (QS)	0.10 in
Toe Quake (QT)	0.08 in
Skin Damping (SD)	0.20 s/ft
Toe Damping (TD)	0.15 s/ft
% Skin Friction	80%
Distribution Shape No. <sup>1</sup>	1
Resistance Distribution Model	Proportional <sup>2</sup>
Pile Penetration	80%
Hammer Energy Range	25 – 60 ft-kips

Note: GRLWEAP (XXXX) was used to perform the wave equation analysis.

<sup>1</sup>Distribution Shape No. varies with depth: 0 at the ground surface (creek bottom); 1 at a depth of 5 ft; and 1 to a depth beyond driving depth below the ground surface.

<sup>2</sup>Pile Installation Chart options – proportional, constant skin friction, constant end bearing

The GEOR shall determine the method of controlling pile installation. If the resistance is to be verified by the PDA and CAPWAP analysis of index piles use the following notes.

Method of controlling installation of piles and verifying their resistance: Resistance and stresses will be verified by Pile Driving Analyzer (PDA) and CAPWAP analysis of index pile(s) during driving. A Pile Installation Chart developed from the analysis will be used to verify the resistance of production piles.

The required minimum tip elevation to achieve critical penetration for the (*PILE TYPE HERE*) at end (interior) bent X is M feet MSL.

Perform Pile Driving Analyzer (PDA) testing on the first production pile driven at the end (interior) bent X. If a CAPWAP analysis determines that resistance has not been achieved, restrike 1 of the production piles. Perform the restrike on the production pile exhibiting the least blows per foot. On initial drive, piles shall be stopped at the highest allowable finished grade on the plans to accommodate a restrike while still remaining within an allowable plan finished grade elevation. Perform PDA testing during the restrike. The time between initial drive and restrike is estimated at D days. Payment for the restrike will be as indicated in the Standard Specifications.

An additional 2 feet, minimum, of (*PROJECT SPECIFIC PILE TYPE HERE*) has been included in order to accommodate the initial PDA testing. (*DO NOT INCLUDE THIS NOTE IF THE EXTRA 2 FEET IS NOT INCLUDED.*)

Perform Pile Driving Analyzer (PDA) testing on the index pile(s) driven at end (interior) bent X. Drive index pile to grade or to practical refusal, whichever occurs first. If a CAPWAP analysis determines that resistance has not been achieved, restrike the index pile(s). Perform PDA testing during the restrike. The time between initial drive and restrike is estimated at D days. Payment for the restrike will be as indicated in the Standard Specifications.

Only 1 of the following notes should be used, if the wave equation without stress measurements is to be used. It is incumbent upon the GEOR to determine which is appropriate.

Method of controlling installation of piles and verifying their resistance: Pile Installation Chart from wave equation analysis without stress wave measurements during driving. Do not strike the pile over 20 blows with less than 1 inch of pile movement.

After excavation of drilled pile foundations have occurred, drive the HP Y (change pile type as appropriate) piling to practical refusal. Do not strike the pile over 20 blows with less than 1 inch of pile movement.

Only 1 of the following notes should be used, it is incumbent upon the GEOR to determine if reinforced pile tips with teeth are required.

Reinforced pile tips are required. Install the reinforced pile tips in accordance with the manufacturer's installation recommendations.

Reinforced pile tips with teeth are required to penetrate partially weathered rock. Install the reinforced pile tips with teeth in accordance with the manufacturer's installation recommendations. Include the cost for providing teeth on the reinforced pile tips in the price bid for Reinforced Pile Tips.

#### 22.2.1.4 Temporary Shoring (Bridge)

The following Plan Notes apply to temporary shoring walls.

Use buoyant unit weights in computations for soils below the water level. Designer shall determine appropriate water level and consider all unbalanced water forces in design. Design shall accommodate live loading. Use the following soil strength parameters for determining earth pressure coefficients.

**Table 22-10, Temporary Shoring Wall Soil Design Parameters**

Depth (ft)	c (psf)	Phi ( $\phi$ ) (degrees)	Saturated Unit Weight ( $\gamma_{sat}$ ) (pcf)	$K_o$	$K_a$	$K_p$
0-7	-	32	100	0.47	0.31	3.25
7-14	343	-	86	1.0	1.0	1.0
14-19	-	30	109	0.50	0.33	3.0
> 19	550	35	120	0.43	0.27	3.69

## 22.2.2 Road Plan Notes

The Plan Notes required on road plans are a relatively recent development in geotechnical practice as the requirements for design of embankments have increased, leading to a requirement for more detailed notes on the plans.

These notes and tables included herein are generic in nature and should be made project specific. Underlined capital letters are used to indicate areas where project specific information is required. In addition, the tables presented herein include numbers; these numbers shall be changed to the requirements of specific projects. Instructions to the GEOR are indicated in *Italics* after the note and shall not be included in the plans. The table provided below presents geotechnical bid items and quantities that should be included in the plans. The Estimated Quantity is the total quantity estimated for a specific item to be used on the project, while the Inclusion Quantity is the quantity that may be required in areas, not previously identified on the plans as needing the item. The difference between the Estimated Quantity and the Inclusion Quantity is quantity of a specific item that is specifically identified on the plans as being required. It is incumbent on the design team to make sure that all bid items required to assure geotechnical performance have been included.

**Table 22-11, Geotechnical Bid Items and Quantities**

Item No.	Pay Item	Estimated Quantity	Inclusion Quantity <sup>1</sup>
2033030	Borrow Material – Controlled Fill	3,000 CY	2,000 CY
2034000	Muck Excavation	200 CY	100 CY
2036020	Geotextile, Separation	362 SY	150 SY
2037030	Geogrid, Stabilization	362 SY	150 SY
2037000	Geogrid Reinforcement (Uniaxial)	1944 SY	2000 SY
2037010	Geogrid Reinforcement (Biaxial)	100 SY	150 SY
2052010	Stone Bridge Lift Material	818 TONS	180 TONS

<sup>1</sup>The inclusion quantities associated with mucking and undercutting, i.e. mucking, stone bridge lift material, geogrid, and geotextile for separation of sub-grade and sub-base are for bid estimation purposes only. Do not purchase or stockpile these items on site without written approval from the RCE unless specific areas and details are defined on the plans.

*(THE NUMBERED FOOTNOTES BENEATH TABLE 22-11 SHALL NOT BE INCLUDED ON THE PLANS)*

### 22.2.2.1 Borrow Materials

The following notes apply to borrow materials that require shear strength in excess of that typically found in the project county. If these notes are to be used, all material shall be called "Borrow Material – Controlled Fill" and shall use Item No.: 2033030. Underlined capital letters are used to indicate areas where project specific information is required.

The following areas have been identified as requiring Borrow Material – Controlled Fill:

Sta. X+XX, Y ft L(R) of Existing Centerline to Sta. U+UU, V ft L(R) of Existing Centerline

Sta. I+II, S ft L(R) of Existing Centerline to Sta. M+MM, N ft L(R) of Existing Centerline

Provide borrow materials meeting the following minimum requirements:

- A material meeting the classifications of A-1, A-2-4, A-2-5, A-2-6(0), A-3 and A-4(0) as defined by AASHTO M145, *Classification of Soil and Soil-Aggregate Mixtures for Highway Construction Purposes* and having a minimum total soil unit weight,  $\gamma_{\text{total}}$  of A pcf at optimum moisture.
- Minimum friction angle,  $\phi'$ , of B° and cohesion,  $c'$ , of D psf.

In addition, determine the moisture-density relationship, classification and soil shear strength parameters of the proposed borrow material and provide to the RPG I GDS for acceptance. An AASHTO certified laboratory is required to perform the testing. Contact the RPG I GDS for a list of locally available AASHTO certified laboratories. The Department may perform independent testing to assure quality.

Determine the soil shear strength parameters using either direct shear testing or consolidated-undrained triaxial shear testing with pore pressure measurements. The borrow material samples shall have the following laboratory tests performed:

#### Classification Testing

- Moisture-density Relationship (Standard Proctor)
- Grain-size Distribution with wash No. 200 Sieve
- Moisture-Plasticity Relationship Determination (Atterberg Limits)
  - Performed only on samples with more than 20 percent passing #200 sieve
- Natural Moisture Content

#### Shear Strength Testing

- Direct Simple Shear Test
  - Performed only on samples with less than or equal to 20 percent passing #200 sieve
  - Sample remolded to 95 percent of Standard Proctor value
  - Sample moisture content shall be between -1 percent to +2 percent of optimum moisture content
  - At normal pressures of X, Y, and Z psi
- Consolidated-Undrained Triaxial Shear Test with pore pressure measurements
  - Performed only on samples with more than 20 percent passing #200 sieve
  - Sample remolded to 95 percent of Standard Proctor value
  - Sample moisture content shall be between -1 percent to +2 percent of optimum moisture content
  - At consolidation stresses of X, Y, and Z psi

Conduct shear strength testing at the initial selection of the borrow pit, any subsequent changes in borrow pits, and for every 50,000 cy of materials placed. Perform classification testing for every R cy of materials placed including the material used for the shear strength testing. Additional shear testing may be required if, in the opinion of the RCE, the materials being placed are different from those originally tested.

If these minimum criteria cannot be met, provide the soil parameters for the intended borrow excavation material for the project site to the RPG I GDS for review and acceptance. After acceptable borrow material is obtained, compact the fill to the required finish grade line using the compactive effort indicated in the Standard Specifications for Highway Construction, Sections 203 (Roadway and Drainage Excavation) and 205 (Embankment Construction).

### 22.2.2.2 Muck Excavation

The following notes apply to muck excavation. Underlined capital letters are used to indicate areas where project specific information is required. The term L is for left and R is for right of either the Existing Centerline as indicated here or the Proposed Centerline, use the appropriate designations. In addition, the elevation for the bottom of the muck excavation may be substituted for depth. A copy of a template drawing may be obtained from the SCDOT website.

The following areas have been identified as requiring muck excavation:

Sta. X+XX, Y ft L(R) of Existing Centerline to Sta. U+UU, V ft L(R) of Existing Centerline to a depth of Z ft beneath the existing ground surface  
Sta. I+II, S ft L(R) of Existing Centerline to Sta. M+MM, N ft L(R) of Existing Centerline to a depth of P ft beneath the existing ground surface

Any additional areas that are discovered to deflect or settle may require muck excavation as directed by the RCE. The RCE will determine the lateral extent of the undercutting. The undercutting should not extend beyond the toe of slope. The final depth of muck excavation shall not exceed 5 feet, unless otherwise specified in the plans and/or Specifications. Contact the Geotechnical Engineer-of-Record (GEOR) if muck excavation needs to exceed 5 feet and it has not been previously specified in the plans or Specifications.

If the undercutting completely removes the materials identified as muck, then bridge lift materials may be placed directly on the firm materials.

If because of the depth of muck, muck materials must be left in place, place a stabilization geosynthetic meeting the requirements of SC-M-203-6, *Geosynthetic Materials for Separation and Stabilization*. After the placement of the initial bridge lift material, expose approximately 1 square foot of the geosynthetic for visual observation to identify any damage caused by the placement of the bridge lift material. After ascertaining that the geosynthetic has not been damaged, replace the bridge lift material excavated to allow observation of the geosynthetic. If the geosynthetic appears to be damaged, expose a larger area and contact the GEOR for instructions. Any damaged areas shall be repaired by the Contractor at no expense to the Department.

Any ruts that develop in bridge lift materials shall be filled in with similar bridge lift materials. Do not blade down the ruts, since this will decrease the thickness of the bridge lift.

In areas that require mucking or undercutting, borrow material soil may be placed as a bridge lift as long as the grade on which the material is being placed is at least 2 feet above the groundwater or surface water level. Place borrow material bridge lifts in single lift thicknesses no greater than 2 feet. Do not place a bridge lift consisting of borrow material within 3 feet of the base of the pavement section. Place only compacted borrow material soil or stone bridge lift within this zone.

In the event that groundwater/surface water does not allow backfilling with borrow material soil, use either stone or granular bridge lift materials meeting the requirements of *Bridge Lift Materials* Supplement Specification. Place the bridge lift materials in single lifts not exceeding a 2-foot thickness. If additional compacted borrow material soil is needed to reach grade, place a geotextile for separation meeting the requirements of SC-M-203-6, *Geosynthetic Materials for Separation and Stabilization* between the stone

bridge lift and the overlying compacted soil. After the placement of the initial lift of compacted material, expose approximately 1 square foot of the geosynthetic for visual observation to identify any damage caused by the placement of the compacted material. After ascertaining that the geosynthetic has not been damaged, replace and compact the material excavated to allow observation of the geosynthetic. If the geosynthetic appears to be damaged, expose a larger area and contact the GEOR for instructions. Any damaged areas shall be repaired by the Contractor at no expense to the Department.

The quantities associated with mucking and undercutting, i.e. mucking, bridge lift material, geogrid, and geotextile for separation of sub-grade and sub-base, are for bid estimation purposes only. Do not purchase or stockpile these bid items on site without prior written approval from the RCE unless specific areas and details are defined in the plans.

### 22.2.2.3 Temporary Shoring (Road)

The following Plan Notes apply to temporary shoring walls.

Use buoyant unit weights in computations for soils below the water level. Designer shall determine appropriate water level and consider all unbalanced water forces in design. Design shall accommodate live loading. Use the following soil strength parameters for determining earth pressure coefficients.

**Table 22-12, Temporary Shoring Wall Soil Design Parameters**

Depth (ft)	c (psf)	Phi ( $\phi$ ) (degrees)	Saturated Unit Weight ( $\gamma_{sat}$ ) (pcf)	$K_o$	$K_a$	$K_p$
0-7	-	32	100	0.47	0.31	3.25
7-14	343	-	86	1.0	1.0	1.0
14-19	-	30	109	0.50	0.33	3.0
> 19	550	35	120	0.43	0.27	3.69

### 22.2.3 Ground Improvement

Because there are many different types of ground improvement methods and the notes required for each method are so varied, Appendix E contains a list of template drawings that can be used for the various ground improvement methods. The notes specific to each ground improvement method are contained on the drawings. The requirement for field verification will be based on the intended use of the ground improvement method. The GEOR will determine what the verification program will consist of and will develop appropriate plan notes to achieve the required results. Copies of template drawings may be obtained from the SCDOT website.

The GEOR shall select 1 of the following notes to be placed on the plans depending on the required Earth-borne Vibration Monitoring level required (see Chapter 24 for level determination).

Level 1 – SCDOT has elected to not monitor the site; therefore, no Earth-borne Vibration Monitoring is required. SCDOT assumes all risk for any potential damage

Level 2 – Earth-borne Vibration Monitoring is required. Earth-borne Vibration Monitoring will be performed by the Department. The RCE or his/her designated representative will coordinate with the Contractor for site access, the schedule of vibration inducing

activities and the placement of the required equipment. The Contractor is required to provide at least 48 hours' notice prior to commencing any vibration inducing activity to the RCE. Any damage caused by vibrations in excess of permitted levels will be the responsibility of the Contractor.

#### **22.2.4 Earth Retaining Structures**

Similar to the ground improvement notes, the notes concerning ERSs are placed on drawings depicting the ERS details. ERS notes specific to the particular structure being designed shall be developed on a case-by-case basis. Copies of template drawings may be obtained from the SCDOT website.

The GEOR shall select 1 of the following notes to be placed on the plans depending on the required Earth-borne Vibration Monitoring level required (see Chapter 24 for level determination).

Level 1 – SCDOT has elected to not monitor the site; therefore, no Earth-borne Vibration Monitoring is required. SCDOT assumes all risk for any potential damage

Level 2 – Earth-borne Vibration Monitoring is required. Earth-borne Vibration Monitoring will be performed by the Department. The RCE or his/her designated representative will coordinate with the Contractor for site access, the schedule of vibration inducing activities and the placement of the required equipment. The Contractor is required to provide at least 48 hours' notice prior to commencing any vibration inducing activity to the RCE. Any damage caused by vibrations in excess of permitted levels will be the responsibility of the Contractor.

### **22.3 PLANS**

From time to time, the GEOR will be required to or find it necessary to develop plans for use on a specific project (see Appendix E). Plan development procedures presented in the Roadway Design Manual (*RDM*) shall be used in the development of plans. All plans prepared at the direction of the GEOR shall be numbered "G-#" for ground improvement and other geotechnical considerations. All plans prepared for ERSs shall be numbered "S-#." The layout of the border shall conform to the latest standard of SCDOT.

**Chapter 23**  
**SPECIFICATIONS AND SPECIAL  
PROVISIONS**

**GEOTECHNICAL DESIGN MANUAL**

*January 2019*





**Table of Contents**

<b><u>Section</u></b>		<b><u>Page</u></b>
23.1	Introduction.....	23-1
23.2	Supplemental Specifications.....	23-1
23.3	Supplemental Technical Specifications.....	23-1
23.4	Special Provisions .....	23-1



# CHAPTER 23

## SPECIFICATIONS AND SPECIAL PROVISIONS

### 23.1 INTRODUCTION

SCDOT has developed the Standard Specifications for Highway Construction (Standard Specifications) to provide requirements, provisions, and direction for use on construction projects. In addition, SCDOT has developed Supplemental Specifications and Supplemental Technical Specifications (STSs) that modify or supplement the Standard Specifications for Highway Construction. The need occasionally arises where modification to the SCDOT specifications or additional specifications are required. A list of Supplemental Specifications and STSs can be found in Appendix F – Geotechnical Specifications List. The purpose of this Chapter is to provide guidance in preparing Supplemental Specifications, STSs and Special Provisions which are project specific.

### 23.2 SUPPLEMENTAL SPECIFICATIONS

Supplemental Specifications are corrections or changes to the Standard Specifications that are required from time to time. These corrections or changes are typically added to the Standard Specifications when the Standard Specifications are rewritten. One of critical features of the Supplemental Specifications is that corrections or changes are required on every project not just specific projects and are not anticipated being changed but every 5 years or so. Supplemental Specifications shall indicate which Section or Subsection of the Standard Specification are being modified or deleted and replaced. Supplemental Specifications are approved in writing by the FHWA South Carolina Division Office. However, prior to being forwarded to FHWA for approval, the Preconstruction Support Engineer or designee shall establish a review process both internal and external to SCDOT. The author of the Supplemental Specification shall follow the review process. The available Supplemental Specifications for the current Standard Specifications may be found on the SCDOT website.

### 23.3 SUPPLEMENTAL TECHNICAL SPECIFICATIONS

Supplemental Technical Specifications (STSs) typically cover new items not covered by the current edition of the Standard Specifications that could be added to the Standard Specifications when the Standard Specifications are rewritten. For new items contact the Letting Preparation Engineer for a Pay Item Number. Include with the request for new Pay Item Number, the anticipated Section of the Standard Specifications where the new item should be placed. In addition, develop and furnish the short and long descriptions as well as the anticipated unit of measure. Once the Pay Item Number has been developed, confirming the Section of the Standard Specification, the new STS should be written. Follow the template format provided in Appendix A as a guide for preparing the STS. All STSs are approved in writing by the FHWA South Carolina Division Office and will become effective either the following January or July lettings. However, prior to being forwarded to FHWA for approval, the Preconstruction Support Engineer or designee shall establish a review process both internal and external to SCDOT. The author of the STS shall follow the review process. The available STSs for the current Standard Specifications may be found on the SCDOT website.

### 23.4 SPECIAL PROVISIONS

Special provisions are additions or revisions to the SCDOT Standard Specifications for Highway Construction, the SCDOT Supplemental Specifications, and the SCDOT STSs, setting forth

conditions and requirements for a special situation on a specific project. Special Provisions are included in the contract documents for that project and are not intended for general use. Any Special Provisions prepared by the GEOR shall be included in the Appendix of either the BGER or RGER as appropriate. Special Provisions supersede all other contract documents. The GEOR prepares the Special Provisions of a geotechnical nature for inclusion in the project documents. Special Provisions prepared by the GEOR shall be sealed by the GEOR as required by SCDOT policy (see Engineering Directive 37, dated 09/04/2007; <http://info2.scdot.org/ED/ED/ED-37.pdf>). See Chapter 9 – Bid Documents of the SCDOT Bridge Design Manual for additional discussion on the guidelines for preparing Special Provisions. In addition, a template format is provided in Appendix A as a guide to preparing the Special Provision. Unless a Pay Item Number was previously established for the item, contact the Letting Preparation Engineer for a new Pay Item Number. Include with the request for new Pay Item Number, the anticipated Section of the Standard Specifications that the Special Provision is modifying. In addition, develop and furnish the short and long descriptions as well as the anticipated unit of measure.

**Chapter 24**  
**CONSTRUCTION SUPPORT**

**GEOTECHNICAL DESIGN MANUAL**

*January 2019*



## Table of Contents

<u>Section</u>		<u>Page</u>
24.1	Introduction.....	24-1
24.2	Quality Control/Quality Assurance .....	24-1
24.3	Shallow Foundations .....	24-1
24.4	Deep Foundations .....	24-1
	24.4.1 Driven Piles.....	24-1
	24.4.2 Drilled Shafts.....	24-3
24.5	Earth-borne Construction Vibration Monitoring .....	24-8
	24.5.1 General .....	24-9
	24.5.2 Structures.....	24-10
	24.5.3 People.....	24-10
	24.5.4 Equipment/Operations.....	24-10
	24.5.5 Impact of Earth-borne Construction Vibrations .....	24-11
	24.5.6 Vibration Prediction .....	24-12
	24.5.7 Vibration Criteria .....	24-14
	24.5.8 Earth-borne Vibration Monitoring Evaluation .....	24-14
	24.5.9 Addressing Earth-borne Vibration Concerns .....	24-17
	24.5.10 Earth-borne Vibration Monitoring Equipment .....	24-17
	24.5.11 Baseline Earth-borne Vibration Study.....	24-17
	24.5.12 Pre- and Post-Construction Condition Survey .....	24-18
	24.5.13 Earth-borne Vibration Monitoring Plan Notes.....	24-18
	24.5.14 Earth-borne Vibration Monitoring Special Provision.....	24-18
24.6	Geotechnical Instrumentation .....	24-19
24.7	Monitoring Plan.....	24-21
	24.7.1 Definition of Project Conditions .....	24-22
	24.7.2 Objectives of Instrumentation .....	24-22
	24.7.3 Predicted Magnitudes of Change .....	24-22
	24.7.4 Define Remedial Actions .....	24-22
	24.7.5 Establish Responsibilities and Chain of Command.....	24-22
	24.7.6 Type of Instruments and Locations.....	24-23
	24.7.7 Recording of Outside Factors.....	24-23
	24.7.8 Procedures for Ensuring Data Validity.....	24-23
	24.7.9 Estimated Costs.....	24-23
	24.7.10 Installation and Protection Plans .....	24-24
	24.7.11 Calibration and Maintenance of Field Instruments.....	24-24
	24.7.12 Data Processing.....	24-24
24.8	Monitoring Plan Execution .....	24-24
	24.8.1 Instrumentation Supplier .....	24-25
	24.8.2 Factory Calibration of Instrumentation.....	24-25
	24.8.3 Pre-Installation Testing Requirements.....	24-25
	24.8.4 Calibration and Maintenance Requirements.....	24-26
	24.8.5 Installation Methods .....	24-26
	24.8.6 Protection Plan.....	24-26
	24.8.7 Installation Records.....	24-26
	24.8.8 Installation Reports .....	24-27
	24.8.9 Data Collection Methods .....	24-27



---

24.8.10	Qualifications of Personnel Collecting Data .....	24-28
24.9	Field Instrumentation .....	24-28
24.9.1	Slope Inclinometers.....	24-28
24.9.2	Settlement Monitoring .....	24-29
24.9.3	Piezometers .....	24-31
24.9.4	Special Instrumentation.....	24-32
24.10	Conclusions .....	24-32
24.11	Shop Plan Review .....	24-33
24.12	References .....	24-33

**List of Tables**

<b><u>Table</u></b>	<b><u>Page</u></b>
Table 24-1, Distance where Vibration drops below 0.1 ips .....	24-11
Table 24-2, Suggested “n” Values Based on Soil Class .....	24-12
Table 24-3, Reference PPV for Various Pieces of Construction Equipment .....	24-13
Table 24-4, Maximum Allowable PPV for Structures .....	24-14
Table 24-5, Maximum Allowable PPV to Avoid Annoyance .....	24-14
Table 24-6, Distance between Vibration Source and Potential Receptors .....	24-15
Table 24-7, STSs Available from SCDOT .....	24-19
Table 24-8, Monitoring Plan Elements .....	24-21
Table 24-9, Monitoring Plan Execution.....	24-24
Table 24-10, Possible Items in Pre-Installation Tests.....	24-25
Table 24-11, Possible Content of Installation Record Sheets .....	24-27

**List of Figures**

<b><u>Figure</u></b>	<b><u>Page</u></b>
Figure 24-1, Pile Installation Chart .....	24-2
Figure 24-2, Bi-Directional Testing Schematic.....	24-5
Figure 24-3, Multiple O-cell Arrangement .....	24-6
Figure 24-4, Rapid Load Test Setup.....	24-7
Figure 24-5, High-Strain Load Testing Apparatus.....	24-8
Figure 24-6, Arrival Time for P-, S-, and R-waves .....	24-9

# CHAPTER 24

## CONSTRUCTION SUPPORT

### 24.1 INTRODUCTION

The purpose of this Chapter is to provide a basic understanding of construction support as it is applied to geotechnical construction issues. Typically geotechnical construction issues are the verification of foundation resistance and integrity, review and acceptance of foundation installation plans, the implementation, review and acceptance of geotechnical instrumentation or the review and acceptance of shop plans.

### 24.2 QUALITY CONTROL/QUALITY ASSURANCE

Construction support performed by the GEOR typically consists of review of Quality Control (QC) and conducting Quality Assurance (QA). QC is a system of routine technical activities implemented by the Contractor to measure and control the quality of the construction materials being used on a project. QA is a systemic review and auditing of procedures and the testing of a select number of samples by the Department to provide an independent verification of the Contractor's QC program and to provide verification that the construction materials meet the project specifications. QC is performed by the Contractor, while QA is performed by the Department. Ultimately the Contractor is responsible for all materials brought on to a project site; however, it is incumbent on the Department to assure that materials meet Departmental criteria. Construction support performed by the GEOR consists of the review of the results of both QC and QA testing to assure that the project specifications are being met. Construction QA/QC is performed on foundations, some ground improvement installations and geotechnical instrumentation.

### 24.3 SHALLOW FOUNDATIONS

Shallow foundations are typically not used to support bridges; however, if shallow foundations are used, contact the PC/GDS for guidance in developing QA/QC procedures for shallow foundation verification.

### 24.4 DEEP FOUNDATIONS

#### 24.4.1 Driven Piles

The Standard Specifications require the Contractor to submit a *Pile Installation Plan (PIP)* for review and acceptance prior to commencing pile installation. The PIP will be submitted to the Department in accordance with the contract documents. For consultant designed projects, the PIP should be forwarded by the RPG/GDS to the GEC for review. The GEOR shall review the PIP for adequacy and for containing the information required by the specifications and plans. The review is to include hammer analysis as described below and should include comments on items such as adjusting hammer fuel settings if needed to protect the pile integrity during driving. On consultant reviewed projects, the GEC will return the PIP to the RPG/GDS with a cover letter containing appropriate comments concerning the PIP. The PIP will be accepted or rejected by the RPG/GDS, regardless of who designed the project, (i.e. either the Department or a consultant) and shall be forwarded to the Bridge Construction Office for distribution to the Contractor. As required, rejected PIPs shall be resubmitted. One of the components of the PIP is the "Pile and Driving Equipment Data Form." Using the information contained on this form,

the GEOR shall perform a Wave Equation Analysis of Pile Driving (WEAP). The WEAP analysis is used to verify that the pile driving hammer should be capable of installing the piles to the correct tip elevation and resistance without inducing excessive stresses in the pile. Piles are typically installed using 1 of 2 criteria, either resistance or elevation (depth). In some cases, both criteria may be required. Resistance driven criteria is typically based on a required blow count being achieved. The exception to this is if practical refusal is achieved. Practical refusal is defined by Section 711.4 of the Standard Specifications as 5 blows per ¼ inch of penetration. Practical refusal driving criteria may be used as long as the minimum tip elevation has been achieved. The wave equation analysis uses a range of resistances, bracketing the required (nominal) resistance, and range of different strokes. A typical Pile Installation Chart (also known as a Bearing Resistance Chart or Graph) providing driving criterion is depicted in Figure 24-1.

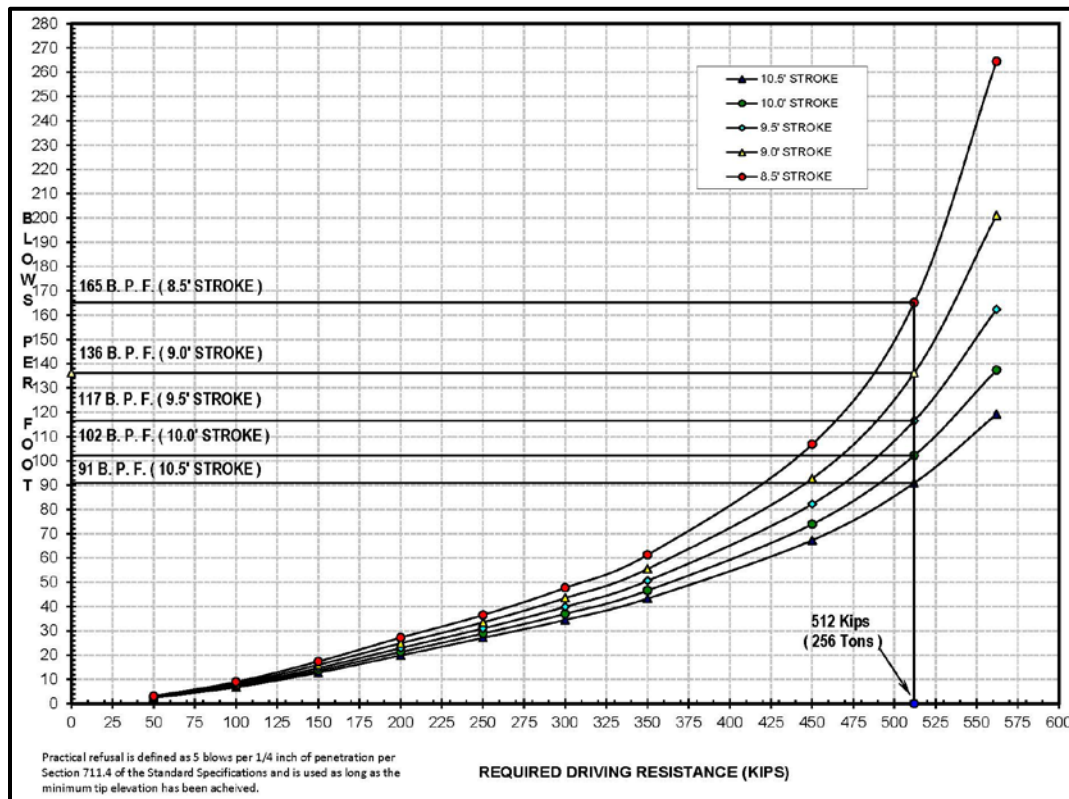


Figure 24-1, Pile Installation Chart

After the GEOR reviews and accepts the PIP, the GEOR shall be responsible for developing Pile Installation Charts as described above or if a PDA or load test is performed as described below. The GEOR shall be responsible for recommending pile lengths as needed based on index pile and/or previous production pile data.

The other criterion to control the installation of a pile is elevation (depth). This criterion is used when it is anticipated that the piles will gain strength with time or the lateral stability of the pile controls the tip elevation. Using both criteria, the GEOR should ensure that the hammer will achieve blow count criteria as set forth in the Standard Specifications. The stresses induced by the hammer should be checked to ensure conformance with the Standard Specifications.

Depending on the resistance factor ( $\phi$ ) selected during design, (refer to Chapter 9), load testing may be required. The load testing may consist of either high-strain (Pile Driving Analyzer (PDA)), rapid (Statnamic®) or static load tests. PDA testing may be conducted during initial driving or on restrike or sometimes both. PDA testing can confirm resistance and driving stresses. However, the resistance obtained from PDA testing is approximate and may require

further refinement by using CAse Pile Wave Analysis Program (CAPWAP). Production piles that are to be tested using PDA should be 2 feet, minimum, longer than production piles to allow for the attachment of the PDA gauges. Index piles should be detailed 2 feet, minimum, longer than production piles to get full driving data to be used in determining pile lengths. Using the results from CAPWAP, a second WEAP analysis should be performed to more accurately model the installation of the pile. This is especially important when the pile is being driven to a specific resistance at a specific blow count. The GEOR shall also develop a Pile Installation Chart for this second WEAP analysis. Monitoring of stresses using the PDA is critical when piles are installed into or through dense formations or partially weathered rock (PWR), or through very soft formations. PDA testing shall conform to the requirements of ASTM D4945 – *Standard Test Method for High-Strain Dynamic Testing of Deep Foundations* as well as the requirements contained in the Standard Specifications.

Statnamic® and static load testing are performed after the installation of the pile, if required. These tests are normally performed prior to production pile driving. Statnamic® is a rapid load test and is different from the PDA, in that the pile is subjected to a “fast push” rather than a sharp blow as would be observed from a pile hammer. Statnamic® load testing of piles can be relatively costly, especially given the capacity requirements. Statnamic® load testing, if used, should follow the standard testing method developed and presented in ASTM D7383 – *Standard Test Methods for Axial Compressive Force Pulse (Rapid) Testing of Deep Foundation* and should also comply with STS SC-M-712-3 for *Rapid Axial Load Testing of Drilled Shafts*. It should be noted that modification of the STS (i.e., a Special Provision) may be required to use this STS with driven piling. In case of conflict between the ASTM and the STS, the STS shall govern. Static load testing, if required, follows the standard testing method developed and presented in ASTM D1143 – *Standard Test Methods for Deep Foundations Static Axial Compressive Load*. Static load testing can not only be expensive, but also time consuming, and is therefore not used except in design testing programs. When static load testing is performed, the results of the testing shall use the Davisson failure criterion.

#### **24.4.2 Drilled Shafts**

Similarly to driven piles, the Standard Specifications require the Contractor to submit a *Drilled Foundation Installation Plan* (DFIP) for review and acceptance prior to commencing drilled foundation installation. The DFIP will be submitted to the Department in accordance with the contract documents. On consultant designed projects, the DFIP should be forwarded by the RPG/GDS to the GEC for review. The GEOR shall review the DFIP for adequacy and for containing the information required by the specifications and plans. On consultant reviewed projects, the GEC will return the DFIP to the RPG/GDS with a cover letter containing appropriate comments concerning the DFIP. The DFIP will be accepted or rejected by the RPG/GDS, regardless of who designed the project (i.e., the Department or a consultant) and shall be forwarded to the Bridge Construction Office for distribution to the Contractor. As required, rejected DFIPs shall be resubmitted.

To verify the acceptability of constructed drilled shafts, crosshole sonic logging (CSL) testing should be required and tubes shall be installed as required by the Standard Specifications, project plans or Special Provisions. A testing report will be generated by a testing firm for review. If the CSL testing indicates no areas of concern, then the drilled shaft is accepted. However, if the CSL testing indicates areas of concern, then the following forms should be requested by the GEOR for review:

- Drilled Shaft Log
- Drilled Shaft Excavation Log
- Slurry Inspection Log
- Drilled Shaft Inspection Log

- Drilled Shaft Concrete Placement Log
- Drilled Shaft Concrete Volumes Log
- Concrete Slump Loss Test

After reviewing these logs, the GEOR should consult with the Bridge Construction Engineer on required actions. On consultant designed projects, the project team shall be responsible for evaluating the drilled foundation to determine if it meets both the structural and load resistance design requirements. The GEOR shall provide written recommendations to the Department concerning drilled foundation acceptance and/or actions to be taken as developed by the project team.

Depending on the resistance factor ( $\phi$ ) selected during design (refer to Chapter 9), a load test may be required. Load tests can be used to verify the existing design or modify the design based on the load test results. The GEOR should evaluate the test results and provide written recommendations concerning the diameter, penetration depth relative to a particular stratum, and/or tip elevation of the production shafts. Drilled foundation load testing consists of static (uni-directional and bi-directional), rapid (Statnamic®) or high-strain (dynamic) load testing. In a uni-directional static load test, the load is applied at the top of the drilled shafts, usually by means of a reaction beam and anchorage foundations. Typically, this type of test is impractical for drilled shafts, unless the drilled shafts have diameters ranging from 3 to 4 feet. Typically drilled shafts in this range have nominal resistances of 1,200 kips, which require a reaction system and jack to have 2,400 kips of reaction capacity. Drilled shafts having larger diameters would require very large reaction systems that would become impractical and potentially unsafe. Therefore, uni-directional static load tests are not normally performed on drilled shafts. Uni-directional testing, if required, follows the standard testing method developed and presented in ASTM D1143 – *Standard Test Methods for Deep Foundations Static Axial Compressive Load*. Uni-directional testing can not only be expensive, but also time consuming, and is therefore not used except in design testing programs. When uni-directional testing is performed, the results of the testing shall use the Davisson failure criterion.

Bi-directional static load tests are performed by applying the load with an expendable jack(s) located between an upper and lower loading plate cast into the drilled shaft. The test is conducted by using the upper portion of the shaft as a reaction element against the base and lower portion of the drilled shaft and vice versa. An effective example of this bi-directional loading system is the Osterberg cell (O-cell) (see Figure 24-2). The maximum test load is limited by the resistance of the shaft above and below the O-cell or the maximum resistance of the O-cell. Therefore, the O-cell should be placed at the point in the shaft where the resistance above the O-cell is approximately equal to the capacity below the O-cell. The use of multiple O-cells may be used to counter the effect of either too much side resistance or too much end resistance, when compared to end or side resistance respectively (see Figure 24-3). The Davisson failure criterion shall be used to interpret the results of uni-directional and bi-directional static load tests. Refer to STS SC-M-712-1 for *Bi-Directional Static Load Testing of Drilled Shafts* construction requirements.

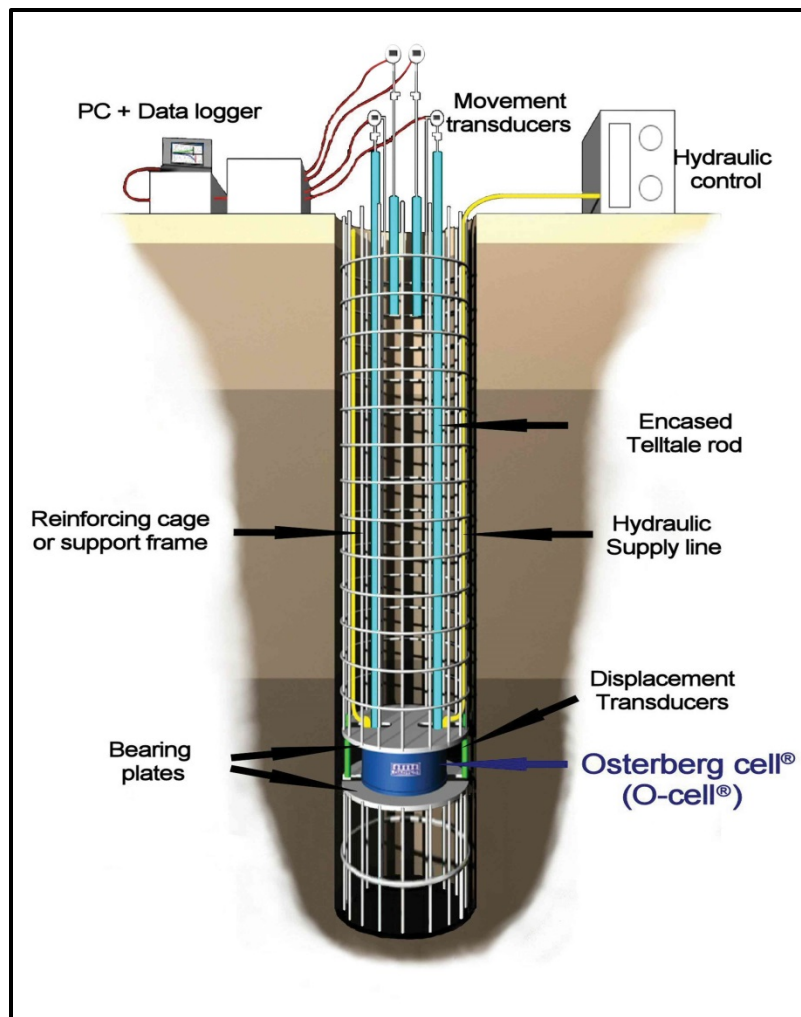


**Figure 24-2, Bi-Directional Testing Schematic  
(LOADTEST, Inc. (2015))**

Listed below are some advantages of the bi-directional static load test:

- Large reaction capacity allows testing of production-sized shafts
- With multiple cells or proper instrumentation, the base and side resistance are isolated from the resistance of other geomaterial layers
- Loading is static and can be maintained to observe creep behavior

Following are some of the disadvantages of bi-directional static load testing:

- The test shaft must be preselected so that the O-cells can be included
- It is not possible to test an existing shaft
- For each installed device, testing is limited to failure of 1 part of the shaft only, unless multiple O-cells are used
- The performance of a production shaft subject to top down loading must be computed and may require extrapolation of data in some cases
- Limitations exist related to using a test shaft as a production shaft
- The effect of upward directed loading compared to top down loading in a rock socket is not completely understood
- Displacement/capacity of shaft is limited by the stroke of the O-cell
- O-cell must be calibrated for anticipated displacement prior to testing or max capacity may not be achieved



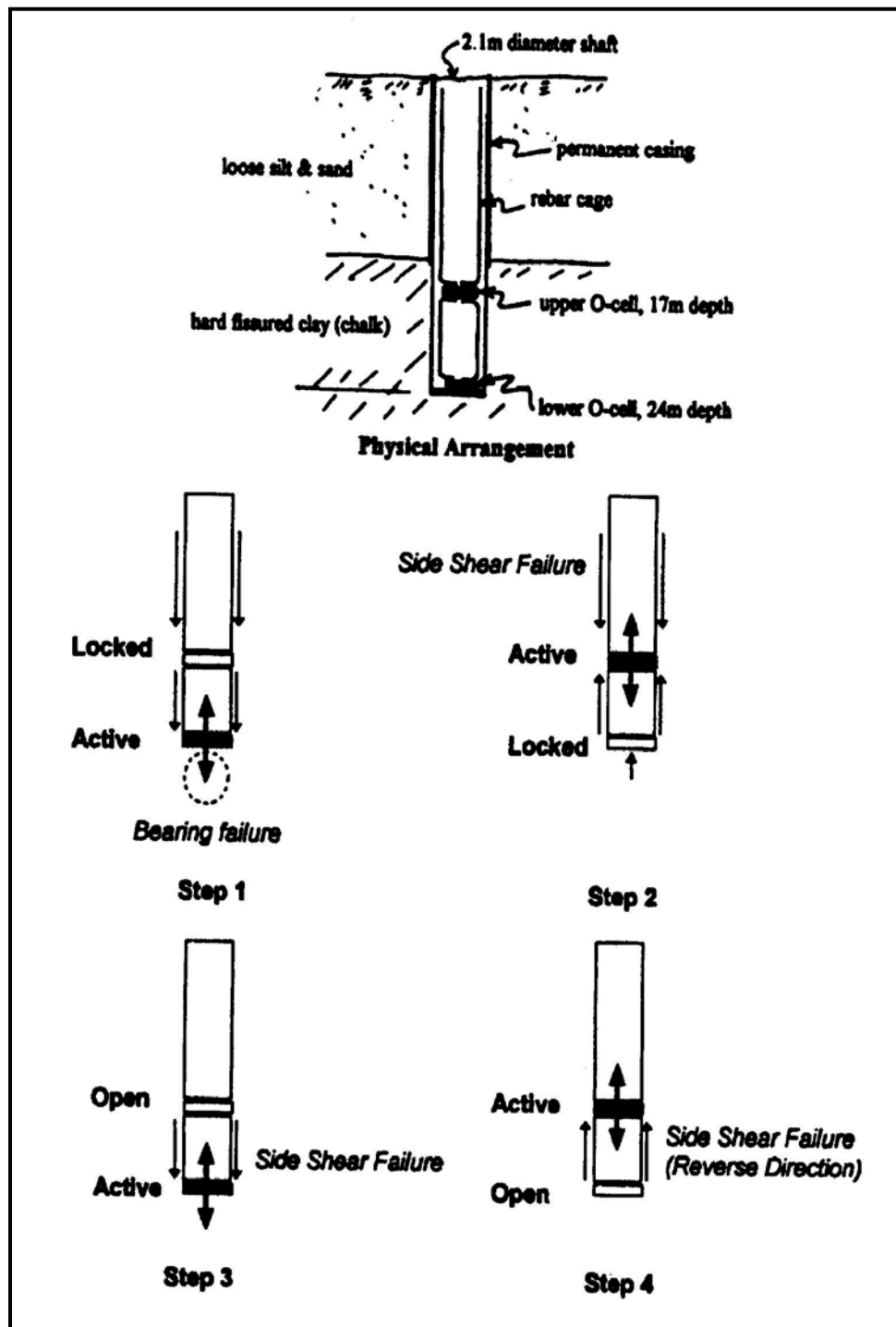
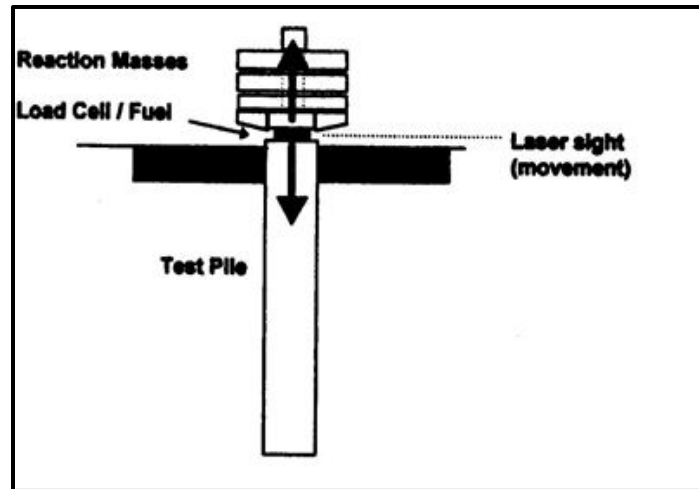


Figure 24-3, Multiple O-cell Arrangement (O’Neil and Reese, 1999)

Rapid load testing is between static load testing and high-strain testing of drilled shafts. Rapid load testing is typically performed on a test shaft that will not be incorporated into the structure. In rapid load testing the drilled shaft is subjected to a “fast push” instead of a sharp blow as would be delivered by a pile driving hammer or a falling weight. In a rapid test, the drilled shaft acts essentially as a rigid body with the top and base of the shaft moving together. Refer to STS SC-M-713-3 for *Rapid Axial Load Testing of Drilled Shafts* construction requirements.

There are 2 methods of inducing load during the rapid test. The first method consists of dropping a weight onto the shaft, but having a soft cushion located at the top of the shaft. The soft cushion causes the weight to decelerate over a required time interval. The second method, and most common, is to accelerate a heavy mass upward using combustion gas pressure, thus pushing the shaft into the ground. Using the second method, commercially available as the Statnamic® load test apparatus, a reaction mass is accelerated vertically while an equal and opposite reaction occurs in the drilled shaft.



**Figure 24-4, Rapid Load Test Setup  
(O'Neil and Reese, 1999)**

Listed below are advantages of the rapid load test method:

- Test resistances up to 10,000 kips (Statnamic®)
- Can test existing or production shafts
- Economies of scale for multiple tests
- Easily used for verification testing on shafts
- Reaction system not needed

Some disadvantages are:

- High capacity, but still limited compared to bi-directional tests
- Rate effects must be considered
- Mobilization costs for reaction weights

High-strain load testing of drilled shafts uses the same equipment and principles as PDA testing and CAPWAP analysis in driven piles. High-strain load testing uses a hammer or weight to strike the top of a shaft inducing a compression wave that propagates the length of the shaft and reflects back to the top. High-strain load testing is typically performed on a test shaft that will not be incorporated into the structure. The impact load can be induced using drop weights (see Figure 24-5) or a large pile driving hammer. If suitable measurements are obtained, then the applied load and drilled shaft response can be determined. The measurements are obtained using transducers and accelerometers mounted directly to the top of the shaft. A computer model of the shaft response to the blow is calibrated to the measurements using a signal matching technique (i.e., CAPWAP). The high-strain dynamic load test setup should always be modeled prior to testing using a wave equation model for specific shaft size and axial capacity. Because the high impact velocity can produce significant compression and tension forces in the shaft, the blow is typically cushioned using a cushioning material such as plywood or a striker plate. Refer to STS SC-M-712-2 for *High Strain Dynamic Load Testing of Drilled Shafts* construction requirements.



**Figure 24-5, High-Strain Load Testing Apparatus  
(GRL Engineers, Inc. (2015))**

Listed below are advantages of high-strain load testing:

- Large load applied at top of shaft
- Can test existing or production shafts
- Economies of scale for multiple tests
- Easily used for verification testing on production shafts
- Reaction system is not needed

Some disadvantages are:

- High resistance possible, but still limited compared to bi-directional tests
- Test includes dynamic effects which must be considered
- The applied force is interpreted from measurements on the shaft rather than from direct measurement of load and therefore is sensitive to the shaft modulus, area, and uniformity in the top 1 to 1-1/2 diameters
- Test must be designed to avoid potential damage to the shaft from driving stresses
- Mobilization costs for a large pile driving hammer or drop hammer
- Location and configuration of reinforcing steel must be accommodated
- Changes in impedance along the length of the shaft can be confused with changes in axial resistance, and therefore the impedance profile of the shaft must be reliably known.
- There may be incomplete mobilization of base resistance at early blows and loss of side resistance after multiple blows, and this issue complicates the interpretation of results.

## **24.5 EARTH-BORNE CONSTRUCTION VIBRATION MONITORING**

Earth-borne vibrations are the motion of a ground particle, at a point in the subsurface or on the ground surface, caused as vibration energy passes through that point. The actual distance that the ground particle moves, either positively or negatively, from its at-rest position is called displacement and is typically very small and is reported in units of inches or mils (thousandth of an inch). Construction induced vibrations may also be described as velocity, measured in

inches per second (ips), and/or acceleration measured in inches per second per second (in/sec<sup>2</sup>). Velocity is the speed at which the ground particle oscillates and should not be confused with the velocity which the wave travels through the ground (i.e. propagation velocity). Acceleration is the rate of change of velocity with time and is often normalized with the gravitational acceleration on the earth's surface (32.2 ft/sec<sup>2</sup> or 386.4 in/sec<sup>2</sup>) and is reported in g's as a percent of gravity. The most common way of determining the impact of earth-borne vibrations is velocity with the peak particle velocity (PPV) being the maximum instantaneous positive or negative peak of the vibration signal. Earth-borne vibrations may be generated by various construction activities including but not limited to: pile driving (both impact and vibratory), compaction efforts (both static and vibratory), drilled shaft installation, normal construction traffic (i.e. loaded dump trucks, bulldozers, etc.), and paving operations including pavement breaking. Monitoring of earth-borne vibrations is a relatively specialized area and may be performed on construction projects that have no other instrumentation; therefore, monitoring of earth-borne vibrations is exempted from the requirements of the Geotechnical Instrumentation Monitoring Plan (GIMP), as discussed in later Sections of this Chapter. However, the GEOR may elect to include the monitoring of earth-borne vibrations in the GIMP if other geotechnical instruments are required during construction.

### 24.5.1 General

Construction induced ground motions are divided into 3 main wave types: compression (P), shear (S) and surface (R – Rayleigh). P- and S-waves are called “body” waves, while the R-wave is “surface” wave. The “surface” may be the ground surface or a boundary of the halfspace. R-waves consist of horizontal and vertical components that attenuate (i.e. dampen out) rapidly with depth. P- and S-waves tend to propagate through the soil in a hemispheric shape, while R-waves tend to propagate cylindrically through the soil. P-, S-, and R-waves travel at different speeds, with the P-wave being the fastest, followed by the S-wave with the R-wave being the slowest. Therefore, the P-wave arrives first at the receptor, then the S-wave, followed lastly by the R-wave (see Figure 24-6). According to Andrews, Buehler, Gill, and Bender (2013) approximately 67 percent of the wave energy is transmitted by the R-wave, 26 percent by the S-wave and the remaining 7 percent by the P-wave.

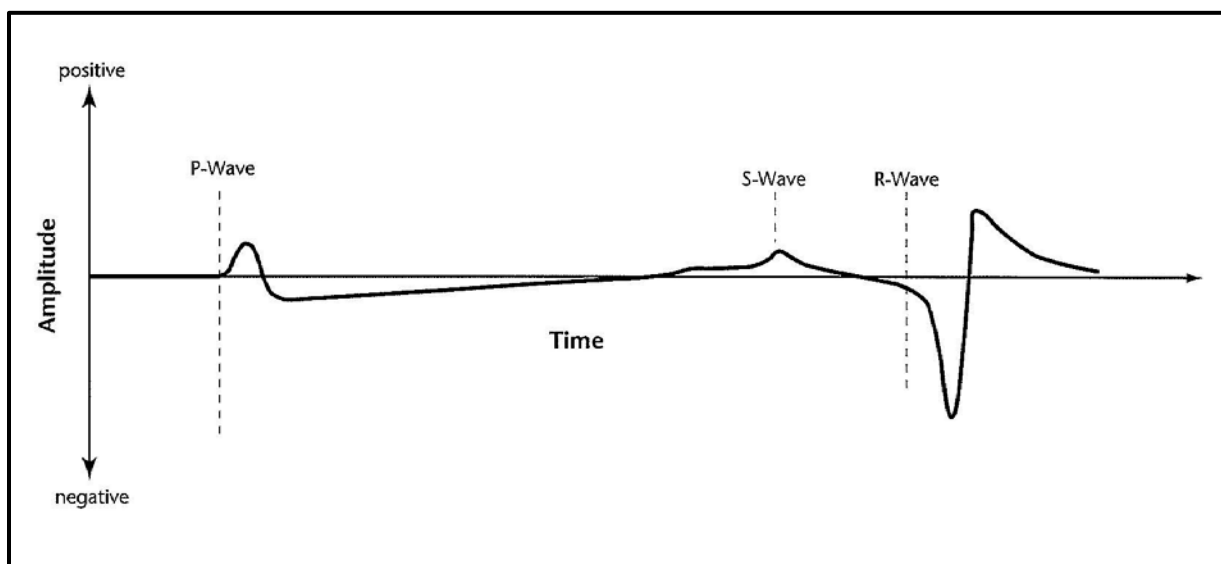


**Figure 24-6, Arrival Time for P-, S-, and R-waves  
(Andrews, et al. (2013))**

To properly describe the ground motion as the earth-borne vibrations passes through it, 3 mutually perpendicular components must be measured. A triaxial geophone has 3 independent transducers, each aligned at mutually perpendicular directions. The longitudinal direction is

aligned with the axis of vibration propagation and the longitudinal geophone measures the compression or P-wave. The transverse direction is at a right angle to the longitudinal direction within the same horizontal plane. The transverse geophone measures the shear or S-wave. The vertical direction measures the movement in the vertical plane, which often has the highest amplitude.

Vibration-producing activities such as blasting, pile driving, vibratory compaction, and the operation of other heavy equipment are common activities on a highway construction project. It may be desirable to monitor the ground vibrations induced by these activities if sensitive equipment or structures are located close to the work zone. Please note that earth-borne vibrations induced by blasting are not included in this Manual, contact the PCS/GDS if blasting is required on a project for specific instructions on design and preparation of a Special Provision to monitor earth-borne vibrations induced by blasting.

Earth-borne construction vibrations can adversely impact 3 types of receivers: structures, people and equipment/operations. Of these 3 types of receivers, structures typically can sustain the highest vibration levels without being impacted; these impacts are normally described as damage. The impacts to humans are best described as annoyance or disturbance, while the impacts to equipment/operations are described in terms of hindering or reducing functionality. The impacts to these receivers are discussed in the following paragraphs.

### **24.5.2 Structures**

The use of the term damage can be a very misleading term since damage can range from hairline cracks in sheetrock walls to complete collapse of the structure. Dowding (1996) provides a more precise definition of damage as generally used by the blasting industry. The definitions are provided below:

- Cosmetic cracking including threshold damage – Opening of old cracks, and formation of new plaster cracks; dislodging of loose structural particles such as loose bricks in chimneys
- Architectural or minor damage – Superficial, not affecting the strength of the building (e.g. broken windows, loosened or fallen plaster), hairline cracks in masonry
- Structural cracking or major damage – Serious weakening of the building or adjacent facilities (e.g. large cracks or shifting of foundations or bearing walls, major settlement resulting in distortion or weakening of the structure, walls out of plumb)

Project vibration limits are typically established to prevent threshold or cosmetic cracking.

### **24.5.3 People**

Earth-borne construction vibrations affect people in 2 ways; the vibrations can annoy people and/or the vibrations cause the perception of damage. People can feel vibrations far below the level that causes damage to structures, but can be very annoying or cause loose items within the structure to rattle (i.e. windows, dishes, etc.). When people feel vibrations or hear items rattling, they almost immediately think of damage and start looking for evidence of damage. Often people discover cracks in walls, ceilings, or foundations that hadn't been previously noticed and now associate the cracks with the earth-borne construction vibrations.

### **24.5.4 Equipment/Operations**

Vibrations can adversely impact sensitive equipment and/or operations, such as hospitals, computerized industries, research centers or industrial machinery. Some equipment (i.e. optical microscopes, cell probing devices, magnetic resonance imaging (MRI) machines, scanning

electron microscopes, photolithography equipment, micro-lathes, and precision milling equipment, etc.) can be more sensitive than humans since the operation of the equipment can be impaired below the vibration perception threshold. However, most of this equipment and/or operations must be isolated within the building housing the equipment or operations to prevent normal building activity from disturbing the equipment and/or operation. Because of this earth-borne construction vibrations rarely impact sensitive equipment/operations.

### **24.5.5 Impact of Earth-borne Construction Vibrations**

Based on research performed by the Minnesota Department of Transportation (MnDOT), cosmetic damage cannot typically be attributed to construction vibration levels below 0.5 ips. Therefore, MnDOT established the distance at which earth-borne construction vibrations will be below 0.1 ips. This level (0.1 ips) was selected since people complain about vibrations having a velocity of more than 0.1 ips. These distances are provided in the following table for various construction activities and may be used for preliminary estimating.

**Table 24-1, Distance where Vibration drops below 0.1 ips  
(MnDOT (2013))**

<b>Construction Activity</b>	<b>Distance<sup>1</sup> (feet)</b>
Embankment Compaction	50
Subgrade Compaction	100
Vibratory Pile Driving <sup>2</sup>	150
Pavement Breaking	180
Bituminous Overlay	200
Impact Pile Driving	200
Construction Blasting	300

<sup>1</sup>For estimating purposes only

<sup>2</sup>SCDOT assumes that vibration of drilled shaft casing would have the same distance

Pile driving can create earth-borne vibrations that can cause damage to structures and disturb people nearby. Other construction activities, such as pavement breaking, vibratory compaction, and the general use of heavy hauling and excavating equipment, typically produce earth-borne vibrations that are below the level necessary to cause damage, unless the source of the vibrations is very close (< 25 feet). Therefore, these lower intensity vibrations can be considered annoying and may cause people to believe that the building is being damaged, when in reality it is not being damaged. However, there are certain conditions such as close proximity to historical buildings or buildings that house historical or antique artifacts that may require special attention to avoid damaging the structure or the artifacts in the structure.

People's perception of vibration is not an accurate gauge of the damage potential of vibration. Therefore, when assessing the potential for impacts due to earth-borne construction vibrations, it is necessary to consider both: the actual potential to cause damage and the potential for causing complaints about being damaged. Vibrations do not affect all structures similarly. Some of the factors that may affect a structures ability to withstand vibrations are: condition, type of construction, geometry, orientation, subsurface geology, etc.

Structures are typically strongest immediately after construction and become weaker through the years as the structure receives many cycles of stress-strain caused by changes in temperature and humidity, ongoing vibration events, and settlement of the foundation soils. Damaged structures are typically more susceptible to additional damage caused by an external vibration event. Historic structures are typically in poorer condition than more modern structures due to their longevity and inferior building materials. Therefore, historic structures are typically

given a lower vibration limit than more modern structures, since materials to make repairs may no longer be available and permanent loss of the historic structure may not be considered tolerable to the public. The existing condition of a historic structure shall always be assessed within a given radius of the source of earth-borne construction vibrations. This radius is normally established based on prior experience; calculations based on damage probability and predicted vibration levels; political concerns; or a combination of all 3.

Structures that have been engineered are typically constructed of stronger, more durable materials (e.g. steel and concrete) than non-engineered structures constructed of materials like wood. The engineered structures are often founded on deep foundations or on improved soil to increase bearing resistance and decrease settlement.

### 24.5.6 Vibration Prediction

Andrews, et al. (2013) provides various equations to estimate the PPV for various pieces of construction equipment at differing distances from the construction equipment. The construction equipment includes impact pile drivers, vibratory pile drivers, hydraulic breakers, and other general construction equipment (i.e. vibratory rollers, bulldozers, loaded trucks, etc.). The equation for estimating the PPV for impact pile driving (IPD) is:

$$PPV_{IPD} = 0.65 * \left(\frac{25}{D}\right)^n * \left(\frac{E_{IPDEquip}}{36,000}\right)^{0.5} \quad \text{Equation 24-1}$$

Where,

PPV<sub>IPD</sub> = Peak Particle Velocity induced by impact pile driving, ips

D = Distance from pile driver to the receiver, ft

n = A value related to the vibration attenuation rate through ground, see Table 24-2

E<sub>IPDEquip</sub> = Rated energy of impact pile driver, foot-pounds (ft-lbs)

The constant 0.65 in the above equation is the reference PPV for the reference pile driver at a distance of 25 feet from the pile driver and has units of ips. The constant 36,000 is the rated energy of the reference pile driver in ft-lbs. The term “n” is determined using Table 24-2 to more accurately account for in-situ soils.

**Table 24-2, Suggested “n” Values Based on Soil Class  
(Andrews, et al. (2013))**

Soil Class	Description of Soil Material	“n”
I	Weak or soft soils: loose soils, dry or partially saturated peat and muck, loose beach sand, and dune sand, recently plowed ground, soft spongy forest or jungle floor, organic soils, top soil. (shovel penetrates easily)	1.4
II	Competent soils: most sands, sandy clays, silty clays, gravel, silts, weathered rock. (can dig with shovel)	1.3
III	Hard soils: dense compacted sand, dry consolidated clay, consolidated glacial till, some exposed rock. (cannot dig with shovel, need pick to break up)	1.1
IV	Hard, competent rock: bedrock, freshly exposed rock. (difficult to brake with hammer)	1.0

The equation for estimating the PPV for vibratory pile driver (VPD) is very similar to the equation for impact pile drivers; with the exception the rated energy of the pile hammer is not required. The equation below is used to estimate the PPV<sub>VPD</sub>:

$$PPV_{VPD} = 0.65 * \left(\frac{25}{D}\right)^n \quad \text{Equation 24-2}$$

Where,

$PPV_{VPD}$  = Peak Particle Velocity induced by vibratory pile driving, ips

D = Distance from pile driver to the receiver, ft

n = A value related to the vibration attenuation rate through ground, see Table 24-2

The constant 0.65 in the above equation is the reference PPV for the reference pile driver at a distance of 25 feet from the pile driver and has units of ips.

The equation for estimating the PPV for hydraulic breakers (HB) (also called hoe-rams, mounted impact hammers, etc.), for the demolition of concrete structure or pavement (i.e., asphaltic concrete or Portland cement concrete) is very similar to the equation for impact pile drivers; with the exception that the referenced energy of the hydraulic breaker is reduced to 5,000 ft-lbs and the  $PPV_{REF}$  is reduced to 0.24 ips for the reference hydraulic breaker. The equation below is used to estimate the  $PPV_{HB}$ :

$$PPV_{HB} = 0.24 * \left(\frac{25}{D}\right)^n * \left(\frac{E_{HBEquip}}{5,000}\right)^{0.5} \quad \text{Equation 24-3}$$

Where,

$PPV_{HB}$  = Peak Particle Velocity induced by hydraulic breaker, ips

D = Distance from hydraulic breaker to the receiver, ft

n = A value related to the vibration attenuation rate through ground, see Table 24-2

$E_{HBEquip}$  = Rated energy of hydraulic breaker, foot-pounds (ft-lbs)

Andrews, et al. (2013) recommend that the PPV for other construction equipment ( $PPV_{ConstEquip}$ ) can be estimated using the following equation. The reference PPV ( $PPV_{Ref}$ ) for different pieces of construction equipment can be obtained from Table 24-3.

$$PPV_{ConstEquip} = PPV_{Ref} * \left(\frac{25}{D}\right)^n \quad \text{Equation 24-4}$$

Where,

$PPV_{ConstEquip}$  = Peak Particle Velocity induced by various pieces of construction equipment, ips

$PPV_{Ref}$  = Reference PPV for various pieces of construction equipment at 25 ft, ips, see Table 24-3

D = Distance from construction equipment to the receiver, ft

n = A value related to the vibration attenuation rate through ground, see Table 24-2

**Table 24-3, Reference PPV for Various Pieces of Construction Equipment  
(Andrews, et al. (2013))**

Equipment	$PPV_{Ref}$ at 25 ft (ips)
Vibratory roller	0.210
Large bulldozer	0.089
Caisson drilling	0.089
Loaded trucks	0.076
Jackhammer	0.035
Small bulldozer	0.003
Crack-and-seat operation	2.400



### 24.5.7 Vibration Criteria

Vibrations can be created by either continuous/frequent intermittent sources or by transient sources. Continuous sources of vibrations include: excavation equipment; static compaction equipment; tracked vehicles; traffic on a highway; vibratory pile drivers; pile-extraction equipment; and vibratory compaction equipment. Transient sources of vibrations include: impact pile drivers; blasting (not covered by this Manual); drop balls; “pogo stick” compactors; and rubbleization (i.e., break-and-seat or crack-and-seat) equipment. Single transient vibration sources will not be considered for developing criteria; however, some of the sources of transient vibrations such as impact pile driving and crack-and-seat operations will be considered frequent intermittent sources for this Manual. Provided in the following table are structure types including condition and the maximum allowable PPV.

**Table 24-4, Maximum Allowable PPV for Structures**

Structure Type and Condition	Maximum PPV <sup>2</sup> (ips)
Extremely fragile historic buildings, ruins, ancient monuments <sup>1</sup>	0.08
Fragile buildings <sup>1</sup> (i.e. sensitive structures and hospitals)	0.10
Historic and some old buildings <sup>1</sup>	0.25
Older residential structures (i.e. built with plaster and lathe)	0.30
New residential structures (i.e. built with sheetrock)	0.50
Modern industrial/commercial buildings (i.e. engineered)	0.50

<sup>1</sup>Contact SCDOT Environmental Services or the Program Manager for a list of historic structures adjacent to the project site.

<sup>2</sup>PPVs will have frequencies in the range of 1 to 100 Hertz.

As indicated previously, people living near a construction site can feel the earth-borne vibrations that are induced by construction. An individual’s reaction may include annoyance and/or the perception that damage is being caused by the vibrations. Provided in the following table are various PPVs that could lead to annoyance of those people who reside around the construction site.

**Table 24-5, Maximum Allowable PPV to Avoid Annoyance**

Human Response	Maximum PPV (ips)
Barely Perceptible	0.01
Distinctly Perceptible	0.04
Strongly Perceptible	0.10
Severe	0.40

No maximum PPV values have been established for sensitive equipment or operations. Project specific PPVs will need to be developed for ultra-sensitive/sensitive equipment or operations.

### 24.5.8 Earth-borne Vibration Monitoring Evaluation

The GEOR shall evaluate the potential impact of earth-borne vibrations from a construction site on the surrounding/adjacent properties. Previous studies have shown that blasting, pile driving and pavement breaking have been documented to have the potential to cause damage to structures. As indicated previously, blasting will not be covered by this Manual. If blasting is required on a project site, contact the PCS/GDS for further instructions. For pile driving and pavement breaking, the potential damage from earth-borne vibration is at locations in relatively close proximity to the activity. However, because the threshold of perception for vibration is much lower than the threshold for damage, claims of damage often arise because of perceptible vibration and not because of actual damage. To limit the potential for damage claims related to earth-borne vibrations, Andrews, et al. (2013) has developed the following process:

- 1) Identify potential problem areas surrounding the project site
- 2) Determine conditions that exist before construction begins
- 3) Inform the public about the project and potential vibration-related consequences
- 4) Schedule work to reduce adverse effects
- 5) Design construction activities to reduce vibrations
- 6) Notify nearby residences and property owners that vibration-generating activity is imminent
- 7) Monitor and record vibration from the activity
- 8) Respond to and investigate complaints

As part of first step, the GEOR shall estimate the PPV at various distances from the project for the various pieces of construction equipment anticipated being used for project construction. These estimated PPVs shall be provided in both the preliminary as well as final geotechnical reports for the project site. The PPVs estimated for the PGER should be anticipated being very approximate since no pile energy requirements will be developed at this stage. The estimated PPVs from this study will be used to determine if there is a potential earth-borne vibration concern at a project site. The distances provided in the table below shall be used. These distances are measured from the source of the vibration (i.e. from either end of the bridge for pile driving). However, it should be noted that the distance between potential vibration sources and receptors may need to be increased, especially if the project is not viewed by the general public as being beneficial or if the project is unpopular. The GEOR shall consult with the project team to determine if there is public perception concern with the project.

**Table 24-6, Distance between Vibration Source and Potential Receptors**

Potential Receptor	Distance (ft)
Sensitive structures	700
Hospitals	500
Extremely fragile historic buildings, ruins, ancient monuments <sup>1</sup> , other historic or old buildings	300
Residential structures: Older residential structures (i.e. built with plaster and lathe) New residential structures (i.e. built with sheetrock)	250
Engineered structures (i.e., modern industrial/commercial buildings)	150

<sup>1</sup>Contact SCDOT Environmental Services or the Program Manager for a list of historic structures adjacent to the project site.

The identification of these potential receptors shall be made during the initial site visit prior to commencing field operations. The GEOR shall attempt to identify all potential receptors within the given radius. For example, if a hospital is located 450 feet from one end of the project, a 500-foot radius from either end of the project will be used and all residential and engineered structures within that radius will be identified. Therefore the larger distance shall be used for potential receptor identification purposes and all structures within that distance shall be considered regardless if the structure is located beyond the limit established for that structure, (i.e., a residential structure located 350 feet from the bridge with a hospital located 450 feet away from the bridge). The identification will include the type of structure (i.e. residential, engineered, historic, etc.), the name of the property owner, the street address of the property and unique identifier for each property. Names of property owners can be obtained from the SCDOT ROW Office or from local property tax records.

For the purpose of this Manual, sensitive receptors have equipment and/or operations similar to optical microscopes, cell probing devices, magnetic resonance imaging (MRI) machines, scanning electron microscopes, photolithography equipment, micro-lathes, and precision milling equipment. This list is not meant to be all inclusive. If industrial facilities are noted within 700

feet, contact the Program Manager for additional information. The Program Manager should either contact the facility or request the ROW Office to contact the facility to determine what the industrial process is and if it is vibration sensitive. A hospital as defined for this Manual is a medical facility that contains surgical suites; operating theatres or MRI machines. This could include some Medical Office Buildings that have the capability for having outpatient procedures performed. As indicated in Table 24-6, contact either the SCDOT Environmental Services Office or the Program Manager for a list of identified historic buildings, ruins and monuments. Residential structures can be single or multi-family. Engineered structures are typically constructed of steel and/or concrete, are used for non-residential purposes and do not contain sensitive operations as previously discussed.

Once the GEOR has identified the potential receptors or lack thereof around a construction site, in the second step, the Director of Construction in consultation with the project team, the SCDOT Construction Office, and the District Construction Engineer (DCE) will determine whether vibration monitoring is required or not.

There will be times when a property owner will not allow their structures to be surveyed. A notation shall be made as to time and date, the specific comment made as well as who made the statement. On some occasions, a property owner may terminate the preconstruction damage assessment survey prior to its completion. This termination shall be noted with the same information as that required when survey isn't permitted.

It may be advantageous to conduct a post construction damage assessment survey to verify that no additional damage has been caused by construction activities. The decision to perform a post construction damage assessment survey should be made by project team in consultation with the Director of Construction, the DCE and the RCE.

The third step in this evaluation process is notifying the public vibrations may be generated during construction. This announcement should be prepared by the project team and sent to all property owners previously identified in Step 1. This announcement will be made in whatever method is deemed appropriate by the project team, including the SCDOT ROW Office.

The fourth step is to schedule work to reduce adverse effects of earth-borne vibrations. For example, if pile driving is to be performed in a primarily residential area, the contract may include a Special Provision indicating that pile driving may only be performed during certain hours, with those hours coinciding with the normal work day. The Contractor will typically be responsible for determining the construction schedule and the Contractor should be aware of the potential impacts on the surrounding properties from earth-borne vibrations induced by construction activities.

The fifth step is to design construction activities to minimize earth-borne vibrations. The GEOR may minimize earth-borne vibrations by using a smaller hammer, requiring a new pile cushion for each pile, etc.

As part of the sixth step, the project team is required to inform all property owners identified previously that vibration inducing activities will commence on a given date. In addition, provide a written notice 7 calendar days prior to the construction activity at a minimum. The notice should consist of a letter sent to each property owner.

Earth-borne vibrations shall be monitored and recorded in accordance with the project specific Special Provision for *Earth-borne Vibration Monitoring*.

The final step is to respond to and investigate all complaints that have been generated as a result of the earth-borne vibrations. The process for handling complaints and the investigation

of the complaints shall be determined by the RCE with consultation with the project team, the Director of Construction the DCE and the RCE.

### **24.5.9 Addressing Earth-borne Vibration Concerns**

SCDOT has developed 2 levels of earth-borne vibration monitoring that can be provided on a project, depending on several things such as structure susceptibility to damage, proximity to vibration producing activities, etc.

**Level 1** – No potential receptors within the specified distances previously provided. No vibration monitoring required.

**Level 2** – Potential receptors are located within the specified distances indicated in Table 24-6. Earth-borne vibration monitoring may be required. The need for earth-borne vibration monitoring will be determined by the project team in conjunction with the Director of Construction, the DCE and the RCE. If required, earth-borne vibration monitoring will be performed by SCDOT. In addition, the project team, the Director of Construction, the DCE and the RCE will jointly decide if a pre-construction baseline vibration monitoring study is required. The RCE in conjunction with the project team, the Director of Construction, and the DCE will determine whether a pre-construction and/or post-construction damage assessment survey will be required and conducted. The GEOR shall prepare a Special Provision for each project that requires earth-borne vibration monitoring.

The appropriate level of Earth-borne Vibration Monitoring shall be indicated on the “General Notes” sheet of bridge plans. In addition, the appropriate level shall also be indicated on the “General Notes” sheet of road plans as required.

### **24.5.10 Earth-borne Vibration Monitoring Equipment**

A vibration-monitoring unit generally consists of some combination of geophones, sound sensors and connecting cables attached to an input and readout unit. Ground vibrations are typically reported in terms of the peak particle velocity (PPV), although other parameters such as peak acceleration, principle frequencies, and peak sound pressure levels can also be obtained with most monitoring units. Vibration monitoring results are then compared with pre-established threshold levels of structures or equipment to determine the level of risk involved.

Portable seismographs are typically used for monitoring the velocities of ground vibrations resulting from construction activities. The seismographs should have the following minimum features:

- Seismic range: 0.01 to 5 ips with an accuracy of  $\pm 5$  percent of the measured PPV or better at frequencies between 1 and 100 Hz and with a resolution of 0.01 ips or less.
- Frequency response ( $\pm 3$  dB (decibels)) : 2 to 200 Hz

Three channels for simultaneous time-domain monitoring of vibration velocities in digital format on 3 perpendicular axes or components: 1 vertical and 2 horizontal (radial and transverse). The seismograph shall be positioned with the longitudinal axis toward the vibration source.

### **24.5.11 Baseline Earth-borne Vibration Study**

For a Level 2 earth-borne vibration monitoring scenario, the project team, the Director of Construction, the DCE and the RCE may require a baseline earth-borne vibration study. This baseline study should be considered if sensitive structures, hospitals or historic buildings are

located within the specified distances given in Table 24-6 of the proposed project site. In addition, the baseline earth-borne vibration study may be considered for other structures around the project. The purpose of the baseline earth-borne vibration study is to establish the background levels of vibration that are induced at a site by existing sources such as traffic, industrial machinery or railroads, etc. In some cases the vibrations from these sources may exceed the limits allowed in this Chapter. The baseline vibration study should be performed for at least 6 months but for no more than 12 months prior to the commencement of construction. The baseline earth-borne vibration study shall be performed by 1 of the consultants selected for the “On Call Structure Foundation Testing and Engineering Services” contract. GECs shall contact the RPG/GDS for list of consultants on the contract. The results of the baseline earth-borne vibration study shall be provided to the GEOR, who shall use the baseline study to prepare an Earth-borne Vibration Monitoring Special Provision.

#### **24.5.12 Pre- and Post-Construction Condition Survey**

As indicated previously, the RCE in consultation with the project team, the Director of Construction and the DCE will determine if Pre- and/or Post-Construction Condition Survey of the structures surrounding the project is required. The Pre- and Post-Construction Condition Survey will occur prior to the commencement of vibration inducing construction activities and immediately after completing vibration inducing construction activities. The purpose of this survey is to determine the condition of the structures surveyed prior to commencing vibration inducing construction activities and serves as evidence of or lack of damage induced by the vibrations. Measure the Source to Potential Receptor distance from both ends of the bridge or source of vibrations. Include documentation of interior floor surfaces whether slab-on-grade or floor with crawl space beneath and above grade accessible walls, ceilings, floors, roofs and the visible exterior as viewed from the ground level. The survey should detail (by engineering sketches (including measurements), digital video, digital photographs and/or field notes) any existing structural, cosmetic, plumbing or electrical damage. All documentation of existing building conditions and information concerning the type and location of crack monitors shall be presented to the GEOR in a report prior to or immediately after any vibration inducing construction activity. If crack monitors are used, the GEOR shall establish the schedule for when the monitors are to read. This schedule shall be provided to the RCE for the actual collection of the data by 1 of the consultants selected for the “On Call Structure Foundation Testing and Engineering Services” contract. The consultant shall provide the results to the RCE who will in-trun provide the results to the GEOR for evaluation. Likewise immediately after the completion of vibration inducing construction activities, conduct a Post-Construction Condition Survey to include documentation of any differences in the defects noted in the Pre-Construction Condition Survey as well as any new defects.

#### **24.5.13 Earth-borne Vibration Monitoring Plan Notes**

The GEOR shall ensure that 1 of the notes provided in Chapter 22 is placed on the appropriate plan sheets.

#### **24.5.14 Earth-borne Vibration Monitoring Special Provision**

The GEOR is required to prepare an Earth-borne Vibration Monitoring Special Provision for inclusion in the construction contract. The Special Provision shall indicate the Level of Earth-borne Vibration Monitoring required for that specific project. For Level 1 no earth-borne vibration monitoring is required since there are no potential receptors present within the indicated distances (see Table 24-6). As indicated previously, the project team, the Director of Construction, the DCE and the RCE will decide if earth-borne vibration monitoring is required for Level 2 based on the number, location and type of potential receptors near the project. Please note that Level 2 will be marked on the appropriate “General Notes” sheets because of the

presence of potential receptors. If the decision is made to not perform earth-borne vibration monitoring, then no Special Provision will be required. If the decision is made to perform earth-borne vibration monitoring, then a Special Provision is prepared indicating to the Contractor that is a Level 2 site and the monitoring will be performed by the Department. The Special Provision should include at a minimum:

- The required threshold PPV to be below
- The distance to the nearest structure of concern
- If earth-borne vibration monitoring affects the Contractor's means and methods, any and all costs associated with changing means and methods are considered incidental to the construction item
- That RCE may halt construction if the threshold PPV is exceeded
- No time or money will be provided to the Contractor if the RCE halts construction due to exceeding the threshold PPV
- The Contractor is required to alter vibration producing activity to obtain PPVs below the threshold PPV
- Indicate if a Pre-Construction Condition Survey is conducted
- Indicate that the RCE will determine if a Post-Construction Condition Survey will be conducted
- All damage that occurs from exceedance of the threshold PPV will be the responsibility of the Contractor to repair at no additional cost to SCDOT
- Any damage that occurs below the threshold PPV will be the responsibility of SCDOT

## 24.6 GEOTECHNICAL INSTRUMENTATION

This Section provides a general overview of the selection and use of geotechnical instrumentation for SCDOT construction projects. There are 2 general classes of geotechnical instrumentation. The first class is those instruments used to investigate and evaluate soil and rock properties. This class of geotechnical instrumentation is presented in Chapter 5 – Field and Laboratory Testing Procedures. The second class is those geotechnical instruments that monitor performance during and after construction. This Section is not intended to provide specifications for individual instruments, but rather to provide a systematic approach to the planning for and implementation of an instrumentation and monitoring plan that includes a discussion of the requirements for the instrumentation, location of the instrumentation and monitoring of the instrumentation. For more specifics regarding the information presented herein, please refer to Dunncliff (1998). Listed below are the Supplemental Technical Specifications (STSs) for selected geotechnical instruments. If a geotechnical instrument is required for which an STS is not written, then the GEOR is required to develop a Special Provision in accordance with Chapter 23.

**Table 24-7, STSs Available from SCDOT**

<b>STS Name</b>	<b>STS Number</b>
Settlement Plates	SC-M-203-4
Vibrating Wire Piezometer	SC-M-203-6
Settlement Sensors	SC-M-203-7
Vibrating Wire Rod Extensometer	SC-M-203-8
Slope Inclinator Casing	SC-M-203-9
Total Pressure Cell	SC-M-203-10
Vibrating Wire Data Collection Centers	SC-M-899-1

This Section also discusses the interpretation of the results of geotechnical instrumentation. The results obtained from geotechnical instrumentation require review by the GEOR in order to determine if the data is meaningful. On projects in which the GEC reviews the results of

geotechnical instrumentation, the GEC shall be responsible for evaluating the geotechnical instrumentation data to determine if it meets the design requirements. The first question concerning the results of geotechnical instrumentation is: “Was the data collected in a manner consistent with the plans, specifications and special provisions?” If the data was not collected in a consistent manner, every effort should be made to determine why not. If the data collected is consistent, next check to determine the numerical accuracy. Finally, the data should be checked for consistency with previous data. If the data is not consistent, does a hypothesis exist that explains all the data? If not, then consideration should be given to the point that the data is bad and should be discarded. The interpretation of data collected from the various forms of geotechnical instrumentation will be discussed within each Subsection that covers a specific geotechnical instrument.

Field instrumentation on highway projects can play several vital roles, including the following:

- Verification of Design Parameters – Data obtained from instrumentation can be used to verify that the constructed embankment, slope, wall, etc. behaves as predicted during and after construction. Initial data can be used to modify the design if necessary.
- Evaluate Performance During Construction – Field instrumentation can be used to monitor construction performance of the embankment, slope, wall, etc. that may affect or be affected by construction activities and that may affect the construction schedule.
- Evaluate Performance of Existing Structures – Existing embankments, slopes, walls, etc. can be instrumented to assess the existing conditions and to guide remediation measures, if necessary.
- Detect short and long-term trends – Before potential problems are visible to observers, instrumentation can provide the first indication of how a structure is going to perform over short-term and long-term periods.
- Safety – Field instrumentation can serve as the first warning sign of a potentially unsafe situation. An instrumentation and monitoring program can also play a role in easing public concerns over safety of areas surrounding the construction site.
- Legal Protection – Instrumentation can provide documentation as to the relationship between construction activities and surrounding structures. In the event of litigation, data from these instruments can be used to prove/disprove connection of damage in surrounding areas to construction activity.

The planning of an instrumentation and monitoring program should be guided by a systematic approach. The steps listed in this Chapter provide a typical list of planning considerations that can be applied to most highway construction projects. The overall objective for the program should be decided before selection of instruments commences. As part of the planning process, the need for instruments should be gauged against such factors as relevance of the data obtained, impedance of construction, and cost.

Although the goal of this Chapter is not to provide specific guidelines on field instrumentation, the general philosophy given in Dunicliff (1998) should be applied to nearly every project where field instrumentation is to be used. First, every instrument should be installed to answer a specific question. More instrumentation than is required produces additional, perhaps harmful, discontinuities in the structure and may provide a false sense of security. Second, in general the simpler the instrumentation is, the more desirable it should be. Although some situations may arise where sophisticated instrumentation cannot be avoided, such as the need for remote monitoring, simpler instruments generally provide data that is just as reliable while having less

chance of malfunction, and at a reduced cost. Third, redundancy, or a system of checks, should always be built into the monitoring program to add another level of reliability beyond what is provided by a single instrument. If sophisticated instruments are to be used, standard, “low-tech” instruments can also be installed to maintain the flow of incoming data in case of malfunction in the sophisticated instruments.

## 24.7 MONITORING PLAN

A Geotechnical Instrumentation Monitoring Plan (GIMP) shall be prepared and submitted by the GEOR when any of the following conditions are met:

- A Vibrating Wire Data Collection Center or other automated monitoring device is to be used for a project
- When more than 2 geotechnical monitoring instruments are required
- When the consequences of failure of the construction being monitored could lead to a potential loss of life
- When a Chain of Command is required
- A GIMP is required by SCDOT

The GIMP should be submitted as part of either the BGER or the RGER, but may be submitted as a stand-alone document if permitted by the PC/GDS. The GIMP shall be submitted at least 3 months prior to the project letting date. After review and acceptance of the GIMP, the GEOR shall convert the GIMP into a Special Provision. The following Section shall be added at the end of the GIMP Special Provision:

### **BASIS OF PAYMENT**

No payment will be made for the Geotechnical Instrumentation Monitoring Plan (GIMP). All payments are considered incidental to the individual Geotechnical Monitoring Instruments required for this project.

The GIMP Special Provision shall be forwarded to the Letting Preparation Engineer for inclusion with the construction contract documents.

The elements to be included in the GIMP are detailed below and generally follow the guidelines set forth in Dunnycliff (1998). Table 24-8 provides a list of the elements used in developing a monitoring plan.

**Table 24-8, Monitoring Plan Elements**

1. Definition of Project Conditions	2. Objectives of Instrumentation
3. Predicted Magnitude of Change	4. Define Remedial Actions
5. Establish Responsibilities and Chain of Command	6. Types of Instruments and Locations
7. Recording of Outside Factors	8. Procedures for Ensuring Data Validity
9. Estimated Costs	10. Installation and Protection Plans
11. Calibration and Maintenance of Field Instruments	12. Data Processing

The monitoring plan as well as certain construction related items, such as monitoring, calibration and maintenance, data collection, processing, presentation, interpretation and reporting, are considered “professional services” and should not be left to the Contractor to perform. On most SCDOT construction projects geotechnical instrumentation is installed by the Contractor under the supervision of a licensed engineer. In addition, in many cases the monitoring, calibration



and maintenance and data collection are made the responsibility of the Contractor. In these cases, the Contractor shall be required to retain the services of a GEC, familiar with the instrumentation being used. The processing, presentation, interpretation and reporting are typically provided by the GEOR.

### **24.7.1 Definition of Project Conditions**

This Section of the instrumentation plan should include a summary of existing conditions and of proposed construction, if applicable. A short summary of the relevant information from BGER or RGER should be included in the monitoring plan. Other information that may be relevant to monitoring, such as condition surveys of existing structures or reports of environmental conditions, should also be summarized in the monitoring plan. All pertinent information about the project related to the monitoring program should be properly referenced in the monitoring plan. If additional information is needed to fully characterize the site, a plan for obtaining this information shall be submitted with the monitoring plan.

### **24.7.2 Objectives of Instrumentation**

The objectives of field instrumentation to be used on the project shall be clearly defined in the monitoring plan. The first step to defining objectives for field instrumentation is to predict potential failure mechanisms that may occur during or after project completion. Secondly, what instruments can be installed to monitor parameters such as pore water pressure, horizontal and/or vertical displacements, in-situ stresses, etc. that are indicative of a failure. Finally, the information gained from the field instruments shall be used to support any further action that may be necessary. If the objectives of the instrumentation cannot be clearly defined, delete the instrumentation. Only use instrumentation that has clearly defined objectives.

### **24.7.3 Predicted Magnitudes of Change**

The lower bound of predicted magnitudes will provide the required accuracy of field instruments, while taking into account the full range of predicted magnitudes will convey the required data range of field instruments. Threshold levels which correspond to escalating need for remedial action shall also be determined and included with the monitoring plan. A table or similar graphic illustrating these levels should be displayed in a prominent place and all personnel associated with monitoring shall be aware of both the threshold level readings and required remedial actions. The threshold values are chosen based on experience with similar projects, similar subsurface conditions or construction methods, case histories of similar projects, and engineering judgment of project personnel.

### **24.7.4 Define Remedial Actions**

In relation to threshold levels, remedial actions corresponding to each escalating level shall be defined in the monitoring plan. Remedial actions will be project specific but may range from simply informing someone higher up the chain of command of a possibly unsafe situation, to stopping work, or to emergency measures in the event of an impending failure. A detailed description of each action may not be feasible at the time the plan is written, but the plan shall at least describe each action in general terms. Pre-project planning ensures that the required labor and materials will be available in case of emergency.

### **24.7.5 Establish Responsibilities and Chain of Command**

The responsible parties for each phase of a monitoring program, from planning to collection and interpretation of data, shall be designated either in the monitoring plan or in another suitable document. Responsibilities and authority of each party in relation to the other parties regarding

the monitoring program shall also be clearly defined. Regardless of their role and level of authority on the project, monitoring personnel shall always have a direct line of communication between themselves, the construction Contractor, and the GEOR in case a situation arises that needs immediate attention.

#### **24.7.6 Type of Instruments and Locations**

The type, number, and manufacturer of each instrument to be used on the project shall be provided in the monitoring plan. The reasons for selecting particular instruments to monitor the conditions described above shall also be explicitly spelled out, keeping in mind that every instrument is installed to answer a specific question. The overriding factor in choosing field instrumentation is reliability. Other factors such as ease of installation, difficulty of interpretation, and cost, may also play a role. Instrument manufacturers can provide valuable information during the instrument selection process about relevance of the instrument to the specific application and limitations of the instrument.

The locations for instrument installation shall be chosen based on potential failure analysis, preexisting information (if for an existing structure or slope), subsurface conditions, and any other pertinent information. If site conditions are generally homogenous, instruments may be installed at selected intervals. If it appears that certain areas will be more critical or have a higher probability of failure, instruments shall be concentrated at these locations. Provisions should be made to order more instruments than necessary to account for damage during installation or malfunction once the instrument is installed. Field instrument locations shall be clearly marked on a plan view of the site. Instrumented cross-sections, if applicable, shall also be included with the monitoring plan.

#### **24.7.7 Recording of Outside Factors**

The recording of all outside factors, that can be reasonably assessed, that may influence field instrument data shall be specified in the monitoring plan. This is especially important for monitoring during construction activities, as heavy construction traffic and altering of the site conditions can have a significant effect on instrument data. Monitoring personnel must keep or have access to a detailed record of construction activities in order to correlate monitoring results and filter out anomalies caused by nearby construction activities. Other outside factors that may influence instrument readings include environmental conditions such as temperature, rainfall, sunlight, and seismic activity.

#### **24.7.8 Procedures for Ensuring Data Validity**

Procedures shall be in place to ensure the validity of each instrument installed for the project. Redundancy is an effective way to reduce error in instrument data. For example, an open-standpipe piezometer can be installed near a pore-pressure transducer, screened at the same interval, to ensure that pore pressure readings are accurate. Optical or GPS surveying of surface monuments can be used to validate apparent movements indicated by subsurface instruments. Visual observation of site conditions by trained personnel can also be an effective means of validating instrument data. Systematic checks of data reliability should be planned for each type of instrument to be installed.

#### **24.7.9 Estimated Costs**

An estimated cost tabulation sheet for both materials and labor associated with the proposed monitoring procedures shall be compiled and submitted either with the monitoring plan or with another suitable document. Contingencies shall also be put in place to cover additional monitoring should the need arise.

### 24.7.10 Installation and Protection Plans

A detailed set of installation plans, including at least a work plan and sketches, shall be included with the monitoring plan. Oftentimes, the instrument manufacturer will provide detailed installation plans for their instruments. If necessary, the appropriate ASTM or AASHTO standard shall be referenced with regard to installation. Included with the installation plan shall also be methods to assure that the instrument is installed correctly and for the initial calibration of the instrument. If the instrument is to be installed in an active construction zone, plans must include methods for handling, protecting and repairing the instrument.

### 24.7.11 Calibration and Maintenance of Field Instruments

The instrument manufacturer is required to provide a recommended schedule for calibration and maintenance of field instrumentation. A calibration schedule of at least once per year is recommended, although many instrument manufacturers recommend shorter time periods between calibrations. Periodic calibration checks should also be performed by monitoring personnel to ensure that the instruments remain in calibration throughout the life of the project.

### 24.7.12 Data Processing

The procedures to be used for data collection, processing, presentation, interpretation, reporting, and implementation shall be provided in the monitoring plan. Field instrument reading schedules shall be detailed out in the monitoring plan, but must remain flexible depending on project progress and the results of initial readings. The plan shall also indicate specific software that may be required for processing data. Typically, field instruments are read on a relatively tight schedule at the beginning of a project and then relaxed as baseline conditions emerge and/or the project progresses beyond critical stages. Management of instrument data from methods of field collection to data storage and backup shall be accounted for in the planning stages of the project. The time needed for post-processing of instrument data will be dependent on instrument type and level of sophistication. Sufficient effort shall be planned for data interpretation by trained personnel. The results of data analysis shall be provided in periodic reports corresponding either to a set time interval (i.e. weekly, monthly, etc.) or to project milestones.

## 24.8 MONITORING PLAN EXECUTION

As discussed previously, the installation of geotechnical instrumentation is typically the responsibility of the Contractor. The Contractor shall be required to submit an installation plan for review. The plan should include the items in Table 24-9.

**Table 24-9, Monitoring Plan Execution**

1. Instrumentation Supplier	2. Factory calibration of instrumentation
3. Pre-Installation testing requirements	4. Calibration and Maintenance Requirements
5. Installation methods	6. Protection plan
7. Installation records	8. Installation report
9. Data Collection methods	10. Qualifications of personnel collecting data

### **24.8.1 Instrumentation Supplier**

The Contractor shall be required to provide the name of the supplier of the geotechnical instrumentation and all literature provided by the supplier. The literature shall be used to verify that the instrumentation selected meets the requirements of the project.

### **24.8.2 Factory Calibration of Instrumentation**

All instrumentation shall be calibrated at the factory prior to shipment and calibration certificates shall be provided by the Contractor. Any additional calibration requirements contained in the STSs or Special Provisions shall also be met.

### **24.8.3 Pre-Installation Testing Requirements**

Due to the potential for rough handling during shipment, all instrumentation shall be checked to ascertain that the equipment is in working order prior to installation. The pre-installation testing shall include a verification of the calibration data provided by the manufacturer, by checking 2 or 3 data points within the instrument measurement range. The verification testing shall be performed at a range of temperatures. Tests at the extreme temperature limits of the instrumentation may reveal malfunctions that could lead to erroneous data if not corrected. The pre-installation testing may consist of testing to determine if the instrumentation is in working order. This type of testing is also called function testing. Table 24-10 indicates some possible items for the pre-installation testing program.

**Table 24-10, Possible Items in Pre-Installation Tests  
(Dunncliff (1998))**

<b>Category</b>	<b>Item</b>
Data Supplied by Manufacturer	<ul style="list-style-type: none"> <li>• Examine factory calibration curve and tabulated data to verify completeness</li> <li>• Examine manufacturer's final quality assurance inspection checklist, to verify completeness</li> </ul>
Documentation	<ul style="list-style-type: none"> <li>• Check, by comparing with procurement document, that model, dimensions, and materials are correct</li> <li>• Check that quantities received correspond to quantities ordered</li> </ul>
Calibration Checks	<ul style="list-style-type: none"> <li>• Check 2 or 3 points, if practicable</li> <li>• Check 0.0 reading, e.g., of vibrating wire piezometers</li> </ul>
Function Checks	<ul style="list-style-type: none"> <li>• Connect to readout and induce change in parameter to be measured</li> <li>• Make and remake connectors several times, to verify correct functioning</li> <li>• Immerse in water, if applicable, and check</li> </ul>
Electrical	<ul style="list-style-type: none"> <li>• Perform resistance and insulation testing, in accordance with criteria provided by the instrument manufacturer</li> </ul>
Mechanical	<ul style="list-style-type: none"> <li>• Check cable length</li> <li>• Check tag numbers on instrument and cable</li> <li>• Verify all components fit together in the correct configuration</li> <li>• Check all components for signs of damage in transit</li> </ul>

#### **24.8.4 Calibration and Maintenance Requirements**

Calibrations or function checks are required throughout the life of the instrumentation. Typically these calibrations are performed by the same personnel responsible for data collection. All calibrations and function checks shall be traceable (i.e. can be checked). The Contractor shall be required to develop a field calibration plan as part of the overall geotechnical instrumentation plan.

In addition to calibration, the personnel collecting the data shall also perform maintenance of the equipment. All maintenance shall be conducted in accordance with the manufacturer's requirements (if any is required).

#### **24.8.5 Installation Methods**

There are numerous ways to install the geotechnical instrumentation. The STSs and Special Provisions will provide some general requirements. The actual installation methods are left to the Contractor and shall be included in the installation plan. As part of the installation methods, the qualifications of the personnel installing the instrumentation shall also be included. The Contractor is solely responsible for installation and the performance of the instrumentation after installation. Badly performing or inoperative instrumentation shall be replaced at no additional cost to SCDOT.

#### **24.8.6 Protection Plan**

Geotechnical instrumentation that terminates at the ground surface (natural or man-made) is subject to damage by construction activities. Therefore, special precautions are required. As part of the installation plan, the Contractor is required to specify how the instrumentation is to be protected, not only from construction activities, but also from vandalism.

#### **24.8.7 Installation Records**

Detailed installation records are required to be submitted by the Contractor. These records fill 2 purposes. First, by requiring detailed installation records, the installation is more likely to be performed in accordance with the accepted installation plan. Secondly, the records function as an "as-built" record and can indicate why the instrumentation is performing poorly or incorrectly, thus aiding the GEOR in determining if less reliance should be placed on a particular instrument. Having the record will also remove doubt if an instrument performs erratically by removing installation concerns as a potential cause of the problem. Presented in Table 24-11 are some items for possible inclusion on the installation record sheet.

**Table 24-11, Possible Content of Installation Record Sheets  
(Dunnicliff (1998))**

<b>Category</b>	<b>Content</b>
Heading	<ul style="list-style-type: none"> <li>• Project Name</li> <li>• Instrument type and number, including readout unit</li> <li>• Personnel responsible for installation</li> <li>• Date and time of start and completion</li> </ul>
Planned Data	<ul style="list-style-type: none"> <li>• Planned location in plan and elevation</li> <li>• Planned orientation</li> <li>• Planned lengths, widths, diameters, depths, and volumes of backfill</li> <li>• Necessary measurements or readings required during installation to ensure that all previous steps have been followed correctly, including post-installation acceptance tests</li> </ul>
As-Built Data	<ul style="list-style-type: none"> <li>• As-built location in plan and elevation</li> <li>• As-built orientation</li> <li>• As-built lengths, widths, diameters, depths, and volumes of backfill</li> <li>• Plant and equipment used, including diameter and depth of any drill casing used</li> <li>• A log of appropriate subsurface data</li> <li>• Type of backfill used</li> <li>• Post-Installation acceptance test</li> </ul>
Weather	<ul style="list-style-type: none"> <li>• Weather conditions</li> </ul>
Notes	<ul style="list-style-type: none"> <li>• Any notes, including problems encountered, delays, unusual features of the installation, and any events that may have a bearing on instrument behavior</li> </ul>

### **24.8.8 Installation Reports**

The purpose of the installation report is to provide a convenient summary of the information that personnel might need who are involved in the data collection, and processing, presentation and interpretation of the data. Listed below are some of the items that should be included in the report:

- Plans and sections sufficient to show instrument numbers and locations
- Appropriate surface and subsurface stratigraphic and geotechnical data
- Descriptions of instruments and readout units, including manufacturer's literature and photographs
- Details of calibration procedures
- Details of installation procedures (photographs are often helpful)
- Initial readings
- A copy of each installation record sheet

### **24.8.9 Data Collection Methods**

Typically on SCDOT projects the collection of data is the responsibility of the Contractor, with the Contractor's personnel meeting the qualifications in the next Section. Data collection is typically obtained manually. In other words, physical measurements are made or the readout device is directly connected to the terminals of the instrument. Automatic Data Acquisition Systems (ADASs) are available, such as Vibrating Wire Data Collection Centers. However, SCDOT does not have much experience in the use of these systems. Therefore, a manual collection system will be required if an ADAS is used. ADASs have the potential for remote downloading of the data, if the communications are properly setup.

### **24.8.10 Qualifications of Personnel Collecting Data**

SCDOT requires that all personnel involved in the collection of instrument data be familiar with the instrumentation being used. These personnel shall be familiar with the installation report, so that if anomalies are encountered, they can provide feedback to the GEC processing the data. In addition, the personnel obtaining the data shall report to a licensed engineer working for the GEC. In the case of settlement plate readings, a licensed land surveyor is required. The qualifications of all personnel involved with the installation, calibration, maintenance and data collections shall be included as part of the Contractor's installation plan.

## **24.9 FIELD INSTRUMENTATION**

The most commonly used types of field instrumentation for highway projects are discussed below. Included in the discussion are the role and typical uses of each instrument, a short description of methods commonly used, and common problems to be aware of with installation, reading, and interpretation of the instrumentation. For more information about particular instruments, the references cited at the end of the Chapter, as well as manufacturer manuals and websites are recommended.

### **24.9.1 Slope Inclinometers**

These instruments are used to monitor the magnitude, direction, and rate of subsurface horizontal deformations. Typical applications include monitoring the rate and extent of horizontal movement of embankments or cut slopes, determining the location of an existing failure surface, and monitoring deflection of retaining walls. Inclinometers can be installed at several levels on an embankment or cut slope to define the extent and nature of subsurface movements. An inclinometer consists of a grooved casing grouted vertically in a borehole. The role of the casing is to deform with the surrounding ground such that readings taken within the casing reflect accurate measurements of ground movement. Typically the grooves are aligned parallel to the direction of movement. The probe is periodically inserted down the casing and deflection of the casing is measured. The inclinometer probe contains accelerometers at either end to measure the parallel and perpendicular tilt of the casing. Successive measurements are plotted to provide a chronological indication of the extent and rate of subsurface movements.

Installation of inclinometer casing must be continued into rock or dense material that is not expected to deform. This will provide a point-of-fixity at the bottom of the casing to which other measurements through the casing can be reliably correlated to. Once drilling has proceeded to the desired depth and the inclinometer casing has been set in the borehole, the annulus between the casing and borehole side is filled with grout that has a similar strength to that of the surrounding soil. Because the grout will induce a buoyant force on the casing, a stabilization method will be required to keep the casing in place during grout placement. Methods involving anchoring or weighting the casing bottom in the borehole are commonly used to overcome this issue. The instrument manufacturer should be consulted for recommended procedures for overcoming buoyancy. Holding the casing in place at the ground surface while grouting will cause the casing to corkscrew within the borehole which may cause errors in future readings. Inclinometers are to be installed and read in accordance with AASHTO Specification R 45-13 – *Standard Practice for Installing, Monitoring, and Processing Data of the Traveling Type Slope Inclinometer* and the manufacturer's specifications. Inclinometer casing conforming to the requirements of STS SC-M-203-9 for *Slope Inclinometer Casing* shall be used.

The review of inclinometer data should indicate first that the bottom of the casing is placed firmly in material that is not moving (i.e., below the potential/actual failure surface). Second, the review should indicate that all subsequent data is indicating movement "downhill." If the data indicates movement in the opposite direction, review the procedures for obtaining the data with

field personnel. In addition, the actual movement data should be compared to the theoretical (design) movements to determine if the predicted is similar to the actual. From this comparison, it may be possible to predict additional movements.

### **24.9.2 Settlement Monitoring**

These instruments are used to record the amount and rate of settlement under load. The most common installation of these instruments is for use with embankments where high settlements are predicted. The instruments listed in the following Subsections are the recommended methods for settlement measurement associated with highway embankments. Some instruments detailed below are designed to measure settlement through depth of strata. Because subsurface settlement instruments are often damaged during construction, some form of long-term settlement monitoring at the top of an embankment should be planned. This will provide a check of the readings obtained from subsurface instruments and can help to fill in the gaps from instruments that have either been damaged or have become unreliable.

The monitoring of settlement is probably the most common type of geotechnical instrumentation used by SCDOT. Typically settlement data consists of either survey (elevation) data or pore pressure data. Survey data is obtained from various points that are compared to established benchmarks, while pore pressure data is obtained from piezometers. The first check of the data is to determine if the numerical calculations are consistent. The second check and more important check, is the trend of the data, i.e. does the data continue to indicate downward movement. With pore pressure data, the second check is whether or not the pore pressures are approaching a static pore pressure level. It should be noted that the before construction pore pressure level will not be obtained, but some higher level will be. Both the survey data and the pore pressure data should approach a trend line where there is very little difference between readings. Once this happens, settlement is assumed to be over. While settlement monitoring is occurring, the amount of actual settlement should be compared to the predicted amount of settlement. One method for determining if settlement (based only on survey data) is complete is to use Taylor's square root of time method. Another method for determining the completion of settlement is the use Asaoka's method.

#### **24.9.2.1 Settlement Plate**

The simplest form of settlement indicator is the settlement plate, which typically consists of a steel plate placed on the ground surface prior to embankment construction. The initial elevation of the plate must be recorded before construction begins to provide a reference point for all future readings. A reference rod and protective casing are then attached to the plate. As fill placement progresses, additional rods and casing are added. Settlement is measured by determining the elevation of the top of the reference rod at specified time intervals by surveying methods. The reference rod and initial platform elevations are determined relative to several benchmarks placed outside the construction area. Settlement plates are often placed in areas where the highest settlements are predicted. Settlement plates conforming to the requirements of STS SC-M-203-4 for *Settlement Plates* shall be used.

#### **24.9.2.2 Extensometers**

The probe extensometer is another instrument commonly used to measure settlement. In a typical arrangement, corrugated polyethylene pipe surrounded by rings of stainless steel wire at selected intervals is lowered into a borehole. A rigid PVC inner pipe is coupled to the corrugated pipe prior to installation. Inclinator casing is often used as the rigid inner pipe, thereby eliminating the need for drilling two separate boreholes for measuring horizontal and vertical displacement. The annulus between the rigid inner pipe and outer corrugated pipe is filled with bentonite slurry to minimize friction and the space between the outer pipe and



borehole side is filled with a grout that conforms as nearly as possible to the properties of the surrounding soils. A more rigid system consisting of PVC pipe with telescopic couplings and steel plates instead of wire rings may be more desirable in situations where the likelihood of crushing the corrugated pipe exists, such as in high fill embankments or where high settlements are predicted.

The reading device in a probe extensometer consists of an induction coil housed within a probe attached to a signal cable that leads to a readout unit at the surface. As the probe is lowered, the operator notes at what depth the probe senses the steel rings, indicated by a buzzer on the readout unit. By comparing these depths to the initial depths, a settlement profile can be obtained. A main advantage of this type of instrument to a conventional settlement plate is that a settlement profile is obtained through the entire depth of the strata in question, not just at the surface. Optical surveying is typically not required so long as the bottom of the extensometer is fixed in stable ground. Drawbacks to this method include disruption to construction activities and cost, as compared to conventional settlement plates. Extensometers conforming to the requirements of STS SC-M-203-8 for *Vibrating Wire Rod Extensometers* shall be used.

### **24.9.2.3 Settlement Sensor**

The settlement sensor, or liquid-level gage instrument, consists of a pressure transducer embedded beneath the embankment with liquid-filled tubes connected to a reservoir and readout unit installed on stable ground. As the transducer settles, greater pressure is imparted on the transducer by the column of liquid. Settlement is measured by converting the increase in pressure to feet or meters of liquid head. This method requires that the liquid-filled tubes be run in trenches to areas outside of the construction area. Although trenching may cause some disruption to construction activity, all readings are taken away from the construction area after the instrument is installed. Settlement sensors are often installed at several depths at the same cross-section to better define the full settlement profile. The ease of automation tends to be highest for this type of settlement measurement, especially if the pressure transducer is of the vibrating-wire type. A limitation to this type of instrument is that the soils surrounding the instrument and in the trench must be installed to specifications similar to that of the surrounding fill. Otherwise harmful discontinuities may be introduced into the embankment. This instrument should be used for short-term monitoring, because this instrument can be extremely temperature sensitive. Settlement sensors conforming to the requirements of STS SC-M-203-7 for *Settlement Sensors* shall be used.

### **24.9.2.4 Settlement Reference Points**

Settlement reference points are installed on structures or embankments upon essential completion of construction or topping out. Settlement reference points are intended to provide long-term settlement data by relatively simple methods at the ground surface. Settlement reference points may also be installed on embankments or structures such as a retaining wall to evaluate distress or unanticipated movement.

Settlement reference points are monitored using conventional surveying methods. Settlement reference points may consist of pins driven into the ground or mounted on a structure, or may simply be a painted reference point on a structure. Data collected over time indicates the amount of settlement that has occurred at each reference point. Care should be taken to protect settlement pins from disturbance by construction equipment or traffic that will affect the validity of data.

### **24.9.2.5 Crack Gauges**

Crack gauges refer to simple commercial devices installed on a structure, such as a retaining

wall, to visually monitor vertical and horizontal movements. Crack gauges permit visual monitoring and measurement of structural movements without requiring the use of survey equipment. Several configurations of the gauges are available, such as gauges mounted on a flat surface, or gauges mounted on either side of a corner.

Typical commercial crack gauges consist of 2 overlapping pieces of acrylic or PVC sheets fixed in place by epoxy. The sheets are installed so that the bottom sheet is fixed to the structure on one side of the crack, and the top sheet is fixed to the structure on the opposite side of the crack. The bottom sheet contains an opaque reference grid, and the top sheet is transparent with an intersecting vertical and horizontal marker. After measuring the width of the crack at the start of the monitoring period, horizontal and vertical movements of the structure can be monitored by noting the movement of the marker over the reference grid.

Crack gauges have some limitations and their use requires judgment and experience. Movements indicated on the gauge facing do not necessarily reflect the true peak movement which may occur in a dimension not recognized by an individual gauge as mounted. Crack gauges are typically only capable of monitoring movement in 2 dimensions; therefore, multiple gauges mounted at several locations on the structure will be required to monitor movement in 3 dimensions. When movements exceed the size of the reference grid, the size of the crack is recorded and new gauges can be installed to continue the monitoring program.

### **24.9.3 Piezometers**

Piezometer applications generally fall into 2 categories: 1) Monitoring the flow of groundwater, or 2) Providing an index of soil strength gain. For highway construction, piezometers are typically installed to monitor pore water pressures associated with fill embankments and existing or cut slopes. Pore water pressure monitoring provides an estimate of effective stress within a slope. An increase in pore pressure indicated by a piezometer in a slope can be a signal of an impending slide. If a dewatering system is installed to stabilize a large excavation, piezometers can be used to gauge the effectiveness of the system. The most common use of piezometers in highway construction is to monitor the initial pore pressure rise and subsequent dissipation associated with consolidation of soils beneath an embankment. Pore pressure readings taken during construction of an embankment can be used to verify design settlement assumptions and to guide further construction activities.

The term piezometer is generally used to describe pore pressure monitoring instruments where seals are placed within the ground at selected depths, so as to monitor pore pressure conditions only within a certain strata. A device that has no seals is generally termed an observation well and should only be used in homogenous and continuously permeable soils. The simplest type of piezometer is an open standpipe piezometer. In this application, a section of slotted pipe attached to riser pipe is lowered to the desired elevation. A filter is generally placed around the slotted pipe and sand is placed in the borehole around the filter to create a reading interval. A bentonite seal is then placed atop the sand and a sealing grout is used to fill the remainder of the borehole. Open standpipe piezometers have a slower response time than some of the more sophisticated instruments described below, but are generally more cost effective to install and are more reliable than other methods.

Vibrating-wire piezometers are often used in applications where fast response to pore pressure changes is desired. Other advantages include less disruption to construction activity, less chance for damage in active construction zones (provided the lead cables are protected properly), and ease of reading and automation. A vibrating-wire piezometer consists of a diaphragm connected to a tensioned wire such that changes in pore-pressure affect the tension of the wire. A readout unit is used to pluck the wire and measure the change in wire tension, which can then be converted to pore-pressure readings. Vibrating-wire piezometers are

typically installed in similar fashion to open-standpipe piezometers with the pressure transducer placed inside the screened reading interval, although recent research suggests that similar results can be obtained in a fully-grouted borehole. Please refer to Dunncliff (1998) for more information on the fully-grouted installation method. Push-in type vibrating-wire piezometers provide a quick and relatively easy installation and are commonly used to monitor pore pressure changes in successive lifts of an embankment. Open standpipe piezometers can also be converted to vibrating-wire piezometers simply by lowering a pressure transducer into the well to a specified depth. Most vibrating-wire type instruments currently come with some form of lightning protection housed inside the body of the instrument, though additional measures may be needed in areas prone to lightning activity. Piezometers conforming to the requirements of STS SC-M-203-6 for *Vibrating Wire Piezometer* shall be used.

Another piezometer type commonly used is the pneumatic piezometer, which consists of a flexible diaphragm and sensor body connected to a junction box at the surface with twin tubes. A filter is commonly used to separate the diaphragm from the surrounding material. Pressurized gas is introduced through the inlet tube. As gas pressure exceeds the pore water pressure, the diaphragm deflects, allowing gas to vent through the outlet tube. When the operator observes a return flow of gas, the gas supply is shut off and the diaphragm returns to its equilibrium position with the pore water pressure. The operator then obtains a reading from a pressure gauge connected to the input tube. This type of instrument also features a relatively short time lag and minimal disruption to construction. Some limitations of this instrument include the complexity of choosing the proper details of instrument, difficulty of reading, and the possibility of minute gas leaks within the system causing errors in data.

Often, it is not immediately known which type of piezometer is better suited to a particular application. One way of narrowing the choice and alleviating concerns over data reliability is to install groups of redundant piezometers of different types at similar locations and depths. Generally, open standpipe piezometers are paired with vibrating-wire or pneumatic piezometers and the data are periodically compared to ensure data validity. This setup also ensures that the flow of data will not be disrupted if 1 instrument malfunctions.

#### **24.9.4 Special Instrumentation**

Situations may arise where field instruments other than those described above are desired for use on a project. Many instruments, such as earth pressure cells or strain gauges, are typically not used in construction projects but only in research and special projects. Other instruments, such as borehole extensometers for monitoring a rock slope or tie-backs, may serve a key role on a project. Less common methods, such as horizontal inclinometers or other specialized instruments, should only be specified in special circumstances and with prior approval from the PC/GDS. The need for special instrumentation and the selection of instruments will be evaluated on a case-by-case basis.

### **24.10 CONCLUSIONS**

After assuring its validity, data from field instruments shall be interpreted relative to other instrument data as well as outside factors that may affect the data. For example, during construction of an embankment on soft ground, pore pressure rises and subsequent drops can be correlated to settlement measurements as well as the level of fill placement. A measured change in a single instrument but not in other corresponding instruments may signal error stemming from either the instrument itself or reading methods. Another effective way to validate instrument readings is through routine visual observation. Observation of the monitored area can provide early warning signals, such as a tension crack or evident seepage, which may not be picked up by nearby field instruments and can also guide remedial actions.

The monitoring program of a highway construction project must be able to adapt to changing conditions. Base line readings of installed instruments may paint a picture that is totally different from what was assumed during the design phase. Components such as reading interval, methods of collecting data, and presentation of data may change dramatically over the course of a project.

## 24.11 SHOP PLAN REVIEW

The Standard Specifications, Supplemental Specifications, Supplemental Technical Specifications, Special Provisions and design drawings occasionally require the Contractor to submit Shop Plans and Installation Plans in addition to the PIP and the DFIP. The GEOR shall review the geotechnical portions of the submitted Shop Plans and Installation Plans for conformance to the Standard Specifications, Supplemental Specifications, Supplemental Technical Specifications, Special Provisions and design drawings. If no review time is specified in the contract, then the GEOR shall conduct the review in 21 calendar days and shall submit the response to the Department.

## 24.12 REFERENCES

Andrews, J., Buehler, D., Gill, H., and Bender, W. L., (2013), Transportation and Construction Vibration Guidance Manual, (CT-HWANP-RT-13-069.25.3), California Department of Transportation, Division of Environmental Analysis, Environmental Engineering, Hazardous Waste, Air, Noise, & Paleontology Office, Sacramento, CA.

Dowding, C. H., (1996), Construction Vibrations, 2<sup>nd</sup> Edition, Prentice Hall, Englewood Cliffs, NJ.

Dunncliff, J., (1998), Geotechnical Instrumentation, (FHWA HI-98-034), U.S. Department of Transportation, National Highway Institute, Federal Highway Administration, Washington D.C.

Elias, V., Welsh, J., Warren, J., Lukas, R., Collin, J.G., and Berg, R.R., (2006), Ground Improvement Methods – Volume I, (FHWA NHI-06-019), U.S. Department of Transportation, National Highway Institute, Federal Highway Administration, Washington D.C.

GRL Engineers, Inc., (2015), *Dynamic Load Testing, Available Apple Systems*, Retrieved January 13, 2015, <http://www.grlengineers.com/services/dlt/appleSystems.aspx?ID=4>.

Hanson, C. E., Towers, D. A. and Meister, L. D., (2006), Transit Noise and Vibration Impact Assessment, (FHWA-VA-90-1003-06), U.S. Department of Transportation, Federal Transit Administration, Washington D.C.

LOADTEST, Inc. (2015), *O-cell Load Testing*, Retrieved January 13, 2015, from <http://www.loadtest.com/services/ocell.htm>.

Minnesota Department of Transportation (MnDOT), (2013), 2013 Geotechnical Engineering Manual, Saint Paul, Minnesota.

O'Neil, M. W. and Reese, L. C., (1999), Drilled Shafts: Construction Procedures and Design Methods, (Publication No. FHWA-IF-99-025), Office of Bridge Technology, U.S. Department of Transportation, Federal Highway Administration, Washington, D.C.

South Carolina Department of Transportation, (2007), Standard Specifications for Highway Construction, [https://www.scdot.org/business/pdf/2007\\_full\\_specbook.pdf](https://www.scdot.org/business/pdf/2007_full_specbook.pdf).

**Chapter 25**  
**RESERVED**

**GEOTECHNICAL DESIGN MANUAL**

*January 2019*



# **CHAPTER 25**

## **RESERVED**

Chapter 25 – Construction Monitoring and Instrumentation of GDM version 1.1, 2010 has been deleted. This Chapter is reserved for future use by SCDOT.

**Chapter 26**  
**GEOTECHNICAL SOFTWARE**

**SCDOT GEOTECHNICAL DESIGN MANUAL**

*January 2019*





**Table of Contents**

<b><u>Section</u></b>		<b><u>Page</u></b>
26.1	Introduction.....	26-1
26.2	Commerical Software .....	26-1
26.3	Non-Commerical Software.....	26-1



# CHAPTER 26

## GEOTECHNICAL SOFTWARE

### 26.1 INTRODUCTION

This Chapter provides a general overview of software used in geotechnical engineering and analysis. Software is used in geotechnical engineering to speed computations and to perform complex analyses. There are 2 types of software used by SCDOT: 1) software packages developed and marketed by universities and software development firms, 2) spreadsheets and customized software packages developed by individuals or companies. Typically the first type of software is commercially available and used by multiple government agencies and private entities. The second type typically is only used by a single agency or entity and is developed locally by the user. SCDOT recognizes that both types of software are used; however, the individually developed software requires QA/QC verification prior to being used on SCDOT projects.

Prior to the use of any software, it is incumbent upon the engineer to understand how the software determines the results and any limitations that are inherent to the software. For example, the SHAKE program becomes unreliable if the strains exceed 3 percent (3%). SCDOT recommends that prior to using a new software program, the user should run at least 1 example and check the results against a set of hand calculations.

Appendix G provides a list of software that is currently used by SCDOT. Consultants are not required to obtain the same software as SCDOT, but all software shall use the models permitted in this Manual.

### 26.2 COMMERCIAL SOFTWARE

As indicated previously, commercially available software packages are typically produced by either a university or software development firm and are sold for profit. Software developed in this manner normally goes through extensive QA/QC prior to being sold. Therefore, the only documentation SCDOT requires for these software packages is the contact information for the developer. Software obtained from the FHWA website requires no additional information.

### 26.3 NON-COMMERCIAL SOFTWARE

Non-commercial software packages are those packages that are developed by and used internally in a single agency or entity. Included in this category are spreadsheets, MathCAD programs or software developed using computer language, such as FORTRAN, C++ or similar. Because these types of packages may not get the same level of review as commercially developed software, additional information and supporting documentation may be required prior to their acceptance by SCDOT. The supporting documentation may include, but is not limited to; an example prepared using the software and a set of hand calculations for the same example. In addition to the example, a QA/QC plan for the development of software packages shall also be prepared, indicating the person or persons who reviewed the software. For software developed internally by the Department, the software should be reviewed by the PCS/GDS.

**APPENDIX A**  
**GEOTECHNICAL DESIGN**  
**FORMS**

**GEOTECHNICAL DESIGN MANUAL**

*January 2019*



**Table of Contents**

<b><u>Section</u></b>		<b><u>Page</u></b>
A.1	Introduction.....	A-1

**List of Tables**

<b><u>Table</u></b>	<b><u>Page</u></b>
Table A-1, Geotechnical Design Forms .....	A-1





## GeoScoping Form

PROJECT INFORMATION	
Project ID:	Date of Trip:
County:	Location:
Rd/Route:	Local Name:
Attendees:	

EXISTING BRIDGE INFORMATION	
Bridge Length:	Bridge Width:
Superstructure Type:	Substructure Type:
Begin Bridge Sta.:	End Bridge Sta.:
Begin Bridge Embankment Sta. <sup>1</sup> :	End Bridge Embankment Sta. <sup>1</sup> :
Structure Number:	Posted Weight Limit:
Crossing:	Skew:
Latitude:	Longitude:
Existing Fill Height:	Approximate Existing Slope Angle:

<sup>1</sup>Begin and End Bridge Embankment 100 feet down station or up station from bridge, respectively

EXISTING ROADWAY EMBANKMENT INFORMATION		
Begin Project Sta.:	Begin Bridge Embankment Sta. <sup>1</sup> :	
Accessibility Issues:		
Ground Cover:		
Existing Fill Height:	Approximate Existing Slope Angle:	
Local Development (undeveloped, developed residential, developed commercial, developed industrial, etc.):		
Topography (level, flat, rolling, steep, hillside, valley, swamp, gully, etc.):		
Traffic Control Necessary (Y/N):		
Surface Soil:	Muck (Y/N):	
Exposed Rock (Y/N):	In Stream Bed (Y/N):	In Banks (Y/N):
Wetlands On-Site (Y/N):	Wetlands Adjacent (Y/N):	
Depth FG to Water:	Water Depth:	
Depth to Existing Ground:		
Scour Condition at EB:	Scour Condition at IB:	
End Bridge Embankment Sta. <sup>1</sup> :	End Project Sta.:	
Accessibility Issues:		
Ground Cover:		
Existing Fill Height:	Approximate Existing Slope Angle:	
Local Development (undeveloped, developed residential, developed commercial, developed industrial, etc.):		
Topography (level, flat, rolling, steep, hillside, valley, swamp, gully, etc.):		
Traffic Control Necessary (Y/N):		
Surface Soil:	Muck (Y/N):	
Exposed Rock (Y/N):	In Stream Bed (Y/N):	In Banks (Y/N):
Wetlands On-Site (Y/N):	Wetlands Adjacent (Y/N):	
Depth FG to Water:	Water Depth:	
Depth to Existing Ground:		
Scour Condition at EB:	Scour Condition at IB:	



## Bridge Load Data Sheet

PROJECT INFORMATION					
<b>Project ID:</b>		<b>County:</b>		<b>Route:</b>	
<b>Description:</b>					
<b>Loads Provided By:</b>				<b>Date Loads Provided:</b>	
<b>Bridge Type:</b>					
<b>No. Spans /Lengths:</b>			<b>Width / No. Lanes:</b>		
<b>Edition of AASHTO LRFD Bridge Design Specifications:</b>					
<b>Edition of SCDOT Seismic Design Specifications for Highway Bridges:</b>					
<b>Bridge Operational Classification (OC):</b>				<b>Scour Report Attached:</b>	
<b>Seismic Design Category (SDC):</b>					
<i>Proposed Foundations (foundation type, size, and number per bent)</i>	<b>End Bent</b>				
	<b>Interior Bent</b>				
<b>Location/Elev. of Applied Loads:<sup>1</sup></b>		<b>End Bent:</b>		<b>Int. Bent:</b>	
<b>Location/Elev. Est. Point of Fixity:</b>		<b>End Bent:</b>		<b>Int. Bent:</b>	

<sup>1</sup>Perferred location of loads is the either the existing ground line for interior bents or the proposed ground line for end bents.

## Bridge Load Data Sheet

	Limit State	Strength			Service		
	Load Cases:	Case 1FL (P=P <sub>max</sub> )	Case 2FL (V=V <sub>max</sub> )	Case 3FL (M=M <sub>max</sub> )	Case 1SL (P=P <sub>max</sub> )	Case 2SL (V=V <sub>max</sub> )	Case 3SL (M=M <sub>max</sub> )
End Bent - Longitudinal	P (kips) =						
	V (kips) =						
	M (ft-kip) =						
End Bent - Transverse	P (kips) =						
	V (kips) =						
	M (ft-kip) =						
Interior Bent - Longitudinal	P (kips) =						
	V (kips) =						
	M (ft-kip) =						
Interior Bent - Transverse	P (kips) =						
	V (kips) =						
	M (ft-kip) =						

	Limit State	Extreme Event I			Extreme Event II <sup>a</sup>			Extreme Event II <sup>b</sup>		
	Load Cases:	Case 1EL (P=P <sub>max</sub> )	Case 2EL (V=V <sub>max</sub> )	Case 3EL (M=M <sub>max</sub> )	Case 1EEL (P=P <sub>max</sub> )	Case 2EEL (V=V <sub>max</sub> )	Case 3EEL (M=M <sub>max</sub> )	Case 1EEL (P=P <sub>max</sub> )	Case 2EEL (V=V <sub>max</sub> )	Case 3EEL (M=M <sub>max</sub> )
End Bent - Longitudinal	P (kips) =									
	V (kips) =									
	M (ft-kip) =									
End Bent - Transverse	P (kips) =									
	V (kips) =									
	M (ft-kip) =									
Interior Bent - Longitudinal	P (kips) =									
	V (kips) =									
	M (ft-kip) =									
Interior Bent - Transverse	P (kips) =									
	V (kips) =									
	M (ft-kip) =									

Notes:

P – Axial; V – Shear; M – Moment; <sup>a</sup> – Check Flood w/o collision loads; <sup>b</sup> – Collision loads w/o check flood





To: Director of Rights-of-Way
From: RPG
Date:
Subject: Access Permission Request

The following project is being prepared for Geotechnical Subsurface Investigation:

County:
Road:
Project ID:
PIN No.:
Location:
Project Name:
Charge Code:
Project Manager:

Project Management has provided us with plans, and we will visit the above referenced site in the coming weeks. Based upon the information provided, we understand the following design concepts are under consideration at this time:

- The proposed bridge will be constructed on the existing horizontal alignment.
The grade will be raised approximately XX ft above the existing finish grade elevation
This project will encompass approximately XX.

Roadway and Bridge borings will need to be performed between Stations XX+XX to XX+XX on Anywhere Road, some of which are on SCDOT Right-of-Way and others that are not. Installation of an accessway will be required for this project. This may entail removal of some trees using heavy equipment to permit access. It may also be necessary for us to bring in fill soil to bridge soft, wet areas. Every effort will be made by the Contractor to minimize damage to property and as few trees as possible will be disturbed in the process. Below is a table of anticipated boring locations for the project site. It must be pointed out that the boring locations are planned and may change if site conditions warrant or utilities such as overhead power lines necessitate relocation of the proposed borings.

Table 1 (Road)

Table with 6 columns: Boring No., Road Cut (C)/ Road Fill (F), Proposed Stationing, Offset Distance (ft)\*, Boring Depth (ft.), Tract No.

\*Offset from construction centerline, both left and right

Table 2 (Bridge)

Table with 4 columns: Boring No., Proposed Stationing, Offset Distance (ft)\*, Tract No.

\*Offset from construction centerline, both left and right



South Carolina  
Department of Transportation

Attached are the Geotechnical Design Section's Scoping forms (Form GDF 000), one (1) full-sized set and one (1) half-sized set of plans depicting the proposed soil test boring locations for the project. Bridge and roadway soil borings will be required as indicated on the plans.

We anticipate the access permission to be available by **Month day, Year** so we can begin mobilizing the drillings. Once signed permission has been obtained, please provide a copy of the signed document to us. We will provide a copy of this document to the drillers, who will be required to maintain copies physically in their possession at all times during drilling operations.

If you have any questions or comments, feel free to contact **Sara Stone at (803) 737-1608**. Or you can email me at [StoneSM@scdot.org](mailto:StoneSM@scdot.org).

**Sara M. Stone**  
**Midlands RPG/GDS**

JCS/SMS: xxx  
cc: BDF, Project Management, Geotech file





South Carolina  
Department of Transportation

Date: **March 10, 2005**

To: **Consultant**

From: **RPG**

Re: Soil Exploration Testing and Compressive Strength Testing of Rock Cores

Soil Exploration and Testing of soil samples and Compressive strength testing of rock core samples is requested for the following project

County:  
Road:  
Route Local Name:  
Project ID:  
Location:  
Project Name:  
Charge Code:  
Priority:

**Lab test information needed April 22, 2005.**  
**Final Boring Logs needed April 29, 2005.**

**Index Testing:**

Boring Number	Sample Depth (ft)	Sample Number	Grain Size with wash #200	Atterberg Limit	Natural Moisture Content
B-1	0 - 2				
	2 - 4				
	4 - 6				
	8 - 10				
	13.5 - 15.0				
	18.5 - 20.0				
	23.5 - 25.0				
	28.5 - 30.0				
	33.5 - 35.0				
B-2	43.5 - 45.0				
	0 - 2				
	2 - 4				
	4 - 6				
	6 - 8				
	8 - 10				
	18.5 - 20.0				
23.5 - 25.0					
B-3	22.0 - 24.0				
	24.0 - 26.0				
	26.0 - 28.0				
	28.0 - 30.0				
	30.0 - 32.0				
	48.5 - 50.0				

Note: \*\* Conduct hydrometer analysis also.

**Electro-Chemical Tests:**

Boring Number	Sample Depth (ft)	Sample Number	pH	Resistivity Testing	Chloride Testing	Sulfate Testing
B-1	<b>Water:</b>					
	Groundwater					
	Surface Water					
	<b>Soil:</b>					
	0 - 2					
	2 - 4					
	13.5 - 15.0					
	33.5 - 35.0					
B-2	<b>Water:</b>					
	Groundwater					
	Surface Water					
	<b>Soil:</b>					
	0 - 2					
	6 - 8					
	8 - 10					
	18.5 - 20.0					
B-3	<b>Water:</b>					
	Groundwater					
	Surface Water					
	<b>Soil:</b>					
	22.0 - 24.0					
	28.0 - 30.0					
	30.0 - 32.0					
	48.5 - 50.0					

**Shear Strength Testing:**

Boring Number	Sample Depth (ft)	Sample Number	Unconfined	Direct Shear	UU	CUw/pp	$\sigma_3$ or N		
B-1	0 - 2								
	2 - 4								
	13.5 - 15.0								
B-2	6 - 8								
	43.5 - 45.0								

Note:  $\sigma_3$  – Confining pressure for UU and CUw/pp.  
N – Normal force applied in Direct Shear.

**Consolidation Testing:**

Boring Number	Sample Depth (ft)	Sample Number	Beginning Load	Load Increment	Ending Load	Begin and End of Reload Cycle
B-1	0 - 2					
	2 - 4					
	13.5 - 15.0					
B-2	6 - 8					
	43.5 - 45.0					

**Note:** There should be 14 to 16 load increments and load increments should be even. Ending load should exceed the first-order estimate of  $\sigma'_p$  by a factor of 8.

**Rock Testing:**

Boring Number	Recovery (%)	RQD(%)	Core Number	Number of Breaks Requested
B-2				
B-3				
B-4				
B-5				
B-6				

Please e-mail an electronic copy and forward a hard copy of the results to **Sara Stone** so that the information can be included in the contract document. If you require any additional information, please contact **Sara Stone at 737-1608**.

Requested by:

**Sara Stone**  
**Geotechnical Professional**

cc: BDF, Geotech

Date

Title

## **1.0 DESCRIPTION**

*This Section of the Special Provision provides a general description of the material and/or construction activity. It is not intended to provide details.*

## **2.0 TESTING STANDARDS**

*This Section is used to indicate which edition of the testing standards within the body of this Special Provision is to be used. In addition, this Section also provides the process for getting substitutions for testing standards approved. Below is an example of a paragraph that may be used:*

Use the latest edition of the testing standards indicated in this specification. Substitution of standards will require the prior written approval of the Materials and Research Engineer (MRE) with concurrence of the GEOR. The Contractor or XX Installer is to provide copies of all substituted standards to the RCE. The RCE will provide the copies to the MRE and GEOR for acceptance.

## **3.0 MATERIALS**

*This Section provides material requirements including specific testing standards that must be met to achieve the required performance. In addition, this Section also provides the required testing standard method. If 2 or more materials are required to be combined to produce a system, this Section should indicate how these materials are to be combined; any required combined performance requirements and any combined testing requirements necessary to verify the required performance.*

## **4.0 SUBMITTALS**

*This Section indicates what submittals are required from the Contractor including, material certifications, qualification certifications, etc. In addition, this Section will also contain a subsection indication the review and acceptance procedure, including, who the certifications are sent to, who reviews and approves the certifications. An example of the submittal review process is provided below:*

Acceptance of the proposed materials will be by the MRE. The equipment, construction sequence, and installation method will be accepted by the GEOR. Acceptance of the XX materials, equipment, construction sequence, or installation method does not relieve the Contractor and XX Installer of its responsibility to install the XXs in accordance with the plans and specifications. Acceptance by the GEOR of the method and equipment to be used to install the XXs is contingent upon satisfactory demonstration of XX installation at the project site. If, at any time, the RCE or the GEOR considers that the method of installation does not produce satisfactory XXs, alter the method and/or equipment as necessary to comply with this Supplemental Technical Specification. The RCE and the GEOR will determine the adequacy of the Contractor's methods and equipment.

**5.0 CONSTRUCTION REQUIREMENTS**

*This Section of the Special Provision provides required submittals, construction requirements and acceptance criteria if required. The required submittals Subsections should include, who gets the submittal, typically the Resident Construction Engineer (RCE), who reviews and accepts the submittal and how long the review should take if different from the requirements of the Standard Specifications. The construction requirements should not dictate means and methods, but should provide general guidance to the Contractor on how the construction should be performed and what the end-result should be achieved. The exception to this is if the Special Provision is written as a method specification, where the Contractor is instructed to use certain methods, equipment and materials. In addition, the Construction Requirements Section may also include a discussion of any equipment requirements. Finally, this Section should provide a means of establishing how acceptance is determined. The acceptance criteria should be something that is achievable during construction and is relatively easy to measure.*

**6.0 METHOD OF MEASUREMENT**

*This Section includes, what is being measured, when it should be measured (if required) and how to measure the item. This Section should also state what is incidental, i.e., what is included in the item, to the measurement of the items*

**7.0 BASIS OF PAYMENT**

*This Section provides for when payment can be requested, e.g., completion of installation of an item; a percentage of completed construction, etc. The following statement and table, please note that the table provided is for example only, are required for all Special Provisions:*

Payments shall be made under:

Item No.	Pay Item	Pay Unit
8012300	Prefabricated Vertical Drain with Fabric	LF

*The Item No. is the provided by the Letting Preparation Engineer and should have requested prior to writing the Special Provision, the Pay Item should be the long description and the Pay Unit is the unit of measurement used for the item.*

---

## Supplemental Technical Specification for

# XX

### SCDOT Designation: SC-M-XXX-X (XX/XX)

---

<b>Instructions for the Title Block above</b>
XX – New Product Title
SCDOT Designation: SC-M-XXX-X (XX/XX)
<i>The first 3 X's above are the first 3 numerals of the Pay Item Number. The next X is a sequential number for multiple STSs that have the same 3 numerals (XX/XX) is the letting date the STS will become effective, typically STSs will only become effective in January and July of each year.</i>

## 1.0 DESCRIPTION

*This Section of the STS provides a general description of the material and/or construction activity. It is not intended to provide details.*

## 2.0 TESTING STANDARDS

*This Section is used to indicate which edition of the testing standards within the body of this STS are to be used. In addition, this Section also provides the process for getting substitutions for testing standards approved. Below is an example of a paragraph that may be used:*

Use the latest edition of the testing standards indicated in this specification. Substitution of standards will require the prior written approval of the Materials and Research Engineer (MRE) with concurrence of the GEOR. The Contractor or XX Installer is to provide copies of all substituted standards to the RCE. The RCE will provide the copies to the MRE and GEOR for acceptance.

## 3.0 MATERIALS

*This Section provides material requirements including specific testing standards that must be met to achieve the required performance. In addition, this Section also provides the required testing standard method. If 2 or more materials are required to be combined to produce a system, this Section should indicate how these materials are to be combined; any required combined performance requirements and any combined testing requirements necessary to verify the required performance.*

## 4.0 SUBMITTALS

*This Section indicates what submittals are required from the Contractor including, material certifications, qualification certifications, etc. In addition, this Section will also contain a subsection indication the review and acceptance procedure, including, who the certifications are sent to, who reviews and approves the certifications. An example of the submittal review process is provided below:*

Acceptance of the proposed materials will be by the MRE. The equipment, construction sequence, and installation method will be accepted by the GEOR. Acceptance of the XX materials, equipment, construction sequence, or installation

method does not relieve the Contractor and XX Installer of its responsibility to install the XXs in accordance with the plans and specifications. Acceptance by the GEOR of the method and equipment to be used to install the XXs is contingent upon satisfactory demonstration of XX installation at the project site. If, at any time, the RCE or the GEOR considers that the method of installation does not produce satisfactory XXs, alter the method and/or equipment as necessary to comply with this Supplemental Technical Specification. The RCE and the GEOR will determine the adequacy of the Contractor's methods and equipment.

## 5.0 CONSTRUCTION REQUIREMENTS

*This Section of the STS provides required submittals, construction requirements and acceptance criteria if required. The required submittals Subsections should include, who gets the submittal, typically the Resident Construction Engineer (RCE), who reviews and accepts the submittal and how long the review should take if different from the requirements of the Standard Specifications. The construction requirements should not dictate means and methods, but should provide general guidance to the Contractor on how the construction should be performed and what the end-result should be achieved. The exception to this is if the STS is written as a method specification, where the Contractor is instructed to use certain methods, equipment and materials. In addition, the Construction Requirements Section may also include a discussion of any equipment requirements. Finally, this Section should provide a means of establishing how acceptance is determined. The acceptance criteria should be something that is achievable during construction and is relatively easy to measure.*

## 6.0 METHOD OF MEASUREMENT

*This Section includes, what is being measured, when it should be measured (if required) and how to measure the item. This Section should also state what is incidental, i.e., what is included in the item, to the measurement of the items*

## 7.0 BASIS OF PAYMENT

*This Section provides for when payment can be requested, e.g., completion of installation of an item; a percentage of completed construction, etc. The following statement and table, please note that the table provided is for example only, are required for all STSs:*

Payments shall be made under:

<b>Item No.</b>	<b>Pay Item</b>	<b>Pay Unit</b>
8012300	Prefabricated Vertical Drain with Fabric	LF

*The Item No. is the provided by the Letting Preparation Engineer and should have requested prior to writing the STS, the Pay Item should be the long description and the Pay Unit is the unit of measurement used for the item.*

**APPENDIX B**  
**RESERVED**

**GEOTECHNICAL DESIGN MANUAL**

*January 2019*





# **APPENDIX B**

## **RESERVED**

Appendix B – Slope Stability Design Charts of GDM version 1.1, 2010 has been deleted. This Appendix is reserved for future use by SCDOT.

**APPENDIX C**  
**MSE WALLS**

**GEOTECHNICAL DESIGN MANUAL**

*January 2019*



## Table of Contents

<u>Section</u>	<u>Page</u>
C.1	Introduction..... C-1
C.2	Design Considerations and Requirements..... C-1
C.3	Site Conditions ..... C-1
C.4	Initial Wall Geometry..... C-1
C.5	Nominal Loads..... C-3
C.5.1	Unfactored Load Estimate..... C-3
C.6	Load Combination Summary ..... C-7
C.7	External Stability ..... C-8
C.7.1	Eccentricity..... C-8
C.7.2	External Sliding Stability..... C-8
C.7.3	Bearing Resistance ..... C-11
C.7.4	Vertical Displacement ..... C-15
C.8	Internal Stability ..... C-15
C.8.1	Select Type of Reinforcement ..... C-16
C.8.2	Critical Slip Surface Location..... C-17
C.8.3	Define Unfactored Loads..... C-19
C.8.4	Establish Vertical Layout of Soil Reinforcements..... C-22
C.8.5	Factored Tensile Forces in Reinforcement Layers ..... C-23
C.8.6	Soil Reinforcement Resistance ..... C-26
C.8.7	Strength and Number of Soil Reinforcements ..... C-37
C.8.8	Calculate Factored Pullout Resistance of Soil Reinforcements ..... C-37
C.8.9	$T_{ac}$ for Connection Strength..... C-43
C.8.10	Estimation of Lateral Movements ..... C-46
C.8.11	Vertical Movement and Bearing Pad Check ..... C-48
C.9	Design of Facing Elements ..... C-48
C.10	Overall Stability..... C-49
C.11	Compound Stability..... C-49
C.12	Wall Drainage System Design ..... C-51
C.12.1	Subsurface Drainage ..... C-51
C.12.2	Surface Water Runoff..... C-51
C.12.3	Scour ..... C-52
C.13	Seismic Design..... C-52
C.14	Computer Software..... C-52
C.15	Plans ..... C-53
C.16	References ..... C-53

**List of Tables**

<b><u>Table</u></b>	<b><u>Page</u></b>
Table C-1, Minimum MSE Wall Embedment Depth .....	C-2
Table C-2, Limiting Differential Settlement for MSE Wall Systems .....	C-15
Table C-3, Minimum Galvanization Thickness by Steel Thickness .....	C-29
Table C-4, Steel Corrosion Rates for Moderately Corrosive Reinforced Fill.....	C-30
Table C-5, Installation Damage Reduction Factors, $RF_{ID}$ .....	C-32
Table C-6, Creep Reduction Factors, $RF_{CR}$ .....	C-33
Table C-7, Anticipated Resistance of Polymers to Specific Environments .....	C-34
Table C-8, $RF_D$ for PET .....	C-35
Table C-9, Minimum Testing Requirements for use $RF_D$ .....	C-36
Table C-10, Typical Values of $\alpha$ .....	C-41

### List of Figures

<u>Figure</u>	<u>Page</u>
Figure C-1, General MSE Wall Schematic.....	C-2
Figure C-2, MSE Wall Earth Pressure for Horizontal Backslope.....	C-4
Figure C-3, MSE Wall Earth Pressure for Sloping Backfill .....	C-5
Figure C-4, MSE Wall Earth Pressure for Broken Backslope.....	C-6
Figure C-5, Notation for Coulomb Active Earth Pressure.....	C-7
Figure C-6, MSE Wall Eccentricity Check for Horizontal Backslope .....	C-13
Figure C-7, MSE Wall Eccentricity Check for Sloping Backfill.....	C-13
Figure C-8, MSE Wall Internal Failure Mechanisms .....	C-16
Figure C-9, Potential Failure Surface Location for Internal Stability of MSE Walls.....	C-18
Figure C-10, Variation of the Coefficient of Lateral Stress Ratio with Depth .....	C-20
Figure C-11, Calculation of $\sigma_2$ for Sloping Backfill for Internal Stability .....	C-21
Figure C-12, Reinforcement Load Contributory Height .....	C-25
Figure C-13, Coverage Ratio.....	C-26
Figure C-14, Geometric Configuration of Metallic Reinforcement .....	C-28
Figure C-15, Long-Term Geosynthetic Reinforcement Strength Concept.....	C-31
Figure C-16, Calculation of Vertical Stress for Internal Stability Analysis.....	C-38
Figure C-17, Calculation of Vertical Confining Pressure beneath Sloping Backfill .....	C-39
Figure C-18, Grid Dimensions for Pullout Capacity .....	C-43
Figure C-19, Bodkin Connection Detail.....	C-44
Figure C-20, Hinge Height of Modular Block MSE Walls .....	C-46
Figure C-21, Empirical Curve for Estimating Lateral Displacement.....	C-47
Figure C-22, Compound Stability MSE Wall Geometries.....	C-50
Figure C-23, Drain Immediately Behind MSE Wall Face .....	C-51





# APPENDIX C

## MECHANICALLY STABILIZED EARTH WALL DESIGN GUIDELINES

### C.1 INTRODUCTION

This Appendix outlines SCDOT's design methodology for MSE Walls. MSE wall structures are internally stabilized, flexible gravity, fill walls constructed of alternating layers of compacted soil and reinforcement. The design of MSE walls follows the design steps provided in Chapter 18. This Appendix governs the design of permanent and temporary MSE wall structures. The design life of both permanent and temporary MSE walls is provided in Chapter 18. The design responsibilities of SCDOT (or its representative) and the MSE wall supplier are outlined with respect to external and internal stability of the MSE wall structure.

### C.2 DESIGN CONSIDERATIONS AND REQUIREMENTS

The first part of the design is determining if an MSE wall is appropriate for the application being planned (see Chapter 18 for ERS selection criteria). If an MSE wall is appropriate, determine the geometry, the external loading conditions, the performance criteria, and any construction constraints. The geometry should include the location relative to the remainder of the project (i.e., to the centerline and specific station) and should establish wall stationing as needed. The geometry should also indicate the anticipated elevation of the top and base of the wall, as well as slopes that tie into the wall. During this step of the design process, external loads should be identified. These loads include, but are not limited to transient (traffic), permanent (weight of pavement surface), and/or seismically induced loads. The Performance Limits are provided in Chapter 10. Any constraints on construction should also be identified during this step (for example, soft ground, standing water, limited ROW, utilities, etc.). These construction constraints should be carefully considered before deciding to use an MSE wall.

### C.3 SITE CONDITIONS

The second step in the design of MSE walls is the evaluation of the topography, subsurface conditions, in-situ soil/rock parameters, and the parameters for the reinforced backfill. The evaluation of the topography should include reviewing the height requirements of the wall, the amount of space between the front of the MSE wall and the anticipated extent of the reinforcement, and the condition of the existing ground surface. This evaluation should identify the need for any temporary shoring that may be required to install the MSE wall (i.e., the grading of the site requires cutting). The subsurface conditions and in-situ soil/rock parameters shall be evaluated using the procedures presented in Chapters 4 through 7. The reinforced backfill to be used to construct the MSE wall shall meet the criteria provided in STS SC-M-713 (latest version) for *Mechanically Stabilized Earth (MSE) Walls*.

### C.4 INITIAL WALL GEOMETRY

The third step in the design of MSE walls is establishing the initial geometry of the MSE wall. Figure C-1 provides the general terminology for MSE wall geometry. The height (H) of an MSE wall is measured vertically from the top of the MSE wall to the top of the leveling pad. MSE wall structures, with panel type facings, should not exceed heights of 40 feet, and with modular block type facings, should not exceed heights of 30 feet. Wall heights in excess of these limits will require approval from the PC/GDS. The length of reinforcement (L) is measured from the back

of MSE wall panels. For modular block type MSE walls the length of reinforcement (B) is measured from the front face of the modular blocks. The minimum reinforcement length is 0.7H (B) or 8 feet whichever is greater. MSE wall structures with sloping surcharge fills or other concentrated loads will generally require longer reinforcement lengths of 0.8H (B) to 1.1H (B). MSE walls may be built to heights mentioned above; however, the external stability requirements may limit MSE wall height due to bearing capacity, settlement, or stability concerns.

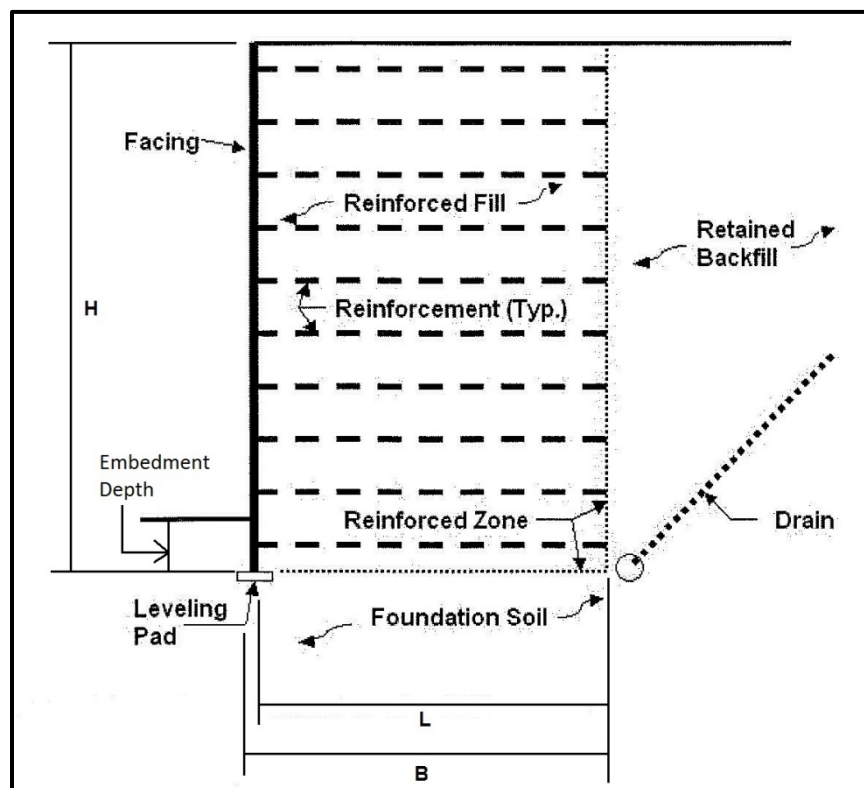


**Figure C-1, General MSE Wall Schematic  
(Modified Berg, Christopher, and Samtani – Volume I (2009))**

The top of the leveling pad will require a minimum embedment below finished grade in front of the wall of 2 feet. Greater embedment depths may be required due to bearing capacity, settlement, stability, erosion, or scour requirements and if utilities, ditches, or other structures are located adjacent to the front of the wall. The minimum embedment depths based on local bearing capacity considerations taking into account the geometry in front of the wall are presented in Table C-1.

**Table C-1, Minimum MSE Wall Embedment Depth  
Based on Local Bearing Capacity**

<b>Slope in Front of Wall</b>	<b>Minimum Embedment Depth</b>
Horizontal (walls)	H/20
Horizontal (abutments)	H/10
3H:1V	H/10
2H:1V	H/7
1.5H:1V	H/5

A minimum horizontal bench of 4 feet is required in front of the MSE wall structure, for MSE walls built on slopes. This minimum bench is required to protect against local instability at the base of the wall.

## C.5 NOMINAL LOADS

The next step is the development of unfactored and factored loads on an MSE wall. The determination of these external loads is normally performed by the GEOR.

### C.5.1 Unfactored Load Estimate

In this step, the GEOR is responsible for developing the unfactored loads that are used in the design of the MSE wall. These loads are the result of earth pressures induced by the retained fill materials (horizontal and vertical earth pressures) and any surcharge loadings. There are 3 cases for the development of earth pressures; these are 1) horizontal backslope with traffic surcharge; 2) sloping backslope; and, 3) broken backslope. The surcharge loadings can include vehicle live loads, the loads imposed by a bridge, etc. These loading conditions are discussed in Chapter 8. In addition, Chapter 8 also provides some unit weights for materials that are used as surcharges as well as the required load factors. If a bridge is to be supported by shallow foundations that bear on top of the MSE wall, then loads induced by the foundations must be included as specialized dead loads in the design of the MSE wall.

#### C.5.1.1 Horizontal Backslope with Traffic Surcharge

The procedure for estimating the earth pressures acting on the back of the reinforced soil mass for the horizontal backslope with traffic surcharge is depicted in Figure C-2. The active earth pressure coefficient ( $K_a$ ) for vertical walls (i.e., walls with less than 8° batter) with horizontal backfill is calculated according to the procedures provided in Chapter 18. The  $K_a$ s used in this Appendix are based on Coulomb earth pressure theory. When considering live loads on MSE walls for this condition, the factored surcharge load is generally included over the reinforced soil mass during the evaluation of foundation bearing resistance, overall (global) stability and tensile resistance of the reinforcement (see Figure C-2). The live load surcharge is not included over the reinforced soil mass in the evaluation of eccentricity, sliding, reinforcement pullout, or other failure mechanisms for which the surcharge load increases the resistance to failure (i.e., increases stability).

$$F_T = \frac{1}{2} * (\gamma_f * h^2 * K_a) \quad \text{Equation C-1}$$

$$F_{TH} = F_T * \cos \delta \text{ and } F_{TV} = F_T * \sin \delta \quad \text{Equation C-2}$$

$$F_q = q * h * K_a \quad \text{Equation C-3}$$

$$F_{qH} = F_q * \cos \delta \text{ and } F_{qV} = F_q * \sin \delta \quad \text{Equation C-4}$$

Where,

$\gamma_f$  = Unit weight of retained fill material

$\delta$  = 2/3 \*  $\phi$  of either reinforced soil or retained fill, whichever is smaller

h = Height of MSE wall above leveling pad (H in Figure C-2)

$K_a$  = Active earth pressure coefficient, determined in accordance with Chapter 18 using the retained fill material properties ( $k_{af}$  in Figure C-2 and C-3)

q = Surcharge load over retained fill

- $F_T$  = Earth pressure induced by retained fill
- $F_{TH}$  = Horizontal component of earth pressure induced by retained fill
- $F_{TV}$  = Vertical component of earth pressure induced by retained fill
- $F_q$  = Earth pressure induced by live load surcharge
- $F_{qH}$  = Horizontal component of earth pressure induced by live load surcharge
- $F_{qV}$  = Vertical component of earth pressure induced by live load surcharge

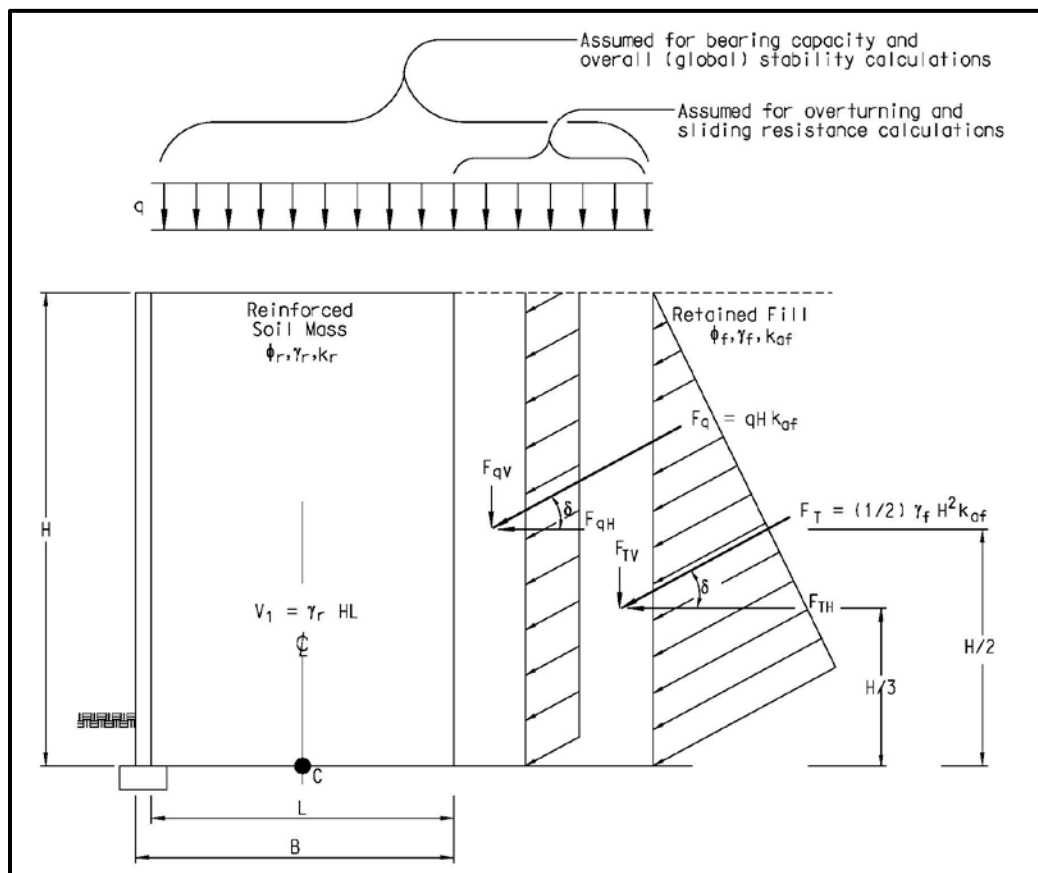


**Figure C-2, MSE Wall Earth Pressure for Horizontal Backslope With Traffic Surcharge (modified AASHTO LRFD Specifications)**

### C.5.1.2 Sloping Backslope

$K_a$  changes when there is a slope behind the MSE wall.  $K_a$  is determined in Chapter 18 and is based on Coulomb earth pressure theory. The force on the rear of the reinforced soil mass ( $P_a$ ) and the resulting horizontal ( $P_H$ ) and vertical ( $P_V$ ) forces are determined from the following equations:

$$F_T = \frac{1}{2} * (\gamma_f * h^2 * K_a) \tag{Equation C-5}$$

$$F_{TH} = F_T * \cos \delta \tag{Equation C-6}$$

$$F_{TV} = F_T * \sin \delta \tag{Equation C-7}$$

Where,

$\delta = 2/3 * \phi$  of either reinforced soil or retained fill, whichever is smaller

- $h$  = Total height of wall including vertical projection of slope above wall (see Figure C-3)  
 $K_a$  = Active earth pressure coefficient, determined in accordance with Chapter 18 using the retained fill material properties  
 $F_T$  = Earth pressure induced by retained fill ( $P_a$  in Figure C-4)  
 $F_{TH}$  = Horizontal component of earth pressure induced by retained fill ( $P_h$  in Figure C-4)  
 $F_{TV}$  = Vertical component of earth pressure induced by retained fill ( $P_v$  in Figure C-4)

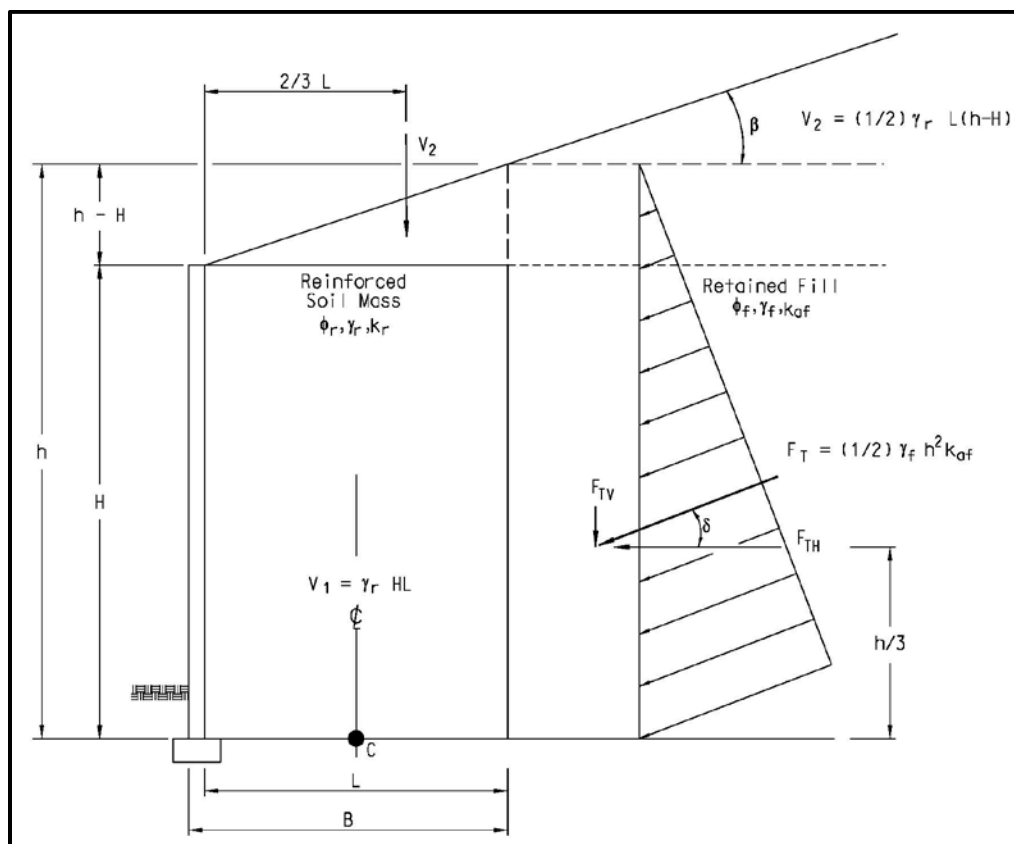


**Figure C-3, MSE Wall Earth Pressure for Sloping Backfill  
(modified AASHTO LRFD Specifications)**

### C.5.1.3 Broken Backslope

For broken backslopes (see Figure C-4), the  $K_a$  is determined as indicated in Chapter 18 and is based on Coulomb earth pressure theory. The AASHTO LRFD Specifications have altered how the  $K_a$  from Coulomb earth pressure theory is developed for a broken backslope. As can be seen in Figure C-4 there are 3 cases for use in determining  $K_a$  for use in the design of MSE walls with broken backslopes. The cases are delineated on the ratio  $L_s$  to  $h$ , where  $L_s$  is the horizontal distance the broken backslope extends from the end of the reinforced soil mass and  $h$  is the vertical distance from the top of the leveling pad (see Figure C-1) to a horizontal line drawn from where the end of the reinforced soil mass intersects the backslope (see Figure C-4).

#### C.5.1.3.1 Case 1

Case 1 (⊙ in Figure C-4) is the condition when  $L_s$  is greater than or equal to  $h$  ( $L_s \geq h$ ). This case is similar to and designed as an MSE wall with a sloping backslope that is infinite as discussed in Section C.5.1.2. In determining the Coulomb active earth pressure coefficient,  $\beta = \beta$  and is termed  $K_{a-Infinitive}$ .

### C.5.1.3.2 Case 3

Case 3 (③ in Figure C-4) is the condition when  $L_s$  is less than or equal to 0 ( $L_s \leq 0$ ) (i.e., slope breaks above the reinforced soil mass (see Figure C-4)). This case is similar to and designed as an MSE wall with a horizontal backslope (Section C.5.1.1 with a traffic surcharge equal to 0 (i.e.,  $q = 0$ )). In determining the Coulomb active earth pressure coefficient,  $\beta = 0$  and is termed  $K_{a-Level}$ .

### C.5.1.3.3 Case 2

Case 2 (② in Figure C-4) is more complicated, since  $L_s$  is greater than 0, but less than  $h$  ( $0 < L_s < h$ ). This case is between Case 1 and Case 3 as far as the development of the Coulomb active earth pressure. The AASHTO LRFD Specifications recommend the following equation be used to develop  $K_a$  for Case 2.

$$K_{a-2} = \left(\frac{L_s}{h}\right) * (K_{a-Infinite} - K_{a-Level}) + K_{a-Level} \quad \text{Equation C-8}$$

Using the  $K_a$  developed from 1 of the 3 cases previously discussed  $P_a$ ,  $P_H$ , and  $P_V$  are determined as indicated in Equations C-5 through C-7. Where,  $P_a$  is the force acting on the rear of the MSE wall.

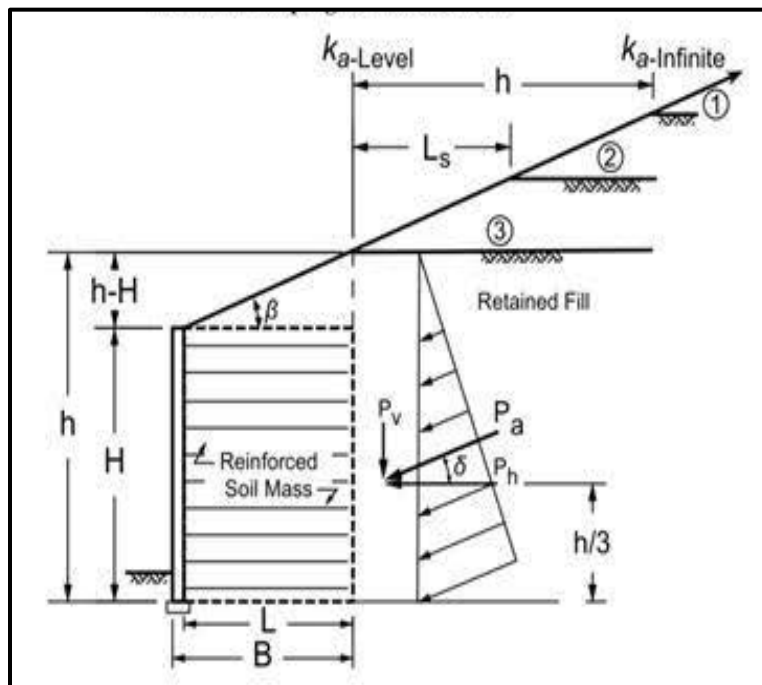


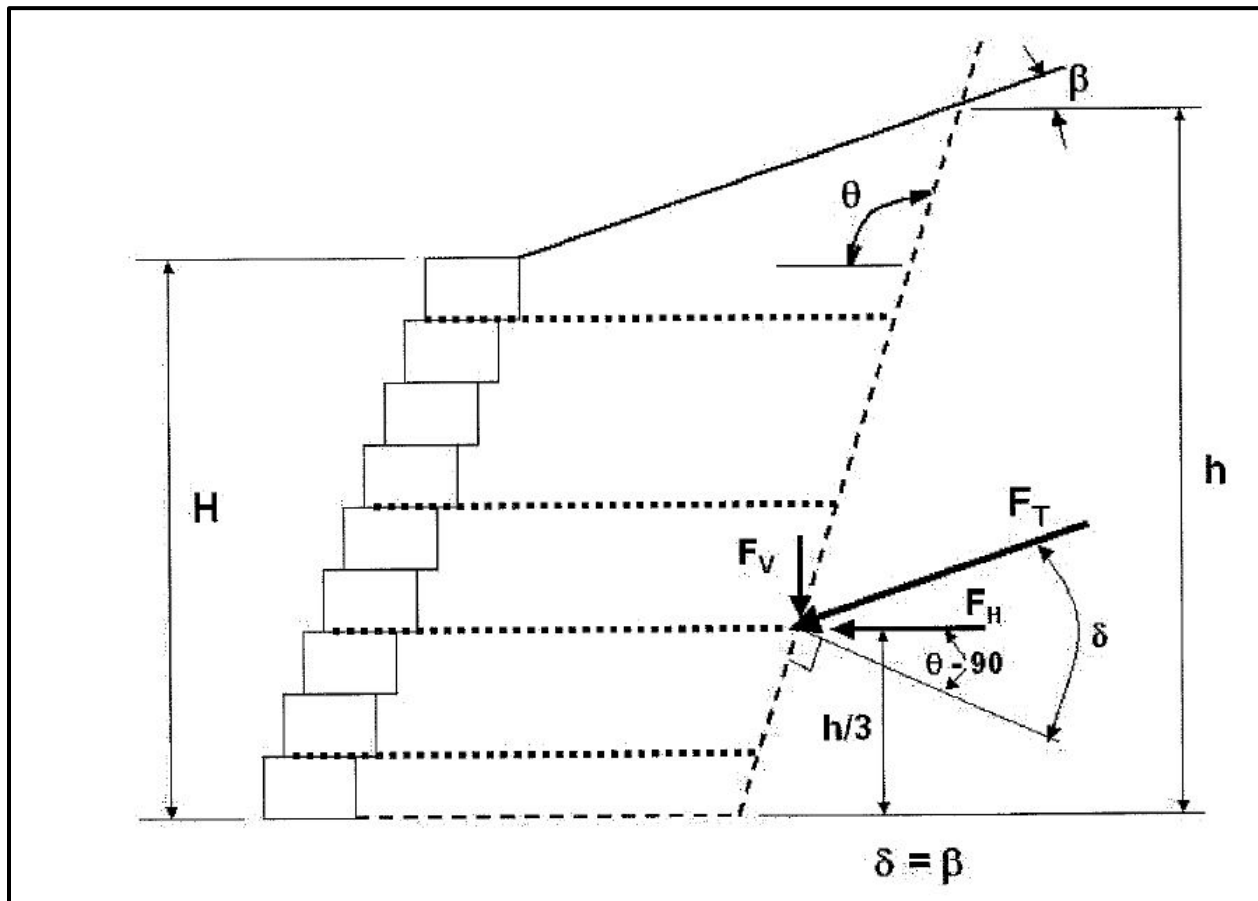
Figure C-4, MSE Wall Earth Pressure for Broken Backslope (AASHTO LRFD Specifications)

### C.5.1.4 Battered Wall with or without Backslope

According to Berg, et al. – Vol. I (2009):

For an inclined front face and reinforced zone (i.e., batter) equal to or greater than  $10^\circ$  from the vertical, the coefficient of earth pressure can be calculated using the procedures contained in Chapter 18, where  $\theta$  is the face inclination

from horizontal, and  $\beta$  is the surcharge slope angle as shown in Figure C-5. The wall friction angle  $\delta$  is assumed to be equal to  $\beta$ .



$\theta \geq 100^\circ$

**Figure C-5, Notation for Coulomb Active Earth Pressure  
(Berg, et al. – Vol. I (2009))**

## C.6 LOAD COMINATION SUMMARY

Portions of the following Section of this Appendix are adopted directly from Tanyu, Sabatini, and Berg (2008) and are used with the permission of the US Department of Transportation, Federal Highway Administration. The italics are added to reflect additions or modifications to the selected text and to supply references to this Manual. According to Tanyu, et al. (2008):

...the unfactored loads from *the previous step* are multiplied by load factors to obtain the factored loads for each limit state. The load factors for the limit state are provided in *Chapter 8*.

Load factors for permanent loads are selected to produce the maximum destabilizing effect for the design check being considered. For example, to produce the maximum destabilizing effect, when checking sliding resistance,  $\gamma_{EV}$  is selected as the minimum value from *Table 8-6* (i.e.,  $\gamma_{EV} = 1.00$ ) and when checking bearing resistance,  $\gamma_{EV}$  is selected as the maximum value from *Table 8-6* (i.e.,  $\gamma_{EV} = 1.35$ ).

## C.7 EXTERNAL STABILITY

The external stability analysis checks eccentricity (Section C.7.1), sliding (Section C.7.2), bearing resistance (C.7.3), and overall (global) stability (Section C.10). The determination of external stability is typically performed by SCDOT or its GEC and is performed for all appropriate limit states (see Chapter 8). The following Sections of this Appendix are adopted directly from the AASTHO LRFD Specifications and Berg, et al. – Vol. I (2009) and are used with the permission of the US Department of Transportation, Federal Highway Administration. The italics are added to reflect additions or modifications to the selected text and to supply references to this Manual.

### C.7.1 Eccentricity

Eccentricity as used in this Section is concerned with overturning centered on the junction of the MSE wall face and the leveling pad. According to AASHTO LRFD Specifications:

Reinforced soil walls are in general too flexible to fail due to excessive eccentricity (i.e., overturning). However, meeting the eccentricity requirements *typically used* for gravity walls...will keep the reinforced soil from being too flexible in its response to lateral earth pressure and other lateral loads that may be present behind the reinforced soil wall.

Therefore,

For foundations on soil, the location of the resultant of the reaction forces shall be within the middle two-thirds (2/3) of the base width.

For foundations on rock, the location of the resultant of the reaction forces shall be within the middle nine-tenths (9/10) of the base width.

For *EE I* eccentricity evaluation of walls with foundations on soil and rock, the location of the resultant of the reaction forces shall be in the middle two-thirds (2/3) of the base for  $\gamma_{EQ} = 0.0$ ... *It is noted that  $\gamma_{EQ} = 0.0$  for all SCDOT projects unless otherwise specified by SCDOT.*

Combining the requirements of Berg, et al. – Vol. I (2009) and AASHTO LRFD Specifications leads to the following equation for an MSE wall with horizontal backslope and traffic surcharge (see Figure C-2):

$$e_c = \frac{[\gamma_{EH-MAX}*(F_{TH})*\left(\frac{H}{3}\right) + \gamma_{LS}*(F_{qH})*\left(\frac{H}{2}\right)] - [\gamma_{EH-MIN}*(F_{TV})*\left(\frac{L}{2}\right) + \gamma_{LS}*(F_{qV})*\left(\frac{L}{2}\right)]}{\gamma_{EV-MIN}*V_1 + \gamma_{EH-MIN}*F_{TV} + \gamma_{LS}*F_{qV}} \quad \text{Equation C-9}$$

Using the same sources leads to the following equation for an MSE wall with a sloping backslope (see Figure C-3):

$$e_c = \frac{[\gamma_{EH-MAX}*(F_{TH})*\left(\frac{h}{3}\right)] - [\gamma_{EH-MIN}*(F_{TV})*\left(\frac{L}{2}\right) + \gamma_{EV-MIN}*(V_2)*\left(\frac{L}{6}\right)]}{\gamma_{EV-MIN}*V_1 + \gamma_{EV-MIN}*V_2 + \gamma_{EH-MAX}*F_{TV}} \quad \text{Equation C-10}$$

### C.7.2 External Sliding Stability

Check external sliding stability of the MSE wall. According to Berg, et al. – Vol. I (2009):



Check the preliminary sizing with respect to sliding of the reinforced zone where the resisting force is the lesser of shear resistance along the base of the wall or of a weak layer near the base of the MSE wall, and the sliding force is the horizontal component of the thrust on the vertical plane at the back of the wall (see Figures C-2 through C-4). The live load surcharge is not considered as a stabilizing force when checking sliding, i.e., the sliding stability check only applies to the live load above the retained backfill, as shown in Figure C-2. The driving forces generally include factored horizontal loads due to earth, water, seismic and surcharges.

Sliding resistance along the base of the wall is evaluated using the same procedures as for spread footings on soil as *indicated in Chapter 15*. The factored resistance against failure by sliding ( $R_r$ ) can be estimated by:

$$R_r = \phi_\tau * R_\tau \quad \text{Equation C-11}$$

Where,

$\phi_\tau$  = Resistance factor for shear resistance between soil and foundation  
(equal to 1.0 for sliding of, see Chapter 9)

$R_\tau$  = Nominal sliding resistance between reinforced fill and foundation soil

Note that any soil passive resistance at the toe due to embedment is ignored due to the potential for the soil to be removed through natural or manmade processes during its service life (e.g., erosion, utility installation, etc.). Also, passive resistance is usually not available during construction. The shear strength of the facing system is also conservatively neglected.

Calculation steps and equations to compute sliding for 2 typical cases follow. These equations should be extended to include other loads and geometries, for other cases, such as additional live and dead load *and* surcharge loads. SOIL

1. Calculate nominal thrust, per unit width, acting on the back of the reinforced zone.

Wall with Horizontal Backfill: (see Figure C-2)

The *horizontal component* of the retained backfill resultant,  $F_{TH}$ , is determined using Equation C-2.

For a uniform surcharge, the *horizontal component of the resultant*,  $F_{qH}$ , is determined using Equation C-4.

Wall with Sloping Backfill: (see Figure C-3)

Calculate *horizontal component of the retained backfill force resultant* per unit width,  $P_H$ , using Equation C-6.

Wall with Broken Backslope: (see Figure C-4)

Use the correct case indicated above and the correct horizontal components indicated.

2. Calculate the nominal and factored horizontal driving forces. For a horizontal backslope and uniform live load surcharge:

$$\sum F = F_{TH} + F_{qH} \quad \text{Equation C-12}$$

$$P_d = \gamma_{EH} * F_{TH} + \gamma_{LS} * F_{qH} \quad \text{Equation C-13}$$

For a sloping backfill, see Equation C-6, therefore:

$$P_d = \gamma_{EH} * P_H \quad \text{Equation C-14}$$

Use the maximum EH load factor (see Chapter 9) in these equations because it creates the maximum driving force effect for the sliding check.

3. Determine the most critical frictional properties at the base. Choose the minimum soil friction angle,  $\phi$  for 3 possibilities:
  - i. Sliding along the foundation soil, if its shear strength (based on  $c'_f$  +  $\tan \phi'_f$  and/or  $c_u$  for cohesive soils) is smaller than that of the reinforced fill material shear strength ( $\tan \phi'_r$ ).
  - ii. Sliding along the reinforced fill ( $\phi'_r$ ).
  - iii. For sheet type reinforcement, sliding along the weaker of the upper and lower soil-reinforcement interfaces. The soil-reinforcement friction angle,  $\rho$ , should preferably be measured by means of interface direct shear tests. In absence of testing, it may be taken as  $(2/3)\tan \phi'_r$ .
4. Calculate the nominal components of resisting force and the factored resisting force per unit length of wall. For a horizontal backslope and uniform live load surcharge, the live load is excluded since it increases sliding stability:

$$R_r = [\gamma_{EV} * (V_1) + \gamma_{EH} * F_{TV}] * \mu \quad \text{Equation C-15}$$

For a sloping backfill condition:

$$R_r = [\gamma_{EV} * (V_1 + V_2) + \gamma_{EH} * F_{TV}] * \mu \quad \text{Equation C-16}$$

$$V_1 = \gamma_r * H * L \quad \text{Equation C-17}$$

$$V_2 = \frac{\gamma_r * (h-H) * L}{2} \quad \text{Equation C-18}$$

Where,

$\gamma_f$  = Unit weight of retained fill material

H = Total wall height above the leveling pad (see Figure C-2)

h = Total height of wall including vertical projection of slope above wall (see Figure C-3)

L = Length of the reinforced soil mass (see Figure C-2)

$F_{TV}$  = Vertical component of earth pressure induced by retained fill ( $P_v$  in Figure C-4) (see Equation C-7)

$\mu$  = Minimum soil friction angle  $\phi$  [ $\tan \phi'_f$ ,  $\tan \phi'_r$ , or (for continuous reinforcement)  $\tan \rho$ ]

Forces  $V_1$  and  $V_2$  are applied through the centroid of the respective soil masses.

External loads that increase sliding resistance should only be included if those loads are permanent.

Use the minimum EV load factor (*see Chapter 9*) in these equations because it results in minimum resistance for the sliding *check*.

5. Compare factored sliding resistance,  $R_r$ , to the factored driving force  $P_d$ , to check that resistance is greater.
6. Check the capacity demand ratio (CDR) for sliding,  $CDR = R_r/P_d$ . If the  $CDR < 1.0$  increase the reinforcement length,  $L$ , and repeat the calculations.

### C.7.3 Bearing Resistance

The bearing resistance of the soil beneath the MSE Wall is the next design check. According to Berg, et al. – Vol. I (2009):

Two modes of bearing capacity failure exist, general shear failure and local shear failure. Local shear is characterized by a punching or squeezing of the foundation soil when soft or loose soils exist below the wall.

Bearing calculations require both a *Strength* limit state and *Service* limit state calculation. Strength limit calculations check that the factored bearing pressure is less than the factored bearing resistance. Service limit calculations are used to compute nominal bearing pressure for use in settlement calculations. It should be noted that the weight and width of the wall facing is typically neglected in the calculations. The bearing check applies live load above both the reinforced zone and the retained backfill, as shown in Figure C-2.

General Shear: To prevent bearing failure on a uniform foundation soil, it is required that the factored vertical pressure at the base of the wall, as calculated with the uniform Meyerhof-type distribution, does not exceed the factored bearing resistance of the foundation soil:

$$q_r \geq q_{uniform} = \sigma_{V-F} \quad \text{Equation C-19}$$

The uniform vertical pressure is calculated as:

$$q_{uniform} = \sigma_{V-F} = \frac{\sum V}{L - 2e_B} \quad \text{Equation C-20}$$

This step requires *the* computation of the eccentricity value. Also note that the bearing check applies the live load above both the reinforced zone and the retained backfill, as shown in Figure C-2. In addition to walls founded on soil, a uniform vertical pressure is also used for walls founded on rock due to the flexibility of MSE walls and their limited ability to transmit moment (Article C11.10.5.4 (*AASHTO LRFD Specifications*)).

Calculation steps for MSE walls with either a horizontal backslope and uniform live load surcharge *or* for sloping backfills follows. Again, note that these equations should be extended to include loads and geometries, for other cases.

1. Calculate the eccentricity,  $e_B$ , of the resulting force at the base of the wall. *Note*, the  $e_C$  value from the eccentricity step *check* cannot be used. Calculate  $e_B$  with factored loads (see *Figure C-6*). For a wall with horizontal backslope and uniform live load surcharge centered about the reinforced zone, the eccentricity is equal to:

**Equation C-21**

$$e_B = \frac{[\gamma_{EH-MAX} * F_{TH} * (\frac{H}{3}) + \gamma_{LS} * F_{qH} * (\frac{H}{2})] - [\gamma_{EH-MAX} * (F_{TV}) * (\frac{L}{2}) + \gamma_{LS} * (F_{qV}) * (\frac{L}{2})]}{\gamma_{EV-MAX} * V_1 + \gamma_{LS} * q * L + \gamma_{EV-MAX} * F_{TV} + \gamma_{LS} * F_{qV}}$$

Where the terms used were previously defined. The maximum load factors for  $\gamma_{EH}$  and  $\gamma_{EV}$  are used to be consistent with the computation for  $\sigma_v$  (below) where the maximum load factors results in the maximum vertical stress.

For walls with sloping backfill see the following equation (see *Figure C-7*). Again, note that these equations should be extended to include other loads and geometries, for other cases.

**Equation C-22**

$$e_B = \frac{[\gamma_{EH-MAX} * (F_{TH}) * (\frac{h}{3})] - [\gamma_{EH-MAX} * (F_{TV}) * (\frac{L}{2}) + \gamma_{EV-MAX} * (V_2) * (\frac{L}{6})]}{\gamma_{EV-MAX} * V_1 + \gamma_{EV-MAX} * V_2 + \gamma_{EH-MAX} * F_{TV}}$$

Note that when checking the various load factors, and load combinations, the value of eccentricity,  $e_B$ , will vary. Also note that when the calculated eccentricity,  $e_B$ , is negative, a value of 0 should be carried in the design stress equation, i.e., set  $L' = L$ , per AASHTO C11.10.5.4 (*AASHTO LRFD Specifications*).

2. Calculate the factored vertical stress  $\sigma_{V-F}$  at the base assuming Meyerhof-type distribution. For a horizontal backslope and uniform live load surcharge the factored bearing pressure is:

$$\sigma_{V-F} = \frac{\gamma_{EV-MAX} * V_1 + \gamma_{LS} * q * L}{L - 2e_B} \quad \text{Equation C-23}$$

This approach, proposed originally by Meyerhof, assumes that a stress distribution due to eccentric loading can be approximated by a uniform stress distribution over a reduced area at the base of the wall. This area is defined by a width equal to the wall width minus twice the eccentricity as shown in *Figures C-6* and *C-7*. The effect of eccentricity and load inclination is addressed with the use of the effective width,  $L - 2e_B$ , in lieu of the full width,  $L$ .

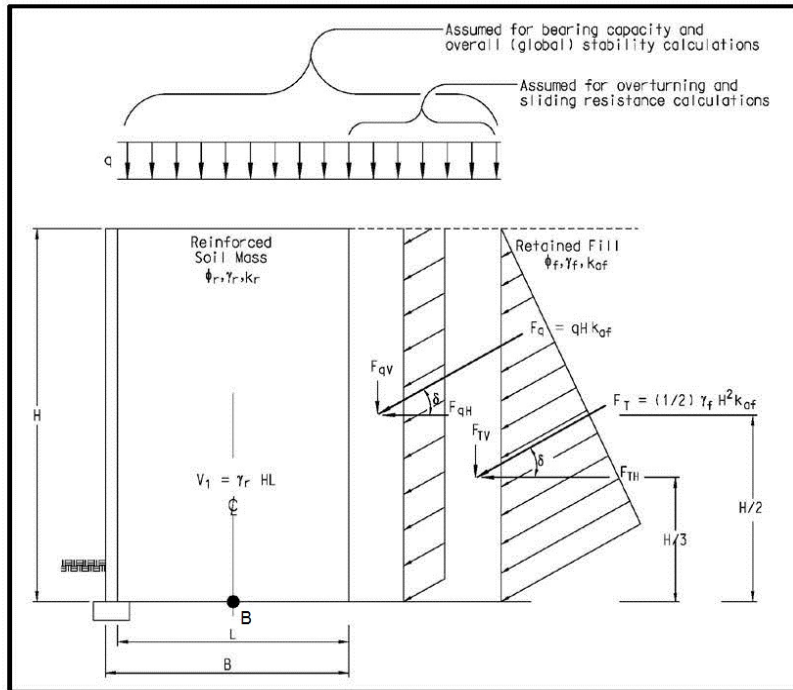


Figure C-6, MSE Wall Eccentricity Check for Horizontal Backslope (Berg, et al. – Vol. I (2009))

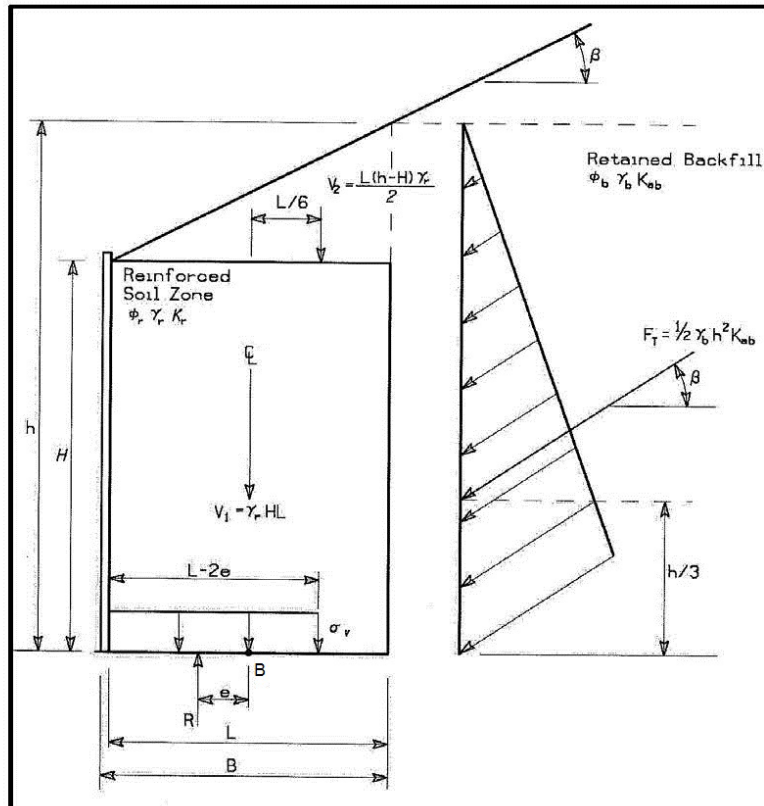


Figure C-7, MSE Wall Eccentricity Check for Sloping Backfill (Berg, et al. – Vol. I (2009))

For wall with sloping backfill the factored bearing stress is:

$$\sigma_{V-F} = \frac{\gamma_{EV-MAX} * V_1 + \gamma_{EV-MAX} * V_2 + \gamma_{EH-MAX} * P_V}{L - 2e_B} \quad \text{Equation C-24}$$

Note the  $(L - 2e_B)$  is set equal to  $L$  when the value of eccentricity is negative. A negative value of eccentricity may be found for some extreme geometries, e.g., a wall section with very long reinforcements and a steep, infinite backslope. Note that when checking the various load factors and load combinations the value of eccentricity,  $e_B$ , will vary and a critical value must be determined by comparisons of applicable load combinations.

Where applicable, in the computation of bearing stress,  $\sigma_{V-F}$ , include the influence of factored surcharge and factored concentrated loads. Maintain consistency with loads and load factors used in the eccentricity calculation and corresponding bearing stress calculation.

3. Determine  $q_n$  per Chapter 15.
4. Check that factored bearing resistance is greater than the factored bearing stress, i.e.,  $q_r \geq \sigma_{V-F}$ . The factored bearing resistance ( $q_r$ ) is given as:

$$q_r = \phi * q_n \quad \text{Equation C-25}$$

5. As indicated previously,  $\sigma_{V-F}$  can be decreased and  $q_r$  increased by lengthening the reinforcements, though only marginally. The nominal bearing resistance often may be increased by additional subsurface investigation and better definition of the foundation soil properties. If adequate support conditions cannot be achieved or lengthening reinforcements significantly increases costs, improvement of the foundation soil may be considered (see Chapter 19).

Local Shear, Punching Shear and Lateral Squeeze. Local shear is a transition between general shear and punching shear, which can occur in loose or compressible soils or in weak soils under slow (drained) loading. If local shear or punching shear is possible, Section 10.6.3.1.2b of *AASHTO LRFD Specifications* requires the use of reduced shear strength parameters for *calculating the* nominal bearing resistance. The reduced effective stress cohesion,  $c^*$  is set equal to  $0.67c'$ . The reduced effective stress soil friction angle,  $\phi^*$  is set equal to  $\tan^{-1}(0.67\tan\phi'_f)$ .

Lateral squeeze is a special case of local shear that can occur when bearing on a weak cohesive soil layer overlying a firm soil layer. Lateral squeeze failure results in significant horizontal movement of the soil under the structure. *Lateral squeeze shall be determined as indicated in Chapter 17.*

If adequate support conditions cannot be achieved, either the soft soils should be removed and replaced with more suitable material or ground improvement of the foundation soils maybe required. Local shear, as well as bearing on 2-layered soil systems in undrained and drained loading, is addressed in Section 10.3.6.1.2 of *AASHTO LRFD Specifications*.

### C.7.4 Vertical Displacement

MSE wall structures can move vertically due to static and seismic loads. The movements caused by static loads (Service limit state) are discussed here. See Chapter 14 for guidance on seismically (EE I limit state) induced movements. Vertical movements (settlement) should be determined using the procedures outlined in Chapter 17. In conditions where the reinforced soil mass will settle more than the face, the reinforcement should be placed on a sloping fill surface, which is higher at the backend of the reinforcement to compensate for the greater vertical movement in this area. The reinforcement connection strength shall be checked if there is any differential settlement between the MSE wall face and the rear of the reinforced soil mass. This differential settlement can induce additional stresses in the connections at the interface between the reinforcement and wall face materials.

Differential settlements perpendicular to the MSE wall facing (along the soil reinforcement) may occur at roadway widening projects. If this type of differential settlement exceeds a ratio of 1/10, the MSE wall suppliers shall be consulted to determine if further analyses are required. The values shown in Table C-2 shall be used as typical limiting differential settlement tolerances along the MSE wall facing for MSE wall structures with precast panel facings.

**Table C-2, Limiting Differential Settlement for MSE Wall Systems with Precast Concrete Panel Facing (along facing)**

Panel Joint Width	Limiting Differential Settlement
$\geq 1/2''$ *	1/300
$< 1/2''$ *	1/600
Full Height Panel	1/600

\* **Note:** Relatively square facing panels

MSE wall structures with modular concrete block facings are typically restricted to a limiting differential settlement of 1/240 along the MSE wall structure. Temporary MSE wall structures with welded wire mesh facing should be restricted to a limiting differential settlement along the MSE wall facing of 1/50.

Slip joints may be used to maintain MSE wall structures within acceptable differential settlement tolerances. When significant differential settlements are anticipated, ground improvement techniques may be needed. Prefabricated Vertical Drains may be required to accelerate the consolidation settlement if construction time is limited. Walls shall be checked for any temporary surcharge loading. When long-term settlements are accelerated during construction, temporary wall facings may be required during this accelerated settlement phase followed by installation of permanent facings after the required level of settlement is achieved. According to Berg, et al. – Vol. I (2009), “Where the anticipated settlements and their duration, cannot be accommodated by these measures, consideration must be given to ... the implementation of 2-phased (-staged) construction in which the first phase (stage) facing is typically a wire facing.”

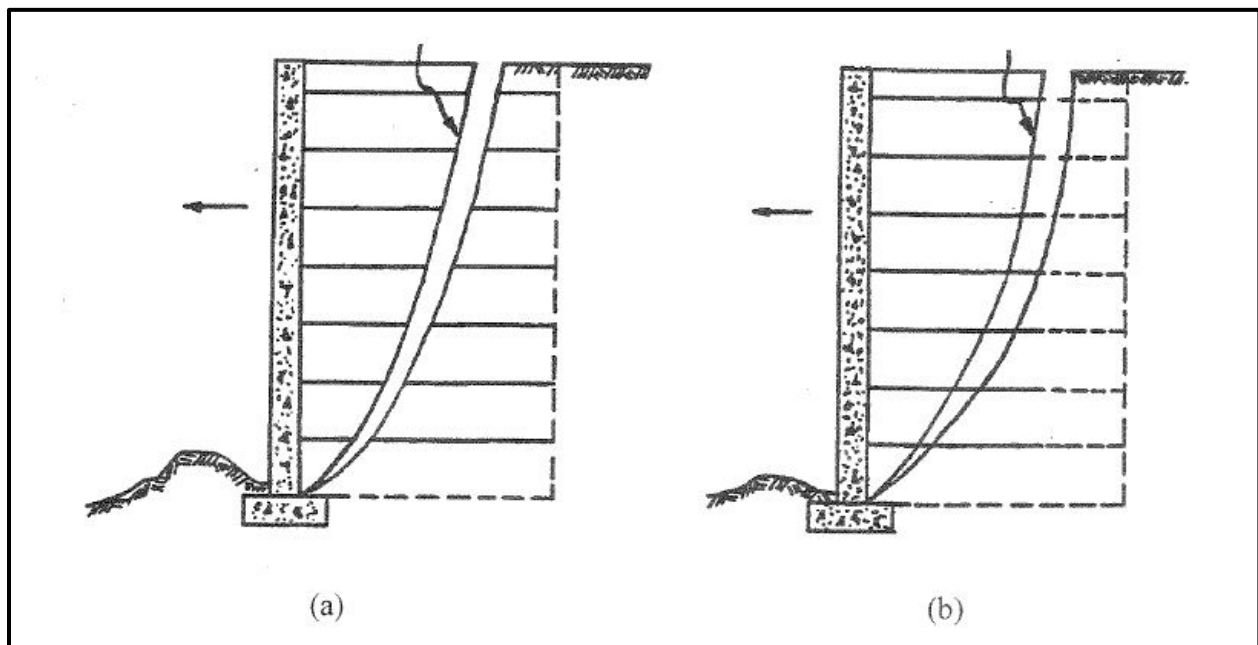
## C.8 INTERNAL STABILITY

The internal stability analysis is the seventh step of the design process provided in Chapter 18. These analyses are typically performed by the MSE wall supplier or manufacturer and reviewed/checked during the shop plan process. According to Berg, et al. – Vol. I (2009):

Internal failure of a MSE wall can occur in 2 different ways (see *Figure C-8*):

- The tensile forces (and, in the case of rigid reinforcements, the shear forces) in the inclusions become so large that the inclusions elongate excessively or break, leading to large movements and/or possible collapse of the structure. This mode of failure is called failure by elongation or breakage of the reinforcements (see *Figure C-8a*).
- The tensile forces in the reinforcements become larger than the pullout resistance, leading to large movements and/or possible collapse of the structure. This mode of failure is called failure by pullout (see *Figure C-8b*).

The process of sizing and designing to preclude internal failure, therefore, consists of determining the maximum developed tension forces, their location along a locus of critical slip surfaces and the resistance provided by the reinforcements both in pullout capacity and tensile strength. Internal stability also includes an evaluation of serviceability requirements such as tolerable lateral movement of supported structures and control of downdrag stress on reinforcement connections.



(a) Tension Failure (b) Pullout Failure

**Figure C-8, MSE Wall Internal Failure Mechanisms  
(Tanyu, et al. (2008))**

### **C.8.1 Select Type of Reinforcement**

The first step in internal stability design is the selection of the type of reinforcement (i.e., inextensible (metallic) or extensible (geosynthetic)). Berg, et al. – Vol. I (2009) describes the selection process as:

Soil reinforcements are either inextensible (i.e., mostly metallic) or extensible (i.e., mostly polymeric materials). The internal wall design model varies by material type due to their extensibility relative to soil at failure. Therefore, the choice of material type should be made at this step of the design. The variations are: whether life prediction is based on metal corrosion or polymeric degradation; critical failure plane geometry assumed for design; and lateral



stress used for design. Distinction can be made between the characteristics on inextensible and extensible reinforcements, as follows:

#### Design Methods, Inextensible (e.g., Metallic) Reinforcements

The current method of limit equilibrium analysis uses a coherent gravity structure approach to determine external stability of the reinforced mass, similar to the analysis for any conventional or traditional gravity structure. For internal stability evaluations, it considers a bi-linear failure surface that divides the reinforced zone in active and resistant zones and requires that an equilibrium state be achieved for successful design.

The lateral earth pressure distribution for **external stability** is assumed to be based on Coulomb's method with a wall friction angle  $\delta$ . For **internal stability** lateral pressure varying from a multiple of  $K_a$  to an active earth pressure state,  $K_a$  is used for design. Previous research (FHWA RD-89-043, *Christopher, et al. (1990)*) has focused on developing the state of stress for internal stability, as a function of  $K_a$ , type of reinforcement used (geotextile, geogrid, metal strip or metal grid), and depth. The results from these and more recent (*Allen, Christopher, Elias, and DiMaggio (2001)*) efforts have been synthesized in a simplified method, which will be used throughout this *Appendix*.

#### Design Methods, Extensible (e.g., Geosynthetic) Reinforcements

For **external stability** calculations, the current method assumes an earth pressure distribution consistent with the method used for inextensible reinforcements.

For **internal stability** computations using the simplified method, the internal coefficient of earth pressure is again a function of the type of reinforcement, where the minimum coefficient ( $K_a$ ) is used for walls constructed with continuous sheets of geotextiles and geogrids. For internal stability, a Rankine failure surface is considered, because the extensible reinforcements can elongate more than the soil, before failure, and do not significantly modify the shape of the soil failure surface.

### **C.8.2 Critical Slip Surface Location**

The second step in internal stability design is selecting the location of the critical slip surface. Berg, et al. – Vol. I (2009) describes the critical slip surface location selection process as:

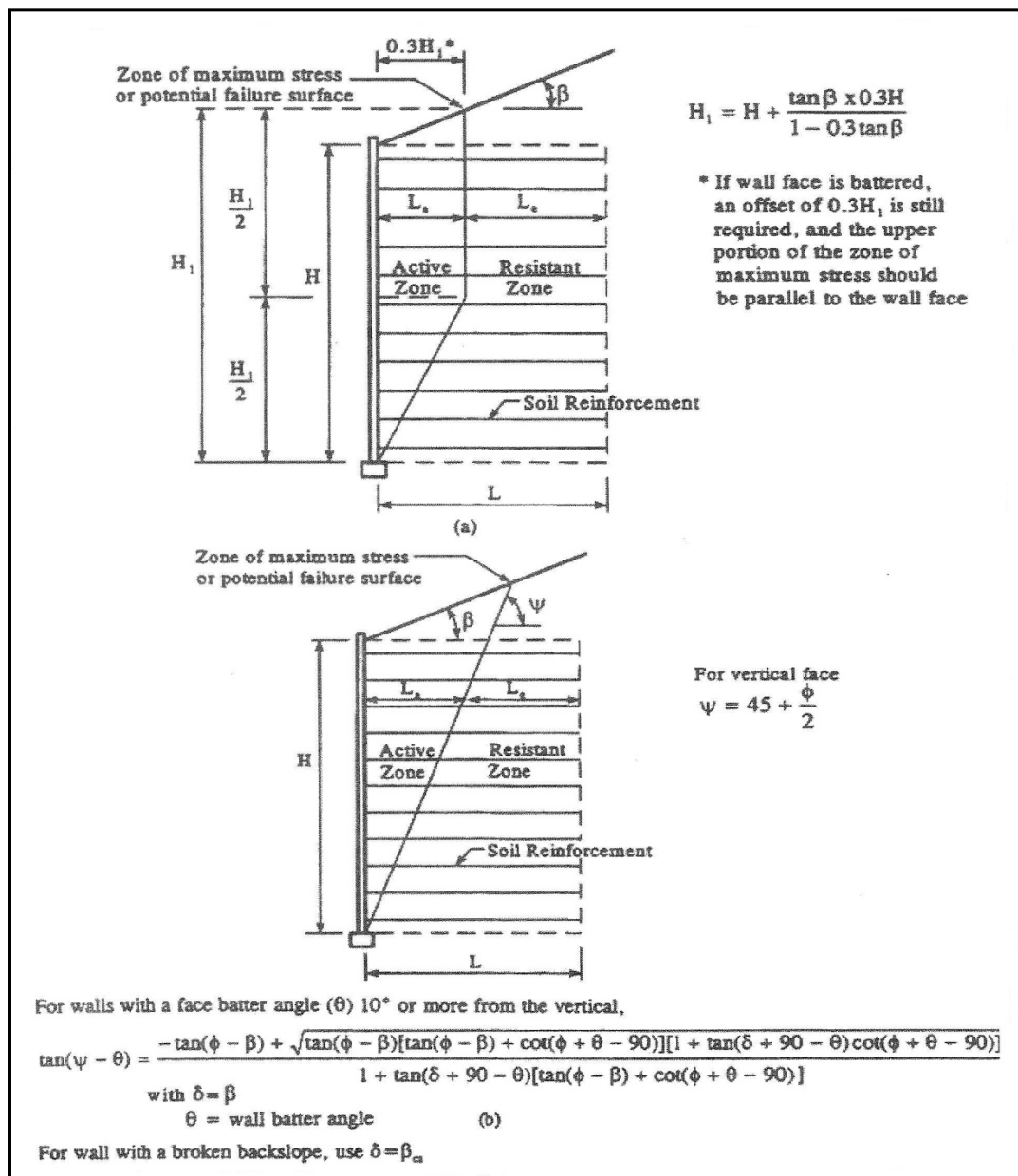
The critical slip surface in a simple reinforced soil wall is assumed to coincide with the locus of the maximum tensile force,  $T_{MAX}$ , in each reinforcement layer. The shape and location of the critical failure surface is based upon instrumented structures and theoretical studies.

The critical failure surface has been assumed to be approximately bilinear in the case of inextensible reinforcements (Figure C-9a), approximately linear in the case of extensible reinforcements (Figure C-9b), and passes through the toe of the wall in both cases.

When failure develops, the reinforcement may elongate and be deformed at its intersection with the failure surface. As a result, the tensile force in the reinforcement would increase and rotate. Consequently, the component in the direction of the failure surface would increase and the normal component may

increase or decrease. Elongation and rotation of the reinforcements may be negligible for stiff inextensible reinforcements such as steel strips but may be significant with geosynthetics. Any reinforcement rotation is ignored for internal wall stability calculations with the simplified method. However, reinforcement rotation may be considered in compound slope stability analysis (see *Berg, et al. – Vol. I (2009)*).

For extensible reinforcements, the Coulomb earth pressure relationship shown in Figure C-9 should be used to define the failure surface, per AASHTO Figure 11.10.6.3.1-1 (*AASHTO LRFD Specifications*), where the wall front batter from vertical is greater than or equal to 10 degrees. For walls with a front batter from the vertical to less than 10° from vertical (i.e.,  $\theta = 90^\circ$  to  $100^\circ$  in Figure C-9), use the Rankine earth pressure relationship (see Chapter 18).



(a) Inextensible reinforcements (b) Extensible reinforcements

**Figure C-9, Potential Failure Surface Location for Internal Stability of MSE Walls (Berg, et al. – Vol. I (2009))**

### **C.8.3 Define Unfactored Loads**

The third step in internal stability design is defining the unfactored loads to be used in design. According to Berg, et al. – Vol. I (2009):

The primary sources of internal loading of an MSE wall is the earth pressure from the reinforced fill and any surcharge loadings on top of the reinforced zone. The unfactored loads for MSE walls may include loads due to vertical earth pressure (EV), live load surcharge (LS), and earth surcharge (ES). Water, seismic, and vehicle impact loads should also be evaluated as appropriate.

Research studies (Collin (1986), Christopher, et al. (1990), Allen, et al. (2001)) have indicated that the maximum tensile force is primarily related to the type of reinforcement in the MSE wall, which, in turn, is a function of the modulus, extensibility and density of reinforcement. Based on this research, a relationship between the type of the reinforcement and the overburden stress has been developed, and shown in Figure C-10. The  $K_r/K_a$  ratio for metallic (inextensible) reinforcements decreases from the top of the reinforced wall fill to a constant value 20 ft below this elevation. In contrast to inextensible reinforcements, the  $K_r/K_a$  for extensible (e.g., geosynthetic) reinforcement is a constant. Note that the resulting  $K_r/K_a$  ratio is referenced to the top of the wall at the face, excluding copings and appurtenances (i.e., the top of the reinforced soil zone at the face) for both walls with level and sloping backfills. The  $K_r/K_a$  starting elevation for an MSE wall supporting a spread footing bridge abutment is the top of the backfill.

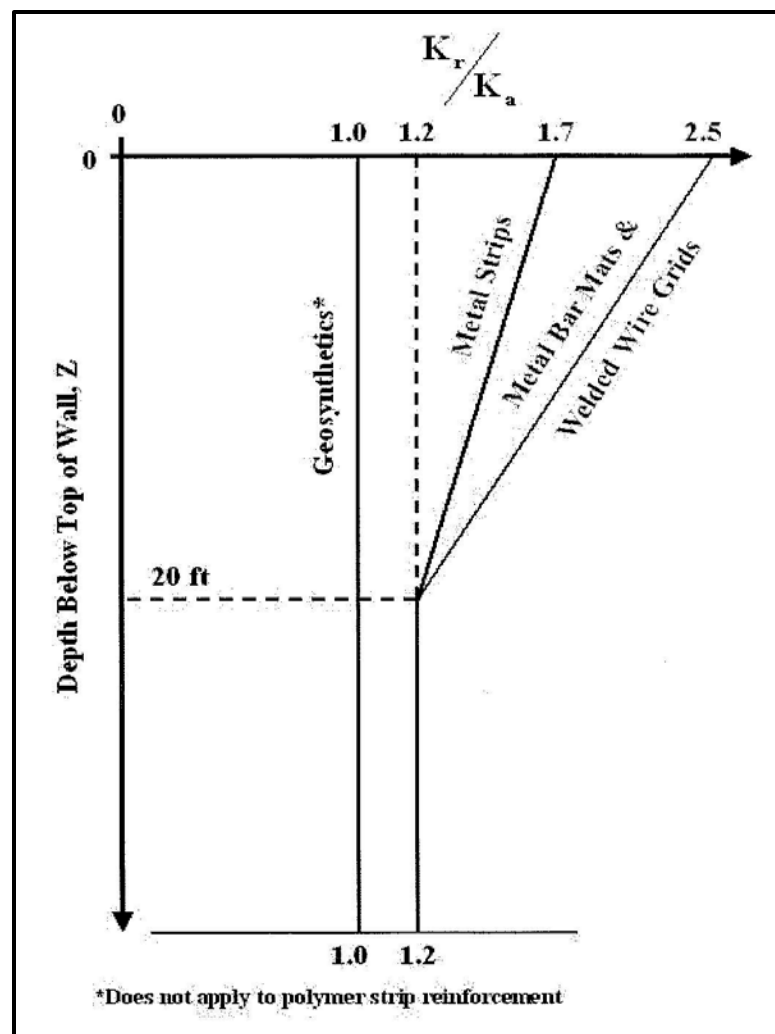


Figure C-10, Variation of the Coefficient of Lateral Stress Ratio with Depth (Berg, et al. – Vol. I (2009))

Figure C-10 was prepared by back analysis of the lateral stress ratio  $K_r$  from available field data where stresses in the reinforcements were measured and normalized as a function of the Rankine active earth pressure coefficient,  $K_a$ . The Rankine active earth pressure theory assumes lateral pressure is independent of backfill slope and interface friction. The ratios shown in Figure C-10 correspond to values representative of the specific reinforcement systems that are known to give satisfactory results assuming that the vertical stress is equal to the weight of the overburden ( $\gamma H$ ). This provides a simplified evaluation method for all cohesionless (*i.e.*, Sand-Like soils) reinforced fill walls. Future data may lead to modifications in Figure C-10, including relationships for newly developed reinforcement types, effect of full height panels, etc. These relationships can be developed by instrumenting structures and using numerical models to verify the  $K_r/K_a$  ratio for routine and complex walls.

The lateral earth pressure coefficient  $K_r$  is determined by applying a multiplier to the active earth pressure coefficient. The active earth pressure coefficient is determined using a Coulomb earth pressure relationship, assuming no wall friction and an  $\beta$  angle equal to 0.0 (*i.e.*, equivalent to the Rankine earth pressure coefficient (see Chapter 18 for determination of active earth pressure coefficient)).

For wall face batters equal to or greater than  $10^\circ$  from the vertical, the following simplified form of the Coulomb equation can be used:

$$K_a = \frac{\sin^2(\theta + \phi'_r)}{\sin^3\theta \left(1 + \frac{\sin\phi'_r}{\sin\theta}\right)} \quad \text{Equation C-26}$$

Where,

$\theta$  = Inclination of back of the facing as measured from the horizontal starting in front of the wall, as shown in Figure C-5, note that  $\theta$  is greater than  $100^\circ$

$\phi'_r$  = Angle of internal friction of reinforced zone

Commentary C11.10.6.2.1 (AASHTO LRFD Specifications) states that the above equation can be used for battered walls. The  $10^\circ$  value recommendation is consistent with the equation to determine the failure surface location for walls with  $10^\circ$  or greater batter [C11.10.6.2.1 (AASHTO LRFD Specifications)].

The stress,  $\sigma_2$ , due to a sloping backfill on top of an MSE wall can be determined as shown in Figure C-11. An equivalent soil height,  $S_{eq}$ , is computed based upon slope geometry. The value of  $S_{eq}$  should not exceed the slope height for broken back sloping fills. A reinforcement length of  $0.7H$  is used to compute the sloping backfill stress,  $\sigma_2$ , on the soil reinforcement, as a greater length would only have minimal effect on the reinforcement. The vertical stress is equal to the product of the equivalent soil height and the reinforced fill unit weight and is uniformly applied across the top of the MSE zone. See Step 3 of Calculate Horizontal Stress in the next Section for an explanation of why the reinforced fill unit weight is used in this calculation.

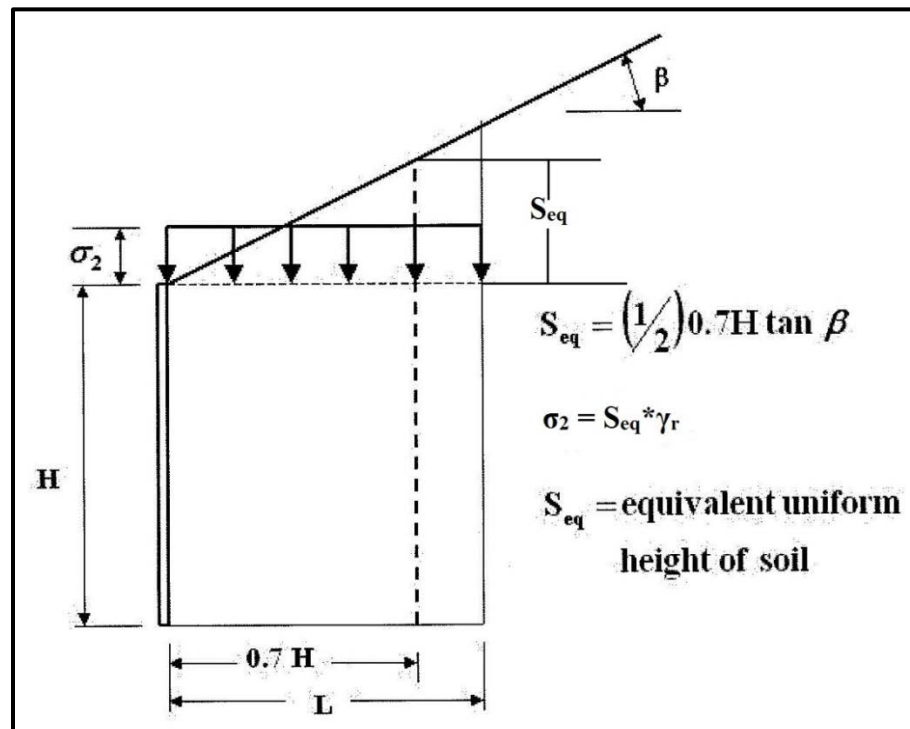


Figure C-11, Calculation of  $\sigma_2$  for Sloping Backfill for Internal Stability (modified Berg, et al. – Vol. I (2009))

### **C.8.4 Establish Vertical Layout of Soil Reinforcements**

The fourth step in internal stability design is defining the vertical layout of the soil reinforcement. Berg, et al. – Vol. I (2009) describes the vertical layout of the soil reinforcement as follows:

Use of a constant reinforcement section and spacing for the full height of the wall usually gives more reinforcement in the upper portion of the wall than is required for stability. Therefore, a more economical design may be possible by varying the reinforcing density with depth. However, to provide a coherent reinforced soil zone, vertical spacing of reinforcement should not exceed 32 inches.

There are generally 2 practical ways to accomplish this for MSE walls:

- For reinforcements consisting of strips, grids, or mats, used with segmental precast concrete facings, the vertical spacing is maintained constant and the reinforcement density is increased with depth by increasing the number and/or the size of the reinforcements. For instance, the typical horizontal spacing of 2-inch X 5/32-inch strips is 30 inches, but this can be decreased by adding horizontal reinforcement locations.
- For continuous sheet reinforcements, made of geotextiles or geogrids, a common way of varying the reinforcement density  $T_{al}/S_v$  is to change the vertical spacing  $S_v$ , especially if wrapped facing is used, because it easily accommodates spacing variations. The range of acceptable spacing is governed by consideration of placement and compaction of the backfill (e.g.,  $S_v$  taken as 1, 2 or 3 times the compacted lift thickness). The reinforcement density  $T_{al}/S_v$  can also be varied by changing the strength ( $T_{al}$ ) especially if wrapped facing techniques requiring a constant wrap height are used.

Low-to-medium-height walls (e.g., < 16 ft) are usually constructed with 1 strength geosynthetic. Taller walls use multiple strength geosynthetics. For example the 41-foot high Seattle preload wall used 4 strengths of geotextiles (*Allen, Christopher, and Holtz (1992)*). A maximum spacing of 16 inches is typical for wrapped faced geosynthetic walls, although a smaller spacing may be desirable to minimize bulging.

For walls constructed with modular blocks, the maximum vertical spacing of reinforcement should be limited to 2 times the block depth (front face to back face) or 32 inches, whichever is less, to assure construction and long-term stability. The top row of reinforcement should be limited to 1.5 the block depth (e.g., 1 unit plus a cap unit).

For large face units, such as 3 feet by 3 feet gabions, a vertical spacing equal to the face height (3 feet) is typically used. The spacing slightly exceeds the limit noted above, but this may be offset by the contributions of the large facing unit to internal (i.e., bulging) stability.

### C.8.5 Factored Tensile Forces in Reinforcement Layers

The fifth step in internal stability design is determining the tensile forces in the reinforcement layers. This determination consists of 2 sub steps, first, calculating the horizontal stress on each reinforcement layer and then determining the maximum tension ( $T_{MAX}$ ). Berg, et al. – Vol. I (2009) describes determining the factored tensile forces as follows:

#### Calculate Horizontal Stress

For internal stability analysis, the distribution of horizontal stress,  $\sigma_H$ , is first established. The horizontal stress at any given depth within the reinforced soil zone is expressed as follows:

$$\sigma_H = K_r * \sigma_v + \Delta\sigma_H \quad \text{Equation C-27}$$

$P_{TMAX-D}$  in Equation C-31

Where,

$K_r$  = Coefficient of lateral earth pressure in the reinforced soil zone (see Figure C-10)

$\sigma_v$  = Factored vertical pressure at depth of interest

$\Delta\sigma_H$  = Supplemental factored horizontal stress due to external surcharges

For internal stability analysis, the following assumptions are made in the computation of factored vertical pressure,  $\sigma_v$ :

1. Vertical pressure due to the weight of the reinforced soil zone is assigned a load type “EV” with a corresponding (maximum) load factor,  $\gamma_{P-EV} = 1.35$ . The maximum load factor of 1.35, and not the minimum load factor of 1.00, is always used to find the critical stress.
2. Any vertical surcharge above the reinforced soil zone is due to soil or considered as an equivalent soil surcharge is assigned a load type “EV”. In this scenario, a live load traffic surcharge that is represented by an equivalent uniform soil surcharge of height  $h_{eq}$  is assumed as a load type “EV”. This is in contrast to the external stability analysis where the live load traffic surcharge is assumed as a load type “LS” because in external stability analysis the MSE wall is assumed to be a rigid block. For internal analysis, the assumption of load type “EV” is used so that the amount of soil reinforcement within the reinforced soil zone is approximately the same as obtained using past working stress design approach (i.e., calibration by fitting).
3. The unit weight of the equivalent soil surcharge is assumed to be the same as the unit weight of the reinforced soil zone,  $\gamma_r$ , which is generally greater than or equal to the unit weight of the retained backfill.
4. Any vertical surcharge that is due to non-soil source is assigned a load type “ES”. Example of such a load is the bearing pressure under a spread footing on top of the reinforced soil zone. However, the application of the load factor of  $\gamma_{P-ES} = 1.50$  that is assigned to load type “ES” is a function of how the vertical pressures are computed as follows:

- If the vertical pressures are based on nominal (i.e., unfactored) loads, then use  $\gamma_{P-ES} = 1.50$ .
- If the vertical pressures were based on factored loads, then use  $\gamma_{P-ES} = 1.00$ . This is because once the loads are factored they should not be factored again.

It is recommended that the factored vertical pressure be evaluated using both the above approaches and the larger value chosen for analysis.

The supplemental factored horizontal pressure,  $\Delta\sigma_H$ , could be from a variety of sources. Two examples of supplemental horizontal pressures are as follows:

1. Horizontal pressures due to the horizontal (shear) stresses at the bottom of a spread footing on top of the reinforced soil zone.
2. Horizontal pressures from deep foundation elements extending through the reinforced soil zone.

Supplemental horizontal pressures are assigned a load type “ES” since they represent surcharges on or within the reinforced soil zone. However, similar to the vertical pressures due to non-soil loads, the application of the maximum load factor of  $\gamma_{P-ES} = 1.50$  that is assigned to the load type “ES” is a function of how the horizontal pressures are computed as follows:

- If the horizontal pressures are based on nominal (i.e., unfactored) loads, the use  $\gamma_{ES-MAX} = 1.50$ .
- If the horizontal pressures were based on factored loads, then use  $\gamma_{P-ES} = 1.00$ . This is because once the loads are factored they should be not factored again.

As with vertical pressure, it is recommended that the factored horizontal pressure be evaluated using both of the approaches and the larger value chosen for analysis.

*Berg, et al. – Vol. I (2009) provides 4 examples of MSE wall configurations ranging from simple to complex geometries as application of the above guidance. In addition, see Chapter 8 for the definition of each load type.*

#### Calculate Maximum Tension ( $T_{MAX}$ )

Calculate the maximum factored tension  $T_{MAX}$  in each reinforcement layer per unit width of wall based on the vertical spacing  $S_v$  from:

$$T_{MAX} = \sigma_H * S_v \quad \text{Equation C-28}$$

The term  $S_v$  is equal to the vertical reinforcement spacing for a layer where vertically adjacent reinforcements are equally spaced from the layer under construction. In this case,  $\sigma_H$ , calculated at the level of the reinforcement, is at the center of the contributory height. The contributory height is defined as the midpoint between vertically adjacent reinforcement elevations, except for the top and bottom layers reinforcement.



For the top and bottom layers of reinforcement,  $S_v$  is the distance from top or bottom of wall, respectively, to the midpoint between the first and second layer (from top or bottom of wall, respectively) of reinforcement.  $S_v$  distances are illustrated in Figure C-12.

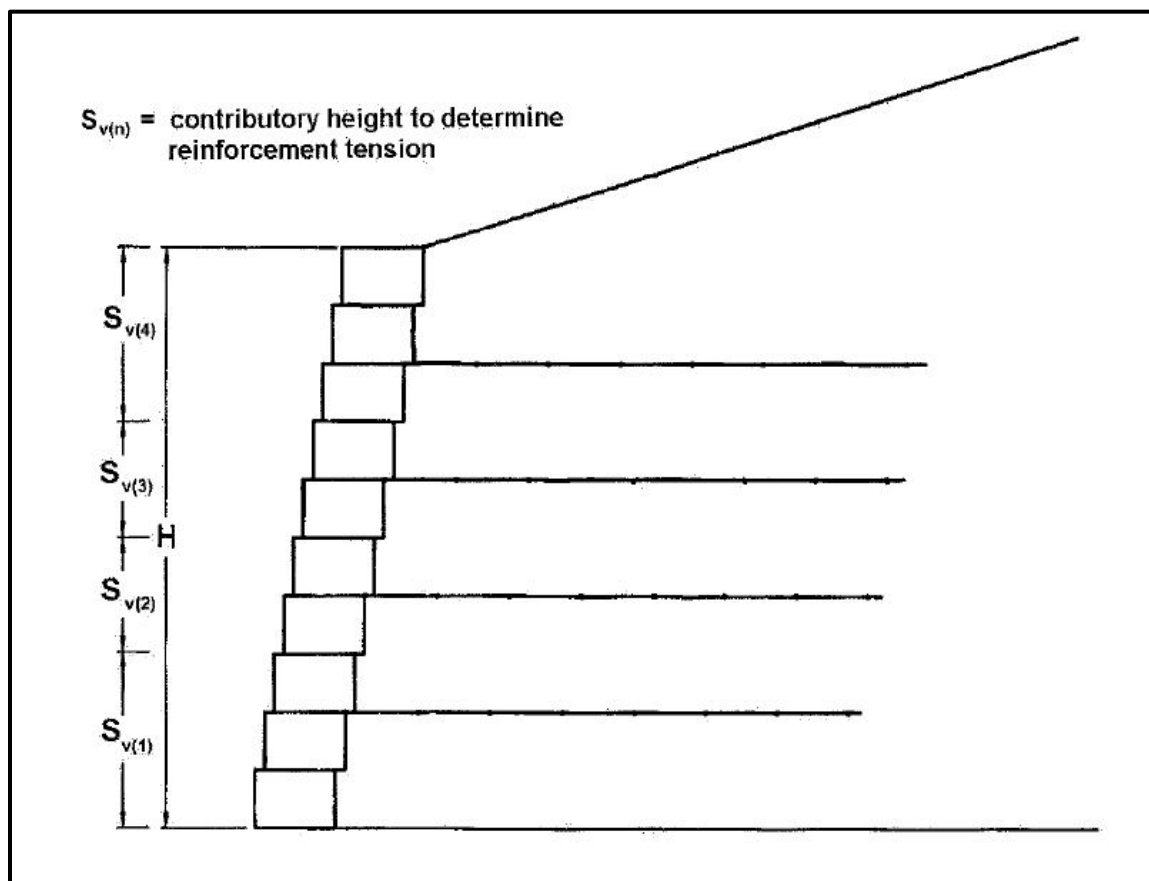


Figure C-12, Reinforcement Load Contributory Height  
(Berg, et al. – Vol. I (2009))

The maximum reinforcement tension,  $T_{MAX}$ , for the top and bottom layers of reinforcement, and for intermediate layers that do not have equally spaced adjacent layers, is calculated as the product of the contributory height and the average factored horizontal stress acting upon that contributory height. The average stress can be calculated based upon the tributary trapezoidal area (i.e., average of the stress at the top and at the bottom of the contributory height) or at the midpoint of the contributory height, as illustrated in Figure C-12.

Alternatively, for discrete reinforcements (metal strips, bar mats, geogrids, etc.),  $T_{MAX}$  (force per unit width) may be calculated at each level as  $P_{TMAX-UWR}$  in terms of force per unit width of reinforcement as:

$$P_{TMAX-UWR} = \frac{\sigma_H S_v}{R_c} \quad \text{Equation C-29}$$

$$R_c = \frac{b}{S_h} \quad \text{Equation C-30}$$

Where,

$R_c$  = Ratio of gross width of strip, sheet or grid to the center-to-center horizontal spacing between strips, sheets, or grids;  $R_c = 1$  for sheet reinforcement; for discrete elements (i.e., strip or bar mat) see Equation C-30

$b$  = Gross width of the reinforcing element (see Figure C-13)

$S_h$  = Center-to-center horizontal spacing between reinforcements (see Figure C-13)

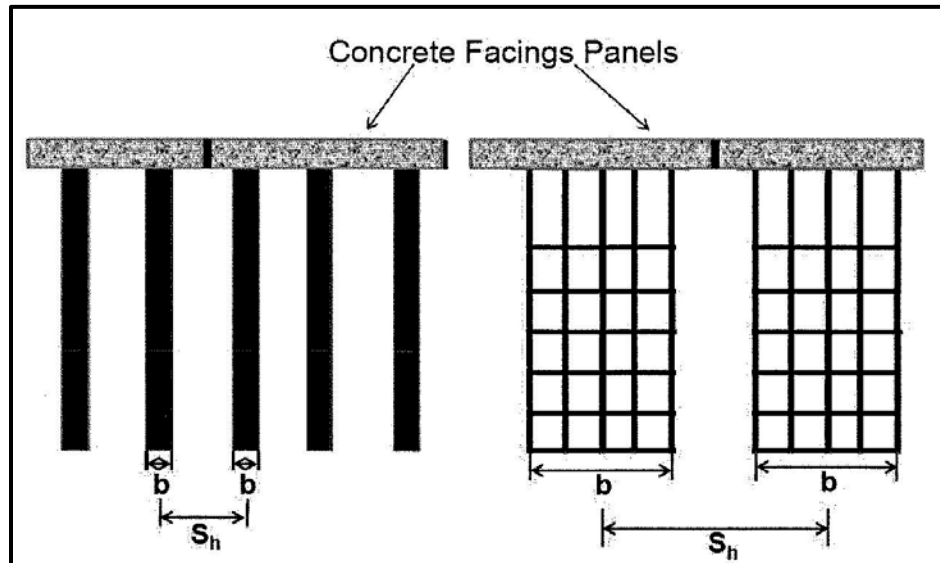


**Figure C-13, Coverage Ratio**  
(Berg, et al. – Vol. I (2009))

For discrete reinforcements of known spacing and segmental precast concrete facing of known panel dimensions,  $T_{MAX}$  (force per unit width) can alternately be calculated per discrete reinforcement,  $P_{TMAX-D}$ , per panel width, defined as:

$$P_{TMAX-D} = \frac{\sigma_H * S_v * W_P}{N_P} \quad \text{Equation C-31}$$

Where,

$P_{TMAX-D}$  = Maximum factored load in discrete reinforcement element

$W_P$  = Width of panel

$N_P$  = Number of discrete reinforcements per panel width

### **C.8.6 Soil Reinforcement Resistance**

The sixth step in internal stability design is determining the soil reinforcement resistance. Berg, et al. – Vol. I (2009) describes determining the soil reinforcement resistance as follows:

The factored soil resistance is the product of the nominal long-term strength, coverage ratio, and applicable resistance factor,  $\phi$ . The resistance factors for tensile rupture in MSE wall soil reinforcements are summarized in Chapter 9. The factored tensile resistance,  $T_r$ , is equal to:

$$T_r = \phi * T_{al} \quad \text{Equation C-32}$$

$T_{al}$  and  $T_r$  may be expressed in terms of strength per unit width or wall, per reinforcement element, or per unit reinforcement width.

Chapter 9 indicates the resistance factors to be used in the internal design of MSE walls. It is noted that the extreme event resistance factors include both EE I and EE II limit state checks. Further, the EE II limit state check includes the impact on the traffic barrier if the traffic barrier is rigidly connected to the MSE wall and relies on the MSE wall to resist the loading. If however, the traffic barrier is designed to not impart any loading on the MSE wall then the EE II limit state check for the MSE wall is not required.

The development of  $T_{al}$  is discussed in the following sections as described by Berg, et al. – Vol. I (2009) for both inextensible (metallic) and extensible (geosynthetic) reinforcements,

The structural design properties of reinforcement materials are a function of geometric characteristics, strength and stiffness, durability, and material type. The 2 most commonly used reinforcement materials, steel (*inextensible*) and geosynthetics (*extensible*) must be considered separately.

#### Strength Properties of Inextensible Reinforcements

For *inextensible* reinforcements, the design life is achieved by reducing the cross-sectional area of the reinforcement used in design calculations by the anticipated corrosion losses over the design life period as follows;

$$E_c = E_n - E_R \quad \text{Equation C-33}$$

Where,

$E_c$  = Thickness of the reinforcement at the end of the design life

$E_n$  = Nominal thickness at construction

$E_R$  = Sacrificial thickness of metal expected to be lost by uniform corrosion during the service life of the structure

The nominal long-term tensile strength of the reinforcement,  $T_{al}$ , is obtained for steel strips and grids as shown in the following equations.  $T_{al}$  in units of force per unit width is used to provide a unified strength approach, which can be applied to any reinforcement. Tensile strength of a known steel or grid reinforcement can also be expressed in terms of the tensile load carried by the reinforcement,  $P_{tal}$ . The designed designation of reinforcement tensile strength ( $T_{al}$  or  $P_{tal}$ ) varies depending on whether one is designing with a known system, designing with an undefined reinforcement, checking a design layout, performing connection design or performing reinforcement pullout calculations. Thus, nominal tensile strength may be calculated and expressed in the following terms:

$$T_{al} = \frac{F_y * A_c}{b} \quad \text{Equation C-34}$$

$$P_{tal} = F_y * A_c \quad \text{Equation C-35}$$

Where,

$b$  = Gross width of strip, sheet or grid (see Figure C-14)

$F_y$  = Yield stress of steel

$A_c$  = Design cross section area of the steel, defined as the original cross section area minus corrosion losses anticipated to occur during the design life of the wall

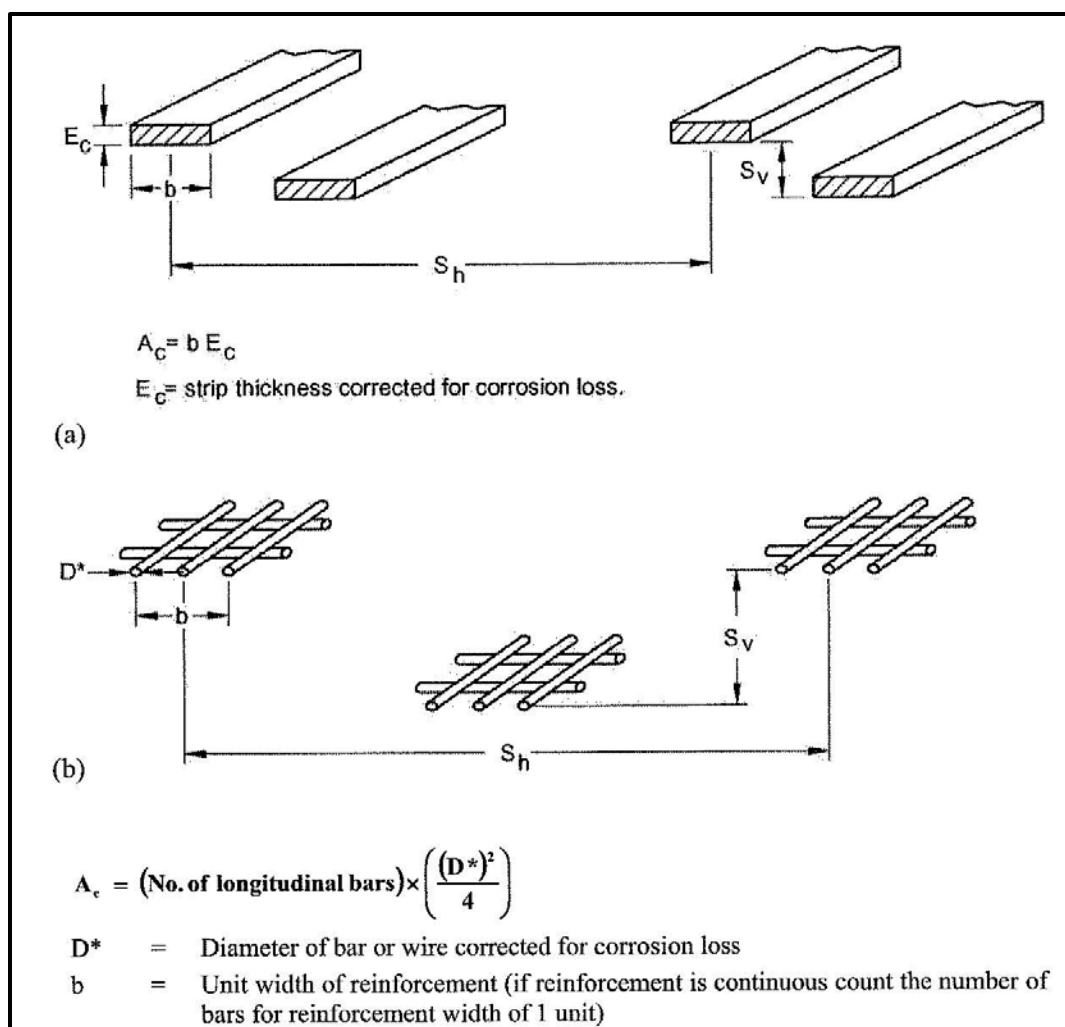


**Figure C-14, Geometric Configuration of Metallic Reinforcement  
(Berg, et al. – Vol. I (2009))**

The LRFD resistance factors for steel reinforcements in MSE walls are listed in *Chapter 9*. The lower resistance factor for grid reinforcing members connected to a rigid facing element (e.g., a concrete panel or block) is used to account for the greater potential for local overstress due to load unconformities for steel grids than for steel strips or bars. Transverse and longitudinal grid members are sized in accordance with *ASTM A1064 – Standard Specification for Carbon-Steel Wire and Welded Wire Reinforcement, Plain and Deformed, for Concrete*.

The quantities needed to determine  $A_c$  for steel strips and grids are shown in Figure C-14. The use of hardened and otherwise low strain (very high strength) steels may increase the potential for catastrophic failure; therefore, a lower resistance factor may be warranted with such materials. *The use of a lower resistance factor shall be approved in writing by the PC/GDS and PC/SDS prior to completing design.*

For metallic reinforcement, the life of the structure will depend on the corrosion resistance of the reinforcement. Practically all the metallic reinforcement used in construction of embankments and walls, whether they are strips, bar mats, or wire mesh, are made of galvanized mild steel. Woven meshes with PVC coatings provide some corrosion protection, provided the coating is not significantly damaged during construction. Epoxy coatings can be used for

corrosion protection, but are susceptible to construction damage, which can significantly reduce the coatings effectiveness. *However, the use of either PVC or epoxy coated reinforcement in MSE walls shall not be allowed on SCDOT projects. This is based on anecdotal evidence that reinforcements coated with these materials do not appear to achieve the required design life required.*

Extensive studies have been made to determine the rate of corrosion of galvanized mild steel bars or strips buried in different types of soils commonly used in reinforced soil. Based on these studies, deterioration of steel strips, mesh, bars, and mats can be estimated and accounted for by using increased metal thickness.

The majority of MSE walls constructed to date have used galvanized steel and backfill materials with low corrosive potential. A minimum galvanization coating of 2.0 oz/ft<sup>2</sup> or 0.0034 inches (3.4 mils) thickness is required per Article 11.10.6.4.2a (AASHTO LRFD Specifications). Galvanization shall be applied in accordance with AASHTO M111 - *Standard Specification for Zinc (Hot-Dip Galvanized) Coatings on Iron and Steel Products* (ASTM A123 – *Standard Specification for Zinc (Hot-Dipped Galvanized) Coatings on Iron and Steel Products*) for strip type, bar mat, or grid type reinforcements and ASTM A153 – *Standard Specification for Zinc Coating (Hot-Dip) on Iron and Steel Hardware* for accessory parts such as bolts and tie strips. Galvanization shall be applied after fabrication in accordance with ASTM A123. The zinc coating provides a sacrificial anode that corrodes while protecting the base metal. Galvanization also assists in preventing the formation of pits in the base metal during the first years of aggressive corrosion (which can occur in non-galvanized or “black” steel). After the zinc is oxidized (consumed) corrosion of the base metal starts.

The ASTM and AASHTO standards for galvanization provide different required minimum galvanization coating thickness as a function of the bar or wire thickness. However, as noted previously AASHTO LRFD Specifications require a minimum thickness of 3.4 mils for MSE walls. Galvanization requirements using this minimum and AASHTO M111 are summarized in Table C-3.

**Table C-3, Minimum Galvanization Thickness by Steel Thickness  
(Berg, et al. – Vol. I (2009))**

Category	Steel Thickness	Minimum Galvanization Thickness
Strip	< ¼ inch	3.4 mils
	> ¼ inch	3.9 mils
Wire <sup>1</sup>	All diameters	3.4 mils

<sup>1</sup> For bar mats fabricated from uncoated steel wire.  
After AASHTO M111 and ASTM A123

The corrosion rates presented in Table C-4 are suitable for conservative design *and are only applicable to galvanized steel*. These values assume a moderately corrosive backfill material having the controlled electro-chemical property limits presented in STS SC-M-713 (latest version) for Mechanically Stabilized Earth (MSE) Walls.

**Table C-4, Steel Corrosion Rates for Moderately Corrosive Reinforced Fill  
(Berg, et al. – Vol. I (2009))**

For zinc/side	0.58 mils/yr (first 2 years)
	0.16 mils/yr (thereafter)
For residual carbon steel/side <sup>1</sup>	0.47 mils/yr (thereafter)

<sup>1</sup>after zinc depletion

For a more detailed discussion of corrosion requirements, refer to Elias, Fishman, Christopher and Berg (2009).

#### Strength Properties of Extensible Reinforcement

Selection of long-term nominal tensile strength,  $T_{al}$ , for *extensible* reinforcement is determined by thorough consideration of all possible strength time dependent strength losses over the design life period. The tensile properties of geosynthetics are affected by factors such as creep, installation damage, aging, temperature, and confining stress. Furthermore, characteristics of geosynthetic products manufactured with the same base polymer can vary widely requiring a  $T_{al}$  determination for each individual product with consideration of all these factors.

Polymeric reinforcement, although not susceptible to corrosion, may degrade due to physiochemical activity in the soil such as hydrolysis, oxidation, and environmental stress cracking depending on polymer type. In addition, these materials are susceptible to installation damage and the effects of high temperature at the facing and connections. Temperature acts to accelerate creep and aging processes and temperature effects are accounted for through their determination. While the normal range of in-ground temperatures vary from 55° F in cold and temperate climates to 85° F in arid desert climates, temperatures at the facing and reinforcement connections can be as high as 120° F. Confining stress is not directly taken into account other than indirectly when installation damage is evaluated. For creep and durability, confining stress generally will tend to improve the long-term strength of the reinforcement.

The available long-term strength,  $T_{al}$ , is calculated as follows:

$$T_{al} = \frac{T_{ult}}{RF} = \frac{T_{ult}}{RF_{ID} * RF_{CR} * RF_D} \quad \text{Equation C-36}$$

Where,

- $T_{ult}$  = Ultimate tensile strength (strength per unit width)
- RF = Product of all applicable reduction factors
- $RF_{ID}$  = Installation damage reduction factor
- $RF_{CR}$  = Creep reduction factor
- $RF_D$  = Durability reduction factor

$RF_{ID}$ ,  $RF_{CR}$ , and  $RF_D$  reflect actual long-term strength losses, analogous to loss of steel strength due to corrosion. This long-term geosynthetic reinforcement strength loss concept is illustrated in Figure C-15. As shown in the figure, some strength losses occur immediately upon installation, and others occur throughout the design life of the reinforcement. Much of the long-term strength loss does not begin to occur until near the end of the reinforcement design life.

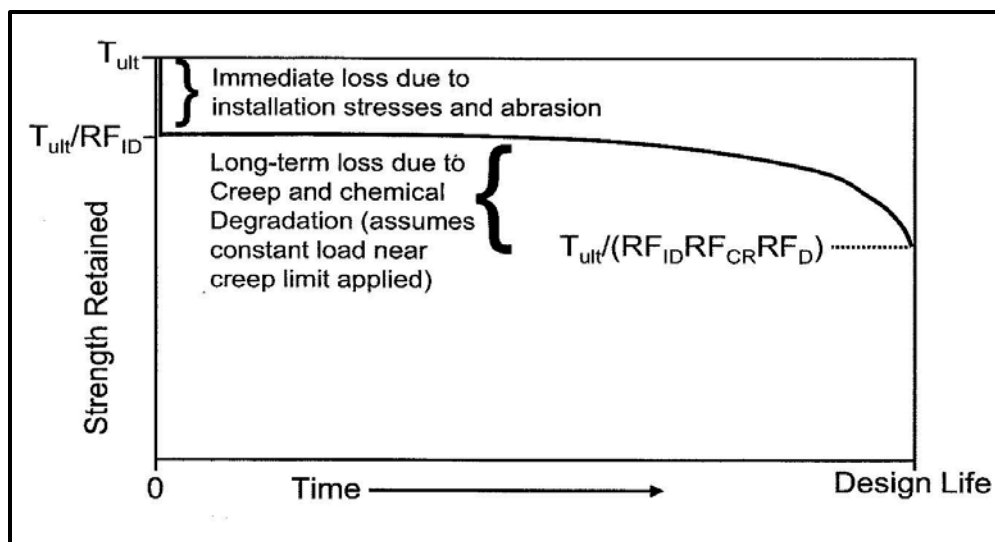


**Figure C-15, Long-Term Geosynthetic Reinforcement Strength Concept (Berg, et al. – Vol. I (2009))**

Because of varying polymer types, quality, additives, and product geometry, each geosynthetic is different in its resistance to aging and attack by different chemical agents. Therefore, each product must be investigated individually, or in the context of product line where the same polymer source and additives are used, and the manufacturing process is the same for all products in the product line. This product line approach makes it possible to interpolate reduction factors for products in the product line not specifically tested using the reduction factors determined for the products in the product line that are specifically tested for each degradation mechanism.

The AASHTO LRFD Specifications provide minimum requirements for the assessment of  $T_{al}$  for use in the design of geosynthetic reinforced soil structures. Protocols for evaluating  $T_{al}$  are included in *Berg, et al. – Vol. I (2009)* with supporting information on testing procedures provided in *Elias, et al. (2009)*.

The determination of reduction factors for each geosynthetic product and product line requires extensive field and/or laboratory testing which can take a year or more to complete. Background regarding the determination of each long-term strength reduction factor is briefly summarized as follows:

**Ultimate Tensile Strength,  $T_{ult}$**  – The value selected for  $T_{ult}$ , for design purposes, is the minimum average roll value (MARV) for the product. *The tensile strength of the reinforcement is determined from wide strip tests for geotextiles per ASTM D4595 – Standard Test Method for Tensile Properties of Geotextiles by the Wide-Width Strip Method or for geogrids per D6637 – Standard Test Method for Determining Tensile Properties of Geogrids by the Single or Multi-Rib Tensile Method based on the MARV for the product.* This MARV accounts for statistical variance in the material strength. Other sources of uncertainty and variability in the long-term strength result from installation damage, creep extrapolation, and the chemical degradation process. It is assumed that the observed variability in the creep rupture envelope is 100 percent correlated with the short-term tensile strength, as the creep strength is typically directly proportional to the short-term tensile strength within a product line. Therefore, the MARV of  $T_{ult}$  adequately takes into account variability in the creep strength. Note that the MARV of  $T_{ult}$  is

the minimum certifiable wide width tensile strength provided by the product manufacturer.

***Installation Damage Reduction Factor,  $RF_{ID}$***  – Damage during handling and construction, such as from abrasion and wear, punching and tear or scratching, notching, and cracking may occur in geosynthetics. These types of damage can only be avoided by using care during handling and construction. Construction equipment should not travel directly on geosynthetic materials.

Damage during reinforced fill placement and compaction operations is a function of the severity of loading imposed on the geosynthetic during construction operations and the size and angularity of the reinforced fill. For MSE walls and RSS construction, lightweight, low strength geotextiles and geogrids should be avoided to minimize damage with ensuing loss of strength.

Protocols for field testing for this reduction factor are detailed in *Elias, et al. (2009)* and in ASTM D5818 – *Standard Practice for Exposure and Retrieval of Samples to Evaluate Installation Damage of Geosynthetics*. These protocols require that the geosynthetic material be subjected to a reinforced fill placement and compaction cycle, consistent with field practice. The ratio of the initial strength, to the strength of retrieved samples defines this reduction factor. For reinforcement applications, a minimum weight of 8.0 oz/yd<sup>2</sup> for geotextiles is recommended to minimize installation damage. This roughly corresponds to a Class 1 geotextile in AASHTO M288 – *Standard Specification for Geotextile Specification for Highway Applications*. In general, the combination of geosynthetic reinforcement, and backfill placement and gradation characteristics, should not result in a value of  $RF_{ID}$  greater than 1.7. If testing indicates that  $RF_{ID}$  will be greater than 1.7 (i.e., an approximate 40 percent strength loss), then that combination of geosynthetic and backfill conditions should not be used, as this or greater levels of damage will cause the remaining strength to be highly variable and therefore not adequately reliable for design.

Table C-5 provides a summary of typical  $RF_{ID}$  values for a range of soil gradations and geosynthetic types.

**Table C-5, Installation Damage Reduction Factors,  $RF_{ID}$**   
(Berg, et al. – Vol. I (2009))

<b>Geosynthetic</b>	<b>Type 1 Backfill Max. Size 4-inch <math>D_{50}</math> about 1-1/4- inch</b>	<b>Type 2 Backfill Max. Size 3/4-inch <math>D_{50}</math> about #30</b>
HDPE uniaxial geogrid	1.20 – 1.45	1.10 – 1.20
PP biaxial geogrid	1.20 – 1.45	1.10 – 1.20
PVC coated PET geogrid	1.30 – 1.85	1.10 – 1.30
Acrylic coated PET geogrid	1.30 – 2.05	1.20 – 1.40
Woven geotextiles (PP & PET) <sup>1</sup>	1.40 – 2.20	1.10 – 1.40
Non-woven geotextiles (PP & PET) <sup>1</sup>	1.40 – 2.50	1.10 – 1.40
Slit film woven PP geotextile <sup>1</sup>	1.60 – 3.00	1.10 – 2.00

<sup>1</sup>Minimum weight 8.0 oz/yd<sup>2</sup>

In general,  $RF_{ID}$  is strongly dependent on the backfill soil gradation characteristics and its angularity, especially for lighter weight geosynthetics. Provided a minimum of 6 inches of backfill material is placed between the reinforcement surface and the compaction and spreading equipment



wheel/tracks, the backfill placement and compaction technique will have a lesser effect on  $RF_{ID}$ . Regarding geosynthetic characteristics, the geosynthetic weight/thickness or tensile strength may have a significant effect on  $RF_{ID}$ . However, for coated polyester geogrids, the coating thickness may overwhelm the effect of the product unit weight or thickness on  $RF_{ID}$ . *A minimum  $RF_{ID}$  of 1.1 shall be used to account for testing uncertainties.*

**Creep Reduction Factor,  $RF_{CR}$**  – The creep reduction factor is required to limit the load in the reinforcement to a level known as the creep limit, that will preclude excessive elongation and creep rupture over the life of the structure. The creep limit strength is thus analogous to yield strength in steel. Creep is essentially a long-term deformation process. As load is applied, molecular chains move relative to each other through straightening out of folded or curved/kinked chains or through breaking of inter-molecular bonds, resulting in no strength loss, but increased elongation.

Essentially, if the load levels are sufficiently high (i.e., constant load near the creep limit), the molecular chains can straighten/elongate no more without breaking the molecular chains. Significant strength loss occurs only when the straightening/slipping process is exhausted. If the load is high enough, molecular chains break, and both elongation and strength loss occur at an accelerating rate, eventually resulting in rupture. Generally this strength loss occurs only near the end of the design life of the geosynthetic under a given load level.

The creep reduction factor is obtained from long-term laboratory creep testing as detailed in *Elias, et al. (2009)*. Creep testing is essentially a constant load test on multiple product samples, loaded to various percentages of the ultimate product load, for periods of up to 10,000 hours. For creep testing 1 of 2 approaches may be used 1) “conventional” creep testing per ASTM D5262 – *Standard Test Method for Evaluating the Unconfined Tension Creep and Creep Rupture Behavior of Geosynthetics*, or 2) a combination of Stepped Isothermal Method (SIM) per ASTM D6992 – *Standard Test Method for Accelerated Tension Creep and Creep-Rupture of Geosynthetic Materials Based on Time-Temperature Superposition Using the Stepped Isothermal Method*, which is an accelerated method using stepped increases in temperature to allow tests to be performed in a matter of days, and “conventional” creep testing. The creep reduction factor is the ratio of the ultimate load to the extrapolated maximum sustainable load (i.e., creep rupture limit) within the design life of the structure (e.g., several years for temporary structures, 75 to 100 years for permanent structures).

Typical ranges of  $RF_{CR}$  as a function of polymer type are provided in *Table C-6*.

**Table C-6, Creep Reduction Factors,  $RF_{CR}$   
(Berg, et al. – Vol. I (2009))**

Polymer Type	$RF_{CR}$
Polyester (PET)	2.5 to 1.6
Polypropylene (PP)	5.0 to 4.0
High Density Polyethylene (HDPE)	5.0 to 2.6

**Durability Reduction Factor,  $RF_D$**  – This reduction factor is dependent on the susceptibility of the geosynthetic to attack by chemicals, thermal oxidation,

hydrolysis, environmental stress cracking, and micro-organisms and can vary typically from 1.1 to 2.0.

Typically, polyester products (PET) are susceptible to aging strength reductions due to hydrolysis (water must be available). Hydrolysis and the resulting fiber dissolution are accelerated in alkaline regimes, percent of water saturation in the surrounding soil, and temperature. Polyolefin products (PP and HDPE) are susceptible to aging strength losses due to oxidation (contact with oxygen). The level of oxygen in reinforced fills is a function of soil porosity, groundwater location, and other factors, and has been found to be slightly less than oxygen levels in the atmosphere (21 percent). Therefore, oxidation of geosynthetics in-ground may proceed at a rate equal to those above ground. Oxidation is accelerated by the presence of transition metals (Fe, Cu, Mn, Co, Cr) in the reinforced fill as found in acid sulphate soils (e.g., pyrite), slag and cinder fills, other industrial wastes or mine tailings containing transition metals, and elevated temperatures. It should be noted that the resistance of polyolefin geosynthetics to oxidation is primarily a function of the proprietary antioxidant package added to the base resin, which differs for each product brand, even when formulated with the same base resin.

The relative resistance of polymers to these identified regimes is shown in Table C-7 and a choice can be made, therefore, consistent with the in-ground regimes indicated.

**Table C-7, Anticipated Resistance of Polymers to Specific Environments  
(Berg, et al. – Vol. I (2009))**

Soil Environment	Polymer		
	PET	HDPE	PP
Acid Sulphate Sols	NE	ETR	ETR
Organic Soils	NE	NE	NE
Saline Soils pH < 9	NE	NE	NE
Ferruginous	NE	ETR	ETR
Calcareous Soils	ETR	NE	NE
Modified Soils/Lime, Cement	ETR	NE	NE
Sodic Soils, pH > 9	ETR	NE	NE
Soils with Transition Metals	NE	ETR	ETR
NE = No effect			
ETR = Exposure Test Required			

Most geosynthetic reinforcement is buried, and therefore ultraviolet (UV) stability is only of concern during construction and when the geosynthetic is used to wrap wall or slope face. If used in exposed locations, geosynthetics should be protected with coatings or facing units to prevent deterioration. UV tests (ASTM D4355 – *Standard Test Method for Deterioration of Geotextiles by Exposure to Light, Moisture and Heat in a Xenon Arc Type Apparatus*) extended beyond the normal 500 hour test duration should be performed on materials that will be directly exposed for long periods of time (more than several months) in order to evaluate the materials anticipated design life. Vegetative covers can also be considered in the case of open weave geotextiles or geogrids. Thick geosynthetics with UV stabilizers can be left exposed for several years or more without protection; however, long-term maintenance should be anticipated because of both UV deterioration and possible vandalism.

Protocols for testing to obtain this reduction factor have been proposed and are detailed in Elias, et al. (1999). In general, for polyolefins, they consist of oven aging polyolefins (PP and HDPE) samples to accelerate oxidation and measure their strength reduction, as a function of time, temperature, and oxygen concentration. This high temperature data must then be extrapolated to a temperature consistent with field conditions. For polyesters (PET) the aging is conducted in an aqueous media at varying pH and relatively high temperature to accelerate hydrolysis, with data extrapolated to a temperature consistent with field conditions. For more detailed explanations, see Elias, et al. (2009).

Due to the long-term nature of these durability evaluation protocols (2 to 3 years could be required to complete such test), it is generally not practical to conduct such tests for typical geosynthetic reinforcement design, but are generally more suited for research activities. However, short-term index type tests can be conducted as indicators of good long-term durability performance, based on correlation to the long-term research results obtained and reported by Elias, et al. (1999). Such index test results, combined with a criteria applied to the test results that can be considered to indicate good long-term performance, can be used to justify the use of a default value of  $RF_D$  that can be used for the determination of  $T_{al}$ .

With respect to aging degradation, current research results suggest the following.

#### Polyester Geosynthetics

PET geosynthetics are recommended for use only in environments characterized by  $3 < \text{pH} \leq 9$ . The reduction factors for PET aging ( $RF_D$ ) listed in Table C-8 are developed for a 100-year design life in the absence of long-term product specific testing. Based on these research results, for polyester reinforcements, the *AASHTO LRFD Specifications* recommend a minimum average molecular weight of 25,000 and a maximum carboxyl end group content (CEG) of 30 to allow the use of the default reduction factor for durability.

**Table C-8,  $RF_D$  for PET  
(Berg, et al. – Vol. I (2009))**

Product <sup>a</sup>	$RF_D$	
	$5 < \text{pH} \leq 8$	$3^b < \text{pH} \leq 5$ $8 < \text{pH} \leq 9$
Geotextiles $M_n < 20,000$ , $40 < \text{CEG} < 50$	1.6	2.0
Coated Geogrids, Geotextiles $M_n > 25,000$ , $\text{CEG} < 30$	1.15	1.3
$M_n$ = Number average molecular weight CEG = Carboxyl end group		
<sup>a</sup> Use of materials outside the indicated molecular property range requires specific product testing. Use of products outside of $3 < \text{pH} < 9$ range is not recommended.		
<sup>b</sup> Lower limit of pH for permanent applications is 4.5 and lower limit for temporary applications is 3, per Article 11.10.6.4.2b (AASHTO LRFD Specifications)		

#### Polyolefin Geosynthetics

To mitigate thermal and oxidative degradative processes, polyolefins (i.e., PP and HDPE) products are stabilized by the addition of antioxidants for both processing stability and long-term functional stability. These antioxidant packages are proprietary to each manufacturer and their type, quantity, and

effectiveness varies. Without residual antioxidant protection (after processing), PP products are vulnerable to oxidation and significant strength loss within a projected 75- to 100-year design life at 68° F. Current data suggests that unsterilized PP has a half-life of less than 50 years.

Therefore the anticipated functional life of a PP geosynthetic is to a great extent a function of the type and post-production antioxidant levels, and the rate of subsequent antioxidant consumption. Antioxidant consumption is related to the in-ground oxygen content, which in fills is only slightly less than atmospheric.

A detailed discussion of the effectiveness of oven aging and other protocols to allow estimation of long-term strength loss due to the combination of heat aging and oxidative degradation of various polyolefins is provided in Elias, et al. (1999) and Elias, et al. (2009).

For both polyester and polyolefins, if the index test criteria are met, a default value of  $RF_D$  of 1.3 could be used to determine  $T_{ai}$  for design purposes. These index criteria are summarized in Table C-9. If the effective in-soil site temperature is anticipated to be approximately 85° F plus or minus a few degrees, a higher default reduction factor for  $RF_D$  should be considered.

**Table C-9, Minimum Testing Requirements for use  $RF_D$   
(modified Berg, et al. – Vol. I (2009))**

<b>Geosynthetic Type</b>	<b>Property</b>	<b>Test Method</b>	<b>Criteria to allow use of Default <math>RF_D</math></b>
Polypropylene (PP) and Polyethylene (HDPE)	UV Oxidation Resistance	ASTM D4355	Min. 70% strength retained after 500 hrs. in weatherometer
Polyester (PET) <sup>1</sup>	Hydrolysis Resistance	Inherent Viscosity Method (ASTM D4603 and GRI Test Method GG8) or Determine Directly Using GEL Permeation Chromatography	Minimum Number ( $M_n$ ) Average Molecular Weight of 25,000
		ASTM D7409	Maximum Carboxyl End Group (CEG) Content of 30
All Polymers	Survivability	Weight per Unit Area, ASTM D5261	Min. 8 oz/yd <sup>2</sup>
All Polymers	Percent Post-consumer Recycled Material by Weight	Certification of Material Used	Maximum 0%
<p><sup>1</sup> Alternatively, a default <math>RF_D = 1.3</math> may be used if product specific installation damage testing is performed and it is determined that <math>RF_{ID} = 1.7</math> or less, and if the other requirements of this table are met.</p> <p>ASTM D4355 – <i>Standard Test Method for Deterioration of Geotextiles by Exposure to Light, Moisture and Heat in a Xenon Arc Type Apparatus</i>  ASTM D4603 – <i>Standard Test Method for Determining Inherent Viscosity of Poly(Ethylene Terephthalate) (PET) by Glass Capillary Viscometer</i>  GRI GG8 – <i>Determination of the Number Average Molecular Weight of PET Yarns Based on Relative Viscosity Value</i>  ASTM D7409 – <i>Standard Test Method for Carboxyl End Group Content of Polyethylene Terephthalate (PET) Yarns</i>  ASTM D5261 – <i>Standard Test Method for Measuring Mass per Unit Area of Geotextiles</i></p>			

Environmental stress cracking is an aging phenomenon that is really as much related to creep as it is to durability. In certain environments, such as when surfactants are present, the creep rupture process, through making it easier for

the tie molecules to pull out of the crystalline structure, can be accelerated, allowing cracks in the polymer to form, and premature rupture. Additional information on this phenomenon is provided in Elias, et al. (2009). For most in ground conditions, the chemicals necessary to cause this to happen are generally not present, and the results from laboratory creep testing are sufficient to address strength loss under constant load.

Note that biological degradation due to micro-organisms is rarely a concern, as most geosynthetic reinforcement products only contain high molecular weight polymers, and the biological agents have great difficulty in finding the molecular chain endings that would allow them to begin consuming the polymer. Therefore, biological degradation is usually not considered in the determination of  $RF_D$ . A minimum  $RF_D$  of 1.1 shall be used to account for testing uncertainties.

### **C.8.7 Strength and Number of Soil Reinforcements**

The seventh step in internal stability design is determining the grade and number of soil reinforcement elements at each level. Berg, et al. – Vol. I (2009) describes this selection process as follows:

The soil reinforcement vertical layout, the factored tensile force at each reinforcement level, and the factored soil reinforcement resistance were defined in the previous steps. With this information, select suitable *strength* of reinforcement, *the number of* (e.g., *discrete (strip) or sheet*) reinforcements, for the defined vertical reinforcement layout; then with this layout check pullout at *Strength and Service limit state loads* and, as applicable, *Extreme Event limit state loadings*. Adjust layout if/as necessary.

Stability with respect to breakage of the reinforcements requires that:

$$T_{MAX} \leq T_r \quad \text{Equation C-37}$$

Where  $T_{MAX}$  is the maximum factored load in a reinforcement (*Equation C-28*) and  $T_r$  is the factored reinforcement tensile resistance (*Equation C-32*).

### **C.8.8 Calculate Factored Pullout Resistance of Soil Reinforcements**

The eighth step in internal stability design is determining the factored pullout resistance of the soil reinforcement elements. Berg, et al. – Vol. I (2009) describes this process as follows:

Stability with respect to pullout of the reinforcement requires that the factored effective pullout length is greater than or equal to the factored tensile load in the reinforcement,  $T_{MAX}$ . Each layer of reinforcement should be checked, as pullout resistance and/or tensile loads may vary with reinforcement layer. Therefore, the following criteria should be satisfied:

$$\phi * L_e = \frac{T_{MAX}}{F^* \alpha * \sigma_v * C * R_c} \quad \text{Equation C-38}$$

Where,

$L_e$  = Length of embedment in the resisting zone. Note that the boundary between the resisting and active zones may be modified by concentrated loadings.

$\phi$  = Resistance factor for soil reinforcement pullout (see Chapter 9)

$T_{MAX}$  = Maximum reinforcement tension (see Equation C-31,  $P_{TMAX-D}$  in Equation C-31)

$F^*$  = Pullout resistance factor with variation in depth starting at the same elevations as that for  $K_r/K_a$  variation (discussed in C.8.8.2)

$\alpha$  = Scale correction factor (discussed in C.8.8.1)

$\sigma_v$  = Nominal (i.e., unfactored) vertical stress at the reinforcement level in the resistant zone, including distributed dead load surcharges, neglecting traffic loads (ksf). See Figure C-16 for computation of horizontal backslope condition and Figure C-17 for the sloping backslope condition.

$C = 2$  for strip, grid, and sheet type reinforcement

$R_c$  = Coverage ratio (see Equation C-30)

The vertical stress,  $\sigma_v$ , used to calculate pullout resistance for level backslope condition shall be determined as shown in Figure C-16 using the following equation.

$$\sigma_v = \gamma_r * Z \quad \text{Equation C-39}$$

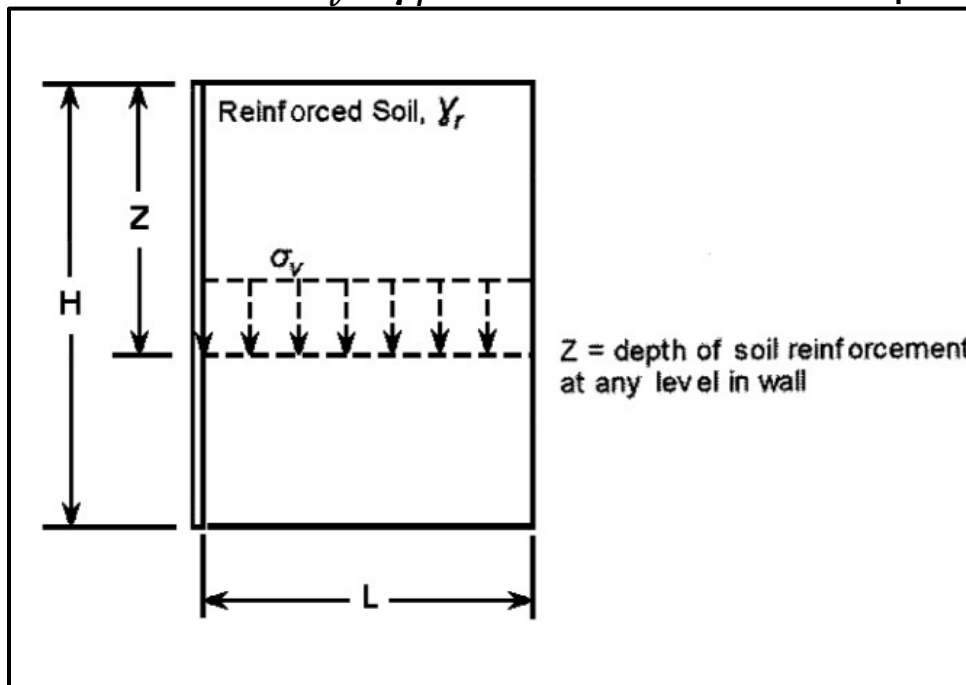


Figure C-16, Calculation of Vertical Stress for Internal Stability Analysis (modified from AASHTO LRFD Specifications (2017))

The vertical stress,  $\sigma_v$ , used to calculate pullout resistance for the sloping backslope condition shall be determined as shown in Figure C-17 using the following equations.

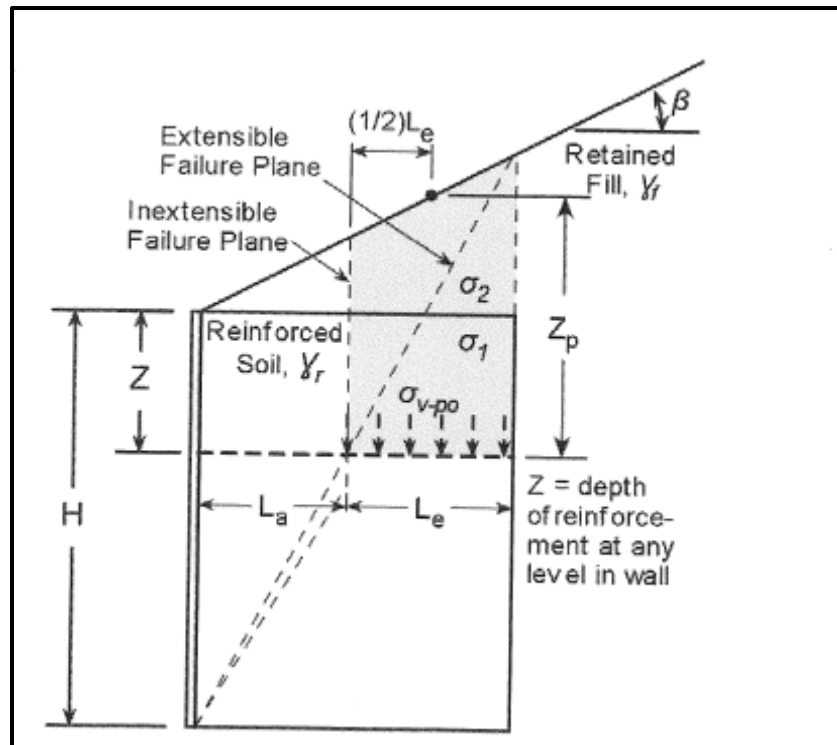


Figure C-17, Calculation of Vertical Confining Pressure beneath Sloping Backfill (AASHTO LRFD Specifications (2017))

$$\sigma_1 = \gamma_r * Z \quad \text{Equation C-40}$$

$$\sigma_2 = \gamma_f * (Z_p - Z) \quad \text{Equation C-41}$$

$$\sigma_v = \sigma_1 + \sigma_2 = \gamma_r * Z + \gamma_f * (Z_p - Z) \quad \text{Equation C-42}$$

Where:

$$Z_p = Z + \left( L_a + \left( \frac{1}{2} \right) L_e \right) \tan \beta \quad \text{Equation C-43}$$

Therefore, the required embedment length in the resistance zone (i.e., beyond the potential failure surface) can be determined from:

$$L_e \geq \frac{T_{MAX}}{\phi * F * \alpha * \sigma_v * C * R_c} \geq 3 \text{ ft} \quad \text{Equation C-44}$$

If traffic or other live load is present, it is recommended that  $T_{MAX}$  be computed with the live loads and that the pullout resistance be computed excluding the live loads. This addresses the possibility of the live loads being present near the front of the wall but not above the reinforcement embedment length. The pullout resistance and the  $T_{MAX}$  can be calculated with the live load excluded if it can be shown that the live load will be on the active and resistant zones at the same time or on the resistant zone alone.

Commentary C11.10.6.2.1 (*AASHTO LRFD Specifications*) notes that traffic loads and other live loads are not included for pullout calculations. Therefore, if  $T_{MAX}$  calculation for checking the reinforcement and connection strengths included a live load surcharge the value must be recomputed, without the surcharge load.

If the criterion is not satisfied for all reinforcement layers, the reinforcement length has to be increased and/or reinforcement with a greater pullout resistance per unit width must be used, or the reinforcement vertical spacing may be reduced which would reduce  $T_{MAX}$ .

The total length of reinforcement,  $L$ , required for internal stability is then determined from:

$$L = L_a + L_e \quad \text{Equation C-45}$$

Where,  $L_a$  is obtained from *Figure C-9* for simple structures not supporting concentrated external loads such as bridge abutments. Based on this figure the following relationships can be obtained for  $L_a$ :

For MSE walls with extensible reinforcement, vertical face and horizontal backfill:

$$L_a = (H - Z) * \tan\left(45 - \frac{\phi'}{2}\right) \quad \text{Equation C-46}$$

Where,

$Z$  = Depth of the reinforcement level

For walls with inextensible reinforcement, vertical face and horizontal backfill, from the base up to  $H/2$ :

$$L_a = 0.6 * (H - Z) \quad \text{Equation C-47}$$

For the upper half of a wall with inextensible reinforcements, vertical face, and horizontal backfill:

$$L_a = 0.3 * H \quad \text{Equation C-48}$$

For construction ease, a final uniform length is commonly chosen, based on the maximum length required. However, if internal stability controls the length, it could be varied from the base, increasing with the height of the wall to the maximum length requirement based on a combination of internal and maximum external stability requirements.

### C.8.8.1 Correction Factor ( $\alpha$ )

The correction factor ( $\alpha$ ) depends primarily upon the strain softening of the compacted granular backfill material, the extensibility, and the length of the reinforcement. Typical values of  $\alpha$  based on reinforcement type are presented in Table C-10. For inextensible reinforcement,  $\alpha$  is approximately 1, but it can be substantially smaller than 1 for extensible reinforcements. The  $\alpha$  factor can be obtained from pullout tests on reinforcements with different lengths or derived using analytical or numerical load transfer models which have been “calibrated” through



numerical test simulations. In the absence of test data, the values included in Table C-10 should be used for geogrids and geotextiles.

**Table C-10, Typical Values of  $\alpha$   
(modified Berg, et al. – Vol. I (2009))**

Reinforcement Type	$\alpha$
All steel reinforcements	1.0
Geogrids	0.8
Geotextiles	0.6

### C.8.8.2 Pullout Friction Factor ( $F^*$ )

The pullout friction factor ( $F^*$ ) can be obtained most accurately from laboratory or field pullout tests performed with the specific material to be used on the project (i.e., select backfill and reinforcement). Alternatively,  $F^*$  can be derived from empirical or theoretical relationships developed for each soil-reinforcement interaction mechanism and provided by the reinforcement supplier. For any reinforcement,  $F^*$  can be estimated using the general equation:

$$F^* = F_q * \alpha_\beta + \tan \rho \quad \text{Equation C-49}$$

Where,

$F_q$  = Embedment (or surcharge) bearing capacity factor (see Figure C-18)

$\alpha_\beta$  = Bearing factor for passive resistance which is based on the thickness per unit width of the bearing member

$\rho$  = Soil-reinforcement interaction friction angle

Equation C-45 represents systems that have both the frictional and passive resistance components of the pullout resistance. In certain systems, however, 1 component is much smaller than the other and can be neglected for practical purposes.

In absence of site-specific pullout test data, it is reasonable to use these semi-empirical relationships in conjunction with the standard specifications for backfill to provide a conservative evaluation of pullout resistance.

For steel ribbed reinforcement,  $F^*$  is commonly estimated as:

$$F^* = \tan \rho = 1.2 + \log C_u \quad \text{Equation C-50}$$

at the top of the structure = 2.0 maximum

$$F^* = \tan \phi \quad \text{Equation C-51}$$

at a depth of 20 feet and below

Where,

$\rho$  = Soil-reinforcement interaction friction angle

$C_u$  = Uniformity coefficient of the backfill (see Chapter 6)

If the specific  $C_u$  for the wall backfill is unknown during design, a  $C_u$  of 4 should be assumed (i.e.,  $F^* = 1.8$  at the top of the wall), for backfill meeting the requirements previously provided.

For steel grid reinforcements with transverse spacing ( $S_t$ )  $\geq$  6 inches,  $F^*$  is a function of a bearing or embedment factor ( $F_q$ ), applied over the contributing bearing factor ( $\alpha_\beta$ ), as follows:

At the top of the structure:

$$F^* = F_q * \alpha_\beta = 40\alpha_\beta = 40 * \left(\frac{t}{2s_t}\right) = 20 * \left(\frac{t}{s_t}\right) \quad \text{Equation C-52}$$

At a depth of 20 feet and below:

$$F^* = F_q * \alpha_\beta = 20\alpha_\beta = 20 * \left(\frac{t}{2s_t}\right) = 10 * \left(\frac{t}{s_t}\right) \quad \text{Equation C-53}$$

Where,

t = Thickness of the transverse bar

S<sub>t</sub> = The distance between individual bars in steel grid reinforcement and shall be uniform throughout the length of the reinforcement, rather than having transverse grid members concentrated only in the resistance zone (see Figure C-18)

For geosynthetic (i.e., geogrid and geotextile) sheet reinforcement, the pullout resistance is based on a reduction in the available soil friction with the reduction factor often referred to as an interaction factor (C<sub>i</sub>). In the absence of test data, the F\* value for geosynthetic reinforcement should conservatively be estimated as:

$$F^* = \left(\frac{2}{3}\right) * \tan \phi \quad \text{Equation C-54}$$

Where,

ϕ = Peak friction angle of the MSE wall backfill

When used in the above relationship, ϕ is the peak friction angle of the soil which, for MSE walls using select granular backfill, is taken as 36° unless project specific test data substantiates higher values. However, ϕ shall not exceed 38° even if specific test data indicates higher friction values.

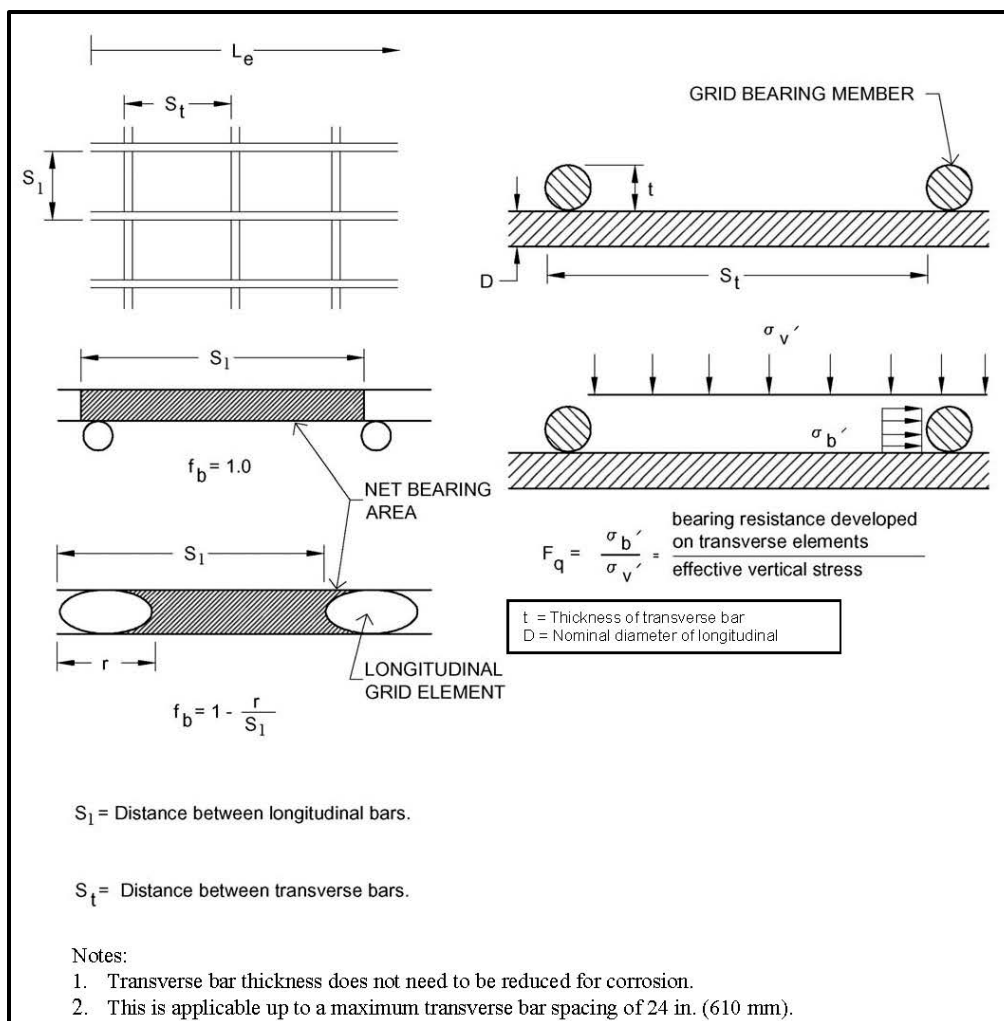


**Figure C-18, Grid Dimensions for Pullout Capacity  
(Berg, et al. – Vol. I (2009))**

### C.8.9 $T_{ac}$ for Connection Strength

The ninth step in internal stability design is determining the connection strength between the facing elements and the soil reinforcement elements. Berg, et al. – Vol. I (2009) describes this process as follows:

The connection of the reinforcements with the facing should be designed for  $T_{MAX}$  for all limit states. The resistance factors ( $\phi$ ) for the connectors are the same as for the reinforcement strength, and are *provided in Chapter 9*.

#### Connections to Concrete Panels

The metallic reinforcements for MSE systems constructed with segmental precast panels are structurally connected to the facing by either bolting the reinforcements to a tie strip cast in the panel or connected with a bar connector to suitable anchorage devices in the panels. The capacity of the embedded connector as an anchorage must be checked by the tests as required by Article 5.11.3 *AASHTO LRFD Specifications* for geometry used. Connections between metallic reinforcements and facing units should be designed in accordance with Article 6.13.5 (*AASHTO LRFD Specifications*), and consider corrosion losses in accordance with Article 11.10.6.4.2A (*AASHTO LRFD Specifications*). The

design load at the connection is equal to the maximum load on the reinforcement.

Polyethylene geogrid reinforcements may be structurally connected to segmental precast panels by casting a tab of the geogrid into the panel and connecting to the full length of geogrid with a bodkin joint, as illustrated in Figure C-19. The capacity of the embedded connector as an anchorage must be checked by tests as required in Article 5.11.3 *AASHTO LRFD Specifications* for each geometry used. A slat of polyethylene is used for the bodkin. Care should be exercised during construction to eliminate slack from this connection.

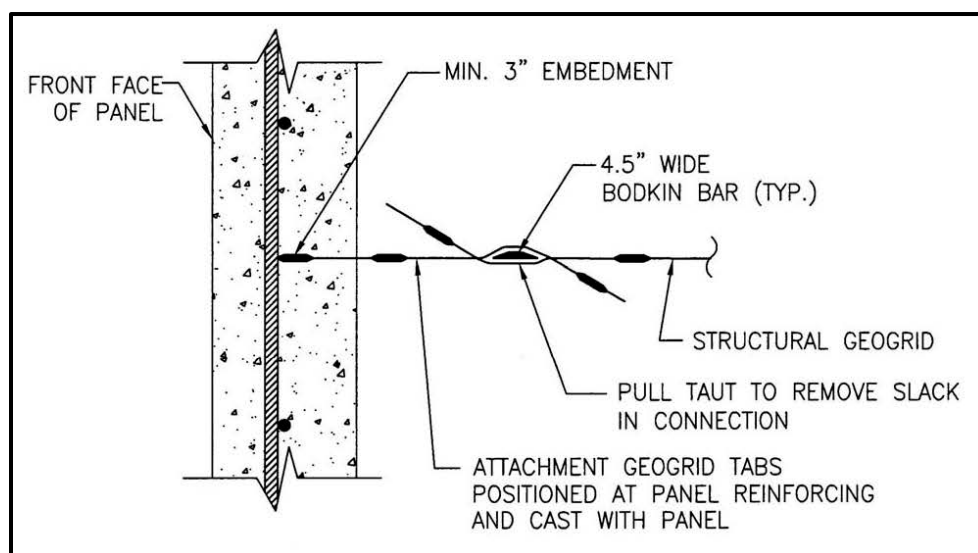


**Figure C-19, Bodkin Connection Detail**  
(Berg, et al. – Vol. I (2009))

Polyester geogrids and geotextiles should not be cast into concrete for connections, due to potential chemical degradation. Other types of geotextiles also are not cast into concrete for connections due to fabrication and field connection requirements.

#### Connections to MBW Units

MSE walls constructed with Modular Block Wall (MBW) units are connected either by (i) a structural connection subject to verification under Article 5.11.3 (*AASHTO LRFD Specifications*), (ii) friction between units and the reinforcement, including the friction developed from the aggregate contained within the core of the units, or, (iii) a combination of friction and shear from connection devices. This strength will vary with each unit depending on its geometry, unit batter, normal pressure, depth of unit, and unit infill gravel (if applicable). The connection strength is therefore specific to each unit/reinforcement combination and must be developed uniquely by test for each combination.

The nominal long-term connection strength,  $T_{alc}$  developed by frictional and/or structural means is determined as follows:

$$T_{alc} = \frac{T_{ult} * CR_{CR}}{RF_{Dc}} \quad \text{Equation C-55}$$

Where,

- $T_{alc}$  = Nominal long-term reinforcement/facing connection strength per unit reinforcement width at a specified confining pressure
- $T_{ult}$  = Ultimate tensile strength of the geosynthetic soil reinforcement, defined as MARV
- $RF_{Dc}$  = Reduction factor to account for chemical and biological degradation at the connection
- $CR_{CR}$  = Reduction factor to account for reduced ultimate strength resulting from the connection

$CR_{CR}$  may be obtained from long-term or short-term tests, as described below.

#### $CR_{CR}$ Defined with Long-Term Testing

A series of connection creep tests are performed over extended periods of time to evaluate creep rupture at the connection. The long-term connection creep rupture data is extrapolated to the specified design life (e.g., 75 years, 100 years) to define the creep reduced connection strength,  $T_{CRc}$ , as the specified design life. Details for long-term testing and interpretation of results are presented in Appendix B of Berg, et al. – Vol. II (2009). With this long-term testing,  $CR_{CR}$  is defined as follows:

$$CR_{CR} = \frac{T_{CRc}}{T_{lot}} \quad \text{Equation C-56}$$

$T_{lot}$  is the ultimate wide width tensile strength of the reinforcement material roll/lot used for the connection strength testing. The  $T_{lot}$  strength, for example, might be 103 percent to 115 percent of the MARV ultimate strength,  $T_{ult}$  (or noted  $T_{ult-MARV}$ ).

#### $CR_{CR}$ Defined with Short-Term Testing

Short-term (i.e., quick) ultimate strength tests, per ASTM D6638 – *Standard Test Method for Determining Connection Strength Between Geosynthetic Reinforcement and Segmental Concrete Units (Modular Concrete Blocks)*, are used to define an ultimate connection strength,  $T_{ultconn}$ , at a specified confining pressure. With short-term testing  $CR_{CR}$  is defined as follows:

$$CR_{CR} = \frac{T_{ultconn}}{RF_{CR} * T_{lot}} \quad \text{Equation C-57}$$

$RF_{CR}$  is the geosynthetic creep reduction factor (see above), and  $T_{lot}$  is the ultimate wide width tensile strength of the reinforcement material roll/lot used for the connection strength testing.

Raw data from short-term connection strength laboratory testing should not be used for design. The wall designer should evaluate the data and define the nominal long-term connection strength,  $T_{alc}$ . Steps for this data reduction are summarized and discussed in Appendix B of Berg, et al. – Vol. II (2009). An example of reduction of short-term connection strength data is presented in Appendix B of Berg, et al. – Vol. II (2009).

Note that the environment between and directly behind modular blocks at the connection may not be the same as the environment with the reinforced soil zone. Therefore, the long-term environmental aging factor ( $RF_{Dc}$ ) may be significantly different than that used in computing the nominal long-term reinforcement strength  $T_{alc}$ .

The connection strength as developed above is a function of normal pressure, which is developed by the weight of the units. Thus, it will vary from a minimum in the upper portion of the structure to a maximum near the bottom of the structure for walls with no batter. Further, since many MBW walls are constructed with a front batter, the column weight above the base of the wall or above any other interface may not correspond to the weight of the facing units above the referenced elevation. The concept is shown in Figure C-20, and is termed a hinge height (*Simac, Bathurst, Berg and Lothspeich (1993)*). Hence, for walls with a nominal batter or more than 8 degrees, the normal stress is limited to the lesser of the hinge height or the height of the wall above the interface. This vertical pressure range should be used in developing  $CR_{CR}$ . This recommendation is based on research findings that indicated that the hinge height concept is overly conservative for walls with small batters (*Bathurst, Walters, Vlachopoulos, Burgess and Allan (2000)*).

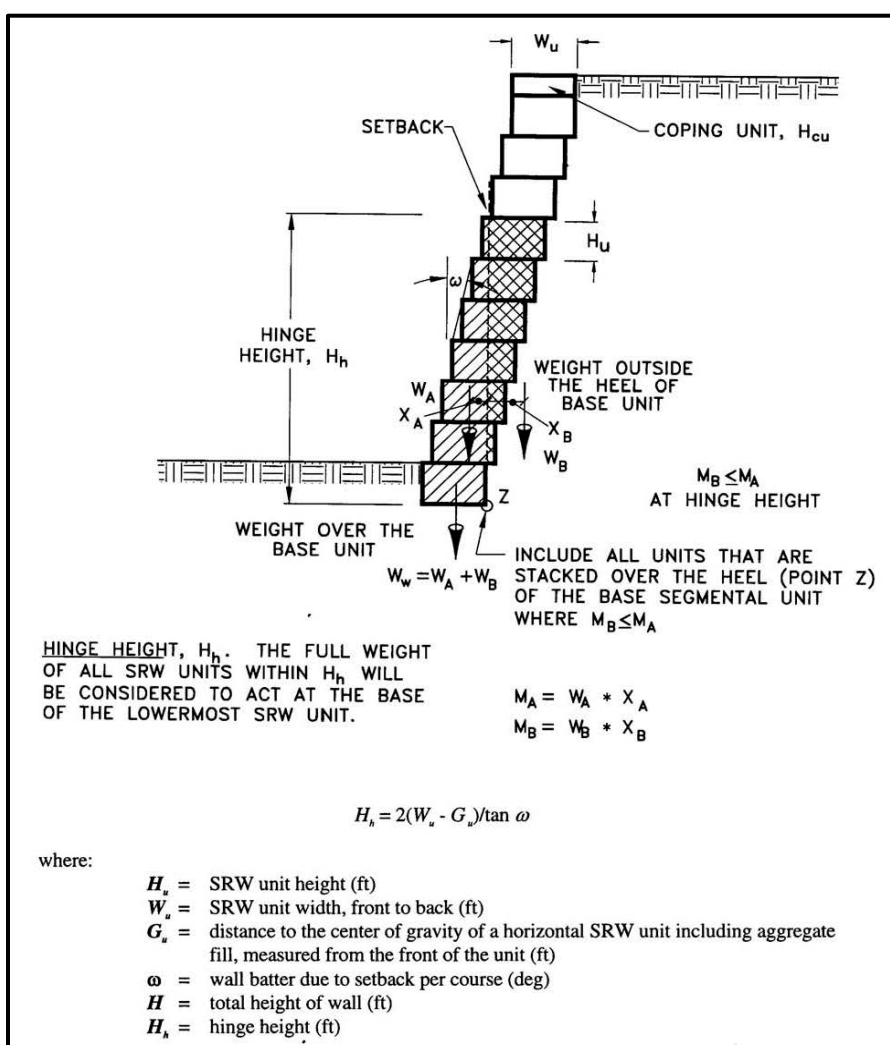


Figure C-20, Hinge Height of Modular Block MSE Walls  
(Berg, et al. – Vol. I (2009))

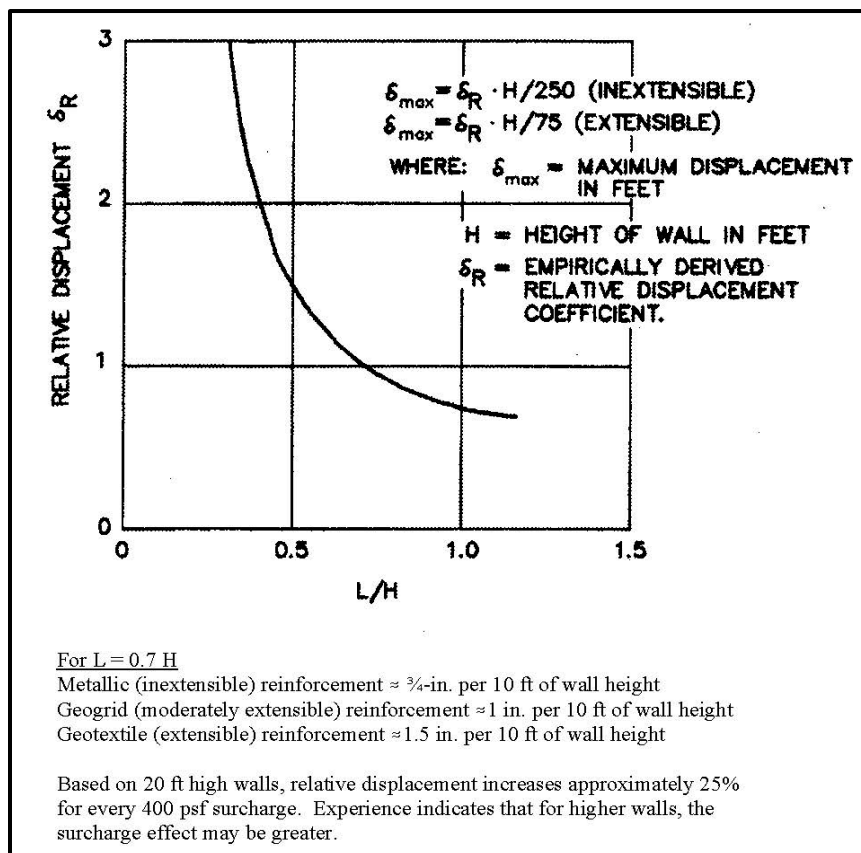
### C.8.10 Estimation of Lateral Movements

The tenth step in internal stability design is estimating the lateral movements that are anticipated to occur within the reinforced soil zone. These movements are required to fully

engage the soil resistance to prevent pullout of the reinforcement. Therefore, the MSE wall face shall be designed and constructed with a positive batter (i.e., the face of the MSE wall shall tilt toward the soil). The required batter shall be clearly indicated on the construction drawings. Berg, et al. – Vol. I (2009) describes lateral movements as follows:

The evaluation of lateral wall movements in LRFD is the same as in ASD as the deformations are evaluated at the Service I limit state. In general, most internal lateral deformations of an MSE wall face usually occur during construction. Post construction movements, however, may take place due to post construction surcharge loads, settlement of wall fill, or long-term settlement of the foundation soils.

The magnitude of lateral displacement depends on fill placement techniques, compaction effects, reinforcement extensibility, reinforcement length, reinforcement-to-facing connection details, and details of the wall facing. The rough estimate of probable lateral displacements of simple MSE walls that may occur during construction can be estimated based on empirical correlations (see *Figure C-21*).



Note: This figure is only a guide. Actual displacement will depend, in addition to the parameters addressed in the figure, on soil characteristics, compaction effort, and contractor workmanship.

**Figure C-21, Empirical Curve for Estimating Lateral Displacement (Berg, et al. – Vol. I (2009))**

In general, increasing the length-to-height ratio of reinforcement, from its theoretical lower limit of  $0.5H$  to the *AASHTO LRFD Specification* specified  $0.7H$  decreases the deformation by about 50 percent. For critical structures requiring

precise tolerances, such as bridge abutments, more accurate calculations using numerical modeling may be warranted.

A deformation response analysis allows for an evaluation of the anticipated performance of the structure with respect to horizontal (and vertical) displacement. Horizontal deformation analyses are the most difficult and least certain of the performed analyses. In many cases, they are done only approximately. The results may impact the choice of facing, facing connections and backfilling sequences.

### **C.8.11 Vertical Movement and Bearing Pad Check**

The final step in internal stability design is checking the vertical movement and bearing pad. Berg, et al. – Vol. I (2009) describes the vertical movement and bearing pad check as follows:

Bearing pads are placed in horizontal joints of segmental precast concrete panels in order to allow the panel and the reinforcement to move down with the reinforced fill as it is placed and settles, mitigate downdrag stress, and provide flexibility for differential foundation settlements. Internal settlement within the reinforced fill is practically immediate with some minor movement occurring after construction due to elastic compression in granular materials. The amount of total movement is the combination of the internal movement and external differential movement. The bearing/compression pad thickness and compressibility could be adjusted according to the anticipated movement. Otherwise concrete panel cracking and/or downdrag on connections resulting in bending of the connections and/or out of plane panel movement can occur. Calculation of the external settlement *is discussed previously*. Normally the internal movement is negligible for well graded, granular fill and external movement will usually control the compression pad requirements. However, when using sand type fill and/or marginal fill containing an appreciable amount of fines, the internal movement can be significant and should be calculated to evaluate additional thickness requirements of the bearing pad. Immediate settlement of granular *material* can be calculated *as indicated in Chapter 17*.

The stiffness (axial and lateral), size, and number of bearing pads should be sized such that the final joint opening will be at least  $3/4 \pm 1/8$ -inch, unless otherwise shown on the plans. A minimum initial joint width of 3/4-inch is recommended. The stiffness (axial and lateral), size, and number of bearing pads should be checked assuming a vertical loading at a given joint is equal to 2 to 3 times the weight of facing panels directly above that level. Laboratory tests in the form of vertical load-vertical strain and vertical load-lateral strain curves of the bearing pads are required for this check.

## **C.9 DESIGN OF FACING ELEMENTS**

Berg, et al. – Vol. I (2009) indicates that the next major design step for an MSE wall is the facing elements. Precast concrete (panels or full height tilt up panels) or MBW units shall be designed by either the SEOR or the MSE wall supplier's engineer. For the design of concrete, steel, or timber facings, Berg, et al. – Vol. I (2009) indicates the following:

Facing elements are designed to resist the horizontal forces *developed previously*. Reinforcement is provided to resist the maximum loading conditions at each depth in accordance with structural design requirements in Sections 5, 6, and 8 of the *AASHTO LRFD Specifications*, for concrete, steel, and timber



facings, respectively. The embedment of the soil reinforcement to panel connector must be developed by test, to ensure that it can resist the  $T_{MAX}$  loads as required in Section 5 of AASHTO LRFD Specifications.

Berg, et al. - Vol. I (2009) indicates the following with regard to the design of MSE walls with flexible facing elements. The use of flexible facing elements is anticipated for temporary and 2-stage MSE walls.

Welded wire or similar facing panels should be designed in a manner that prevents the occurrence of excessive bulging as backfill behind the facing elements compresses due to compaction stresses, self-weight of the backfill or lack of section modulus. Bulging at the face between soil reinforcement elements in both the horizontal and vertical direction generally should be limited to 1 to 2 inches as measured from the theoretical wall line. Specification requirements and design detailing to help achieve this tolerance might include limiting the face panel height to 18 inches or less, the placement of a nominal 2-foot wide zone of rockfill or cobbles directly behind the facing, decreasing the vertical and horizontal spacing between reinforcements, increasing the section modulus of the facing material, and/or by providing sufficient overlap between adjacent facing panels. Furthermore, the top of the flexible facing panel at the top of the wall should be attached to a soil reinforcement layer to provide stability to the top of the facing panel.

Geosynthetic facing elements generally should not be left exposed to sunlight (specifically UV radiation) for permanent walls. If geosynthetic facing elements must be left exposed permanently to sunlight, the geosynthetic should be stabilized to be resistant to UV radiation. Furthermore, product specific test data should be provided which can be extrapolated to the intended design life and which proves that the product will be capable of performing as intended in an exposed environment. Alternatively a protective facing should be constructed in addition (e.g., concrete, shotcrete, etc.).

## C.10 OVERALL STABILITY

The overall (global) stability is typically determined by the GEOR. This stability shall be determined using classical slope stability analyses (see Chapter 17). The failure surfaces may be circular or non-circular and both should be checked. Typically, it is assumed, in overall stability that the failure surface does not pass through the reinforced mass of the MSE structure; therefore, the MSE structure is given strength parameters greater than the retained and foundation soils to prevent the failure plane from passing through the reinforced soil mass. Overall stability analyses are performed for the Service limit state and are normally performed once the initial estimate of the reinforcement length is determined. The results of the overall stability analysis can and do affect the reinforcement length used in the design. It should be noted that it is assumed that all MSE walls are free draining and that pore water pressures are not allowed to build up behind the wall.

## C.11 COMPOUND STABILITY

Prior to submission of the final design plans, a compound global stability analysis shall be performed by the MSE wall supplier. Compound stability analyses and failure surfaces are described by Berg, et al. – Vol. I (2009) as follows:

Additional slope stability analyses should be performed for MSE walls to investigate potential compound failure surfaces, i.e., failure planes that pass behind or under and through a portion of the reinforced soil zone as illustrated in Figure C-22. For simple structures with rectangular geometry, relatively uniform reinforcement spacing, and a near vertical face, compound failures passing both through the unreinforced and reinforced zones will not generally be critical. However, if complex conditions exist such as changes in reinforced soil types or reinforcement lengths, high surcharge loads, seismic loading, sloping faced structures, significant slopes at the toe or above the wall or stacked (tiered) structures, compound failures must be considered.

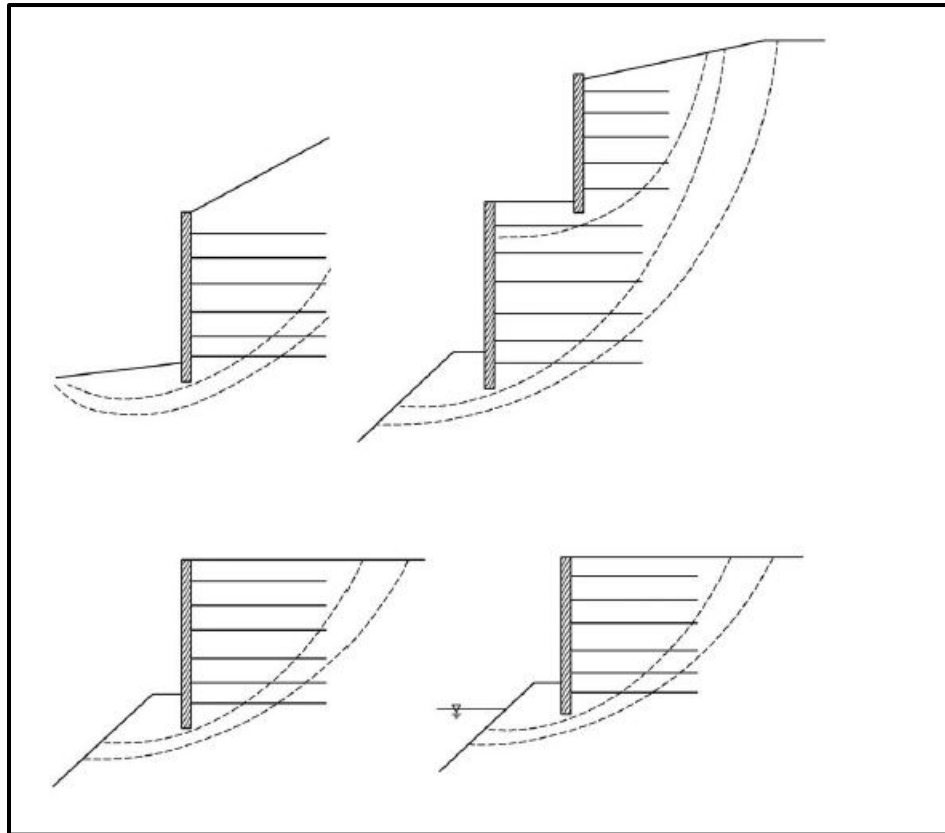


**Figure C-22, Compound Stability MSE Wall Geometries  
(Berg, et al. – Vol. I (2009))**

As indicated in Figure C-22, a compound stability analysis examines failure surfaces that pass through either the retained fill and reinforced soil mass to exit through the MSE wall face or that pass through the retained fill, reinforced soil mass, and the foundation soil to exit beyond the toe of the MSE wall. The actual strength parameters that the reinforced soil mass is based on shall be used in the analysis. These analyses can only be performed once a specific MSE wall type is selected. The GEOR will show on the plans the necessary soil parameters for the retained fill and the foundation soils. The compound analysis shall be performed by the MSE wall supplier using the information supplied by the GEOR. In addition, the MSE wall supplier should use the MSEW software package as prepared and provided by ADAMA Engineering, Inc.

The resistance factors ( $\phi$ ) for global stability analyses are provided in Chapter 9. MSE wall structures are considered Flexible Gravity Retaining Walls.

## C.12 WALL DRAINAGE SYSTEM DESIGN

The following Section is adopted directly from Berg, et al. – Vol. I (2009) and is used with the permission of the US Department of Transportation, Federal Highway Administration. The italics are added to reflect additions or modifications to the selected text and to supply references to this Manual.

### C.12.1 Subsurface Drainage

Subsurface drainage must be addressed in design. The primary component of an MSE wall is soil. Water has a profound effect on this primary component, as it can both decrease the soil shear strength (i.e., resistance) and increase destabilizing forces (i.e., load). Thus, FHWA recommends drainage features be required in all walls unless the engineer determines such feature is, or features are, not required for a specific project or structure.

Drainage design and detailing is addressed in *Berg, et al. – Vol. I (2009)*. Note that MSE walls using free draining reinforced fill do not typically need a full drainage system, but do need a method for discharging water collected within the reinforced wall fill (see *Figure C-23*). Also note that MSE walls can be designed for water loads, if needed. Basic soil mechanics principles should be used to determine the effect or phreatic surface on wall loads. See *Berg, et al. – Vol. I (2009)* for a discussion of the required design of MSE walls for flood and scour events.

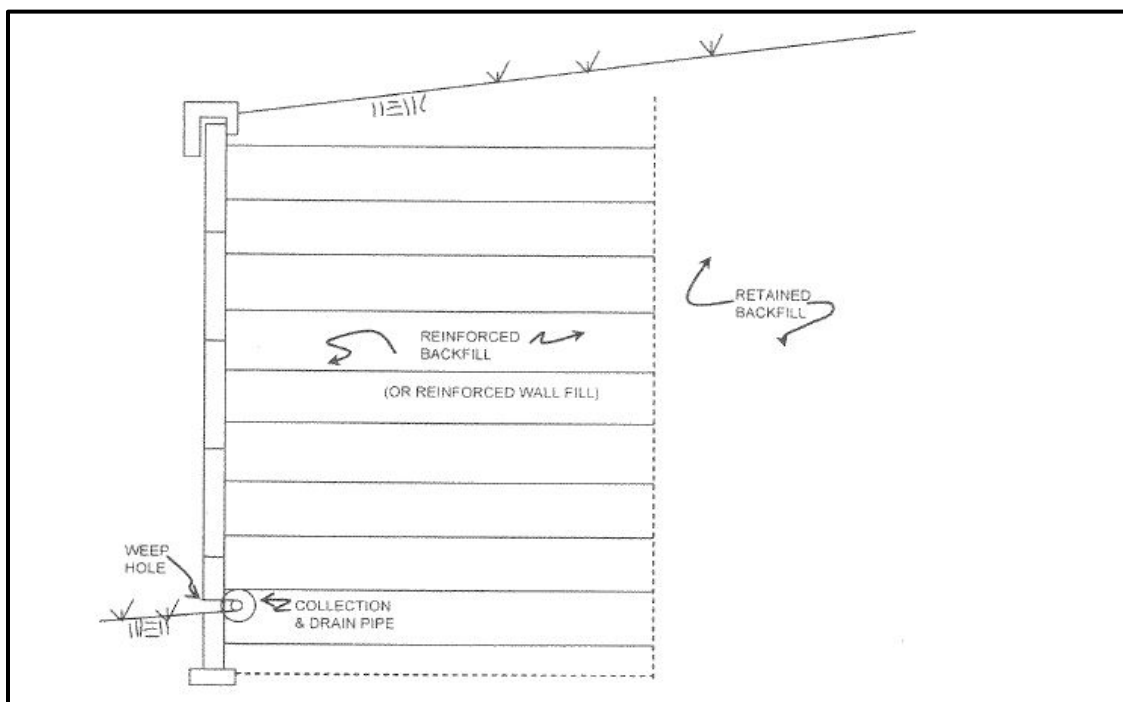


**Figure C-23, Drain Immediately Behind MSE Wall Face  
(Tanyu, et al. (2008))**

### C.12.2 Surface Water Runoff

Surface drainage is an important aspect of ensuring wall performance and must be addressed during design and during construction. Appropriate drainage

measures to prevent surface water from *excessively* infiltrating into the wall fill should be included in the design of a MSE wall structure. Surface drainage design and detailing are addressed in *Berg, et al. – Vol. I (2009)*.

### C.12.3 Scour

There are additional detailing considerations for walls that are exposed to potential scour. The wall embedment depth must be below the predicted *or estimated* scour depth. Wall initiation and termination detailing should consider and should be designed to protect from scour *that may be caused by surface water runoff*. Riprap may be used to protect the base and ends of a wall. A coarse stone wall fill may be desired to drain rapidly. The reinforced wall fill at the bottom of the structure may be wrapped with a geotextile filter to minimize loss of fill should scour exceed design predictions. These items are discussed in detail by *Berg, et al. – Vol. I (2009)*, and should be included on the plans.

## C.13 SEISMIC DESIGN

The seismic external stability design shall conform to the requirements of Chapters 13 and 14. The seismic internal stability calculations shall conform to the requirements contained in the AASHTO LRFD Specifications (Section 11.10 – Mechanically Stabilized Earth Walls), except all accelerations used shall conform to the requirements of this Manual. Additionally, all load and resistance factors shall conform to Chapters 8 and 9 and all displacements should conform to Chapter 10.

## C.14 COMPUTER SOFTWARE

A complete set of the MSE wall system supplier's design calculations prepared in accordance with this Appendix shall be provided by the MSE wall system supplier. The determination of all loading conditions and assumptions shall be fully documented with all design calculations. Submitted calculations (including computer runs) shall include all load cases that exist during construction including staging and at the end of construction for any surcharges, hydraulic conditions, live loads, combinations, and obstructions within the reinforced backfill. Computer generated designs made by software other than FHWA's MSEW computer program shall meet the requirements of Chapter 26 and shall require verification that the computer program's design methodology meets the requirements provided herein. This shall be accomplished by either:

1. Complete, legible, calculations that show the design procedure step-by-step for the most critical geometry and loading condition that will govern each design section of the MSE wall structure. Calculations may be computer generated provided that all input, equations, and assumptions used are shown clearly.
2. Provide an electronic file with the input files and the full computer output of the FHWA sponsored computer program MSEW (latest version) for the governing loading condition for each design section of the MSE wall structure. This software may be obtained at:

**ADAMA Engineering, Inc.**  
33 The Horseshoe, Covered Bridge Farms  
Newark, Delaware 19711, USA  
Tel. (302) 368-3197, Fax (302) 731-1001

## C.15 PLANS

This Section details the information that should be placed on construction drawings related to MSE walls. The GEOR should review the template drawings available on the SCDOT website at:

<https://www.scdot.org/business/geotech.aspx>

Select “713 Series – Mechanically Stabilized Earth Walls” in the drop down menu. The requirements for plans for MSE Walls are contained in Chapter 22.

## C.16 REFERENCES

Allen, T., Christopher, B. R., Elias, V. E., and DiMaggio, J., (2001), *Development of the Simplified Method for Internal Stability Design of Mechanically Stabilized Earth Walls*, Washington State Department of Transportation Research Report WA-RD 513.1, 108p.

Allen, T., Christopher, B. R., and Holtz, R. D., (1992), *Performance of a 41-foot High Geotextile Wall*, Washington State Department of Transportation Research Report WA-RD 257.1, 64p.

American Association of State Highway and Transportation Officials, (2017), *LRFD Bridge Design Specifications Customary U.S. Units, 8<sup>th</sup> Edition*, American Association of State Highway and Transportation Officials, Washington, D.C.

Bathurst, R. J., Walters, D., Vlachopoulos, N., Burgess, P., and Allan, T. M., (2000), “Fullscale Testing of Geosynthetic Reinforced Walls”, *Proceedings of GeoDenver: Advances in Transportation and Geoenvironmental Systems Using Geosynthetics*, Geotechnical Special Publication No. 103, ASCE, pp. 201-217.

Berg, R. R., Christopher, B. R., and Samtani, N. C., (2009), *Design of Mechanically Stabilized Earth Walls and Reinforced Soil Slopes - Volume I*, Geotechnical Engineering Circular No. 11 – Volume I, (Publication No. FHWA-NHI-10-024), U.S. Department of Transportation, National Highway Institute, Federal Highway Administration, Washington D.C.

Berg, R. R., Christopher, B. R., and Samtani, N. C., (2009), *Design of Mechanically Stabilized Earth Walls and Reinforced Soil Slopes - Volume II*, Geotechnical Engineering Circular No. 11 – Volume I, (Publication No. FHWA-NHI-10-025), U.S. Department of Transportation, National Highway Institute, Federal Highway Administration, Washington D.C.

Christopher, B. R., Gill, S. A. Giroud, J.-P., Juran, I., Mitchell, J. K., Schlosser, F., and Dunicliff, J., (1990), *Reinforced Soil Structures Volume I Design and Construction Guidelines*, (Publication No. FHWA-RD-89-043), U.S. Department of Transportation, Office of Engineering and Highway Operations R&D, Federal Highway Administration, Washington D.C.

Collin, J. G., (1986) “Earth Wall Design”, Ph.D. Dissertation, University of California – Berkeley, 419 p.

Elias, V., Fishman, K. L., Christopher, B. K., and Berg, R. R., (2009), *Corrosion/Degradation of Soil Reinforcements for Mechanically Stabilized Earth Walls and Reinforced Soil Slopes*, (Publication No. FHWA-NHI-09-087), U.S. Department of Transportation, National Highway Institute, Federal Highway Administration, Washington D.C.

Elias, V., Salman, A., Juran, I., Pearce, E., and Lu, S. (1999), Testing Protocols for Oxidation and Hydrolysis of Geosynthetics, (Publication No. FHWA RD-97-144), U.S. Department of Transportation, Office of Engineering and Highway Operations R&D, Federal Highway Administration, Washington D.C.

Simac, M. R., Bathurst, R. J., Berg, R. R., and Lothspeich, S. E., (1993), Design Manual for Segmental Retaining Walls, National Concrete Masonry Association, Herndon, VA., 336 p.

Tanyu, B. F., Sabatini, P. J., and Berg, R. R., (2008), Earth Retaining Structures, (Publication No. FHWA-NHI-07-071), U.S. Department of Transportation, National Highway Institute, Federal Highway Administration, Washington D.C.

**APPENDIX D**  
**REINFORCED SOIL SLOPES**

**GEOTECHNICAL DESIGN MANUAL**

*January 2019*





## Table of Contents

<u>Section</u>	<u>Page</u>
D.1 Introduction.....	D-1
D.2 Design Considerations and Requirements.....	D-1
D.3 Site Conditions .....	D-2
D.4 Reinforced Fill Material Properties .....	D-3
D.5 Design Parameters for Reinforcement.....	D-3
D.5.1 Reinforcement Pullout Resistance .....	D-3
D.6 Unreinforced Stability.....	D-13
D.7 Reinforcement Design .....	D-15
D.7.1 Estimating $L_e$ .....	D-20
D.7.2 Correction Factor ( $\alpha$ ) .....	D-21
D.7.3 Pullout Friction Factor ( $F^*$ ) .....	D-21
D.7.4 Selection of Reinforcement .....	D-23
D.8 External Stability .....	D-24
D.8.1 Sliding Resistance.....	D-24
D.8.2 Global (Deep-Seated) Stability .....	D-26
D.8.3 Local Bearing Failure at Toe .....	D-26
D.8.4 Foundation Settlement .....	D-27
D.8.5 Seismic Stability .....	D-27
D.9 Drainage System Design .....	D-27
D.9.1 Subsurface Water Control .....	D-27
D.9.2 Surface Water Runoff.....	D-28
D.10 Computer Software.....	D-29
D.11 References .....	D-30

**List of Tables**

<b><u>Table</u></b>	<b><u>Page</u></b>
Table D-1, Steel Corrosion Rates for Moderately Corrosive Reinforced Fill.....	D-7
Table D-2, Creep Reduction Factors .....	D-12
Table D-3, Minimum Testing Requirements for use $RF_D$ .....	D-13
Table D-4, Typical Values of $\alpha$ .....	D-21

**List of Figures**

<b>Figure</b>	<b>Page</b>
Figure D-1, RSS Design Requirements and Geometry.....	D-2
Figure D-2, Mechanisms of Pullout Resistance .....	D-4
Figure D-3, Cross Section Area for Strips.....	D-6
Figure D-4, Cross Section Area for Bars .....	D-7
Figure D-5, Long-Term Geosynthetic Reinforcement Strength Concept.....	D-9
Figure D-6, Critical Zone .....	D-14
Figure D-7, Geometry of Rotational Shear Failure Surface.....	D-16
Figure D-8, Reinforcement Strength Requirements Chart Solution - A .....	D-16
Figure D-9, Reinforcement Strength Requirements Chart Solution - B .....	D-17
Figure D-10, Reinforcing Zone Vertical Layout.....	D-18
Figure D-11, Definitions of $b$ , $S_h$ and $S_v$ .....	D-23
Figure D-12, Sliding Stability Analysis .....	D-25
Figure D-13, Local Bearing Failure (Lateral Squeeze).....	D-26
Figure D-14, Groundwater and Surface Drainage .....	D-27



# APPENDIX D

## REINFORCED SOIL SLOPE DESIGN GUIDELINES

### D.1 INTRODUCTION

This Appendix outlines SCDOT's design methodology for Reinforced Soil Slopes (RSS). RSSs are internally stabilized fill slopes, constructed of alternating layers of compacted soil and reinforcement. An RSS is different from an MSE wall or a conventional slope in that the slope has an inclination ranging from 1H:1V to 70° and will require a facing element. This Appendix governs the design of permanent and temporary RSSs. The design life of both permanent and temporary RSS is provided in Chapter 17. The procedures contained in this Appendix may also be used to design a reinforced embankment (2H:1V to 1H:1V).

This design process assumes that the existing subgrade soils provide a stable foundation for the founding of the RSS. If improvement is required, see Chapters 19 and 20. This procedure assumes that classical limit equilibrium slope stability methods are applicable (see Chapter 17).

### D.2 DESIGN CONSIDERATIONS AND REQUIREMENTS

The first part of the design is determining the geometry, the external loading conditions, the performance criteria, and any construction constraints. The geometry should include the location relative to the remainder of the project (i.e., to the centerline and specific station). The geometry should also indicate the anticipated toe and crest of the slope (see Figure D-1). During this step of the design, external loads should be identified. These loads include, but are not limited to transient (traffic), permanent (weight of pavement surface) and/or seismically induced loads. The performance criteria are based on whether the RSS is a bridge or road embankment. Bridge embankment RSSs are further subdivided by OC (see Chapter 8) to meet the Performance Objectives for the bridge contained in the Seismic Specs. RSSs shall be designed for the appropriate limit state indicated in Chapter 8. The load and resistance factors are determined from Chapters 8 and 9, respectively. The Performance Limits are provided in Chapter 10. Any constraints on construction (i.e., soft ground, standing water, limited ROW, etc.) should also be identified during this step. These construction constraints should be carefully considered before deciding to use an RSS.

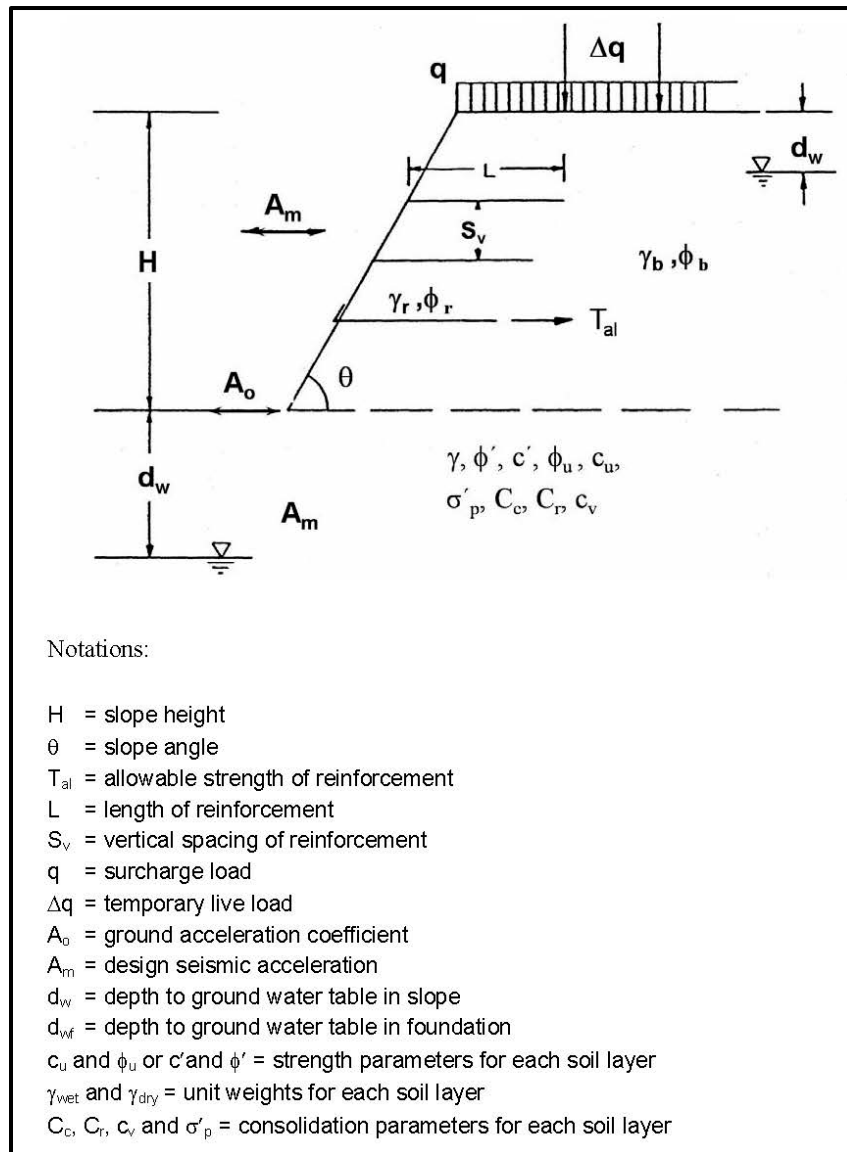


**Figure D-1, RSS Design Requirements and Geometry  
(Berg, Christopher and Samtani – Vol. II (2009))**

### D.3 SITE CONDITIONS

The second step in the design of an RSS is the evaluation of the topography, subsurface conditions, and in-situ soil/rock parameters. The topography evaluation should include reviewing the height requirements of the slope, the amount of space between the toe of the slope and the anticipated extent of the reinforcement, and the condition of the existing ground surface. This evaluation should identify the need for any temporary shoring that may be required to install the RSS (i.e., the grading of the site requires cutting). The subsurface conditions and in-situ soil/rock parameters shall be evaluated using the procedures presented in Chapters 4 through 7.

## D.4 REINFORCED FILL MATERIAL PROPERTIES

The fill materials to be used to construct a permanent RSS shall meet the criteria provided in STS SC-M-206-1 (latest version) for *Reinforced Soil Slopes (RSS)*. The GEOR shall provide, in the plans, the fill material requirements for temporary RSSs. The soil strength parameters ( $\phi$ ,  $c$  and  $\gamma_t$ ) shall be determined in accordance with Chapter 5.

## D.5 DESIGN PARAMETERS FOR REINFORCEMENT

Portions of the following sections of this Appendix are adopted directly from Tanyu, Sabatini and Berg (2008), and Berg, Christopher and Samtani – Volumes I and II (2009) and are used with the permission of the US Department of Transportation, Federal Highway Administration. Italics have been added to reflect additions or modifications to the selected text and to supply references to this Manual. According to Berg, et al. – Vol. I (2009):

### D.5.1 Reinforcement Pullout Resistance

A reinforced soil mass is somewhat analogous to reinforced concrete in that the mechanical properties of the mass are improved by reinforcement placed parallel to the principal strain direction to compensate for soil's lack of tensile resistance. The improved tensile properties are a result of the interaction between the reinforcement and the soil. The composite material has the following characteristics:

- Stress transfer between the soil and reinforcement takes place continuously along the reinforcement
- Reinforcements are distributed throughout the soil zone with a degree of regularity

Stresses are transferred between soil and reinforcement by friction (*Figure D-2A*) and/or passive resistance (*Figure D-2B*) depending on the reinforcement geometry.

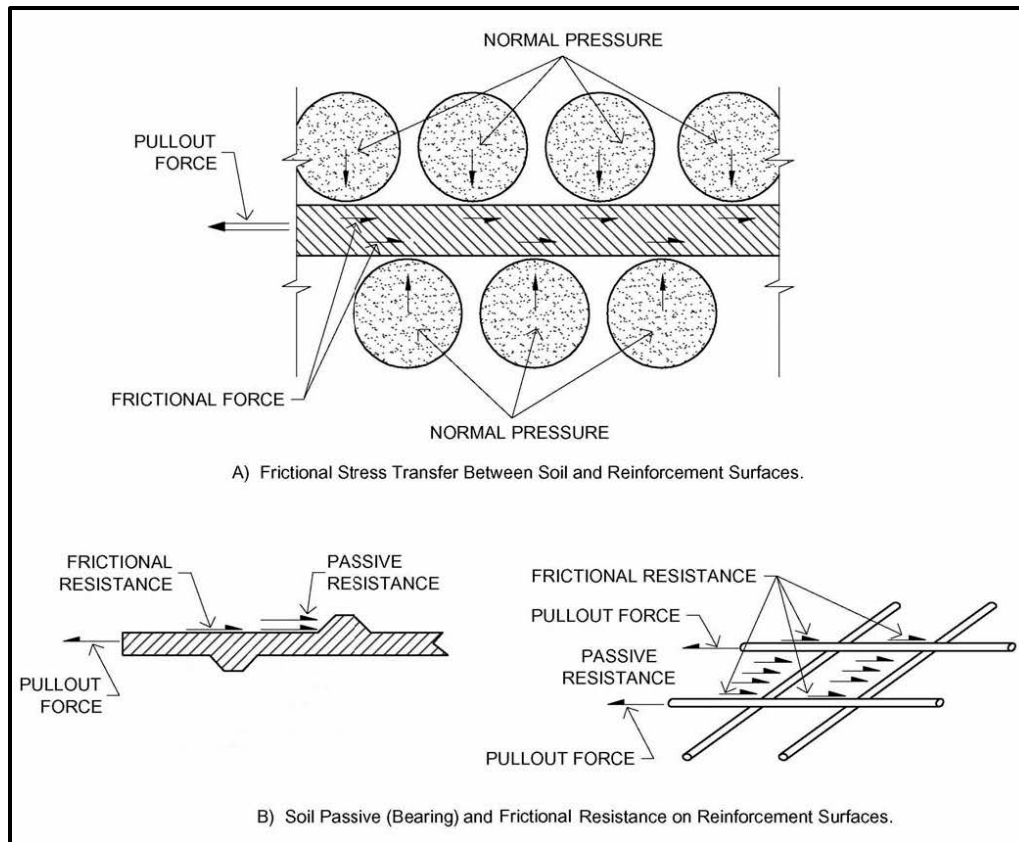


**Figure D-2, Mechanisms of Pullout Resistance  
(Berg, et al. – Vol. I (2009))**

**Friction** develops at locations where there is a relative shear displacement and corresponding shear stress between soil and reinforcement surface. Reinforcing elements dependent on friction should be aligned with the direction of soil reinforcement relative movement. Examples of such reinforcing elements are steel strips, longitudinal bars in grids, geotextile, and some geogrid layers.

**Passive Resistance** occurs through the development of bearing type stresses on “transverse” reinforcement surfaces normal to the direction of soil reinforcement relative movement. Passive resistance is generally considered to be the primary interaction for bar mat, wire mesh reinforcements, and geogrids with relatively stiff cross machine direction ribs. The transverse ridges on “ribbed” strip reinforcements also provide some passive resistance.

The contribution of each transfer mechanism for a particular reinforcement will depend on the roughness of the surface (skin friction), normal effective stress, grid opening dimensions, thickness of the transverse members, and elongation characteristics of the reinforcement. Equally important for interaction development are the soil characteristics, including grain size and grain size distribution, particle shape, density, water content, cohesion, and stiffness.

The primary function of reinforcement is to restrain soil deformations. In doing so, stresses are transferred from the soil to the reinforcement. These stresses are resisted by the reinforcement tension and/or shear and bending.

Two types of reinforcement material can be considered:



- **Strips, bars, and steel grids** – A layer of steel strips, bars or grids is characterized by the cross-sectional area, the thickness and perimeter of the reinforcement element, and the center-to-center horizontal distance between elements (for steel grids, an element is considered to be a longitudinal member of the grid that extends into the wall).
- **Geotextiles and geogrids** – A layer of geosynthetic strips is characterized by the width of the strips and the center-to-center horizontal distance between them. The cross-sectional area is not needed, since the strength of the geosynthetic is expressed by a tensile force per unit width, rather than by stress. Difficulties in measuring the thickness of these thin and relatively compressible materials preclude reliable estimates of stress.

The structural design properties of reinforcement materials are a function of geometric characteristics, strength and stiffness, durability, and material type. The 2 most commonly used reinforcement materials, steel and geosynthetics, must be considered separately as *discussed in the following Sections*:

### D.5.1.1 Inextensible Reinforcements

For steel reinforcements, the design life is achieved by reducing the cross-sectional area of the reinforcement used in the design calculations by the anticipated corrosion (*see next Section*) losses over the design life period as follows:

$$E_c = E_n - E_R \quad \text{Equation D-1}$$

Where,

$E_c$  = Thickness of the reinforcement at the end of the design life

$E_n$  = Nominal thickness at construction

$E_R$  = Sacrificial thickness of metal expected to be lost by uniform corrosion during the service life of the structure

The nominal long-term design strength of inextensible reinforcement is obtained for steel strips and grids as shown in the following equation.  $T_{al}$  in units of force per unit width is used to provide a unified strength approach, which can be applied to any reinforcement. Tensile strength of a known steel or grid reinforcement can also be expressed in terms of the tensile load carried by the reinforcement,  $P_{tal}$ . Thus, nominal tensile strength may be calculated and expressed in the following terms:

$$T_{al} = \frac{F_y * A_c}{b} \quad \text{Equation D-2}$$

$$P_{tal} = F_y * A_c \quad \text{Equation D-3}$$

Where,

$F_y$  = Minimum yield strength of steel

$b$  = Unit width of sheet, grid, bar or mat

$A_c$  = Design cross sectional area corrected for corrosion loss

$T_{al}$  = Strength per unit reinforcement width

$P_{tal}$  = Strength per reinforcement element

The LRFD resistance factors for steel reinforcements in RSSs are listed in *Chapter 9*. The resistance factor for strip reinforcement under static conditions is 0.75 (see *Chapter 9*). The resistance factor for steel grid reinforcement, for static loading, is 0.65 (see *Chapter 9*) when reinforcement is connected to a rigid facing element and is 0.75 when connected to a flexible facing. The lower resistance factor for grid reinforcing members connected to a rigid facing element (e.g., a concrete panel or block) is used to account for the greater potential for local overstress due to load unconformities for steel grids than for steel strips or bars. Transverse and longitudinal grid members are sized in accordance with ASTM A1064 – *Standard Specification for Carbon-Steel Wire and Welded Wire Reinforcement, Plain and Deformed, for Concrete*.

$A_c$  for strips is determined as:

$$A_c = b * E_c = b * (E_n - E_R) \quad \text{Equation D-4}$$

Where,

$b$  = Unit width of sheet, grid, bar or mat

$E_c$  = Thickness at end of design life (see Figure D-3)

$E_n$  = Thickness at end of construction

$E_R$  = Sacrificial thickness of metal expected to be lost by uniform corrosion during the service life of the structure

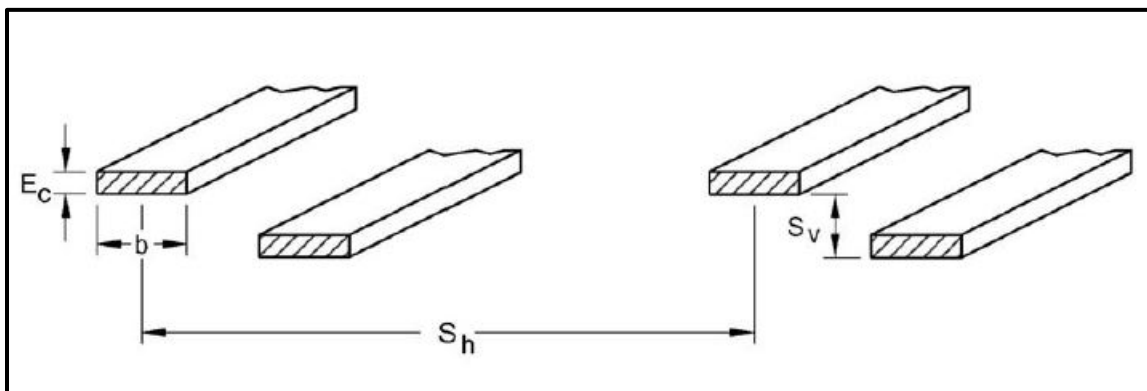


**Figure D-3, Cross Section Area for Strips  
(Berg, et al. – Vol. I (2009))**

When estimating  $E_R$ , it may be assumed that equal loss occurs from the top and bottom of the strip.

$A_c$  for bars is determined as:

$$A_c = N_b * \left( \frac{\pi * (D^*)^2}{4} \right) \quad \text{Equation D-5}$$

Where,

$N_b$  = Number of bars per unit width  $b$

$D^*$  = Bar diameter after corrosion loss (Figure D-4)

When estimating  $D^*$ , it may be assumed that corrosion losses occur uniformly over the area of the bar.

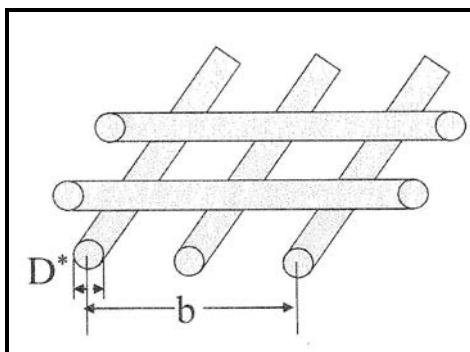


**Figure D-4, Cross Section Area for Bars  
(Berg, et al. – Vol. I (2009))**

### D.5.1.2 Corrosion Rates Inextensible Reinforcements

According to Berg, et al. – Vol. I (2009):

The corrosion rates presented *below* are suitable for conservative design. These rates assume a mildly corrosive backfill material having the controlled electrochemical property limits as discussed in the STS SC-M-206-1.

**Table D-1, Steel Corrosion Rates for Moderately Corrosive Reinforced Fill  
(Berg, et al. – Vol. I (2009))**

For zinc/side	0.58 mils/yr (first 2 years)
	0.16 mils/yr (thereafter)
For residual carbon steel/side <sup>1</sup>	0.47 mils/yr (thereafter)

<sup>1</sup>after zinc depletion

Based on these rates, complete corrosion of galvanization with the minimum required thickness of *0.0034 inches (3.4 mils)* (AASHTO M111) is estimated to occur during the first 16 years and a carbon steel thickness or diameter loss of 0.055 inches to 0.08 inches would be anticipated over the remaining 75- to 100-year design life, respectively. Galvanization can be damaged during handling and construction by abrasion, scratching, notching, and cracking. Construction equipment should not travel directly on reinforcing elements and elements should not be dragged, excessively bent, or field cut. Galvanized reinforcement should be well supported during lifting and handling to prevent excessive bending. Any damaged section should be field repaired by coating the damaged area with a field grade zinc-rich paint.

The designer of an *RSS* structure should also consider the potential for changes in the reinforced backfill environment during the structure's service life. In certain parts of *South Carolina*, it can be expected that deicing salts might cause such an environment change. For this problem, the depth of chloride infiltration and concentration are of concern.

For permanent structures directly supporting roadways exposed to deicing salts, limited data indicates that the upper 8 feet of the reinforced backfill (as measured from the roadway surface) or greater depths, depending on the gradation and compaction of the fill, are affected by higher corrosion rates not presently defined. Under these conditions, it is recommended that a 30 mil (minimum) geomembrane be placed below the road base and tied into a drainage system to mitigate the penetration of the deicing salts in lieu of higher corrosion rates. Alternatively free draining reinforced fill (e.g., No. 57 stone) has been found to

allow salts to “flush out” and limit corrosion as discussed in *Elias, Fishman, Christopher and Berg (2009)*. Note that value of “higher” corrosion rate for deicing salt exposure is not defined.

The following project situations lie outside the scope of the previously presented values:

- Structures exposed to a marine or other chloride-rich environment. (Excluding locations where de-icing salts are used). For marine saltwater structures, carbon steel losses on the order of 3.2 mils per side or radius should be anticipated in the first few years, reducing to 0.67 to 0.70 mils thereafter. Zinc losses are likely to be quite rapid as compared to losses in reinforced fills meeting the *RSS* electro-chemical criteria. Total loss of zinc (3.4 mils) should be anticipated in the first year.
- Structures exposed to stray currents, such as from nearby underground power lines, and structures supporting or located adjacent to electrical railroads.
- Structures exposed to acidic water emanating from mine waste, abandoned coal mines, or pyrite-rich soil and rock strata.

Each of these situations creates a special set of conditions that should be specifically analyzed by a corrosion specialist.

### D.5.1.3 Extensible Reinforcements

According to Berg, et al. – Vol. I (2009):

Selection of long-term nominal tensile strength,  $T_{al}$ , for geosynthetic reinforcement is determined by thorough consideration of all possible ... time dependent strength losses over the design life period. The tensile properties of geosynthetics are affected by factors such as creep, installation damage, aging, temperature, and confining stress. Furthermore, characteristics of geosynthetic products manufactured with the same base polymer can vary widely requiring a  $T_{al}$  determination for each individual product with consideration of all these factors. *The GEOR for the RSS should refer to STSs SC-M-203-2 for Geogrid Soil Reinforcement and SC-M-203-3 for Geotextile Soil Reinforcement for the  $T_{al}$  that are assigned to specific geogrid and geotextile designations.*

Polymeric reinforcement, although not susceptible to corrosion, may degrade due to physiochemical activity in the soil such as hydrolysis, oxidation, and environmental stress cracking depending on the polymer type. In addition, these materials are susceptible to installation damage and the effects of high temperature at the facing and connections. Temperature acts to accelerate creep and aging processes and temperature effects are accounted through their determination. While the normal range of in-ground temperature vary from 55° F in cold and temperate climates to 85° F in arid desert climates, temperatures at the facing and reinforcement connections can be as high as 120° F. Confining stress is not directly taken into account other than indirectly when installation damage is evaluated. For creep and durability, confining stress generally will tend to improve the long-term strength of the reinforcement.

The available long-term strength,  $T_{al}$ , is calculated as follows:

$$T_{al} = \frac{T_{ult}}{RF} = \frac{T_{ult}}{RF_{ID} * RF_{CR} * RF_D} \quad \text{Equation D-6}$$

Where,

$T_{ult}$  = Ultimate tensile strength (strength per unit width).

RF = Reduction factor. The product of all applicable reduction factors

$RF_{ID}$  = Installation damage reduction factor accounts for the damaging effects of placement and compaction of soil or aggregate over the geosynthetic material during installation. A minimum reduction factor 1.1 should be used to account for testing uncertainties.

$RF_{CR}$  = Creep reduction factor accounts for the effect of creep resulting from long-term sustained tensile load applied to the geosynthetic.

$RF_D$  = Durability reduction factor accounts for the strength loss caused by chemical degradation (aging) of the polymer used in the geosynthetic reinforcement (e.g., oxidation of polyolefins, hydrolysis of polyesters, etc.). A minimum reduction factor 1.1 should be used to account for testing uncertainties.

$RF_{ID}$ ,  $RF_{CR}$  and  $RF_D$  reflect actual long-term strength losses, analogous to loss of steel strength due to corrosion. This long-term geosynthetic reinforcement strength loss concept is illustrated in Figure D-5. As shown in the figure, some strength losses occur immediately upon installation, and others occur throughout the design life of the reinforcement. Much of the long-term strength loss does not begin to occur until near the end of the reinforcement design life.

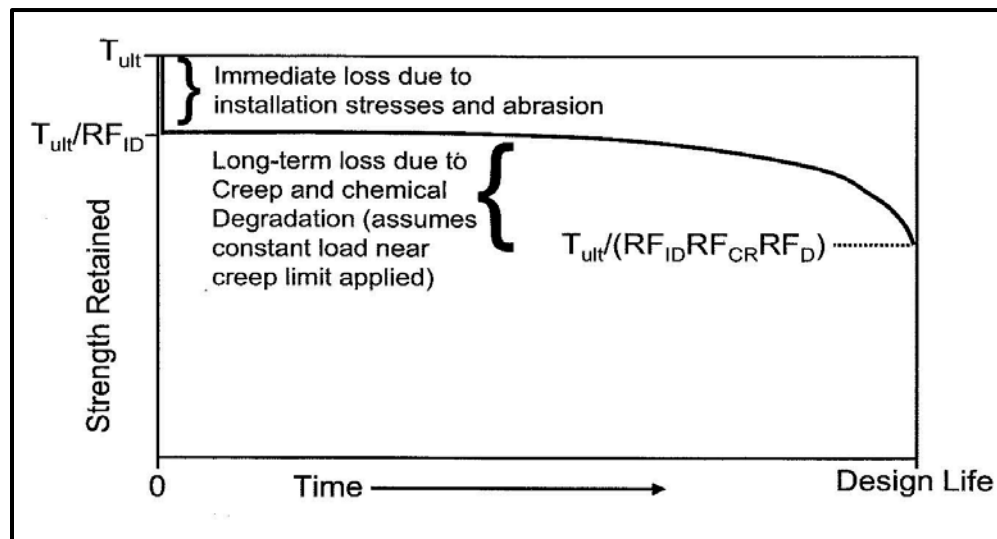


Figure D-5, Long-Term Geosynthetic Reinforcement Strength Concept  
(Berg, et al. – Vol. I (2009))

Because of varying polymer types, quality, additives and product geometry, each geosynthetic is different in its resistance to aging and attack by different chemical agents. Therefore, each product must be investigated individually, or in the context of product line where the same polymer source and additives are used, and the manufacturing process is the same for all products in the product line. This product line approach makes it possible to interpolate reduction factors for products in the product line not specifically tested using the reduction factors determined for the products in the product line that are specifically tested for each degradation mechanism.

The AASHTO LRFD Specifications provide minimum requirements for the assessment of  $T_{al}$  for use in the design of geosynthetic reinforced soil structures. Protocols for evaluating  $T_{al}$  are included in Berg, et al. – Vol. I (2009) with supporting information on testing procedures provided in Elias, et al. (2009).

The determination of reduction factors for each geosynthetic product and product line requires extensive field and/or laboratory testing which can take a year or more to complete.

#### **D.5.1.4 Ultimate Tensile Strength, $T_{ult}$**

The value selected for  $T_{ult}$ , for design purposes, is the minimum average roll value (MARV) for the product. The tensile strength of the reinforcement is determined from wide strip tests for geotextiles per ASTM D4595 – *Standard Test Method for Tensile Properties of Geotextiles by the Wide-Width Strip Method* or for geogrids per D6637 – *Standard Test Method for Determining Tensile Properties of Geogrids by the Single or Multi-Rib Tensile Method* based on the MARV for the product. This MARV accounts for statistical variance in the material strength. Other sources of uncertainty and variability in the long-term strength result from installation damage, creep extrapolation, and the chemical degradation process. It is assumed that the observed variability in the creep rupture envelope is 100 percent correlated with the short-term tensile strength, as the creep strength is typically directly proportional to the short-term tensile strength within a product line. Therefore, the MARV of  $T_{ult}$  adequately takes into account variability in the creep strength. Note that the MARV of  $T_{ult}$  is the minimum certifiable wide-width tensile strength provided by the product manufacturer.

#### **D.5.1.5 Reduction Factors**

The following Sections of this Appendix are adopted directly from Berg, et al. – Vol. I (2009) and are used with the permission of the US Department of Transportation, Federal Highway Administration. Italics have been added to reflect additions or modifications to the selected text and to supply references to this Manual.

##### **D.5.1.5.1 Installation Damage Reduction Factor, $RF_{ID}$**

According to Berg, et al. – Vol. I (2009):

Damage during handling and construction, from abrasion and wear, punching and tear or scratching, notching, and cracking may occur in geosynthetics. These types of damage can only be avoided by using care during handling and construction. Construction equipment should not travel directly on geosynthetic materials.

Damage during reinforced fill placement and compaction operations is a function of the severity of the loading imposed on the geosynthetic during construction operations and the size and angularity of the reinforced fill. For RSS construction, lightweight, low strength geotextiles and geogrids should be avoided to minimize damage with ensuing loss of strength.

Protocols for field testing for this reduction factor are detailed in *Elias, et al. (2009)* and in ASTM D5818 – *Standard Practice for Exposure and Retrieval of Samples to Evaluate Installation Damage of Geosynthetics*. These protocols require that the geosynthetic material be subjected to a reinforced fill placement and compaction cycle, consistent with field practice. The ratio of the initial strength, to the strength of retrieved samples defines this reduction factor. For

reinforcement applications, a minimum weight of 8.0 oz/yd<sup>2</sup> for geotextiles is recommended to minimize installation damage. In general, the combination of geosynthetic reinforcement, and backfill placement and gradation characteristics, should not result in a value of  $RF_{ID}$  greater than 1.7. If testing indicates that  $RF_{ID}$  will be greater than 1.7 (approximately a 40 percent strength loss); then that combination of geosynthetic and backfill conditions should not be used, as this or greater levels of damage will cause the remaining strength to be highly variable and therefore not adequately reliable for design.

In general,  $RF_{ID}$  is strongly dependent on the backfill soil gradation characteristics and its angularity, especially for lighter weight geosynthetics. Provided a minimum of 6 inches of backfill material is placed between the reinforcement surface and the compaction and spreading equipment wheels/tracks, the backfill placement and compaction technique will have a lesser effect on  $RF_{ID}$ . Regarding geosynthetic characteristics, the geosynthetic weight/thickness or tensile strength may have a significant effect on  $RF_{ID}$ . However, for coated polyester geogrids, the coating thickness may overwhelm the effect of the product unit weight or thickness on  $RF_{ID}$ . *Even with product specific testing results a minimum  $RF_{ID}$  1.1 shall be used to account for testing uncertainties.*

#### D.5.1.5.2 Creep Reduction Factor, $RF_{CR}$

The creep reduction factor is required to limit the load in the reinforcement to a level known as the creep limit that will preclude excessive elongation and creep rupture over the life of the structure. The creep limit strength is thus analogous to yield strength in steel. Creep is essentially a long-term deformation process. As load is applied, molecular chains move relative to each other through straightening out of folded or curved/kinked chains or through breaking of inter-molecular bonds, resulting in no strength loss, but increased elongation.

Eventually, if the load levels are sufficiently high (i.e., constant load near the creep limit), the molecular chains can straighten/elongate no more without breaking the molecular chains. Significant strength loss occurs only when the straightening/slipping process is exhausted. If the load is high enough, molecular chains break, and both elongation and strength loss occur at an accelerating rate, eventually resulting in rupture. Generally this strength loss occurs only near the end of the design life of the geosynthetic under a given load level.

The creep reduction factor is obtained from long-term laboratory creep testing as detailed in Appendix D of *Berg, et al. – Vol. II (2009)*. Creep testing is essentially a constant load test on multiple product samples, loaded to various percentages of the ultimate product load, for periods of up to 10,000 hours. For creep testing 1 of 2 approaches may be used: 1) “conventional” creep testing per ASTM D5262 – *Standard Test Method for Evaluating the Unconfined Tension Creep and Creep Rupture Behavior for Geosynthetics*, or 2) a combination of Stepped Isothermal Method (SIM) per ASTM D6992 – *Standard Test Method for Accelerated Tensile Creep and Creep-Rupture of Geosynthetic Materials Based on Time-Temperature Superposition Using the Stepped Isothermal Method*, which is an accelerated method using stepped increases in temperatures to allow tests to be performed in a matter of days, and “conventional” creep testing. The creep reduction factor is the ratio of the ultimate load to the extrapolated maximum sustainable load (i.e., creep rupture limit) within the design life of the

structure (e.g., several years for temporary structures (*less than 5 years*), 75 to 100 years for permanent structures).

Typical ranges of  $RF_{CR}$  as a function of polymer type are *indicated in Table D-2*.

**Table D-2, Creep Reduction Factors  
(Berg, et al. – Vol. I (2009))**

Polymer Type	$RF_{CR}$
Polyester (PET)	1.6 to 2.5
Polypropylene (PP)	4.0 to 5.0
High Density Polyethylene (HDPE)	2.6 to 5.0

If no product specific creep reduction factors are provided, then the maximum creep reduction factor for a specific polymer shall be used. If the polymer is unknown, then an  $RF_{CR}$  of 5.0 shall be used.

#### **D.5.1.5.3 Durability Reduction Factor, $RF_D$**

According to Berg, et al. – Vol. I (2009):

This reduction factor is dependent on the susceptibility of the geosynthetic to be attacked by chemicals, thermal oxidation, hydrolysis, environment stress cracking, and microorganisms, and can vary typically from 1.1 to 2.0. *Even with product specific tests results, the minimum reduction factor shall be 1.1. Protocols for testing to obtain this reduction factor has been described in Elias, et al. (1999) and Elias, et al. (2009).*

Due to the long-term nature of these durability evaluation protocols (2 to 3 years could be required to complete such tests), it is generally not practical to conduct such tests for typical geosynthetic reinforcement design, but are generally more suited for research activities. However, short-term index type tests can be conducted as indicators of good long-term durability performance, based on correlation to the long-term research results obtained and reported by Elias, et al. (1999). Such index test results, combined with a criteria applied to the test results that can be considered to indicate good long-term performance, can be used to justify a default value for  $RF_D$  that can be used for the determination of  $T_{al}$ .

Table D-3 provides the minimum testing requirements for the use of the default  $RF_D$  for geosynthetic reinforcement.



**Table D-3, Minimum Testing Requirements for use  $RF_D$   
(modified Berg, et al. – Vol. I (2009))**

Geosynthetic Type	Property	Test Method	Criteria to allow use of Default $RF_D$
Polypropylene (PP) and Polyethylene (HDPE)	UV Oxidation Resistance	ASTM D4355	Min. 70% strength retained after 500 hrs. in weatherometer
Polyester (PET) <sup>1</sup>	Hydrolysis Resistance	Inherent Viscosity Method (ASTM D4603 and GRI Test Method GG8) or Determine Directly Using GEL Permeation Chromatography	Minimum Number ( $M_n$ ) Average Molecular Weight of 25,000
		ASTM D7409	Maximum Carboxyl End Group (CEG) Content of 30
All Polymers	Survivability	Weight per Unit Area, ASTM D5261	Min. 8 oz/yd <sup>2</sup>
All Polymers	Percent Post-consumer Recycled Material by Weight	Certification of Material Used	Maximum 0%

<sup>1</sup>Alternatively, a default  $RF_D = 1.3$  may be used if product specific installation damage testing is performed and it is determined that  $RF_{ID} = 1.7$  or less, and if the other requirements of this table are met.

ASTM D4355 – *Standard Test Method for Deterioration of Geotextiles by Exposure to Light, Moisture and Heat in a Xenon Arc Type Apparatus*  
 ASTM D4603 – *Standard Test Method for Determining Inherent Viscosity of Poly(Ethylene Terephthalate) (PET) by Glass Capillary Viscometer*  
 GRI GG8 – *Determination of the Number Average Molecular Weight of PET Yarns Based on Relative Viscosity Value*  
 ASTM D7409 – *Standard Test Method for Carboxyl End Group Content of Polyethylene Terephthalate (PET) Yarns*  
 ASTM D5261 – *Standard Test Method for Measuring Mass per Unit Area of Geotextiles*

## D.6 UNREINFORCED STABILITY

The overall (global) stability of the unreinforced slope is checked first to determine if reinforcement is required, if the potential for deep-seated failure surfaces is possible, and to determine the approximate limit of reinforcement. If the resistance factor is less than required in Chapter 9, then, the unreinforced slope is stable and no reinforcement is required. It is noted that the resistance factor ( $\phi$ ) is the inverse of the Factor of Safety (i.e.,  $\phi = 1/FS$ ). If  $\phi$  is greater than indicated in Chapter 9, then the slope is considered unstable and reinforcement of the slope is required. According to Berg, et al. – Vol. II (2009):

Determine the size of the critical zone to be reinforced.

- Examine the full range of potential failure surfaces found to have:  
Unreinforced safety factor,  $FS_u (\phi_u) \leq$  Required safety factor,  $FS_r (\phi_r)$
- Plot all of these surfaces on the cross-section of the slope.
- The surfaces that just meet the required resistance factor ( $\phi$ ) roughly envelope the limits of the critical zone to be reinforced as shown in *Figure D-6*.

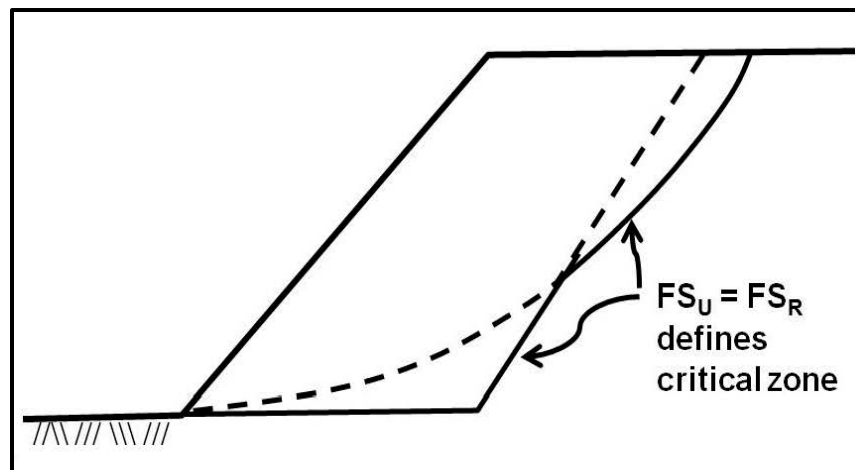


**Figure D-6, Critical Zone**  
(Berg, et al. – Vol. II (2009))

Further, this stability check also identifies potential deep-seated failures. Deep-seated failure surfaces extend into the foundation soil and may be used to determine the first estimate of the length of reinforcement required to stabilize the slope. Depending on the length of reinforcement required some form of ground improvement (see Chapters 19 and 20) may be necessary.

This stability can be determined using classical slope stability analyses. The failure surfaces may be circular or non-circular (sliding block) and both should be checked. Overall stability analyses are performed for the Service limit state roadway embankments only. RSSs located within bridge embankments require both Service and EE I limit state checks. It should be noted that it is assumed that all RSSs are free draining and that pore water pressures are not allowed to build up behind the face of the slope. In addition to checking deep seated failure potential, the potential for lateral squeeze at the toe should also be checked (see Chapter 17). If the potential for lateral squeeze is indicated, ground improvement at the toe may be required. Ground improvement may consist of the following options; please note that this is not an all-inclusive list, but is meant as an example of ground improvement options,

- Undercut and replace soft soils
- Toe berm construction
- Vertically stage construction the embankment to allow for strength gain with time
- Construction of a shear key beneath the toe of the embankment
- Use vertical reinforcing elements (i.e., stone columns, driven piling, deep mixing method columns, etc.)
- Improve subsurface drainage (i.e., use wick drains)

After the development of the final design, a compound global stability analysis shall be performed. As defined in Chapter 18, a compound stability analysis examines failure surfaces that pass through either the retained fill and reinforced soil mass to exit through the RSS face, or that pass through the retained fill, reinforced soil mass, and the foundation soil to exit either at or beyond the toe of the RSS. The actual strength parameters for the reinforced soil mass shall be used in the analysis. These analyses can only be performed once a specific reinforcement strength and type is selected.

## D.7 REINFORCEMENT DESIGN

The reinforcement used in RSS may consist of either extensible (geosynthetics) or inextensible (metallic) reinforcement. While the use of inextensible (metallic) reinforcement is permitted, it is noted that the current STS for RSS is written based on the use of extensible (geogrid) reinforcement being used. The GEOR is required to write a Special Provision to SC-M-206-1 to allow the use of geotextiles in addition to geogrids, if the GEOR wants to allow the use of geotextiles as well as geogrids. If inextensible reinforcement is to be used, the GEOR shall write a Special Provision indicating the soil and inextensible properties required. It is noted that the GEOR may review and use the latest version of STS SC-M-714 for *Mechanically Stabilized Earth (MSE) Walls* for information regarding soils and inextensible material properties. Inextensible reinforcement may only be used with wire baskets and must be connected to the baskets. In this step, the reinforcement is designed to provide a stable slope that meets the requirements of the project. According to Berg, et al. – Vol. II (2009):

Calculate the total reinforcement tension per unit width of slope  $T_S$  required to obtain the required *resistance factor*  $1/\phi_r$  for each potential failure surface inside the critical zone in *the previous step* that extends through or below the toe of the slope using the following equation:

$$T_S = \left( \frac{1}{\phi_r} - \frac{1}{\phi_u} \right) * \left( \frac{M_D}{D} \right) \quad \text{Equation D-7}$$

Where,

$T_S$  = The sum of the required tensile force per unit width of reinforcement (considering rupture and pullout) in all reinforcement layers intersecting the failure surface

$M_D$  = Driving moment about the center of the failure surface

$D$  = The moment arm of  $T_S$  about the center of the failure circle, where,

= Radius of circle  $R$  for continuous, sheet type extensible reinforcement (i.e., assumed to act tangentially to the circle) (*see Figure D-7*)

= Radius of circle  $R$  for continuous, sheet type inextensible reinforcement (e.g., wire mesh reinforcement) to account for normal stress increase on adjacent soil (*see Figure D-7*)

= Vertical distance,  $Y$ , to the centroid of  $T_S$  for discrete element, strip type reinforcement. Assume  $H/3$  above slope base for preliminary calculations (i.e., assumed to act in a horizontal plane intersecting the failure surface at  $H/3$  above the slope base) (*see Figure D-7*)

$1/\phi_r$  = Target minimum slope *resistance factor* which is applied to both the soil and reinforcement

$1/\phi_u$  = Unreinforced slope *resistance factor*

$T_{S-MAX}$  = The largest  $T_S$  calculated establishes the total design tension

Note: The maximum unreinforced resistance factor usually does not control the location of  $T_{S-MAX}$ ; the most critical surface is the surface requiring the greatest amount of reinforcement strength.

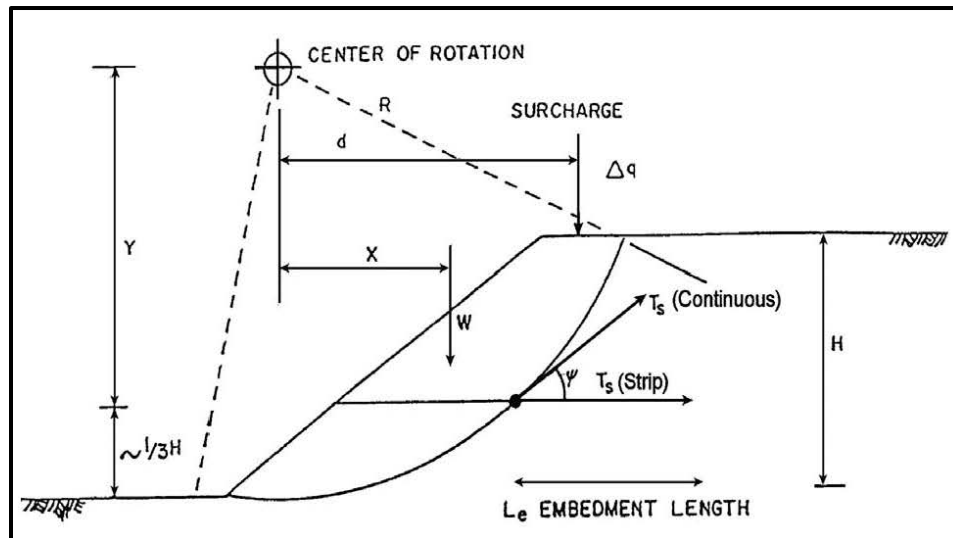


**Figure D-7, Geometry of Rotational Shear Failure Surface (Berg, et al. – Vol. II (2009))**

Determine the total design tension per unit width of slope ( $T_{S-MAX}$ ) using Figures D-8 and D-9 and compare  $T_{S-MAX}$  from the chart to  $T_{S-MAX}$  calculated from Equation D-7. If significantly different, check the validity of the charts based on the limiting assumptions listed in the figure and recheck the calculations in the previous step (Unreinforced Stability) and Equation D-7.

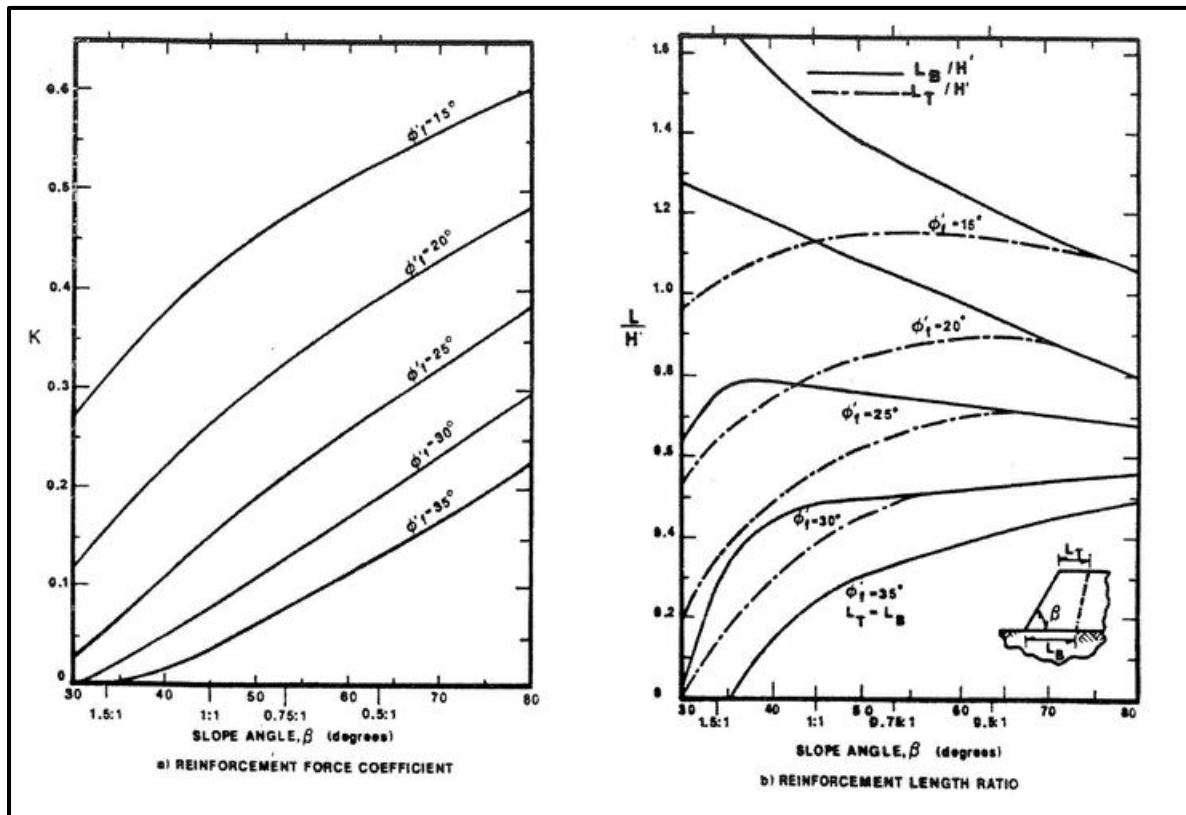


**Figure D-8, Reinforcement Strength Requirements Chart Solution - A (Berg, et al. – Vol. II (2009))**

CHART PROCEDURE:

- 1) Determine force coefficient K from figure above, where  $\phi_r$  = friction angle of reinforced fill:
 
$$\phi_f = \tan^{-1} \left( \frac{\tan \phi_r}{FS_R} \right)$$
- 2) Determine:
 
$$T_{S-MAX} = 0.5 K \gamma_r (H')^2$$

where:  $H' = H + q/\gamma_r$   
 $q = \text{a uniform load}$
- 3) Determine the required reinforcement length at the top  $L_T$  and bottom  $L_B$  of the slope from the figure above.

LIMITING ASSUMPTIONS

- Extensible reinforcement.
- Slopes constructed with uniform, cohesionless soil,  $c = 0$ .
- No pore pressures within slope.
- Competent, level foundation soils.
- No seismic forces.
- Uniform surcharge not greater than  $0.2 \gamma_r H$ .
- Relatively high soil/reinforcement interface friction angle,  $\phi_{sg} = 0.9 \phi_r$  (may not be appropriate for some geotextiles).

Note:  $FS_R = 1/\phi_R$ , where  $\phi_R$  is the resistance factor (see Chapter 9)

**Figure D-9, Reinforcement Strength Requirements Chart Solution - B  
(Berg, et al. – Vol. II (2009))**

According to Berg, et al. – Vol. II (2009):

*Figures D-8 and D-9* is provided for a quick check of computer-generated results. The figure presents a simplified method based on a 2-part wedge type failure surface and is limited by the assumptions noted on the figure.

Note that *Figures D-8 and D-9* is not intended to be a single design tool. Other design charts that are available from the literature could also be used (e.g., Ruegger, 1986; Leshchinsky and Boedeker, 1989; and Jewell, 1990). Several computer programs are also available (see *Section D.10*) for analyzing a slope with a given reinforcement and can be used as a check. Judgment in selection of other appropriate design methods (i.e., most conservative or experience) is required.

After determining the maximum required tensile strength of the reinforcement, the determination of the distribution of the reinforcement comes next. According to Berg, et al. – Vol. II (2009):

For low slopes ( $H \leq 20$  feet) assume a uniform reinforcement distribution and use  $T_{S-MAX}$  to determine the spacing or the required tension,  $T_{MAX}$ , requirements for each reinforcement layer.

For high slope ( $H > 20$  feet), either a uniform reinforcement distribution may be used (preferable) or the slope may be divided *into* 2 (top and bottom) or 3 (top, middle and bottom) reinforcement zones of equal height, and use a factored  $T_{S-MAX}$  in each zone for spacing or design tension requirements (see *Figure D-9*). The total required tension in each zone is found from:

For 1 zone:

Use  $T_{S-MAX}$

For 2 zones:

$$T_{Bottom} = \frac{3}{4} * (T_{S-MAX}) \quad \text{Equation D-8}$$

$$T_{Top} = \frac{1}{4} * (T_{S-MAX}) \quad \text{Equation D-9}$$

For 3 zones:

$$T_{Bottom} = \frac{1}{2} * (T_{S-MAX}) \quad \text{Equation D-10}$$

$$T_{Middle} = \frac{1}{3} * (T_{S-MAX}) \quad \text{Equation D-11}$$

$$T_{Top} = \frac{1}{6} * (T_{S-MAX}) \quad \text{Equation D-12}$$

The force is assumed to be uniformly distributed over the entire zone.

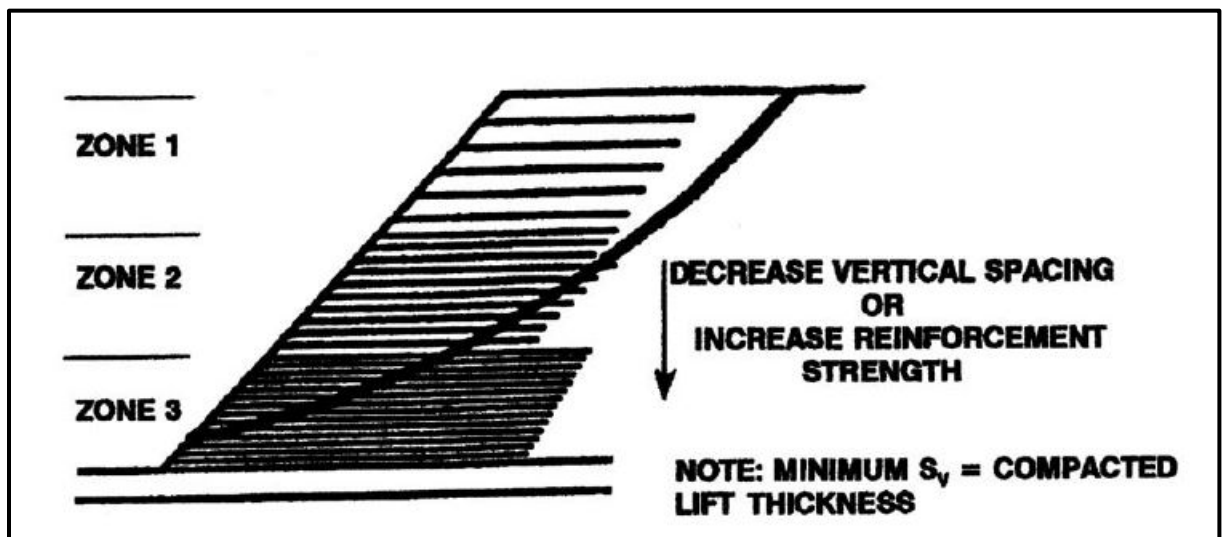


Figure D-10, Reinforcing Zone Vertical Layout  
(Berg, et al. – Vol. II (2009))

Determine reinforcement vertical spacing ( $S_v$ ) or the maximum design tension ( $T_{MAX}$ ) requirements for each reinforcing layer.

For each zone, calculate  $T_{MAX}$  for each reinforcing layer in that zone based on an assumed  $S_v$ , or, if the allowable reinforcement strength is known, calculate the

minimum vertical spacing and number of reinforcing layers  $N$  required for each zone based on:

$$T_{MAX} = \frac{T_{zone} * S_V}{H_{zone}} = \frac{T_{zone}}{N} \leq T_{al} * R_c \quad \text{Equation D-13}$$

Where,

$R_c$  = Coverage ratio of the reinforcement which equals the width of the reinforcement  $b$  divided by the horizontal spacing  $S_h$

$S_V$  = Vertical Spacing of reinforcement; multiples of compacted layer thickness of ease of construction (see Figure D-10)

$T_{zone}$  = Maximum reinforcement tension required for each zone;  $T_{S-MAX}$  for low slopes ( $H \leq 20$  feet)

$T_{al} = T_{ult}/RF$  (see Equation D-6)

$H_{zone}$  = Height of zone;  $T_{Top}$ ,  $T_{Middle}$ , and  $T_{Bottom}$  for high slopes ( $H > 20$  feet)

$N$  = Number of reinforcement layers

Use short 4 to 6.5 feet lengths of intermediate reinforcement layers to maintain a maximum vertical spacing of 16 inches or less for face stability and compaction quality. For slopes flatter than 1H:1V ( $45^\circ$ ), closer spaced reinforcements (i.e., every lift or every other lift, but no greater than 16 inches) preclude having to wrap the face in well graded soils (e.g., sandy gravel and silty and clayey sands). Wrapped faces are required for steeper slopes and uniformly graded soils to prevent face sloughing. Alternative vertical spacing could be used to prevent face sloughing, but in these cases a face stability analysis should be performed either using the method presented in this chapter or by evaluating the face as an infinite slope using:

Equation D-14

$$\phi = \frac{\gamma_g H z \cos \beta \sin \beta}{c' H + (\gamma_g - \gamma_w) H z \cos^2 \beta \tan \phi' + F_g (\cos \beta \sin \beta + \sin^2 \beta \tan \phi')}$$

Where,

$c'$  = Effective cohesion

$\phi'$  = Effective friction angle

$\gamma_g$  = Saturated unit weight

$\gamma_w$  = Unit weight of water

$z$  = Vertical depth to failure plane defined by the depth to saturation

$H$  = Vertical slope height

$\beta$  = Slope angle

$F_g$  = Summation of geosynthetic resisting force

Intermediate reinforcement should be placed in continuous layers and does not need to be as strong as the primary reinforcement, but it must be strong enough to survive construction (e.g., minimum survivability requirements for geotextiles in road stabilization applications in AASHTO M288) and provide localized tensile reinforcement to the surficial soils.

If the interface friction angle of the intermediate reinforcements,  $\rho_{sr}$ , is less than that of the primary reinforcement  $\rho_r$ , then  $\rho_{sr}$  should be used in the analysis for the portion of the failure surface intersecting the reinforced soil zone.

To ensure that the rule-of-thumb reinforcement distribution is adequate for critical or complex structures, recalculate  $T_S$  using *Equation D-7* to determine potential failure above each layer of primary reinforcement.

Check that the sum of the reinforcement forces passing through each failure surface is greater than  $T_S$  required for that surface. Only count reinforcement that extends *more than 3 feet* beyond the surface to account for pullout resistance. If the available reinforcement force is not sufficient, increase the length of reinforcement not passing through the surface or increase the strength of lower-level reinforcement. Simplify the layout by lengthening some reinforcement layers to create 2 or 3 sections of equal reinforcement length for ease of construction and inspection. Reinforcement layers do not generally need to extend to the limits of the critical zone, except for the lowest levels of each reinforcement section. Check the length using *Figure D-8(b)*. Note:  $L_e$  is already included in the total length,  $L_T$  and  $L_B$  from *Figure D-8(b)*.

When checking a design that has zones of different reinforcement lengths, lower zones may be over reinforced to provide reduced lengths of upper reinforcement levels. In evaluating the length of requirements for such cases, the pullout stability for the reinforcement must be carefully checked in each zone for the critical surfaces exiting at the base of each length zone.

### D.7.1 Estimating $L_e$

According to Berg, et al. – Vol. II (2009):

The embedment length  $L_e$  of each reinforcement layer beyond the critical sliding surface (i.e., circle found for  $T_{S-MAX}$ ) must be sufficient to provide adequate pullout resistance based on:

$$L_e = \frac{T_{S-MAX}}{\varphi * (F^*) * \alpha * \sigma'_v * R_c * C} \quad \text{Equation D-15}$$

Where,

$T_{S-MAX}$  = Maximum factored tensile load in the reinforcement (calculated in *Equation D-7*)

$\varphi$  = Resistance factor for reinforcement pullout (see *Chapter 9*)

$\alpha$  = Scale effect correction factor (discussed in D.7.2)

$F^*$  = Pullout friction factor (discussed in D.7.3)

$\sigma'_v$  = Unfactored effective vertical stress at the reinforcement level in the resistance zone

$C$  = Overall reinforcement surface area geometry factor (2 for strip, grid and sheet-type reinforcement)

$R_c$  = Reinforcement coverage ratio

*For continuous geosynthetic reinforcement  $R_c = 1$*

$$R_c = \frac{b}{S_h} \quad \text{Equation D-16}$$

Where,

$b$  = Gross width of the reinforcing element



$S_h$  = Center-to-center horizontal spacing between reinforcements (see Figure D-10)

“Minimum value of  $L_e$  is 3 feet. For cohesive soils, check  $L_e$  for both short- and long-term pullout conditions, when using the semi-empirical equations to obtain  $F^*$ . For long-term design use  $\phi'$  of the reinforced fill with  $c' = 0$ . For short-term evaluation, conservatively use  $\phi$  of the reinforced fill with  $c = 0$  from consolidated undrained triaxial or direct shear tests or *perform* pullout tests.

When checking a design that has zones of different reinforcement length, lower zones may be over reinforced to provide reduced lengths of upper reinforcement levels. In evaluating the length requirements for such cases, the pullout stability for the reinforcement must be carefully checked in each zone for the critical surfaces existing at the base of each length zone.

### D.7.2 Correction Factor ( $\alpha$ )

According to Berg, et al. – Vol. I (2009):

The correction factor ( $\alpha$ ) depends primarily upon the strain softening of the compacted granular backfill material, the extensibility, and the length of the reinforcement. For inextensible (*metallic*) reinforcement,  $\alpha$  is approximately 1, but it can be substantially smaller than 1 for extensible (*geosynthetic*) reinforcements. The  $\alpha$  factor can be obtained from pullout tests on reinforcements with different lengths or derived using analytical or numerical load transfer models, which have been “calibrated” through numerical test simulations. In the absence of test data, *the values included in Table D-4 should be used for geogrids and geotextiles.*

**Table D-4, Typical Values of  $\alpha$   
(According to Berg, et al. – Vol. I (2009))**

Reinforcement Type	$\alpha$
All metallic reinforcements	1.0
Geogrids	0.8
Geotextiles	0.6

### D.7.3 Pullout Friction Factor ( $F^*$ )

According to Berg, et al. – Vol. I (2009):

The pullout friction factor can be obtained most accurately from laboratory or field pullout tests performed with the specific material to be used on the project (*i.e., select backfill and reinforcement*). Alternatively,  $F^*$  can be derived from empirical or theoretical relationships developed for each soil-reinforcement interaction mechanism and provided by the reinforcement supplier. For any reinforcement,  $F^*$  can be estimated using the general equation:

$$F^* = F_q * \alpha_\beta + \tan \rho \quad \text{Equation D-17}$$

Where,

$F_q$  = The embedment (or surcharge) bearing capacity factor

- $\alpha_\beta$  = A bearing factor for passive resistance which is based on the thickness per unit width of the bearing member  
 $\rho$  = The soil-reinforcement interaction friction angle

In absence of site-specific pullout testing data, it is reasonable to use these semi-empirical relationships in conjunction with the standard specifications for backfill to provide a conservative evaluation of pullout resistance.

For steel ribbed reinforcement,  $F^*$  is commonly estimated as:

$$F^* = \tan \rho = 1.2 + \log C_u \quad \text{Equation D-18}$$

It is noted that at the top of the RSS,  $F^*$  is at a maximum of 2.0.

For reinforcement located at a depth of 20 feet or more below the top of the RSS  $F^*$  may be estimated using:

$$F^* = \tan \phi_r \quad \text{Equation D-19}$$

Where,

$\rho$  = Interface friction angle mobilized along the reinforcement

$\phi_r$  = Reinforced backfill peak friction angle

$C_u$  = Uniformity coefficient of the backfill (see Chapter 6)

If the specific  $C_u$  for the wall backfill is unknown during design, a  $C_u$  of 4 should be assumed (i.e.,  $F^* = 1.8$  at the top of the wall), for backfill meeting the requirements *previously provided*.

For steel grid reinforcements with transverse spacing ( $S_t$ )  $\geq 6$  inches,  $F^*$  is a function of a bearing or embedment factor ( $F_q$ ), applied over the contributing bearing factor ( $\alpha_\beta$ ), as follows at the top of the structure:

$$F^* = F_q * \alpha_\beta = 40 * \alpha_\beta = 40 * \left(\frac{t}{2S_t}\right) = 20 * \left(\frac{t}{S_t}\right) \quad \text{Equation D-20}$$

While, for reinforcement located at a depth of 20 feet or more below the top of the RSS  $F^*$  may be estimated using:

$$F^* = F_q * \alpha_\beta = 20 * \alpha_\beta = 20 * \left(\frac{t}{2S_t}\right) = 10 * \left(\frac{t}{S_t}\right) \quad \text{Equation D-21}$$

Where,

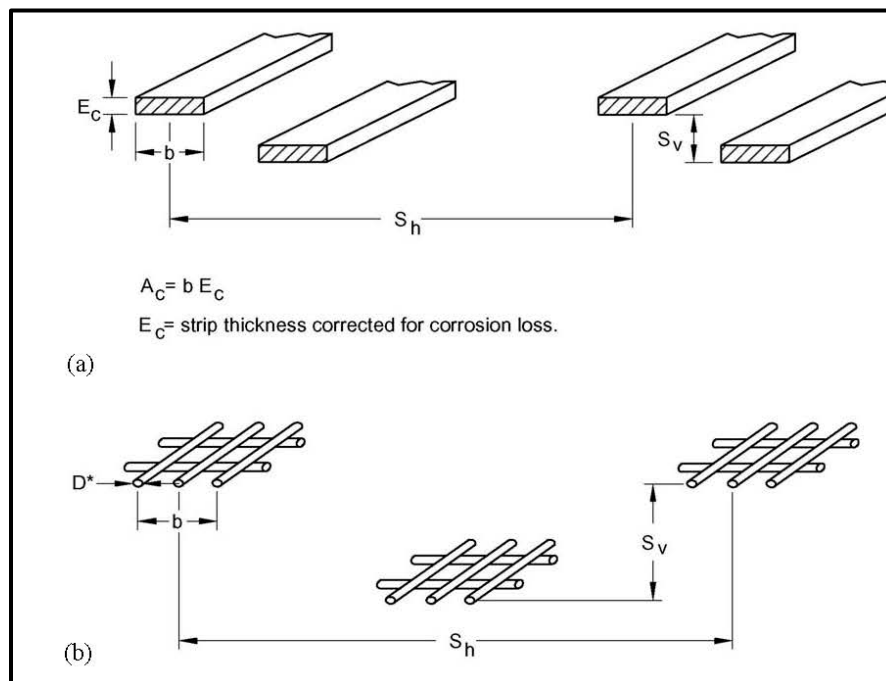
$t$  = The thickness of the transverse bar

$S_t$  = *The distance between individual bars in steel grid reinforcement and shall be uniform throughout the length of the reinforcement, rather than having transverse grid members concentrated only in the resistance zone*

For geosynthetic (i.e., geogrid and geotextile) sheet reinforcement, the pullout resistance is based on a reduction in the available soil friction. In the absence of test data, the  $F^*$  value for geosynthetic reinforcement should conservatively be estimated as:

$$F^* = 0.67 * \tan \phi_r$$

Equation D-22



<sup>1</sup>For geosynthetic strips use (a)

<sup>2</sup>Please note that geosynthetic strips have no measureable thickness.

**Figure D-11, Definitions of  $b$ ,  $S_h$  and  $S_v$   
 (Berg, et al. – Vol. I (2009))**

#### D.7.4 Selection of Reinforcement

The type of reinforcement to be used in the RSS shall be determined. The 2 types of reinforcement are extensible and inextensible. Extensible reinforcements consist of geosynthetic materials, typically geogrids (biaxial or uniaxial) and geotextiles. These reinforcements are a wrapped face consisting of a layer of geogrid that wraps around the face and a layer of geotextile to prevent erosion of the reinforced soil materials. Inextensible reinforcements consist of bars or bar mats (metallic grids) and shall meet the requirements in STS SC-M-713 (latest version) for *Mechanically Stabilized Earth (MSE) Walls* for the inextensible material properties. These reinforcements are typically connected to wire baskets at the front face to provide anchorage at the face of the slope. The selection of the type of reinforcement is influenced by the strength required to maintain stability and the aesthetic appearance required at the completion of the project.

When extensible reinforcements are used, the continuity of the reinforcement shall be assured. For geogrid used as the extensible reinforcement, the geogrid shall be placed so that the strong axis is perpendicular to the face of the RSS. The geogrid reinforcement materials to be used to construct an RSS shall meet the criteria provided in STS SC-M-203-2 (latest version) for *Geogrid Soil Reinforcement*. Indicate on the plans the required  $T_{ai}$  for the geogrid soil reinforcement. Overlapping of geogrids in the strong axis direction is not permitted. The use of a mechanical connection (i.e., a bodkin connector) will be permitted, provided the strength of the connection is equal to the required geogrid strength or if reduced geogrid strength equal to the connection is used. Prior to using a mechanical connection obtain written permission from the PC/GDS. Geogrids may be overlapped in the transverse (i.e., parallel to the RSS face). The minimum overlap in RSS shall be 12 inches. If a mechanical connection is allowed in the strong axis direction, the GEOR is reminded that the location, type and material for the connection,

should be shown on the plans. In addition, the plans should also include a requirement for the Contractor to provide the results of testing of the mechanical connection.

When geotextiles are used as the extensible reinforcement, the geotextile shall be placed so that the strong axis is perpendicular to the face of the RSS. The geotextile reinforcement materials to be used to construct an RSS shall meet the criteria provided in STS SC-M-203-3 (latest version) for *Geotextile Soil Reinforcement*. Indicate on the plans the required  $T_{ai}$  for the geotextile soil reinforcement. Overlapping of the geotextiles in the strong axis direction is not permitted. The use of sew seams may be permitted in the strong axis direction; however, the strength of the geotextile will be reduced to the strength of the sewn seam. The sewn seam strength (whether field or factory sewn) shall be at least 25 percent of  $T_{ult}$  (ASTM D4884 – *Standard Test Method for Strength of Sewn or Bonded Seams of Geotextiles*) in machine direction. Prior to using a sewn seams obtain written permission from the PC/GDS. For sewn seams use thread that consists of either polypropylene or polyester polymers and which has a strength matching the strength of the geotextile being seamed. Do not use nylon thread. Use thread that is of contrasting color to that of the geotextile itself. Use a double row of double-thread chain stitch, Type 401 (see ASTM D6193 – *Standard Practice for Stitches and Seams*). Use 150 to 400 stitches per yard depending on the weight of the geotextile. The GEOR should consult with a geotextile manufacturer or supplier to determine the appropriate stitch density. Use either a “butterfly” seam (Type SSd) or “J” seam (Type SSn) (see ASTM D6193). Geotextiles may be overlapped in the transverse direction. The minimum overlap shall be 12 inches. If a sewn seam in the cross machine (i.e., transverse) direction is to be used as opposed to overlapping, the sewn seam strength (whether field or factory sewn) shall be at least 25 percent of  $T_{ult}$  (ASTM D4884) in the cross machine direction. If sewn seams are allowed, the GEOR is reminded that the ultimate strength of the seam in the machine and cross machine directions, the location of the sewn seam, the type of thread, the color contrast of the thread, the type and density of stitching, and the seam type shall be shown on the plans. In addition, the plans should also include a requirement for the Contractor to provide the results of sewn seam testing.

## D.8 EXTERNAL STABILITY

### D.8.1 Sliding Resistance

According to Berg, et al. – Vol. II (2009):

Evaluate the width of the reinforced soil mass at any level to resist sliding along the reinforcement. Use a 2-part wedge type failure surface defined by the limits of the reinforcement (the length of reinforcement at the depth of evaluation defined *previously*). The analysis can best be performed using a computerized method which takes into account all soil strata and interface friction values. If the computer program does not account for the presence of reinforcement, the back of the wedge should be angled at  $45^\circ + \phi/2$  (see *Figure D-11*) or parallel to the back of the reinforced zone, whichever is flatter (i.e., the wedge should not pass through layers of reinforcement to avoid an overly conservative design). The frictional resistance provided by the weakest layer, either the reinforced soil, the foundation soil or the soil-reinforcement interface, should be used in the analysis.

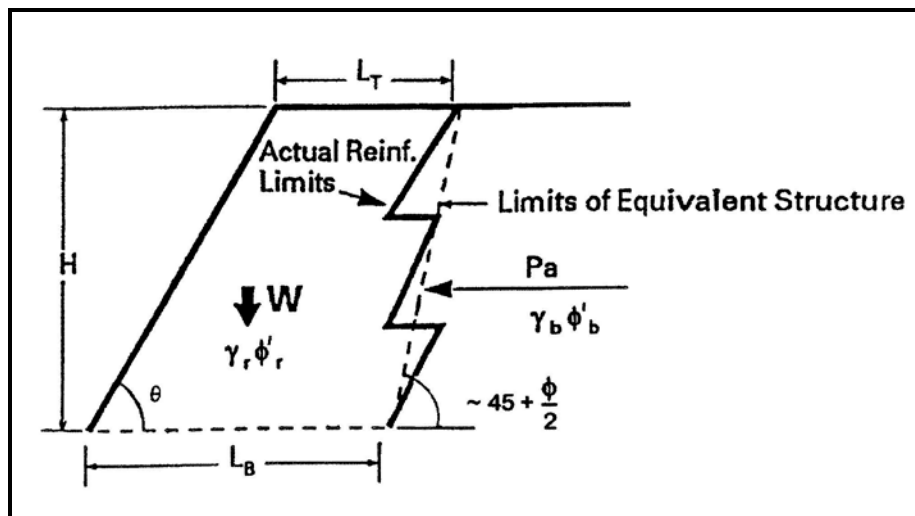


**Figure D-12, Sliding Stability Analysis  
(Elias, Christopher and Berg (2001))**

A simple analysis using a sliding block method can be performed as a check. The method also assumes that the reinforcement layers are truncated along a plane parallel to the slope face, which may or may not be the case. The analysis is based on a 2-part wedge model to predict  $L_B$  assuming that the reinforcement interface is the weakest plane. The frictional resistance provided by the weakest layer in contact with either, the geosynthetics and reinforced soil (*i.e.*, the interface friction) or between the reinforced soil and the foundation soil.

The frictional resistance between the reinforced soil and the foundation soil will depend on whether the foundation soil is Sand-Like or Clay-Like. Regardless of which soil comprises the foundation soil the following equation is required to be balanced:

$$\text{Horizontal Driving Forces} \leq \varphi * \text{Horizontal Resisting Forces} \quad \text{Equation D-23}$$

For Sand-Like soils use the following equations:

$$P_a * \cos \phi_b \leq \varphi * (W + P_a * \sin \phi_b) * \tan \phi_{min} \quad \text{Equation D-24}$$

For  $L < H$

$$W = \frac{1}{2} L^2 * \gamma_r * \tan \theta \quad \text{Equation D-25}$$

Or for  $L > H$

$$W = \left[ L * H - \frac{H^2}{(2 \tan \theta)} \right] * \gamma_r \quad \text{Equation D-26}$$

$$P_a = \frac{1}{2} \gamma_b * H^2 * K_a \quad \text{Equation D-27}$$

Where,

$L$  = Length of bottom reinforcing layer in each level where there is a reinforcement length change

$H$  = Height of Slope

$\varphi$  = Resistance Factor (see Chapter 9)

- $\phi_{\min}$  = Minimum angle of shearing friction either between reinforced soil and reinforcement or the friction angle of the foundation soil  
 $\theta$  = Slope angle  
 $\gamma_r$  &  $\gamma_b$  = Unit weight of the reinforced backfill and retained backfill, respectively  
 $\phi_b$  = Friction angle of retained fill (Note: If drains/filters are placed on the backslope, then  $\phi_b$  equals the interface friction angle between the geosynthetic and retained fill)

For Clay-Like soils use the following equation:

$$P_a \leq \varphi * c * L_B \quad \text{Equation D-28}$$

Where,

- $\varphi$  = Resistance Factor (see Chapter 9)  
 $c$  = Cohesion  
 $L_B$  = Length of base of RSS  
 $P_a$  = Active earth pressure (see Equation D-27)

### D.8.2 Global (Deep-Seated) Stability

This sub-step is to evaluate the potential for deep-seated failure surfaces beyond or below the reinforced soil mass to provide resistance factors that meet the requirements of Chapter 9. This check is similar to and may use the results of the Unreinforced Stability analysis discussed previously.

### D.8.3 Local Bearing Failure at Toe

According to Berg, et al. – Vol. II (2009):

If a weak layer exists beneath the embankment to limited depth  $D_s$ , which is less than the width of the slope  $b'$  (see *Figure D-12*), the *resistance factor against failure by squeezing may be calculated using the procedures contained in Chapter 17.*

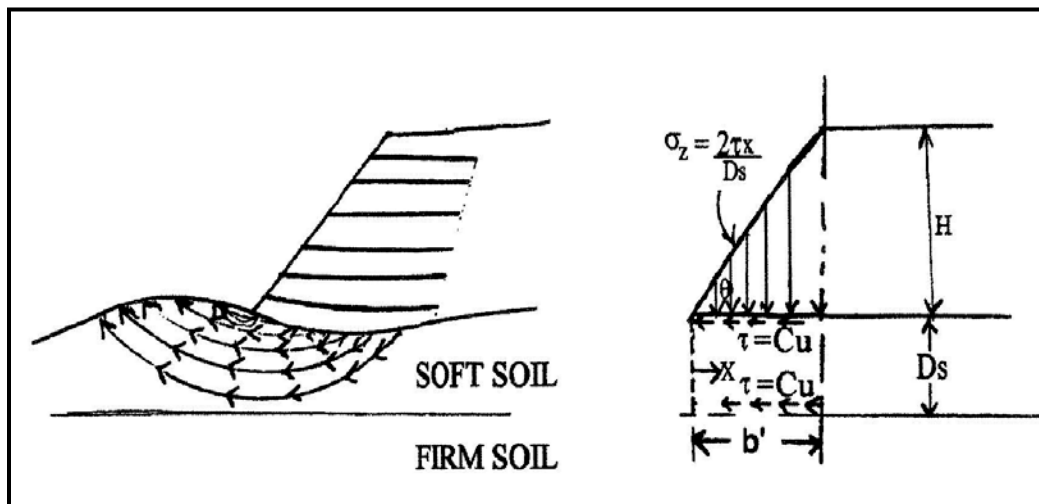


Figure D-13, Local Bearing Failure (Lateral Squeeze)  
 (Berg, et al. – Vol. II (2009))

Caution is advised and rigorous analysis (i.e., numerical modeling) should be performed when the *resistance factor* ( $\phi$ ) is greater than 0.5. This approach is somewhat conservative as it does not provide any influence from the reinforcement. When the depth of the soft layer,  $D_s$ , is greater than the base width of the slope,  $b'$ , general slope stability will govern design.

#### D.8.4 Foundation Settlement

The settlement (total, differential and time for settlement to occur) of the RSS shall be determined using the procedures provided in Chapter 17.

#### D.8.5 Seismic Stability

RSSs located within bridge embankments shall be designed seismically according to the procedures contained in Chapter 13. In addition, the RSS shall meet the requirements of Chapters 9 and 10 for resistance factors and displacements, respectively.

### D.9 DRAINAGE SYSTEM DESIGN

The following Section of this Appendix is adopted directly from Berg, et al. – Vol. II (2009) and is used with the permission of the US Department of Transportation, Federal Highway Administration. Italics have been added to reflect additions or modifications to the selected text and to supply references to this Manual.

#### D.9.1 Subsurface Water Control

According to Berg, et al. – Vol. II (2009):

Design of subsurface water drainage features should address flow rate, filtration, placement, and other details. Drains are typically placed at the rear of the reinforced soil mass in Figure D-13. Geocomposite drainage systems or conventional granular blanket and trench drains could be used. *Granular drainage systems are not addressed in this Appendix.*

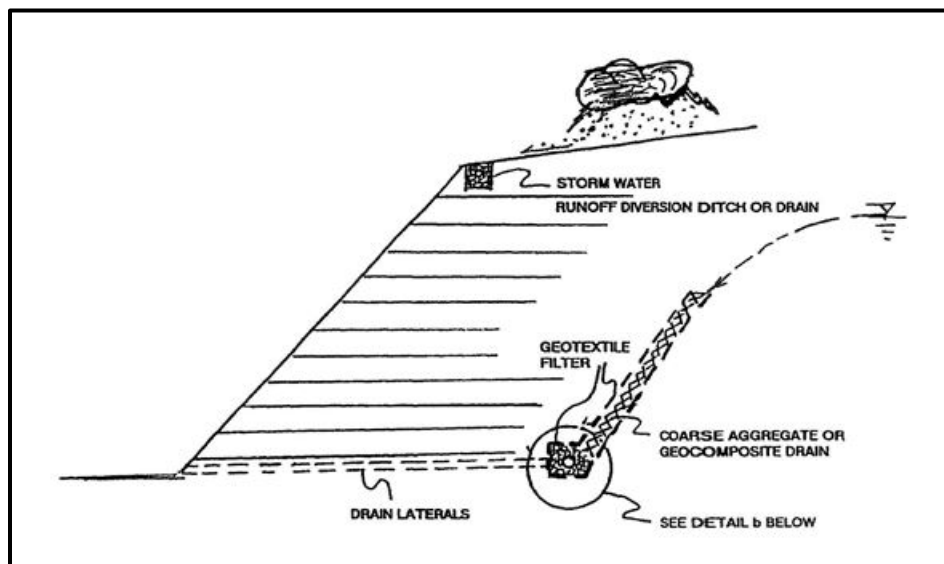


Figure D-14, Groundwater and Surface Drainage  
(Berg, et al. – Vol. II (2009))

Lateral spacing of outlets is dictated by site geometry and estimated flow. Outlet design should address long-term performance and maintenance requirements. Geosynthetic drainage composites can be used in subsurface water drainage design. Drainage composites should be designed with consideration for:

- Geotextile filtration/clogging
- Long-term compressive strength of polymeric core
- Reduction of flow capacity due to intrusion of geotextile into the core
- Long-term inflow/outflow capacity

Procedures for checking geotextile permeability and filtration/clogging criteria are presented in Geosynthetic Design and Construction Guidelines, Holtz, Christopher and Berg (2008), FHWA NHI-07-092. Long-term compressive stress and eccentric loadings on the core of a geocomposite should be considered during design and selection. Though not yet addressed in standardized test methods or standards of practice, the following criteria are suggested for addressing core compression. The design pressure on a geocomposite core should be limited to either:

- The maximum pressure sustained on the core in a test of 10,000 hours minimum duration
- The crushing pressure of a core, as defined with a quick loading test, *multiplied by a resistance factor of 0.2*

Note that crushing pressure can only be defined for some core types. For cases where a crushing pressure cannot be defined, suitability should be based on the maximum load resulting in a residual thickness of the core adequate to provide the required flow after 10,000 hours, or the maximum loading resulting in a residual thickness of the core adequate to provide the required flow as defined with the quick loading test *multiplied by a resistance factor of 0.2*.

Intrusion of the geotextiles into the core and long-term outflow capacity should be measured with a sustained transmissivity test. Slope stability analyses should account for interface shear strength along a geocomposite drain. The geocomposite/soil interface will most likely have a friction value that is lower than that of the soil. Thus, a potential failure surface may be induced along the interface. Geotextile reinforcements (primary and intermediate layers) must be more permeable than the reinforced fill material to prevent a hydraulic build up above the geotextile layers during precipitation. Special emphasis on the design and construction of subsurface drainage features is recommended for structures where drainage is critical for maintaining slope stability. Redundancy in the drainage system is also recommended for these cases.

### **D.9.2 Surface Water Runoff**

Surface water runoff should be collected above the reinforced slope and channeled or piped below the base of the slope. This applies to be both permanent as well as temporary RSSs. Wrapped faces and/or intermediate layers of secondary reinforcement may be required at the face of reinforced slopes to prevent local sloughing. Intermediate layers of reinforcement help achieve compaction at the face, thus increasing soil shear strength and erosion resistance. These layers also act as reinforcement against shallow or sloughing types of slope failures. Intermediate reinforcement is typically placed on each or



every other soil lift, except at lifts where primary structural reinforcement is placed. Intermediate reinforcement also is placed horizontally, adjacent to primary reinforcement and at the same elevation as the primary reinforcement when primary reinforcement is placed at less than 100 percent coverage in plan view. The intermediate reinforcement should extend 4 to 7 feet into the fill from the face. Select a long-term facing system to prevent or minimize erosion due to rainfall and runoff on the face.

Calculated flow-induced tractive shear stress on the face of the reinforced slope by:

$$\lambda = d * \gamma_w * s \quad \text{Equation D-29}$$

Where,

$\lambda$  = Tractive shear stress, psf

d = Depth of water flow, ft

$\gamma_w$  = Unit weight of water, pcf

s = The vertical to horizontal angle of slope face, ft/ft

For  $\lambda < 2$  psf, consider vegetation with temporary or permanent erosion control mat. For  $\lambda > 2$  psf, consider vegetation with permanent erosion control mat or other armor type systems (e.g., riprap, gunite, prefabricated modular units, fabric-formed concrete, etc.). Select vegetation based on local horticultural and agronomic considerations and maintenance. Select synthetic (permanent) erosion control mat that is stabilized against ultraviolet light and is inert to naturally occurring soil-born chemicals and bacteria. Erosion control mats and blankets vary widely in type, cost, and more importantly, applicability to project conditions. Slope protection should not be left to the construction contractor or vendor's discretion.

## D.10 COMPUTER SOFTWARE

The following Section of this Appendix is adopted directly from Berg, et al. – Vol. II (2009) and is used with the permission of the US Department of Transportation, Federal Highway Administration. Italics have been added to reflect additions or modifications to the selected text and to supply references to this Manual.

An alternative to reinforcement design is to develop a trial layout of reinforcement and analyze the reinforced slope with a computer program. Layout includes number, length, design strength, and vertical distribution of the geosynthetic reinforcement. The charts presented in Figure D-8 provide a method for generating a preliminary layout. Note that these charts were developed with the specific assumptions noted in this figure.

Analyze the reinforced soil slope with the trial geosynthetic reinforcement layouts. The most economical reinforcement layout must provide the *maximum stability resistance factors* for internal, external and compound failure planes. A contour plot of the *highest resistance factor* values about the trial failure circle centroids is recommended to map and locate the *maximum resistance factor* values for the 3 modes of failure.

Computer generated designs made by software other than FHWA's ReSSA computer program shall meet the requirements of Chapter 26 and shall require verification that the computer

program's design methodology meets the requirements provided herein. This shall be accomplished by either:

1. Provide complete, legible, calculations that show the design procedure step-by-step for the most critical geometry and loading condition that will govern each design section of the RSS structure. Calculations may be computer generated provided that all input, equations, and assumptions used are shown clearly.
2. Provide an electronic file with the input files and the full computer output of the FHWA sponsored computer program ReSSA (latest version) for the governing loading condition for each design section of the RSS structure. This software may be obtained at:

**ADAMA Engineering, Inc.**  
33 The Horseshoe  
Newark, Delaware 19711, USA  
Tel. (302) 368-3197, Fax (302) 731-1001

## D.11 REFERENCES

Berg, R. R., Christopher, B. R., and Samtani, N. C. (2009), Design of Mechanically Stabilized Earth Walls and Reinforced Soil Slopes – Volume I, Geotechnical Engineering Circular No. 11 – Volume I, (Publication No. FHWA NHI-10-024), National Highway Institute, Federal Highway Administration, U.S. Department of Transportation, Washington D.C.

Berg, R. R., Christopher, B. R., and Samtani, N. C. (2009), Design of Mechanically Stabilized Earth Walls and Reinforced Soil Slopes – Volume II, Geotechnical Engineering Circular No. 11 – Volume II, (Publication No. FHWA NHI-10-025), National Highway Institute, Federal Highway Administration, U.S. Department of Transportation, Washington D.C.

Elias, V., Christopher, B. R., and Berg, R. R. (2001), Mechanically Stabilized Earth Walls and Reinforced Soil Slopes Design and Construction, (Publication No. FHWA NHI-00-043), National Highway Institute, Federal Highway Administration, U.S. Department of Transportation, Washington D.C.

Elias, V., Fishman, K. L., Christopher, B. R., and Berg, R. R. (2009), Corrosion/Degradation of Soil Reinforcements for Mechanically Stabilized Earth Walls and Reinforced Soil Slopes, (Publication No. FHWA-NHI-09-087), National Highway Institute, Federal Highway Administration, U.S. Department of Transportation, Washington D.C.

Elias, V., Salman, I., Juran, E., Pearce, E., and Lu, S. (1999), Testing Protocols for Oxidation and Hydrolysis of Geosynthetics, (Publication No. FHWA-RD-97-144, Office of Engineering R & D, Federal Highway Administration, U. S. Department of Transportation, Washington D.C.

Holtz, R. D., Christopher, B. R., and Berg, R. R. (2008), Geosynthetic Design and Construction Guidelines, (Publication No. FHWA NHI-97-092), National Highway Institute, Federal Highway Administration, U.S. Department of Transportation, Washington D.C.

Jewell, R. A., (1990), "Revised Design Charts for Steep Reinforced Slopes, Reinforced Embankments: Theory and Practice in the British Isles", *Thomas Telford*, London, United Kingdom.

Leshchinsky, E. and Boedeker, R. H., (1989) "Geosynthetic Reinforced Soil Structures", *Journal of Geotechnical Engineering*, ASCE, Volume 115, Issue 10, p. 1459-1478.

Ruegger, R., (1986), "Geotextile Reinforced Soil Structures on which Vegetation can be Established", *Proceedings of the 3<sup>d</sup> International Conference on Geotextiles*, Vienna, Austria, Volume II.

SCDOT Standard Specifications for Highway Construction (2007), South Carolina Department of Transportation, [https://www.scdot.org/business/pdf/2007\\_full\\_specbook.pdf](https://www.scdot.org/business/pdf/2007_full_specbook.pdf).

Tanyu, B. F., Sabatini, P. J., and Berg, R. R. (2008), Earth Retaining Structures, (Publication No. FHWA NHI-07-071), National Highway Institute, Federal Highway Administration, U.S. Department of Transportation, Washington D.C.

**APPENDIX E**  
**GEOTECHNICAL TEMPLATE**  
**PLANS**

**GEOTECHNICAL DESIGN MANUAL**

*January 2019*



# APPENDIX E

## GEOTECHNICAL TEMPLATE PLANS


### E.1 GEOTECHNICAL TEMPLATE DRAWING POLICY

1. Geotechnical Template Drawings are not Standards. Engineering analysis and design is still required prior to completing/using the drawings.
2. Geotechnical Template Drawings are developed by the PCS/GDS and are anticipated to be used on multiple projects. PCS/GDS will ask for the Preconstruction Support Engineer (PCSE) for manpower help to perform drawing tasks.
3. If no Geotechnical Template Drawing exists, the GEOR will develop project-specific drawings as required.
4. PCS/GDS will coordinate with PCS/Design Automation to get template drawings on the SCDOT website. Any moving, updating or changes to existing template drawings or the SCDOT website will require written documentation prior to PCS/Design Automation taking action. PCS/Design Automation will coordinate with ITS to accomplish this task as necessary. Please note that this task could take several weeks to a month or more.
5. All Geotechnical Template Drawing numbers will be assigned by PCS/GDS and will be based partially on the pay item number that the template most closely relates to. The follow-on numbers will be sequential order. Alpha designations will be used after the follow-on number to indicate that the temple drawings are typically issued concurrently (e.g. 713-01a and 713-01b).
6. Geotechnical Template Drawings will be made available in both .PDF as well as in Microstation formats.
7. The GEOR will be responsible for completing the drawings and for determining the applicability to the specific project. The GEOR is also responsible for recommending and/or providing any of these drawings into the contract documents.
8. The PCS/GDS will occasionally solicit the RPG/GDSs for suggestion on additional template drawings.

### E.2 EXSITING GEOTECHINCAL TEMPLATE DRAWINGS

The following list contains the currently available Geotechnical Template Plans. Consultants can obtain any of these plans via the SCDOT internet website at:

<https://www.scdot.org/business/geotech.aspx>

 <b>SCDOT Geotechnical Design Drawings and Details Master List</b>		
Drawing Number:	Posted Date	Description
203-05	04/04/18	Geotechnical General Notes
205-05	04/04/18	Stone Columns
205-10	07/10/10	Earthquake Drains
711-01	04/01/14	LRFD Pile Record
711-02	04/01/14	ASD Pile Record
712-05	03/07/11	Axial Shaft Load Test – XX" Dia. Statnamic
712-10	03/07/11	Lateral Shaft Load Test – XX" Dia. Statnamic
712-15	03/07/11	Axial Shaft Load Test – XX" Dia. Osterberg Cell
713-01	08/17/15	MSE Wall Notes and Details – Panel Face
713-02	08/17/15	MSE Wall Notes and Details – Block Face
713-03	03/29/18	Flexible Gravity Wall With Block Face for Low Volume Bridge Replacements
801-01	04/04/18	Prefabricated Vertical Drains (PVD)

**Figure E-1, Geotechnical Table of Contents**

**APPENDIX F**

**GEOTECHNICAL  
SPECIFICATIONS LIST**

**GEOTECHNICAL DESIGN MANUAL**

*January 2019*





# APPENDIX F

## GEOTECHNICAL SPECIFICATIONS LIST

The following list contains the currently available Geotechnical Specifications including Supplemental Specifications and Supplemental Technical Specifications (STSs). All of these Specifications can be obtained from the SCDOT website: <https://www.scdot.org/business/business-landing.aspx>. In the list below, the Specifications without numbers are Supplemental Specifications, while the specifications with numbers are STSs. In addition, the GEC can obtain the word files for any of these specifications by contacting the PC/GDS in order to make project specific Special Provisions. Any changes made to the specifications, regardless of whether the change is made by the GEOR, shall be highlighted prior to the review process to facilitate the review. If a Special Provision does not exist contact the PCS/GDS for possible draft versions.

<b><u>Name</u></b>	<b><u>Number</u></b>	<b><u>Let Date</u></b>
Bridge Lift Materials	-	03/08/2016
Muck Excavation	-	07/01/2017
Geosynthetic Materials – Separation & Stabilization	SC-M-203-1	07/17
Geogrid Soil Reinforcement	SC-M-203-2	07/17
Geotextile Soil Reinforcement	SC-M-203-3	07/17
Settlement Plates	SC-M-203-4	07/17
Lightweight Aggregates	SC-M-203-5	07/17
Vibrating-Wire Piezometer	SC-M-203-6	07/17
Settlement Sensors	SC-M-203-7	07/17
Vibrating Wire Rod Extensometer	SC-M-203-8	07/17
Slope Inclinator Casing	SC-M-203-9	07/17
Earthquake Drains	SC-M-205-1	07/16
Stone Columns	SC-M-205-2	07/17
Reinforced Soil Slopes	SC-M-206-1	04/16
Bi-Directional Static Load Testing of Drilled Shafts	SC-M-712-1	01/18
High Strain Static Load Testing of Drilled Shafts	SC-M-712-2	09/15
Rapid Axial Load Testing of Drilled Shafts	SC-M-712-3	09/15
Mechanically Stabilized Earth (MSE) Walls	SC-M-713	01/19
Prefabricated Vertical Drains	SC-M-801-1	07/16
Geocomposite Wall Drain	SC-M-802-1	07/18

**APPENDIX G**  
**SCDOT SOFTWARE LIST**

**GEOTECHNICAL DESIGN MANUAL**

*January 2019*



# APPENDIX G

## SCDOT SOFTWARE LIST

The following list contains the software (both commercially available and non-commercial) used by SCDOT. Consultants are not required to have the same software as the Department. This is provided for reference to the consultants. The non-commercial software is used exclusively internal to the Department.

### Commercial Software

GSTABL7 with STEDwin  
Slide  
PYWall  
MSEW  
ReSSA  
FoSSA  
SNAP2  
APILE  
LPILE  
Shaft  
GRLWEAP  
FB Deep  
RSPile  
DEEPSOIL  
SHAKE2000  
D-MOD2000  
RspMatchEDT  
SLAMMER  
CLiq  
gINT  
CPeT-IT2  
SectionMaker

### Non-Commercial Software

SCENARIO-PC  
SCDOT SHAKE  
ADRS - Site Class & Andrus (Excel spreadsheet)  
SPT-SSL\_Idriss and Boulanger (Excel spreadsheet)  
SPLiq (Excel Spreadsheet)  
Bridge Abutment Backwall Seismic Passive Pressures (Excel spreadsheet)  
ERS-Grd Imp Selection Matrix (Excel Spreadsheet)

**APPENDIX H**  
**SHEAR WAVE VELOCITY**  
**PROFILES**

**GEOTECHNICAL DESIGN MANUAL**

*January 2019*



**Table of Contents**

<b><u>Section</u></b>		<b><u>Page</u></b>
H.1	Introduction.....	H-1
	H.1.1 South Carolina Reference Shear Wave Profiles.....	H-1
H.2	References .....	H-155



**List of Tables**

<b><u>Table</u></b>	<b><u>Page</u></b>
Table H-1, USGS Shear Wave Profile Summary.....	H-3

### List of Figures

<u>Figure</u>	<u>Page</u>
Figure H-1, USGS Nine Study Locations.....	H-2
Figure H-2, USGS Shear Wave $V_s$ Profile.....	H-3
Figure H-3, USGS Sites 1, 2, 5, 9, 7, and 8.....	H-4
Figure H-4, USGS Sites 6, 4, 3.....	H-5
Figure H-5, Site Response Categories and Depth To Pre-Cretaceous Rock.....	H-6
Figure H-6, Piedmont/Blue Ridge Site Response Category Base Vs Profile .....	H-7
Figure H-7, Savannah River Site Response Category Base Vs Profile .....	H-8
Figure H-8, Charleston Site Response Category Base Vs Profile .....	H-9
Figure H-9, Myrtle Beach Site Response Category Base Vs Profile.....	H-10
Figure H-10, SCPT Piedmont Profile - NGES Opelika, Alabama.....	H-11
Figure H-11, Geophysical $V_s$ Piedmont Profile - NGES Opelika, Alabama.....	H-12
Figure H-12, SCPT Profile Savannah River, South Carolina .....	H-12
Figure H-13, SCPT Profile (DS-1) Cooper River Bridge, Charleston, SC .....	H-13
Figure H-14, Shear Wave Profile US 17, Beaufort County, South Carolina .....	H-13
Figure H-15, SCPT (B-14) US 17 Bridge 1, Beaufort County, South Carolina .....	H-14
Figure H-16, SCPT (B-5A) US 17 Bridge 3, Beaufort County, South Carolina.....	H-14
Figure H-17, Shear Wave Profile (SC3) - US 378, Lake City, South Carolina .....	H-15
Figure H-18, SCPT (SC3) - US 378, Lake City, South Carolina .....	H-15
Figure H-19, Shear Wave Profile (SC4) - US 378, Lake City, South.....	H-16
Figure H-20, SCPT (SC4) - US 378, Lake City, South Carolina .....	H-16
Figure H-21, Deep Hole Location Map .....	H-17
Figure H-22, Soil Test Boring DHT-1/B-6 .....	H-19
Figure H-23, Soil Test Boring DHT-1/B-6 (con't) .....	H-20
Figure H-24, Soil Test Boring DHT-1/B-6 (con't) .....	H-21
Figure H-25, Soil Test Boring DHT-1/B-6 (con't) .....	H-22
Figure H-26, Soil Test Boring DHT-1/B-6 (con't) .....	H-23
Figure H-27, Soil Test Boring DHT-1/B-6 (con't) .....	H-24
Figure H-28, Soil Test Boring DHT-1/B-6 (con't) .....	H-25
Figure H-29, $V_s$ and $V_p$ Profile – DHT-1/B-6 .....	H-26
Figure H-30, Soil Test Boring B-2A .....	H-27
Figure H-31, Soil Test Boring B-2A (con't) .....	H-28
Figure H-32, Soil Test Boring B-2A (con't) .....	H-29
Figure H-33, Soil Test Boring B-2A (con't) .....	H-30
Figure H-34, $V_s$ Profile B-2A.....	H-31
Figure H-35, Tabulated $V_s$ Results – B-2A .....	H-32
Figure H-36, Soil Test Boring B-2.....	H-33
Figure H-37, $V_s$ Profile B-2 .....	H-34
Figure H-38, Tabulated $V_s$ Results – B-2.....	H-35
Figure H-39, Soil Test Boring STB-1 .....	H-36
Figure H-40, Soil Test Boring STB-1 (con't) .....	H-37
Figure H-41, Soil Test Boring STB-1 (con't) .....	H-38
Figure H-42, Soil Test Boring STB-1 (con't) .....	H-39
Figure H-43, Soil Test Boring STB-1 (con't) .....	H-40
Figure H-44, Soil Test Boring STB-1 (con't) .....	H-41
Figure H-45, Soil Test Boring STB-1 (con't) .....	H-42

Figure H-46, Soil Test Boring STB-1 (con't) .....	H-43
Figure H-47, Soil Test Boring STB-1 (con't) .....	H-44
Figure H-48, Soil Test Boring STB-1 (con't) .....	H-45
Figure H-49, Soil Test Boring STB-1 (con't) .....	H-46
Figure H-50, $V_s$ and $V_p$ Profile – STB-1 .....	H-47
Figure H-51, Tabulated $V_s$ and $V_p$ Results – STB-1 .....	H-48
Figure H-52, Tabulated $V_s$ and $V_p$ Results – STB-1 (con't) .....	H-49
Figure H-53, Tabulated $V_s$ and $V_p$ Results – STB-1 (con't) .....	H-50
Figure H-54, Tabulated $V_s$ and $V_p$ Results – STB-1 (con't) .....	H-51
Figure H-55, Tabulated $V_s$ and $V_p$ Results – STB-1 (con't) .....	H-52
Figure H-56, Tabulated $V_s$ and $V_p$ Results – STB-1 (con't) .....	H-53
Figure H-57, Tabulated $V_s$ and $V_p$ Results – STB-1 (con't) .....	H-54
Figure H-58, Tabulated $V_s$ and $V_p$ Results – STB-1 (con't) .....	H-55
Figure H-59, Soil Test Boring G-B-1 .....	H-56
Figure H-60, Soil Test Boring G-B-1 (con't) .....	H-57
Figure H-61, Soil Test Boring G-B-1 (con't) .....	H-58
Figure H-62, Soil Test Boring G-B-1 (con't) .....	H-59
Figure H-63, Soil Test Boring G-B-1 (con't) .....	H-60
Figure H-64, Soil Test Boring G-B-1 (con't) .....	H-61
Figure H-65, Soil Test Boring G-B-1 (con't) .....	H-62
Figure H-66, Soil Test Boring G-B-1 (con't) .....	H-63
Figure H-67, Soil Test Boring G-B-1 (con't) .....	H-64
Figure H-68, Soil Test Boring G-B-1 (con't) .....	H-65
Figure H-69, Soil Test Boring G-B-1 (con't) .....	H-66
Figure H-70, $V_s$ and $V_p$ Profile – G-B-1 .....	H-67
Figure H-71, Tabulated $V_s$ and $V_p$ Results – G-B-1 .....	H-68
Figure H-72, Tabulated $V_s$ and $V_p$ Results – G-B-1 (con't) .....	H-69
Figure H-73, Tabulated $V_s$ and $V_p$ Results – G-B-1 (con't) .....	H-70
Figure H-74, Tabulated $V_s$ and $V_p$ Results – G-B-1 (con't) .....	H-71
Figure H-75, Tabulated $V_s$ and $V_p$ Results – G-B-1 (con't) .....	H-72
Figure H-76, Tabulated $V_s$ and $V_p$ Results – G-B-1 (con't) .....	H-73
Figure H-77, Tabulated $V_s$ and $V_p$ Results – G-B-1 (con't) .....	H-74
Figure H-78, Soil Test Boring SB-1 .....	H-75
Figure H-79, Soil Test Boring SB-1 (con't) .....	H-76
Figure H-80, Soil Test Boring SB-1 (con't) .....	H-77
Figure H-81, Soil Test Boring SB-1 (con't) .....	H-78
Figure H-82, Soil Test Boring SB-1 (con't) .....	H-79
Figure H-83, Soil Test Boring SB-1 (con't) .....	H-80
Figure H-84, Soil Test Boring SB-1 (con't) .....	H-81
Figure H-85, Soil Test Boring SB-1 (con't) .....	H-82
Figure H-86, Soil Test Boring SB-1 (con't) .....	H-83
Figure H-87, Soil Test Boring SB-1 (con't) .....	H-84
Figure H-88, Soil Test Boring SB-1 (con't) .....	H-85
Figure H-89, $V_s$ and $V_p$ Profile – SB-1 .....	H-86
Figure H-90, Tabulated $V_s$ and $V_p$ Results – SB-1 .....	H-87
Figure H-91, Tabulated $V_s$ and $V_p$ Results – SB-1 (con't) .....	H-88
Figure H-92, Tabulated $V_s$ and $V_p$ Results – SB-1 (con't) .....	H-89

Figure H-93, Tabulated $V_s$ and $V_p$ Results – SB-1 (con't)	H-90
Figure H-94, Tabulated $V_s$ and $V_p$ Results – SB-1 (con't)	H-91
Figure H-95, Tabulated $V_s$ and $V_p$ Results – SB-1 (con't)	H-92
Figure H-96, Tabulated $V_s$ and $V_p$ Results – SB-1 (con't)	H-93
Figure H-97, SCPT-2	H-94
Figure H-98, $V_s$ Profile – SCPT-2	H-95
Figure H-99, Tabulated $V_s$ Results – SCPT-2	H-96
Figure H-100, SCPT-11	H-97
Figure H-101, $V_s$ Profile – SCPT-11	H-98
Figure H-102, Tabulated $V_s$ Results – SCPT-11	H-99
Figure H-103, Soil Test Boring B-11GEO	H-100
Figure H-104, Soil Test Boring B-11GEO (con't)	H-101
Figure H-105, Soil Test Boring B-11GEO (con't)	H-102
Figure H-106, Soil Test Boring B-11GEO (con't)	H-103
Figure H-107, Soil Test Boring B-11GEO (con't)	H-104
Figure H-108, Soil Test Boring B-11GEO (con't)	H-105
Figure H-109, Soil Test Boring B-11GEO (con't)	H-106
Figure H-110, Soil Test Boring B-11GEO (con't)	H-107
Figure H-111, Soil Test Boring B-11GEO (con't)	H-108
Figure H-112, $V_s$ and $V_p$ Profile – B-11GEO	H-109
Figure H-113, Tabulated $V_s$ and $V_p$ Results – B-11GEO	H-110
Figure H-114, Tabulated $V_s$ and $V_p$ Results – B-11GEO (con't)	H-111
Figure H-115, Tabulated $V_s$ and $V_p$ Results – B-11GEO (con't)	H-112
Figure H-116, Tabulated $V_s$ and $V_p$ Results – B-11GEO (con't)	H-113
Figure H-117, Tabulated $V_s$ and $V_p$ Results – B-11GEO (con't)	H-114
Figure H-118, Tabulated $V_s$ and $V_p$ Results – B-11GEO (con't)	H-115
Figure H-119, Tabulated $V_s$ and $V_p$ Results – B-11GEO (con't)	H-116
Figure H-120, Tabulated $V_s$ and $V_p$ Results – B-11GEO (con't)	H-117
Figure H-121, Tabulated $V_s$ and $V_p$ Results – B-11GEO (con't)	H-118
Figure H-122, Tabulated $V_s$ and $V_p$ Results – B-11GEO (con't)	H-119
Figure H-123, Tabulated $V_s$ and $V_p$ Results – B-11GEO (con't)	H-120
Figure H-124, Soil Test Boring GEI 4	H-121
Figure H-125, Soil Test Boring GEI 4 (con't)	H-122
Figure H-126, Soil Test Boring GEI 4 (con't)	H-123
Figure H-127, Soil Test Boring GEI 4 (con't)	H-124
Figure H-128, Soil Test Boring GEI 4 (con't)	H-125
Figure H-129, Soil Test Boring GEI 4 (con't)	H-126
Figure H-130, Soil Test Boring GEI 4 (con't)	H-127
Figure H-131, Soil Test Boring GEI 4 (con't)	H-128
Figure H-132, $V_s$ and $V_p$ Profile – GEI-4	H-129
Figure H-133, Tabulated $V_s$ and $V_p$ Results – GEI-4	H-130
Figure H-134, Tabulated $V_s$ and $V_p$ Results – GEI-4 (con't)	H-131
Figure H-135, Tabulated $V_s$ and $V_p$ Results – GEI-4 (con't)	H-132
Figure H-136, Tabulated $V_s$ and $V_p$ Results – GEI-4 (con't)	H-133
Figure H-137, SCPT-01	H-134
Figure H-138, $V_s$ Profile – SCPT-01	H-135
Figure H-139, SCPT-02	H-136

Figure H-140, $V_s$ Profile – SCPT-02 .....	H-137
Figure H-141, Soil Test Boring STB-09 .....	H-138
Figure H-142, Soil Test Boring STB-09 (con't) .....	H-139
Figure H-143, Soil Test Boring STB-09 (con't) .....	H-140
Figure H-144, Soil Test Boring STB-09 (con't) .....	H-141
Figure H-145, Soil Test Boring STB-09 (con't) .....	H-142
Figure H-146, $V_s$ and $V_p$ Profile – STB-09 .....	H-143
Figure H-147, $V_s$ Profile – STB-09.....	H-144
Figure H-148, $V_s$ Profile – Maybank .....	H-145
Figure H-149, Tabulated $V_s$ Results – Maybank.....	H-146
Figure H-150, Soil Test Boring SC-85 – B-11.....	H-147
Figure H-151, Soil Test Boring SC-85 – B-11 (con't).....	H-148
Figure H-152, Soil Test Boring SC-85 – B-11 (con't).....	H-149
Figure H-153, $V_s$ Profile – SC-85 – DHT-1 .....	H-150
Figure H-154, Tabulated $V_s$ Results – SC-85 – DHT-1.....	H-151
Figure H-155, Soil Test Boring Withers Swash – STB2.....	H-152
Figure H-156, Soil Test Boring Withers Swash – STB2 (con't).....	H-153
Figure H-157, $V_s$ Profile and Tabulated Results – Withers Swash – DHT-1 .....	H-154

# APPENDIX H

## SHEAR WAVE VELOCITY PROFILES

### H.1 INTRODUCTION

#### H.1.1 South Carolina Reference Shear Wave Profiles

The shear wave profiles presented in this Appendix are provided for reference purposes only. Project specific shear wave profiles to depths of at least 100 feet beneath either the existing ground surface or the approximate original ground surface shall be developed from in-situ shear wave measurements as required in Chapter 4. These shear wave profiles shall be extended to the anticipated B-C Boundary as required, for performing a site-specific seismic response analysis, using geologic publications, previous investigations, and the reference shear wave profiles presented in this Appendix.

A number of seismic studies have been performed in South Carolina and have yielded shear wave profiles for different parts of the state. The majority of the published shear wave profiles are in the Coastal Plain. The shear wave velocity profiles were obtained by one of the following testing methods: Seismic Refraction, Seismic Reflection, Surface Wave (SASW and MASW), Downhole (including Seismic CPT), or Crosshole techniques as described in Chapter 5. When shear wave measurements are not available for soil formations beyond the shear wave testing capabilities, estimates are typically made by using available shear wave data from formations previously tested or by using geologic information. Regardless of the data available all shear wave profiles shall be measured to a depth of at least 100 feet.

The shear wave velocity profile information contained in this Appendix has been divided into 3 sections: USGS Shear Wave Velocity Data, South Carolina Emergency Management Division (SCEMD) Seismic Risk and Vulnerability Study, and Published / SCDOT Shear Wave Velocity Profiles. A brief review of these reference shear wave velocity profiles is presented in the following Sections.

#### H.1.1.1 USGS Shear Wave Velocity Data

The U.S. Geologic Survey (USGS) has compiled shear wave profiles in South Carolina in a report prepared by Odum, Williams, Stepheson and Worley (2003). Shear wave measurements were obtained by seismic refraction/reflection profiling techniques for nine locations in South Carolina as indicated in Figure H-1 and listed below:

1. Lake Murray Dam Spillway, Columbia, SC: Paleozoic Rocks of the Carolina Slate Group.
2. Fort Jackson Military Base, Columbia, SC: Cretaceous Tuscaloosa Formation (Middendorf Formation)
3. Deep Creek School: Peedee Formation (Upper Cretaceous)
4. Black Mingo: Black Mingo Formation (lower Eocene-Wilcox Group)
5. Santee Limestone: Santee Limestone (Middle Eocene-Clayborne Group)
6. The Citadel, Charleston, SC: Quaternary deposits (barrier sand facies) overlying Upper Tertiary Cooper Group (Ashley and Parkers Ferry Formations) - The Citadel
7. U.S. Highway 17 Overpass next to Ashley River Memorial Bridge: Quaternary deposits overlying Upper Tertiary Cooper Group (Ashley and Parkers Ferry Formations)

8. Isle of Palms, Charleston, SC: Quaternary deposits (beach and barrier-island sand facies) overlying Upper Tertiary Cooper Group (Ashley and Parkers Ferry Formations)
9. U.S. National Seismograph Network (USNSN) installation site: Quaternary deposits overlying Upper Tertiary Cooper Group (Ashley and Parkers Ferry Formations)

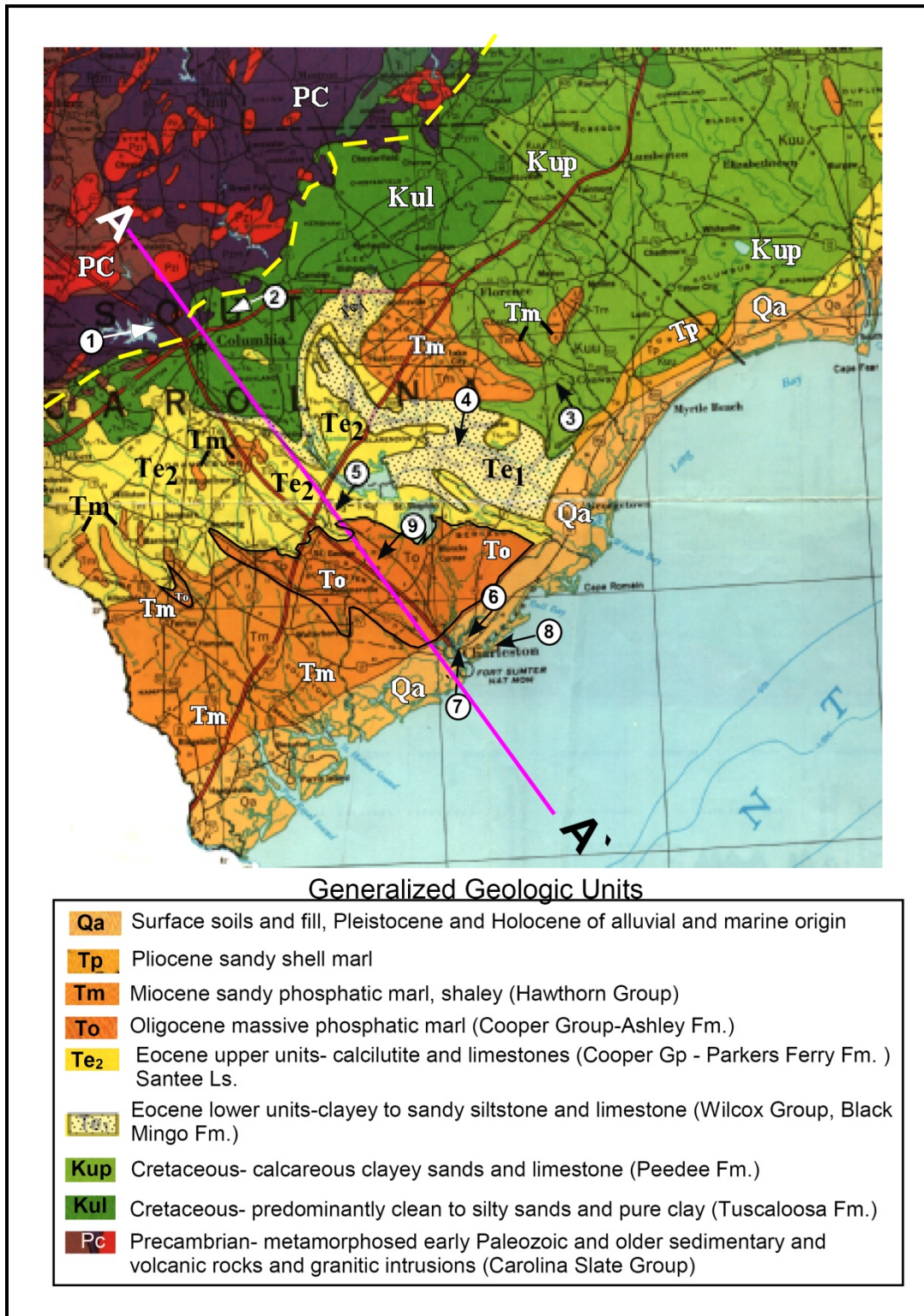


**Figure H-1, USGS Nine Study Locations  
(Odum, et al. (2003))**

Shear wave ( $V_s$ ) profiles for the 9 USGS sites are summarized in Table H-1 and shown in Figure H-2.

**Table H-1, USGS Shear Wave Profile Summary  
(Odum, et al. (2003))**

Site No.	Site Name	Latitude (degrees)	Longitude (degrees)	Surficial Geology <sup>(1)</sup>	Highest $V_s$ in Upper 164' (50 m)		Description <sup>(1)</sup>
					(m/s)	(ft/sec)	
1	Lake Murray Spillway	35.052	81.210	Fill, P <sub>z</sub>	2,674 @ 23 m	8,770 @ 75 ft	Carolina Slate Group (P <sub>z</sub> )
2	Fort Jackson	34.028	90.912	K <sub>u</sub>	866 @ 27 m	2,840 @ 89 ft	Tuscaloosa Fm
3	Deep Creek School	33.699	79.351	Q?, K <sub>u</sub>	710 @ 22 m	2,330 @ 72 ft	Q over Peedee Fm
4	Black Mingo	33.551	79.933	Q, T <sub>l</sub>	855 @ 9 m	2,805 @ 30 ft	Q over Eocene Wilcox Group
5	Santee Ls	33.235	80.433	T <sub>l</sub>	932 @ 7 m	3,057 @ 23 ft	Santee Limestone
6	The Citadel, Charleston	32.798	79.958	Q, T <sub>u</sub>	795 @ 78 m	2,608 @ 256 ft	Q over T <sub>u</sub> (Cooper Group)
7	US Hwy. 17, Charleston	32.785	79.955	Fill, Q	247 @ 11 m	810 @ 36 ft	Q over T <sub>u</sub> (Cooper Group)
8	Isle of Palms	32.795	79.775	Q <sub>h</sub> , T <sub>u</sub>	497 @ 23 m	1,630 @ 75 ft	Q over T <sub>u</sub> (Cooper Group)
9	USNSN	33.106	80.178	Q, T <sub>u</sub>	792 @ 10 m	2,598 @ 33 ft	Q over T <sub>u</sub> (Cooper Group)

<sup>(1)</sup> Definitions: Q – Quaternary; T<sub>u</sub> – upper Tertiary; T<sub>l</sub> – lower Tertiary; K<sub>u</sub> – upper Cretaceous; P<sub>z</sub> - Paleozoic

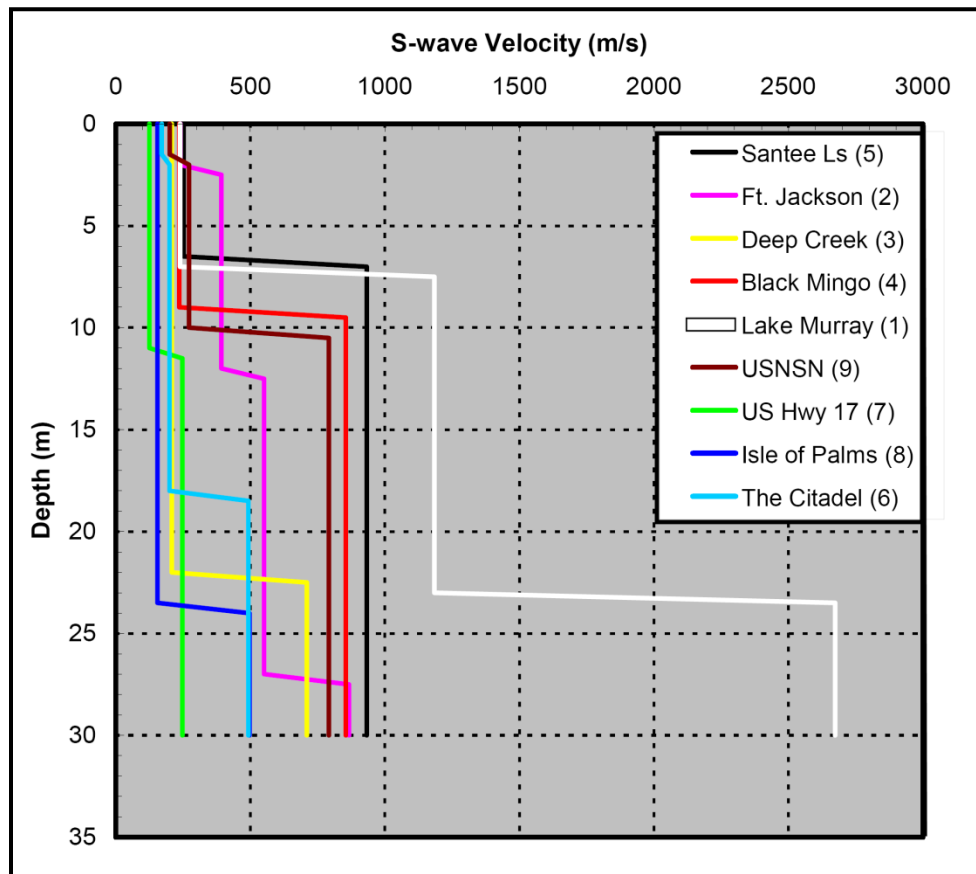


**Figure H-2, USGS Shear Wave  $V_s$  Profile  
(Odum, et al. (2003))**



The shear wave ( $V_s$ ) and compression wave ( $V_p$ ) profiles developed for the 9 sites are shown in Figures H-3 and H-4. The columns show successively higher velocity layers V1, V2, and V3, indicated by yellow, blue, and light brown, respectively. For a detailed interpretation of the results shown in these profiles refer to Odum et al. (2003).

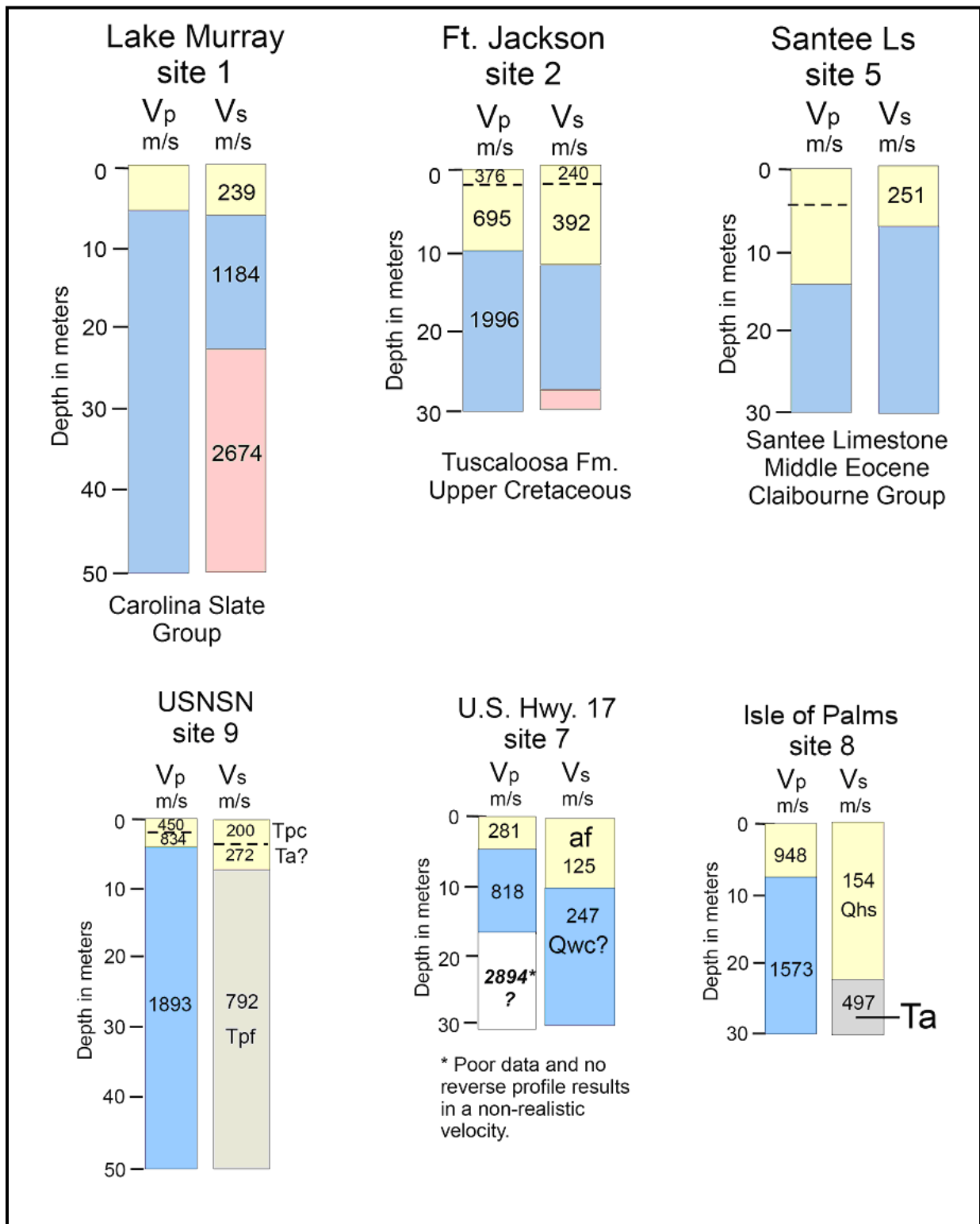


Figure H-3, USGS Sites 1, 2, 5, 9, 7, and 8 (Odum, et al. (2003))

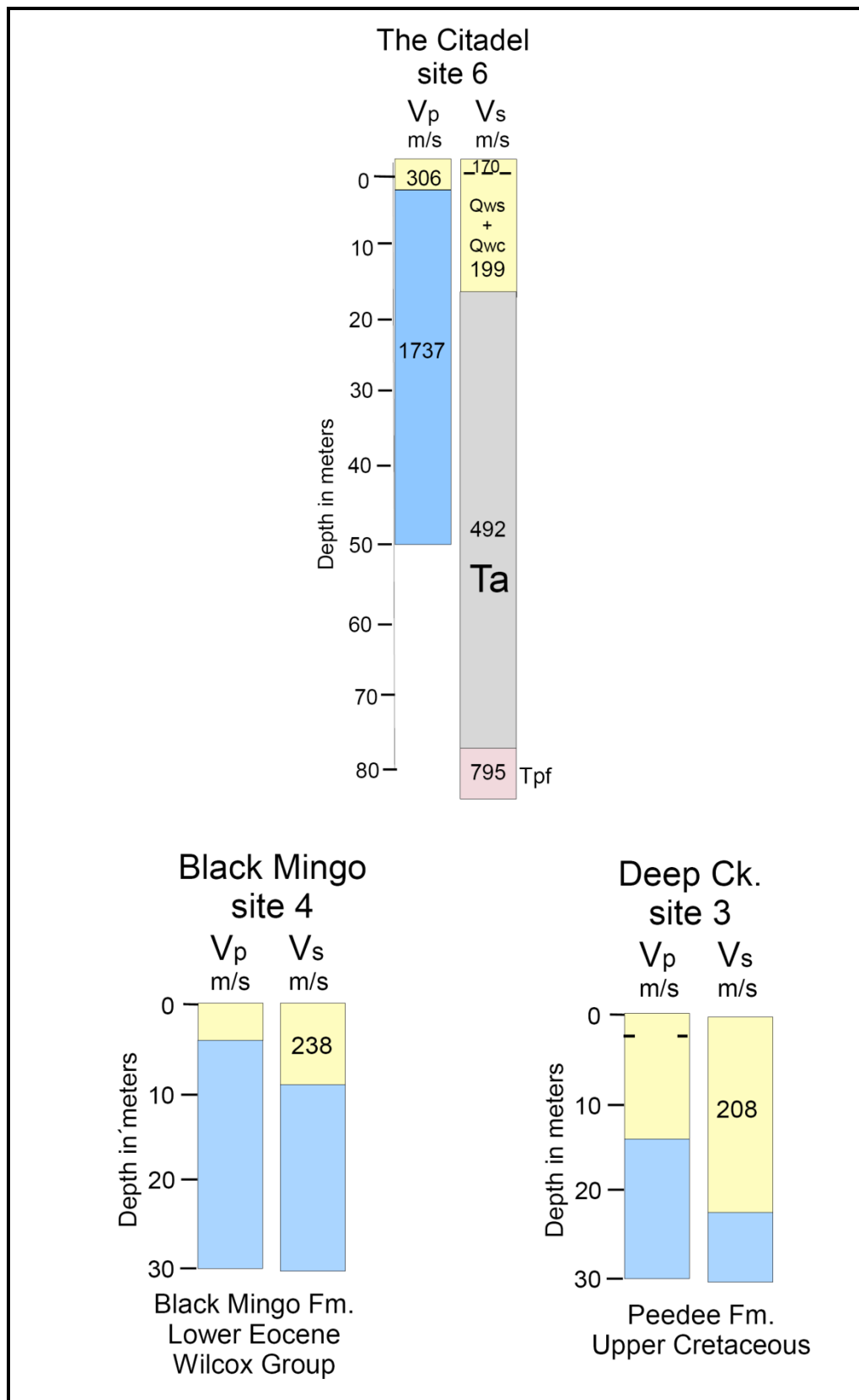
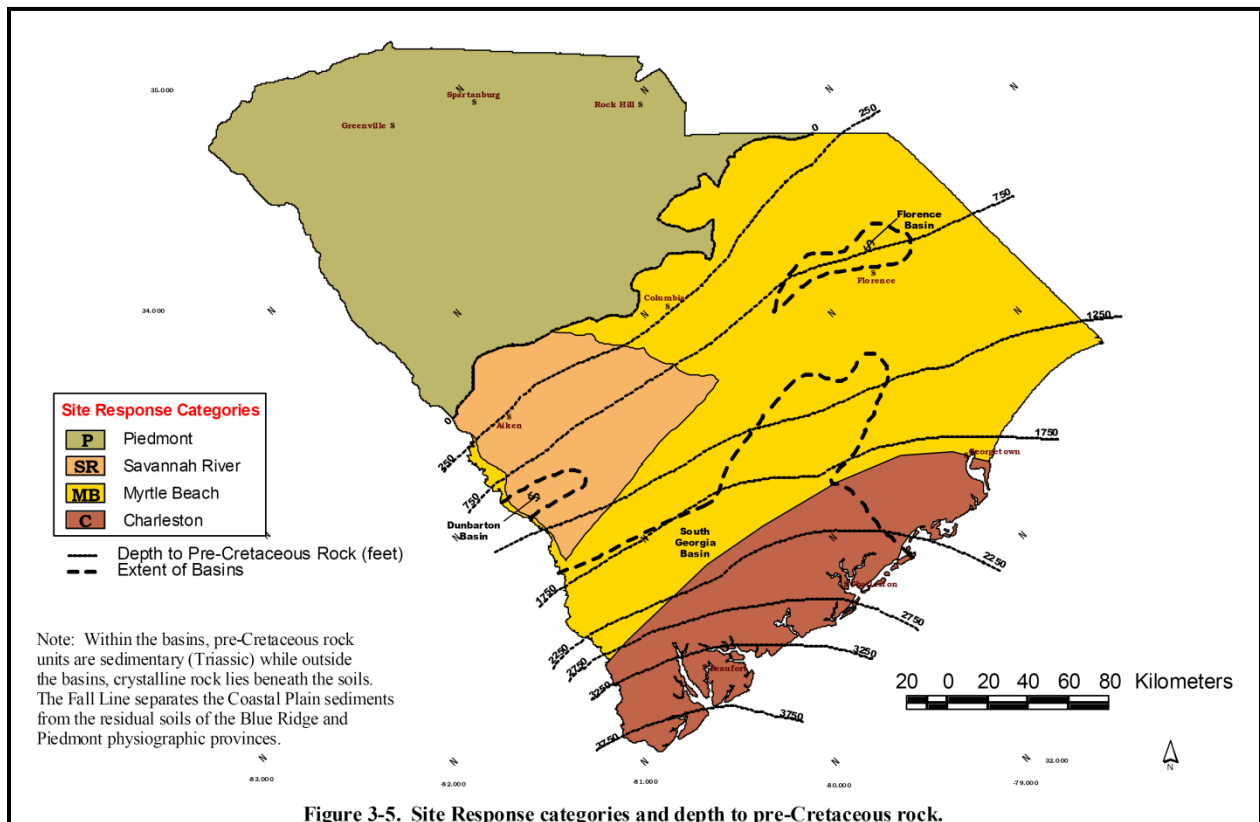


Figure H-4, USGS Sites 6, 4, 3  
(Odum, et al. (2003))

### H.1.1.2 SCEMD Seismic Risk and Vulnerability Study

A study was prepared by URS Corporation (2001) for SCEMD. This study evaluated the potential losses resulting from 4 scenario earthquakes that may occur in South Carolina sometime in the future. South Carolina was divided into 4 site response categories based on physiographic provinces, surficial geology, and trends in subsurface data. The 4 site categories that were selected for this study are: Piedmont, Savannah River, Charleston, and Myrtle Beach. The extent of these site response categories are shown on a South Carolina map in Figure H-5. The shear wave profiles for the Piedmont, Savannah River, Charleston, and Myrtle Beach are shown in Figures H-6, H-7, H-8, and H-9, respectively. For a detailed explanation of the base shear wave profiles used in this study refer to SCEMD report prepared by URS Corporation (2001).



**Figure H-5, Site Response Categories and Depth To Pre-Cretaceous Rock (URS Corporation (2001))**

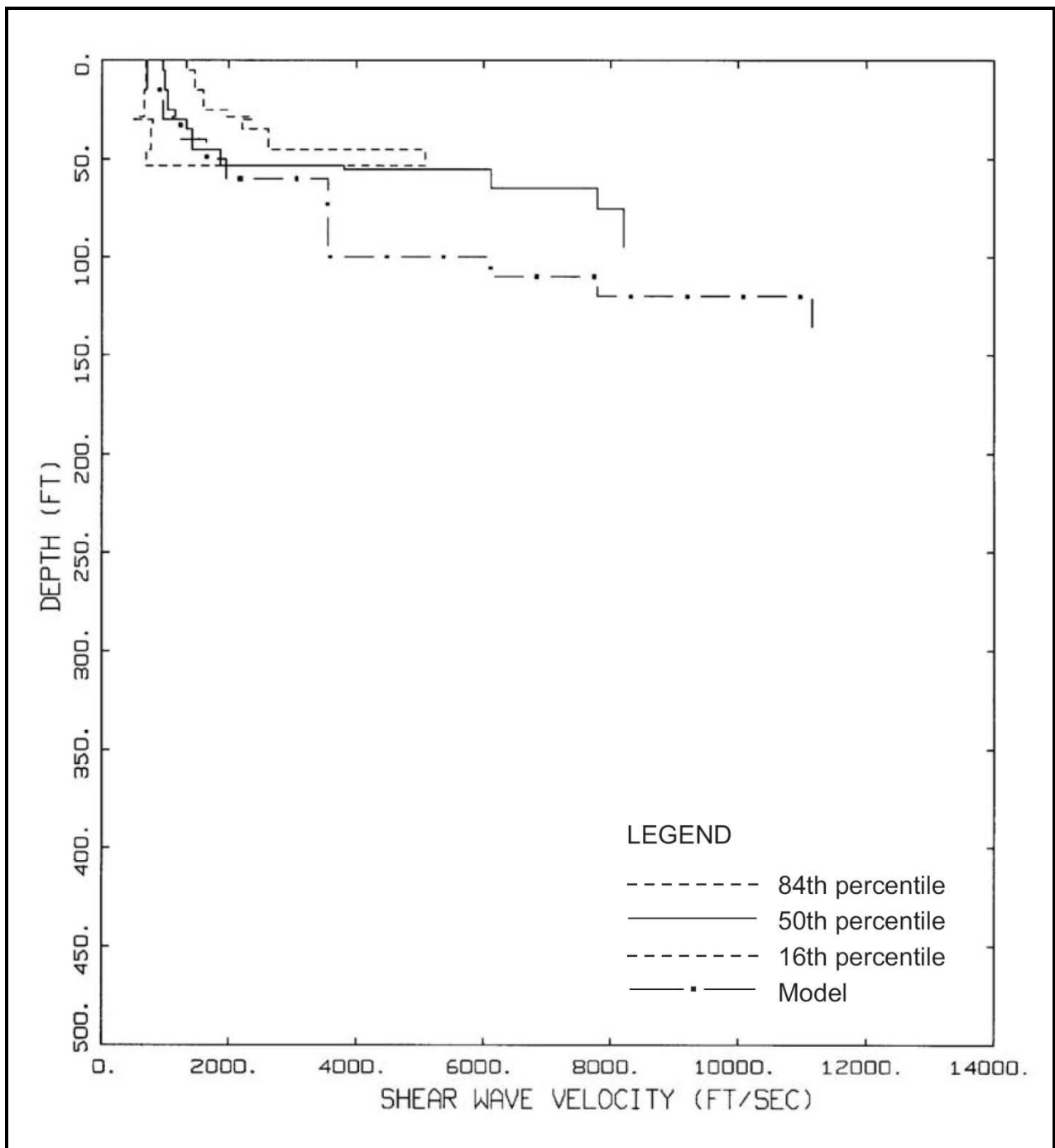


**Figure H-6, Piedmont/Blue Ridge Site Response Category Base Vs Profile (URS Corporation (2001))**

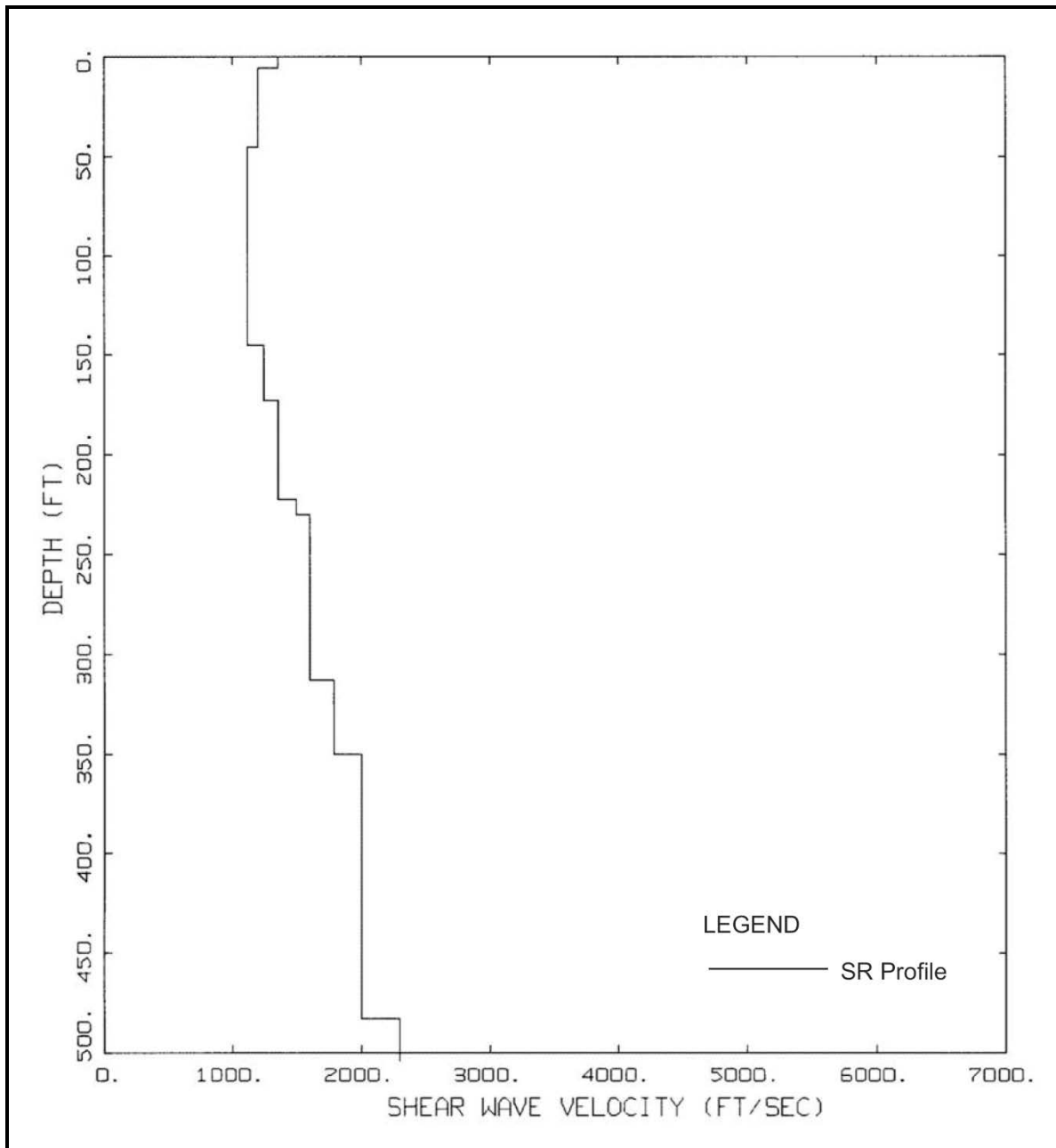


**Figure H-7, Savannah River Site Response Category Base Vs Profile (URS Corporation (2001))**

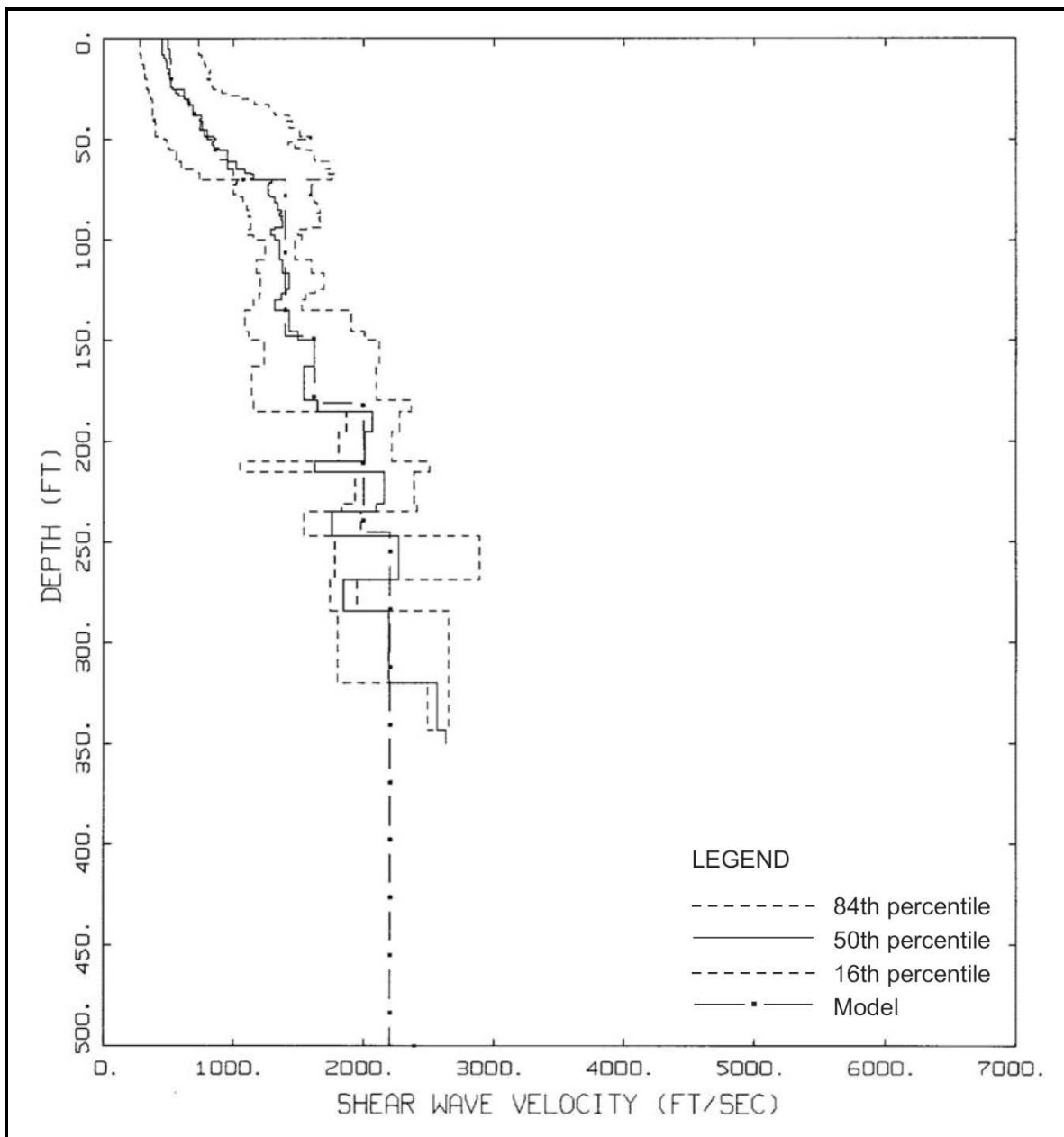


**Figure H-8, Charleston Site Response Category Base Vs Profile (URS Corporation (2001))**

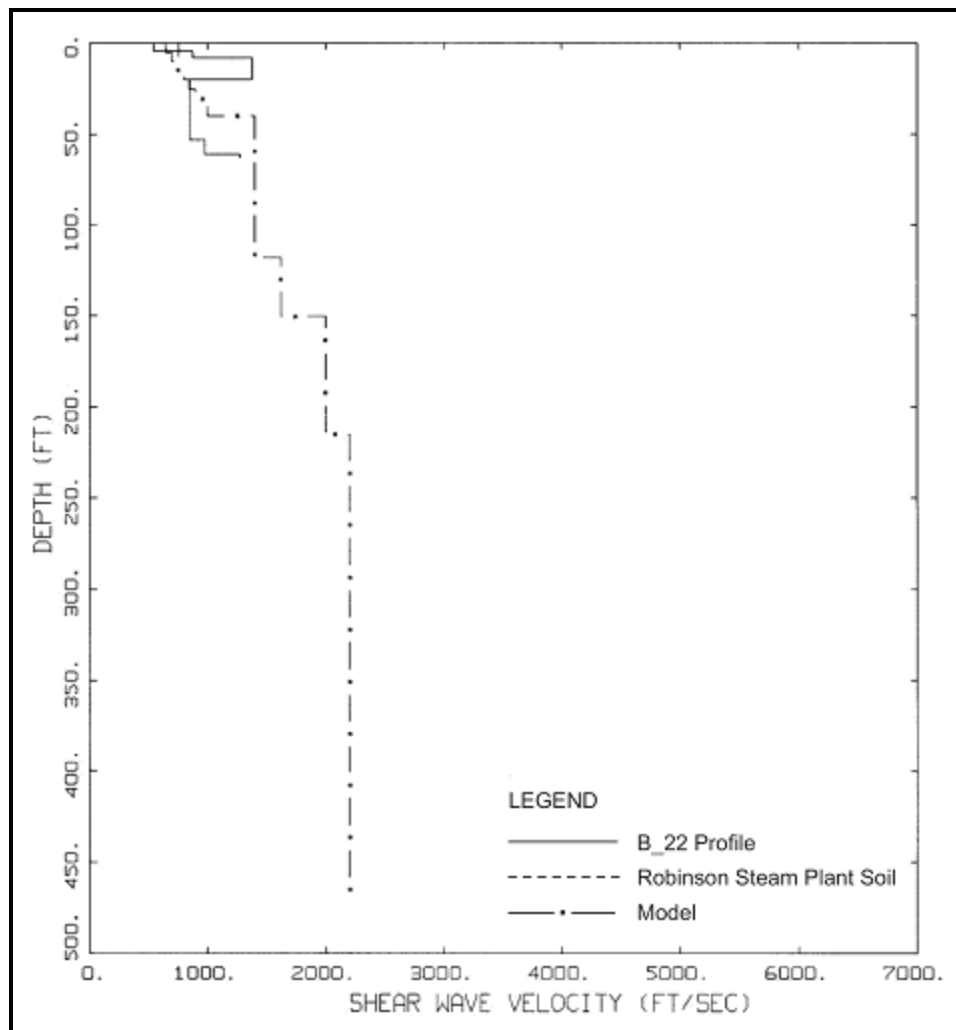


**Figure H-9, Myrtle Beach Site Response Category Base Vs Profile (URS Corporation (2001))**

### H.1.1.3 Published / SCDOT Shear Wave Velocity Profiles

A partial review of published shear wave velocity profiles has been compiled to provide additional reference data for use in characterizing sites in South Carolina. The shear wave profiles are provided as references. For a detailed description of the geologic formation and geotechnical investigation, refer to the source documents. The list of the shear wave profiles compiled is provided below:

1. Seismic CPT and Geophysical shear wave profiles taken in Piedmont soils from the National Geotechnical Experimentation Sites (NGES) located at Opelika, Alabama. The Seismic CPT is shown in Figure H-10 and the geophysical testing is shown in Figure H-11. This site is generally accepted to be representative of Piedmont surface soils.
2. Seismic CPT shear wave profile taken at the Savannah River site in South Carolina is shown in Figure H-12. This shear wave profile is generally representative of the soils at the U.S. Department of Energy Savannah River Site.
3. Seismic CPT shear wave profile taken at the Ravenel Bridge (Cooper River Bridge), located in Charleston, South Carolina, is shown in Figure H-13.
4. Seismic CPT shear wave profiles taken at Wetland Bridges 1 and 3 on US 17 between US Highway 21 intersection in Gardens Corner and the Combahee

River. Two shear wave profiles were developed for Bridges 1 & 2 and Bridges 3 & 4 as shown in Figure H-14. The SCPT B-14 taken at Bridge 1 is shown in Figure H-15 and B-5A taken at Bridge 3 is shown in Figure H-16.

5. Seismic CPT shear wave profiles taken for a new bridge on US 378 over Great Pee Dee River, approximately 18 miles east of Lake City, South Carolina. Representative shear wave profiles from two SCPT SC3 and SC4 are shown in Figure H-17 and H-19, respectively. The corresponding SCPT logs for SC3 and SC4 are shown in Figures H-18 and H-20, respectively.

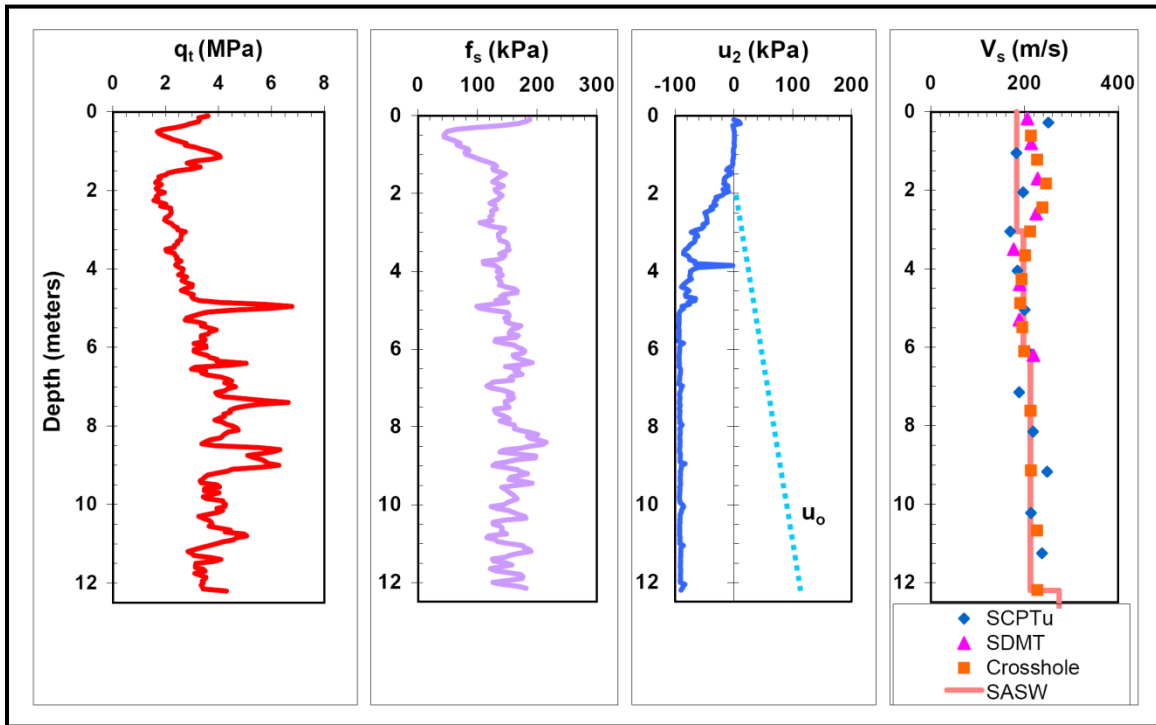


**Figure H-10, SCPT Piedmont Profile - NGES Opelika, Alabama  
(Mayne, et al. (2000) with permission from ASCE)**



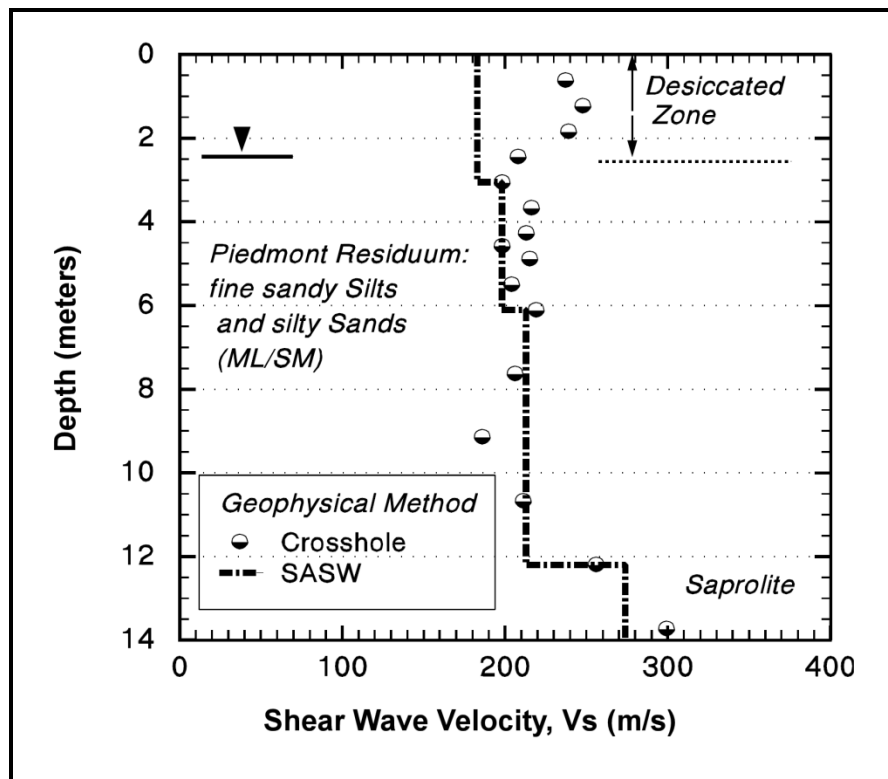


Figure H-11, Geophysical  $V_s$  Piedmont Profile - NGES Opelika, Alabama (Mayne, et al. (2000) with permission from ASCE)

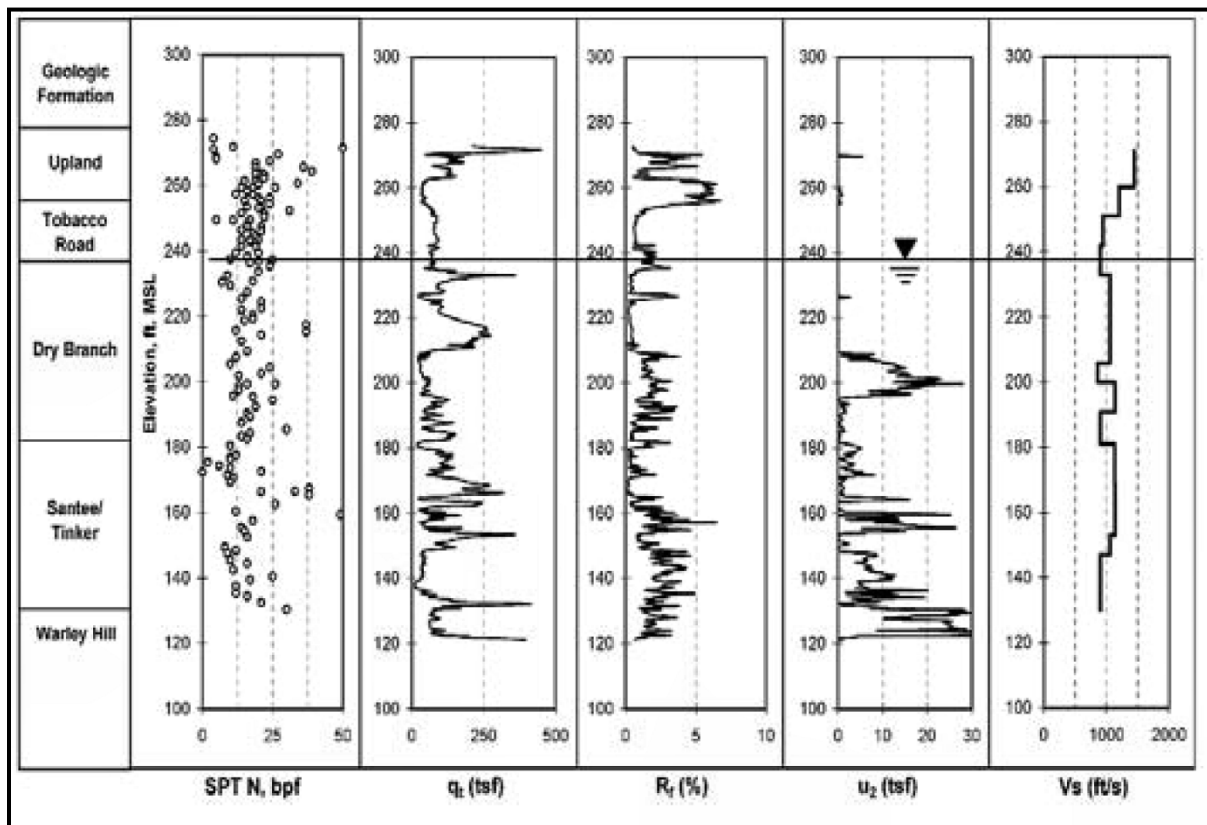


Figure H-12, SCPT Profile Savannah River, South Carolina (Lewis, et al. (2004))

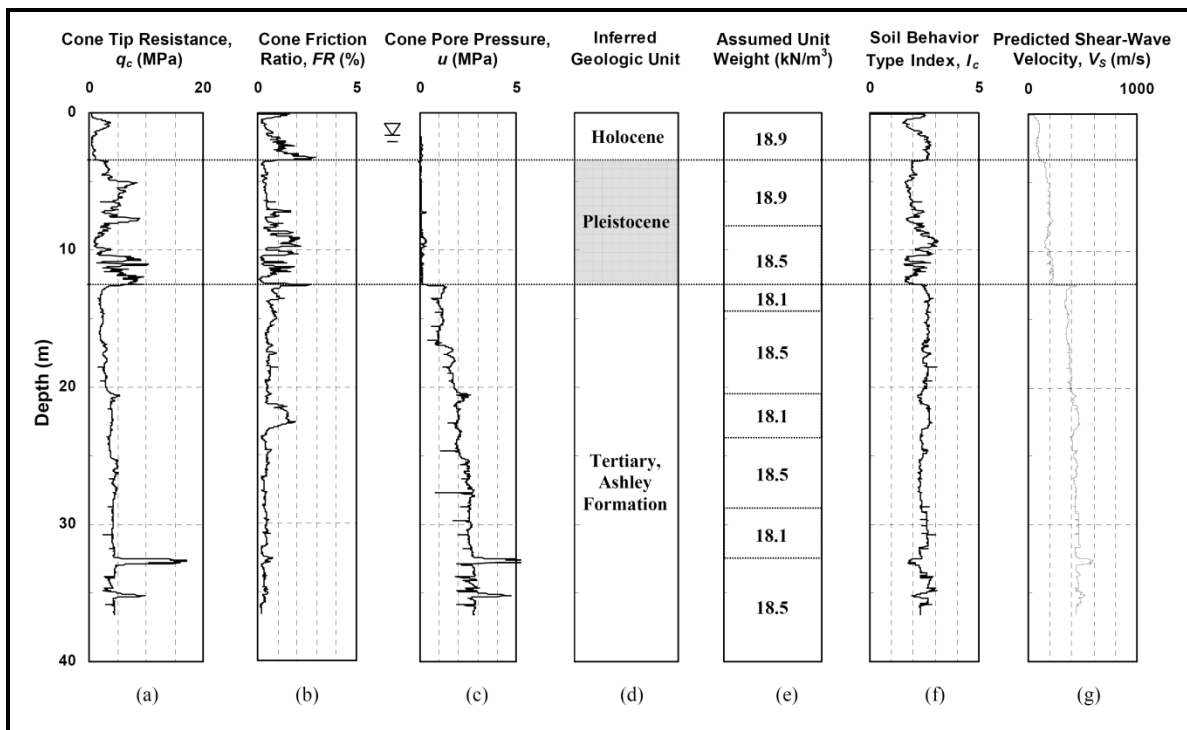


Figure H-13, SCPT Profile (DS-1) Cooper River Bridge, Charleston, SC (S&ME (2000))

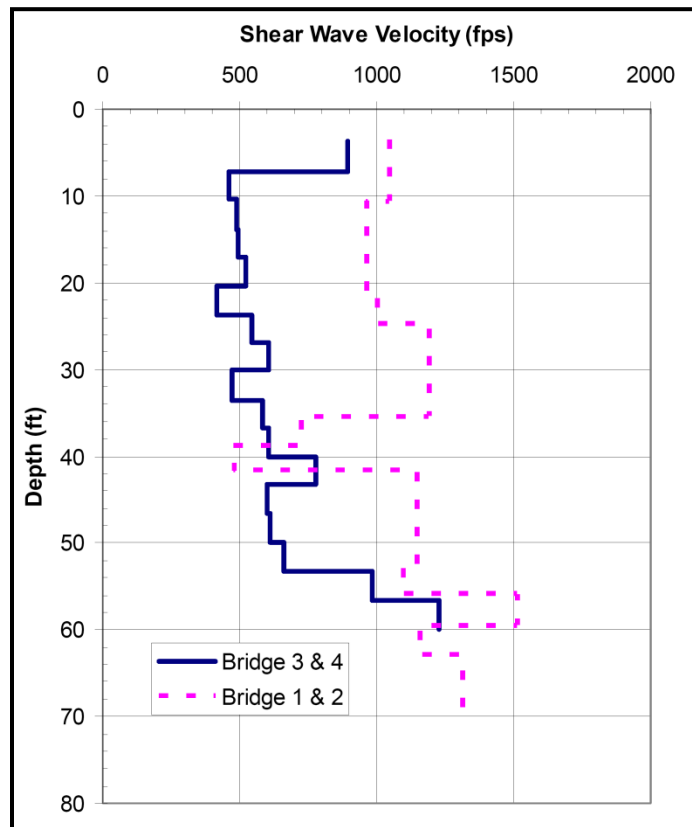


Figure H-14, Shear Wave Profile US 17, Beaufort County, South Carolina (S&ME (2007))

Geologic profiles provided in Figures H-15 and H-16

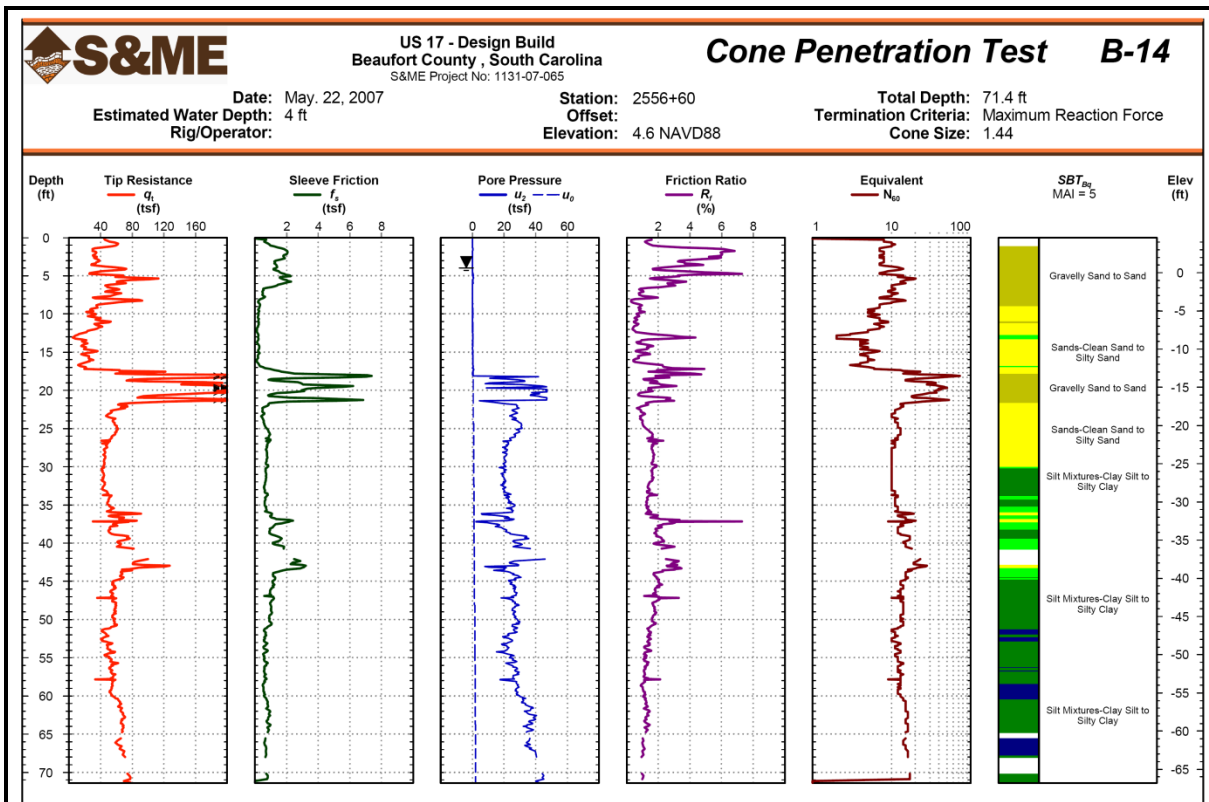


Figure H-15, SCPT (B-14) US 17 Bridge 1, Beaufort County, South Carolina (S&ME (2007))

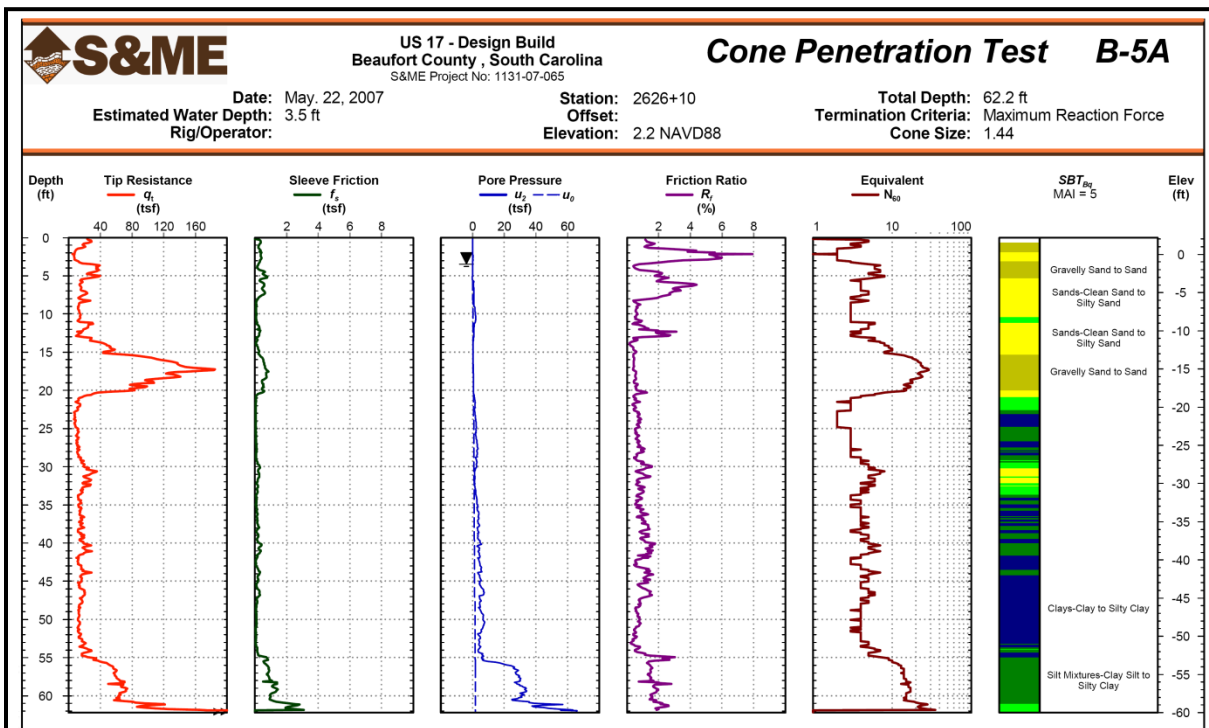


Figure H-16, SCPT (B-5A) US 17 Bridge 3, Beaufort County, South Carolina (S&ME (2007))

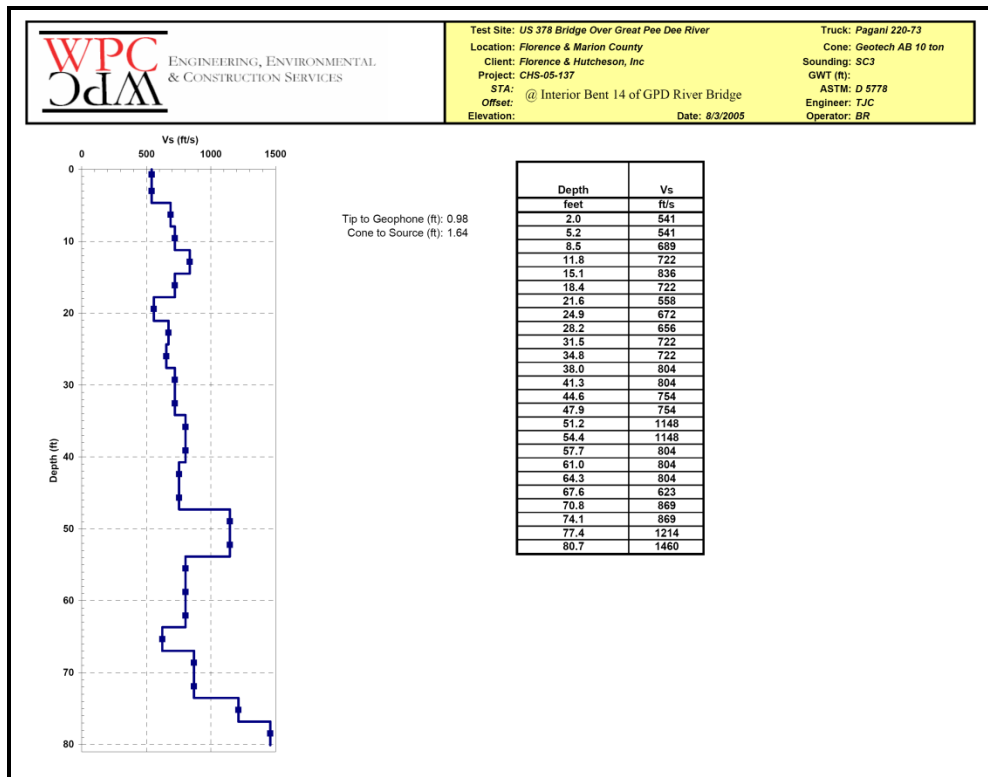


Figure H-17, Shear Wave Profile (SC3) - US 378, Lake City, South Carolina (Florence & Hutcheson (2006))

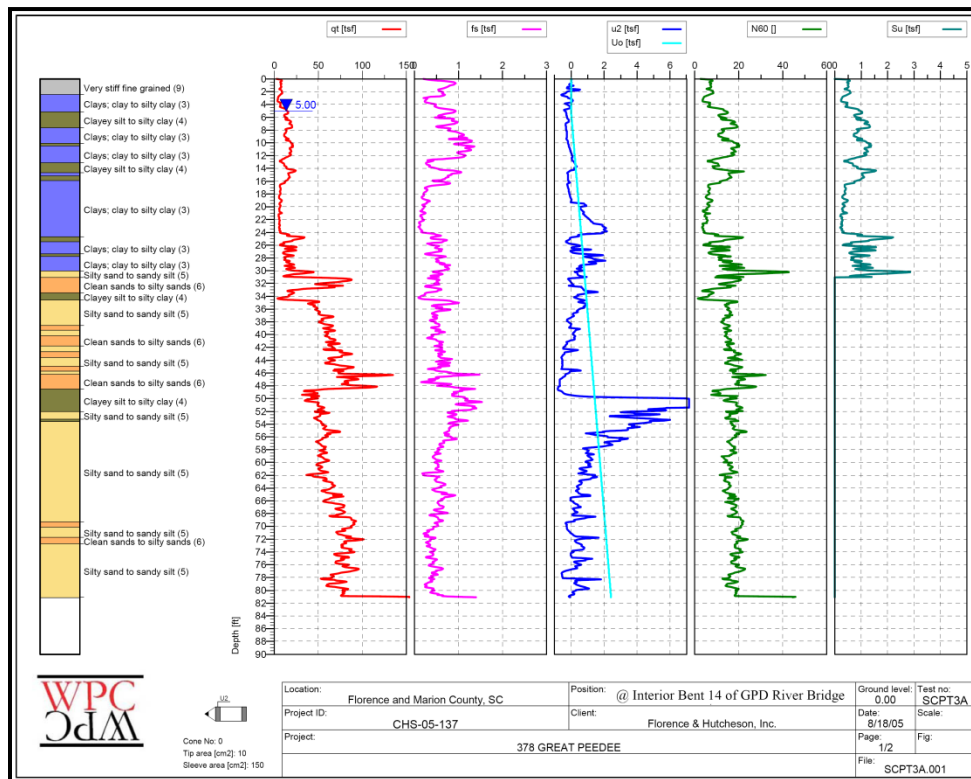


Figure H-18, SCPT (SC3) - US 378, Lake City, South Carolina (Florence & Hutcheson (2006))

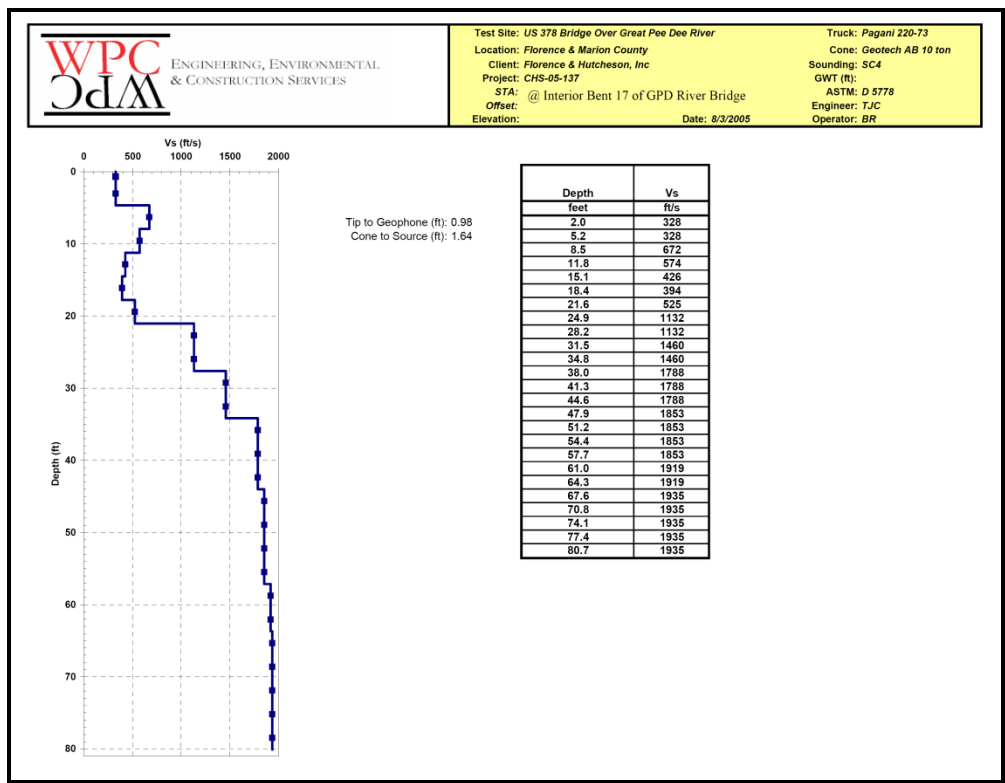


Figure H-19, Shear Wave Profile (SC4) - US 378, Lake City, South (Florence & Hutcheson (2006))

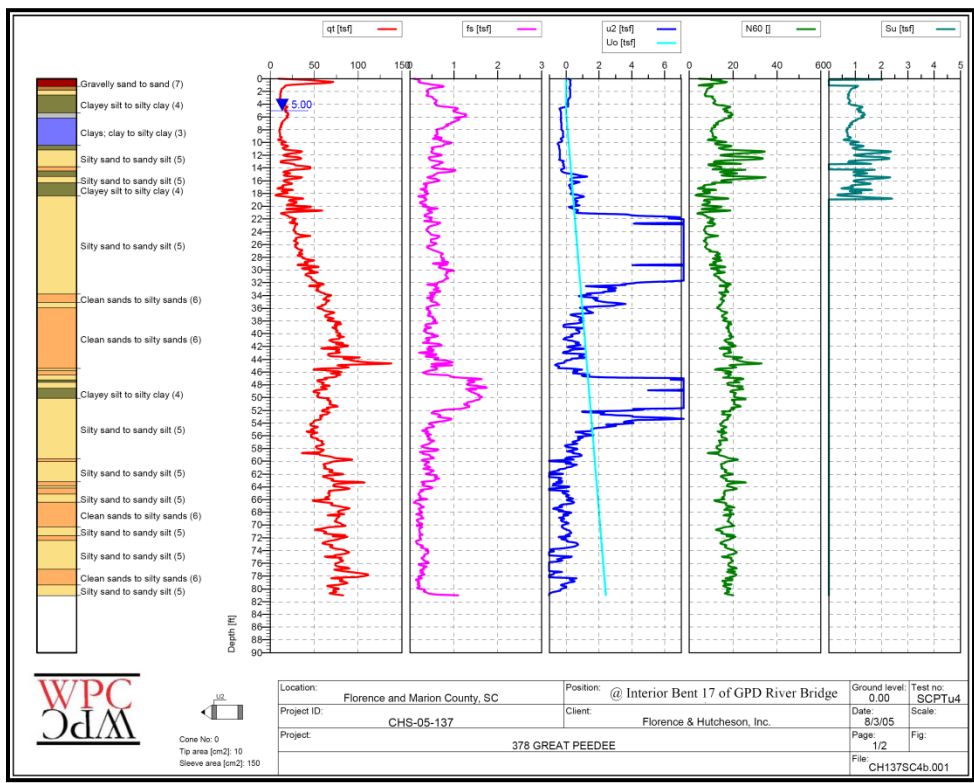


Figure H-20, SCPT (SC4) - US 378, Lake City, South Carolina (Florence & Hutcheson (2006))





- SCPT-01 and SCPT-02 located in Myrtle Beach, SC at the intersection of Carolina Bays Parkway (SC 31) and SC 544. This site is located in the Lower Coastal Plain Physiographic Province.
- SB-09 is located in York County, S-655 (Auten Road) over Fishing Creek. This site is located in the Piedmont Physiographic Province.
- Maybank Highway (SC 700) is located near Charleston, SC and is located in the Lower Coastal Plain Physiographic Province.
- SC-85 is located in Spartanburg, SC over Norfolk-Southern Railway, S-995 and S-2. This site is located in the Piedmont Physiographic Province.
- Withers Swash is located in Myrtle Beach, SC and is located in the Lower Coastal Plain Physiographic Province.

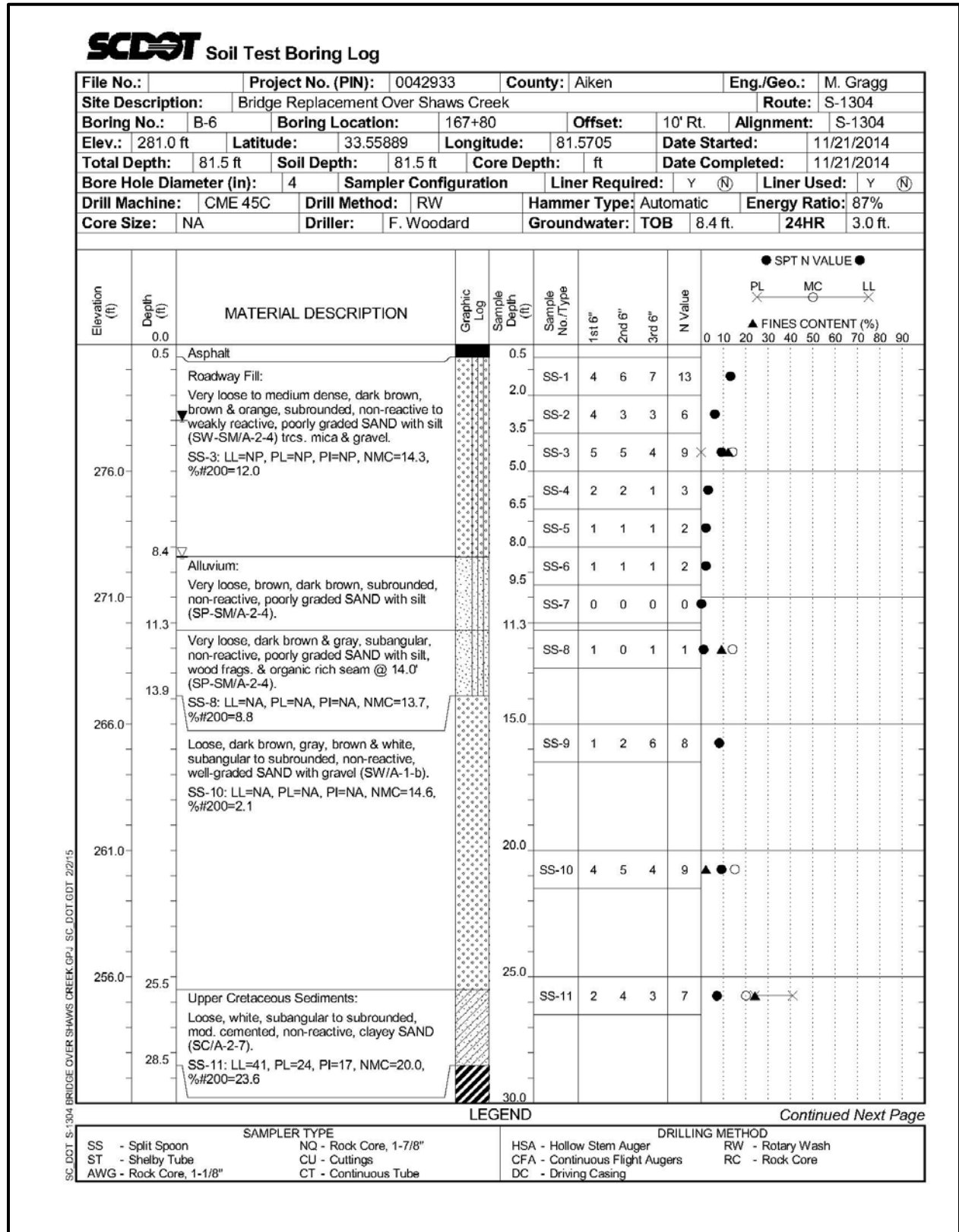


Figure H-22, Soil Test Boring DHT-1/B-6



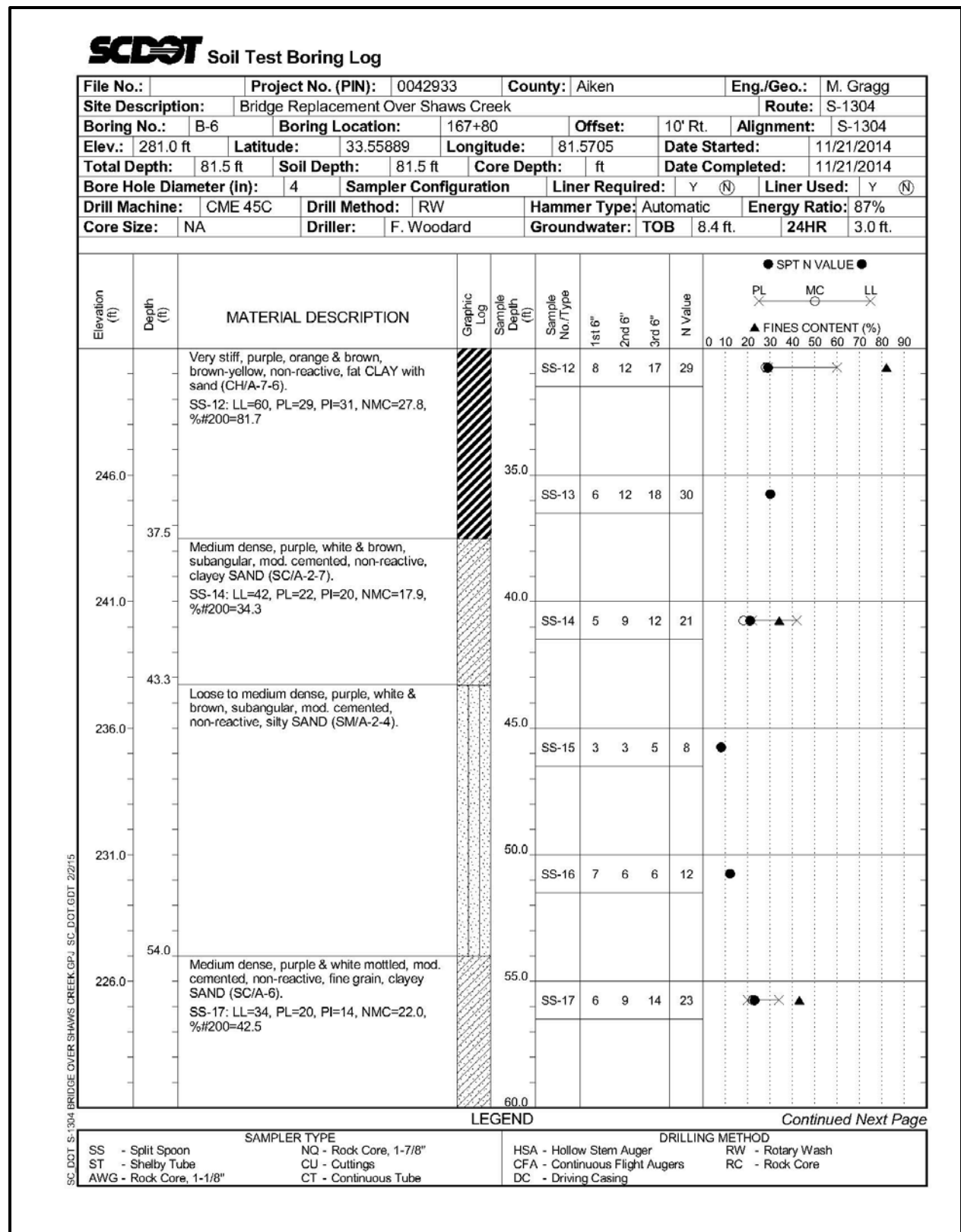


Figure H-23, Soil Test Boring DHT-1/B-6 (con't)

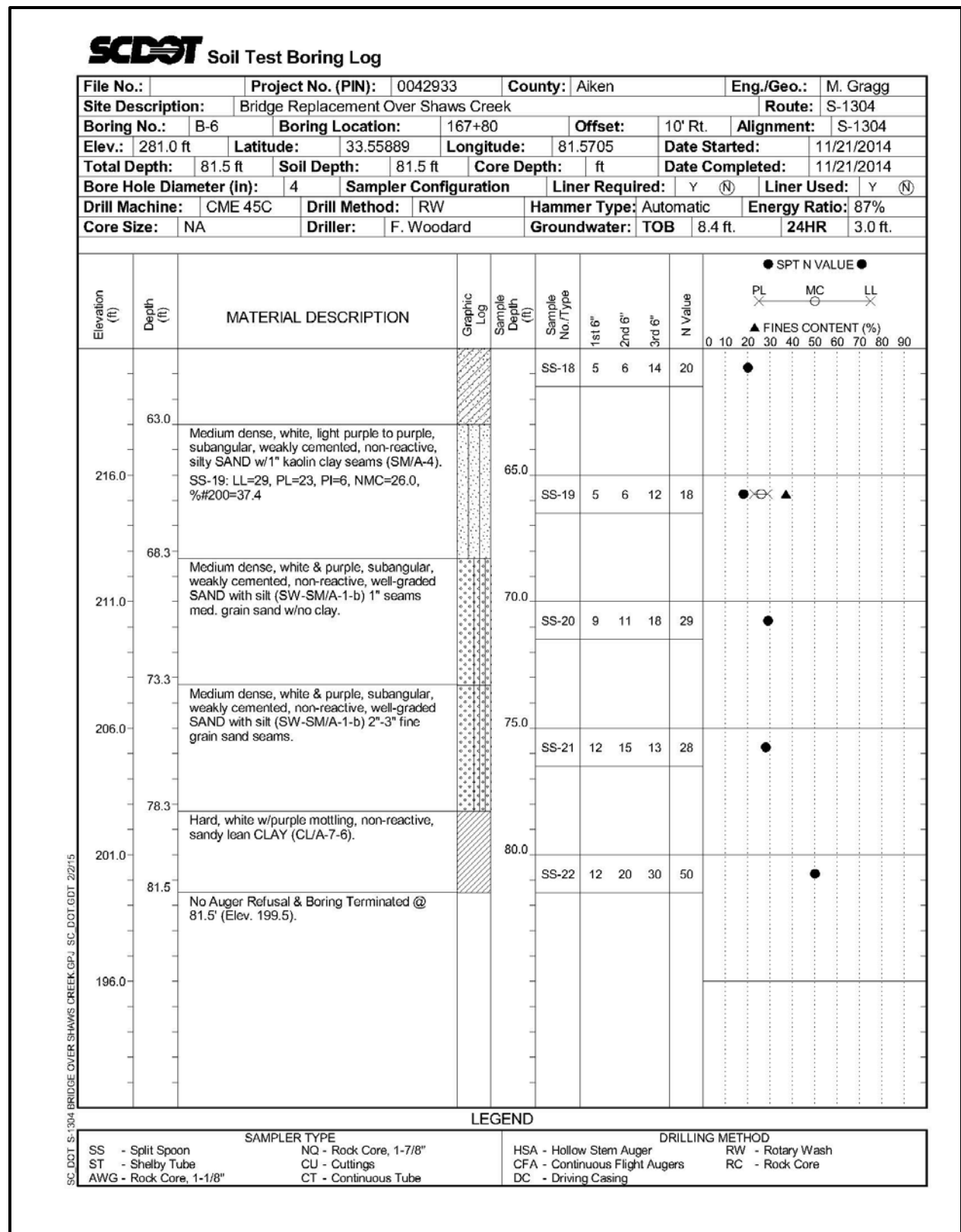


Figure H-24, Soil Test Boring DHT-1/B-6 (con't)

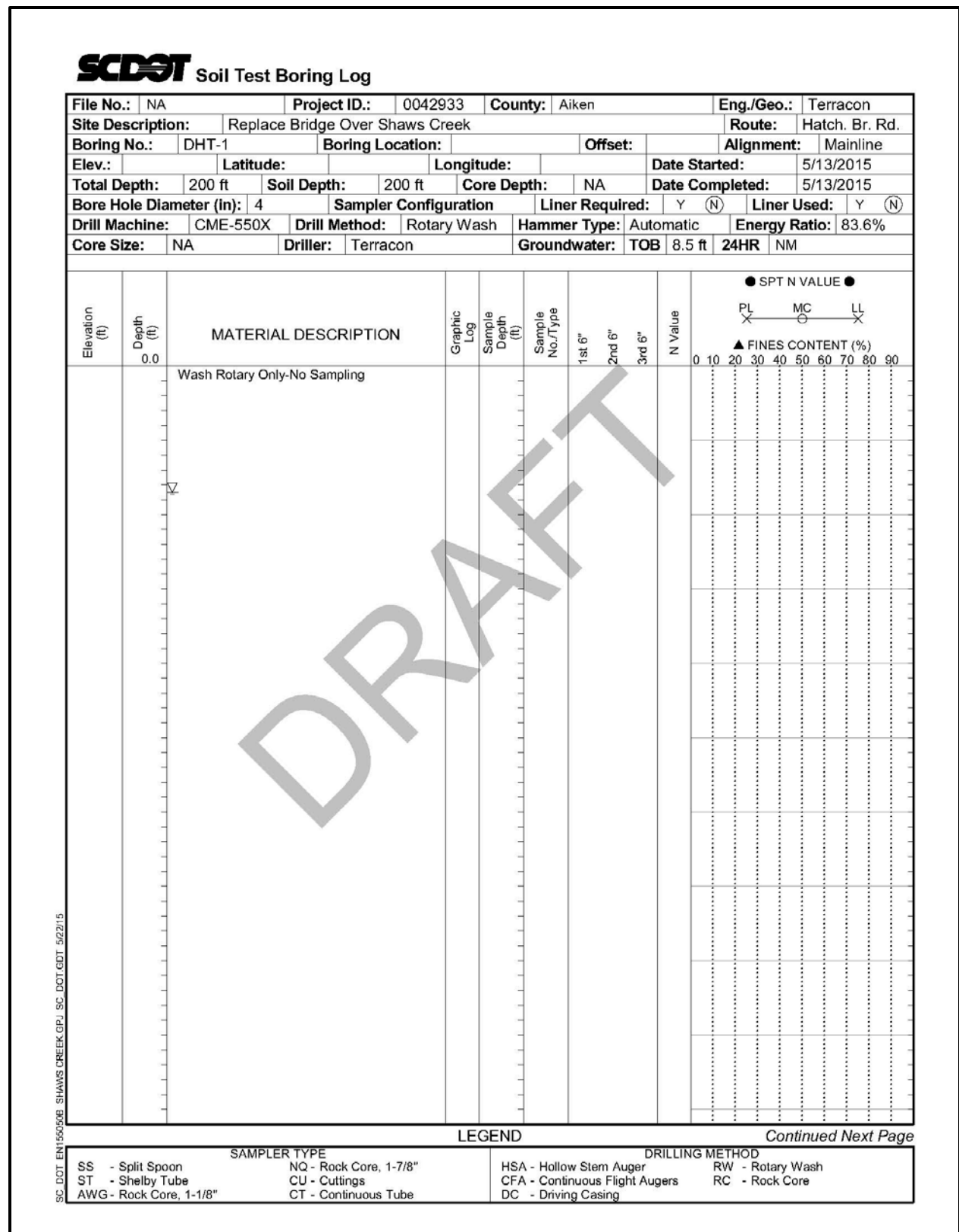


Figure H-25, Soil Test Boring DHT-1/B-6 (con't)

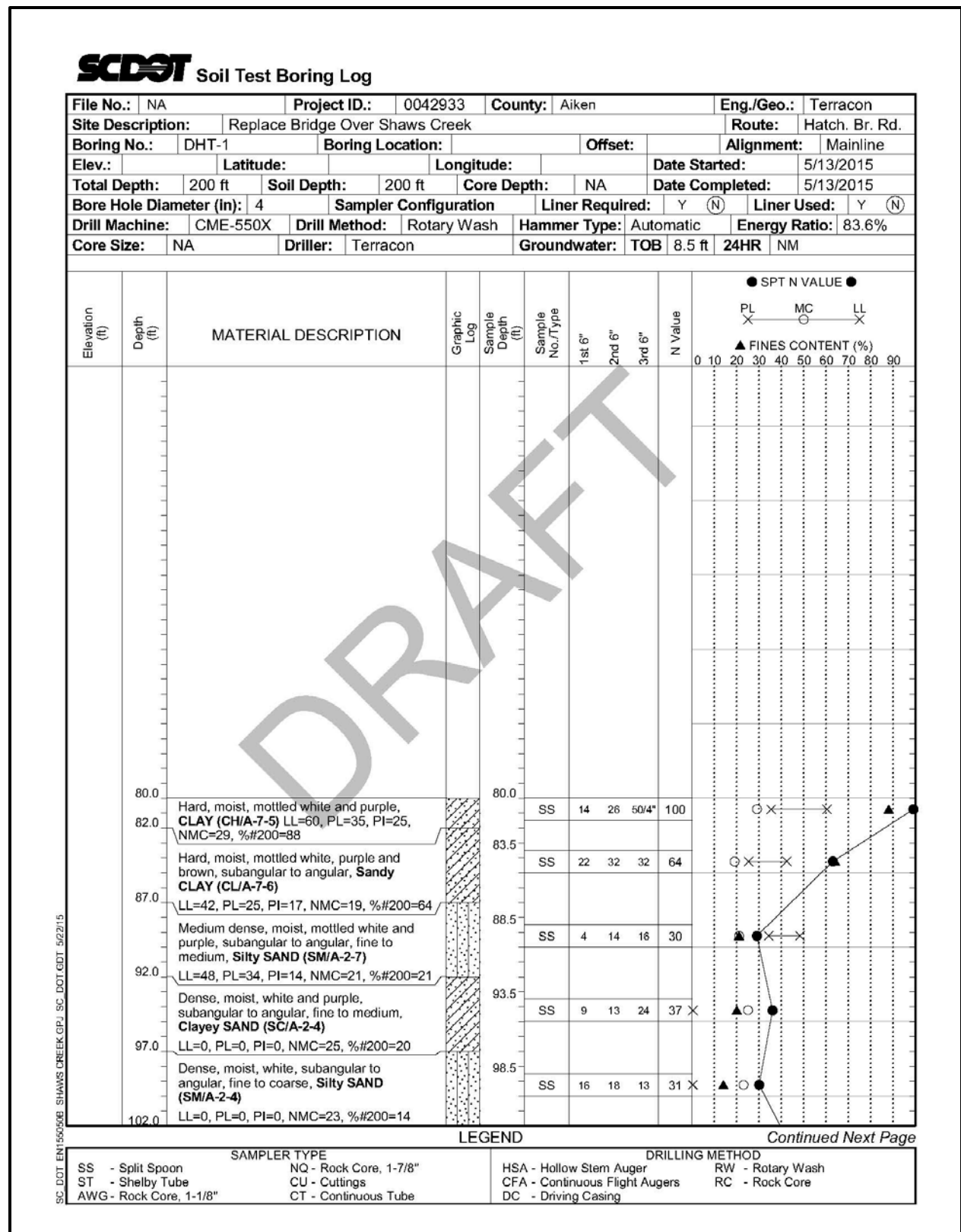


Figure H-26, Soil Test Boring DHT-1/B-6 (con't)

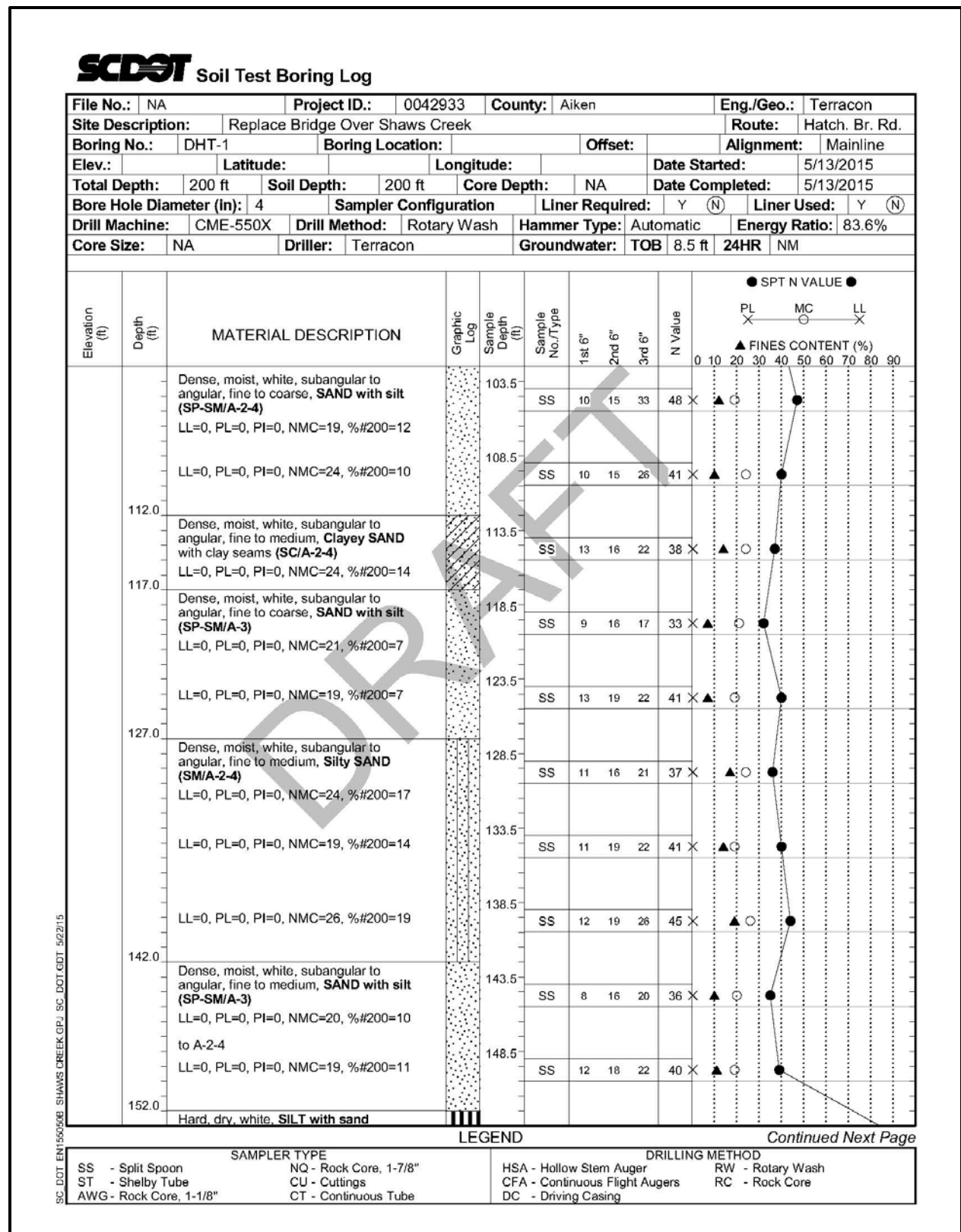


Figure H-27, Soil Test Boring DHT-1/B-6 (con't)

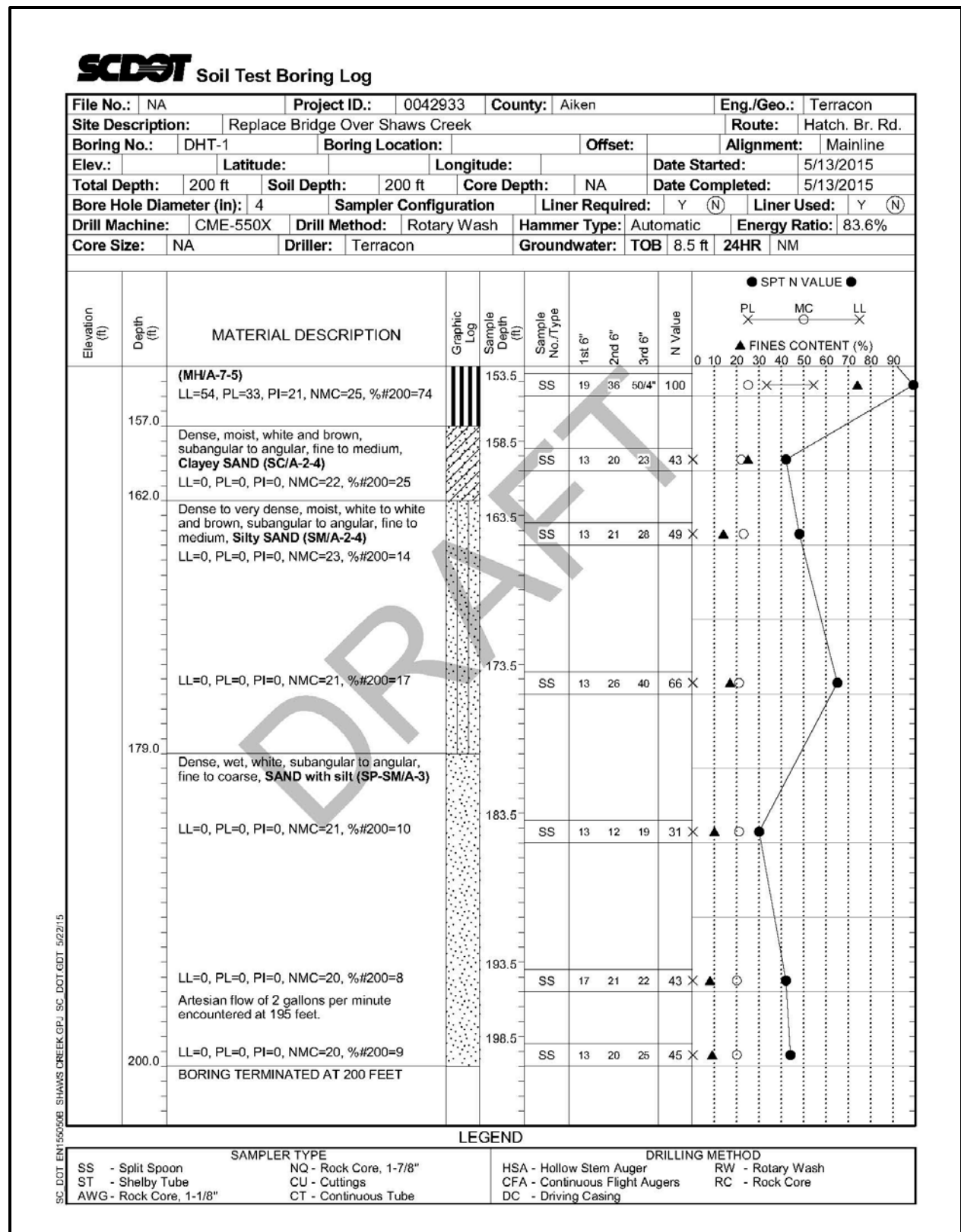


Figure H-28, Soil Test Boring DHT-1/B-6 (con't)

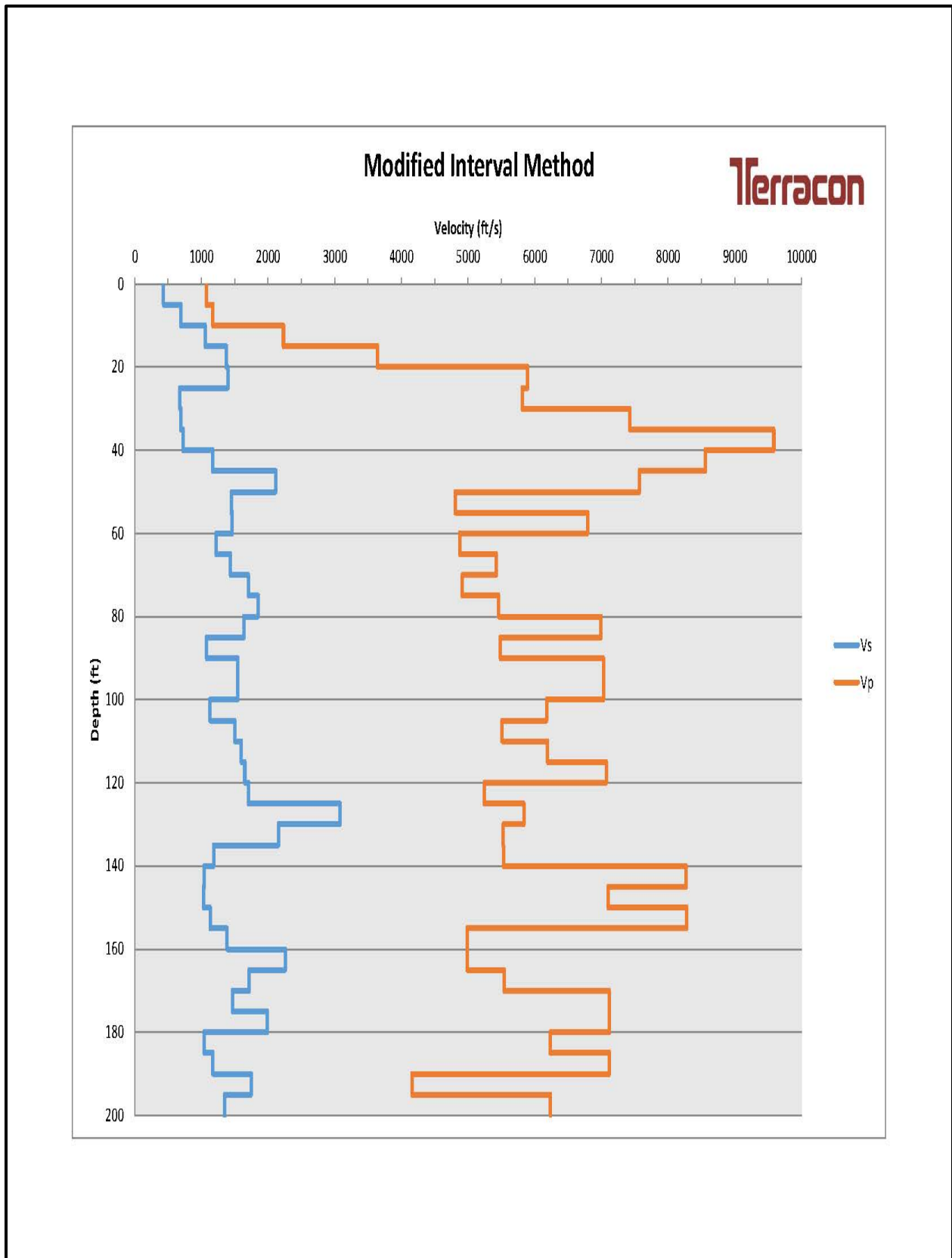


Figure H-29,  $V_s$  and  $V_p$  Profile – DHT-1/B-6

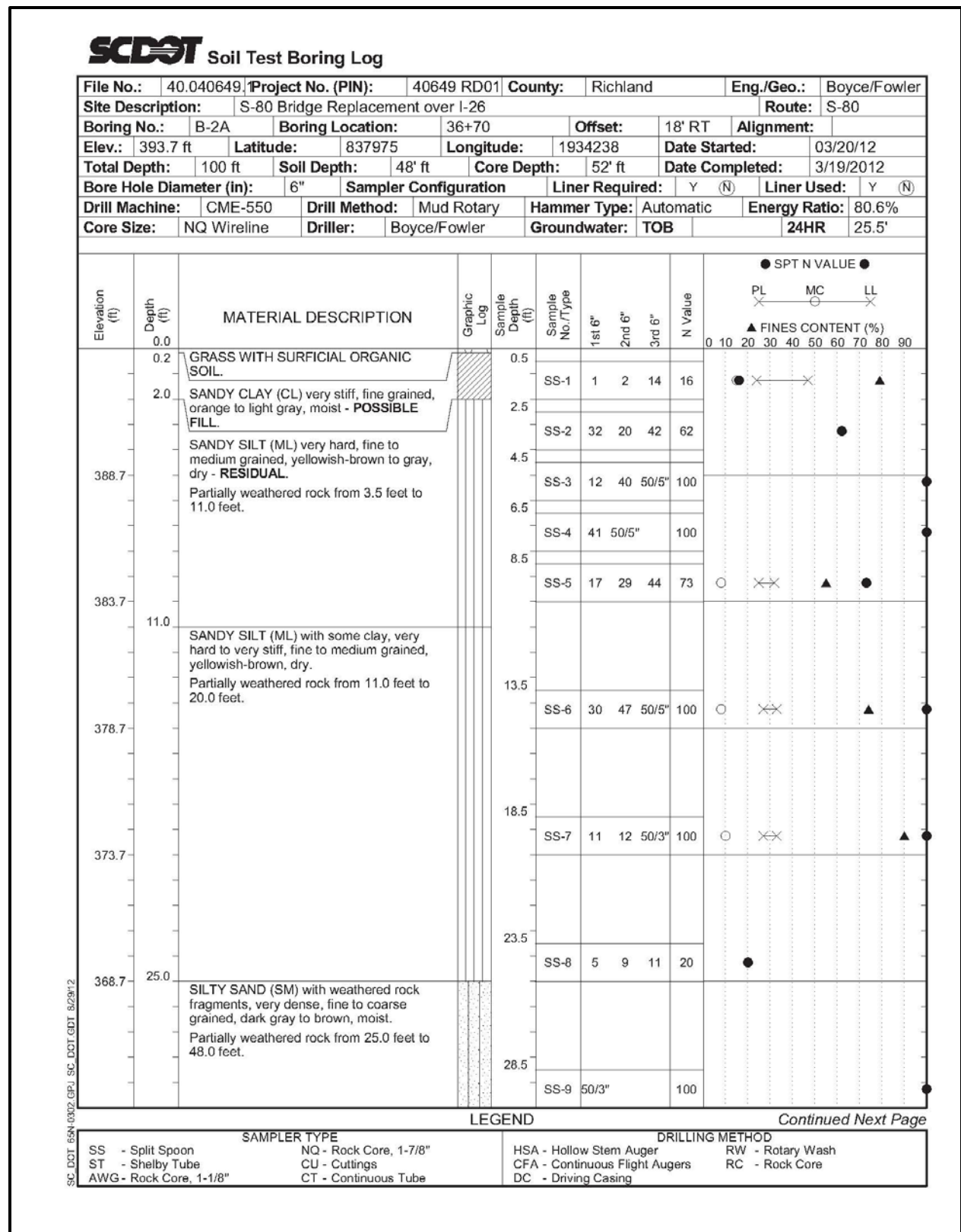


Figure H-30, Soil Test Boring B-2A



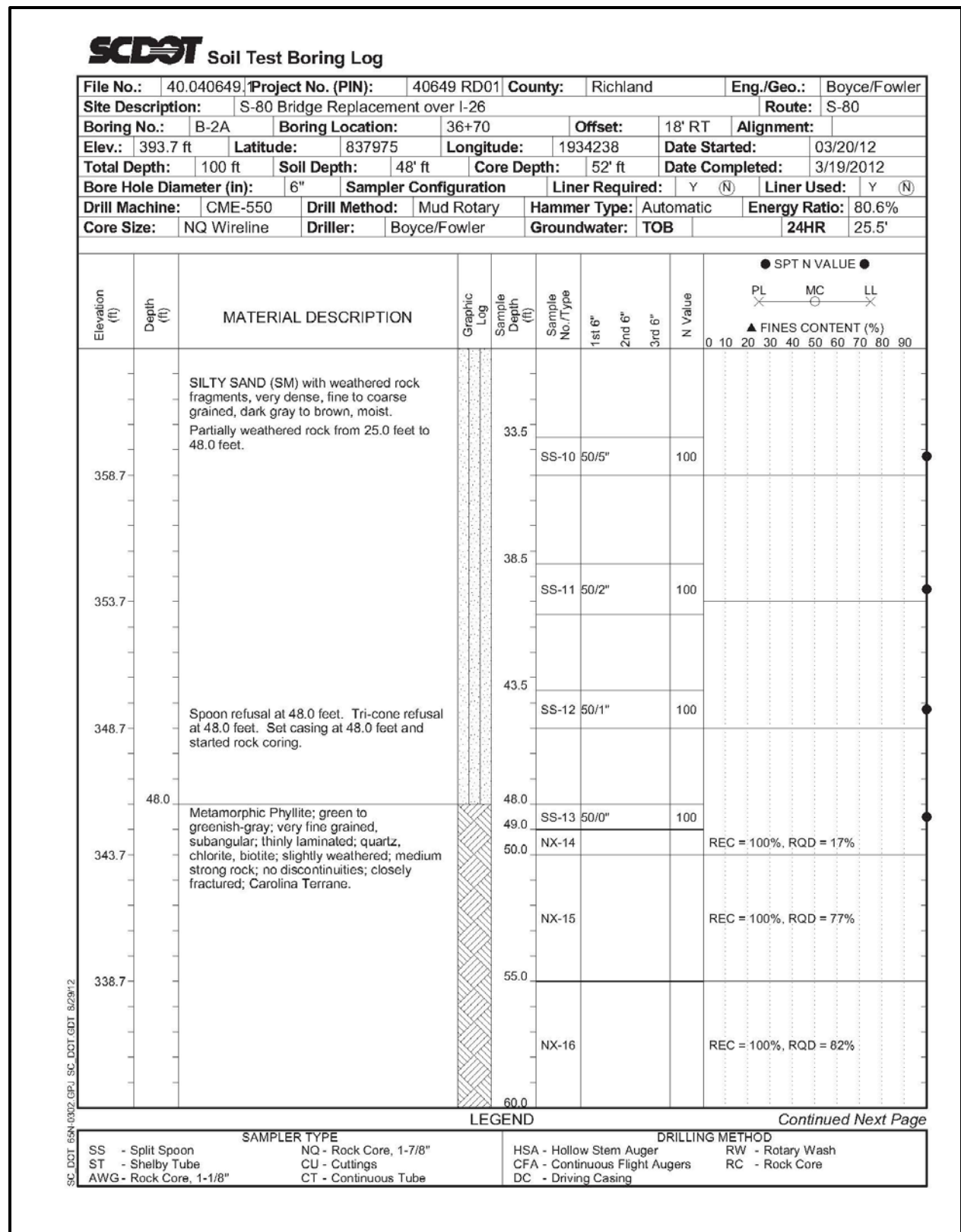


Figure H-31, Soil Test Boring B-2A (con't)

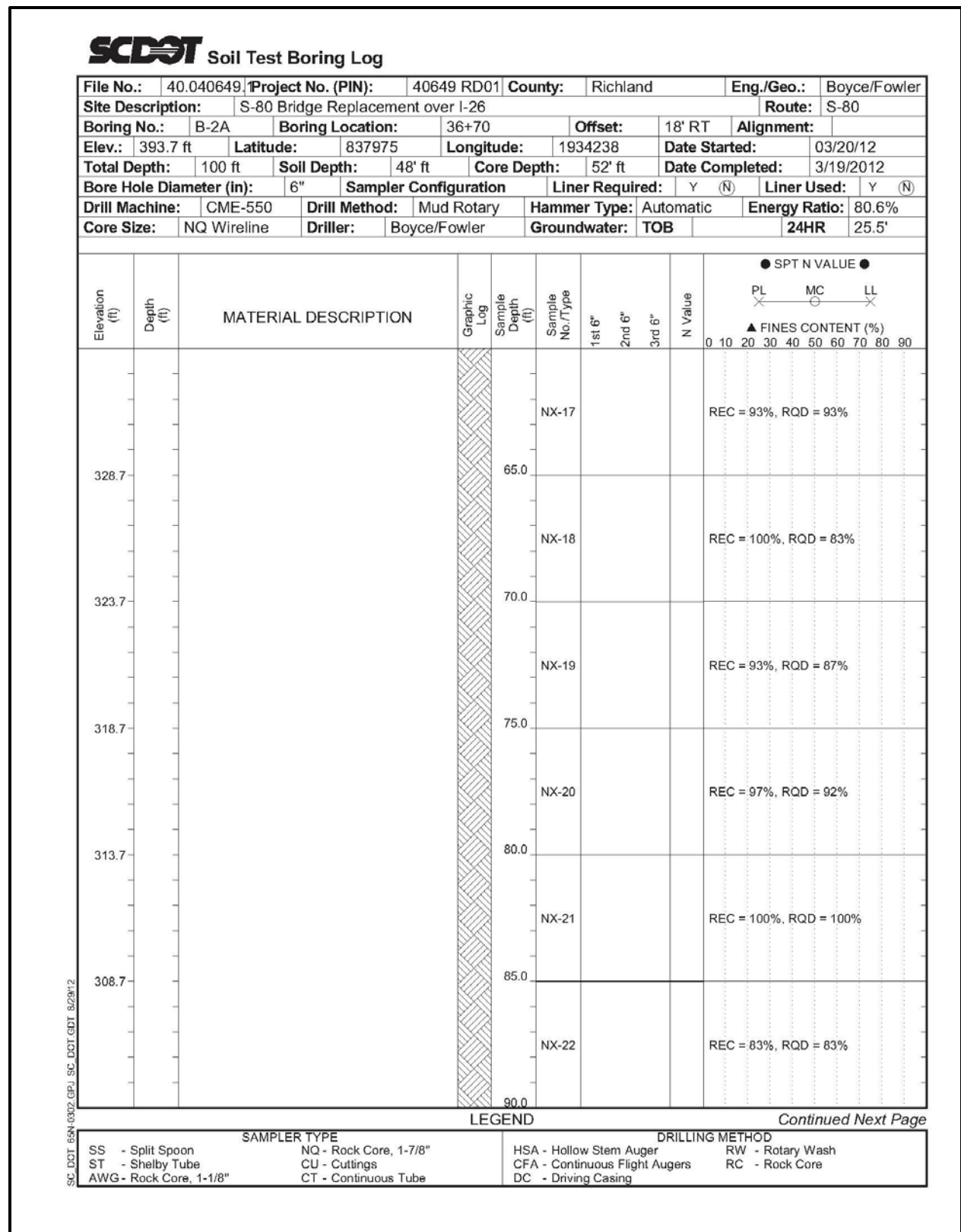


Figure H-32, Soil Test Boring B-2A (con't)

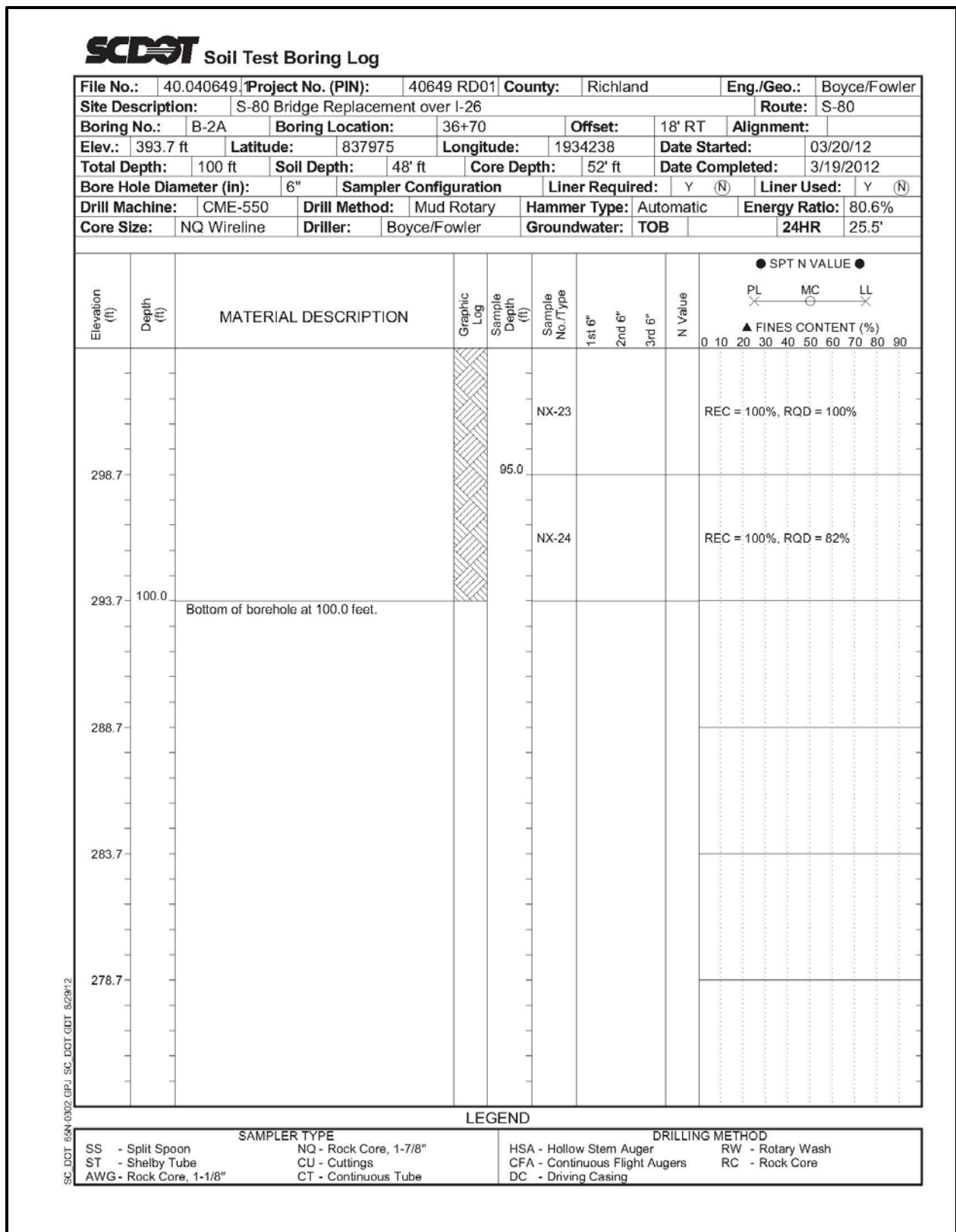


Figure H-33, Soil Test Boring B-2A (con't)

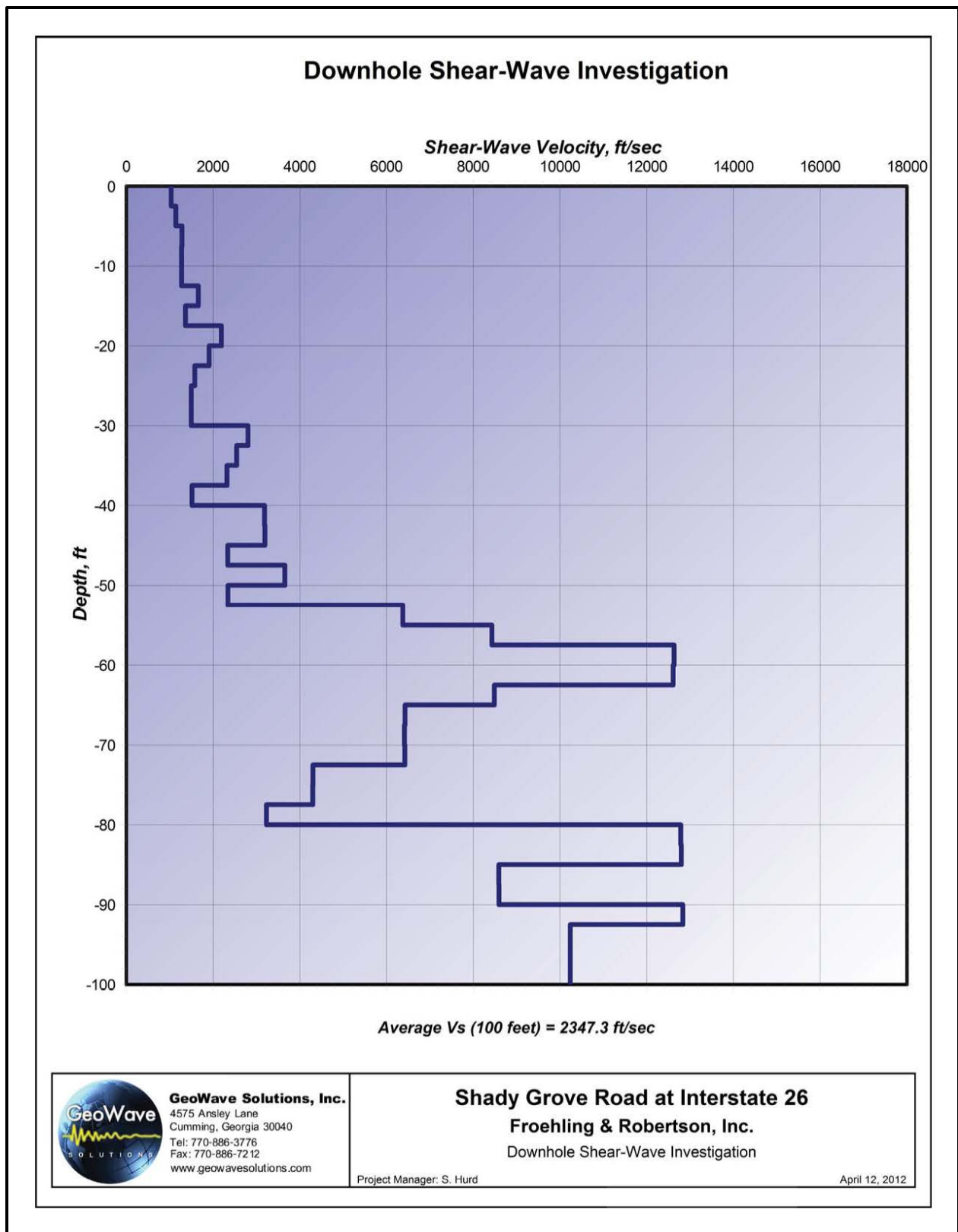



Figure H-34,  $V_s$  Profile B-2A

### Downhole Shear-Wave Investigation

Depth (ft)	Vs ( ft/sec)
0.0	1034.80
-2.5	1034.80
-5.0	1141.90
-7.5	1283.00
-12.5	1276.70
-15.0	1662.00
-17.5	1367.10
-20.0	2193.30
-22.5	1910.20
-25.0	1581.50
-27.5	1498.90
-30.0	1498.90
-32.5	2808.00
-35.0	2546.80
-37.5	2325.40
-40.0	1516.90
-42.5	3189.60
-45.0	3200.60
-47.5	2339.30
-50.0	3660.40
-52.5	2343.30
-55.0	6377.60
-57.5	8434.80
-60.0	12636.10
-62.5	12614.70
-65.0	8490.90
-67.5	6430.10
-70.0	6419.70
-72.5	6425.20
-75.0	4306.30
-77.5	4300.50
-80.0	3234.60
-82.5	12792.40
-85.0	12805.30
-87.5	8592.60
-90.0	8597.10
-92.5	12837.20
-93.5	10241.30
-100.0	10241.30

*Average Vs (100 feet) = 2347.3 ft/sec*

	<b>GeoWave Solutions, Inc.</b> 4575 Ansley Lane Cumming, Georgia 30040 Tel: 770-886-3776 Fax: 770-886-7212 www.geowavesolutions.com	<b>Shady Grove Road at Interstate 26</b> <b>Froehling &amp; Robertson, Inc.</b> Downhole Shear-Wave Investigation  PI Project Manager: S. Hurd	April 12, 2012
---	--	--	----------------

**Figure H-35, Tabulated V<sub>s</sub> Results – B-2A**

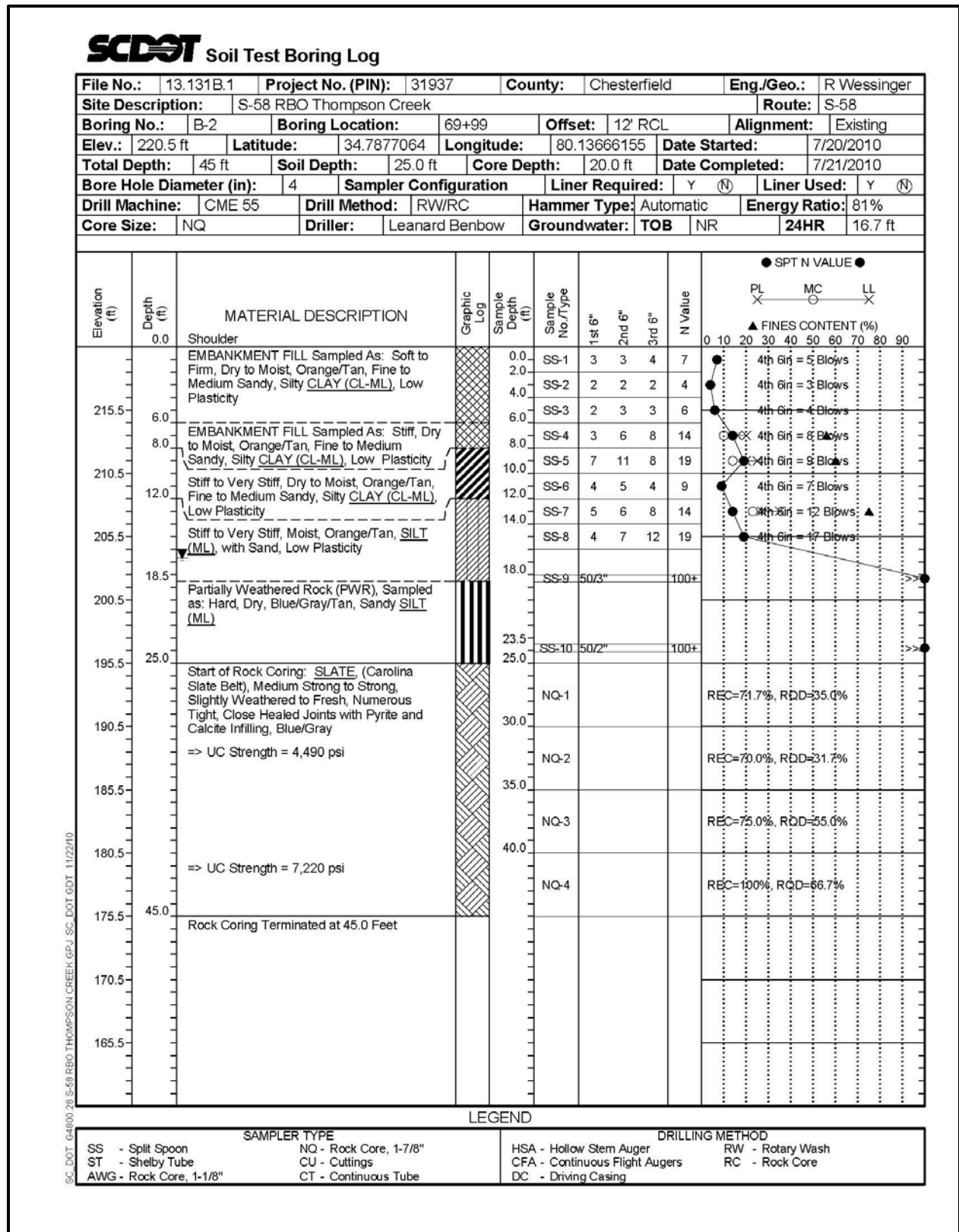
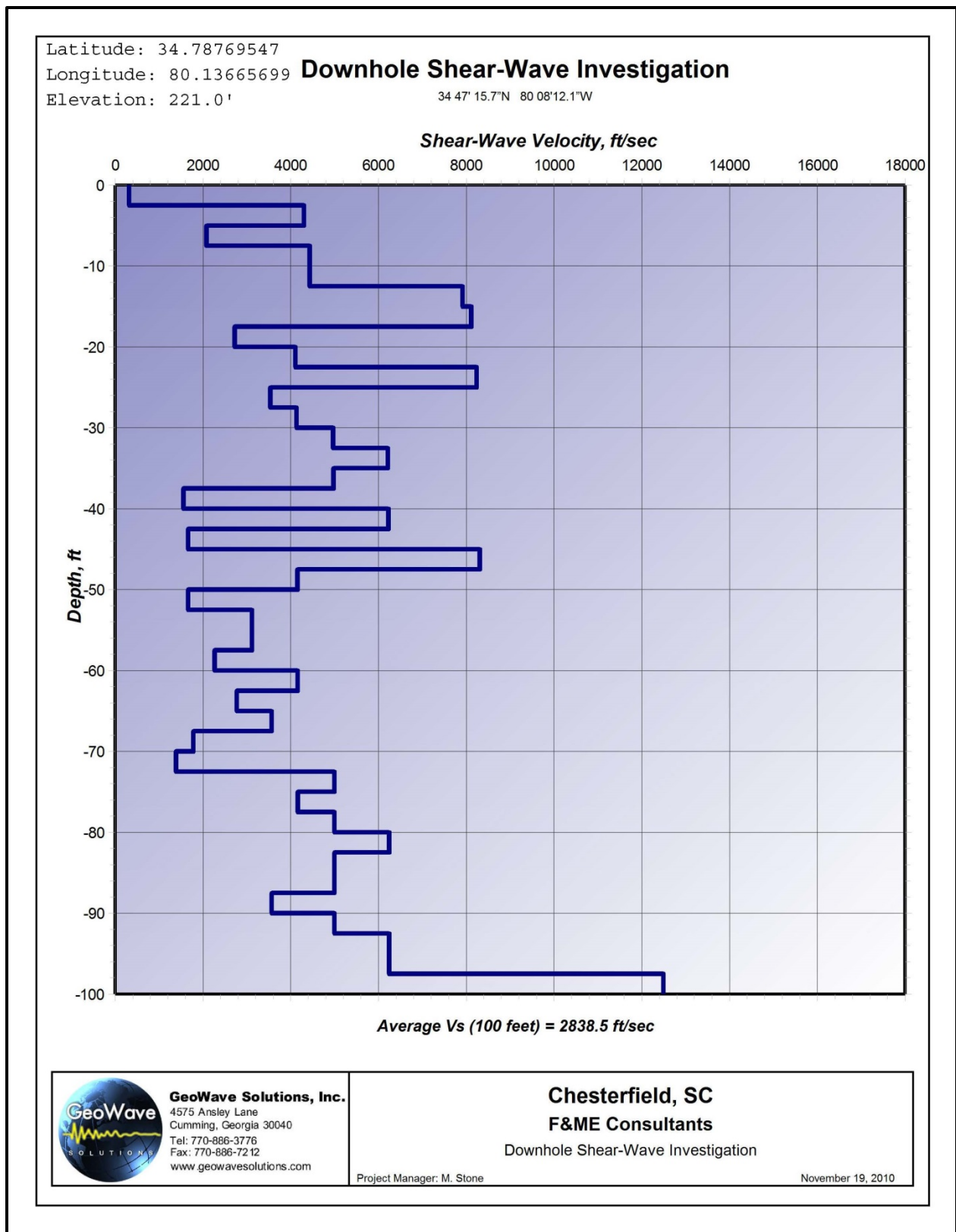


Figure H-36, Soil Test Boring B-2





**Figure H-37, Vs Profile B-2**

### Downhole Shear-Wave Investigation

34 47' 15.7"N 80 08'12.1"W

Depth (ft)	Vs ( ft/sec)
0.0	320.00
-2.5	4303.94
-5.0	2083.93
-7.5	4435.62
-12.5	7914.93
-15.0	8114.78
-17.5	2725.14
-20.0	4107.03
-22.5	8240.11
-25.0	3539.36
-27.5	4135.98
-30.0	4969.26
-32.5	6217.44
-35.0	4977.65
-37.5	1556.44
-40.0	6228.78
-42.5	1661.67
-45.0	8311.11
-47.5	4156.72
-50.0	1663.09
-52.5	3118.92
-55.0	3119.47
-57.5	2269.06
-60.0	4160.50
-62.5	2773.99
-65.0	3566.94
-67.5	1783.63
-70.0	1387.39
-72.5	4994.96
-75.0	4162.75
-77.5	4995.60
-80.0	6244.85
-82.5	4996.13
-85.0	4996.35
-87.5	3568.97
-90.0	4996.75
-92.5	6246.16
-95.0	6246.36
-97.5	12493.10
-100.0	12493.44

**Average Vs (100 feet) = 2838.5 ft/sec**



**GeoWave Solutions, Inc.**  
 4575 Ansley Lane  
 Cumming, Georgia 30040  
 Tel: 770-886-3776  
 Fax: 770-886-7212  
 www.geowavesolutions.com

**Chesterfield, SC**  
**F&ME Consultants**  
 Downhole Shear-Wave Investigation

Project Manager: M. Stone

November 19, 2010

**Figure H-38, Tabulated Vs Results – B-2**



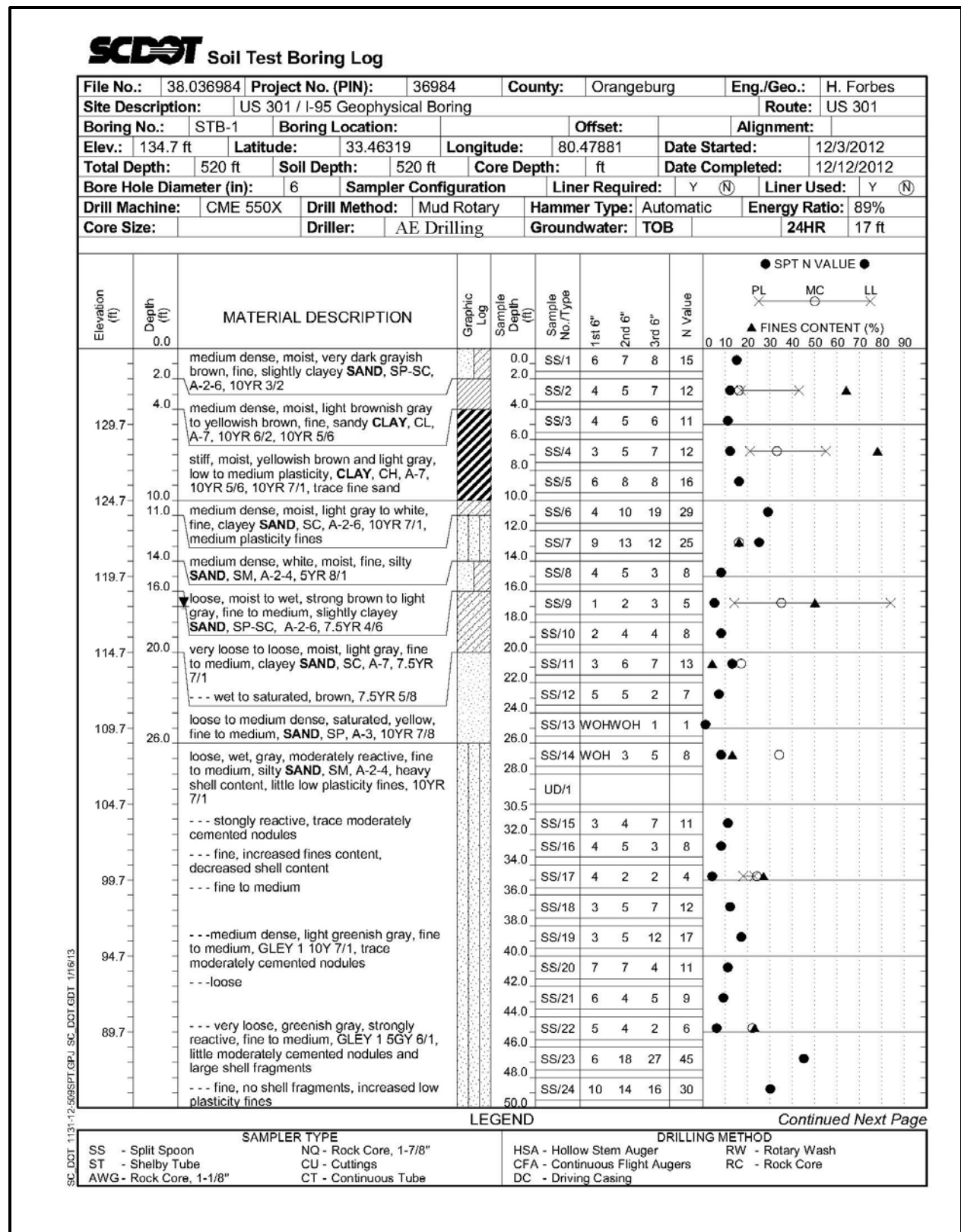


Figure H-39, Soil Test Boring STB-1

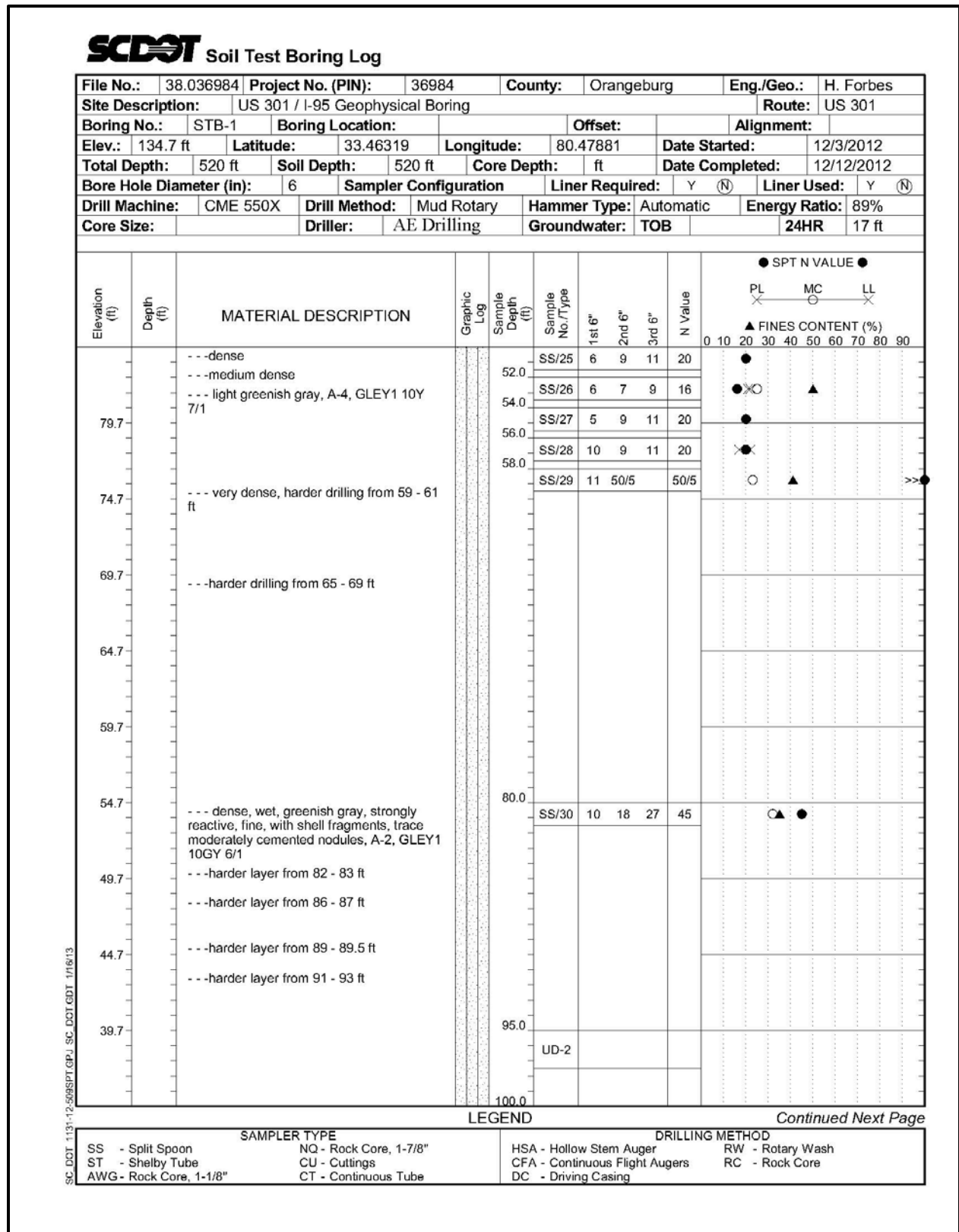


Figure H-40, Soil Test Boring STB-1 (con't)

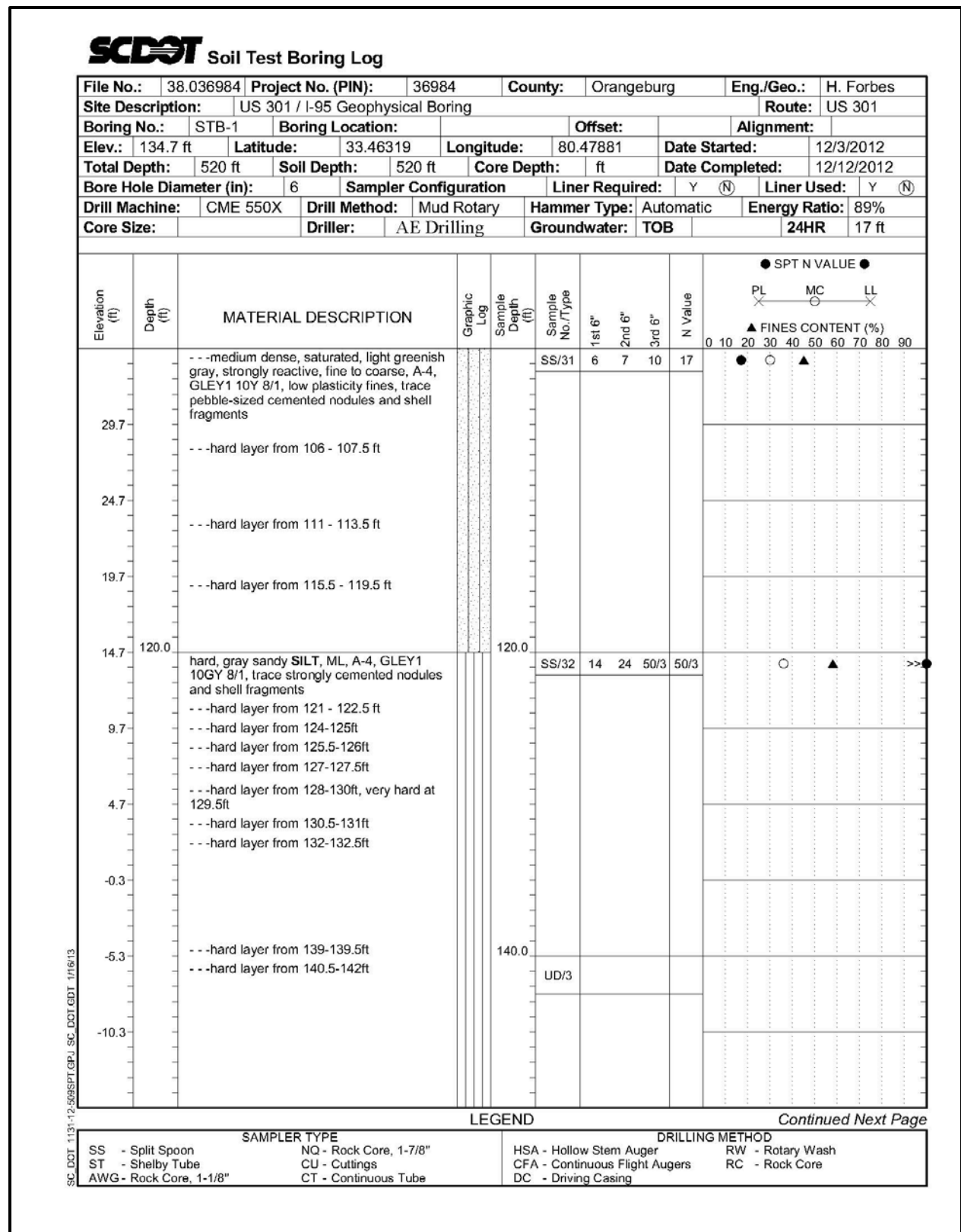


Figure H-41, Soil Test Boring STB-1 (con't)

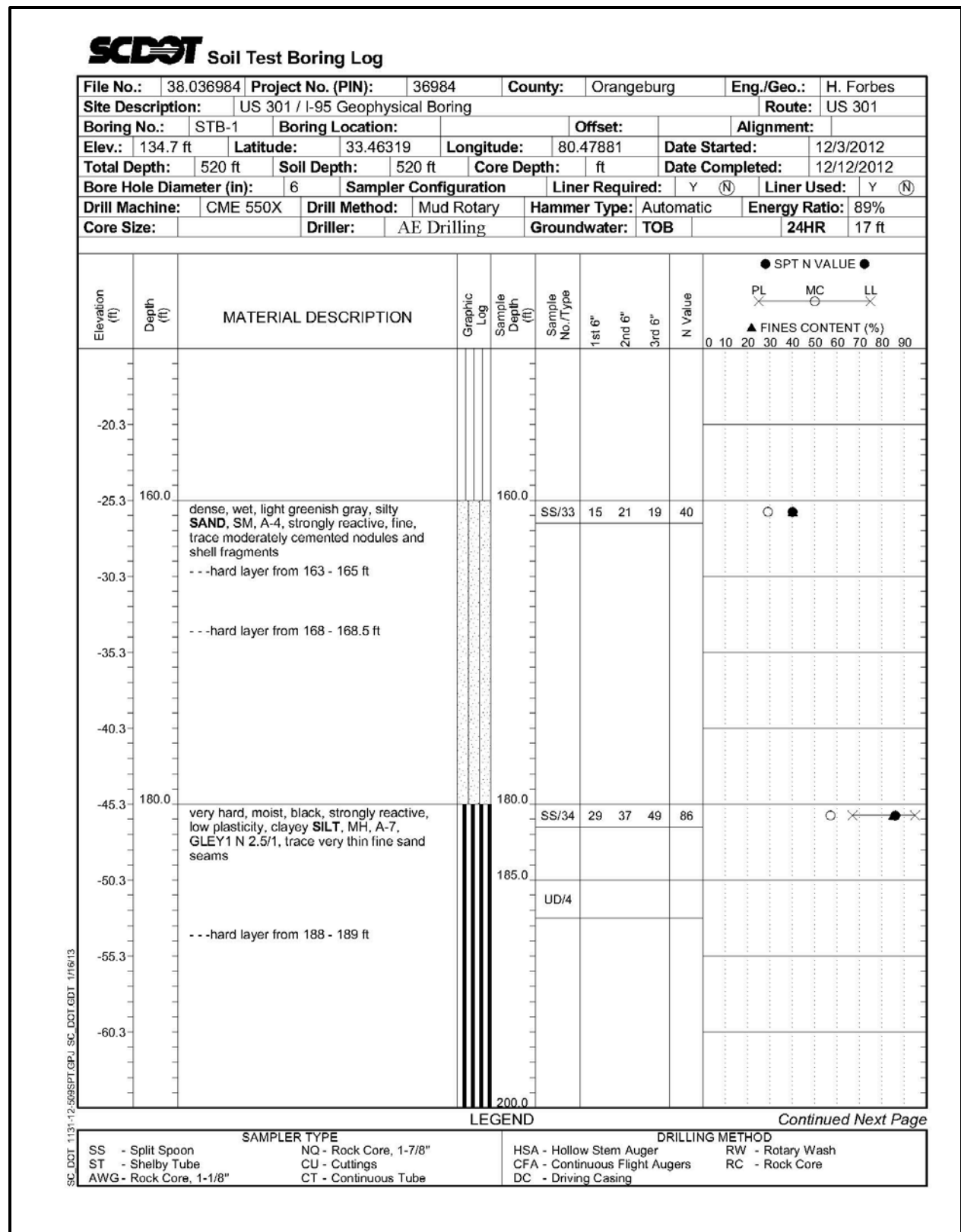


Figure H-42, Soil Test Boring STB-1 (con't)

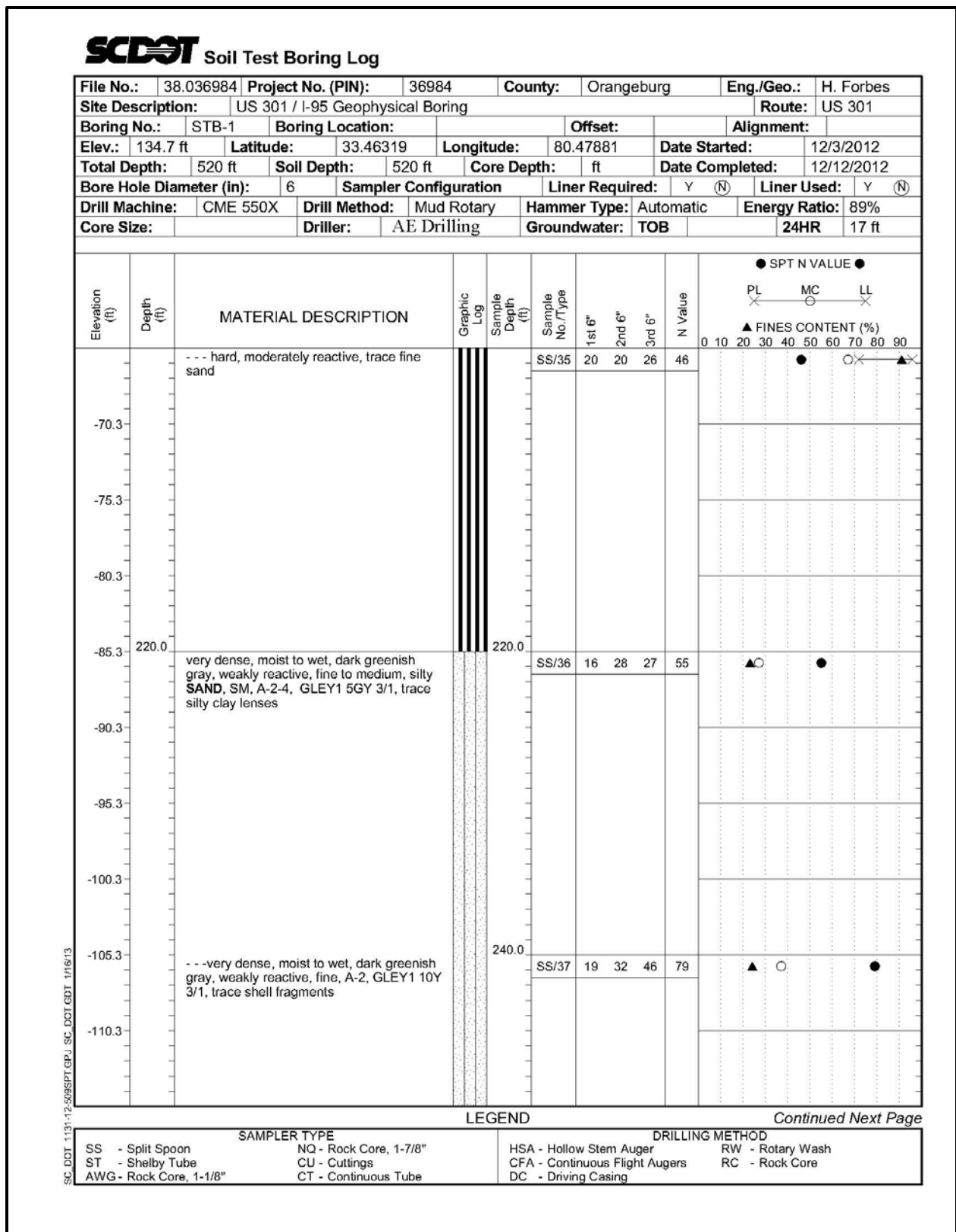


Figure H-43, Soil Test Boring STB-1 (con't)

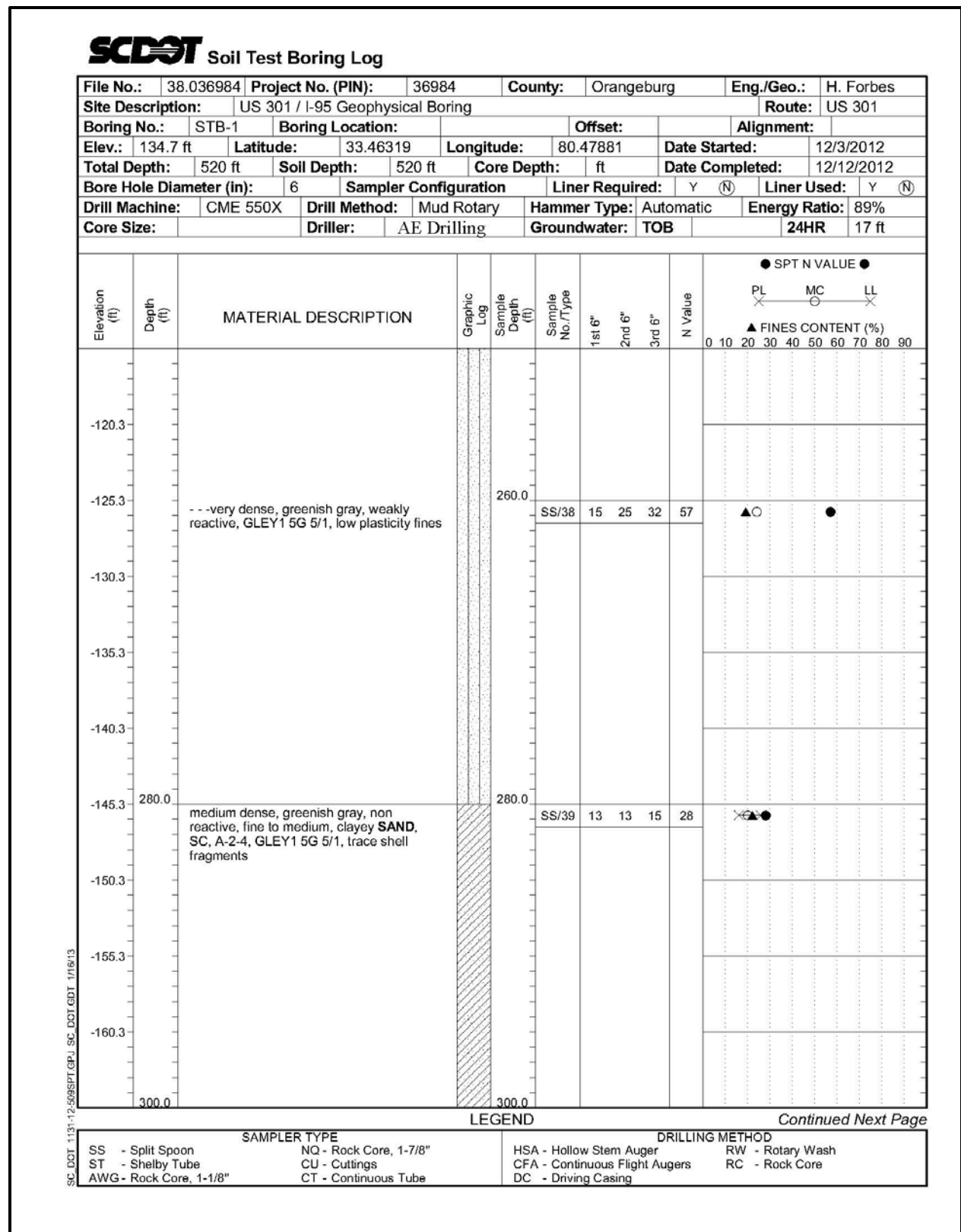


Figure H-44, Soil Test Boring STB-1 (con't)

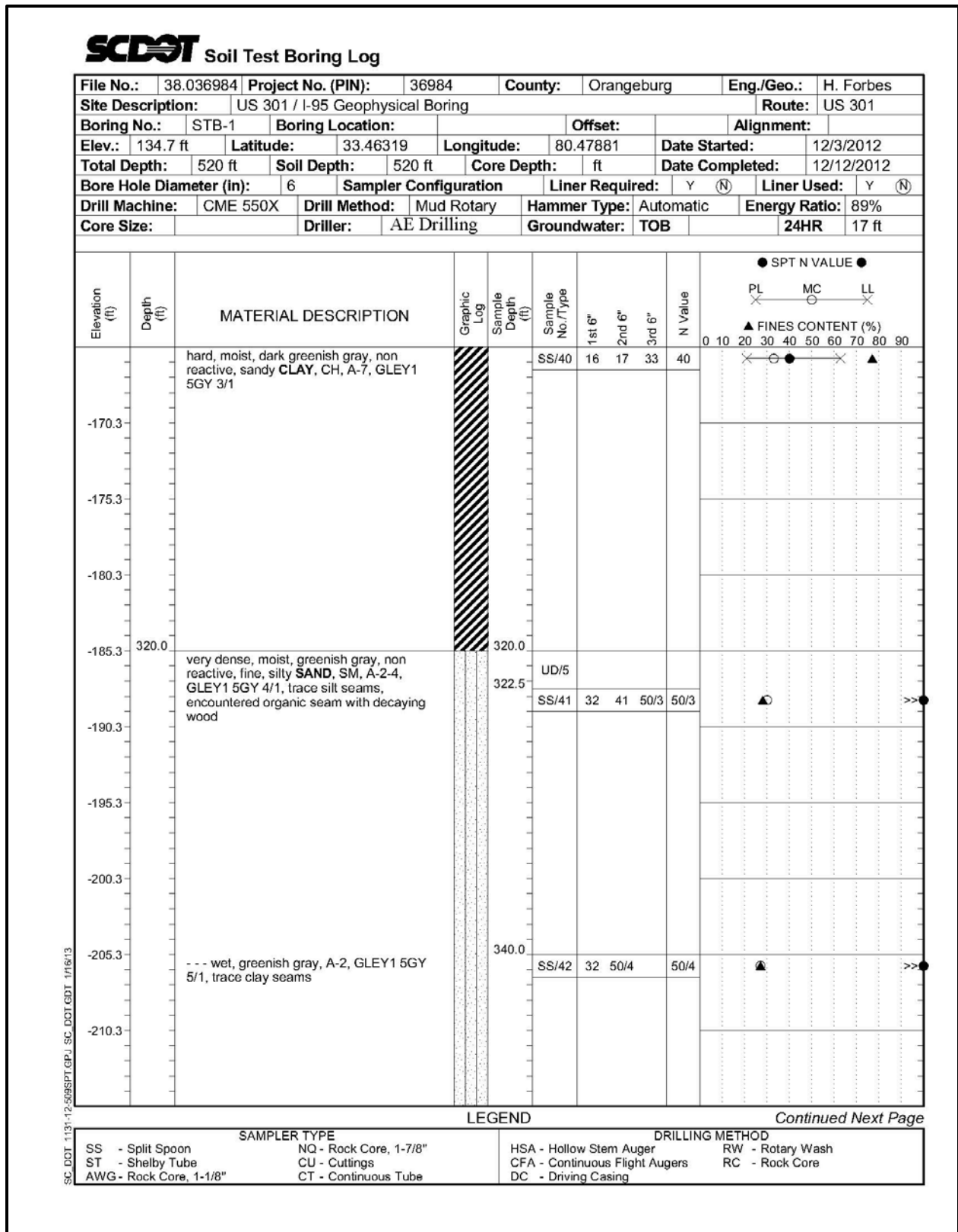


Figure H-45, Soil Test Boring STB-1 (con't)

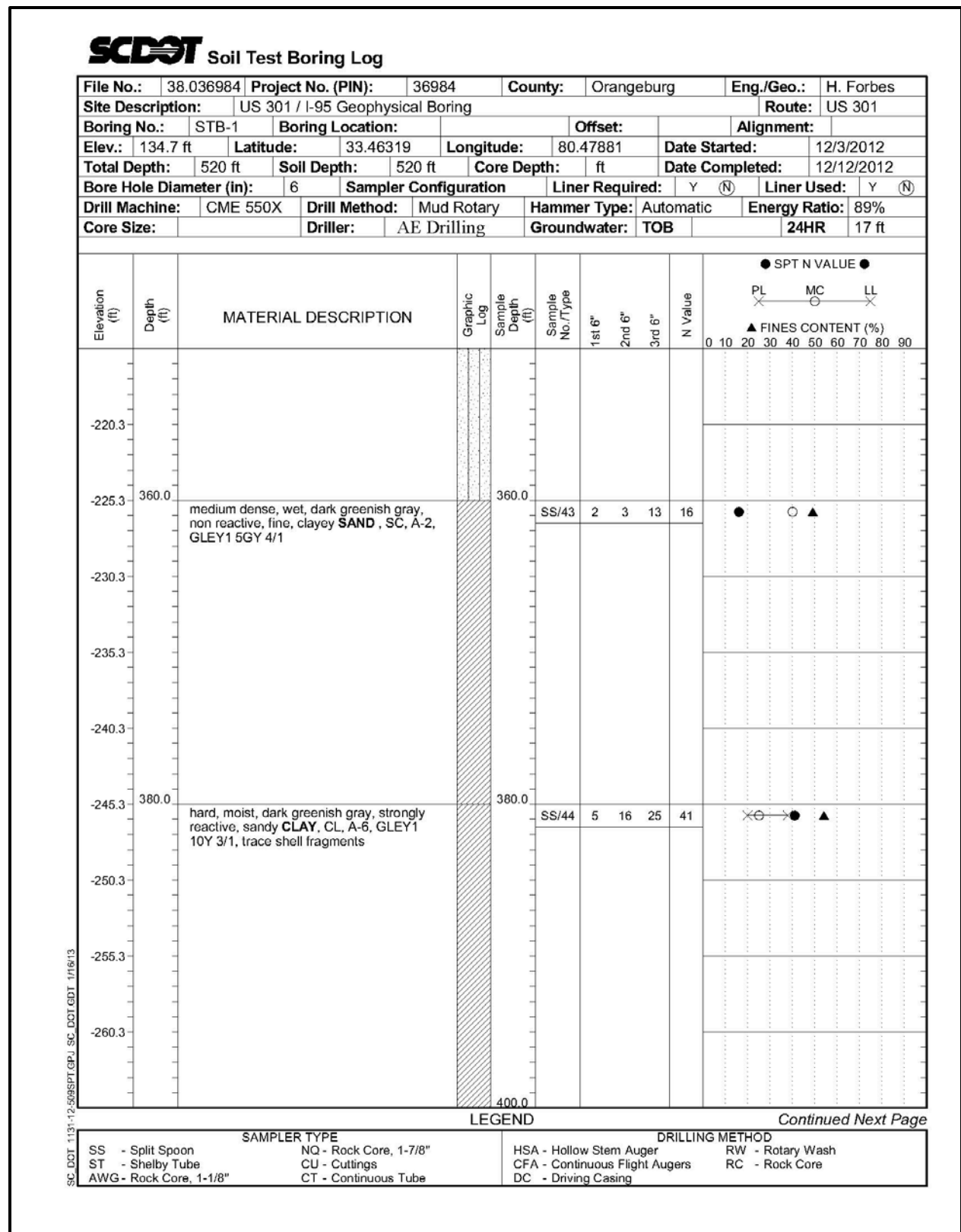


Figure H-46, Soil Test Boring STB-1 (con't)



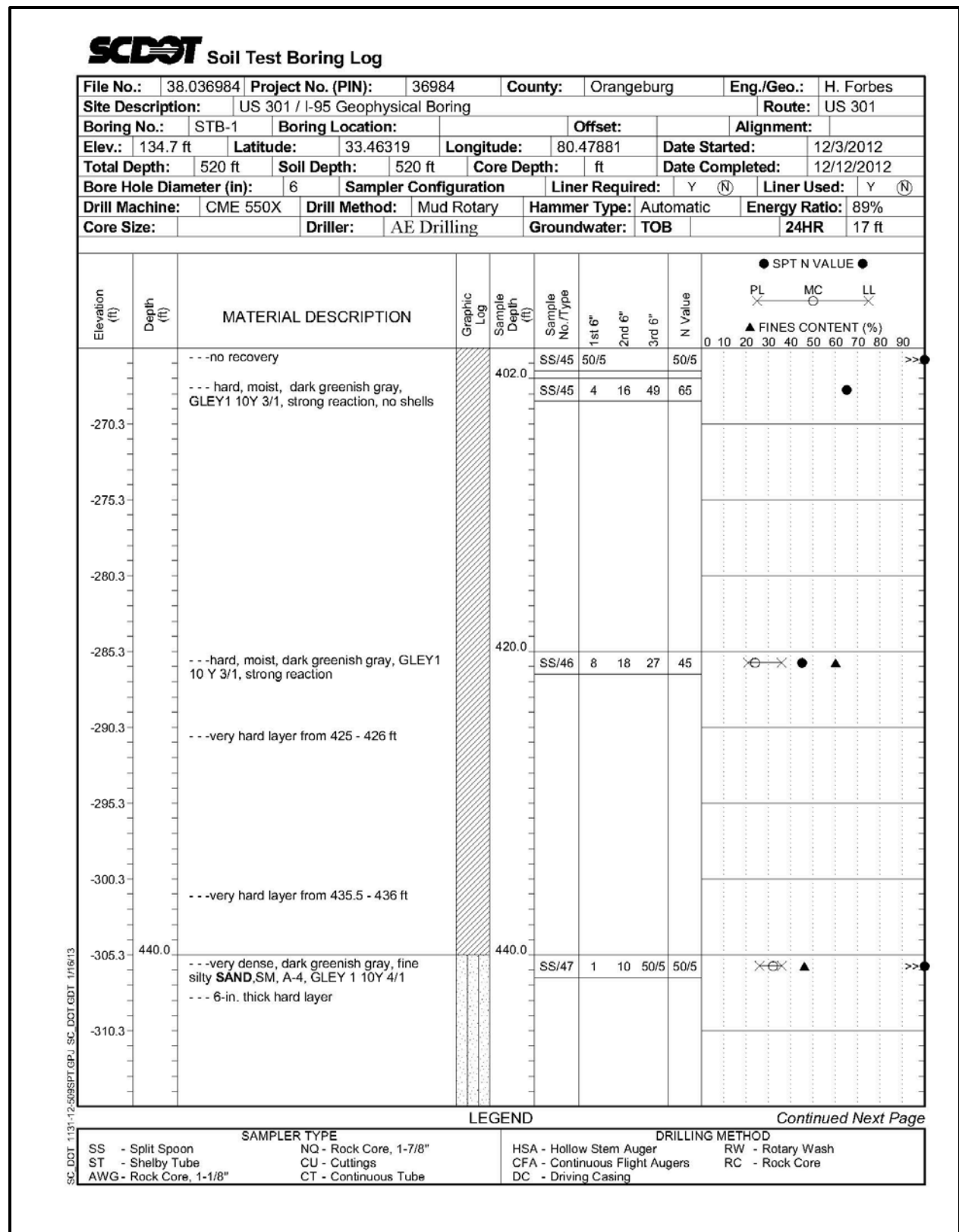


Figure H-47, Soil Test Boring STB-1 (con't)

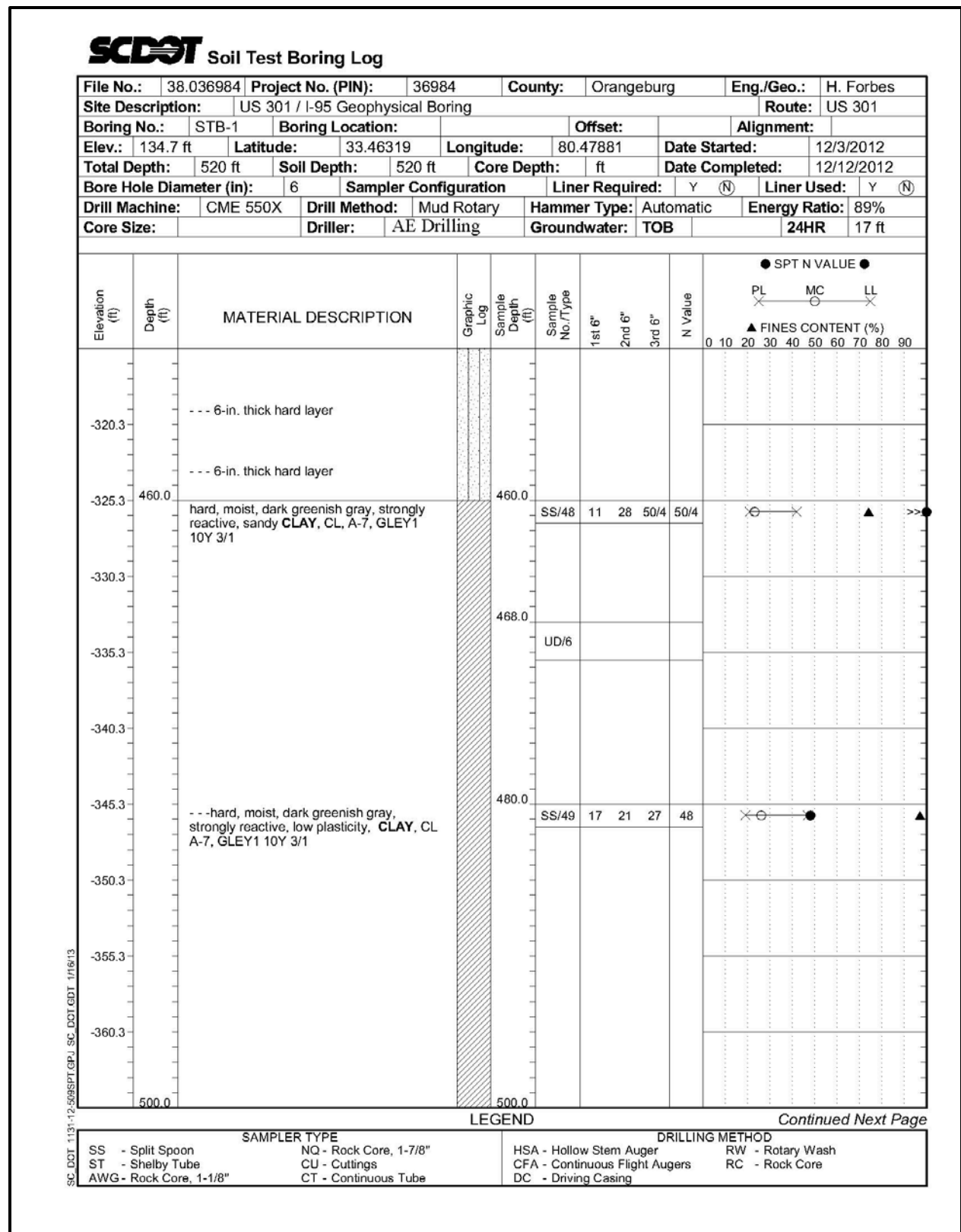


Figure H-48, Soil Test Boring STB-1 (con't)

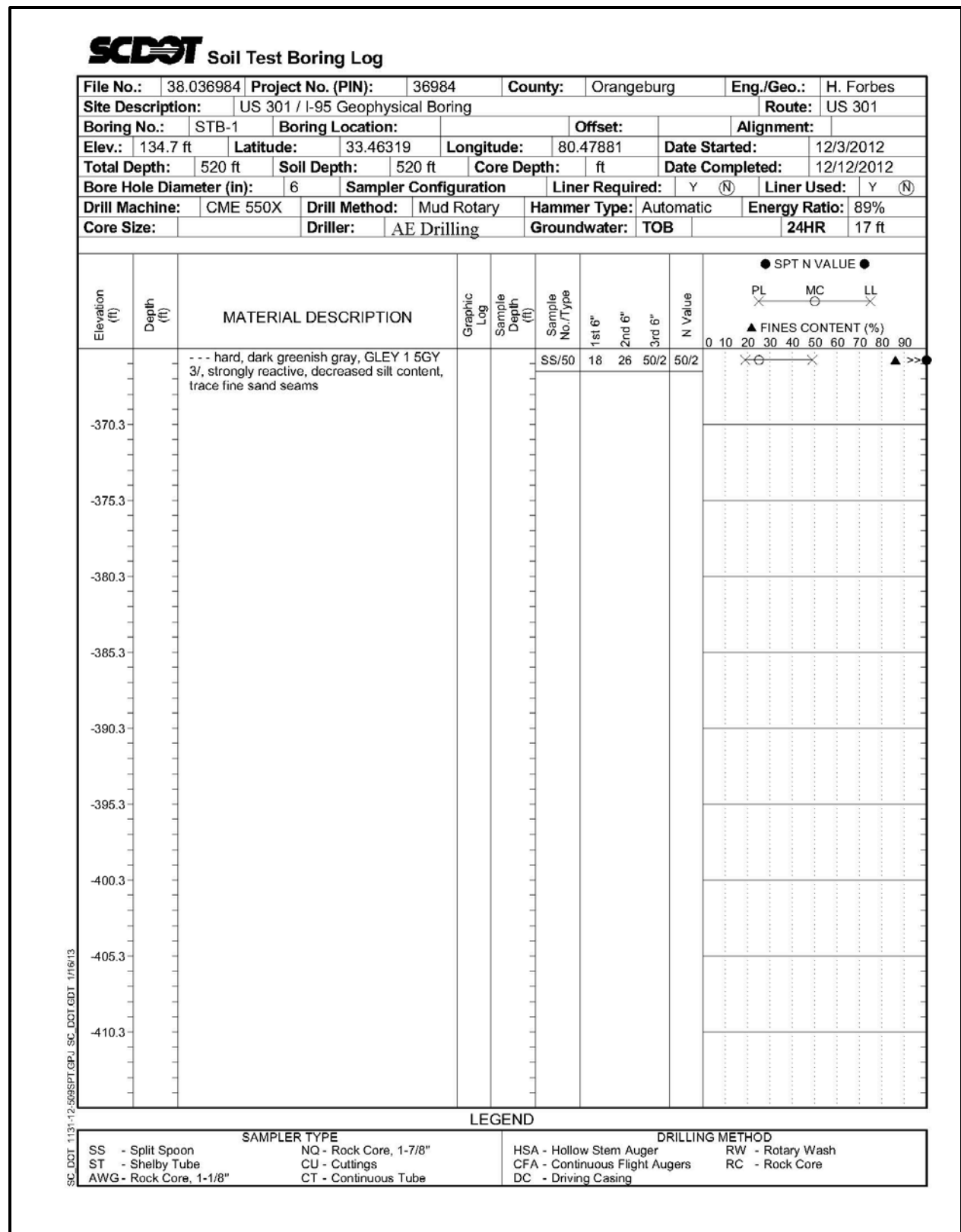
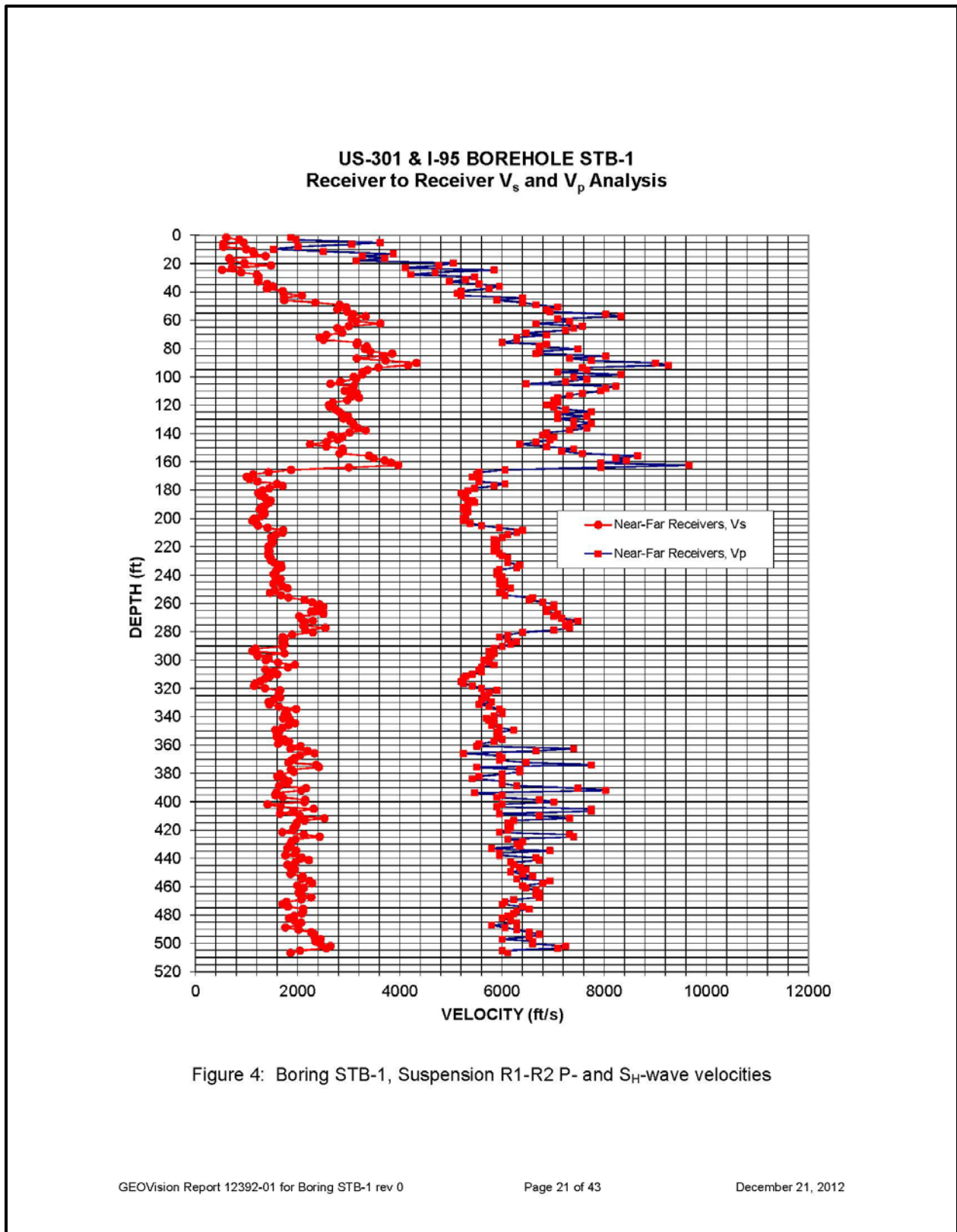


Figure H-49, Soil Test Boring STB-1 (con't)



**Figure H-50,  $V_s$  and  $V_p$  Profile – STB-1**

Table 3. Boring STB-1, Suspension R1-R2 depths and P- and S<sub>H</sub>-wave velocities

Summary of Compressional Wave Velocity, Shear Wave Velocity, and Poisson's Ratio  
Based on Receiver-to-Receiver Travel Time Data - Borehole STB-1

American Units				Metric Units			
Depth at Midpoint Between Receivers	Velocity		Poisson's Ratio	Depth at Midpoint Between Receivers	Velocity		Poisson's Ratio
	V <sub>s</sub>	V <sub>p</sub>			V <sub>s</sub>	V <sub>p</sub>	
(ft)	(ft/s)	(ft/s)		(m)	(m/s)	(m/s)	
1.6	610	1870	0.44	0.5	180	570	0.44
3.3	860	1970	0.38	1.0	260	600	0.38
5.3	940	3620	0.46	1.6	290	1100	0.46
6.6	540	3060	0.48	2.0	170	930	0.48
8.2	550	2010	0.46	2.5	170	610	0.46
9.8	1000	1530	0.13	3.0	300	470	0.13
11.5	1130	2510	0.37	3.5	340	760	0.37
13.1	1150	3880	0.45	4.0	350	1180	0.45
14.8	1370	3270	0.39	4.5	420	1000	0.39
16.4	660	3700	0.48	5.0	200	1130	0.48
18.0	690	3140	0.47	5.5	210	960	0.47
19.7	960	5050	0.48	6.0	290	1540	0.48
21.3	1480	4760	0.45	6.5	450	1450	0.45
23.0	720	4120	0.48	7.0	220	1250	0.48
24.6	520	5850	0.50	7.5	160	1780	0.50
26.3	890	4690	0.48	8.0	270	1430	0.48
27.9	1200	4220	0.46	8.5	370	1290	0.46
29.5	1240	5460	0.47	9.0	380	1670	0.47
31.2	1230	5290	0.47	9.5	380	1610	0.47
32.8	1230	4980	0.47	10.0	370	1520	0.47
34.5	1410	5560	0.47	10.5	430	1690	0.47
36.1	1520	5950	0.47	11.0	460	1810	0.47
37.7	1400	5750	0.47	11.5	430	1750	0.47
39.4	1710	5210	0.44	12.0	520	1590	0.44
41.0	1730	5130	0.44	12.5	530	1560	0.44
42.7	2080	5210	0.40	13.0	640	1590	0.40
44.3	1740	6410	0.46	13.5	530	1950	0.46
45.9	1740	5900	0.45	14.0	530	1800	0.45
47.6	2350	6410	0.42	14.5	720	1950	0.42
49.2	2820	6670	0.39	15.0	860	2030	0.39
50.9	2950	7090	0.40	15.5	900	2160	0.40
52.5	2780	6870	0.40	16.0	850	2090	0.40
54.1	2980	6940	0.39	16.5	910	2120	0.39
55.8	3090	8030	0.41	17.0	940	2450	0.41
57.4	3330	8330	0.40	17.5	1020	2540	0.40
59.1	3060	7090	0.39	18.0	930	2160	0.39

Figure H-51, Tabulated V<sub>s</sub> and V<sub>p</sub> Results – STB-1

**Summary of Compressional Wave Velocity, Shear Wave Velocity, and Poisson's Ratio  
Based on Receiver-to-Receiver Travel Time Data - Borehole STB-1**

American Units				Metric Units			
Depth at Midpoint Between Receivers	Velocity		Poisson's Ratio	Depth at Midpoint Between Receivers	Velocity		Poisson's Ratio
	V <sub>s</sub>	V <sub>p</sub>			V <sub>s</sub>	V <sub>p</sub>	
(ft)	(ft/s)	(ft/s)		(m)	(m/s)	(m/s)	
60.7	3140	7330	0.39	18.5	960	2230	0.39
62.3	3620	6670	0.29	19.0	1100	2030	0.29
64.3	3000	7580	0.41	19.6	920	2310	0.41
65.6	2780	7410	0.42	20.0	850	2260	0.42
67.3	2850	7250	0.41	20.5	870	2210	0.41
68.9	2870	6470	0.38	21.0	880	1970	0.38
70.5	2560	6870	0.42	21.5	780	2090	0.42
72.2	2430	6290	0.41	22.0	740	1920	0.41
73.8	2510	6290	0.41	22.5	760	1920	0.41
75.8	3170	6010	0.31	23.1	970	1830	0.31
77.1	3160	6870	0.37	23.5	960	2090	0.37
78.7	3350	6730	0.34	24.0	1020	2050	0.34
80.4	3320	7490	0.38	24.5	1010	2280	0.38
82.0	3420	6730	0.33	25.0	1040	2050	0.33
83.7	3850	6670	0.25	25.5	1170	2030	0.25
85.3	3680	8030	0.37	26.0	1120	2450	0.37
86.9	3160	7330	0.39	26.5	960	2230	0.39
88.6	3720	7750	0.35	27.0	1140	2360	0.35
90.2	4330	9010	0.35	27.5	1320	2750	0.35
91.9	4170	9260	0.37	28.0	1270	2820	0.37
93.5	3580	7580	0.36	28.5	1090	2310	0.36
95.1	3370	7660	0.38	29.0	1030	2340	0.38
96.8	3270	7090	0.37	29.5	1000	2160	0.37
98.4	3270	8330	0.41	30.0	1000	2540	0.41
100.1	3100	7410	0.39	30.5	950	2260	0.39
101.7	3140	7660	0.40	31.0	960	2340	0.40
103.4	2840	7250	0.41	31.5	860	2210	0.41
105.0	2650	6470	0.40	32.0	810	1970	0.40
106.6	3100	8230	0.42	32.5	950	2510	0.42
108.3	3060	8030	0.42	33.0	930	2450	0.42
109.9	2920	7940	0.42	33.5	890	2420	0.42
111.6	3160	7580	0.39	34.0	960	2310	0.39
113.2	3040	7330	0.40	34.5	930	2230	0.40
114.8	3210	7090	0.37	35.0	980	2160	0.37
116.5	2980	7020	0.39	35.5	910	2140	0.39
118.1	2690	7090	0.42	36.0	820	2160	0.42
119.8	2610	6870	0.42	36.5	800	2090	0.42
121.4	2640	7020	0.42	37.0	800	2140	0.42
123.0	2740	7250	0.42	37.5	840	2210	0.42

**Figure H-52, Tabulated V<sub>s</sub> and V<sub>p</sub> Results – STB-1 (con't)**

**Summary of Compressional Wave Velocity, Shear Wave Velocity, and Poisson's Ratio  
Based on Receiver-to-Receiver Travel Time Data - Borehole STB-1**

American Units				Metric Units			
Depth at Midpoint Between Receivers	Velocity		Poisson's Ratio	Depth at Midpoint Between Receivers	Velocity		Poisson's Ratio
	V <sub>s</sub>	V <sub>p</sub>			V <sub>s</sub>	V <sub>p</sub>	
(ft)	(ft/s)	(ft/s)		(m)	(m/s)	(m/s)	
124.7	2810	7750	0.42	38.0	860	2360	0.42
126.3	2860	7090	0.40	38.5	870	2160	0.40
128.0	2990	7660	0.41	39.0	910	2340	0.41
129.6	2900	7090	0.40	39.5	880	2160	0.40
131.2	3030	7410	0.40	40.0	920	2260	0.40
132.9	3090	7750	0.41	40.5	940	2360	0.41
134.5	3100	7410	0.39	41.0	950	2260	0.39
136.2	3170	7660	0.40	41.5	970	2340	0.40
137.8	3330	7330	0.37	42.0	1020	2230	0.37
139.4	3020	6870	0.38	42.5	920	2090	0.38
141.1	2660	6800	0.41	43.0	810	2070	0.41
142.7	2870	7020	0.40	43.5	880	2140	0.40
144.4	2790	6940	0.40	44.0	850	2120	0.40
146.0	2570	6670	0.41	44.5	780	2030	0.41
147.6	2240	6350	0.43	45.0	680	1940	0.43
149.3	2560	6870	0.42	45.5	780	2090	0.42
150.9	2890	7410	0.41	46.0	880	2260	0.41
152.6	2890	7170	0.40	46.5	880	2180	0.40
154.2	2820	7580	0.42	47.0	860	2310	0.42
155.8	3400	8660	0.41	47.5	1040	2640	0.41
157.5	3490	8230	0.39	48.0	1060	2510	0.39
159.1	3700	8440	0.38	48.5	1130	2570	0.38
160.8	3830	7940	0.35	49.0	1170	2420	0.35
162.4	3970	9660	0.40	49.5	1210	2940	0.40
164.0	3000	7940	0.42	50.0	920	2420	0.42
165.7	1870	6060	0.45	50.5	570	1850	0.45
167.3	1430	5560	0.46	51.0	440	1690	0.46
169.0	1130	5510	0.48	51.5	340	1680	0.48
170.6	1000	5420	0.48	52.0	310	1650	0.48
172.2	1060	5560	0.48	52.5	320	1690	0.48
173.9	1220	5560	0.47	53.0	370	1690	0.47
175.5	1590	6060	0.46	53.5	490	1850	0.46
177.2	1710	5850	0.45	54.0	520	1780	0.45
178.8	1450	5460	0.46	54.5	440	1670	0.46
180.5	1310	5330	0.47	55.0	400	1630	0.47
182.1	1230	5210	0.47	55.5	370	1590	0.47
183.7	1270	5250	0.47	56.0	390	1600	0.47
185.4	1360	5290	0.46	56.5	410	1610	0.46
187.3	1470	5420	0.46	57.1	450	1650	0.46

**Figure H-53, Tabulated V<sub>s</sub> and V<sub>p</sub> Results – STB-1 (con't)**

**Summary of Compressional Wave Velocity, Shear Wave Velocity, and Poisson's Ratio  
Based on Receiver-to-Receiver Travel Time Data - Borehole STB-1**

American Units				Metric Units			
Depth at Midpoint Between Receivers	Velocity		Poisson's Ratio	Depth at Midpoint Between Receivers	Velocity		Poisson's Ratio
	V <sub>s</sub>	V <sub>p</sub>			V <sub>s</sub>	V <sub>p</sub>	
(ft)	(ft/s)	(ft/s)		(m)	(m/s)	(m/s)	
188.7	1460	5460	0.46	57.5	440	1670	0.46
190.3	1380	5330	0.46	58.0	420	1630	0.46
191.9	1310	5250	0.47	58.5	400	1600	0.47
193.6	1260	5250	0.47	59.0	380	1600	0.47
195.2	1340	5330	0.47	59.5	410	1630	0.47
196.9	1360	5290	0.46	60.0	410	1610	0.46
198.5	1290	5290	0.47	60.5	390	1610	0.47
200.1	1150	5250	0.47	61.0	350	1600	0.47
201.8	1110	5250	0.48	61.5	340	1600	0.48
203.4	1190	5380	0.47	62.0	360	1640	0.47
205.1	1230	5600	0.47	62.5	370	1710	0.47
206.7	1410	5950	0.47	63.0	430	1810	0.47
208.3	1720	6410	0.46	63.5	520	1950	0.46
210.0	1710	6290	0.46	64.0	520	1920	0.46
211.6	1570	6120	0.46	64.5	480	1860	0.46
213.3	1490	6010	0.47	65.0	450	1830	0.47
214.9	1490	5850	0.47	65.5	460	1780	0.47
216.5	1520	5900	0.46	66.0	460	1800	0.46
218.2	1490	5900	0.47	66.5	450	1800	0.47
219.8	1430	5850	0.47	67.0	440	1780	0.47
221.5	1440	5900	0.47	67.5	440	1800	0.47
223.1	1450	5850	0.47	68.0	440	1780	0.47
224.7	1420	5950	0.47	68.5	430	1810	0.47
226.4	1430	6010	0.47	69.0	440	1830	0.47
228.0	1470	6120	0.47	69.5	450	1860	0.47
229.7	1480	6120	0.47	70.0	450	1860	0.47
231.3	1540	6120	0.47	70.5	470	1860	0.47
232.9	1680	6350	0.46	71.0	510	1940	0.46
234.6	1680	6290	0.46	71.5	510	1920	0.46
236.2	1590	5950	0.46	72.0	490	1810	0.46
237.9	1570	5900	0.46	72.5	480	1800	0.46
239.5	1530	5900	0.46	73.0	470	1800	0.46
241.1	1580	6010	0.46	73.5	480	1830	0.46
242.8	1670	5950	0.46	74.0	510	1810	0.46
244.4	1560	6060	0.46	74.5	480	1850	0.46
246.1	1530	5950	0.46	75.0	470	1810	0.46
247.7	1700	6060	0.46	75.5	520	1850	0.46
249.3	1800	6170	0.45	76.0	550	1880	0.45
251.0	1550	6010	0.46	76.5	470	1830	0.46

**Figure H-54, Tabulated V<sub>s</sub> and V<sub>p</sub> Results – STB-1 (con't)**



**Summary of Compressional Wave Velocity, Shear Wave Velocity, and Poisson's Ratio  
Based on Receiver-to-Receiver Travel Time Data - Borehole STB-1**

American Units				Metric Units			
Depth at Midpoint Between Receivers	Velocity		Poisson's Ratio	Depth at Midpoint Between Receivers	Velocity		Poisson's Ratio
	V <sub>s</sub>	V <sub>p</sub>			V <sub>s</sub>	V <sub>p</sub>	
(ft)	(ft/s)	(ft/s)		(m)	(m/s)	(m/s)	
252.6	1460	5950	0.47	77.0	450	1810	0.47
254.3	1680	6060	0.46	77.5	510	1850	0.46
255.9	1820	6600	0.46	78.0	560	2010	0.46
257.6	2140	6540	0.44	78.5	650	1990	0.44
259.2	2280	6800	0.44	79.0	700	2070	0.44
260.8	2430	7020	0.43	79.5	740	2140	0.43
262.5	2510	7020	0.43	80.0	760	2140	0.43
264.1	2380	6870	0.43	80.5	730	2090	0.43
265.8	2270	6870	0.44	81.0	690	2090	0.44
267.4	2510	7090	0.43	81.5	760	2160	0.43
269.0	2030	7020	0.45	82.0	620	2140	0.45
270.7	2070	7170	0.45	82.5	630	2180	0.45
272.3	2300	7490	0.45	83.0	700	2280	0.45
274.0	2140	7330	0.45	83.5	650	2230	0.45
275.6	2110	7250	0.45	84.0	640	2210	0.45
277.2	2540	7330	0.43	84.5	780	2230	0.43
278.9	2150	7020	0.45	85.0	660	2140	0.45
280.5	2300	6410	0.43	85.5	700	1950	0.43
282.2	1890	6120	0.45	86.0	580	1860	0.45
283.8	1710	5950	0.46	86.5	520	1810	0.46
285.4	1750	6120	0.46	87.0	530	1860	0.46
287.1	1700	6290	0.46	87.5	520	1920	0.46
288.7	1750	6170	0.46	88.0	530	1880	0.46
290.4	1710	6010	0.46	88.5	520	1830	0.46
292.0	1170	5850	0.48	89.0	360	1780	0.48
293.6	1120	5750	0.48	89.5	340	1750	0.48
295.3	1750	5850	0.45	90.0	530	1780	0.45
296.9	1220	5800	0.48	90.5	370	1770	0.48
298.6	1430	5750	0.47	91.0	440	1750	0.47
300.2	1380	5650	0.47	91.5	420	1720	0.47
301.8	1620	5750	0.46	92.0	490	1750	0.46
303.5	1950	5850	0.44	92.5	590	1780	0.44
305.1	1810	5600	0.44	93.0	550	1710	0.44
306.8	1370	5560	0.47	93.5	420	1690	0.47
308.4	1540	5600	0.46	94.0	470	1710	0.46
310.0	1600	5420	0.45	94.5	490	1650	0.45
311.7	1460	5290	0.46	95.0	440	1610	0.46
313.3	1360	5250	0.46	95.5	410	1600	0.46
315.0	1270	5210	0.47	96.0	390	1590	0.47

**Figure H-55, Tabulated V<sub>s</sub> and V<sub>p</sub> Results – STB-1 (con't)**

**Summary of Compressional Wave Velocity, Shear Wave Velocity, and Poisson's Ratio  
Based on Receiver-to-Receiver Travel Time Data - Borehole STB-1**

American Units				Metric Units			
Depth at Midpoint Between Receivers	Velocity		Poisson's Ratio	Depth at Midpoint Between Receivers	Velocity		Poisson's Ratio
	V <sub>s</sub>	V <sub>p</sub>			V <sub>s</sub>	V <sub>p</sub>	
(ft)	(ft/s)	(ft/s)		(m)	(m/s)	(m/s)	
316.6	1170	5250	0.47	96.5	360	1600	0.47
318.2	1150	5420	0.48	97.0	350	1650	0.48
319.9	1360	5600	0.47	97.5	410	1710	0.47
321.5	1660	5900	0.46	98.0	510	1800	0.46
323.2	1630	5750	0.46	98.5	500	1750	0.46
324.8	1630	5650	0.45	99.0	500	1720	0.45
326.4	1660	5700	0.45	99.5	510	1740	0.45
328.1	1540	5600	0.46	100.0	470	1710	0.46
329.7	1440	5800	0.47	100.5	440	1770	0.47
331.4	1450	5560	0.46	101.0	440	1690	0.46
333.0	1630	5750	0.46	101.5	500	1750	0.46
334.7	1970	5950	0.44	102.0	600	1810	0.44
336.3	1780	6010	0.45	102.5	540	1830	0.45
337.9	1750	6010	0.45	103.0	530	1830	0.45
339.6	1810	5850	0.45	103.5	550	1780	0.45
341.2	1720	5700	0.45	104.0	520	1740	0.45
342.9	1860	5750	0.44	104.5	570	1750	0.44
344.5	1950	5850	0.44	105.0	590	1780	0.44
346.1	1820	5800	0.45	105.5	560	1770	0.45
347.8	1710	5950	0.46	106.0	520	1810	0.46
349.4	1560	6230	0.47	106.5	480	1900	0.47
351.1	1630	5900	0.46	107.0	500	1800	0.46
352.7	1590	5950	0.46	107.5	490	1810	0.46
354.3	1590	5900	0.46	108.0	490	1800	0.46
356.0	1730	6010	0.45	108.5	530	1830	0.45
357.6	1830	5850	0.45	109.0	560	1780	0.45
359.3	1620	5560	0.45	109.5	490	1690	0.45
360.9	2060	5510	0.42	110.0	630	1680	0.42
362.5	1860	7410	0.47	110.5	570	2260	0.47
364.2	2190	6670	0.44	111.0	670	2030	0.44
365.8	2330	5250	0.38	111.5	710	1600	0.38
367.5	2040	5950	0.43	112.0	620	1810	0.43
369.1	1950	6010	0.44	112.5	590	1830	0.44
370.7	1880	5950	0.44	113.0	570	1810	0.44
372.4	1820	6470	0.46	113.5	560	1970	0.46
374.0	2360	7750	0.45	114.0	720	2360	0.45
375.7	2420	5510	0.38	114.5	740	1680	0.38
377.3	1870	6350	0.45	115.0	570	1940	0.45
378.9	1930	6350	0.45	115.5	590	1940	0.45

**Figure H-56, Tabulated V<sub>s</sub> and V<sub>p</sub> Results – STB-1 (con't)**

**Summary of Compressional Wave Velocity, Shear Wave Velocity, and Poisson's Ratio  
Based on Receiver-to-Receiver Travel Time Data - Borehole STB-1**

American Units				Metric Units			
Depth at Midpoint Between Receivers	Velocity		Poisson's Ratio	Depth at Midpoint Between Receivers	Velocity		Poisson's Ratio
	V <sub>s</sub>	V <sub>p</sub>			V <sub>s</sub>	V <sub>p</sub>	
(ft)	(ft/s)	(ft/s)		(m)	(m/s)	(m/s)	
380.6	1660	6010	0.46	116.0	510	1830	0.46
382.2	1600	5560	0.45	116.5	490	1690	0.45
383.9	1730	5420	0.44	117.0	530	1650	0.44
385.5	1820	6010	0.45	117.5	560	1830	0.45
387.1	1780	6010	0.45	118.0	540	1830	0.45
388.8	1640	6290	0.46	118.5	500	1920	0.46
390.4	2160	7490	0.45	119.0	660	2280	0.45
392.1	2070	8030	0.46	119.5	630	2450	0.46
393.7	1590	5460	0.45	120.0	480	1670	0.45
395.3	1560	6010	0.46	120.5	480	1830	0.46
397.0	1710	5900	0.45	121.0	520	1800	0.45
398.6	2150	6730	0.44	121.5	660	2050	0.44
400.3	2140	7020	0.45	122.0	650	2140	0.45
401.9	1410	6010	0.47	122.5	430	1830	0.47
403.5	1670	5900	0.46	123.0	510	1800	0.46
405.2	2310	7750	0.45	123.5	710	2360	0.45
406.8	1920	7750	0.47	124.0	580	2360	0.47
408.5	1660	5950	0.46	124.5	510	1810	0.46
410.1	2040	6730	0.45	125.0	620	2050	0.45
411.8	2530	7330	0.43	125.5	770	2230	0.43
413.4	2140	6230	0.43	126.0	650	1900	0.43
415.0	1980	6120	0.44	126.5	600	1860	0.44
416.7	1970	6120	0.44	127.0	600	1860	0.44
418.3	1930	6170	0.45	127.5	590	1880	0.45
420.0	1920	6120	0.45	128.0	580	1860	0.45
421.6	1700	5950	0.46	128.5	520	1810	0.46
423.2	2120	7330	0.45	129.0	650	2230	0.45
424.9	2430	7410	0.44	129.5	740	2260	0.44
426.5	1960	6120	0.44	130.0	600	1860	0.44
428.2	1880	6410	0.45	130.5	570	1950	0.45
429.8	1870	6290	0.45	131.0	570	1920	0.45
431.4	1830	6350	0.45	131.5	560	1940	0.45
433.1	1800	5800	0.45	132.0	550	1770	0.45
434.7	1970	6940	0.46	132.5	600	2120	0.46
436.4	1960	5950	0.44	133.0	600	1810	0.44
438.0	1760	5950	0.45	133.5	540	1810	0.45
439.6	2080	6670	0.45	134.0	640	2030	0.45
441.3	2220	6730	0.44	134.5	680	2050	0.44
442.9	1960	6170	0.44	135.0	600	1880	0.44

**Figure H-57, Tabulated V<sub>s</sub> and V<sub>p</sub> Results – STB-1 (con't)**

**Summary of Compressional Wave Velocity, Shear Wave Velocity, and Poisson's Ratio  
Based on Receiver-to-Receiver Travel Time Data - Borehole STB-1**

American Units				Metric Units			
Depth at Midpoint Between Receivers	Velocity		Poisson's Ratio	Depth at Midpoint Between Receivers	Velocity		Poisson's Ratio
	V <sub>s</sub>	V <sub>p</sub>			V <sub>s</sub>	V <sub>p</sub>	
(ft)	(ft/s)	(ft/s)		(m)	(m/s)	(m/s)	
444.6	1800	6230	0.45	135.5	550	1900	0.45
446.2	1850	6350	0.45	136.0	560	1940	0.45
447.8	1950	6470	0.45	136.5	590	1970	0.45
449.5	1900	6170	0.45	137.0	580	1880	0.45
451.1	1860	6410	0.45	137.5	570	1950	0.45
452.8	2100	6600	0.44	138.0	640	2010	0.44
454.4	2080	6290	0.44	138.5	640	1920	0.44
456.0	2240	6940	0.44	139.0	680	2120	0.44
457.7	2280	6800	0.44	139.5	700	2070	0.44
459.3	2000	6410	0.45	140.0	610	1950	0.45
461.0	2120	6470	0.44	140.5	650	1970	0.44
462.6	2060	6670	0.45	141.0	630	2030	0.45
464.2	2020	6730	0.45	141.5	620	2050	0.45
465.9	2080	6670	0.45	142.0	640	2030	0.45
467.5	2270	6730	0.44	142.5	690	2050	0.44
469.2	2070	6230	0.44	143.0	630	1900	0.44
470.8	1780	6060	0.45	143.5	540	1850	0.45
472.4	1700	6010	0.46	144.0	520	1830	0.46
474.1	1810	6410	0.46	144.5	550	1950	0.46
475.7	2110	6540	0.44	145.0	640	1990	0.44
477.4	2110	6290	0.44	145.5	640	1920	0.44
479.0	2080	6230	0.44	146.0	640	1900	0.44
480.6	1940	6120	0.44	146.5	590	1860	0.44
482.3	1830	6010	0.45	147.0	560	1830	0.45
483.9	1940	6170	0.45	147.5	590	1880	0.45
485.6	2070	6290	0.44	148.0	630	1920	0.44
487.2	2010	5800	0.43	148.5	610	1770	0.43
488.9	1760	6060	0.45	149.0	540	1850	0.45
490.5	2020	6290	0.44	149.5	620	1920	0.44
492.1	2270	6540	0.43	150.0	690	1990	0.43
493.8	2330	6730	0.43	150.5	710	2050	0.43
495.4	2330	6540	0.43	151.0	710	1990	0.43
497.1	2450	6010	0.40	151.5	750	1830	0.40
498.7	2350	6600	0.43	152.0	720	2010	0.43
500.3	2450	6600	0.42	152.5	750	2010	0.42
502.0	2650	7250	0.42	153.0	810	2210	0.42
503.6	2560	7090	0.42	153.5	780	2160	0.42
505.3	2040	6010	0.43	154.0	620	1830	0.43
506.9	1860	6120	0.45	154.5	570	1860	0.45

**Figure H-58, Tabulated V<sub>s</sub> and V<sub>p</sub> Results – STB-1 (con't)**

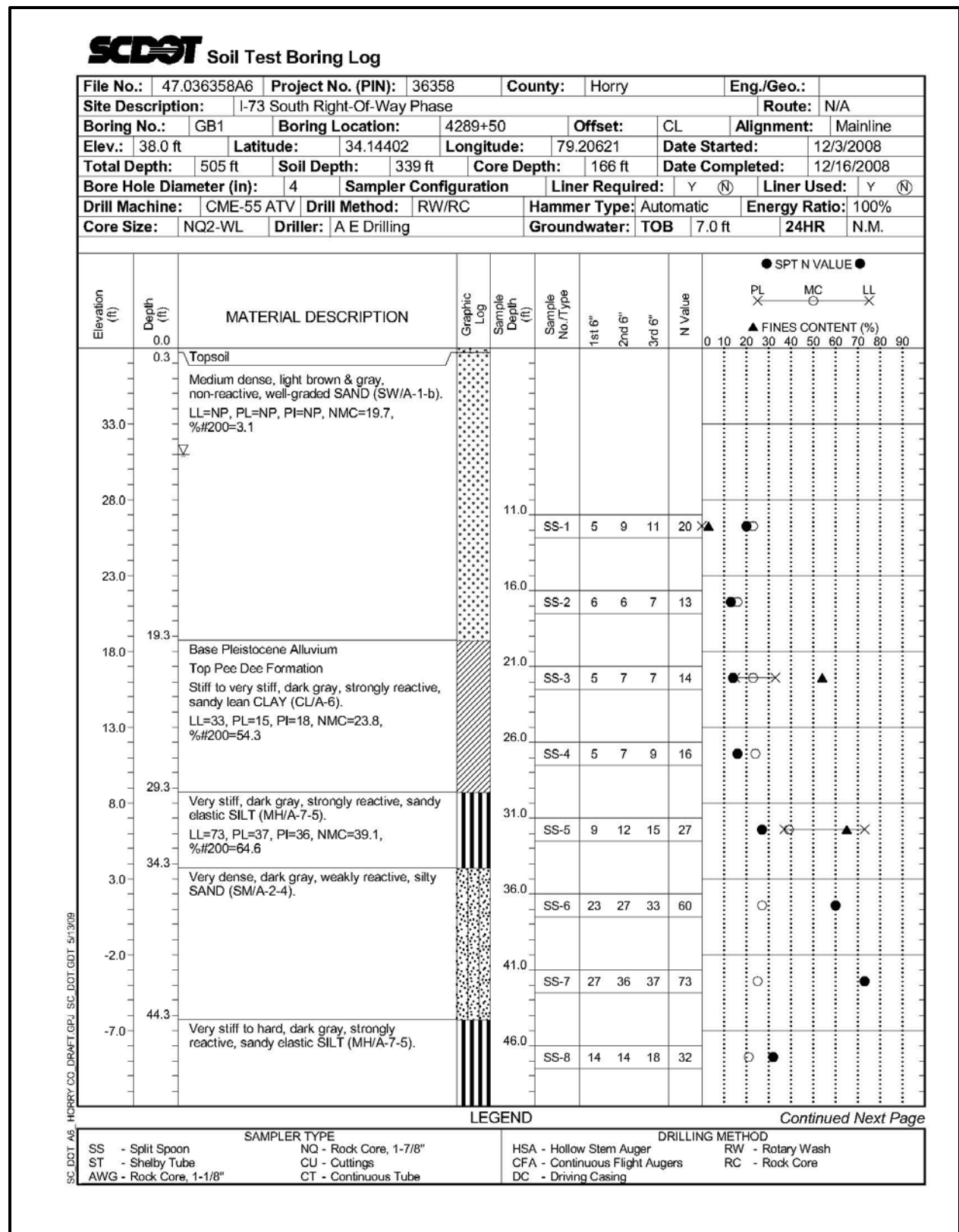


Figure H-59, Soil Test Boring G-B-1

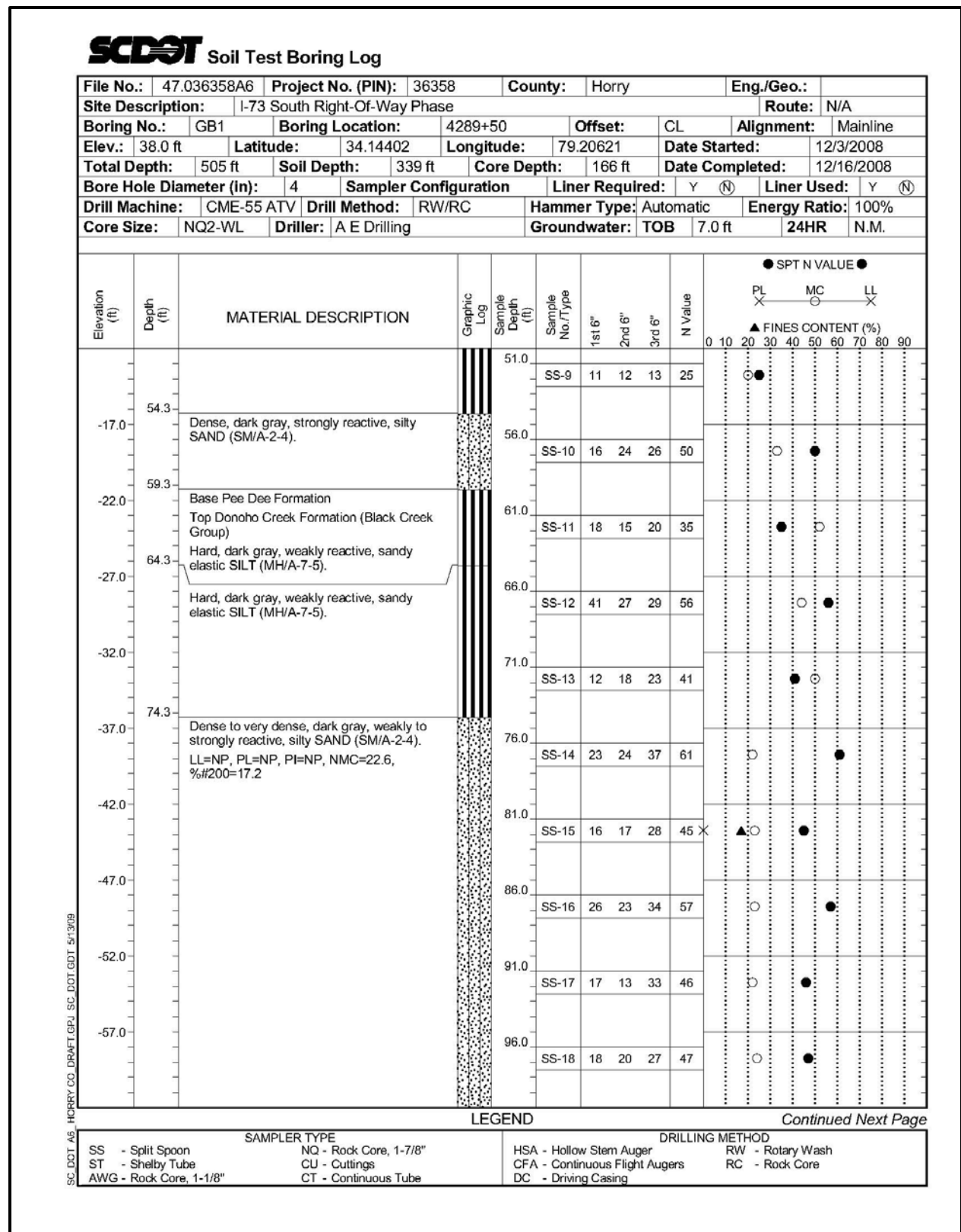


Figure H-60, Soil Test Boring G-B-1 (con't)

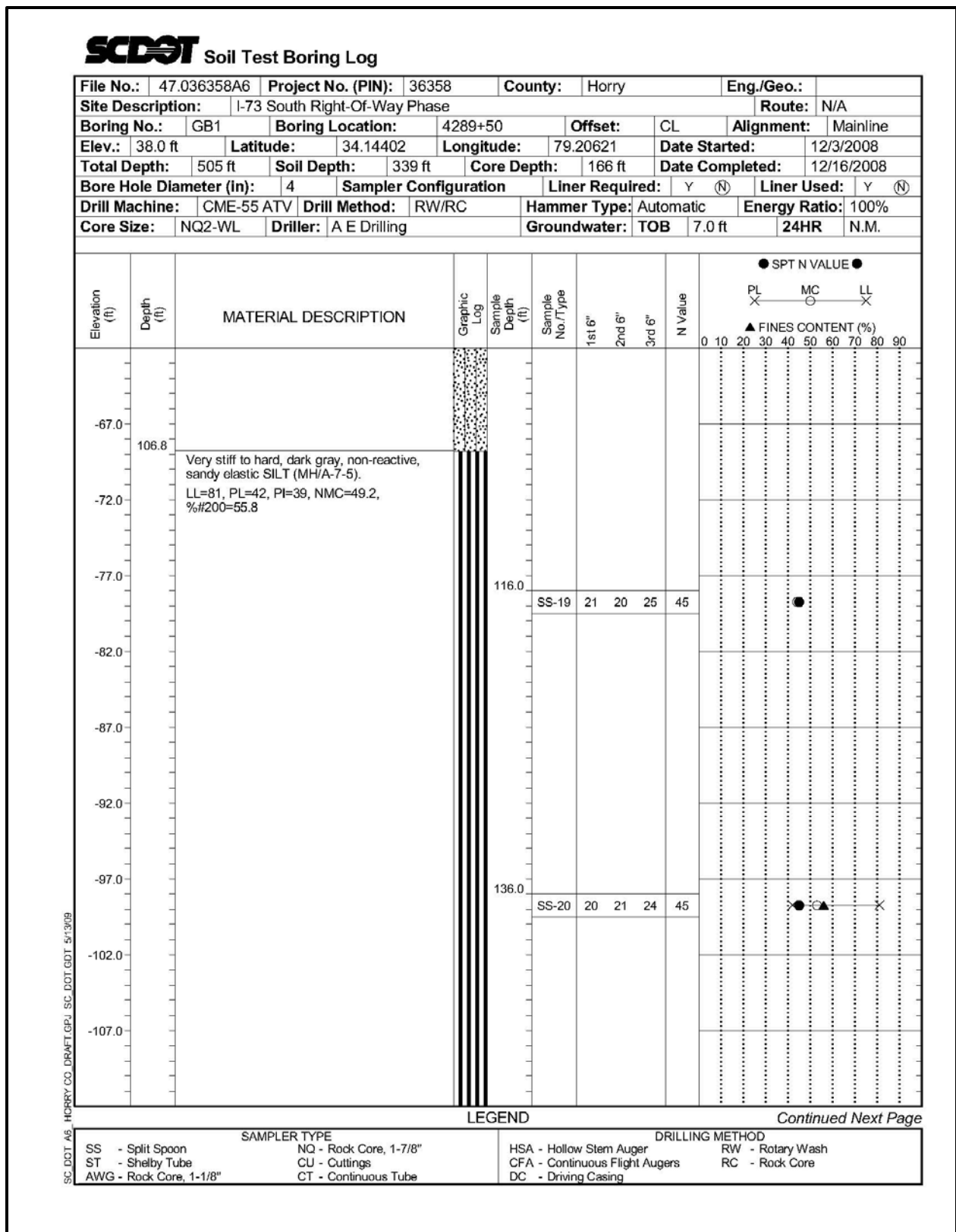


Figure H-61, Soil Test Boring G-B-1 (con't)

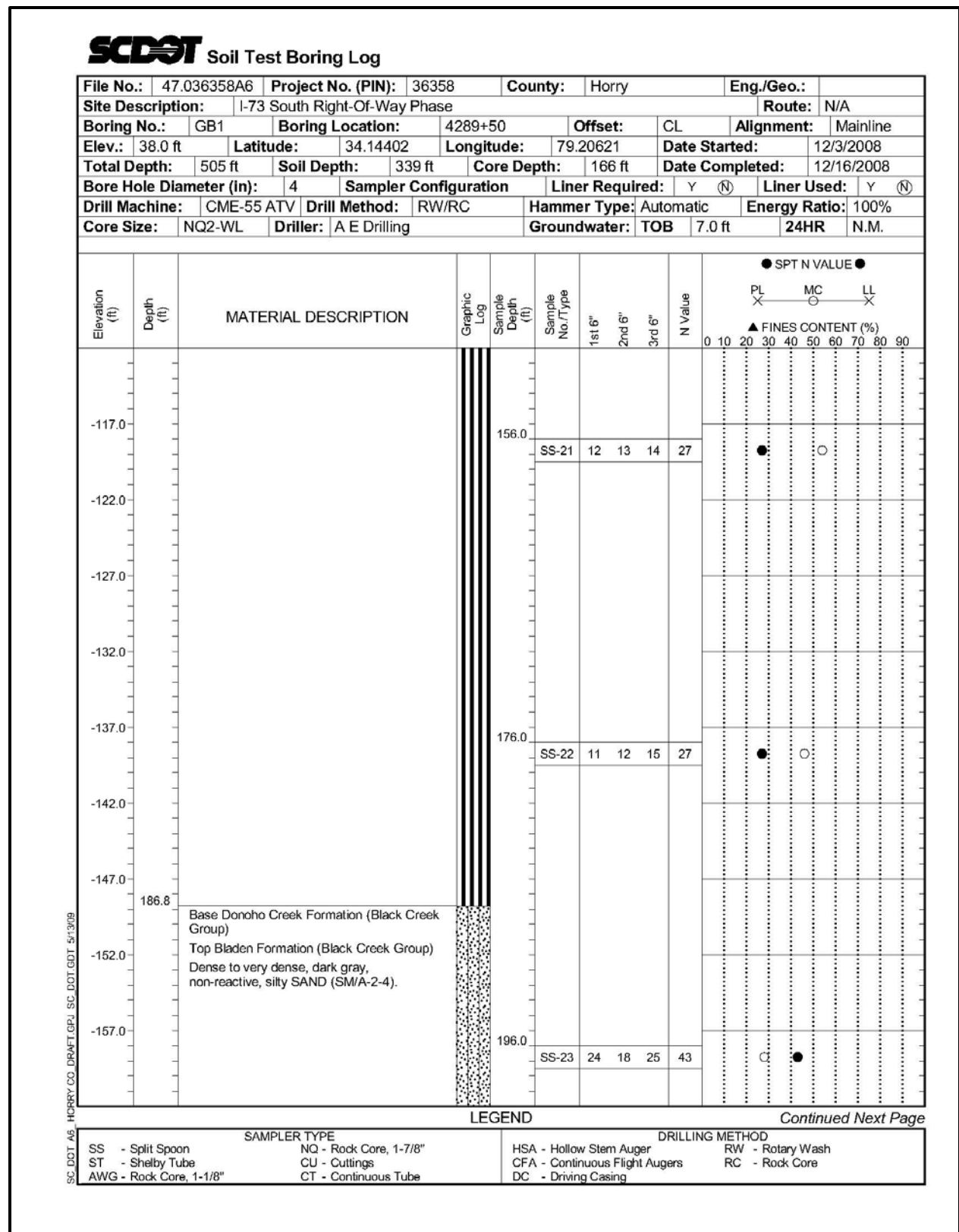


Figure H-62, Soil Test Boring G-B-1 (con't)



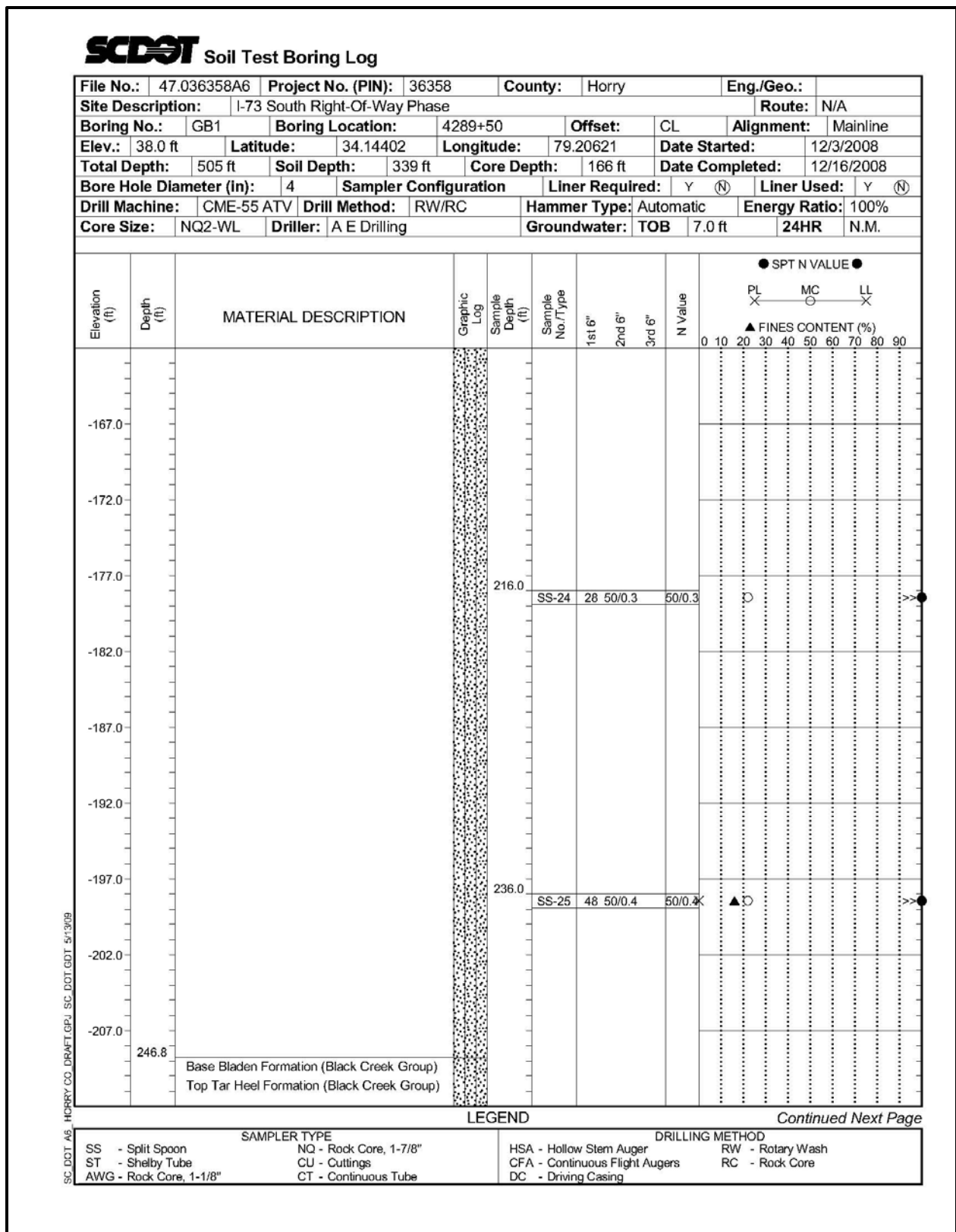


Figure H-63, Soil Test Boring G-B-1 (con't)

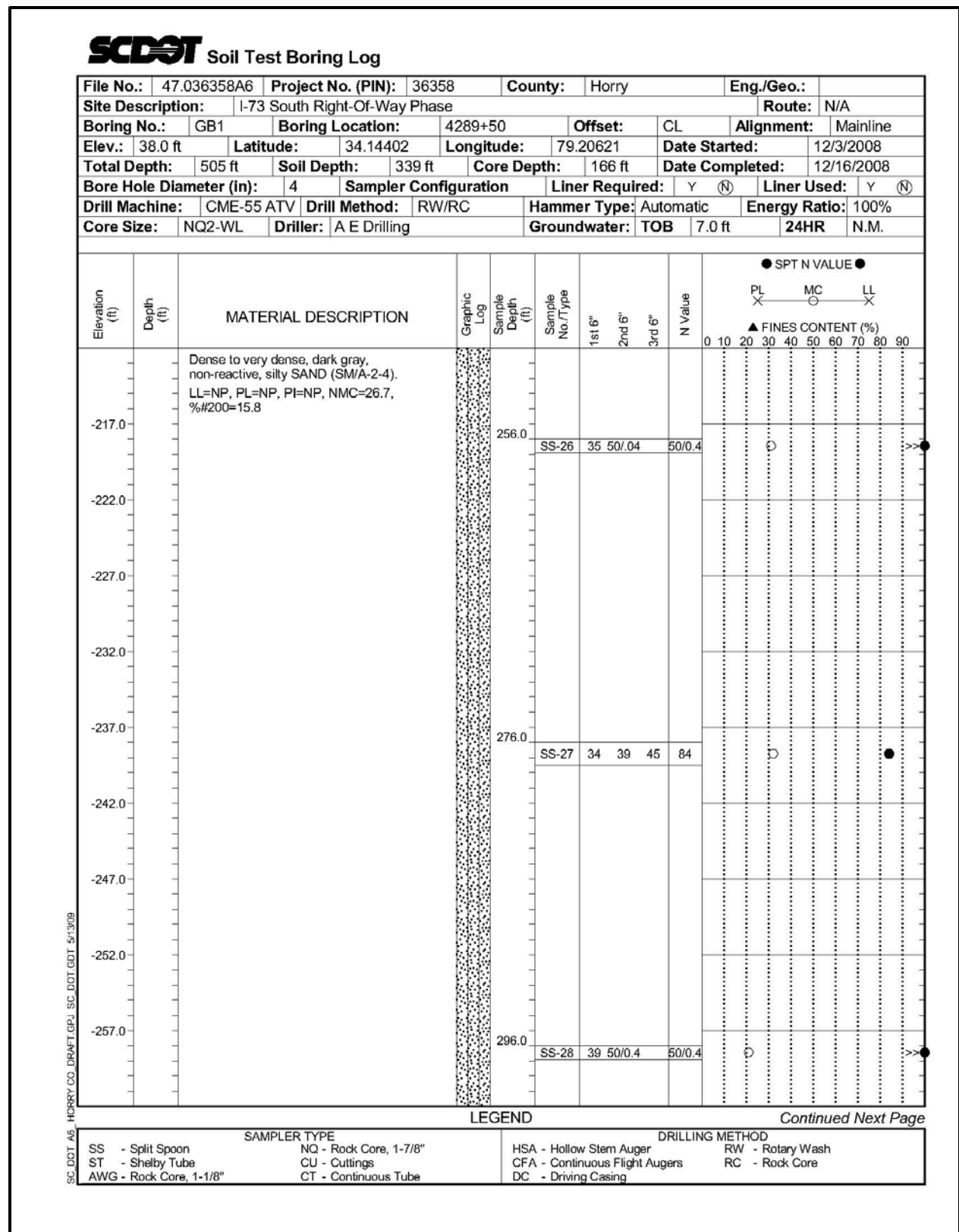


Figure H-64, Soil Test Boring G-B-1 (con't)



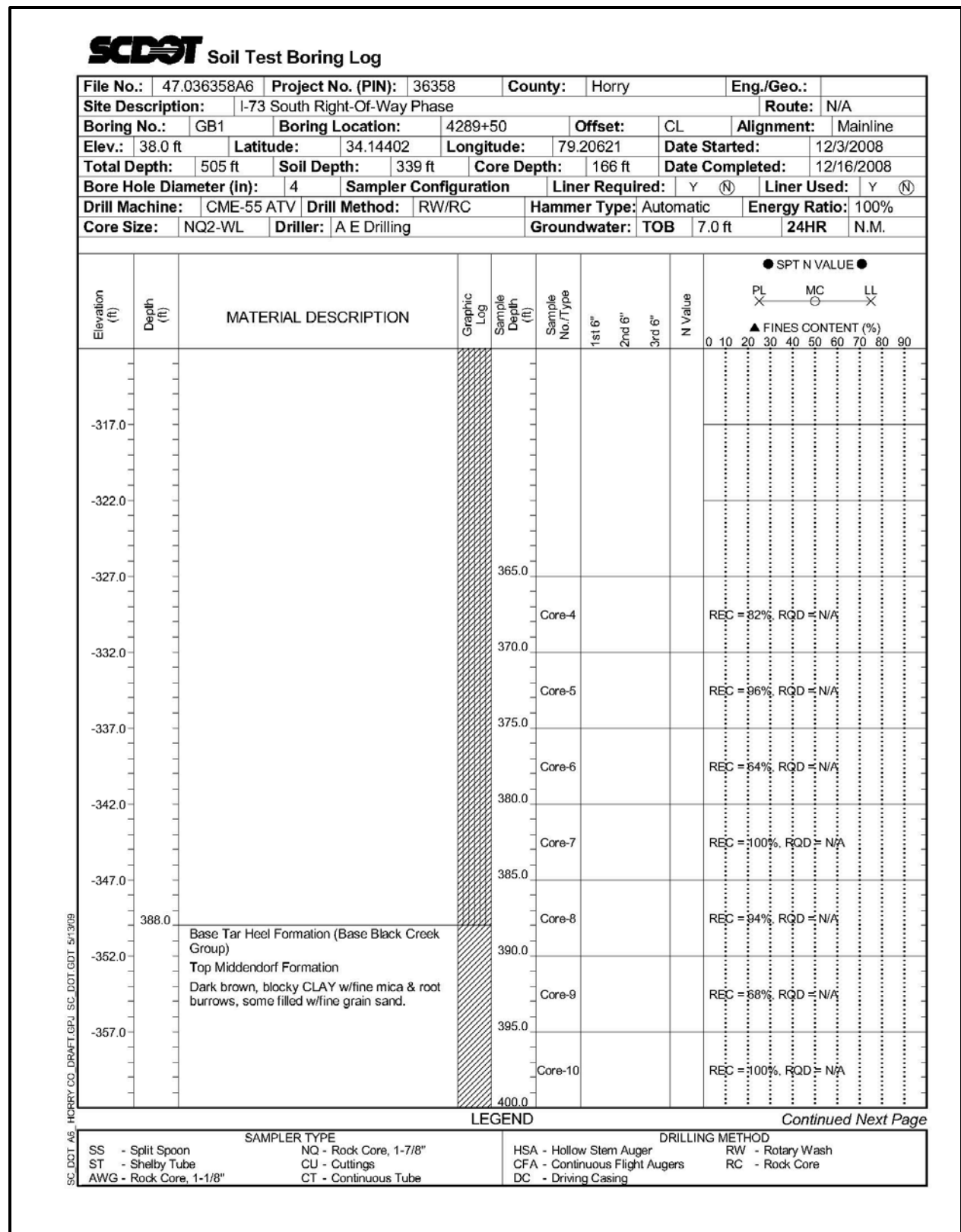


Figure H-66, Soil Test Boring G-B-1 (con't)

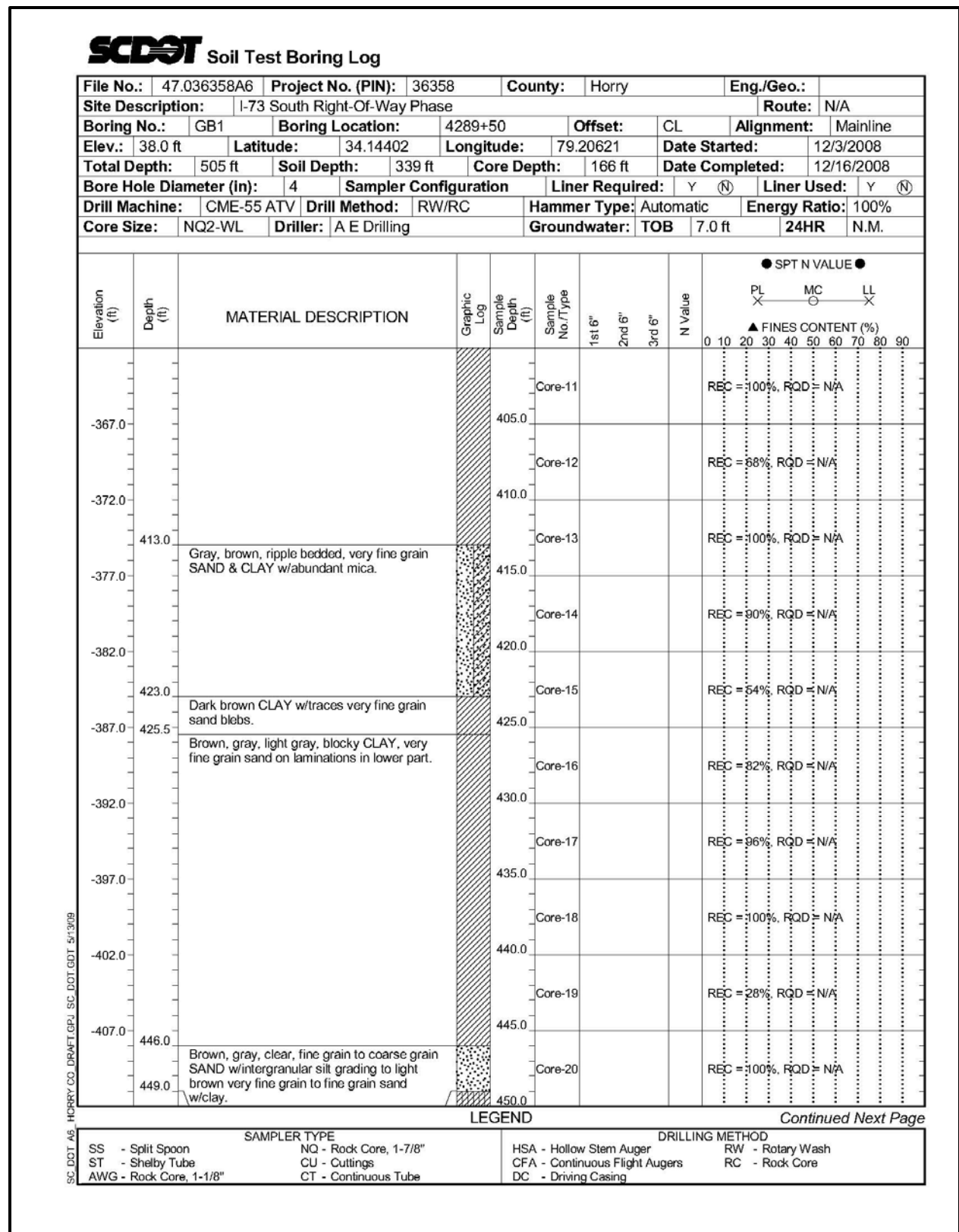


Figure H-67, Soil Test Boring G-B-1 (con't)

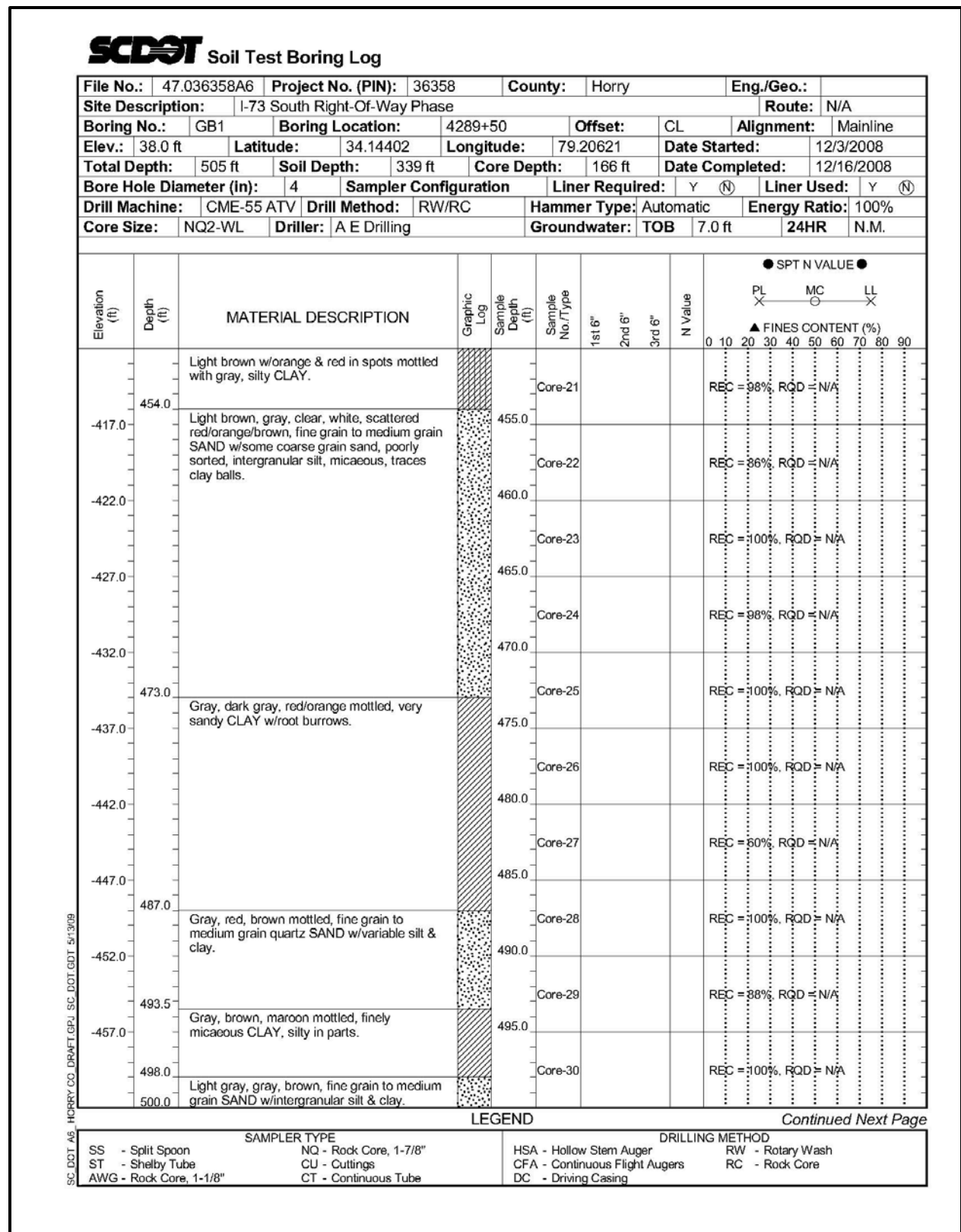


Figure H-68, Soil Test Boring G-B-1 (con't)

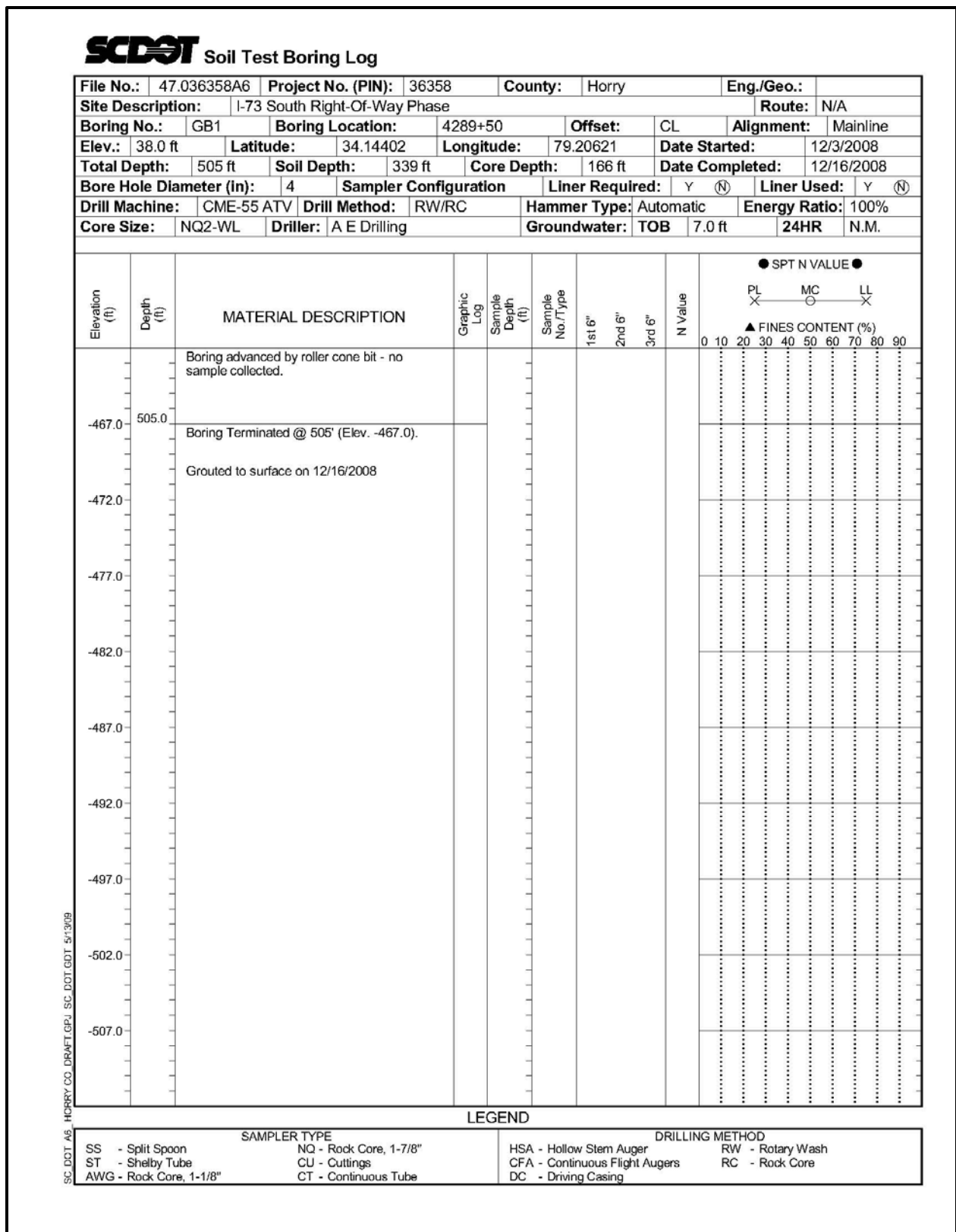
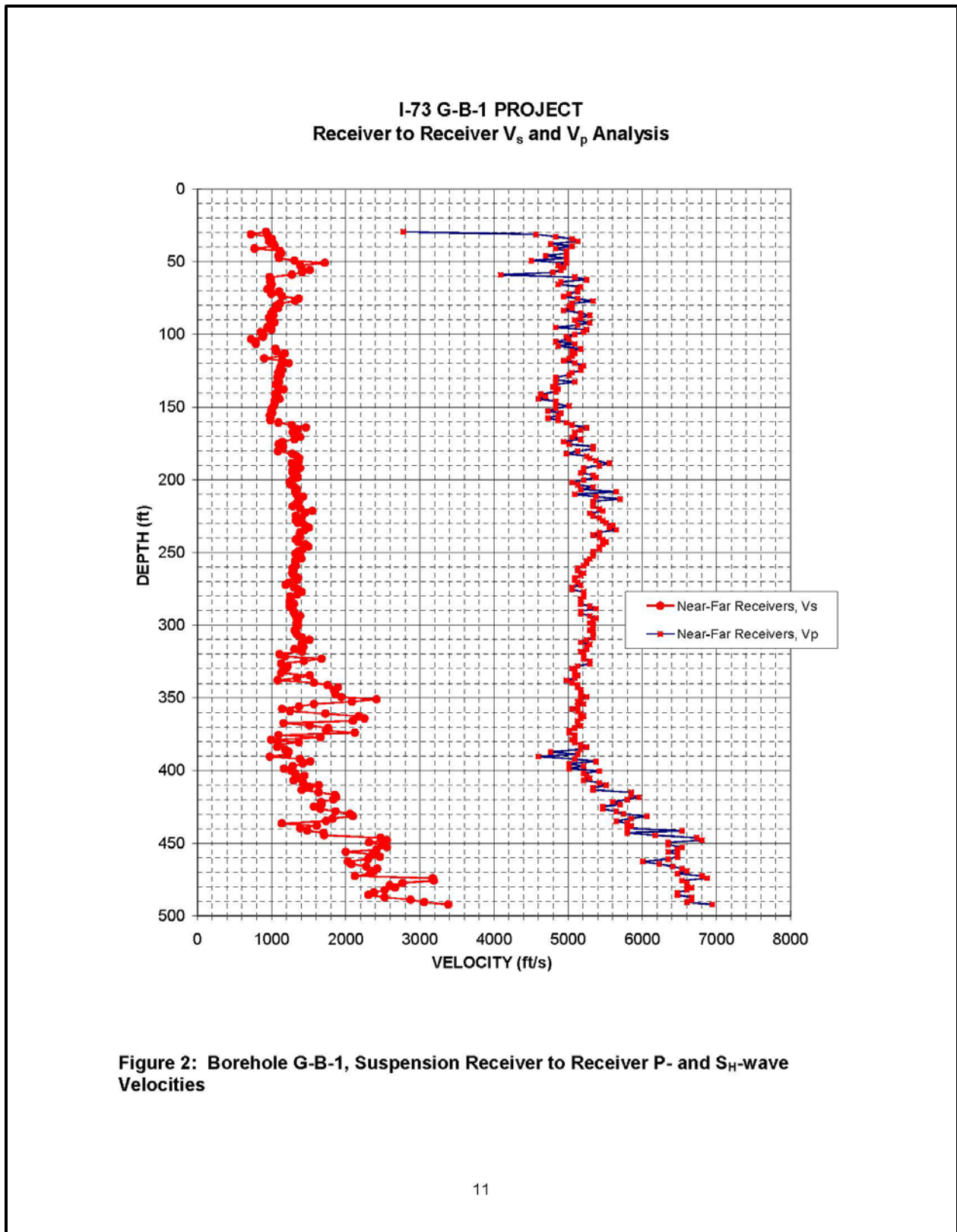


Figure H-69, Soil Test Boring G-B-1 (con't)



**Figure H-70,  $V_s$  and  $V_p$  Profile – G-B-1**



**Table 2: Summary of Shear and Compressional Wave Velocity Based on Receiver-to-Receiver Travel Time Data - Borehole G-B-1, SC-917, Mullins, SC**

Summary of Compressional Wave Velocity, Shear Wave Velocity, and Poisson's Ratio Based on Receiver-to-Receiver Travel Time Data - Borehole B-1							
American Units				Metric Units			
Depth at Midpoint Between Receivers	Velocity		Poisson's Ratio	Depth at Midpoint Between Receivers	Velocity		Poisson's Ratio
(ft)	V <sub>s</sub> (ft/s)	V <sub>p</sub> (ft/s)		(m)	V <sub>s</sub> (m/s)	V <sub>p</sub> (m/s)	
29.5	930	2780	0.44	9.0	280	850	0.44
31.2	720	4570	0.49	9.5	220	1390	0.49
32.8	960	4830	0.48	10.0	290	1470	0.48
34.5	1000	5050	0.48	10.5	310	1540	0.48
36.1	970	5130	0.48	11.0	290	1560	0.48
37.7	1030	4760	0.48	11.5	310	1450	0.48
39.4	1040	5050	0.48	12.0	320	1540	0.48
41.0	770	4830	0.49	12.5	230	1470	0.49
42.7	1110	4980	0.47	13.0	340	1520	0.47
44.3	1130	4980	0.47	13.5	340	1520	0.47
45.9	1090	4690	0.47	14.0	330	1430	0.47
47.6	1100	4980	0.47	14.5	340	1520	0.47
49.2	1310	4500	0.45	15.0	400	1370	0.45
50.9	1720	4980	0.43	15.5	520	1520	0.43
52.5	1380	4870	0.46	16.0	420	1480	0.46
54.1	1410	4940	0.46	16.5	430	1510	0.46
55.8	1520	4900	0.45	17.0	460	1490	0.45
57.4	1410	4800	0.45	17.5	430	1460	0.45
59.1	1270	4090	0.45	18.0	390	1250	0.45
60.7	970	5090	0.48	18.5	300	1550	0.48
62.3	990	5250	0.48	19.0	300	1600	0.48
64.0	980	4900	0.48	19.5	300	1490	0.48
65.6	1000	4870	0.48	20.0	310	1480	0.48
67.3	990	5170	0.48	20.5	300	1580	0.48
68.9	940	5130	0.48	21.0	290	1560	0.48
70.5	1100	5130	0.48	21.5	340	1560	0.48
72.2	1000	5010	0.48	22.0	300	1530	0.48
73.8	1140	4940	0.47	22.5	350	1510	0.47
75.5	1370	5130	0.46	23.0	420	1560	0.46
77.1	1320	5330	0.47	23.5	400	1630	0.47
78.7	1110	5050	0.47	24.0	340	1540	0.47
80.4	1060	5010	0.48	24.5	320	1530	0.48
82.0	1090	5050	0.48	25.0	330	1540	0.48
83.7	1030	4940	0.48	25.5	310	1510	0.48
85.3	1000	5170	0.48	26.0	300	1580	0.48
86.9	1020	5290	0.48	26.5	310	1610	0.48
88.6	970	5170	0.48	27.0	290	1580	0.48
90.2	990	5090	0.48	27.5	300	1550	0.48
91.9	1040	5290	0.48	28.0	320	1610	0.48
93.5	980	5130	0.48	28.5	300	1560	0.48
95.1	940	4830	0.48	29.0	290	1470	0.48
96.8	1000	5250	0.48	29.5	300	1600	0.48

**Figure H-71, Tabulated V<sub>s</sub> and V<sub>p</sub> Results – G-B-1**

Summary of Compressional Wave Velocity, Shear Wave Velocity, and Poisson's Ratio Based on Receiver-to-Receiver Travel Time Data - Borehole B-1							
American Units				Metric Units			
Depth at Midpoint Between Receivers	Velocity		Poisson's Ratio	Depth at Midpoint Between Receivers	Velocity		Poisson's Ratio
(ft)	V <sub>s</sub> (ft/s)	V <sub>p</sub> (ft/s)		(m)	V <sub>s</sub> (m/s)	V <sub>p</sub> (m/s)	
98.4	850	5210	0.49	30.0	260	1590	0.49
100.1	890	5090	0.48	30.5	270	1550	0.48
101.7	880	4980	0.48	31.0	270	1520	0.48
103.4	720	5010	0.49	31.5	220	1530	0.49
105.0	780	4830	0.49	32.0	240	1470	0.49
106.6	790	5090	0.49	32.5	240	1550	0.49
107.9	1010	4870	0.48	32.9	310	1480	0.48
109.9	1050	5170	0.48	33.5	320	1580	0.48
111.6	1060	5050	0.48	34.0	320	1540	0.48
113.2	1180	5090	0.47	34.5	360	1550	0.47
114.8	1140	5050	0.47	35.0	350	1540	0.47
116.5	900	5010	0.48	35.5	270	1530	0.48
118.1	1140	4940	0.47	36.0	350	1510	0.47
119.8	1230	5090	0.47	36.5	370	1550	0.47
121.4	1130	5210	0.48	37.0	340	1590	0.48
123.0	1120	5170	0.48	37.5	340	1580	0.48
124.7	1140	5170	0.47	38.0	350	1580	0.47
126.3	1090	5050	0.48	38.5	330	1540	0.48
128.0	1120	5010	0.47	39.0	340	1530	0.47
129.6	1080	4830	0.47	39.5	330	1470	0.47
131.2	1090	4830	0.47	40.0	330	1470	0.47
132.9	1100	5090	0.48	40.5	340	1550	0.48
134.5	1060	4830	0.47	41.0	320	1470	0.47
136.2	1090	4800	0.47	41.5	330	1460	0.47
137.8	1160	4870	0.47	42.0	350	1480	0.47
139.4	1080	4830	0.47	42.5	330	1470	0.47
141.1	1050	4630	0.47	43.0	320	1410	0.47
142.7	1080	4690	0.47	43.5	330	1430	0.47
144.4	1110	4600	0.47	44.0	340	1400	0.47
146.0	1040	4830	0.48	44.5	320	1470	0.48
147.6	1040	4830	0.48	45.0	320	1470	0.48
149.3	1030	5010	0.48	45.5	310	1530	0.48
150.9	1010	4830	0.48	46.0	310	1470	0.48
152.6	1000	4730	0.48	46.5	300	1440	0.48
154.2	1010	4900	0.48	47.0	310	1490	0.48
155.8	980	4870	0.48	47.5	300	1480	0.48
157.5	990	4730	0.48	48.0	300	1440	0.48
159.1	980	4870	0.48	48.5	300	1480	0.48
160.8	1090	4980	0.47	49.0	330	1520	0.47
162.4	1270	5050	0.47	49.5	390	1540	0.47
164.0	1460	5250	0.46	50.0	450	1600	0.46
165.7	1340	5170	0.46	50.5	410	1580	0.46
167.3	1290	5090	0.47	51.0	390	1550	0.47
169.0	1330	5090	0.46	51.5	410	1550	0.46

Figure H-72, Tabulated V<sub>s</sub> and V<sub>p</sub> Results – G-B-1 (con't)

Summary of Compressional Wave Velocity, Shear Wave Velocity, and Poisson's Ratio Based on Receiver-to-Receiver Travel Time Data - Borehole B-1							
American Units				Metric Units			
Depth at Midpoint Between Receivers	Velocity		Poisson's Ratio	Depth at Midpoint Between Receivers	Velocity		Poisson's Ratio
(ft)	V <sub>s</sub> (ft/s)	V <sub>p</sub> (ft/s)		(m)	V <sub>s</sub> (m/s)	V <sub>p</sub> (m/s)	
170.6	1380	5050	0.46	52.0	420	1540	0.46
172.2	1310	5170	0.47	52.5	400	1580	0.47
173.9	1140	4940	0.47	53.0	350	1510	0.47
175.5	1100	5010	0.47	53.5	330	1530	0.47
177.2	1160	5330	0.48	54.0	350	1630	0.48
178.8	1140	5330	0.48	54.5	350	1630	0.48
180.5	1090	5130	0.48	55.0	330	1560	0.48
182.1	1280	4980	0.46	55.5	390	1520	0.46
183.7	1340	5250	0.47	56.0	410	1600	0.47
185.4	1370	5290	0.46	56.5	420	1610	0.46
187.0	1370	5380	0.47	57.0	420	1640	0.47
188.7	1270	5560	0.47	57.5	390	1690	0.47
190.3	1360	5420	0.47	58.0	410	1650	0.47
191.9	1380	5210	0.46	58.5	420	1590	0.46
193.6	1280	5210	0.47	59.0	390	1590	0.47
195.2	1290	5170	0.47	59.5	390	1580	0.47
196.9	1340	5330	0.47	60.0	410	1630	0.47
198.5	1350	5380	0.47	60.5	410	1640	0.47
200.1	1280	5210	0.47	61.0	390	1590	0.47
201.8	1240	5050	0.47	61.5	380	1540	0.47
203.4	1260	5130	0.47	62.0	380	1560	0.47
205.1	1310	5330	0.47	62.5	400	1630	0.47
206.7	1340	5170	0.46	63.0	410	1580	0.46
208.3	1320	5650	0.47	63.5	400	1720	0.47
210.0	1330	5090	0.46	64.0	410	1550	0.46
211.6	1420	5380	0.46	64.5	430	1640	0.46
213.3	1370	5700	0.47	65.0	420	1740	0.47
214.9	1370	5330	0.46	65.5	420	1630	0.46
216.5	1330	5330	0.47	66.0	410	1630	0.47
218.2	1290	5330	0.47	66.5	390	1630	0.47
219.8	1390	5420	0.46	67.0	420	1650	0.46
221.5	1550	5460	0.46	67.5	470	1670	0.46
223.1	1450	5290	0.46	68.0	440	1610	0.46
224.7	1330	5330	0.47	68.5	400	1630	0.47
226.4	1410	5420	0.46	69.0	430	1650	0.46
228.0	1330	5460	0.47	69.5	400	1670	0.47
229.7	1360	5510	0.47	70.0	410	1680	0.47
231.3	1450	5600	0.46	70.5	440	1710	0.46
232.9	1500	5560	0.46	71.0	460	1690	0.46
234.6	1450	5650	0.46	71.5	440	1720	0.46
236.2	1380	5420	0.47	72.0	420	1650	0.47
237.9	1380	5330	0.46	72.5	420	1630	0.46
239.5	1380	5420	0.47	73.0	420	1650	0.47
241.1	1330	5460	0.47	73.5	400	1670	0.47

Figure H-73, Tabulated V<sub>s</sub> and V<sub>p</sub> Results – G-B-1 (con't)

Summary of Compressional Wave Velocity, Shear Wave Velocity, and Poisson's Ratio Based on Receiver-to-Receiver Travel Time Data - Borehole B-1							
American Units				Metric Units			
Depth at Midpoint Between Receivers	Velocity		Poisson's Ratio	Depth at Midpoint Between Receivers	Velocity		Poisson's Ratio
(ft)	V <sub>s</sub> (ft/s)	V <sub>p</sub> (ft/s)		(m)	V <sub>s</sub> (m/s)	V <sub>p</sub> (m/s)	
242.8	1360	5510	0.47	74.0	410	1680	0.47
244.4	1460	5460	0.46	74.5	440	1670	0.46
246.1	1490	5420	0.46	75.0	460	1650	0.46
247.7	1420	5420	0.46	75.5	430	1650	0.46
249.3	1360	5330	0.47	76.0	410	1630	0.47
251.0	1320	5330	0.47	76.5	400	1630	0.47
252.6	1390	5330	0.46	77.0	420	1630	0.46
254.3	1400	5290	0.46	77.5	430	1610	0.46
255.9	1320	5250	0.47	78.0	400	1600	0.47
257.6	1320	5250	0.47	78.5	400	1600	0.47
259.2	1330	5210	0.47	79.0	400	1590	0.47
260.8	1280	5130	0.47	79.5	390	1560	0.47
262.5	1300	5130	0.47	80.0	400	1560	0.47
264.1	1280	5210	0.47	80.5	390	1590	0.47
265.8	1300	5170	0.47	81.0	400	1580	0.47
267.4	1360	5090	0.46	81.5	410	1550	0.46
269.0	1340	5090	0.46	82.0	410	1550	0.46
270.7	1230	5130	0.47	82.5	380	1560	0.47
272.3	1190	5170	0.47	83.0	360	1580	0.47
274.0	1300	5050	0.46	83.5	400	1540	0.46
275.6	1360	5050	0.46	84.0	410	1540	0.46
277.2	1410	5210	0.46	84.5	430	1590	0.46
278.9	1350	5210	0.46	85.0	410	1590	0.46
280.5	1250	5210	0.47	85.5	380	1590	0.47
282.2	1260	5170	0.47	86.0	380	1580	0.47
283.8	1240	5170	0.47	86.5	380	1580	0.47
285.4	1300	5170	0.47	87.0	400	1580	0.47
287.1	1240	5290	0.47	87.5	380	1610	0.47
288.7	1280	5380	0.47	88.0	390	1640	0.47
290.4	1300	5170	0.47	88.5	400	1580	0.47
292.0	1310	5170	0.47	89.0	400	1580	0.47
293.6	1380	5290	0.46	89.5	420	1610	0.46
295.3	1340	5380	0.47	90.0	410	1640	0.47
296.9	1360	5330	0.47	90.5	410	1630	0.47
298.6	1340	5290	0.47	91.0	410	1610	0.47
300.2	1360	5330	0.47	91.5	410	1630	0.47
301.8	1330	5330	0.47	92.0	410	1630	0.47
303.5	1310	5290	0.47	92.5	400	1610	0.47
305.1	1330	5330	0.47	93.0	400	1630	0.47
306.8	1350	5330	0.47	93.5	410	1630	0.47
308.4	1410	5330	0.46	94.0	430	1630	0.46
310.0	1510	5250	0.46	94.5	460	1600	0.46
311.7	1410	5170	0.46	95.0	430	1580	0.46
313.3	1410	5290	0.46	95.5	430	1610	0.46

Figure H-74, Tabulated V<sub>s</sub> and V<sub>p</sub> Results – G-B-1 (con't)

Summary of Compressional Wave Velocity, Shear Wave Velocity, and Poisson's Ratio Based on Receiver-to-Receiver Travel Time Data - Borehole B-1							
American Units				Metric Units			
Depth at Midpoint Between Receivers	Velocity		Poisson's Ratio	Depth at Midpoint Between Receivers	Velocity		Poisson's Ratio
(ft)	V <sub>s</sub> (ft/s)	V <sub>p</sub> (ft/s)		(m)	V <sub>s</sub> (m/s)	V <sub>p</sub> (m/s)	
315.0	1430	5250	0.46	96.0	440	1600	0.46
316.6	1310	5250	0.47	96.5	400	1600	0.47
318.2	1410	5170	0.46	97.0	430	1580	0.46
319.9	1110	5210	0.48	97.5	340	1590	0.48
321.5	1180	5210	0.47	98.0	360	1590	0.47
323.2	1680	5210	0.44	98.5	510	1590	0.44
324.8	1440	5290	0.46	99.0	440	1610	0.46
326.4	1130	5290	0.48	99.5	340	1610	0.48
328.1	1220	5130	0.47	100.0	370	1560	0.47
329.7	1200	5050	0.47	100.5	370	1540	0.47
331.4	1160	5090	0.47	101.0	350	1550	0.47
333.0	1130	5090	0.47	101.5	340	1550	0.47
334.7	1520	5130	0.45	102.0	460	1560	0.45
336.3	1340	5090	0.46	102.5	410	1550	0.46
337.9	1080	4980	0.48	103.0	330	1520	0.48
339.6	1570	5050	0.45	103.5	480	1540	0.45
341.2	1750	5130	0.43	104.0	530	1560	0.43
342.9	1890	5130	0.42	104.5	580	1560	0.42
344.5	1840	5170	0.43	105.0	560	1580	0.43
346.1	1850	5170	0.43	105.5	560	1580	0.43
347.8	1860	5170	0.43	106.0	570	1580	0.43
349.4	1940	5250	0.42	106.5	590	1600	0.42
351.1	2420	5170	0.36	107.0	740	1580	0.36
352.7	2080	5130	0.40	107.5	640	1560	0.40
354.3	1570	5210	0.45	108.0	480	1590	0.45
356.0	1370	5130	0.46	108.5	420	1560	0.46
357.6	1140	5050	0.47	109.0	350	1540	0.47
359.3	1250	5130	0.47	109.5	380	1560	0.47
360.9	1730	5170	0.44	110.0	530	1580	0.44
362.5	2180	5210	0.39	110.5	660	1590	0.39
364.2	2250	5170	0.38	111.0	690	1580	0.38
365.8	2100	5130	0.40	111.5	640	1560	0.40
367.5	1160	5130	0.47	112.0	350	1560	0.47
369.1	1520	5170	0.45	112.5	460	1580	0.45
370.7	1760	5090	0.43	113.0	540	1550	0.43
372.4	1740	5010	0.43	113.5	530	1530	0.43
374.0	2120	5010	0.39	114.0	650	1530	0.39
375.7	1090	5090	0.48	114.5	330	1550	0.48
377.3	1660	5090	0.44	115.0	510	1550	0.44
378.9	1000	5050	0.48	115.5	300	1540	0.48
380.6	1370	5090	0.46	116.0	420	1550	0.46
382.2	1090	5170	0.48	116.5	330	1580	0.48
383.9	1080	5250	0.48	117.0	330	1600	0.48
385.5	1180	5170	0.47	117.5	360	1580	0.47

Figure H-75, Tabulated V<sub>s</sub> and V<sub>p</sub> Results – G-B-1 (con't)

Summary of Compressional Wave Velocity, Shear Wave Velocity, and Poisson's Ratio Based on Receiver-to-Receiver Travel Time Data - Borehole B-1							
American Units				Metric Units			
Depth at Midpoint Between Receivers	Velocity		Poisson's Ratio	Depth at Midpoint Between Receivers	Velocity		Poisson's Ratio
(ft)	V <sub>s</sub> (ft/s)	V <sub>p</sub> (ft/s)		(m)	V <sub>s</sub> (m/s)	V <sub>p</sub> (m/s)	
387.1	1230	4760	0.46	118.0	370	1450	0.46
388.8	1210	5130	0.47	118.5	370	1560	0.47
390.4	980	4600	0.48	119.0	300	1400	0.48
392.1	1380	5090	0.46	119.5	420	1550	0.46
393.7	1520	5380	0.46	120.0	460	1640	0.46
395.3	1420	5010	0.46	120.5	430	1530	0.46
397.0	1290	5210	0.47	121.0	390	1590	0.47
398.6	1170	5010	0.47	121.5	360	1530	0.47
400.3	1270	5420	0.47	122.0	390	1650	0.47
401.9	1320	5210	0.47	122.5	400	1590	0.47
403.5	1440	5250	0.46	123.0	440	1600	0.46
405.2	1330	5290	0.47	123.5	410	1610	0.47
406.8	1300	5210	0.47	124.0	400	1590	0.47
408.5	1420	5420	0.46	124.5	430	1650	0.46
410.1	1630	5510	0.45	125.0	500	1680	0.45
411.8	1510	5330	0.46	125.5	460	1630	0.46
413.4	1410	5330	0.46	126.0	430	1630	0.46
415.0	1630	5850	0.46	126.5	500	1780	0.46
416.7	1850	5850	0.44	127.0	560	1780	0.44
418.3	1870	5950	0.45	127.5	570	1810	0.45
420.0	1830	5800	0.44	128.0	560	1770	0.44
421.6	1670	5600	0.45	128.5	510	1710	0.45
423.2	1680	5700	0.45	129.0	510	1740	0.45
424.9	1570	5460	0.45	129.5	480	1670	0.45
426.5	1660	5460	0.45	130.0	510	1670	0.45
428.2	1860	5650	0.44	130.5	570	1720	0.44
429.8	2060	5750	0.43	131.0	630	1750	0.43
431.4	2100	6060	0.43	131.5	640	1850	0.43
433.1	1820	5850	0.45	132.0	560	1780	0.45
434.7	1740	5650	0.45	132.5	530	1720	0.45
436.4	1140	5800	0.48	133.0	350	1770	0.48
438.0	1610	5850	0.46	133.5	490	1780	0.46
439.6	1380	5800	0.47	134.0	420	1770	0.47
441.3	1480	6540	0.47	134.5	450	1990	0.47
442.9	1700	5800	0.45	135.0	520	1770	0.45
444.6	1710	6170	0.46	135.5	520	1880	0.46
446.2	2470	6730	0.42	136.0	750	2050	0.42
447.8	2550	6800	0.42	136.5	780	2070	0.42
449.5	2310	6350	0.42	137.0	710	1940	0.42
451.1	2490	6350	0.41	137.5	760	1940	0.41
452.8	2550	6540	0.41	138.0	780	1990	0.41
454.4	2420	6470	0.42	138.5	740	1970	0.42
456.0	2000	6350	0.44	139.0	610	1940	0.44
457.7	2360	6470	0.42	139.5	720	1970	0.42

Figure H-76, Tabulated V<sub>s</sub> and V<sub>p</sub> Results – G-B-1 (con't)

Summary of Compressional Wave Velocity, Shear Wave Velocity, and Poisson's Ratio Based on Receiver-to-Receiver Travel Time Data - Borehole B-1							
American Units				Metric Units			
Depth at Midpoint Between Receivers	Velocity		Poisson's Ratio	Depth at Midpoint Between Receivers	Velocity		Poisson's Ratio
(ft)	V <sub>s</sub> (ft/s)	V <sub>p</sub> (ft/s)		(m)	V <sub>s</sub> (m/s)	V <sub>p</sub> (m/s)	
459.3	2460	6470	0.42	140.0	750	1970	0.42
461.0	2300	6350	0.42	140.5	700	1940	0.42
462.6	2030	6010	0.44	141.0	620	1830	0.44
464.2	2080	6230	0.44	141.5	630	1900	0.44
465.9	2280	6410	0.43	142.0	690	1950	0.43
467.5	2420	6540	0.42	142.5	740	1990	0.42
469.2	2380	6600	0.43	143.0	730	2010	0.43
470.8	2330	6470	0.43	143.5	710	1970	0.43
472.4	2120	6800	0.45	144.0	650	2070	0.45
474.1	3170	6870	0.36	144.5	970	2090	0.36
475.7	3190	6540	0.34	145.0	970	1990	0.34
477.4	2770	6600	0.39	145.5	840	2010	0.39
479.0	2590	6600	0.41	146.0	790	2010	0.41
480.6	2670	6670	0.40	146.5	810	2030	0.40
482.3	2530	6600	0.41	147.0	770	2010	0.41
483.9	2380	6470	0.42	147.5	730	1970	0.42
485.6	2310	6470	0.43	148.0	700	1970	0.43
487.2	2530	6670	0.42	148.5	770	2030	0.42
488.9	2870	6670	0.39	149.0	880	2030	0.39
490.5	3060	6600	0.36	149.5	930	2010	0.36
492.1	3380	6940	0.34	150.0	1030	2120	0.34

**Notes:** "." means no data available at that particular interval of depth.

Figure H-77, Tabulated V<sub>s</sub> and V<sub>p</sub> Results – G-B-1 (con't)

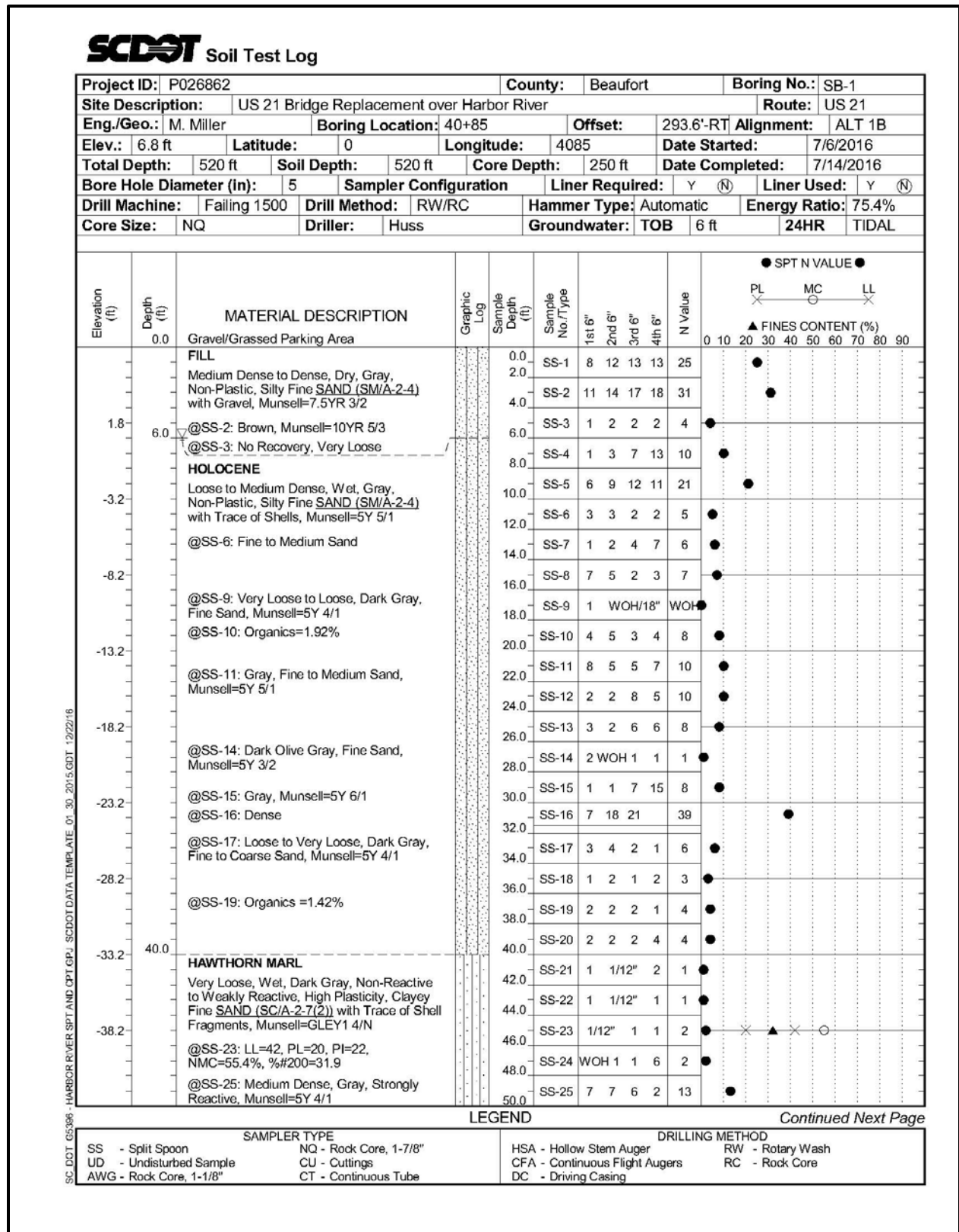


Figure H-78, Soil Test Boring SB-1



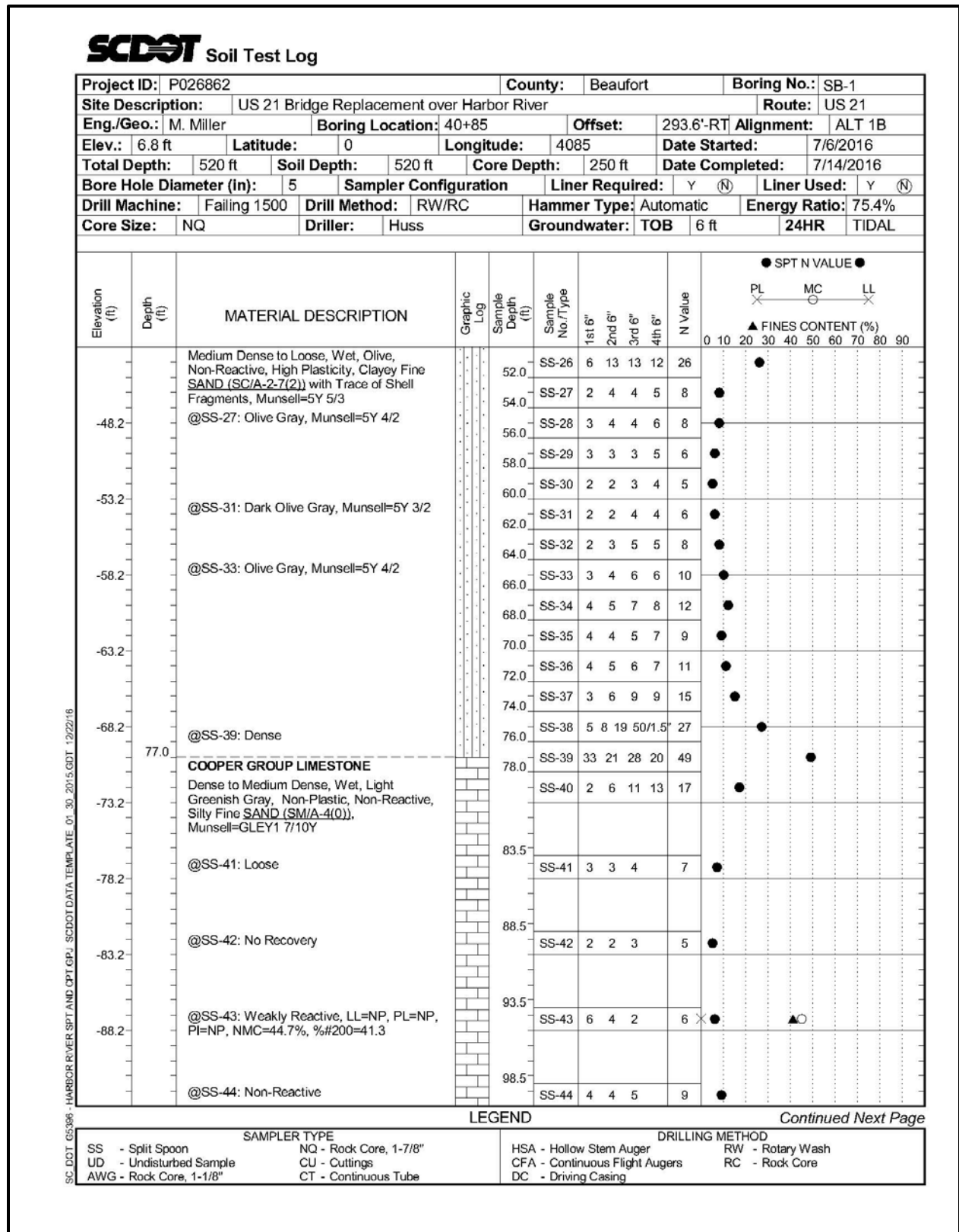


Figure H-79, Soil Test Boring SB-1 (con't)

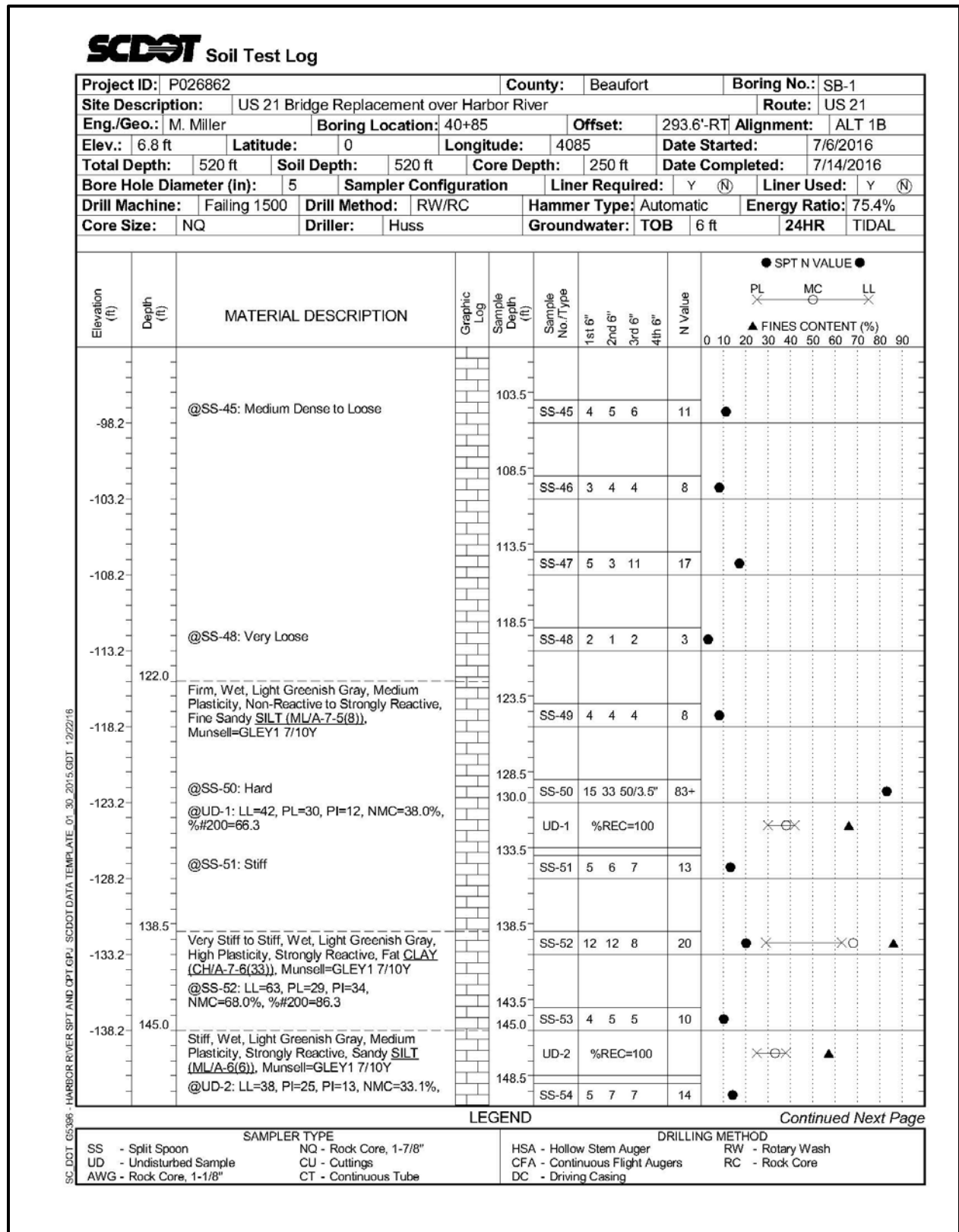


Figure H-80, Soil Test Boring SB-1 (con't)

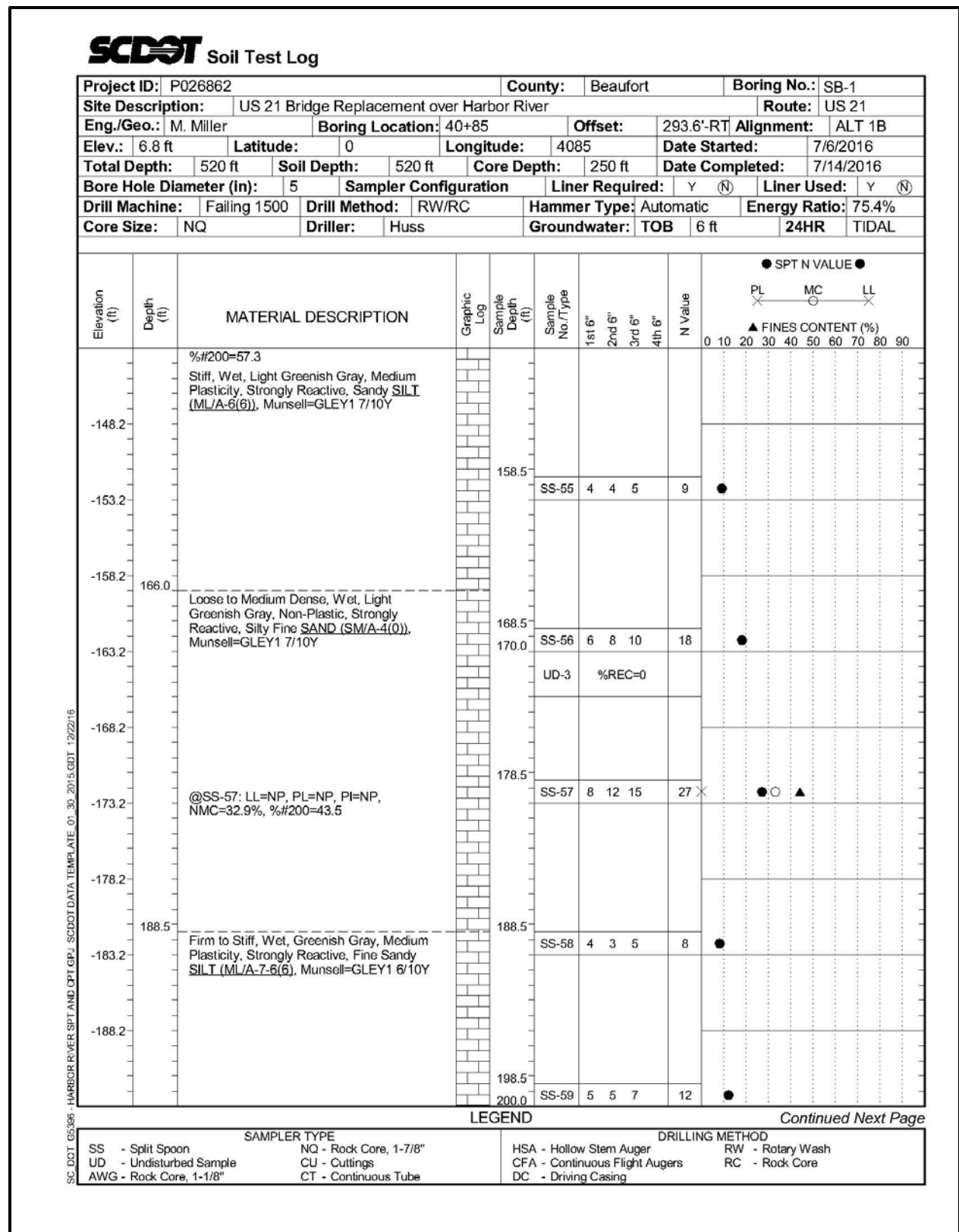


Figure H-81, Soil Test Boring SB-1 (con't)

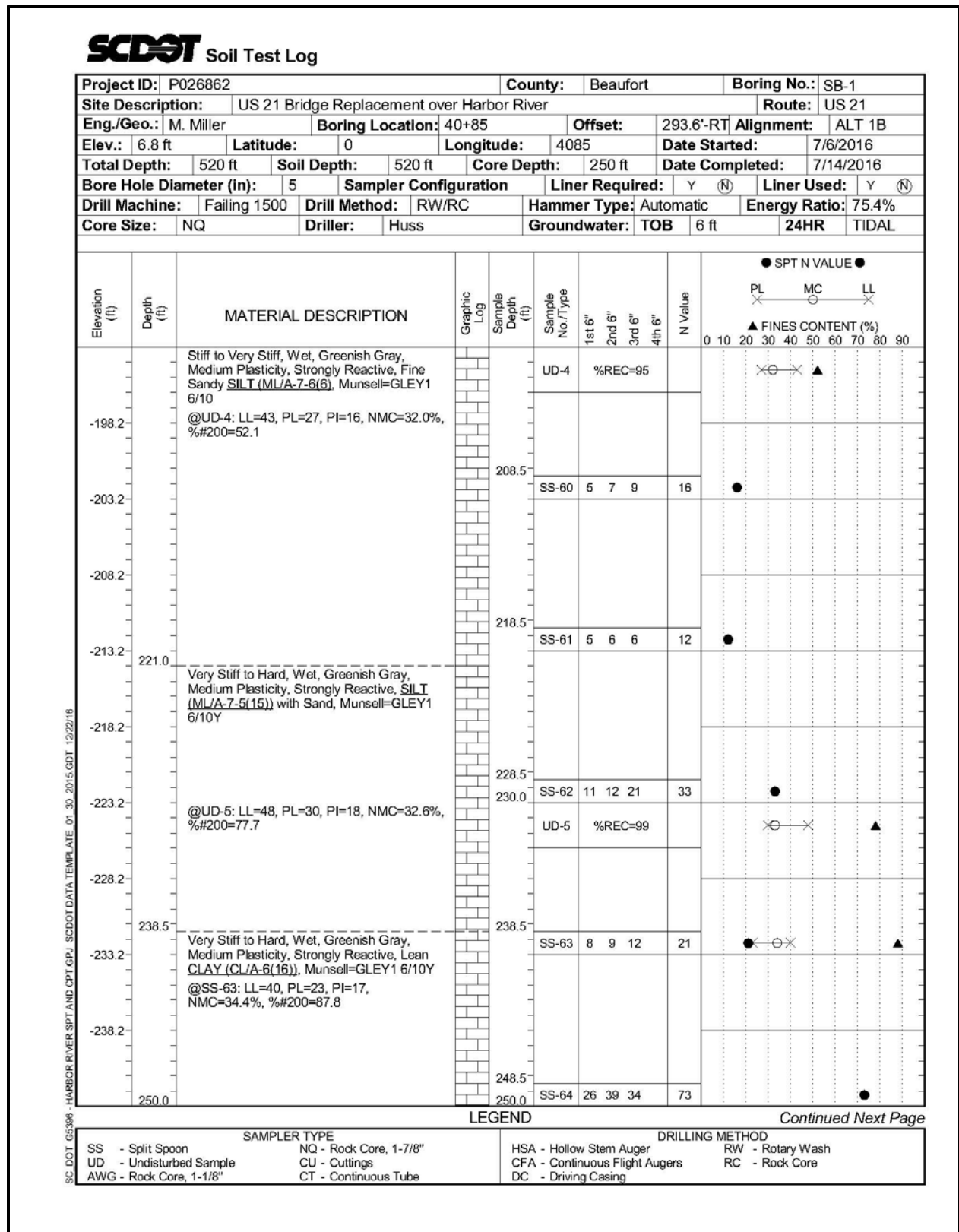


Figure H-82, Soil Test Boring SB-1 (con't)



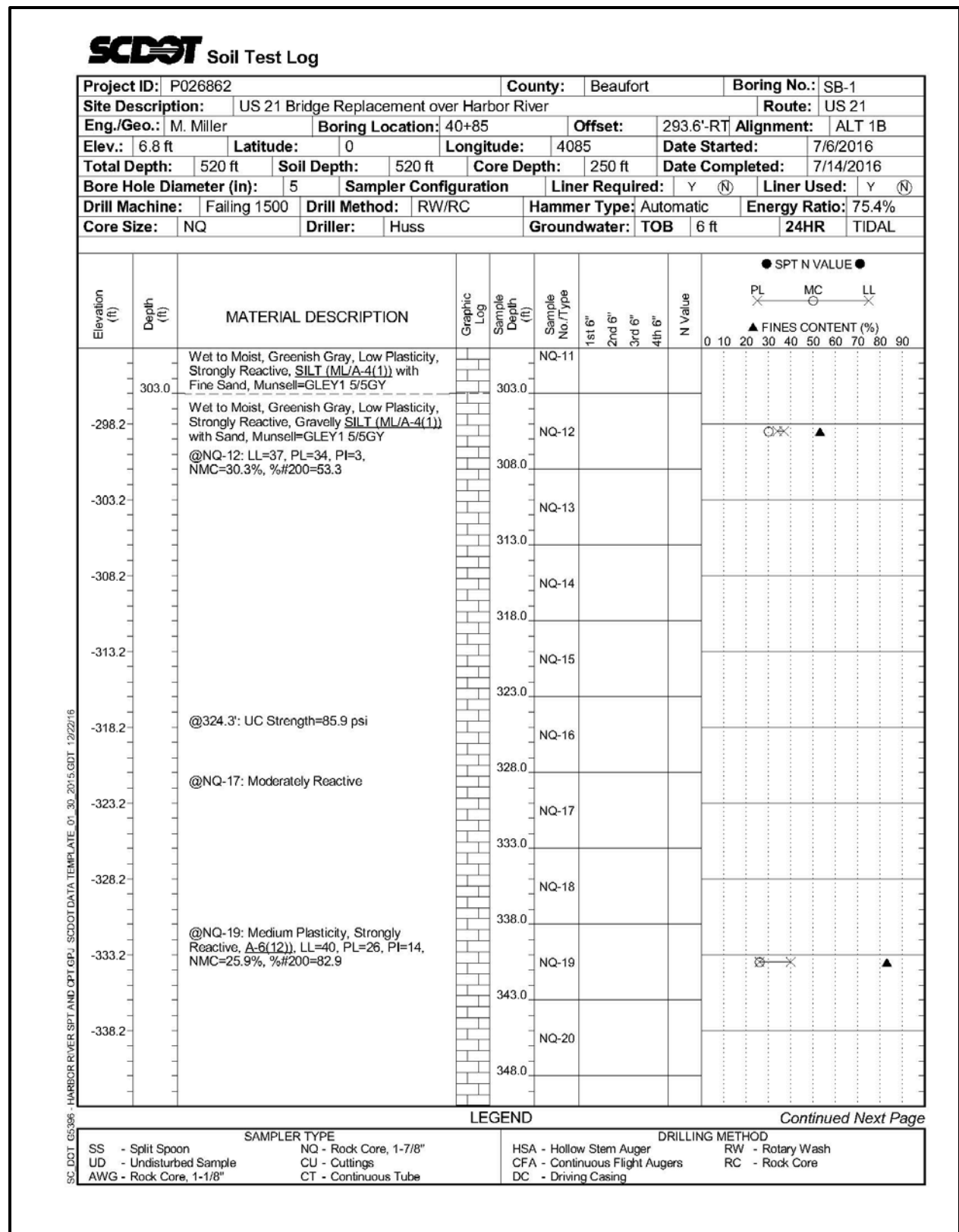


Figure H-84, Soil Test Boring SB-1 (con't)

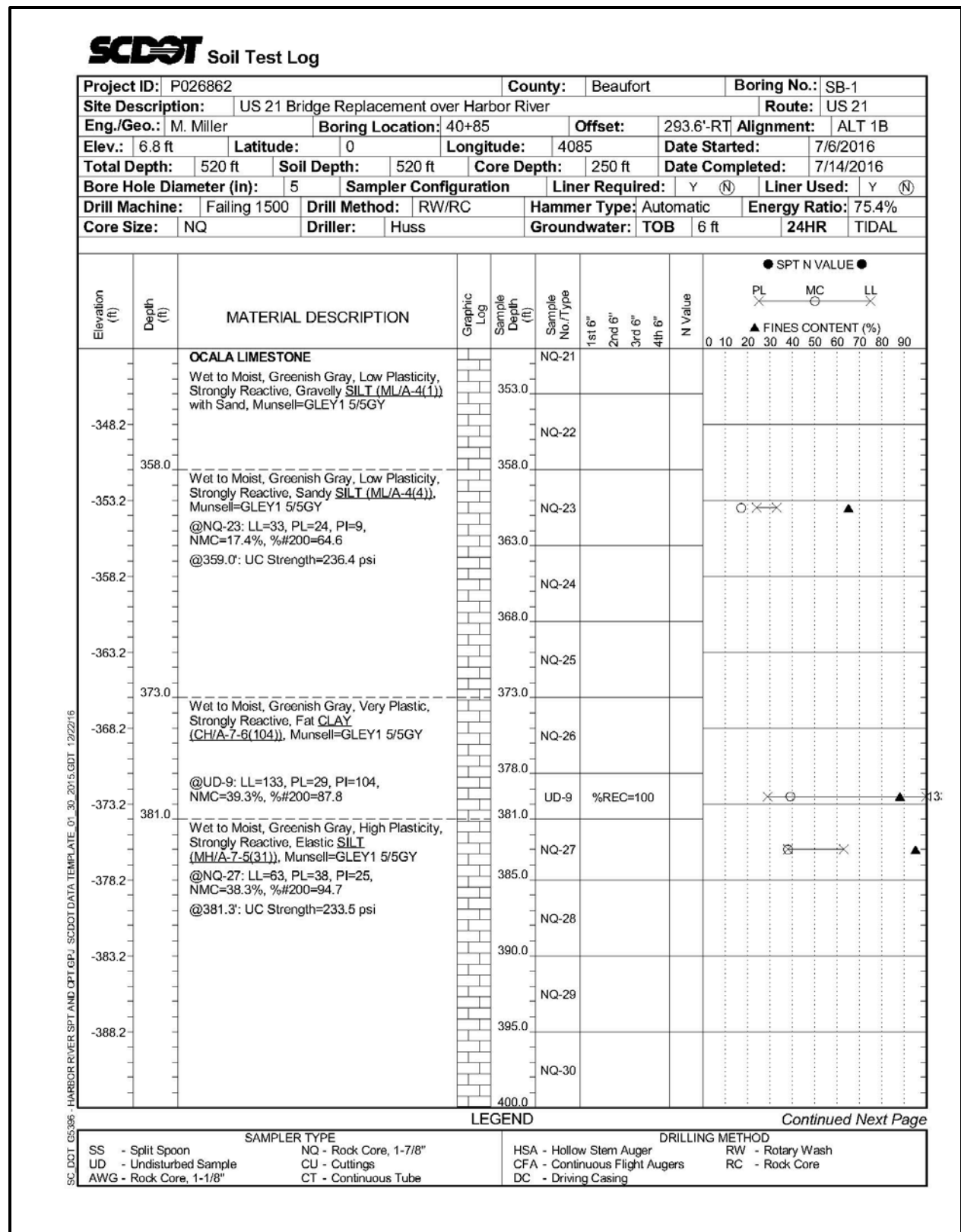


Figure H-85, Soil Test Boring SB-1 (con't)







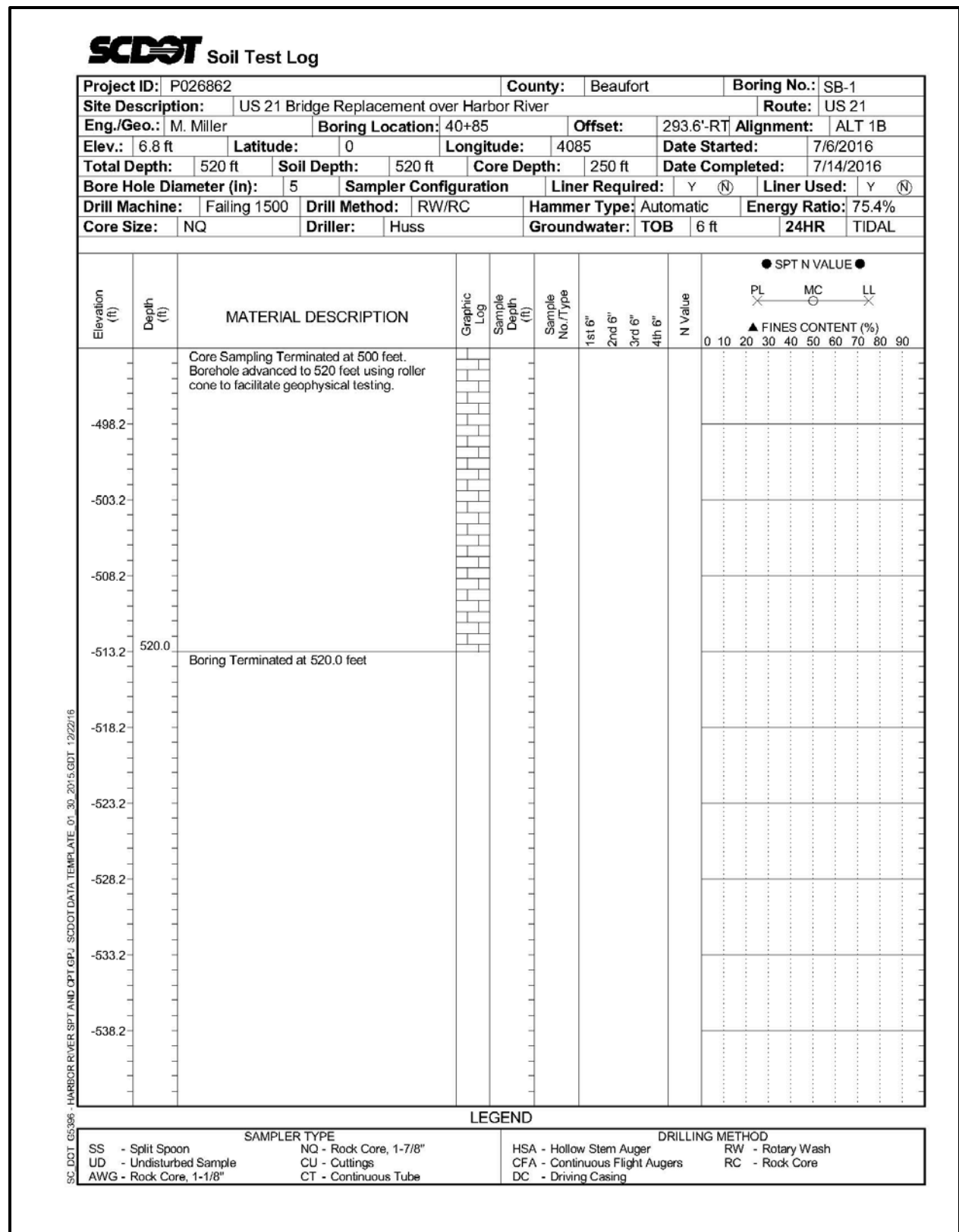
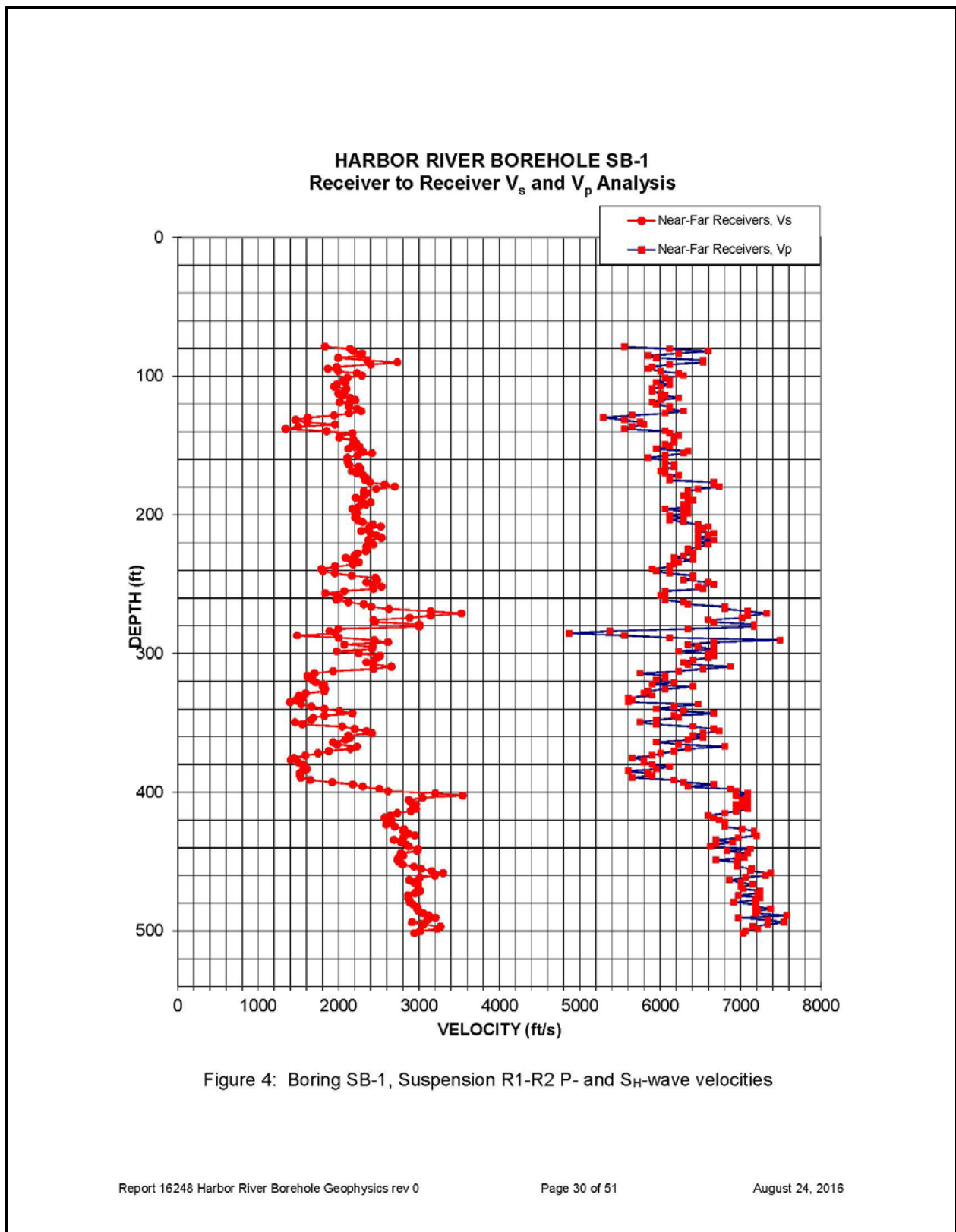


Figure H-88, Soil Test Boring SB-1 (con't)



**Figure H-89,  $V_s$  and  $V_p$  Profile – SB-1**

Table 3. Boring SB-1, Suspension R1-R2 depths and P- and SH-wave velocities

Summary of Compressional Wave Velocity, Shear Wave Velocity, and Poisson's Ratio  
Based on Receiver-to-Receiver Travel Time Data - Borehole SB-1

American Units				Metric Units			
Depth at Midpoint Between Receivers	Velocity		Poisson's Ratio	Depth at Midpoint Between Receivers	Velocity		Poisson's Ratio
	V <sub>s</sub>	V <sub>p</sub>			V <sub>s</sub>	V <sub>p</sub>	
(ft)	(ft/s)	(ft/s)		(m)	(m/s)	(m/s)	
78.9	1830	5560	0.44	24.0	560	1690	0.44
80.5	2140	6120	0.43	24.5	650	1860	0.43
82.1	2190	6600	0.44	25.0	670	2010	0.44
83.7	2290	6230	0.42	25.5	700	1900	0.42
85.3	2270	5850	0.41	26.0	690	1780	0.41
86.9	2000	5950	0.44	26.5	610	1810	0.44
88.5	2360	6540	0.43	27.0	720	1990	0.43
90.1	2730	6540	0.39	27.5	830	1990	0.39
91.7	2400	6120	0.41	27.9	730	1860	0.41
93.3	1980	5900	0.44	28.4	600	1800	0.44
94.9	1870	5850	0.44	28.9	570	1780	0.44
96.5	2000	6010	0.44	29.4	610	1830	0.44
98.1	2230	6230	0.43	29.9	680	1900	0.43
99.7	2290	6290	0.42	30.4	700	1920	0.42
101.3	2110	6060	0.43	30.9	640	1850	0.43
102.9	2060	6120	0.44	31.4	630	1860	0.44
104.5	2080	5950	0.43	31.8	640	1810	0.43
106.1	1980	6120	0.44	32.3	600	1860	0.44
107.7	1940	6010	0.44	32.8	590	1830	0.44
109.3	2100	5900	0.43	33.3	640	1800	0.43
110.9	2080	5900	0.43	33.8	630	1800	0.43
112.5	2000	6010	0.44	34.3	610	1830	0.44
114.1	2040	6060	0.44	34.8	620	1850	0.44
115.7	2140	6230	0.43	35.3	650	1900	0.43
117.3	2210	6010	0.42	35.8	670	1830	0.42
118.9	2010	5900	0.43	36.2	610	1800	0.43
120.5	2130	5950	0.43	36.7	650	1810	0.43
122.1	2130	6120	0.43	37.2	650	1860	0.43
123.7	2230	6120	0.42	37.7	680	1860	0.42
125.3	2280	6290	0.42	38.2	700	1920	0.42
126.9	2130	6060	0.43	38.7	650	1850	0.43
128.5	1940	5650	0.43	39.2	590	1720	0.43
130.1	1620	5290	0.45	39.7	490	1610	0.45
131.7	1470	5560	0.46	40.1	450	1690	0.46
133.3	1610	5750	0.46	40.6	490	1750	0.46
134.9	1960	5800	0.44	41.1	600	1770	0.44
136.5	1500	5650	0.46	41.6	460	1720	0.46

Figure H-90, Tabulated V<sub>s</sub> and V<sub>p</sub> Results – SB-1

**Summary of Compressional Wave Velocity, Shear Wave Velocity, and Poisson's Ratio  
Based on Receiver-to-Receiver Travel Time Data - Borehole SB-1**

American Units				Metric Units			
Depth at Midpoint Between Receivers	Velocity		Poisson's Ratio	Depth at Midpoint Between Receivers	Velocity		Poisson's Ratio
	V <sub>s</sub>	V <sub>p</sub>			V <sub>s</sub>	V <sub>p</sub>	
(ft)	(ft/s)	(ft/s)		(m)	(m/s)	(m/s)	
138.1	1340	5560	0.47	42.1	410	1690	0.47
139.7	1850	6060	0.45	42.6	560	1850	0.45
141.3	2170	6120	0.43	43.1	660	1860	0.43
142.9	2020	6230	0.44	43.6	620	1900	0.44
144.5	2010	6170	0.44	44.1	610	1880	0.44
146.1	2190	6170	0.43	44.5	670	1880	0.43
147.7	2210	6170	0.43	45.0	680	1880	0.43
149.3	2180	6060	0.43	45.5	660	1850	0.43
150.9	2260	6120	0.42	46.0	690	1860	0.42
152.5	2120	5950	0.43	46.5	650	1810	0.43
154.1	2300	6350	0.42	47.0	700	1940	0.42
155.7	2420	6290	0.41	47.5	740	1920	0.41
157.3	2240	6060	0.42	48.0	680	1850	0.42
158.9	2110	5850	0.43	48.4	640	1780	0.43
160.5	2110	6060	0.43	48.9	640	1850	0.43
162.1	2120	6060	0.43	49.4	650	1850	0.43
163.8	2130	6170	0.43	49.9	650	1880	0.43
165.4	2250	6170	0.42	50.4	690	1880	0.42
167.0	2280	6060	0.42	50.9	690	1850	0.42
168.6	2160	6010	0.43	51.4	660	1830	0.43
170.2	2220	6060	0.42	51.9	680	1850	0.42
171.8	2310	6230	0.42	52.4	700	1900	0.42
173.4	2340	6120	0.41	52.8	710	1860	0.41
175.0	2330	6120	0.42	53.3	710	1860	0.42
176.6	2390	6670	0.43	53.8	730	2030	0.43
178.2	2570	6670	0.41	54.3	780	2030	0.41
179.8	2700	6730	0.40	54.8	820	2050	0.40
181.4	2470	6470	0.41	55.3	750	1970	0.41
183.0	2310	6350	0.42	55.8	710	1940	0.42
184.6	2350	6350	0.42	56.3	720	1940	0.42
186.2	2310	6290	0.42	56.7	710	1920	0.42
187.8	2210	6350	0.43	57.2	680	1940	0.43
189.4	2280	6410	0.43	57.7	700	1950	0.43
191.0	2400	6350	0.42	58.2	730	1940	0.42
192.6	2340	6290	0.42	58.7	710	1920	0.42
194.2	2250	6350	0.43	59.2	690	1940	0.43
195.8	2170	6060	0.43	59.7	660	1850	0.43
197.4	2200	6290	0.43	60.2	670	1920	0.43
199.0	2230	6350	0.43	60.7	680	1940	0.43
200.6	2210	6120	0.42	61.1	680	1860	0.42

**Figure H-91, Tabulated V<sub>s</sub> and V<sub>p</sub> Results – SB-1 (con't)**

**Summary of Compressional Wave Velocity, Shear Wave Velocity, and Poisson's Ratio  
Based on Receiver-to-Receiver Travel Time Data - Borehole SB-1**

American Units				Metric Units			
Depth at Midpoint Between Receivers	Velocity		Poisson's Ratio	Depth at Midpoint Between Receivers	Velocity		Poisson's Ratio
	V <sub>s</sub>	V <sub>p</sub>			V <sub>s</sub>	V <sub>p</sub>	
(ft)	(ft/s)	(ft/s)		(m)	(m/s)	(m/s)	
202.2	2210	6290	0.43	61.6	670	1920	0.43
203.8	2240	6120	0.42	62.1	680	1860	0.42
205.4	2300	6290	0.42	62.6	700	1920	0.42
207.0	2420	6470	0.42	63.1	740	1970	0.42
208.6	2530	6600	0.41	63.6	770	2010	0.41
210.2	2370	6540	0.42	64.1	720	1990	0.42
211.8	2280	6470	0.43	64.6	700	1970	0.43
213.4	2400	6670	0.43	65.0	730	2030	0.43
215.0	2470	6600	0.42	65.5	750	2010	0.42
216.6	2530	6470	0.41	66.0	770	1970	0.41
218.2	2370	6670	0.43	66.5	720	2030	0.43
219.8	2410	6470	0.42	67.0	730	1970	0.42
221.4	2430	6600	0.42	67.5	740	2010	0.42
223.0	2350	6470	0.42	68.0	720	1970	0.42
224.6	2360	6350	0.42	68.5	720	1940	0.42
226.2	2340	6350	0.42	69.0	710	1940	0.42
227.8	2240	6410	0.43	69.4	680	1950	0.43
229.4	2200	6290	0.43	69.9	670	1920	0.43
231.0	2090	6170	0.44	70.4	640	1880	0.44
232.6	2160	6410	0.44	70.9	660	1950	0.44
234.2	2250	6230	0.42	71.4	690	1900	0.42
235.8	2180	6170	0.43	71.9	660	1880	0.43
237.4	1960	6120	0.44	72.4	600	1860	0.44
239.0	1790	5900	0.45	72.9	540	1800	0.45
240.6	1810	5950	0.45	73.3	550	1810	0.45
242.2	1960	6120	0.44	73.8	600	1860	0.44
243.8	2160	6410	0.44	74.3	660	1950	0.44
245.4	2460	6410	0.41	74.8	750	1950	0.41
247.0	2480	6290	0.41	75.3	760	1920	0.41
248.7	2350	6600	0.43	75.8	720	2010	0.43
250.3	2420	6670	0.42	76.3	740	2030	0.42
251.9	2530	6470	0.41	76.8	770	1970	0.41
253.5	2430	6540	0.42	77.3	740	1990	0.42
255.1	2070	6060	0.43	77.7	630	1850	0.43
256.7	1840	6060	0.45	78.2	560	1850	0.45
258.3	1980	6010	0.44	78.7	600	1830	0.44
259.9	2010	6060	0.44	79.2	610	1850	0.44
261.5	1970	6060	0.44	79.7	600	1850	0.44
263.1	2120	6290	0.44	80.2	650	1920	0.44
264.7	2310	6350	0.42	80.7	710	1940	0.42

Report 16248 Harbor River Borehole Geophysics rev 0

Page 33 of 51

August 24, 2016

**Figure H-92, Tabulated V<sub>s</sub> and V<sub>p</sub> Results – SB-1 (con't)**

**Summary of Compressional Wave Velocity, Shear Wave Velocity, and Poisson's Ratio  
Based on Receiver-to-Receiver Travel Time Data - Borehole SB-1**

American Units				Metric Units			
Depth at Midpoint Between Receivers	Velocity		Poisson's Ratio	Depth at Midpoint Between Receivers	Velocity		Poisson's Ratio
	V <sub>s</sub>	V <sub>p</sub>			V <sub>s</sub>	V <sub>p</sub>	
(ft)	(ft/s)	(ft/s)		(m)	(m/s)	(m/s)	
266.3	2410	6800	0.43	81.2	730	2070	0.43
267.9	2620	6800	0.41	81.6	800	2070	0.41
269.5	3140	7090	0.38	82.1	960	2160	0.38
271.1	3530	7330	0.35	82.6	1080	2230	0.35
272.7	3140	7090	0.38	83.1	960	2160	0.38
274.3	2890	7020	0.40	83.6	880	2140	0.40
275.9	2430	6600	0.42	84.1	740	2010	0.42
277.5	2450	6670	0.42	84.6	750	2030	0.42
279.1	3000	7170	0.39	85.1	920	2180	0.39
280.7	3000	7170	0.39	85.6	920	2180	0.39
282.3	2000	6350	0.45	86.0	610	1940	0.45
283.9	1890	5380	0.43	86.5	580	1640	0.43
285.5	1960	4870	0.40	87.0	600	1480	0.40
287.1	1480	5560	0.46	87.5	450	1690	0.46
288.7	2000	6120	0.44	88.0	610	1860	0.44
290.3	2440	7490	0.44	88.5	740	2280	0.44
291.9	2610	6670	0.41	89.0	800	2030	0.41
293.5	2070	6350	0.44	89.5	630	1940	0.44
295.1	2420	6470	0.42	89.9	740	1970	0.42
296.7	2420	6670	0.42	90.4	740	2030	0.42
298.3	1980	6230	0.44	90.9	600	1900	0.44
299.9	2250	6600	0.43	91.4	690	2010	0.43
301.5	2520	6670	0.42	91.9	770	2030	0.42
303.1	2490	6600	0.42	92.4	760	2010	0.42
304.7	2440	6410	0.42	92.9	740	1950	0.42
306.3	2350	6290	0.42	93.4	720	1920	0.42
307.9	2430	6350	0.41	93.9	740	1940	0.41
309.5	2660	6870	0.41	94.3	810	2090	0.41
311.1	2430	6540	0.42	94.8	740	1990	0.42
312.7	1930	6230	0.45	95.3	590	1900	0.45
314.3	1700	5750	0.45	95.8	520	1750	0.45
315.9	1610	6060	0.46	96.3	490	1850	0.46
317.5	1630	6060	0.46	96.8	500	1850	0.46
319.1	1680	5950	0.46	97.3	510	1810	0.46
320.7	1720	6170	0.46	97.8	520	1880	0.46
322.3	1820	5900	0.45	98.2	550	1800	0.45
323.9	1800	6410	0.46	98.7	550	1950	0.46
325.5	1830	6060	0.45	99.2	560	1850	0.45
327.1	1820	5850	0.45	99.7	560	1780	0.45
328.7	1590	5800	0.46	100.2	480	1770	0.46

Report 16248 Harbor River Borehole Geophysics rev 0

Page 34 of 51

August 24, 2016

**Figure H-93, Tabulated V<sub>s</sub> and V<sub>p</sub> Results – SB-1 (con't)**

**Summary of Compressional Wave Velocity, Shear Wave Velocity, and Poisson's Ratio  
Based on Receiver-to-Receiver Travel Time Data - Borehole SB-1**

American Units				Metric Units			
Depth at Midpoint Between Receivers	Velocity		Poisson's Ratio	Depth at Midpoint Between Receivers	Velocity		Poisson's Ratio
	V <sub>s</sub>	V <sub>p</sub>			V <sub>s</sub>	V <sub>p</sub>	
(ft)	(ft/s)	(ft/s)		(m)	(m/s)	(m/s)	
330.3	1510	5900	0.47	100.7	460	1800	0.47
331.9	1560	5600	0.46	101.2	470	1710	0.46
333.6	1470	5650	0.46	101.7	450	1720	0.46
335.2	1390	5600	0.47	102.2	430	1710	0.47
336.8	1540	6470	0.47	102.6	470	1970	0.47
338.4	1660	6170	0.46	103.1	510	1880	0.46
340.0	1830	5950	0.45	103.6	560	1810	0.45
341.6	2010	6290	0.44	104.1	610	1920	0.44
343.2	2170	6670	0.44	104.6	660	2030	0.44
344.8	1820	6170	0.45	105.1	560	1880	0.45
346.4	1680	6230	0.46	105.6	510	1900	0.46
348.0	1660	5950	0.46	106.1	510	1810	0.46
349.6	1460	5750	0.47	106.5	440	1750	0.47
351.2	1550	5950	0.46	107.0	470	1810	0.46
352.8	2040	6410	0.44	107.5	620	1950	0.44
354.4	2200	6670	0.44	108.0	670	2030	0.44
356.0	2350	6730	0.43	108.5	720	2050	0.43
357.6	2420	6540	0.42	109.0	740	1990	0.42
359.2	2120	6410	0.44	109.5	650	1950	0.44
360.8	2140	6540	0.44	110.0	650	1990	0.44
362.4	2080	6350	0.44	110.5	640	1940	0.44
364.0	1930	5950	0.44	110.9	590	1810	0.44
365.6	1980	6230	0.44	111.4	600	1900	0.44
367.2	2230	6800	0.44	111.9	680	2070	0.44
368.8	2150	6350	0.44	112.4	660	1940	0.44
370.4	1880	6170	0.45	112.9	570	1880	0.45
372.0	1750	6010	0.45	113.4	530	1830	0.45
373.6	1590	5900	0.46	113.9	480	1800	0.46
375.2	1450	5650	0.46	114.4	440	1720	0.46
376.8	1410	5800	0.47	114.8	430	1770	0.47
378.4	1490	5800	0.46	115.3	460	1770	0.46
380.0	1570	5900	0.46	115.8	480	1800	0.46
381.6	1560	6120	0.47	116.3	480	1860	0.47
383.2	1610	5950	0.46	116.8	490	1810	0.46
384.8	1550	5600	0.46	117.3	470	1710	0.46
386.4	1520	5850	0.46	117.8	460	1780	0.46
388.0	1520	5900	0.46	118.3	460	1800	0.46
389.6	1530	5650	0.46	118.8	470	1720	0.46
391.2	1650	6170	0.46	119.2	500	1880	0.46
392.8	1920	6290	0.45	119.7	590	1920	0.45

Report 16248 Harbor River Borehole Geophysics rev 0

Page 35 of 51

August 24, 2016

**Figure H-94, Tabulated V<sub>s</sub> and V<sub>p</sub> Results – SB-1 (con't)**



**Summary of Compressional Wave Velocity, Shear Wave Velocity, and Poisson's Ratio  
Based on Receiver-to-Receiver Travel Time Data - Borehole SB-1**

American Units				Metric Units			
Depth at Midpoint Between Receivers	Velocity		Poisson's Ratio	Depth at Midpoint Between Receivers	Velocity		Poisson's Ratio
	V <sub>s</sub>	V <sub>p</sub>			V <sub>s</sub>	V <sub>p</sub>	
(ft)	(ft/s)	(ft/s)		(m)	(m/s)	(m/s)	
394.4	2180	6670	0.44	120.2	660	2030	0.44
396.0	2300	6350	0.42	120.7	700	1940	0.42
397.6	2510	6870	0.42	121.2	760	2090	0.42
399.2	2610	6940	0.42	121.7	800	2120	0.42
400.8	3210	7090	0.37	122.2	980	2160	0.37
402.4	3550	6940	0.32	122.7	1080	2120	0.32
404.0	3040	7090	0.39	123.1	930	2160	0.39
405.6	2870	7020	0.40	123.6	880	2140	0.40
407.2	2900	7090	0.40	124.1	880	2160	0.40
408.8	2960	6940	0.39	124.6	900	2120	0.39
410.4	2920	7020	0.39	125.1	890	2140	0.39
412.0	2960	7090	0.39	125.6	900	2160	0.39
413.6	2900	6940	0.39	126.1	880	2120	0.39
415.2	2730	6800	0.40	126.6	830	2070	0.40
416.8	2650	6600	0.40	127.1	810	2010	0.40
418.5	2570	6670	0.41	127.5	780	2030	0.41
420.1	2660	6730	0.41	128.0	810	2050	0.41
421.7	2610	6800	0.41	128.5	800	2070	0.41
423.3	2590	6800	0.41	129.0	790	2070	0.41
424.9	2700	6800	0.41	129.5	820	2070	0.41
426.5	2810	7020	0.40	130.0	860	2140	0.40
428.1	2800	7170	0.41	130.5	850	2180	0.41
429.7	2860	7170	0.41	131.0	870	2180	0.41
431.3	2950	7200	0.40	131.5	900	2190	0.40
432.9	2800	6970	0.40	131.9	850	2130	0.40
434.5	2690	6690	0.40	132.4	820	2040	0.40
436.1	2780	6900	0.40	132.9	850	2100	0.40
437.7	2840	6690	0.39	133.4	860	2040	0.39
439.3	2870	6630	0.38	133.9	880	2020	0.38
440.9	2990	7120	0.39	134.4	910	2170	0.39
442.5	2980	6830	0.38	134.9	910	2080	0.38
444.1	2780	7090	0.41	135.4	850	2160	0.41
445.7	2800	6970	0.40	135.8	850	2130	0.40
447.3	2740	7050	0.41	136.3	840	2150	0.41
448.9	2730	6690	0.40	136.8	830	2040	0.40
450.5	2750	6960	0.41	137.3	840	2120	0.41
452.1	2800	6960	0.40	137.8	850	2120	0.40
453.7	2940	6960	0.39	138.3	900	2120	0.39
455.3	3020	7140	0.39	138.8	920	2180	0.39
456.9	3160	7120	0.38	139.3	960	2170	0.38

Report 16248 Harbor River Borehole Geophysics rev 0

Page 36 of 51

August 24, 2016

**Figure H-95, Tabulated V<sub>s</sub> and V<sub>p</sub> Results – SB-1 (con't)**

**Summary of Compressional Wave Velocity, Shear Wave Velocity, and Poisson's Ratio  
Based on Receiver-to-Receiver Travel Time Data - Borehole SB-1**

American Units				Metric Units			
Depth at Midpoint Between Receivers	Velocity		Poisson's Ratio	Depth at Midpoint Between Receivers	Velocity		Poisson's Ratio
	V <sub>s</sub>	V <sub>p</sub>			V <sub>s</sub>	V <sub>p</sub>	
(ft)	(ft/s)	(ft/s)		(m)	(m/s)	(m/s)	
458.5	3300	7370	0.37	139.8	1010	2250	0.37
460.1	3200	7310	0.38	140.2	970	2230	0.38
461.7	3010	7060	0.39	140.7	920	2150	0.39
463.3	2880	6860	0.39	141.2	880	2090	0.39
464.9	2930	7000	0.39	141.7	890	2130	0.39
466.5	2990	7150	0.39	142.2	910	2180	0.39
468.1	2990	7000	0.39	142.7	910	2130	0.39
469.7	2990	7030	0.39	143.2	910	2140	0.39
471.3	3020	7250	0.40	143.7	920	2210	0.40
472.9	2950	7220	0.40	144.1	900	2200	0.40
474.5	2860	6970	0.40	144.6	870	2130	0.40
476.1	2860	7250	0.41	145.1	870	2210	0.41
477.7	2880	7180	0.40	145.6	880	2190	0.40
479.3	2890	6920	0.39	146.1	880	2110	0.39
480.9	2920	7180	0.40	146.6	890	2190	0.40
482.5	2980	7180	0.40	147.1	910	2190	0.40
484.1	2980	7370	0.40	147.6	910	2250	0.40
485.7	3000	7220	0.40	148.1	910	2200	0.40
487.3	3050	7180	0.39	148.5	930	2190	0.39
488.9	3120	7580	0.40	149.0	950	2310	0.40
490.5	3210	6970	0.37	149.5	980	2130	0.37
492.1	3110	7340	0.39	150.0	950	2240	0.39
493.7	2910	7540	0.41	150.5	890	2300	0.41
495.3	3060	7340	0.40	151.0	930	2240	0.40
496.9	3270	7150	0.37	151.5	1000	2180	0.37
498.5	3230	7220	0.37	152.0	980	2200	0.37
500.1	3020	7060	0.39	152.4	920	2150	0.39
501.8	2940	7030	0.39	152.9	900	2140	0.39

**Figure H-96, Tabulated V<sub>s</sub> and V<sub>p</sub> Results – SB-1 (con't)**

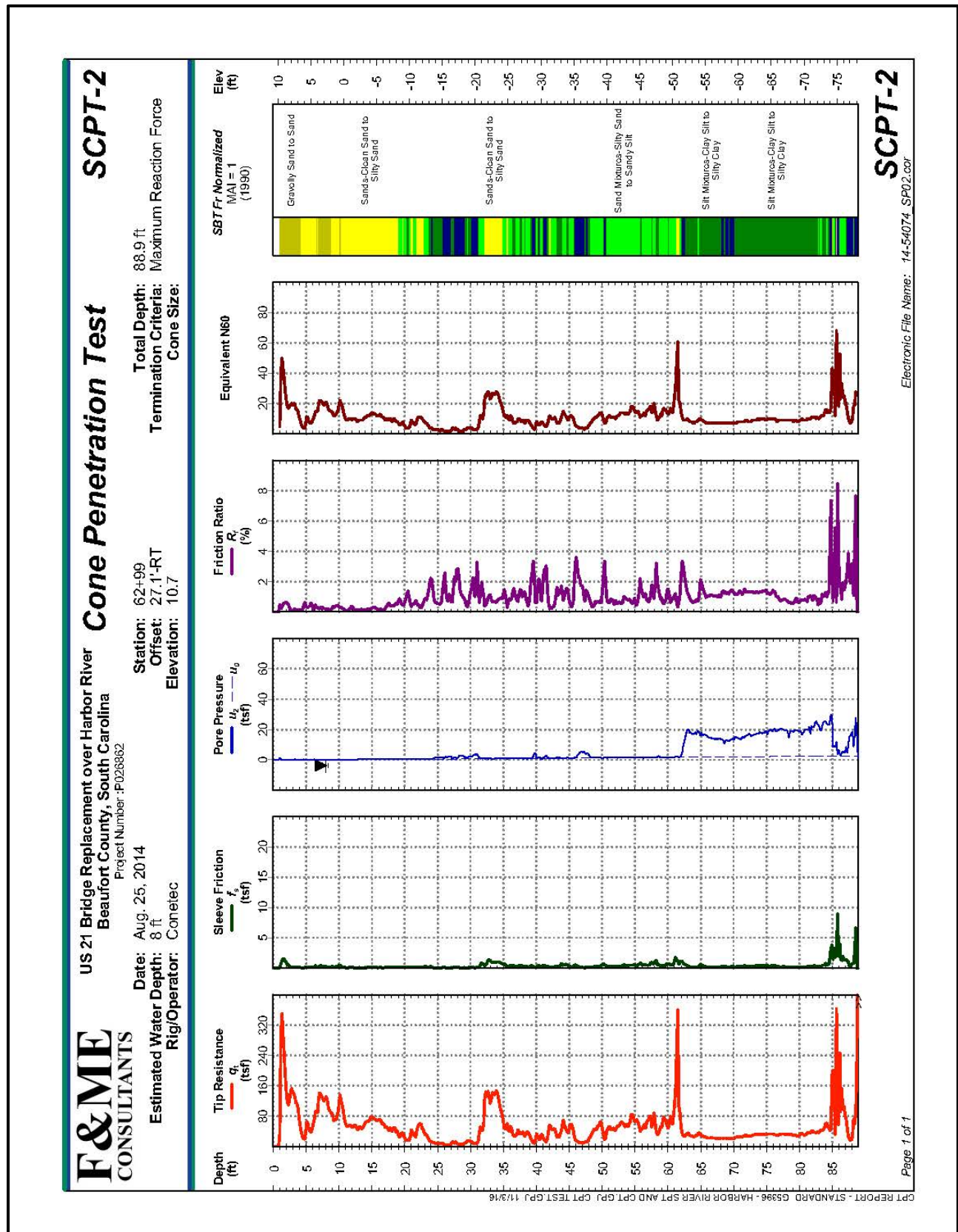


Figure H-97, SCPT-2

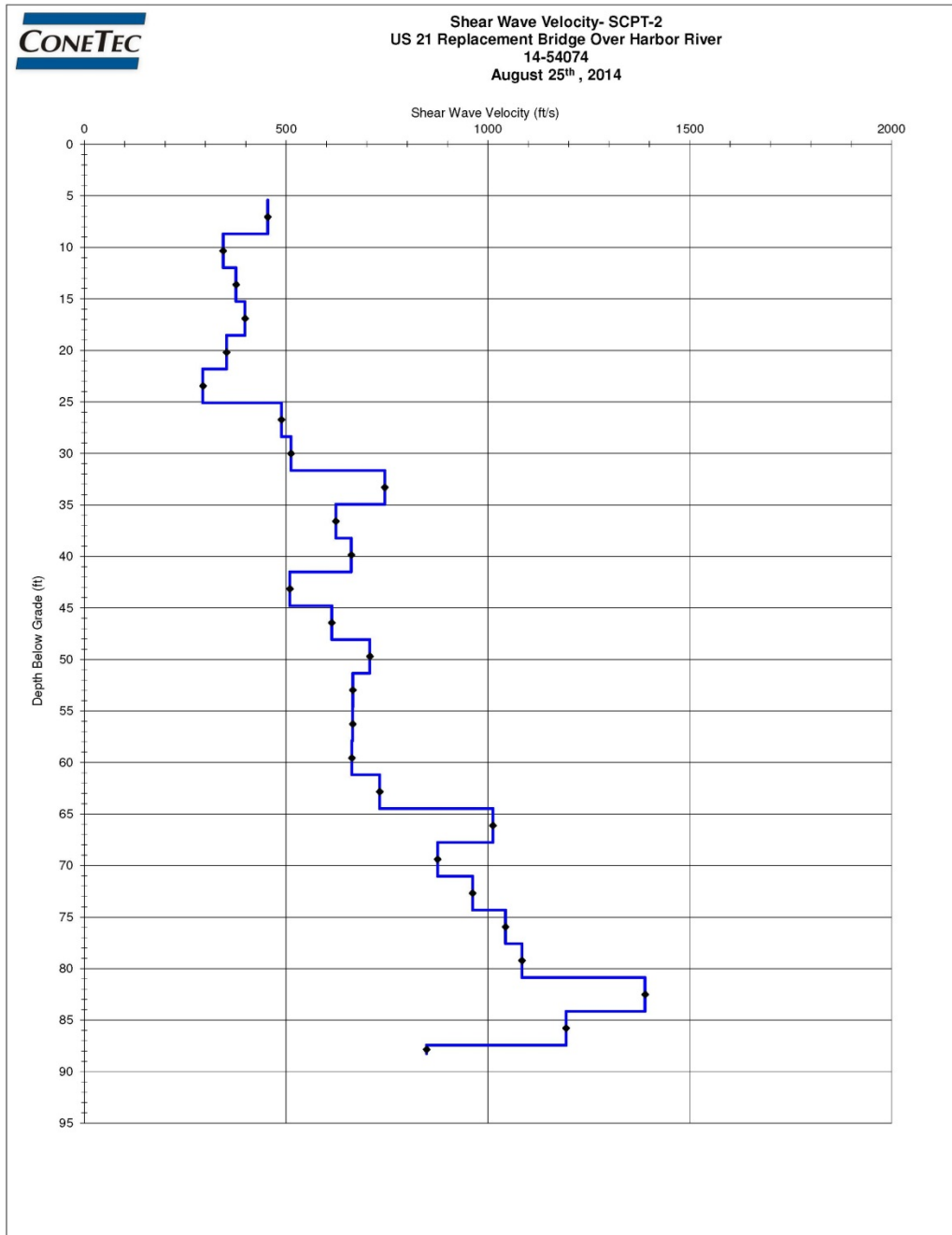


Figure H-98,  $V_s$  Profile – SCPT-2

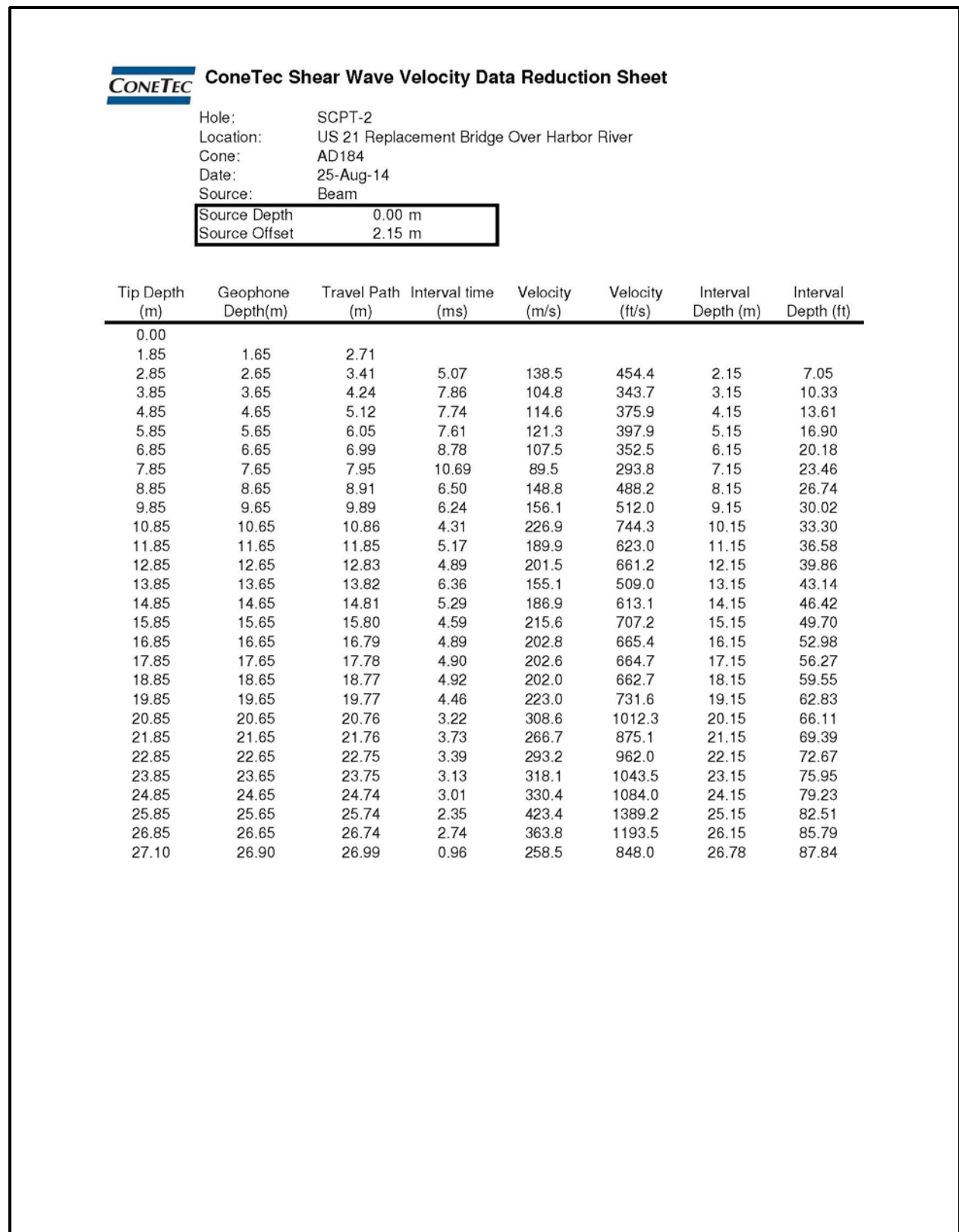


Figure H-99, Tabulated  $V_s$  Results – SCPT-2



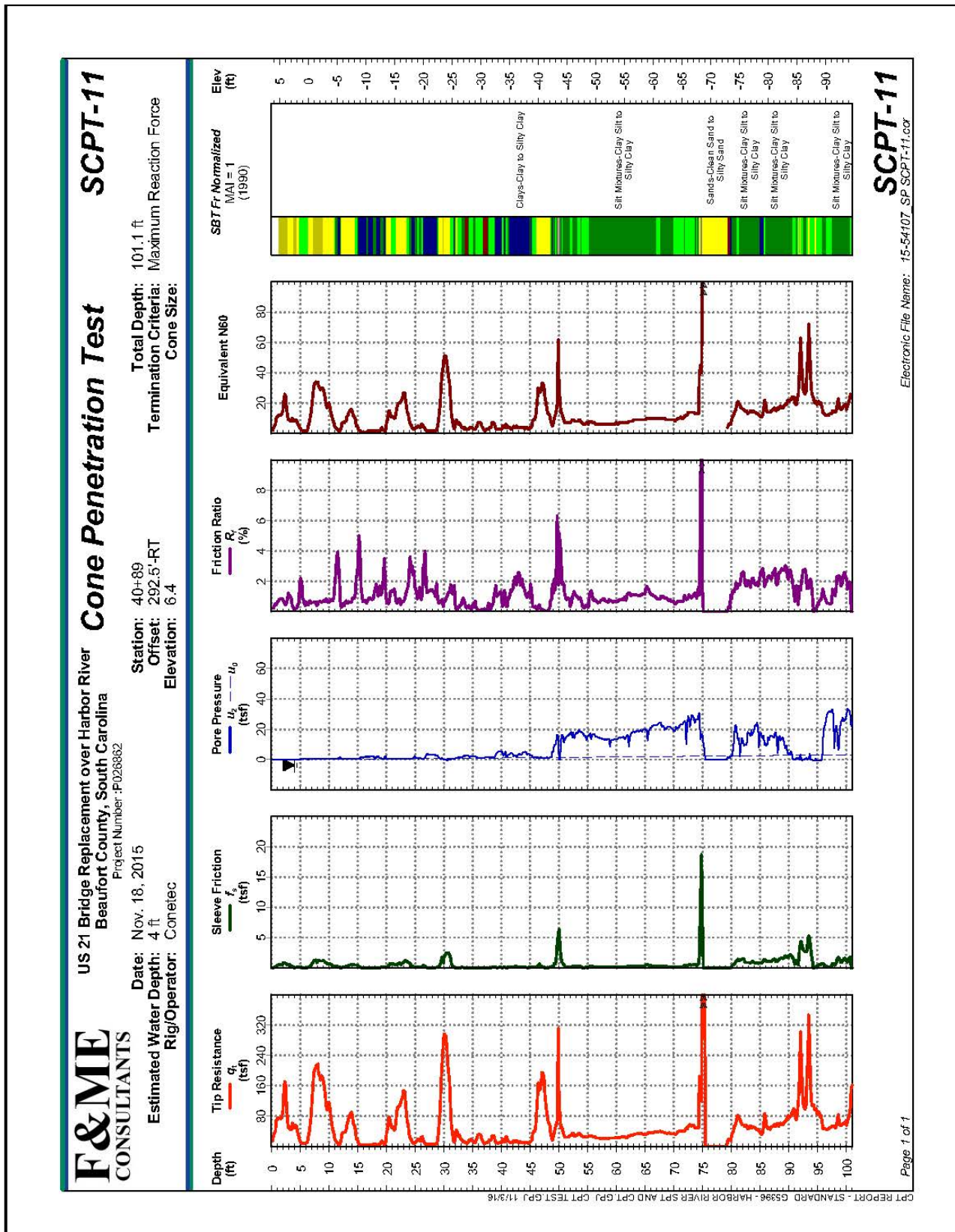


Figure H-100, SCPT-11

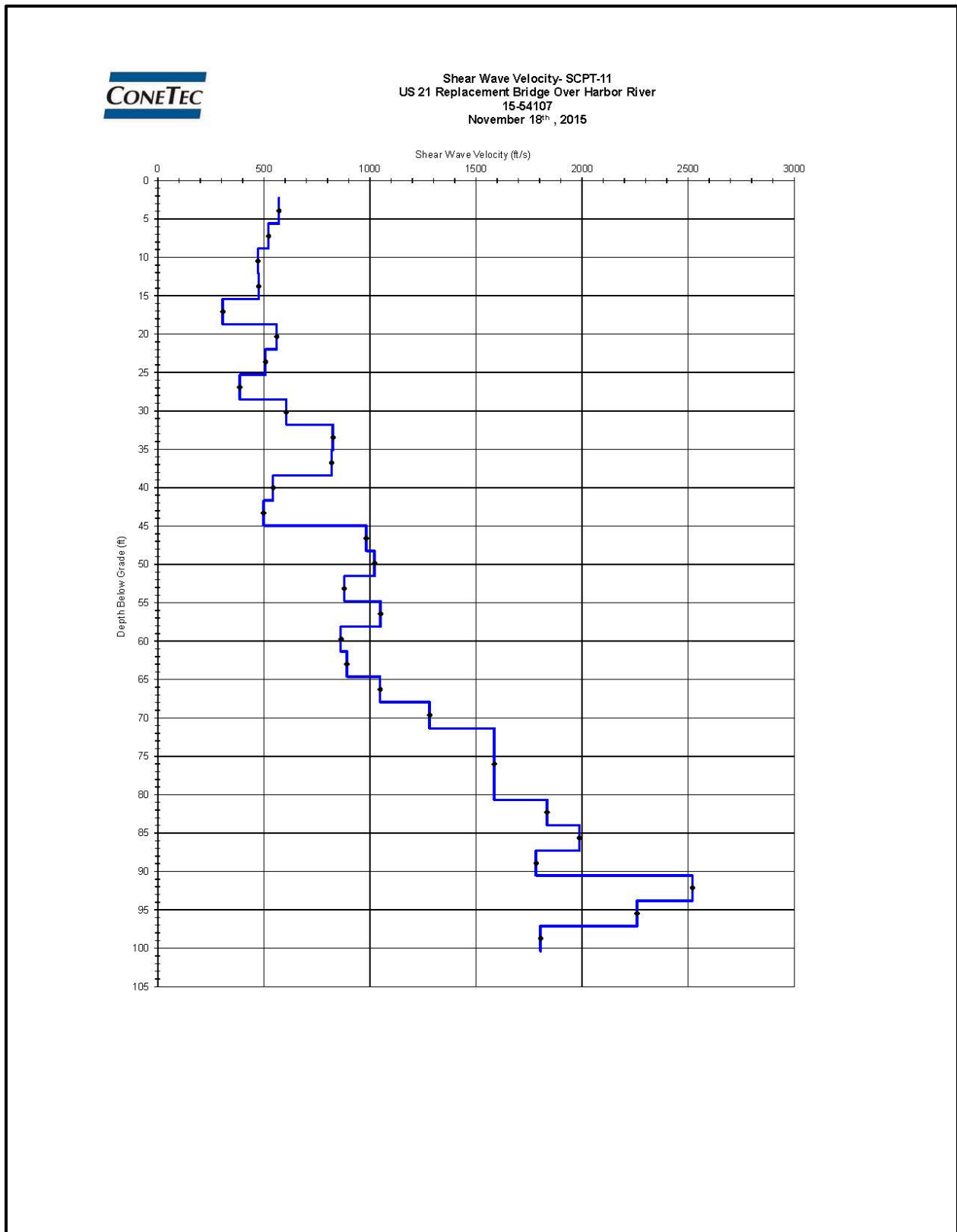


Figure H-101,  $V_s$  Profile – SCPT-11



Job No: 15-54107  
 Client: F&ME  
 Project: Harbor River  
 Sounding ID: SCPT-11  
 Date: 11/18/2015

Seismic Source: Beam  
 Source Offset (ft): 4.75  
 Source Depth (ft): 0.00  
 Geophone Offset (ft): 0.66

**SCPT<sub>u</sub> SHEAR WAVE VELOCITY TEST RESULTS - V<sub>s</sub>**

Tip Depth (ft)	Geophone Depth (ft)	Ray Path (ft)	Ray Path Difference (ft)	Travel Time Interval (ms)	Interval Velocity (ft/s)
2.95	2.30	5.28			
6.23	5.58	7.33	2.05	3.59	571
9.51	8.86	10.05	2.73	5.23	521
12.80	12.14	13.04	2.98	6.32	472
16.08	15.42	16.13	3.10	6.52	475
19.36	18.70	19.29	3.16	10.35	305
22.64	21.98	22.49	3.19	5.71	559
25.92	25.26	25.71	3.22	6.34	507
29.20	28.54	28.94	3.23	8.38	386
32.48	31.82	32.18	3.24	5.36	605
35.76	35.10	35.42	3.25	3.94	825
39.04	38.39	38.68	3.25	3.97	820
42.32	41.67	41.94	3.26	6.00	543
45.60	44.95	45.20	3.26	6.55	498
48.88	48.23	48.46	3.26	3.32	982
52.17	51.51	51.73	3.27	3.20	1020
55.45	54.79	55.00	3.27	3.72	879
58.73	58.07	58.26	3.27	3.12	1049
62.01	61.35	61.53	3.27	3.79	862
65.29	64.63	64.81	3.27	3.67	892
68.57	67.91	68.08	3.27	3.12	1047
72.01	71.36	71.52	3.44	2.69	1280
81.36	80.71	80.85	9.33	5.89	1585
84.65	83.99	84.12	3.28	1.79	1834
87.93	87.27	87.40	3.28	1.65	1987
91.21	90.55	90.68	3.28	1.84	1783
94.49	93.83	93.95	3.28	1.30	2520
97.77	97.11	97.23	3.28	1.45	2260
101.05	100.39	100.51	3.28	1.82	1804

Sheet 1 of 1

**Figure H-102, Tabulated V<sub>s</sub> Results – SCPT-11**



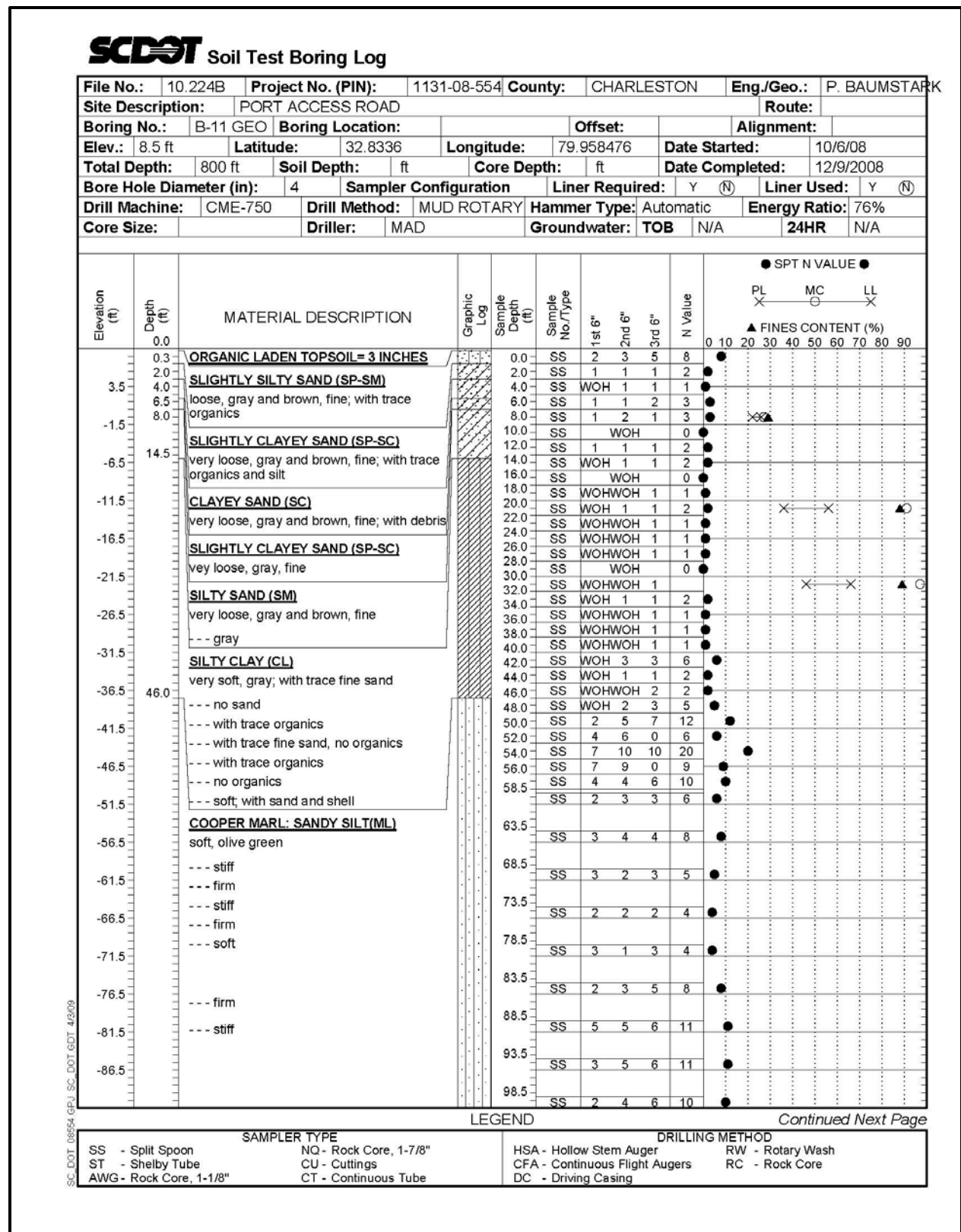


Figure H-103, Soil Test Boring B-11GEO

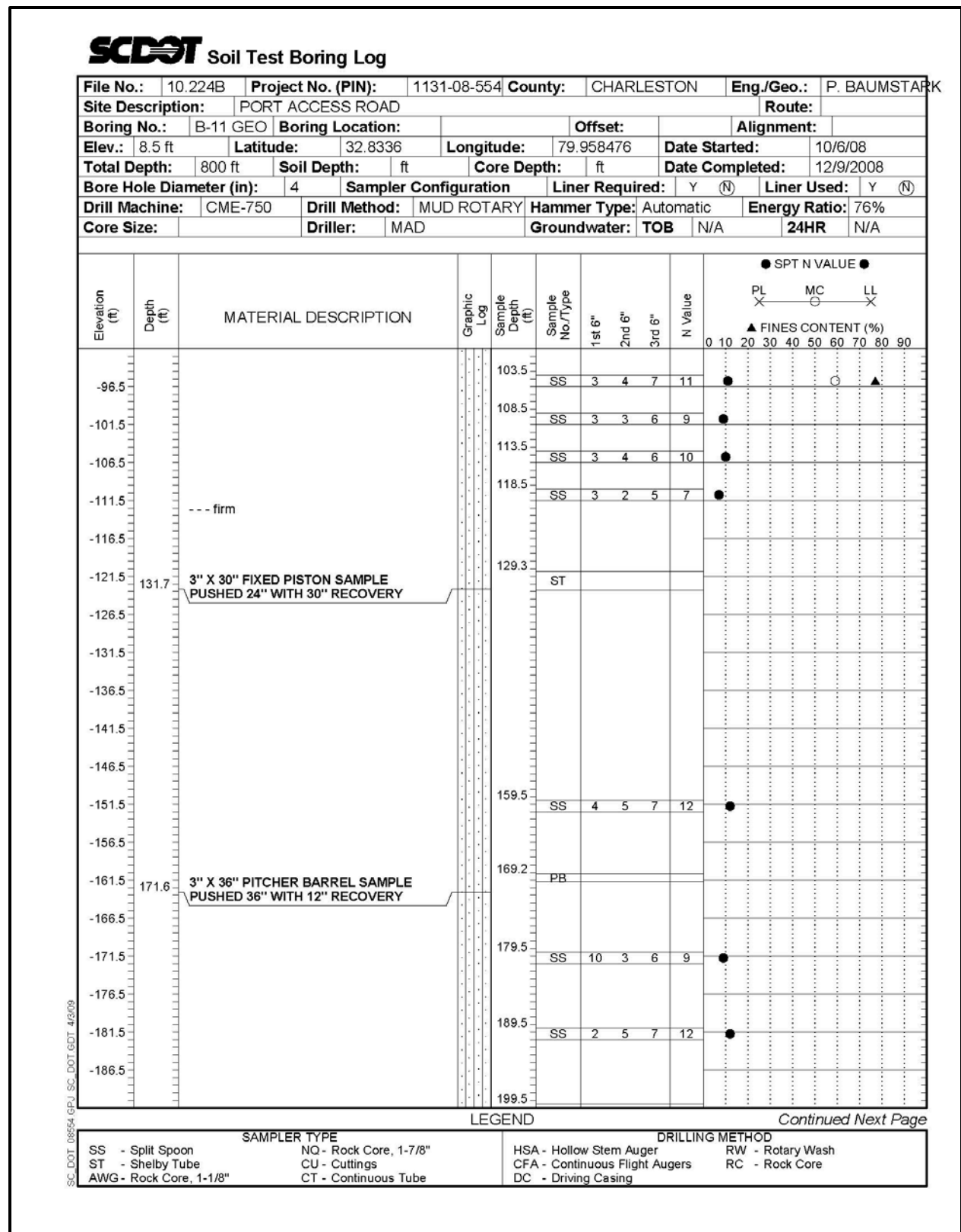


Figure H-104, Soil Test Boring B-11GEO (con't)

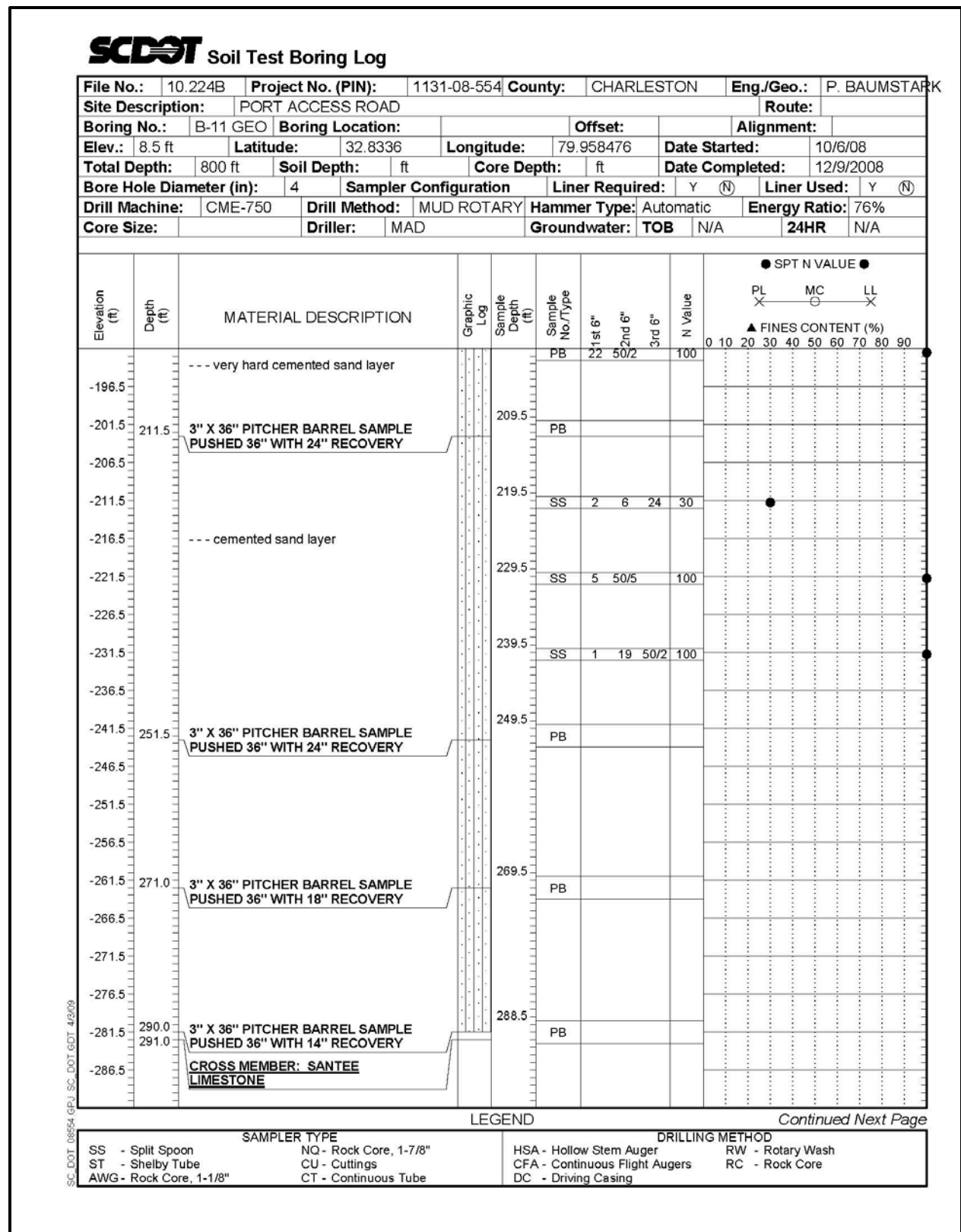


Figure H-105, Soil Test Boring B-11GEO (con't)



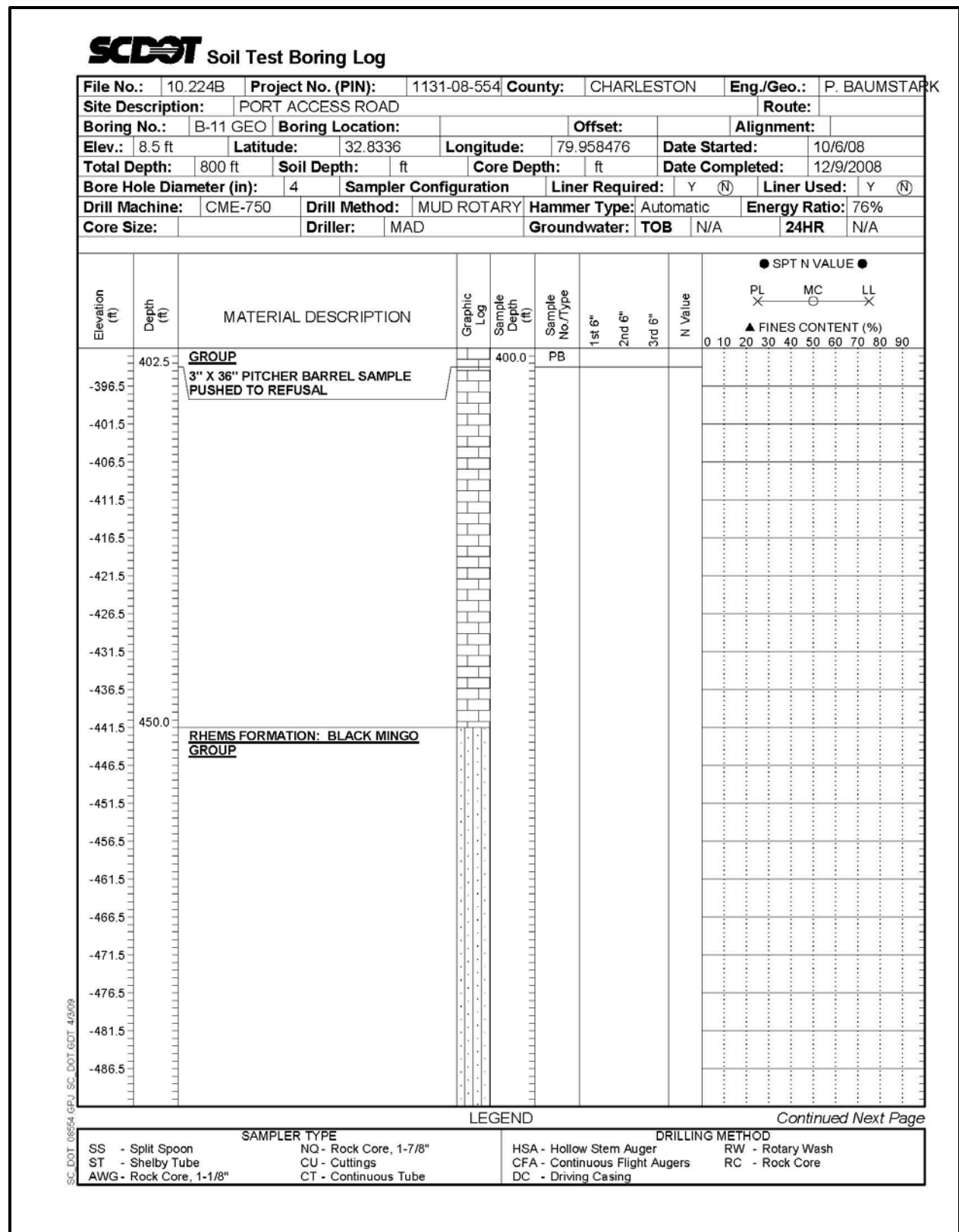
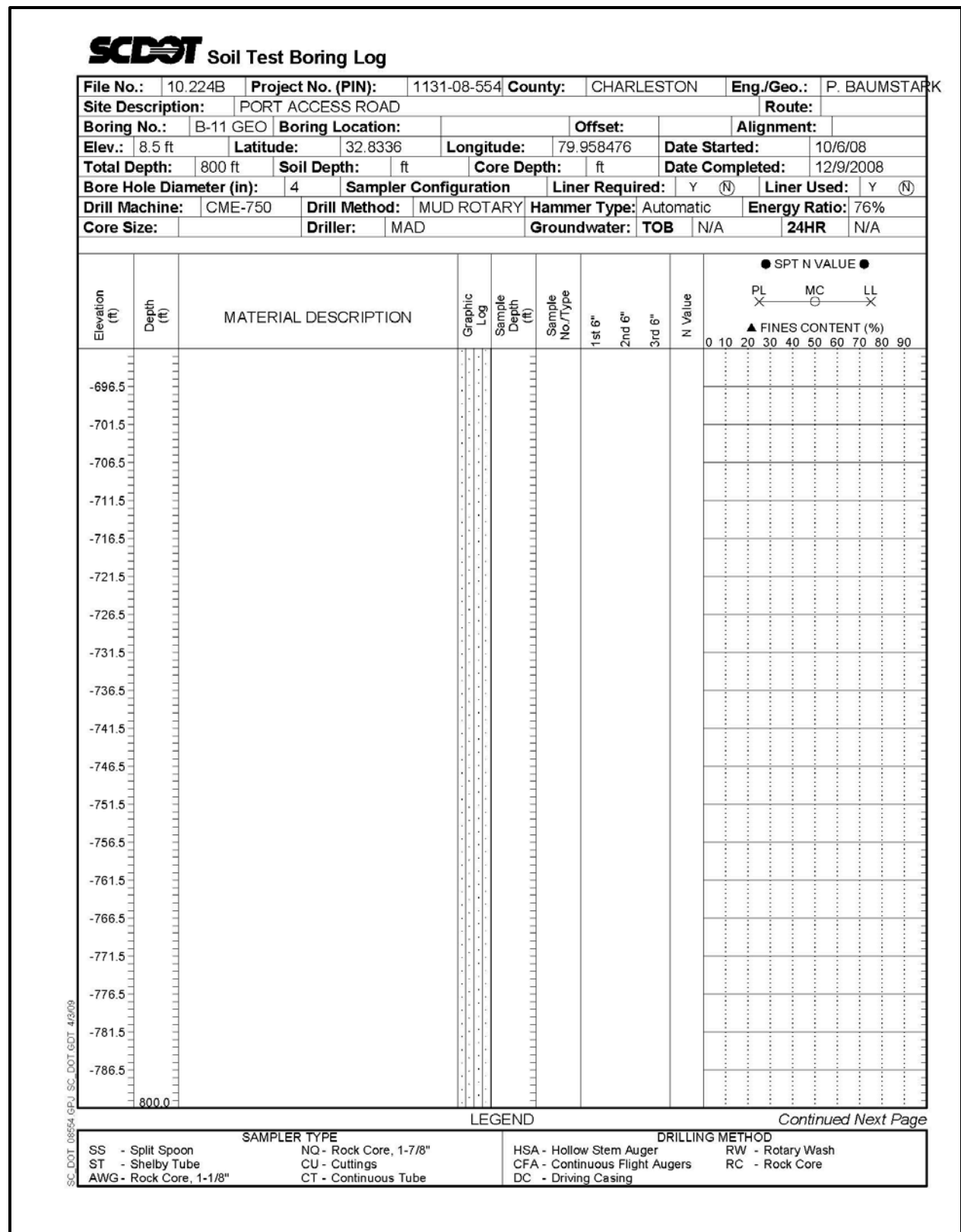


Figure H-107, Soil Test Boring B-11GEO (con't)







**Figure H-110, Soil Test Boring B-11GEO (con't)**





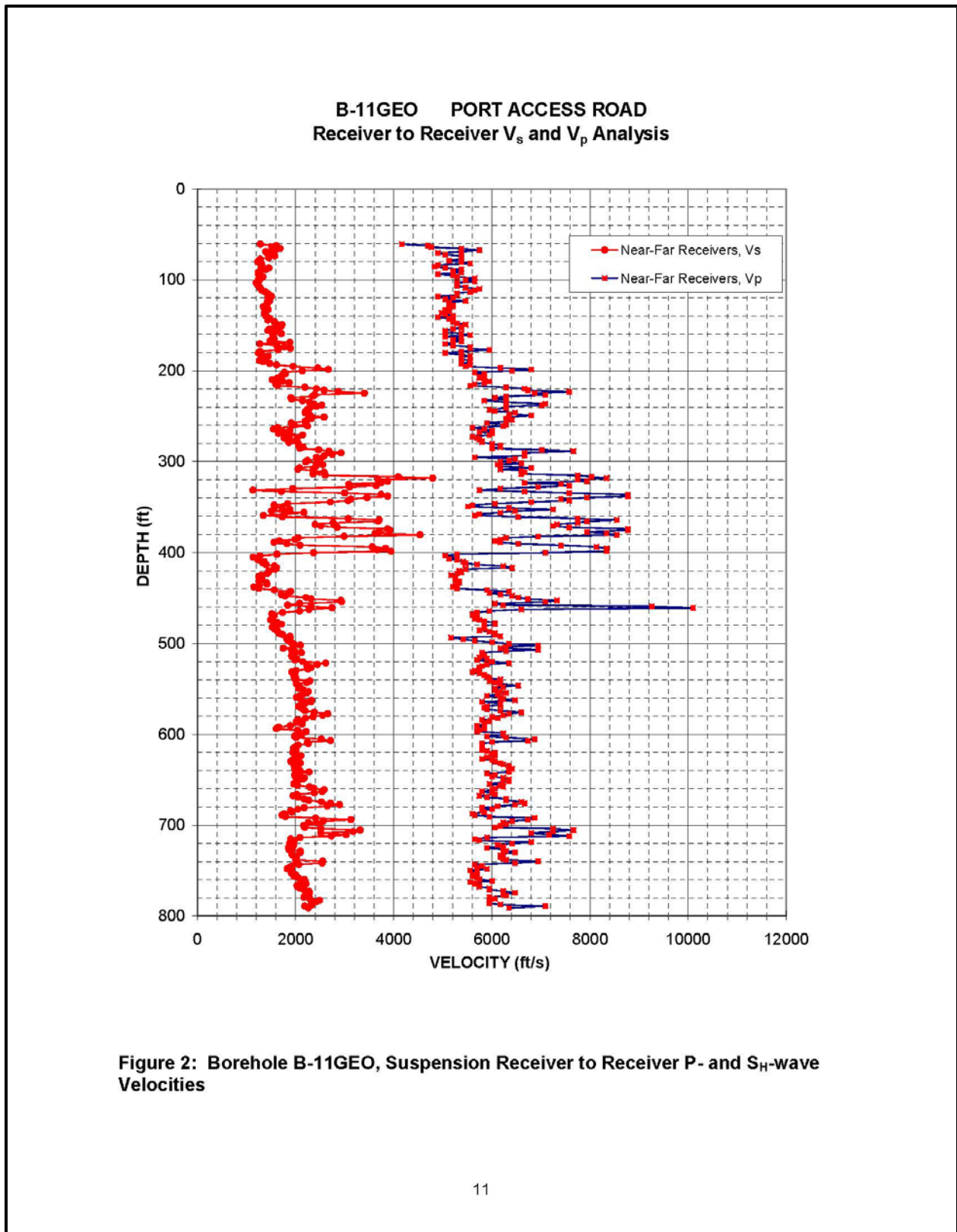


**Figure H-112,  $V_s$  and  $V_p$  Profile – B-11GEO**

**Table 2: Summary of Shear and Compressional Wave Velocity Based on Receiver-to-Receiver Travel Time Data - Borehole B-11GEO, Port Access Road, North Charleston**

**Summary of Compressional Wave Velocity, Shear Wave Velocity, and Poisson's Ratio Based on Receiver-to-Receiver Travel Time Data - Borehole B-11GEO**

American Units				Metric Units			
Depth at Midpoint Between Receivers	Velocity		Poisson's Ratio	Depth at Midpoint Between Receivers	Velocity		Poisson's Ratio
	V <sub>s</sub>	V <sub>p</sub>			V <sub>s</sub>	V <sub>p</sub>	
(ft)	(ft/s)	(ft/s)		(m)	(m/s)	(m/s)	
60.7	1280	4170	0.45	18.5	390	1270	0.45
62.3	1610	4690	0.43	19.0	490	1430	0.43
64.0	1520	4760	0.44	19.5	460	1450	0.44
65.6	1680	5380	0.45	20.0	510	1640	0.45
67.3	1580	5750	0.46	20.5	480	1750	0.46
68.9	1390	5380	0.46	21.0	430	1640	0.46
70.5	1420	4900	0.45	21.5	430	1490	0.45
72.2	1520	5050	0.45	22.0	460	1540	0.45
73.8	1570	5380	0.45	22.5	480	1640	0.45
75.5	1460	5380	0.46	23.0	440	1640	0.46
77.1	1280	5380	0.47	23.5	390	1640	0.47
78.7	1260	5130	0.47	24.0	380	1560	0.47
80.4	1230	5380	0.47	24.5	370	1640	0.47
82.0	1300	5560	0.47	25.0	400	1690	0.47
83.7	1310	4900	0.46	25.5	400	1490	0.46
85.3	1300	4830	0.46	26.0	400	1470	0.46
86.9	1460	5050	0.45	26.5	440	1540	0.45
88.6	1390	5380	0.46	27.0	430	1640	0.46
90.2	1280	5210	0.47	27.5	390	1590	0.47
91.9	1240	5380	0.47	28.0	380	1640	0.47
93.5	1240	4900	0.47	28.5	380	1490	0.47
95.1	1280	5210	0.47	29.0	390	1590	0.47
96.8	1330	5290	0.47	29.5	410	1610	0.47
98.4	1300	5650	0.47	30.0	400	1720	0.47
100.1	1240	5460	0.47	30.5	380	1670	0.47
101.7	1250	5650	0.47	31.0	380	1720	0.47
103.4	1200	5290	0.47	31.5	370	1610	0.47
105.0	1230	5290	0.47	32.0	370	1610	0.47
106.6	1240	5290	0.47	32.5	380	1610	0.47
108.3	1270	5460	0.47	33.0	390	1670	0.47
109.9	1290	5750	0.47	33.5	390	1750	0.47
111.6	1310	5650	0.47	34.0	400	1720	0.47
113.2	1380	5560	0.47	34.5	420	1690	0.47
114.8	1430	5290	0.46	35.0	440	1610	0.46
116.5	1460	5290	0.46	35.5	440	1610	0.46
118.1	1510	4900	0.45	36.0	460	1490	0.45
119.8	1440	5210	0.46	36.5	440	1590	0.46
121.4	1470	5050	0.45	37.0	450	1540	0.45
123.0	1470	5460	0.46	37.5	450	1670	0.46
124.7	1420	5130	0.46	38.0	430	1560	0.46
126.6	1420	5130	0.46	38.6	430	1560	0.46

**Figure H-113, Tabulated V<sub>s</sub> and V<sub>p</sub> Results – B-11GEO**

**Summary of Compressional Wave Velocity, Shear Wave Velocity, and Poisson's Ratio  
Based on Receiver-to-Receiver Travel Time Data - Borehole B-11GEO**

American Units				Metric Units			
Depth at Midpoint Between Receivers	Velocity		Poisson's Ratio	Depth at Midpoint Between Receivers	Velocity		Poisson's Ratio
	V <sub>s</sub>	V <sub>p</sub>			V <sub>s</sub>	V <sub>p</sub>	
(ft)	(ft/s)	(ft/s)		(m)	(m/s)	(m/s)	
128.0	1400	5210	0.46	39.0	430	1590	0.46
129.6	1340	5210	0.46	39.5	410	1590	0.46
131.2	1370	5130	0.46	40.0	420	1560	0.46
132.9	1440	5050	0.46	40.5	440	1540	0.46
134.5	1400	5130	0.46	41.0	430	1560	0.46
136.2	1370	4980	0.46	41.5	420	1520	0.46
137.8	1370	5050	0.46	42.0	420	1540	0.46
139.4	1390	5210	0.46	42.5	430	1590	0.46
141.1	1420	4900	0.45	43.0	430	1490	0.45
142.7	1470	5130	0.46	43.5	450	1560	0.46
144.4	1440	5210	0.46	44.0	440	1590	0.46
146.0	1560	5210	0.45	44.5	480	1590	0.45
147.6	1590	5290	0.45	45.0	490	1610	0.45
149.3	1720	5460	0.45	45.5	520	1670	0.45
150.9	1710	5380	0.44	46.0	520	1640	0.44
152.6	1570	5380	0.45	46.5	480	1640	0.45
154.2	1470	5210	0.46	47.0	450	1590	0.46
155.8	1440	5050	0.46	47.5	440	1540	0.46
157.5	1670	5050	0.44	48.0	510	1540	0.44
159.1	1710	5380	0.44	48.5	520	1640	0.44
160.8	1540	5560	0.46	49.0	470	1690	0.46
162.4	1540	5050	0.45	49.5	470	1540	0.45
164.0	1560	5380	0.45	50.0	470	1640	0.45
165.7	1560	5210	0.45	50.5	480	1590	0.45
167.3	1480	5380	0.46	51.0	450	1640	0.46
169.0	1880	5210	0.42	51.5	570	1590	0.42
170.6	1270	5050	0.47	52.0	390	1540	0.47
172.2	1620	5210	0.45	52.5	490	1590	0.45
173.9	1770	5560	0.44	53.0	540	1690	0.44
175.5	1890	5560	0.43	53.5	580	1690	0.43
177.2	1640	5950	0.46	54.0	500	1810	0.46
178.8	1280	5380	0.47	54.5	390	1640	0.47
180.5	1240	5050	0.47	55.0	380	1540	0.47
182.1	1310	5380	0.47	55.5	400	1640	0.47
183.7	1440	5560	0.46	56.0	440	1690	0.46
185.4	1410	5380	0.46	56.5	430	1640	0.46
187.0	1290	5380	0.47	57.0	390	1640	0.47
188.7	1270	5560	0.47	57.5	390	1690	0.47
190.3	1340	5560	0.47	58.0	410	1690	0.47
191.9	1470	5380	0.46	58.5	450	1640	0.46
193.6	1610	5560	0.45	59.0	490	1690	0.45
195.2	1950	5460	0.43	59.5	590	1670	0.43
196.9	2450	6170	0.41	60.0	750	1880	0.41

**Figure H-114, Tabulated V<sub>s</sub> and V<sub>p</sub> Results – B-11GEO (con't)**

**Summary of Compressional Wave Velocity, Shear Wave Velocity, and Poisson's Ratio  
Based on Receiver-to-Receiver Travel Time Data - Borehole B-11GEO**

American Units				Metric Units			
Depth at Midpoint Between Receivers	Velocity		Poisson's Ratio	Depth at Midpoint Between Receivers	Velocity		Poisson's Ratio
	V <sub>s</sub>	V <sub>p</sub>			V <sub>s</sub>	V <sub>p</sub>	
(ft)	(ft/s)	(ft/s)		(m)	(m/s)	(m/s)	
198.5	2670	6800	0.41	60.5	810	2070	0.41
200.1	2140	6410	0.44	61.0	650	1950	0.44
201.8	1770	5650	0.45	61.5	540	1720	0.45
203.4	1790	5850	0.45	62.0	550	1780	0.45
205.1	1720	5850	0.45	62.5	530	1780	0.45
206.7	1710	5750	0.45	63.0	520	1750	0.45
208.0	1630	5750	0.46	63.4	500	1750	0.46
210.0	1530	5850	0.46	64.0	460	1780	0.46
211.6	1730	5950	0.45	64.5	530	1810	0.45
213.3	1870	5850	0.44	65.0	570	1780	0.44
214.9	1600	5650	0.46	65.5	490	1720	0.46
216.5	1630	5560	0.45	66.0	500	1690	0.45
218.2	2190	6290	0.43	66.5	670	1920	0.43
219.8	2420	6670	0.42	67.0	740	2030	0.42
221.5	2580	6730	0.41	67.5	790	2050	0.41
223.1	2870	7580	0.42	68.0	880	2310	0.42
224.7	3400	6870	0.34	68.5	1040	2090	0.34
226.4	2390	7090	0.44	69.0	730	2160	0.44
228.0	2350	6290	0.42	69.5	720	1920	0.42
229.7	1900	6060	0.45	70.0	580	1850	0.45
231.3	1920	6290	0.45	70.5	590	1920	0.45
232.9	2140	5850	0.42	71.0	650	1780	0.42
234.6	2280	6290	0.42	71.5	700	1920	0.42
236.2	2370	7090	0.44	72.0	720	2160	0.44
237.9	2530	7020	0.42	72.5	770	2140	0.42
239.5	2420	6290	0.41	73.0	740	1920	0.41
241.1	2290	6290	0.42	73.5	700	1920	0.42
242.8	2240	5950	0.42	74.0	680	1810	0.42
244.4	2210	6060	0.42	74.5	670	1850	0.42
246.1	2190	6470	0.44	75.0	670	1970	0.44
247.7	2270	6350	0.43	75.5	690	1940	0.43
249.3	2300	6800	0.44	76.0	700	2070	0.44
251.0	2580	6350	0.40	76.5	790	1940	0.40
252.6	2320	6290	0.42	77.0	710	1920	0.42
254.3	2240	6410	0.43	77.5	680	1950	0.43
255.9	2190	6290	0.43	78.0	670	1920	0.43
257.6	1910	5900	0.44	78.5	580	1800	0.44
259.2	1960	6290	0.45	79.0	600	1920	0.45
260.8	2240	6230	0.43	79.5	680	1900	0.43
262.5	1630	5600	0.45	80.0	500	1710	0.45
264.1	1550	5850	0.46	80.5	470	1780	0.46
265.8	1890	6010	0.45	81.0	580	1830	0.45
267.4	1750	5750	0.45	81.5	530	1750	0.45

**Figure H-115, Tabulated V<sub>s</sub> and V<sub>p</sub> Results – B-11GEO (con't)**

**Summary of Compressional Wave Velocity, Shear Wave Velocity, and Poisson's Ratio  
Based on Receiver-to-Receiver Travel Time Data - Borehole B-11GEO**

American Units				Metric Units			
Depth at Midpoint Between Receivers	Velocity		Poisson's Ratio	Depth at Midpoint Between Receivers	Velocity		Poisson's Ratio
	V <sub>s</sub>	V <sub>p</sub>			V <sub>s</sub>	V <sub>p</sub>	
(ft)	(ft/s)	(ft/s)		(m)	(m/s)	(m/s)	
269.0	1650	6010	0.46	82.0	500	1830	0.46
270.7	2140	5950	0.43	82.5	650	1810	0.43
272.3	1820	5600	0.44	83.0	560	1710	0.44
274.0	1770	5700	0.45	83.5	540	1740	0.45
275.6	2030	5750	0.43	84.0	620	1750	0.43
277.2	1920	5800	0.44	84.5	580	1770	0.44
278.9	1860	5800	0.44	85.0	570	1770	0.44
280.5	2060	6010	0.43	85.5	630	1830	0.43
282.2	2060	6170	0.44	86.0	630	1880	0.44
283.8	2150	6170	0.43	86.5	660	1880	0.43
285.4	2090	6010	0.43	87.0	640	1830	0.43
287.1	2470	7020	0.43	87.5	750	2140	0.43
288.7	2680	7660	0.43	88.0	820	2340	0.43
290.4	2920	6670	0.38	88.5	890	2030	0.38
292.0	2740	6670	0.40	89.0	840	2030	0.40
293.6	2580	6670	0.41	89.5	790	2030	0.41
295.3	2420	5650	0.39	90.0	740	1720	0.39
296.9	2510	6470	0.41	90.5	760	1970	0.41
298.9	2240	6350	0.43	91.1	680	1940	0.43
300.2	2210	6170	0.43	91.5	670	1880	0.43
301.8	2430	6600	0.42	92.0	740	2010	0.42
303.5	2550	6120	0.39	92.5	780	1860	0.39
305.1	2420	6170	0.41	93.0	740	1880	0.41
306.8	2080	6800	0.45	93.5	640	2070	0.45
308.4	2040	6170	0.44	94.0	620	1880	0.44
310.0	2360	6600	0.43	94.5	720	2010	0.43
311.7	2580	6670	0.41	95.0	790	2030	0.41
313.3	2360	6600	0.43	95.5	720	2010	0.43
315.0	2600	7750	0.44	96.0	790	2360	0.44
316.6	4090	8030	0.32	96.5	1250	2450	0.32
318.2	4800	8330	0.25	97.0	1460	2540	0.25
319.9	3680	7750	0.35	97.5	1120	2360	0.35
321.5	3880	7940	0.34	98.0	1180	2420	0.34
323.2	3750	6670	0.27	98.5	1140	2030	0.27
324.8	3090	7410	0.39	99.0	940	2260	0.39
326.4	3640	7580	0.35	99.5	1110	2310	0.35
328.1	3100	6940	0.38	100.0	950	2120	0.38
329.7	1940	6170	0.44	100.5	590	1880	0.44
331.4	1130	5750	0.48	101.0	340	1750	0.48
333.0	1710	6670	0.46	101.5	520	2030	0.46
334.7	3000	7580	0.41	102.0	920	2310	0.41
336.3	3750	8770	0.39	102.5	1140	2670	0.39
337.9	3880	8770	0.38	103.0	1180	2670	0.38

**Figure H-116, Tabulated V<sub>s</sub> and V<sub>p</sub> Results – B-11GEO (con't)**

**Summary of Compressional Wave Velocity, Shear Wave Velocity, and Poisson's Ratio  
Based on Receiver-to-Receiver Travel Time Data - Borehole B-11GEO**

American Units				Metric Units			
Depth at Midpoint Between Receivers	Velocity		Poisson's Ratio	Depth at Midpoint Between Receivers	Velocity		Poisson's Ratio
	V <sub>s</sub>	V <sub>p</sub>			V <sub>s</sub>	V <sub>p</sub>	
(ft)	(ft/s)	(ft/s)		(m)	(m/s)	(m/s)	
339.6	3450	7940	0.38	103.5	1050	2420	0.38
341.2	3130	7410	0.39	104.0	950	2260	0.39
342.9	3070	7580	0.40	104.5	940	2310	0.40
344.5	2710	6800	0.41	105.0	830	2070	0.41
346.1	1840	6060	0.45	105.5	560	1850	0.45
347.8	1560	5600	0.46	106.0	480	1710	0.46
349.4	1580	5510	0.45	106.5	480	1680	0.45
351.1	1730	6350	0.46	107.0	530	1940	0.46
352.7	1880	7250	0.46	107.5	570	2210	0.46
354.3	1510	6470	0.47	108.0	460	1970	0.47
356.0	2170	6170	0.43	108.5	660	1880	0.43
357.6	1770	5750	0.45	109.0	540	1750	0.45
359.3	1340	5650	0.47	109.5	410	1720	0.47
360.9	1730	6540	0.46	110.0	530	1990	0.46
362.5	3070	7750	0.41	110.5	940	2360	0.41
364.2	3700	8550	0.38	111.0	1130	2610	0.38
365.8	3680	7940	0.36	111.5	1120	2420	0.36
367.5	2770	7750	0.43	112.0	840	2360	0.43
369.1	2400	7330	0.44	112.5	730	2230	0.44
370.7	2520	7250	0.43	113.0	770	2210	0.43
372.4	2850	7580	0.42	113.5	870	2310	0.42
374.0	3880	8770	0.38	114.0	1180	2670	0.38
375.7	3920	8770	0.38	114.5	1200	2670	0.38
377.3	3700	7940	0.36	115.0	1130	2420	0.36
378.9	3620	8330	0.38	115.5	1100	2540	0.38
380.6	4540	8550	0.30	116.0	1380	2610	0.30
382.2	2990	6940	0.39	116.5	910	2120	0.39
383.9	2050	6290	0.44	117.0	630	1920	0.44
385.5	1990	6170	0.44	117.5	610	1880	0.44
387.1	1670	6060	0.46	118.0	510	1850	0.46
388.8	1560	6170	0.47	118.5	480	1880	0.47
390.4	1830	6540	0.46	119.0	560	1990	0.46
392.1	2090	7410	0.46	119.5	640	2260	0.46
393.7	3570	8130	0.38	120.0	1090	2480	0.38
395.3	3830	8330	0.37	120.5	1170	2540	0.37
397.0	3660	8330	0.38	121.0	1120	2540	0.38
398.6	3940	8330	0.36	121.5	1200	2540	0.36
400.3	2360	7090	0.44	122.0	720	2160	0.44
401.9	1620	5290	0.45	122.5	490	1610	0.45
403.5	1270	5050	0.47	123.0	390	1540	0.47
405.2	1140	5290	0.48	123.5	350	1610	0.48
406.8	1220	5130	0.47	124.0	370	1560	0.47
408.5	1230	5290	0.47	124.5	380	1610	0.47

**Figure H-117, Tabulated V<sub>s</sub> and V<sub>p</sub> Results – B-11GEO (con't)**

**Summary of Compressional Wave Velocity, Shear Wave Velocity, and Poisson's Ratio  
Based on Receiver-to-Receiver Travel Time Data - Borehole B-11GEO**

American Units				Metric Units			
Depth at Midpoint Between Receivers	Velocity		Poisson's Ratio	Depth at Midpoint Between Receivers	Velocity		Poisson's Ratio
	V <sub>s</sub>	V <sub>p</sub>			V <sub>s</sub>	V <sub>p</sub>	
(ft)	(ft/s)	(ft/s)		(m)	(m/s)	(m/s)	
410.1	1360	5420	0.47	125.0	410	1650	0.47
411.8	1340	5460	0.47	125.5	410	1670	0.47
413.4	1400	5700	0.47	126.0	430	1740	0.47
415.0	1570	6230	0.47	126.5	480	1900	0.47
416.7	1610	6410	0.47	127.0	490	1950	0.47
418.3	1580	5460	0.45	127.5	480	1670	0.45
420.0	1470	5330	0.46	128.0	450	1630	0.46
421.6	1450	5380	0.46	128.5	440	1640	0.46
423.2	1420	5290	0.46	129.0	430	1610	0.46
424.9	1300	5170	0.47	129.5	400	1580	0.47
426.5	1250	5250	0.47	130.0	380	1600	0.47
428.2	1310	5250	0.47	130.5	400	1600	0.47
429.8	1290	5250	0.47	131.0	390	1600	0.47
431.4	1260	5330	0.47	131.5	380	1630	0.47
433.1	1410	5330	0.46	132.0	430	1630	0.46
434.7	1420	5290	0.46	132.5	430	1610	0.46
436.4	1260	5250	0.47	133.0	380	1600	0.47
438.0	1150	5210	0.47	133.5	350	1590	0.47
439.6	1250	5290	0.47	134.0	380	1610	0.47
441.3	1570	5900	0.46	134.5	480	1800	0.46
442.9	1900	6350	0.45	135.0	580	1940	0.45
444.6	1850	5950	0.45	135.5	560	1810	0.45
446.2	1710	6170	0.46	136.0	520	1880	0.46
447.8	1790	6410	0.46	136.5	540	1950	0.46
449.5	2210	6540	0.44	137.0	680	1990	0.44
451.1	2310	6730	0.43	137.5	710	2050	0.43
452.8	2920	7330	0.41	138.0	890	2230	0.41
454.4	2940	7090	0.40	138.5	900	2160	0.40
456.0	2080	6060	0.43	139.0	640	1850	0.43
457.7	1840	6230	0.45	139.5	560	1900	0.45
459.3	2310	9260	0.47	140.0	710	2820	0.47
461.0	2740	10100	0.46	140.5	840	3080	0.46
462.6	2280	6600	0.43	141.0	690	2010	0.43
464.2	2080	5950	0.43	141.5	640	1810	0.43
465.9	1740	5700	0.45	142.0	530	1740	0.45
467.5	1520	5600	0.46	142.5	460	1710	0.46
469.2	1570	5600	0.46	143.0	480	1710	0.46
470.8	1540	5700	0.46	143.5	470	1740	0.46
472.4	1540	5650	0.46	144.0	470	1720	0.46
474.1	1490	5750	0.46	144.5	450	1750	0.46
475.7	1540	5850	0.46	145.0	470	1780	0.46
477.4	1630	6060	0.46	145.5	500	1850	0.46
479.0	1710	6060	0.46	146.0	520	1850	0.46

**Figure H-118, Tabulated V<sub>s</sub> and V<sub>p</sub> Results – B-11GEO (con't)**



**Summary of Compressional Wave Velocity, Shear Wave Velocity, and Poisson's Ratio  
Based on Receiver-to-Receiver Travel Time Data - Borehole B-11GEO**

American Units				Metric Units			
Depth at Midpoint Between Receivers	Velocity		Poisson's Ratio	Depth at Midpoint Between Receivers	Velocity		Poisson's Ratio
	V <sub>s</sub>	V <sub>p</sub>			V <sub>s</sub>	V <sub>p</sub>	
(ft)	(ft/s)	(ft/s)		(m)	(m/s)	(m/s)	
480.6	1610	5850	0.46	146.5	490	1780	0.46
482.3	1530	5850	0.46	147.0	470	1780	0.46
483.9	1560	5850	0.46	147.5	480	1780	0.46
485.6	1610	5750	0.46	148.0	490	1750	0.46
487.2	1640	5950	0.46	148.5	500	1810	0.46
488.9	1660	6060	0.46	149.0	510	1850	0.46
490.5	1740	6060	0.46	149.5	530	1850	0.46
492.1	1890	6170	0.45	150.0	580	1880	0.45
493.8	1890	5170	0.42	150.5	580	1580	0.42
495.4	1830	5420	0.44	151.0	560	1650	0.44
497.1	1860	5650	0.44	151.5	570	1720	0.44
498.7	1900	6010	0.44	152.0	580	1830	0.44
500.3	1960	6350	0.45	152.5	600	1940	0.45
502.0	2100	6940	0.45	153.0	640	2120	0.45
503.6	1950	6290	0.45	153.5	590	1920	0.45
505.3	1750	6170	0.46	154.0	530	1880	0.46
506.9	1920	6940	0.46	154.5	580	2120	0.46
508.5	1980	6290	0.45	155.0	600	1920	0.45
510.2	2120	5800	0.42	155.5	650	1770	0.42
511.8	1970	5800	0.43	156.0	600	1770	0.43
513.5	1920	5850	0.44	156.5	580	1780	0.44
515.1	1930	5750	0.44	157.0	590	1750	0.44
516.7	2020	5900	0.43	157.5	620	1800	0.43
518.4	1990	5700	0.43	158.0	610	1740	0.43
520.0	2140	6010	0.43	158.5	650	1830	0.43
521.7	2610	6350	0.40	159.0	800	1940	0.40
523.3	2440	5900	0.40	159.5	740	1800	0.40
524.9	2230	5800	0.41	160.0	680	1770	0.41
526.6	2310	5750	0.40	160.5	710	1750	0.40
528.2	2250	5750	0.41	161.0	690	1750	0.41
529.9	2010	5650	0.43	161.5	610	1720	0.43
531.5	1920	5600	0.43	162.0	590	1710	0.43
533.1	1990	5750	0.43	162.5	610	1750	0.43
534.8	1970	5850	0.44	163.0	600	1780	0.44
536.4	1970	5900	0.44	163.5	600	1800	0.44
538.1	2000	5950	0.44	164.0	610	1810	0.44
539.7	2000	6170	0.44	164.5	610	1880	0.44
541.3	2290	5950	0.41	165.0	700	1810	0.41
543.0	2220	6060	0.42	165.5	680	1850	0.42
544.6	2020	6170	0.44	166.0	620	1880	0.44
546.3	2040	6540	0.45	166.5	620	1990	0.45
547.9	2090	6230	0.44	167.0	640	1900	0.44
549.5	2060	6060	0.43	167.5	630	1850	0.43

**Figure H-119, Tabulated V<sub>s</sub> and V<sub>p</sub> Results – B-11GEO (con't)**

**Summary of Compressional Wave Velocity, Shear Wave Velocity, and Poisson's Ratio  
Based on Receiver-to-Receiver Travel Time Data - Borehole B-11GEO**

American Units				Metric Units			
Depth at Midpoint Between Receivers	Velocity		Poisson's Ratio	Depth at Midpoint Between Receivers	Velocity		Poisson's Ratio
	V <sub>s</sub>	V <sub>p</sub>			V <sub>s</sub>	V <sub>p</sub>	
(ft)	(ft/s)	(ft/s)		(m)	(m/s)	(m/s)	
551.2	2150	6060	0.43	168.0	660	1850	0.43
552.8	2260	6170	0.42	168.5	690	1880	0.42
554.5	2230	6290	0.43	169.0	680	1920	0.43
556.1	2140	6120	0.43	169.5	650	1860	0.43
557.7	2080	5900	0.43	170.0	640	1800	0.43
559.4	2020	6170	0.44	170.5	620	1880	0.44
561.0	2100	6230	0.44	171.0	640	1900	0.44
562.7	2320	6470	0.43	171.5	710	1970	0.43
564.3	2310	5800	0.41	172.0	710	1770	0.41
565.9	2200	6170	0.43	172.5	670	1880	0.43
567.6	2120	6170	0.43	173.0	650	1880	0.43
569.2	2060	5900	0.43	173.5	630	1800	0.43
570.9	2100	5850	0.43	174.0	640	1780	0.43
572.5	2160	5900	0.42	174.5	660	1800	0.42
574.2	2190	6170	0.43	175.0	670	1880	0.43
575.8	2380	6600	0.43	175.5	730	2010	0.43
577.4	2660	6350	0.39	176.0	810	1940	0.39
579.1	2550	6230	0.40	176.5	780	1900	0.40
580.7	2360	6010	0.41	177.0	720	1830	0.41
582.4	2200	6120	0.43	177.5	670	1860	0.43
584.0	2040	5800	0.43	178.0	620	1770	0.43
585.6	2020	5950	0.43	178.5	620	1810	0.43
587.3	2140	5850	0.42	179.0	650	1780	0.42
588.9	2130	5850	0.42	179.5	650	1780	0.42
590.6	1890	5700	0.44	180.0	580	1740	0.44
592.2	1660	5850	0.46	180.5	510	1780	0.46
593.8	1610	5850	0.46	181.0	490	1780	0.46
595.5	2040	5750	0.43	181.5	620	1750	0.43
597.1	2210	5700	0.41	182.0	680	1740	0.41
598.8	2110	6230	0.44	182.5	640	1900	0.44
600.4	2120	6230	0.43	183.0	650	1900	0.43
602.0	1980	5900	0.44	183.5	600	1800	0.44
603.7	2010	6290	0.44	184.0	610	1920	0.44
605.3	2530	6870	0.42	184.5	770	2090	0.42
607.0	2710	6730	0.40	185.0	830	2050	0.40
608.6	2240	6010	0.42	185.5	680	1830	0.42
610.2	2260	5800	0.41	186.0	690	1770	0.41
611.9	2050	5800	0.43	186.5	630	1770	0.43
613.5	2010	5800	0.43	187.0	610	1770	0.43
615.2	1960	5800	0.44	187.5	600	1770	0.44
616.8	2010	5800	0.43	188.0	610	1770	0.43
618.4	2010	5900	0.43	188.5	610	1800	0.43
620.1	1940	6060	0.44	189.0	590	1850	0.44

**Figure H-120, Tabulated V<sub>s</sub> and V<sub>p</sub> Results – B-11GEO (con't)**

**Summary of Compressional Wave Velocity, Shear Wave Velocity, and Poisson's Ratio  
Based on Receiver-to-Receiver Travel Time Data - Borehole B-11GEO**

American Units				Metric Units			
Depth at Midpoint Between Receivers	Velocity		Poisson's Ratio	Depth at Midpoint Between Receivers	Velocity		Poisson's Ratio
	V <sub>s</sub>	V <sub>p</sub>			V <sub>s</sub>	V <sub>p</sub>	
(ft)	(ft/s)	(ft/s)		(m)	(m/s)	(m/s)	
621.7	2010	6010	0.44	189.5	610	1830	0.44
623.4	2110	6060	0.43	190.0	640	1850	0.43
625.0	2070	5900	0.43	190.5	630	1800	0.43
627.0	1980	5800	0.43	191.1	600	1770	0.43
628.3	1940	6010	0.44	191.5	590	1830	0.44
629.9	1900	6060	0.45	192.0	580	1850	0.45
631.6	2100	6170	0.43	192.5	640	1880	0.43
633.2	2050	6230	0.44	193.0	630	1900	0.44
634.8	1970	6350	0.45	193.5	600	1940	0.45
636.5	1990	6350	0.45	194.0	610	1940	0.45
638.1	1980	6410	0.45	194.5	600	1950	0.45
639.8	2090	6350	0.44	195.0	640	1940	0.44
641.4	2280	6350	0.43	195.5	690	1940	0.43
643.0	2090	5900	0.43	196.0	640	1800	0.43
644.7	1980	6060	0.44	196.5	600	1850	0.44
646.3	1990	6010	0.44	197.0	610	1830	0.44
648.0	2180	6230	0.43	197.5	660	1900	0.43
649.6	2140	6350	0.44	198.0	650	1940	0.44
651.3	2030	6350	0.44	198.5	620	1940	0.44
652.9	2000	6230	0.44	199.0	610	1900	0.44
654.5	1970	5950	0.44	199.5	600	1810	0.44
656.2	2040	6170	0.44	200.0	620	1880	0.44
657.8	2280	6230	0.42	200.5	700	1900	0.42
659.5	2370	6060	0.41	201.0	720	1850	0.41
661.1	2580	6010	0.39	201.5	790	1830	0.39
662.7	2540	5800	0.38	202.0	780	1770	0.38
664.4	2380	6010	0.41	202.5	730	1830	0.41
666.0	2030	6060	0.44	203.0	620	1850	0.44
667.7	1950	5750	0.44	203.5	590	1750	0.44
669.3	2050	5900	0.43	204.0	630	1800	0.43
670.9	2170	6290	0.43	204.5	660	1920	0.43
672.6	2270	6290	0.43	205.0	690	1920	0.43
674.2	2530	6600	0.41	205.5	770	2010	0.41
675.9	2710	6670	0.40	206.0	830	2030	0.40
677.5	2900	6470	0.37	206.5	880	1970	0.37
679.1	2650	6120	0.38	207.0	810	1860	0.38
680.8	2180	5800	0.42	207.5	660	1770	0.42
682.4	2040	6010	0.43	208.0	620	1830	0.43
684.1	1900	5800	0.44	208.5	580	1770	0.44
685.7	1930	5850	0.44	209.0	590	1780	0.44
687.3	1770	5600	0.44	209.5	540	1710	0.44
689.0	1720	5650	0.45	210.0	530	1720	0.45
690.6	1790	5950	0.45	210.5	550	1810	0.45

**Figure H-121, Tabulated V<sub>s</sub> and V<sub>p</sub> Results – B-11GEO (con't)**

**Summary of Compressional Wave Velocity, Shear Wave Velocity, and Poisson's Ratio  
Based on Receiver-to-Receiver Travel Time Data - Borehole B-11GEO**

American Units				Metric Units			
Depth at Midpoint Between Receivers	Velocity		Poisson's Ratio	Depth at Midpoint Between Receivers	Velocity		Poisson's Ratio
	V <sub>s</sub>	V <sub>p</sub>			V <sub>s</sub>	V <sub>p</sub>	
(ft)	(ft/s)	(ft/s)		(m)	(m/s)	(m/s)	
692.3	2410	6870	0.43	211.0	730	2090	0.43
693.9	3130	6730	0.36	211.5	950	2050	0.36
695.5	2560	6410	0.40	212.0	780	1950	0.40
697.2	2260	6230	0.42	212.5	690	1900	0.42
698.8	2490	6290	0.41	213.0	760	1920	0.41
700.5	2160	6170	0.43	213.5	660	1880	0.43
702.4	2190	6060	0.43	214.1	670	1850	0.43
703.7	2520	7250	0.43	214.5	770	2210	0.43
705.4	3320	7660	0.38	215.0	1010	2340	0.38
707.0	3170	7250	0.38	215.5	970	2210	0.38
708.7	2520	6800	0.42	216.0	770	2070	0.42
710.3	3030	7170	0.39	216.5	920	2180	0.39
711.9	2730	7580	0.43	217.0	830	2310	0.43
713.6	2090	5900	0.43	217.5	640	1800	0.43
715.2	1900	5650	0.44	218.0	580	1720	0.44
716.9	1970	5750	0.43	218.5	600	1750	0.43
718.5	1940	6800	0.46	219.0	590	2070	0.46
720.1	1880	6410	0.45	219.5	570	1950	0.45
721.8	1970	6120	0.44	220.0	600	1860	0.44
723.4	1940	6230	0.45	220.5	590	1900	0.45
725.1	1850	5900	0.45	221.0	560	1800	0.45
726.7	1870	6230	0.45	221.5	570	1900	0.45
728.4	2100	6290	0.44	222.0	640	1920	0.44
730.0	2100	6470	0.44	222.5	640	1970	0.44
731.6	1920	6230	0.45	223.0	590	1900	0.45
733.3	1940	6170	0.44	223.5	590	1880	0.44
734.9	2020	6170	0.44	224.0	620	1880	0.44
736.6	2000	6230	0.44	224.5	610	1900	0.44
738.2	2000	6290	0.44	225.0	610	1920	0.44
739.8	2550	6940	0.42	225.5	780	2120	0.42
741.5	2540	6470	0.41	226.0	780	1970	0.41
743.1	2060	5650	0.42	226.5	630	1720	0.42
744.8	1940	5800	0.44	227.0	590	1770	0.44
746.4	1880	5700	0.44	227.5	570	1740	0.44
748.0	1830	5900	0.45	228.0	560	1800	0.45
749.7	1920	5560	0.43	228.5	580	1690	0.43
751.3	1910	5700	0.44	229.0	580	1740	0.44
753.0	1920	5700	0.44	229.5	580	1740	0.44
754.6	2000	5600	0.43	230.0	610	1710	0.43
756.2	1970	5600	0.43	230.5	600	1710	0.43
757.9	2060	5700	0.43	231.0	630	1740	0.43
759.5	2180	5750	0.42	231.5	660	1750	0.42
761.2	2110	6010	0.43	232.0	640	1830	0.43

**Figure H-122, Tabulated V<sub>s</sub> and V<sub>p</sub> Results – B-11GEO (con't)**

**Summary of Compressional Wave Velocity, Shear Wave Velocity, and Poisson's Ratio  
Based on Receiver-to-Receiver Travel Time Data - Borehole B-11GEO**

American Units				Metric Units			
Depth at Midpoint Between Receivers	Velocity		Poisson's Ratio	Depth at Midpoint Between Receivers	Velocity		Poisson's Ratio
	V <sub>s</sub>	V <sub>p</sub>			V <sub>s</sub>	V <sub>p</sub>	
(ft)	(ft/s)	(ft/s)		(m)	(m/s)	(m/s)	
762.8	2160	5560	0.41	232.5	660	1690	0.41
764.4	2210	5650	0.41	233.0	680	1720	0.41
766.1	2030	5750	0.43	233.5	620	1750	0.43
767.7	2040	5750	0.43	234.0	620	1750	0.43
769.4	2090	5950	0.43	234.5	640	1810	0.43
771.0	2160	5950	0.42	235.0	660	1810	0.42
772.6	2270	6230	0.42	235.5	690	1900	0.42
774.3	2280	6470	0.43	236.0	700	1970	0.43
775.9	2240	6230	0.43	236.5	680	1900	0.43
777.6	2200	6290	0.43	237.0	670	1920	0.43
779.2	2170	5950	0.42	237.5	660	1810	0.42
780.8	2290	6060	0.42	238.0	700	1850	0.42
782.5	2490	5950	0.39	238.5	760	1810	0.39
784.1	2420	5950	0.40	239.0	740	1810	0.40
785.8	2320	5950	0.41	239.5	710	1810	0.41
787.4	2340	6170	0.42	240.0	710	1880	0.42
789.0	2190	7090	0.45	240.5	670	2160	0.45
791.0	2260	6350	0.43	241.1	690	1940	0.43

**Notes:**        "-" means no data available at that particular interval of depth.

**Figure H-123, Tabulated V<sub>s</sub> and V<sub>p</sub> Results – B-11GEO (con't)**

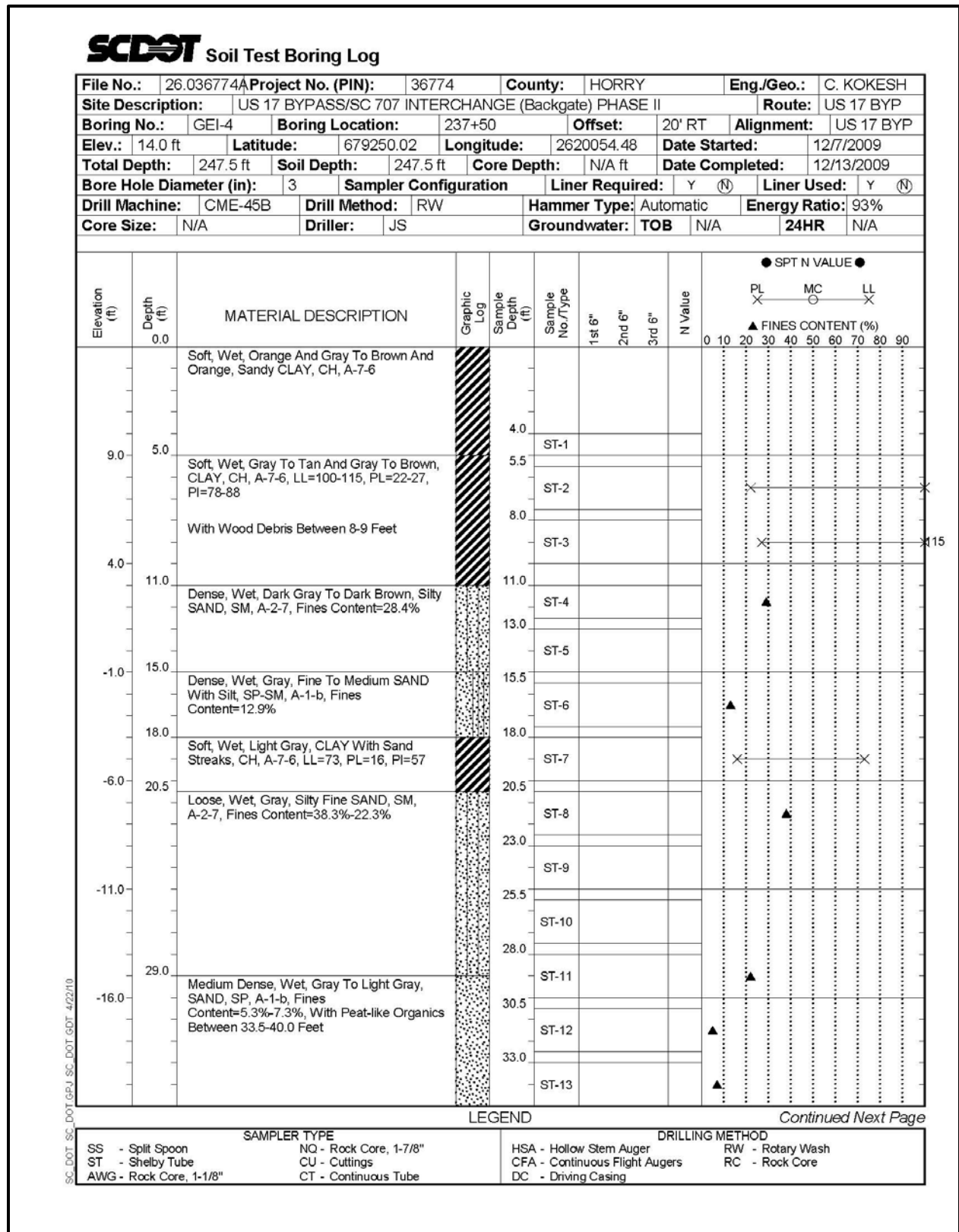


Figure H-124, Soil Test Boring GEI 4

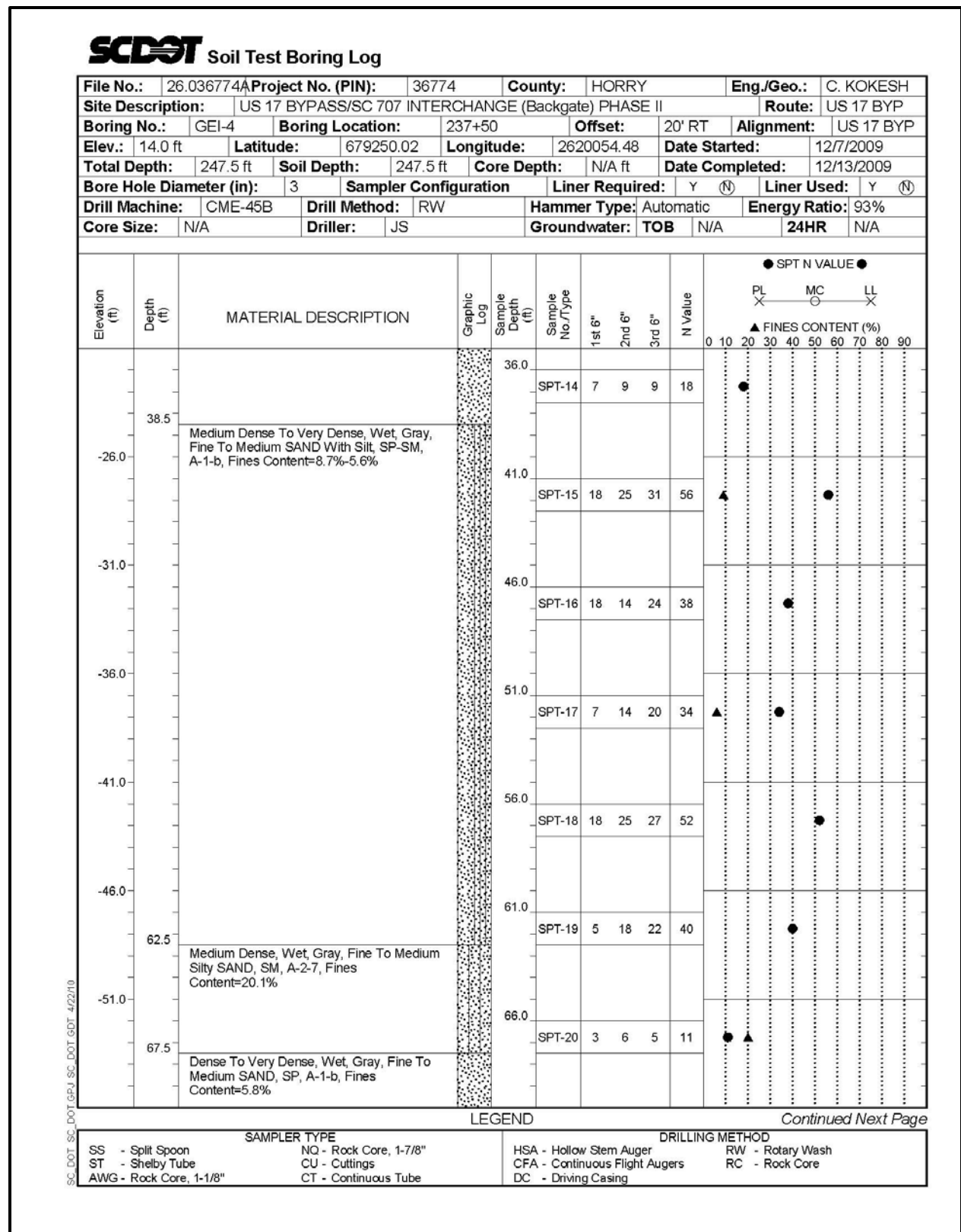


Figure H-125, Soil Test Boring GEI 4 (con't)

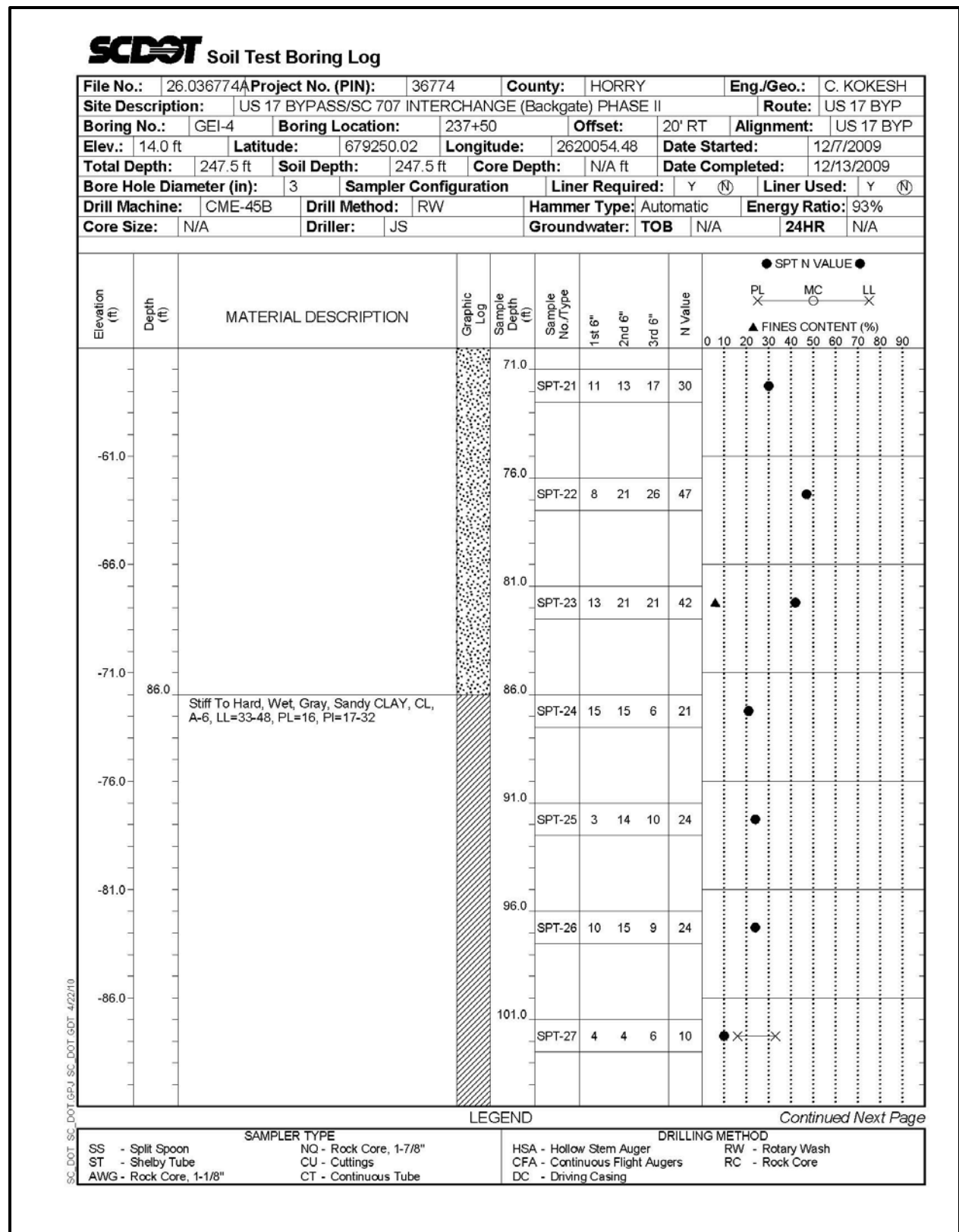


Figure H-126, Soil Test Boring GEI 4 (con't)



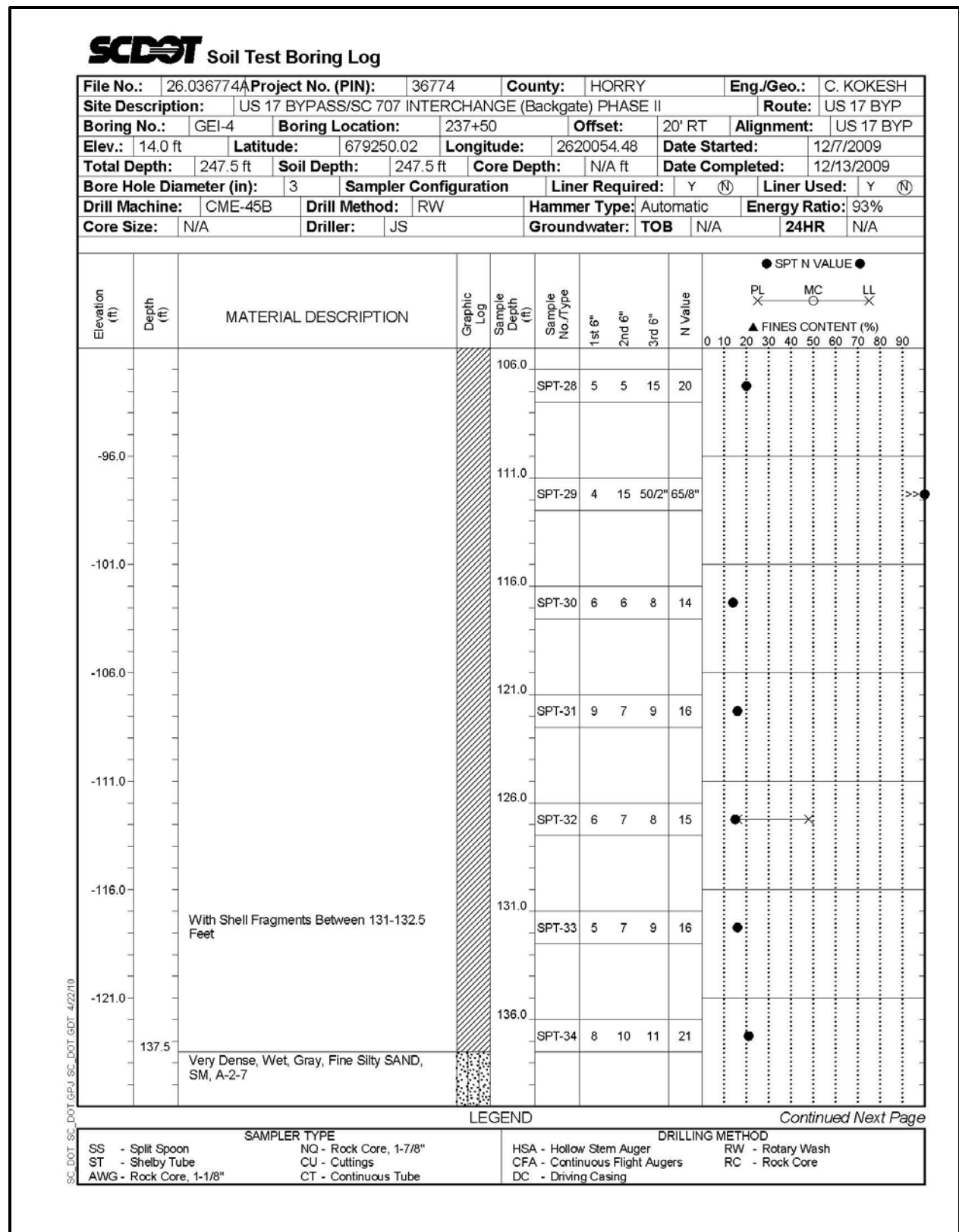


Figure H-127, Soil Test Boring GEI 4 (con't)

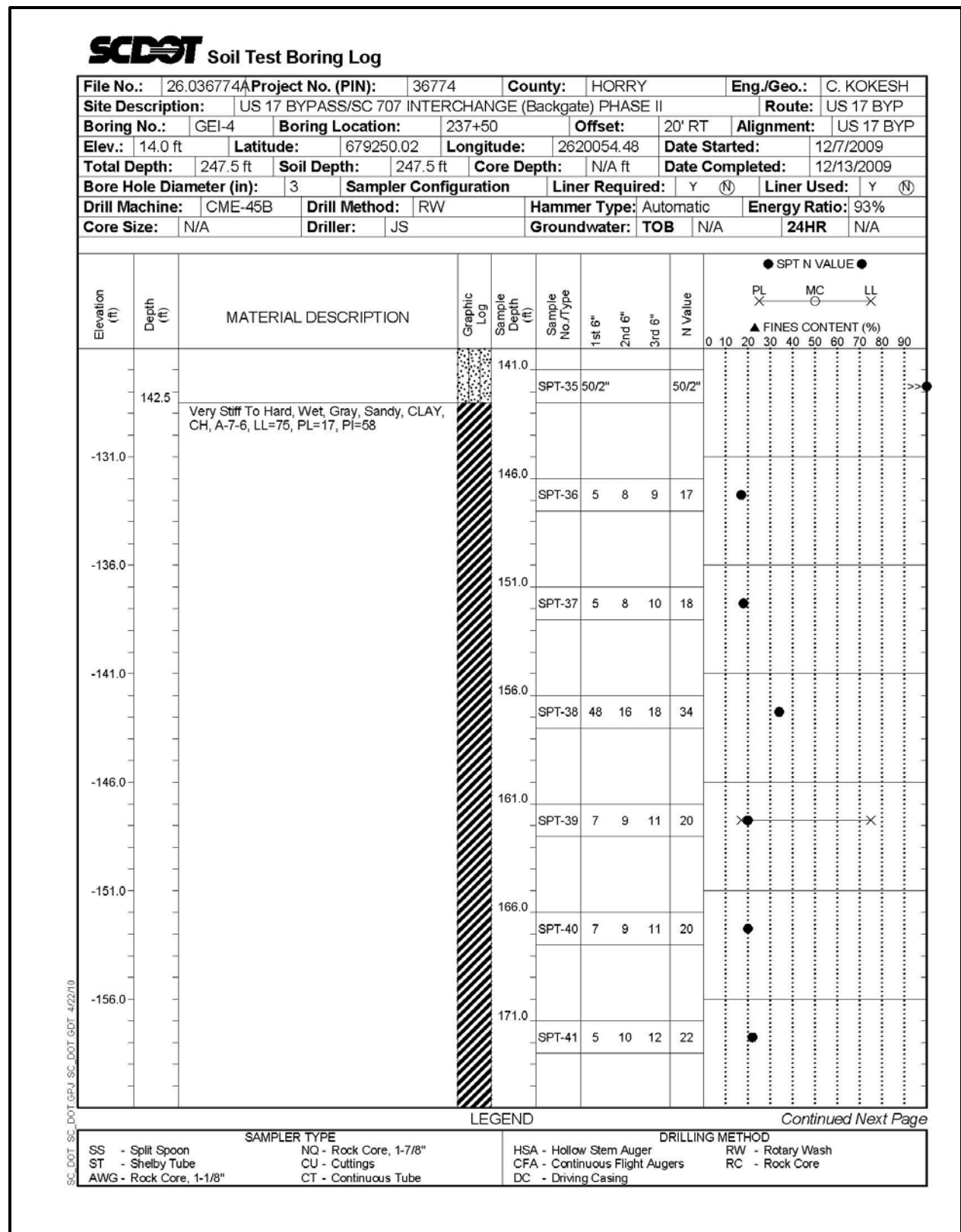


Figure H-128, Soil Test Boring GEI 4 (con't)

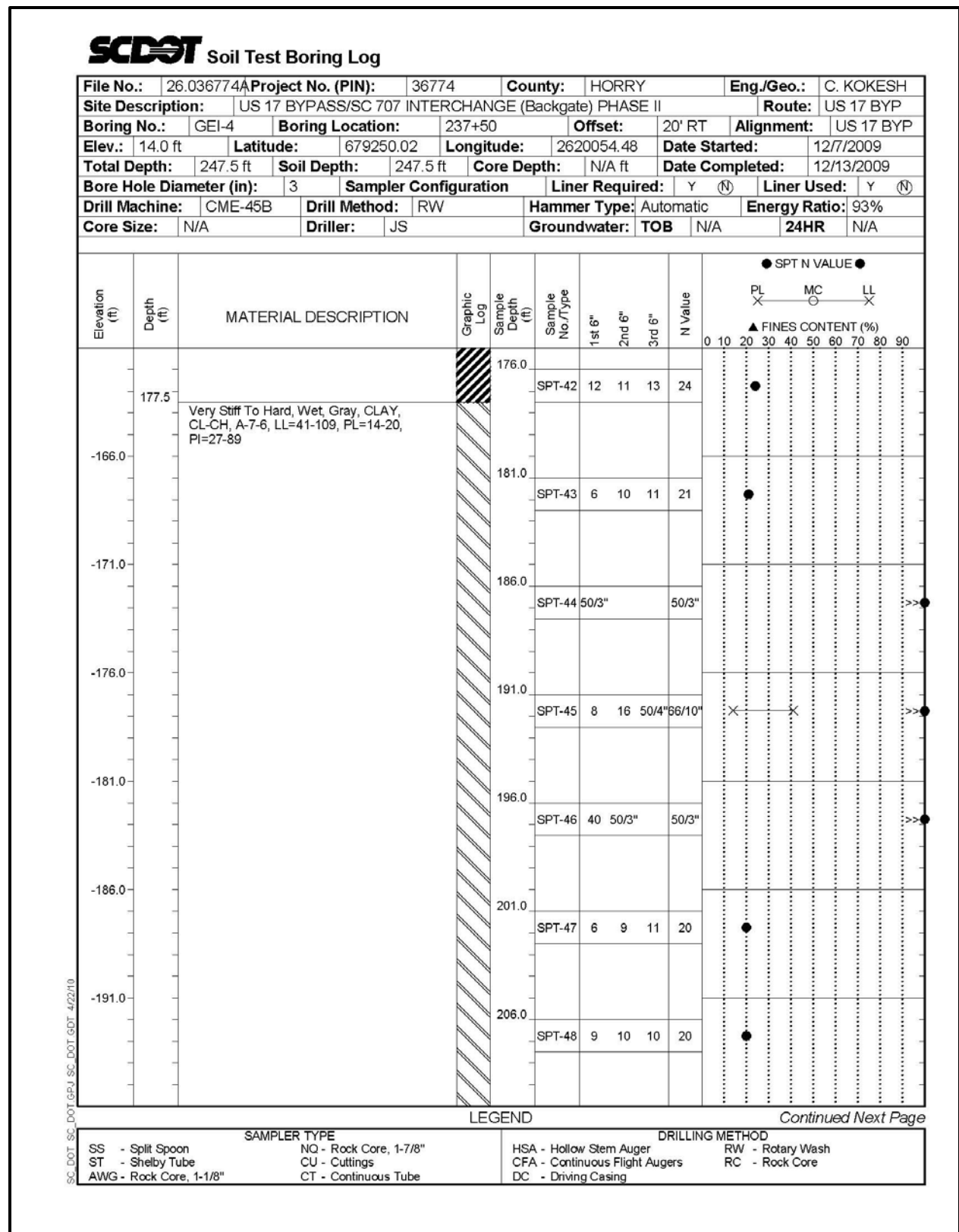


Figure H-129, Soil Test Boring GEI 4 (con't)

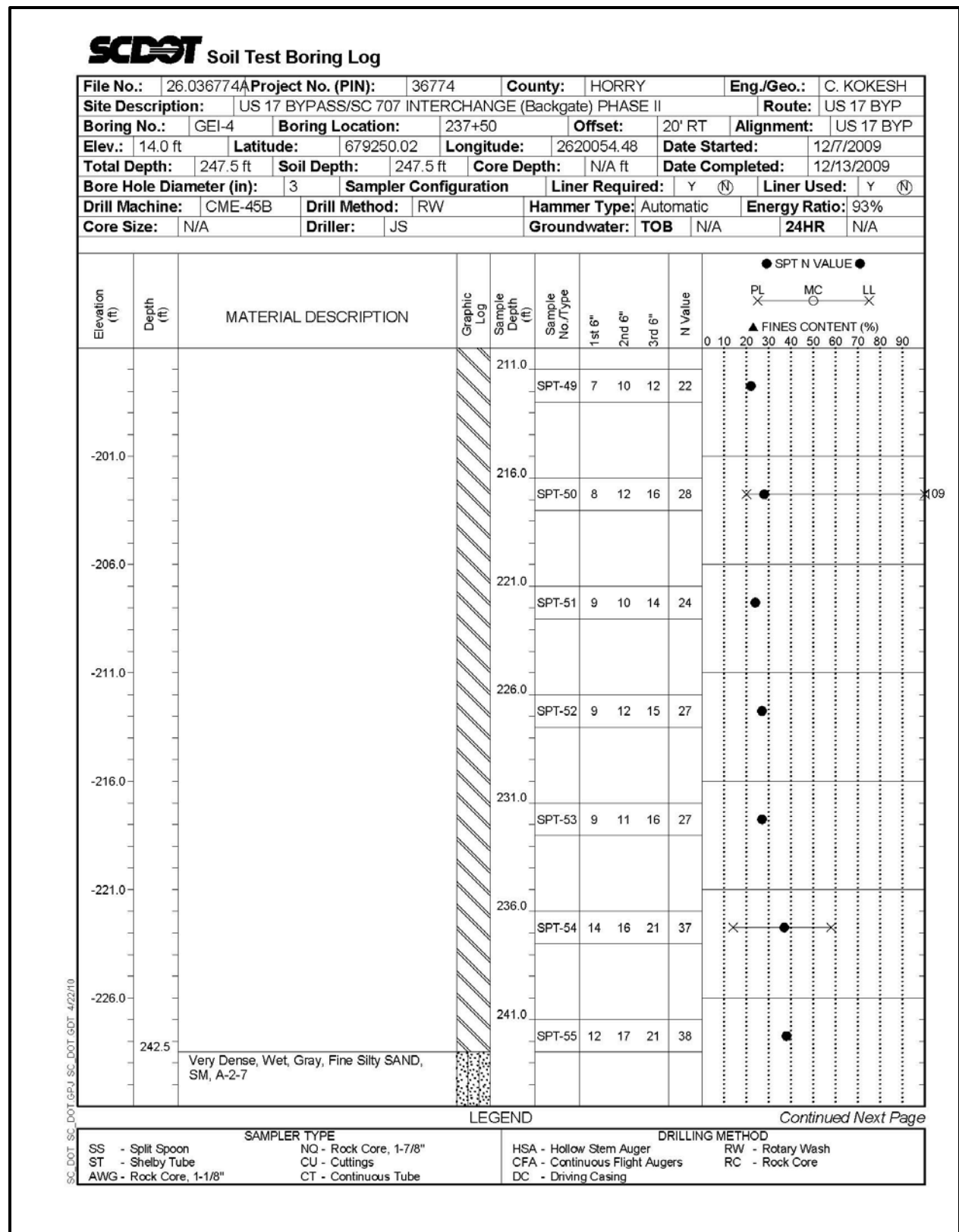


Figure H-130, Soil Test Boring GEI 4 (con't)

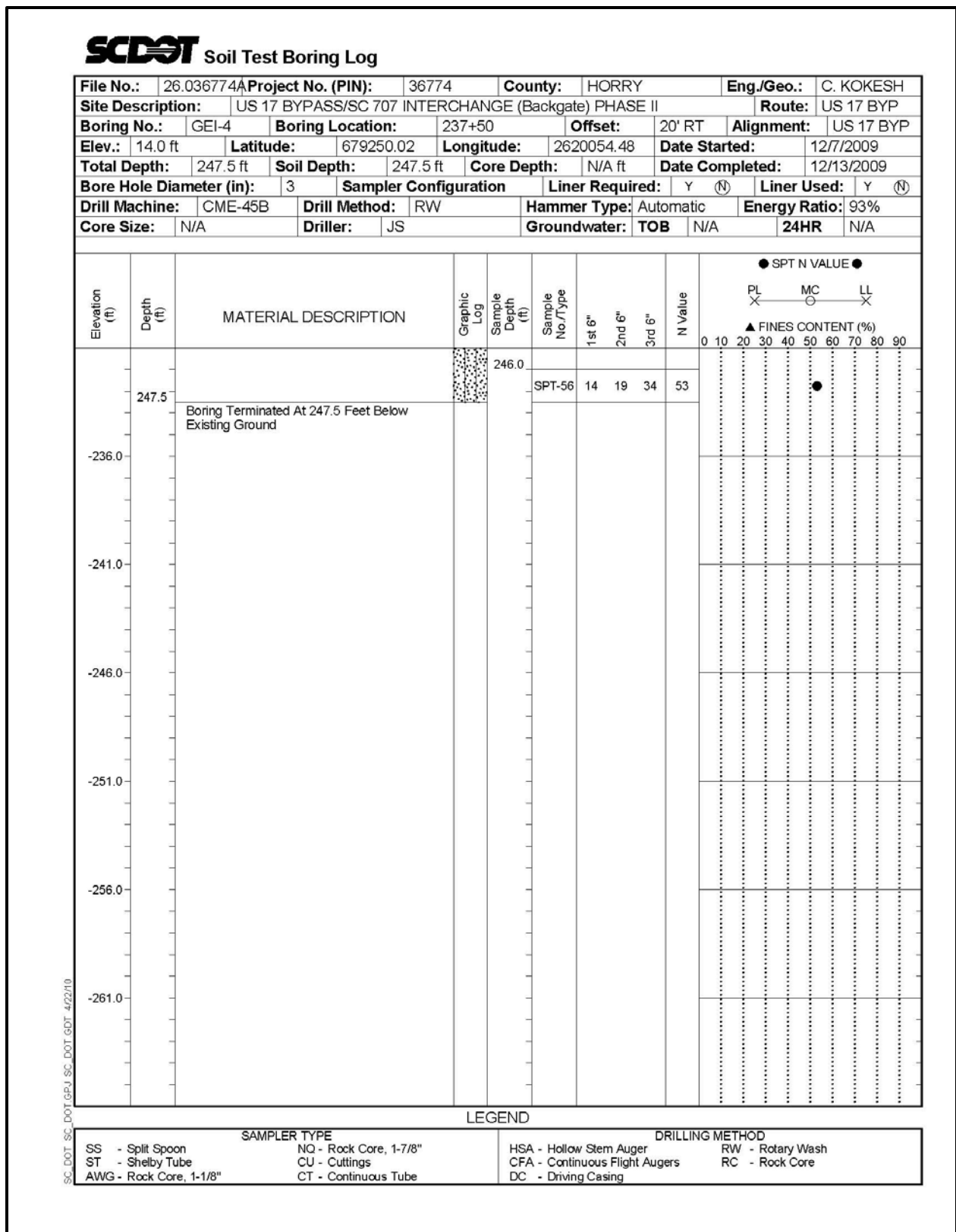
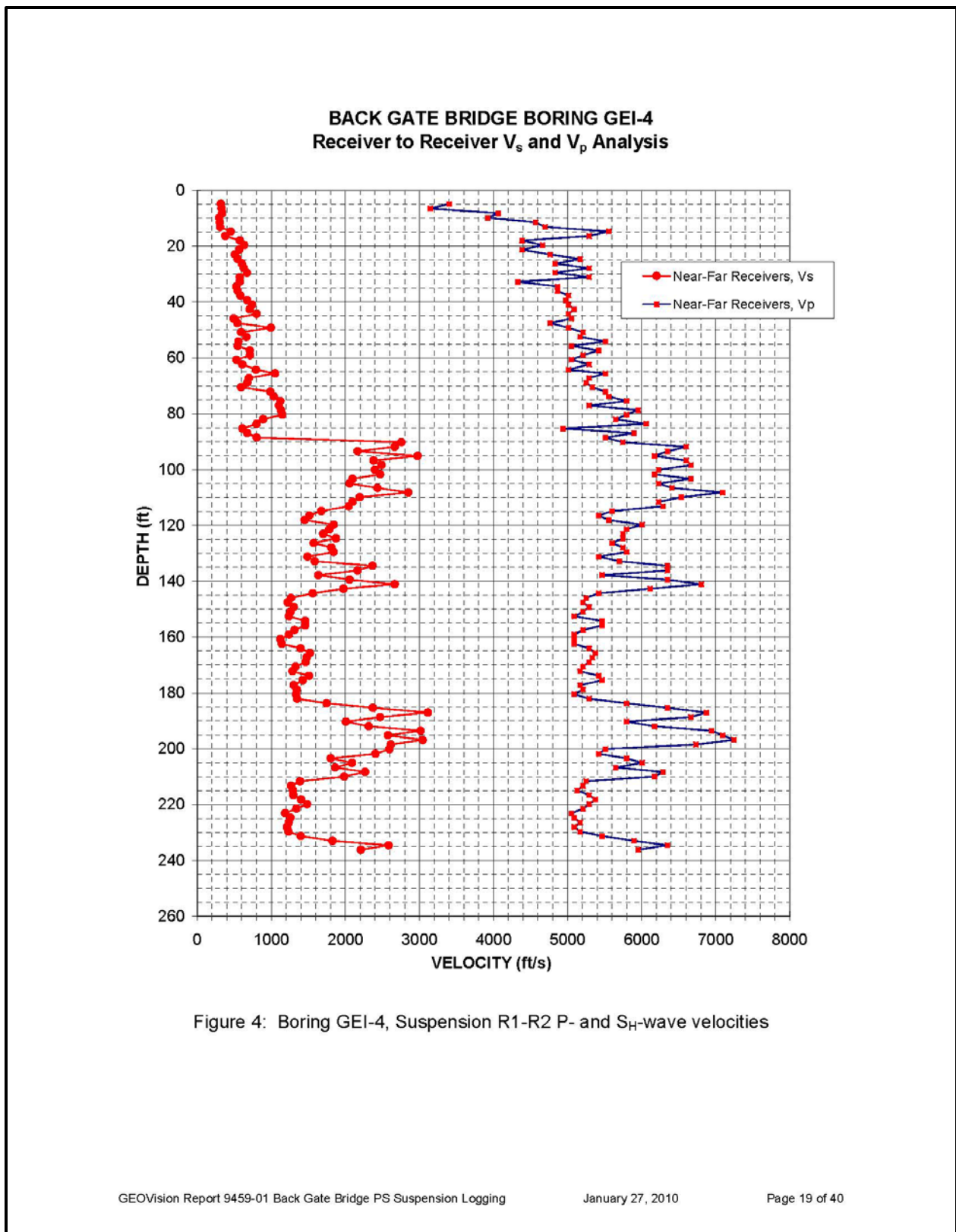


Figure H-131, Soil Test Boring GEI 4 (con't)



**Figure H-132,  $V_s$  and  $V_p$  Profile – GEI-4**

Table 3. Boring GEI-4, Suspension R1-R2 depths and P- and S<sub>H</sub>-wave velocities

Summary of Compressional Wave Velocity, Shear Wave Velocity, and Poisson's Ratio  
Based on Receiver-to-Receiver Travel Time Data - Borehole GEI-4

American Units				Metric Units			
Depth at Midpoint Between Receivers	Velocity		Poisson's Ratio	Depth at Midpoint Between Receivers	Velocity		Poisson's Ratio
	V <sub>s</sub>	V <sub>p</sub>			V <sub>s</sub>	V <sub>p</sub>	
(ft)	(ft/s)	(ft/s)		(m)	(m/s)	(m/s)	
4.9	320	3400	0.50	1.5	100	1040	0.50
6.6	330	3140	0.49	2.0	100	960	0.49
8.2	340	4070	0.50	2.5	100	1240	0.50
9.8	300	3920	0.50	3.0	90	1200	0.50
11.5	310	4570	0.50	3.5	90	1390	0.50
13.1	310	4690	0.50	4.0	90	1430	0.50
14.8	450	5560	0.50	4.5	140	1690	0.50
16.4	380	5290	0.50	5.0	120	1610	0.50
18.0	570	4390	0.49	5.5	180	1340	0.49
19.7	630	4660	0.49	6.0	190	1420	0.49
21.3	560	4390	0.49	6.5	170	1340	0.49
23.0	510	4760	0.49	7.0	160	1450	0.49
24.6	550	5170	0.49	7.5	170	1580	0.49
26.3	600	4830	0.49	8.0	180	1470	0.49
27.9	630	5290	0.49	8.5	190	1610	0.49
29.5	670	4830	0.49	9.0	200	1470	0.49
31.2	570	5290	0.49	9.5	180	1610	0.49
32.8	570	4330	0.49	10.0	170	1320	0.49
34.5	530	4870	0.49	10.5	160	1480	0.49
36.1	550	4870	0.49	11.0	170	1480	0.49
37.7	580	5010	0.49	11.5	180	1530	0.49
39.4	670	4980	0.49	12.0	210	1520	0.49
41.0	740	5010	0.49	12.5	230	1530	0.49
42.7	710	5090	0.49	13.0	220	1550	0.49
44.3	800	5010	0.49	13.5	240	1530	0.49
45.9	490	5050	0.50	14.0	150	1540	0.50
47.6	540	4760	0.49	14.5	170	1450	0.49
49.2	1000	5010	0.48	15.0	300	1530	0.48
50.9	590	5210	0.49	15.5	180	1590	0.49
52.5	660	5170	0.49	16.0	200	1580	0.49
54.1	560	5510	0.49	16.5	170	1680	0.49
55.8	550	5050	0.49	17.0	170	1540	0.49
57.4	710	5420	0.49	17.5	220	1650	0.49
59.1	710	5210	0.49	18.0	220	1590	0.49
60.7	530	5050	0.49	18.5	160	1540	0.49
62.3	610	5290	0.49	19.0	190	1610	0.49
64.3	790	5010	0.49	19.6	240	1530	0.49
65.6	1050	5510	0.48	20.0	320	1680	0.48
67.3	700	5290	0.49	20.5	210	1610	0.49
68.9	680	5250	0.49	21.0	210	1600	0.49

Figure H-133, Tabulated V<sub>s</sub> and V<sub>p</sub> Results – GEI-4

**Summary of Compressional Wave Velocity, Shear Wave Velocity, and Poisson's Ratio  
Based on Receiver-to-Receiver Travel Time Data - Borehole GEI-4**

American Units				Metric Units			
Depth at Midpoint Between Receivers	Velocity		Poisson's Ratio	Depth at Midpoint Between Receivers	Velocity		Poisson's Ratio
	V <sub>s</sub>	V <sub>p</sub>			V <sub>s</sub>	V <sub>p</sub>	
(ft)	(ft/s)	(ft/s)		(m)	(m/s)	(m/s)	
70.5	590	5330	0.49	21.5	180	1630	0.49
72.2	990	5510	0.48	22.0	300	1680	0.48
73.8	1030	5560	0.48	22.5	320	1690	0.48
75.5	1120	5800	0.48	23.0	340	1770	0.48
77.1	1100	5290	0.48	23.5	340	1610	0.48
78.7	1130	5950	0.48	24.0	340	1810	0.48
80.4	1150	5800	0.48	24.5	350	1770	0.48
82.0	890	5650	0.49	25.0	270	1720	0.49
83.7	800	6060	0.49	25.5	240	1850	0.49
85.3	610	4940	0.49	26.0	190	1510	0.49
86.9	670	5900	0.49	26.5	210	1800	0.49
88.6	800	5510	0.49	27.0	240	1680	0.49
90.2	2750	5750	0.35	27.5	840	1750	0.35
91.9	2670	6600	0.40	28.0	810	2010	0.40
93.5	2160	6350	0.43	28.5	660	1940	0.43
95.1	2980	6170	0.35	29.0	910	1880	0.35
96.8	2380	6600	0.43	29.5	730	2010	0.43
98.4	2490	6670	0.42	30.0	760	2030	0.42
100.1	2400	6230	0.41	30.5	730	1900	0.41
101.7	2470	6170	0.40	31.0	750	1880	0.40
103.4	2100	6670	0.45	31.5	640	2030	0.45
105.0	2060	6230	0.44	32.0	630	1900	0.44
106.6	2430	6410	0.42	32.5	740	1950	0.42
108.3	2850	7090	0.40	33.0	870	2160	0.40
109.9	2190	6540	0.44	33.5	670	1990	0.44
111.6	2100	6230	0.44	34.0	640	1900	0.44
113.2	2040	6290	0.44	34.5	620	1920	0.44
114.8	1680	5600	0.45	35.0	510	1710	0.45
116.5	1520	5420	0.46	35.5	460	1650	0.46
118.1	1450	5560	0.46	36.0	440	1690	0.46
119.8	1840	6010	0.45	36.5	560	1830	0.45
121.4	1780	5800	0.45	37.0	540	1770	0.45
123.0	1700	5750	0.45	37.5	520	1750	0.45
124.7	1870	5750	0.44	38.0	570	1750	0.44
126.3	1570	5600	0.46	38.5	480	1710	0.46
128.0	1810	5750	0.44	39.0	550	1750	0.44
129.6	1840	5800	0.44	39.5	560	1770	0.44
131.2	1490	5420	0.46	40.0	450	1650	0.46
132.9	1590	5700	0.46	40.5	480	1740	0.46
134.5	2360	6350	0.42	41.0	720	1940	0.42
136.2	2160	6350	0.43	41.5	660	1940	0.43
137.8	1630	5460	0.45	42.0	500	1670	0.45
139.4	2060	6350	0.44	42.5	630	1940	0.44

**Figure H-134, Tabulated V<sub>s</sub> and V<sub>p</sub> Results – GEI-4 (con't)**



**Summary of Compressional Wave Velocity, Shear Wave Velocity, and Poisson's Ratio  
Based on Receiver-to-Receiver Travel Time Data - Borehole GEI-4**

American Units				Metric Units			
Depth at Midpoint Between Receivers	Velocity		Poisson's Ratio	Depth at Midpoint Between Receivers	Velocity		Poisson's Ratio
	V <sub>s</sub>	V <sub>p</sub>			V <sub>s</sub>	V <sub>p</sub>	
(ft)	(ft/s)	(ft/s)		(m)	(m/s)	(m/s)	
141.1	2670	6800	0.41	43.0	810	2070	0.41
142.7	1970	6120	0.44	43.5	600	1860	0.44
144.4	1560	5420	0.45	44.0	470	1650	0.45
146.0	1270	5250	0.47	44.5	390	1600	0.47
147.6	1220	5210	0.47	45.0	370	1590	0.47
149.3	1300	5290	0.47	45.5	400	1610	0.47
150.9	1260	5210	0.47	46.0	380	1590	0.47
152.6	1240	5090	0.47	46.5	380	1550	0.47
154.2	1460	5460	0.46	47.0	440	1670	0.46
155.8	1460	5460	0.46	47.5	440	1670	0.46
157.5	1310	5210	0.47	48.0	400	1590	0.47
159.1	1240	5090	0.47	48.5	380	1550	0.47
160.8	1120	5090	0.47	49.0	340	1550	0.47
162.4	1140	5090	0.47	49.5	350	1550	0.47
164.0	1390	5290	0.46	50.0	430	1610	0.46
165.7	1520	5380	0.46	50.5	460	1640	0.46
167.3	1470	5330	0.46	51.0	450	1630	0.46
169.0	1460	5290	0.46	51.5	450	1610	0.46
170.6	1330	5210	0.47	52.0	400	1590	0.47
172.2	1290	5170	0.47	52.5	390	1580	0.47
173.9	1510	5420	0.46	53.0	460	1650	0.46
175.5	1420	5460	0.46	53.5	430	1670	0.46
177.2	1300	5170	0.47	54.0	400	1580	0.47
178.8	1340	5210	0.46	54.5	410	1590	0.46
180.5	1330	5090	0.46	55.0	410	1550	0.46
182.1	1350	5290	0.47	55.5	410	1610	0.47
183.7	1750	5800	0.45	56.0	530	1770	0.45
185.4	2370	6350	0.42	56.5	720	1940	0.42
187.0	3120	6870	0.37	57.0	950	2090	0.37
188.7	2470	6670	0.42	57.5	750	2030	0.42
190.3	2010	5800	0.43	58.0	610	1770	0.43
191.9	2310	6170	0.42	58.5	710	1880	0.42
193.6	3020	6940	0.38	59.0	920	2120	0.38
195.2	2570	7090	0.42	59.5	780	2160	0.42
196.9	3040	7250	0.39	60.0	930	2210	0.39
198.5	2610	6730	0.41	60.5	800	2050	0.41
200.1	2590	5510	0.36	61.0	790	1680	0.36
201.8	2410	5420	0.38	61.5	730	1650	0.38
203.4	1800	5800	0.45	62.0	550	1770	0.45
205.1	2090	6010	0.43	62.5	640	1830	0.43
206.7	1860	5650	0.44	63.0	570	1720	0.44
208.3	2270	6290	0.43	63.5	690	1920	0.43
210.0	1980	6170	0.44	64.0	600	1880	0.44

**Figure H-135, Tabulated V<sub>s</sub> and V<sub>p</sub> Results – GEI-4 (con't)**

**Summary of Compressional Wave Velocity, Shear Wave Velocity, and Poisson's Ratio  
Based on Receiver-to-Receiver Travel Time Data - Borehole GEI-4**

American Units				Metric Units			
Depth at Midpoint Between Receivers	Velocity		Poisson's Ratio	Depth at Midpoint Between Receivers	Velocity		Poisson's Ratio
	V <sub>s</sub>	V <sub>p</sub>			V <sub>s</sub>	V <sub>p</sub>	
(ft)	(ft/s)	(ft/s)		(m)	(m/s)	(m/s)	
211.6	1390	5250	0.46	64.5	420	1600	0.46
213.3	1270	5210	0.47	65.0	390	1590	0.47
214.9	1290	5130	0.47	65.5	390	1560	0.47
216.5	1300	5290	0.47	66.0	400	1610	0.47
218.2	1400	5380	0.46	66.5	430	1640	0.46
219.8	1480	5290	0.46	67.0	450	1610	0.46
221.5	1340	5210	0.46	67.5	410	1590	0.46
223.1	1190	5050	0.47	68.0	360	1540	0.47
224.7	1260	5090	0.47	68.5	380	1550	0.47
226.4	1230	5170	0.47	69.0	380	1580	0.47
228.0	1210	5090	0.47	69.5	370	1550	0.47
229.7	1230	5170	0.47	70.0	380	1580	0.47
231.3	1400	5460	0.47	70.5	430	1670	0.47
232.9	1830	5900	0.45	71.0	560	1800	0.45
234.6	2580	6350	0.40	71.5	790	1940	0.40
236.2	2210	5950	0.42	72.0	670	1810	0.42

**Figure H-136, Tabulated V<sub>s</sub> and V<sub>p</sub> Results – GEI-4 (con't)**

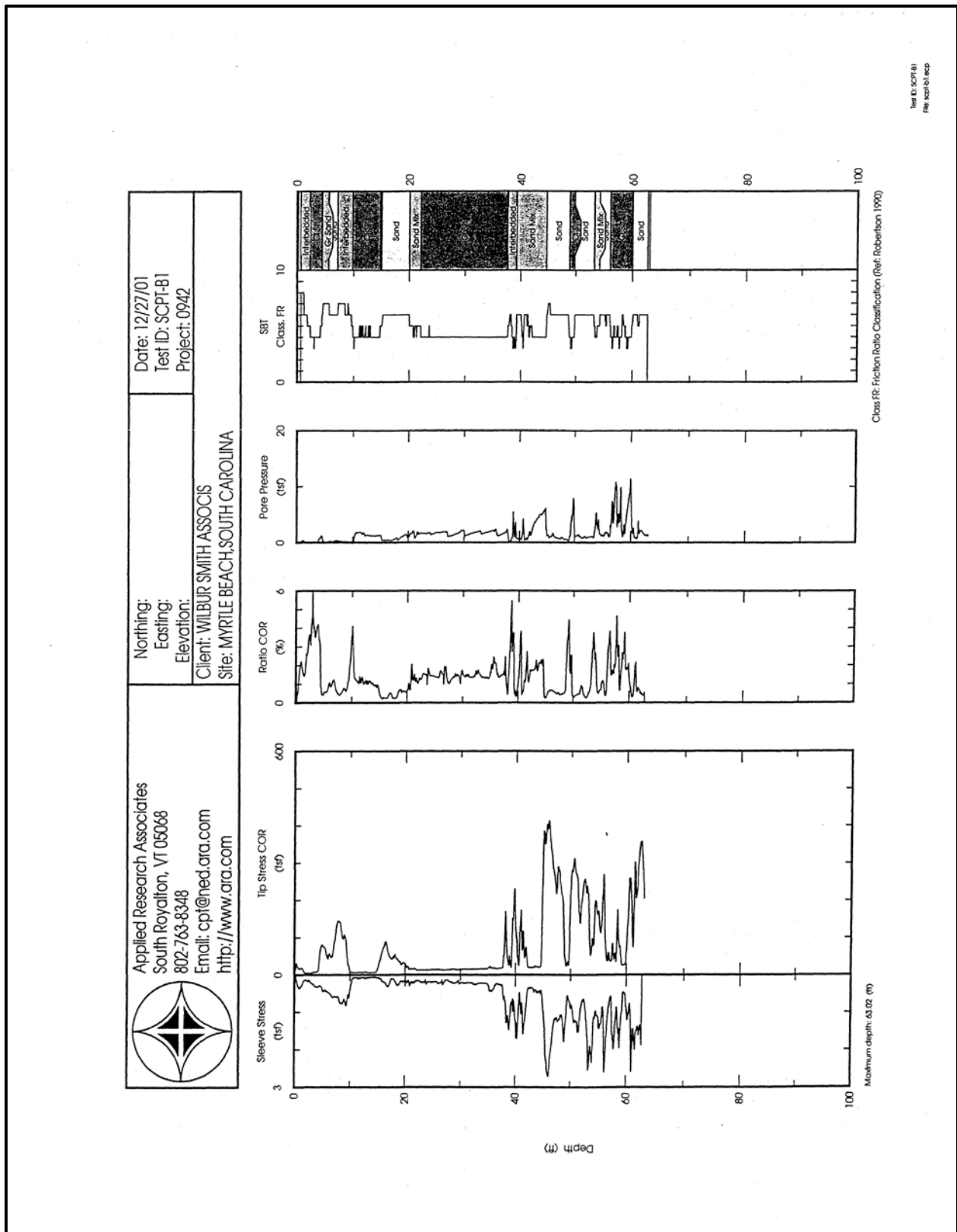
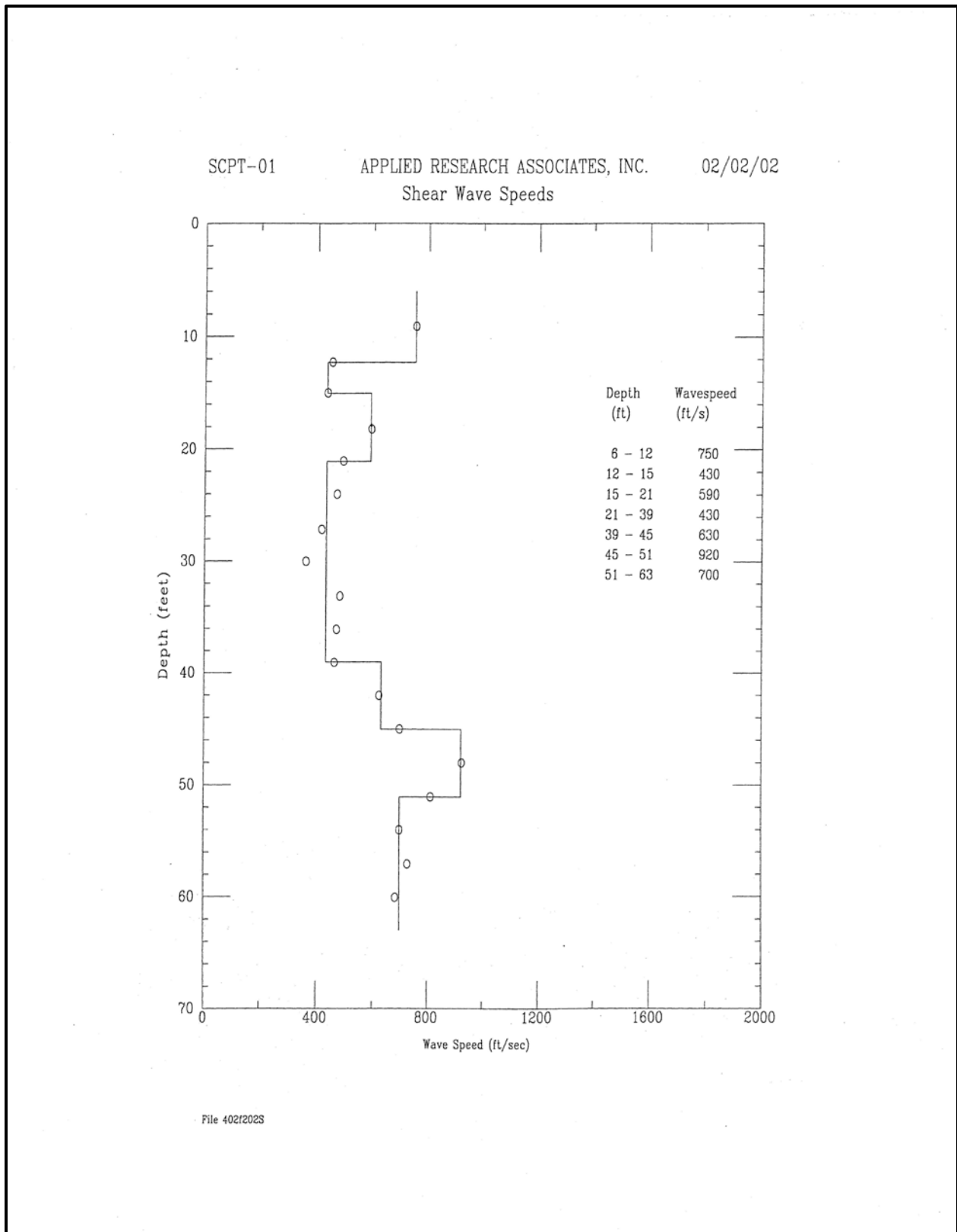


Figure H-137, SCPT-01



**Figure H-138,  $V_s$  Profile – SCPT-01**

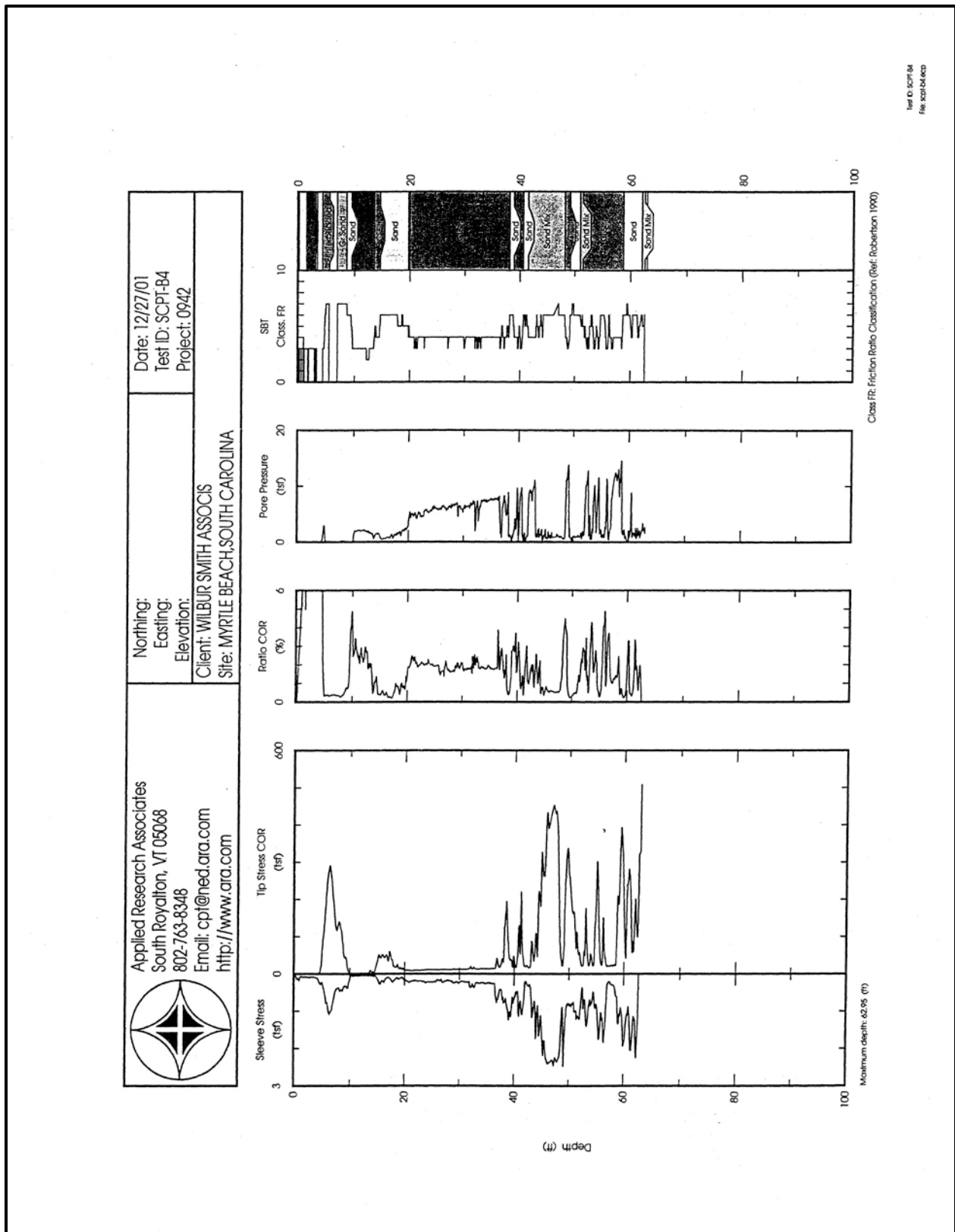
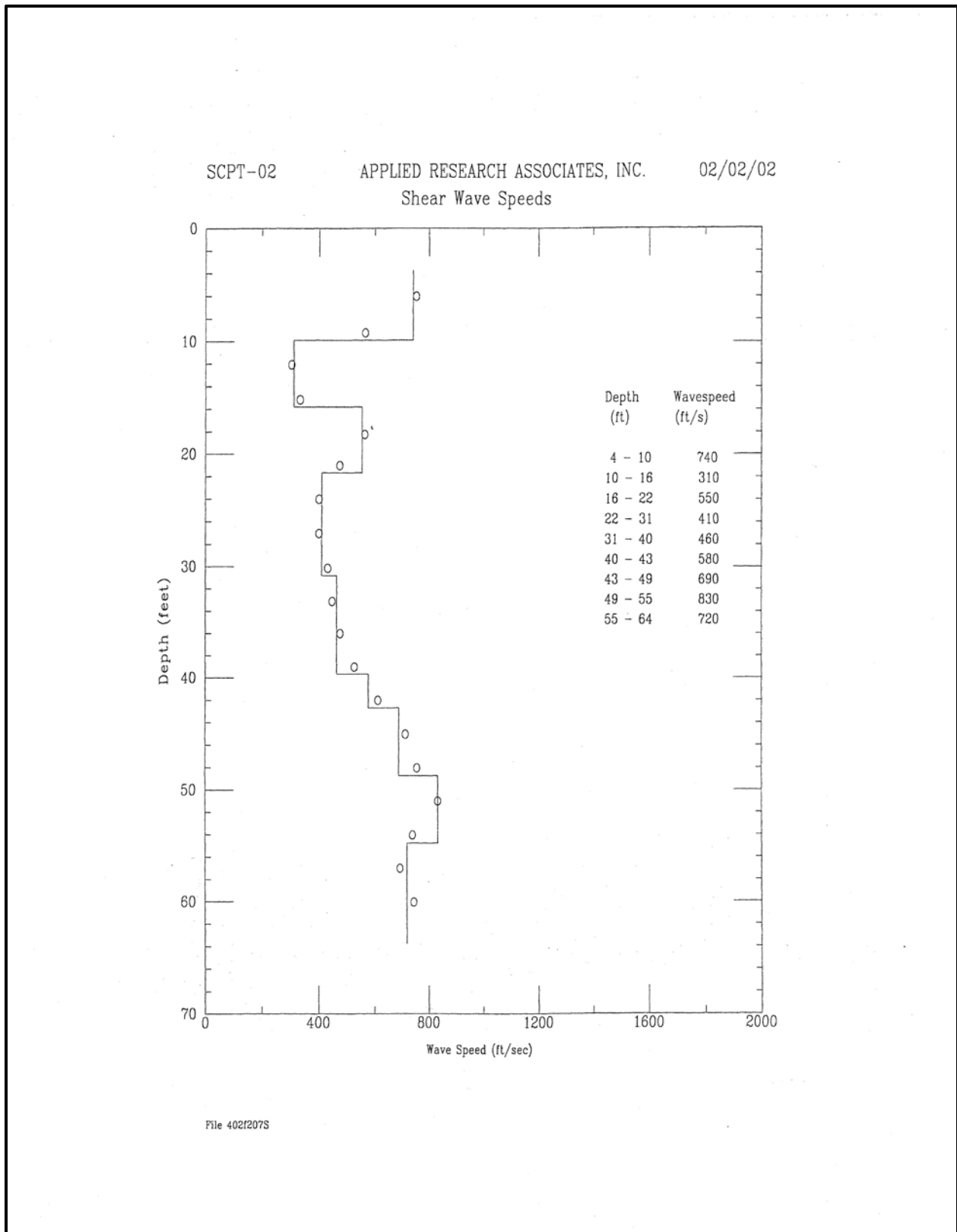


Figure H-139, SCPT-02



**Figure H-140,  $V_s$  Profile – SCPT-02**

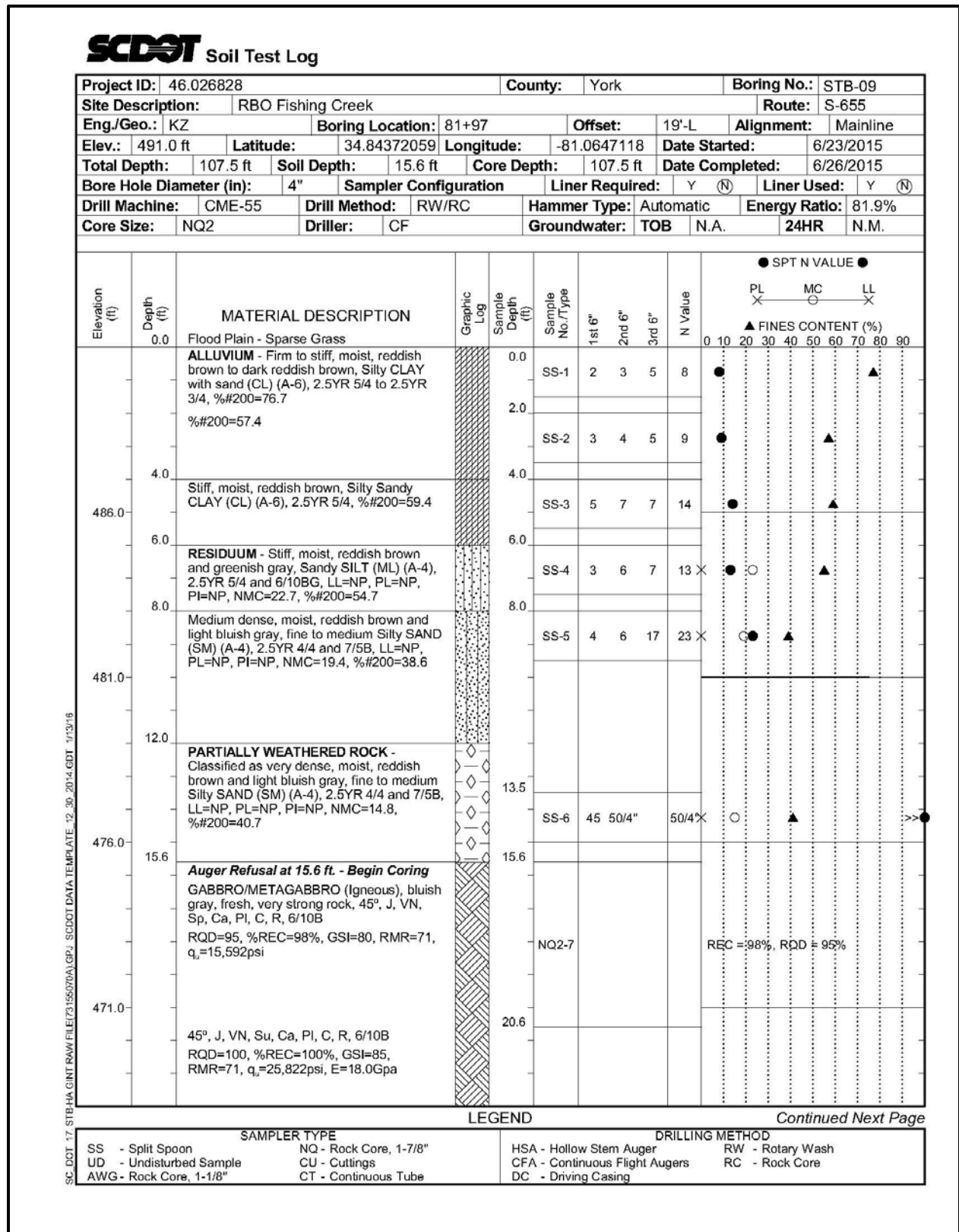


Figure H-141, Soil Test Boring STB-09

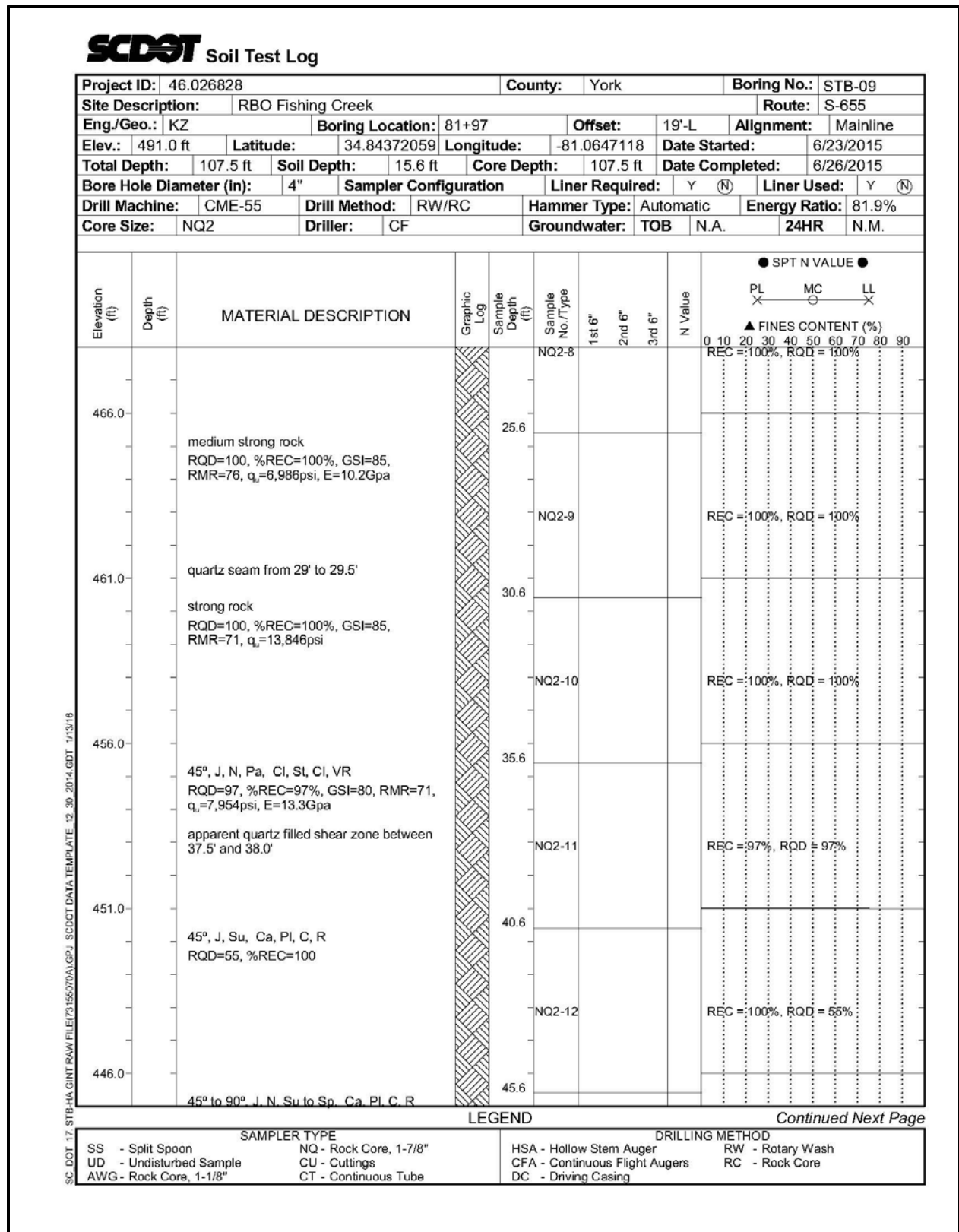


Figure H-142, Soil Test Boring STB-09 (con't)



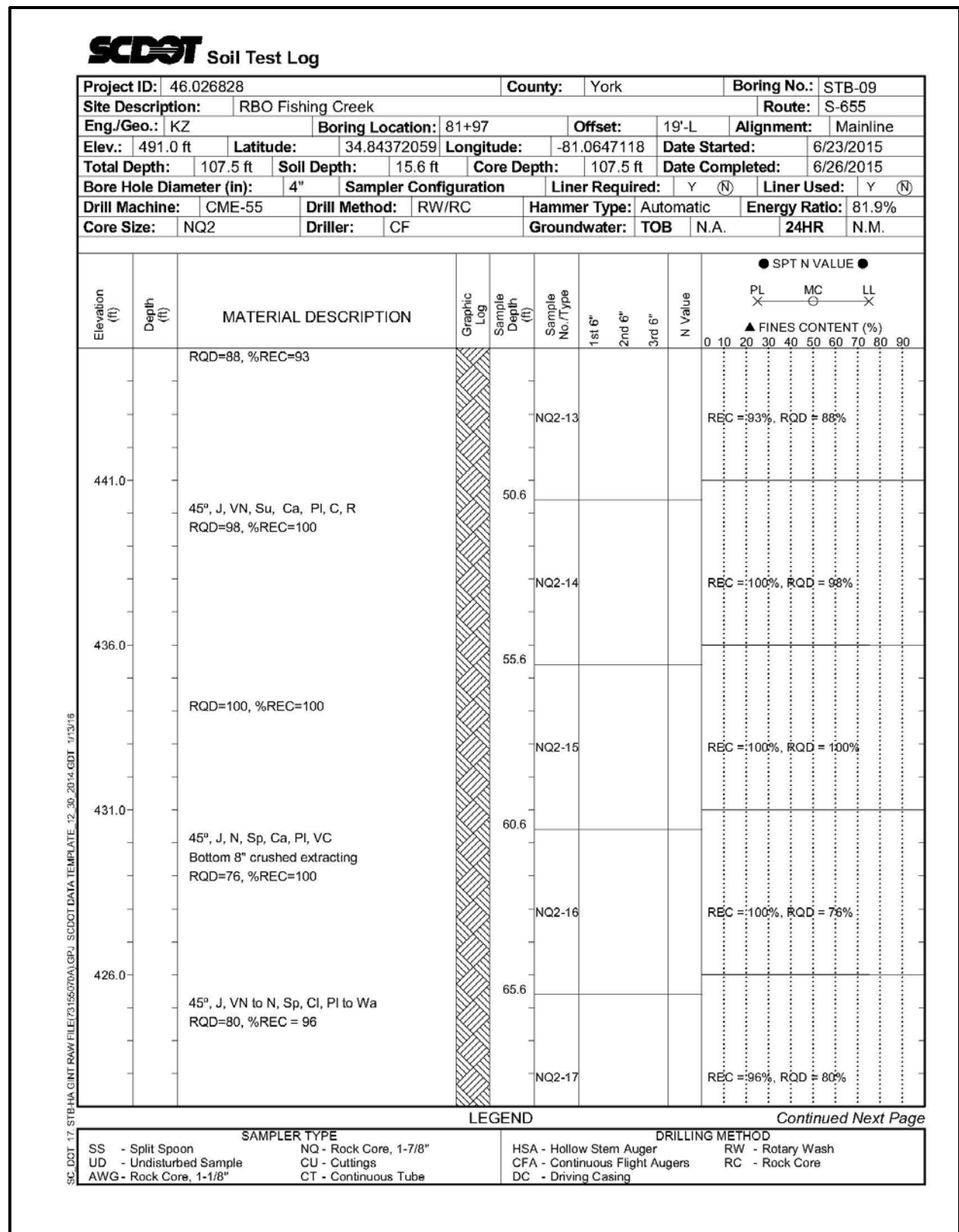


Figure H-143, Soil Test Boring STB-09 (con't)

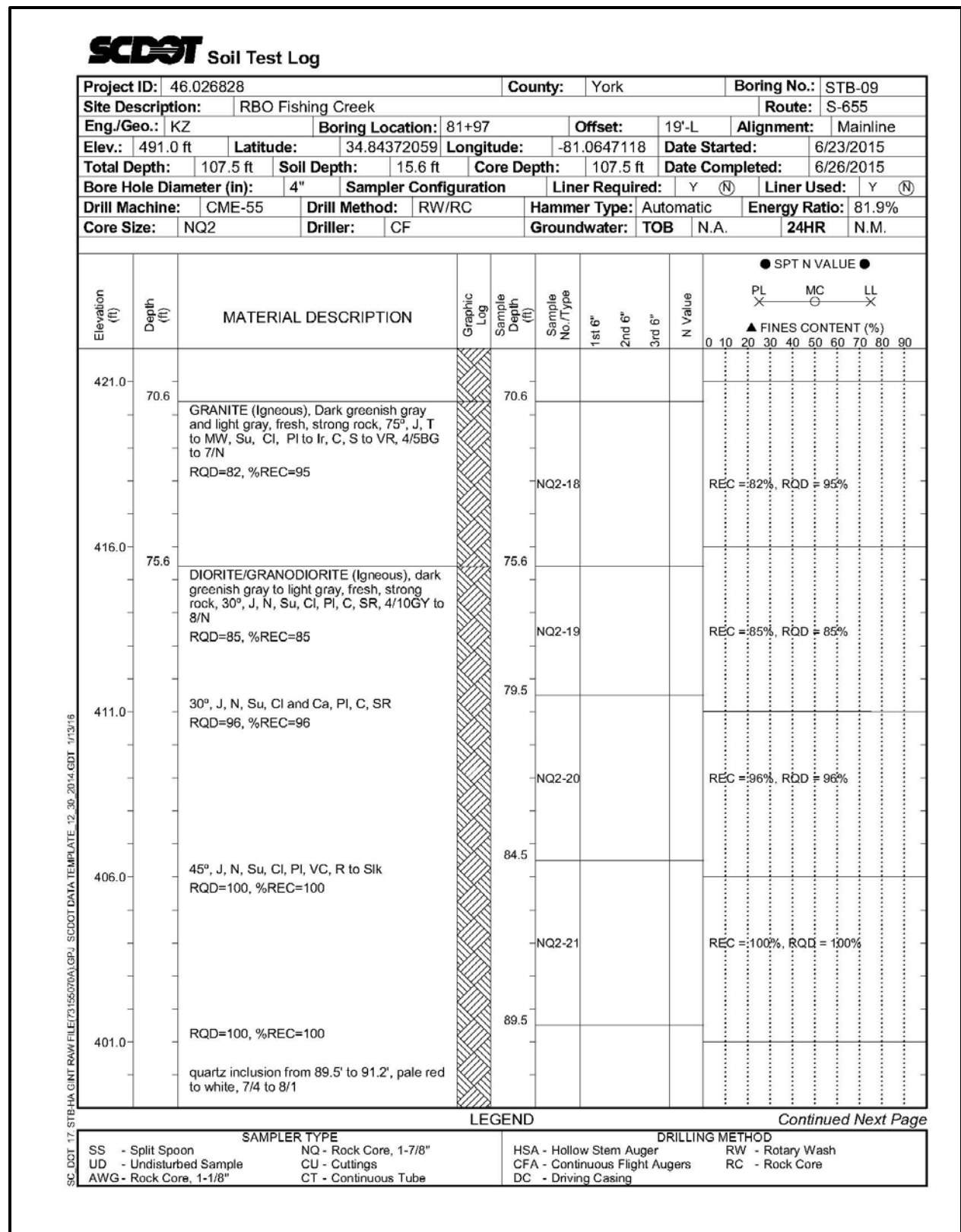


Figure H-144, Soil Test Boring STB-09 (con't)

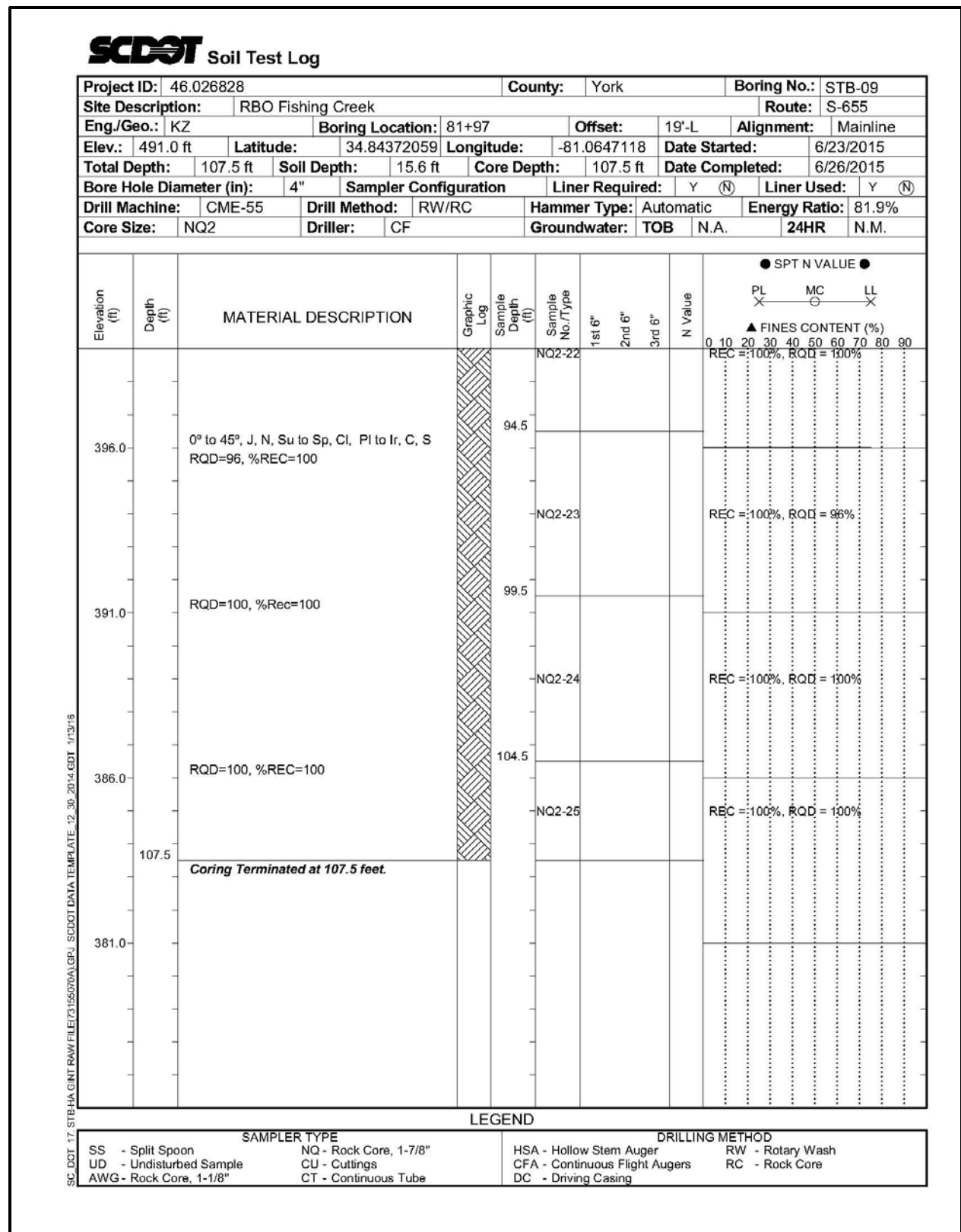
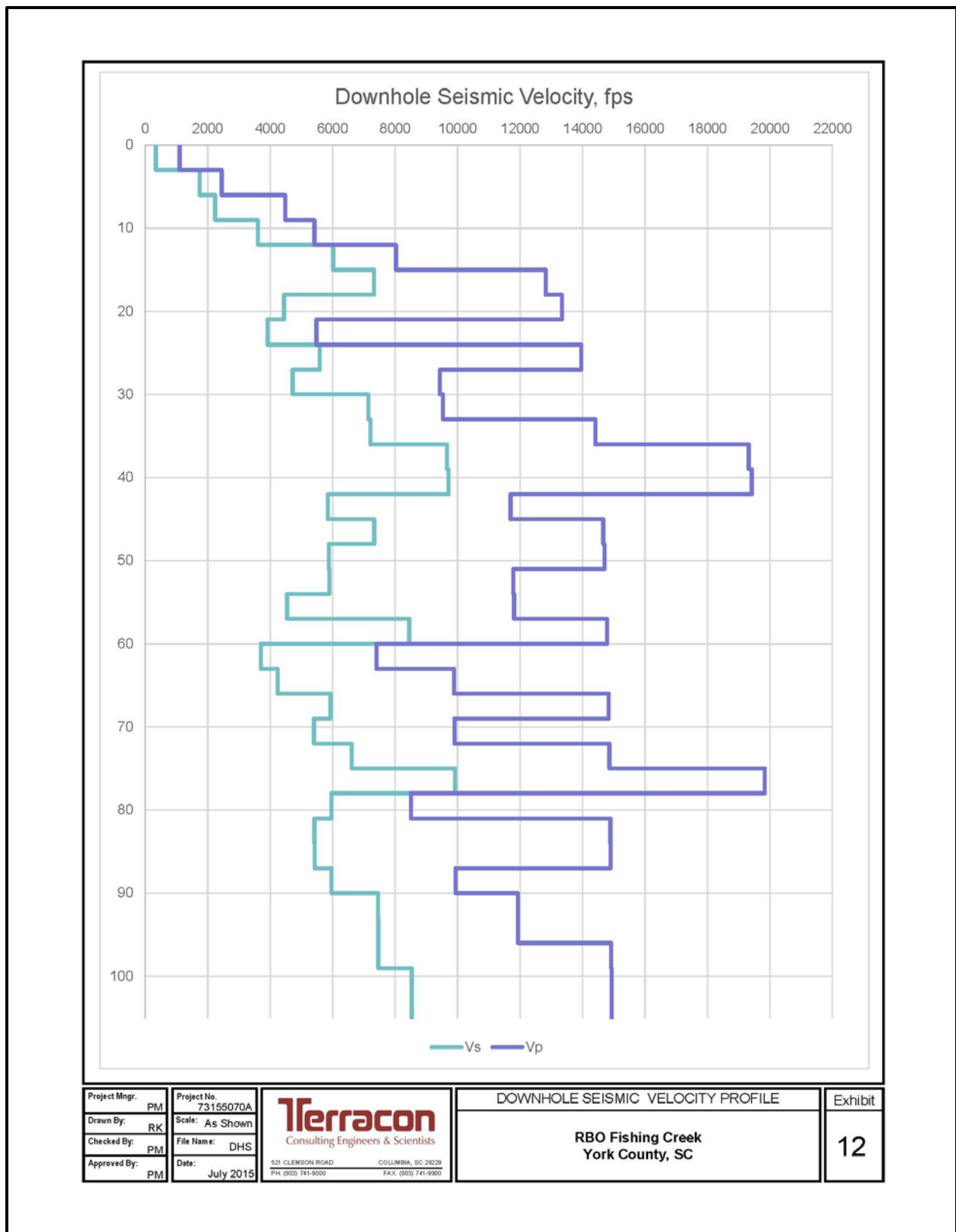


Figure H-145, Soil Test Boring STB-09 (con't)



Project Mngr: PM	Project No. 73155070A	 521 CLEMSON ROAD COLUMBIA, SC 29229 PH: (803) 741-9000 FAX: (803) 741-9900	DOWNHOLE SEISMIC VELOCITY PROFILE	Exhibit
Drawn By: RK	Scale: As Shown		RBO Fishing Creek York County, SC	12
Checked By: PM	File Name: DHS			
Approved By: PM	Date: July 2015			

Figure H-146,  $V_s$  and  $V_p$  Profile – STB-09

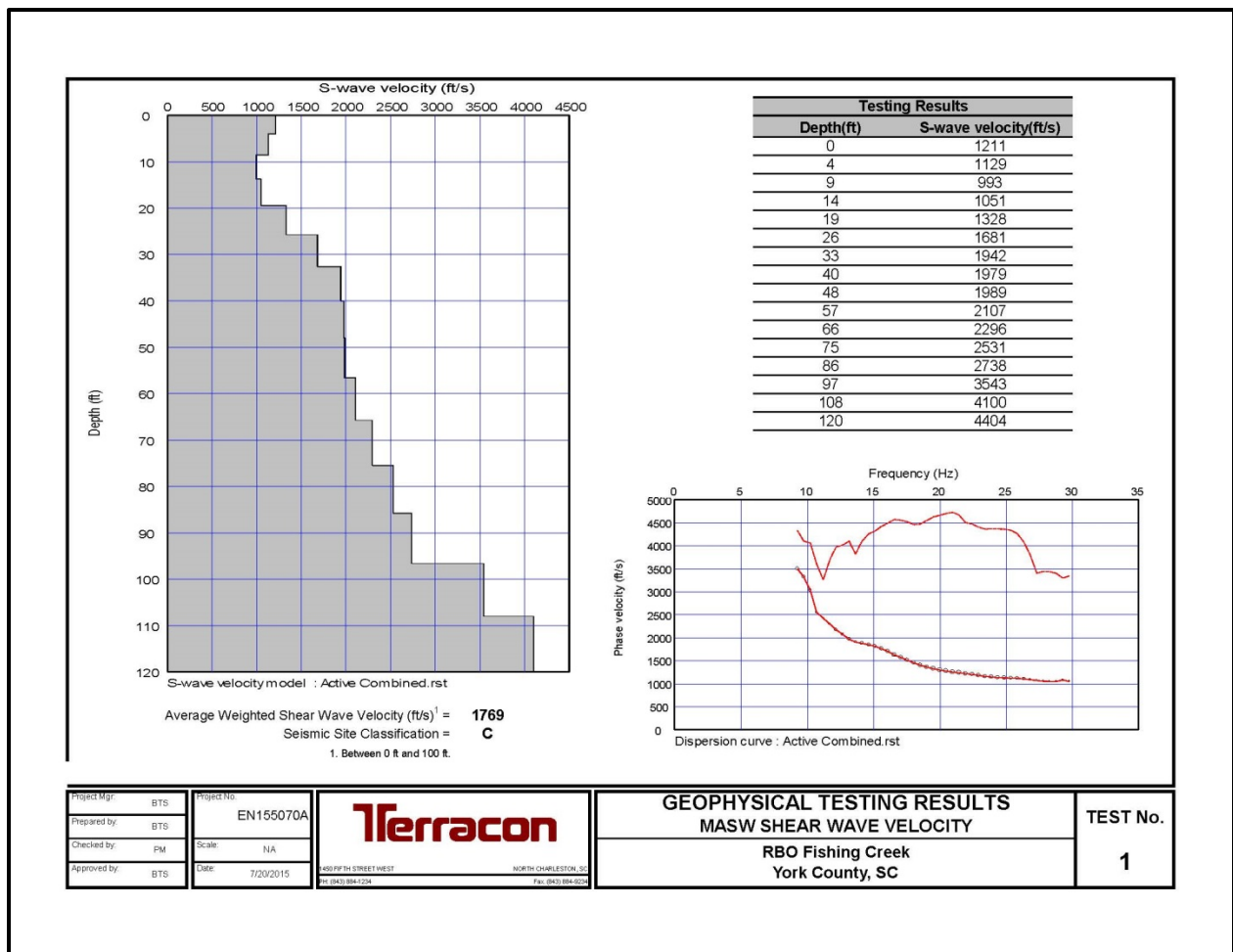


Figure H-147,  $V_s$  Profile – STB-09

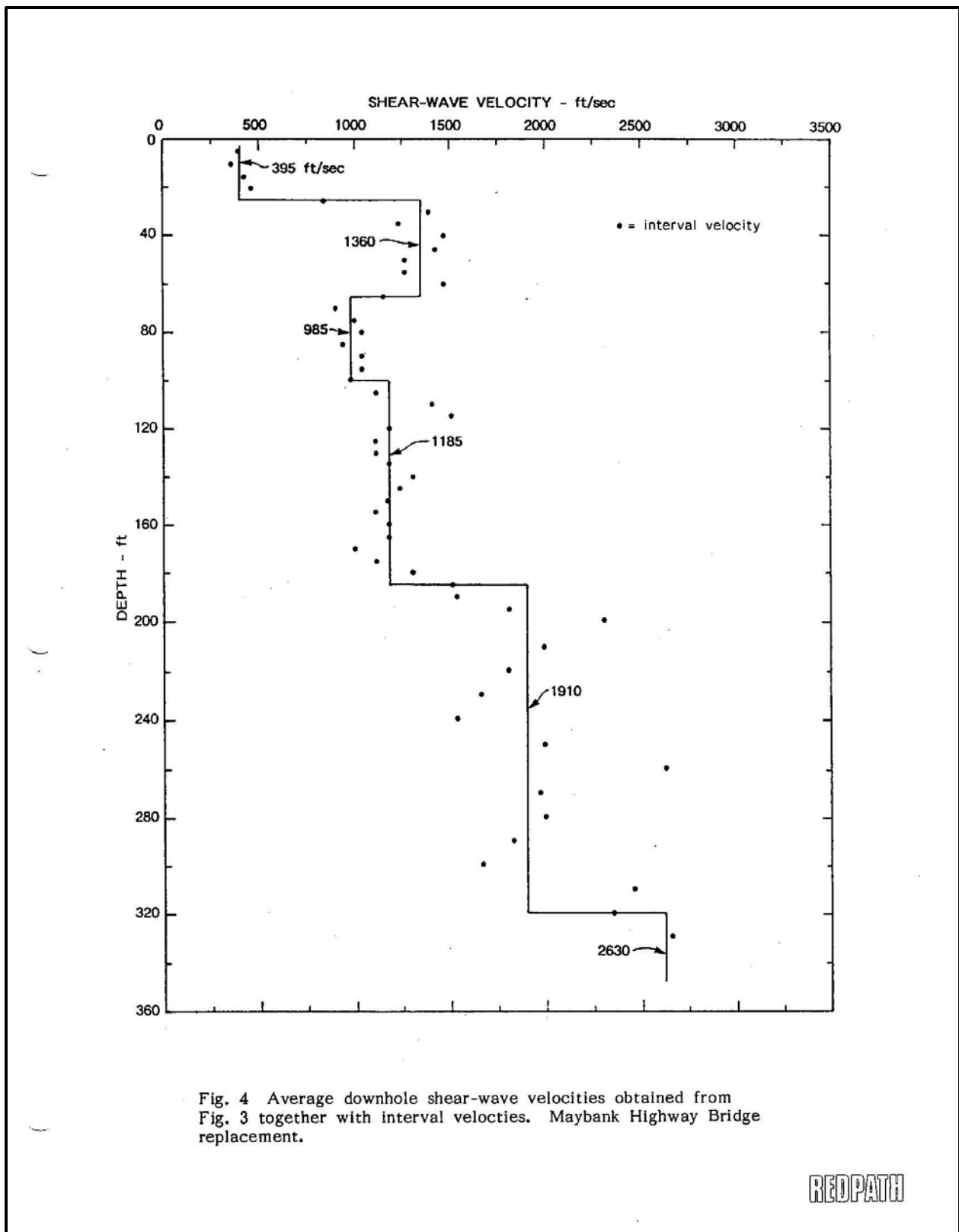


Fig. 4 Average downhole shear-wave velocities obtained from Fig. 3 together with interval velocities. Maybank Highway Bridge replacement.

REDPATH

Figure H-148,  $V_s$  Profile – Maybank

**TABLE I**  
Maybank River Bridge Replacement  
Downhole Velocities Measured in Borehole PS-1

<u>Depth Interval</u>	<u>Shear-Wave Velocity</u>	<u>Compression-Wave Velocity</u>
0 - 25 ft	395 ft/sec	4715 ft/sec
25 - 65	1360	6630
65 - 100	985	5340
100 - 185	1185	5340
185 - 320	1910	6110
320 - 350	2630	7465

REDPATH

Figure H-149, Tabulated  $V_s$  Results – Maybank

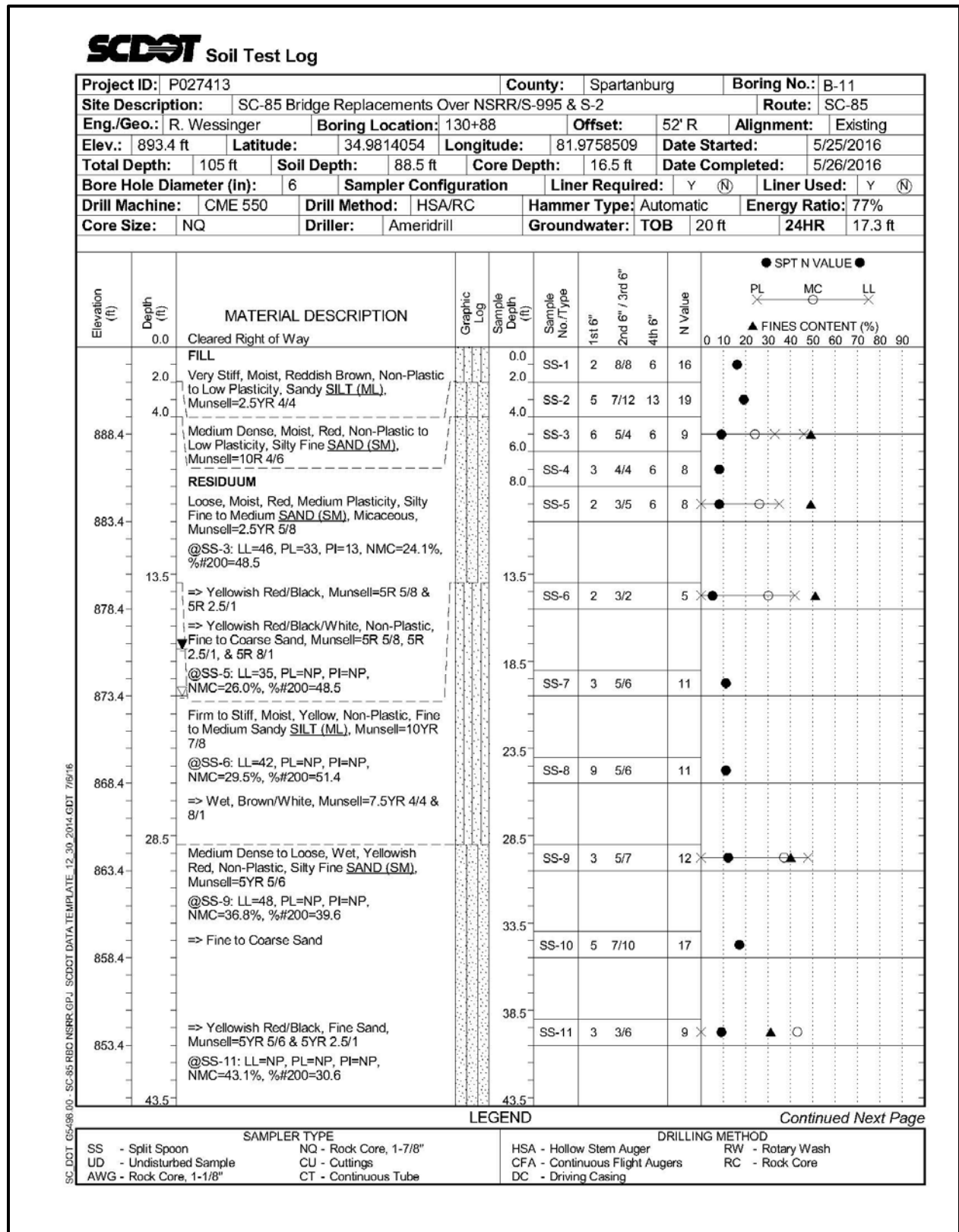


Figure H-150, Soil Test Boring SC-85 – B-11



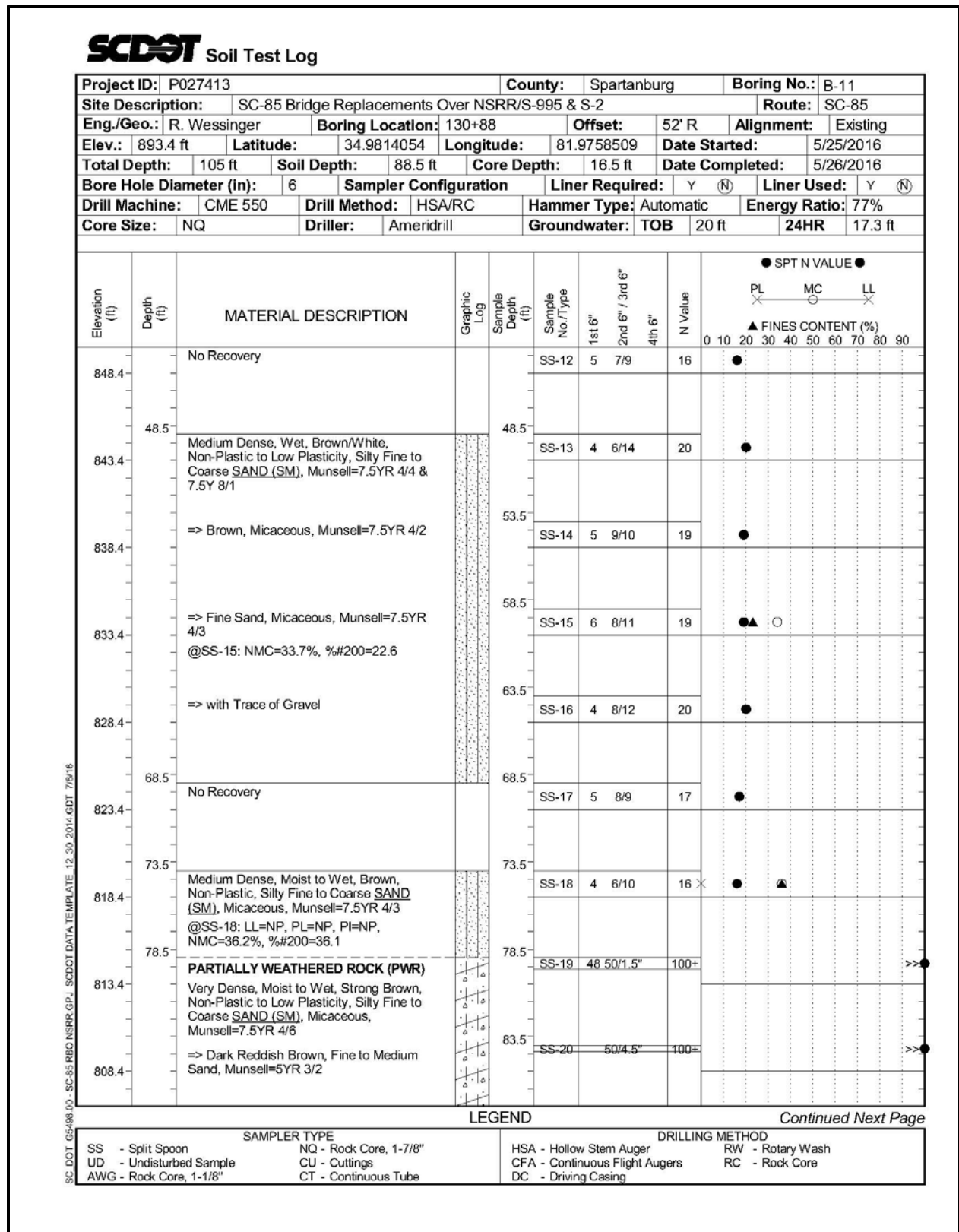


Figure H-151, Soil Test Boring SC-85 – B-11 (con't)

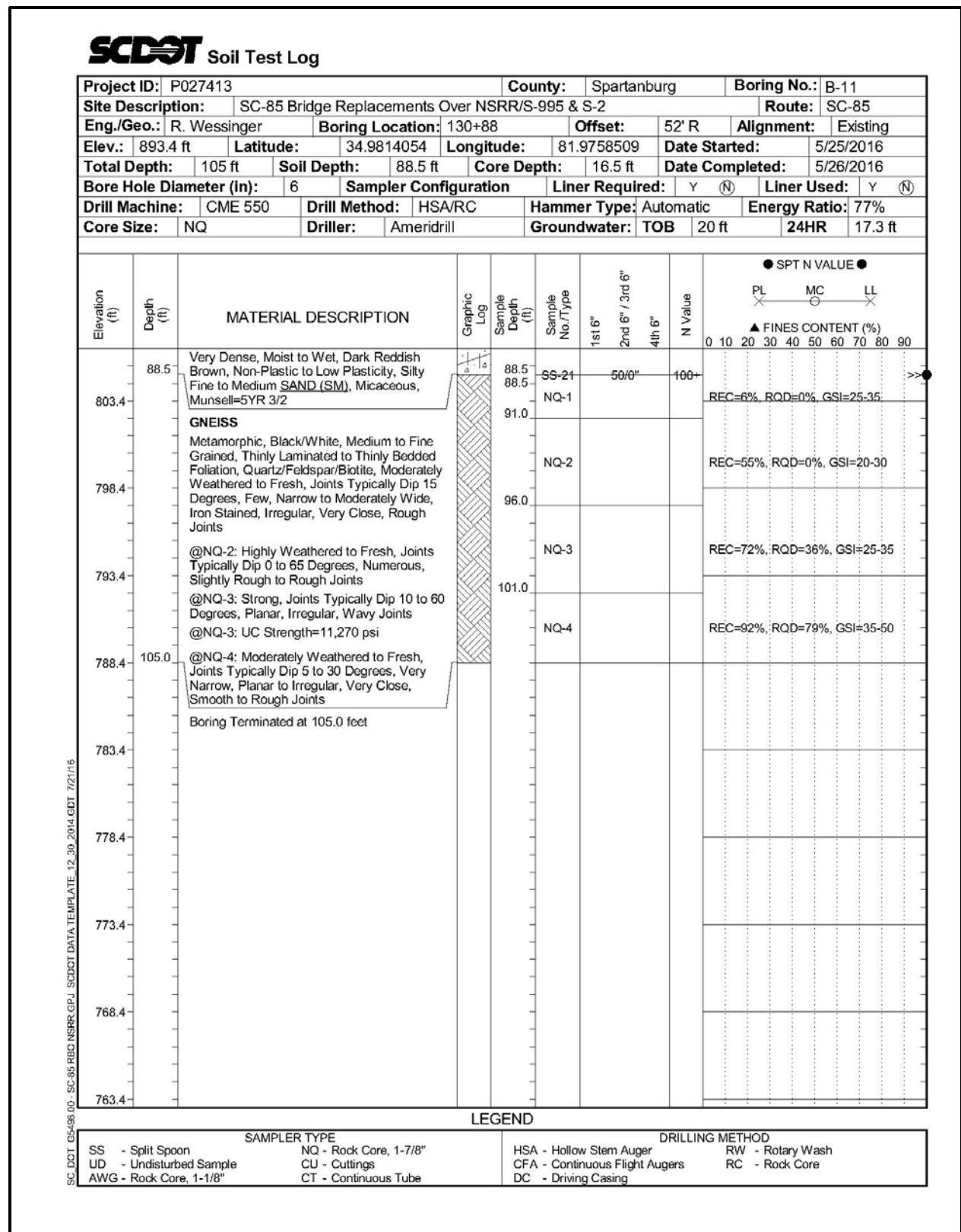


Figure H-152, Soil Test Boring SC-85 – B-11 (con't)

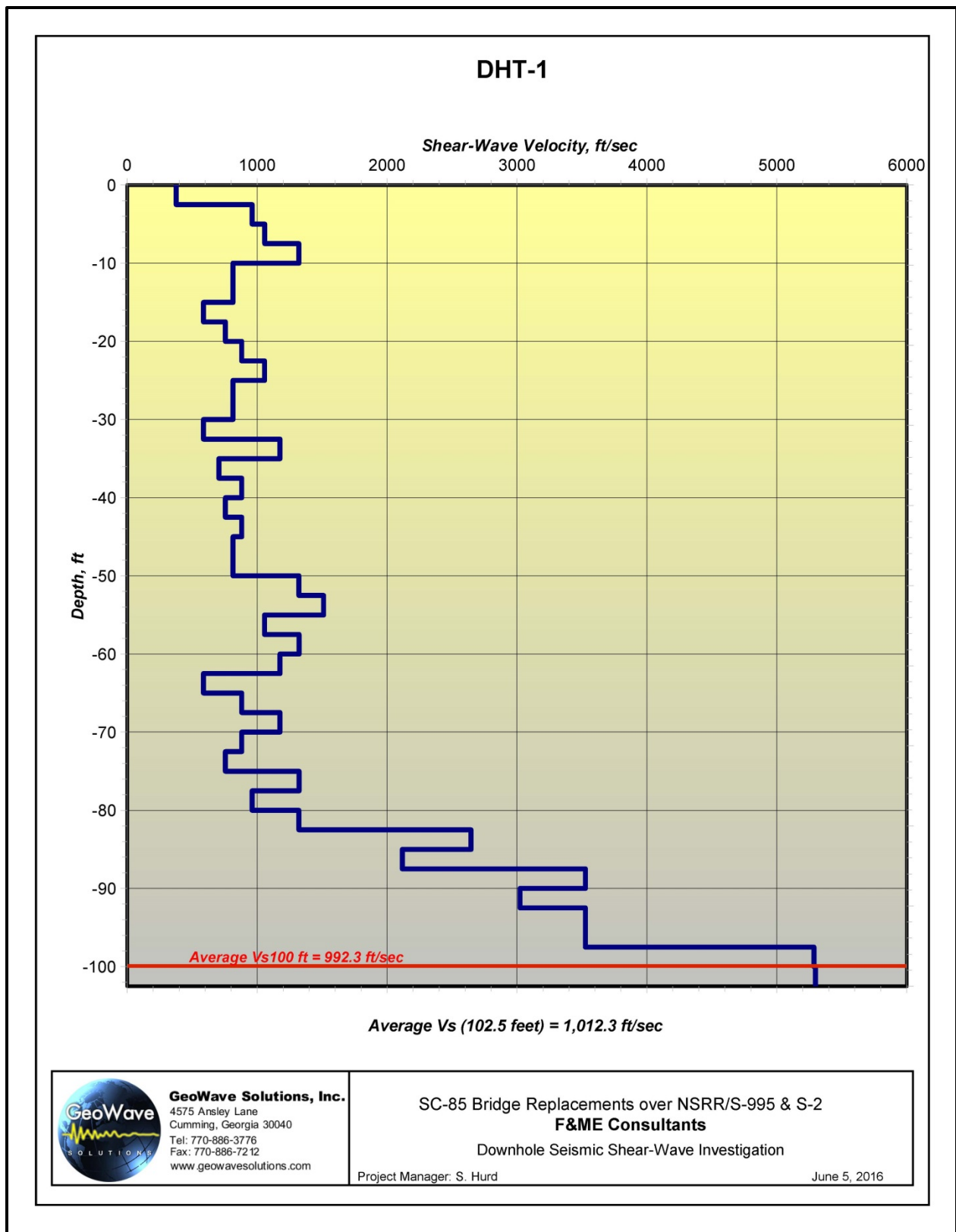



Figure H-153,  $V_s$  Profile – SC-85 – DHT-1

**DHT-1**

Depth (ft)	Vs ( ft/sec)
-2.5	377.9
-5.0	961.5
-7.5	1058.4
-10.0	1322.1
-12.5	813.8
-15.0	814.1
-17.5	587.7
-20.0	755.7
-22.5	881.8
-25.0	1058.0
-27.5	813.8
-30.0	813.8
-32.5	587.8
-35.0	1175.4
-37.5	705.4
-40.0	881.5
-42.5	755.7
-45.0	881.5
-47.5	814.1
-50.0	813.8
-52.5	1322.1
-55.0	1511.5
-57.5	1058.0
-60.0	1322.8
-62.5	1175.4
-65.0	587.8
-67.5	881.5
-70.0	1175.9
-72.5	881.5
-75.0	755.7
-77.5	1322.7
-80.0	961.9
-82.5	1322.1
-85.0	2645.5
-87.5	2116.9
-90.0	3526.1
-92.5	3023.0
-95.0	3526.1
-97.5	3526.1
-100.0	5285.4
-102.5	5296.7

 <p><b>GeoWave Solutions, Inc.</b>                  4575 Ansley Lane                  Cumming, Georgia 30040                  Tel: 770-886-3776                  Fax: 770-886-7212                  www.geowavesolutions.com</p>	<p>SC-85 Bridge Replacements over NSRR/S-995 &amp; S-2  <b>F&amp;ME Consultants</b>                  Downhole Seismic Shear-Wave Investigation                  Project Manager: S. Hurd                  June 5, 2016</p>
---	--

**Figure H-154, Tabulated Vs Results – SC-85 – DHT-1**

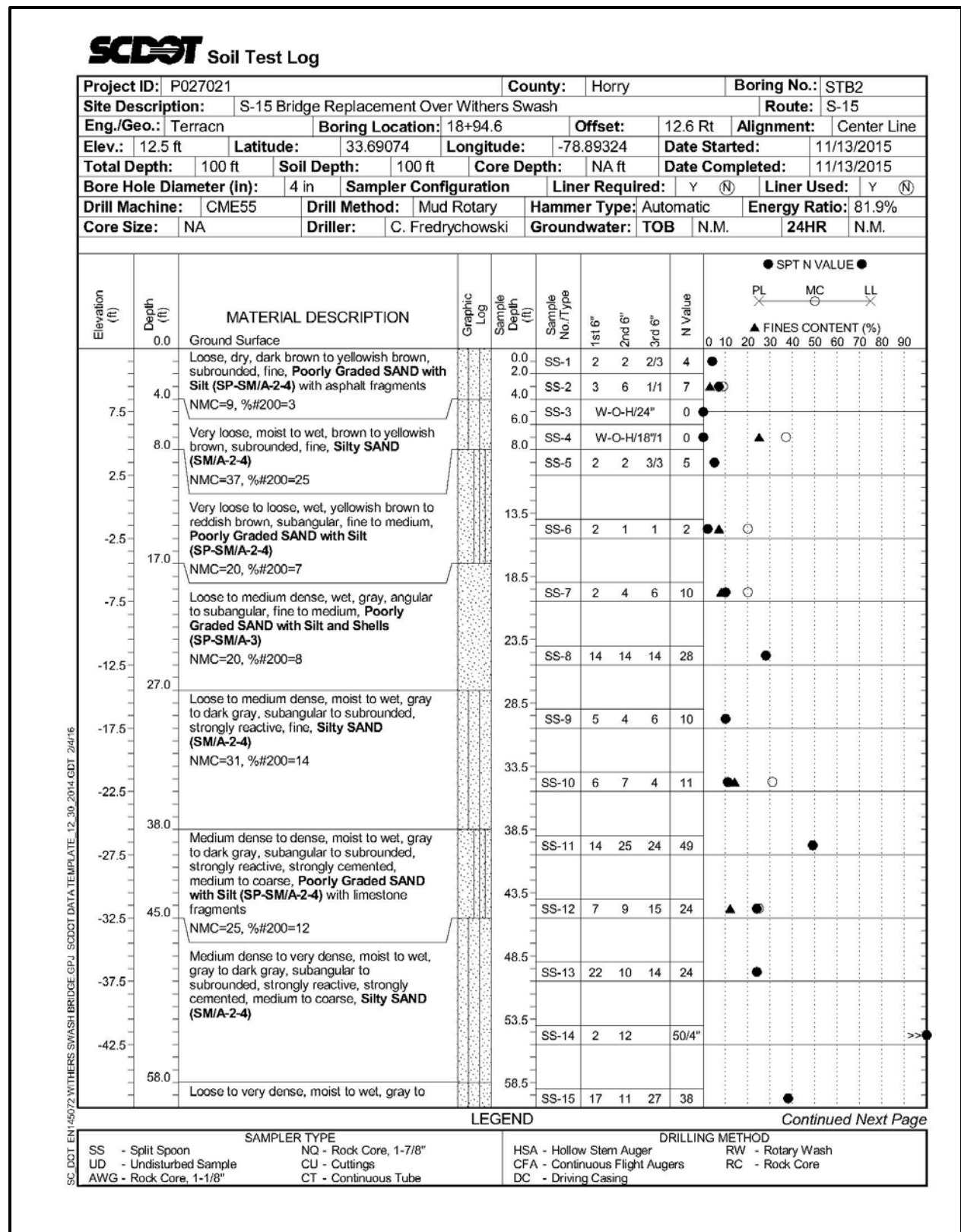


Figure H-155, Soil Test Boring Withers Swash – STB2

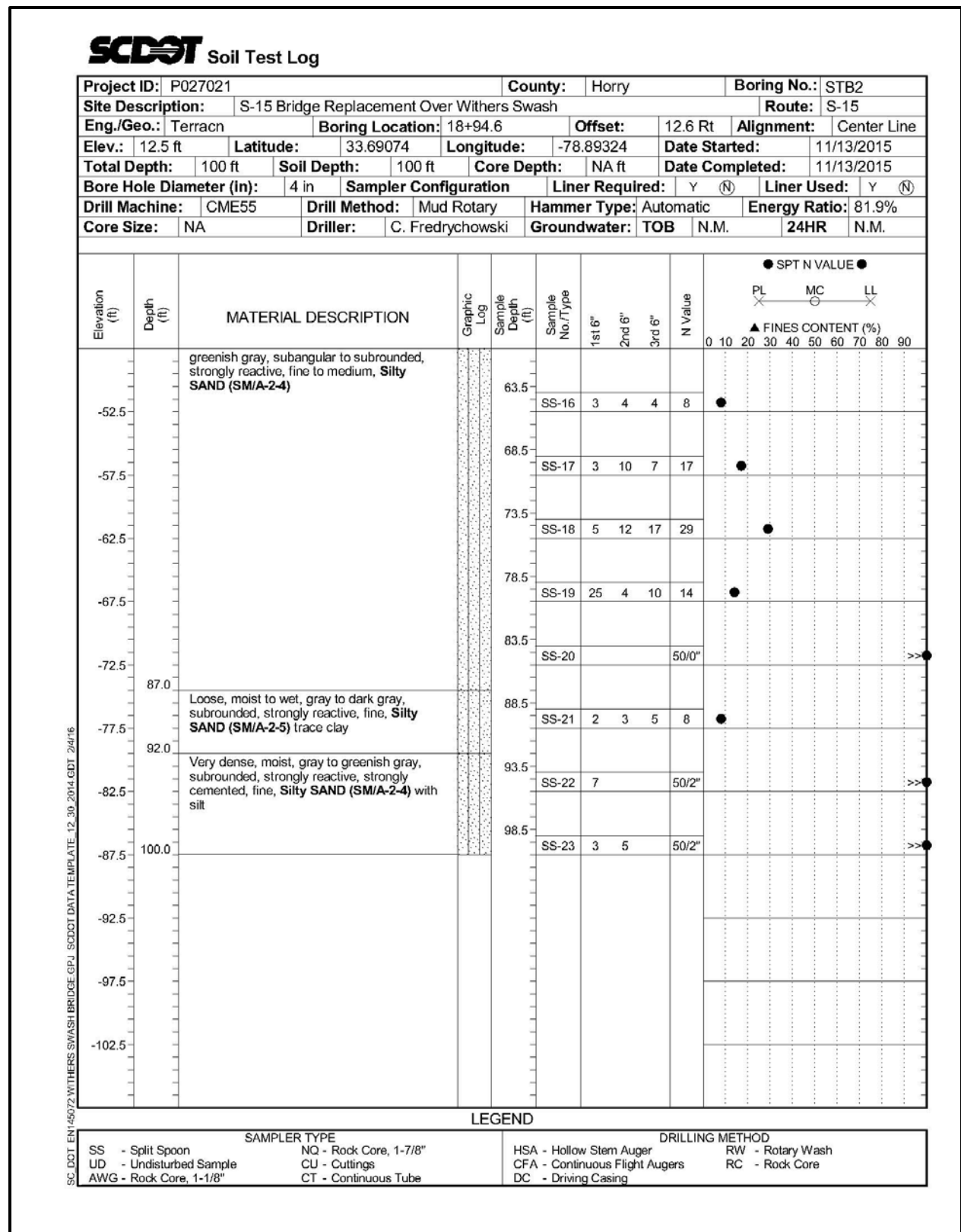


Figure H-156, Soil Test Boring Withers Swash – STB2 (con't)

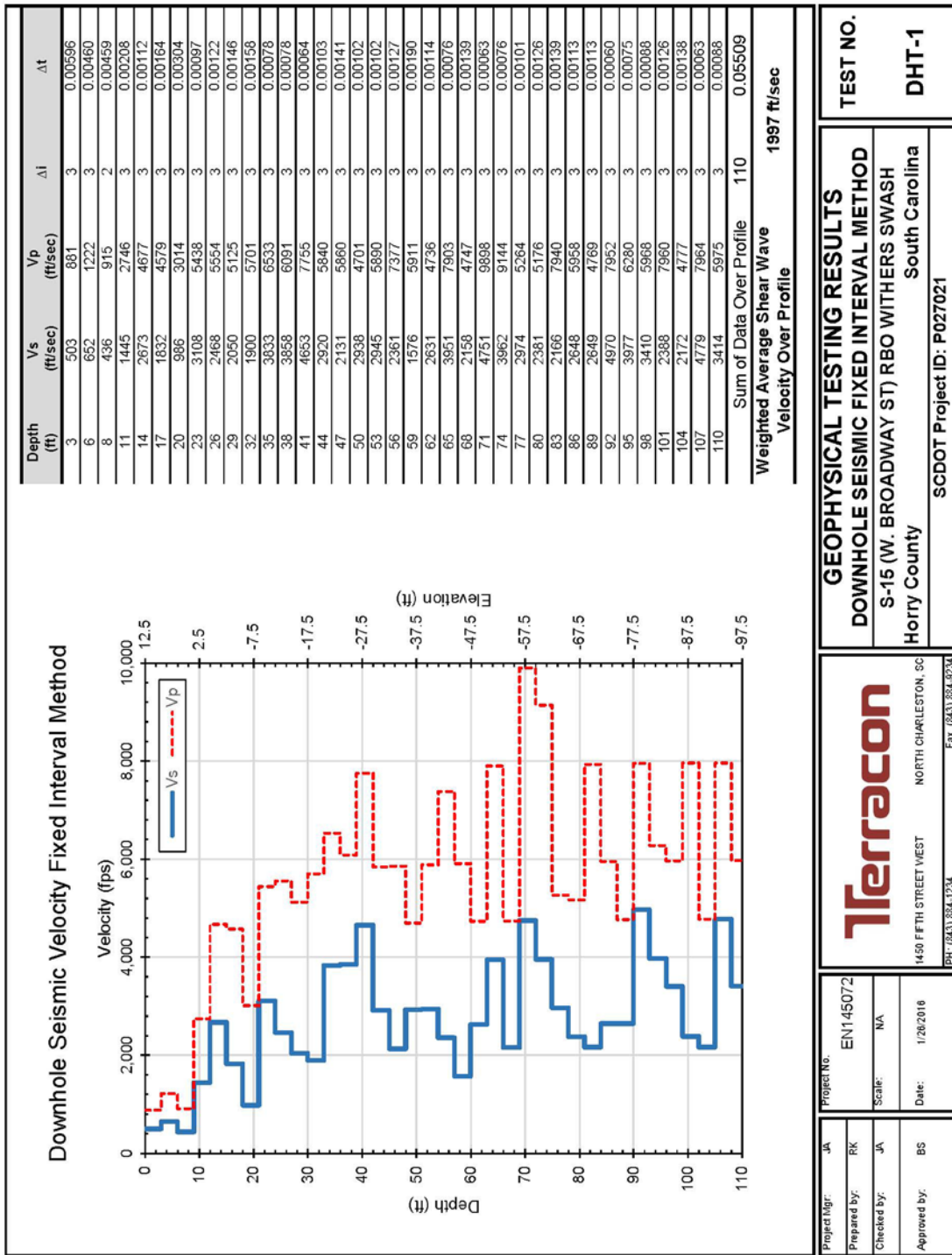


Figure H-157, Vs Profile and Tabulated Results – Withers Swash – DHT-1

Project Mgr: JA	Project No. EN145072	<b>Terracon</b> 1450 FIFTH STREET WEST NORTH CHARLESTON, SC PH: (843) 834-1234 Fax: (843) 834-9234	TEST NO. <b>DHT-1</b>
Prepared by: RK	Scale: NA		
Checked by: JA	Date: 1/26/2016	GEOPHYSICAL TESTING RESULTS DOWNHOLE SEISMIC FIXED INTERVAL METHOD S-15 (W. BROADWAY ST) RBO WITHERS SWASH Horry County South Carolina SCDOT Project ID: P027021	
Approved by: BS			

## H.2 REFERENCES

Florence & Hutcheson (2008), "Site-Specific Seismic Response Study US 378 Bridge Replacements over the Great Pee Dee River and the CSX Railroad, Florence and Marion Counties, South Carolina", SCDOT File No. 21.182B.1 (PIN 30597), Columbia, SC.

Lewis, M. R., McHood, M. D., and Arango, I., (2004), "Liquefaction Evaluation at the Savannah River Site – A Case History", Proceedings: *Fifth International Conference on Case Histories in Geotechnical Engineering*, New York, NY, April 13-17, 2004, Paper No. 3.21.

Mayne, P. W., Brown, D., Vinson, J., Schneider, J. A., and Finke, K. A., (2000), "Site characterization of Piedmont residual soils at the NGES, Opelika, Alabama", *National Geotechnical Experimentation Sites*, (GSP No. 93), American Society of Civil Engineers, Reston/VA, 160-185.

Odum, J. K., Williams, R. A., Stepheson, W. J., and Worley, D. M., (2003), "Near-surface S-wave and P-wave seismic velocities of primary geological formations on the Piedmont and Atlantic Coastal Plain of South Carolina, USA", United States Geological Survey Open-File Report 03-043, 14p.

S&ME (2000), "Phase II Geotechnical Data Summary Report – Cooper River Bridge Replacement Project, Charleston, South Carolina", S&ME Job No. 1131-97-741, Mount Pleasant, SC.

S&ME (2007), "Site Specific Seismic Study – Wetland Bridges 1, 2, 3, & 4", Charleston, South Carolina, U.S. Route 17 – Design Build, Beaufort County, South Carolina", SCDOT File No. 7.412B, S&ME Job No. 1131-07-065, Mount Pleasant, SC.

URS Corporation (2001), "Comprehensive Seismic Risk and Vulnerability Study for the State of South Carolina", South Carolina Emergency Management Division (SCEMD).



**APPENDIX I**

**SHEAR STRENGTH RATIO  
TRIGGERING METHODS**

**SCDOT GEOTECHNICAL DESIGN MANUAL**

*January 2019*



## Table of Contents

<u>Section</u>	<u>Page</u>
I.1 Introduction.....	I-1
I.2 Olson and Stark Method.....	I-1
I.2.1 Screening of Sand-Like Soils For Contractive Behavior.....	I-1
I.2.2 Evaluate Soil SSL SSR Triggering Model .....	I-2
I.3 References.....	I-4

**List of Figures**

<b><u>Figure</u></b>	<b><u>Page</u></b>
Figure I-1, Contractive Soil Behavior Evaluation .....	I-2

# APPENDIX I

## SHEAR STRENGTH RATIO TRIGGERING METHOD

### I.1 INTRODUCTION

The Shear Strength Ratio (SSR) triggering method computes the ratio of shear stress demand on the soil layer susceptible to soil SSL, to the soil's yield strength. This method, developed by Olson and Stark (2003), uses the yield shear strength ratio and soil SSL ratio to evaluate the triggering of soil SSL. This method shall be used when the maximum initial static shear stress ratio ( $\alpha$ ) is greater than 0.35 ( $\alpha > 0.35$ ). Where  $\alpha$  is determined as indicated in Chapter 13.

### I.2 OLSON AND STARK METHOD

The SSR method proposed by Olson and Stark (2003) has been adapted to evaluate cyclic liquefaction triggering for Sand-Like soils and cyclic softening of Clay-Like soils with a static shear stress in excess of 0.35. This soil SSL triggering method consists of the following 2 parts:

1. Screen Sand-Like soils for Contractive behavior based on Contractive/Dilative correlations with in-situ testing (SPT and CPT) for Sand-Like soils (Section I.2.1).
2. Evaluate soil SSL triggering of Sand-Like and Clay-Like soils by dividing the static (Section 13.9.6.1), seismic, and other shear stresses that the soil is exposed to (Demand, D) by the undrained shear strength of the soil (Capacity, C) to obtain the SSL ratio  $(D/C)_{SL}$  and determine if the soil SSL triggering potential exists. The overall procedure is presented in Section I.2.2.

#### I.2.1 Screening of Sand-Like Soils For Contractive Behavior

In addition to the soil SSL susceptibility screening criteria indicated in Chapter 13, this method requires the screening of Sand-Like soils for contractive behavior. Sand-Like soils must have contractive behavior in order to be subject to slope instability that could lead to flow failure. The screening for contractive behavior is accomplished by plotting either SPT ( $N_{1,60}^*$ ) or CPT ( $q_{c,1}$ ) values on the horizontal axis as a function of the pre-failure vertical effective stress ( $\sigma'_{vo}$ ) as indicated in Figure I-1. After the in-situ testing values have been plotted, the Fear and Robertson (1995) soil boundary behavior relationship is plotted on the graph as indicated to determine which Sand-Like soil layers meet the contractive soil requirement of the SSR method. The Fear and Robertson (1995) soil boundary for contractive/dilative behavior relationship equations are provided below for CPT and SPT in-situ testing.

$$(\sigma'_{vo})_{SPT-Boundary} = 9.58 * 10^{-4} * (N_{1,60}^*)^{4.79} \quad \text{Equation I-1}$$

$$(\sigma'_{vo})_{CPT-Boundary} = 1.10 * 10^{-2} (q_{c,1})^{4.79} \quad \text{Equation I-2}$$

Where,

- $\sigma'_{vo}$  = Effective overburden stress (or  $\sigma'_v$ ), units of kPa.  
 $N_{1,60}^*$  = Normalized SPT-N values (Blows/foot) See Chapter 7 for SPT corrections.  
 $q_{c,1}$  = CPT corrected tip resistance, units of MPA. See Chapter 7 for CPT corrections.

SPT or CPT values of Sand-Like soils that plot on the *Contractive* side of the boundary (left of boundary) are confirmed to be susceptible to flow failure as indicated by the liquefaction case histories evaluated by Olson and Stark (2003) plotted in Figure I-1.

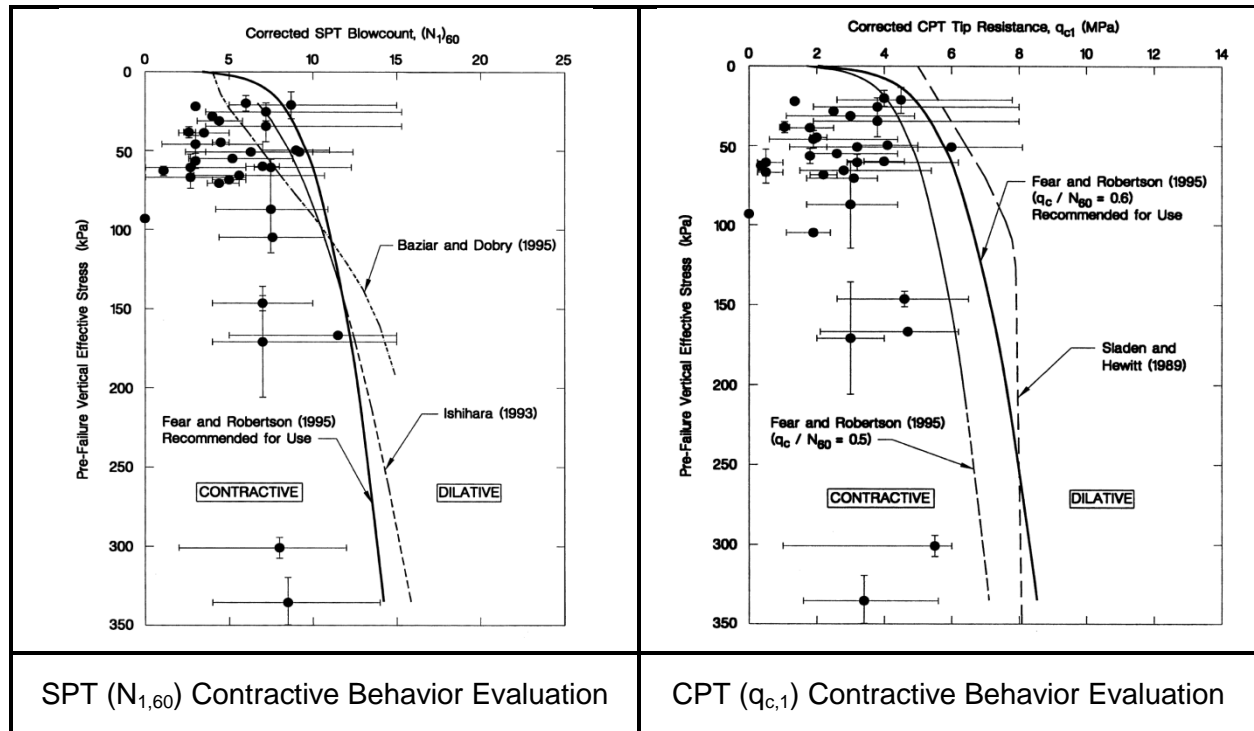


Figure I-1, Contractive Soil Behavior Evaluation (Olson and Stark, 2003 with permission from ASCE)

### I.2.2 Evaluate Soil SSL SSR Triggering Model

Soil SSL triggering of Sand-Like and Clay-Like soils is determined by dividing the static, seismic, and other shear stresses that the soil is subjected to (Demand, D) by the undrained shear strength of the soil (Capacity, C) to obtain the strength loss ratio (D/C)<sub>SL</sub>. The LRFD equation that is used to evaluate the onset of strength loss (SL) at steeply sloped ground site conditions is provided below:

$$\left(\frac{D}{C}\right)_{SL} \leq \phi_{SL} \tag{Equation I-3}$$

The Demand (D) is computed by adding the static driving shear stress ( $\tau_{Static}$ ), average seismic shear stress ( $\tau_{Seismic}$ ), and other shear stresses ( $\tau_{Other}$ ) as indicated by the following equation.

$$D = \gamma * (\tau_{Static} + \tau_{Seismic} + \tau_{Other}) \tag{Equation I-4}$$

The Capacity (C) of the soil is the undrained peak shear strength ( $\tau_{Peak}$ ) as determined for either Sand-Like soils (Cohesionless) or Clay-Like soils (Cohesive) as determined from Chapter 7. The peak undrained shear strength for cohesionless soils should be estimated based on the yield shear strength ( $\tau_{Yield} = S_u(\text{yield})$ ) and the peak undrained shear strength ( $\tau = \tau_{Yield}$ ) for cohesive soils should be estimated from either laboratory testing or in-situ testing.

The triggering of soil SSL occurs when the strength loss ratio (D/C)<sub>SL</sub> is greater than the strength loss resistance factor ( $\phi_{SL}$ ) provided in Chapter 9.

$$\left(\frac{D}{C}\right)_{SL} = \frac{(\tau_{Static} + \tau_{Seismic} + \tau_{Other})}{\tau_{Peak}} > \phi_{SL} \quad \text{Equation I-5}$$

Since the SSR method for evaluating soil SSL triggering at a project site is a deterministic procedure, a load factor,  $\gamma$ , of unity (1.0) is used and the resistance factor,  $\phi_{SL}$ , accounts for the site variability and the level of acceptable risk of soil SSL. As research advances and soil SSL analytical models are calibrated for LRFD design methodology, adjustments will be made in the implementation of the LRFD design methodology.

The process to evaluate triggering of soil SSL is as follows:

1. The triggering of soil SSL begins by conducting a slope stability of the pre-failure geometry. The slope stability search should evaluate both circular and sliding wedge potential failure surfaces in accordance with Chapter 17. Spencer's Slope Stability method is required.
2. The critical failure surface is then divided into  $n$  slices (typically 10 to 15 slices) of length,  $L_i$ .
3. Compute the static shear stress ( $\tau_{Static}$ ) for each slope stability slice (length,  $L_i$ ) susceptible to soil SSL at the onset of flow failure, in accordance with Section 13.9.6.1.
4. Compute the average, magnitude weighted, seismic induced stress ( $\tau_{Seismic}$ ) for each slice (length,  $L_i$ ) susceptible to soil SSL in accordance with the following equation.

$$\tau_{Seismic} = \frac{0.65 * \tau_{max}}{MSF} \quad \text{Equation I-6}$$

Where,

- $\tau_{max}$  = Maximum earthquake induced shear stress.  $\tau_{max}$  is computed using the methodologies discussed in Chapter 13.
- MSF = Magnitude Scaling Factor computed in accordance with Chapter 13.

5. Compute any other shear stresses ( $\tau_{Other}$ ) that may be applicable such as those induced by surcharges, foundation loadings, etc.
6. Determine the value of the peak undrained shear strength ratio ( $\tau_{Peak}/\sigma'_{vo} = \tau_{Yield}/\sigma'_{vo}$ ) for Sand-Like soils (cohesionless soils) or the undrained shear strength ratio ( $\tau_{Peak}/\sigma'_{vo} = S_u/\sigma'_{vo}$ ) for Clay-Like soils (cohesive soils) in accordance with Chapter 7. Compute the undrained shear strength for Sand-Like soils ( $\tau = \tau_{Yield} = S_u(\text{yield})$ ) or Clay-Like soils ( $\tau = S_u$ ) for each slice of the critical failure surface by multiplying the peak undrained shear strength ratio ( $\tau/\sigma'_{vo}$ ) by the effective overburden stress ( $\sigma'_{vi}$ ) for each slice.
7. Compute the soil SSL resistance ratio  $(D/C)_{SL}$  as indicated by the following equation for each slice.

$$\left(\frac{D}{C}\right)_{SL} = \frac{(\tau_{Static} + \tau_{Seismic} + \tau_{Other})}{\tau} \quad \text{Equation I-7}$$

8. The onset of cyclic liquefaction in Sand-Like soils or cyclic softening in Clay-Like soils, occurs when the strength loss ratio  $(D/C)_{SL-i}$  for each slice (length,  $L_i$ )

susceptible to soil SSL is greater than the LRFD resistance factor ( $\phi_{SL}$ ) presented in Chapter 9 as indicated by the following equation.

$$\left(\frac{D}{C}\right)_{SL-i} > \phi_{SL} \quad \text{Equation I-8}$$

### I.3 REFERENCES

Fear, C. E., and Robertson, P. K. (1995). "Estimating the undrained strength of sand: A theoretical framework," *Canadian Geotechnical Journal*, 32(4), 859–870.

Olson, S. M., and Stark, T. D., (2003), "Yield Strength Ratio and Liquefaction Analysis of Slopes and Embankments," *Journal of Geotechnical and Geoenvironmental Engineering*, ASCE, Volume 129, Issue 8, pp. 727-737.



# **APPENDIX J**

## **FLOW CHARTS**

### **GEOTECHNICAL DESIGN MANUAL**

*January 2019*



# APPENDIX J

## FLOW CHARTS

The following list contains the Flow Charts used by SCDOT in the development of seismic design procedures. Please note that these Flow Charts are available at <https://www.scdot.org/business/geotech.aspx> and that the Flow Charts are setup to be printed on an “E” (Arch E (36-inch by 48-inch)) size sheet of paper.

- Figure J-1 – ADRS Curve Development Decision Chart
- Figure J-2 – Geotechnical Seismic Evaluation Process Master Flowchart – Part A
- Figure J-3 – Geotechnical Seismic Evaluation Process Master Flowchart – Part B
- Figure J-4 – Embankment and ERS Design Methodology Chart – Embankments
- Figure J-5 – Embankment and ERS Design Methodology Chart – ERSs (under construction)

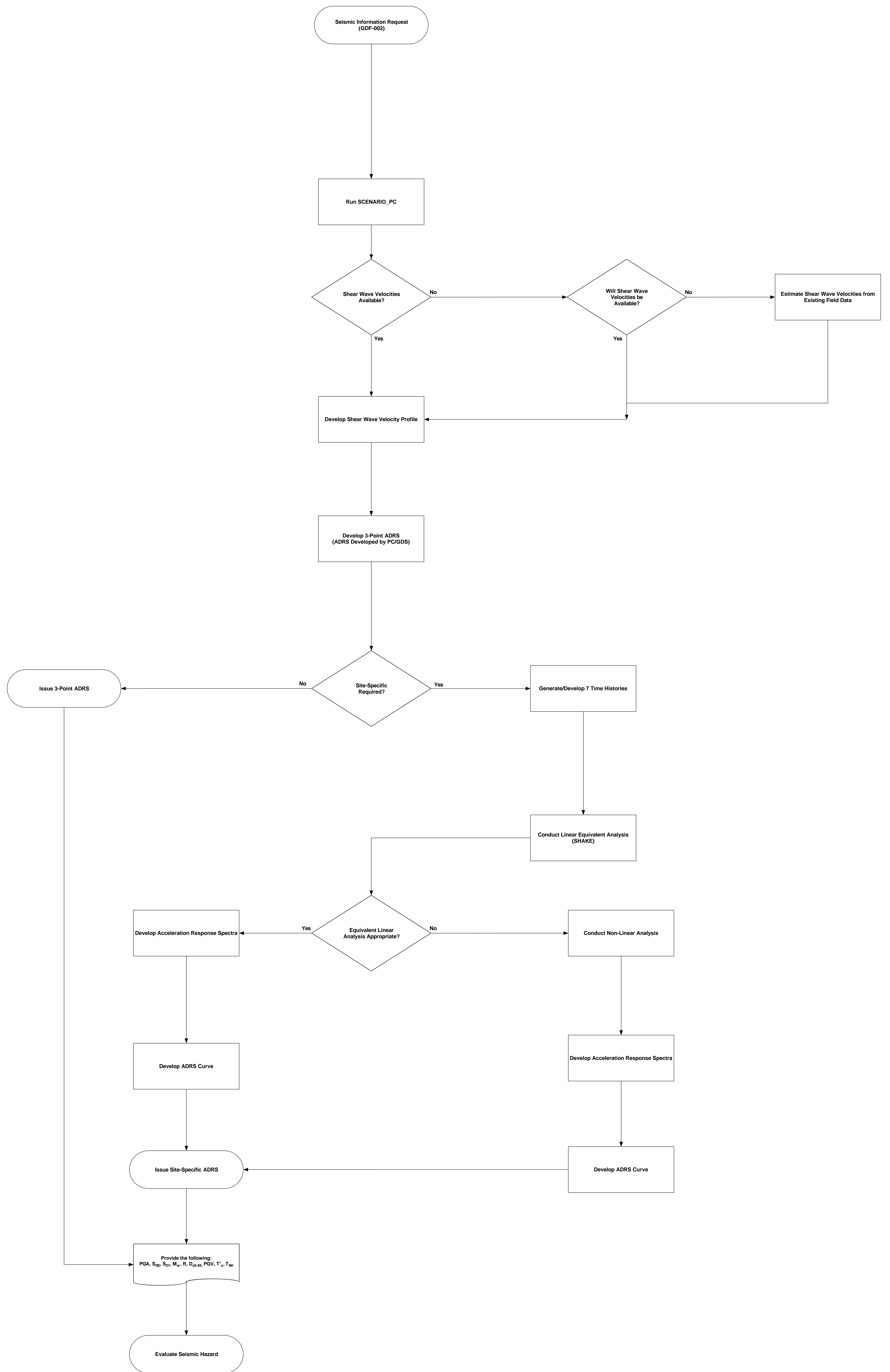


Figure J-1



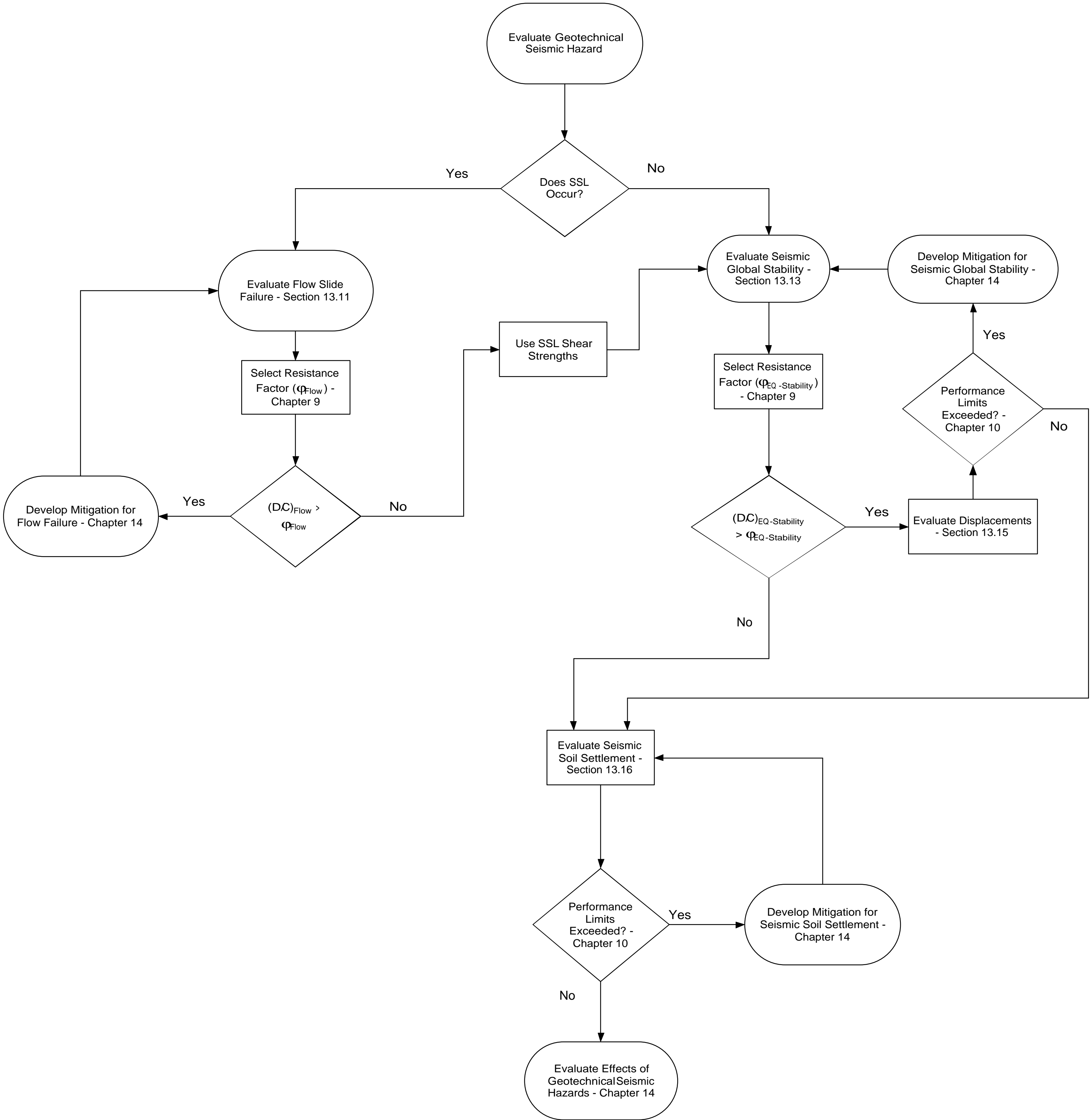


Figure J-3

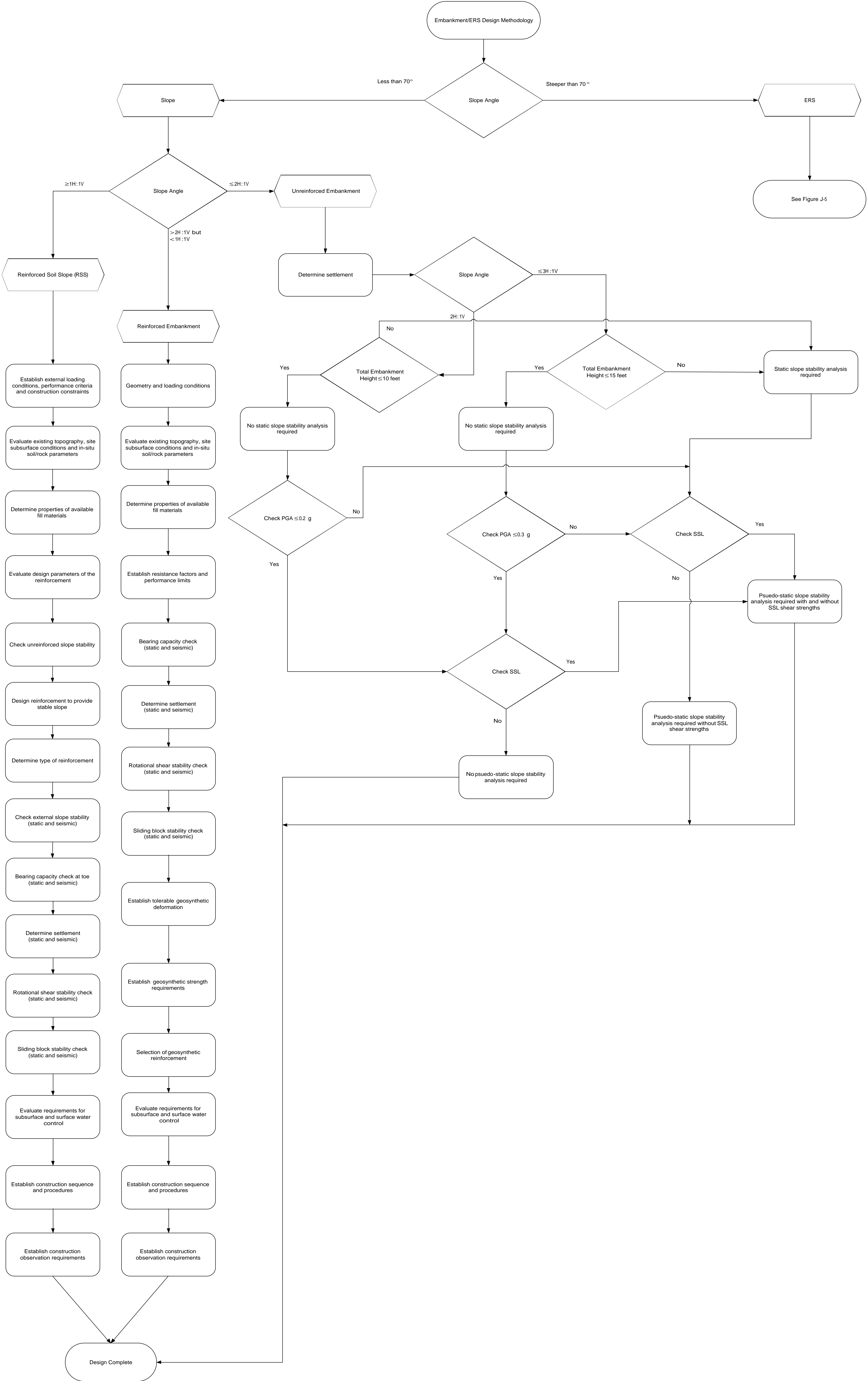


Figure J-4

**APPENDIX K**  
**PERFORMANCE OBJECTIVE**  
**DEVELOPMENT**

**GEOTECHNICAL DESIGN MANUAL**

*January 2019*





**Table of Contents**

<b><u>Section</u></b>		<b><u>Page</u></b>
K.1	Introduction.....	K-1
K.2	Safety .....	K-1
K.3	Operational Classification .....	K-1
K.4	Design Life .....	K-1
K.5	Functionality .....	K-1
K.6	Aesthetics.....	K-2
K.7	Construction .....	K-2
K.8	Maintenance.....	K-2
K.9	Risk .....	K-2



# APPENDIX K

## PERFORMANCE OBJECTIVE DEVELOPMENT

### K.1 INTRODUCTION

Performance Objectives have been previously developed (see Seismic Specs and Chapter 10) for bridges, ERSs and embankments. However, it is possible that additional Performance Objectives will be required and it will be the responsibility of the design team to develop these additional Performance Objectives. All additional Performance Objectives should be submitted to the PC/SDS and PC/GDS for review and acceptance prior to being used in design. Provided in the following Sections are general guidelines that should be used in the development of Performance Objectives.

### K.2 SAFETY

The structure must be designed for safety so as not to collapse when loads are applied to the structure and to control structural damage caused by these loads so that the risk of loss of life is reduced to an acceptable level (see Risk in the following Sections). The reliability of the design to maintain this objective is addressed by designing for the Strength limit state that takes into account the variability of the applied load and the available resistance. Structures that are designed for the Strength limit state will have component/members and foundations that are sized for larger loadings than loadings observed at the Service limit state. Having components/members and foundations of a structure that are sized for Strength limit state typically improves the performance of the structure by increasing the stiffness of the members. Thus resulting in smaller deformations and improved performance and service loads.

### K.3 OPERATIONAL CLASSIFICATION

SCDOT has established operational classifications for typical bridges (OC) to allow for differentiation between structures of higher and lower operational requirements to the South Carolina transportation infrastructure. The OC has 3 levels (I, II, and III), where OC I is the highest and OC III is the lowest. The OC is defined in the Seismic Specs. This classification allows SCDOT to vary the reliability, design requirements and performance expectations between structures that have relatively high operational requirements such as the Interstate system to those on low volume roads that are typically part of the secondary roadway system during the EE I limit state check.

### K.4 DESIGN LIFE

Design Life is the anticipated life expectancy of the structure, typically 75 years for bridges, 100 years for embankments and ERSs and 20 years for pavements. Typically at the end of the Design Life the existing structure will require either replacement by a new structure or extensive rehabilitation. It is assumed that the structure has periodic inspection and maintenance so as not to reduce the expected Design Life.

### K.5 FUNCTIONALITY

Functionality of a structure requires acceptable performance of the structure in order to be useable by the traveling public. This is accomplished by establishing performance limits (traffic projections, deformation limits, rideability requirements, etc.) for the Design Life of the structure.

In order to maintain the required functionality of the structure, periodic maintenance will be required.

## **K.6 AESTHETICS**

The aesthetics of a structure should be consistent with the environment where the structure will be placed. The aesthetic requirement of a structure located in an urban setting with high visibility will be different from those aesthetic requirements of a structure located in a rural setting with low visibility by the traveling public. Aesthetics of the structure are also defined by public perception of how visually safe or appealing a structure appears. A structure that is structurally stable but has cracks, excessive deformations in the form of bulges, out-of-plumbness, etc. is not aesthetically satisfactory. Satisfying aesthetic objectives requires proper planning (public hearings, timely information, etc.), good construction specifications that specify construction tolerances, finish requirements, proper inspection during construction, and periodic maintenance.

## **K.7 CONSTRUCTION**

The development of plans and construction specifications should be clear and take into account the constructability of the design and any construction monitoring. Construction specifications should include construction tolerances, construction methods, and field performance monitoring of the structure such as settlement monitoring.

## **K.8 MAINTENANCE**

A Maintenance Plan should be in place that consists of periodic inspections of the structure and communication with designers to evaluate the results of the inspections. The Maintenance Plan should also provide for the development of the appropriate responses required to meet the serviceability requirements of the structure for the remainder of its design life. Design details of the structure should allow for periodic inspection of vital components that would affect the structure's performance.

## **K.9 RISK**

The selection of the type of structure to be used in the design should consider any associated risk that would affect the performance of the structure. Some factors that increase the risk of unsatisfactory structure performance are presented below:

- **Construction:** Common types of structures are usually associated with less construction risk due to the familiarity of the construction procedures.
- **Structure Selection:** Failure to consider the limitations of the structure type selected in relation to the desired performance may lead to unsatisfactory performance. A common misapplication in construction is the use of cantilever sheetpiling for temporary shoring of deep excavations. The deformations typically exceed acceptable performance for adjacent structures.
- **Design/Construction Methodology:** Misapplication of methodologies in design (i.e. using unaccepted design methods) or construction (i.e. misapplication of ground improvement method).
- **Design Experience:** Insufficient design experience in either the design of the structure or of any ground improvement required can lead to unsatisfactory performance. Insufficient design experience includes untested designs, new design methodologies, and designer's inexperience.
- **Geotechnical Investigation:** A subsurface geotechnical investigation that does not adequately describe the foundation soils can lead to construction delays, "changes in

soil/subsurface conditions,” redesign of foundations that unfortunately results in contractor claims, increased construction costs, not meeting schedules, litigation, etc. The long-term impacts of an inadequate geotechnical investigation can result in poor long-term performance of the structure that results in higher maintenance costs and in many cases replacement of the structure before it has reached its anticipated design life.

- **Change in Soil/Subsurface Conditions:** These are unforeseen field conditions that typically cannot be accounted for during design. When changes in soil/subsurface conditions occur, they can be addressed during construction with proper communication between Construction and Design personnel. Field conditions that fall into this category are subsurface soil variability, and environmental factors (weather, etc.). Performing an adequate geotechnical subsurface investigation during the design phase of structure development is the most cost effective method of reducing the risk of having a “change in soil/subsurface conditions” occur during construction.

Quantifiable Performance Objectives are first developed and then Performance Limits are developed to meet these Performance Objectives. The Performance Limits are based on Design Life and Deformation Limits that are defined to meet the Performance Objectives of the Service limit state. Where possible, the factors listed above have been taken into consideration in the development of the Performance Limits listed for the Service limit state.